Helmut Popper

Pathology of Lung Disease

Morphology – Pathogenesis – Etiology

Springer

Pathology of Lung Disease

Helmut Popper

Pathology of Lung Disease

Morphology – Pathogenesis – Etiology

With contribution by Prof. Fiorella Calabrese

Springer

Helmut Popper
Institute of Pathology
Medical University Graz
Graz
Austria

ISBN 978-3-662-50489-5 ISBN 978-3-662-50491-8 (eBook)
DOI 10.1007/978-3-662-50491-8

Library of Congress Control Number: 2016948439

© Springer-Verlag Berlin Heidelberg 2017
This work is subject to copyright. All rights are reserved by the Publisher, whether the whole or part of the material is concerned, specifically the rights of translation, reprinting, reuse of illustrations, recitation, broadcasting, reproduction on microfilms or in any other physical way, and transmission or information storage and retrieval, electronic adaptation, computer software, or by similar or dissimilar methodology now known or hereafter developed.
The use of general descriptive names, registered names, trademarks, service marks, etc. in this publication does not imply, even in the absence of a specific statement, that such names are exempt from the relevant protective laws and regulations and therefore free for general use.
The publisher, the authors and the editors are safe to assume that the advice and information in this book are believed to be true and accurate at the date of publication. Neither the publisher nor the authors or the editors give a warranty, express or implied, with respect to the material contained herein or for any errors or omissions that may have been made.

Printed on acid-free paper

This Springer imprint is published by Springer Nature
The registered company is Springer-Verlag GmbH Germany
The registered company address is Heidelberger Platz 3, 14197 Berlin, Germany

Preface

Scio, me nihil scire (a phrase attributed to the Greek philosopher Socrates)

As an academic pathologist, I see this phrase not as discouraging but instead encouraging. In almost every disease, there are many unanswered questions, so when our students ask about it, we have to answer that we do not know. But many of the "I do not know answers" can be the starting point for a new research proposal – in this sense I mean our missing knowledge "is not discouraging" at all.

Pathology has reached an important crossroad: there is danger of losing competence on one hand but also a bright revival of the importance of pathology. Many new discoveries have shed light into pathogenesis, which we had previously simply described from our understanding of morphology, but which now we can interpret with a completely different perspective of understanding underlying molecular processes.

In tumors, we have learned a lot about the importance of genetic abnormalities and what the results from these alterations are. We are just learning to separate driver mutations and alterations of genes from cooperating mutations and use some of these genetic abnormalities to treat our patients in a completely new way with fewer side effects.

In inflammatory and immune diseases, we have learned that lymphocytes can act in an opposite way, either bringing good or bad actions in a given disease. Lymphocytes can aggravate the damage of lesions initiated by infectious organisms or help to defend against the organisms. Developments in immunology research have broadened our understanding of regulations between the many types of regulatory lymphocytes and antigen-presenting cells. This will not only enable us to more precisely diagnose immune diseases but also to promote immune attack toward tumor cells in patients. In addition, immunooncology has entered tumor therapy, and pathologists are faced with new challenges in the interpretation of anti- or pro-tumor action of the patient's immune system.

Has this changed our recognition? If you do an Internet research looking for basic science investigations, pathologists are hardly in the forefront of this type of research; they are rarely leading. Most often, if ever they are coauthors, because they have contributed some tissues for the investigation, or sometimes have made the diagnosis, so the research material could be grouped.

And many pathologists are just happy to contribute on this small scale. Some are even happy to outsource molecular pathologic diagnostics to private companies instead of doing this investigation "in-house." Other pathologists have developed a pseudoscientific habit: By changing classifications every 4–5 years, they assume they will be regarded as important. But this old style of changing little diagnostic boxes and giving them new names, without creating new information, will not last for more than a few years. Will this increase our reputation? I think not. This behavior will finally degrade pathology departments into a tissue repository, and pathologists into biobank curators, who do not care what this tissue is used for.

Is there an alternative? Where is the bright light and future?

We need to learn the biology of the diseases, and we need to familiarize with their genetic abnormalities and what impact genetic changes might have. In our daily practice, we often see a time sequence of pathogenetic events in a given disease. We need to assemble these single-time events like pictures into a movie (early–intermediate–late, resolving–recurrent). For example, early on, hyperplasia might be the first step into neoplasia. The cells acquire better access to nutrition and oxygen supply, which enables them to grow faster and outrange their normal neighbors. Some of these cells develop atypia; among them are tissue stem cells, which can move out, settle down at another focus, and establish another hyperplastic focus. Some of these colonies will develop into preneoplastic lesions, others will be whipped out by the immune system, and others will die due to defective DNA repair and apoptosis. All these events will leave footprints in the tissue, and we as pathologists should read and interpret these footprints and correlate this with the underlying genetic changes: phenotypic genotypic correlation is a key to better understanding and better diagnostics. The same is true for immune diseases. Understanding the interaction of immune cells in an autoimmune disease and analyzing the cells present at a given time sequence might not only provide a more accurate diagnosis but also might provide understanding of the disease progression and finally pave ways for better treatment. So a successful new type of pathologist will understand the biology behind a given morphology and in this way will be a welcomed partner in research as well as in the patient management team.

It will be impossible to describe all aspects of etiology and pathogenesis in all diseases we will cover; this would go beyond the scope of this book on lung diseases. However, I will summarize as good as possible pathogenesis and etiology in each of the entities, being aware that I am not able to give a complete overview.

This book is based on my experience of dealing with lung diseases for more than 35 years. I present a one-author book instead of the common multiauthor books, because all the chapters will be in line with my perspective of interpreting pathology. And this can be summarized as follows: pattern recognition is a first step of analysis, but looking into the pathogenesis and etiology of a disease is what makes a good pathologist. One chapter is an exception: My practice in transplant pathology is limited. In Austria, lung transplantation is concentrated in Vienna, which results to less tissues being studied. So I was happy that Fiorella was willing to contribute this chapter.

I encourage you as the reader and user of this book to communicate with me on your critiques, as this is important for future improvements. I have learned more from mistakes than from everything else. Misdiagnosis was my best teacher. As in every scientific discipline, mistakes and misinterpretations do occur, sometimes simply overlooked.

Graz, Austria Helmut Popper

Acknowledgments

I am indebted to my family especially to my wife Ursula for her understanding during my increasing commitment with lung pathology.

I am also grateful to my teachers Helmut Denk, Liselotte Hochholzer (AFIP), and Hans Becker for their encouragement to study lung pathology in depth and promoting me to go abroad to learn new technologies and learn new ways of interpreting lung tissue reactions. I would also like to thank numerous colleagues with whom I shared my enthusiasm and time to discuss lung pathology during international conferences. Many of them became friends during the process to form the European Working Group on Pulmonary Pathology. It would be impossible to name them all personally.

Contents

1 Development of the Lung 1
1.1 Genetic Control of the Development 4
1.2 Comparison of Lung Development Across Species 4
References 4

2 Normal Lung 7
2.1 Gross Morphology 7
2.2 The Airways 9
2.3 Lymphoreticular Tissue and the Immune System of the Lung 18
2.4 Comparison of Human Lung to Other Species 18
References 19

3 Pediatric Diseases 21
3.1 Developmental and Inherited Lung Diseases 21
3.1.1 Aplasia and Acinar/Alveolar Dysgenesis 21
3.1.2 Growth Retardation 24
3.1.3 Vascular Malformations 24
3.1.4 Malformations of the Airway System 33
3.1.5 Lung Pathology in Chromosomal Abnormalities 41
3.1.6 Inborn Errors of Metabolism 42
3.1.7 Cystic Fibrosis 47
3.1.8 Neuroendocrine Cell Hyperplasia of Infancy (NEHI) . . 48
3.2 Pneumonia in Childhood Including Noninfectious Interstitial Pneumonias 50
3.2.1 Chronic Pneumonia of Infancy (CPI) 50
3.2.2 Mendelson Syndrome in Children and Silent Nocturnal Aspiration 51
References 53

4 Edema 59
4.1 Gross Morphology 59
4.2 Histology 59
4.3 High-Altitude Edema (HAPE) 59
References 61

5 Air Filling Diseases 63
5.1 Atelectasis 63
5.1.1 Gross Morphology 64
5.1.2 Histology 64
5.2 Emphysema 65
5.2.1 Gross Morphology 65
5.2.2 Histology 66
5.3 Emphysema and Lung Function 72
5.3.1 Factors Contributing to Emphysema Development 73
References 74

6 Airway Diseases 77
6.1 Tracheitis and Bronchitis 77
6.1.1 Gross Morphology 77
6.1.2 Histology 78
6.2 Bronchial Asthma 80
6.2.1 Etiology 80
6.2.2 Immune Mechanisms 80
6.2.3 Gross Morphology 82
6.2.4 Histology 82
6.3 Bronchiolitis 84
6.4 The Classification 84
References 100

7 Smoking-Related Lung Diseases 103
7.1 Langerhans Cell Histiocytosis 103
7.1.1 Histology 103
7.1.2 Molecular Biology 104
7.1.3 Function of LH Cells 106
7.1.4 Differential Diagnosis 106
7.2 Respiratory Bronchiolitis: Interstitial Lung Disease (RBILD) 106
7.2.1 Histology 107
7.3 Desquamative Interstitial Pneumonia (DIP) 109
7.3.1 Histology 111
7.4 Smoking-Induced Interstitial Fibrosis (SRIF)/Respiratory Bronchiolitis-Associated Interstitial Lung Disease (RBILD) 112
7.5 Chronic Obstructive Pulmonary Disease (COPD) 113
7.5.1 What Are the Mechanisms? Why Not Every Smoker Develops COPD? 114
References 116

8 Pneumonia 121
8.1 Alveolar Pneumonias (Lobar and Bronchopneumonia) 121
8.1.1 Clinical Symptoms of Pneumonias 123
8.1.2 Alveolar Pneumonias (Bronchopneumonia and Lobar Pneumonia; Adult and Childhood) 123

8.1.3 Diffuse Alveolar Damage (DAD) and Acute Interstitial Pneumonia 126
8.1.4 Lymphocytic Interstitial Pneumonia (LIP) 131
8.1.5 Giant Cell Interstitial Pneumonia (GIP; See Also Under Pneumoconiosis) 133
8.1.6 The Infectious Organisms 133
8.1.7 Bronchopulmonary Dysplasia (BPD) 142
8.1.8 Aspiration Pneumonia 142
8.1.9 HIV Infection 142
8.2 Granulomatous Pneumonias 144
8.2.1 Introduction 144
8.2.2 What Influences Granuloma Formation? Why Necrosis? 144
8.2.3 Morphologic Spectrum of Epithelioid Cell Granulomas 146
8.2.4 The Causes of Epithelioid Cell Granulomas and Their Differential Diagnosis 147
8.2.5 Methods to Be Used for a Definite Diagnosis of Infectious Organisms 170
8.3 Fibrosing Pneumonias (Interstitial Pneumonias) 173
8.3.1 Historical Remarks on Interstitial Pneumonia Classification 173
8.3.2 Usual Interstitial Pneumonia (UIP)/Idiopathic Pulmonary Fibrosis (IPF) 174
8.3.3 Familial IPF (FIPF) 182
8.3.4 Nonspecific Interstitial Pneumonia (NSIP) 184
8.3.5 Organizing and Cryptogenic Organizing Pneumonia (OP, COP) 187
8.3.6 Airway-Centered Interstitial Fibrosis (ACIF) 189
References 191

9 Immunological Lung Diseases 199
9.1 Introduction into Interstitial Lung Diseases 199
9.2 Autoimmune Diseases 200
9.2.1 Rheumatoid Lung Disease 200
9.2.2 Systemic Lupus Erythematosus 207
9.2.3 Systemic Sclerosis 211
9.2.4 Dermatomyositis/Polyserositis 215
9.2.5 Sjøgren's Syndrome 217
9.2.6 Mixed Collagen Vascular Diseases (CVD) 220
9.2.7 Goodpasture Syndrome 221
9.2.8 Other Autoimmune Diseases Affecting the Lung 223
9.2.9 Surfactant-Related Interstitial Pneumonias: Alveolar Proteinosis 225
9.3 Diseases of the Innate Immune System Based in Genetic Abnormalities 226
9.3.1 Idiopathic Pulmonary Hemosiderosis 226
9.3.2 Lymphangioleiomyomatosis (LAM) 227

9.3.3 Hermansky-Pudlak Syndrome 232
9.3.4 Erdheim-Chester Disease 234
9.4 Allergic Diseases 234
9.4.1 Allergic Bronchopulmonary Mycosis 234
9.5 Drug Allergy 234
References 236

10 Eosinophilic Lung Diseases 239
10.1 Introduction 239
10.2 Allergic or Hyperreactive Diseases 239
10.2.1 Allergic Bronchopulmonary Mycosis (Aspergillosis) 239
10.3 Eosinophilic Pneumonias (EP) 241
10.3.1 Epidemiology and Incidence 241
10.3.2 Clinical Presentation and CT 241
10.3.3 Pathogenesis and Etiology 242
10.3.4 Immunohistochemistry, Genetics, and Immunology 247
References 248

11 Vascular Lung Diseases 251
11.1 Infarct and Thromboembolic Disease 251
11.1.1 Gross Examination and Histology 251
11.2 Vasculitis 251
11.2.1 Classification of Vasculitis 251
11.2.2 Granulomatosis with Polyangiitis 253
11.2.3 Eosinophilic Granulomatosis with Polyangiitis (EGPA, Formerly Called Churg-Strauss Vasculitis) 255
11.2.4 Microscopic Polyangiitis 256
11.2.5 Panarteritis Nodosa 258
11.3 Secondary Vasculitis with Infection 260
11.4 Secondary Vasculitis Without Infection 261
11.5 Vascular Diseases and Malformation 262
11.5.1 Histology 262
11.6 Malformation and Systemic (Inborn) Vascular Diseases in Children 263
11.7 Pulmonary Hypertension 263
11.7.1 Mechanisms of PAH 269
11.8 Alveolar Hemorrhage 270
11.9 Diseases of the Lymphatics (Adult and Childhood) 270
11.10 Malformation 270
11.11 Obstruction 271
11.12 Inflammation 271
References 272

12 Metabolic Lung Diseases 275
12.1 Amyloidosis 275
12.2 Disturbed Calcium Metabolism 277
12.3 Lipid and Surfactant Metabolism 282
12.4 Iron and Elastin Metabolism 288
References 289

13 Pneumoconiosis and Environmentally Induced Lung Diseases 291
13.1 Introduction 291
13.2 Silicosis 292
13.3 Silicatosis 294
13.3.1 Asbestosis 295
13.3.2 Other Silicatoses 296
13.4 Metal-Induced Pneumoconiosis and Disease 300
13.4.1 Hard Metal Lung Disease 302
13.4.2 Aluminosis 302
13.4.3 Chromium and Vanadium 305
13.4.4 Tungsten 305
13.4.5 Cobalt 306
13.4.6 Other Metals 307
13.4.7 Mercury 308
13.4.8 Nickel 308
13.4.9 Arsenic, Tin 308
13.4.10 Indium, Tin 308
13.4.11 Siderosis 309
13.4.12 Rare Metals and Chronic Allergic Metal Diseases . . 309
13.5 Cotton Dust, Flock Workers' Lung, and Byssinosis 312
13.6 Manmade Fibers, Hydrocarbon Compounds, and Polyvinyls 312
13.7 Pesticides and Insecticides 312
13.8 Inhalation of Combustibles 313
13.9 Cocaine and Marijuana 313
References 315

14 Iatrogenic Lung Diseases 321
14.1 Drug-Induced Interstitial Lung Diseases 321
14.2 Action of Drugs and Morphologic Changes Associated with Drug Metabolism 321
14.2.1 Granulomatous Reactions 323
14.2.2 DAD Pattern 323
14.2.3 Organizing Pneumonia Pattern 323
14.2.4 NSIP and LIP Patterns 323
14.2.5 UIP Pattern 323
14.2.6 Vasculitis 328
14.2.7 Edema 328
14.2.8 Fibrinous Pneumonia 328

14.3 Iatrogenic Pathology by Radiation 328
References 329

15 Bronchoalveolar Lavage as a Diagnostic and Research Tool 331
15.1 Where and When Doing BAL? 331
15.2 Processing of BAL 332
References 334

16 Lung Transplantation-Related Pathology 335
16.1 Explant Pathology 335
16.1.1 Obstructive Diseases 335
16.1.2 Restrictive Diseases 336
16.1.3 Vascular Disease (Pulmonary Hypertension) 338
16.2 Perioperative Complications 338
16.3 Lung Allograft Rejection 339
16.3.1 Hyperacute Lung Rejection 339
16.3.2 Acute Rejection (Grade A, B) 339
16.3.3 Chronic Rejection (Grade C and D) 339
16.3.4 Emerging Immunological Lesions 342
16.4 Infections 344
16.4.1 Viral Infection 344
16.4.2 Bacterial Infection 345
16.4.3 Fungal Infections 345
16.5 Tumors 346
16.5.1 Other Tumors 346
16.6 Other Complications 347
16.6.1 Graft-Versus-Host Disease (GVHD) 347
16.6.2 Disease Recurrence in the Graft 347
16.6.3 Drug Injury 347
References 347

17 Lung Tumors 353
17.1 Epithelial Tumors 353
17.1.1 Benign Epithelial Tumors 353
17.2 In Situ Carcinoma and Precursor Lesions 382
17.2.1 Preneoplastic Lesions – Squamous Cell Dysplasia . . 382
17.2.2 Atypical Adenomatous Hyperplasia 385
17.2.3 Bronchiolar Columnar Cell Dysplasia 385
17.2.4 Atypical Goblet Cell Hyperplasia 388
17.2.5 Neuroendocrine Cell Hyperplasia 388
17.3 Malignant Epithelial Tumors 392
17.3.1 Epidemiology 392
17.3.2 Carcinogenesis: Our Current Sight on the Development of Cancer 393
17.3.3 Common Carcinomas 398
17.3.4 Carcinomas with Clear Cells 448
17.3.5 Rhabdoid Carcinoma 449
17.3.6 LC of Hepatoid Phenotype 449
17.3.7 Lymphoepithelioma-like Carcinoma 449

17.3.8 Adenosquamous Carcinoma. 452
17.3.9 Diagnosis on Small Biopsies and Cytology Preparations 452
17.3.10 Salivary Gland-Type Carcinomas 454
17.3.11 The Sarcomatoid Carcinomas 461
17.3.12 Primary Intrapulmonary Germ Cell Neoplasms 465
17.3.13 NUT Carcinoma. 469
17.3.14 Staging of Pulmonary Carcinomas 470
17.4 Benign and Malignant Mesenchymal Tumors. 470
17.4.1 Hamartoma. 470
17.4.2 Smooth Muscle Tumors 471
17.4.3 Fibromatous Tumors 480
17.4.4 PEComa (Clear Cell Tumor and Sugar Tumor) 491
17.4.5 Chondroma, Osteoma, and Lipoma 493
17.4.6 Tumors with Nervous Differentiation 494
17.4.7 Triton Tumor 499
17.4.8 Paraganglioma 500
17.4.9 Pulmonary Meningioma. 502
17.4.10 Vascular Tumors. 503
17.4.11 Primary Melanoma of the Bronchus 524
17.5 Hematologic Tumors Primarily Arising in the Lung. 527
17.5.1 Lymphomas 527
17.5.2 Dendritic Cell and Histiocytic Tumors 535
17.6 Childhood Tumors. 542
17.6.1 Congenital Peribronchial Myofibroblastic Tumor . . . 542
17.6.2 Fetal Lung Interstitial Tumor (FLIT). 547
17.6.3 Pleuropulmonary Blastoma 547
17.6.4 Adenocarcinoma of the Lung Arising in CPAM 551
17.6.5 Squamous Cell Papilloma and Papillomatosis. 552
17.6.6 Capillary Hemangiomatosis. 553
References. 553

18 Metastasis. 577
18.1 Tumor Establishment and Cell Migration. 577
18.1.1 Angiogenesis, Hypoxia, and Stroma (Microenvironment). 577
18.1.2 The Role of Hypoxia in Tumor Cell Migration and Metastasis 579
18.1.3 Escaping Immune Cell Attack 582
18.1.4 Migration 582
18.2 Vascular Invasion: Lymphatic/Hematologic 586
18.2.1 Blood Vessels 586
18.2.2 Lymphatic Vessels 587
18.3 Extravasation. 587
18.4 Preparing the Distant Metastatic Focus 588
18.4.1 Angiogenesis 589
18.5 Metastasis 589
18.5.1 Brain Metastasis. 590
18.5.2 Lung Metastasis 593
18.5.3 Bone Metastasis 593

18.5.4 Pleural Metastasis 594
18.5.5 Lymph Node Metastasis. 595
18.6 Metastasis to the Lung 596
References. 605

19 Molecular Pathology of Lung Tumors 611
19.1 Introduction. 611
19.2 Therapy Relevant Molecular Changes in Pulmonary Carcinomas 611
19.2.1 NSCLC and Angiogenesis 611
19.2.2 NSCLC and Cisplatin Drugs: The Effect of Antiapoptotic Signaling 612
19.2.3 Thymidylate Synthase Blocker 612
19.2.4 Receptor Tyrosine Kinases in Lung Carcinomas 613
19.2.5 TP53: The Tumor Suppressor Gene. 613
19.3 Adenocarcinomas 613
19.3.1 EGFR 614
19.3.2 KRAS. 614
19.3.3 EML4ALK1 and Additional Fusion Partners 615
19.3.4 ROS1 615
19.3.5 KIF5B and RET 616
19.3.6 MET 616
19.3.7 Others Genes 616
19.4 Squamous Cell Carcinomas 617
19.4.1 FGFR1 617
19.4.2 DDR2 and FGFR2 617
19.4.3 SOX2 Amplification. 617
19.4.4 PTEN Mutation-Deletion. 618
19.4.5 PDGFRA Amplification. 618
19.4.6 CDKN2A (p16) Mutation, Deletion, and Methylation 618
19.4.7 Notch1 Mutation 618
19.4.8 REL Amplification 618
19.5 Large Cell Carcinoma 618
19.6 Other Types of Large Cell Carcinomas. 619
19.7 The Neuroendocrine Carcinomas 619
19.7.1 Small Cell Neuroendocrine Carcinoma 619
19.7.2 Large Cell Neuroendocrine Carcinoma 620
19.7.3 Carcinoids 620
19.8 Salivary Gland Type Carcinomas 621
19.8.1 Mucoepidermoid Carcinoma 621
19.8.2 Adenoid Cystic Carcinoma 621
19.9 Sarcomatoid Carcinomas (SC) 622
19.10 Preneoplastic Lesions 622
19.10.1 Hyperplasia of Goblet Cells and Squamous Metaplasia/Dysplasia 623
19.10.2 Genetic Aberrations in AAH 623
19.10.3 Neuroendocrine Cell Hyperplasia 624

19.11 Selected Examples of Benign and Mesenchymal Lung Tumors . . . 624
19.11.1 Benign Epithelial Tumors . . . 624
19.11.2 Sclerosing Pneumocytoma . . . 624
19.12 Tumors Induced by Mutations of the TSC Genes (Related to Tuberous Sclerosis) . . . 625
19.12.1 Multifocal Nodular Pneumocyte Hyperplasia (MNPH) . . . 625
19.12.2 Lymphangioleiomyomatosis (LAM) . . . 625
19.12.3 Clear Cell Tumor (Sugar Tumor, PEComa = Perivascular Epithelioid Cell Tumor) . . . 625
19.13 Malignant Tumors of Childhood . . . 626
19.13.1 Pleuropulmonary Blastoma . . . 626
19.13.2 Congenital Myofibroblastic Tumor . . . 626
19.14 Final Remarks . . . 626
References . . . 626

20 Immunotherapy of Lung Tumors . . . 639
20.1 Systems Known to Be Able to Induce Immune Tolerance Toward Foreign Antigens . . . 640
References . . . 642

21 Diseases of the Pleura . . . 645
21.1 Hemorrhage . . . 645
21.2 Effusion . . . 645
21.3 Inflammation: Pleuritis . . . 645
21.3.1 Purulent Pleuritis . . . 645
21.3.2 Hemorrhagic Pleuritis . . . 646
21.3.3 Chronic Pleuritis . . . 646
21.4 Tumors . . . 646
21.4.1 Mesothelioma . . . 649
21.4.2 Multicystic Mesothelioma . . . 662
21.4.3 Adenomatoid Tumor . . . 663
21.4.4 Solitary Fibrous Tumor of the Pleura (Fibroma, SFT) . . . 663
21.4.5 Desmoid Tumor . . . 665
21.4.6 Calcifying (Fibrous) Pleura Tumor (CPT) . . . 666
21.4.7 Primary Squamous Cell Carcinoma of the Pleura . . . 666
21.4.8 Primary Fibrosarcoma . . . 667
21.4.9 Undifferentiated Sarcoma Arising in the Lung and/or Pleura (Formerly Malignant Fibrous Histiocytoma, MFH) . . . 667
21.4.10 Desmoplastic Round Cell Tumor . . . 668
21.5 Metastasis to the Pleura . . . 668
References . . . 671

22 Experimental Lung Tumors . . . 675
22.1 History . . . 675
22.2 Tobacco Inhalation Experiments . . . 675

22.3 Why Adenocarcinomas in Mice and Rats? 675
22.4 Xenograft Transplantation of Human Carcinomas/Cell Cultures into Nude Mice 676
22.5 Differences in Chemically Induced Lung Tumors Compared to Humans 676
22.6 The Urethane Model 676
22.7 Genetically Engineered Mouse Models of Lung Cancer 677
22.7.1 The Pulmonary Adenocarcinoma Models 677
22.7.2 Histopathology of Adenocarcinomas 678
22.7.3 Immunohistochemistry as an Aid to Identify the Precursor Cell Population 682
22.7.4 Progression of Adenocarcinomas 683
22.7.5 Specific Changes Induced by Genetic Modifications 684
22.7.6 Do Mouse Adenocarcinomas Resemble Human Adenocarcinomas? 685
22.7.7 Differences in Mouse and Human Lung Morphology as Explanation for Different Adenocarcinoma Appearance 686
22.7.8 Genetic Differences Between Mouse and Human Adenocarcinomas 686
22.7.9 Cellular Origin of Adenocarcinomas 687
22.7.10 The Small-Cell Carcinoma Models 687
22.8 Models of Metastasis 690
References 691

23 Handling of Tissues and Cells 697
23.1 Biopsies 697
23.2 Videothoracic Lung Biopsy (VATS) and Open Lung Biopsy (OLB) 697
23.3 Resection Specimen 698
23.4 Frozen Section Handling and Evaluation 698
23.5 Handling of Cells 699
23.6 Microbiology 699

Development of the Lung

1

The lung develops from the foregut. At the highness of the later larynx, the single tube splits into two buds for the esophagus and the lower respiratory tract, the "Lungenanlage" [1] (around gestational week 4). Out of this primitive bud, the larynx and the trachea develop, and the trachea finally separates into two bronchial buds. As in general, organogenesis recapitulates also the developmental stages of mammalian lung: a bronchial bud is also formed for a possible mediastinal lobe, as it is found in sheep, swine, and other mammalians. If this bud persists, a median mediastinal bronchial cyst can result [2]. Supernumerary buds are usually deleted by apoptotic mechanisms [3, 4]. Sometimes these buds can give rise to communications with the esophagus [5] or also to bronchogenic cysts [2, 6].

The bronchial buds give rise to several generations of bronchi, starting with the main bronchi, lobar bronchi, segmental bronchi, and so on. In the human lung, approximately 16 generations are formed around the seventh week. After that, bronchioli are formed with an additional of four generations, as membranous, and three generations of terminal respiratory bronchioli. These open into alveolar ducts on which alveoli are grouped.

For the bronchial and alveolar development, the mesenchyme derived from the mesoderm is essential. Each primitive bronchus is surrounded by splanchnopleuromesoderm. Without the connection to the mesoderm, no alveoli develop [7]. Some mediators have been identified, which are responsible for this cooperation between bronchial sprouting and mesenchyme development, such as epimorphin and fibroblast growth factor 7 (FGF7). If this is knocked out, no sprouting does occur [8, 9].

The different developmental stages of the lung are the embryonic stage, where the lung consists of branching tubules (gestational weeks 4–8). These tubules are lined by a single row of high columnar epithelium. In the pseudoglandular phase (weeks 8–16), the branching bronchial tree is embedded in a primitive immature mesenchyme; however, there are so many tubules that it mimics glandular structures (Figs. 1.1 and 1.2).

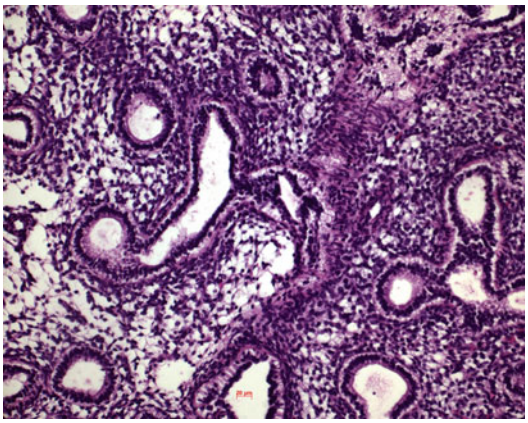

Fig. 1.1 Lung specimen in the early developmental tubular stage, eight week of gestation; the bronchial buds are separated by a primitive mesenchyme, only few primitive endothelial precursor cells can be identified, and capillaries have not been formed. A pulmonary artery has been cut tangentially and is seen between two bronchial buds (*right upper border to middle lower border*). H&E, bar 20 μm

© Springer-Verlag Berlin Heidelberg 2017

H. Popper, *Pathology of Lung Disease*, DOI 10.1007/978-3-662-50491-8_1

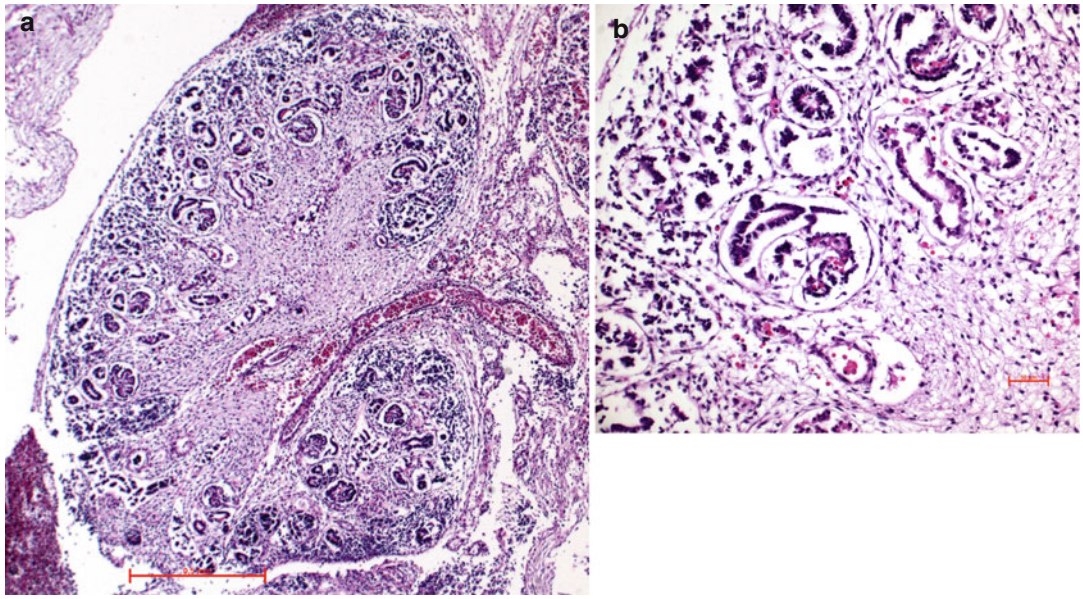

Fig. 1.2 (**a**, **b**) Lung specimen in early developmental glandular stage, 12th gestation week; (**a**) bronchial buds are seen embedded in a primitive mesenchymal stroma, (**b**) but early glands are already formed. H&E, bar 500 and 50 µm

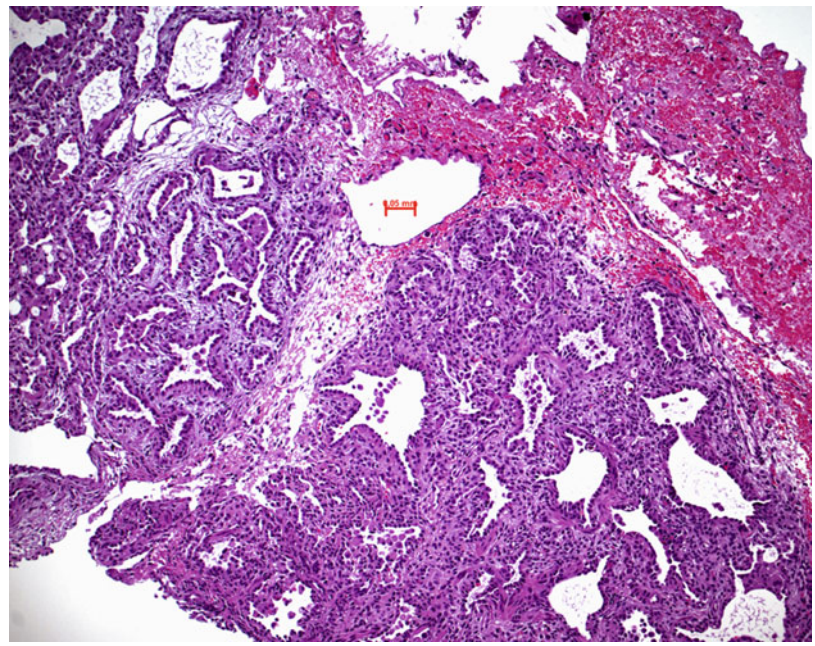

Fig. 1.3 Lung specimen in a premature child (gestation week 24); in transition from canalicular to saccular stage with primitive alveoli, which have not branched, the epithelium already shows pneumocytes in type II, and capillaries are already present; in this case the child developed bronchopulmonary dysplasia. H&E, bar 50 µm

Around the 13th week, the canalicular stage begins lasting until the 25th week. In this stage, the last generations of bronchioli are formed, the epithelium starts to differentiate into pneumocytes type I and II, capillaries are formed around the alveoli, and the bronchi are folded to form the first primitive lobules (Fig. 1.3). The bronchial epithelium also starts from few layers of cells, which expand during development and maturation. Columnar epithelia on H&E-stained section appear as clear cells due to abundant glycogen storage in the cytoplasm, and the nuclei

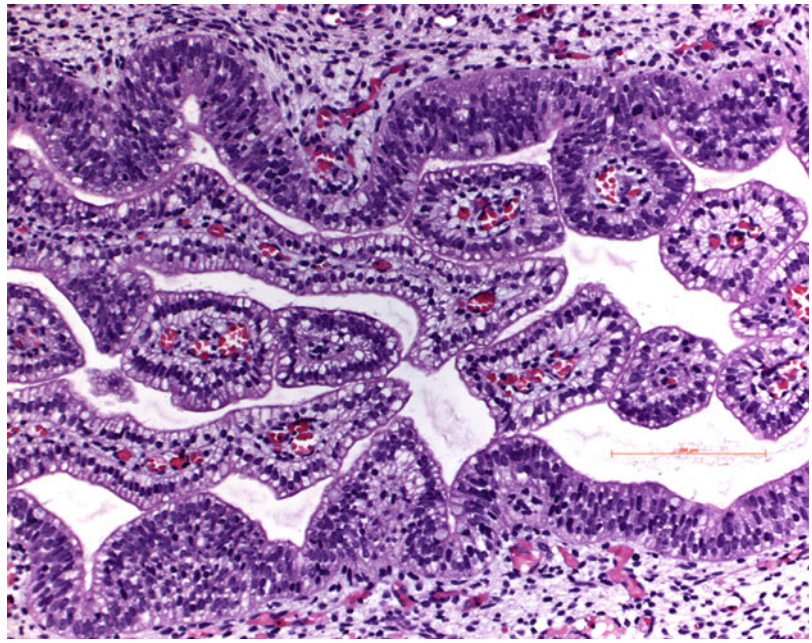

Fig. 1.4 Lung specimen at the development age of 18th gestation week; the bronchial epithelium shows nicely the clear cell pattern with apical positioned nuclei; this changes during maturation: nuclei start to move from the apical to the final basal location within the cell. The clear cell pattern results from abundant glycogen storage, which is dissolved during tissue section processing (alcohol). H&E, bar 200 µm

are positioned at the apical cell portion (Fig. 1.4). During maturation, nuclei move toward the basal portion of the cell, and other structures and proteins replace glycogen granules. In the saccular or terminal sac stage (gestational weeks 24–36), the alveoli are formed, expanded, and capillarized, and surfactant synthesis is started. During the last 2 weeks (alveolar phase), alveoli are expanded, filled by amniotic fluid, secondary septation starts (proceeding still after birth), and respiration starts. In this phase, the fetus already can take up oxygen from the amniotic fluid and release carbon hydroxide. Even after birth bronchial generations and alveoli can be generated [9]. The newborn human has approximately 50 million alveoli at birth, which represents approximately one-sixth of the number of an adult.

The vascular structures arise in two different ways: the large arteries start from the sixth branchial arch and grow along the bronchial tree down to the periphery behind the ductus arteriosus. The veins develop later by sprouting from the left atrium into the mediastinum but in addition also from the sinus venosus. The veins reach the developing primitive lobules and surround them at the surface. Veins primarily form sinusoidal islands and coalesce into conducting structures following the interlobular septa [8, 9]. In contrast the capillaries develop from the mesoderm [10, 11].

Bronchial arteries can be found from the ninth week of gestation. They form a plexus around the bronchi and form anastomoses with the pulmonary veins, whereas a specialized form of blood vessels, the contractile arteries, organizes the connection with the pulmonary arteries. During the saccular stage of the development, the central and peripheral vascular structures are joined. If this program is disturbed, pulmonary sequestration can result, where a part of the peripheral vascular bed is joined to a systemic artery. Also other vascular malformations such as Scimitar syndrome can be based on program failure in this period.

Lymphatic vessels are formed as a plexus in the hilar region together with the ductus thoracicus and are developed at the fifth fetal month.

Nerves are primarily formed out of ganglia of nervus vagus and truncus sympathicus/parasympathicus. An outer and inner plexus is formed around the bronchi, which is finally fused into one plexus at the site of the bronchioles. At the eight month, nerves and ganglia are mature;

neurofilaments can be demonstrated. The nerves can be separated into secretory and sensory as well as motoric fibers. They are close to the bronchial muscles and also around blood vessels.

Neuroendocrine cells (NEC) can be found from the eight gestational weeks on, whereas in bronchioles and alveoli, they can be first demonstrated by neuroendocrine markers around the fifth month (chromogranin A, synaptophysin, PGP9.5). NECs are essential for the proper development and maturation of the bronchial tree.

The other mesenchymal structures, such as myoblasts and chondroblasts, develop from the coelom (splanchnopleura), which surrounds the developing bronchial tree.

The pleura also starts from the coelom (splanchnopleura), which surrounds the "Lungenanlage" [8, 9]. From there the visceral pleura develop. From the pericardo-peritoneal channel, which is the lateral portion of the splanchnopleura, the parietal pleura arises. Primarily the parietal pleura fills both lateral thoracic cavities, since the developing bronchi occupy only small portions of the cavity. The recessus pleura pulmonalis is the only portion, which is free of lung structures.

1.1 Genetic Control of the Development

The organogenesis and maturation of the lung are under the control of genes, which are still only marginally explored. Thyroid transcription factor 1 (TTF1), hepatocyte nuclear factor (HNF3ß), retinoic acid receptor (RAR), Kruppel-like factor 5 (KLF5), and GATA6 all have been identified as differentiation factors for the developing lung [7, 12, 13]. HOX genes and sonic hedgehog (Shh-Gli) are responsible for organogenesis [14]. More specifically FGF2, FGF7, and FGF10 engineer bronchial sprouting [7, 15]. From mouse studies, many more factors are known: The genes listed above act more general, but in the developing bronchial bud, more fine-tuning is required, which is regulated by the interaction of the epithelium and the surrounding mesenchyme. Also NEC play a role: by secreting adrenocorticotropin, in the embryonic and fetal period – rather a growth hormone than an endocrine protein – local growth stimuli are directed toward the dividing bronchial bud, whereas apoptotic mechanisms counteract and abolish supernumerary buds [16–18].

1.2 Comparison of Lung Development Across Species

Within the mammalian family, wide variations are known. In marsupials the young are born with a lung in the pseudoglandular phase; the whole lung development starts after birth. In mice, rats, and hamsters, the young are delivered with lungs in the canalicular phase, and alveoli are formed after birth. In guinea pigs and also in carnivores and sheep, the young have a fully developed lung before birth. Human beings are in between these groups: The alveolar/terminal saccular phase already starts before birth but continues after birth until the fourth to fifth year of postnatal life. After that, the lung still grows in size but the numerical structure is reached [8, 9].

References

1. Miura T. Modeling lung branching morphogenesis. Curr Top Dev Biol. 2008;81:291–310.
2. St-Georges R, Deslauriers J, Duranceau A, Vaillancourt R, Deschamps C, Beauchamp G, Page A, Brisson J. Clinical spectrum of bronchogenic cysts of the mediastinum and lung in the adult. Ann Thorac Surg. 1991;52:6–13.
3. Zylak CJ, Eyler WR, Spizarny DL, Stone CH. Developmental lung anomalies in the adult: radiologic-pathologic correlation. Radiographics. 2002; 22(Spec No):S25–43.
4. Tian J, Mahmood R, Hnasko R, Locker J. Loss of Nkx2.8 deregulates progenitor cells in the large airways and leads to dysplasia. Cancer Res. 2006;66: 10399–407.
5. Srikanth MS, Ford EG, Stanley P, Mahour GH. Communicating bronchopulmonary foregut malformations: classification and embryogenesis. J Pediatr Surg. 1992;27:732–6.
6. Stocker JT. Cystic lung disease in infants and children. Fetal Pediatr Pathol. 2009;28:155–84.
7. Kumar VH, Ryan RM. Growth factors in the fetal and neonatal lung. Front Biosci. 2004;9:464–80.
8. O'Rahilly R, Mueller F. Die Lunge. Edited by Bern, Goettingen, Toronto, Seattle, H. Huber; 1999, p. 275–88.

9. Moore KL, Persaud TVN. Lung development. Elsevier; 2003. p. 267–80.
10. Schachtner SK, Wang Y, Scott Baldwin H. Qualitative and quantitative analysis of embryonic pulmonary vessel formation. Am J Respir Cell Mol Biol. 2000;22: 157–65.
11. de Mello DE, Reid LM. Embryonic and early fetal development of human lung vasculature and its functional implications. Pediatr Dev Pathol. 2000;3:439–49.
12. DeFelice M, Silberschmidt D, DiLauro R, Xu Y, Wert SE, Weaver TE, Bachurski CJ, Clark JC, Whitsett JA. TTF-1 phosphorylation is required for peripheral lung morphogenesis, perinatal survival, and tissue-specific gene expression. J Biol Chem. 2003;278: 35574–83.
13. Wan H, Luo F, Wert SE, Zhang L, Xu Y, Ikegami M, Maeda Y, Bell SM, Whitsett JA. Kruppel-like factor 5 is required for perinatal lung morphogenesis and function. Development. 2008;135:2563–72.
14. Grier DG, Thompson A, Lappin TR, Halliday HL. Quantification of Hox and surfactant protein-B transcription during murine lung development. Neonatology. 2009;96:50–60.
15. Yu S, Poe B, Schwarz M, Elliot SA, Albertine KH, Fenton S, Garg V, Moon AM. Fetal and postnatal lung defects reveal a novel and required role for Fgf8 in lung development. Dev Biol. 2010;347:92–108.
16. Borges M, Linnoila RI, van de Velde HJ, Chen H, Nelkin BD, Mabry M, Baylin SB, Ball DW. An achaete-scute homologue essential for neuroendocrine differentiation in the lung. Nature. 1997;386: 852–5.
17. Cutz E, Yeger H, Pan J. Pulmonary neuroendocrine cell system in pediatric lung disease-recent advances. Pediatr Dev Pathol. 2007;10:419–35.
18. McGovern S, Pan J, Oliver G, Cutz E, Yeger H. The role of hypoxia and neurogenic genes (Mash-1 and Prox-1) in the developmental programming and maturation of pulmonary neuroendocrine cells in fetal mouse lung. Lab Invest. 2010;90:180–95.

Normal Lung

2

In this chapter, we will focus on all aspects of the anatomy and histology of the lung as far as necessary to understand lung function in disease. This chapter does not aim to replace textbooks on anatomy, histology, and lung physiology. More detailed information can be found in these books.

2.1 Gross Morphology

In humans two lungs are formed. In some mammalians, an additional mediastinal lobe is generated, which has its own bronchus directly branching off from the trachea. Both lungs fill the thoracic cavities leaving the midportion for the mediastinal structures and the heart and the posterior midportion for the esophagus and other structures of the posterior mediastinum. The lungs are covered by the visceral pleura, whereas the thoracic wall is internally covered by the parietal pleura. Both merge at the hilum of each lung. The right lung consists of three lobes, the left of two lobes, upper, middle, and lower lobes (Fig. 2.1). The normal lung of an adult weighs 350 (right) to 250 g (left); the lung volume varies individually between 3.5 and 8 L.

Each lobe is further divided into segments (Fig. 2.2). Each upper lobe has three segments, apical, posterior, and anterior, usually numbered accordingly from 1 to 3. In the right lung, the middle lobe is divided into a lateral (4) and a medial (5) segments. On the left side, two further bronchi are found supporting the lingula with a superior (4) and inferior (5) segment. Both lower lobes are divided into a superior (6), mediobasal (7), anterobasal (8), laterobasal (9), and posterobasal (10) segment. The segments are composed of subsegments, which can, however, anatomically not be separated.

Fig. 2.1 Paper mount section of the right lung; the fissure between the upper and lower lobe is seen; the central hilar structures are represented by pulmonary arteries and bronchi

© Springer-Verlag Berlin Heidelberg 2017
H. Popper, *Pathology of Lung Disease*, DOI 10.1007/978-3-662-50491-8_2

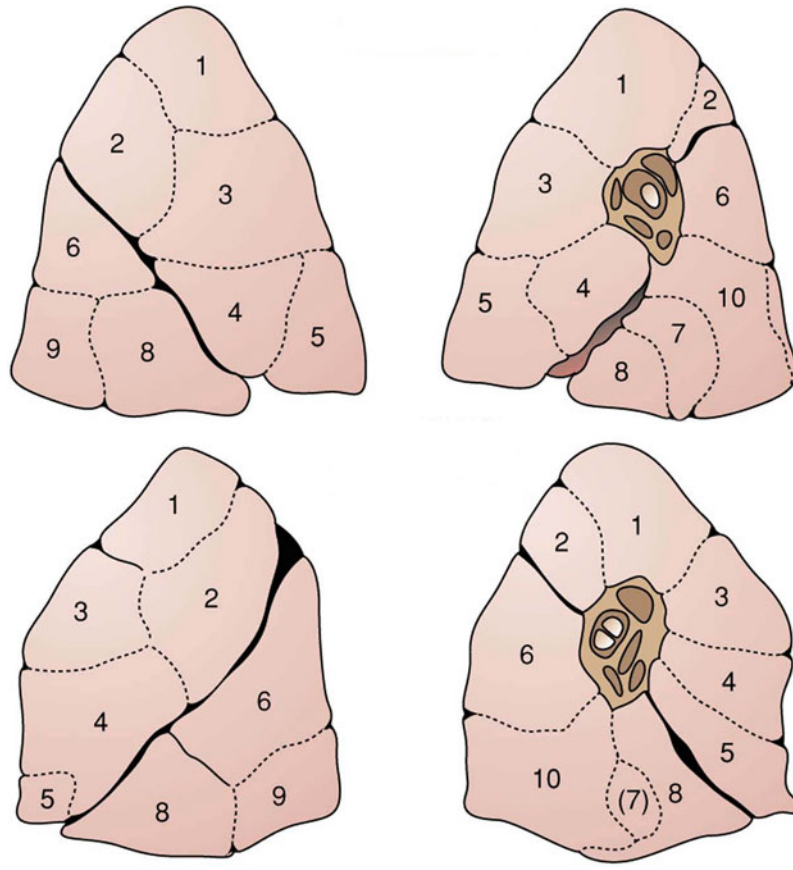

Fig. 2.2 Schematic representation of lung segments, *right upper panel*, *left lower panel*

An alveolar duct together with his alveoli forms the primary lobule. This lobule is difficult to identify on histology (easier in children's lung) and impossible on CT scan. A terminal bronchiole III splits into several alveolar ducts, is larger, and can be identified on CT scan. Histologically this secondary lobule can also be identified by its interlobular septa. Between alveoli pores do exist (pores of Kohn), which permit gas exchange between primary lobules (Fig. 2.3). Between lobules another connecting structure, the channels of Lambert, permits gas exchange.

Fissures are separating the lobes on each site. These are formed by visceral pleura. The fissures between the lower and the middle/lingula and upper lobe are usually well developed and can be followed almost to the hilum. The fissure between the upper and middle lobe clearly separates the

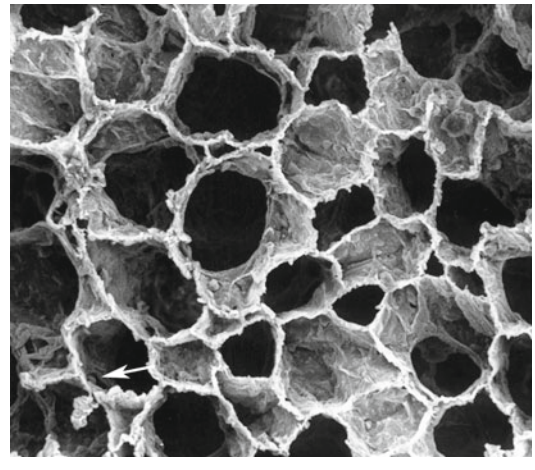

Fig. 2.3 Scanning electron micrograph showing alveolar tissue. The epithelial layer is characterized by *grayish color*, whereas the stroma is more dense and therefore *white*. An *arrow* points to a pore of Kohn

lobes, but also other variations can occur, where the fissure is shallow and both lobes are less well separated. In addition accessory fissures can be found separating segments from their respective lobe. All these are individual variations and have no importance for disease processes.

2.2 The Airways

The airways start with the trachea, which divides into the two main bronchi. The angle of the first bifurcation is 20–30° for the right and 45° for the left main bronchus. The next bifurcation is that of the lobar bronchi: the right main bronchus gives rise to the right upper lobe bronchus and builds a short intermediate bronchus, which further on divides into the mid lobe and the lower lobe bronchus. On the left side, the main bronchus splits into the upper and lower lobe bronchus, respectively. These further on give rise to 16 generations of bronchi as an average (there are some variations between the different lobes), from lobar to segmental, subsegmental, and so on. In humans the bronchial division is asymmetric: the diameter of the upper lobe bronchus is one third and the intermediate bronchus two thirds of the diameter of the main bronchus (Fig. 2.4). This asymmetric branching is found in all subsequent bronchial generations. This has important functional meaning (see below).

Finally there are four generations of bronchioli, membranous, and three generations of respiratory bronchioles. These finally give rise to alveolar ducts on which the alveoli are opened (Fig. 2.5). The alveolar periphery is built by approximately 300 millions of alveoli.

Each bronchus has its epithelial lining, which sits on a basal lamina. Next in the bronchial wall is loose connective tissue followed by a smooth muscle layer. Within the connective tissue, bronchial glands are embedded. Finally the cartilage separates the bronchial wall from adjacent structures.

The definition of bronchioles is still not solved. Most investigators agree that they should microscopically be defined by a diameter of 1 mm and less, being devoid of cartilage and having only two layers of smooth muscle cells. The size of the internal lumen can also be used macroscopically [1].

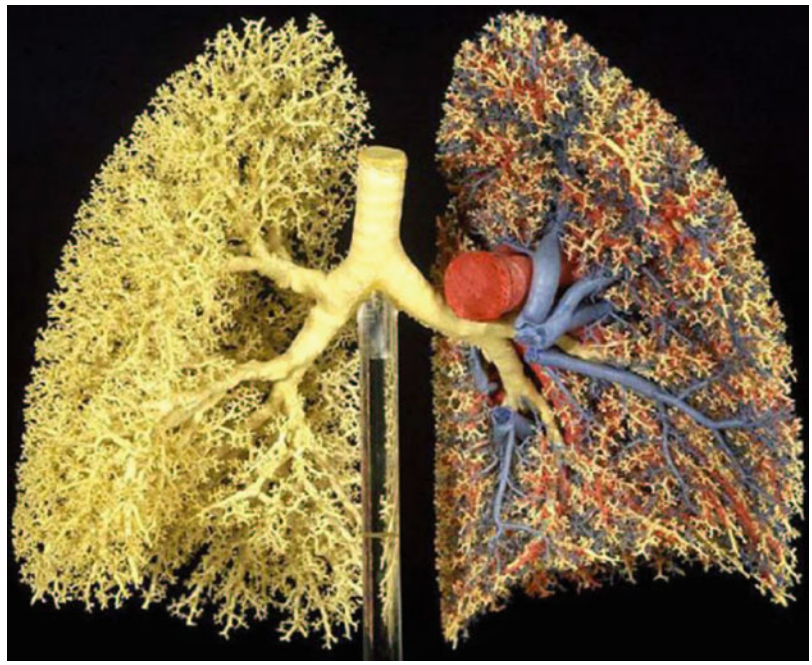

Fig. 2.4 Plastic cast of both lungs. Left side the branching of the bronchial tree is shown, right the branching of the pulmonary arteries and veins, and their association with bronchi and bronchioles is highlighted by *red*, *blue*, and *yellow colors*

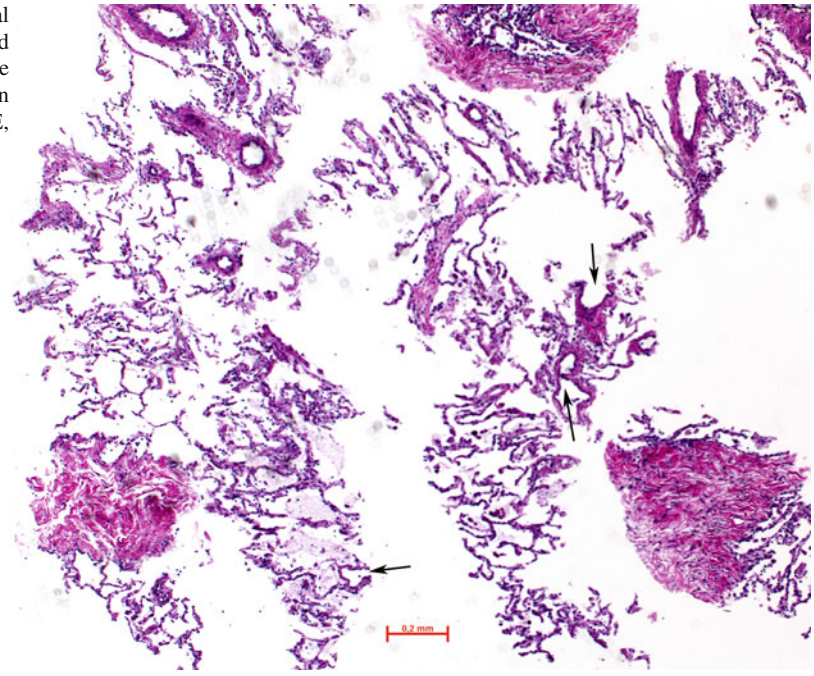

Fig. 2.5 Transbronchial biopsies. Small bronchi and respiratory bronchioles are seen with an opening into an alveolar duct (*arrow*). H&E, bar 200 µm

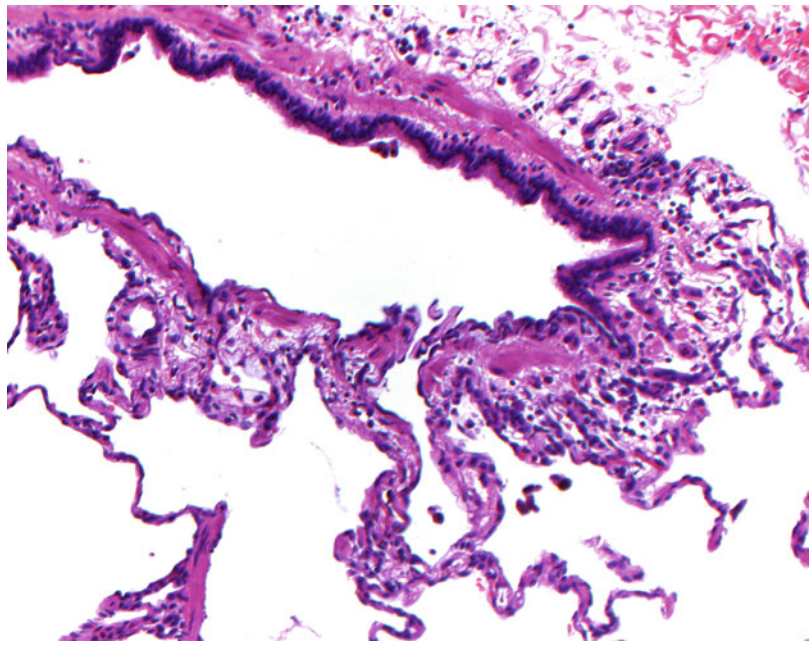

Fig. 2.6 Open lung biopsy. The membranous bronchiole changes into a terminal bronchiole (*right side*); the epithelium shows only a single layer, which is also flattened. At the *bottom side*, the terminal bronchiole opens into a recurrent bronchiole. These recurrent bronchioles together with their usually reduced number of alveoli fill the space adjacent to the larger bronchioles and small bronchi. H&E, bar 100 µm

The epithelial lining changes in thickness as well as cell composition from one bronchial generation to the next one: large bronchi have usually five layers of cells, whereas in the terminal respiratory bronchiole, there is only one single layer (Fig. 2.6). In large bronchi several cell types can be discerned in an H&E-stained section: ciliated cells, goblet cells (Fig. 2.7), secretory cells, basal

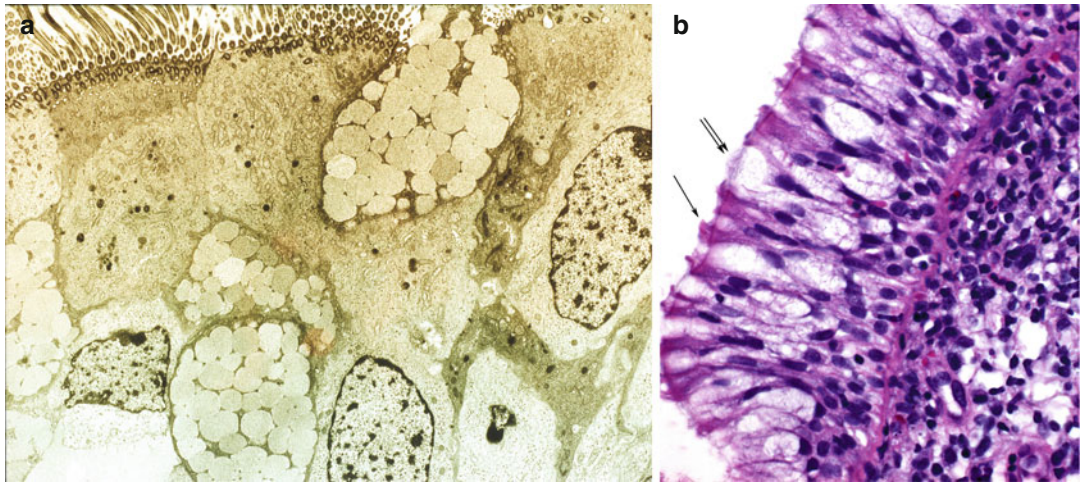

Fig. 2.7 (**a**) Transmission electron micrograph showing ciliated and goblet cells. In the middle portion, one reserve cell is seen (*right border*). One goblet cell is just secreting mucus into the lumen (×9,000). (**b**) Ciliated and goblet cells in light microscopy, *arrow* points to cilia, *double arrow* to a goblet cell; case with chronic bronchitis and hyperplasia of goblet cells. H&E, ×600

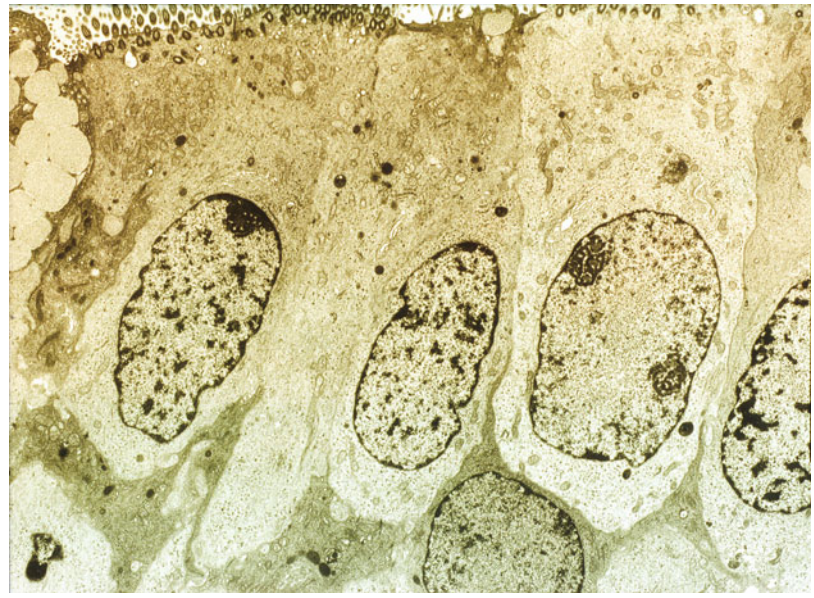

Fig. 2.8 Transmission electron micrograph showing a secretory columnar cell in the *middle*, characterized by microvilli; a basal cell is seen at the *bottom*. The basal cells are triangular in shape and have only few subcellular organelles. × 9,000

cells (Fig. 2.8), intermediate cells, and neuroendocrine cells (clear cells). The proportion of ciliated cells to goblet cells in humans is normally 6–8:1. Clara cells in humans are almost absent in large bronchi, while they form a major proportion in small bronchi and bronchioles (Fig. 2.9). In contrast ciliated cells are rare in small bronchi and bronchioles and finally disappear in terminal bronchioles. Neuroendocrine cells are scattered as single cells within the bronchial mucosa; few can be found in a submucosal position (Fig. 2.10). In the alveolar periphery, neuroendocrine cells usually form neuroepithelial bodies: they consist of four to six neuroendocrine cells covered by

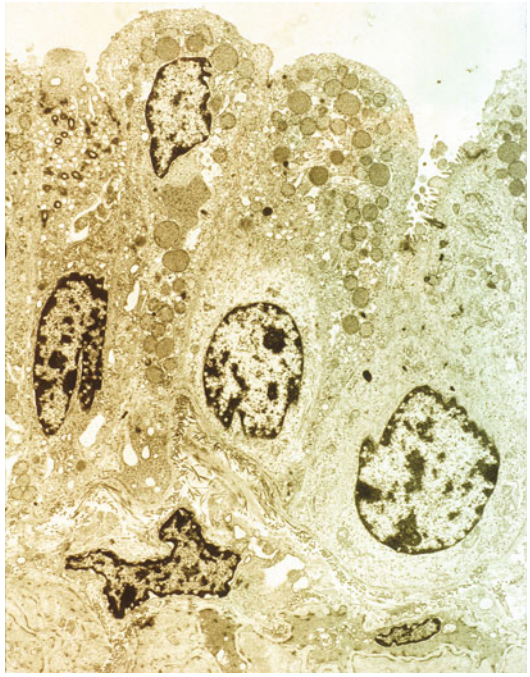

Fig. 2.9 Bronchiole with Clara cells. Clara cells are characterized by their basally located nucleus and large electron dense granules containing Clara cell proteins, but also lipids. At the bottom the basal lamina is seen and two stroma cells. ×12,000

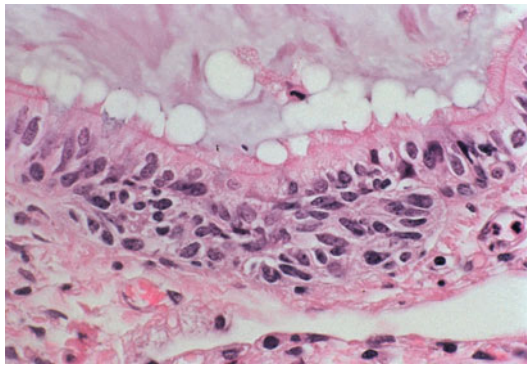

Fig. 2.10 Neuroendocrine cell hyperplasia (NEH) in a bronchus. In this case the reason for NEH was bronchiectasis and emphysema in a patient with COPD. H&E ×200

cuboidal epithelial cells (Fig. 2.11). In children these bodies are easily found, whereas in adult lung, neuroepithelial bodies are rarely discovered. This might be due to the increased size of an adult lung.

Ciliated cells are specialized cells, which cannot divide anymore (Fig. 2.7). They have to be replaced by regenerating reserve cells which differentiate into the ciliated type. The ciliated cell is attached with a small cytoplasmic "foot process" to the basal lamina and moreover held in its position by intercellular connections with the basal and the intermediate cells. On the surface numerous cilia are formed. These cilia have a double outer membrane, eight to nine outer doublets of axonemata, and one central. From the central axonema, radial spokes radiate toward the outer axonemata. On the right side of each axonema pair, there are electron dense hornlike structures, the dynein arms, which represent a topically fixed calcium-activated ATPase (Fig. 2.12) [2]. The ATPase functions as the energy provider for the axonemata movement. All cilia coordinately beat toward the upper respiratory tract and thus move the mucus up and out. In the mucus embedded are particulates, which have been inhaled. The system is usually referred as the mucociliary escalator or clearance system and represents one of the oldest clearance systems to remove harmful material from the respiratory tract.

Goblet cells are also tall columnar cells, characterized by many mucin-containing vacuoles in the apical portion of the cytoplasm (Fig. 2.7). The nucleus is small often appearing as compressed and located at the basis of the cell. As ciliated cells, goblet cells also are fixed by long slender cytoplasmic processes to the basement membrane, and adhesion molecules fix goblet cells to basal and intermediate cells. The mucus secreted by the goblet cells consists of a three-dimensional polymer network of glycoproteins. Mucin macromolecules are 70–80 % carbohydrate, predominantly glycosaminoglycans, some of them are bound to hyaluronic acid, another 20 % are proteins, and 1–2 % sulfate are bound to oligosaccharide side chains. The protein backbones of mucins are encoded by mucin genes (MUC genes), at least eight of which are expressed in the respiratory tract, although MUC5AC and MUC5B are the two principal gel-forming mucins secreted in the airway [3].

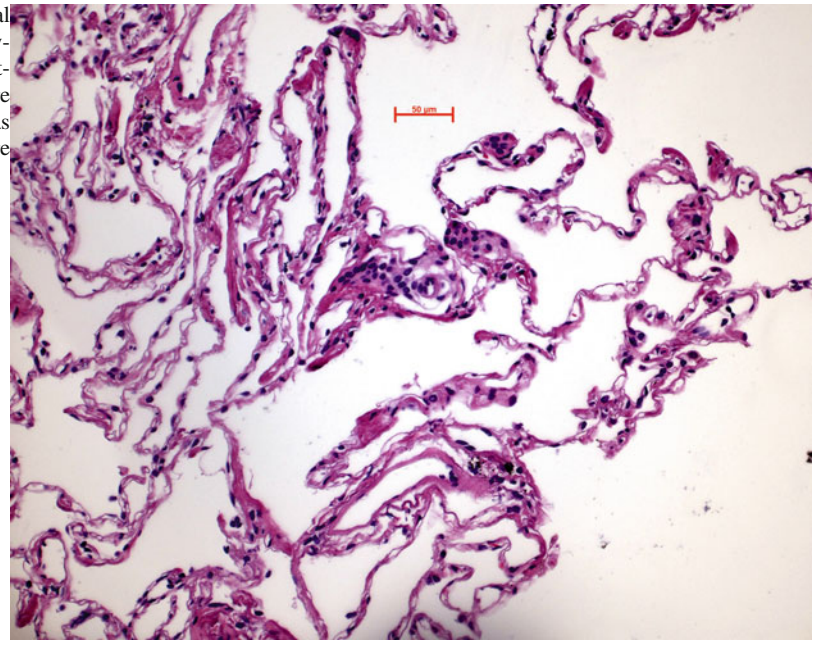

Fig. 2.11 Neuroepithelial body in the lung with emphysema. The cells with light-stained cytoplasm are neuroendocrine cells, whereas the darker-stained cells are Clara cells. H&E, bar 50 µm

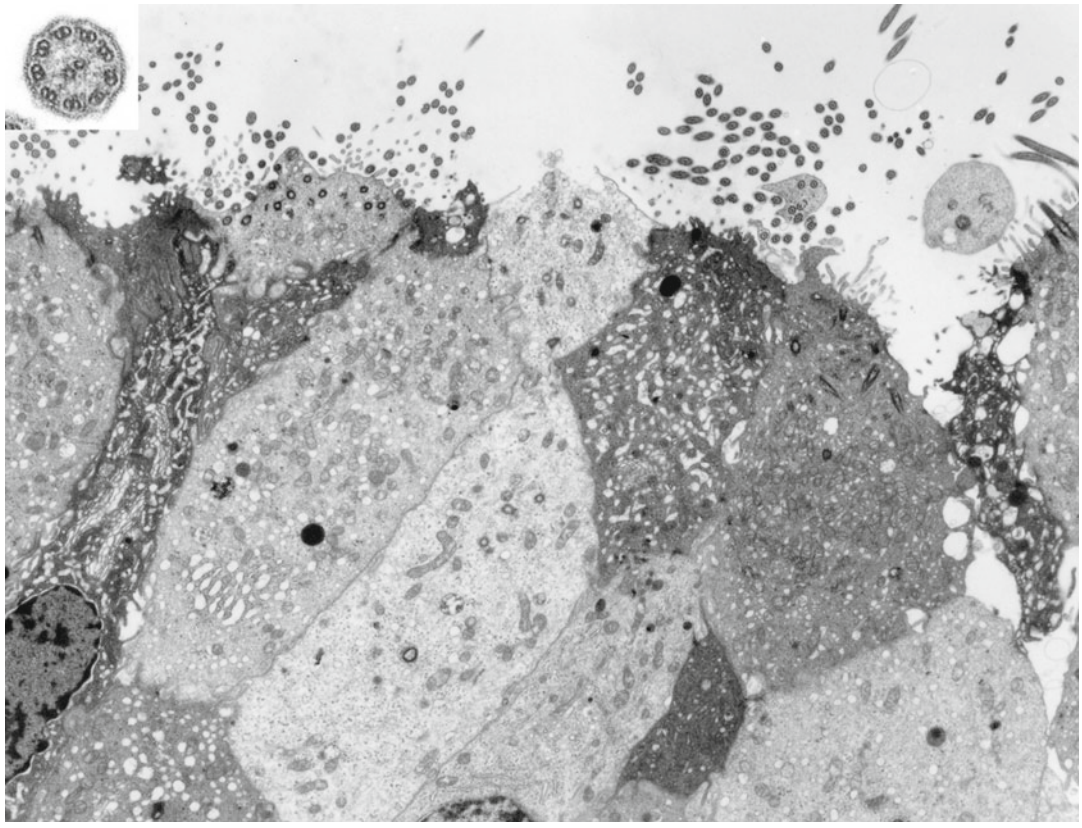

Fig. 2.12 Transmission electron micrograph showing ciliated cells with rootlets. Some cilia are cross-sectioned and look normal. ×9,000; in the inset (*left upper corner*), a single cilium is shown in cross section; there are nine outer axonema doublets and one central. From the lower axonema, two electron dense hornlike structures are arising, which represent dynein arms. ×19,000

Columnar secretory cells are the third tall columnar cell species (Fig. 2.8). They are characterized by short microvilli and secretory vacuoles. They are involved into the assembly of the immunoglobulin A (IgA) with the secretory piece [4], but might also contribute to the correct consistency of the bronchial surface fluid by secreting a more watery portion to be mixed with the mucins from the goblet cells. In animal experiments, these cells have been erroneously called pneumocytes type III or tufted cells and attributed to alveoli [5]. This is incorrect, because these cells as others of the terminal bronchioli will repopulate denuded alveolar walls in many cases of regeneration, such as alveolar damage, toxic injury, etc. However, the function of these cells is still not completely understood and will need further investigation.

Intermediate cells have a polygonal shape and fill the middle portion of the bronchial epithelial layers (Fig. 2.7). The nuclei are large and have a finely distributed chromatin, and nucleoli are inconspicuous. Within this cell layers, the bronchial or central lung stem cells are expected to exist. In experimental settings, the proliferation activity within this cell layer is upregulated [6].

Basal cells: The major function of the triangular-shaped basal cells is adherence (Fig. 2.8). They sit with their long axis firmly attached to the basal membrane and with their side axis provide attachment for several other cells especially for tall columnar cells such as the ciliated and goblet cells. The basal cells are only marginally able to divide and reproduce themselves. They are not forming the stem cell pool as previously supposed (personal communication G.R. Johnson, Lovelace Respiratory Research Institute, Albuquerque, NM).

Clara cells are one of the main cell types in bronchioles in humans (in some mammals, Clara cells can be found up to the trachea). They together with pneumocytes were for a long time supposed to be the peripheral stem cells (Fig. 2.9). They are cuboidal in shape, the nucleus is positioned in the middle of the cell, and the cytoplasm forms a dome-shaped apical portion, protruding into the lumen of the bronchioles. By electron microscopy in the apical portion, vesicles can be demonstrated, which contain proteinaceous material. This adds also in the eosinophilic staining of the cells. Clara cell proteins are involved in the defense system of the bronchiole epithelial lining but also are functioning as immune modulators [7–11]. In addition Clara cell proteins are involved in growth modulation and differentiation of the developing lung [12–14]. Clara cells can divide and differentiate into cells of the bronchioles; however, they are not peripheral stem cells.

Pneumocytes are forming the epithelial layer of alveoli. The main cell population are pneumocytes type I, whereas type 2 is usually found in edges between adjacent alveoli. Type I cell is flat and thin (Fig. 2.13). By light microscopy, they can be seen when their nucleus is in the focus of the section. By electron microscopy, the cytoplasm forms a thin layer of the basal lamina. Together with endothelial cells and the basal lamina, they form the air-blood barrier. In areas where the capillary is close to the surface, the two basal laminae are fused into one, thus providing a short diffusion distance between the surface, the cytoplasm of the pneumocyte, the basal lamina, and the endothelial cell. To keep this diffusion distance short is essential for oxygenation. Pneumocytes types II are polygonal in shape and have a round large nucleus and a granular cytoplasm. On electron microscopy, these granules in part correspond to lamellar bodies, which are the storage form of surfactant and surfactant-associated proteins (Fig. 2.14). Pneumocytes type II are capable of regeneration in as far as they are formed out of the peripheral stem cell pool and further on differentiate into type I cells.

Stem cells: Only recently it was shown that those peripheral stem cells do exist in niches at the bronchioloalveolar junction. They can be visualized due to their coexpression of stem cell markers CD34 and Oct3/Oct4 together with Clara cell protein 10 and surfactant apoprotein C (also prepro-proteins can be demonstrated) [15–17]. In mouse models using toxicants directed against Clara cells and pneumocytes, it could be shown that the epithelial lining is repopulated by stem cells undergoing differentiation into either pneumocytes type II or Clara cells, respectively [18, 19]. From these studies, there is some evidence

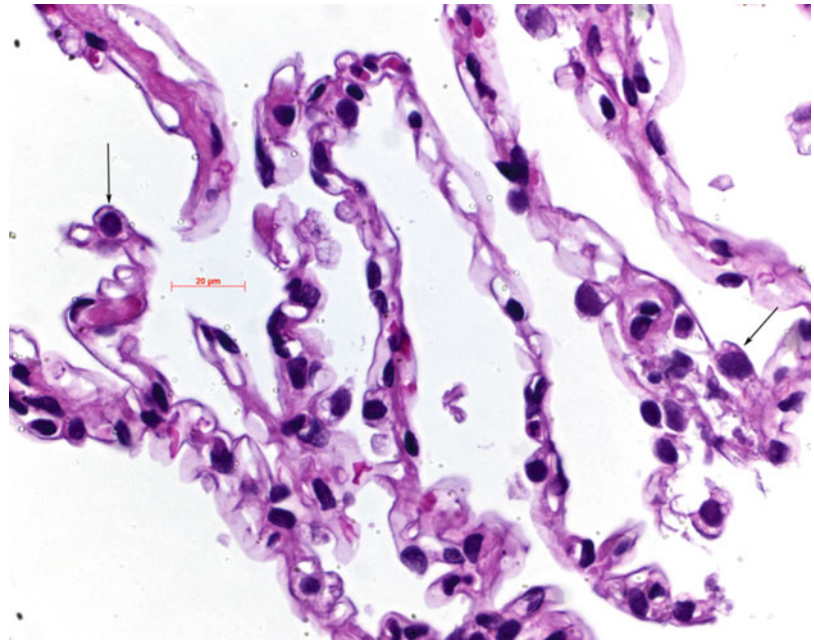

Fig. 2.13 Peripheral lung tissue showing pneumocytes types I and II. The type I cells are only visible by their knob-like protruding nuclei, whereas type II cells (*arrow*) are positioned in edges of alveoli. Recognize also the capillary loops. H&E, bar 20 μm

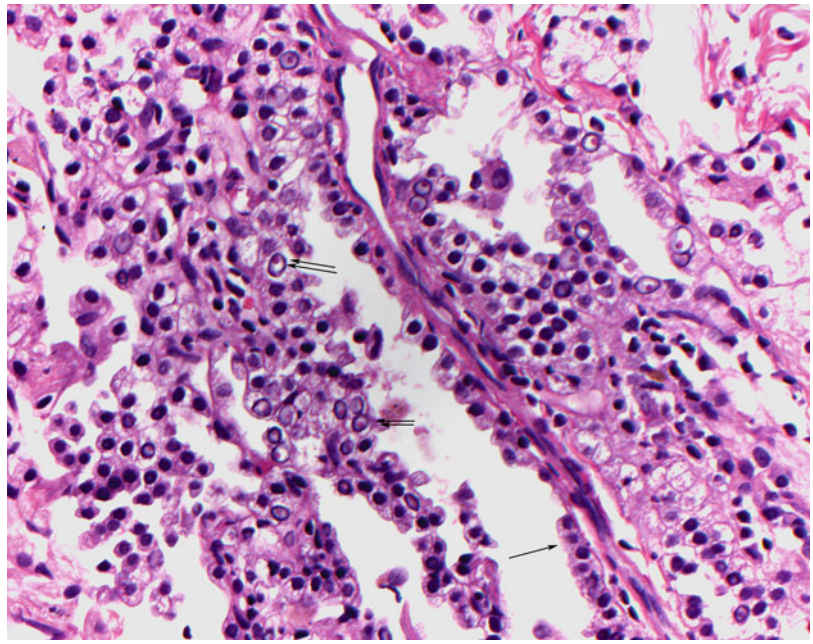

Fig. 2.14 Terminal bronchiole (row of Clara cells, *arrow*) and opening into adjacent alveoli. There is a hyperplasia of type II pneumocytes; several of them show pseudoinclusion of pink material within their nuclei (*double arrow*). This in reality is surfactant proteins located in the cytoplasm, due to convoluted nuclei giving the impression as being within the nucleus. H&E, ×200

that Clara cells as well as pneumocytes type II can still divide and differentiate into either the other cell types of bronchioles or pneumocytes type I, respectively. Whereas data are available on peripheral stem cells, the central stem cells as well as stem cells in larger bronchi have not been identified. In one study cells within the trachea were thought to represent central lung stem cells, but this has not been confirmed so far [20]. In one of the experimental small cell carcinoma models, the authors used embryonal stem cells to induce this type of carcinoma, but it is still unclear if

central stem cells of the mouse lung contribute to this tumor development [21]. Within the bronchial epithelium, p63-expressing cells within the basal and intermediate layer are also discussed representing the central lung stem cell pool [22]. However, these findings are mainly based on findings within tumors, which might not reflect the developing lung exactly. Another open question is if there are epithelial and mesenchymal central stem cells or only one type of stem cell, which is able to differentiate into all various lung cells.

Neuroendocrine cells (NEC) and neuroepithelial bodies (NEB) are part of the diffuse neuroendocrine system first described by F. Feyrter [23, 24]. They are dispersed within the bronchial epithelium; a few cells can also be found in the subepithelial layer. In the alveolar periphery, NEC are usually clustered into NEB: cuboidal cells (predominantly Clara cells) cover small cluster of NEC, thus forming the NEB (Figs. 2.10 and 2.11). The function of NEC is not fully understood. In the fetal period, they most probably are involved in fine-tuning of the growth and differentiation of the bronchial tree and the development of the blood vessels and probably also nerves. They are also associated with chemosensitivity and probably via secretion of motility peptides influence the tone of smooth muscle cells in the bronchial wall [25–27]. Most studies have focused on a few neuroendocrine markers, such as chromogranin A and synaptophysin, but many more peptides and hormones can be released from NEC. Adrenocorticotropin is the most widespread hormone, which in fetal lung acts as a growth hormone; others are gastrin-releasing peptide, a growth hormone as well, calcitonin, serotonin, motilin, vasointestinal peptide, etc. The physiological function of the latter is largely unknown; however, they can be expressed and released in pulmonary carcinoids [28, 29]. Achaete-scute homolog-1 (ASH1) has been shown to be essential for the differentiation of cells into a neuroendocrine phenotype [30].

Smooth muscle cells form bundles around large bronchi and, however, are not ordered longitudinal but in a spiral form. This enables them not only to contract the bronchial wall but also to shorten bronchi. This assists in coughing, as a mechanism to get rid of inhaled particulate material and mucus. Toward the periphery, the muscular layer gets thinner; in bronchioles two cell layers form the muscular coat. In addition smooth muscle cells are replaced by myofibrocytes in alveolar ducts and alveolar walls. These cells are capable of synthesizing collagen, but also have myofilaments in their cytoplasm [31–33]. Matrix proteins expressed at the epithelium-mesenchymal interface facilitate smooth muscle cell formation and differentiation. Decorin, lumican, and several collagen types form a sleeve around the bronchiolar ducts. Thus, the distribution pattern of collagen and proteoglycans in the early developmental stages of the human lung may be closely related to the process of dichotomous division of the bronchial tree [34].

Bronchial glands are present along the large bronchi (main, lobar, segmental), but vanish already at the site of subsegmental bronchi. These glands consist of groups of secretory cells with eosinophilic secretory cells and mucus-secreting goblet cells forming several acini. These acini together are grouped into one bronchial gland field. The acini secrete their products into a collecting duct, which opens into the bronchial surface. The composition of secretory cells and goblet cells is normally 1:1. Large areas of connective tissues separate bronchial glands from each other. Normally in a circular section of a bronchus, there are two to three bronchial gland fields visible. They consist of a cluster of acinar cells and one duct. In bronchial gland hyperplasia, more glands are found and they also form clusters of acini with more than one duct (Fig. 2.15).

Cartilages are present as semicircular rings around large bronchi. In medium-sized bronchi usually from subsegmental bronchi downward, cartilages are no longer semicircular, but are placed like islands around the bronchi, forming a spiral. Toward small bronchi, cartilages are finally not anymore present. However, it should be reminded that this is an adaptation to the environment: sea mammals have complete cartilaginous rings down to their bronchioles to keep the lumen open during diving.

Blood vessels are structured differently in the lung. Arteries are found along the bronchovas-

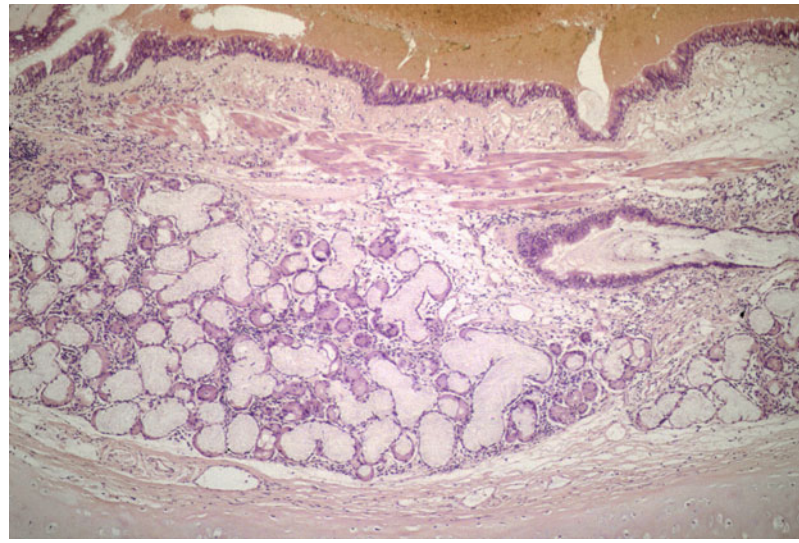

Fig. 2.15 Longitudinal section of a bronchus. At the bottom parts of a cartilage is seen, above bronchial glands – in this case hyperplasia in chronic bronchitis. Within the glands two cell types can be seen, the pale goblet cell and the pinkish-stained serous cell. The former produces sticky mucus, the latter a soluble fluid; the mix of both forms part of the thin mucus layer on the bronchial epithelium. H&E, ×100

cular bundle, whereas veins collect blood along the interlobular septa. Blood from the right heart flows along the pulmonary arteries along the bronchovascular bundle. These arteries divide together with the bronchi/bronchioles until they form arterioles, which finally open into capillaries. Each capillary runs into an alveolar septum forming a loop and finally opens into a venule. Venules are collected in the lobular septum, which drains into interlobular, subsegmental, segmental, and lobar septa and finally drains into a pulmonary vein. Only the large vein is close to the bronchovascular bundle in the hilum; otherwise, veins are strictly separated from the arteries. Bronchial arteries and veins are in close proximity to the bronchial wall; their capillaries are within the mucosa, underneath the epithelium. In a normal adult lung, no anastomoses between the different vascular beds are found; however, in different diseases, these anastomosing vessels from the fetal period can be "reopened," connecting arterial and venous bloodstreams. Under certain circumstances, also the position of the blood vessels can change (see developmental diseases). The formation of the pulmonary vascular bed is also quite interesting: whereas the central blood vessels form out of the branchial arch (arteries) and the sinus venosus (veins), the peripheral blood vessels are formed from the coelomic wall. Large blood vessels are under the control of several genes, especially the VEGF receptor type 1, whereas VEGR2 and 3 control the growth of the coelomic blood vessels [35–37]. This has also therapeutic implication in patients with vasculopathy in adults.

Lymphatics are formed together with the capillary bed out of the coelom wall. They start as open lymphatic channels or slits, which drain into small lymphatic vessels/capillaries. Usually lymphatic vessels can be found along the pulmonary arteries, following them toward the hilum close to the arterial walls. Other lymphatics follow veins and connect to the lymphatic net of the pleura. Lymphatic channels can only be visualized by experimental injection techniques, whereas an endothelial cell layer and a thin capillary wall formed by myofibrocytes and pericytes characterize lymphatic capillaries.

Nerves are easily found along the large bronchi, whereas they are hardly identified in peripheral airways. However, from studies of chronic obstructive pulmonary disease and asthma, bronchial hyperplastic nerves can be demonstrated along small bronchi. Sympathetic as well as parasympathetic innervation has been demonstrated, whereas the occurrence of C-fiber type has not been proven. Ganglia can be found around the hilum. Different types of receptors are known, such as adrenergic and cholinergic receptors,

however, there is still an open dispute on C-fiber types and pain receptors.

2.3 Lymphoreticular Tissue and the Immune System of the Lung

Under normal condition, lymphoreticular tissue cannot be demonstrated within the lung, neither aggregates of lymphocytes nor clusters of dendritic cells. Different types of antigen-presenting and modulating cells are usually found as single cells within the airway wall and in the peripheral parenchyma. B lymphocytes can be found as single cells moving along the bronchial tree either coming from the circulation of moving out toward regional lymph nodes. T lymphocytes are also found as single cells most often within the alveolar periphery. Macrophages are the most common leukocytes encountered in the lung. They are derived from the macrophage-monocyte cell system. Some of these cells enter the lung from the circulation; others reside within the alveolar interstitium as resident cells. These cells usually undergo a differentiation where they acquire the enzymatic repertoire, enabling them to control the integrity of the alveolar lumina and the terminal bronchiolar system. The lung is essentially a T-lymphocyte controlled organ, which means that T lymphocytes are a major part of the inflammatory response. Aggregates of lymphocytes point to an injury, most often a previous infection. Plasma cells have their physiologic role along the bronchial system by releasing IgA, which is taken up by the secretory columnar cells: two molecules of IgA are joined by the secretory piece, and this complex is released into the surface liquid layer, where it exerts its anti-inflammatory function. It is necessary for the opsonization of bacteria and a prerequisite for phagocytosis by macrophages.

In immunodeficiency syndromes involving the T and NK lymphocyte system, a hyperplasia of the B-cell system can be seen with lymph follicles along the bronchial tree.

Pleura: The pleura develops out of the coelom and forms two layers, a visceral pleura covering the lung and a parietal pleura separating the pleura cavity against the thoracic wall. The pleura is formed by a single layer of mesothelial cells, followed by a mesenchymal layer containing fibrocytes and few scattered histiocytes and dendritic cells. There is no basal lamina, but two layers of elastic fibers.

2.4 Comparison of Human Lung to Other Species

Tracheal lobe: In several mammalian species, a separate bronchus develops and grows toward the mediastinum giving rise to a mediastinal lung lobe. In humans and apes, this bronchial "anlage" is also present, but during lung development is deleted by apoptosis. However, persistence of this tracheal branch without concomitant lung lobe might give rise to bronchial cysts isolated lying in the mediastinum.

Dichotomous branching in mammalians: In most mammalians as well as in reptiles and birds, bronchial branching is symmetric; this means one bronchus divides into two next generation bronchi, which are similarly sized (Fig. 2.16). In humans and also some primates, bronchi divide asymmetrically into one main next generation bronchus and one smaller "side" bronchus. Due to this asymmetric division, the airflow is not laminar but turbulent at the bifurcations, and therefore particulates are deposited in this area. Impaction of particulates at bronchial bifurcations induces a cough reflex and by that particulates can be removed early on. In many other animals, large nasal sinuses serve as a filter mechanism, where particulates are deposited and removed by sneezing. Probably in humans this is an evolutionary compensation for our small nasal sinuses and helps to clean the inhaled air.

There are other dissimilarities in the evolution and adaptation of the lungs: short and long trachea might be adaptations to the species needs; short trachea and bronchi are usually found in carnivores, hunting birds, and reptiles, which require immediate increase of oxygen supply for their hunting activity ("small death room"). In others, humans and primates included, large conducting airways result in an increase of dead space, which

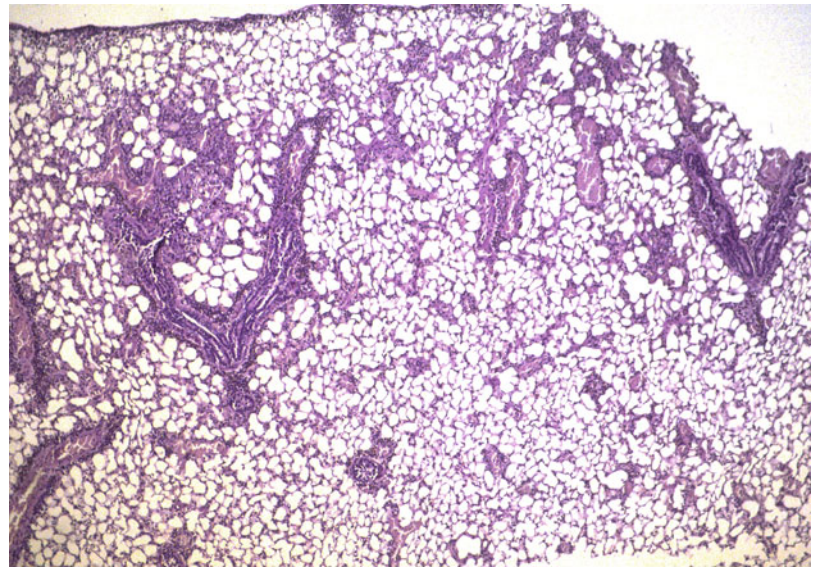

Fig. 2.16 Mouse lung showing the dichotomous branching of airways. H&E, ×100

requires forced inspiration for maximal activity. In reptiles and birds, there are few generation of bronchi, in some species even no bronchi are present as in snakes, and bronchioles directly arise from the trachea and main bronchus.

It is beyond the aim of this book to discuss in depth the structure and function relationships during evolution of the lung, because besides modification of genes, adaptation to specific environmental condition plays an important role for lung development.

References

1. Lamb D, McLean A, Gillooly M, Warren PM, Gould GA, MacNee W. Relation between distal airspace size, bronchiolar attachments, and lung function. Thorax. 1993;48:1012–7.
2. Popper H, Jakse R, Loidolt D. Problems in the differential diagnosis of Kartagener's syndrome and ATPase deficiency. Pathol Res Pract. 1985;180:481–5.
3. Lillehoj ER, Kim KC, Foster WM, Rubin BK. Airway mucus: its components and function Mucociliary transport and cough in humans Physiology of airway mucus clearance. Arch Pharm Res. 2002;25:770–80.
4. Petrache I, Natarajan V, Zhen L, Medler TR, Richter AT, Cho C, Hubbard WC, Berdyshev EV, Tuder RM. Ceramide upregulation causes pulmonary cell apoptosis and emphysema-like disease in mice. Nat Med. 2005;11:491–8.
5. Kish JK, Ro JY, Ayala AG, McMurtrey MJ. Primary mucinous adenocarcinoma of the lung with signet-ring cells: a histochemical comparison with signet-ring cell carcinomas of other sites. Hum Pathol. 1989;20:1097–102.
6. Singh G, Katyal SL. An immunologic study of the secretory products of rat Clara cells. J Histochem Cytochem. 1984;32:49–54.
7. Sakamoto H, Shimizu J, Horio Y, Ueda R, Takahashi T, Mitsudomi T, Yatabe Y. Disproportionate representation of KRAS gene mutation in atypical adenomatous hyperplasia, but even distribution of EGFR gene mutation from preinvasive to invasive adenocarcinomas. J Pathol. 2007;212:287–94.
8. Sato K, Ueda Y, Shikata H, Katsuda S. Bronchioloalveolar carcinoma of mixed mucinous and nonmucinous type: immunohistochemical studies and mutation analysis of the p53 gene. Pathol Res Pract. 2006;202:751–6.
9. Katavolos P, Ackerley CA, Clark ME, Bienzle D. Clara cell secretory protein increases phagocytic and decreases oxidative activity of neutrophils. Vet Immunol Immunopathol. 2011;139:1–9.
10. Snyder JC, Reynolds SD, Hollingsworth JW, Li Z, Kaminski N, Stripp BR. Clara cells attenuate the inflammatory response through regulation of macrophage behavior. Am J Respir Cell Mol Biol. 2010;42:161–71.
11. Awaya H, Takeshima Y, Yamasaki M, Inai K. Expression of MUC1, MUC2, MUC5AC, and MUC6 in atypical adenomatous hyperplasia, bronchioloalveolar carcinoma, adenocarcinoma with mixed subtypes, and mucinous bronchioloalveolar carcinoma of the lung. Am J Clin Pathol. 2004;121:644–53.
12. Londhe VA, Maisonet TM, Lopez B, Jeng JM, Li C, Minoo P. A subset of epithelial cells with CCSP

promoter activity participates in alveolar development. Am J Respir Cell Mol Biol. 2011;44:804–12.
13. Melamed MR. Mucinous (so-called colloid) carcinoma of the lung. Am J Surg Pathol. 2004;28:1397; author reply 1397.
14. Coppens JT, Plopper CG, Murphy SR, Van Winkle LS. Postnatal lung development of rhesus monkey airways: cellular expression of Clara cell secretory protein. Dev Dyn. 2009;238:3016–24.
15. Banerjee ER, Henderson Jr WR. Characterization of lung stem cell niches in a mouse model of bleomycin-induced fibrosis. Stem Cell Res Ther. 2012;3:21.
16. Giangreco A, Reynolds SD, Stripp BR. Terminal bronchioles harbor a unique airway stem cell population that localizes to the bronchoalveolar duct junction. Am J Pathol. 2002;161:173–82.
17. Kim CF, Jackson EL, Woolfenden AE, Lawrence S, Babar I, Vogel S, Crowley D, Bronson RT, Jacks T. Identification of bronchioalveolar stem cells in normal lung and lung cancer. Cell. 2005;121:823–35.
18. Volckaert T, Dill E, Campbell A, Tiozzo C, Majka S, Bellusci S, De Langhe SP. Parabronchial smooth muscle constitutes an airway epithelial stem cell niche in the mouse lung after injury. J Clin Invest. 2011; 121:4409–19.
19. Van Winkle LS, Buckpitt AR, Nishio SJ, Isaac JM, Plopper CG. Cellular response in naphthalene-induced Clara cell injury and bronchiolar epithelial repair in mice. Am J Physiol. 1995;269:L800–18.
20. Cole BB, Smith RW, Jenkins KM, Graham BB, Reynolds PR, Reynolds SD. Tracheal Basal cells: a facultative progenitor cell pool. Am J Pathol. 2010;177:362–76.
21. Huijbers IJ, Bin Ali R, Pritchard C, Cozijnsen M, Kwon MC, Proost N, Song JY, de Vries H, Badhai J, Sutherland K, Krimpenfort P, Michalak EM, Jonkers J, Berns A. Rapid target gene validation in complex cancer mouse models using re-derived embryonic stem cells. EMBO Mol Med. 2014;6:212–25.
22. Moreira AL, Gonen M, Rekhtman N, Downey RJ. Progenitor stem cell marker expression by pulmonary carcinomas. Mod Pathol. 2010;23:889–95.
23. Feyrter F. Argyrophilia of bright cell system in bronchial tree in man. Z Mikrosk Anat Forsch. 1954;61:73–81.
24. Merigo F, Benati D, Di Chio M, Osculati F, Sbarbati A. Secretory cells of the airway express molecules of the chemoreceptive cascade. Cell Tissue Res. 2007; 327:231–47.
25. Cutz E, Yeger H, Pan J. Pulmonary neuroendocrine cell system in pediatric lung disease-recent advances. Pediatr Dev Pathol. 2007;10:419–35.
26. Stevens TP, McBride JT, Peake JL, Pinkerton KE, Stripp BR. Cell proliferation contributes to PNEC hyperplasia after acute airway injury. Am J Physiol. 1997;272:L486–93.
27. Miki M, Ball DW, Linnoila RI. Insights into the achaete-scute homolog-1 gene (hASH1) in normal and neoplastic human lung. Lung Cancer. 2012;75: 58–65.
28. McGovern S, Pan J, Oliver G, Cutz E, Yeger H. The role of hypoxia and neurogenic genes (Mash-1 and Prox-1) in the developmental programming and maturation of pulmonary neuroendocrine cells in fetal mouse lung. Lab Invest. 2010;90:180–95.
29. Klemen HS-JF, Popper HH. Morphological and immunohistochemical study of typical and atypical carcinoids of the lung, on the bases of 55 cases with clinico-pathological correlation and proposal of a new classification. Endocr Relat Cancer. 1994;1:53–62.
30. Borges M, Linnoila RI, van de Velde HJ, Chen H, Nelkin BD, Mabry M, Baylin SB, Ball DW. An achaete-scute homologue essential for neuroendocrine differentiation in the lung. Nature. 1997;386:852–5.
31. Selman M, Pardo A. Idiopathic pulmonary fibrosis: misunderstandings between epithelial cells and fibroblasts? Sarcoidosis Vasc Diffuse Lung Dis. 2004;21: 165–72.
32. Ramos C, Montano M, Garcia-Alvarez J, Ruiz V, Uhal BD, Selman M, Pardo A. Fibroblasts from idiopathic pulmonary fibrosis and normal lungs differ in growth rate, apoptosis, and tissue inhibitor of metalloproteinases expression. Am J Respir Cell Mol Biol. 2001;24:591–8.
33. King Jr TE, Pardo A, Selman M. Idiopathic pulmonary fibrosis. Lancet. 2011;378:1949–61.
34. Godoy-Guzman C, San Martin S, Pereda J. Proteoglycan and collagen expression during human air conducting system development. Eur J Histochem. 2012;56:e29.
35. Erber R, Thurnher A, Katsen AD, Groth G, Kerger H, Hammes HP, Menger MD, Ullrich A, Vajkoczy P. Combined inhibition of VEGF and PDGF signaling enforces tumor vessel regression by interfering with pericyte-mediated endothelial cell survival mechanisms. Faseb J. 2004;18:338–40.
36. Yahata Y, Shirakata Y, Tokumaru S, Yamasaki K, Sayama K, Hanakawa Y, Detmar M, Hashimoto K. Nuclear translocation of phosphorylated STAT3 is essential for vascular endothelial growth factor-induced human dermal microvascular endothelial cell migration and tube formation. J Biol Chem. 2003;278: 40026–31.
37. Zhang X, Groopman JE, Wang JF. Extracellular matrix regulates endothelial functions through interaction of VEGFR-3 and integrin alpha5beta1. J Cell Physiol. 2005;202:205–14.

Pediatric Diseases

3

3.1 Developmental and Inherited Lung Diseases

Developmental and inherited lung diseases are rare events and therefore not many cases are seen in single institutions. This has resulted in a vast amount of single case reports, but only rarely have these been collected and studied with the focus on classification. A few studies came out from the Armed Forces Institute of Pathology (T. Stocker), which for a long time was one of the major pathology institutes with a vast amount of collected cases. Only recently initiatives were started in the USA and Europe to collect interstitial and developmental childhood cases and classify them accordingly [1–4]. As soon as cases have been analyzed, it was apparent that there are two peaks when diseases are recognized in children: The first peak occurs in the first 2 years of life comprising mainly developmental diseases and some acquired infections transmitted intrauterine or immediately postnatal. The second peak occurs in the period between 3 and 6 years of life and is composed predominantly by infections, genetic inherited diseases such as cystic fibrosis, and miscellaneous others.

In this chapter, we follow the proposed classification by the American CHILD group, however, include some modifications in as far as we additionally group the diseases into vascular malformations, malformations of the airways including components of the bronchial wall and the alveolar septa, malformations associated to chromosomal abnormalities, metabolic diseases, and finally a group of diseases with miscellaneous causes (Table 3.1).

3.1.1 Aplasia and Acinar/Alveolar Dysgenesis

Aplasia of both lungs is a rare developmental disorder, which is incompatible with life [5]. Aplasia of one lung in contrast can result in normal birth. Most often the left lung is involved. This disease is associated with other malformations such as aplasia of the left-sided diaphragm resulting in misplacement of abdominal organs into the left thoracic cavity. Most important in these cases, the coelom is also missing on the left side [5]. Another rare cause of single lung agenesis is Holt-Oram syndrome [6]. This is normally a combination of a congenital heart malformation (atrial or septum defect) combined with malformations on the fingers or lower arm based on mutations found at 12q23-24.1 (location of the TBX5 gene).

Hypoplasia of one or both lungs is not so uncommon. If both lungs are reduced in size, the newborn will require immediate assisted ventilation due to hypoxia. There are many underlying causes of hypoplasia, such as oligohydramnios, congenital diaphragmatic hernia, thoracic mass lesions, and neuromuscular dysfunction, which in concert with low levels of connective tissue growth factor could result in lung hypoplasia [7, 8]. Another factor identified as being associated

© Springer-Verlag Berlin Heidelberg 2017

H. Popper, *Pathology of Lung Disease*, DOI 10.1007/978-3-662-50491-8_3

Table 3.1 Modified classification of childhood diseases

Disease group	Name of disease	Known genetic abnormality
General malformation of whole lungs or lobes	Aplasia of the lung (partial or total)	
	Holt-Oram syndrome and aplasia	12q23-24.1, TBX5
	Hypoplasia	TTF1?
	Congenital acinar/alveolar dysgenesis/ dysplasia	SOX genes?
Growth retardation	Growth arrest, immature lung lobules, or subsegments, associated with heart diseases	
General malformation of whole lungs or lobes combined with vascular malformations	Alveolar capillary dysplasia with/without misalignment of pulmonary veins	FOXF1, PTEN
Vascular malformations	Diffuse and localized AV anastomoses	
	Morbus Rendu-Osler (hereditary hemorrhagic telangiectasia)	Endoglin and activin receptor-like kinase genes
	Ehlers-Danlos syndrome type IV	Collagen synthase
	Marfan disease	
	Veno-occlusive disease and pulmonary arterial hypertension	ElF2AK4 coding for GCN PERK, PKR, HRI
	Anomalous systemic arterial supply, including sequestration	
	Anomalous venous return	
Malformations of the airway system	Congenital pulmonary adenomatoid malformation (CPAM, formerly CCAM)	Fatty acid-binding protein-7, FGFs
	Bronchogenic cyst	
	Congenital lobar emphysema	
	William-Campbell syndrome	
	Mounier-Kuhn syndrome	
Lung malformation in chromosomal abnormalities	Trisomy 21	
	Trisomy 1q	
	Trisomy 8	
Inborn errors of metabolism		
Cystic fibrosis		
Neuroendocrine cell hyperplasia of infancy		
Pneumonias in infancy		

with acinar development and hypoplasia is phosphorylated TTF-1 [9, 10]. A reduction of Clara cell protein 16 in amniotic fluid has been found being associated with lung hypoplasia [11]; however, in this case it is unclear if this finding is primarily responsible for hyperplasia or a secondary effect due to maturation stop of the epithelia. Macroscopically the lung is reduced in size with respect to the developmental age. Microscopically the lung lobules are also reduced in size and numbers of alveoli per lobule (primary lobule). Otherwise the different structures of the lung are present, and no element is missing. On microscopy it might be difficult to assess hypoplasia: if uncertain look for two adjacent bronchioles and count the alveolar septa in between them. There are usually less than four septa present (Fig. 3.1).

Congenital alveolar dysplasia is characterized by a regular bronchial development but no acinar/alveolar development, resembling the pseudoglandular phase of 16 weeks gestation [4, 12] (Fig. 3.2). Usually these children already die intrauterine or immediately after birth. The

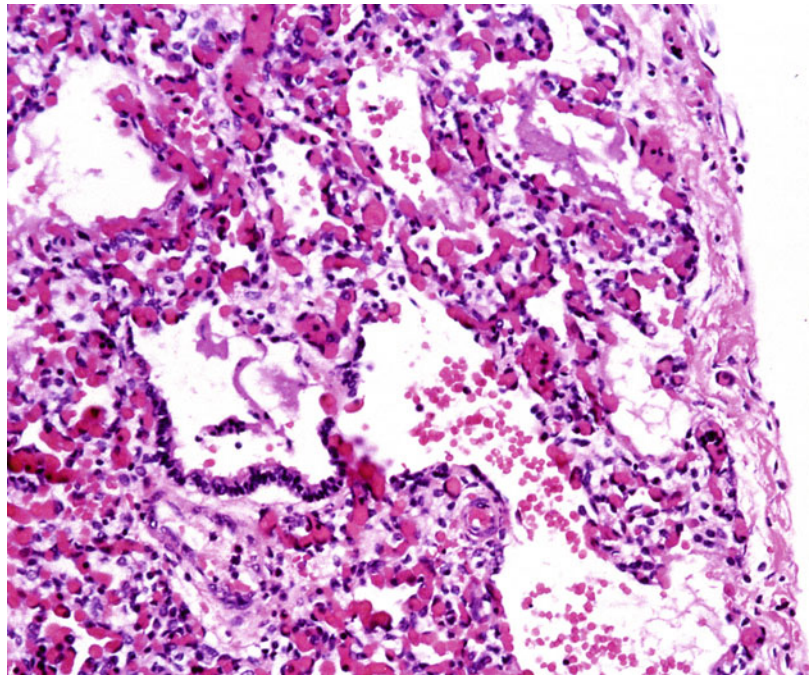

Fig. 3.1 Hypoplasia of one lung lobe; the number of alveoli is reduced and their size is increased. H&E, ×150

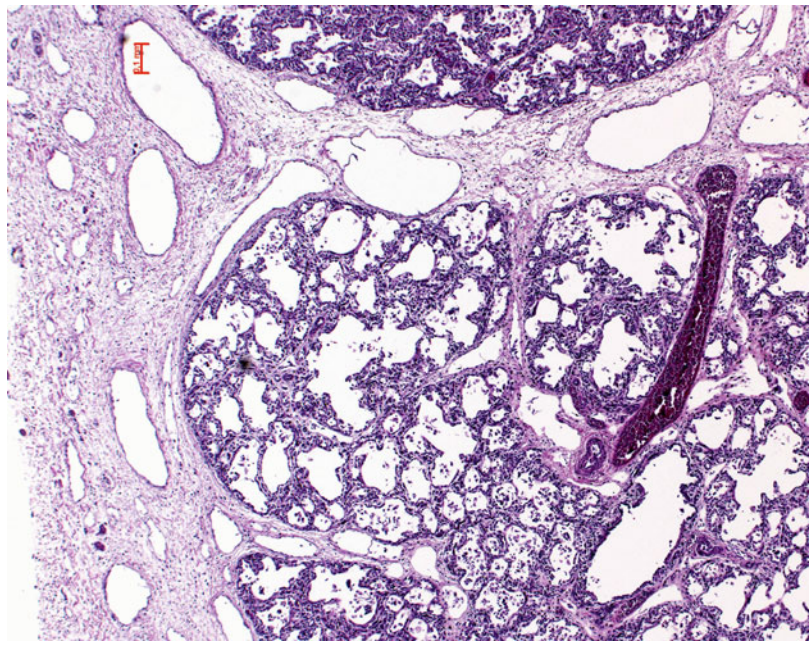

Fig. 3.2 Congenital alveolar dysplasia in a newborn, mild form; the lung lobules are developed, the bronchi and bronchioles are normal, but bronchioles open in cystic pseudoglandular to saccular spaces. H&E, bar 100 µm

underlying genetic defect might be associated with defective coelom development, missing cross talk between epithelial and mesenchymal cells, or impaired signaling of SOX genes, but so far these genetic defects have not been identified. Congenital alveolar dysplasia corresponds to CPAM type 0 in the Stocker classification but in contrast to the other CPAM types results in the generalized failure of forming bronchial and alveolar structures.

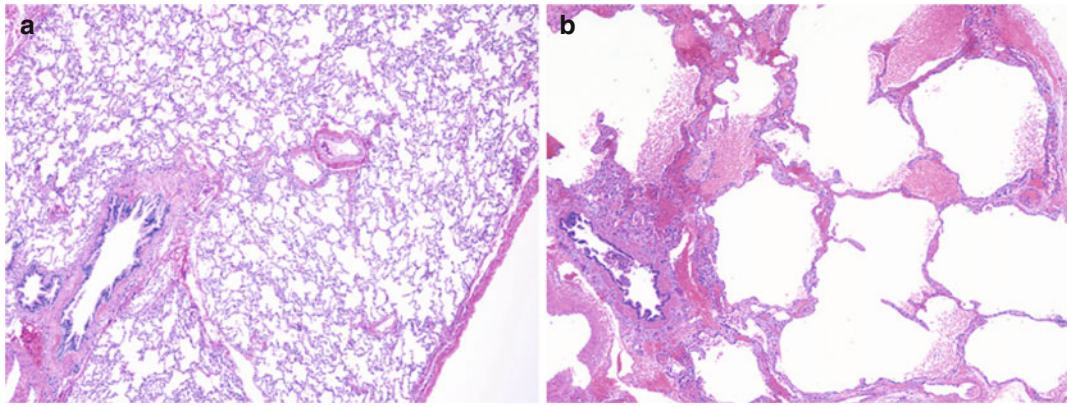

Fig. 3.3 Mild form of congenital alveolar dysplasia with rudimentary alveolar septation (*right*, **b**). For comparison a normal lung from an autopsy case (same age) is shown to the *left* (**a**). H&E, ×50

A more mild form of congenital alveolar dysplasia can be found where the alveolar development has started, but alveolar septation has stopped resulting in ill-formed alveoli with a few septa (Fig. 3.3). Thus lung development has stopped differentiation at the saccular stage. This results in a reduced respiratory surface and thus reduced oxygenation. These children even with mechanical ventilation are hard to oxygenate. They are also prone to postnatal infections.

3.1.2 Growth Retardation

Focally retardation and growth arrest is not uncommon in children with congenital heart disease with or without an association to chromosomal abnormalities. It might be due to impaired blood supply resulting in growth and differentiation retardation. These children present with focal immature lung lobules or subsegments detected during radiological evaluation before heart surgery.

3.1.3 Vascular Malformations

3.1.3.1 Alveolar Capillary Dysplasia with/Without Misalignment of Pulmonary Veins

Alveolar capillary dysplasia is a life-threading disease of newborns. Babies are born without symptoms, but immediately after birth will show symptoms of hypoxia and pulmonary hypertension. Mechanical ventilation and oxygenation in an intensive care unit will improve the clinical situation; however, immediately after withdrawal the symptoms will worse again [13]. There is no cure for this disease.

Histologically the number of capillaries is dramatically reduced or they might be almost absent. Larger arteries will show mild increase of vessel wall thickness. On step section AV anastomoses can be proven. In those cases where there is also misalignment of the veins, these run parallel with the arteries within alveolar septa, and they are anastomosing focally. Veins are closely attached to pulmonary arterioles and small arteries and are widened (Figs. 3.4. 3.5, 3.6, and 3.7). As a result the blood flow is shunted from the arterial bed to the veins without a significant flow into the capillaries resulting in severe hypoxia [14]. Recently microdeletions resulting in frameshift, nonsense, and stop mutations of the FOXF1 gene have been identified probably underlying this disease [15–17]. Another genetic abnormality possibly also leading to the same phenotype was identified as PTEN loss in mesodermal cells inhibiting the proliferation of angioblasts, and a relationship was identified with FOXF1 mutation [18]. So it is most likely that not just a single gene causes this disease but more than one, disrupting the cross talk between different cells involved in the correct alignment of the peripheral vascular bed. In a case report, trisomy 21 was described in a child with alveolar capillary dysplasia and misalignment of veins [19], but again cardiac

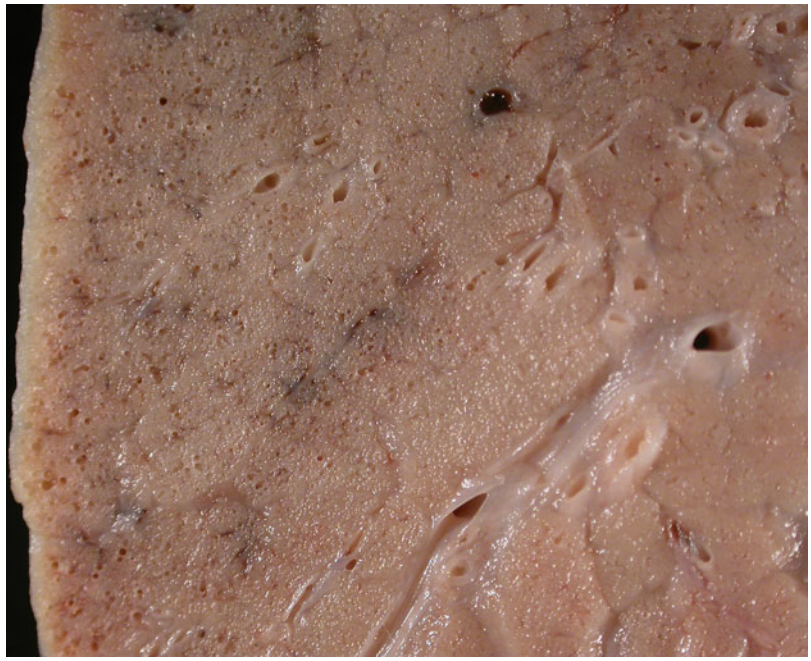

Fig. 3.4 Macroscopic picture of alveolar capillary dysplasia with misalignment of pulmonary veins; open lung biopsy taken after 3 weeks of mechanical ventilation and oxygenation, which started immediately after birth. The holes in the periphery represent widened blood vessels

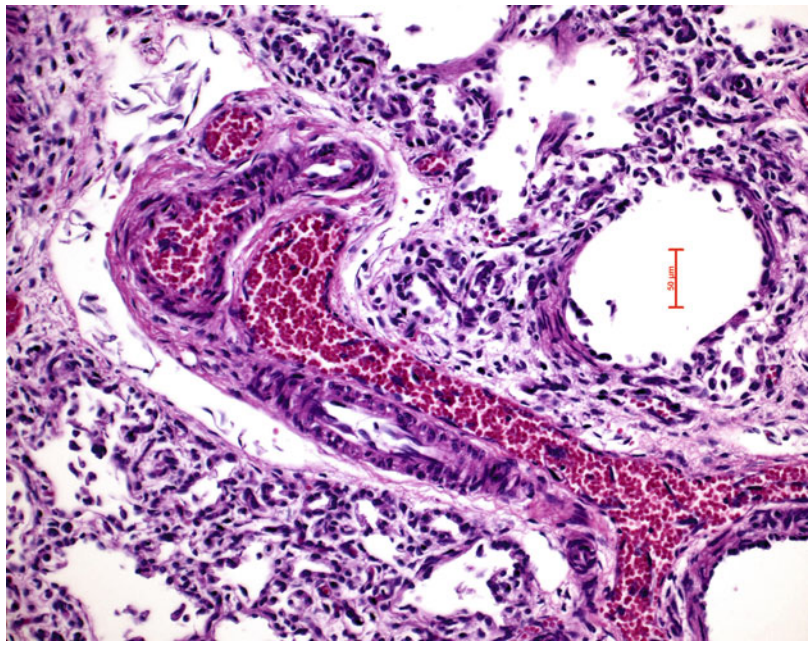

Fig. 3.5 Histological findings in alveolar capillary dysplasia with misalignment of pulmonary veins: in the *middle* there is a pulmonary artery accompanied by a large dilated vein. The alveoli are ill formed and in most capillaries are missing. H&E, bar 50 µm

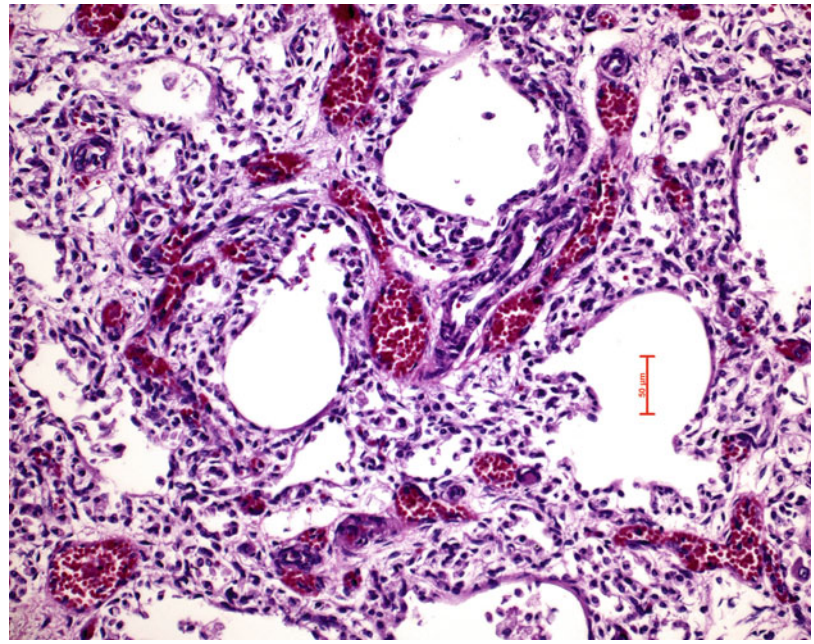

Fig. 3.6 Histological findings in alveolar capillary dysplasia with misalignment of pulmonary veins: here anastomosis of the pulmonary artery and the accompanying vein could be proven on serial sections. H&E, bar 50 µm

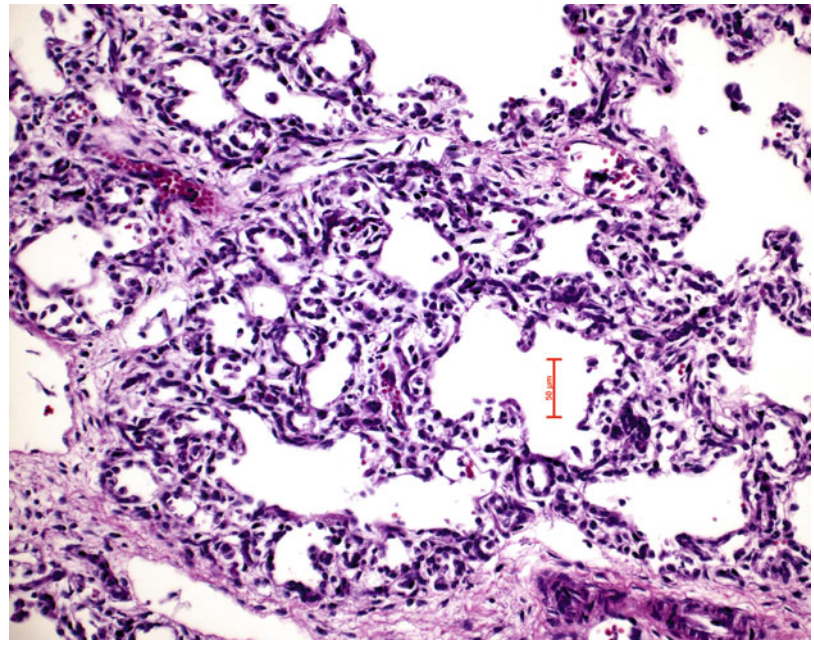

Fig. 3.7 Histological findings in alveolar capillary dysplasia with misalignment of pulmonary veins: In this micrograph the ill-formed alveoli are shown, and in addition the capillaries in the alveolar septa are missing. H&E, bar 50 µm

malformations were also present, which makes it difficult to assign a chromosomal abnormality to one of the different organ abnormalities.

3.1.3.2 Diffuse and Localized AV Anastomoses

Pulmonary arteries and veins can be affected by different malformations, which are presently ill defined. Usually patients present with alveolar hemorrhage, which sometimes can be life threatening [20]. Pulmonary hypertension is usually present in diffuse non-tumor cases. All ages can be affected; however, diffuse AV anastomoses such as in Rendu-Osler disease usually present at an early age [21–23], whereas localized AV anastomoses (i.e., within one lobe) are seen at an

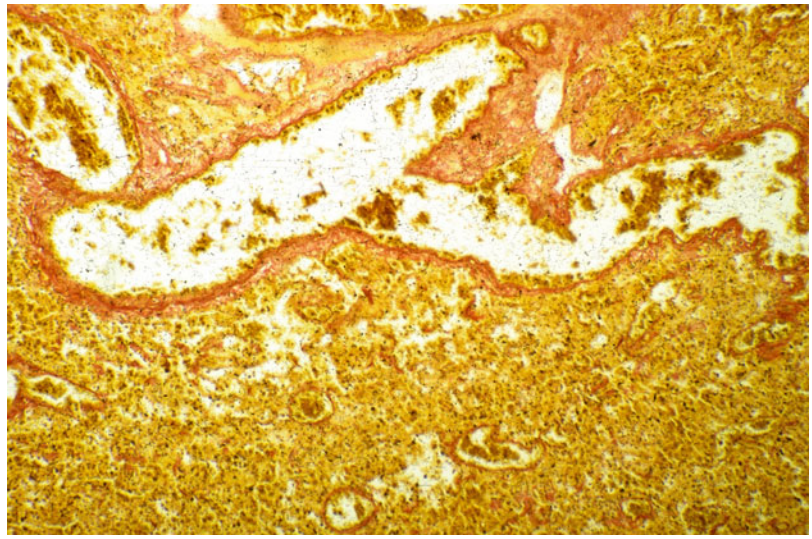

Fig. 3.8 AV angiomatosis in a young adult. There were several AV anastomoses in both lungs. The patient died with massive hemorrhage. Elastica van Gieson, ×50

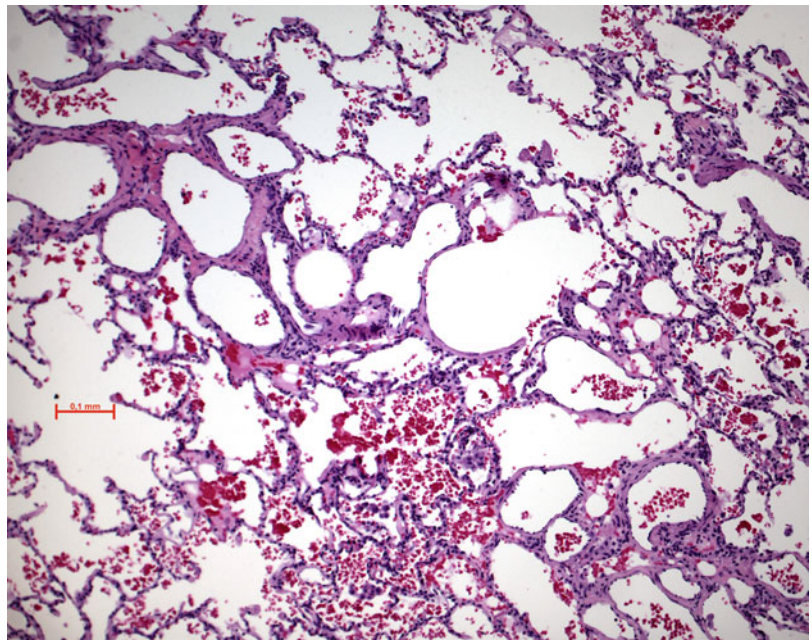

Fig. 3.9 Mb. Rendu-Osler in a child; there are anastomosing cavernous blood vessels; in this case the lesion was located only in the right upper lobe. H&E, bar 100 µm

older age (above 12 years; Fig. 3.8). The underlying pathology can be capillary or cavernous hemangiomas, arteriovenous malformations, or angiomas. Usually a careful examination is necessary to find the underlying cause of bleeding. In my experience one should select those areas where massive hemorrhage is present. Take many sections and start searching for malformations.

Morbus Rendu-Osler (hereditary hemorrhagic telangiectasia) is an autosomal dominant systemic vascular disorder presenting with vascular malformations including thin-walled ill-formed small blood vessels (telangiectasia) and diffuse AV anastomoses (Figs. 3.9, 3.10, and 3.11). Most often the small and large bowel are affected, but other organs might be involved too – the affection of the lung is rare [22, 23]. It can cause life-threatening bleeding, but also hypertension. A constant clinical finding is an impaired vascular flow, which can be visualized by tracers showing a time difference in the venous flow between the affected and the normal lung lobe (short turnover due to AV anastomoses). Treatment is still experimental; however, we significantly improved the symptoms in a

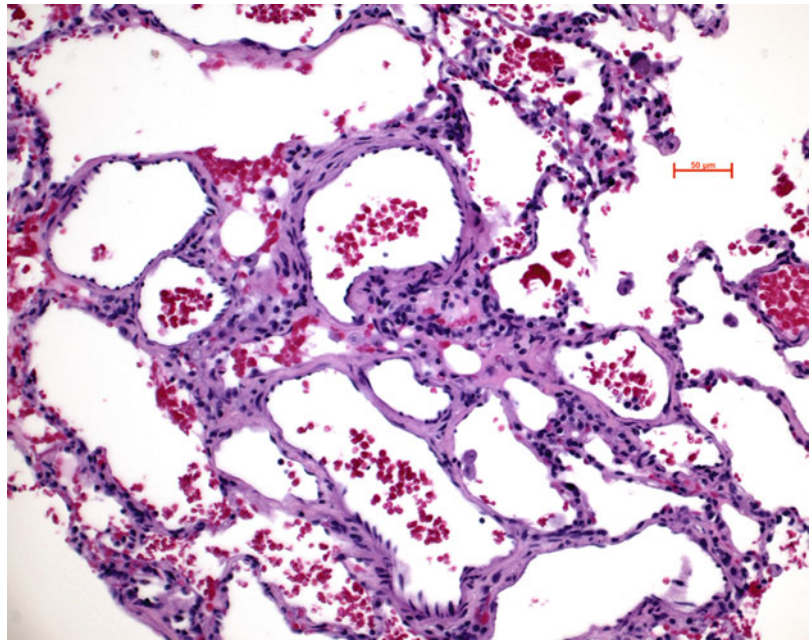

Fig. 3.10 Mb. Rendu-Osler in a child; higher magnification of the angiomatosis. H&E, bar 50 µm

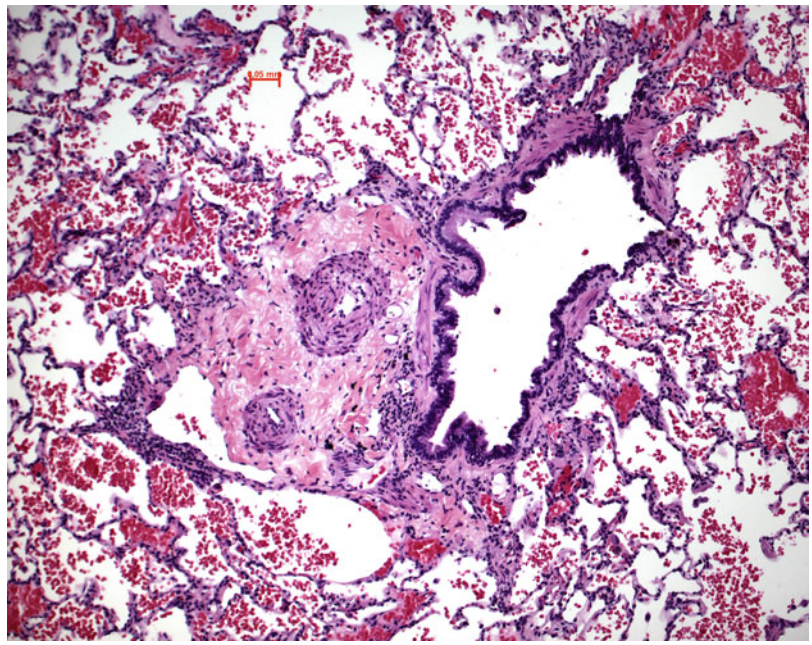

Fig. 3.11 Mb. Rendu-Osler in a child; here the severe sclerosis of the pulmonary arteries is shown. There is severe muscular hyperplasia in the vessels wall and massive narrowing of the lumina. H&E bar 500 µm

young boy using a treatment protocol for arterial hypertension (bosentan) [24]. Recently mutations in the endoglin and activin receptor-like kinase genes were discovered, which might open a new line of treatment in this rare disease [25–29].

Ehlers-Danlos syndrome type IV as well as *Marfan disease* can affect the pulmonary blood vessels [30, 31]. The symptoms are usually life-threatening bleedings (alveolar hemorrhage). It might be necessary to resect a lung lobe or do even a pneumonectomy, to rescue the patient, although the disease will recur affecting other lung lobes and finally cause death. Histologically these diseases are most difficult to prove. Of

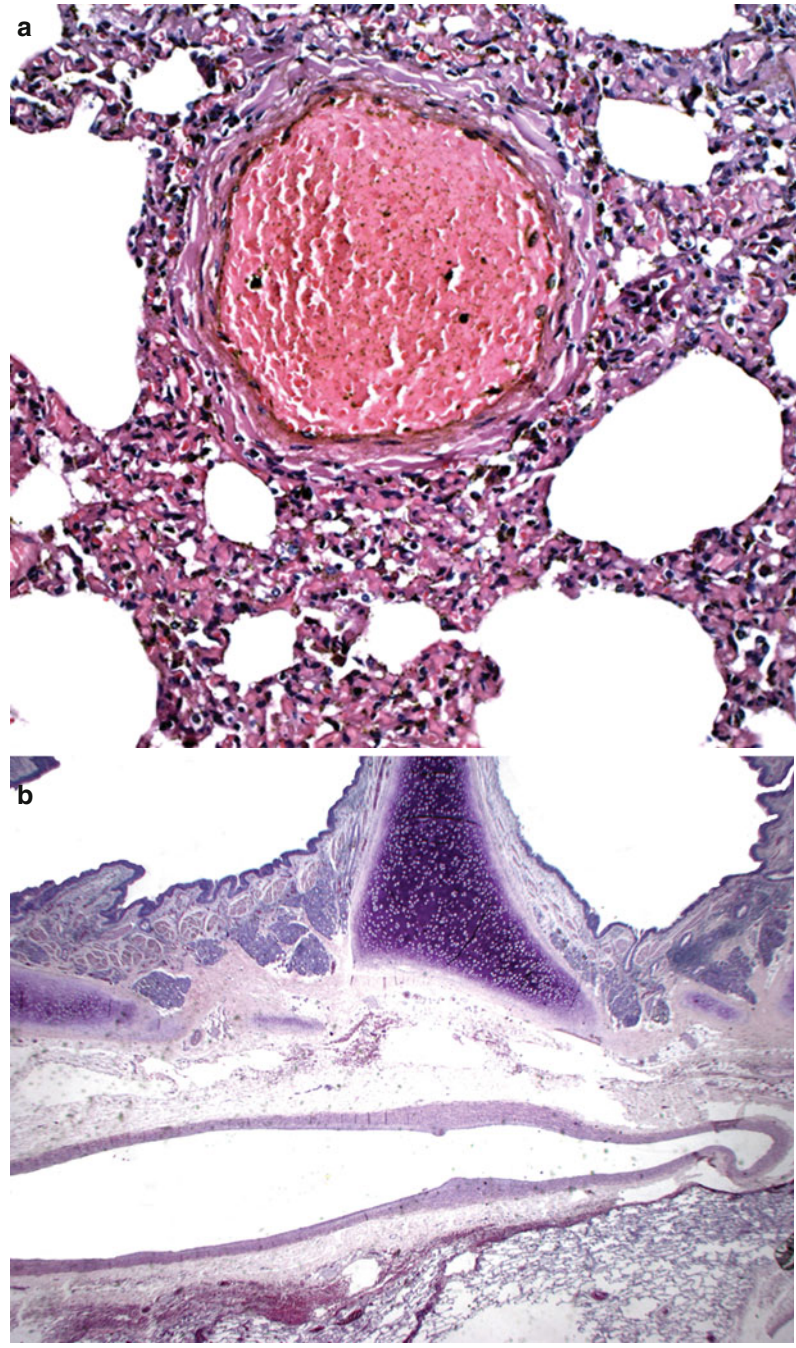

Fig. 3.12 (**a**) Marfan disease; in the pulmonary arteries, the elastic laminae are completely missing, which will result in hemorrhage, and depending on the size of the ruptured vessel can be life threatening. H&E, 100. (**b**) Ehlers-Danlos syndrome IV in a 20-year-old male patient; the only important finding here is the thin-walled pulmonary artery; any stain, which highlight collagen and elastic fibers, will show the ill-formed collagen. H&E ×50

diagnostic help is the young age of the patients. All other causes of alveolar hemorrhage have to be excluded, such as vasculitis, localized hemangioma, trauma, etc. A typical feature of both diseases is the thin wall of the large pulmonary arteries. In Marfan disease, an elastic stain will highlight the nearly absent or ill-formed elastic fibers (Fig. 3.12a); in Ehlers-Danlos disease type IV, collagen and elastic fibers are very thin and sometimes form an incomplete rim around the vascular smooth muscles, whereas the lamina elastic is normal (Figs. 3.12b and 3.13). The synthesis of type III procollagen is impaired in this latter disease [31].

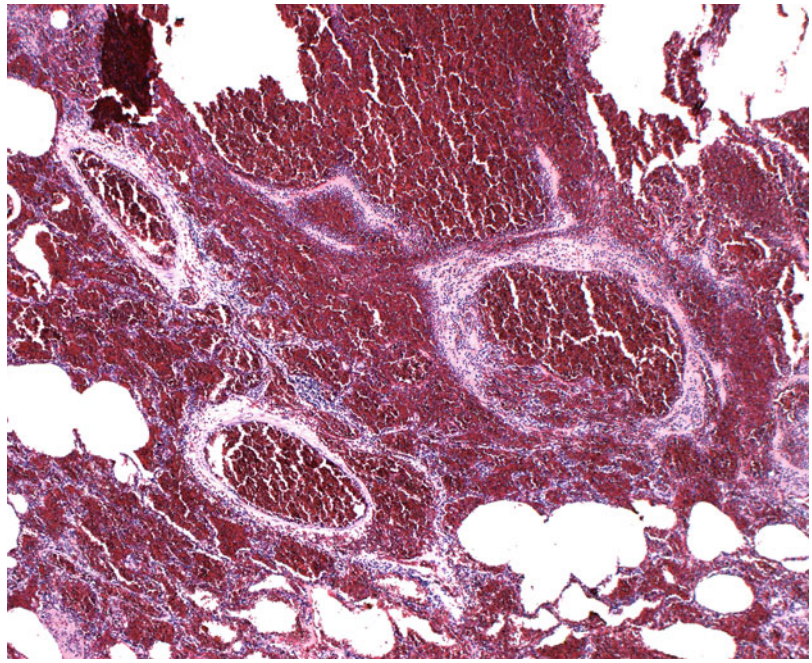

Fig. 3.13 Ehlers-Danlos syndrome IV; in the peripheral lung, massive alveolar hemorrhage was found; however, no cause for bleeding could be demonstrated. H&E ×100

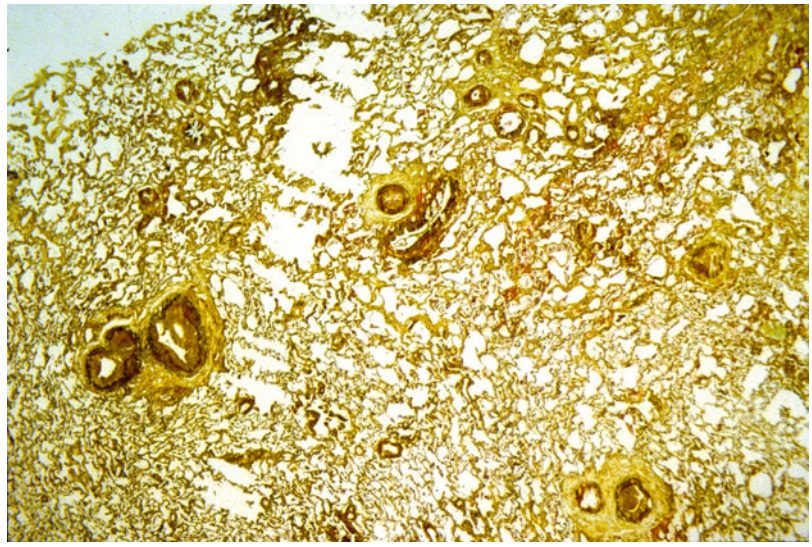

Fig. 3.14 Veno-occlusive disease; the peripheral lung tissue looks normal, only the blood vessels present with pathological abnormalities. Movat stain ×25

Veno-occlusive disease is characterized by venous stenosis and/or occlusion. Most often also arteries will show thickened walls (Figs. 3.14 and 3.15). Veno-occlusive disease can present with pulmonary arterial hypertension and capillary hemangiomatosis in children and adults, but rarely is found as an isolated disease. In children it is most often found in complex malformations of the heart. Veno-occlusive disease will be covered in detail also in the chapter on vascular disorders.

3.1.3.3 Anomalous Systemic Arterial Supply Including Sequestration

Sequestration was originally regarded as a malformation of the lung blood system. During lung development an artery from the branchial arch of

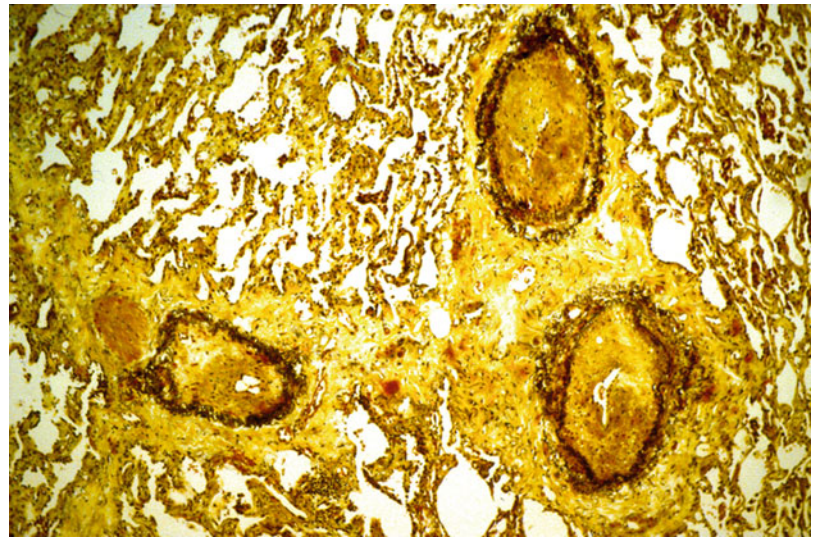

Fig. 3.15 Veno-occlusive disease; on higher magnification the veins within these interlobular septa are almost occluded, only slit-like spaces are left. Otherwise the lung is normal. Movat stain, ×60

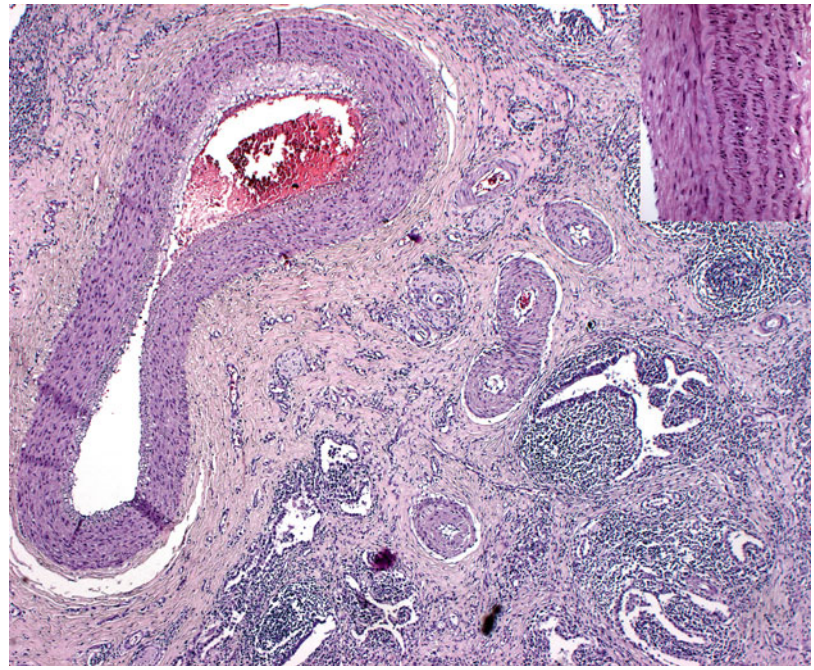

Fig. 3.16 Pulmonary sequestration; the picture shows thickened arteries and in addition also inflammation and fibrosis; increase of elastic laminae is even seen on H&E-stained section and highlighted in the inset (*upper right corner*). H&E, ×100, inset ×400

the primitive blood supply persists and therefore a segment or even a lung lobe gets it blood supply from an aortic branch (A. mammaria interna, AA. intercostales, etc.) or the aorta directly. Recent surveys have shown that associated with this condition are other malformations, such as stenosis or atresia of the segmental bronchus and congenital cystic adenomatoid malformation (type I or II) [32, 33]. Surgeons will usually cut the bronchus at the atresia site and thus this lesion is usually not present at the resected segment. Sequestration can be intralobar (within the lung) or extralobar (thoracic cavity) or even within the abdominal cavity (below the diaphragm). On macroscopic examination a thick-walled artery is found entering the lung from the pleura. Macroscopically as well as microscopically, there is most often hemorrhage overlaying the specific histologic features. A diagnostic feature is elastosis of the involved arteries (Fig. 3.16). There is multilayering of

Fig. 3.17 Scimitar syndrome; open lung resection; there are several arteries and veins entering the upper lobe from outside the lung. On histology these blood vessels merge with the regular vascular structures at the level of small arteries and veins

Fig. 3.18 Large AV angioma in a female child of 4 years of age. There was a surgical correction of a ventricular malformation several months ago. Hemorrhage caused surgical resection of the angioma

elastic laminae. The increase of the vessel wall thickness is quite characteristic and not seen in that severity in other diseases such as pulmonary hypertension. The arterial wall looks like that of a large systemic artery. Often there is considerable inflammation in the lung tissue, so resection will much improve the overall situation of these patients [34–39]. In more than 50 % of cases, sequestration is associated with cystic pulmonary malformation (discussed below).

A rare anomalous venous return to the right atrium or the inferior vena cava has been described as Scimitar syndrome (Fig. 3.17). It can be combined with other abnormalities, especially the heart [40–42]. Arteriovenous angiomas have been seen in congenital heart malformations (Fig. 3.18).

Different other variants of anomalous arterial and venous blood supplies have been reported as single cases. Following the description of these cases, they are most probably based on the same organogenesis pathway: branches of the bronchogenic pouch remain and get fused to the peripheral lung blood vessels [14], and formation of veins out of the left atrium and sinus venosus is impaired [37, 43].

Other vascular malformations either inborn or acquired such as capillary hemangiomatosis and lymphangiomatosis will be discussed in the chapter on tumor pathology, vascular tumors.

3.1.4 Malformations of the Airway System

3.1.4.1 Congenital Pulmonary Adenomatoid Malformation (CPAM, Formerly CCAM) Types I, II, and III

Congenital cystic/pulmonary adenomatoid malformation is a developmental disease, which predominantly occurs in children; however, it has been diagnosed also in young adults and occasionally in older patients. Originally three types have been described, types I–III. Type I is characterized by large cysts, >2 cm, often multilocular, and type II is more uniform with smaller cysts, less than 2 cm, whereas type III is microcystic and not visible macroscopically. Stocker has added types 0 and IV several years ago, because not all lesions fitted into one of the three categories [44]. In a recent review, Langston critically discussed CCAM/CPAM. First of all, the Stocker classification was primarily based on autopsy cases and primarily characterized macroscopically. Second, today more cases come in as resected specimen, because by clinical investigation these lesions are diagnosed even intrauterine. In her series of cases, Langston has nicely shown that CPAM quite often is associated with other developmental abnormalities, as bronchial atresia and sequestration (see above). She proposed a simplified classification into large cyst type (CPAM I) [1, 33]. The cysts are multilocular, larger than 2 cm in diameter, and covered by bronchial epithelium overlying fibromuscular stroma (Figs. 3.19, 3.20, and 3.21). In contrast to bronchial cysts, there is no cartilage. CPAM I communicate with the peripheral lung tissue, also in contrast to the situation of bronchial cysts (no alveolar tissue), which is the main differential diagnosis. Within CPAM I and II foci of atypical goblet cell, hyperplasia does exist, which might give rise to childhood adenocarcinoma (Fig. 3.22) [45–47].

The small cyst type (CPAM II) is usually associated with airway obstruction, such as atresia, but also frequently with sequestration or even both. Cysts are found in a regional distribution; the cysts are lined by bronchiolar epithelium. Between the cysts normal alveolar lobules can be found (Figs. 3.23, 3.24, and 3.25).

The solid form of CPAM type III (CCAM III) is completely different from types I and II, because it appears macroscopically solid not cystic. Histologically it presents as an immature lung with tubular bronchioles organized into

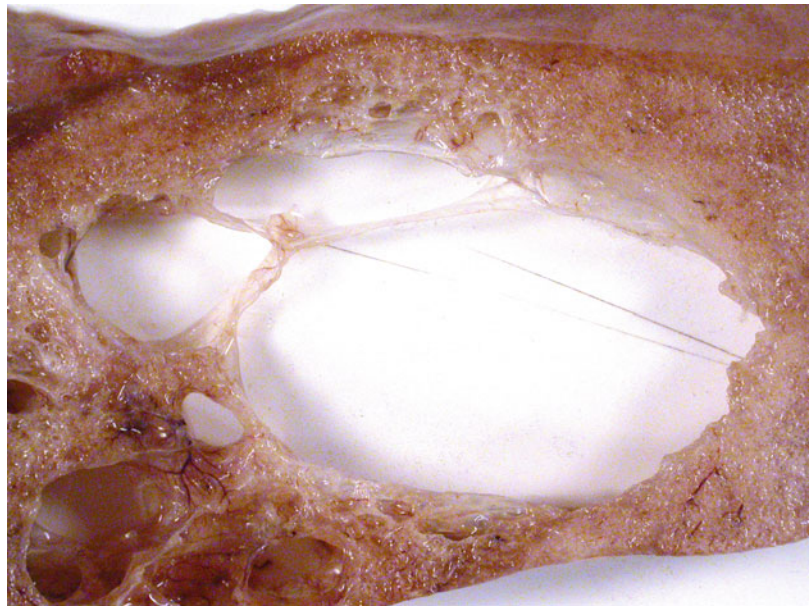

Fig. 3.19 CPAM I; macroscopic picture of a resection; there are several large cysts, some of them multilocular

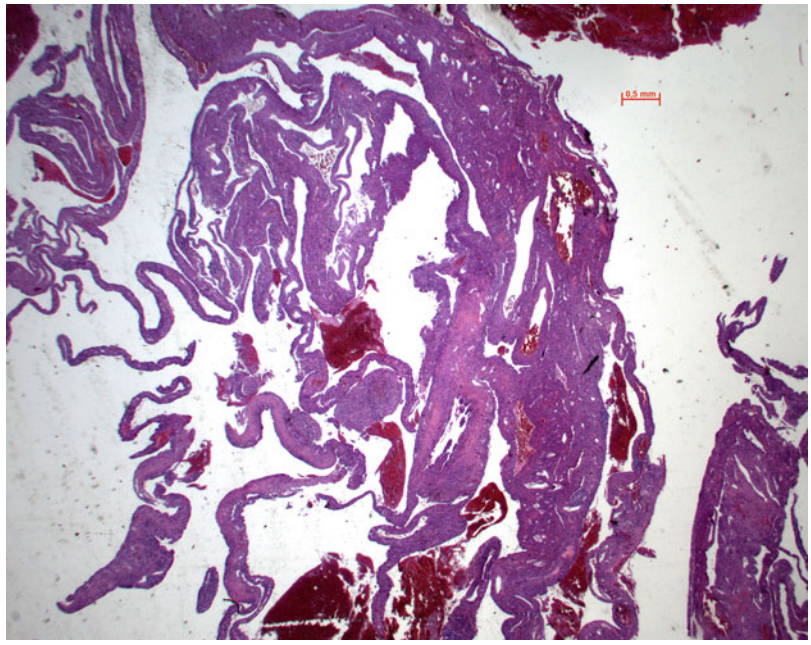

Fig. 3.20 CPAM I; on histology large cysts are seen covered by bronchial epithelium. H&E, bar 500 µm

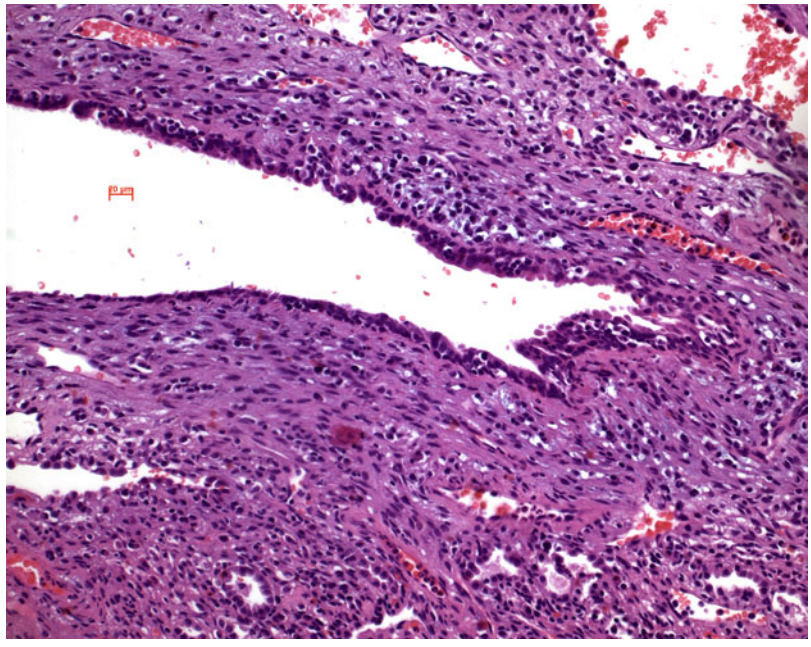

Fig. 3.21 CPAM I; on higher magnification the bronchial epithelium is seen covering the cyst surface. Underneath the epithelium there are thick bundles of smooth muscle cells; the cartilage is most often missing, but can occur in rare cases. H&E, bar 20 µm

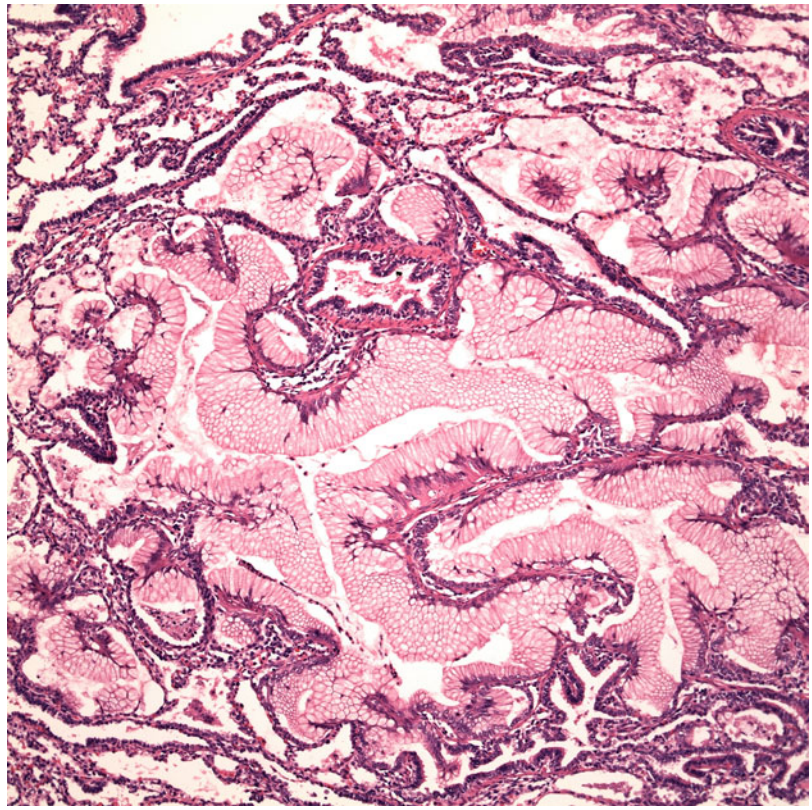

Fig. 3.22 CPAM II; an area of atypical goblet cell dysplasia is shown. Single layer of high columnar goblet cells replacing the normal epithelium totally covers the cyst epithelium. H&E, ×150

Fig. 3.23 Macroscopic picture of CPAM II; numerous small cysts are seen, most of them communicating with each other

lung lobules without an alveolar part. It resembles fetal lung at the tubular stage (Figs. 3.26 and 3.27). It can be found combined with laryngeal atresia, according to Langston [1]. Therefore, CPAM III should be taken as a different non-cystic lesion best under a different name and not subcategorized under CPAM. The only thing in common with CPAM I and II is that it is also a growth and differentiation abnormality related to developmental genes. In a recent report, trisomy 13 was identified in a child; however, there were also several other malformations as holoprosencephaly, arhinencephaly, cleft palate, ventricular septal defect, and bilateral clubfeet [48]. In another case CPAM was described combined with cardiac and renal abnormalities [49].

CPAM 0 and IV are ill defined, and Stocker's classification could not be reproduced in our experience (European Rare disease group). According to Stocker CPAM 0 is a malformation at the level of the tracheal bud and corresponds most likely to alveolar dysgenesis, which is discussed above, whereas CPAM IV in our experience is indistinguishable from congenital lobar emphysema. Both are not correctly placed into

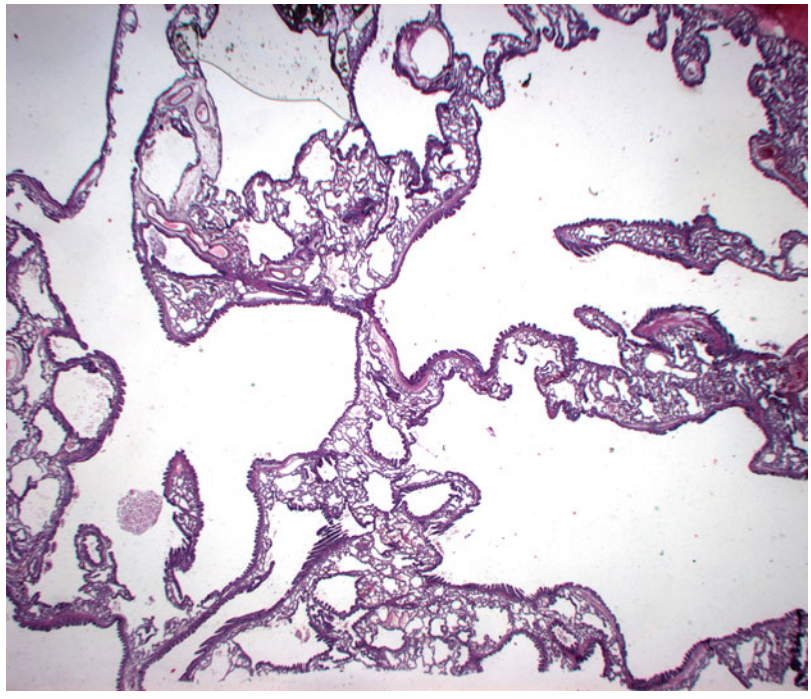

Fig. 3.24 CPAM II; the cysts are covered by regular bronchial epithelium; a thin smooth muscle layer can be present, cartilage is absent. Between the cysts normal lung parenchyma is embedded; however, the cysts most often do not communicate with the normal lobules. H&E, ×100

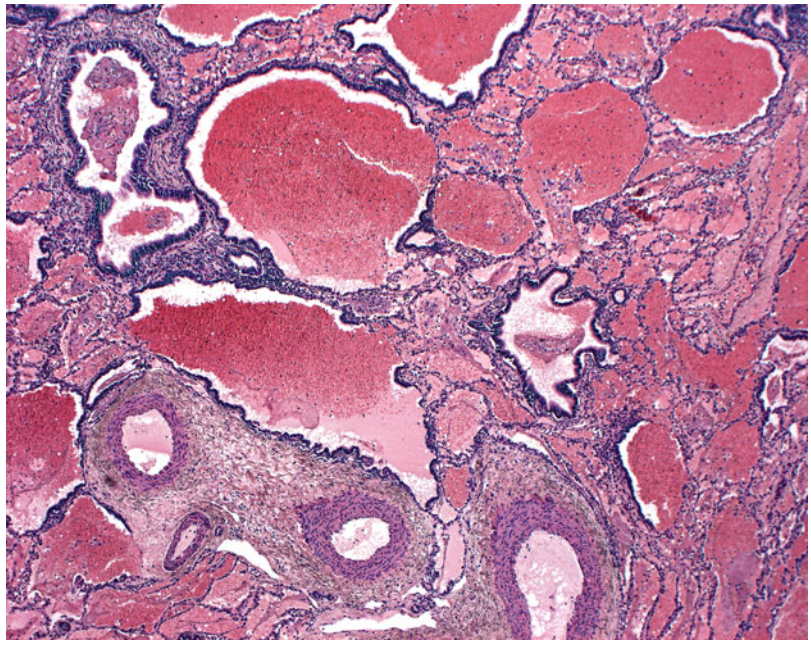

Fig. 3.25 CPAM II combined with sequestration; see the thick-walled arteries with elastosis. H&E, ×100

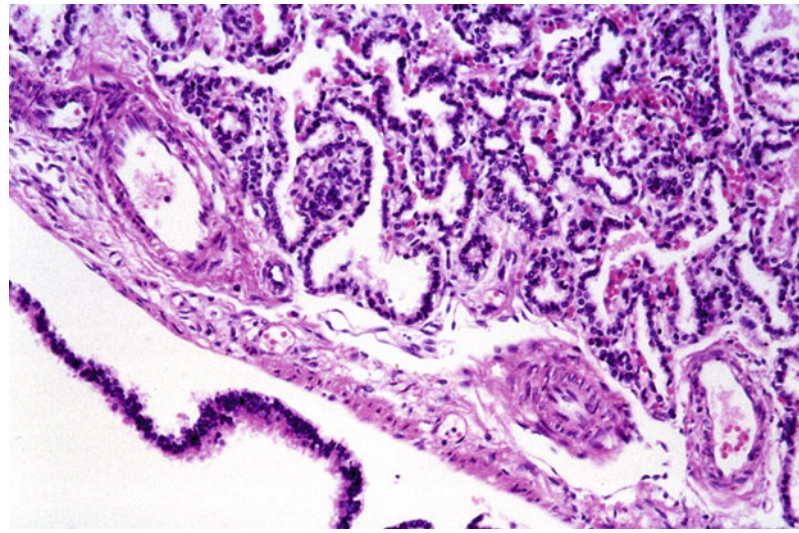

Fig. 3.26 CPAM III; the lesion is composed of small cystic structures composed of immature bronchioles. There is no alveolar tissue. The cysts neither communicate with the central airways nor the periphery. H&E, ×100

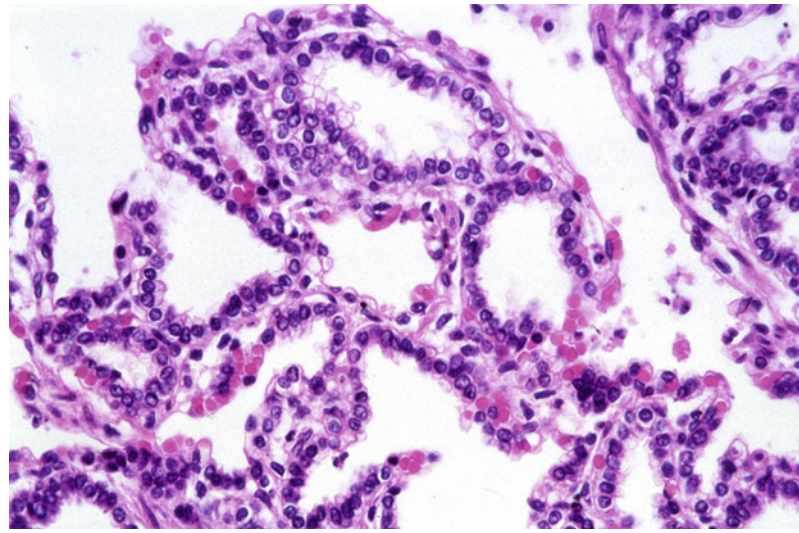

Fig. 3.27 CPAM III; higher magnification of this lesion showing the immature bronchioles completely covered by Clara cells. H&E, ×250

cystic malformations: CPAM 0 is not cystic and CPAM IV is emphysematous, so we will discuss these lesions under the appropriate term of alveolar dysgenesis and congenital emphysema, although at present we do not have enough data about pathogenesis and the genetic background.

In contrast, CPAM types I–III represent examples of growth and differentiation arrest, which could be highlighted by some recent molecular genetic studies. In the study by Wagner et al., fatty acid-binding protein-7 was found underexpressed in CPAM [50]; in the study by Jancelewicz, a fourfold expression of FGF9 was found in fetal epithelia of CPAM compared to normal fetal lung. By immunohistochemistry a decreased FGF7 expression was detected in CPAM mesenchyme [51]. However, both studies failed to classify the subtypes of CPAM, which they analyzed in their respective investigations. This might have contributed to understand better the pathogenesis and would have improved the present day classification (different time points of developmental stops/defects).

3.1.4.2 Bronchogenic Cyst

Bronchial cysts do occur usually extrapulmonary (most often within mediastinum), rarely within the lung. They are characterized by a cystic space covered by bronchial epithelium, usually with well-formed muscular layer. Cartilage most often is present. There is no peripheral lung tissue present (Fig. 3.28). It might be assumed that bronchial cysts represent supernumerary bronchi of the ontogenesis of the lung, not having been abolished by apoptosis during bronchial budding. In several mammals but also birds (sheep, goat, etc.), there exist a mediastinal lung lobe, the bronchus arising directly from the trachea. Since the lung development is recapitulated during morphogenesis, it might be that this bronchus persists, looses its communication with the trachea, and finally transforms into a cyst.

Congenital lobar emphysema (corresponding to Stocker's CPAM type IV) is inborn or acquired emphysema for which no cause has been defined. It is similar to panacinar emphysema in adults, showing an even distension of alveoli. However, it affects only lung lobes or segments, not the whole lung (Fig. 3.29). Symptoms are caused by compression of the adjacent lung lobes. Newborn will present with hypoxia. A resection usually cures the patient, because the other lobes will expand and later on grow, and thus replaces what was resected.

William-Campbell syndrome is characterized by the absence or malformation of cartilages in peripheral bronchi. The cartilages in the trachea and main bronchi are normally developed; however, below the segmental bronchi, the cartilages are either totally absent or ill developed. This causes bronchial collapse during expiration and symptoms of bronchial obstruction in a very young-aged population. The diagnosis even on VATS biopsies is not easy, because VATS take usually peripheral lung tissue below the order of segmental or subsegmental bronchi (see schema below). Therefore, in these tissues, only small bronchi, which normally have ill-formed cartilage or none at all, are seen. Therefore, before the biopsy is taken, the thoracic surgeon needs to be advised, to take a tissue fragment, which contains at least one subsegmental bronchus. Also the largest bronchus should be marked, so that the tissue can be cut vertically to get cross sections of the bronchus.

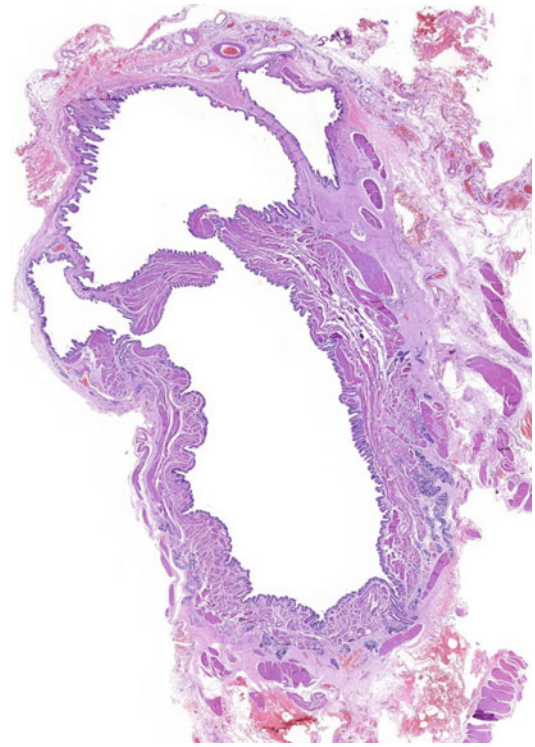

Fig. 3.28 Bronchogenic cyst, here within the mediastinum; the cyst is lined by bronchial epithelium, a thick muscular coat is also present, cartilages are absent. H&E, ×25

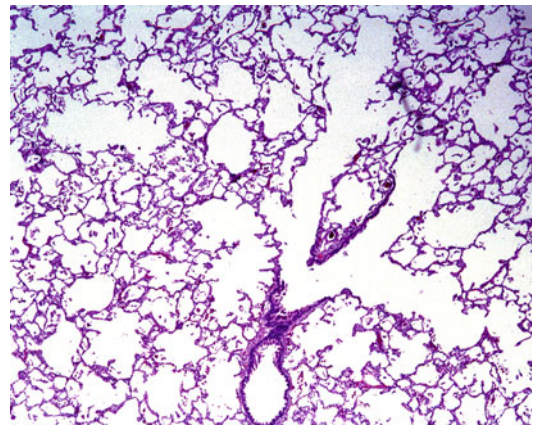

Fig. 3.29 Congenital lobar emphysema/CPAM IV; there is widening of alveolar ducts and the centroacinar alveolar region. H&E, ×25

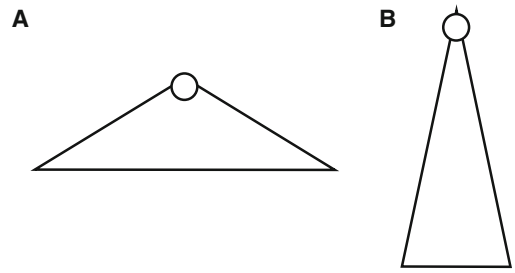

Schema: Normally VATS biopsies are shallow and therefore only small bronchi and bronchioles are included as in schema A; for WC syndrome a steep section is required to get larger bronchi into the specimen as in B; in addition the tip containing the largest bronchus should be marked.

Histologically there might be no cartilage in a medium-sized bronchus or ill-developed immature cartilage islands (Fig. 3.30). These immature cartilage islands are most helpful in establishing the correct diagnosis.

Mounier-Kuhn syndrome (tracheobronchopulmonary megaly) is characterized by large dilated central bronchi and trachea. There is usually a degeneration of elastic fibers within the bronchial mucosa. All other elements are normal. From the subsegmental bronchi downward, the structure of the lung is normal. The clinician will report about an unusual wideness of the main bronchial system (Fig. 3.31). The patients will suffer from obstructive symptoms. In some cases a functional stenosis of the esophagus can be the dominant symptom. The disease is found in a young-aged population. Insertions of a stent might help in preventing airflow impairment.

Birt-Hogg-Dube (*BHD*) *syndrome* is a rare inherited genodermatosis characterized by distinctive cutaneous lesions, an increased risk of renal and colonic neoplasia, and the development of pleuropulmonary blebs and cysts. Within the

Fig. 3.30 Cross section of a bronchus of a 5-years old boy with William Campbell syndrome. See the immature cartilage island (*beginning of arrow*). For comparison in the inset a bronchus and cartilage is shown derived from a newborn child (*tip of the arrow*). Compare the already much more mature looking cartilage in comparison to the immature one in the disease

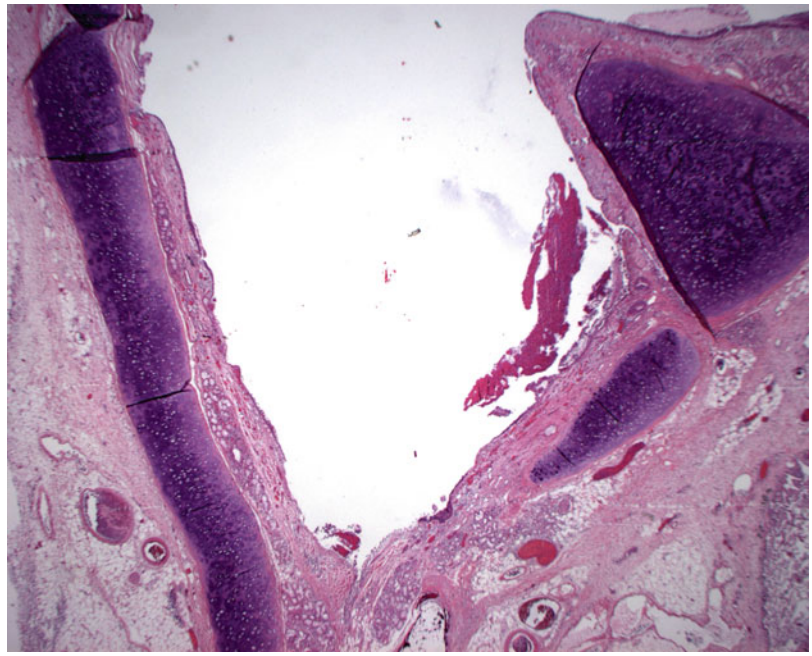

Fig. 3.31 Mounier-Kuhn syndrome (tracheobronchomegaly); there is no pathology in this section, only the dimension of the bronchus is abnormal; this is best seen by macroscopy. H&E, ×25

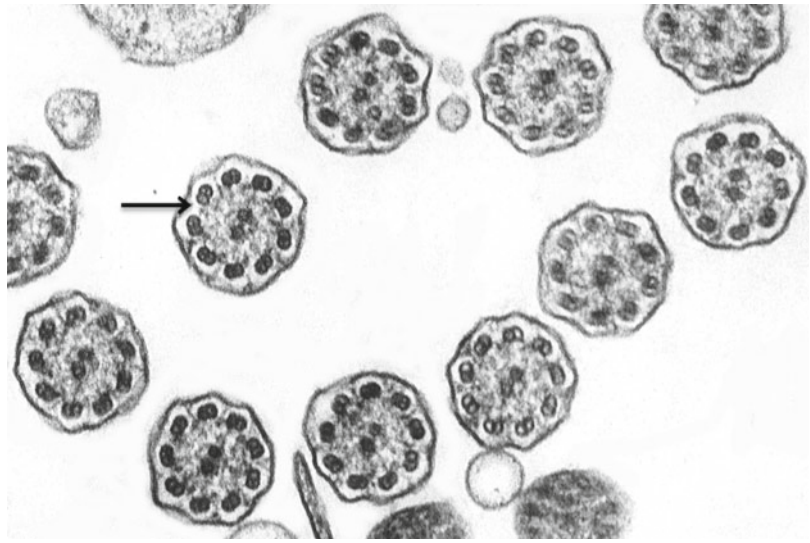

Fig. 3.32 ICS in a young female with complete situs inversus (Kartagener syndrome); the cilia show a complete loss of dynein arms (*arrows*). ×19,000

lung with a predominant basal location, cysts are seen surrounded by normal lung parenchyma. These cysts present with thin fibrous walls and are a source of pneumothorax. Other cystic lesions may radiologically mimic BHD [52].

3.1.4.3 Immotile Cilia Syndrome

Immotile cilia syndrome also called primary ciliary dyskinesia is based on different mutations. So far four genes have been identified, DNAH5 and DNAI1 are involved in 28 % and 10 % of PCD cases, respectively, while two other genes, DNAH11 and TXNDC3, have been identified as causal in one PCD family each [53]. It results in a loss of dynein arms in cilia of different organs, such as bronchial epithelial cells (Fig. 3.32), cells of the uterine tubes, and also sperm cilia. Within the dynein arms, specific calcium-activated

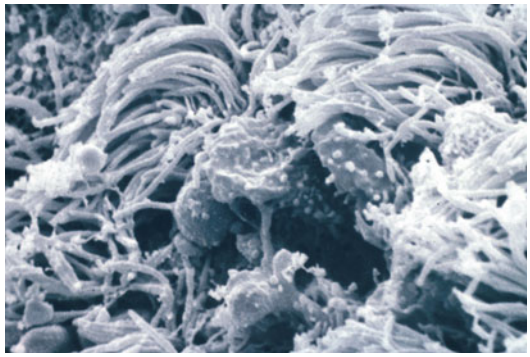

Fig. 3.33 Scanning electron microscopy of ciliated cells from a patient with ICS. Note the totally disorganized cilia of these bronchial cells, which results in disorganized beating and inability to remove mucus into the proximal direction. ×2,500

ATPase is located, which is responsible for proper cilia beating. In these patients cilia are beating in a non-coordinated fashion, resulting in accumulation of mucus on the bronchial mucosa surface (Fig. 3.33). ISC can be associated with complete or partial situs inversus (Kartagener syndrome). In male this results in infertility due to the inability of sperm movement. Females usually act as carriers.

The symptoms are related to early development of bronchiectasis and recurrent infections. The diagnosis can be made either classically by electron microscopy demonstrating the loss of either the inner or outer dynein arms or both together (total loss). By inverse microscopy using bronchial or nasal biopsies covered by physiological fluid, the discoordinated beating of cilia can be demonstrated. With the loss of dynein arms, also the calcium-activated ATPase is lost, which can be demonstrated by enzyme histochemistry.

3.1.5 Lung Pathology in Chromosomal Abnormalities

Trisomy 21 (*Down's syndrome*) is associated with a variety of pulmonary malformations, none of them specific for this chromosomal abnormality. In most reports, children with this syndrome have been reported to be prone to recurrent infections, such as RSV and adenovirus [54]; however, cystic lung lesions have been reported too [55–59]. In other studies pulmonary hypertensive lung disease has been demonstrated, but this most probably is related to the high incidence of valvular heart diseases and factors involving the coagulation system in trisomy 21 [60–62]. In single case reports, trisomy 21 was associated with alveolar capillary dysplasia [19, 63], but this might be due to not identified complex genetic aberrations. In a case seen by the author, there was focal retardation of alveolar growth and differentiation, resulting in areas of immature lobules (saccular stage) adjacent to normally developed lobules. Pulmonary hypertension was also diagnosed resulting from malformation and insufficiency of the pulmonary valve. In one case report, trisomy 21 was associated with homozygous mutation for the cystic fibrosis gene (F508del) [64]. In some cases lymphangiectasis has been found in patients with trisomy 21. Some are associated with a mutation in the FOXC2 gene, others not [65–67]; however, as discussed above in these cases with known mutations, there are also other abnormalities such as hydrops, and so the mutations are difficult to attribute to any specific abnormality. Hennekam syndrome is a systemic disease with intestinal and pulmonary lymphangiectasis (Fig. 3.34), congenital lymphedema, and facial anomalies. These patients present with severe respiratory distress due to nonimmune hydrops fetalis, congenital chylothorax, and pulmonary lymphangiectasis [68].

A trisomy 1q combined with monosomy X was reported in a fetus with CPAM type III and hydrops fetalis [69].

A trisomy 8 was found being associated with giant cystic pulmonary malformation in a 5-year-old girl. This lesion could not be placed in any of the known malformation and probably represents a new entity within the group of cystic lung lesions. Morphologically it was characterized by a highly disorganized proliferation of numerous cartilage islands, abundant mesenchymal tissue with abundant adipose differentiation, and cysts lined by a primitive epithelium.

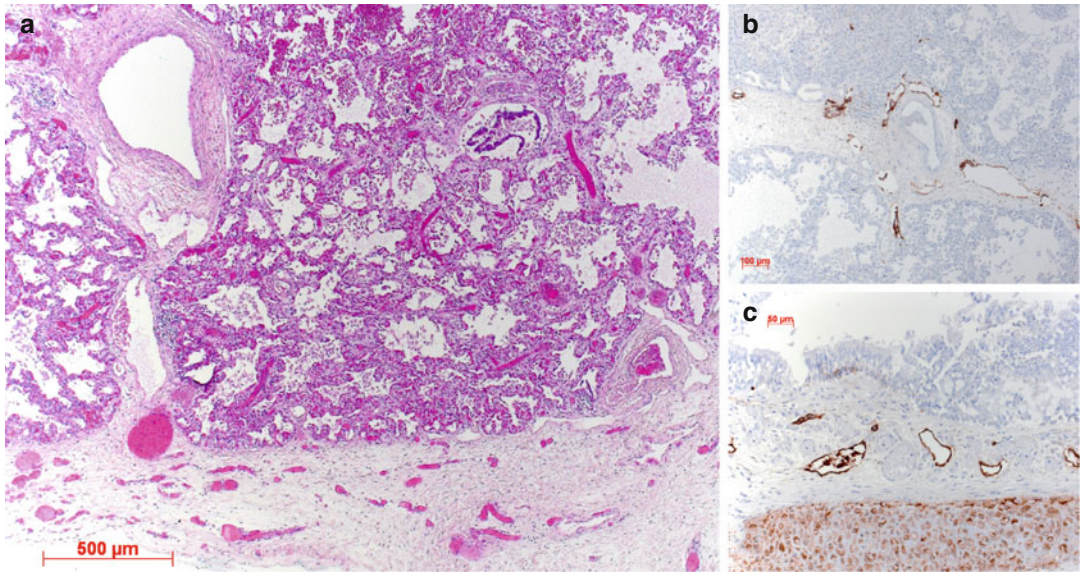

Fig. 3.34 Trisomy 21 and Hennekam syndrome showing lymphangiectasis in the lung; in (**a**) there is an immature lung and dilated lymphatics adjacent to a pulmonary vein. In (**b**, **c**) lymphatics are highlighted by podoplanin stain, showing dilated lymphatics along an interlobular septum close to veins, but also within the bronchial mucosa. H&E, bar 500 µm, immunohistochemistry for Podoplanin (D2-40), bars 100 and 50 µm, respectively

3.1.6 Inborn Errors of Metabolism

Pulmonary interstitial glycogenosis (also known as infantile cellular interstitial pneumonitis/histiocytoid pneumonia) is an inborn error of metabolism of glycogen resulting in accumulation of glycogen in primitive mesenchymal cell in the alveolar septa. The cells have a spindle cell morphology, are positive for vimentin, but are negative for macrophagocytic and histiocytic markers [70]. This glycogen most probably is taken up from the circulation, because no glycogen storage is seen in pneumocytes (Fig. 3.35, courtesy of E. Bruder, Basel). Clinically children within the first year of life (most often first month) are affected and present with tachypnea, hypoxia, and radiologically with interstitial infiltrates. Treatment with corticosteroids most often results in improvement of the condition [70–72]. In some cases, pulmonary interstitial glycogenosis was associated with congenital heart disease; however, this most probably are associations by chance and not found in the majority of cases [73, 74]. Therefore, a separation of pulmonary interstitial glycogenosis into primary and secondary forms (associated with other diseases) at present seems not to be based on sound data.

Niemann-Pick syndrome is another inborn metabolic disease characterized by the accumulation of macrophages and histiocytes within the alveolar septa and the bronchial walls [30]. In Niemann-Pick syndrome, mutations of the sphingomyelin phosphodiesterase 1 gene (SMPD1) encoding for sphingomyelinase are associated with a marked decrease in lysosomal stability and consequent deposition of sphingomyelin in different organ systems. The histiocytes and macrophages present with foamy cytoplasm; histochemically sphingomyelin can be demonstrated by Sudan black B stain and furthermore confirmed biochemically (Figs. 3.36 and 3.37). Respiratory symptoms were recorded in all patients in the largest published series of patients [75]. Signs of interstitial lung disease were seen on chest X-ray and lung CT scan, no lung biopsy was analyzed in these patients, but analysis of bronchoalveolar lavage revealed an accumulation of foamy macrophages (Niemann-Pick cells) in all. One of the ten patients died of the disease; all

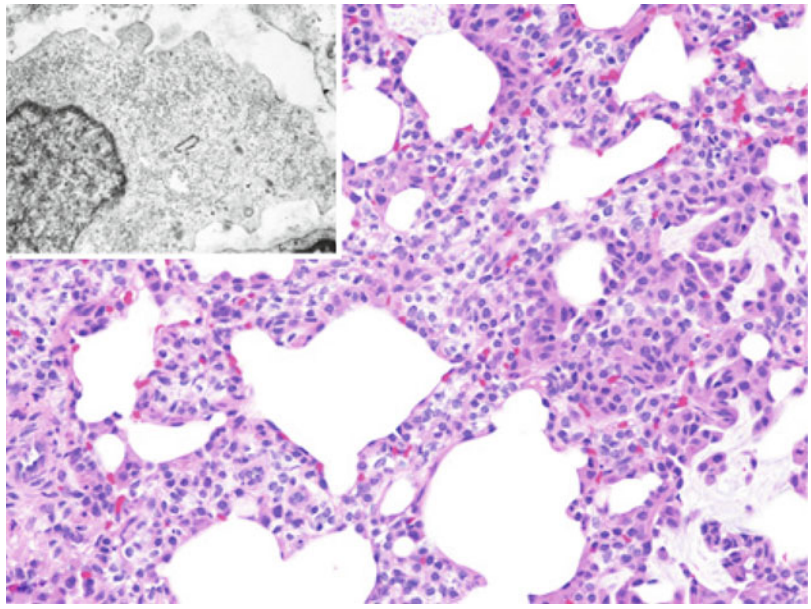

Fig. 3.35 Pulmonary interstitial glycogenosis: showing cells with eosinophilic cytoplasm infiltrating the interstitium; *inset* = electron microscopy of such a cell with abundant glycogen in the cytoplasm. H&E, ×25 and 200, respectively, PAS ×200 (Courtesy of Elisabeth Bruder, Basle)

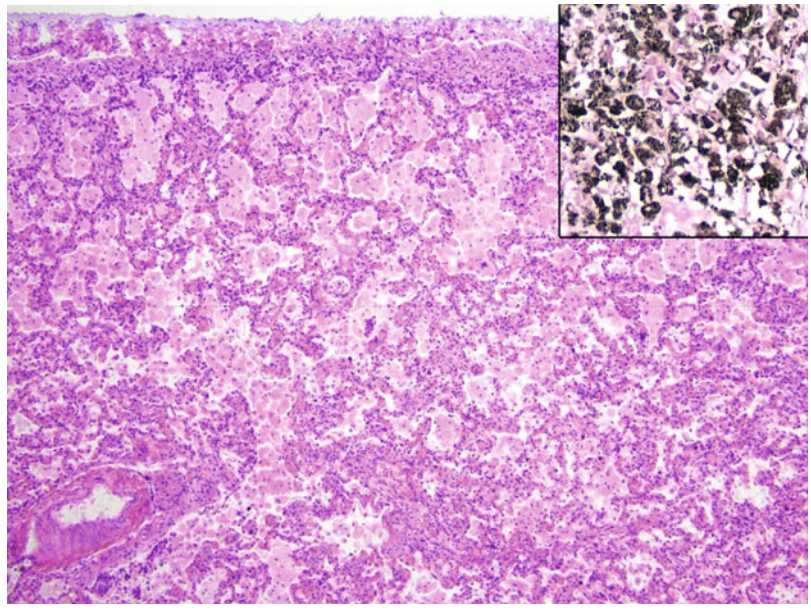

Fig. 3.36 Niemann-Pick syndrome in a 3-year-old child; the alveolar lumina are filled with macrophages, which show a pink cytoplasm. H&E, ×50; *inset*: Sudan black B stain highlighting the fatty substances stored in the macrophages, Sudan black B, ×200

others had severe complication requiring oxygen therapy due to chronic obstructive pulmonary disease or chronic cough. In a recent study by Kirkegaard et al., the reduced sphingomyelinase activity in cells from patients with Niemann-Pick disease A and B can be effectively corrected by treatment with recombinant Hsp70 [76] thus providing a new treatment option for this disease.

Pulmonary involvement in *Gaucher's disease* (mucopolysaccharidosis) type I GD is rare; in the

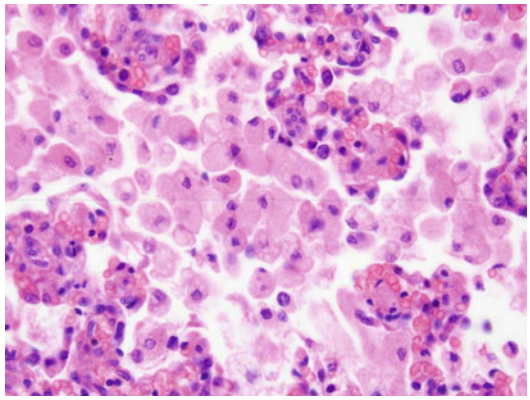

Fig. 3.37 Niemann-Pick syndrome in a 3-year-old child; higher magnification shows foamy macrophages with eosinophilic material, which on Sudan black B stain were positively stained. Chemically sphingomyelin could be proven. H&E, ×400

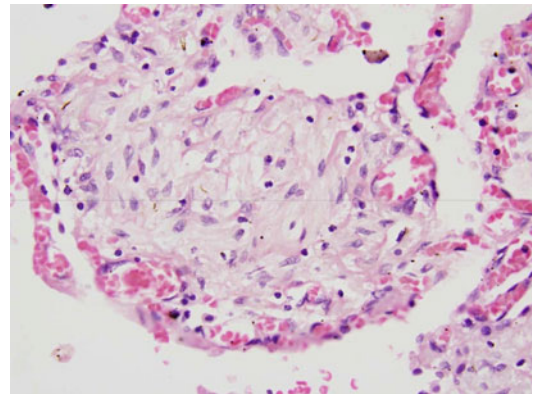

Fig. 3.38 Gaucher disease, autopsy case; the interstitium is widened by infiltrations of spindle cell-like histiocytes which contain pale eosinophilic material identified by special stains as mucopolysaccharides. H&E, ×400

largest published series 5 in a survey of 150 patients presented with pulmonary involvement. The patients showed diffuse interstitial infiltrates with spindle cells/histiocytes with pale eosinophilic staining of the cytoplasm (Fig. 3.38). Due to the widening of the interstitium and thus increase of the alveolocapillary distance, clinical symptoms are dyspnea, low diffusion capacity, excessive ventilation, and increased dead space. Responses on exercise testing were interpreted clinically as consistent with circulation impairment [30, 77].

Surfactant-related disorders in children will be discussed briefly in this chapter. A more extensive discussion is provided in the chapter on the adult form (see chapter on metabolic diseases). In children almost all cases are due to mutations in genes responsible for the synthesis, transport, or degradation of surfactant proteins and lipids. Mutations of the surfactant apoprotein genes B (on chromosome 2) and C (on chromosome 8) are known for quite a while [78, 79]; recently a new mutation in the ATP-binding cassette transporter protein ABCA3 [80, 81] has been reported to result also in alveolar lipoproteinosis (chromosome 16). The prevalent form underlying lipoproteinosis in adults, namely, a defect in the granulocyte-macrophage colony-stimulating factor (GM-CSF, mutations on chromosome 5 or 22), seems to be exceedingly rare in children [82, 83]. Morphologically alveolar lipoproteinosis in children was originally subsummarized under chronic interstitial pneumonia of infancy, but now is regarded as a separate entity. The characteristic findings are eosinophilic debris in the alveoli sometimes simulating hyaline membranes (less in SPC, more severe in SPB and ABCA3 disease), a lymphohistiocytic infiltration of the alveolar walls resulting in widening of the wall [84] (Figs. 3.39, 3.40, and 3.41). In some cases a pattern of desquamative interstitial pneumonia with many alveolar macrophages has been described; others have assigned a pattern of nonspecific interstitial pneumonia to their cases [85, 86]. On electron microscopic examination, atypical and giant lamellar bodies can be seen and by their form and structure can be assigned to the underlying genetic defect [87]. The disease is seen in newborn, which present with severe hypoxia and dyspnea immediately after birth. The babies do not show signs of infection, which would histologically be the major differential diagnosis. Children with apoprotein C gene mutations in contrast to those with ApoB and ABCA3 mutations have a better prognosis and can reach adulthood. They will require therapeutic bronchoalveolar lavage to remove the surfactant lipids and proteins from their lungs. Over time interstitial fibrosis can develop, which might ultimately cause death of the patient (Fig. 3.42).

Many patients with *lysinuric protein intolerance* will also present with alveolar lipoproteinosis on histologic examination. There can be additional morphological features, such as hemorrhage and cholesterol granulomas. Later on fibrosis can develop, similar to patients with the

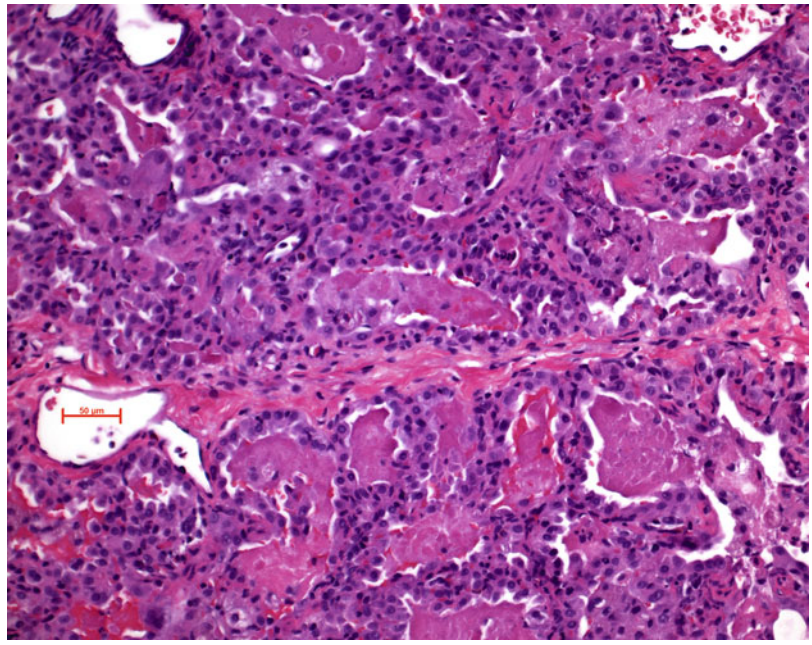

Fig. 3.39 Surfactant apoprotein B gene mutation; this is a typical picture which can also be diagnosed on frozen sections. Alveoli are filled with eosinophilic debris, usually only few dying nuclei might be seen. The interstitium is widened by an infiltration of histiocytes and few lymphocytes. The pneumocytes type II are hyperplastic, covering almost exclusively the alveolar surfaces. H&E, bar 50 µm

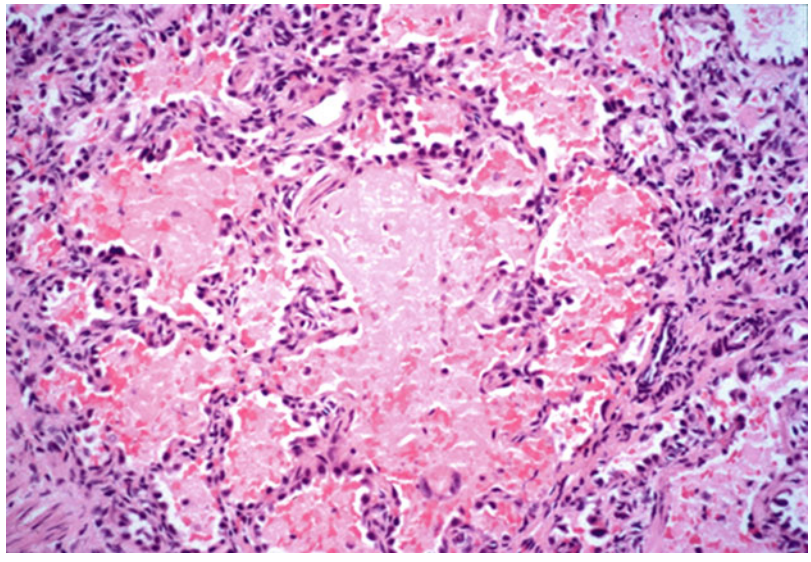

Fig. 3.40 Surfactant apoprotein C gene mutation; in this case the eosinophilic debris is less dense and also more uneven distributed. The lymphohistiocytic infiltration of the alveolar walls is similar, the pneumocyte type II hyperplasia is less pronounced. H&E, ×200

classical alveolar lipoproteinosis. Clinically the patients will often present with acute respiratory symptoms with dyspnea, hypoxia, and chest pain. The onset of the disease is in early childhood [88]. Mutations of SLC7A7/y+LAT1 impair the system for the transport of cationic amino acids. In a recent study, the expression and function of y+LAT1 was investigated in monocytes and

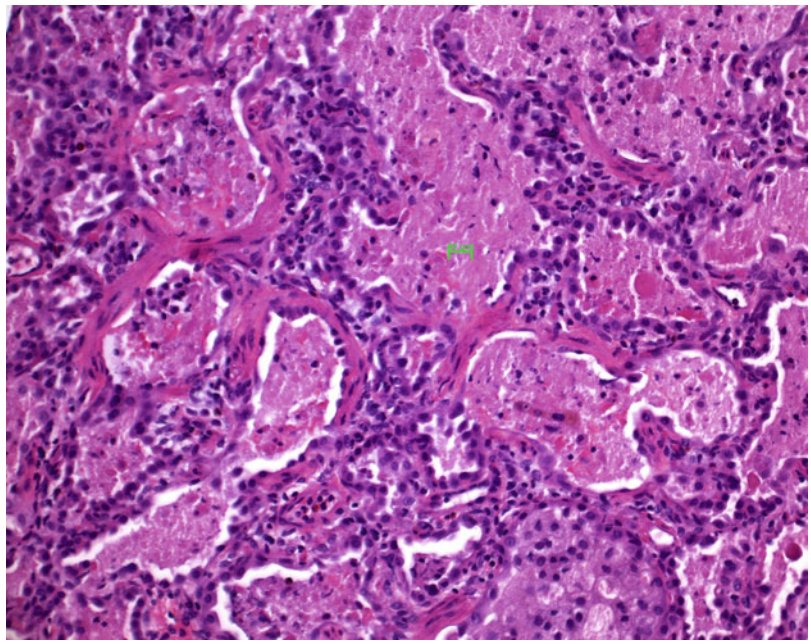

Fig. 3.41 Mutation of ABCA3 gene, resulting in a picture almost identical to surfactant ApoB gene mutation; again there is a dense eosinophilic debris within alveoli, the septa are widened by a lymphohistiocytic infiltration, and pneumocytes type II cover most of the alveoli. H&E, bar 20 μm

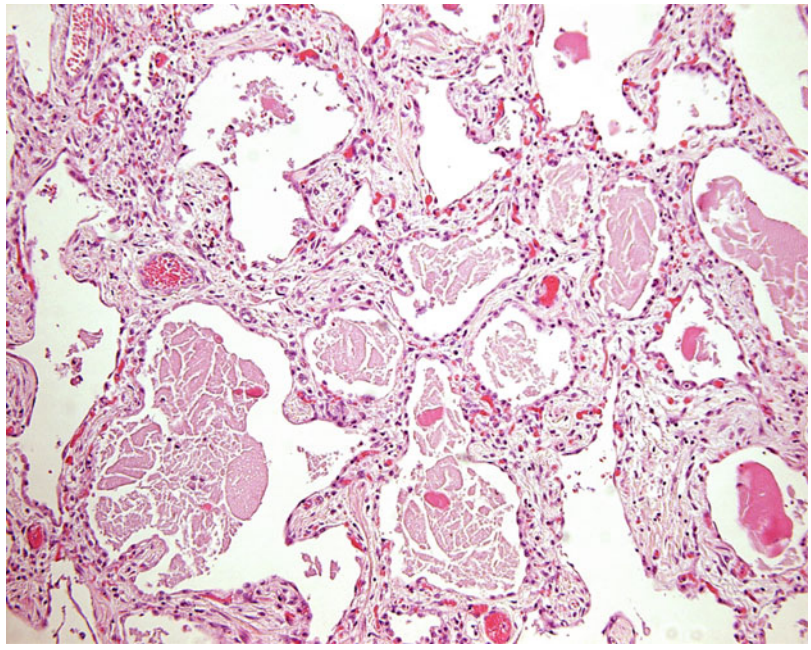

Fig. 3.42 Surfactant apoprotein C gene mutation in a 19-year-old male patient. The patient was treated over time with therapeutic bronchoalveolar lavages and also with drugs. Due to developing interstitial fibrosis and accumulation of surfactant material in the alveoli, he died with respiratory insufficiency (Courtesy of Abida Haque, Galveston). H&E, ×200

macrophages isolated from an affected patient. y+LAT1 activity was markedly lowered in monocytes and alveolar macrophages, because of the prevailing expression of SLC7A7/y+LAT1. It was also shown that GM-CSF induces the expression of SLC7A7, so GM-CSF in monocytes of patients with lysinuric protein intolerance with deficient y+LAT1 might have a role in the pathogenesis of alveolar proteinosis in this disease [89].

3.1.7 Cystic Fibrosis

Cystic fibrosis is another disease of inborn metabolic error. It is caused by a defect in the cystic fibrosis transmembrane conductance regulator (CFTR), which controls the balance of sodium transport. The gene for CFTR resides at chromosome 7q31.2 and consists of 520501 nucleotides with several exons. Within the gene, there are two salt bridges essential for the chloride ion channel's normal function (Arg(352)-Asp(993) and Arg(347)-Asp(924). Published data suggest that Arg(347) not only interacts with Asp(924) but also interacts with Asp(993). The tripartite interaction Arg(347)-Asp(924)-Asp(993) mainly contributes to maintaining a stable s2 open subconductance state [90].

Point mutations do exist on several positions of the gene; the most frequent mutation is an out-of-frame deletion of three nucleotides (CTT). This mutation leads to the loss of phenylalanine-508 (DeltaF508) and a silent codon change (SCC) for isoleucine-507. DeltaF508 CFTR is misfolded and degraded by endoplasmic reticulum-associated degradation. Depending on homozygous double allele mutations or single allele mutations in heterozygous patients will present with severe or mild disease, respectively.

Cystic fibrosis affects all organs where mucus is produced and secreted toward a mucosal surface, such as small and large intestines, the pancreas, and upper and lower respiratory tract. With respect to the airways, patients will present with bronchial obstruction and bronchiectasis with recurrent infections (Fig. 3.43).

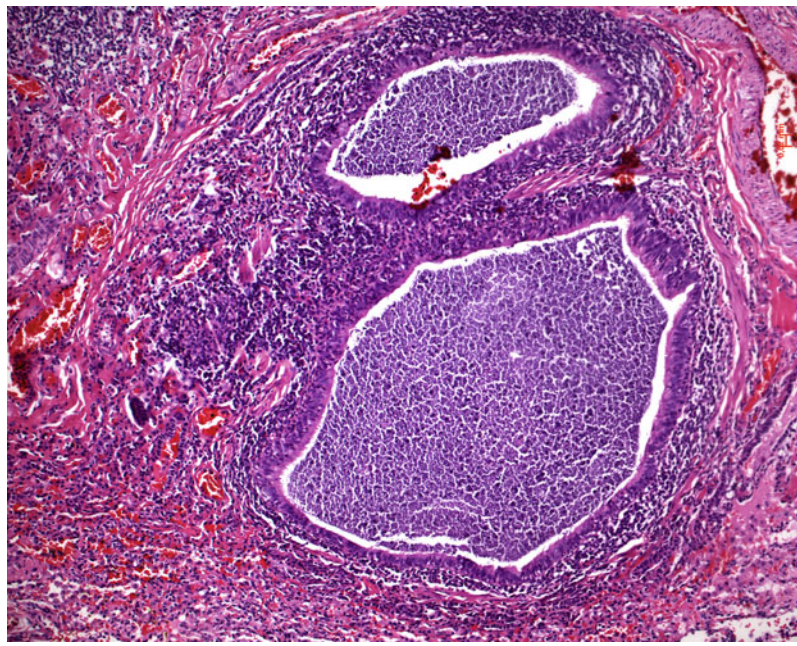

Fig. 3.43 Cystic fibrosis; one of the characteristics is shown here, namely, the mucus impaction of the bronchi. Within the lumina there is mucus mixed with nuclear debris, in the bronchial wall usually a dense lymphocytic infiltration is seen. In contrast to allergic bronchopulmonary mycosis and also bronchial asthma, there are no prominent eosinophilic infiltrations. H&E, ×150

Cystic fibrosis was one of the first diseases where gene transfer was applied using adenoviral vectors. However, over time the patients developed antibodies against the adenovirus vector, thus making gene transfer ineffective. New approaches using better designed adenovirus vectors and also trials with Lipofectamine might open new opportunities to treat this disease.

3.1.8 Neuroendocrine Cell Hyperplasia of Infancy (NEHI)

NEHI (also known as persistent tachypnea of infancy and chronic bronchiolitis) is an infant disease with unknown etiology. The affected children present with tachypnea [91, 92]. Macroscopically the lung tissue looks normal. On microscopy not much pathologic changes are seen (Fig. 3.44). One must focus on high-power magnification to recognize clear cell proliferations within the mucosa of bronchi and bronchioles (Fig. 3.45). In the periphery also some neuroendocrine cell clusters can be seen, but this is much more difficult to identify without immunohistochemistry. By immunohistochemistry a diffuse hyperplasia of neuroendocrine cells can be highlighted using antibodies for chromogranin A, gastrin-releasing peptide (GRP), NCAM, PGP9.5, and/or synaptophysin (Fig. 3.46). Each of these antibodies will show some neuroendocrine cell clusters but never all of them, suggesting that different types of neuroendocrine cells with different proteins are involved in this disease. There are no data about secretion of vasoactive or neurogenic hormones/biogenic amines in the neuroendocrine cells – reactions for serotonin are negative in my experience. Since cells of the diffuse neuroendocrine system are capable of synthesizing and secreting a wide variety of neurotransmitters, it could well be that these cells secrete

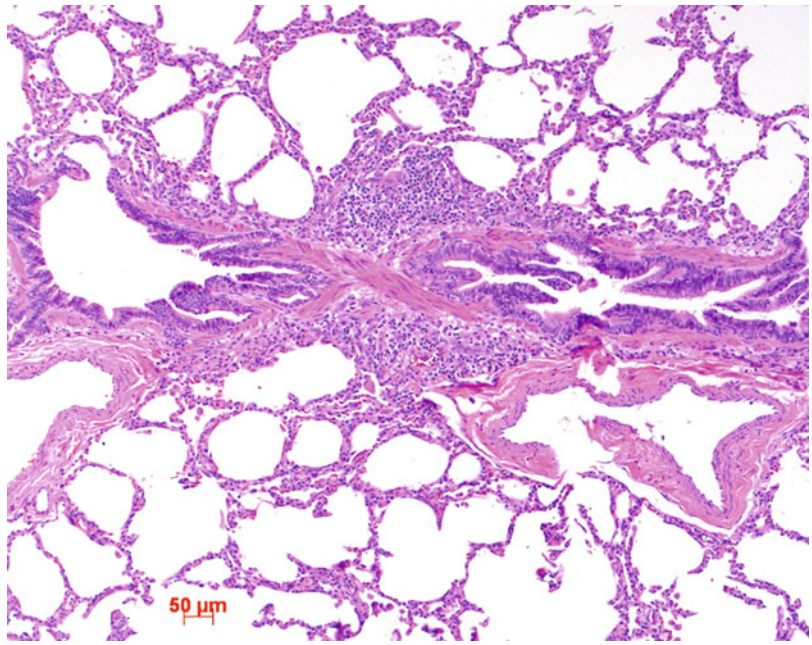

Fig. 3.44 Neuroendocrine cell hyperplasia of infancy; the lung looks almost normal; there is only a minimal lymphohistiocytic infiltration around the bronchi. H&E, bar 50 µm

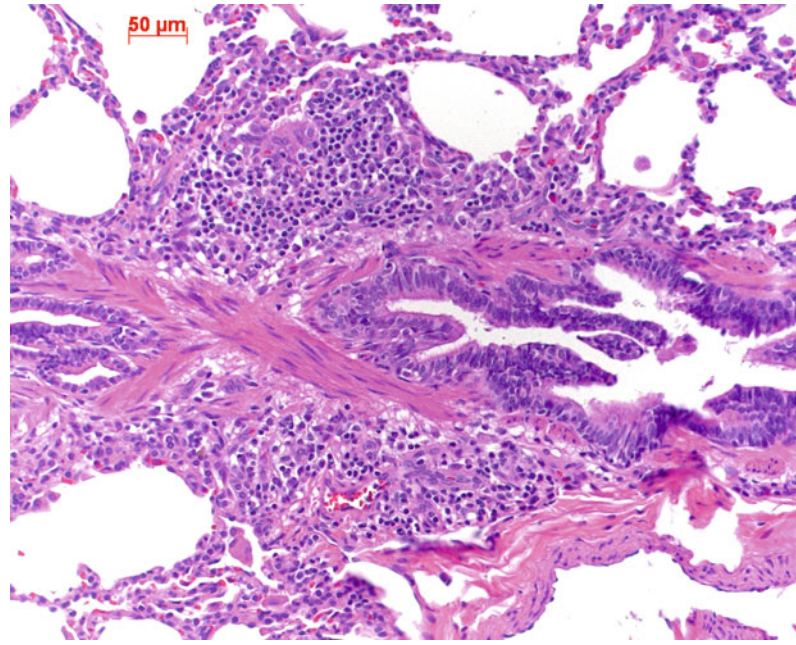

Fig. 3.45 Neuroendocrine cell hyperplasia of infancy; on higher magnification within the bronchial epithelium, there are cells with pale eosinophilic cytoplasm, corresponding to neuroendocrine calls. H&E, bar 50 µm

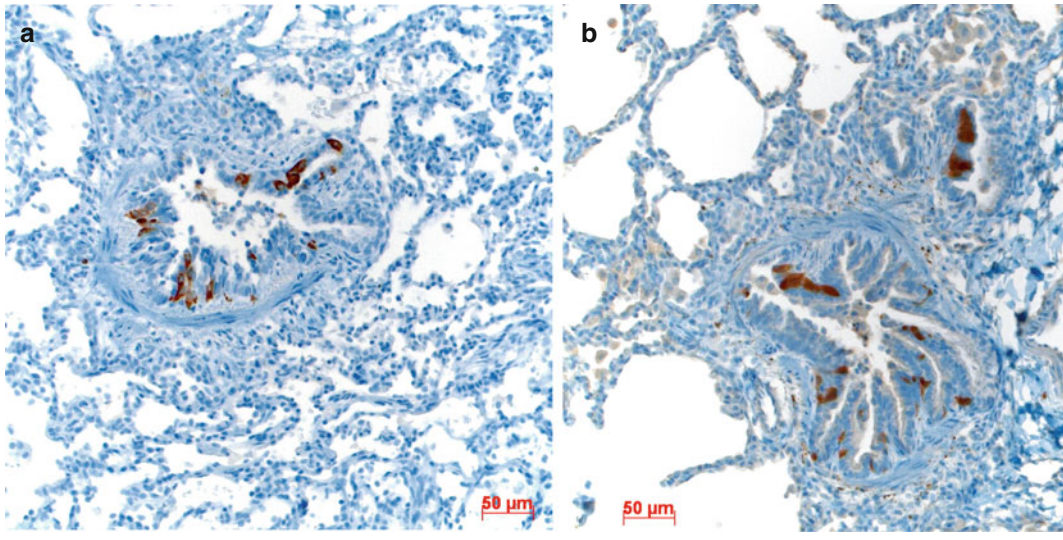

Fig. 3.46 Neuroendocrine cell hyperplasia of infancy; using immunohistochemistry for chromogranin A (CGA) or neural cell adhesion molecule (NCAM) and other markers for neuroendocrine differentiation, the amount of neuroendocrine cells is apparent. (**a**) CGA, (**b**) NCAM, bars 50 µm

peptides of the tachykinin family causing the clinical symptoms (at present no antibodies are available, which give consistent results on formalin-fixed paraffin-embedded tissues). Despite that possibility what causes neuroendocrine hyperplasia in these children remains unclear.

3.2 Pneumonia in Childhood Including Noninfectious Interstitial Pneumonias

3.2.1 Chronic Pneumonia of Infancy (CPI)

Originally surfactant-related interstitial pneumonias with alveolar proteinosis were included into CPI; however, since the different causes of alveolar proteinosis were discovered, it has been excluded. Therefore, CPI has been reduced to those pediatric interstitial diseases with unknown cause. It is now quite rare. CPI predominantly occurs in newborn or small children [93, 94]. In many instances, a careful investigation of the biopsies might uncover underlying infectious diseases, such as Wilson-Mikity syndrome, infections caused by respirotropic viruses, *Chlamydiae*, or *Ureaplasma* [95]; another cause might be gastroesophageal reflux [96]. In rare instances interstitial glycogenosis might be the cause of CPI [3, 72]. However, it should be reminded that although the clinical symptoms in affected children are severe, the density of the inflammatory cells is much less compared to pneumonias in adults. CPI is characterized by mild lymphocytic and a variable amount of histiocytic infiltrations in the alveolar septa all causing thickening of the septa and impaired gas exchange. The septa are widened by these infiltrations but also by a proliferation of primitive mesenchymal cells, causing impairment of oxygenation. Pneumocytes type II also proliferate at the surface, within alveoli few to numerous macrophages can be seen (Figs. 3.47 and 3.48). In addition intra-alveolar eosinophilic debris can be seen in some cases; however, lipoproteinosis has to be excluded, for example, by a negative PAS stain [93, 97]. Outcome is fatal in many cases; however, others can respond to high-dose corticoid or immunosuppressive therapy.

Nonspecific interstitial pneumonia (*NSIP*) has been described in children. Most often this is found in different forms of autoimmune diseases. Prognosis is very often poor. Therapy requires high-dose corticosteroid treatment, which in itself increases the risk of infections. Usual interstitial (UIP) and desquamative interstitial pneumonias (DIP) are rarely found in children, with exception of familial forms of idiopathic pulmonary fibrosis (NSIP and DIP will be discussed in Chap. 8, UIP in the context of familial interstitial lung fibrosis).

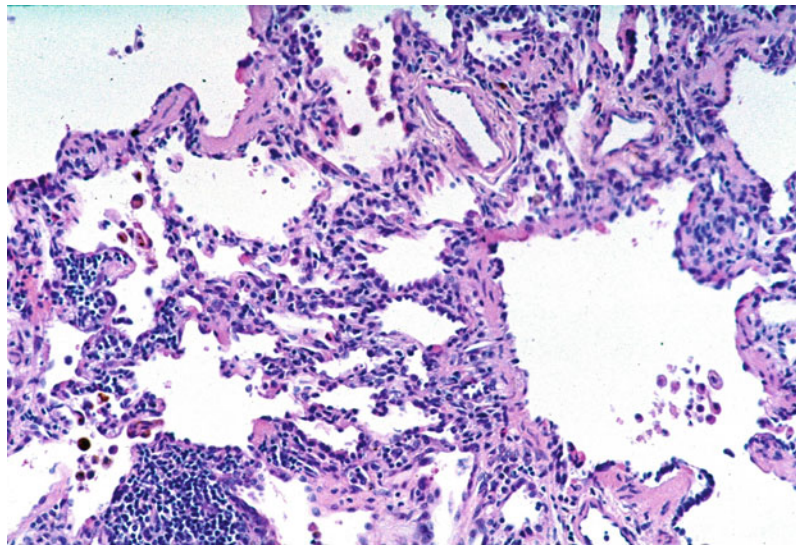

Fig. 3.47 Chronic interstitial pneumonia of infancy; this young 6-month-old boy presented with clinical symptoms of impaired development and hypoxia. On open lung biopsy, a focally dense lymphohistiocytic infiltration was noted. Infectious organisms and metabolic diseases were all excluded, resulting in the diagnosis of CPI. H&E, ×100

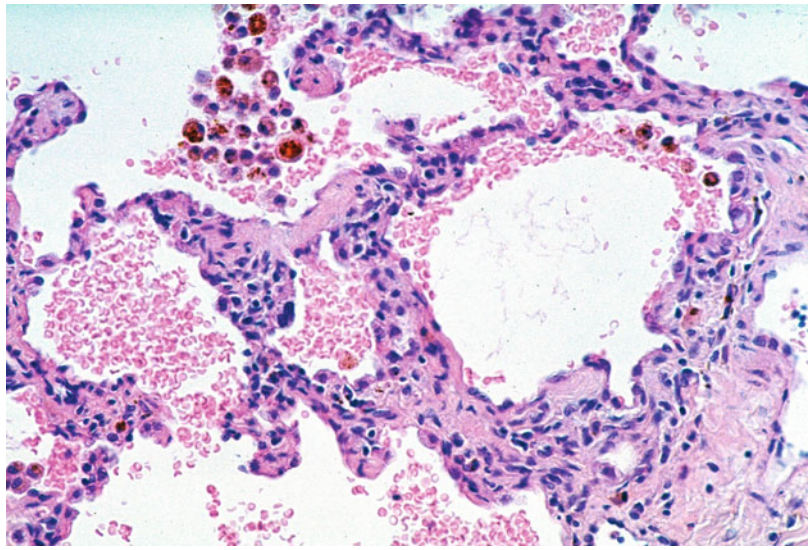

Fig. 3.48 Chronic interstitial pneumonia of infancy; another focus is demonstrated here with some debris, siderin-laden macrophages, and also focal fibrosis. H&E, ×200

Lymphocytic interstitial pneumonia (*LIP*) not uncommonly is seen in children at the school age. It is not different from the adult form; however, in contrast to the adult situation, lymphoma is exceedingly rare in children, whereas most often these children present with early onset of juvenile rheumatoid arthritis, extrinsic allergic alveolitis (hypersensitivity pneumonia), or with HIV infection (LIP will be more extensively discussed in Chap. 8).

Acute interstitial pneumonia in *Hamman-Rich syndrome* has been reported in children [98]. But, since the morphology of Hamman-Rich syndrome has not been clarified and the original cases are not available anymore for review, the only information accessible is the rapid and progressive course of the disease with progressive fibrosis.

Bronchopulmonary dysplasia (*BPD*) is a chronic inflammatory disease with florid septal fibrosis, due to surfactant deficiency. It occurs in children born before maturation of the pneumocytes types II, often at gestation weeks 26–30. At this time there is no surfactant synthesis in the fetal lung. This results in a collapse of the alveolar septa due to increased alveolar tension, followed by an acute interstitial pneumonia with formation of hyaline membranes (diffuse alveolar damage, DAD, IRDS; Fig. 3.49). The therapeutic management usually included mechanical ventilation with high oxygen pressure, which in itself acted fibrogenic. In recent investigations genetic and environmental factor have been added to the etiologic spectrum of the disease. In the chronic phase, a florid proliferation of fibroblasts causes a distortion of the alveolar architecture [99–105]. Children with BPD often catch a secondary infection, either viral or bacterial, and in former times often died from secondary superimposed infection (Fig. 3.50). Nowadays due to surfactant replacement therapy as well as treatment of the mothers by corticosteroids, BPD turned into a rare disease in most European countries. Corticosteroids given to pregnant woman, in whom premature birth is suspected will increase maturation of the fetal pneumocytes II and thus help to prevent BPD.

3.2.2 Mendelson Syndrome in Children and Silent Nocturnal Aspiration

Gastric juice aspiration (*Mendelson*) *syndrome* can occur in children, although it is much more common in adults, and few decades ago was

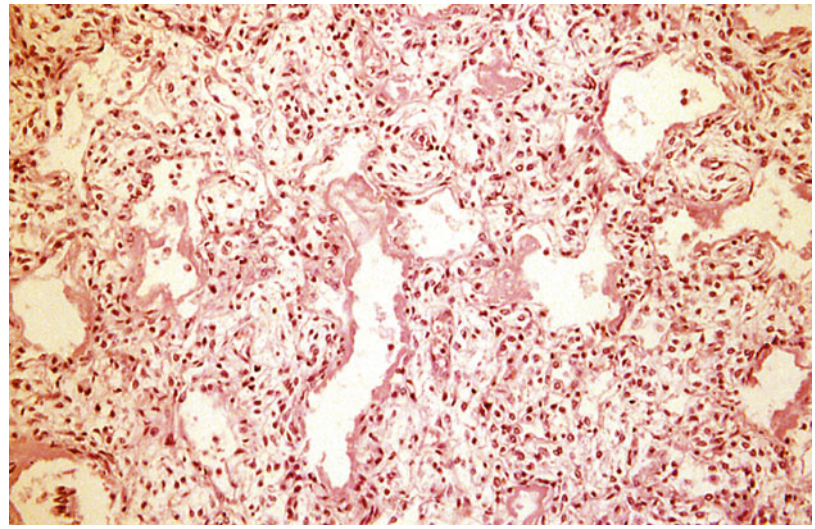

Fig. 3.49 Broncho-pulmonary dysplasia; this child has survived a few days, therefore DAD has developed with formation of hyaline membranes. Alveolar septa are widened by a mild lymphocytic infiltration and a more pronounced proliferation of myofibroblasts. H&E, ×100

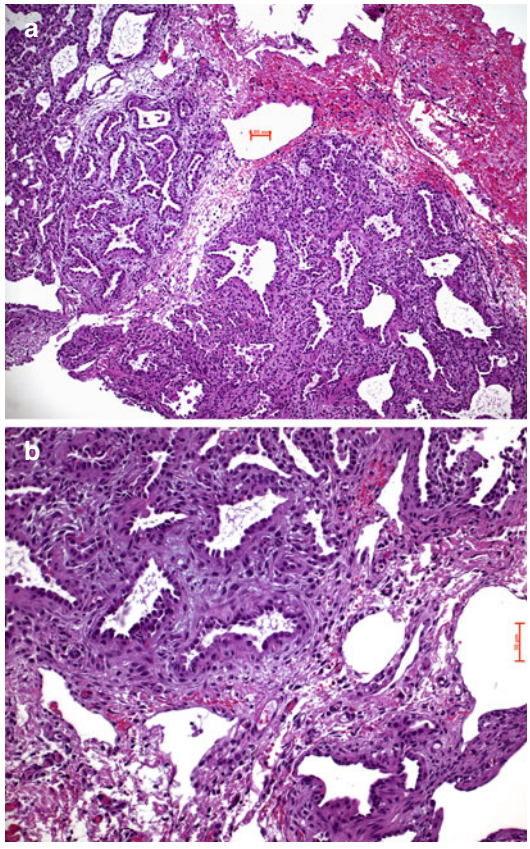

Fig. 3.50 (**a**) Bronchopulmonary dysplasia; in this case the child did not develop hyaline membranes, but there is still a mild lymphocytic infiltration, but more pronounced in this case is the proliferation of myofibroblasts with deposition of immature collagen. In addition the alveolar collapse is seen in (**a**). (**b**) is another area in the same lung. H&E, bars 50 μm

often seen in pregnant woman. Aspiration of gastric juice, especially in patients with hyperacidism cause acute interstitial pneumonia with diffuse alveolar damage (DAD) and hyaline membrane formation. The alveolar walls are denuded, fibrin is abundant in alveoli, and inflammatory infiltrates are scarce. Within a few hours, the patients develop acute respiratory failure and will need mechanical ventilation and oxygen supply. If the patient survives the acute phase, a chronic phase follows, which is characterized by an organizing pneumonia with granulation tissue growing into alveoli and bronchioles, finally partly or completely occluding the lumina [106]. The major acting agents are proteases such as elastase and collagenase, activated by hydrochloric acid. In the very early phase, this can be prevented by antiprotease treatment [106]; more recently treatment with extracorporeal oxygenation or NO application has shown improvement.

In contrast *nocturnal silent aspiration* is much more common in newborns. Most often the disease is based on weakness of the gastric sphincter muscles. This usually vanishes during the next few months. Since the gastric juice is much less acidic and also buffered by milk, the pulmonary symptoms are less severe. In this age, milk fat proteins and some fatty substances are aspirated, which cause a macrophage-dominated alveolar reaction, similar to DIP but much more focally and with abundant foam cells. In bronchoalveolar

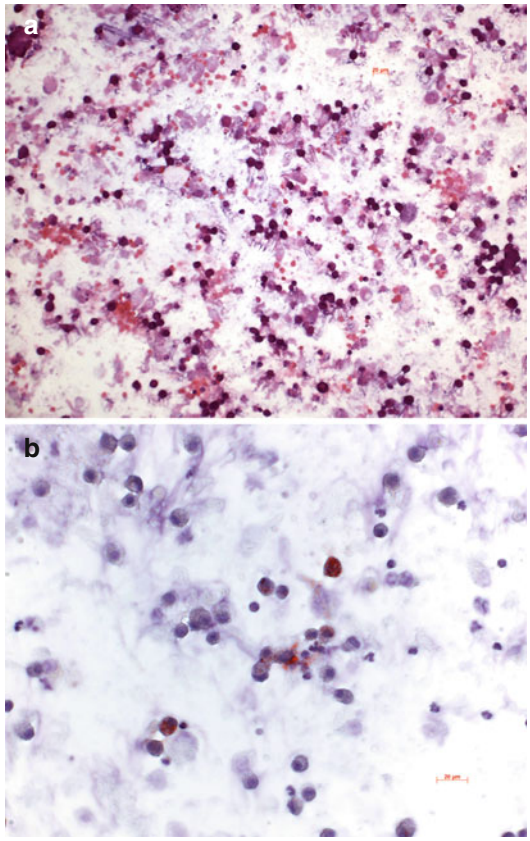

Fig. 3.51 Silent nocturnal aspiration in a breast-fed child; on bronchoalveolar lavage numerous macrophages are seen together with lots of debris. H&E, bar 20 µm. In (**b**) the lavage cells are stained with oil red O. Many macrophages contain lipid droplets within their cytoplasm. Oil red O, bar 20 µm

lavage (BAL) these macrophages can be found, representing the major cell population. They contain abundant fatty substances (derived from milk fats), which can be demonstrated by a fat stain such as oil red O. Their percentage in BAL is usually over 10 % and therefore is diagnostic for this disorder (Fig. 3.51).

There are other diseases, which are included into pediatric lung diseases by some authors. However, since these are also seen in adults and are not much different in their morphology, we will discuss this in the respective chapters. These are:

Diseases of the normal host will be discussed under the respective chapter together with the adult forms. *Infectious pneumonias* in childhood will be discussed together with the adult pneumonias in Chap. 8. Organizing phases such as organizing pneumonia (formerly bronchiolitis obliterans/organizing pneumonia (BOOP)) are also a focus in this chapter as eosinophilic and inhalation-associated pneumonias. Familial interstitial pulmonary fibrosis also will be discussed in Chap. 8.

Diseases of the immunocompromised host: Disorders related to therapeutic intervention – chemotherapeutic drug and radiation injury will be discussed in toxic reaction due to drugs and inhalation. Opportunistic infections are part of the infectious pneumonias in immunocompromised patients. Disorders related to the solid organ, lung, and bone marrow transplantation are also described in the pneumonia chapter.

Autoimmune diseases are discussed in the respective chapter.

Vascular diseases, such as Wegener's granulomatosis, panarteritis nodosa, vasculitis in ductus thoracicus occlusion, lymphangiectasis, lymphangiomatosis, arterial hypertensive vasculopathy, and congestive vasculopathy including veno-occlusive disease, are discussed in the chapter on vascular diseases.

References

1. Biko DM, Schwartz M, Anupindi SA, Altes TA. Subpleural lung cysts in Down syndrome: prevalence and association with coexisting diagnoses. Pediatr Radiol. 2008;38:280–4.
2. Deutsch GH, Young LR, Deterding RR, Fan LL, Dell SD, Bean JA, Brody AS, Nogee LM, Trapnell BC, Langston C, Albright EA, Askin FB, Baker P, Chou PM, Cool CM, Coventry SC, Cutz E, Davis MM, Dishop MK, Galambos C, Patterson K, Travis WD, Wert SE, White FV. Diffuse lung disease in young children: application of a novel classification scheme. Am J Respir Crit Care Med. 2007;176:1120–8.
3. Langston C, Dishop MK. Diffuse lung disease in infancy: a proposed classification applied to 259 diagnostic biopsies. Pediatr Dev Pathol. 2009;12:421–37.
4. Dishop MK. Paediatric interstitial lung disease: classification and definitions. Paediatr Respir Rev. 2011;12:230–7.
5. Schwartz MZ, Ramachandran P. Congenital malformations of the lung and mediastinum – a quarter century of experience from a single institution. J Pediatr Surg. 1997;32:44–7.
6. Hennrick KT, Keeton AG, Nanua S, Kijek TG, Goldsmith AM, Sajjan US, Bentley JK, Lama VN, Moore BB, Schumacher RE, Thannickal VJ, Hershenson MB. Lung cells from neonates show a mesenchymal stem cell phenotype. Am J Respir Crit Care Med. 2007;175:1158–64.

7. Burgos CM, Nord M, Roos A, Didon L, Eklof AC, Frenckner B. Connective tissue growth factor expression pattern in lung development. Exp Lung Res. 2010;36:441–50.
8. Pasutto F, Sticht H, Hammersen G, Gillessen-Kaesbach G, Fitzpatrick DR, Nurnberg G, Brasch F, Schirmer-Zimmermann H, Tolmie JL, Chitayat D, Houge G, Fernandez-Martinez L, Keating S, Mortier G, Hennekam RC, von der Wense A, Slavotinek A, Meinecke P, Bitoun P, Becker C, Nurnberg P, Reis A, Rauch A. Mutations in STRA6 cause a broad spectrum of malformations including anophthalmia, congenital heart defects, diaphragmatic hernia, alveolar capillary dysplasia, lung hypoplasia, and mental retardation. Am J Hum Genet. 2007;80:550–60.
9. DeFelice M, Silberschmidt D, DiLauro R, Xu Y, Wert SE, Weaver TE, Bachurski CJ, Clark JC, Whitsett JA. TTF-1 phosphorylation is required for peripheral lung morphogenesis, perinatal survival, and tissue-specific gene expression. J Biol Chem. 2003;278:35574–83.
10. Zhou H, Morotti RA, Profitt SA, Langston C, Wert SE, Whitsett JA, Greco MA. Expression of thyroid transcription factor-1, surfactant proteins, type I cell-associated antigen, and Clara cell secretory protein in pulmonary hypoplasia. Pediatr Dev Pathol. 2001;4:364–71.
11. Kakegawa S, Shimizu K, Sugano M, Miyamae Y, Kaira K, Araki T, Nakano T, Kamiyoshihara M, Kawashima O, Takeyoshi I. Clinicopathological features of lung adenocarcinoma with KRAS mutations. Cancer. 2011;117:4257–66.
12. Davidson LA, Batman P, Fagan DG. Congenital acinar dysplasia: a rare cause of pulmonary hypoplasia. Histopathology. 1998;32:57–9.
13. Gutierrez C, Rodriguez A, Palenzuela S, Forteza C, Rossello JL. Congenital misalignment of pulmonary veins with alveolar capillary dysplasia causing persistent neonatal pulmonary hypertension: report of two affected siblings. Pediatr Dev Pathol. 2000;3:271–6.
14. Pucci A, Zanini C, Ferrero F, Arisio R, Valori A, Abbruzzese P, Forni M. Misalignment of lung vessels: diagnostic role of conventional histology and immunohistochemistry. Virchows Arch. 2003;442:597–600.
15. Stankiewicz P, Sen P, Bhatt SS, Storer M, Xia Z, Bejjani BA, Ou Z, Wiszniewska J, Driscoll DJ, Bolivar J, Bauer M, Zackai EH, McDonald-McGinn D, Nowaczyk MM, Murray M, Shaikh TH, Martin V, Tyreman M, Simonic I, Willatt L, Paterson J, Mehta S, Rajan D, Fitzgerald T, Gribble S, Prigmore E, Patel A, Shaffer LG, Carter NP, Cheung SW, Langston C, Shaw-Smith C. Genomic and genic deletions of the FOX gene cluster on 16q24.1 and inactivating mutations of FOXF1 cause alveolar capillary dysplasia and other malformations. Am J Hum Genet. 2009;84:780–91.
16. Laux D, Malan V, Bajolle F, Boudjemline Y, Amiel J, Bonnet D. FOX gene cluster defects in alveolar capillary dysplasia associated with congenital heart disease. Cardiol Young. 2013;23(5):697–704.
17. Wambach JA, Wegner DJ, Depass K, Heins H, Druley TE, Mitra RD, An P, Zhang Q, Nogee LM, Cole FS, Hamvas A. Single ABCA3 mutations increase risk for neonatal respiratory distress syndrome. Pediatrics. 2012;130:e1575–82.
18. Poggi C, Giusti B, Vestri A, Pasquini E, Abbate R, Dani C. Genetic polymorphisms of antioxidant enzymes in preterm infants. J Matern Fetal Neonatal Med. 2012;25 Suppl 4:131–4.
19. Alkhorayyef A, Ryerson L, Chan A, Phillipos E, Lacson A, Adatia I. Pulmonary interstitial glycogenosis associated with pulmonary hypertension and hypertrophic cardiomyopathy. Pediatr Cardiol. 2013;34:462–6.
20. Fraga JC, Favero E, Contelli F, Canani F. Surgical treatment of congenital pulmonary arteriovenous fistula in children. J Pediatr Surg. 2008;43:1365–7.
21. Pouwels HM, Janevski BK, Penn OC, Sie HT, ten Velde GP. Systemic to pulmonary vascular malformation. Eur Respir J. 1992;5:1288–91.
22. Varnholt H, Kradin R. Pulmonary capillary hemangiomatosis arising in hereditary hemorrhagic telangiectasia. Hum Pathol. 2004;35:266–8.
23. Giordano P, Nigro A, Lenato GM, Guanti G, Suppressa P, Lastella P, DE Mattia D, Sabba C. Screening for children from families with Rendu-Osler-Weber disease: from geneticist to clinician. J Thromb Haemost. 2006;4:1237–45.
24. Mache CJ, Gamillscheg A, Popper HH, Haworth SG. Early-life pulmonary arterial hypertension with subsequent development of diffuse pulmonary arteriovenous malformations in hereditary haemorrhagic telangiectasia type 1. Thorax. 2008;63:85–6.
25. Letteboer TG, Zewald RA, Kamping EJ, de Haas G, Mager JJ, Snijder RJ, Lindhout D, Hennekam FA, Westermann CJ, Ploos van Amstel JK. Hereditary hemorrhagic telangiectasia: ENG and ALK-1 mutations in Dutch patients. Hum Genet. 2005;116:8–16.
26. Shovlin CL, Guttmacher AE, Buscarini E, Faughnan ME, Hyland RH, Westermann CJ, Kjeldsen AD, Plauchu H. Diagnostic criteria for hereditary hemorrhagic telangiectasia (Rendu-Osler-Weber syndrome). Am J Med Genet. 2000;91:66–7.
27. Assis AM, Costa FF, Arruda VR, Annichino-Bizzacchi JM, Bertuzzo CS. Three novel mutations in the activin receptor-like kinase 1 (ALK-1) gene in hereditary hemorrhagic telangiectasia type 2 in Brazilian patients. J Hum Genet. 2007;52:237–43.
28. Grimmer G, Abel U, Brune H, Deutsch-Wenzel R, Emura M, Heinrich U, Jacob J, Kemena A, Misfeld J, Mohr U, et al. Evaluation of environmental carcinogens by carcinogen-specific test systems. Exp Pathol. 1986;29:65–76.
29. Albinana V, Bernabeu-Herrero ME, Zarrabeitia R, Bernabeu C, Botella LM. Estrogen therapy for hereditary haemorrhagic telangiectasia (HHT): effects of raloxifene, on Endoglin and ALK1 expression in endothelial cells. Thromb Haemost. 2010;103:525–34.

30. Dinwiddie R, Sonnappa S. Systemic diseases and the lung. Paediatr Respir Rev. 2005;6:181–9.
31. Watanabe A, Kawabata Y, Okada O, Tanabe N, Kimura H, Hatamochi A, Shinkai H, Sakai N, Shimada T, Hiroshima K, Kuriyama T. Ehlers-Danlos syndrome type IV with few extrathoracic findings: a newly recognized point mutation in the COL3A1 gene. Eur Respir J. 2002;19:195–8.
32. Bertrand P, Navarro H, Caussade S, Holmgren N, Sanchez I. Airway anomalies in children with Down syndrome: endoscopic findings. Pediatr Pulmonol. 2003;36:137–41.
33. Fukushima H, Kosaki K, Sato R, Yagihashi T, Gatayama R, Kodo K, Hayashi T, Nakazawa M, Tsuchihashi T, Maeda J, Kojima Y, Yamagishi H, Takahashi T. Mechanisms underlying early development of pulmonary vascular obstructive disease in Down syndrome: an imbalance in biosynthesis of thromboxane A2 and prostacyclin. Am J Med Genet A. 2010;152A:1919–24.
34. Fusonie D, Molnar W. Anomalous pulmonary venous return, pulmonary sequestration, bronchial atresia, aplastic right upper lobe, pericardial defect and intrathoracic kidney. An unusual complex of congenital anomalies in one patient. Am J Roentgenol Radium Ther Nucl Med. 1966;97:350–4.
35. Carter R. Pulmonary sequestration. Ann Thorac Surg. 1969;7:68–88.
36. Gwinn JL, Lee FA. Pulmonary sequestration – intralobar. Am J Dis Child. 1974;127:233–4.
37. Thilenius OG, Ruschhaupt DG, Replogle RL, Bharati S, Herman T, Arcilla RA. Spectrum of pulmonary sequestration: association with anomalous pulmonary venous drainage in infants. Pediatr Cardiol. 1983;4:97–103.
38. Juettner FM, Pinter HH, Lammer G, Popper H, Friehs GB. Bilateral intralobar pulmonary sequestration: therapeutic implications. Ann Thorac Surg. 1987;43:660–2.
39. Lee ML, Tsao LY, Chaou WT, Yang AD, Yeh KT, Wang JK, Wu MH, Lue HC, Chiu IS, Chang CI. Revisit on congenital bronchopulmonary vascular malformations: a haphazard branching theory of malinosculations and its clinical classification and implication. Pediatr Pulmonol. 2002;33:1–11.
40. Currarino G, Williams B. Causes of congenital unilateral pulmonary hypoplasia: a study of 33 cases. Pediatr Radiol. 1985;15:15–24.
41. Dupuis C, Charaf LA, Breviere GM, Abou P. "Infantile" form of the scimitar syndrome with pulmonary hypertension. Am J Cardiol. 1993;71:1326–30.
42. Namvar M, Zoroufian A, Shirani S, SalehiOmran A, Davoodi G, Yazdanifard P. Scimitar vein anomaly with total right-side pulmonary vein return to inferior vena cava concomitant with atresia of upper right-side pulmonary vein and secundum atrial septal defect. Heart Surg Forum. 2009;12:E235–7.
43. Pfleger A, Gamillscheg A, Popper HH, Smolle-Juttner FM, Zach MS. Diffuse pulmonary arteriovenous malformations in a teenager with corrected total anomalous pulmonary venous drainage. Respiration. 2007;74:106–9.
44. Stocker JT, Madewell JE, Drake RM. Congenital cystic adenomatoid malformation of the lung. Classification and morphologic spectrum. Hum Pathol. 1977;8:155–71.
45. Stacher E, Ullmann R, Halbwedl I, Gogg-Kammerer M, Boccon-Gibod L, Nicholson AG, Sheppard MN, Carvalho L, Franca MT, Macsweeney F, Morresi-Hauf A, Popper HH. Atypical goblet cell hyperplasia in congenital cystic adenomatoid malformation as a possible preneoplasia for pulmonary adenocarcinoma in childhood: a genetic analysis. Hum Pathol. 2004;35:565–70.
46. Lantuejoul S, Nicholson AG, Sartori G, Piolat C, Danel C, Brabencova E, Goldstraw P, Brambilla E, Rossi G. Mucinous cells in type 1 pulmonary congenital cystic adenomatoid malformation as mucinous bronchioloalveolar carcinoma precursors. Am J Surg Pathol. 2007;31:961–9.
47. Ota H, Langston C, Honda T, Katsuyama T, Genta RM. Histochemical analysis of mucous cells of congenital adenomatoid malformation of the lung: insights into the carcinogenesis of pulmonary adenocarcinoma expressing gastric mucins. Am J Clin Pathol. 1998;110:450–5.
48. Orsini A, Stahl A, Sansot M, Giraud F, Perrimond H, Bernard PJ, Brusquet Y, Taramasco H. Pulmonary hemosiderosis in a 9-year-old child with a trisomy 18. Exploration with radiochromium-51 and radioiron-59. Pediatrie. 1969;24:339–49.
49. Banerjea MC, Wirbelauer J, Adam P, Trusen A, Marx A, Speer C. Bilateral cystic adenomatoid lung malformation type III – a rare differential diagnosis of pulmonary hypertension in neonates. J Perinat Med. 2002;30:429–36.
50. Wagner AJ, Stumbaugh A, Tigue Z, Edmondson J, Paquet AC, Farmer DL, Hawgood S. Genetic analysis of congenital cystic adenomatoid malformation reveals a novel pulmonary gene: fatty acid binding protein-7 (brain type). Pediatr Res. 2008;64:11–6.
51. Jancelewicz T, Nobuhara K, Hawgood S. Laser microdissection allows detection of abnormal gene expression in cystic adenomatoid malformation of the lung. J Pediatr Surg. 2008;43:1044–51.
52. Butnor KJ, Guinee Jr DG. Pleuropulmonary pathology of Birt-Hogg-Dube syndrome. Am J Surg Pathol. 2006;30:395–9.
53. Geremek M, Schoenmaker F, Zietkiewicz E, Pogorzelski A, Diehl S, Wijmenga C, Witt M. Sequence analysis of 21 genes located in the Kartagener syndrome linkage region on chromosome 15q. Eur J Hum Genet. 2008;16:688–95.
54. Schloo BL, Vawter GF, Reid LM. Down syndrome: patterns of disturbed lung growth. Hum Pathol. 1991;22:919–23.
55. Popler J, Lesnick B, Dishop MK, Deterding RR. New coding in the International Classification of Diseases, Ninth Revision, for children's interstitial lung disease. Chest. 2012;142:774–80.

56. Pham TT, Benirschke K, Masliah E, Stocker JT, Yi ES. Congenital pulmonary airway malformation (congenital cystic adenomatoid malformation) with multiple extrapulmonary anomalies: autopsy report of a fetus at 19 weeks of gestation. Pediatr Dev Pathol. 2004;7:661–6.
57. Deutsch GH, Young LR. Histologic resolution of pulmonary interstitial glycogenosis. Pediatr Dev Pathol. 2009;12:475–80.
58. Chen CP, Chuang CY, Chang YC, Tzen CY. Type III congenital cystic adenomatoid malformation of the lung detected through maternal serum screening positive for Down's syndrome. Acta Obstet Gynecol Scand. 1997;76:378–9.
59. Smets K, Dhaene K, Schelstraete P, Meersschaut V, Vanhaesebrouck P. Neonatal pulmonary interstitial glycogen accumulation disorder. Eur J Pediatr. 2004;163:408–9.
60. de Krijger RR, Claessen SM, van der Ham F, van Unnik AJ, Hulsbergen-van de Kaa CA, van Leuven L, van Noesel M, Speel EJ. Gain of chromosome 8q is a frequent finding in pleuropulmonary blastoma. Mod Pathol. 2007;20:1191–9.
61. Deterding RR. Infants and young children with children's interstitial lung disease. Pediatr Allergy Immunol Pulmonol. 2010;23:25–31.
62. Cooney TP, Thurlbeck WM. Pulmonary hypoplasia in Down's syndrome. N Engl J Med. 1982; 307:1170–3.
63. Radman MR, Goldhoff P, Jones KD, Azakie A, Datar S, Adatia I, Oishi PE, Fineman JR. Pulmonary interstitial glycogenosis: an unrecognized etiology of persistent pulmonary hypertension of the newborn in congenital heart disease? Pediatr Cardiol. 2013;34(5):1254–7.
64. Taeger D, Johnen G, Wiethege T, Tapio S, Mohner M, Wesch H, Tannapfel A, Muller KM, Bruning T, Pesch B. Major histopathological patterns of lung cancer related to arsenic exposure in German uranium miners. Int Arch Occup Environ Health. 2009;82:867–75.
65. Rettwitz-Volk W, Schlosser R, Ahrens P, Horlin A. Congenital unilobar pulmonary lymphangiectasis. Pediatr Pulmonol. 1999;27:290–2.
66. Rutigliani M, Boccardo F, Campisi C, Bonioli E, Fulcheri E, Bellini C. Immunohistochemical studies in a hydroptic fetus with pulmonary lymphangiectasia and trisomy 21. Lymphology. 2007;40:114–21.
67. de Bruyn G, Casaer A, Devolder K, Van Acker G, Logghe H, Devriendt K, Cornette L. Hydrops fetalis and pulmonary lymphangiectasia due to FOXC2 mutation: an autosomal dominant hereditary lymphedema syndrome with variable expression. Eur J Pediatr. 2012;171:447–50.
68. Bellini C, Mazzella M, Arioni C, Campisi C, Taddei G, Toma P, Boccardo F, Hennekam RC, Serra G. Hennekam syndrome presenting as nonimmune hydrops fetalis, congenital chylothorax, and congenital pulmonary lymphangiectasia. Am J Med Genet A. 2003;120A:92–6.
69. Ding M, Chen F, Shi X, Yucesoy B, Mossman B, Vallyathan V. Diseases caused by silica: mechanisms of injury and disease development. Int Immunopharmacol. 2002;2:173–82.
70. Quijano G, Drut R. Multiple congenital infantile hemangiomas of the lung in partial trisomy D. J Clin Pathol. 2007;60:943–5.
71. Chng WJ, Remstein ED, Fonseca R, Bergsagel PL, Vrana JA, Kurtin PJ, Dogan A. Gene expression profiling of pulmonary mucosa-associated lymphoid tissue lymphoma identifies new biologic insights with potential diagnostic and therapeutic applications. Blood. 2009;113:635–45.
72. Castillo M, Vade A, Lim-Dunham JE, Masuda E, Massarani-Wafai R. Pulmonary interstitial glycogenosis in the setting of lung growth abnormality: radiographic and pathologic correlation. Pediatr Radiol. 2010;40:1562–5.
73. Roque L, Rodrigues R, Martins C, Ribeiro C, Ribeiro MJ, Martins AG, Oliveira P, Fonseca I. Comparative genomic hybridization analysis of a pleuropulmonary blastoma. Cancer Genet Cytogenet. 2004;149:58–62.
74. Turan O, Hirfanoglu IM, Beken S, Biri A, Efeturk T, Atalay Y. Prenatally detected congenital cystic adenomatoid malformation and postnatally diagnosed trisomy 13: case report and review of the literature. Turk J Pediatr. 2011;53:337–41.
75. Guillemot N, Troadec C, de Villemeur TB, Clement A, Fauroux B. Lung disease in Niemann-Pick disease. Pediatr Pulmonol. 2007;42:1207–14.
76. Kirkegaard T, Roth AG, Petersen NH, Mahalka AK, Olsen OD, Moilanen I, Zylicz A, Knudsen J, Sandhoff K, Arenz C, Kinnunen PK, Nylandsted J, Jaattela M. Hsp70 stabilizes lysosomes and reverts Niemann-Pick disease-associated lysosomal pathology. Nature. 2010;463:549–53.
77. Miller A, Brown LK, Pastores GM, Desnick RJ. Pulmonary involvement in type 1 Gaucher disease: functional and exercise findings in patients with and without clinical interstitial lung disease. Clin Genet. 2003;63:368–76.
78. Tredano M, Griese M, Brasch F, Schumacher S, de Blic J, Marque S, Houdayer C, Elion J, Couderc R, Bahuau M. Mutation of SFTPC in infantile pulmonary alveolar proteinosis with or without fibrosing lung disease. Am J Med Genet. 2004;126A:18–26.
79. Whitsett JA, Wert SE, Weaver TE. Alveolar surfactant homeostasis and the pathogenesis of pulmonary disease. Annu Rev Med. 2010;61:105–19.
80. Somaschini M, Castiglioni E, Presi S, Volonteri C, Ferrari M, Carrera P. Genetic susceptibility to neonatal lung diseases. Acta Biomed. 2012;83 Suppl 1:10–4.
81. Zscheppang K, Liu W, Volpe MV, Nielsen HC, Dammann CE. ErbB4 regulates fetal surfactant phospholipid synthesis in primary fetal rat type II cells. Am J Physiol Lung Cell Mol Physiol. 2007;293:L429–35.
82. Price A, Manson D, Cutz E, Dell S. Pulmonary alveolar proteinosis associated with anti-GM-CSF antibodies in a child: successful treatment with inhaled GM-CSF. Pediatr Pulmonol. 2006;41:367–70.

83. Latzin P, Tredano M, Wust Y, de Blic J, Nicolai T, Bewig B, Stanzel F, Kohler D, Bahuau M, Griese M. Anti-GM-CSF antibodies in paediatric pulmonary alveolar proteinosis. Thorax. 2005;60:39–44.
84. Ioachimescu OC, Kavuru MS. Pulmonary alveolar proteinosis. Chron Respir Dis. 2006;3:149–59.
85. Stevens PA, Pettenazzo A, Brasch F, Mulugeta S, Baritussio A, Ochs M, Morrison L, Russo SJ, Beers MF. Nonspecific interstitial pneumonia, alveolar proteinosis, and abnormal proprotein trafficking resulting from a spontaneous mutation in the surfactant protein C gene. Pediatr Res. 2005;57:89–98.
86. Bhagwat AG, Wentworth P, Conen PE. Observations on the relationship of desquamative interstitial pneumonia and pulmonary alveolar proteinosis in childhood: a pathologic and experimental study. Chest. 1970;58:326–32.
87. DeBoer EM, Keene S, Winkler AM, Shehata BM. Identical twins with lethal congenital pulmonary airway malformation type 0 (acinar dysplasia): further evidence of familial tendency. Fetal Pediatr Pathol. 2012;31:217–24.
88. Parto K, Svedstrom E, Majurin ML, Harkonen R, Simell O. Pulmonary manifestations in lysinuric protein intolerance. Chest. 1993;104:1176–82.
89. Barilli A, Rotoli BM, Visigalli R, Bussolati O, Gazzola GC, Kadija Z, Rodi G, Mariani F, Ruzza ML, Luisetti M, Dall'asta V. In Lysinuric Protein Intolerance system y+L activity is defective in monocytes and in GM-CSF-differentiated macrophages. Orphanet J Rare Dis. 2010;5:32.
90. Ramos M, Trujillano D, Olivar R, Sotillo F, Ossowski S, Manzanares J, Costa J, Gartner S, Oliva C, Quintana E, Gonzalez M, Vazquez C, Estivill X, Casals T. Extensive sequence analysis of CFTR, SCNN1A, SCNN1B, SCNN1G and SERPINA1 suggests an oligogenic basis for cystic fibrosis-like phenotypes. Clin Genet. 2014;86(1):91–5.
91. Popler J, Gower WA, Mogayzel Jr PJ, Nogee LM, Langston C, Wilson AC, Hay TC, Deterding RR. Familial neuroendocrine cell hyperplasia of infancy. Pediatr Pulmonol. 2010;45:749–55.
92. Glasser SW, Hardie WD, Hagood JS. Pathogenesis of interstitial lung disease in children and adults. Pediatr Allergy Immunol Pulmonol. 2010;23:9–14.
93. Katzenstein AL, Gordon LP, Oliphant M, Swender PT. Chronic pneumonitis of infancy. A unique form of interstitial lung disease occurring in early childhood. Am J Surg Pathol. 1995;19:439–47.
94. Mak H, Moser RL, Hallett JS, Robotham JL. Usual interstitial pneumonitis in infancy. Clinical and pathologic evaluation. Chest. 1982;82:124–6.
95. Reiterer F, Dornbusch HJ, Urlesberger B, Reittner P, Fotter R, Zach M, Popper H, Muller W. Cytomegalovirus associated neonatal pneumonia and Wilson-Mikity syndrome: a causal relationship? Eur Respir J. 1999;13:460–2.
96. Euler AR, Byrne WJ, Ament ME, Fonkalsrud EW, Strobel CT, Siegel SC, Katz RM, Rachelefsky GS. Recurrent pulmonary disease in children: a complication of gastroesophageal reflux. Pediatrics. 1979;63:47–51.
97. Kavantzas N, Theocharis S, Agapitos E, Davaris P. Chronic pneumonitis of infancy. An autopsy study of 12 cases. Clin Exp Pathol. 1999;47:96–100.
98. Swaye P, Van Ordstrand HS, McCormack LJ, Wolpaw SE. Familial Hamman-Rich syndrome. Report of eight cases. Dis Chest. 1969;55:7–12.
99. Parton LA, Strassberg SS, Qian D, Galvin-Parton PA, Cristea IA. The genetic basis for bronchopulmonary dysplasia. Front Biosci. 2006;11:1854–60.
100. Chess PR, D'Angio CT, Pryhuber GS, Maniscalco WM. Pathogenesis of bronchopulmonary dysplasia. Semin Perinatol. 2006;30:171–8.
101. Kevill KA, Bhandari V, Kettunen M, Leng L, Fan J, Mizue Y, Dzuira JD, Reyes-Mugica M, McDonald CL, Baugh JA, O'Connor CL, Aghai ZH, Donnelly SC, Bazzy-Asaad A, Bucala RJ. A role for macrophage migration inhibitory factor in the neonatal respiratory distress syndrome. J Immunol. 2008;180:601–8.
102. Torday JS, Rehan VK. Developmental cell/molecular biologic approach to the etiology and treatment of bronchopulmonary dysplasia. Pediatr Res. 2007;62:2–7.
103. Hilgendorff A, Heidinger K, Bohnert A, Kleinsteiber A, Konig IR, Ziegler A, Lindner U, Frey G, Merz C, Lettgen B, Chakraborty T, Gortner L, Bein G. Association of polymorphisms in the human surfactant protein-D (SFTPD) gene and postnatal pulmonary adaptation in the preterm infant. Acta Paediatr. 2009;98:112–7.
104. Chen S, Rong M, Platteau A, Hehre D, Smith H, Ruiz P, Whitsett J, Bancalari E, Wu S. CTGF disrupts alveolarization and induces pulmonary hypertension in neonatal mice: implication in the pathogenesis of severe bronchopulmonary dysplasia. Am J Physiol Lung Cell Mol Physiol. 2011;300:L330–40.
105. Somaschini M, Castiglioni E, Volonteri C, Cursi M, Ferrari M, Carrera P. Genetic predisposing factors to bronchopulmonary dysplasia: preliminary data from a multicentre study. J Matern Fetal Neonatal Med. 2012;25 Suppl 4:127–30.
106. Popper H, Juettner F, Pinter J. The gastric juice aspiration syndrome (Mendelson syndrome). Aspects of pathogenesis and treatment in the pig. Virchows Arch A Pathol Anat Histopathol. 1986; 409:105–17.

Edema

4

Lung edema is defined as an accumulation of fluid within alveoli and small bronchi/bronchioles. Edema fluid enters the peripheral lung from the circulation via the interstitium into alveoli. It can be induced by various causes. The most common form is due to congestion of the pulmonary circulation, most often caused by heart failure either due to infarction, valvular diseases, and the like. In these cases the venous flow into the left atrium is reduced, resistance in the venous part of the circulation increases, and leakage of the pulmonary veins increase. The gaps between the endothelial cells increase in size and serum gets into the interstitium and causes interstitial edema. In this case the composition of proteins and electrolytes are essentially similar to their concentration within the bloodstream. However, large proteins usually are lacking, because their large size prevents transudation in the early phases of edema development. In late phase of edema, this changes and also large proteins can be found within the fluid. Edema impairs respiration. Due to hypoxia patients will start with forced breathing. Air mixes with edema fluid resulting in foamy fluid, which can be easily recognized on patient inspection. Reduced oxygenation of the red blood cells and increased resistance in the peripheral circulation finally causes right ventricular failure and death.

4.1 Gross Morphology

Lungs are heavy, sometimes double the weight of normal, and the color is dark red. In cut surface foamy fluid is immediately starting to flow.

4.2 Histology

The alveoli are filled with fluid, most often acellular. A few macrophages might be seen, some of them containing hemosiderin. In more severe cases, also red blood cells will enter the alveoli. The capillaries are dilated and filled with blood. Within the vascular bed, there is no increase of leukocytes (Fig. 4.1).

4.3 High-Altitude Edema (HAPE)

High-altitude edema is a condition, which morphologically resembles edema due to cardiac insufficiency; however the mechanisms are different. Mountaineering over 3,500 m of altitude can cause headache, vomiting, and finally edema of brain and lung. Mountaineers have to leave the altitude immediately to be rescued. Several drugs have been tested and several of them such as nifedipine will help in therapy as well as in prevention. Research in HAPE has highlighted two main factors responsible for pulmonary edema. One of them is stress failure of pulmonary capillaries resulting in a high-permeability form of edema or even frank hemorrhage [1]. Another factor is defective alveolar fluid clearance. This most likely is based on nonfunctioning endothelial and epithelial nitric oxide synthesis predisposing to hypoxic pulmonary vasoconstriction, capillary stress failure, and alveolar fluid flooding [2]. Asymptomatic

© Springer-Verlag Berlin Heidelberg 2017
H. Popper, *Pathology of Lung Disease*, DOI 10.1007/978-3-662-50491-8_4

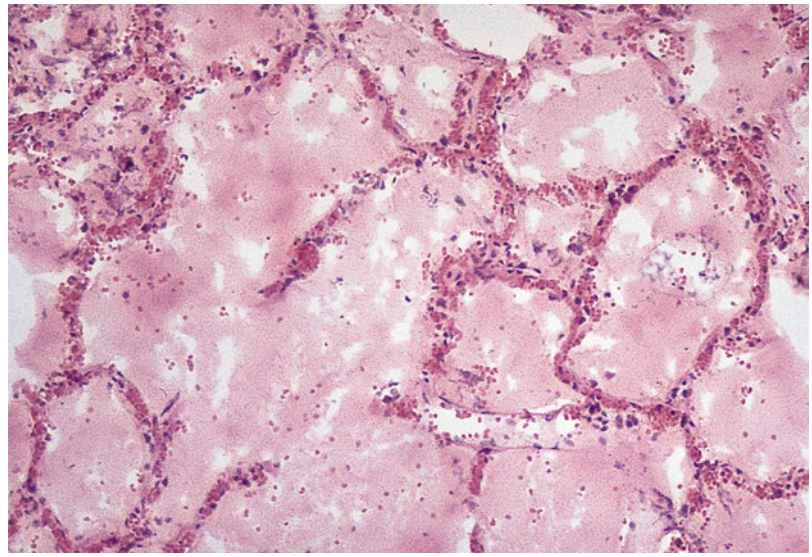

Fig. 4.1 Lung edema due to cardial insufficiency; the capillaries are dilated, within the alveoli is an eosinophilic fluid and scattered red blood cells. There is no inflammatory cell infiltration. H&E, ×100

alveolar fluid accumulation may be a normal phenomenon in healthy humans shortly after arrival at high altitude. Two fundamental mechanisms determine whether fluid accumulation is cleared or progresses to HAPE: the quantity of liquid escaping from the pulmonary vasculature and the rate of its clearance by the alveolar respiratory epithelium. The former is directly related to the degree of hypoxia-induced pulmonary hypertension, whereas the latter is determined by the alveolar epithelial sodium transport [3]. Several investigations have shaded light on mechanisms underlying these defects.

Potassium voltage channels (Kv1.2, Kv1.5, and Kv2.1) are sensitive to subacute hypoxia. Decreased expression has physiologic effects on membrane potential and cytosolic calcium. K^+ channels may also be involved in the mechanism of high-altitude pulmonary edema and hypertension [4]. During normoxia, the redox mediator hydrogen peroxide maintains voltage-gated O_2-sensitive K^+ channels (Kv) in an oxidized open state. Hypoxic withdrawal of ROS inhibits Kv channels, activates voltage-gated Ca^{2+} channels, enhances Ca^{2+} influx, and promotes vasoconstriction. The unique occurrence of hypoxic vasoconstriction in the pulmonary circulation relates to the co-localization of an O_2-sensor and O_2-sensitive Kv channels in resistance pulmonary arteries [5]. Oxygen tension sensing mechanisms are involved in hypoxic adaptation such as hypoxia-inducible factor-1 (HIF1). Genes involved in adaptation to hypoxia are angiotensin-1-converting enzyme, tyrosine hydroxylase, serotonin transporter, and endothelial NO synthase genes [6].

When the epithelial barrier is compromised at high altitude, the normally high level of VEGF in the alveolar epithelial fluid has access to the pulmonary endothelium, due to openings of tight junctions, where it acutely alters permeability, markedly exacerbating high-altitude pulmonary edema [7]. In the experimental study by Kolluru, leakiness of the endothelial monolayer was increased by twofold under hypoxia compared to cells under normoxia. F-actin stress fibers were depolymerized under hypoxia. Nitric oxide, cyclic guanosine monophosphate (cGMP), and a phosphodiesterase type 5 inhibitor led to recovery from hypoxia-induced leakiness of the endothelial monolayers [8]. Insufficient NO synthesis is also related to augmented oxidative stress and may represent an underlying mechanism predisposing to pulmonary hypertension [9]. Finally the study by Comellas pointed to increased endothelin-1 (ET-1) and decreased alveolar fluid reabsorption in patients with high-altitude pulmonary edema. If the endothelin receptor ETB is blocked, alveolar fluid reabsorption can be reestablished. Exposing endothelial

cell cultures to ET-1 resulted in increased NO. ET-1, via an endothelial-epithelial interaction, leads to decreased alveolar fluid reabsorption by activation of endothelial ETB receptors and NO generation [10].

Inflammation-associated edema is a different process. It is induced by hyperemia and widening of the precapillary, capillary, and venular bed, which slows down the blood flow. Again the endothelial gaps increase in size and fluid can enter the interstitium. In this condition also leukocytes actively leave the vascular bed and enter the interstitium. In inflammatory edema the composition of the fluid changes: pro-inflammatory proteins, immunoglobulins, and many other molecules are dominant components. Release of enzymes and other inflammation-associated molecules from leukocytes joins with molecules from the circulation. In addition the coagulation cascade is activated early on and plays an integral part in inflammation [11].

There are many causes of inflammation-associated edema:

Every infectious pneumonia starts with edema due to the hyperemia of the blood vessels, which is caused by inflammation-induced synthesis of cytokines.

Endogenous noxes will induce edema formation, as in bacteremia, viremia, shock, and release of enzymes into the circulation as in necrotizing pancreatitis.

Exogenous noxes such as air pollutants can induce edema. However, in almost all cases, this edema requires high concentrations of noxious gases, fumes, and particulates. Examples are:

- SO_x released by coal combustion and environmental fire [12]:
- NO_x released during accidents with NO_x-filled containers – NO_x released by car traffic does not reach a concentration, which causes edema; however, in heavily infested cities, smog containing high NO_x concentrations might cause edema.
- Insecticides and pesticides if inhaled in large concentration will cause edema followed by acute interstitial pneumonia.

Other causes of edema caused by exogenous noxes are inhalation of toxic metal fumes [13, 14], inhalation of organic fumes [15], inhalation of halogenated carbohydrates [16], and inhalation of organic and inorganic toxic particulates [17–19].

The consequences of inflammatory edema if not treated are similar to the other edema forms: impaired oxygenation and increased peripheral resistance in the vascular bed.

References

1. West JB, Mathieu-Costello O. Stress failure of pulmonary capillaries: role in lung and heart disease. Lancet. 1992;340:762–7.
2. Sartori C, Allemann Y, Scherrer U. Pathogenesis of pulmonary edema: learning from high-altitude pulmonary edema. Respir Physiol Neurobiol. 2007;159:338–49.
3. Scherrer U, Rexhaj E, Jayet PY, Allemann Y, Sartori C. New insights in the pathogenesis of high-altitude pulmonary edema. Prog Cardiovasc Dis. 2010;52:485–92.
4. Hong Z, Weir EK, Nelson DP, Olschewski A. Subacute hypoxia decreases voltage-activated potassium channel expression and function in pulmonary artery myocytes. Am J Respir Cell Mol Biol. 2004;31:337–43.
5. Michelakis ED, Thebaud B, Weir EK, Archer SL. Hypoxic pulmonary vasoconstriction: redox regulation of O2-sensitive K+ channels by a mitochondrial O2-sensor in resistance artery smooth muscle cells. J Mol Cell Cardiol. 2004;37:1119–36.
6. Mortimer H, Patel S, Peacock AJ. The genetic basis of high-altitude pulmonary oedema. Pharmacol Ther. 2004;101:183–92.
7. Kaner RJ, Crystal RG. Pathogenesis of high altitude pulmonary edema: does alveolar epithelial lining fluid vascular endothelial growth factor exacerbate capillary leak? High Alt Med Biol. 2004;5:399–409.
8. Kolluru GK, Tamilarasan KP, Rajkumar AS, Geetha Priya S, Rajaram M, Saleem NK, Majumder S, Jaffar Ali BM, Illavazagan G, Chatterjee S. Nitric oxide/cGMP protects endothelial cells from hypoxia-mediated leakiness. Eur J Cell Biol. 2008;87:147–61.
9. Scherrer U, Turini P, Thalmann S, Hutter D, Salmon CS, Stuber T, Shaw S, Jayet PY, Sartori-Cucchial C, Villena M, Allemann Y, Sartori C. Pulmonary hypertension in high-altitude dwellers: novel mechanisms, unsuspected predisposing factors. Adv Exp Med Biol. 2006;588:277–91.
10. Comellas AP, Briva A, Dada LA, Butti ML, Trejo HE, Yshii C, Azzam ZS, Litvan J, Chen J, Lecuona E, Pesce LM, Yanagisawa M, Sznajder JI. Endothelin-1 impairs alveolar epithelial function via endothelial ETB receptor. Am J Respir Crit Care Med. 2009;179:113–22.

11. Kim KJ, Malik AB. Protein transport across the lung epithelial barrier. Am J Physiol Lung Cell Mol Physiol. 2003;284:L247–59.
12. Viswanathan S, Eria L, Diunugala N, Johnson J, McClean C. An analysis of effects of San Diego wildfire on ambient air quality. J Air Waste Manag Assoc. 2006;56:56–67.
13. Nemery B. Metal toxicity and the respiratory tract. Eur Respir J. 1990;3:202–19.
14. Leininger JR, Farrell RL, Johnson GR. Acute lung lesions due to zirconium and aluminum compounds in hamsters. Arch Pathol Lab Med. 1977;101:545–9.
15. Final Report on Carcinogens Background Document for Formaldehyde, Rep Carcinog Backgr Doc 2010, i-512.
16. Van de Louw A, Jean D, Frisdal E, Cerf C, d'Ortho MP, Baker AH, Lafuma C, Duvaldestin P, Harf A, Delclaux C. Neutrophil proteinases in hydrochloric acid- and endotoxin-induced acute lung injury: evaluation of interstitial protease activity by in situ zymography. Lab Invest. 2002;82:133–45.
17. Bachelet M, Pinot F, Polla RI, Francois D, Richard MJ, Vayssier-Taussat M, Polla BS. Toxicity of cadmium in tobacco smoke: protection by antioxidants and chelating resins. Free Radic Res. 2002;36:99–106.
18. Moller W, Hofer T, Ziesenis A, Karg E, Heyder J. Ultrafine particles cause cytoskeletal dysfunctions in macrophages. Toxicol Appl Pharmacol. 2002;182:197–207.
19. Wang XR, Pan LD, Zhang HX, Sun BX, Dai HL, Christiani DC. A longitudinal observation of early pulmonary responses to cotton dust. Occup Environ Med. 2003;60:115–21.

Air Filling Diseases

5

5.1 Atelectasis

Atelectasis is defined as an alveolar collapse due to lack of air filling. In newborns there exists a condition of primary atelectasis (Fig. 5.1); however, normally the lung extends with the first inspiration and the alveoli are filled with air. In rare cases, this inspiration does not happen, mainly caused by severe cerebral malformations. In other cases, primary lung injury, such as meconium aspiration, sepsis, or persistent pulmonary hypertension, can also cause severe or partial atelectasis [1].

Secondary atelectasis can occur at any age after birth. The causes of atelectasis in childhood are infantile myofibromatosis [2], infantile bronchial obstruction or atresia [3, 4], or compression by cysts as in congenital adenomatoid pulmonary malformation (type 1 and 2; Fig. 5.2) [5].

In adults several diseases can cause atelectasis. The most common is stenosis of the bronchi by tumors or aspirated foreign bodies. The lung segment(s) peripheral to the stenosis undergoes resorption of the air followed by lung collapse. Another common cause is severe emphysema:

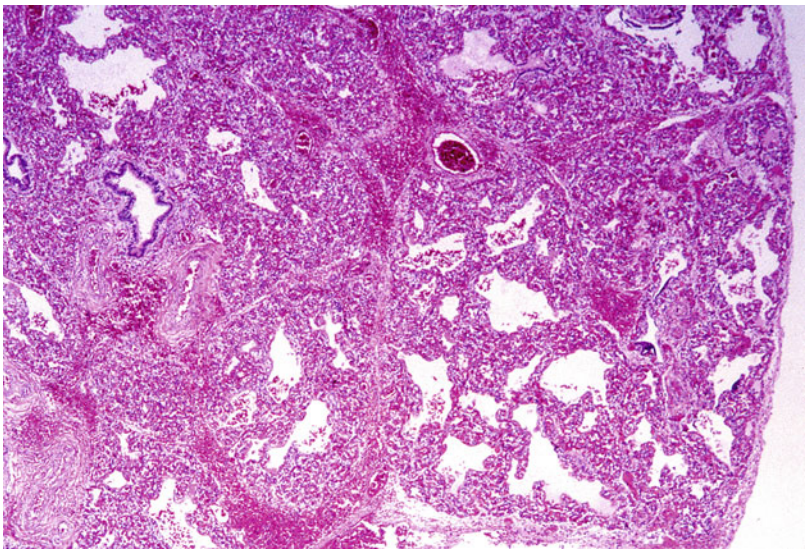

Fig. 5.1 Primary atelectasis in a case of single lung hypoplasia due to defect of the diaphragm and subsequent compression of the left lung by intestinal organs; H&E, ×50

© Springer-Verlag Berlin Heidelberg 2017
H. Popper, *Pathology of Lung Disease*, DOI 10.1007/978-3-662-50491-8_5

here large blebs compress adjacent lung parenchyma causing focal atelectasis (Fig. 5.3). Empyema and also severe pleural effusion cause localized atelectasis by compression of parts of the lung. A rare cause of localized or even one-sided atelectasis has been reported in severe scoliosis [6].

Fig. 5.2 Secondary atelectasis in a case of CPAM type 2. The cysts compress the adjacent lung parenchyma

5.1.1 Gross Morphology

Macroscopically atelectasis is characterized by a dark blue-red color of the lung. On the surface, the atelectatic areas are beneath adjacent lung areas with normal air content. In resorption atelectasis, the border of the atelectatic areas is sharp following the lobular borders, whereas in compression atelectasis, the border is blurred.

5.1.2 Histology

Histologically the alveoli are collapsed, and the capillaries are usually prominent, filled with blood. Cave: collapsed alveoli can only be seen, when the lung tissue is properly fixed (see Chap. 23).

The consequences of atelectasis are largely dependent on the size of atelectasis: small foci might not cause symptoms at all. Larger atelectatic areas will cause impaired blood flow and congestion. Long-standing atelectasis is also prone to secondary infection. If the area is large involving a whole lobe or more, also hypertension can result.

Fig. 5.3 Secondary atelectasis in a case of bullous emphysema in an adult. Note the compressed lung parenchyma (*arrows*). Papermount whole lung section, no counterstain

5.2 Emphysema

Emphysema is defined as an enlargement of alveolar spaces combined with the destruction and remodeling of the alveolar septa usually resulting also in numerical loss of alveoli. A simple enlargement is not emphysema, but hyperinsufflation, such as seen in status asthmaticus [7]. Also so-called emphysema of the elderly is not emphysema, at least in the early stages, but hyperinsufflation due to loss of elastic fibers, resulting in overextension of alveoli and impaired retraction in expiration. When septa rupture and subsequently get repaired, hyperinsufflation can shift into real emphysema.

5.2.1 Gross Morphology

Macroscopically emphysema can be diagnosed if the enlarged alveoli can be seen with the naked eye – this is the main and most reliable criterion (Fig. 5.4); normal alveoli are just below the size a human eye can recognize, so they are invisible. Another but less reliable sign is protrusion of the emphysematous segments over adjacent ones. In old German pathology books, there is always a description of depigmentation and of "knistern" (crackles) when pressing the lung: both are not signs of emphysema. As the lung is an organ filled with air, any kind of pressure will cause the air to bypass into other segments/saccules. By applying pressure, channels of Lambert and

Fig. 5.4 Centrilobular emphysema; the enlarged alveoli can be seen on this native section as translucent small spaces. *Arrows* point to some of these alveoli at the peripheral lung

pores of Kohn are opened and cause these crackles. A normal lung has a rosy-red color. Deposition of pigments from the ambient air causes pigmentation of the lungs over the years. In case of emphysema, there is some depigmentation; however, again this is not a reliable sign of emphysema.

5.2.2 Histology

On histologic examination, a proper fixation is required; otherwise, only high grades of emphysema can be diagnosed. Emphysema can be diagnosed, if there is increased size of alveoli with any kind of remodeling of the architecture of the lung. Linear intercept can be used for the diagnosis: a line is drawn between two adjacent bronchioles, which should cross at least seven alveolar walls. Everything below this value can be attributed to emphysema. Emphysema grading can be done according to the work of W. Thurlbeck into grades 1–9 [8]. It can easily be done without morphometry; even the most significant morphometric parameter, linear intercept, can be included. The classification has a good correlation with lung function and HRCT (see below). However, still a lot of correlation studies have to be done.

Emphysema can be classified into:

1. Panlobular (panacinar) emphysema (diffuse, symmetric)
2. Centrilobular (centriacinar) emphysema (often combined with COPD, asymmetric, irregular)
3. Scar emphysema
4. Juvenile emphysema
5. Congenital or lobar emphysema (already discussed in childhood diseases)
6. Interstitial emphysema (no longer seen in developed countries, because of much improved computer-assisted mechanical ventilation in newborn and premature children)
7. Emphysema and chronic bronchitis, chronic obstructive lung disease (COPD)

There are other classifications, such as by size into vesicular and bullous emphysema or by the underlying cause, i.e., obstructive emphysema. None has gained a significant acceptance.

Panlobular (*panacinar*) *emphysema* is caused by an inherited α1-antitrypsin deficiency. Usually mutations are located on exons 2–5 of the α1-antitrypsin gene, located on chromosome 14 (SERPINA1). There are different degrees of deficiency, depending on the type of mutation [9]. The most severe form is caused by missense mutations resulting in a truncated nonfunctioning protein. Other mutations, usually base exchange, will result in a change of the amino acid composition of α1-antitrypsin. If the amino-terminal portion of the protein is affected, this causes a biologically less efficient protein. α1-antitrypsin is responsible in counteracting the action of inflammatory proteins/peptides and is thus responsible for maintaining the structure of the lung. Each time a toxic substance is inhaled, an inflammatory response is started, but the action of the inflammation is terminated by α1-antitrypsin and some other anti-inflammatory molecules. Thus, the way for regeneration is paved.

Panlobular emphysema development starts in alveoli, affecting peripheral portions of the primary lobule, but leaving bronchioles and alveolar ducts unaffected. There is no visible inflammatory reaction/infiltration. In later stages, more and more lobules are involved, and also central portions with their alveolar ducts and respiratory bronchioles are included in cyst formation and enlargement. At the final stage, such as in explanted lung at transplantation, it might be almost impossible to separate panlobular from centrilobular emphysema (Figs. 5.5, 5.6, and 5.7).

Fig. 5.5 Panlobular emphysema; note the generalized emphysematous alveolar spaces, whereas the bronchial structures almost appear normal. Papermount whole lung section, no counterstain

An enlargement of the bronchioloalveolar unit characterizes *centrilobular* (*centriacinar*) *emphysema*: terminal bronchioles, alveolar ducts, and the centrally located alveoli are widened. Inflammation is often present, especially chronic bronchiolitis. In later stages, the more peripherally located alveoli are also included into the emphysema, and this results in the formation of large vesiculae or bullae. The alveolar septa usually rupture, and remnants can easily be seen

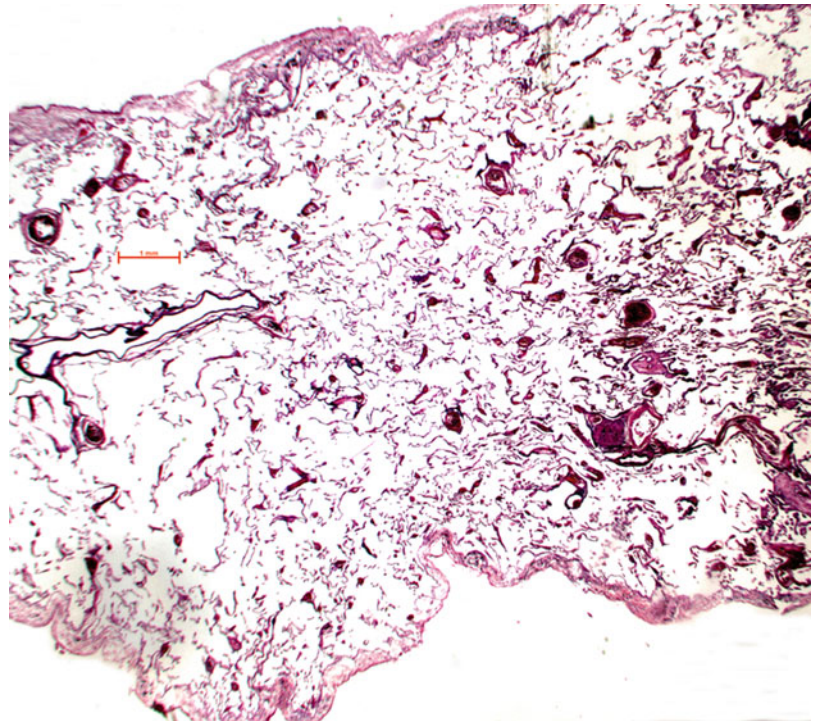

Fig. 5.6 Panlobular emphysema; note the destruction of the alveoli without an inflammatory component in the bronchi; in the left upper corner, an pulmonary artery is seen with thickened wall, a common finding pointing to arterial hypertension in these patients; H&E, bar 1 mm

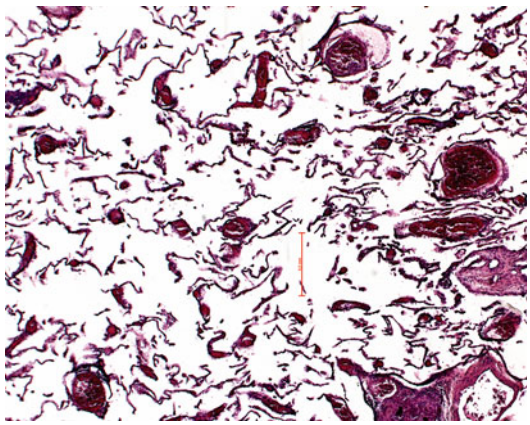

Fig. 5.7 Panlobular emphysema; see the destruction of the alveoli; many of them have already formed large confluent blebs including alveolar ducts; the septa are lost. There is no inflammation along the airways. H&E, bar 0.5 mm

(Figs. 5.8 and 5.9) [10]. As a consequence of chronic bronchiolitis, fibrosis of the bronchial and bronchiolar walls can be seen.

In cases of chronic bronchitis and bronchiolitis combined with centrilobular emphysema, the diagnosis of chronic obstructive pulmonary disease (COPD) can be rendered also pathologically. Centrilobular emphysema is most often associated and caused by cigarette smoking. The mechanism is not entirely understood, but there are some data pointing that cigarette smoking shifts the balance of pro-inflammatory and anti-inflammatory proteins toward the pro-inflammatory side, and thus lung tissue is destroyed gradually. Several other factors may interplay, such as defects of degradation-associated enzymes in alveolar macrophages and also phenotypic variation in the expression of different metalloproteinases [11–13]. Recent investigations have shed light on the role of immune mechanisms in emphysema development (detailed discussion below).

Scar emphysema is caused by scars, which result in distortion of the bronchioles. Since scar tissue does not follow the lung movement during respiration, bronchioles are periodically occluded during expiration, and air trapping results. In the next inspiration cycle, the peripheral saccules are overextended and septa eventually rupture.

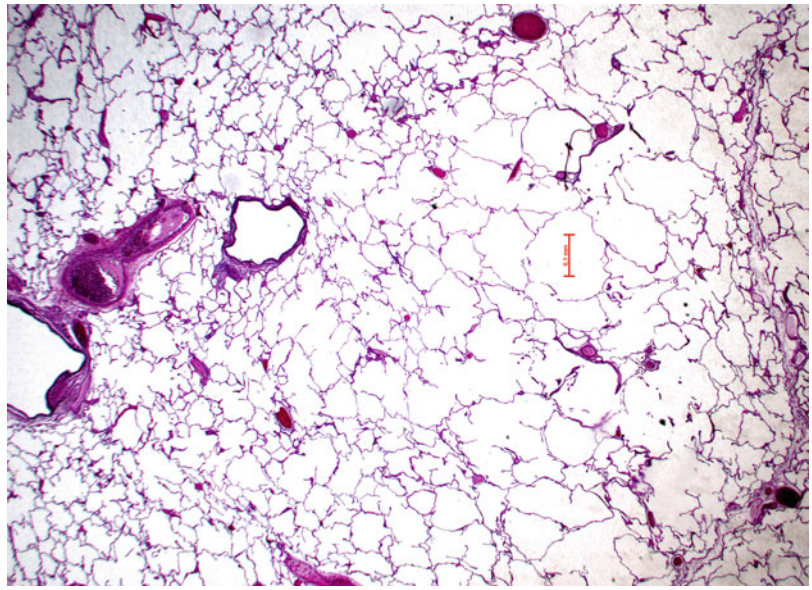

Fig. 5.8 Centrilobular emphysema; in contrast to panlobular emphysema, the bronchial walls are thickened and widened, due to inflammation. H&E, bar 0.1 mm

Fig. 5.9 Centrilobular emphysema; note the widened terminal bronchiole with fibrosis of the wall; the connected alveolar duct is widened, several alveoli are already incorporated into the duct forming a bleb; of note are also some normal peripheral alveoli to the left of the bronchiole. H&E, bar 0.2 mm

Morphologically the emphysema usually looks like centrilobular emphysema (Fig. 5.10).

Smoking-related interstitial fibrosis (SRIF), recently published by Katzenstein [14], presents also with scar emphysema; however, scarring and interstitial fibrosis are more diffuse compared to classical scarring. We will discuss this new entity under smoking-related diseases.

Juvenile emphysema is confined to the upper lobes. It occurs in young adults, most often in their teens and twenties. Patients most commonly present with spontaneous pneumothorax. No

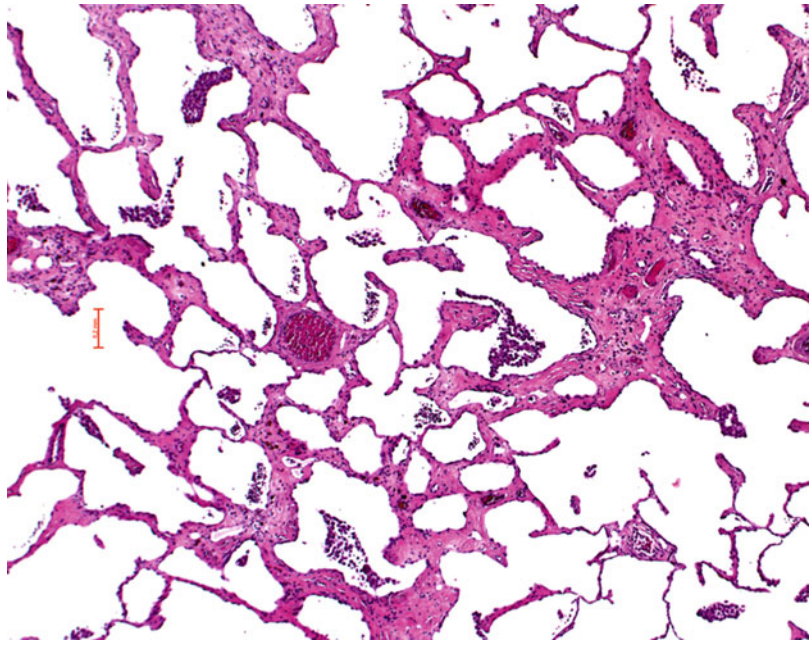

Fig. 5.10 Scar emphysema in a case of smoking-related interstitial fibrosis; here the emphysema is localized around scarred lung tissue; H&E, bar 0.2 mm

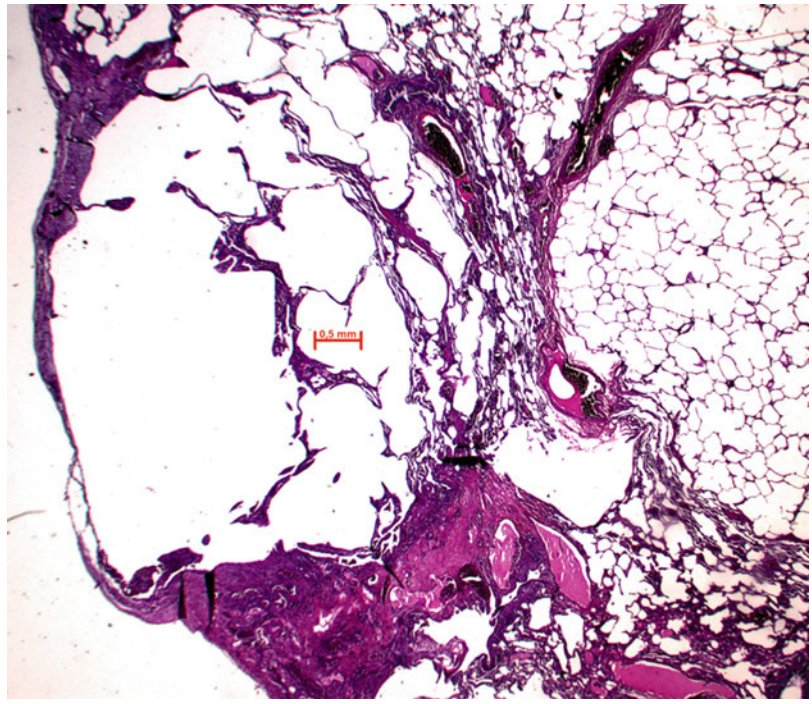

Fig. 5.11 Juvenile emphysema; this is a localized emphysema exclusively occurring in the upper lobes in a juvenile population presenting with unexplained pneumothorax; the emphysema is surrounded by normal lung parenchyma. Fibrosis of the pleura with or without inflammation is due to previous pneumothorax. H&E, bar 0.5 mm

underlying disease is found clinically. When resected, localized subpleural emphysema is seen at the periphery of the upper lobes. The adjacent areas show normal lung. Usually there is no bronchiolitis and no interstitial inflammatory infiltration (Fig. 5.11). However, within the pleura, inflammatory infiltrates can be seen, with a predominance of eosinophils – this is a sign of

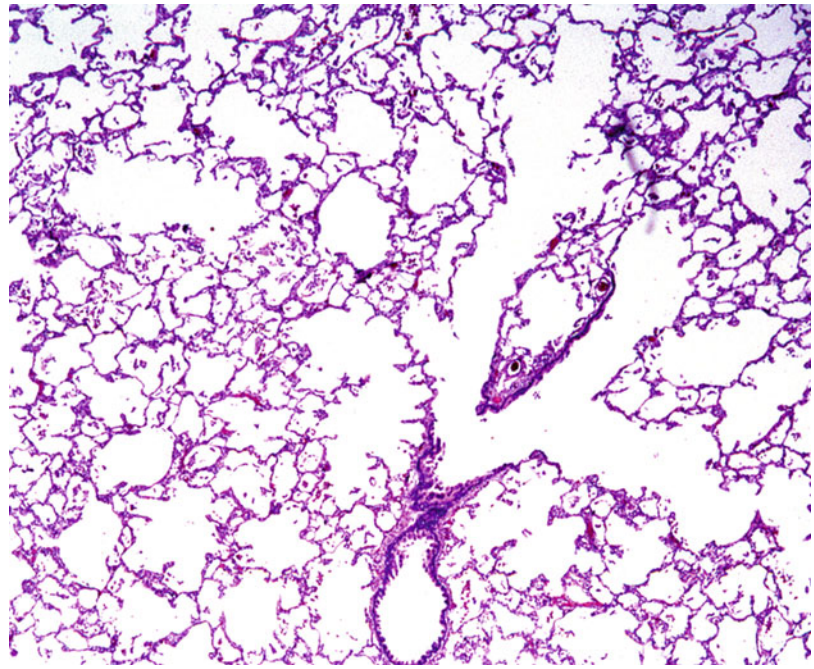

Fig. 5.12 Congenital emphysema (alternatively called lobar emphysema) in a child. Note the widened small airways extending into alveoli, which already fused with alveolar ducts into blebs. H&E, ×50

recent rupture (pneumothorax). In a few cases with the history of recurrent pneumothorax, also focal scar formation is seen at the borders of the emphysema.

Most probably this type of emphysema is based on a malformation of peripheral lung tissue, which causes enlargement of small lobules and consequently rupture and pneumothorax. After resection, these patients are cured; there will be no recurrence at the same site. In some cases, a subsequent pneumothorax can occur at the contralateral site. In these cases, juvenile emphysema does exist bilaterally. Again the resection causes complete healing without recurrence.

Congenital or lobar emphysema is an inborn defect in lung development. During organogenesis, a segment, rarely a lobe, is less well developed and the alveoli are enlarged. This type of emphysema can cause severe hypoxia, because the enlarged or cystic emphysematous segment compresses the normal lung and thus impairs oxygenation. On CT scan a focal translucent area is seen; often large cysts are formed. Surgical resection completely cures this disease. In children the remaining lung grows and develops normally and compensates completely the defect. Nowadays the diagnosis is often made intrauterine by CT or ultrasound examination (Fig. 5.12).

Interstitial emphysema is rarely seen in developed countries. In the past this disease was seen in newborn, often preterm children, which required assisted mechanical ventilation. Interstitial emphysema was caused by increased mechanical pressure, which at that time could not be controlled so precisely as today. Mechanical ventilation resulted in rupture of alveolar septa and air was trapped in the interstitium. In this disease large cysts can be seen most often within the interlobular septa. The cyst wall is covered by a foreign body giant cell reaction, which is almost pathognomonic in this condition (Fig. 5.13).

Birt-Hogg-Dube syndrome is another process characterized by cysts comprised of intraparenchymal collections of air surrounded by the normal parenchyma or a thin fibrous wall and blebs consisting of collections of air within the pleura. The emphysematous cysts are characteristically basally located, which separates them from other forms of emphysema [15].

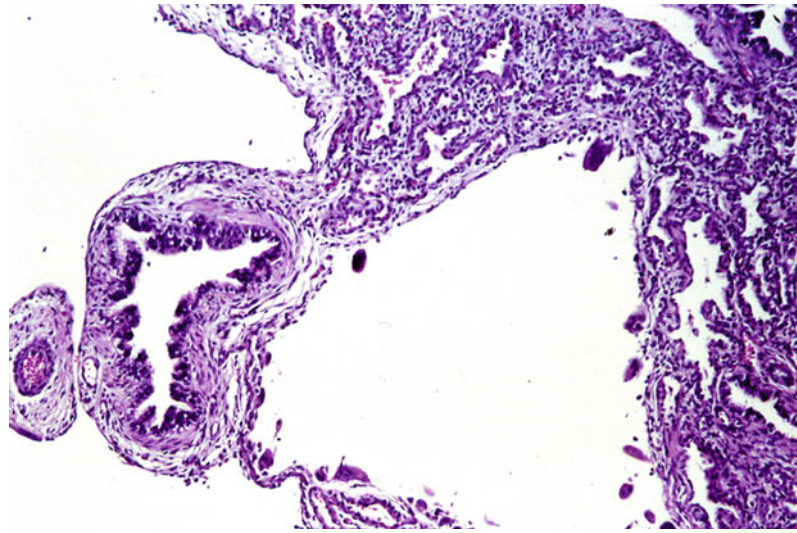

Fig. 5.13 Interstitial emphysema in a child, which has been under pressure ventilation causing rupture of airways. The interstitial air bleb is covered by a foreign body giant cell reaction. H&E, ×50

5.3 Emphysema and Lung Function

There are several dismal consequences of emphysema. The most important is reduced oxygenation of the blood. Oxygenation depends on a given surface for exchange of oxygen from the circulation, CO_2 transported into the alveoli and O_2 taken up through the alveolo-capillary membranes into the capillaries. A normal speed of circulating red blood cells in capillaries enables them to be loaded with oxygen. Normally the alveolar wall is very thin: type I pneumocytes are flat cells with almost invisible cytoplasm on light microscopy, the basal lamina of an alveolus and the adjacent capillary is fused, so the thickness of an alveolus at this site is thin (Fig. 5.14). Due to the many alveoli, there is a huge area for gas exchange. In emphysema the number of alveoli is reduced due to the loss of alveolar walls. Although an emphysema bleb is large, it misses the alveolar septation, which results in a reduced surface. In addition an emphysema bleb compresses adjacent alveoli, thus also reducing the surface available for oxygen uptake. Another problem is the reduction of the total number of capillaries. With each alveolar septum lost, also its capillary loop is lost. Therefore, in severe emphysema, up to >50 % of the total capillary diameter or volume is lost. This results in hypoxia and in addition increased peripheral resistance. The pulmonary blood pressure is raised, the speed of the blood flow is increased, and right heart hypertrophy (cor pulmonale) results. Hypoxia can result in further loss of alveolar septa and fibrosis. In the final stage, right heart failure and dilation are the consequence.

Clinically emphysema most often present with obstructive lung function test results. This, however, is not characteristic for all emphysema types: the most prevalent form is centrilobular emphysema, and this is always associated with chronic bronchitis/bronchiolitis, which results in either constriction of airways due to inflammatory infiltrations and muscular hyperplasia or fibrosis of bronchiolar walls, resulting in collapse during expiration. Narrowing of the airways causes impaired airflow, which is seen in severe forms of emphysema, centrilobular, as well as scar types. In panlobular emphysema, the function tests might result in restrictive changes, because there is no narrowing of airways, but distension and loss of alveoli, causing impaired oxygenation. However, lung function tests are not able to detect early changes and also not localized changes, because there is an enormous reserve in both lungs. There needs to be severe loss of alveoli until this results in a pathologic function tests.

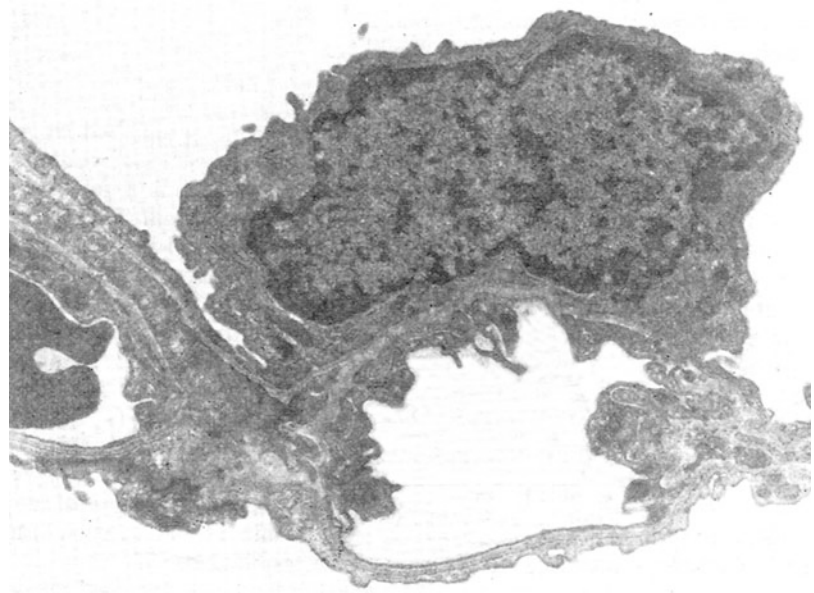

Fig. 5.14 Electron micrograph showing the wall of an alveolus. Note the thin cytoplasm of a type I pneumocyte and the fusion of the basement membrane of the epithelium and that of the underlying capillary. ×3,500

5.3.1 Factors Contributing to Emphysema Development

Although the association of small airway inflammation by cigarette smoke is well established in centrilobular emphysema and α1-antitrypsin deficiency in panlobular emphysema, how and why emphysema develops is still not understood. There are many more smokers, which do not develop emphysema or COPD, but develop diseases in other organ systems such as arteriosclerosis of coronary arteries. So smoking-induced epithelial injury and resulting airway inflammation are only one part of emphysema induction. There must be modifiers within the lung, which direct the tissue response. Decades ago emphysema was experimentally induced in animals by instillation of elastase into the lung [16, 17]. At this time, the research focus was on the reaction of alveolar macrophages being the major source for elastase. A release of elastase was thought to be linked to emphysema development [11, 18]. This has been confirmed recently [19].

The classic disease paradigm suggests that an imbalance of pulmonary matrix proteases versus anti-proteases underlies tissue destruction and inflammation associated with COPD. However, there is a growing appreciation of the complex and multifaceted nature of the pathological mechanisms associated with disease progression. Recently, there has been mounting evidence indicating that COPD patients exhibit many of the characteristics of a classical autoimmune response [20]. Questioning the role of macrophages and lymphocytes as well as autoimmunity has opened a new focus on emphysema research. α1-antitrypsin (AAT) has been shown to posses other functions besides the well-known anti-inflammatory capacity: in diabetic mice AAT treatment resulted in specific immune tolerance with increased FOXP3-positive Treg cells, immature dendritic cells (CD86 low), and lower CD3-positive T lymphocytes [21]. This provoked further studies into the role of immune cells in emphysema induction. In emphysema patients, antielastin antibodies have been detected associated with a T-helper type 1 (Th1) responses, which correlate with emphysema severity. These findings link emphysema to adaptive immunity against a specific lung antigen [22].

AAT is also a liver-derived acute-phase protein that, in vitro and in vivo, reduces production of pro-inflammatory cytokines, inhibits apoptosis, blocks leukocyte degranulation and migration, and modulates local and systemic inflammatory responses. In monocytes, AAT has

been shown to increase intracellular cAMP, regulate expression of CD14, and suppress NFκB nuclear translocation. These effects may be mediated by AAT's serpin activity or by other protein-binding activities. In preclinical models of autoimmunity and transplantation, AAT therapy prevents or reverses autoimmune disease and graft loss, and these effects are accompanied by tolerogenic changes in cytokine and transcriptional profiles and T-cell subsets [23].

Patients with tobacco smoke-induced emphysema have been shown to exhibit classical signs of T-cell-mediated autoimmunity characterized by autoantibody production and Th1 type responses. The role of Th17 type, a subset of Th1 cells, was studied in a murine model of emphysema. Exposure of mice to inhalation of mainstream cigarette smoke led to progressive airspace enlargement. Analysis of the bronchoalveolar lavage (BAL) from these mice demonstrated a significant increase in the overall number of both $CD4^+$ and $CD8^+$ T cells. Distinct populations of BAL $CD4^+$T cells were found to express IFN-γ or IL17 demonstrating the presence of both a Th1- and Th17-type response. Further analysis of this Th17 subset demonstrated that the majority of cells with this effector phenotype express the chemokine receptor CCR6. Together these data identify a novel T-cell subset associated with pulmonary inflammation as a result of cigarette smoke exposure. This subset may play an important role in the pathogenesis of cigarette smoke-induced autoimmunity [24].

Patients with chronic obstructive pulmonary disease and emphysema showed a lower expression of CD46. CD46 not only regulates the production of regulatory T cells, which suppresses $CD8^+$T-cell proliferation, but also the complement cascade by degradation of C3b. These results were replicated in the murine smoking model, which showed increased C5a that suppressed IL12-mediated bias to Th1 cells and elastin coprecipitation with C3b, suggesting that elastin could be presented as an antigen. Similarly 43 % of patients with severe early onset of chronic obstructive pulmonary disease tested positive for IgG to elastin in their serum compared to healthy controls. These data suggest that higher expression of CD46 in the lungs of ex-smoker protects them from emphysema and chronic obstructive pulmonary disease by clearing the inflammation impeding the proliferation of $CD8^+$T cells and necrosis, achieved by production of T regulatory cells and degradation of C3b; restraining the complement cascade favors apoptosis over necrosis, protecting them from autoimmunity and chronic inflammation [25]. Future research will bring up new insights into the development of emphysema and also identify cigarette-smoking patients who are at risk of developing emphysema and COPD.

References

1. Guarnieri M, Balmes JR. Outdoor air pollution and asthma. Lancet. 2014;383:1581–92.
2. Acharya KR, Ackerman SJ. Eosinophil granule proteins: form and function. J Biol Chem. 2014;289:17406–15.
3. Fusonie D, Molnar W. Anomalous pulmonary venous return, pulmonary sequestration, bronchial atresia, aplastic right upper lobe, pericardial defect and intrathoracic kidney. An unusual complex of congenital anomalies in one patient. Am J Roentgenol Radium Ther Nucl Med. 1966;97:350–4.
4. Riedlinger WF, Vargas SO, Jennings RW, Estroff JA, Barnewolt CE, Lillehei CW, Wilson JM, Colin AA, Reid LM, Kozakewich HP. Bronchial atresia is common to extralobar sequestration, intralobar sequestration, congenital cystic adenomatoid malformation, and lobar emphysema. Pediatr Dev Pathol. 2006;9:361–73.
5. Zylak CJ, Eyler WR, Spizarny DL, Stone CH. Developmental lung anomalies in the adult: radiologic-pathologic correlation. Radiographics. 2002, 22 Spec No:S25–43
6. Brusselle GG, Provoost S, Bracke KR, Kuchmiy A, Lamkanfi M. Inflammasomes in respiratory disease: from bench to bedside. Chest. 2014;145:1121–33.
7. Matsuba K, Thurlbeck WM. The number and dimensions of small airways in emphysematous lungs. Am J Pathol. 1972;67:265–75.
8. Saito K, Thurlbeck WM. Measurement of emphysema in autopsy lungs, with emphasis on interlobar differences. Am J Respir Crit Care Med. 1995;151:1373–6.
9. Stoller JK, Aboussouan LS. Alpha1-antitrypsin deficiency. Lancet. 2005;365:2225–36.
10. Demeo DL, Mariani TJ, Lange C, Srisuma S, Litonjua AA, Celedon JC, Lake SL, Reilly JJ, Chapman HA, Mecham BH, Haley KJ, Sylvia JS, Sparrow D, Spira AE, Beane J, Pinto-Plata V, Speizer FE, Shapiro SD, Weiss ST, Silverman EK. The SERPINE2 gene is

associated with chronic obstructive pulmonary disease. Am J Hum Genet. 2006;78:253–64.
11. Churg A, Wang RD, Tai H, Wang X, Xie C, Dai J, Shapiro SD, Wright JL. Macrophage metalloelastase mediates acute cigarette smoke-induced inflammation via tumor necrosis factor-alpha release. Am J Respir Crit Care Med. 2003;167:1083–9.
12. Wallace AM, Sandford AJ. Genetic polymorphisms of matrix metalloproteinases: functional importance in the development of chronic obstructive pulmonary disease? Am J Pharmacogenomics. 2002;2:167–75.
13. Barnes PJ, Shapiro SD, Pauwels RA. Chronic obstructive pulmonary disease: molecular and cellular mechanisms. Eur Respir J. 2003;22:672–88.
14. Katzenstein AL, Mukhopadhyay S, Zanardi C, Dexter E. Clinically occult interstitial fibrosis in smokers: classification and significance of a surprisingly common finding in lobectomy specimens. Hum Pathol. 2010;41:316–25.
15. Butnor KJ, Guinee Jr DG. Pleuropulmonary pathology of Birt-Hogg-Dube syndrome. Am J Surg Pathol. 2006;30:395–9.
16. Niewoehner DE, Kleinerman J. Effects of experimental emphysema and bronchiolitis on lung mechanics and morphometry. J Appl Physiol. 1973;35:25–31.
17. Ip MP, Kleinerman J, Ranga V, Sorensen J, Powers JC. The effects of small doses of oligopeptide elastase inhibitors on elastase-induced emphysema in hamsters: a dose-response study. Am Rev Respir Dis. 1981;124:714–7.
18. Padilla ML, Galicki NI, Kleinerman J, Orlowski M, Lesser M. High cathepsin B activity in alveolar macrophages occurs with elastase-induced emphysema but not with bleomycin-induced pulmonary fibrosis in hamsters. Am J Pathol. 1988;131:92–101.
19. Morris DG, Huang X, Kaminski N, Wang Y, Shapiro SD, Dolganov G, Glick A, Sheppard D. Loss of integrin alpha(v)beta6-mediated TGF-beta activation causes Mmp12-dependent emphysema. Nature. 2003; 422:169–73.
20. Stefanska AM, Walsh PT. Chronic obstructive pulmonary disease: evidence for an autoimmune component. Cell Mol Immunol. 2009;6:81–6.
21. Lewis EC, Mizrahi M, Toledano M, Defelice N, Wright JL, Churg A, Shapiro L, Dinarello CA. alpha1-Antitrypsin monotherapy induces immune tolerance during islet allograft transplantation in mice. Proc Natl Acad Sci U S A. 2008;105:16236–41.
22. Lee SH, Goswami S, Grudo A, Song LZ, Bandi V, Goodnight-White S, Green L, Hacken-Bitar J, Huh J, Bakaeen F, Coxson HO, Cogswell S, Storness-Bliss C, Corry DB, Kheradmand F. Antielastin autoimmunity in tobacco smoking-induced emphysema. Nat Med. 2007;13:567–9.
23. Ehlers MR. Immune-modulating effects of alpha-1 antitrypsin. Biol Chem. 2014;395:1187–93.
24. Harrison OJ, Foley J, Bolognese BJ, Long 3rd E, Podolin PL, Walsh PT. Airway infiltration of CD4+ CCR6+ Th17 type cells associated with chronic cigarette smoke induced airspace enlargement. Immunol Lett. 2008;121:13–21.
25. Grumelli S, Lu B, Peterson L, Maeno T, Gerard C. CD46 protects against chronic obstructive pulmonary disease. PLoS ONE. 2011;6, e18785.

Airway Diseases

6

6.1 Tracheitis and Bronchitis

Tracheitis and bronchitis are one of the most common diseases in all ages. Acute tracheobronchitis is common in children as well as in old patients, less common in middle ages. The causes are in most instances infections. In children viral infections dominate the infectious spectrum. It usually starts at kindergarten age as a first peak. Later on children also get in contact with bacterial organisms, but most often develop immune protection. In most developed countries, due to vaccination programs, classical infections are decreasing. However, in some countries because of refusal of vaccination by parents, the situation can change.

6.1.1 Gross Morphology

In acute tracheitis/bronchitis, the mucosa is red; hemorrhage can be present especially in viral infections (Fig. 6.1). Later on, in bacterial infections, purulent exudate can be seen and necrosis of the mucosa can develop (Fig. 6.2).

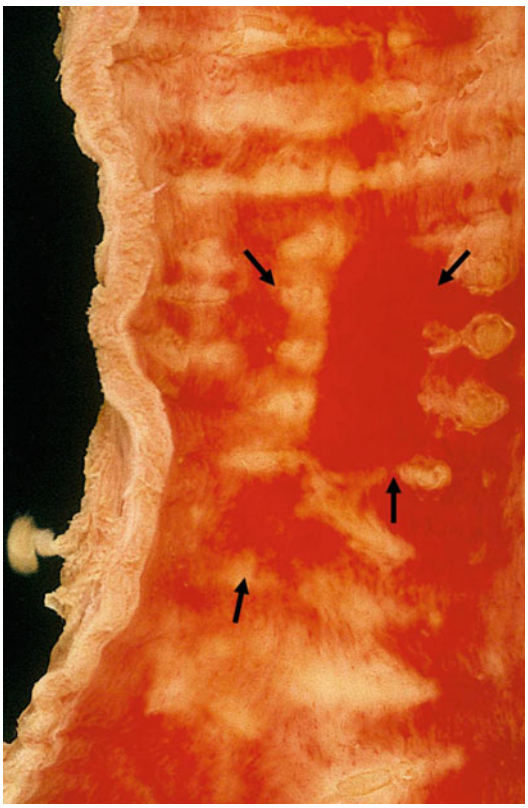

Fig. 6.1 Macroscopic picture of acute tracheitis; most likely this inflammation is caused by viral infection

© Springer-Verlag Berlin Heidelberg 2017
H. Popper, *Pathology of Lung Disease*, DOI 10.1007/978-3-662-50491-8_6

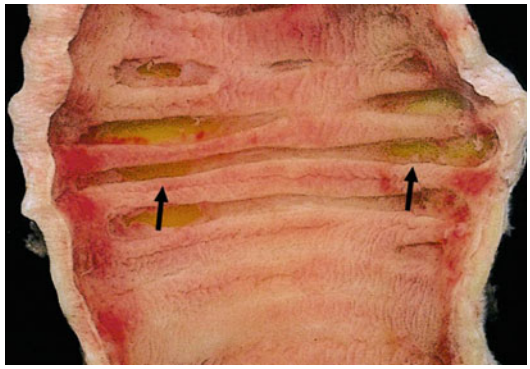

Fig. 6.2 Necrotizing tracheitis. Note the necrosis focally reaching the cartilages (*arrows*). On the surface also fibrinopurulent exudate is present

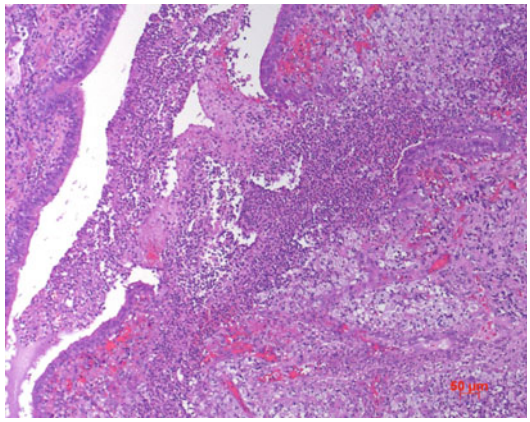

Fig. 6.3 Purulent bronchitis. Focal ulceration of the bronchial mucosa; numerous neutrophils are in the lumen but also infiltrating the necrosis. H&E, bar 50 μm

6.1.2 Histology

In acute bronchitis and tracheitis, the mucosa is infiltrated by numerous neutrophils and will show epithelial damage with/without disruption of the basal lamina (Fig. 6.3). In chronic bronchitis, lymphocytes and plasma cells dominate (Fig. 6.4), and in addition hyperplasia of smooth muscle cells is seen. In recurrent bronchitis, the basal lamina might be thickened, and smooth muscle cells are gradually replaced by fibrocytes depositing collagen, resulting in scarring of the mucosa. Hyperplasia of goblet cells of the mucosa and within bronchial glands is usually a sign of recurrent chronic bronchitis. Hyperplasia

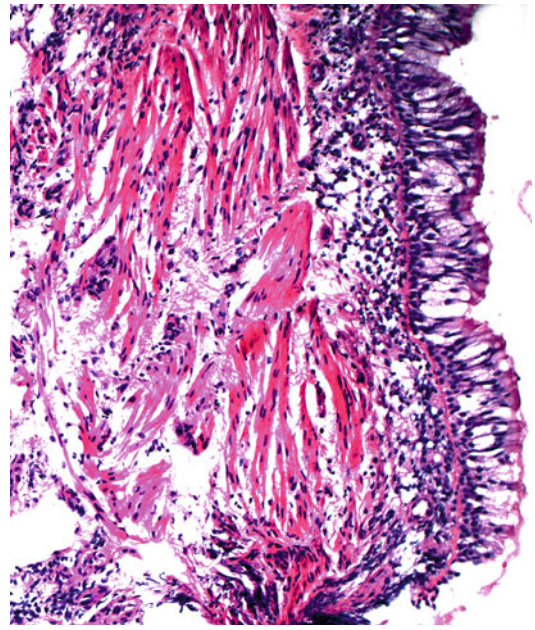

Fig. 6.4 Chronic bronchitis. The infiltration is dominated by lymphocytes and few plasma cells, some of them within the epithelial layer. There is also thickening of the smooth muscle layer. H&E, ×100

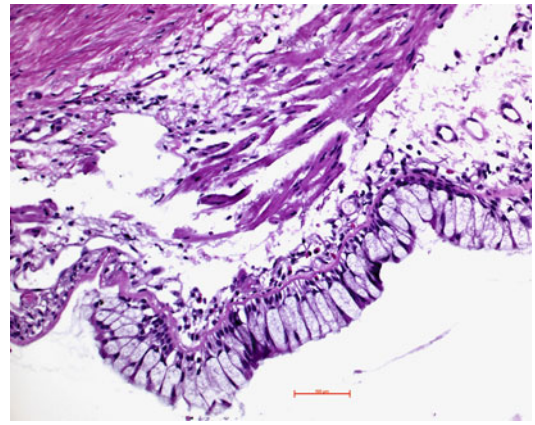

Fig. 6.5 Hyperplasia of goblet cells is a sign of recurrent chronic bronchitis. There are only few lymphocytes, some eosinophils. The ratio of ciliated to goblet cells is changed to approximately 1:3, whereas the normal ratio is 6–8:1. H&E, bar 100 μm

of bronchial glands does occur in those cases where the large bronchi are dominantly involved (Figs. 6.5 and 6.6). In some cases, the morphologic picture might be almost indistinguishable from asthma bronchitis. However, there are

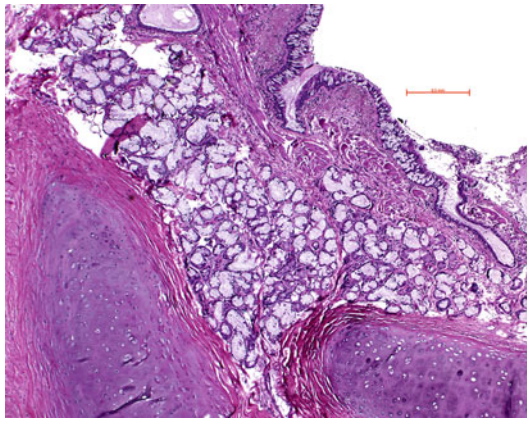

Fig. 6.6 Hyperplasia of bronchial glands. The whole glands are expanded and increased in size. Within the glands, there is also an increase of goblet cells over the serous cells – there should be an equal amount of both cell types. H&E, bar 500 µm

Fig. 6.7 Bronchiectasis with purulent bronchitis. The lumina of the bronchi is filled with pus

differences: squamous metaplasia and hyperplasia of bronchial glands and smooth muscle layer are quite characteristic in chronic bronchitis and chronic obstructive lung disease (COPD) and much less pronounced in asthma bronchitis, where a dense eosinophilic infiltration in the mucosa and submucosa is pronounced. However, in the course of the diseases, this might overlap [1].

In chronic recurrent bronchitis, some additional changes can occur: bronchiectasis can develop, which might pave the way for bacterial colonization and repeated bacterial infections, resulting finally in purulent bronchiectasis

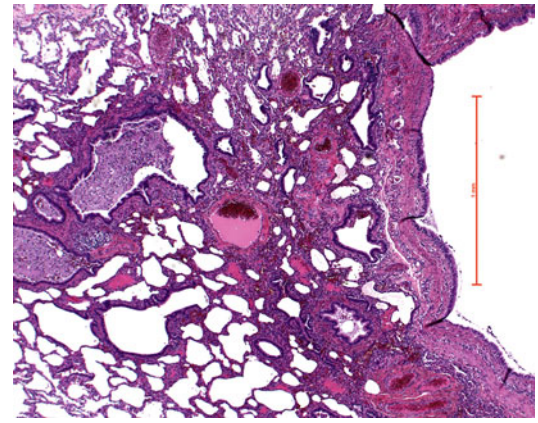

Fig. 6.8 Bronchiectasis and purulent bronchitis. H&E, bar 1 mm

(Figs. 6.7 and 6.8). Another but rare finding is thickening and degeneration of nerves (Fig. 6.9). If this phenomenon is associated with a special form of chronic bronchitis and is accompanied by a characteristic type of cough, it needs to be explored.

Acute bronchitis is most often caused by bacterial or viral infection, in rare instances by inhalation of noxious gases. By far the most common cause of chronic bronchitis is tobacco smoke, followed by air pollution and occupational exposure to noxious substances (will be discussed in the chapters on pneumonia, pneumoconiosis, and environmentally induced diseases). Many of the constituents of tobacco smoke are toxic to the respiratory epithelium, especially to the ciliated cells [2]. In addition heat slows down the beating frequency of the cilia. Loss of ciliated cells and lowered beating frequency together result in prolonged contact of the toxic substances to the epithelium, followed by toxic injury of increasing numbers of cells. Air pollution now very common in megacities of the developing countries is composed of gaseous substances and particulate matter. The gaseous phase is composed of combinations of sulfuric and nitric oxides, but also low amounts of ozone and polyaromatic hydrocarbons can be found [3–5]. Within the particle fraction, many different substances can be found: coal ash particles from combustion, metal oxides from industrial waste and automobile exhaust, and silica and silicates [6–10].

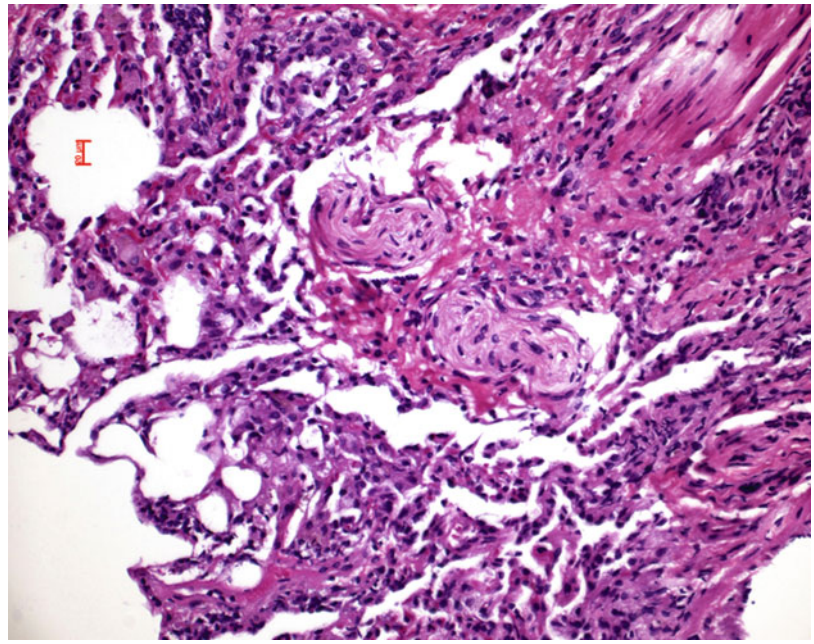

Fig. 6.9 Within the bronchial wall, thickened (hyperplastic) nerves can be seen. Most likely this represents degeneration, as there are too many Schwann cells. The type of these nerves cannot be analyzed, because antibodies for kininogens and adrenergic substances do not work on FFPE tissues. H&E, bar 20 µm

6.2 Bronchial Asthma

6.2.1 Etiology

Bronchial asthma is a chronic inflammatory disease of the conducting airways, in which the epithelium and cells of the innate and adaptive immune system are involved. Asthma affects approximately 300 million people worldwide, and its incidence is increasing especially in developed countries. The leading symptom is hyperreactivity of the airway smooth muscle cells. Clinically it is characterized by shortness of breath, wheezing, and chest tightness. Traditionally asthma was separated into allergic (intrinsic) and nonallergic (extrinsic) asthma, but in recent years within nonallergic asthma, several so-called endotypes have been identified. So asthma is no longer regarded as a single disease but rather a syndrome [11]. These endotypes differ with respect to genetic susceptibility, environmental risk factors, age of onset, clinical presentation, prognosis, and response to treatment [12].

6.2.2 Immune Mechanisms

A huge amount of literature has accumulated on different immune mechanisms involved in asthma. It is impossible to discuss these data in this book; therefore, the reader is directed to several relevant reviews on the subject [11–20]. Here we will try to summarize the most relevant aspects.

Allergic asthma is a Th_2-driven disease, however, in patients Th_2^{high} and Th_2^{low} clusters have been identified [21], characterized by high IL4, IL5, and IL13 and eosinophilia in blood and tissues. In Th_2^{high} clusters, there is also high IgE, which characterizes these asthma patients as driven by IL4-induced class switching of immunoglobulins synthesized by B cells – these patients will also present with a history of atopy [22]. These patients are sensitized against a wide array of allergens, such as house dust mite, tree pollen, animal dander, and fungal spores [23]. Children in a family with atopy have a higher propensity to develop asthma. These children can present with allergic eczema already within the

first year of life and in a high proportion will develop asthma later in their life. A good marker for this asthma endotype is a high serum level of IL25 and periostin, which also correlates well with tissue eosinophilia [24]. In these patients, new treatment options have been opened, such as blockade of IL4 and IL5 receptors. In addition to a specific allergen-oriented immune reaction by primed lymphocytes, also cells of the innate immune system are involved: in asthma innate lymphoid cell 2 (ILC2) plays a major role. ILC2 do not have antigen-specific receptors, but they similarly produce IL13, IL5, and IL9 as Th_2 cells when stimulated by epithelial-derived IL25, IL33, and thymic stromal lymphopoietin (TSLP) [12, 25, 26]. ILC2 are activated early on after allergen exposure, but can also respond to viral infection: in influenza infection, they produce IL5 and elicit an eosinophil infiltration. A recently detected player in asthma is Th_9 cells; they secrete IL9 which is a survival factor for ILC2 and a proliferation factor for mast cells; IL9 also promotes IL4-driven antibody production by B cells.

Much research has also been done evaluating the role of regulatory T cells (Treg). Treg are decreased and functionally impaired in asthma; experimentally it has been shown that they can suppress asthma by secretion of IL10 and suppress IL17-induced bronchial hyperreactivity. However, their role is not entirely clear, probably because there are different populations of Treg acting such as $ICOS1^+$Treg, which are probably the important population capable of counteracting asthma [17, 27].

One of the most important cells in asthma are dendritic cells (DCs). In the bronchial mucosa, three different types have been identified: common DC expressing $CD11b^+CD172^+$(SIRP1alpha) sufficient to induce allergic sensitization and DC expressing $CD103^+XCR1^+$ which will need additional IRF8 and BATF3 stimulation for sensitization; in contrast plasmacytoid DC counteract by inducing tolerance via $FOXP3^+$ Treg [17, 18, 28]. However, DCs always interact with epithelial cells from the mucosa.

Epithelia among other functions are responsible to maintain an intact epithelial barrier. Many allergens possess a protease activity; for example, papain decreases epithelial barrier by cleaving tight junction proteins and stimulating innate cytokine response. Aspergillus fumigatus spore protease leads to fibrinogen cleavage, and these metabolites activate Toll-receptor 4 on epithelia; airway cells in response secrete IL33 and TSLP and GM-CSF, which in turn activates DC-$CD11b^+$ and also ILC2. This again induces a Th_2 polarization, thus orchestrating the allergic response [16, 17, 29–31]. Some allergen also can contain an endotoxin fraction. In this case an additional Th_1 reaction is mounted. This links to so-called neutrophil asthma. An example has been shown in high exposure to diesel exhaust. This type of asthma is associated with Th_{17} cells; secretion of IL17 is also found in exacerbation in asthmatic children, which again can be stimulated by polluted air. This simultaneous activation of Th_2 and Th_{17} profile producing $CD4^+$ cells ($CD4^+IL4^+IL17^+$ cells) has been termed overlap syndrome [12, 32–34]. It could also be produced in experimental models.

A reduced barrier function has been shown recently by genetic studies. In atopic children, a single nucleotide polymorphism has been found for filaggrin, a protein functioning in tight junction stability; filaggrin controls the production of TSLP and IL1RL1 (the receptor for IL33); this modified protein does not function properly. In this context, nonallergic asthma caused by smoking, viral infection, and air pollution acts similarly on downregulation of the epithelial barrier function and subsequently epithelial-DC interaction.

Recently also an overlap of asthma and COPD has been described [35, 36]. Probably this again refers to a combination of Th_2 and Th17 polarization of the adaptive immune system and epithelial barrier disruption induced by cigarette smoke. However, much more has to be learned until this phenomenon is really understood. Initially mast cells were regarded as important in asthma. Recently the role of mast cells has been

mainly attributed to Th_2^{high}, IgE^{high}, and atopy-associated asthma. But more likely basophils within the epithelia play a more prominent role. Both cells interact with eosinophils in promoting the release of cytotoxic eosinophilic granules [37]. Thus they are responsible for some of the morphologic changes seen in asthma biopsies.

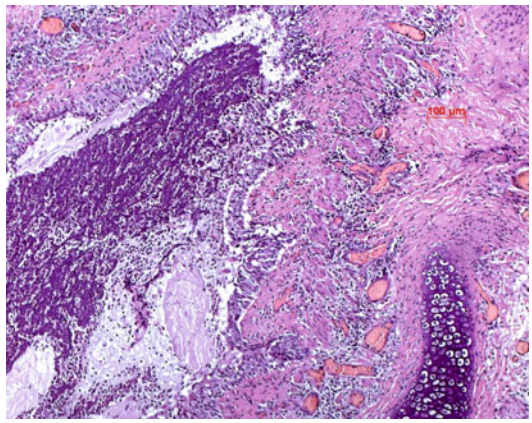

Fig. 6.10 Bronchial asthma in a 2-year-old girl dying in asthma attack. There is an inspissated mucus mixed with numerous eosinophils in the bronchial lumen; eosinophils and lymphocytes are seen within the mucosa. The muscular layer is thickened, although not as much as it is seen in long-standing asthma. H&E, bar 100 µm

6.2.3 Gross Morphology

The main finding of lung specimen of patients dying of asthma usually asthma attacks is hyperinsufflation of both lungs. Usually both lungs completely overlap the heart. Alveoli are visible at the surface. The pleura is normal unaffected. On cut surface, the only important finding is mucus impaction in the bronchi and bronchioles. If the lung is left for an hour, the trapped air vanishes and the lung shrinks to normal.

6.2.4 Histology

Biopsies or autopsy lung specimen of patients with bronchial asthma will show infiltration by eosinophils within the bronchial mucosa, spissated mucus with masses of eosinophils, Curshmann's spirals (Figs. 6.10, 6.11, and 6.12), and different amounts of lymphocytes (depending to the disease activity). Mast cells and more important basophils highlighted by immunostains for tryptase and chymotryptase are seen in IgE^{high} atopic asthma. Goblet cells within the mucosa and the bronchial glands are increased; smooth muscle cells are hyperplastic in early

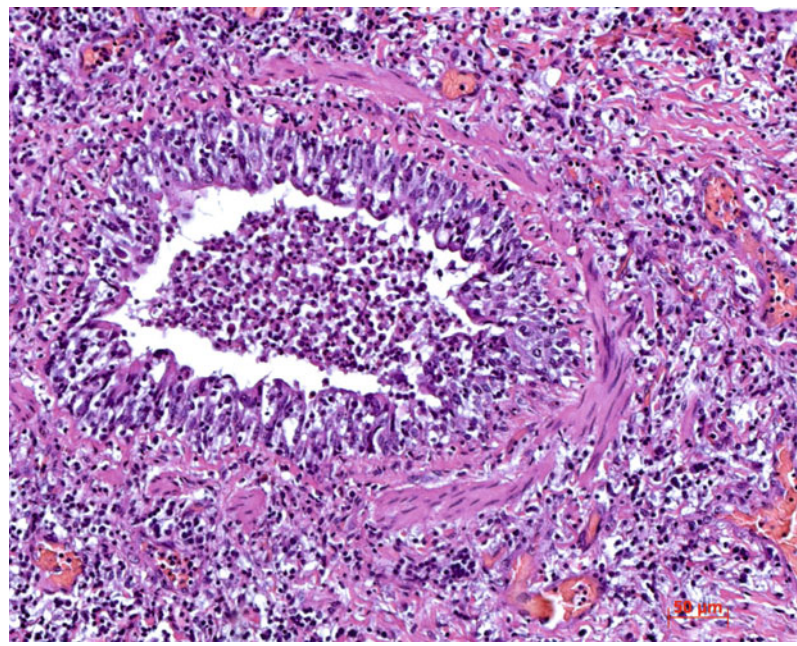

Fig. 6.11 Same case, showing a small bronchus densely infiltrated by eosinophils in the lumen and bronchial mucosa. There are also many lymphocytes within the bronchial wall. H&E, bar 50 µm

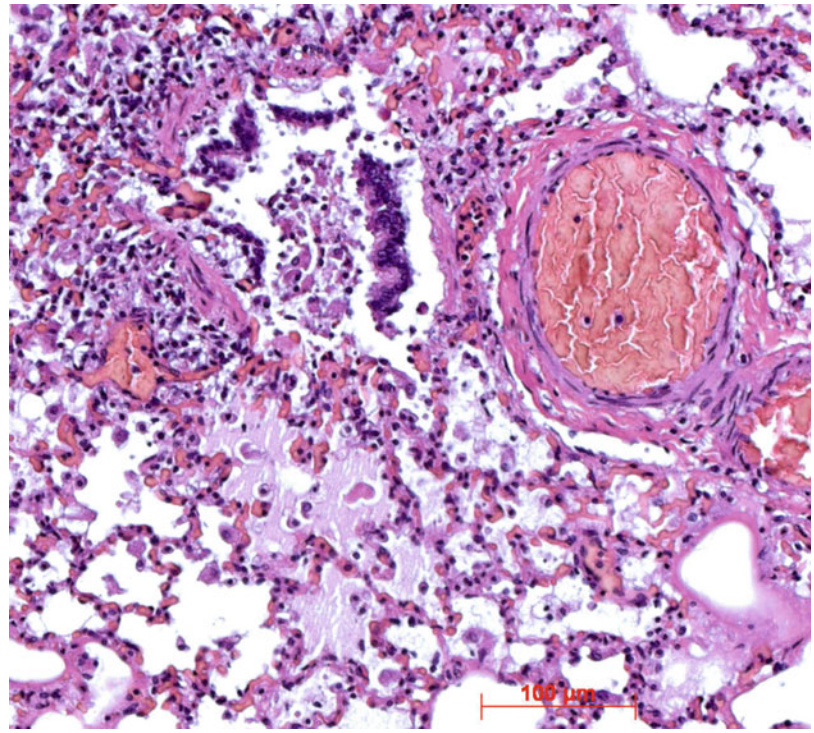

Fig. 6.12 Same case, the inflammatory infiltrate can be seen down to the bronchioles. H&E, bar 100 µm

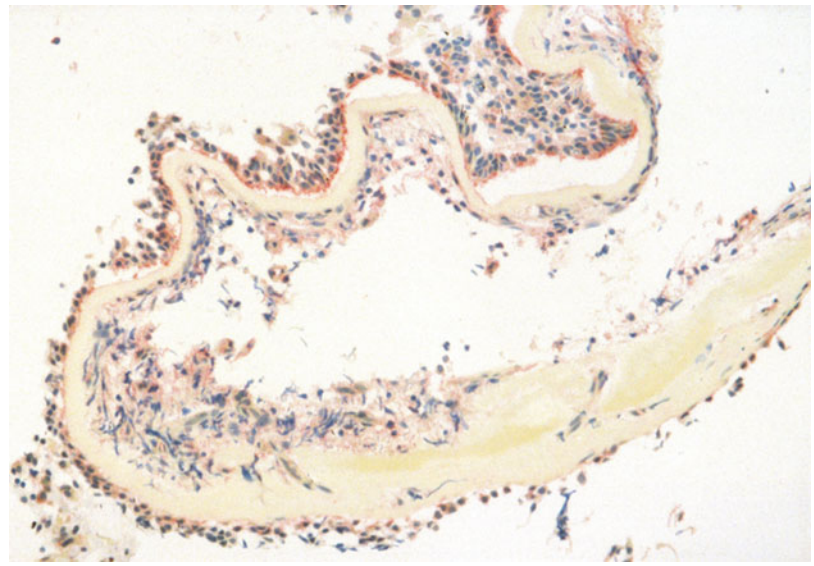

Fig. 6.13 Bronchial biopsy in bronchial asthma. Within the mucosa, there is shedding of columnar cells including ciliated ones. Another feature is massive thickening of the basal lamina. Although thickening does occur also in COPD bronchitis, it is much more pronounced in asthma. Immunohistochemistry for ICAM-1 showing downregulation of this molecule in the columnar cells but not in basal cells, ×100

stages, but may be replaced by fibrosis in long-standing asthma. Epithelial disruption is another characteristic feature of asthma bronchitis: the epithelial layer shows shedding of columnar cells; only basal cells remain firmly attached to the basal membrane. The basal lamina is typically thickened and on electron microscopy will show several layers, each newly formed after repair of an acute asthma attack and induced by TGF-β (also called airway remodeling; Fig. 6.13).

The major differential diagnosis is chronic bronchitis in COPD. There is no single feature

which allows a certain distinction of both diseases; however, a combination of features can most likely be of help: eosinophilia, epithelial shedding, hyperplasia of smooth muscle cells, and extreme thickening of the basal membrane are together in favor of asthma bronchitis [1].

6.3 Bronchiolitis

Bronchioles are small airways defined by an inner diameter ≤1 mm. Bronchioles have a thin muscular layer and are devoid of cartilage. Bronchioles start at the 16th generation of airways. The epithelial layer is composed of a mixture of Clara, ciliated and secretory columnar, and few goblet cells. At the basal lamina, there is also a layer of triangular-shaped basal cells and atop of them polygonal reserve cells. At the larger bronchioles, the thickness of the epithelial layer is three cell layers, but toward the terminal bronchioles, the epithelial layer is reduced to two layers, basal cells and Clara cells with a few interspersed columnar cells [38]. Regeneration starts from Clara cells and reserve cells, whereas basal cells are functioning to serve as attachments for the columnar cells [39–41]. At the bronchioloalveolar junction zone (BJZ), a terminal stem cell has been identified, which expresses Clara cell protein 10 (CC10), surfactant apoprotein C, and stem cell markers [42].

Bronchiolitis most often is associated with either bronchitis such as in asthma or is associated with pneumonia; an example is organizing pneumonia. However, there are two reasons to discuss bronchiolitis separately: bronchiolitis is the underlying pathology in clinically called small airways disease, and it does occur sometimes as an isolated disease confined only to bronchioles.

6.4 The Classification

At present we best classify bronchiolitis into:

A. **Acute bronchiolitis**
B. **Chronic bronchiolitis**
C. **COPD-associated bronchiolitis**
D. **Distinct forms of bronchiolitis**

A. The term cellular bronchiolitis is sometimes used. However, chronic bronchiolitis can also be cellular; therefore, this term will not be used throughout this chapter. If no specific inflammatory pattern is recognized, an acute bronchiolitis NOS (not otherwise specified) can be diagnosed. It is characterized by a dense granulocytic and/or lymphocytic infiltrate within the epithelium, the subepithelial, as well as the muscular layers. The epithelium can show different degrees of degenerative as well as reactive changes, but there should be no metaplasia or hyperplasia. Usually a mixture of granulocytes and cellular debris fills the lumen. Acute bronchiolitis can be caused by a variety of infectious organisms, as respirotropic viruses, bacteria, and inhaled toxic substances. The degree of the inflammatory infiltrate might be used to sort the etiology: if granulocytic infiltrates predominate within the surface layer of the mucosa, the cause of bronchiolitis is most often infectious. If eosinophils predominate with necrosis of the epithelium, either an immune mechanism such as asthma is the underlying condition or a parasitic infection. If the inflammatory infiltrate is more pronounced in deeper layers of the mucosa, i.e., within the muscularis, other etiologies have to be considered. Within acute bronchiolitis, specific entities can be separated:

A1. *Eosinophilic or asthmatic bronchiolitis*
A2. *Pseudomembranous and necrotizing bronchiolitis*
A3. *Granulomatous bronchiolitis*

A1. **Eosinophilic or asthmatic bronchiolitis** is characterized by a mixed infiltration of eosinophils, mast cells/basophils, plasma cells, and lymphocytes within the bronchiolar wall. The most characteristic feature is eosinophilia, which can be highlighted by a Congo red stain, picking up the basic cytotoxic proteins of eosinophilic granules. By this stain, even degranulation and extracellular granules can be seen (Fig. 6.14). Other

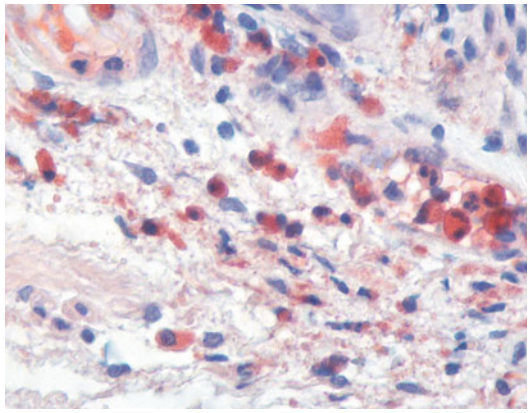

Fig. 6.14 Degranulation of eosinophils in asthma. The basic proteins are stained by Congo red, and released granules and content are still visible in the stroma of this small bronchus. Congo red stain, ×630

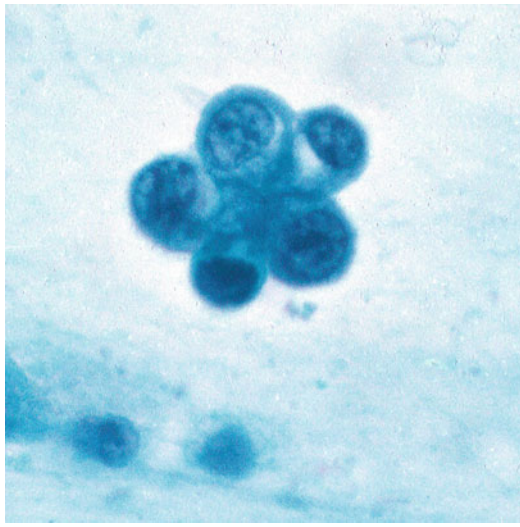

Fig. 6.15 Induced sputum cytology in a patient with asthma. A cluster of bronchiolar Clara cells is seen. Giemsa stain, ×630

diagnostic features of asthma bronchiolitis are mucus plugs in the lumen containing cellular debris, eosinophils, Curshmann's spirals, and Charcot-Leyden crystals, a prominent thickening and even hyalinization of the basal lamina, and a shedding of the columnar cells. Sometimes clusters of peripheral bronchiolar cells can be seen, mainly Clara and goblet cells (Fig. 6.15). Immunohistochemically there is an upregulation of VCAM-1 on the endothelial cells of

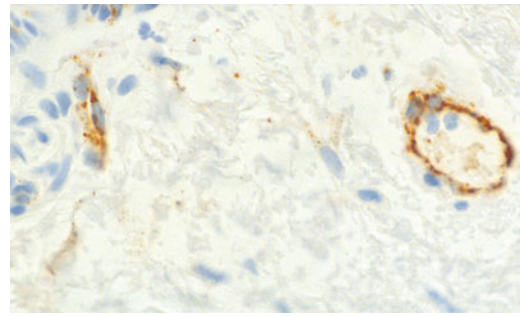

Fig. 6.16 Upregulation of VCAM-1 in epithelial as well as endothelial cells in asthma. VCAM-1 facilitates the influx of eosinophils into the bronchial mucosa. Immunohistochemistry with VCAM-1 antibodies, ×250

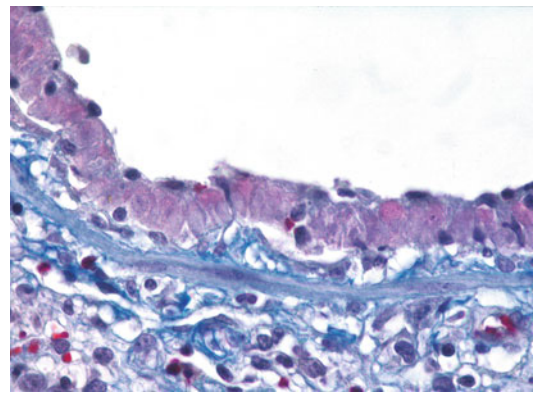

Fig. 6.17 Necrotizing bronchiolitis. Experimental gastric aspiration syndrome in pigs. The mucosa is completely necrotic and denuded. The basal lamina remains in part intact. Trichrome stain, ×400

small blood vessels (Fig. 6.16) as well as a disease-specific upregulation of VLA 4 and ICAM-3 on lymphocytes and eosinophils. The shedding of columnar cells might be due to a loss of intercellular adhesion molecules like VLA 1–3, 5, and 6, and an upregulation of ICAM-1 on these cells, by which they lose contact especially to the triangular-shaped basal cells. The muscular coat can either show hyperplasia or atrophy, most likely related to the duration of the disease.

A2. **Acute necrotizing and pseudomembranous bronchiolitis** is characterized by necrosis of the epithelial layer with or without disruption of the basal lamina (Fig. 6.17).

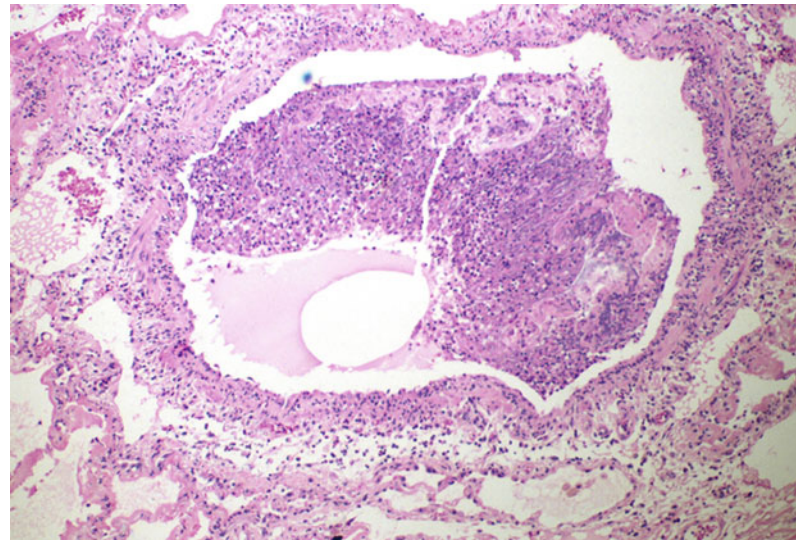

Fig. 6.18 Necrotizing bronchiolitis in a case of influenza A virus infection. See also the hyaline membranes in the nearby alveoli. H&E, 160

Cellular infiltrates may be predominantly neutrophilic or lymphocytic or a mixture of both. The cellular composition reflects most often the specific response to the causing agent, like lymphocytic infiltration early on in viral infection. The necrotic debris is mixed with fibrin leaking out from the capillaries beneath the basal lamina. In the case of pseudomembranous bronchiolitis, this fibrin together with debris forms the pseudomembrane on the bronchiolar surface. There are certain organisms, which can cause this condition: influenza and parainfluenza and also herpes viruses (Fig. 6.18). A classical example of pseudomembranous bronchiolitis caused by a bacterium is *Bordetella pertussis* bronchiolitis. Pseudomembranous bronchiolitis can progress into bronchiolitis obliterans with complete or incomplete occlusion of the bronchiolar lumen. The same kind of viruses can cause also necrotizing bronchiolitis. These viruses probably belong to more virulent strains. Some inhaled toxins like SO_X, NO_X, and O_3 at higher than ambient air concentrations can cause necrotizing bronchiolitis. Some acidic aerosols can cause this bronchiolitis, as in Mendelson syndrome, where hydrochloric acid together with pepsin is the noxious agents. Due to the fact that the basal lamina is destroyed or at least interrupted, this kind of bronchiolitis will never heal "ad integrum" and will progress into bronchiolitis obliterans organizing pneumonia.

A3. **Granulomatous bronchiolitis/bronchitis** is a condition often seen in sarcoidosis and tuberculosis; however, other kinds of granulomatoses should be kept in mind. Granulomatous bronchiolitis may show the classic sarcoid granuloma with or without necrosis or a mixture of sarcoid and palisading histiocytic granulomas (Fig. 6.19). If there is necrosis, tuberculosis should be suspected, and being without necrosis mycobacteriosis or sarcoidosis is the major differential diagnoses to be considered. In rare cases, occupational exposure to beryllium or zirconium oxides may mimic sarcoidosis. If mixtures of histiocytic and epithelioid cell granulomas together with infiltrating granulocytes are seen, a diagnosis of broncho- and bronchiolocentric granulomatosis can be made. If there is substantial eosinophilic infiltration, an allergic bronchopulmonary mycosis (aspergillosis, ABPA) might be the underlying disease; however, parasitic infection has to be ruled out. If a neutrophilic infiltration predominates, bacterial infection is the most likely

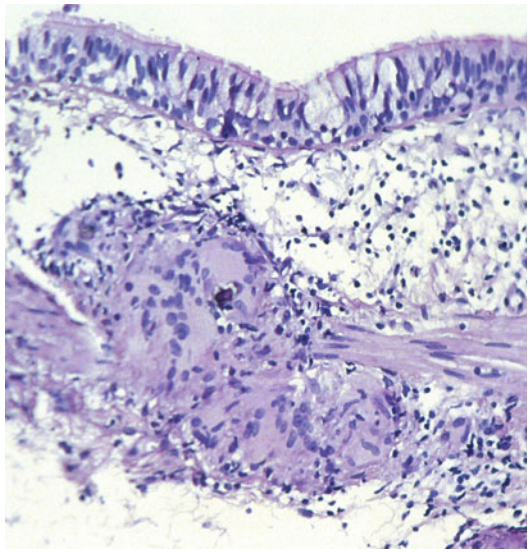

Fig. 6.19 Granulomatous bronchitis/bronchiolitis with two epithelioid cell granulomas. Due to the fact that the granulomas are close to the surface epithelium and these cells do not show any inflammation-associated changes, an infectious cause is unlikely. Here it is sarcoidosis. H&E, ×200

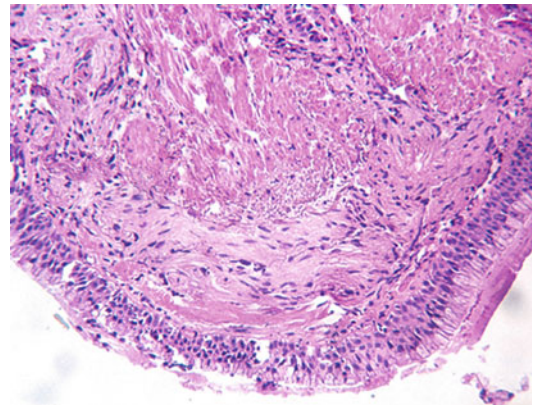

Fig. 6.20 Chronic bronchitis/bronchiolitis; hyperplasia of the muscle cell layer, but toward the surface fibrosis is already focally present. H&E, ×200

cause, very often mycobacterial infection. If there is a pure histiocytic granulomatous bronchiolitis, rare infectious diseases and occupational lung disease have to be considered. Granulomatous leprosy very rarely involves the lungs; more often *M. avium* and other slow-growing mycobacteria in the setting of immunocompromised patients might induce a pure histiocytic granulomatous bronchiolitis. Other rare examples of infectious histiocytic granulomatous bronchiolitis are involvement of the lung in Whipple's disease and infections with *Listeria monocytogenes*.

Histiocytic granulomatous bronchiolitis is seen in occupational lung disease. It can be found in silicosis, silicatosis, coal worker's pneumoconiosis, and asbestosis. However, granulomas are usually early lesions, more related to exposure, and not encountered in full-blown disease. In most instances, the etiologic diagnosis can be made easily by either polarized microscopy or by the proof of foreign material.

In rare instances, autoimmune disorders may underlie palisading histiocytic granulomatous bronchiolitis, especially rheumatoid arthritis with lung involvement. Most other collagen vascular diseases do not induce granuloma formation.

B. **Chronic bronchiolitis** can be defined by a predominant lymphoplasmacytic infiltrate, a goblet cell, and a smooth muscle hyperplasia. Goblet cell hyperplasia is defined by a change of the ciliated to goblet cell ratio in favor of goblet cells (normal 6–8:1). Since there is an individual variation of this ratio in humans, a clear cutoff point is a ratio of ≤4:1 (Fig. 6.5). Muscle cell hyperplasia is not always present (Fig. 6.20): in long-standing chronic bronchiolitis and in some special forms (concentric bronchiolitis), the muscle layer may be replaced by fibrous tissue. Other features seen sometimes in chronic bronchiolitis but more often in bronchitis are nodular thickening of nerves (Figs. 6.9 and 6.21) and fibrosis of the basal lamina. The later one never reaches the extent seen in asthma bronchiolitis. Eosinophils may be present in chronic bronchiolitis, especially in bronchiolectasis; however, they do not stain with VLA 4 and ICAM-3 antibodies, as in asthma [43].

In the etiology of chronic bronchiolitis, the same causes as in acute forms are encountered: infections

with respirotropic viruses, bacteria, fungi, allergic reactions, autoimmune diseases, graft versus host disease (GVHD), inhalation of toxic substances, and airborne dust. Over all chronic bronchiolitis in the majority of patients is induced by continuous tobacco smoke inhalation. In some cases, a causative agent cannot be identified, and therefore the etiology remains unknown (clinically referred to as cryptogenic bronchiolitis).

In young-aged patients with recurrent bronchitis/bronchiolitis and combined rhinosinusitis, an i**mmotile cilia syndrome** (**ICS**) might be suspected. This disease is characterized by a partial or total loss of the inner and/or outer dynein arms of the cilia axonemata [44] (Fig. 6.22). This results in uncoordinated cilia beats and subsequentially loss of ciliated cells due to recurrent infection. One of the clearance mechanisms of the lung, the mucus escalator system, does not function properly. There may be inflammation-related features, like giant cilia, loss of one layer of cilia membranes, loss of spikes, and axonemata.

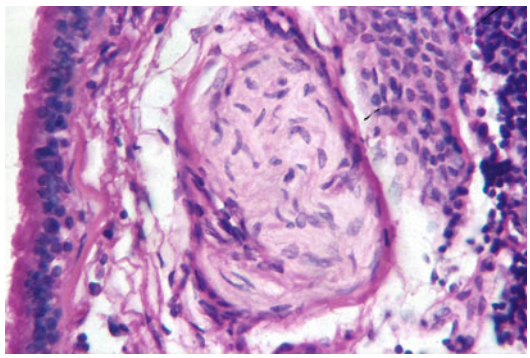

Fig. 6.21 Nodular thickening of nerve fibers by a proliferation of Schwann cells; this more likely is due to a degeneration of nerve fibers. H&E, ×400

C. **Chronic bronchiolitis combined with COPD** might be defined by a combination of pathologic and clinical features; however, the diagnosis can also be made by pathological examination alone: if there is centrilobular emphysema combined with chronic bronchitis/bronchiolitis, a diagnosis of COPD can be established (Fig. 6.23). This will not match with the clinical diagnosis in every case, because the clinical assessment is based on lung function studies, which are much less sensitive than morphologic analysis of the tissue. Especially in those cases where an open lung biopsy specimen is eval-

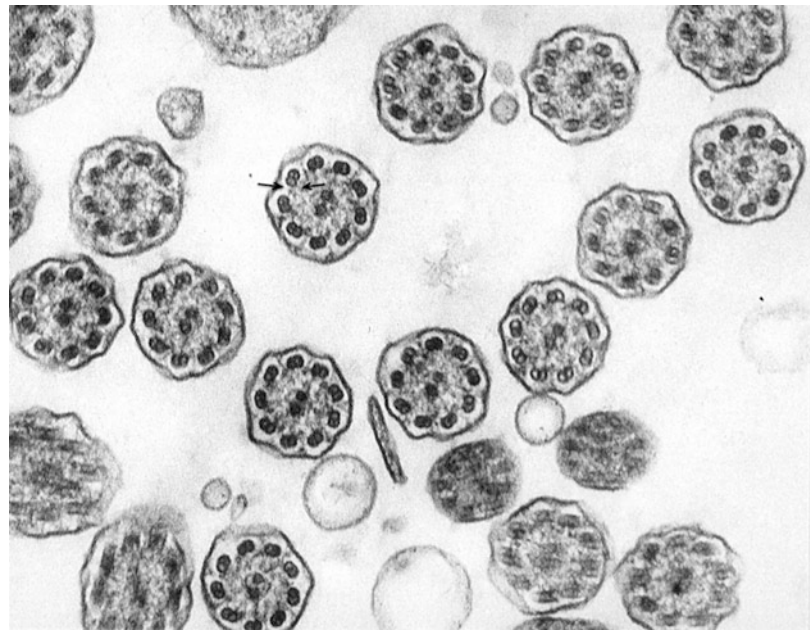

Fig. 6.22 Immotile cilia syndrome; both dynein arms are lost in this case. The arrows point to the area, where the dynein arms are usually located. Electron micrograph, ×19000

Fig. 6.23 Surgical resection specimen in a case of chronic bronchitis, bronchiectasis, and emphysema. In the *upper panel*, chronic purulent bronchitis/bronchiolitis is seen, combined with bronchiectasis (*left side*). In the lower panels, the peripheral lung tissue with centrilobular emphysema is demonstrated. In such a case, the diagnosis of "chronic obstructive pulmonary disease" (COPD) can be made

uated (due to pneumothorax, recurrent pneumonia, or volume reduction surgery) and bronchiolectases and centrilobular emphysema are seen, the diagnosis can be made with confidence.

D. **Special variants of bronchiolitis**. All these variants either arise from an acute bronchiolitis or have a distinctive acute phase. Our knowledge, why and how these variants develop, is still limited. Some of these forms have a narrow spectrum of etiologic causes, like respiratory bronchiolitis, whereas others are seen in a variety of infectious and noninfectious conditions like bronchiolitis obliterans organizing pneumonia. However, they all have in common some unique features, by which they can be differentiated from ordinary bronchiolitis, and due to their special etiologic background must be sorted out. These different variants have to be considered:

D1	*Bronchiolitis obliterans*
D2	*(Bronchiolitis obliterans combined) organizing pneumonia*
D3	*Constrictive bronchiolitis*
D4	*Respiratory bronchiolitis*
D5	*Respiratory bronchiolitis combined interstitial lung disease*
D6	*Follicular bronchiolitis*
D7	*Diffuse panbronchiolitis*
D8	*Airway-centered lung fibrosis*

It might be considered to include Langerhans cell histiocytosis also in this spectrum of bronchiolitis, because bronchioles are predominantly involved. But since Langerhans cell histiocytosis does involve the bronchi, bronchioles, and alveolar tissues and also is almost exclusively a smoking-related disease, it will be discussed in another chapter. In addition a reactive form has to be separated from a tumor-like form in Langerhans cell histiocytosis.

D1. **Bronchiolitis obliterans** (**BO**) can arise from acute bronchiolitis, like necrotizing bronchiolitis, or starts as a focal necrosis of the epithelial layer and submucosal tissue, with disruption of the basal lamina. This defect is subsequently organized by an inflammatory granulation tissue, growing into the bronchial lumen like an inflammatory polyp (Fig. 6.24). The cellular infiltrates are composed of macrophages, lymphocytes, fibroblasts, and myofibroblasts. The granulation tissue can either completely occlude the bronchiolar lumen or leave a narrow slit-like space. When the granulation tissue matures, more matrix proteins are deposited and less inflammatory cells are seen. There may be an epithelial regeneration overgrowing the polyp. The end stage is

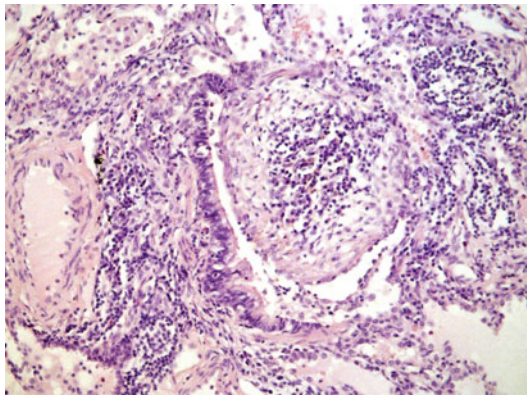

Fig. 6.24 Bronchiolitis obliterans (BO). A granulation tissue is growing into the bronchiolar lumen, completely obstructing the lumen. H&E, ×250

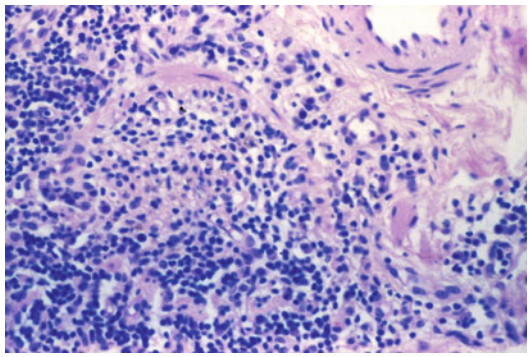

Fig. 6.25 BO in a 4-year-old girl due to graft versus host disease (GVHD); there was a bone marrow transplantation because of leukemia. H&E, ×200

Table 6.1 Causes of specific forms of bronchiolitis

Type of bronchiolitis	Etiology
Bronchiolitis obliterans	Graft versus host disease, collagen vascular diseases, rejection in heart-lung transplantation, idiopathic
Organizing pneumonia	Non-resolved infectious pneumonias, toxic gas inhalation, inhalation of insecticides/pesticides, gastric juice inhalation, autoimmune diseases, drug toxicity, idiopathic
Constrictive bronchiolitis	Graft versus host disease, collagen vascular diseases, rejection in heart-lung transplantation, drug reaction
Respiratory bronchiolitis and RB combined interstitial lung disease	Tobacco smoking, rare idiopathic
Follicular bronchiolitis	Recurrent viral infection, immunodeficiency, autoimmune diseases, immune defects (T cell or NK), idiopathic; part of HP/EAA
Diffuse panbronchiolitis	Immune defect associated with the HLA system
Airway-centered interstitial fibrosis (ACIF)	Hypersensitivity pneumonia, collagen vascular diseases, inhalation of toxic substances, idiopathic

partial or complete obliteration of the lumen. From a functional aspect, airflow is impaired in either case. The etiologic background in BO includes chronic rejection of lung and heart-lung transplants, graft versus host reaction in bone marrow transplants (Fig. 6.25), collagen vascular diseases (lung involvement in rheumatoid arthritis or polymyositis), and idiopathic, respectively (see Table 6.1).

D2. **Bronchiolitis obliterans organizing pneumonia**, **now organizing pneumonia** (**OP**), is characterized by BO as described above and in addition by inflammatory granulation tissue within alveoli (Figs. 6.26 and 6.27). As in the bronchioles, OP can be preceded by alveolar cell damage, including disruption of the basal lamina. But there are also cases, where this granulation tissue extends along terminal bronchioles and alveolar ducts into alveoli; and no primary defect can be seen in the alveolar wall. From a functional standpoint, this organizing alveolar process results in gas exchange and diffusion abnormalities. OP is a classical reaction pattern of non-resolved acute bronchiolitis combined with interstitial or alveolar pneumonia. For a long time, it was known in the German pathologic literature as "carnification," although it should be mentioned that other types of interstitial pneumonia were also included in that entity.

A wide variety of diseases can process along OP-morphology: non-resolved infectious diseases,

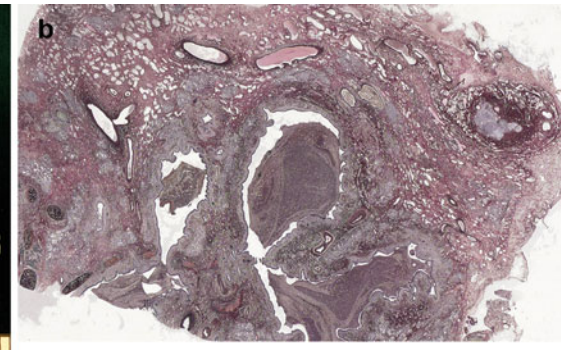

Fig. 6.26 Organizing pneumonia (OP); (**a**) a resection specimen is shown with consolidation of lung tissue; note the loss of the bronchi and bronchioli. (**b**) Corresponding tissue section showing the occlusion of bronchi and bronchioles, but also the consolidation of alveolar spaces by granulation tissue. Movat stain, ×16

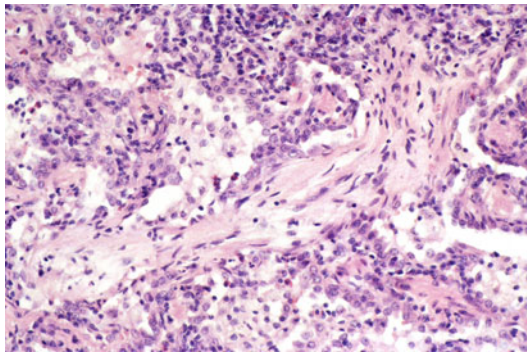

Fig. 6.27 OP; the growth of the granulation tissue within the alveoli is shown. There is a scattered infiltration by lymphocytes and a few eosinophils; pneumocytes type II are covering many alveoli as a sign of regeneration. H&E, ×160

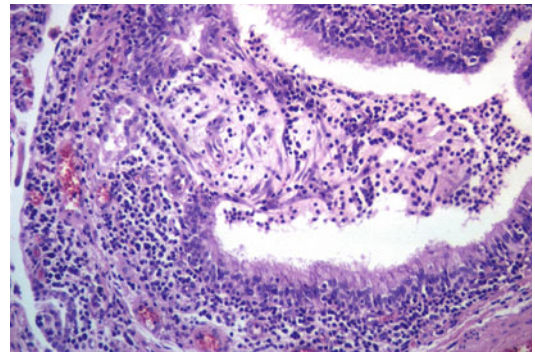

Fig. 6.28 OP in a case of toxic NO_x inhalation; car accident of the patient with a tank truck filled with NO_x. The patient was squeezed in the car for 6 h until he could be released, but died 2 days later. H&E, ×150

viral, bacterial, fungal, or parasitic. Other causes are inhaled toxic gases like SO_x, NO_x (Fig. 6.28), and gastric juice aspiration syndrome (Mendelson disease), which in the organizing phase progress into OP (Fig. 6.29). In most of these cases, focal remnants of the acute phase can persist, for example, a necrotizing bronchiolitis combined with an acute interstitial pneumonia and diffuse alveolar damage in viral infection. This preceding viral infection might also be suspected, because of virus-induced proliferations of type II pneumocytes and bronchiolar epithelial cells, which can persist for some time. This can be proven by immunohistochemical or in situ hybridization

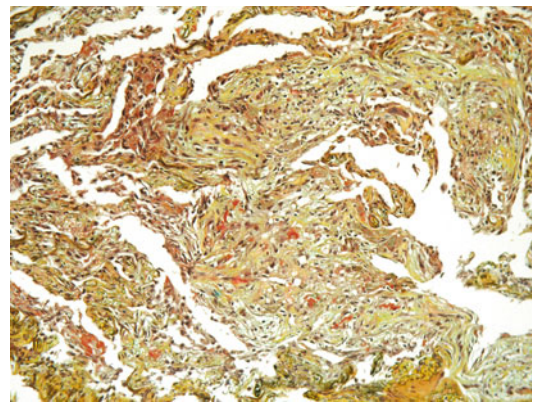

Fig. 6.29 Gastric juice aspiration syndrome. OP is the main finding in this case. Granulation tissue has already been replaced by fibrosis. Movat stain, ×100

analysis. Autoimmune diseases such as rheumatoid arthritis, polymyositis, and systemic lupus erythematosus very often affect the lungs by an OP pattern. In rare cases, Wegener's granulomatosis can present with OP morphology. And hemophagocytic syndrome, either acquired or inborn, in late stages shows OP morphology.

A wide variety of drugs can induce OP. Among them are many cytotoxic drugs like cyclophosphamide, mitomycin, methotrexate, chlorozotocin, and bleomycin. But also noncytotoxic drugs can induce OP, like gold salts, sulfasalazine, penicillamine, amiodarone, tocainide, hexamethonium, phenytoin, and "street drugs" like cocaine.

Having excluded all these causes, there remains idiopathic OP (Fig. 6.30), which clinically behaves less aggressive and responds better to corticosteroid treatment than the above secondary forms of OP (see Table 6.1).

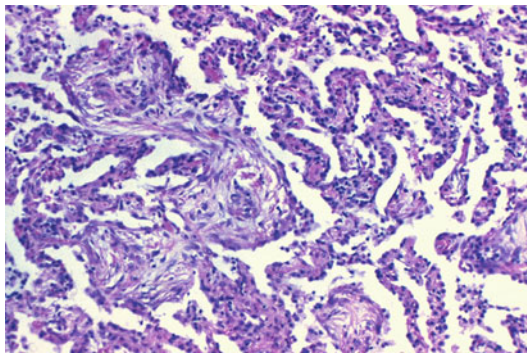

Fig. 6.30 Cryptogenic organizing pneumonia. In this patient's biopsy, no cause for OP was found, and all possible underlying diseases were excluded by clinical, radiological, and pathological examination. H&E, ×100

D3. **Constrictive bronchiolitis** (**CB**) is a recently reinvented entity, in the old German pathologic literature called fibrosing bronchiolitis. It involves preferentially membranous bronchioles. It is characterized by a lymphoplasmacytic infiltrate within the bronchiolar wall, mural thickening, and fibrosis of the stroma, narrowing the lumen in a concentric fashion. The muscle layer may be hypertrophic in early lesions, but atrophic in late stages, and finally is replaced by fibrotic tissue (Figs. 6.31 and 6.32). This is in contrast to BO where usually remnants of the muscular layer are found even in late stages of the disease. In the lumen, there is considerable mucostasis. In end stages, the bronchiolar lumen might be completely occluded. The early stage of CB is not well defined. We have seen few cases at an early

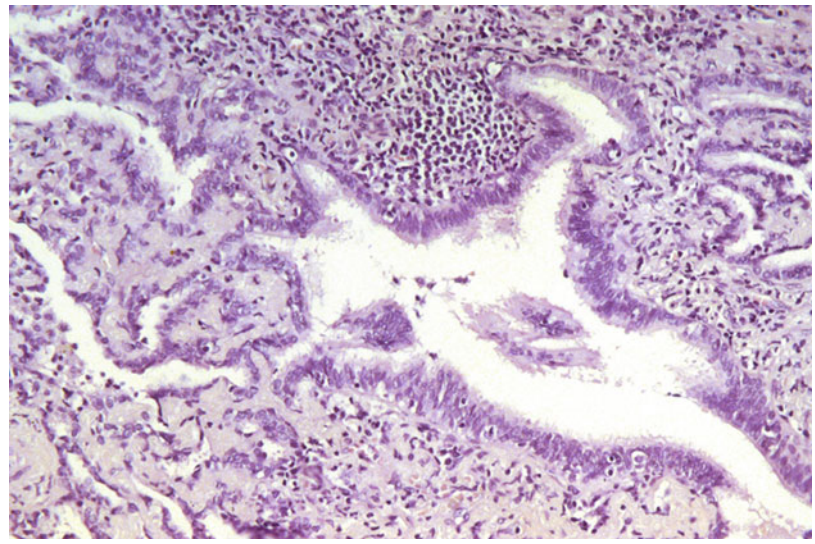

Fig. 6.31 Constrictive bronchiolitis (CB). A chronic inflammatory infiltrate is only focally seen; most of the walls of these bronchioles are replaced by scar tissue. H&E, ×100

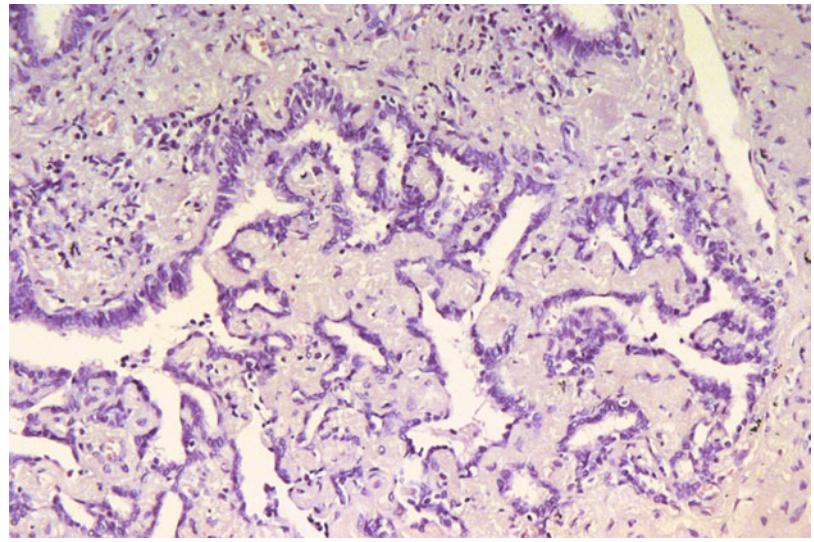

Fig. 6.32 CB end stage. The muscular coat has completely been destroyed and replaced by scar tissue. This results in collapse of the bronchioles during expiration. H&E, ×100

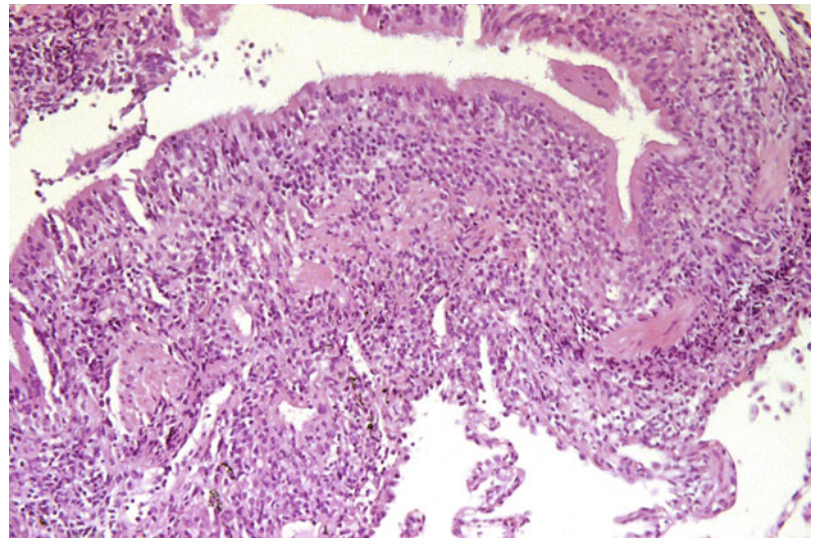

Fig. 6.33 Early CB; the neutrophilic infiltration is concentrated within the muscle layer, destroying the smooth muscle cells. There is much less infiltration within the epithelial layer. H&E, ×150

stage: There is a dense neutrophilic infiltration in the mucosa increasing toward the muscular layer. Only mild degenerative changes are found in the epithelium, very few neutrophils in the lumen, but a dense infiltration in the subepithelial and muscular layers (Fig. 6.33). There is a muscular destruction. CB has been described in cases of chronic rejection of lung and heart-lung transplants; GVHD in bone marrow recipients; collagen vascular diseases, mainly rheumatoid arthritis; and drug reactions (gold salts, Table 6.1). However, we still have to await further reports, before coming up with an established list of possible causes of CB. And the pathogenesis of this form of bronchiolitis awaits further clarification.

D3.1. Recently cases of *Sauropus androgynus* juice-induced bronchiolitis were reported, which closely mimics CB [45–47]. Bronchiolitis starts with myxoid degeneration of matrix proteins, followed by a mixed infiltrate of eosinophils, histiocytes/macrophages

and foam cells, occasional histiocytic giant cells, and few lymphocytes (Figs. 6.34 and 6.35). This is followed by epithelial necrosis. The bronchioles are then replaced by granulation tissue and finally by a scar. In contrast to concentric bronchiolitis, the muscular coat is retained in this form even in the occlusive stage (Fig. 6.36). Bronchiolar lumen obstruction starts in an eccentric fashion. Therefore **eccentric destructive bronchiolitis** would be an appropriate name for it. A similar process can be seen in larger bronchi and in blood vessel walls. The mechanism by which the ingredients of Sauropus juice interfere with the metabolism of matrix proteins is incompletely understood [48]. But given the

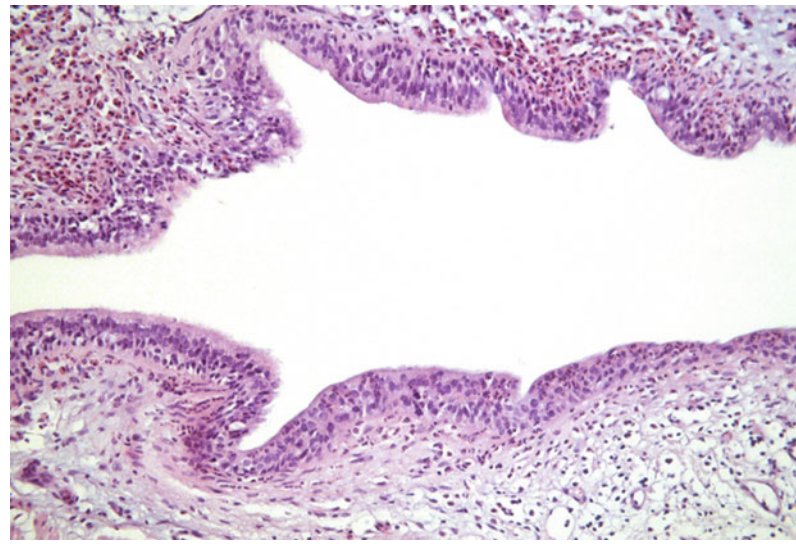

Fig. 6.34 CB in Sauropus poisoning; there are myxoid changes in the mucosa and infiltrates composed of eosinophils, lymphocytes, and histiocytes. H&E, ×200

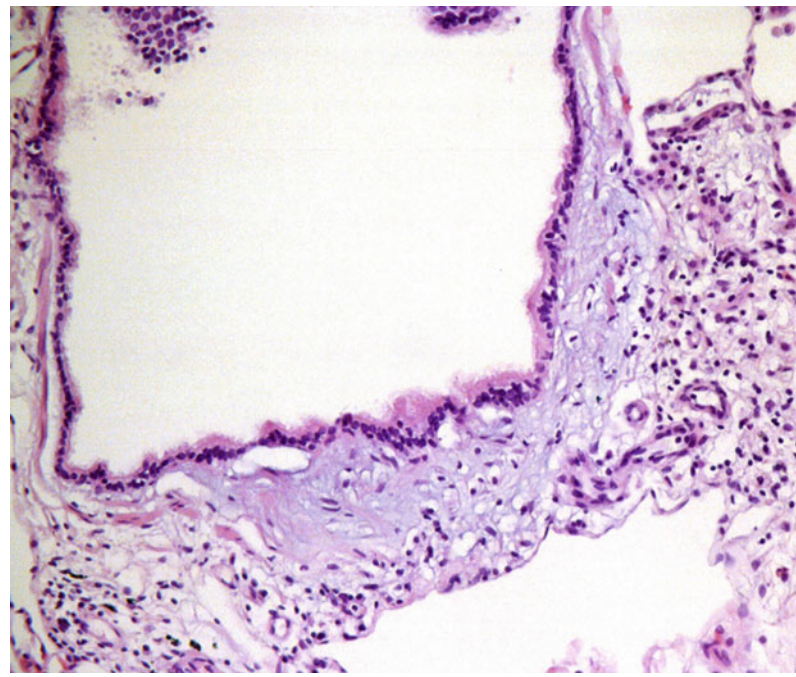

Fig. 6.35 CB in Sauropus poisoning; in this focus, the myxoid changes in the mucosa dominate. H&E, ×100

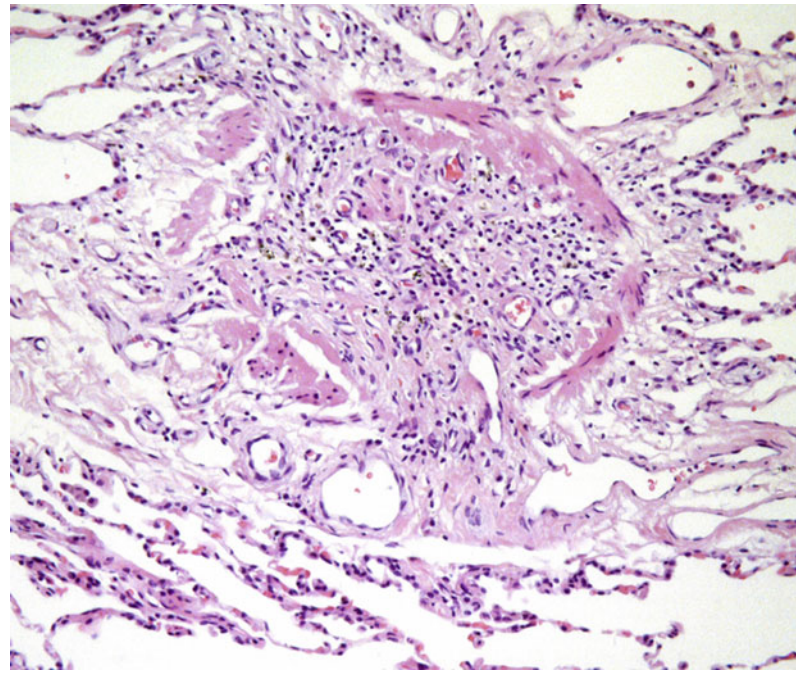

Fig. 6.36 Late stage of CB in Sauropus poisoning. The bronchiolar lumen is completely lost, respectively, replaced by granulation tissue; in contrast to classical CB, the muscular coat is retained. H&E, ×100

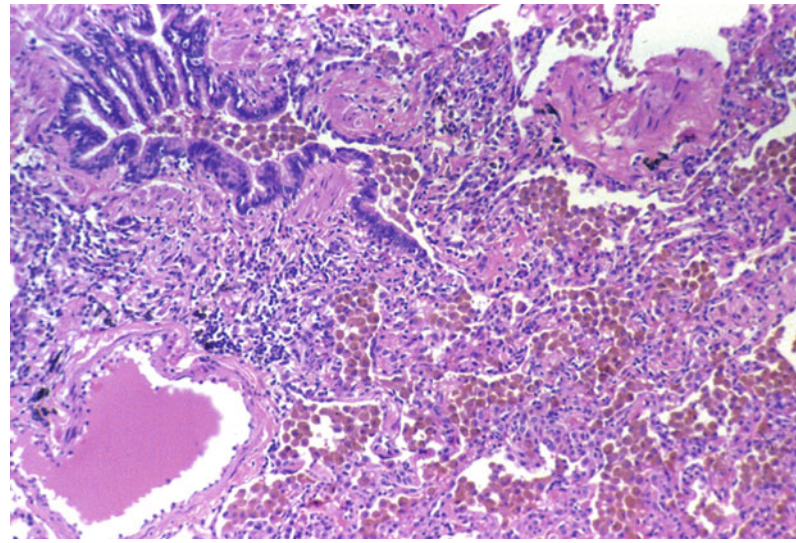

Fig. 6.37 Respiratory bronchiolitis; numerous pigmented alveolar macrophages almost completely occlude the terminal bronchioles and extend into the centroacinar alveoli. H&E, ×250

cellular infiltrate, a combined allergic/toxic reaction might be anticipated.

D4. **Respiratory bronchiolitis** (**RB**) is characterized by a predominantly intraluminal infiltration of pigment-laden macrophages at the bronchioloalveolar border with extension into the central alveolar region (Fig. 6.37). There is no necrosis of the epithelial layer, but an infiltration of the mucosa by histiocytes, macrophages, and few lymphocytes. Mild degenerative and reactive changes of epithelial cells can be seen. The pigment in alveolar macrophages is finely granular and of light olive to yellow color (Figs. 6.37 and 6.38). By electron microscopy, thin needles can be

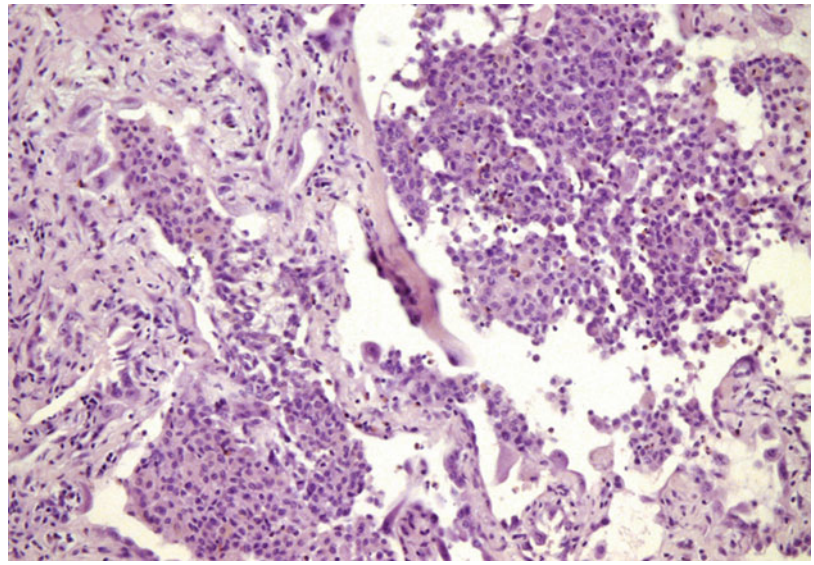

Fig. 6.38 Numerous pigmented alveolar macrophages not only occlude the bronchioles but also major portions of the alveolar tissues. H&E, ×150

found within the macrophages. It is well established that this pigment represents metabolites and waste from tobacco smoke-related compounds. RB is usually found in smokers less than 35 years of age. In some cases, the lymphocytic infiltrate may increase, forming lymph follicles with activated germinal centers, which then points to an additional chronic allergic reaction for some of the tobacco products. Since heavy smokers have been seen some decades before, when RB was considered a rare disease, it might be related to the earlier onset of smoking, which was not seen in the 1940s–1960s, but was quite common in the 1980s–1990s up to the present time. In RB patients might be treated with corticosteroids, which can reduce inflammation, but the only effective treatment is smoking cessation.

In the new classification on interstitial pneumonias, the term RB-ILD is regarded as clinical diagnosis; however, usually RB-ILD is diagnosed morphologically by the extension of the macrophage accumulation into the alveolar region. It is usually associated with more aggravated clinical symptoms and therefore should be made also on tissue evaluation [49]. In exceptional cases, RB can be found in patients without any tobacco smoke inhalation. In these patients, other causes of inhalation of noxious gases should be excluded.

Fig. 6.39 Resection specimen of follicular bronchiolitis (FB). The yellow tissue surrounding the bronchi and bronchioles represents lymphoid tissues

D5. **Follicular bronchiolitis** is characterized by a hyperplasia of lymphoid tissue along the airways (including the large bronchi, Fig. 6.39) and by the development of follicles and follicular centers (Figs. 6.40 and 6.41). The lymphocytes are polyclonal on immunohistochemical analysis. The follicles

usually obstruct the bronchiolar lumen, and when this happens, secondary infection and peribronchiolar pneumonia may result [38, 50, 51]. It should be pointed out that in follicular bronchitis/bronchiolitis, no other component of the other special bronchiolitis variants is allowed, whereas the reverse might happen in other variants: follicular bronchiolitis can be present in the other forms of bronchiolitis without altering the diagnostic label.

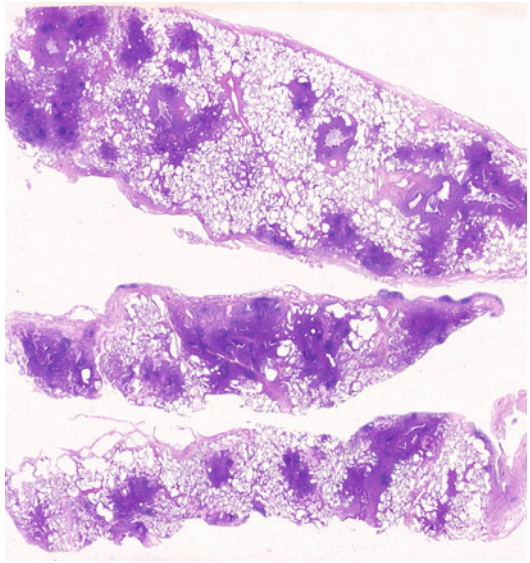

Fig. 6.40 FB, VATS biopsy. Most of the peripheral lung tissue looks normal; however, dense lymphoid tissues with lymph follicles are seen along the bronchial tree, starting from small bronchi and following the airways into bronchioles. H&E, ×5

Follicular bronchiolitis as an entity is seen in recurrent viral infections, in different types of immunodeficiency syndromes and in collagen vascular diseases. Follicular bronchiolitis together with lymphocytic interstitial pneumonia and epithelioid cell granulomas is part of the morphologic reaction spectrum of extrinsic allergic alveolitis/hypersensitivity pneumonia, which is important to know, when one is dealing with bronchial biopsies. If follicular bronchiolitis is encountered, also the differential diagnosis of BALT lymphoma should come into one's mind. Differentiation is facilitated by the presence of lymphoepithelial lesions and monoclonality of lymphocytes found in BALT lymphoma.

In childhood the etiologic background of follicular bronchiolitis is of prognostic importance: in cases of recurrent viral infections, the prognosis is usually a good one. If maintained under good anti-infectious prevention, the children

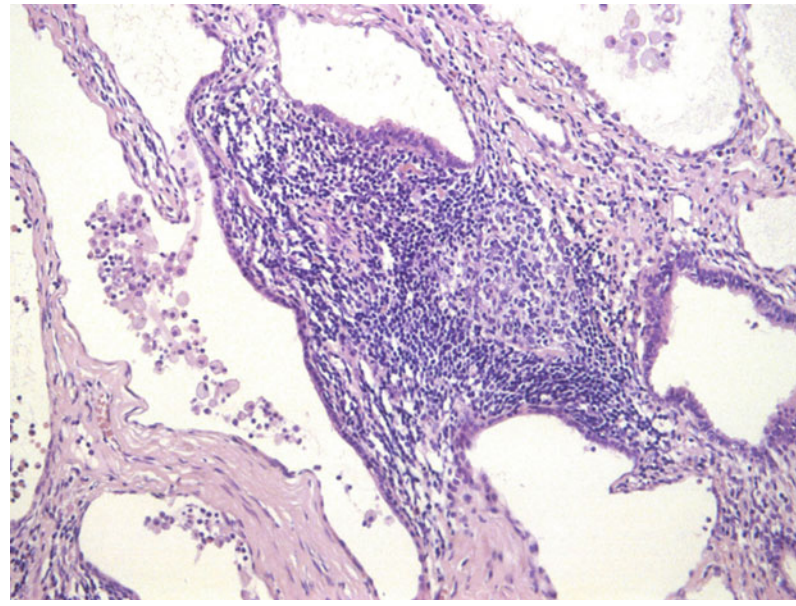

Fig. 6.41 FB in a child. A lymph follicle is seen with well-developed germinal center. There is already fibrosis in areas of former inflammation. H&E, ×100

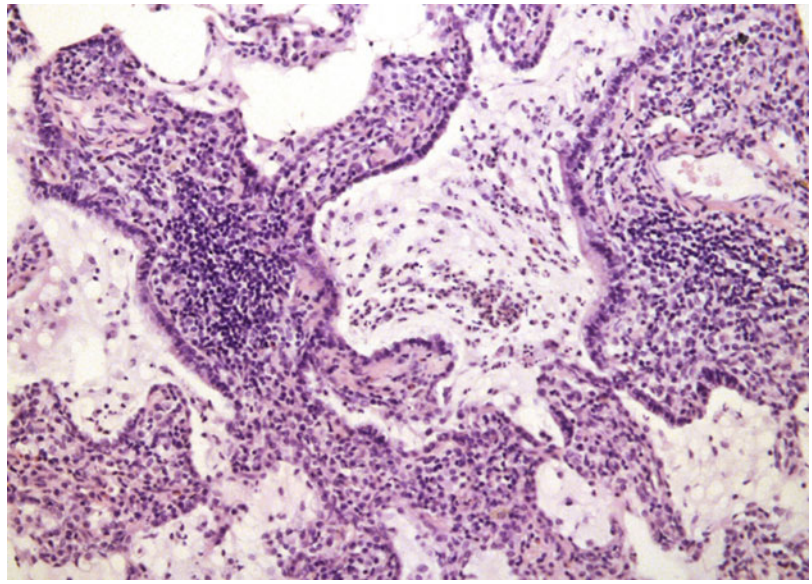

Fig. 6.42 FB in a 5-year-old boy with active inflammation. Several lymph follicles are seen and a dense lymphocytic infiltration. Within the bronchiolar and alveolar lumina, macrophages and a few neutrophils are seen. In this case primarily panbronchiolitis was suspected clinically; however, an NK-cell defect was finally diagnosed as the underlying cause of FB. H&E, 200

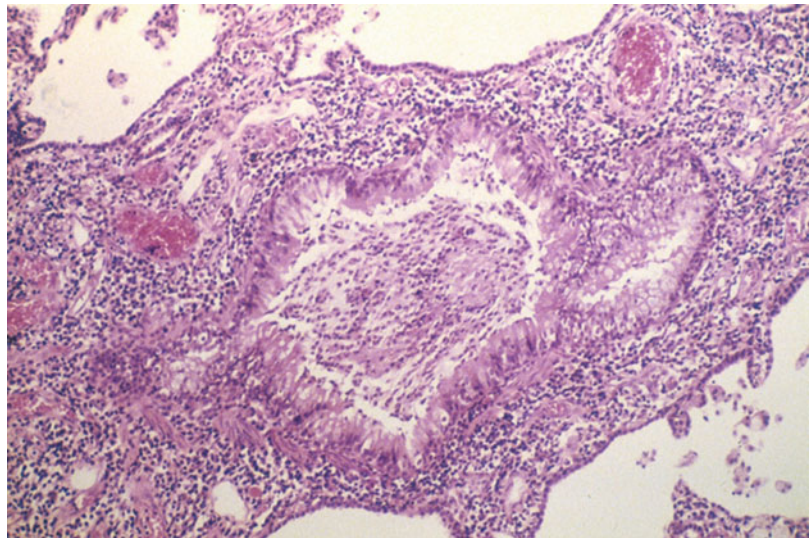

Fig. 6.43 Diffuse panbronchiolitis in a 4-year-old Turkish boy. HLA-BW54 association was established. The bronchioles are infiltrated by lymphocytes, plasma cells, and macrophages; the bronchiolar lumen is narrowed by this infiltrate. In the lumen are foamy macrophages and cell detritus. H&E, ×100

grew older, the immune system matures, and they develop normally. In cases of an inborn or acquired immunodeficiency, the prognosis is worse (Fig. 6.42), and in idiopathic follicular bronchiolitis, the prognosis is worst. In these cases, usually no therapy can stop the process, and most children die within a few years from the onset of the disease [50, 51].

D6. **Diffuse panbronchiolitis** was first described in patients from Southeast Asia. It is characterized by an accumulation of macrophages within bronchioles and a lymphoplasmacytic infiltration within the bronchiolar walls. Macrophages are predominantly transformed into foam cells (Fig. 6.43). Bacteria can usually be identified within the macrophages. Hyperplasia of BALT does occur; follicle centers might be present, usually related to recurrent infections [52]. Sometimes it resembles follicular bronchiolitis. In contrast to LIP, the infiltration is always concentrated along the bronchi and bronchioles. Healing occurs by the formation of intrabronchial

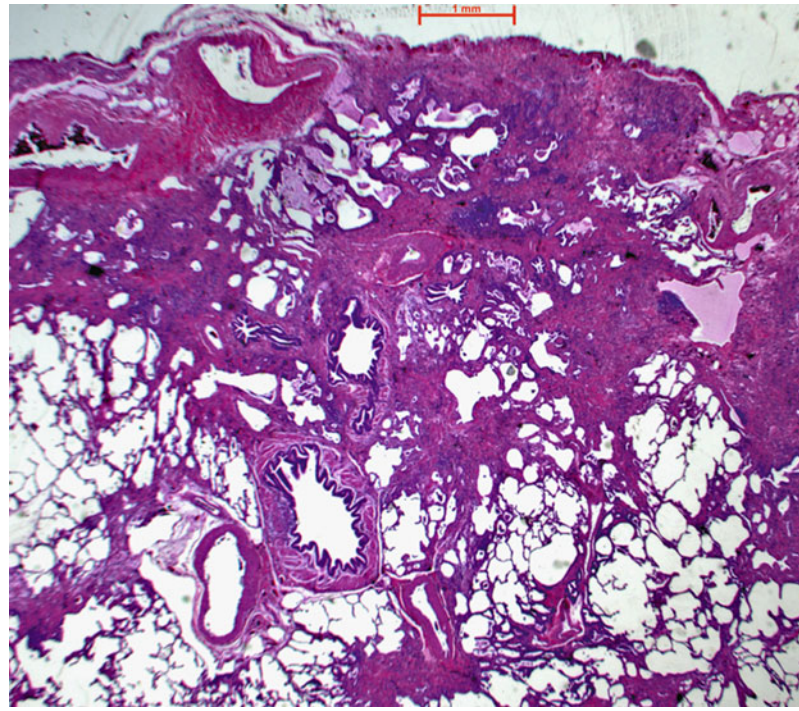

Fig. 6.44 Airway-centered interstitial fibrosis (ACIF). In this low-power magnification, the fibrosis can be appreciated starting from the bronchi and following the airways down to the bronchioles and finally close to the pleura. H&E, bar 1 mm

granulation tissue, similar to early BO. The bacterial infection found in these patients most likely represents an epiphenomenon and not the cause of the disease. It seems that these patients are unable to completely clear their lungs from this bacterial burden and therefore develop a persisting chronic infectious bronchiolitis. In rare instances, DPB has been identified in children of Caucasian and Turkish descendance. These children need to be protected by antibiotics whenever an infection starts.

DPB might be difficult to separate from other forms of bronchiolitis. However, there are some features which are of help: in DPB the obstructive lesions are confined to the respiratory bronchiole; chronic parasinusitis is common; follicular bronchiolitis is a common finding [53]. The cause is a phenotypic variation in the HLA system involving HLA-BW54, HLA-A11, and HLA-DRB5*010/020 [54], residing on chromosome 6. This leads to susceptibility to otherwise nonpathogenic bacterial infection in immunocompetent children. Children with this HLA type need to be treated with erythromycin every time a respiratory tract infection occurs. In non-treated children, the disease will cause secondary destruction of the peripheral lung with cyst formation and fibrosis. Initially DPB was mainly identified in children of Asian descendance; however, meanwhile this disease has been diagnosed also in Caucasians [55]. But it should be mentioned that the diagnosis should be confirmed by morphologic analysis, because of similarity with other forms of bronchiolitis, seen by HRCT [38, 50].

D7. **Airway-centered interstitial fibrosis (ACIF)** is characterized by interstitial fibrosis centered on small airways (bronchioles and small bronchi) with an addition of smooth muscle hyperplasia. Often the bronchiolar epithelium exhibit metaplastic changes even squamous cell metaplasia (Figs. 6.44, 6.45 and 6.46). Clinically, patients presented with chronic cough and progressive dyspnea. In the initial description, Churg et al. reported inhalation exposures (wood smoke, birds, cotton, pasture, chalk dust, agrochemical compounds, and cocaine) in their patients [56]. BAL showed a mild increase in lymphocytes in a

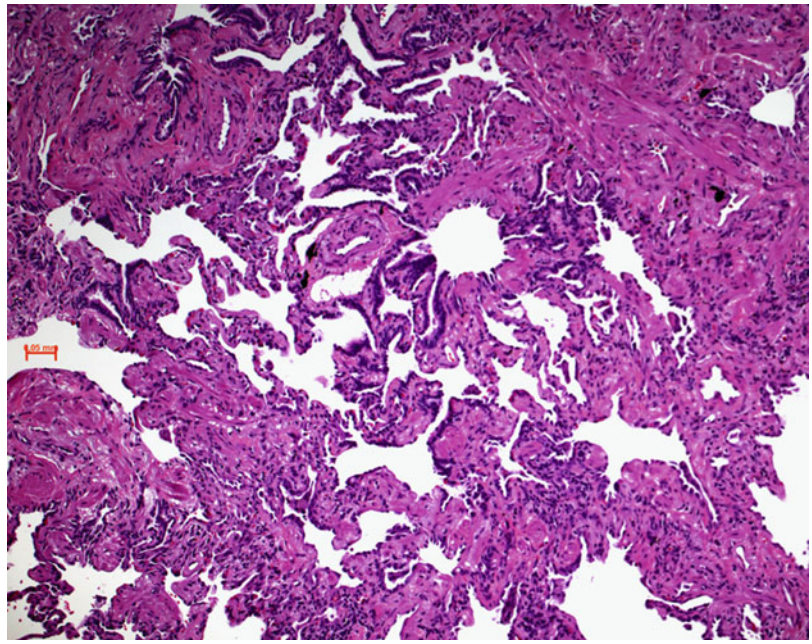

Fig. 6.45 ACIF, showing more closely fibrosis and muscular hyperplasia along the airways. H&E, bar 50 µm

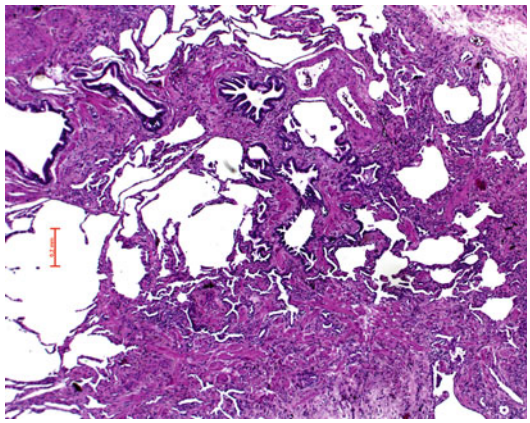

Fig. 6.46 ACIF with fibrosis and muscular hyperplasia along the airways. The whole subsegment is involved. H&E, bar 200 µm

minority of the patients. Treatment was done with corticosteroids and bronchodilators; however, the outcome was dismal with disease progression and death in many patients.

ACIF could be either placed into idiopathic interstitial pneumonias or into bronchiolitis. Since interstitial inflammatory infiltrates have not been described, it is best placed into bronchiolar disorders, although the early disease stages have not been identified yet.

References

1. Fattahi F, Vonk JM, Bulkmans N, Fleischeuer R, Gouw A, Grunberg K, Mauad T, Popper H, Felipe-Silva A, Vrugt B, Wright JL, Yang HM, Kocks JW, Hylkema MN, Postma DS, Timens W, Ten Hacken NH. Old dilemma: asthma with irreversible airway obstruction or COPD. Virchows Arch. 2015;467:583–93.
2. Regland B, Cajander S, Wiman LG, Falkmer S. Scanning electron microscopy of the bronchial mucosa in some lung diseases using bronchoscopy specimens. A pilot study including cases of bronchial carcinoma, sarcoidosis, silicosis and tuberculosis. Scand J Respir Dis. 1976;57:171–82.
3. Viswanathan S, Eria L, Diunugala N, Johnson J, McClean C. An analysis of effects of San Diego wildfire on ambient air quality. J Air Waste Manag Assoc. 2006;56:56–67.
4. Massolo L, Muller A, Tueros M, Rehwagen M, Franck U, Ronco A, Herbarth O. Assessment of mutagenicity and toxicity of different-size fractions of air particulates from La Plata, Argentina, and Leipzig, Germany. Environ Toxicol. 2002;17:219–31.
5. Shi T, Duffin R, Borm PJ, Li H, Weishaupt C, Schins RP. Hydroxyl-radical-dependent DNA damage by ambient particulate matter from contrasting sampling locations. Environ Res. 2006;101:18–24.

6. Becker S, Soukup JM, Gallagher JE. Differential particulate air pollution induced oxidant stress in human granulocytes, monocytes and alveolar macrophages. Toxicol In Vitro. 2002;16:209–18.
7. Oberdorster G. Toxicokinetics and effects of fibrous and nonfibrous particles. Inhal Toxicol. 2002;14:29–56.
8. Ma JY, Ma JK. The dual effect of the particulate and organic components of diesel exhaust particles on the alteration of pulmonary immune/inflammatory responses and metabolic enzymes. J Environ Sci Health Part C Environ Carcinog Ecotoxicol Rev. 2002;20:117–47.
9. Becker S, Dailey LA, Soukup JM, Grambow SC, Devlin RB, Huang YC. Seasonal variations in air pollution particle-induced inflammatory mediator release and oxidative stress. Environ Health Perspect. 2005;113: 1032–8.
10. Hannigan MP, Busby Jr WF, Cass GR. Source contributions to the mutagenicity of urban particulate air pollution. J Air Waste Manag Assoc. 2005;55:399–410.
11. Kontakioti E, Domvri K, Papakosta D, Daniilidis M. HLA and asthma phenotypes/endotypes: a review. Hum Immunol. 2014;75:930–9.
12. Anderson GP. Endotyping asthma: new insights into key pathogenic mechanisms in a complex, heterogeneous disease. Lancet. 2008;372:1107–19.
13. Hall S, Agrawal DK. Key mediators in the immunopathogenesis of allergic asthma. Int Immunopharmacol. 2014;23:316–29.
14. Erle DJ, Sheppard D. The cell biology of asthma. J Cell Biol. 2014;205:621–31.
15. DeKruyff RH, Yu S, Kim HY, Umetsu DT. Innate immunity in the lung regulates the development of asthma. Immunol Rev. 2014;260:235–48.
16. Holgate ST. Mechanisms of asthma and implications for its prevention and treatment: a personal journey. Allergy, Asthma Immunol Res. 2013;5:343–7.
17. Lambrecht BN, Hammad H. Asthma: the importance of dysregulated barrier immunity. Eur J Immunol. 2013;43:3125–37.
18. Gaurav R, Agrawal DK. Clinical view on the importance of dendritic cells in asthma. Expert Rev Clin Immunol. 2013;9:899–919.
19. Kumar Y, Bhatia A. Immunopathogenesis of allergic disorders: current concepts. Expert Rev Clin Immunol. 2013;9:211–26.
20. Grotenboer NS, Ketelaar ME, Koppelman GH, Nawijn MC. Decoding asthma: translating genetic variation in IL33 and IL1RL1 into disease pathophysiology. J Allergy Clin Immunol. 2013;131:856–65.
21. Roy MG, Livraghi-Butrico A, Fletcher AA, McElwee MM, Evans SE, Boerner RM, Alexander SN, Bellinghausen LK, Song AS, Petrova YM, Tuvim MJ, Adachi R, Romo I, Bordt AS, Bowden MG, Sisson JH, Woodruff PG, Thornton DJ, Rousseau K, De la Garza MM, Moghaddam SJ, Karmouty-Quintana H, Blackburn MR, Drouin SM, Davis CW, Terrell KA, Grubb BR, O'Neal WK, Flores SC, Cota-Gomez A, Lozupone CA, Donnelly JM, Watson AM, Hennessy CE, Keith RC, Yang IV, Barthel L, Henson PM, Janssen WJ, Schwartz DA, Boucher RC, Dickey BF, Evans CM. Muc5b is required for airway defence. Nature. 2014;505:412–6.
22. Jackola DR. Random allergen-specific IgE expression in atopic families: evidence for inherited "stochastic bias" in adverse immune response development to non-infectious antigens. Mol Immunol. 2007;44:2549–57.
23. Tan J, Bernstein JA. Occupational asthma: an overview. Curr Allergy Asthma Rep. 2014;14:431.
24. Woodruff PG, Boushey HA, Dolganov GM, Barker CS, Yang YH, Donnelly S, Ellwanger A, Sidhu SS, Dao-Pick TP, Pantoja C, Erle DJ, Yamamoto KR, Fahy JV. Genome-wide profiling identifies epithelial cell genes associated with asthma and with treatment response to corticosteroids. Proc Natl Acad Sci U S A. 2007;104:15858–63.
25. Holtzman MJ, Byers DE, Alexander-Brett J, Wang X. The role of airway epithelial cells and innate immune cells in chronic respiratory disease. Nat Rev Immunol. 2014;14:686–98.
26. Kumar RK, Foster PS, Rosenberg HF. Respiratory viral infection, epithelial cytokines, and innate lymphoid cells in asthma exacerbations. J Leukoc Biol. 2014;96:391–6.
27. Vadasz Z, Haj T, Toubi E. The role of B regulatory cells and Semaphorin3A in atopic diseases. Int Arch Allergy Immunol. 2014;163:245–51.
28. van Helden MJ, Lambrecht BN. Dendritic cells in asthma. Curr Opin Immunol. 2013;25:745–54.
29. Heijink IH, Nawijn MC, Hackett TL. Airway epithelial barrier function regulates the pathogenesis of allergic asthma. Clin Exp Allergy. 2014;44: 620–30.
30. Vermeer PD, Denker J, Estin M, Moninger TO, Keshavjee S, Karp P, Kline JN, Zabner J. MMP9 modulates tight junction integrity and cell viability in human airway epithelia. Am J Physiol Lung Cell Mol Physiol. 2009;296:L751–62.
31. de Boer WI, Sharma HS, Baelemans SM, Hoogsteden HC, Lambrecht BN, Braunstahl GJ. Altered expression of epithelial junctional proteins in atopic asthma: possible role in inflammation. Can J Physiol Pharmacol. 2008;86:105–12.
32. Yu S, Kim HY, Chang YJ, DeKruyff RH, Umetsu DT. Innate lymphoid cells and asthma. J Allergy Clin Immunol. 2014;133:943–50, quiz 951.
33. Alexis NE, Carlsten C. Interplay of air pollution and asthma immunopathogenesis: a focused review of diesel exhaust and ozone. Int Immunopharmacol. 2014;23:347–55.
34. Message SD, Johnston SL. The immunology of virus infection in asthma. Eur Respir J. 2001;18:1013–25.
35. Lambrecht BN, Hammad H. Allergens and the airway epithelium response: gateway to allergic sensitization. J Allergy Clin Immunol. 2014;134:499–507.
36. Postma DS, Reddel HK, ten Hacken NH, van den Berge M. Asthma and chronic obstructive pulmonary disease: similarities and differences. Clin Chest Med. 2014;35:143–56.

37. Popper H. Experimental monoarthritis. Modulatory effect of injected eosinophils on influx of various types of inflammatory cells. Inflammation. 1984;8: 301–12.
38. Popper HH. Bronchiolitis, an update. Virchows Arch. 2000;437:471–81.
39. Tam A, Sin DD. Pathobiologic mechanisms of chronic obstructive pulmonary disease. Med Clin N Am. 2012;96:681–98.
40. Shan M, Yuan X, Song LZ, Roberts L, Zarinkamar N, Seryshev A, Zhang Y, Hilsenbeck S, Chang SH, Dong C, Corry DB, Kheradmand F. Cigarette smoke induction of osteopontin (SPP1) mediates T(H)17 inflammation in human and experimental emphysema. Sci Transl Med. 2012;4:117ra119.
41. Cole BB, Smith RW, Jenkins KM, Graham BB, Reynolds PR, Reynolds SD. Tracheal Basal cells: a facultative progenitor cell pool. Am J Pathol. 2010; 177:362–76.
42. Banerjee ER, Henderson Jr WR. Characterization of lung stem cell niches in a mouse model of bleomycin-induced fibrosis. Stem Cell Res Ther. 2012;3:21.
43. Popper HH, Pailer S, Wurzinger G, Feldner H, Hesse C, Eber E. Expression of adhesion molecules in allergic lung diseases. Virchows Arch. 2002;440: 172–80.
44. Popper H, Jakse R, Loidolt D. Problems in the differential diagnosis of Kartagener's syndrome and ATPase deficiency. Pathol Res Pract. 1985;180:481–5.
45. Chang YL, Yao YT, Wang NS, Lee YC. Segmental necrosis of small bronchi after prolonged intakes of Sauropus androgynus in Taiwan. Am J Respir Crit Care Med. 1998;157:594–8.
46. Chang H, Wang JS, Tseng HH, Lai RS, Su JM. Histopathological study of Sauropus androgynus-associated constrictive bronchiolitis obliterans: a new cause of constrictive bronchiolitis obliterans. Am J Surg Pathol. 1997;21:35–42.
47. Lai RS, Chiang AA, Wu MT, Wang JS, Lai NS, Lu JY, Ger LP, Roggli V. Outbreak of bronchiolitis obliterans associated with consumption of Sauropus androgynus in Taiwan. Lancet. 1996;348:83–5.
48. Hashimoto I, Imaizumi K, Hashimoto N, Furukawa H, Noda Y, Kawabe T, Honda T, Ogawa T, Matsuo M, Imai N, Ito S, Sato M, Kondo M, Shimokata K, Hasegawa Y. Aqueous fraction of Sauropus androgynus might be responsible for bronchiolitis obliterans. Respirology. 2013;18:340–7.
49. Travis WD, Costabel U, Hansell DM, King Jr TE, Lynch DA, Nicholson AG, Ryerson CJ, Ryu JH, Selman M, Wells AU, Behr J, Bouros D, Brown KK, Colby TV, Collard HR, Cordeiro CR, Cottin V, Crestani B, Drent M, Dudden RF, Egan J, Flaherty K, Hogaboam C, Inoue Y, Johkoh T, Kim DS, Kitaichi M, Loyd J, Martinez FJ, Myers J, Protzko S, Raghu G, Richeldi L, Sverzellati N, Swigris J, Valeyre D. An official American Thoracic Society/European Respiratory Society statement: update of the international multidisciplinary classification of the idiopathic interstitial pneumonias. Am J Respir Crit Care Med. 2013;188:733–48.
50. Benesch M, Kurz H, Eber E, Varga EM, Gopfrich H, Pfleger A, Popper H, Setinek-Liszka U, Zach MS. Clinical and histopathological findings in two Turkish children with follicular bronchiolitis. Eur J Pediatr. 2001;160:223–6.
51. Nicholson AG, Kim H, Corrin B, Bush A, du Bois RM, Rosenthal M, Sheppard MN. The value of classifying interstitial pneumonitis in childhood according to defined histological patterns. Histopathology. 1998;33:203–11.
52. Kudoh S, Keicho N. Diffuse panbronchiolitis. Semin Respir Crit Care Med. 2003;24:607–18.
53. Homma S, Sakamoto S, Kawabata M, Kishi K, Tsuboi E, Motoi N, Hebisawa A, Yoshimura K. Comparative clinicopathology of obliterative bronchiolitis and diffuse panbronchiolitis. Respiration. 2006;73:481–7.
54. She J, Sun Q, Fan L, Qin H, Bai C, Shen C. Association of HLA genes with diffuse panbronchiolitis in Chinese patients. Respir Physiol Neurobiol. 2007;157:366–73.
55. Anthony M, Singham S, Soans B, Tyler G. Diffuse panbronchiolitis: not just an Asian disease: Australian case series and review of the literature. Biomed Imaging Interv J. 2009;5, e19.
56. Churg A, Myers J, Suarez T, Gaxiola M, Estrada A, Mejia M, Selman M. Airway-centered interstitial fibrosis: a distinct form of aggressive diffuse lung disease. Am J Surg Pathol. 2004;28:62–8.

Smoking-Related Lung Diseases 7

Under the term of smoking-related diseases, several diseases with quite different morphological features are discussed, but all of them are related to cigarette smoke exposure, most often in young-aged heavy smokers. Some present with interstitial fibrosis, others show granulomas centered on the airways, and others present with an inflammatory cell infiltration along the airways. Combinations of these diseases are currently more often seen, probably due to the wide variety of differential diagnosis including malignant disease seen at HRCT followed by open lung biopsy. Although clinically most of these diseases are characterized by coughing and mucus plugs, they also have different symptomatologies: some patients present with symptoms related to chronic bronchitis affecting predominantly the large airways, other patients present with small airway disease (clinically vague and ill defined), and some patients present with restrictive in contrast to the predominant obstructive lung diseases of the two former groups.

Why cigarette smoking can present with so many different faces is still not understood, but individual mechanisms associated with metabolism of tobacco smoke substances as well as protective mechanisms including anti-inflammatory enzymes might provide some explanation (see last paragraph of this chapter and Chap. 5 on emphysema).

7.1 Langerhans Cell Histiocytosis

Langerhans cell histiocytosis (LHCH, histiocytosis X, eosinophilic granuloma) is caused by excessive inhalation of tobacco smoke. It occurs predominantly in young-aged people. It has been postulated that tobacco plant antigens present within tobacco smoke (incomplete combustion) might cause this accumulation and proliferation of Langerhans cells, which are part of the antigen-presenting reticulum cell population [1–3]. So the continuous exposure of Langerhans cells to plant proteins in susceptible persons might cause proliferation of these cells to keep up with the increasing amount of antigens to be processed. Patients sometimes present with acute respiratory failure and the subjective impression of asphyxia.

7.1.1 Histology

Langerhans cells proliferate within bronchial mucosa as well as in the peripheral lung. The cells have an ill-defined border, nuclei are convoluted often elongated, chromatin is vesicular, and nucleoli are small. In bronchi this proliferation causes necrosis of the mucosa, occlusion of the lumen, and finally scar tissue [4] (Fig. 7.1). Langerhans cell proliferation is accompanied by

© Springer-Verlag Berlin Heidelberg 2017
H. Popper, *Pathology of Lung Disease*, DOI 10.1007/978-3-662-50491-8_7

an infiltration of eosinophils, hence the old name eosinophilic granuloma (Fig. 7.2). These eosinophils are attracted by cytokines such as interleukin 4 secreted by the Langerhans cells (LH cells) [5]. Eosinophilic granulocytes might be the main cause of cytotoxicity releasing eosinophilic basic proteins and destroy the epithelium (Fig. 7.3). The granulomas undergo regression especially in patients with smoking cessation. The resulting scar has a stellate-like appearance and is surrounded by bronchiolectasis and emphysema blebs (Fig. 7.4). On CT scan this results in a characteristic picture called starry sky, where the dense scar shows tiny extensions (Fig. 7.5).

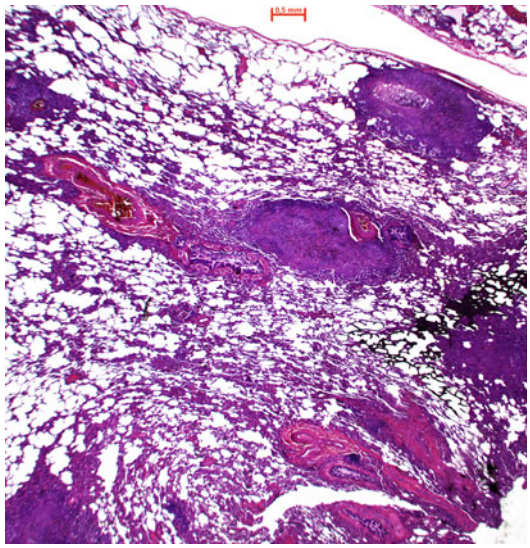

Fig. 7.1 Early lesions of Langerhans cell histiocytosis (LHCH). The lesions are centered on small bronchi and bronchioles. A dense cellular infiltrate is seen. Peripheral lung tissue is much less infiltrated. H&E, bar 0.5 mm

7.1.2 Molecular Biology

An underlying genetic abnormality, i.e., mutation in the BRAF gene, has recently been identified [6–8]. These mutations resulted in discussions, if LHCH should be regarded as a tumor. However, several issues remain to be solved, before this view can be accepted: lung cases are most often induced by smoking and in many patients will undergo regression in case of smoking cessation, which is unlikely in a tumor [3]. BRAF mutations are found in a minority of cases. On the contrary there exists a tumorous form, characterized by a multi-organ involvement, seen in children and young adults and not related to smoking [9, 10]. So probably we are confronted with two

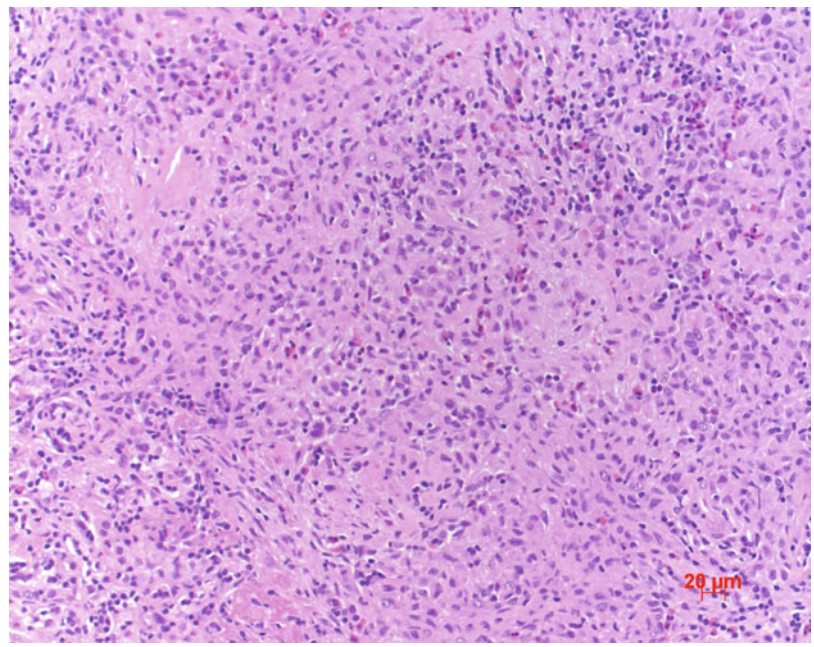

Fig. 7.2 LHCH showing a granuloma-like accumulation of Langerhans cells mixed with eosinophils. The LH cells have pale eosinophilic cytoplasm and elongated nuclei. H&E, bar 20 µm

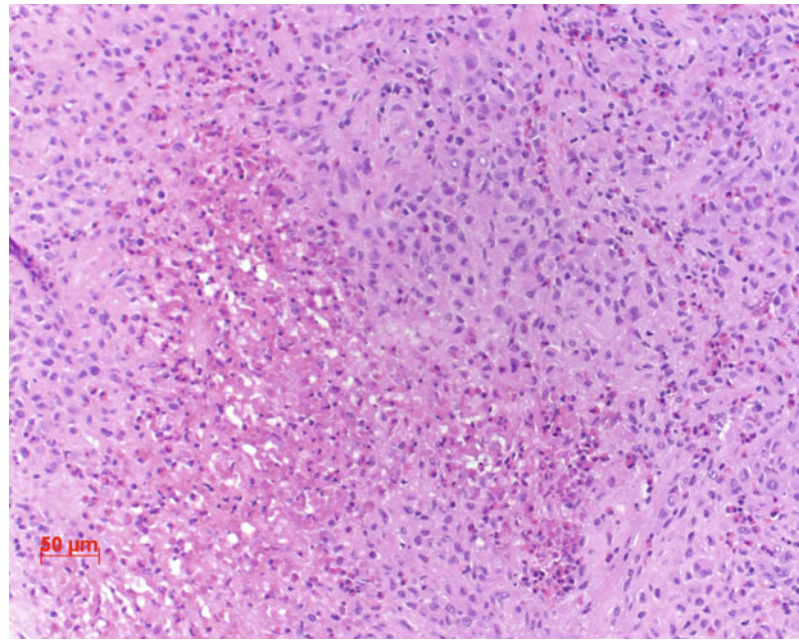

Fig. 7.3 Necrosis induced by the inflammatory infiltrate composed of eosinophils and Langerhans cells. H&E, bar 50 µm

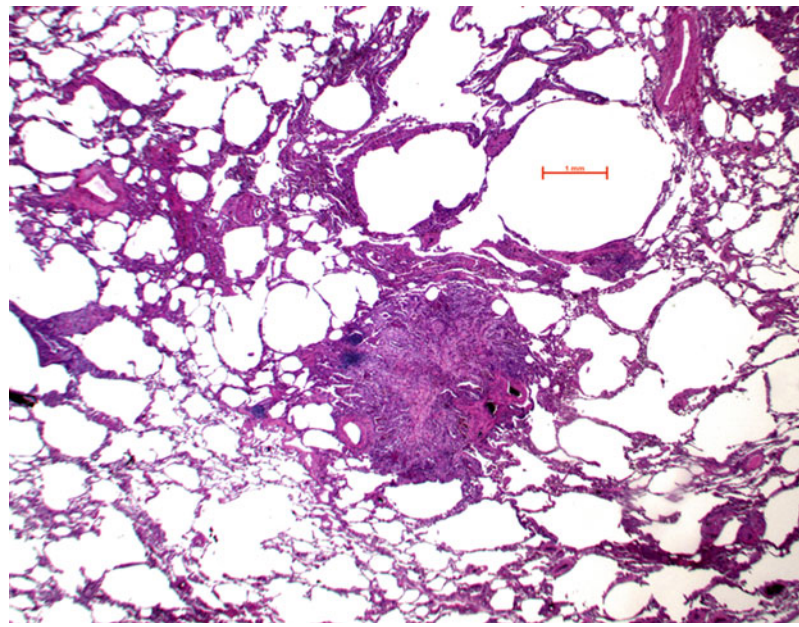

Fig. 7.4 Late LHCH with developing stellate-like scar and many cystic (emphysematous) spaces surrounding the scar. H&E, bar 1 mm

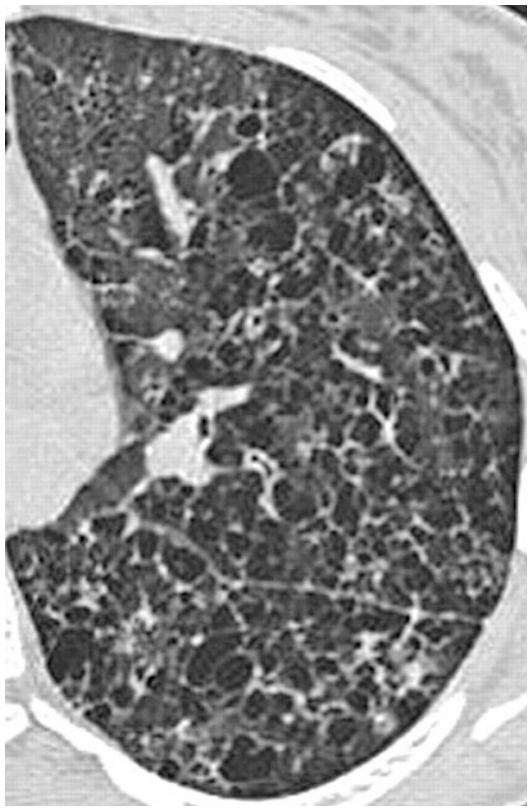

Fig. 7.5 HRCT scan showing the stellate-like scars and the many cysts, making this late stage of LHCH easy to diagnose by radiologists

different diseases. Morphologically the reactive form cannot be discerned from the tumor form other than by involvement of at least two organ systems [11, 12]. Further investigations hopefully will increase our knowledge about this disease.

7.1.3 Function of LH Cells

LH cells are part of the antigen-presenting cell system. Inhaled antigens are presented to LH cells and are taken up and processed by specific mechanisms involving Toll receptors and Langerin, a molecule with C-type lectin domain [13–15]. LH cells can interact with the specific as well as the innate immune system and play a role in control of infections as well as in the pathogenesis of asthma [16–18].

7.1.4 Differential Diagnosis

In the differential diagnosis, LHCH has to be separated from other histiocytosis or reticulum cell proliferations by their positive staining for CD1a and Langerin [19, 20] (Fig. 7.6), whereas the positivity for S100 protein is not specific. On electron microscopy the characteristic feature are the Birbeck granules, which resemble a tennis racket (Fig. 7.7). LHCH might be also diagnosed in samples of bronchoalveolar lavage: on cytology, usually macrophages and lymphocytes can be seen, but also increased numbers of eosinophils. By immunocytology using antibodies for either Langerin or CD1a, the number of positive cells should be >6/HPF; at least six field should be counted and a mean established (Fig. 7.8). Other histiocytoses need to be separated from LHCH. The histiocytes in Erdheim-Chester disease are negative for Langerin and CD1a, although BRAF mutations can be found as well in this disease. Systemic LHCH cannot be differentiated from the reactive pulmonary form as the cells express the same markers. Probably the proof of JL1 epitope of CD43 might help in this respect, as this epitope is expressed only on immature LH cells [21]. Histiocytic sarcomas are easier to separate, as they will present with nuclear atypia, increased mitosis, and invasive growth. However, it should be reminded that Langerhans cell sarcoma although rare does exist, showing the same marker expression as LHCH (see chapter on tumor).

7.2 Respiratory Bronchiolitis: Interstitial Lung Disease (RBILD)

Respiratory bronchiolitis (RB) with or without interstitial lung disease is a common disease in heavy smokers. RB can be seen in a majority of cigarette smokers with lung carcinoma, if nontumorous lung tissue is evaluated. RB can be combined with LHCH [22, 23]. On CT scan widening and thickening of the airways associated with cystic spaces are seen (Fig. 7.9).

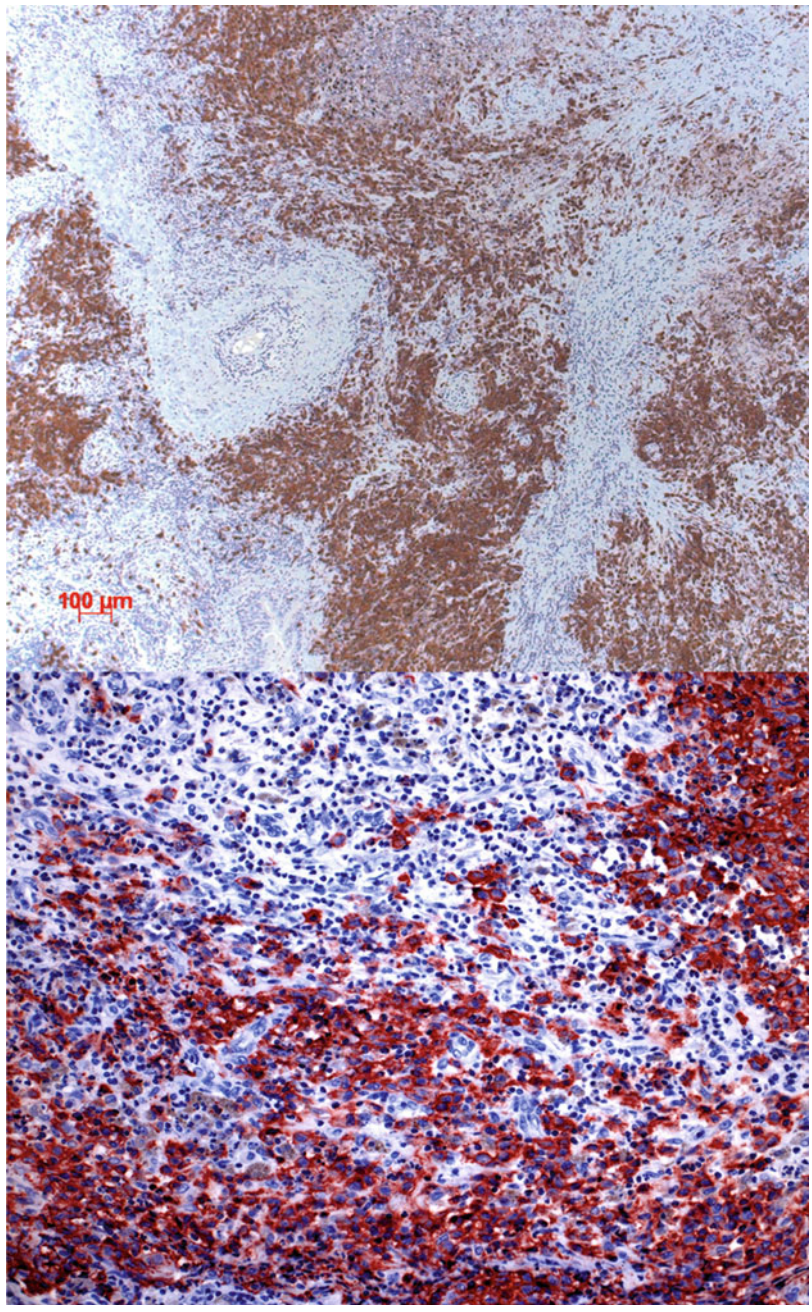

Fig. 7.6 Immunohistochemistry in LHCH: *upper panel* stain for Langerin antigen showing huge amounts of Langerhans cells; bar 100 µm. *Lower panel* stain for CD1a antigen, showing the infiltration of Langerhans cell into the bronchial wall. ×250

7.2.1 Histology

An accumulation of alveolar macrophages within respiratory bronchioles and the adjacent centrilobular region of the lung lobules characterize RBILD (Figs. 7.10 and 7.11). The macrophages usually contain dirty brownish-yellow fine granular pigment (Fig. 7.12). Ultrastructurally this

pigment represents phagolysosomes filled with tobacco waste including also some metal oxides such as cadmium oxide [24–26]. Functionally this macrophage accumulation obstructs the terminal bronchioles and impairs airflow, resulting in distension of alveoli and eventually rupture of septa.

Some authors use the diagnosis of RB only in those cases, where no other pathology is present; others this author included follow the morphology and accept RB diagnosis also in heavy smokers with lung carcinoma, in whom also RB is present. The argument is that RB is a disease of smokers, and there is no good argument why smokers are not allowed to have more than one disease, e.g., RB, carcinoma, LHCH, and emphysema. However, this results in different statistical figures: if RB diagnosis is only accepted presenting as a singular disease, it is rare; if diagnosed by its morphological features regardless of other smoking-induced diseases, it is a common disease, present in many patients with lung cancer. RB and RBILD in my opinion are subsequent stages of the same disease. In early stages accumulation of alveolar macrophages are concentrated within bronchioles. If tobacco smoke exposure goes on, more and more areas of the centroacinar region of alveoli are occupied by these macrophages, resulting in radiological ground-glass opacities, clinically called RBILD. Whereas the clinical symptoms of RB might be mild, the symptoms in RBILD are much more severe.

Fig. 7.7 Electron microscopy of a Langerhans cell with one tennis racket-shaped Birbeck granule (*arrow*). ×11,000

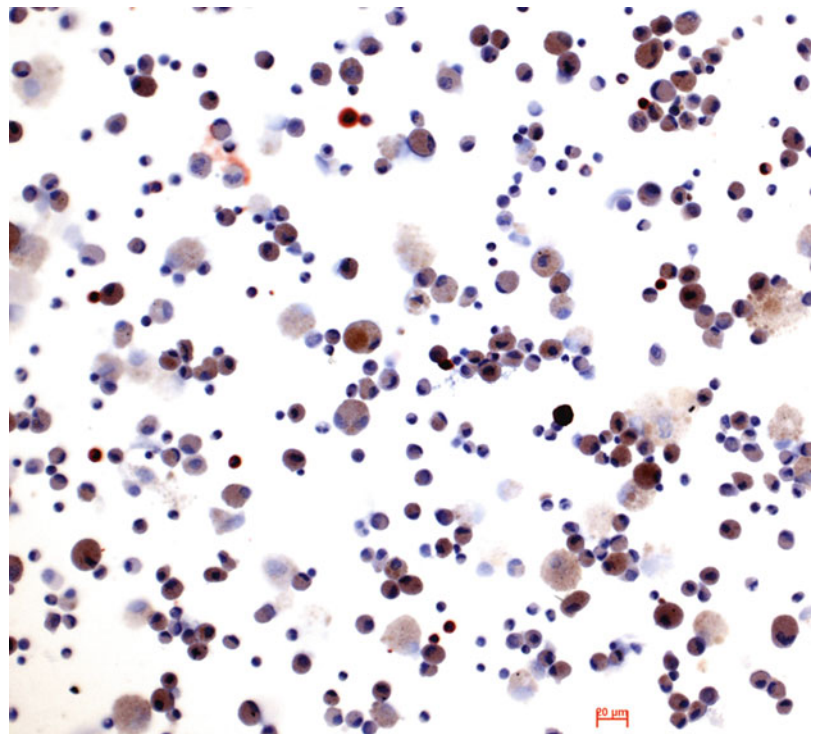

Fig. 7.8 Bronchoalveolar lavage in a case of LHCH; note the positively stained Langerhans cells by CD1a antibodies (*red*). Bar 20 µm

The mechanism of RB/RBILD is still not understood. However, there exists an experimental condition, which shows similar features: in previous experimental inhalation, study investigators used titanium oxide as an inert nontoxic control substance. In these studies it was shown that increasing the dosage of TiO_2 does cause a toxic reaction within the lung by an accumulation of macrophages resulting in obstruction of small bronchi and bronchioles and extension of the infiltrates into the centrilobular lung areas. Macrophages by phagocytosing TiO_2 released cytotoxic enzymes, which subsequently destroyed the wall of bronchi, bronchioles, and alveolar septa and finally resulted in scar formation and fibrosis of alveolar septa. This phenomenon was called overload [27, 28]. Morphologically it resembles RBILD. So probably RBILD is caused by an overload with toxic tobacco smoke products resulting in this accumulation of macrophages. However, it should be reminded that additional factors are acting, since RBILD is not seen in every smoker.

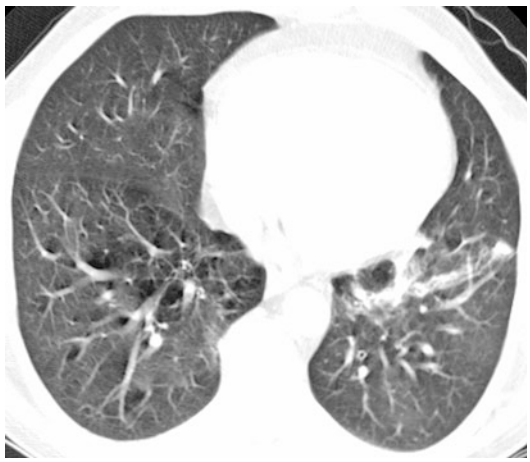

Fig. 7.9 CT scan of RBILD. Note the thickened airway walls and the cystic spaces around the airways. There are also focal areas of ground-glass opacities

7.3 Desquamative Interstitial Pneumonia (DIP)

The term desquamative interstitial pneumonia was created by Liebow in 1965 [29], long before immunohistochemistry was invented. Liebow misinterpreted the cells accumulating within the alveoli as pneumocytes type II, therefore the term desquamative. These cells were later on identified as macrophages [4, 30, 31]. Therefore the name macrophagocytic pneumonia would have been more appropriate.

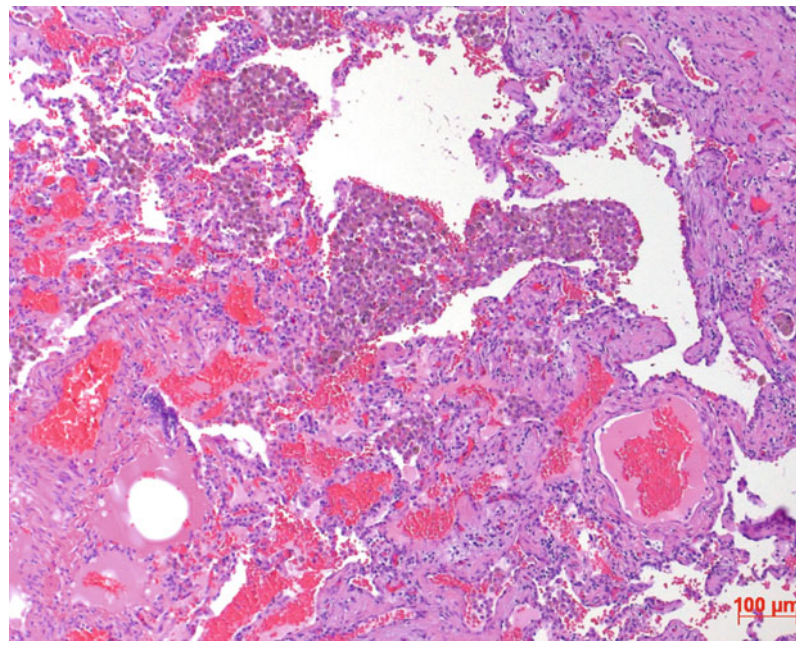

Fig. 7.10 Respiratory bronchiolitis; pigmented alveolar macrophages fill the lumen of this respiratory bronchiole. H&E, bar 100 µm

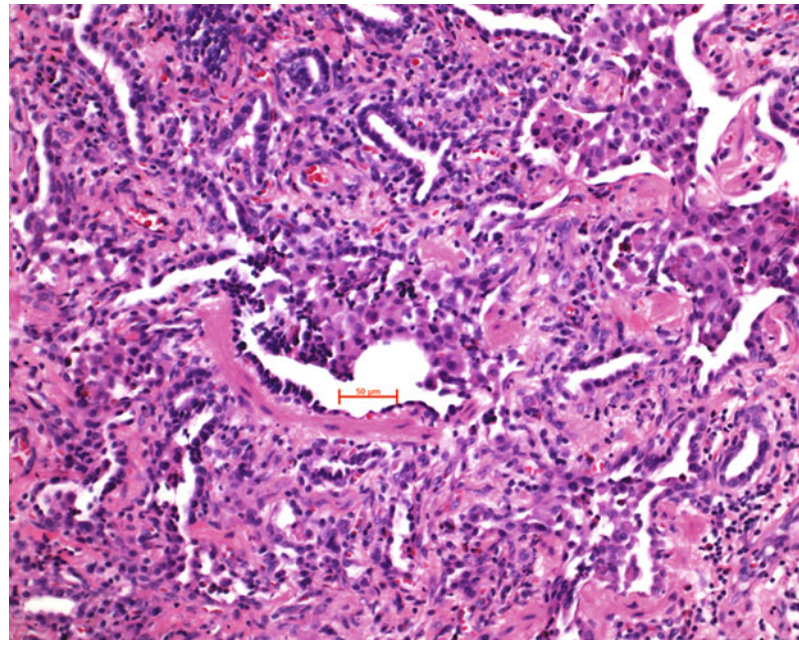

Fig. 7.11 Here the accumulation of macrophages extends into the adjacent lung tissue, which will result in more pronounced symptoms. H&E, bar 50 µm

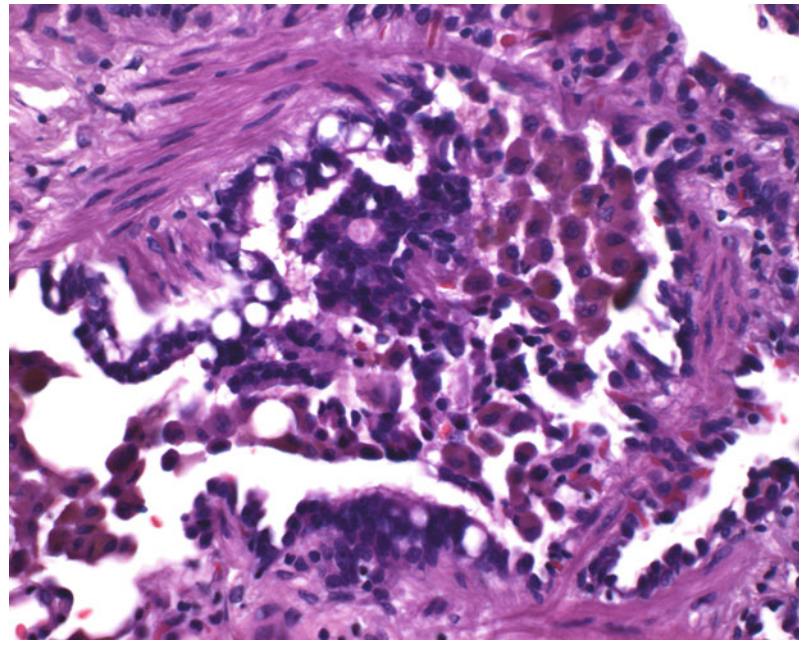

Fig. 7.12 Respiratory bronchiolitis showing pigmented alveolar macrophages filling the lumen of this bronchiole. H&E, ×400

In most patients diagnosed with DIP, heavy cigarette smoking is reported; however, approximately 10–42 % of patients with DIP are nonsmokers. In children some of the reported cases were second-hand exposures to cigarette smoke, but again a few cases reported had no association with tobacco smoke exposure [32–35].

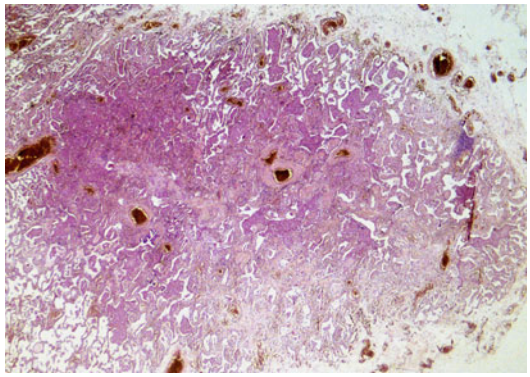

Fig. 7.13 Desquamative interstitial pneumonia (DIP). Almost all alveoli are filled with a cellular infiltrate. H&E, ×16

7.3.1 Histology

By definition DIP is characterized by an accumulation of pigmented smoker macrophages within alveoli, completely obscuring the peripheral airspaces. No infiltration of bronchioles is present (Figs. 7.13 and 7.14). Fibrosis of alveolar septa if present is mild. DIP can radiologically simulate a tumor with ground-glass opacity, not uncommonly misdiagnosed as adenocarcinoma in situ [22]. Only by immunohistochemistry using anti-CD68 antibodies the nature of the accumulating cells is becoming clear (Fig. 7.15).

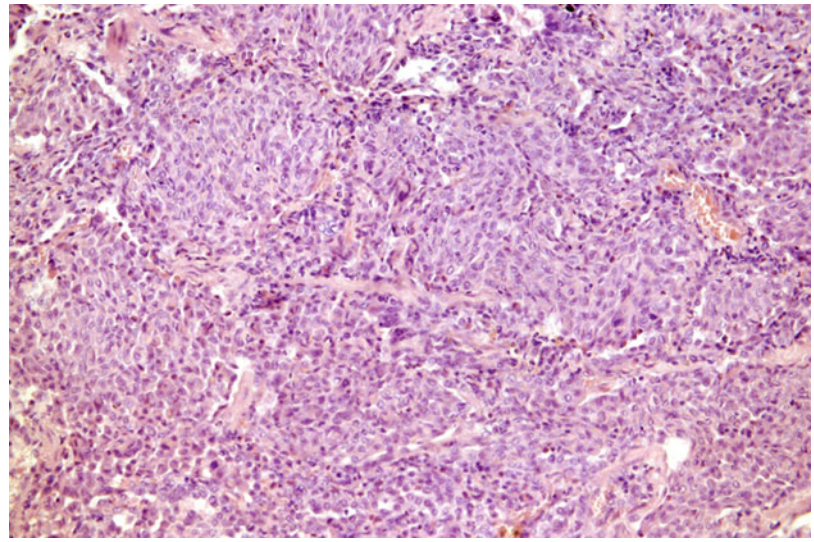

Fig. 7.14 DIP; at higher magnification the alveoli are almost obscured by the infiltrating cells. Not surprisingly this might cause a misinterpretation as tumor. H&E, ×250

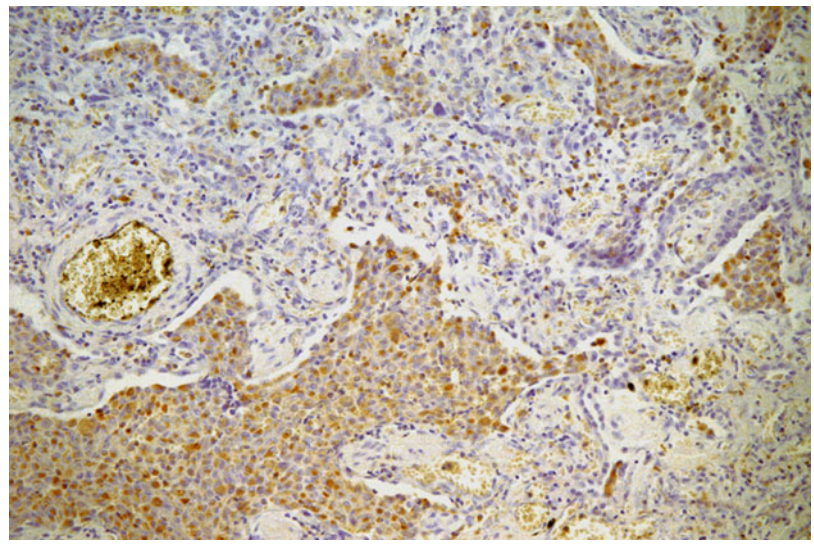

Fig. 7.15 DIP, immunohistochemistry for CD68. Here the nature of the cells belonging to alveolar macrophages is demonstrated; in addition the alveolar walls are now visible. ×250

For several decades, the discussion, if RBILD could be the early form of DIP or vice versa, is unsolved. But there are some aspects, which clearly separates both entities: DIP is a rare, whereas RBILD a common disease. Respiratory bronchiolitis is not seen in DIP and extension of macrophage accumulation beyond the centrilobular region is not seen in RBILD. If one disease arises from the other entities, some overlap features should be present. So I think this debate can be closed, just on logical aspects.

The reason of DIP might be explained similar to RBILD; however, as DIP is rare, there might be some other underlying disease modifiers, which we do not know. A few other causes have been reported in the literature such as steel welding fumes [36], waterproofing sprays [37], and toxin inhalation, as well as certain drugs [35].

Bronchoalveolar lavage can be of help in the diagnosis of DIP and RBILD. However, in both diseases pigmented alveolar macrophages dominate the cytological findings. Alveolar macrophages can be seen in up to 85 % of the total cells. Staining for hemosiderin can be positive in these macrophages; however, this is a mild finely granular staining, not coarse granular as in previous episodes of hemorrhage.

7.4 Smoking-Induced Interstitial Fibrosis (SRIF)/Respiratory Bronchiolitis-Associated Interstitial Lung Disease (RBILD)

SRIF and RBILD might represent the same disease characterized by a respiratory bronchiolitis and a paucicellular eosinophilic collagenous thickening of alveolar septa with a subpleural distribution [38, 39]. In some areas the disease resembles fibrotic NSIP, but the typical association with tobacco smoking points to this underlying etiology. In looking up several cases of respiratory bronchiolitis, we also recognized similar reactions as described by S. Yousem and A. L. Katzenstein, but in addition also cases showing fibroblastic foci associated with emphysema blebs and fibrosis (Figs. 7.16 and 7.17), which were also mentioned by Katzenstein in her original case description [38]. In these cases also respiratory bronchiolitis could be seen in different areas. In contrast to UIP, there were no honeycomb lesions, and almost all lobules showed changes of centrilobular emphysema (Fig. 7.18). Some of these patients were clinically diagnosed as having COPD, in others the lesions were found incidentally because of pneumothorax. So this

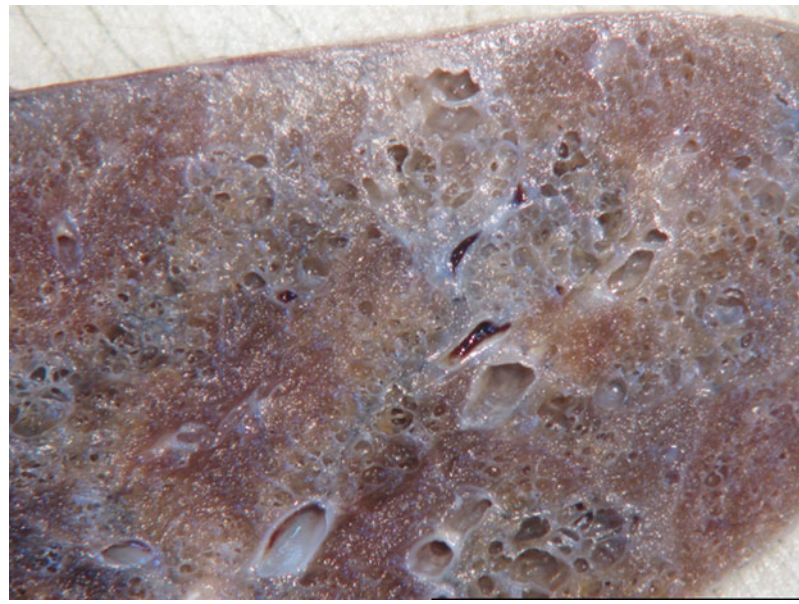

Fig. 7.16 Macroscopic features of smoking-related interstitial fibrosis (SRIF); the emphysematous cysts are easily recognized. The wall of bronchi and bronchioles are thickened, and whitish fibrotic areas can be discerned

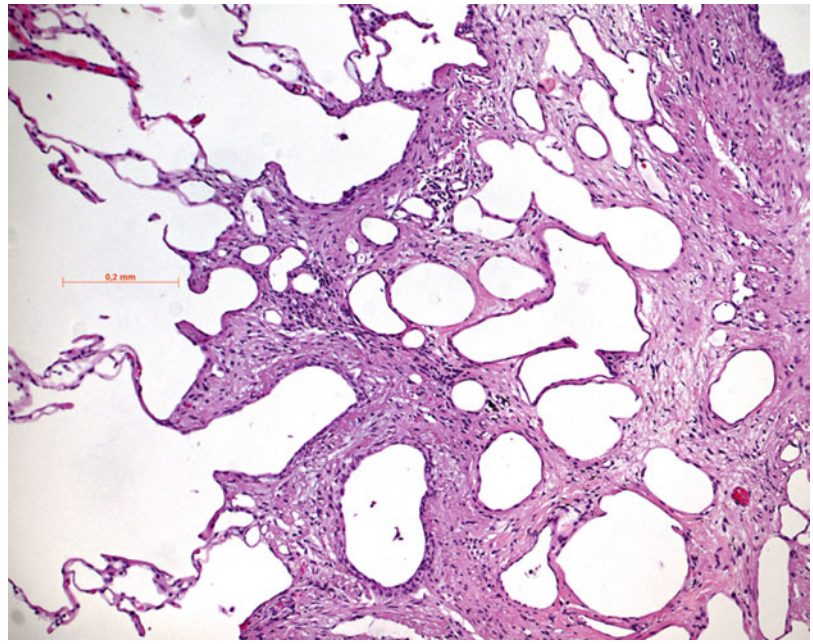

Fig. 7.17 Corresponding morphology to fibrosis and emphysematous blebs. Note also myofibroblastic foci. H&E, bar 200 µm

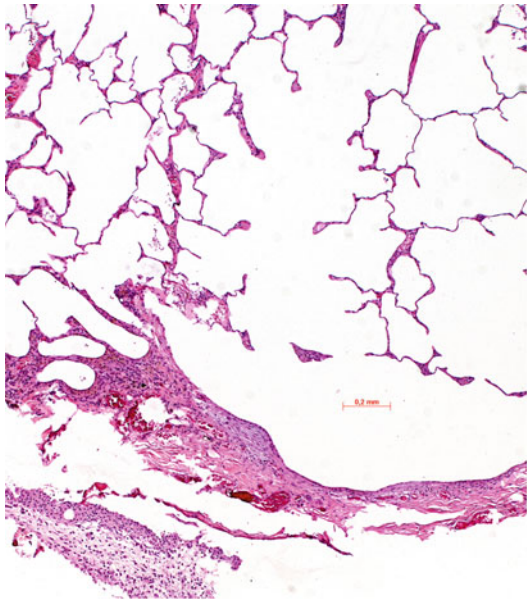

Fig. 7.18 SRIF showing a fibroblastic focus associated with centrilobular emphysema. In contrast to UIP, there are no cystic remodeled areas, and there is no temporal heterogeneity. H&E, bar 200 µm

might represent another form of smoking-induced lung fibrosis, probably resulting from release of toxic enzymes from macrophages and subsequent destruction and repair of alveolar septa.

7.5 Chronic Obstructive Pulmonary Disease (COPD)

COPD is clinically characterized by prolonged coughing and mucus expectoration within two consecutive seasonal periods and at least one episode in two following years. Although this subject has been discussed in the emphysema chapter and also in airway diseases, we will summarize the main features here and also discuss the etiology and pathogenesis more in detail. The two main pathological features of COPD to be seen are chronic bronchitis and emphysema; chronic bronchitis can be diagnosed if one of the following features is present (Fig. 7.19):

1. Lymphocytic and plasmacytic infiltrates within the mucosa
2. Goblet cell hyperplasia within the mucosa and/or the bronchial glands (Fig. 7.20)
3. Hyperplasia of bronchial glands (can only be evaluated in resection specimen; Fig. 7.21)

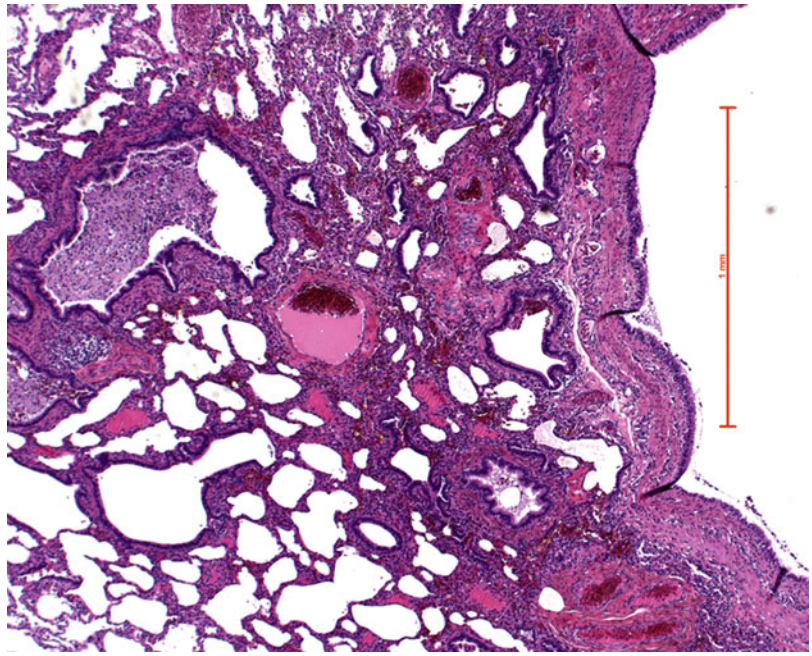

Fig. 7.19 Chronic obstructive pulmonary disease (COPD). There is chronic bronchitis, focally with bronchiectasis, and there is emphysema (best seen in lower half). H&E, bar 1 mm

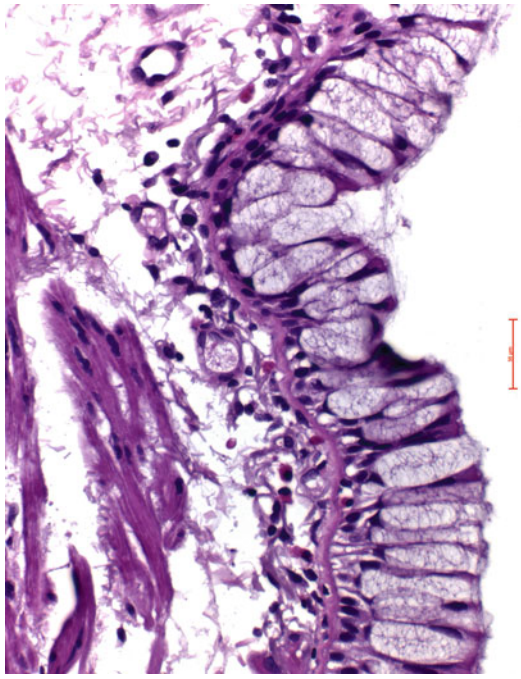

Fig. 7.20 COPD, goblet cell hyperplasia in a bronchus; note also the thickening of the basal lamina. H&E, bar 50 µm

An enlargement of alveoli and reduction in number characterizes emphysema. One of the easiest measurements is the linear intercept: draw a line from one bronchiole to the next one; the line should pass seven alveolar septa. Less than five septa already qualifies for emphysema, which is a structural remodeling of the peripheral lung. In COPD the emphysema corresponds to the centrilobular type (Fig. 7.22).

The incidence of COPD is increasing worldwide. It is estimated that by 2025, COPD might be the number one disease in most developed countries, outnumbering cardiovascular diseases [40–51].

7.5.1 What Are the Mechanisms? Why Not Every Smoker Develops COPD?

To answer these questions, we need not only to focus on toxic mechanisms of tobacco smoke but also on the different protective mechanisms the lung has developed to keep the airways clean.

As with any toxic substance, tobacco smoke acts by a mixture of different components, either physically or chemically. Tobacco smoke at the burning tip of the cigarette has a temperature of

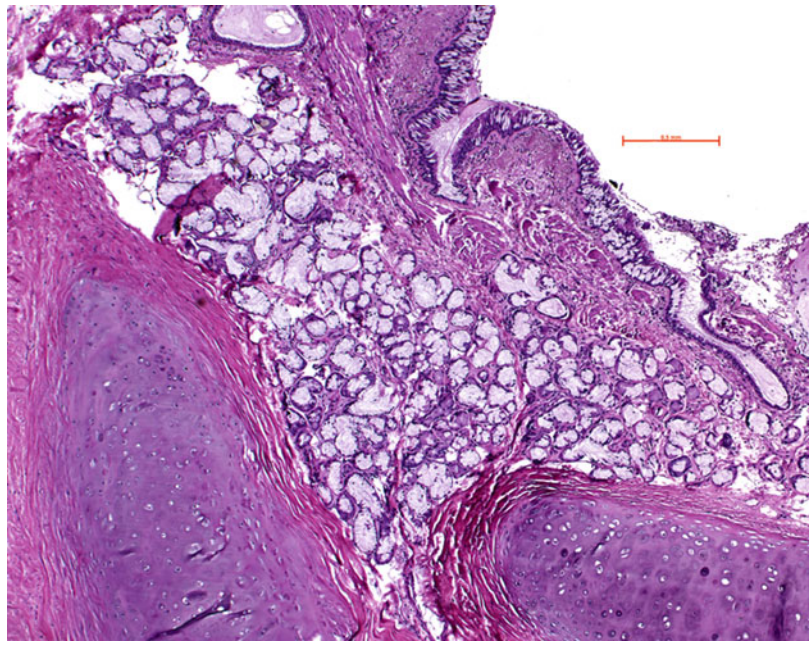

Fig. 7.21 COPD, hyperplasia of bronchial glands, and concomitant hyperplasia of goblet cells within the glands. H&E, bar 500 µm

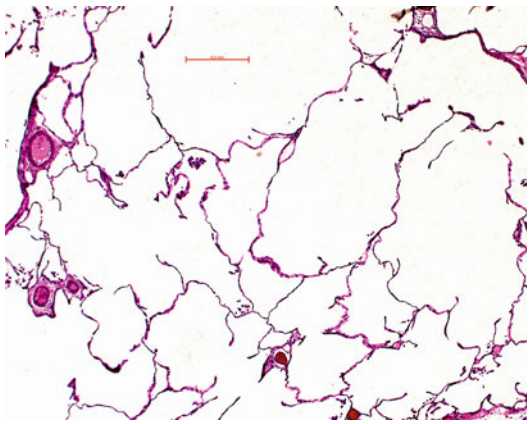

Fig. 7.22 COPD, the peripheral lung tissue shows centrilobular emphysema. H&E, bar 500 µm

approximately 400–600 °C; the inhaled smoke has a temperature between 60 and 80 °C, which by itself already will cause injury to the epithelial layer of the airways. Tobacco smoke constituents contain acidic as well as basophilic substances. These will cause injury to the epithelia. Many of the polyaromatic hydrocarbons act acidic by their SO_3 groups or N = N double or triple bounds, which will dissociate into NO_x groups, but also can be basic by NH_2 groups, depending on the availability of either oxidizing or aminating enzymes.

However, there are defense mechanisms at the epithelial layer preventing epithelial injury. The evolutionary oldest mechanisms are the mucus escalator system and phagocytosis by macrophages. Goblet and secretory cells at the surface and in bronchial glands secrete mucus. It covers the epithelia as a thin film, which is constantly moved toward the larynx by the beating cilia (mucociliary clearance). Many toxic substances, tobacco smoke constituents included, stick within this mucus and are transported toward the upper airways and coughed out. But high temperature by tobacco smoke will slow down and even block ciliary beating, resulting in prolonged contact of toxic substances with the epithelia. Chronic tobacco smoke inhalation will also cause apoptosis of ciliated columnar cells, which are consecutively replaced by goblet and secretory cells. This will primarily result in an increase of mucus thickness protecting the epithelia, but later on in more sticky mucus, which cannot be rapidly moved by the cilia. This again results in slowed mucus transport and thus more contact time for toxic substances to injure the epithelia.

Another protection, as old as the former, is phagocytosis/pinocytosis of substances by alveolar macrophages in the alveolar periphery. Macrophages constantly move within the alveoli and remove foreign material. This material will be degraded in phagolysosomes. Some of the tobacco smoke waste can be seen in the phagolysosomes such as carcinogenic cadmium compounds (needlelike material under electron microscopic magnification). These substances can still act on the cells and might even be liberated from dying macrophages.

Less well known are the enzymatic defense mechanisms. Along the airways different enzymes are found in varying concentrations, including individual variations. Whereas the concentration is low in the trachea, the enzymes are more concentrated in bronchiolar and alveolar epithelia [52–56]. Two groups of enzymes can be found: phase 1 enzymes are mainly oxidases such as cytochrome p450 oxidases and phase 2 enzymes as hydrolases, sulfatases, and glutathione transferases. Oxidases play a major role in the defense against bacterial infection by oxidizing bacterial capsules molecules and thus paving the way for opsonization and degradation. In tobacco smoke-induced injury, these oxidases can toxify polyaromatic hydrocarbons creating oxygen radicals, which can cause apoptosis of cells but also can induce DNA strand breaks, paving the way for carcinogenesis. On the other hand, phase 2 enzymes can detoxify many polyhydrocarbons by hydrolyzing CH_2 groups, breaking double bounds on N = N, or may prevent toxicity of oxygen radicals by increasing the glutathione pool in epithelial cells [54, 56–61]. In some individuals, group 1 enzymes and in others group 2 enzymes dominate, which can explain why one group of patients is prone to develop pulmonary carcinomas, whereas others seem to be protected, but instead develop arteriosclerosis or other diseases related to tobacco smoke exposure.

Finally immune mechanisms came into focus recently. It is well known that neutrophils and macrophages contribute to emphysema development. But recently it was shown that the presence of CD8+ T cells could distinguish between smokers with and without COPD. If T cells are responsible for the lung injury and progression of COPD, this would point to an antigenic stimulus originating in the lung, and consequently COPD has to be considered as an autoimmune disease [62]. This concept was further strengthened by experiments using endothelial cells (EC) as antigen. Immunization with ECs causes pneumocyte apoptosis and activation of matrix metalloproteases MMP9 and MMP2. Anti-EC antibodies caused emphysema in passively immunized mice. Adoptive transfer of $CD4^+$ cells into naïve animals resulted in emphysema. Therefore, it was proven that humoral and $CD4^+$ lymphocyte-dependent immune mechanisms are sufficient to trigger the development of emphysema [63]. In other experiments, chemokine receptor 6 (CCR6), usually expressed on dendritic cells, neutrophils, and T lymphocytes, was knocked out. In the lung tissue of CCR6 KO mice, the inflammatory action of dendritic cells, activated $CD8^+$ T lymphocytes, and granulocytes was impaired. This attenuated inflammatory response partially protected against emphysema and correlated with impaired production of MMP12. This study showed that the interaction of CCR6 with its ligand MIP3α contributes to the pathogenesis of cigarette smoke-induced emphysema and COPD [64]. In experiments done decades ago, instillation of elastase was used to induce emphysema [65]. Recently antielastin antibodies and T-helper-1 (Th1) responses in COPD patients were shown to correlate with emphysema severity. These findings link emphysema to adaptive immunity against a specific lung antigen associated with cigarette smoking [66]. Finally the study of Ehlers et al. pointed to new biological functions of α1-antitrypsin as a modulator of immune reactions. In these studies, AAT therapy prevents or reverses autoimmune disease and graft loss and induces immune tolerance [67].

References

1. Koethe SM, Kuhnmuench JR, Becker CG. Neutrophil priming by cigarette smoke condensate and a tobacco anti-idiotypic antibody. Am J Pathol. 2000;157:1735–43.

2. Youkeles LH, Grizzanti JN, Liao Z, Chang CJ, Rosenstreich DL. Decreased tobacco-glycoprotein-induced lymphocyte proliferation in vitro in pulmonary eosinophilic granuloma. Am J Respir Crit Care Med. 1995;151:145–50.
3. Friedman PJ, Liebow AA, Sokoloff J. Eosinophilic granuloma of lung. Clinical aspects of primary histiocytosis in the adult. Medicine (Baltimore). 1981;60:385–96.
4. Sundar KM, Gosselin MV, Chung HL, Cahill BC. Pulmonary Langerhans cell histiocytosis: emerging concepts in pathobiology, radiology, and clinical evolution of disease. Chest. 2003;123:1673–83.
5. Egeler RM, Favara BE, van Meurs M, Laman JD, Claassen E. Differential in situ cytokine profiles of Langerhans-like cells and T cells in Langerhans cell histiocytosis: abundant expression of cytokines relevant to disease and treatment. Blood. 1999;94: 4195–201.
6. Badalian-Very G, Vergilio JA, Degar BA, MacConaill LE, Brandner B, Calicchio ML, Kuo FC, Ligon AH, Stevenson KE, Kehoe SM, Garraway LA, Hahn WC, Meyerson M, Fleming MD, Rollins BJ. Recurrent BRAF mutations in Langerhans cell histiocytosis. Blood. 2010;116:1919–23.
7. Badalian-Very G, Vergilio JA, Degar BA, Rodriguez-Galindo C, Rollins BJ. Recent advances in the understanding of Langerhans cell histiocytosis. Br J Haematol. 2012;156:163–72.
8. Wilejto M, Abla O. Langerhans cell histiocytosis and Erdheim-Chester disease. Curr Opin Rheumatol. 2012;24:90–6.
9. Chikwava KR, Hunt JL, Mantha GS, Murphy JE, Jaffe R. Analysis of loss of heterozygosity in single-system and multisystem Langerhans' cell histiocytosis. Pediatr Dev Pathol. 2007;10:18–24.
10. Mehes G, Irsai G, Bedekovics J, Beke L, Fazakas F, Rozsa T, Kiss C. Activating BRAF V600E mutation in aggressive pediatric Langerhans cell histiocytosis: demonstration by allele-specific PCR/direct sequencing and immunohistochemistry. Am J Surg Pathol. 2014;38:1644–8.
11. Nezelof C, Basset F. Langerhans cell histiocytosis research. Past, present, and future. Hematol Oncol Clin N Am. 1998;12:385–406.
12. Shahla A, Parvaneh V, Hossein HD. Langerhans cells histiocytosis in one family. Pediatr Hematol Oncol. 2004;21:313–20.
13. Chabrol E, Nurisso A, Daina A, Vassal-Stermann E, Thepaut M, Girard E, Vives RR, Fieschi F. Glycosaminoglycans are interactants of Langerin: comparison with gp120 highlights an unexpected calcium-independent binding mode. PLoS ONE. 2012;7, e50722.
14. Feinberg H, Rowntree TJ, Tan SL, Drickamer K, Weis WI, Taylor ME. Common polymorphisms in human langerin change specificity for glycan ligands. J Biol Chem. 2013;288:36762–71.
15. Lenormand C, Spiegelhalter C, Cinquin B, Bardin S, Bausinger H, Angenieux C, Eckly A, Proamer F, Wall D, Lich B, Tourne S, Hanau D, Schwab Y, Salamero J, de la Salle H. Birbeck granule-like "organized smooth endoplasmic reticulum" resulting from the expression of a cytoplasmic YFP-tagged langerin. PLoS ONE. 2013;8, e60813.
16. Egeler RM, van Halteren AG, Hogendoorn PC, Laman JD, Leenen PJ. Langerhans cell histiocytosis: fascinating dynamics of the dendritic cell-macrophage lineage. Immunol Rev. 2010;234:213–32.
17. Salazar F, Ghaemmaghami AM. Allergen recognition by innate immune cells: critical role of dendritic and epithelial cells. Front Immunol. 2013;4:356.
18. Lambrecht BN, Hammad H. Allergens and the airway epithelium response: gateway to allergic sensitization. J Allergy Clin Immunol. 2014;134:499–507.
19. Fisher GM, Iqball S, Knight SC. Gene expression during differentiation of human dendritic cells from cord blood cd34 stem cells. Cytokine. 1999;11:111–7.
20. Dziegiel P, Dolilnska-Krajewska B, Dumanska M, Weclawek J, Jelen M, Podhorska-Okolow M, Jagoda E, Fic M, Zabel M. Coexpression of CD1a, langerin and Birbeck's granules in Langerhans cell histiocytoses (LCH) in children: ultrastructural and immunocytochemical studies. Folia Histochem Cytobiol. 2007;45:21–5.
21. Park HJ, Jeon YK, Lee AH, Oh YH, Park SH, Jung KC. Use of the JL1 epitope, which encompasses the nonglycosylation site of CD43, as a marker of immature/neoplastic Langerhans cells. Am J Surg Pathol. 2012;36:1150–7.
22. Vassallo R, Jensen EA, Colby TV, Ryu JH, Douglas WW, Hartman TE, Limper AH. The overlap between respiratory bronchiolitis and desquamative interstitial pneumonia in pulmonary Langerhans cell histiocytosis: high-resolution CT, histologic, and functional correlations. Chest. 2003;124:1199–205.
23. Scheidl SJ, Kusej M, Flick H, Stacher E, Matzi V, Kovacs G, Popper HH, Costabel U, Olschewski H. Clinical manifestations of respiratory bronchiolitis as an incidental finding in surgical lung biopsies: a retrospective analysis of a large Austrian registry. Respiration. 2016;91:26–33.
24. Fraig M, Shreesha U, Savici D, Katzenstein AL. Respiratory bronchiolitis: a clinicopathologic study in current smokers, ex-smokers, and never-smokers. Am J Surg Pathol. 2002;26:647–53.
25. Popper HH. Bronchiolitis, an update. Virchows Arch. 2000;437:471–81.
26. Ryu JH, Colby TV, Hartman TE, Vassallo R. Smoking-related interstitial lung diseases: a concise review. Eur Respir J. 2001;17:122–32.
27. Allison AC. Pathogenic effects of inhaled particles and antigens. Ann N Y Acad Sci. 1974;221:299–308.
28. Oberdorster G. Lung particle overload: implications for occupational exposures to particles. Regul Toxicol Pharmacol. 1995;21:123–35.
29. Liebow AA, Steer A, Billingsley JG. Desquamative interstitial pneumonia. Am J Med. 1965;39: 369–404.
30. Valdivia E, Hensley G, Leory EP, Wu J, Jaeschke W. Morphology and pathogenesis of desquamative interstitial pneumonitis. Thorax. 1977;32:7–18.

31. Singh G, Katyal SL, Whiteside TL, Stachura I. Desquamative interstitial pneumonitis. The intra-alveolar cells are macrophages. Chest. 1981;79:128.
32. Crotty Alexander LE, Shin S, Hwang JH. Inflammatory diseases of the lung induced by conventional cigarette smoke: a review. Chest. 2015;148:1307–22.
33. Kroll RR, Flood DA, Srigley J. Desquamative interstitial pneumonitis in a non-smoker: a rare diagnosis. Can Respir J. 2014;21:86–8.
34. Ischander M, Fan LL, Farahmand V, Langston C, Yazdani S. Desquamative interstitial pneumonia in a child related to cigarette smoke. Pediatr Pulmonol. 2014;49:E56–8.
35. Godbert B, Wissler MP, Vignaud JM. Desquamative interstitial pneumonia: an analytic review with an emphasis on aetiology. Eur Respir Rev. 2013;22: 117–23.
36. Cosgrove MP. Pulmonary fibrosis and exposure to steel welding fume. Occup Med (Lond). 2015;65: 706–12.
37. Nakazawa A, Hagiwara E, Harada S, Yoshida M, Baba T, Okudela K, Takemura T, Ogura T. Surgically proven desquamative interstitial pneumonia induced by waterproofing spray. Intern Med. 2014;53:2107–10.
38. Katzenstein AL, Mukhopadhyay S, Zanardi C, Dexter E. Clinically occult interstitial fibrosis in smokers: classification and significance of a surprisingly common finding in lobectomy specimens. Hum Pathol. 2010;41:316–25.
39. Yousem SA. Respiratory bronchiolitis-associated interstitial lung disease with fibrosis is a lesion distinct from fibrotic nonspecific interstitial pneumonia: a proposal. Mod Pathol Off J US Can Acad Pathol Inc. 2006;19:1474–9.
40. Lozano R, Naghavi M, Foreman K, Lim S, Shibuya K, Aboyans V, Abraham J, Adair T, Aggarwal R, Ahn SY, Alvarado M, Anderson HR, Anderson LM, Andrews KG, Atkinson C, Baddour LM, Barker-Collo S, Bartels DH, Bell ML, Benjamin EJ, Bennett D, Bhalla K, Bikbov B, Bin Abdulhak A, Birbeck G, Blyth F, Bolliger I, Boufous S, Bucello C, Burch M, Burney P, Carapetis J, Chen H, Chou D, Chugh SS, Coffeng LE, Colan SD, Colquhoun S, Colson KE, Condon J, Connor MD, Cooper LT, Corriere M, Cortinovis M, de Vaccaro KC, Couser W, Cowie BC, Criqui MH, Cross M, Dabhadkar KC, Dahodwala N, De Leo D, Degenhardt L, Delossantos A, Denenberg J, Des Jarlais DC, Dharmaratne SD, Dorsey ER, Driscoll T, Duber H, Ebel B, Erwin PJ, Espindola P, Ezzati M, Feigin V, Flaxman AD, Forouzanfar MH, Fowkes FG, Franklin R, Fransen M, Freeman MK, Gabriel SE, Gakidou E, Gaspari F, Gillum RF, Gonzalez-Medina D, Halasa YA, Haring D, Harrison JE, Havmoeller R, Hay RJ, Hoen B, Hotez PJ, Hoy D, Jacobsen KH, James SL, Jasrasaria R, Jayaraman S, Johns N, Karthikeyan G, Kassebaum N, Keren A, Khoo JP, Knowlton LM, Kobusingye O, Koranteng A, Krishnamurthi R, Lipnick M, Lipshultz SE, Ohno SL, Mabweijano J, MacIntyre MF, Mallinger L, March L, Marks GB, Marks R, Matsumori A, Matzopoulos R, Mayosi BM, McAnulty JH, McDermott MM, McGrath J, Mensah GA, Merriman TR, Michaud C, Miller M, Miller TR, Mock C, Mocumbi AO, Mokdad AA, Moran A, Mulholland K, Nair MN, Naldi L, Narayan KM, Nasseri K, Norman P, O'Donnell M, Omer SB, Ortblad K, Osborne R, Ozgediz D, Pahari B, Pandian JD, Rivero AP, Padilla RP, Perez-Ruiz F, Perico N, Phillips D, Pierce K, Pope 3rd CA, Porrini E, Pourmalek F, Raju M, Ranganathan D, Rehm JT, Rein DB, Remuzzi G, Rivara FP, Roberts T, De Leon FR, Rosenfeld LC, Rushton L, Sacco RL, Salomon JA, Sampson U, Sanman E, Schwebel DC, Segui-Gomez M, Shepard DS, Singh D, Singleton J, Sliwa K, Smith E, Steer A, Taylor JA, Thomas B, Tleyjeh IM, Towbin JA, Truelsen T, Undurraga EA, Venketasubramanian N, Vijayakumar L, Vos T, Wagner GR, Wang M, Wang W, Watt K, Weinstock MA, Weintraub R, Wilkinson JD, Woolf AD, Wulf S, Yeh PH, Yip P, Zabetian A, Zheng ZJ, Lopez AD, Murray CJ, AlMazroa MA, Memish ZA. Global and regional mortality from 235 causes of death for 20 age groups in 1990 and 2010: a systematic analysis for the Global Burden of Disease Study 2010. Lancet. 2012;380:2095–128.
41. Lou P, Zhu Y, Chen P, Zhang P, Yu J, Zhang N, Chen N, Zhang L, Wu H, Zhao J. Vulnerability, beliefs, treatments and economic burden of chronic obstructive pulmonary disease in rural areas in China: a cross-sectional study. BMC Public Health. 2012;12:287.
42. Mehta AJ, Miedinger D, Keidel D, Bettschart R, Bircher A, Bridevaux PO, Curjuric I, Kromhout H, Rochat T, Rothe T, Russi EW, Schikowski T, Schindler C, Schwartz J, Turk A, Vermeulen R, Probst-Hensch N, Kunzli N. Occupational exposure to dusts, gases, and fumes and incidence of chronic obstructive pulmonary disease in the Swiss Cohort Study on Air Pollution and Lung and Heart Diseases in Adults. Am J Respir Crit Care Med. 2012;185:1292–300.
43. Adeloye D, Basquill C, Papana A, Chan KY, Rudan I, Campbell H. An estimate of the prevalence of COPD in Africa: a systematic analysis. COPD. 2015;12(1):71–81.
44. Ciapponi A, Alison L, Agustina M, Demian G, Silvana C, Edgardo S. The epidemiology and burden of COPD in Latin America and the Caribbean: systematic review and meta-analysis. COPD. 2014;11:339–50.
45. Pallasaho P, Kainu A, Sovijarvi A, Lindqvist A, Piirila PL. Combined effect of smoking and occupational exposure to dusts, gases or fumes on the incidence of COPD. COPD. 2014;11:88–95.
46. Blanchette CM, Dalal AA, Mapel D. Changes in COPD demographics and costs over 20 years. J Med Econ. 2012;15:1176–82.
47. Lam KB, Yin P, Jiang CQ, Zhang WS, Adab P, Miller MR, Thomas GN, Ayres JG, Lam TH, Cheng KK. Past dust and GAS/FUME exposure and COPD in Chinese: the Guangzhou Biobank Cohort Study. Respir Med. 2012;106:1421–8.
48. Vanfleteren LE, Franssen FM, Wesseling G, Wouters EF. The prevalence of chronic obstructive pulmonary

disease in Maastricht, the Netherlands. Respir Med. 2012;106:871–4.
49. Ringshausen FC, de Roux A, Pletz MW, Hamalainen N, Welte T, Rademacher J. Bronchiectasis-associated hospitalizations in Germany, 2005–2011: a population-based study of disease burden and trends. PLoS ONE. 2013;8, e71109.
50. Falzon C, Soljak M, Elkin SL, Blake ID, Hopkinson NS. Finding the missing millions – the impact of a locally enhanced service for COPD on current and projected rates of diagnosis: a population-based prevalence study using interrupted time series analysis. Prim Care Respir J. 2013;22:59–63.
51. El Hasnaoui A, Rashid N, Lahlou A, Salhi H, Doble A, Nejjari C. Chronic obstructive pulmonary disease in the adult population within the Middle East and North Africa region: rationale and design of the BREATHE study. Respir Med. 2012;106 Suppl 2:S3–15.
52. Vanderslice RR, Domin BA, Carver GT, Philpot RM. Species-dependent expression and induction of homologues of rabbit cytochrome P-450 isozyme 5 in liver and lung. Mol Pharmacol. 1987;31:320–5.
53. Cohen GM. Pulmonary metabolism of foreign compounds: its role in metabolic activation. Environ Health Perspect. 1990;85:31–41.
54. Bartsch H, Petruzzelli S, De Flora S, Hietanen E, Camus AM, Castegnaro M, Alexandrov K, Rojas M, Saracci R, Giuntini C. Carcinogen metabolism in human lung tissues and the effect of tobacco smoking: results from a case – control multicenter study on lung cancer patients. Environ Health Perspect. 1992;98:119–24.
55. Dinsdale D. Lung injury: cell-specific bioactivation/deactivation of circulating pneumotoxins. Int J Exp Pathol. 1995;76:393–401.
56. Mace K, Bowman ED, Vautravers P, Shields PG, Harris CC, Pfeifer AM. Characterisation of xenobiotic-metabolising enzyme expression in human bronchial mucosa and peripheral lung tissues. Eur J Cancer. 1998;34:914–20.
57. Nakajima T, Elovaara E, Anttila S, Hirvonen A, Camus AM, Hayes JD, Ketterer B, Vainio H. Expression and polymorphism of glutathione S-transferase in human lungs: risk factors in smoking-related lung cancer. Carcinogenesis. 1995;16:707–11.
58. Risch A, Wikman H, Thiel S, Schmezer P, Edler L, Drings P, Dienemann H, Kayser K, Schulz V, Spiegelhalder B, Bartsch H. Glutathione-S-transferase M1, M3, T1 and P1 polymorphisms and susceptibility to non-small-cell lung cancer subtypes and hamartomas. Pharmacogenetics. 2001;11:757–64.
59. Stucker I, Hirvonen A, de Waziers I, Cabelguenne A, Mitrunen K, Cenee S, Koum-Besson E, Hemon D, Beaune P, Loriot MA. Genetic polymorphisms of glutathione S-transferases as modulators of lung cancer susceptibility. Carcinogenesis. 2002;23:1475–81.
60. Reszka E, Wasowicz W, Rydzynski K, Szeszenia-Dabrowska N, Szymczak W. Glutathione S-transferase M1 and P1 metabolic polymorphism and lung cancer predisposition. Neoplasma. 2003;50:357–62.
61. Castell JV, Donato MT, Gomez-Lechon MJ. Metabolism and bioactivation of toxicants in the lung. The in vitro cellular approach. Exp Toxicol Pathol. 2005;57 Suppl 1:189–204.
62. Cosio MG, Majo J. Inflammation of the airways and lung parenchyma in COPD: role of T cells. Chest. 2002;121:160S–5.
63. Taraseviciene-Stewart L, Scerbavicius R, Choe KH, Moore M, Sullivan A, Nicolls MR, Fontenot AP, Tuder RM, Voelkel NF. An animal model of autoimmune emphysema. Am J Respir Crit Care Med. 2005;171:734–42.
64. Bracke KR, D'Hulst AI, Maes T, Moerloose KB, Demedts IK, Lebecque S, Joos GF, Brusselle GG. Cigarette smoke-induced pulmonary inflammation and emphysema are attenuated in CCR6-deficient mice. J Immunol. 2006;177:4350–9.
65. Schuyler MR, Rynbrandt DJ, Kleinerman J. Physiologic and morphologic observations of the effects of intravenous elastase on the lung. Am Rev Respir Dis. 1978;117:97–102.
66. Lee SH, Goswami S, Grudo A, Song LZ, Bandi V, Goodnight-White S, Green L, Hacken-Bitar J, Huh J, Bakaeen F, Coxson HO, Cogswell S, Storness-Bliss C, Corry DB, Kheradmand F. Antielastin autoimmunity in tobacco smoking-induced emphysema. Nat Med. 2007;13:567–9.
67. Ehlers MR. Immune-modulating effects of alpha-1 antitrypsin. Biol Chem. 2014;395:1187–93.

Pneumonia

8

8.1 Alveolar Pneumonias (Lobar and Bronchopneumonia)

The lung is constantly exposed to airborne infectious agents due to the large surface area of approximately 100 m^2. Therefore pneumonia is one of the most common lung diseases. Understanding infection requires understanding the routes of infections, the way invading organisms infect epithelial cells, as well as defense mechanisms of the lung tissue acquired during evolution.

By the double arterial supply via pulmonary and bronchial arteries, neutrophil granulocytes or lymphocytes and monocytes can be directed into an area of infection rapidly. In addition the diameter of the pulmonary capillaries of approximately 5–6 μm requires adaptation of leukocytes and thus also slows their passage time, providing more time for contact with adhesion molecules expressed on endothelial cells, required for migration into the infected tissue [1].

Defense system: The mucociliary escalator system can remove infectious organisms before they might act on the epithelia. The more viscous layer of mucus is at the surface, the more liquid layer at the ciliary site. Bacteria, for example, stick within this viscous mucus and can be transported toward the larynx. The cough reflex in addition helps to expel this material from the airways. An example how important this system works can be seen in patients with immotile cilia syndrome, where an inherent gene defect causes uncoordinated ciliary beating and results in defective clearance of mucus and subsequent recurrent infections [2, 3].

Innate immune system: The innate immune system consists of complement activation (often via alternative pathway), surfactant apoproteins capable of bacterial inactivation, and the cellular constituents such as macrophages, granulocytes, and epithelial cells. Here we will briefly discuss this system. For more detailed information, the reader is referred to the vast amount of immunological reviews on this subject.

There are three known activation pathways for complement: the alternative, the classic, and the lectin pathway. Opsonization seems to be the most important function of complement C3. This leads to enhanced phagocytosis of bacteria. The system seems to be self-regulated as phagocytosis of apoptotic neutrophils by macrophages leads to less C3 activation and cytokine release by macrophages and consequently less inflammation [4].

Several surfactant apoproteins (SP) are produced by type II pneumocytes and secreted toward the alveolar surface. Two of them SPA and SPD are members of the collectin family proteins. At their C-terminal end, they have a lectin moiety, which is able to recognize bacterial oligosaccharides (galactosylceramide, glucosylceramide) present on the capsule of bacteria such as staphylococci. This binding causes aggregation and growth arrest of the

© Springer-Verlag Berlin Heidelberg 2017
H. Popper, *Pathology of Lung Disease*, DOI 10.1007/978-3-662-50491-8_8

bacteria and enhances phagocytosis by alveolar macrophages [5, 6].

Epithelial cells form a barrier for the entry of infectious organisms and thus protect the underlying mesenchymal structures, essential for lung function. Although many organisms have developed binding sites for respiratory epithelia, such as ICAM1 used by rhinoviruses, the epithelia have developed response mechanisms such as cytokine release, for example, proinflammatory interleukin 1β (IL1β), tumor necrosis factor α (TNFα), IL6, IL16, chemokines as IL8, macrophage inflammatory protein (MIP1α), RANTES, granulocyte-macrophage colony-stimulating factor (GMCSF), and others [7]. By the release of these mediators, neutrophils, macrophages, lymphocytes, and especially also cytotoxic T and NK cells are attracted and might initially already kill the invading organisms.

Monocytes/macrophages and granulocytes: Macrophages are the primary source of defense against any type of infectious organism. Macrophages constantly patrol throughout the lung, ingesting every inhaled foreign material. Macrophages in contrast to monocytes live longer due to a genetic shift toward antiapoptosis by downregulating PTEN [8]. Macrophages also express Toll-like receptors (TLR2, TLR4) and CD14 and interact with SPA and CD44 to exert different functions such as release of antibacterial proteins/peptides [9]. Granulocytes interact with macrophages: if large amount of bacteria are inhaled, macrophages direct neutrophils to the site of infection, whereas small amounts of bacteria might be cleared by macrophages alone. Removal of apoptotic neutrophils requires macrophages, and this in turn decreases the inflammatory response and neutrophil influx [4]. Neutrophils are able to kill many phagocytosed bacteria by producing large amounts of oxygen radicals (superoxide anions) in their lysosomes and fusing them with the phagosomes. Neutrophils are produced in the bone marrow and released from there by cytokine stimuli. Once they enter the circulation, their apoptotic program is activated. They enter the infectious site using adhesion molecules on endothelia in due time and exert their function. This is facilitated by integrins and also other adhesins. Once within the interstitium, neutrophils move along gradients of chemokines and also acidic pH.

Eosinophils are specifically seen in parasitic infections. This is usually mediated by T lymphocytes and will be discussed below.

Adaptive immune system: The adaptive immune system is a late invention in evolution. It requires different types of lymphocytes, such as B lymphocytes for an antibody-mediated reaction and T lymphocytes and NK cells for a direct cell-mediated toxic reaction. In addition this system also requires classical dendritic cells for antigen processing and antigen presentation; these cells get in contact with invading organisms at the site of first contact or in lymph nodes.

Within the bronchial mucosa, IgA-producing B lymphocytes are found. Secreted IgA is a complex, where two molecules of IgA are joined by a secretory component. In combination with other molecules such as albumin, transferrin, ceruloplasmin, and IgG, these are antioxidants and have a mucosal defense function. These molecules are increased secreted in lung injury and inflammation [10]. In cigarette smokers the immune barrier function is impaired by a decreased release of secretory component, which in turn also decreases the transcytosis of IgA [11]. One of the most important functions of IgA secreted at the lining fluid is opsonization of different bacteria [12].

Different types of dendritic cells can be found in the bronchial and alveolar system such as classical, follicular, Langerhans, and interdigitating reticulum cells. These cells are thought to play a role in antigen uptake and processing. Dendritic cells also direct the type of immune reaction by interacting with different Toll receptors. Under inflammatory conditions a Thelper1 response is favored, whereas Thelper2 responses require another mechanism [13]. Dendritic cells, for example, confronted with mycobacteria will induce differentiation of $CD4^+$ to $CD4^+17^+$ cells and also induce Toll receptor 9 expression resulting in granuloma formation [14]. Some subpopulations of dendritic cells can induce immune tolerance and exhaustion, which might play a role in certain diseases, but this will be discussed in another chapter.

8.1.1 Clinical Symptoms of Pneumonias

There are some key features characterizing pneumonias, such as fever, cough, and fatigue. Fever will give some information about possible organisms: above 39.5 °C most likely this is caused by a viral infection, whereas bacterial pneumonias present with temperatures between 38 and 39 °C. Cough can be productive with either serous or purulent expectoration. Laboratory evaluation will show inflammatory parameters, such as leukocytosis, etc.

Radiologically the lung will show ground glass opacities and consolidations, depending on the age of the inflammatory infiltrate. Clinically pneumonias are separated into typical and atypical pneumonia. Atypical pneumonia can have different meanings, either an atypical infiltration pattern on CT scans or atypical presentation with rare infectious organisms.

8.1.2 Alveolar Pneumonias (Bronchopneumonia and Lobar Pneumonia; Adult and Childhood)

Although infectious pneumonia is a common disease, biopsies and surgical resections are rarely seen in pathologic practice. Most of these cases are diagnosed clinically and treated accordingly by antibiotics. If biopsied or resected, these cases usually turn out as unusual pneumonia caused by unusual organisms. Pneumonias are commonly seen at autopsy. The evaluation of infectious organisms will be discussed after the granulomatous pneumonias.

8.1.2.1 Gross Morphology

Pneumonia develops in stages, starting with hemorrhage. The lung is dark red, consistency is firm, and on the cut surface, there is some granularity seen, corresponding to fibrin cloths out of the alveoli (Fig. 8.1). In the next stage, the color of the lung changes to gray and grayish yellow. This is induced by the influx of leukocytes, dying of leukocytes, and release of lipid substances (Fig. 8.2). The consistency of the lung is comparable to liver tissue, hence the old name "hepatization." Finally

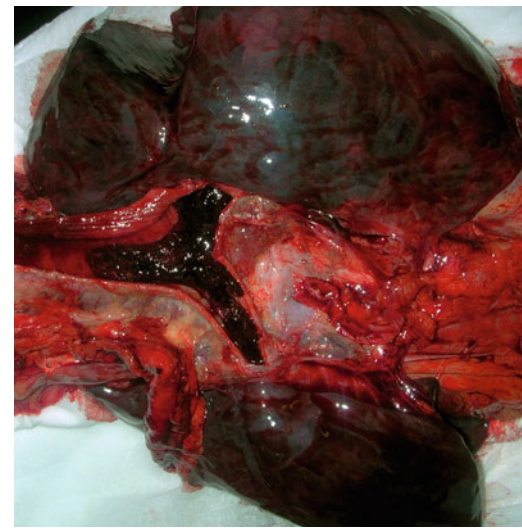

Fig. 8.1 Early pneumonia with hemorrhage; autopsy specimen

Fig. 8.2 Macroscopy of purulent bronchopneumonia. At lower right there is abscess formation; the pleura shows purulent pleuritis

in the best scenario, the exudate is reabsorbed, the alveoli are filled with air, and the lung changes back to normal (lysis). Most often these classical stages are not anymore seen, because pneumonia is immediately treated with antibiotics and therefore do not develop into the yellow "hepatization" stage but resolve out of the gray-red one. However, complications of bronchopneumonia can be seen such as abscess formation (Fig. 8.3) and pneumonia with infarcts due to infectious vasculitis (see below; Fig. 8.4).

Histology and development of bronchopneumonia: Bronchopneumonia in the initial stages starts with an influx of macrophages from the interstitial cell pool as well as from the blood vessels (monocytoid cells; Fig. 8.5). Capillaries are widened (hyperemia) and the endothelial gaps are opened. Fluid from the blood enters into the alveolar spaces (inflammatory edema) and proteins start to coagulate (fibrin cloths). This initial stage is followed by an entry of red blood cells, which undergo lysis, contributing to fibrinogenesis. In this stage fibrin nets are seen mixed with red blood cells, scattered macrophages, and neutrophils. This corresponds to the macroscopic picture of hemorrhagic pneumonia (dark red cut surface, heavy lung, edematous fluid rinsing from the cut surface). After 1 day dense infiltrations by neutrophils appear, mixed with fibrin nets completely filling the alveolar spaces (Fig. 8.6). Capillaries are still hyperemic and widened. Macroscopically the cut surface changes to a gray-red color, due to the massive infiltration by granulocytes. Since the alveoli are completely filled by cells and fibrin, the consistency is similar to liver (hepatic consolidation or hepatization). Granulocytes ingesting and degrading bacteria also die because of liberation of toxic lysosomal enzymes accumulate lipids within their cytoplasm, which macroscopically gives the cut surface a yellow tone (usually by day 2–3; Fig. 8.7). After 6–7 days clearance of the alveoli starts: neutrophils have degraded the bacteria, macrophages clear the debris from dying neutrophils, fibrin is lysed by the enzymes from macrophages and granulocytes, and finally the alveoli are filled by air again. Under normal condition the pneumonia resolves within 10–14 days without remnants of the infectious episode.

If for several reasons no resolution occurs, acute bronchopneumonia will undergo organization. The resulting morphologic picture is organizing pneumonia (see below).

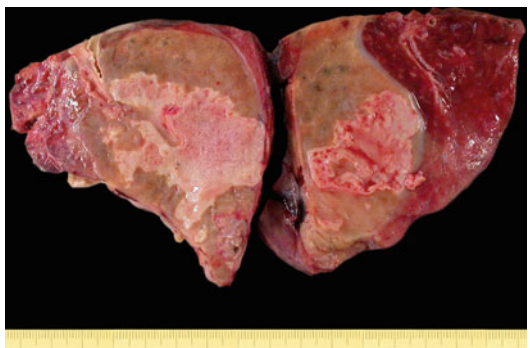

Fig. 8.3 Purulent pneumonia with abscess formation

Fig. 8.4 Purulent pneumonia with multiple infarcts due to infectious vasculitis

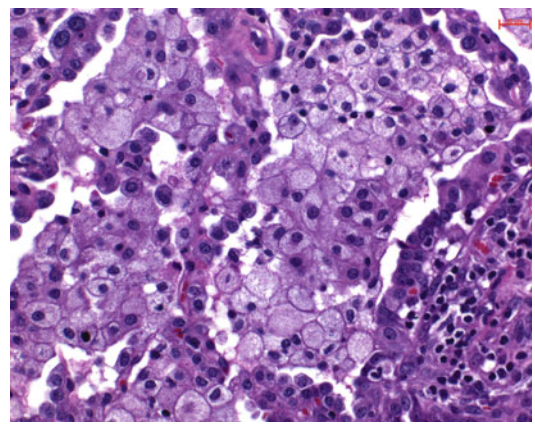

Fig. 8.5 Early bronchopneumonia with influx of macrophages into the alveolar lumen. H&E, bar 20 µm

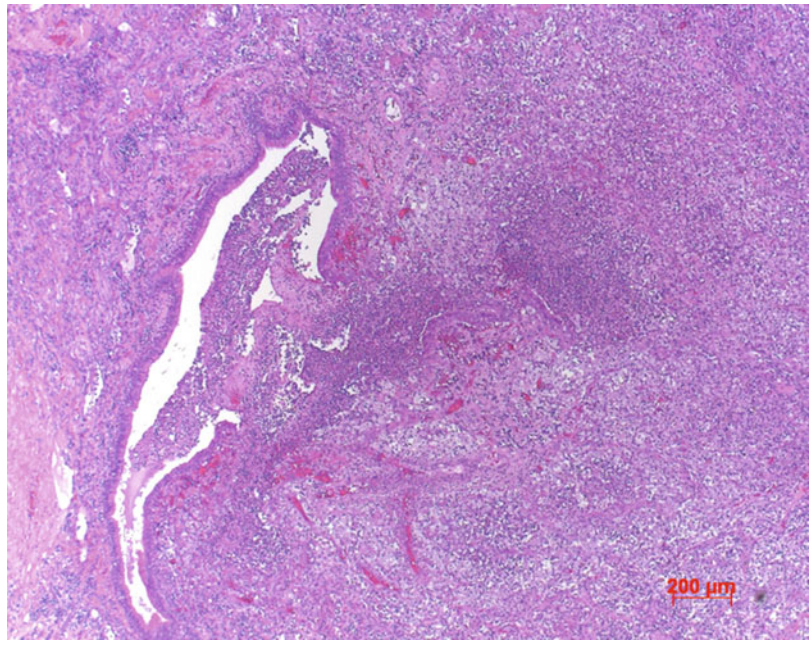

Fig. 8.6 Full blown bronchopneumonia. There is necrosis of the bronchial mucosa and dense infiltration of the bronchial wall and the alveolar tissue by neutrophils. H&E, bar 200 µm

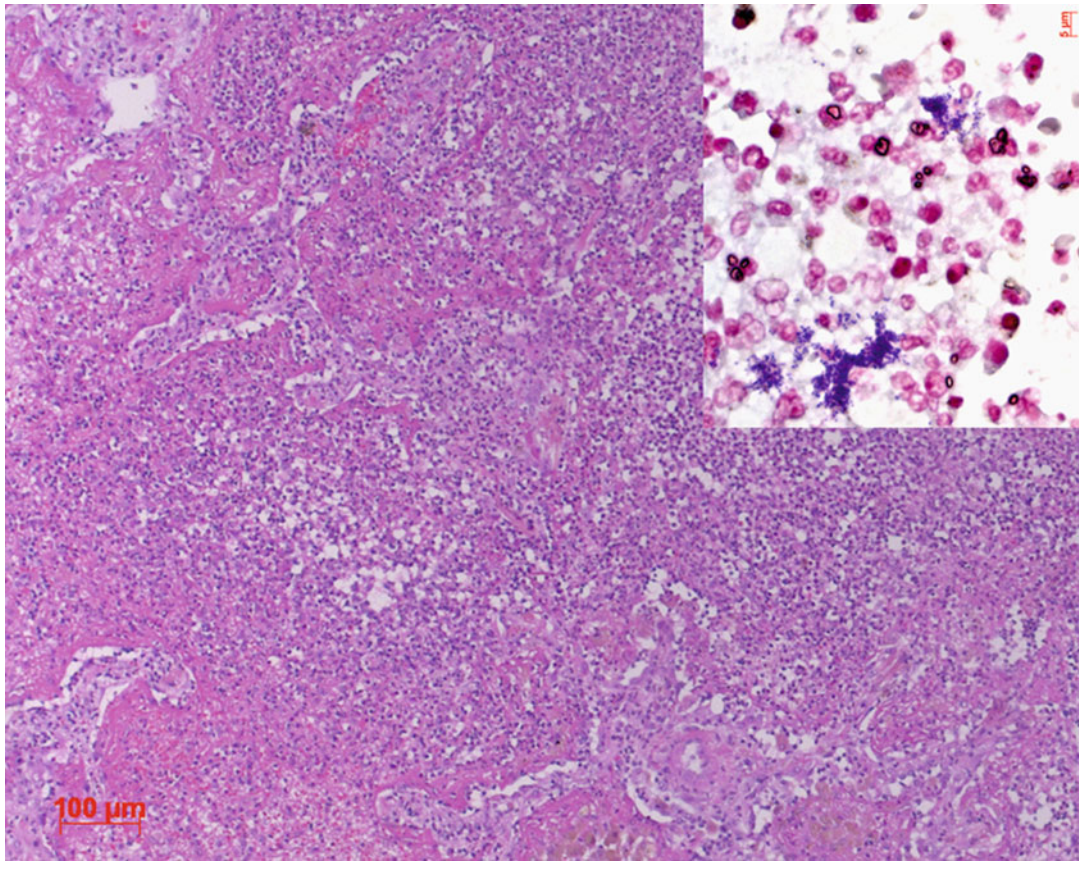

Fig. 8.7 Purulent bronchopneumonia due to bacterial infection; H&E, bar 100 µm; inset gram stain of the same area showing gram-positive cocci. Gram, bar 5 µm

8.1.2.2 Variants of Bronchopneumonias (Purulent Pneumonia (PN))

Lobar pneumonia is characterized by a uniform inflammatory infiltration of the lung. Bacteria are distributed early on by an edema within a whole lobe or several segments. The pneumonia therefore will show the same timely development in all areas involved. This means that the developmental stage of the inflammation is identical in each area investigated. Most often biopsies or resection specimen will present with dense neutrophilic infiltrations and fibrin cloths filling the alveoli. Bacteria can easily be identified using a Gram stain (Fig. 8.7).

Bronchopneumonia in contrast will show different developmental stages in different areas, depending on the amount of bacteria present in a given segment. This will result in a colorful picture on macroscopy with dark red, grayish, and even yellowish areas and the same on histology: areas of hemorrhage, areas of mixed fibrinous and granulocytic infiltrations, areas of granulocytic debris, and macrophage infiltration.

Pneumonias with abscess formation are another form of bronchopneumonia, which most often is seen in infections with certain species of bacteria. These abscesses are based on localized necrosis, either directly induced by the bacteria or by an interaction of bacteria with the coagulation system.

8.1.3 Diffuse Alveolar Damage (DAD) and Acute Interstitial Pneumonia

Clinically acute interstitial pneumonia (AIP, also adult respiratory distress syndrome (ARDS)) is characterized by an acute onset of severe hypoxia, with the radiological appearance of white lung. Histologically there is edema and fibrinous exudate, widened edematous alveolar septa (see also below acute fibrinous pneumonia). Later on hyaline membranes are formed – this was called diffuse alveolar damage (DAD) (Fig. 8.8). Depending on the cause of DAD, scattered neutrophilic and/or eosinophilic granulocytes can be found in bacterial, toxic, or drug-induced DAD, or few lymphocytes are seen in viral and rickettsia infections, respectively [15, 16]. Inflammatory infiltrates may be even absent such as in various kinds of shock. Rarely cases of "idiopathic AIP" have been reported. Probably some of these cases represent cases of undiagnosed SLE or drug toxicity. In the author's experience in all cases sent for consultation and primarily labeled as idio-

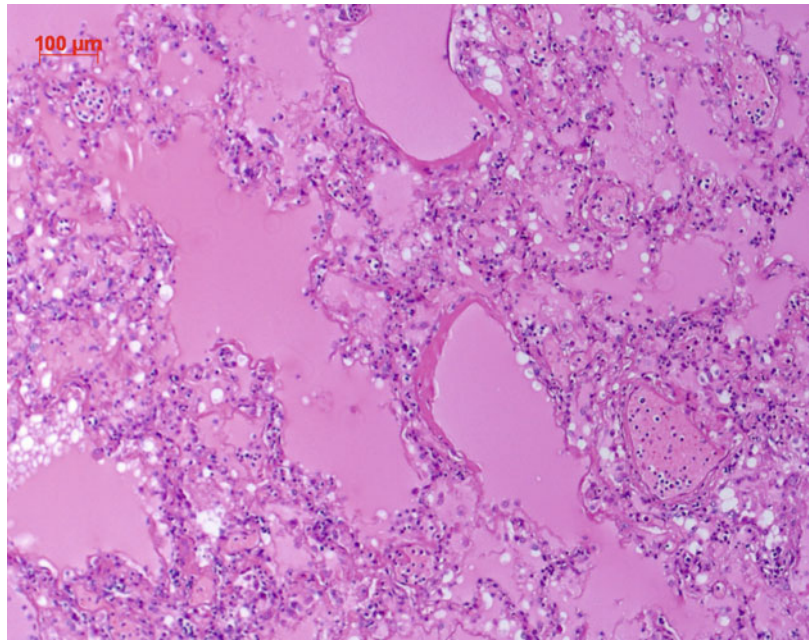

Fig. 8.8 Diffuse alveolar damage (DAD)/acute interstitial pneumonia in this case induced by Puumala virus. There is edema, mild infiltration by lymphocytes, and development of hyaline membranes. H&E, bar 100 µm

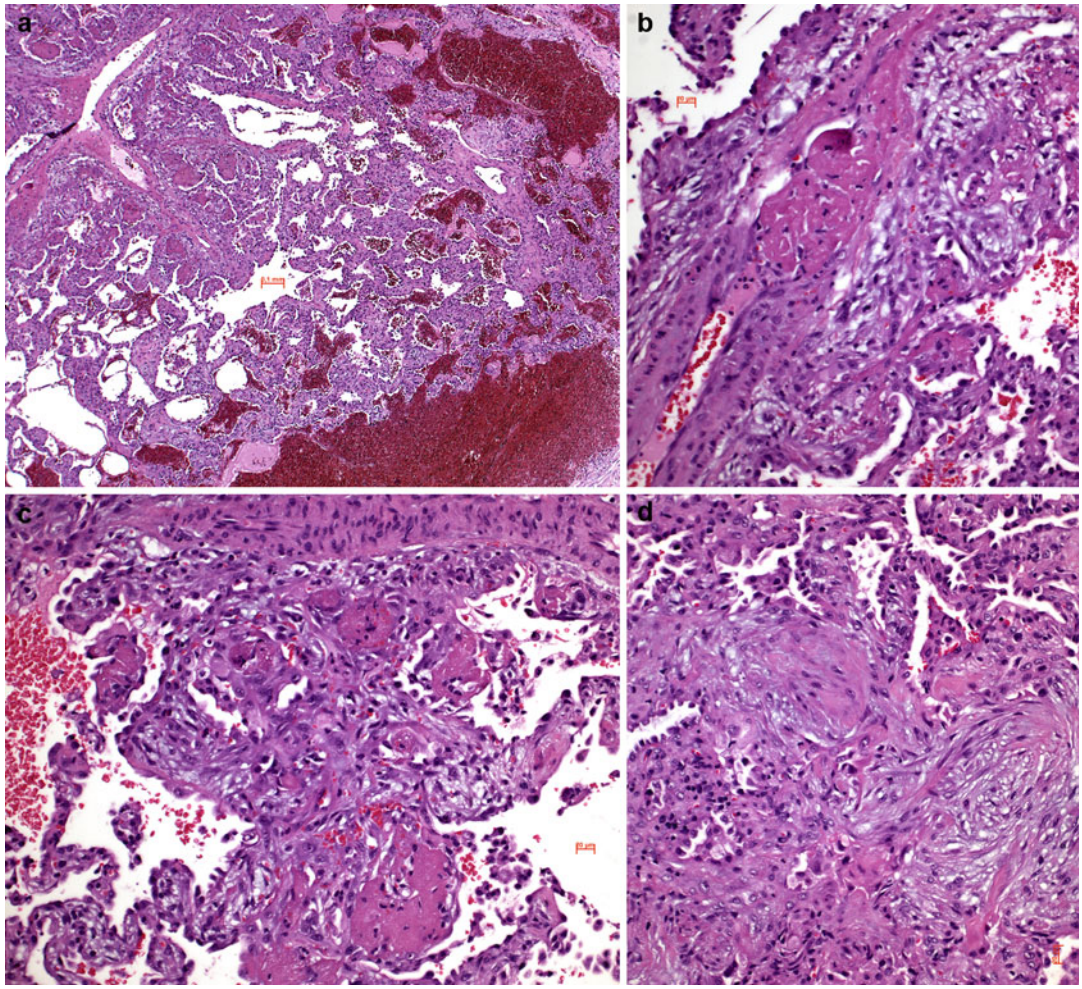

Fig. 8.9 Drug-induced DAD (neuroleptic). In (**a**) areas of interstitial infiltrations by lymphocytes and histiocytes are seen, as well as fibrin cloths in alveoli. There is also alveolar hemorrhage. In (**b**) there is endothelial damage and fibrin cloth, which points to the etiology (toxic substance from circulation). In (**c**) fibrin cloths are seen within the septa as well as outside in alveoli, and in (**d**) there are hyaline membranes already in organization. H&E, bar 100 µm, and 20 µm in (**b**–**d**)

pathic DAD, an etiology could finally be established. So it might be questioned if idiopathic DAD does exist [17].

Hamman-Rich described an interstitial pneumonia with fulminant course leading to death in their six cases within 6 months. In the author's description, there was no hyaline membrane mentioned but a proliferation of fibroblasts. Since the tissues from these cases were all lost, this disease cannot be reconstructed and remains an enigma [18].

The sequence of events in DAD is largely dependent on the cause: Toxic metabolites of drugs or released collagenase and elastase from necrotizing pancreatitis will cause endothelial damage, followed by leakage of the small peripheral blood vessels. This causes edema, followed by pneumocyte cell death due to hypoxia. Serum proteins will pass into the alveolar lumina, coagulate there, and by the breathing movements are compressed into hyaline membranes (Figs. 8.9 and 8.10). In case of airborne disease, e.g., infection or inhaled toxins, pneumocytes type I die followed by type II. Due to the lack of surfactant lipids, the alveoli collapse. The basement membrane is either preserved or also destroyed (especially in viral infection). This again causes

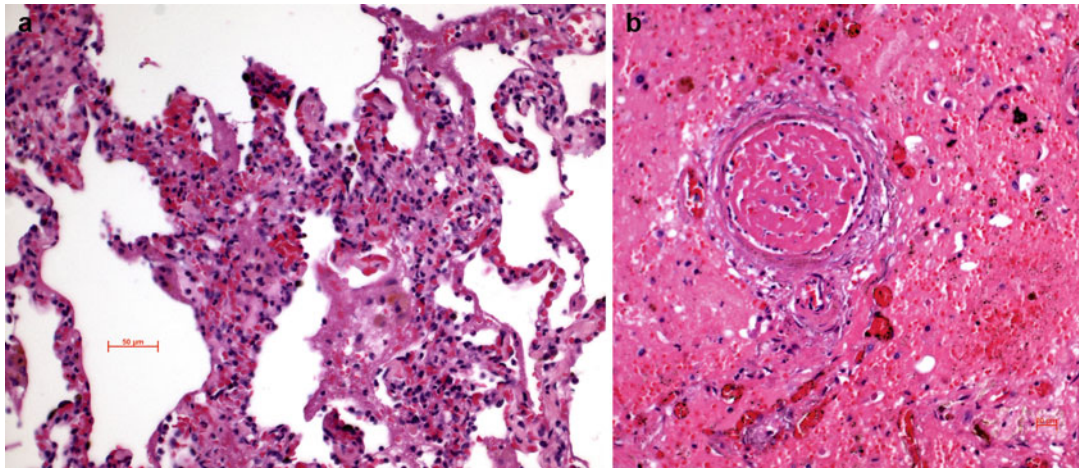

Fig. 8.10 DAD in cardiac shock. There is congestion of blood in the capillaries, also hyaline membranes have developed (**a**); in (**b**) there is another typical feature of shock, namely, intravascular fibrin clothing. H&E, bars 50 μm and 20 μm, respectively

Fig. 8.11 DAD in organization. Macroscopic picture showing areas of consolidation. Not much normal lung tissue is left. On the cut surface, numerous tiny little nodules are seen, which represent granulation tissue

leakage of capillaries, edema with/without bleeding, protein extravasation into the alveoli, and finally formation of hyaline membranes.

The lethality of DAD is still high despite improvements, which have been made in the past decade. In some cases the progression of the disease might be blocked by antiprotease treatment [19]. In more recent time extracorporeal oxygenation or NO treatment has shown some benefit. If the patient survives the acute phase, DAD will be organized, which is essentially an organizing pneumonia, by some authors also labeled organizing DAD: granulation tissue grows into the alveoli and hyaline membranes are incorporated into the plugs. Remnants of hyaline membranes can be demonstrated several weeks after the initial injury (Figs. 8.11, 8.12, and 8.13). If a tissue biopsy or an autopsy specimen is available early on in the course of the disease, the etiology might be elaborated: in viral infection inclusion bodies can be seen, which can present either as nice large inclusion bodies (CMV, RSV) or by

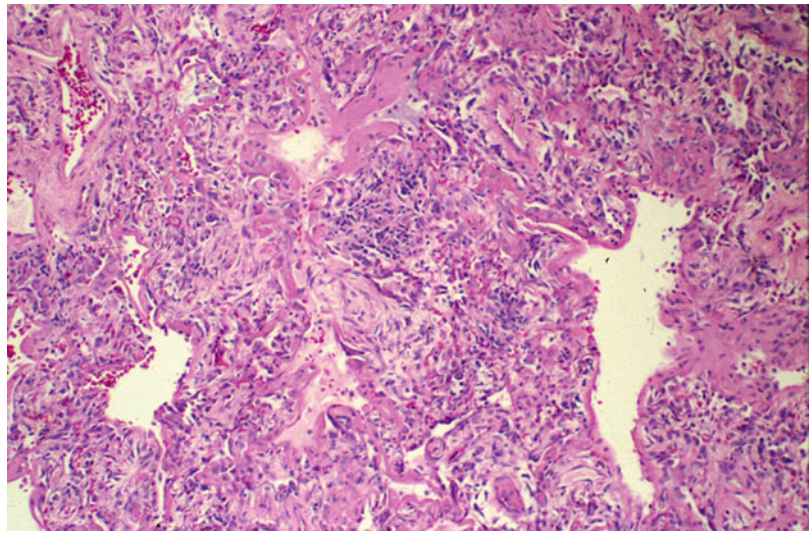

Fig. 8.12 DAD in organization, this is essentially an organizing pneumonia. Hyaline membranes are still visible but organized by granulation tissue, which grows within alveoli and finally will fill the lumina

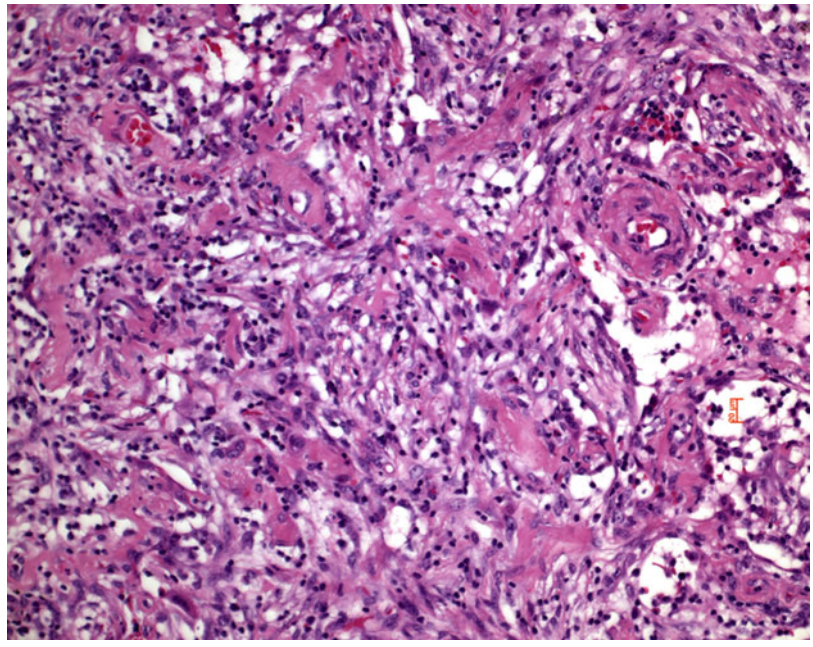

Fig. 8.13 DAD in organization. In this case the granulation tissue has filled the alveoli, leaving only slit-like spaces. Remnants of hyaline membranes are still visible. H&E, bar 20 µm

red-violet stained nucleic acids forming ill-defined speckles in nuclei and/or cytoplasm (adenovirus) [20]. This is followed by atypical proliferation and transformation of pneumocytes type II (Fig. 8.14). Typically the infected cell shows enlargement, an atypical large bizarre nucleus, and an accentuated nuclear membrane due to increased nucleic acid traffic induced by the virus. These cellular features can last for several months. In contrast to atypical pneumocyte hyperplasia (AAH), these atypical cells are singles and do not form a continuous layer along the alveolar wall. Rickettsia infection results in less pronounced proliferation of pneumocytes. In shock and drug-induced DAD, the endothelia will undergo apoptosis and necrosis, and fibrin cloths might be seen in capillaries (Fig. 8.10). In these cases the alveolar septa are widened and edematous. Inflammatory cells are scarce or absent. In later stages of drug pneumonia, scattered eosinophils are encountered – their function being completely unknown.

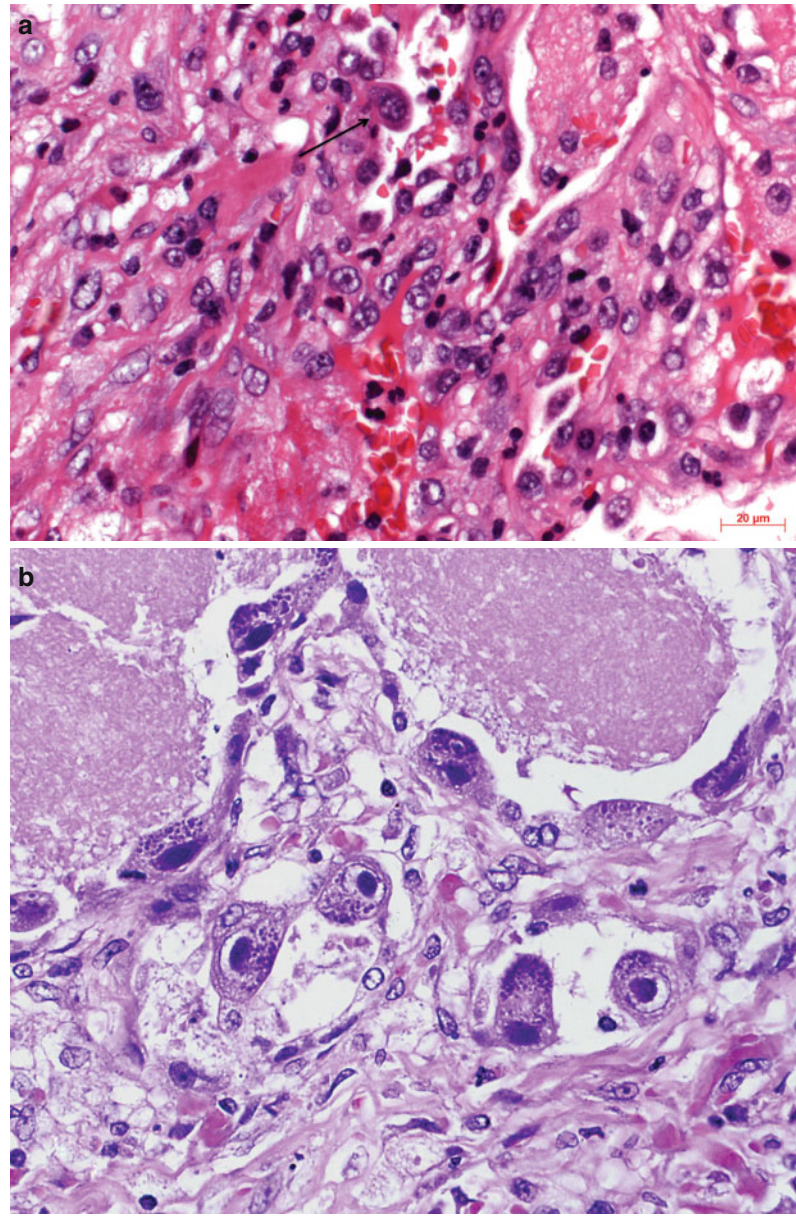

Fig. 8.14 DAD in viral infection; in (**a**) proven infection by adenovirus type 5 (*infected cell arrow*); there are no inclusion bodies, because these viruses form tiny pseudocrystalline intracytoplasmic structures. H&E, bar 20 µm, in (**b**) cytomegalovirus infection combined with *Pneumocystis jirovecii*. Note the characteristic large intranuclear inclusion bodies in CMV. Giemsa, ×630

What are the characteristics of DAD?

- Edematous fluid accumulation in alveoli and in the interstitium (depending on the time course)
- Fibrin cloths in alveoli with/without hyaline membranes
- Scarce inflammatory infiltrates (neutrophils and/or lymphocytes, etiology dependent)
- Minor diagnostic but etiologically important features are damage of pneumocytes, endothelial cells, fibrin thrombi in small blood vessels, and regeneration ± atypia

Acute fibrinous and organizing pneumonia (AFOP) was recently described as a variant of DAD: the dominant pattern is accumulation of intra-alveolar fibrin and concomitant organizing pneumonia [21]. Also pneumocyte type II hyperplasia, edema, and inflammatory infiltrates were described. Clinically the symptoms were identi-

cal to ARDS/AIP. The main difference stated by the author was the absence of hyaline membranes and the presence of fibrin cloths. The underlying causes were similar to classical DAD/AIP, so the author concluded that this might be a variant of DAD. However, some aspects have never been clarified: Fibrin exudation and clothing is seen early in DAD (see also Fig. 8.9), so the earliest phase of DAD does not present with hyaline membranes – these are formed later on due to respiration, which compresses fibrin into hyaline membranes. Rarely DAD might also present with a multifocal pattern, which includes a timely heterogeneity: acute fibrinous exudation in one, organizing DAD in another area [22]. Within the underlying cause, similar diseases as in DAD were found, including rare cases of acute hypersensitivity pneumonia [21, 23].

8.1.4 Lymphocytic Interstitial Pneumonia (LIP)

LIP almost vanished from the literature in the last 5 years. The major problem is the separation from NSIP. When NSIP was described, it was never clearly separated from LIP [24]. When comparing my own cases and reports from the literature, it becomes evident that differences do exist: in LIP the lymphocytic and plasmacytic infiltration is dense, hyperplasia of the bronchus-associated lymphoid tissue (BALT) is common, and within lymph follicles germinal centers are usually present [24]. The infiltration in LIP is more diffuse, architectural distortion is common, and scarring does occur. Histiocytic and monocytic cellular infiltrations are much less pronounced compared to NSIP. Lymphoepithelial lesions do occur similar to lymphomas, in some entities aggressively infiltrating and destroying the epithelium; in other cases no epithelial disruption does occur. In contrast to NSIP, the architecture of the peripheral lung is remodeled, especially in later stages (Fig. 8.15).

The clinical presentation depends on the underlying disease, and the CT scan usually shows ground glass opacities, in subacute and chronic stages, and also areas of fibrosis.

On gross morphology scattered areas of consolidations are seen.

Within the etiologic spectrum, similar diseases are found as in NSIP: autoimmune diseases especially collagen vascular diseases, allergic diseases as extrinsic allergic alveolitis/hypersensitivity pneumonia (EAA/HP) (acute and subacute), allergic drug reactions, HIV infection, and in children different types of immunodeficiency (T-cell defect, NK-cell defect). The most important differential diagnoses, however, are extranodal marginal zone lymphoma of MALT/BALT type and lymphomatoid granulomatosis type I. In all cases the clonality has to be evaluated and a lymphoma needs to be excluded by proof of multiclonality.

LYG type I can be difficult to separate: large blasts are rare and can be obscured within a dense infiltrate by small lymphocytes. The lymphocytic infiltration is polyclonal, so this does not help in the separation. Therefore a search for EBV-positive blasts is essential. Also it is important to exclude posttransplant lymphoproliferative disease [25], which can present in a similar pattern (large lymphoid cells usually EBV positive). However, it should be reminded that some of the autoimmune diseases have a high propensity of developing non-Hodgkin lymphomas later in the course [26]. Within the autoimmune diseases, Sjøgren's disease most often presents with LIP pattern [27, 28].

What are the morphologic characteristics?

- Diffuse dense lymphoplasmocytic infiltrates in alveolar septa and bronchial/bronchiolar walls. In some cases the lymphocytic infiltration can form concentric rows encasing capillaries and venules.
- Hyperplasia of BALT with well-formed follicular centers.
- Focal fibrosis and scarring with distortion of the peripheral lung architecture.
- Lymphoepithelial lesions.
- Eccentric sclerosis of vessel walls with narrowing of lumina: this is usually a sign of deposition of immune complexes in the vessel walls and should prompt the search for diseases associated with the production of autoantibodies, such as Sjøgren's disease and systemic sclerosis.

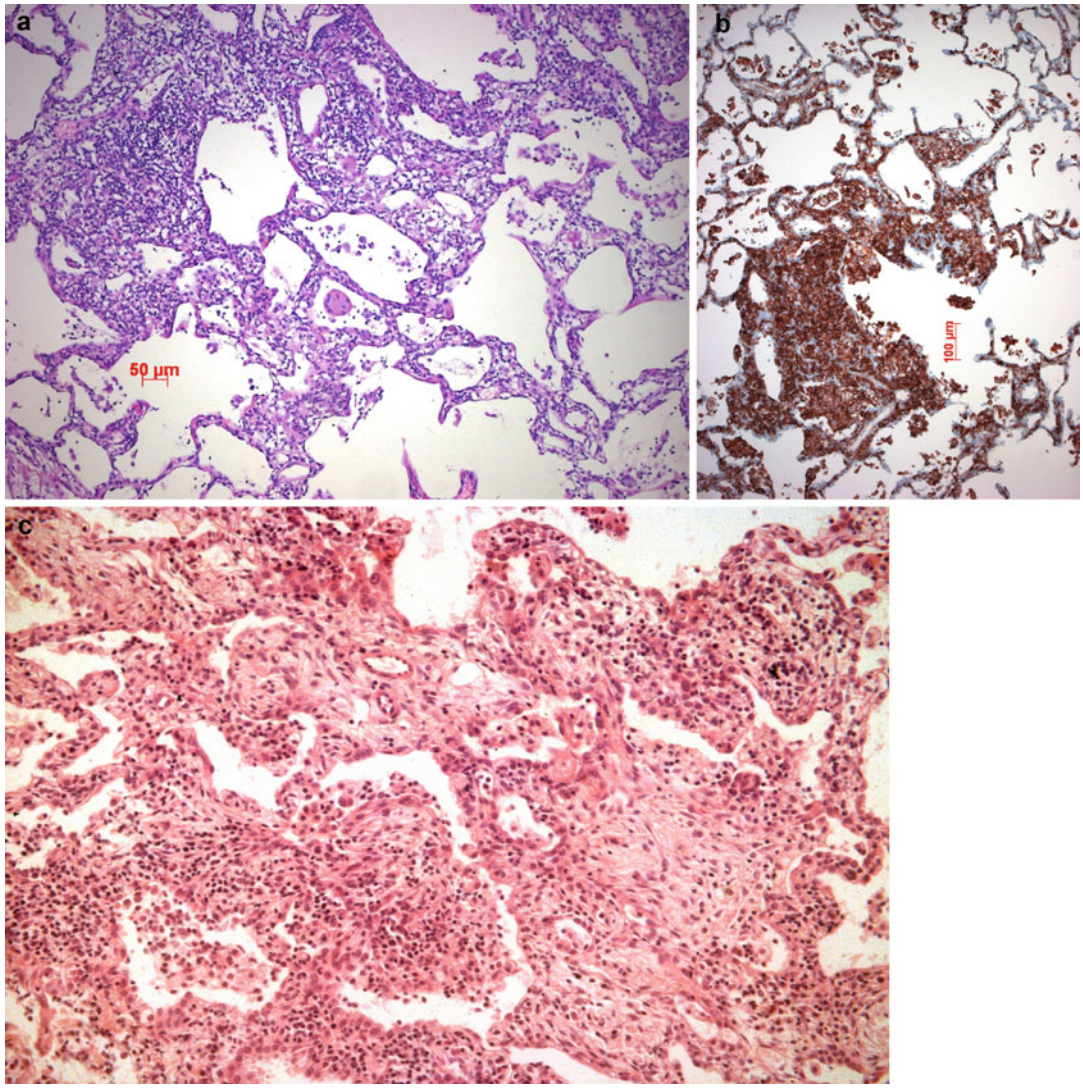

Fig. 8.15 Lymphocytic interstitial pneumonia. Dense lymphocytic infiltrates with ill-formed primary lymph follicles are seen in (**a**). In (**b**) the infiltration was dominated by CD4+ lymphocytes ruling out hypersensitivity pneumonia in this case. In (**c**) the infiltrate is composed of lymphocytes, plasma cells. Focally fibrosis has started with proliferating myofibroblasts. H&E, bar 50 µm (**a**) and ×200 (**c**), immunohistochemistry for CD4, bar 100 µm in (**b**)

Immunohistochemistry

Every case of LIP needs an evaluation for clonality using antibodies or in situ hybridization for kappa and lambda. As soon as a lymphoma is ruled out, further evaluation can be directed toward the underlying etiology. In a first step, lymphocytes should be subtyped into B and T lymphocytes and furthermore into CD4+ and CD8+ T lymphocytes. An evaluation of regulatory T cells using FOXP3 antibodies will also help in sorting the etiology. EAA/HP is dominated by CD8+ T lymphocytes at least in acute stages, whereas in autoimmune diseases the lymphocytic infiltrate is usually mixed. The absence of Treg cells can be of help for the diagnosis of some of the autoimmune diseases, such as rheumatoid arthritis.

8.1.5 Giant Cell Interstitial Pneumonia (GIP; See Also Under Pneumoconiosis)

GIP has a quite narrow etiologic spectrum either being caused by hard metal dust or by viral infection. The former will be discussed later. Several viruses can cause GIP, the classical one being measles virus. However, in contrast to pneumoconiosis in infections, the giant cells are mixed epithelial as well as macrophagocytic. The epithelial giant cells (Hecht cells) are transformed pneumocytes type II in whom nuclear division was not followed by cell division giving rise to multinucleation [29]. The additional features are identical to DAD as described above. Especially within the epithelial cells, viral inclusion bodies can be found (Fig. 8.16). Besides measles, also respiratory syncytial virus (RSV) can present with this picture predominantly in children [30].

Alveolar and interstitial pneumonias can be induced by a wide variety of organisms. According to that they can be classified as bacterial, viral, rickettsia, or parasitic. Parasitoses will be covered in eosinophilic pneumonias (Chap. 10).

Infectious pneumonias in childhood are quite common but are rarely biopsied. There are some differences in so far as the density of leukocytic infiltrations is much less compared to the adult form.

Opportunistic infections as part of the infectious pneumonias in immunocompromised patients will be mentioned in the tables under the different organisms and in the chapter on transplantation pathology. Disorders related to therapeutic intervention, chemotherapeutic drug, and radiation injury will be discussed in toxic reaction due to drugs and inhalation.

8.1.6 The Infectious Organisms

Bacterial pneumonias are most often purulent; the dominant inflammatory cell is the neutrophil. In early stages the infiltration starts with macrophages and fibrin exudation followed by infiltration by neutrophils. Abscess formation is common; cavitation is induced by some bacteria and most likely is induced by vasculitis and thrombosis. A few bacteria cause DAD and fibrinous pneumonia, other lymphocytic pneumonia – these tissue reactions can point to the underlying type of infection (Table 8.1). A scattered type of neutrophilic infiltration is seen in some infections such as *Nocardia* or *Legionella*

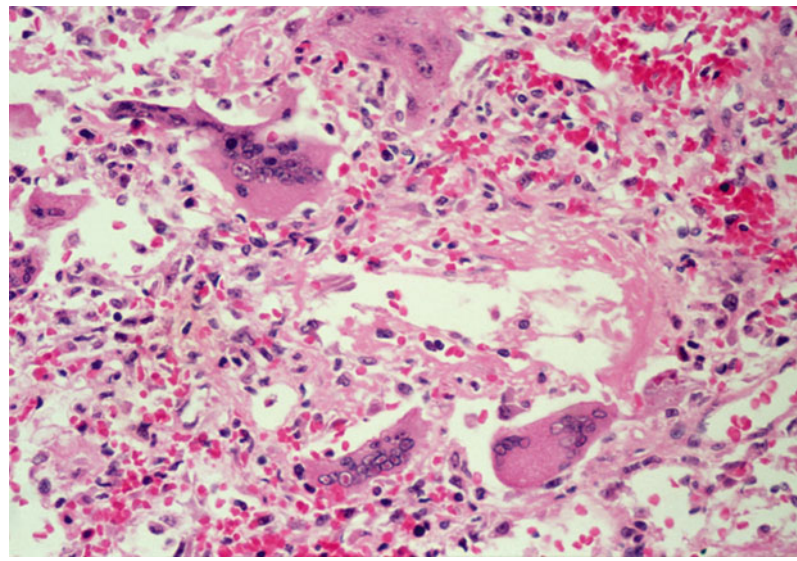

Fig. 8.16 Giant cell interstitial pneumonia (GIP) here in a 2-year-old girl, which died due to measles pneumonia. There is DAD with hyaline membrane formation, but in addition there are multiple multinucleated giant cells, which show intranuclear violet-red viral inclusion bodies. H&E, ×400

Table 8.1 Gram-negative and gram-positive bacteria and types of pneumonias

Type of bacterium	Tissue reaction	Proof by	Children/adult
Actinomyces israelii and other subspec.	Abszeding PN, necrotizing histiocytic/epithelioid granulomatous PN	Pos. Gram or Brown-Brenn stain	No/yes
Bacillus anthracis	DAD, hemorrhage, necrotizing purulent PN	IHC, culture	No/yes wool sorters disease
Chlamydia pneumoniae, *Chlamydophila psittaci*	Lymphocytic and eosinophilic bronchitis, DAD, LIP	IHC, ISH, PCR (two forms: EB and RB	Yes/no
Corynebacterium diphtheriae	Pseudomembranous bronchitis, purulent PN	Gram pos	Yes/yes
Haemophilus influenzae	Purulent PN	Gram neg, methylene blue, IHC	Yes/yes
Klebsiella pneumoniae	Abszeding necrotizing purulent PN (lobar or lobular)	Gram neg, culture	Yes/yes
Legionella pneumophila	Fibrinous, hemorrhagic, necrotizing purulent PN	Warthin-Starry, Brown-Hopps, EM, IHC	No/yes
Listeria monocytogenes	DAD (transplacental transmission), purulent PN	Gram pos	Yes/no
Burkholderia pseudomallei, *B. cepacia*	Abszeding purulent PN, histiocytic granulomatous PN	Gram neg	Rarely/rarely (opportunistic)
Mycobacterium tuberculosis complex (see also below)	Granulomatous PN, necrotizing PN	ZN, RA, IHC, PCR	Yes/yes
Non-tuberculosis Mycobacteria (MOTT)	Granulomatous PN	ZN, RA, IHC, PCR	Yes/yes
Mycoplasma pneumoniae	Lymphocytic necrotizing bronchiolitis, LIP, DAD	IHC, PCR	No/yes
Nocardia asteroides	Purulent absceding PN	Modified ZN, GMS, Brown-Brenn (Gram pos), PCR	Rare/yes
Pseudomonas aeruginosa	Hemorrhagic PN, absceding purulent PN. Combined purulent vasculitis and cavitation	Gram neg, Brown-Hopps, culture	Rare/yes
Rhodococcus equi	Absceding PN, cavitation	PAS, GMS, Brown-Hopps (Gram pos)	No/yes (opportunistic, HIV)
Staphylococcus aureus	Purulent PN	Gram pos	No/yes
Streptococcus pneumoniae, *S. viridans*[*]	Purulent PN, DAD (infants), [*]abscesses	Gram pos	Yes/yes
Treponema pallidum	Epithelioid and neutrophilic granulomatous PN with abscesses and vasculitis	Warthin-Starry	
Francisella tularensis	DAD with neutrophils and macrophages, later epithelioid cell granulomas, necrosis, cavitation	Gram neg, Brown-Hopps, Warthin-Starry, IHC	No/yes
Bordetella pertussis	Necrotizing bronchitis, bronchiolitis, peribronchiolar purulent PN	Gram neg, Giemsa, PCR	Yes/no

[*]*GRAM* gram stain, *GMS* Grocott methenamine silver impregnation, *ZN* Ziehl-Neelsen stain, *RA* rhodamine-auramine stain, *PAS* periodic acid-Schiff reaction, *IHC* immunohistochemistry, *PCR* polymerase chain reaction, *EM* electron microscopy, *EB* elementary body, *RB* reticulate body

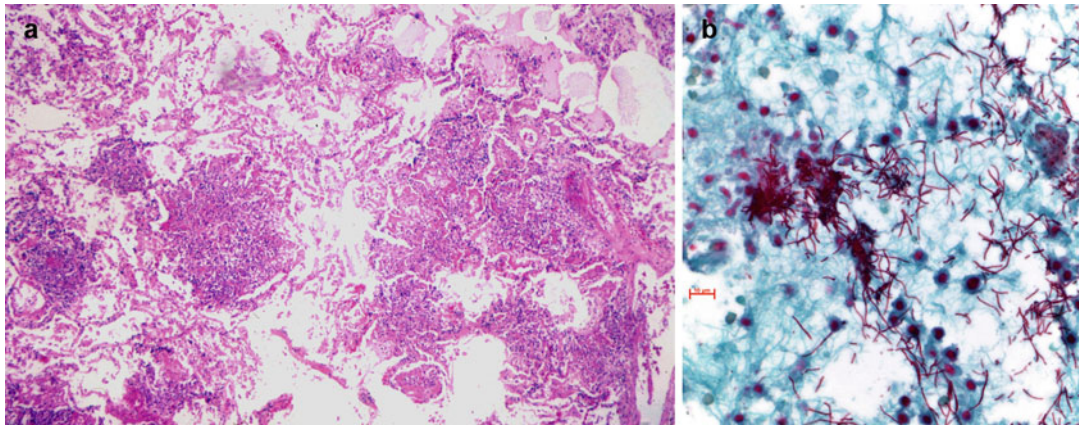

Fig. 8.17 (**a**) Bacterial pneumonia with scattered nodular aggregates of neutrophils. This should prompt one for special stains such as silver stains and modified acid-fast stains. (**b**) The infectious organism in this case was identified as *Nocardia asteroides*. (**a**) H&E, ×50, (**b**) Fite stain, bar 10 μm

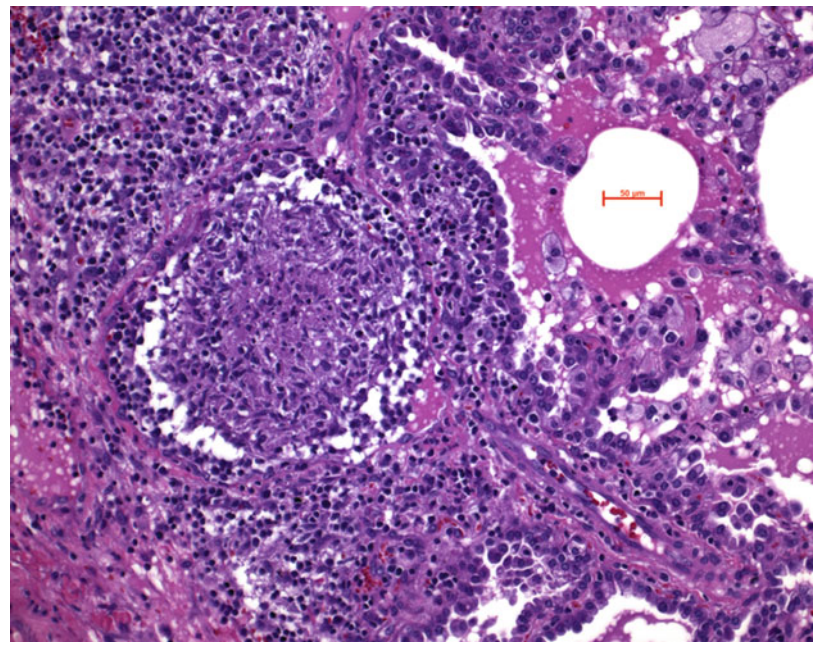

Fig. 8.18 Acute bacterial pneumonia with unusual features. There are histiocytic granulomas in the bronchial wall extending into the lumen, a dense macrophagocytic infiltration in alveoli, and a mixture of lymphocytic and neutrophilic infiltrations within the alveolar septa and bronchial wall. Special stains and culture identified the organisms as *Listeria monocytogenes*. H&E, bar 50 μm

pneumonia (Fig. 8.17) and a mixed infiltration of leukocytes but dominated by macrophages seen in such rare bacterial infections as listeriosis (Fig. 8.18, Table 8.1).

Fungal pneumonias are caused by a variety of fungal organisms. Most often fungal infection does not proceed into infections of deep organs, but stay confined to the skin, oral cavity, or the upper respiratory tract. In immunocompromised patients or in infants, however, fungal infections can cause lethal widespread multiorgan infections (Figs. 8.19 and 8.20). Since many of the fungi have developed some capsular structures and also can undergo different developmental stages, the host tissue often needs to develop different strategies to keep the infection under control. In the normal host, fungi are usually controlled by an influx of neutrophils, which are capable of eliminating the fungi before they can cause pneumonia.

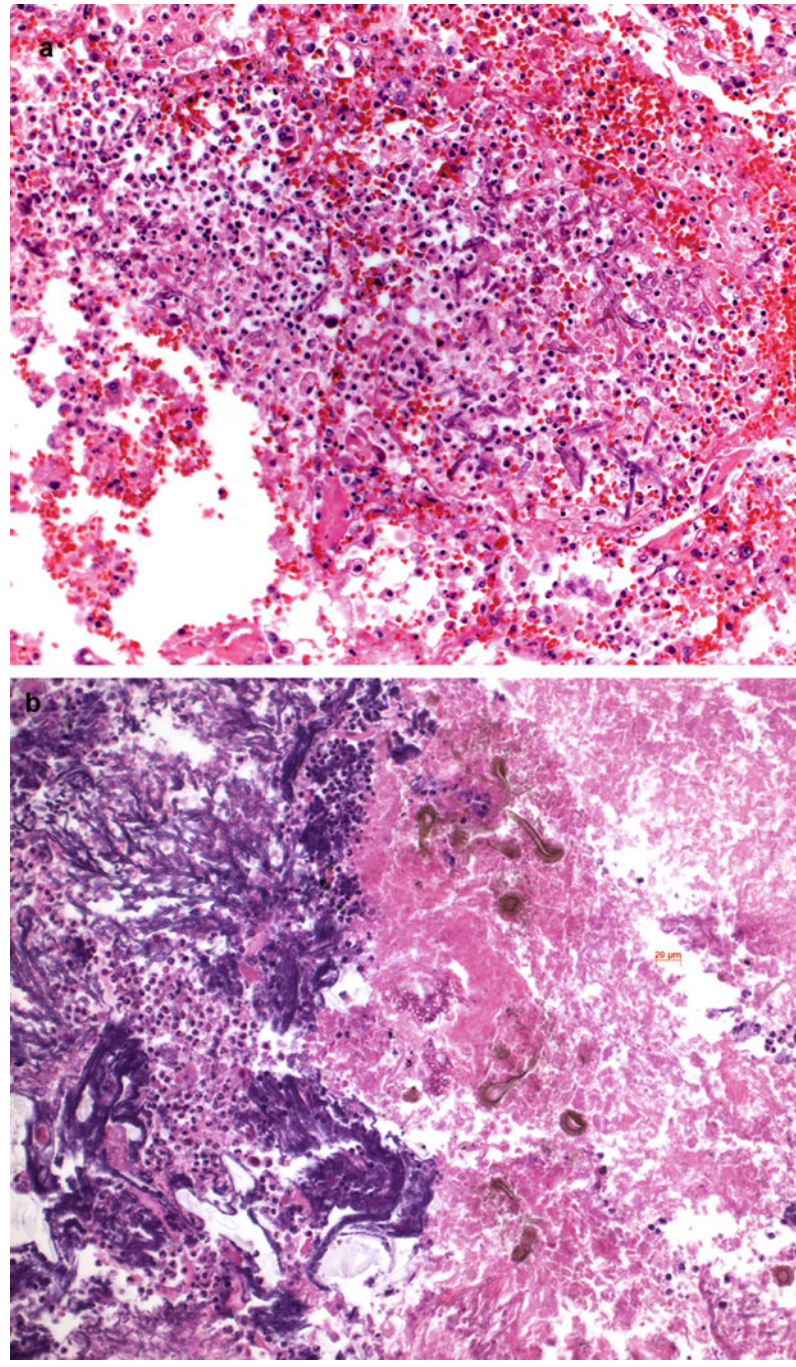

Fig. 8.19 (**a**) Purulent pneumonia due to fungal infection in a child being treated for leukemia. Note that the hyphae have already reached the blood vessels, which is a risk for developing sepsis. Although the size of the hyphae, the 45° angle of growth, and the septation would favor an *Aspergillus* type of fungus, be aware that many other fungi can look alike. In (**b**) the fungus could be identified as *Aspergillus niger*, due to the presence of conidia. H&E, ×200, bar 20 µm

In conditions where the fungi cannot be controlled, such as in bronchiectasis, the lung encases the infection by granulation tissue, starting as an organizing pneumonia, and later on a fibrous capsule separates the infectious focus from the normal lung – a mycetoma has been formed (Fig. 8.21). Normally there is a steady-state situation, i.e., no invasion of the fungus in deep areas of the lung occur, but the lung cannot get rid of the fungus. However,

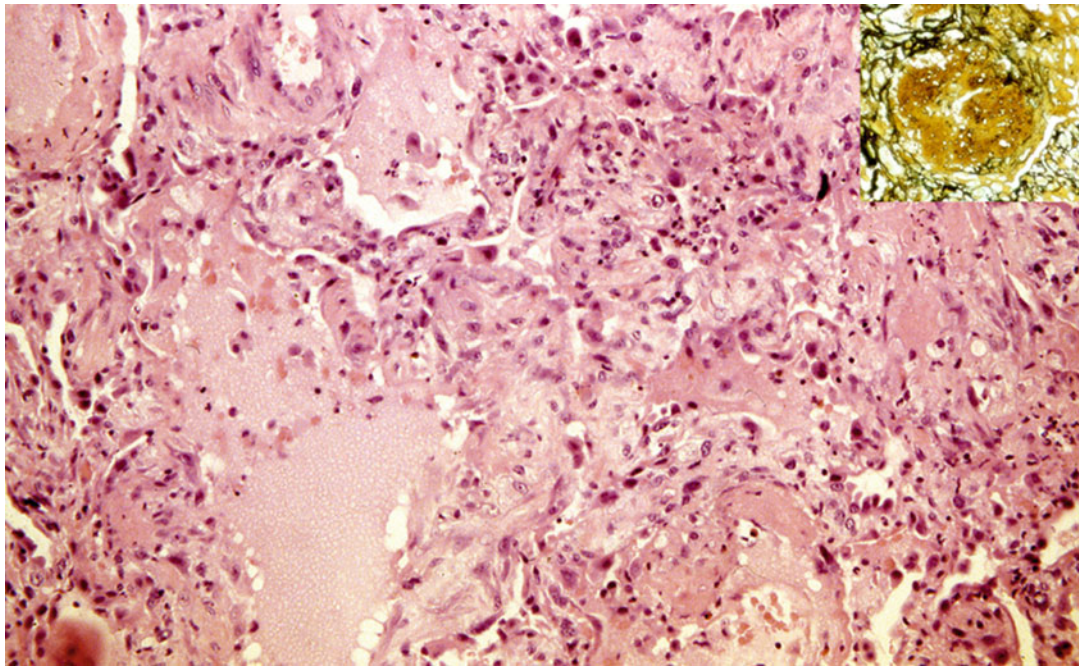

Fig. 8.20 Infection in an immunocompromised patient treated with high-dose corticosteroids. Within the alveoli there is a foamy eosinophilic material, which is suggestive for *Pneumocystis* infection. In the inset *Pneumocystis jirovecii* is demonstrated by Grocott methenamine silver stain. H&E, ×200, Grocott, ×400

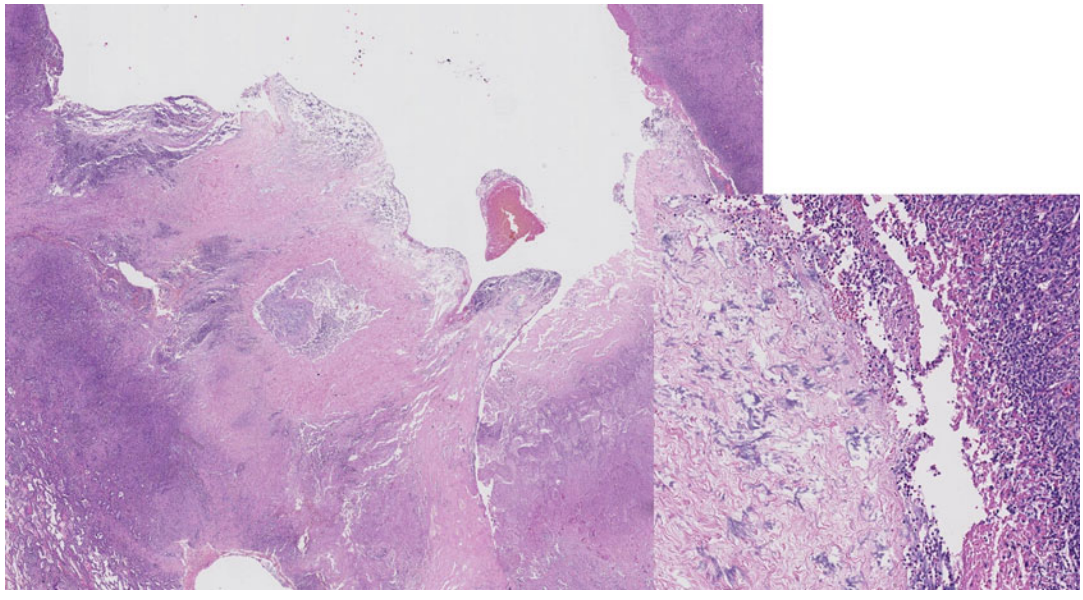

Fig. 8.21 Mycetoma in a preformed bronchiectasis. Overview shows necrosis and a dense infiltrate in the wall of this bronchus. In the inset numerous hyphae are shown and the neutrophilic reaction within the bronchial wall. H&E, ×12.5 and 100, respectively

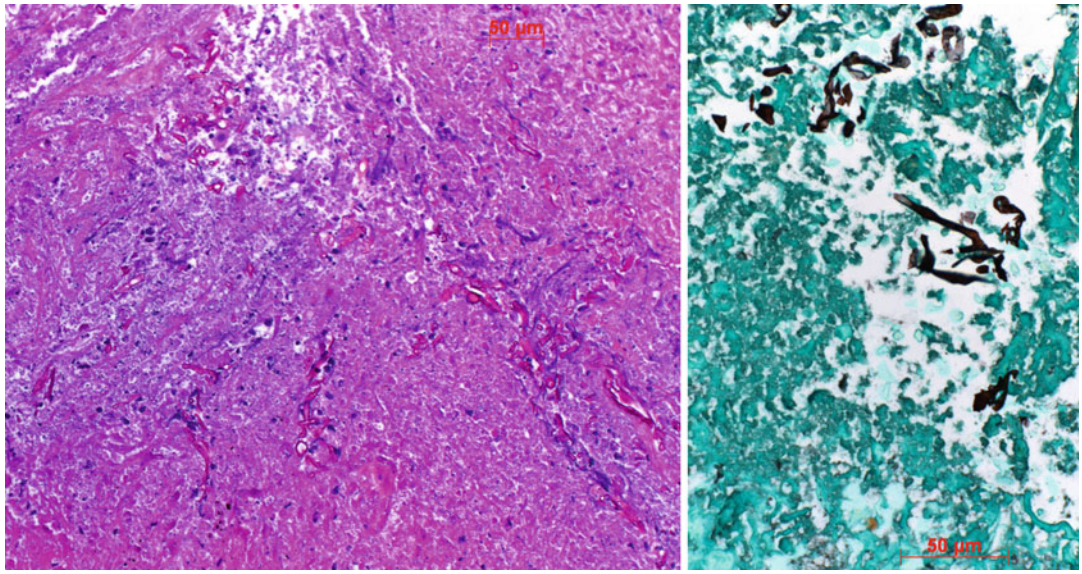

Fig. 8.22 Mucormycosis here with widespread necrosis and nuclear debris from leukocytes. The organisms can be seen on H&E (*left side*) but better by silver impregnation (*right side*). H&E, bar 50 µm, Grocott methenamine, bar 50 µm

there are rare conditions where invasion does occur and a chronic slowly progressing pneumonia develops – called chronic necrotizing mycosis. A few fungi pathogenic in humans can cause life-threatening infections: an example is mucormycosis. Again infection most often occurs in immunocompromised patients. The patients develop cough, occasionally mild hemorrhage, fever and shortness of breath is common. The major problem is that this fungus does not respond to many antifungal drugs therefore amphotericin B is applied, which has many toxic side effects. Pneumonia in *Mucor* infection presents with an infiltration of macrophages and neutrophils, necrosis is widespread, pleura is often involved, or the infection can even enter the pleural cavity (Fig. 8.22, Table 8.2).

Finally the reaction of the lung tissue against some specific forms of fungi can also be granulomatous. This reaction can be an innate immune reaction with histiocytes, macrophages, and foreign body giant cells or develop into a specific immune reaction with lymphocytes and epithelioid granuloma formation. However, this specific immune reaction depends on a functioning non-impaired immune system capable of producing different types of T lymphocytes (see below). Many fungi exhibit an angioinvasive growth behavior, i.e., their hyphae will grow toward arteries and veins directed by increase of pO_2 and immediately will invade through the vessels wall, resulting in sepsis. There exist also an allergic mycosis, called allergic bronchopulmonary mycosis (ABPA, ABPM), which is based on a sensitization against fungal proteins; this will be discussed in Chap. 10.

Respirotropic viruses and *Rickettsia* cause viral and rickettsial pneumonias. One of the most common tissue reactions is DAD with hyaline membranes. In virus infections only scattered lymphocytes are seen in tissue sections, but in BAL there can be a lymphocytosis with up to 30 % of lymphocytes, predominantly $CD8^+$ ones. Some viruses such as influenza type A strains can destroy the basal lamina of the epithelial layer and the capillaries by their enzymes. In these cases diffuse hemorrhage is seen with bleeding from capillaries, giving the macroscopic surface of the mucosa a dark red color. The distribution of inflammatory changes is also important: influenza virus usually causes trachea-broncho-pneumonia,

Table 8.2 Fungal organisms causing pneumonias

Type of fungus	Tissue reaction	Proof by	Children/adult
Aspergillus fumigatus, A. flavus, A. niger, other spec.	BCG, necrotizing bronchitis, mycetoma, chronic necrotizing PN, purulent PN with vasculitis	GMS, PAS, PCR	Yes/yes
Mucor 5 species	Necrotizing purulent PN, pleural involvement common	GMS, PCR	Yes/yes
Blastomyces dermatiditis	Purulent PN with abscesses, epithelioid granulomatous PN	GMS, IHC	No/yes
Candida species	Purulent PN, focal abscess	PAS, GMS, calcofluor-white, IHC	Yes/yes; immunocompromised
Coccidioides immitis	Purulent PN with microabscesses, necrotizing epithelioid granulomatous PN	GMS, IHC, ISH,	No/yes
Cryptococcus neoformans	Necrotizing epithelioid granulomatous PN	GMS, PAS, Fontana-Masson, IHC, Mucicarmine	No/yes
Histoplasma capsulatum,	Necrotizing epithelioid or histiocytic, granulomatous PN	GMS, Wright-Giemsa, IHC	Yes/yes
Paracoccidioides brasiliensis	Necrotizing epithelioid granulomatous PN, may be mixed with purulent PN	GMS, IHC	Yes/yes

GMS Grocott methenamine silver impregnation, *PAS* periodic acid-Schiff reaction, *IHC* immunohistochemistry, *PCR* polymerase chain reaction

whereas adenovirus is more likely causing bronchiolo-pneumonia. In cases of less virulent types of strains of viruses, a lymphocytic interstitial pneumonia can be seen (Figs. 8.23, 8.24, and 8.25). As a rule one should always try to find viral inclusion bodies. They can be prominent and easily seen as in CMV or HSV infection, whereas in adenovirus infection this can be difficult, because of intracytoplasmic bodies. Since the virions are very small and invisible, the package is ill defined. Viral inclusion bodies are stained violet red due to their high content of either DNA or RNA, and viral inclusions change the internal structure of a nucleus: the nuclear membrane is less sharp, and the chromatin structure is blurred.

8.1.6.1 HIV Infection and the Lung

Clinically early pulmonary involvement appears as interstitial infiltration with progression to nodular tumor masses obliterating the lung. As with other viral infections, mild diffuse alveolar damage to frank interstitial fibrosis is the prominent finding [31]. However, due to the specific attack of the virus toward CD4+ lymphocytes, concomitant infections are common. This also will change the histology of HIV-induced pneumonia. There can be an overlay by *Pneumocystis jirovecii* or cytomegalovirus pneumonia, a lymphoid interstitial pneumonia, and a desquamative interstitial pneumonia [32]. Children as well as adults can be involved. Early interstitial fibrosis and even complete resolution of the pulmonary changes can be seen early on in the disease development. Kaposi's sarcoma as a consequence of long-standing HIV infection is one of the most serious complications in these patients (this will be discussed in the tumor chapter) [33] (Table 8.3).

Pneumonia in children occurs in two peak ages: in early childhood and later in school children. Whereas pneumonia in school children is not much different from that in adults, pneumonia in early childhood is different. In small children the infiltration by leukocytes is much less pronounced compared to adults; however, the symptoms are much more pronounced. When

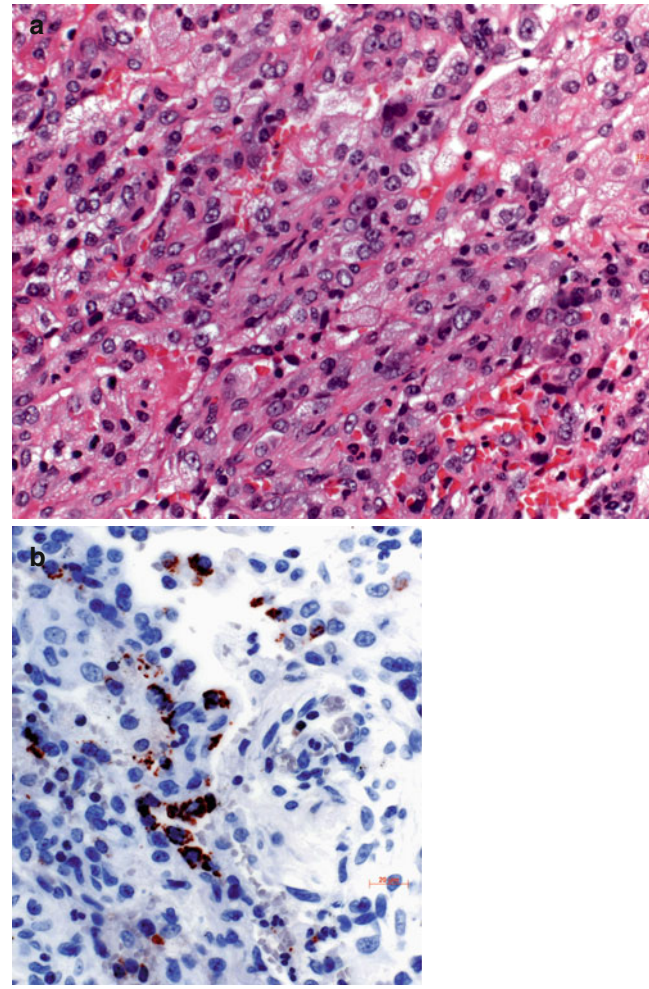

Fig. 8.23 Adenovirus-induced pneumonia. (**a**) There are many transformed pneumocytes with large nuclei. A few show dark stained nuclei and a red-violet cytoplasm. This should prompt further evaluation for viruses. (**b**) Immunohistochemistry for adenovirus showing many infected cells with granular cytoplasmic inclusion bodies. H&E, bar 10 μm; Immunohistochemistry, bar 20 μm pneumonia.

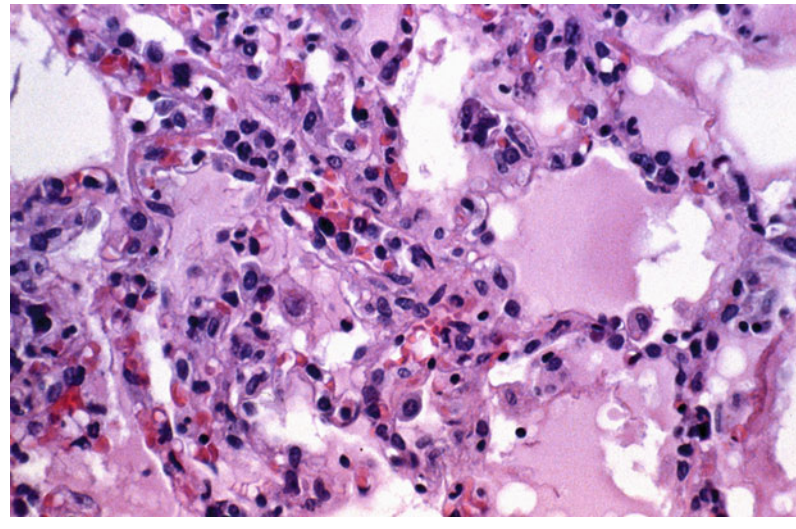

Fig. 8.24 *Hantavirus*-induced pneumonia. There is edema, mild lymphocytic infiltration, only few pneumocytes show enlargement of nuclei, and abnormal chromatin pattern. H&E, ×250 (Courtesy of Prof. Walker, Galveston)

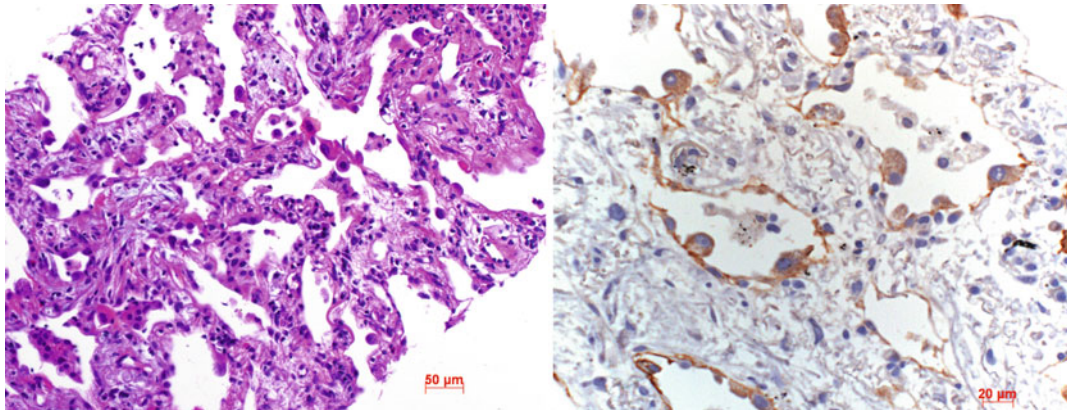

Fig. 8.25 Pneumonia induced by *Chlamydia trachomatis*. The lung tissue is infiltrated by scattered lymphocytes, the pneumocytes II show abnormal nuclei some with blurred contours, and a red-violet cytoplasm. By immunohistochemistry the *Chlamydia* infection was proven. H&E, bar 50 µm, Immunohistochemistry, bar 20 µm

Table 8.3 Virus and *Rickettsia*, causing pneumonia

Type of virus	Tissue reaction	Proof by	Children/adult
Adenovirus	Hemorrhagic PN, DAD	IHC or ISH	Yes/yes
Cytomegalovirus	DAD, hemorrhagic PN	H&E, IHC, ISH	Yes/rare (AIDS, immunocompromised)
Echovirus	Hemorrhagic PN, DAD	IHC, ISH	Yes/no
Epstein-Barr virus	Mild lymphocytic PN	IHC, ISH	Yes/no
Hantavirus	Hemorrhagic PN	ISH, PCR	No/yes
Herpes simplex virus	DAD, hemorrhagic PN with necrosis	ISH, PCR, IHC	Yes/yes
Influenza/parainfluenza virus	DAD	ISH, PCR, IHC, cell culture	Yes/yes
Measles virus	GIP, DAD	H&E, ISH, IHC	Yes/no
Respiratory syncytial virus	DAD, hemorrhagic PN, GIP	H&E, IHC, ISH	Yes/no
Rubella virus	LIP, DAD	ISH, PCR	Yes, congenital/no
Hemorrhagic fever viruses (Ebola, Marburg HF, Kyasanur HF, Omsk HF)	Hemorrhagic PN	ISH, PCR	No/yes
Human immunodeficiency virus (HIV)	DAD, LIP, interstitial fibrosis	ISH, PCR	Yes/yes
Rickettsia rickettsii, R. prowazekii, R. typhi	Edema, DAD, LIP, vasculitis	IHC, PCR	No/yes

IHC immunohistochemistry, *ISH* in situ hybridization, *PCR* polymerase chain reaction, *HF* hemorrhagic fever

calculating the density of leukocytes in alveolar septa, a mild infiltration by lymphocytes can be accompanied by dramatic shortness of breath and severe hypoxia, even requiring assisted ventilation. Infection in children in the first 2 years of life can happen as intrauterine infection or as an infection shortly after birth (Fig. 8.26).

8.1.6.2 Transplacental Infection Causing Pneumonias in Childhood

Infections can occur in children already in the fetal period via transplacental infection. Some of these infections such as measles when occurring during the first 3 months of gestation will cause

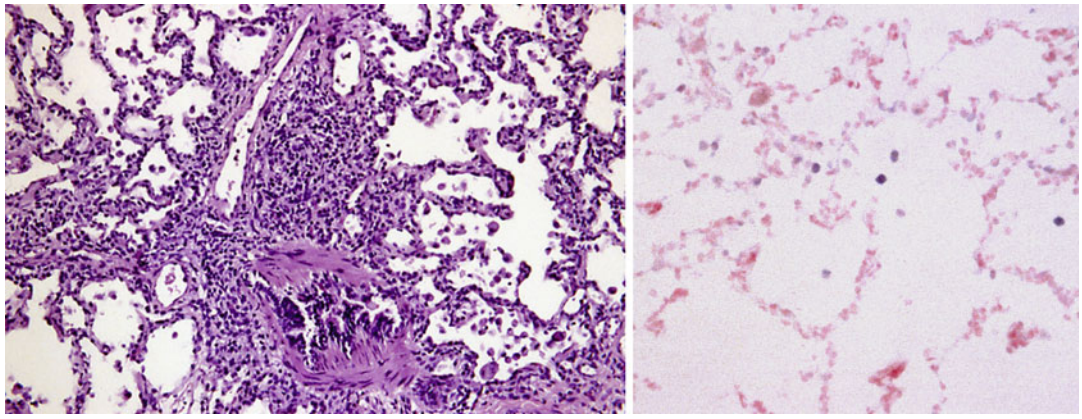

Fig. 8.26 Perinatal infection and pneumonia with EBV in a 6-month-old child. *Left side* photograph shows a mild lymphocytic infiltration, predominantly peribronchiolar. *Right*: In situ hybridization for EBV. H&E, ×100, ISH, ×100

developmental defects especially in the brain. Bacterial and fungal infections will not occur in this period, because for an infection a fully developed placenta is necessary. Whereas bacterial infections via the placenta will cause placentitis and amniitis [34] and cause premature delivery or intrauterine death, infections with viruses and *Rickettsia* will be transmitted to the fetus. Most common although in general rare infections are caused by ureaplasma (different serotypes), CMV, EBV, and *Chlamydia trachomatis* and *pneumoniae* [34–40]. The disease is also known under the name of Wilson-Mikity syndrome (Fig. 8.27).

8.1.7 Bronchopulmonary Dysplasia (BPD)

Bronchopulmonary dysplasia is a specific condition found in premature children. Inflammation is a major contributor to the pathogenesis of BPD, which is often initiated by a respiratory distress response and exacerbated by mechanical ventilation and exposure to supplemental oxygen [41]. Similar to Wilson-Mikity syndrome, infectious organisms such as ureaplasma and CMV have been reported to cause BPD [34, 42, 43]. In BPD sometimes remnants of infant DAD can be seen (hyaline membranes; Fig. 8.28), but the characteristic feature is interstitial fibrosis (Fig. 8.29).

8.1.8 Aspiration Pneumonia

Aspiration in children can be seen in two different forms: meconium aspiration during delivery causing severe respiratory distress and postnatal aspiration, most often as silent nocturnal aspiration in breast-fed babies. Risk factors for severe meconium aspiration are fetal distress and birth asphyxia [44, 45]. The diagnosis is most often made at autopsy. In addition to DAD, also a foreign body granulomatous reaction might be seen, depending on the time the child has survived. In silent nocturnal aspiration, children swallow milk from breast-feeding and aspirate small amounts. This causes scattered ground glass opacities on CT scan and lipid pneumonia on histology. However, the diagnosis can be made by bronchoalveolar lavage: macrophages laden with lipid droplets in their cytoplasm in more than 10 % are diagnostic in this setting (Fig. 8.30).

8.1.9 HIV Infection

HIV infection transmitted by HIV-positive mothers can cause also HIV in the child. It has been shown that HIV-infected women as well as HIV-infected family members coinfected with opportunistic pathogens might transmit these infections more likely to their infants than

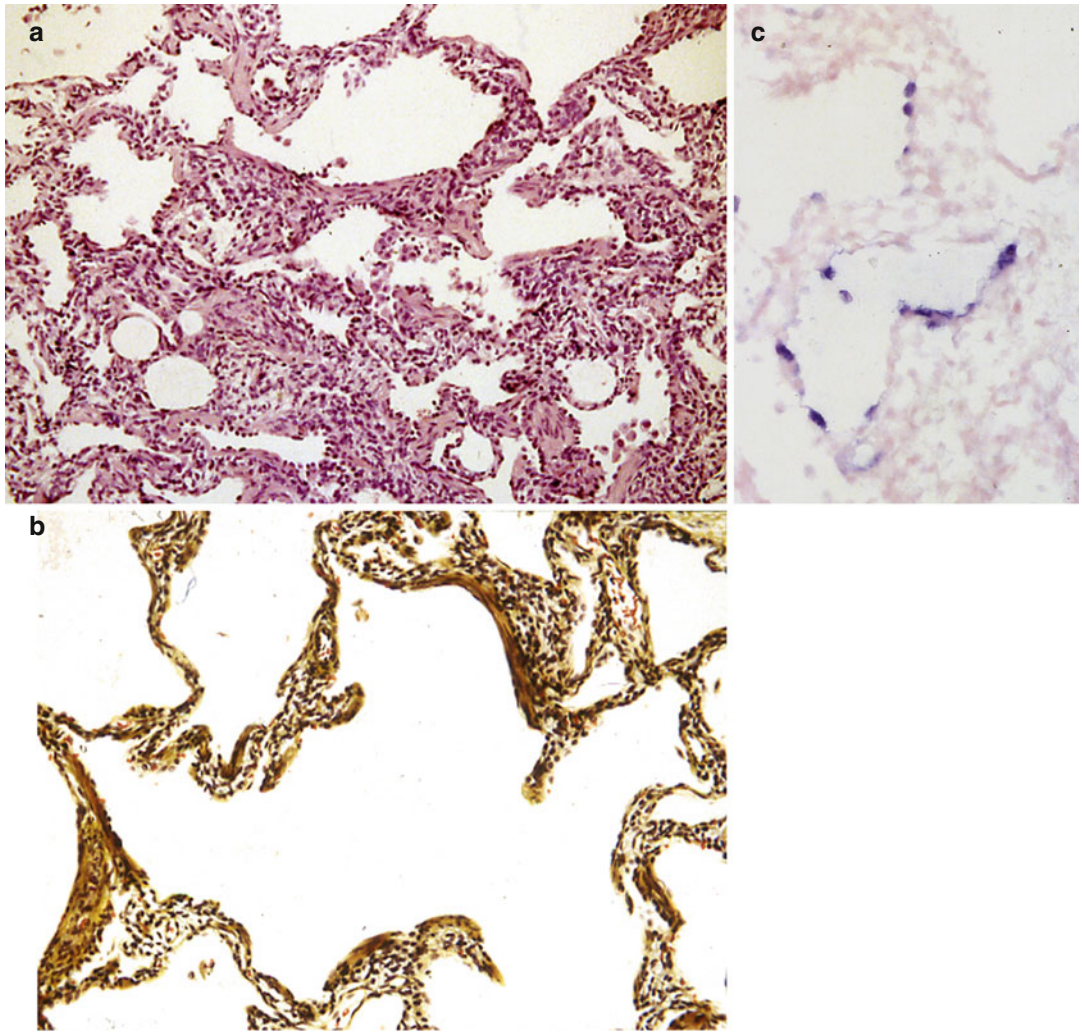

Fig. 8.27 Wilson-Mikity syndrome is another viral infection here in a 2-month-old baby. The child was transplacentally infected by the mother and developed pneumonia. Note the thickening of the alveolar septa by a lymphocytic infiltration but in addition also a proliferation of smooth muscle cells (**a**). In (**b**) the muscular proliferation is highlighted by Movat stain. Normal are single cells whereas here two to four layers of smooth muscle cells are seen. (**c**) In situ hybridization for CMV turned out positively. H&E, ×100, Movat pentachrome stain, ×100, ISH, ×200

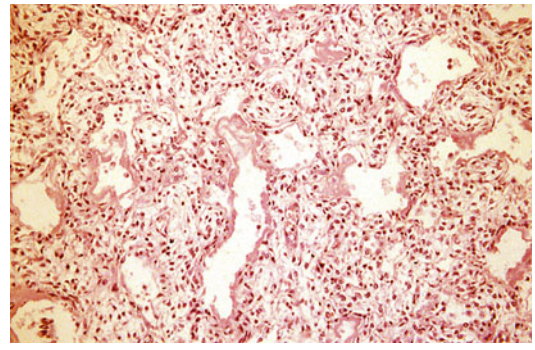

Fig. 8.28 Bronchopulmonary dysplasia (BPD) in a prematurely born child, which died with respiratory distress syndrome. There are hyaline membranes pointing to previous DAD but in addition mild inflammatory lymphocytic infiltrates and most important fibroblast proliferation in the septa. H&E, ×150

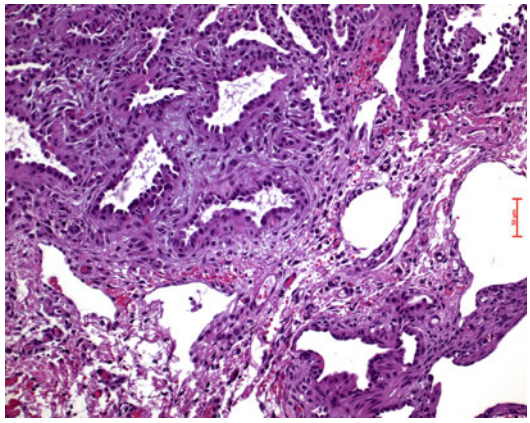

Fig. 8.29 BPD in another prematurely born child. Here fibrosis of the interstitium is striking. Prematurity of the lung is evident by hyperplastic type II pneumocytes. H&E, bar 50 µm

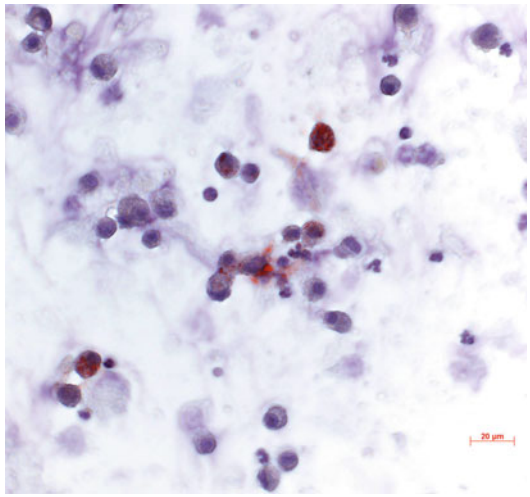

Fig. 8.30 Silent nocturnal aspiration. The suspected clinical diagnosis was confirmed by BAL showing >10 % of macrophages with lipid droplets in their cytoplasm. Oil red O stain, bar 20 µm

women without HIV infection, resulting in increased acquisition of such infections in the young child [46]. Otherwise HIV infection in children is morphologically similar to that in adults. Within the spectrum of opportunistic infections, *Pneumocystis jirovecii* is the most common.

8.2 Granulomatous Pneumonias

8.2.1 Introduction

The name granuloma is derived from the Latin word granulum, which means grain. The ending -oma is a Greek ending, used to designate a nodular swelling. Therefore granuloma is a nodular, well-circumscribed macroscopic lesion. With the invention of microscopy, this term has been extended to small nodular aggregates of cells. Over the decades the definition has undergone different interpretations. Some use granuloma strictly for well-circumscribed lesions, whereas others also designate a more loose aggregate of inflammatory cells as granuloma.

Epithelioid cell granulomas originally were recognized as a granulomatous inflammatory reaction elicited by infectious organisms. The first organisms identified were *Mycobacterium tuberculosis* and *bovis* and *Treponema pallidum* [47]. In the nineteenth century, Schaumann, Besnier, and Boeck recognized another epithelioid cell granulomatosis, which, due to the macroscopic resemblance to dermal sarcoma, they called sarcoidosis [48]. In the following decades, various epithelioid cell granulomatoses have been added, and even in the 1990s, new diseases have been reported, like zirconiosis [49–52].

8.2.2 What Influences Granuloma Formation? Why Necrosis?

The formation of epithelioid cell granulomas requires a combination of at least two different sets of stimulants: (a) stimulants for granuloma formation and (b) stimulants for epithelioid and Langhans cell differentiation. So what are the driving forces?

Granuloma formation is an old phylogenetic process by which complex organisms protect themselves against invading organisms or toxic substances. The invader or a toxic substance is isolated by granulation tissue or is phagocytosed and degraded simply by macrophages as part of the innate immune system. If these cells can kill the invading organism, no further defense line is

required. If the invader cannot be ingested and degraded by these cells, histiocytes and macrophages can form foreign body giant cells, which are more efficient in phagocytosis and degradation. These cells together form foreign body granulomas. In every case the invading organism cannot be killed by phagocytosis, another defense line is activated, which includes immune mechanisms. This more powerful line of defense is the epithelioid cell granuloma. The driving forces, which induce granuloma formation, are the macrophages, the antigen-presenting cells, such as Langerhans and dendritic reticulum cells, and the T and B lymphocytes [53–56]. Among the different cytokines released are interleukins 1β, 2, 3, 8, 10, 12, 17, macrophage migration inhibitory factor 1 (MIF1), IFNγ, and TNFα. How these factors act and interact is still not understood; however, macrophages and lymphocytes are activated and immobilized. This is followed by the cytokine-induced transformation of macrophages into epithelioid and foreign body giant cells [57–62]. Giant cells can be either formed by fusion of macrophages or by nuclear division without cell division. Foreign body giant cells further on differentiate into Langhans giant cells. This process of transformation is maintained by the same secretory factors, which are produced in larger quantities by the epithelioid cells and by infiltrating lymphocytes [63].

But why do we find non-necrotizing and necrotizing epithelioid cell granulomas even in the presence of the same organism?

Different substances either actively liberated from mycobacteria or passively by degradation can induce granuloma formation. Among them are trehalose-6,6′-dimycolate, lipoarabinomannan, and 65 kDa antigen of mycobacterial capsule (a chaperonin) [61, 62]. These products stimulate granuloma formation by the induction of cytokine gene expression, mainly IL1β or TNFα. In addition they have other effects, like induction of apoptosis, enhancing coagulation, and together release TNFα, which subsequently induce necrosis by occlusion of small blood vessels. The mycobacterial chaperonin also stimulates monocytes to express mRNA for TNFα and to release IL6 and IL8, cytokines which are chemoattractants for lymphocytes. In some patients necrotizing and non-necrotizing epithelioid cell granulomas, induced by *M. tuberculosis*, can be found side by side. The underlying mechanism is not completely understood. One possible explanation might be the mycobacterial burden: large amounts of mycobacteria release large quantities of coagulation factors and thus induce infarct-like necrosis. Another explanation is within the interaction of virulent stains of mycobacteria and host defense cells [63].

When we go back to morphology, we can see three different settings, in which we encounter necrosis: *M. tuberculosis* escape the immune defense, multiply, invade vessel walls, and are in part degraded by leukocytes, and by this a massive liberation of capsule constituents occurs; epithelioid cell granulomas develop in vessels walls and obstruct or occlude the vessel lumen, and ischemic necrosis follows; an imbalance of the virulence of the mycobacteria and the immune defense capability of the host is in favor of the invading organism. These factors together might lead to higher concentration of TNFα, as well as trehalose-6,6′-dimycolate, lipoarabinomannan, and chaperonin. In addition vasculitis-associated and released thrombogenic factors may synergistically act together to induce this characteristic caseous necrosis (Fig. 8.31).

Fig. 8.31 Macroscopy of nodular tuberculosis with many large and small nodules with caseous necrosis

When classifying granulomatous pneumonias, we will discern epithelioid from histiocytic granulomas and as a second step differentiate infectious from noninfectious forms.

8.2.3 Morphologic Spectrum of Epithelioid Cell Granulomas

Epithelioid cell granulomas are a specific form of granulomas, composed of epithelioid cells, giant cells, and lymphocytes (epithelioid: epithel = the stem of epithelium and oid = similar to). This type of granuloma can be induced by a variety of quite different stimuli. Epithelioid and giant cells are specialized members of the monocyte/macrophage lineage, the first a differentiated secretory cell (Fig. 8.32) and the second a specialized phagocytic cell (Fig. 8.33). Giant cells can be either formed by cell fusion or by incomplete cell division (no cytoplasmic division). Both ways have been proven experimentally [56, 64, 65]. First foreign body giant cells are formed, which later reorganize into Langhans cells. These are characterized by a nuclear row opposite to the phagocytic pole of the cell. Lymphocytes are usually layered at the outer granuloma shell and can be numerous or sparse. Phenotypically these are T lymphocytes, whereas B lymphocytes are loosely arranged outside the granulomas. T-helper-1 and T-helper-2 and cytotoxic T lymphocytes ($CD8^+$) can be present in the granulomas, with the composition depending on the type of underlying disease. This will be discussed later.

We can encounter different stages of granuloma formation: first we see a loose aggregation of macrophages, histiocytes, lymphocytes, and even neutrophils. During each step the granuloma becomes more compact, and the margins are better circumscribed. During aging, epithelioid cell granulomas might undergo fibrosis and hyalinization (Figs. 8.34, 8.35, and 8.36). However, in some diseases like extrinsic allergic alveolitis, the

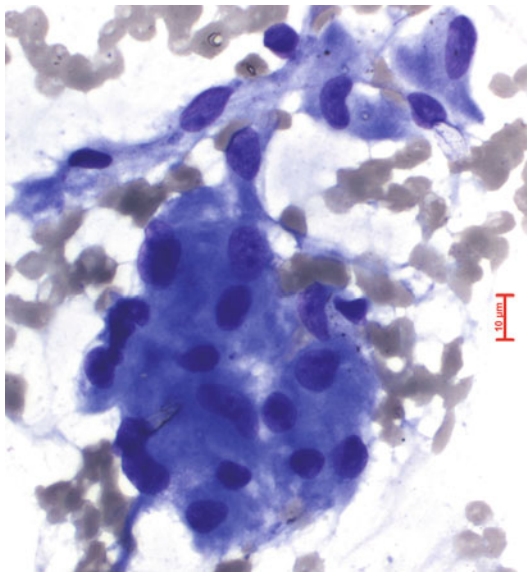

Fig. 8.32 Cytology of epithelioid cells. The nuclei are curved, the cytoplasmic border is ill defined. Giemsa, bar 10 µm

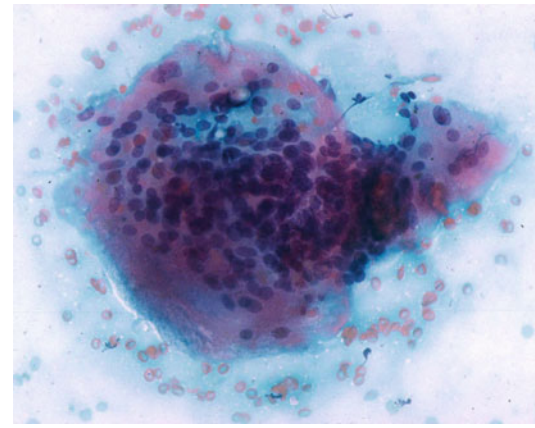

Fig. 8.33 Cytology of a giant cell with numerous nuclei. Pap stain, ×400

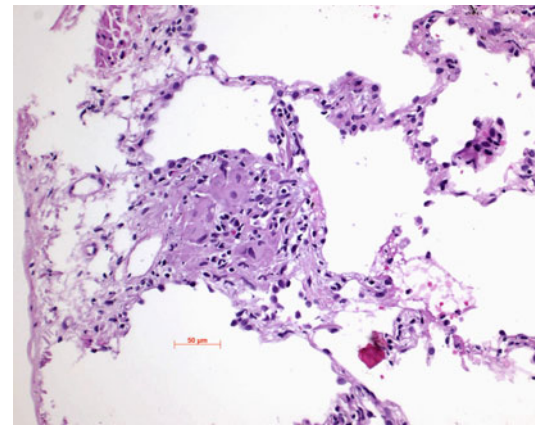

Fig. 8.34 Early epithelioid cell granuloma, here in a case of sarcoidosis. Note the scattered lymphocytes within and outside the granuloma. H&E, bar 50 µm

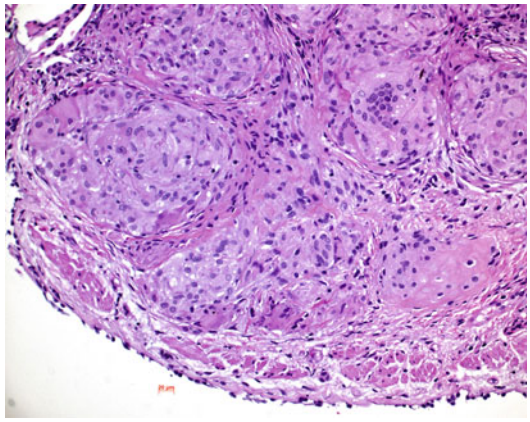

Fig. 8.35 Well-developed epithelioid cell granuloma in sarcoidosis. Epithelioid and Langhans cells are easily seen; lymphocytes are now scarce. H&E, bar 20 μm

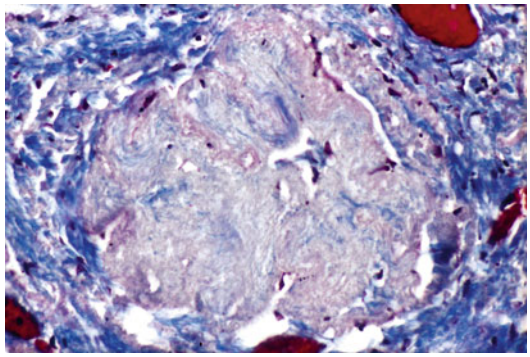

Fig. 8.36 Old epithelioid cell granuloma in a patient with long-standing sarcoidosis. Almost all cells vanished, a few epithelioid cells are seen. Trichrome stain, ×150

epithelioid cell granulomas remain less well delineated and tend to be more loosely arranged. Also a spillover of lymphocytes into adjacent alveolar septa is seen.

A very important finding is central necrosis, defining the necrotizing epithelioid cell granuloma. Small necrobiotic foci or few apoptotic cells are not regarded as necrosis. The necrosis is either stained eosinophilic with minimal amounts of nuclear debris, or may contain larger amounts of nuclear debris, or stained blue violet by H&E. In early necrosis neutrophils can be found. The descriptive term caseous necrosis is often used; however, it should be reminded that this term was invented to describe these necroses macroscopically: a caseous necrosis is characterized by a yellowish color and soft, cheese-like consistency (Fig. 8.31).

8.2.4 The Causes of Epithelioid Cell Granulomas and Their Differential Diagnosis

Pathologists usually differentiate granulomatoses by their morphologic appearance: if there is an epithelioid cell granuloma with necrosis, primarily infectious diseases are to be discussed, whereas in non-necrotizing granulomas, other diagnoses are to be added. Although this rule will be true in most cases, it should be reminded that sometimes necrosis is not associated with infection, as in necrotizing sarcoid granulomatosis and some cases of bronchocentric granulomatosis.

The distribution pattern of the granulomas may assist in sorting out specific diseases: the distribution of granulomas along lymphatic vessels is quite characteristic in sarcoidosis, whereas an airspace-oriented pattern is seen in most infectious epithelioid cell granulomatoses. However, the distribution pattern might not be apparent in transbronchial biopsies.

8.2.4.1 Infectious Epithelioid Cell Granulomas

Tuberculosis

Members of the *M. tuberculosis* complex, i.e., *M. tuberculosis*, *M. bovis* and BCG, *M. africanum*, and *M. microti*, cause tuberculosis. These mycobacteria belong to a group of fast-growing mycobacteria (Table 8.4). Virulence of these mycobacteria varies from medium- to high-virulent strains. Depending on the virulence on the one hand and the competence of the hosts'

Table 8.4 Types of mycobacteria in tuberculosis type, which are pathogenic for humans

M. tuberculosis
M. bovis and Bacillus Calmette-Guerin
M. africanum with subtypes *M. suricattae* and *M. mungi*
M. microti
M. canetti
M. pinnipedii

immune system, the morphology is reflected by widespread necrosis or by non-necrotizing epithelioid cell granulomas (Figs. 8.37, 8.38, and 8.39). The faith of the granulomas depends on stabilization or destabilization of this balance between virulence of the mycobacteria and the immune system of the host (see schema below): improved immune competence combined with antituberculous therapy is accompanied by inhibition of mycobacterial growth, stabilization of granulomas, fibrosis, and hyalinization. The opposite results when a decrease of immunocompetence and increase of virulence occur. This is reflected by necrosis up to necrotizing pneumonia with abscess formation and the inability to mount a granulomatous response, as it can be seen in end-stage AIDS patients infected with *M. tuberculosis*.

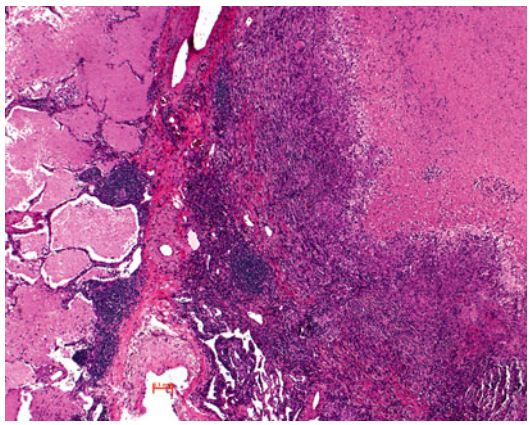

Fig. 8.37 Tuberculosis with large necrosis and concomitant alveolar proteinosis, which results in widespread distribution of the mycobacteria. This condition is based on an impaired immune function and usually also highly virulent strains of *M. tuberculosis*. H&E, bar 0.1 mm

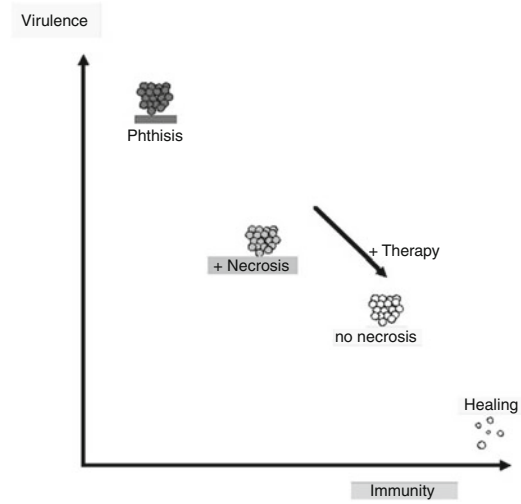

Schema: The balance of the host's immune system capability and the virulence of the mycobacterial strain: extensive necrosis in tuberculosis associated with alveolar proteinosis points to impaired immune reaction, whereas a good functioning immune system and slowly growing mycobacteria will result in healing or scar.

A wide variety of responses and patterns can occur in tuberculosis. Infection in the European

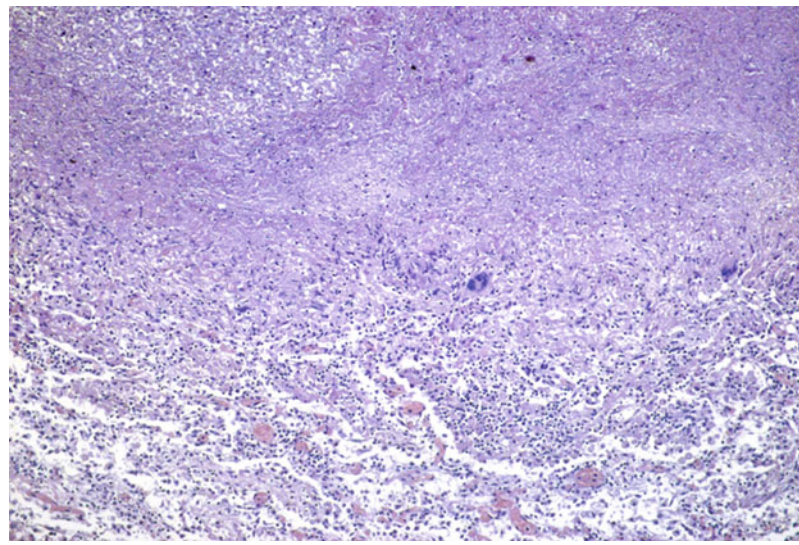

Fig. 8.38 Tuberculosis in an immunocompromised patient. There is widespread necrosis and the granuloma formation is impaired. The granuloma wall is broken down at two areas in this section, and mycobacteria can escape the host's immune defense. H&E, ×100

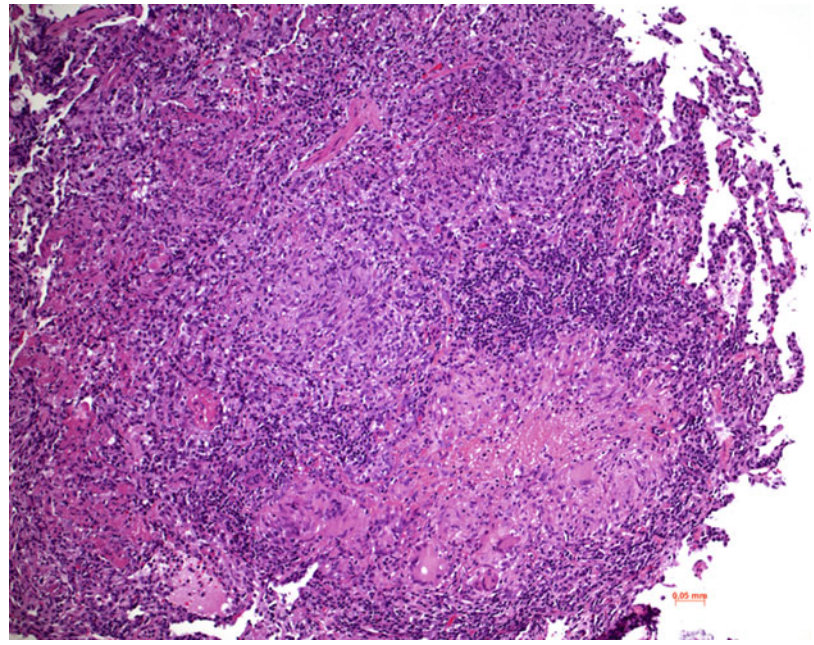

Fig. 8.39 Tuberculosis in a normal host. One of the granulomas present with a small focus of necrosis, whereas most of the granulomas not. Transbronchial biopsy, H&E, bar 50 μm

population is frequent; up to 90 % of the population acquire a mycobacterial infection in early adulthood; however, only 1–3 % of this population will present with symptoms. In the majority of the population, this infection will cause tiny granulomas in the mid and upper portion of the lower lobes. These granulomas undergo fibrosis, and a scar is all what can be found quite frequently in this location at autopsies decades later.

Clinical symptoms are cough, night sweats, temperature around 38 °C, and fatigue. Radiologically tuberculosis presents with single or multinodular densities but also often simulates lung cancer. Even on CT scan, the differential diagnosis cannot be made with certainty.

In patients presenting with tuberculosis, the initial form is most often a multinodular disease with caseous necrosis but located in one of the lung lobes (usually lower lobes). Depending on the ability of the patient's immune system, vasculitis can occur. Under tuberculostatic treatment this type of tuberculosis usually heals leaving scars and bronchiectasis. These in later life can be the preformed cystic structures prone to mycetoma.

In rare instances the primary infection had destroyed large areas of the lung and the necrotic focus cannot be replaced by scar tissue. In this case the necrotic focus is encased by granulation tissue, which is subsequently replaced by scar tissue. In the center the necrotic focus is still present, and mycobacteria are viable. This lesion is called tuberculoma (Fig. 8.40).

Fig. 8.40 Tuberculoma detected incidentally during X-ray and removed because clinically suspected for malignancy. Resection specimen formalin fixed

Secondary tuberculosis can occur in some patients in later life either as an exacerbation from a tuberculoma or by a secondary infection. In these cases the upper lobes are more often affected. Usually in this condition, miliary tuberculosis occurs: myco-

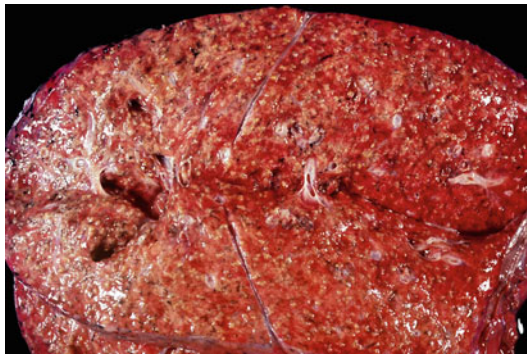

Fig. 8.41 Miliary tuberculosis, autopsy specimen. Numerous small nodules are scattered in this lung, each representing a granuloma with necrosis

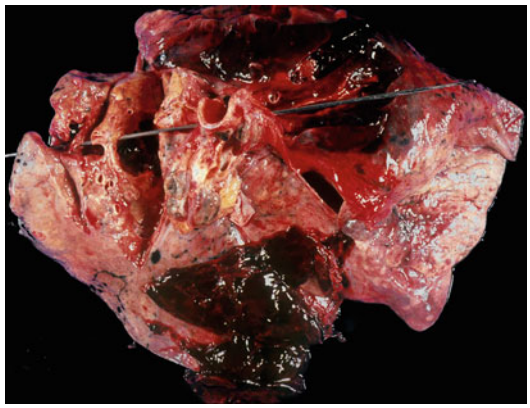

Fig. 8.42 Autopsy specimen showing massive hemorrhage from an erosion of a large pulmonary artery caused by caseous tuberculosis

bacteria get access to the blood vessels causing vasculitis, and the organisms are disseminated within the lung but also to other organs (Fig. 8.41).

There are some complications from tuberculosis, such as hemorrhage, when the necrotizing granuloma destroys the wall of larger pulmonary arteries. This will cause diffuse bleeding and ultimately the death of the patient (Fig. 8.42). Another complication is access of the granulomas and their mycobacterial content to larger airways, which will result in aerogenous spreading of the organisms, but also infection of other humans within the patient's living area (Fig. 8.43).

Diagnosis is established first by the demonstration of an epithelioid granulomatous reaction, followed by the proof of mycobacteria within the granuloma or in cytological material (BAL, smear) and by culture or PCR. This will be discussed in detail at the end.

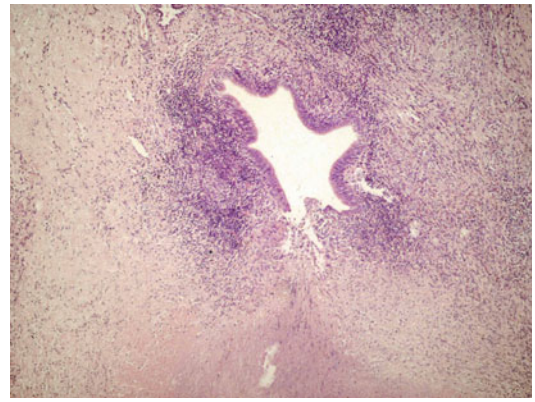

Fig. 8.43 Tuberculosis-induced necrosis has opened this bronchus and the infectious organisms can now be distributed through the airways but also will be expectorated and can infect other people. H&E, ×100

Mycobacteriosis

This is an infection with atypical mycobacteria (other than *M. tuberculosis* complex (MOTT)). It was once a rare disease, causing epithelioid cell granulomas in newborn and young children. It now has become a well-recognized disease in patients suffering from AIDS, or in otherwise immunocompromised patients. Many different mycobacteria can induce predominantly non-necrotizing epithelioid cell granulomas, among them *M. avium*-intracellulare, *M. fortuitum*, *M. gordonae*, *M. kansasii*, and *M. xenopi*, to name just the more common species. Some cause local disease, like skin lesions by *M. marinum*, whereas others cause systemic disease, like *M. avium* (Fig. 8.44). The diagnosis of mycobacteriosis can be made by acid-fast stains but in most instances requires culture or molecular biology techniques for species definition. In cases of severe immunodeficiency, the host's reaction might be impaired, which results in the inability to form epithelioid cell granulomas. In these cases macrophage granulomas are found, similar to granulomas in lepromatous lepra.

The reproductive cycle of MOTT species is quite variable: *M. avium*-intracellulare is a very slow-growing organism, which requires a culture for up to 11 weeks until the organism can be

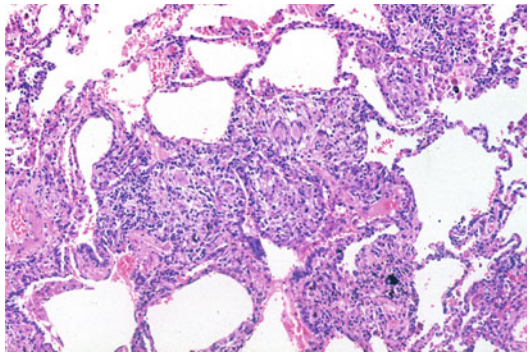

Fig. 8.44 Mycobacteriosis with non-necrotizing epithelioid cell granulomas. Note the proximity of the granulomas to the airspace, which points to an airborne infection. *M. gordonae* was identified by acid-fast stain and PCR. H&E, ×160

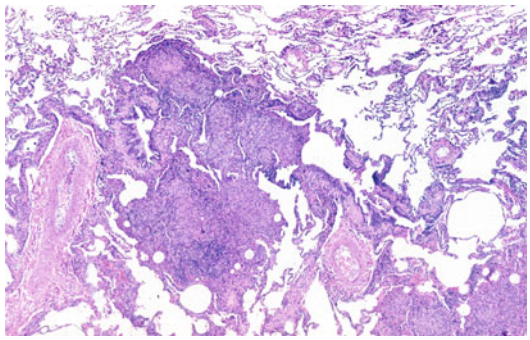

Fig. 8.45 Mycobacteriosis in hot tub disease. Within the VATS specimen, non-necrotizing epithelioid cell granulomas are seen. The granulomas are confluent and show many infiltrating lymphocytes, which are also present in adjacent alveolar septa. H&E, ×50

identified, whereas *M. fortuitum* is a fast-growing organism, which can be identified within 2 weeks. Necrotizing granulomas are usually found in these fast-growing species.

Recently a new disease was described as hot tub lung disease. Mycobacteria of the MOTT complex were identified as the causing agent [66, 67]. If this is an infectious disease caused by slow-growing MOTT, species in otherwise immunocompetent patients or a hypersensitivity reaction is not clear. An answer to this question is complicated as a hyperreactivity or allergic reaction can occur in mycobacterial infections as part of the immune defense and thus is not a proof of an allergy (Fig. 8.45). Biopsies from patients suffering from this type of disease will show exposure-related symptoms, i.e., increase of symptoms during the weekend (exposure to mycobacteria in hot tub) and relief of symptoms during the week. Morphologically the lesions present as non-necrotizing epithelioid cell granulomas, similar to classical mycobacteriosis with slow-growing mycobacteria such as *M. avium*-intracellulare (Table 8.5).

Table 8.5 Mycobacteria other than tuberculosis complex (MOTT), ordered according to pigment production in culture and also speed of growth

Producing photochromogens, slow growing	*M. kansasii*
	M. asiaticum
	M. simiae
Scotochromogen producing, slow growing	*M. gordonae*
	M. scrofulaceum
	M. szulgai
	M. xenopi
Non-pigmented, slow growing	*M. avium*-intracellulare
	M. malmoense
Fast growing	*M. fortuitum*
	M. abscessus
	M. chelonae
	M. leprae

Granulomatous or Tuberculoid Leprosy

In certain areas of the world, *M. leprae* is still widespread and infection due to bad hygiene conditions does occur. Areas with still high prevalence are in tropical Africa and Asia, less frequently South and Central America. Predilections are found in skin, upper respiratory tract, nerves, and testes. Lung lesions and involvement of other organ systems are rarely encountered; however, they do occur in end-stage disease (personal communication). Whereas in lepromatous leprosy, there is an unspecified macrophage-dominated host reaction, in granulomatous leprosy the host is able to mount an epithelioid cell reaction. Necrosis in these granulomas is uncommon; in most instances the granulomas resemble those seen in sarcoidosis. In cases of borderline tuberculoid reaction (mixture of tuberculoid and lepromatous leprosy), the granulomas tend to be more loose than those in tuberculosis (Fig. 8.46). The differentiation of macrophages and histiocytes into epithelioid

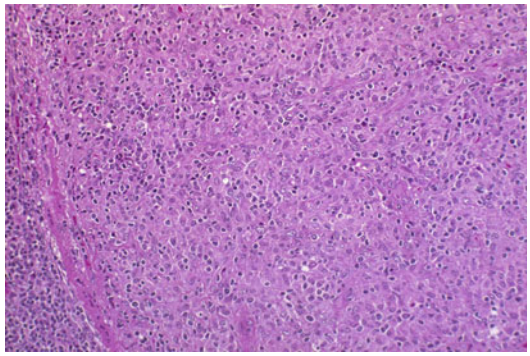

Fig. 8.46 Diffuse histiocytic and epithelioid cell reaction in a lung lymph node in tuberculoid leprosy. There are no well-circumscribed granulomas, and most cells are histiocytic, but some already have undergone epithelioid cell transformation. The organisms were identified by PCR. H&E, ×260

cells is not as pronounced as in the tuberculoid form. *M. leprae* are packed in bundles of organisms within macrophages or epithelioid and Langhans cells. They are less acid fast than other mycobacteria.

Rare Bacterial Infections

There are a few bacteria, other than mycobacteria, which can induce the formation of epithelioid cell granulomas. Among these *Treponema pallidum* is the best known.

Treponema pallidum, the causative agent of syphilitic gumma, still exists, although rare in Western countries. In recent years a rise of syphilis is seen in Asian and South American countries,

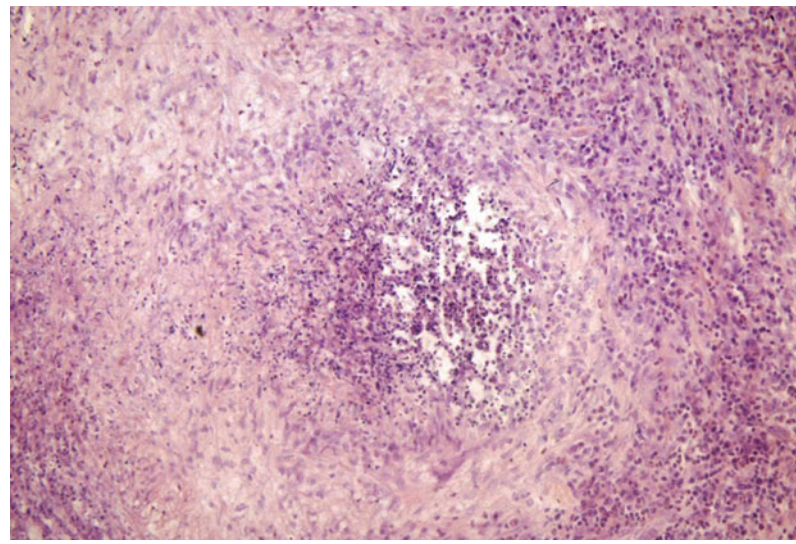

Fig. 8.47 Epithelioid cell granulomas with central necrosis. The necrosis contains numerous neutrophils, which point to an infectious organism other than mycobacteria. Here *Treponema pallidum* was identified. H&E, ×160

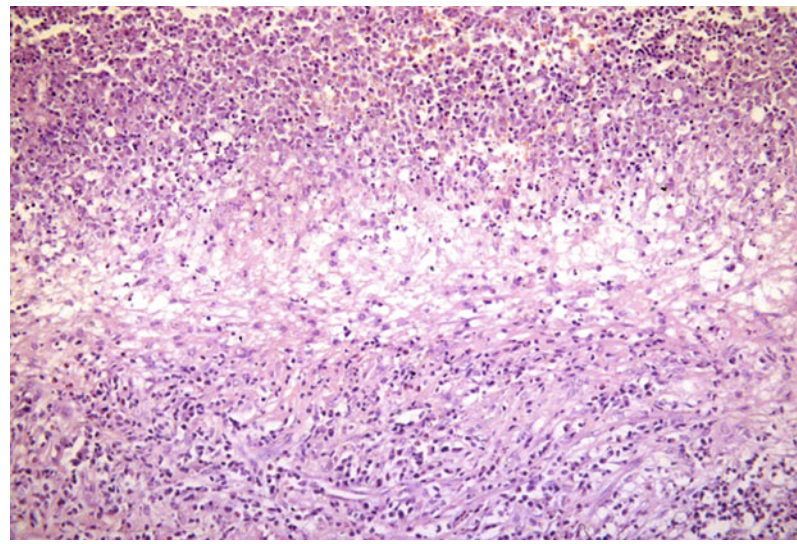

Fig. 8.48 Higher magnification of the same case. In the center of the necrosis, numerous neutrophils are seen; epithelioid cells and lymphocytes form the border. H&E, ×250

and new cases appear in Europe due to "sex tourism." In most instances it might be difficult to get the proper information from the patients. The primary infection sites are the external genitalia, where a granulomatous and ulcerating inflammation starts. After bacteremia the organisms can enter the lungs. Inflammation is characterized by necrotizing epithelioid cell granulomas with numerous neutrophils within the central necrosis (Figs. 8.47, 8.48, and 8.49). Vasculitis is commonly seen in this granulomas causing vascular obstruction. The name gumma, used for these granulomas, is derived from their macroscopic appearance: the central necrosis is not caseous as in tuberculosis but has a gumlike consistency, hence the name (gummi arabicum). The *Treponema* organisms can be stained by silver impregnation (modified Warthin-Starry stain, Fig. 8.50) or immunohistochemically by specific antibodies.

Other bacteria able to mount an epithelioid granulomatous reaction are other members of the *Spirochaetae* family, like *Leptospirochaetae*.

In rare instances atypical bacteria form a histiocytic granulomatous inflammation. Some of these were initially included in malakoplakia. However, infectious organisms have been identified in some of these, such as *Rhodococcus equi* and *Tropheryma whipplei*, the causing organism of Whipple's disease (Fig. 8.51). *Actinomyces* another rare bacterium can cause either purulent pneumonia with abscess formation or also a histiocytic granulomatous reaction (Fig. 8.52).

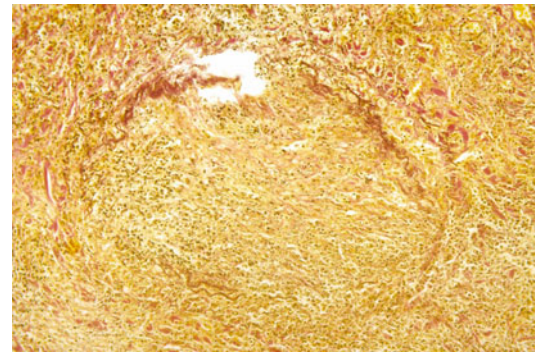

Fig. 8.49 Necrotizing epithelioid cell granulomatous vasculitis. Same case as Fig. 8.47. The pulmonary artery is occluded by the granuloma and the lamina elastic is partially destroyed. Elastica v. Gieson, ×100

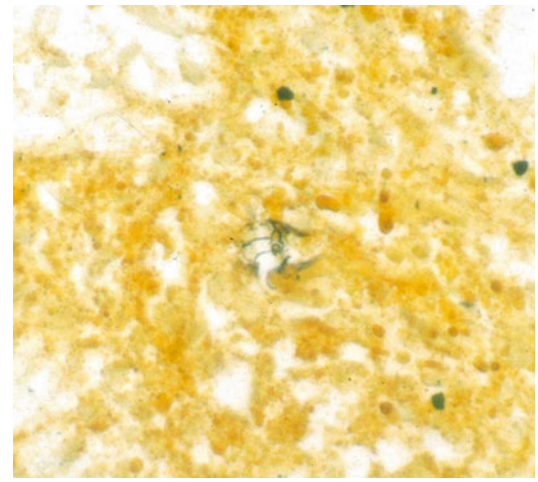

Fig. 8.50 *Treponema pallidum* identified in the necrotic center of the granuloma. Warthin-Starry, ×1000

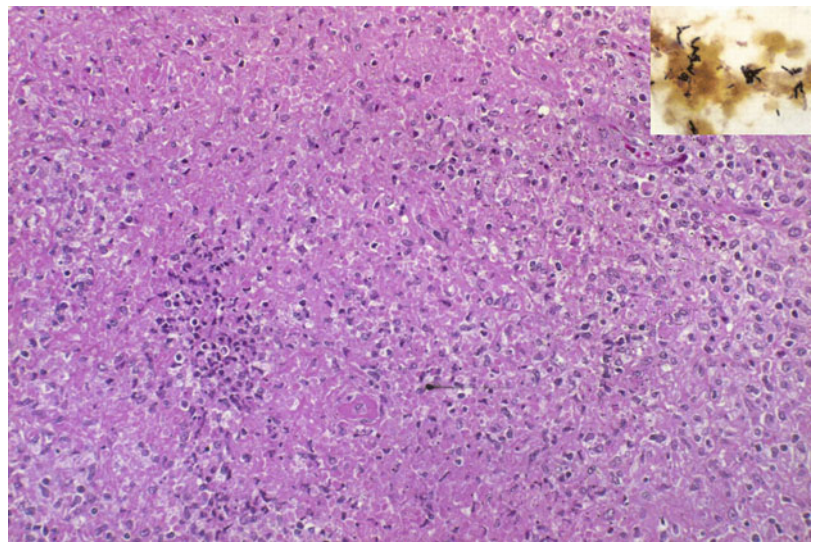

Fig. 8.51 Histiocytic granulomatosis with focal necrobiosis (dying of few cells) due to infection with *Rhodococcus equi*. H&E, ×260. Inset silver impregnation of the organisms, Warthin-Starry, ×1000

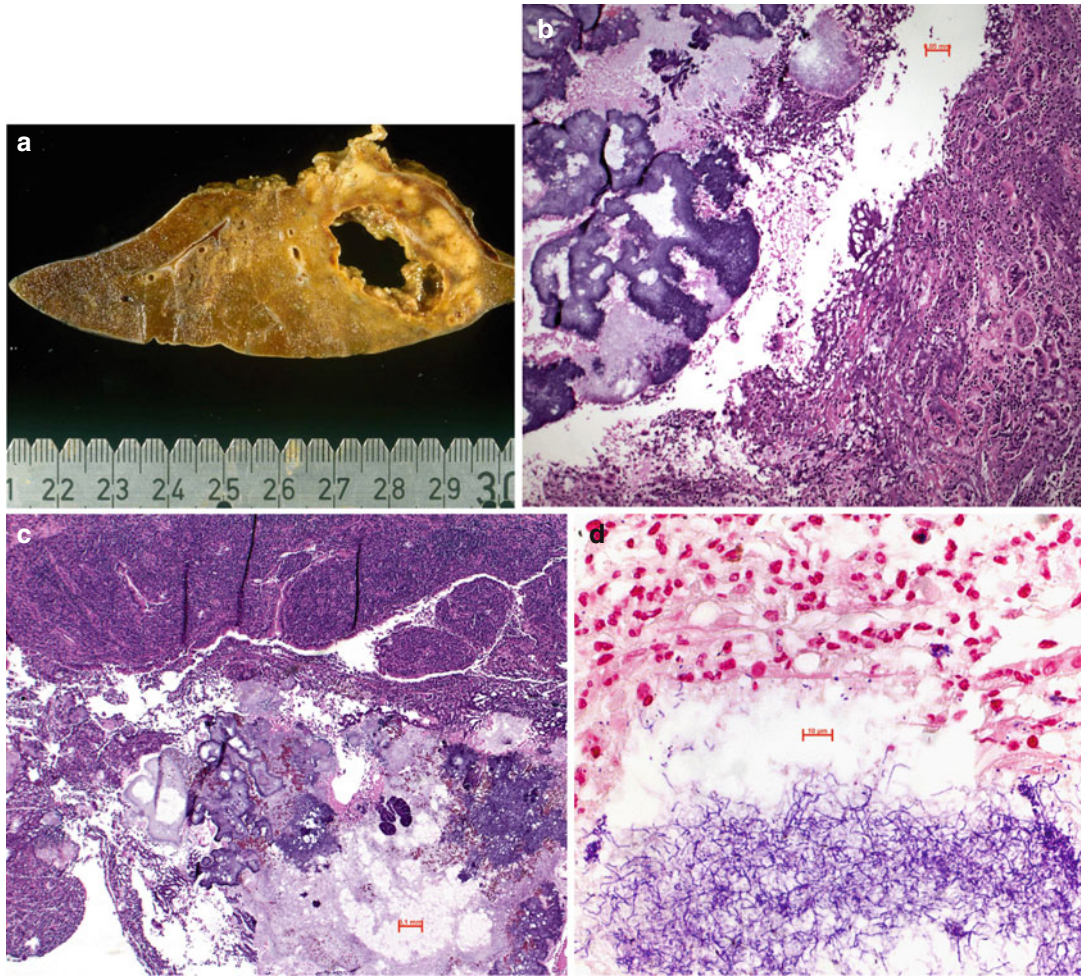

Fig. 8.52 Actinomycosis with a mixed infiltration in the wall of the airways composed of histiocytes, foreign body giant cells, neutrophils, plasma cells, and lymphocytes. In the lumen a basophilic material is seen. (**a**) Macroscopic picture of a resection specimen. (**b**) Wall of the necrosis with a mixed inflammatory infiltrate, besides remnant of the bronchial epithelium also some giant cells are seen. (**c**) Dense lymphocytic infiltration and basophilic material in the lumen. (**d**) Gram stain highlighting *Actinomyces* species. (**b+c**) H&E, bars 50 µm and 100 µm, (**d**) Gram, bar 10 µm

Mycosis

Most often fungi cause either a localized mycetoma or a diffuse bronchopneumonia. Rarely they will cause a granulomatous reaction. However there are species, such as *Histoplasma*, which more often induce granuloma formation. Information on the epidemiology, the distribution, reproduction cycles, and much more can be found at the website of the Center for Disease Control and Prevention (CDC: www.cdc.gov). Clinical symptoms are similar to tuberculosis. On X-ray and CT scan, nodules of different size can be seen, often in both lungs. Based on the different forms of cysts and sporozoites, and with the aid of additional stains, the following mycoses can be differentiated:

Histoplasmosis

Histoplasma organisms are found in wet lowland areas. *H. capsulatum* is widespread in the soil of North American river valleys, especially in valleys flooded annually, for example, the Mississippi river and its main tributaries. For reproduction this organism requires periodic flooding, after which spores are produced. These spores will resist deterioration for a long time and are the source for infection. In certain areas of Mesoamerica, animals such as bats are another source of infections, and outbreaks have been reported [68]. Its occurrence in Europe has been described in humans (Fig. 8.53) but also in animals. *Histoplasma capsulatum* is a yeastlike uni-

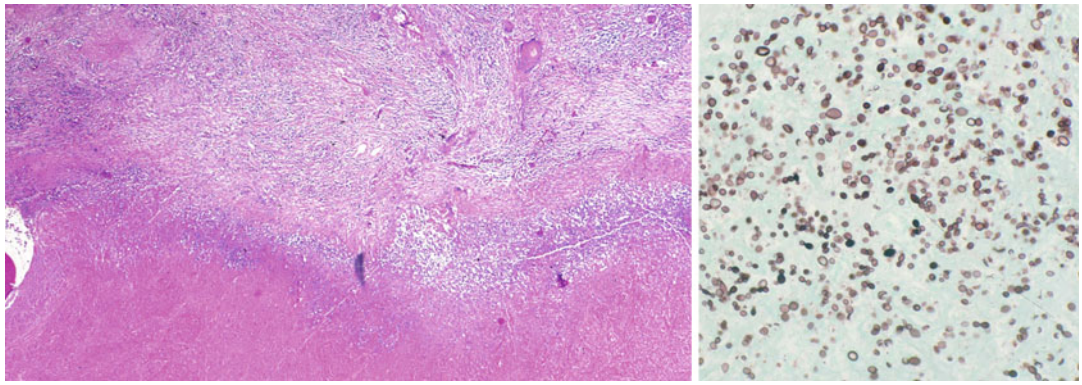

Fig. 8.53 Epithelioid cell granulomatosis with large necrotic area, very much looking like tuberculosis. Even Langhans cell can be seen at this magnification. H&E, ×25. (**b**) By silver impregnation a fungus can be seen, in this case *Histoplasma capsulatum*. GMS, ×400

nucleate organism, 2–4 μm in diameter. It reproduces by budding or by endospores. The organisms are usually found within macrophages and histiocytes but also in the necrotic debris. Capsules of *Histoplasma* can be stained by GMS and by PAS, leaving the center unstained. With Giemsa the nuclei of the sporozoites are stained, leaving the capsule more or less unstained.

The African variant is *Histoplasma duboisii*, which is larger than *H. capsulatum. H. duboisii* similar to *H. capsulatum* exists in the soil of river valleys, along the large African rivers, like the Niger. Lung lesions in African histoplasmosis are less frequent than with the North American form. Acute histoplasmosis presents with bronchopneumonia and abscess formation; the reaction is dominated by neutrophils and macrophages. In chronic forms epithelioid cell granulomas are seen in both; however, necrotizing granulomas are more frequent in *H. capsulatum*-induced lesions. This form of histoplasmosis can look identical to necrotizing tuberculosis; only the stain for the organisms will tell the difference.

Cryptococcosis (European Blastomycosis)

Cryptococcus neoformans and *C. gattii* are distributed worldwide, except the arctic and antarctic circles. The organisms are found in the soil or in the droppings from pigeons. Airborne spores are inhaled but usually cause infection in patients with weakened immune system. The organisms are 4–7 μm in diameter, their cell walls can be stained by H&E, but the mucinous capsule is usually unstained. Mucicarmine or PAS stains are helpful in highlighting the capsule. The organisms reproduce by budding. The small or large yeastlike organisms are found side by side, and buds might be small or large and show prominent fragmentation, which distinguish them from *Histoplasma* and *Blastomyces*. In the acute setting, cryptococcosis causes a bronchopneumonia with abscess formation but also accumulations of macrophages within their cytoplasm, the organisms can be demonstrated. In the subacute and chronic form, epithelioid granulomas are formed [69]. The organisms are usually found within Langhans giant cells, but may also be found lying free within necrosis (Fig. 8.54).

Blastomycosis

Blastomyces dermatitidis can be found in North America and Africa. The fungus lives in moist soil where decomposing organic matter supplies its nutrients. It is a thick-walled round 8–15 μm organism, which reproduces by budding. The buds are numerous and are broad based attached to the parent yeast. The fungus has many nuclei, which distinguish it from *Cryptococcus* and the *Coccidioides* organisms. GMS stain the whole yeast; the capsule can be highlighted by PAS or mucicarmine stains. Infection occurs by inhalation of airborne spores. The symptoms of acute blastomycosis are similar to flu. Blastomyces regularly induce a granulomatous reaction with and without necrosis; however, the necroses are not of the classical caseous type: they contain cellular debris and many neutrophils.

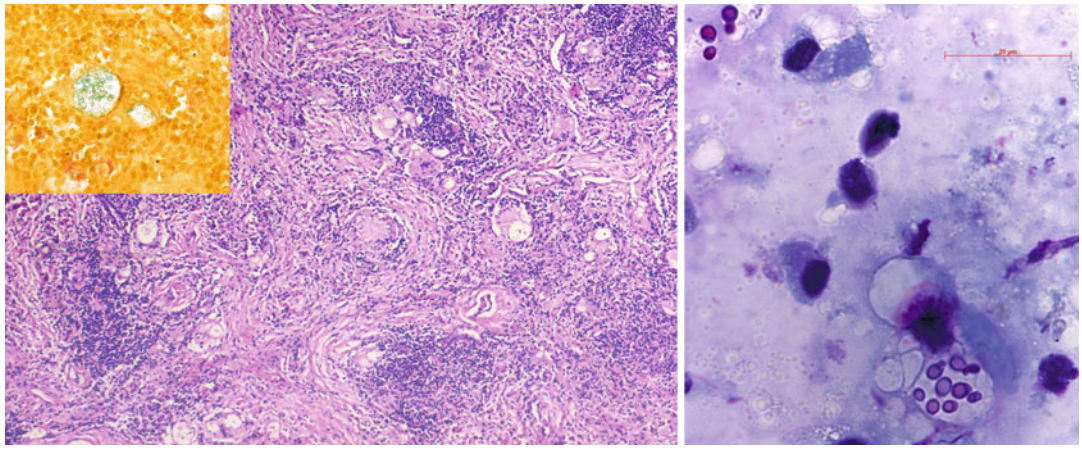

Fig. 8.54 Epithelioid cell granulomatous pneumonia due to *Cryptococcus* infection. Within the Langhans cells but also outside in the granulomas cysts are seen with some pale eosinophilic material. H&E, ×160. *Inset*: GMS stain identifying sporozoites within the cysts, ×260. *Right*: BAL specimen showing sporozoites of *Cryptococcus neoformans*, Giemsa, bar 20 µm

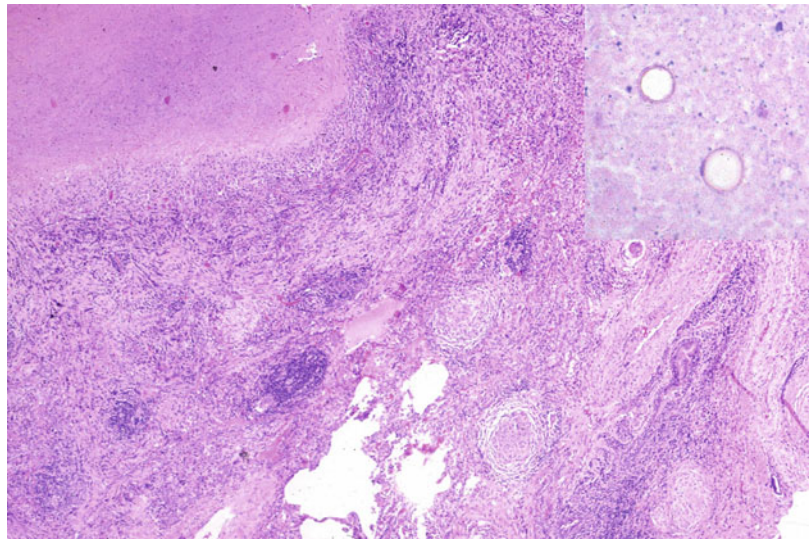

Fig. 8.55 Epithelioid cell necrotizing granulomatosis due to *Coccidioides* infection. Numerous granulomas are formed, many of them without necrosis; however, a large necrosis is seen in the *upper left corner*. Inset PAS stain of the cyst wall. In this case *Coccidioides immitis* was identified. H&E, ×100, PAS, ×400

Coccidio- and Paracoccidiomycosis

Coccidioides immitis is found in the soil of dry, desertlike areas in the southwestern parts of the USA, but also in Central and South America. It is also known as valley fever and is a common cause of pneumonias in these endemic areas. It is characterized by large sporangia, 30–60 µm in diameter, the endospores are each 1–5 µm. They can be identified in H&E-stained sections; however, GMS and PAS also stain them (Fig. 8.55). The sporangia can be found within giant cells or free within necrosis. In some cases an acute bronchopneumonia with a dominant neutrophilic and macrophagocytic infiltration is seen; in other cases classic epithelioid cell granulomas are developed.

Paracoccidioides brasiliensis – found in South America – is characterized by multiple buds growing out of one organism. The single fungus is 5–15 µm in diameter but by budding may approach 20–40 µm (Fig. 8.56). The fungus is uninucleate and the buds are of varying size

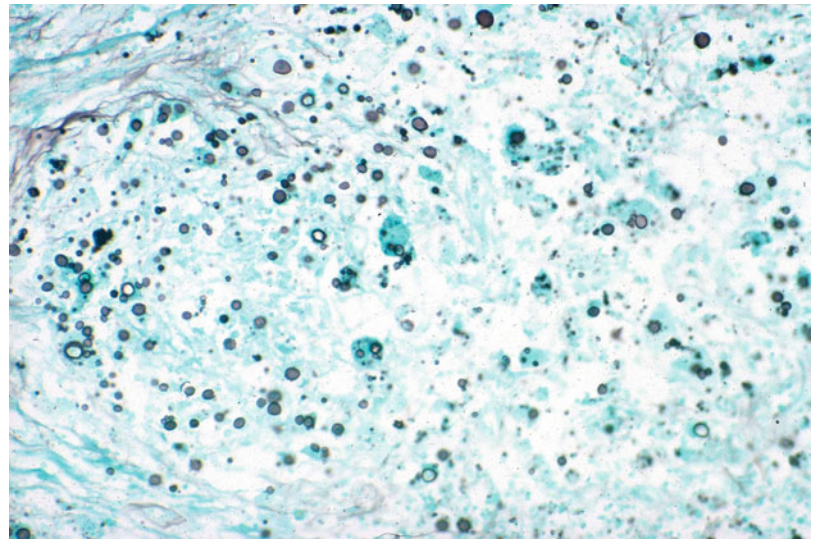

Fig. 8.56 GMS stain of *Paracoccidioides brasiliensis* in a case showing similar morphology as in Fig. 8.54. GMS stain, ×400

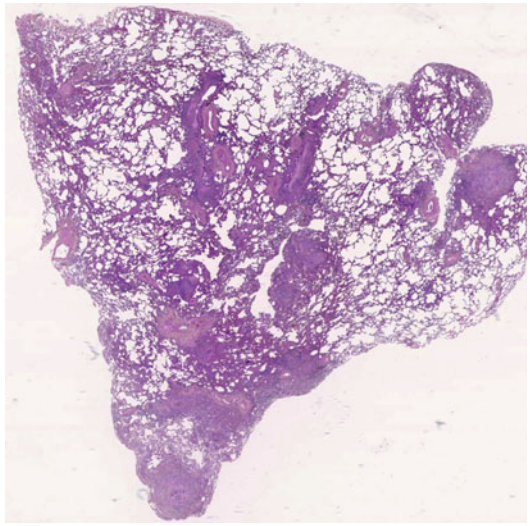

Fig. 8.57 A rare case of *Aspergillus*-induced epithelioid cell granulomatous pneumonia. H&E, ×2.5

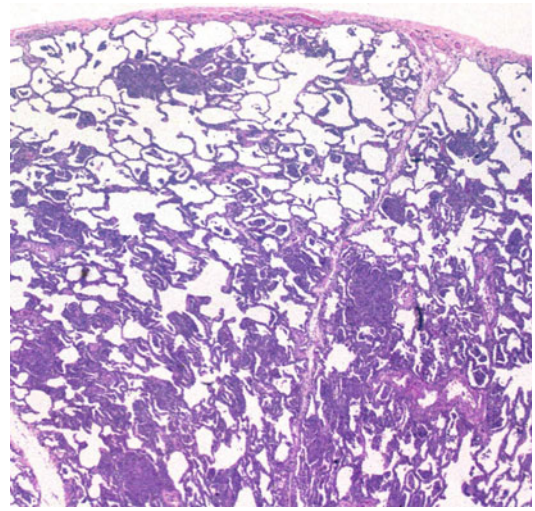

Fig. 8.58 Rare form of epithelioid cell granulomas in *Pneumocystis jirovecii* pneumonia. H&E, ×50

and shape. The organisms can be demonstrated by H&E, PAS, and GMS.

Other fungi causing deep mycosis rarely induce epithelioid cell granulomas. In most instances organisms, like *Aspergillus*, *Candida*, *Pneumocystis*, and others, cause a localized mycetoma, or a diffuse invasive mycosis, or an allergic reaction (allergic bronchopulmonary aspergillosis/mycosis). The cause for organisms like *Aspergillus* or *Pneumocystis* to induce an epithelioid cell granulomatous inflammation is largely unknown (Figs. 8.57 and 8.58).

8.2.4.2 The Noninfectious Epithelioid Cell Granuloma

These granulomas are characterized by the absence of central necrosis; however, necrobiotic foci can occur. It is important to rule out neutrophilic, eosinophilic, and mixed granulocytic and lymphocytic vasculitis, which is the hallmark of a

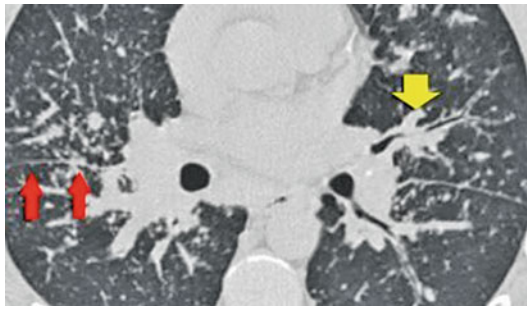

Fig. 8.59 CT scan of sarcoidosis; there are scattered nodules in both lungs; the hilar nodes are enlarged. *Red arrows* point to small nodules along the airways (bronchovascular bundle), *yellow arrow* points to aggregates of nodules

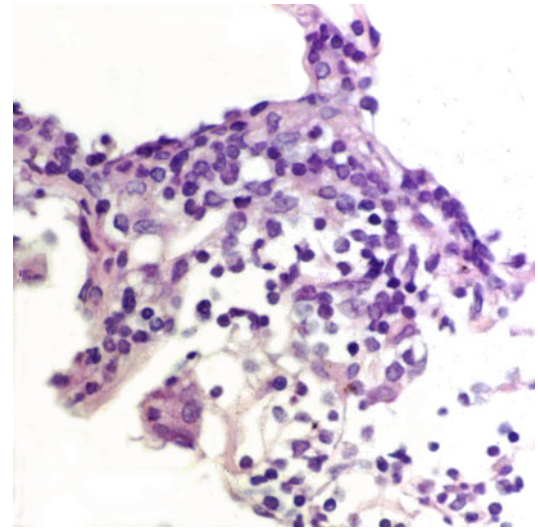

Fig. 8.60 Early granuloma in sarcoidosis. There are many lymphocytes but a few histiocytes and epithelioid cells are there. H&E, ×400

group of diseases, like granulomatosis with polyangiitis (GPA). However, granulomatous vasculitis showing epithelioid cell granulomas in the wall of different-sized blood vessels is not infrequently encountered in all variants of epithelioid cell granulomatosis (see below).

Sarcoidosis

Clinics and Radiology

The diagnosis is based on the exclusion of cultivable and/or stainable organisms. Important are the clinical picture and the radiological data, like bilateral hilar lymphadenopathy on X-ray. The granulomas are most frequently found along bronchovascular bundles, pulmonary veins, and lymphatics. High-resolution CT scans are useful to highlight this distribution pattern (Fig. 8.59).

In sarcoidosis the earliest lesion is characterized by an accumulation of macrophages/monocytes and lymphocytes within alveolar septa and underneath the bronchial mucosa (Fig. 8.60). These monocytoid cells differentiate into epithelioid and giant cells. Early on foreign body as well as Langhans giant cells can be seen. Later on lymphocytes become scarce, and the granulomas stick out from an otherwise not inflamed parenchyma (Figs. 8.61, 8.62, and 8.63). Well-formed granulomas undergo fibrosis, which usually starts from the outside of the granuloma in a concentric fashion. Finally a hyalinized granuloma remains, which will show an occasional epithelioid cell (Fig. 8.36). In fully developed granulomas, lymphatic vessels can be seen transversing the granuloma, sometimes also capillaries. A granulomatous vasculitis pattern can be seen in some cases (Fig. 8.64). Granulomas are usually within the interstitium and do not show any association with the airway epithelium. Some features have been regarded as specific, like asteroid, Schaumann, and conchoid bodies in the Langhans cells. However, these structures can be seen in all Langhans cell containing granulomas of diverse etiology and are of no help in making the diagnosis of sarcoidosis. Calcium oxalate, carbonate, and pyrophosphate crystals can be found in granulomas and in Schaumann bodies; however, they are not diagnostic too (Fig. 8.65). A T-helper lymphocyte ($CD3^+CD4^+$)-dominated alveolitis in the BAL might supplement the histologic diagnosis.

Diagnosis on small biopsies and cytological specimen is easy in sarcoidosis. Due to the predominant distribution pattern along the bronchovascular bundles, transbronchial biopsies are most often diagnostic (Fig. 8.66). Since sarcoidosis also involves the hilar lymph nodes, EBUS-derived fine needle aspiration is also most often diagnostic (Fig. 8.67).

A variant of sarcoidosis has been described as *nodular sarcoidosis*. In this form of sarcoidosis,

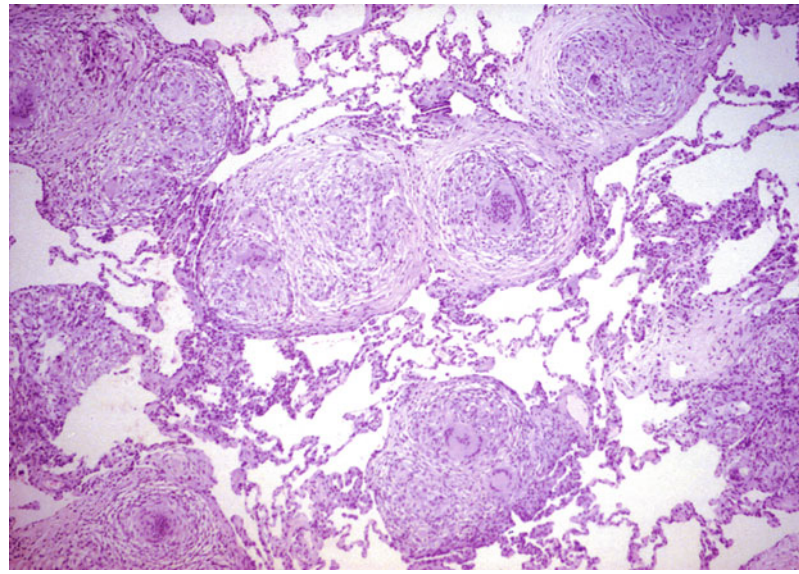

Fig. 8.61 Well-formed epithelioid cell granulomas in sarcoidosis. The granulomas are all centered within the interstitium and do not show an association with the alveoli. In the center a transversing lymphatic capillary is seen, which points to the etiology of an antigen coming from the circulation. H&E, ×250

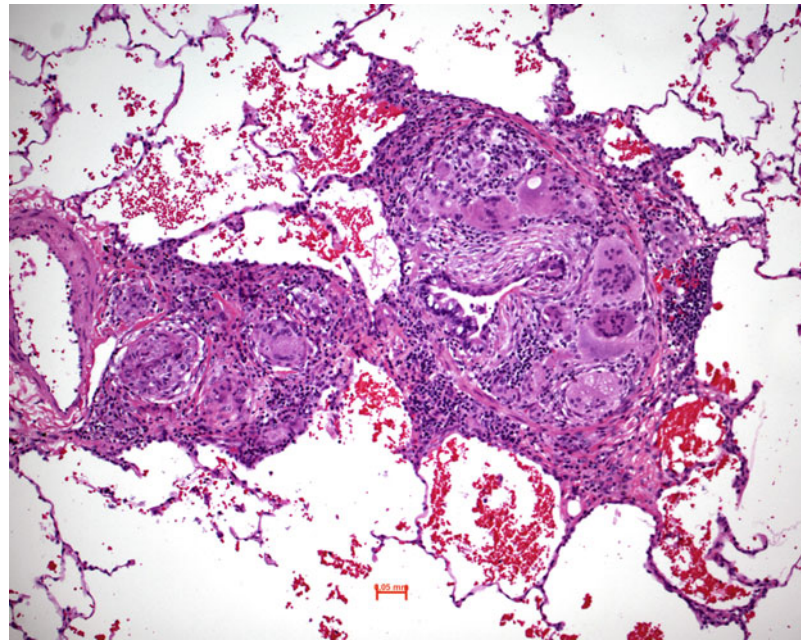

Fig. 8.62 Epithelioid cell granulomas in sarcoidosis. The location of the granulomas within bronchovascular bundles is seen here. Again the granulomas are centered in the middle of the interstitium. The adjacent alveolar septa are normal, not even a lymphocytic infiltration is noticed. H&E, bar 50 µm

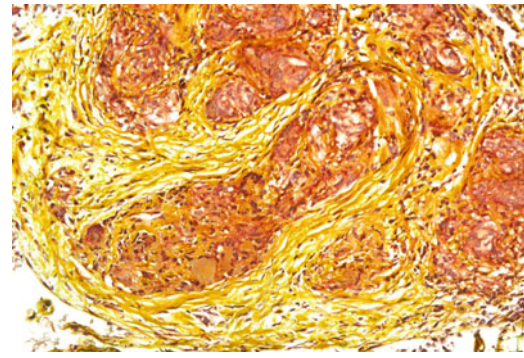

Fig. 8.63 Fibrosis in epithelioid cell granulomas in sarcoidosis. The granulomas are not dissected by fibrosis as this is often seen in tuberculosis – the fibrosis in sarcoidosis starts outside the granulomas and gradually encase them. Movat pentachrome, ×250

the granulomas coalesce forming large aggregates, which can reach a diameter of up to 3 cm (Fig. 8.68) [70, 71]. Clinically nodular sarcoidosis does not behave different from common sarcoidosis. Also the therapy and prognosis is similar.

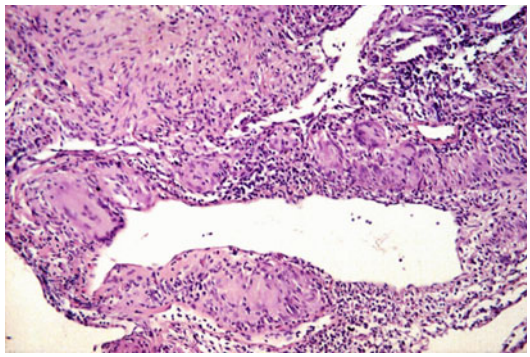

Fig. 8.64 Sarcoidosis with epithelioid cell granulomatous vasculitis, here in the wall of a small vein. H&E, ×200

Another variant of sarcoidosis is *necrotizing sarcoid granulomatosis* (NSG). In NSG non-caseating epithelioid cell granulomas are found. The distribution is similar to sarcoidosis with a dominant involvement of the bronchovascular bundle. In addition there is an epithelioid granulomatous vasculitis causing ischemic infarcts. The granulomas can usually confluent, forming large nodules identical to nodular sarcoidosis; the lymphocytic rim is usually prominent (Figs. 8.69 and 8.70). Liebow originally described this disease as a separate entity [72], because he assumed that it has features in between Wegener's granulomatosis (vasculitis, ischemic necrosis) and sarcoidosis (nodular aggregates of epithelioid cell granulomas). Based on our own observation and research, we proposed NSG as a variant of sarcoidosis, characterized by nodular aggregates of epithelioid cell granulomas, granulomatous vasculitis, and ischemic infarcts [73,

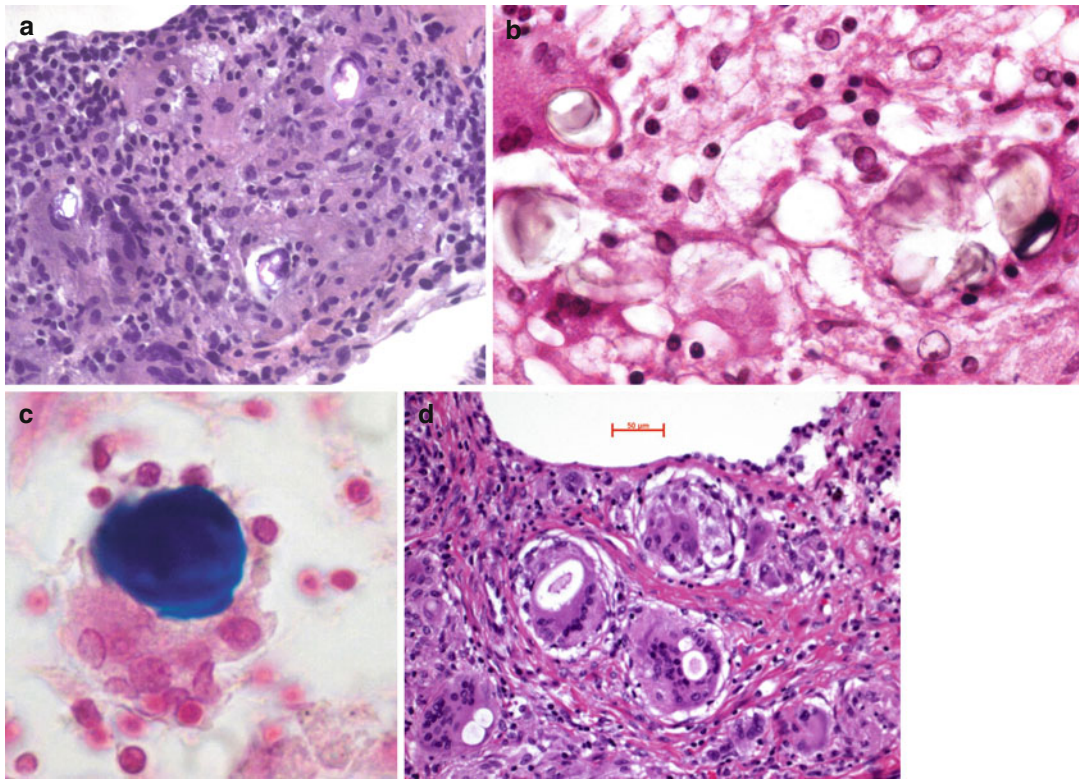

Fig. 8.65 Substances and organelles in sarcoidosis: (**a**) Calcium compounds, most frequent oxalates and pyrophosphates (partially polarized), (**b+c**) Schaumann bodies, which can stain with Prussian blue for iron, (**d**) asteroid bodies which are giant centrosomes. H&E, ×200, ×400, bar 50 µm, Prussian blue stain, ×400

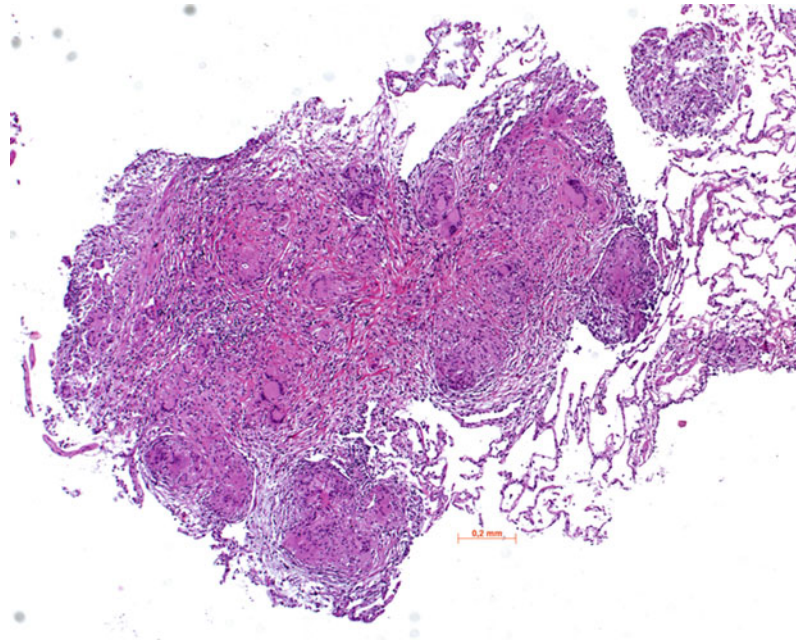

Fig. 8.66 Transbronchial lung biopsy showing a large piece with many epithelioid cell granulomas. After excluding infectious organisms the diagnosis of sarcoidosis was made. H&E, bar 200 µm

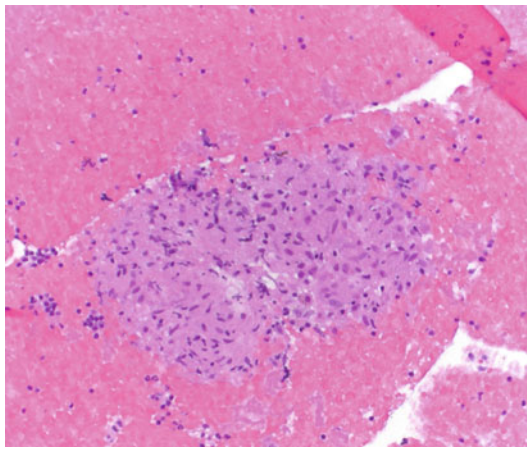

Fig. 8.67 EBUS-derived fine needle aspiration from a hilar lymph node showing a well-preserved epithelioid cell granuloma. Using cellblock technique also infectious organisms could be excluded and a diagnosis of sarcoidosis made. H&E, ×250

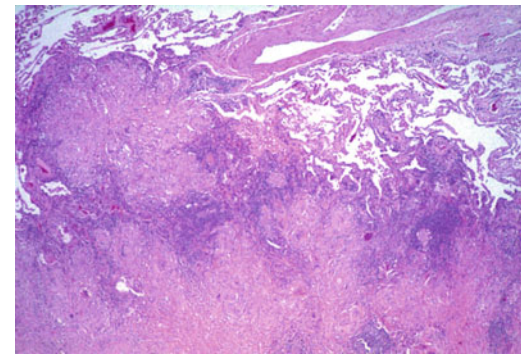

Fig. 8.68 Nodular sarcoidosis. In this case the large nodule measuring almost 3 cm in diameter is composed of numerous confluent granulomas. H&E, ×50

74]: granulomatous vasculitis is a feature in NSG and sarcoidosis, ischemic necrosis in NSG is due to lumen obstruction induced by vasculitis, and finally like sarcoidosis NSG is also a systemic disease involving several organs (liver, spleen, ocular adnexa, lymph nodes, etc.).

The *etiology of sarcoidosis* is presently a matter of debate. It has been shown that in some cases, mycobacteria could be cultured from sarcoidosis granulomas of the skin after subculture [75, 76]. Different investigators succeeded in demonstrating mycobacterial DNA and RNA in sarcoidosis. We have found mycobacterial DNA other than tuberculosis complex (MOTT-DNA) in one third of sarcoidosis cases. Others could demonstrate DNA of *Propionibacterium acnes* [77–83]. Neither mycobacteria nor propionibacteria could be cultured directly from the granulomas. So how to interpret this? Is the finding of bacterial DNA in sarcoidosis granulomas incidental? Could it be causative for

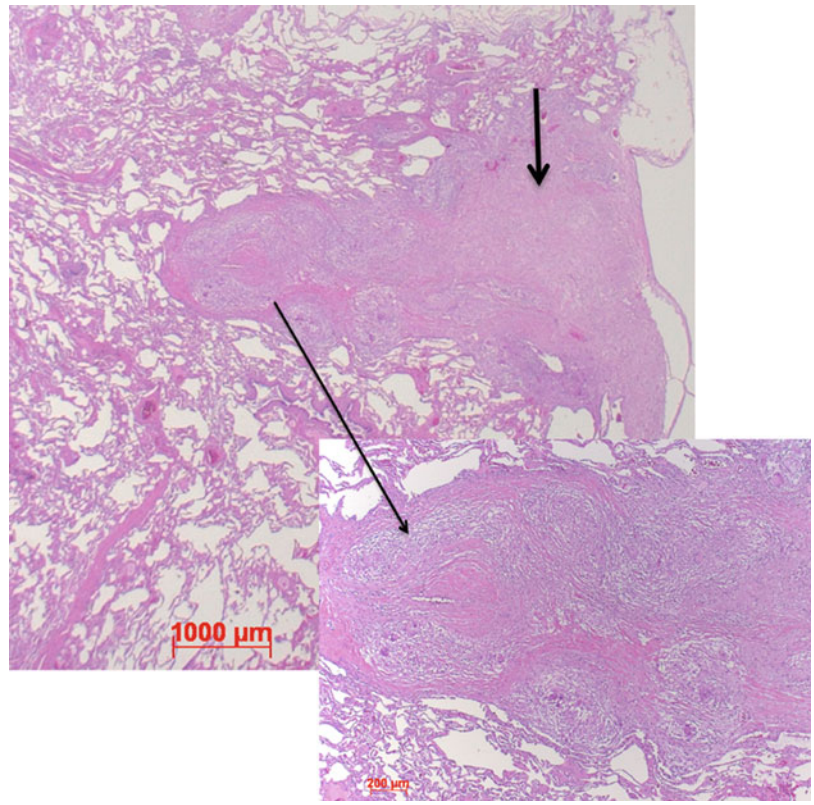

Fig. 8.69 Necrotizing sarcoid granulomatosis (NSG). Multiple sarcoid granulomas are formed, many of them obstructing a large pulmonary artery. An ischemic infarct has developed (*arrow*). Inset figure shows enlarged the area of granulomatous vasculitis, leading to the infarct. H&E, bars 1 mm and 200 µm

sarcoidosis? How can this be merged with the delayed-type immune reaction in sarcoidosis, based on a dominant action of T-helper-1 lymphocytes?

It has been speculated that cell wall-deficient mycobacteria, unable to grow, might induce sarcoidosis. We have shown that in some cases, DNA insertion sequences, characteristic for *M. avium*, could be amplified from granulomas. In three cases of recurrent sarcoidosis in lung transplants, mycobacterial DNA other than tuberculosis complex could be found [84]. Other recent reports have demonstrated that naked mycobacterial DNA is capable of inducing a strong immune response [85–87]. And it is known that mycobacteria can preferentially persist in macrophages. In a working hypothesis, we assume that slow-growing members of mycobacteria might elicit an allergic reaction, in the background of a host's hyperergic predisposition. Via circulation these allergens could be distributed to different organ systems, eliciting the well-known perivascular granulomatous reaction.

By gene profiling we have identified genetic deregulation of proliferation and apoptosis. In sarcoidosis patients with active disease, proliferation pathways involving the phosphoinositol-3-kinase-Akt2 pathway, including Src kinase, and crk-oncogene, as well as fatty acid-binding proteins 4 and 5 together with PPARβδ, induce proliferation of macrophages and lymphocytes of Th1 lineage. In addition the apoptosis pathway is downregulated by protein 14-3-3. So probably the underlying defect in sarcoidosis might be a prolonged proliferation of lymphocytes and macrophages and a longer survival of these activated cells, which then causes disease [88]. The mechanism by which mycobacteria or propionibacteria can trigger this inflammatory reaction is still unclear, but the answer might be found in the mechanisms of antigen processing and presentation. Other

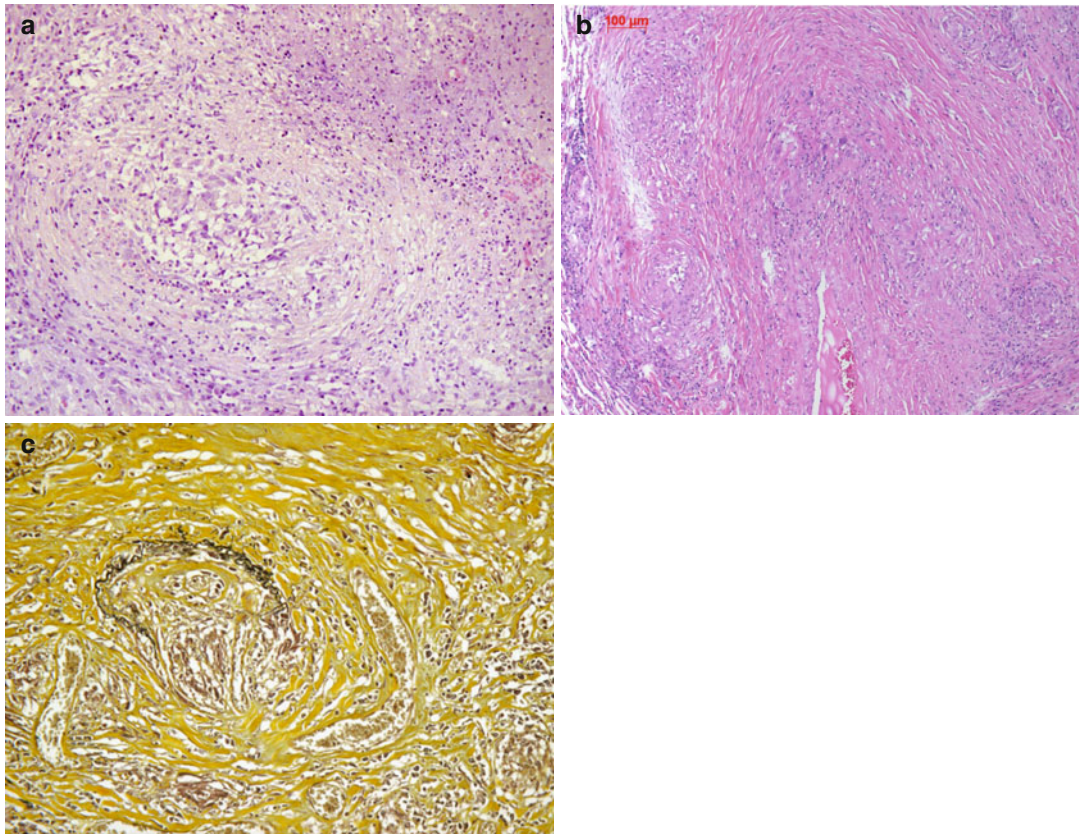

Fig. 8.70 NSG showing the different developmental stages of granulomatous vasculitis. (**a**) Early vasculitis with epithelioid cells occluding the lumen of this small artery; to the *right upper corner*, ischemic necrosis is already seen. (**b**) Sarcoid granulomas within the wall of this large pulmonary artery, the lumen is fully occluded. (**c**) Small pulmonary artery completely occluded by a sarcoid granuloma. (**a+b**) H&E, ×150, bar 100 µm, (**c**) Movat stain, ×150

theories are focusing on polymorphisms of different genes such as TNFβ and HSP70 [89]. A lot of research has focused on polymorphisms within the HLA system. HLADRB1*0301/DQB1*0201 has been linked to good prognosis and Lofgren syndrome; a linkage study found genetic alterations on chromosome 5 in African American sarcoidosis patients, whereas another linkage to chromosome 6 (identified as BTNL2 gene) was found in a German population [90]. Finally studies have focused on the Toll-like receptor (TLR) family, which are responsible for the processing of antigens and also dictate the type of immune reactions. Modifications within the TLR4 might be associated with the susceptibility for sarcoidosis [91].

The proof of mycobacterial DNA in sarcoid granulomas has serious diagnostic implications: molecular proof of mycobacterial DNA does neither rule out sarcoidosis nor confirm mycobacteriosis. The clinical setting, the radiological data, and the histological and microbiological proof of stainable/viable mycobacteria are required. In recurrent sarcoidosis in lung transplants, even DNA sequencing is necessary, to discern MOTT-DNA positive cases of sarcoidosis from secondary mycobacterial infection in the transplant.

Chronic Allergic Metal Disease

Chronic berylliosis is an allergic epithelioid cell granulomatosis. The granulomas tend to be larger than in EAA/HP or sarcoidosis; however,

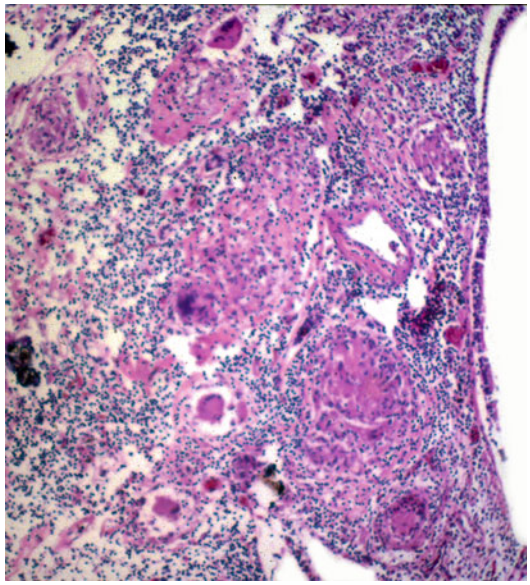

Fig. 8.71 Epithelioid cell granulomatosis in chronic berylliosis. The epithelioid granulomas are distributed along the bronchovascular bundles like in sarcoidosis. The lymphocytic infiltrate is CD4+ dominated as in sarcoidosis. H&E, ×200

it is impossible to differentiate them morphologically from sarcoidosis. The granuloma itself is identical to the granuloma in sarcoidosis (Fig. 8.71). As in sarcoidosis no infectious organisms can be demonstrated in the granulomas. No larger series of BAL have been reported in berylliosis so far. However, in an experimental investigation, a predominance of T-helper lymphocytes has been reported, making BAL an unsuitable tool for the differentiation of berylliosis and sarcoidosis. For the diagnosis a lymphocyte transformation test is usually recommended, and an exposure history is necessary. The exact cause of berylliosis is still unclear. Beryllium oxide is a molecule, too small to induce an allergic reaction. Beryllium-protein complexes most probable induce this reaction. Beryllium might form tetrameric complexes with amino acids and alter the tertiary structure of proteins, subsequently eliciting an allergic reaction [92, 93]. A genetic predisposition for chronic allergic berylliosis has been proven [94], and recently tetramers of beryllium-loaded HLADP2-mimotope and HLADP2-plexin A4 have been detected in patients. This tetramers bind specifically to $CD4^+$T cells and might elicit the allergic reaction [95]. By electron microscopy and EDAX analysis, beryllium oxide can be proven in the granulomas. It should be reminded that in routinely processed specimen, the beryllium oxide is often leached out from the tissue by the solvents used for fixation, dehydration, and embedding. The same is true for an analysis, using laser-assisted mass spectrophotometry (LAMA) in paraffin-embedded tissues.

Another rare occupational allergic granulomatous reaction against metal compounds was reported for zirconium. Zirconium dust can induce non-necrotizing epithelioid cell granulomas, similar to beryllium oxide, probably based on a similar mechanism.

Extrinsic Allergic Alveolitis/ Hypersensitivity Pneumonia (EAA, HP)

This is a granulomatous lung disease, induced by an allergic reaction against different fungi, plant pollen and proteins, and also animal proteins. In open lung biopsies, epithelioid cell granulomas are frequently seen in EAA/HP, whereas they are quite rare in transbronchial biopsies. This might be a technical and distribution phenomenon: whereas granulomas in sarcoidosis are easily found in the bronchial mucosa, in EAA/HP the granulomas are more frequent in the periphery of the lung, usually distributed along small blood vessels (venules, capillaries; Fig. 8.72). Granulomas are, however, not the diagnostic requirement of EAA/HP: a dense lymphocytic interstitial infiltration centered upon small blood vessels alone raises the differential diagnosis of EAA/HP (Fig. 8.72a). As in sarcoidosis all special stains for infectious organisms are negative. In contrast to sarcoidosis, the granulomas in EAA/HP are more loosely organized; they have usually a broader rim of lymphocytes, and the lymphocytic infiltration spills over into the adjacent alveolar septa. In active disease there may be a lymphocytic interstitial infiltration with or without lymph follicle hyperplasia. Very helpful is the BAL: in EAA/HP there is a lymphocytic alveolitis with a predominance of

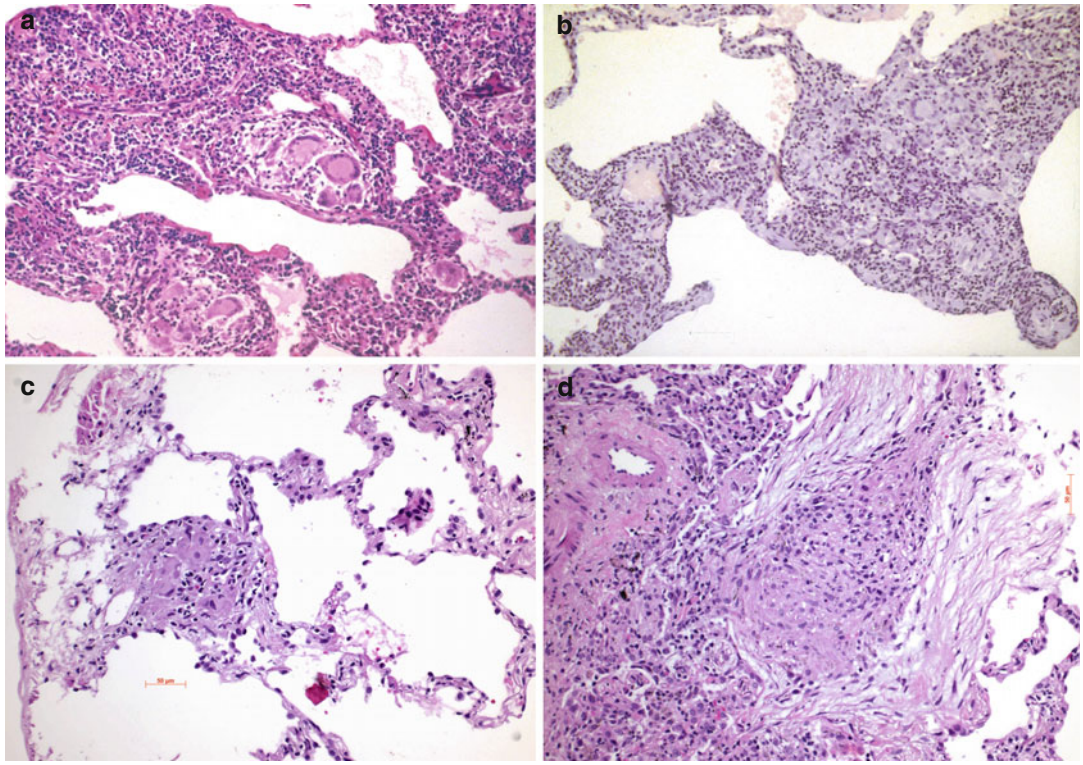

Fig. 8.72 Hypersensitivity pneumonia/extrinsic allergic alveolitis (HP, EAA). Different granulomas are shown, in (**a**) dense lymphocytic infiltration qualifying for LIP, in (**b**) less dense lymphocytic infiltration, in (**c**) an early epithelioid granuloma, and in (**d**) a granuloma surrounded by organizing pneumonia. In all cases the granulomas are loosely formed, not as compact as in sarcoidosis. H&E, ×160, ×160, ×200, ×200, respectively

cytotoxic T lymphocytes ($CD8^+$, $CD11a^+$). The CD4/CD8 ratio should be <0.8. However, it should be mentioned that a few exceptions to this rule have been reported. There is also a time effect: under antigen restriction the helper-suppressor ratio normalizes within a week and in some cases may even become >1.0 within a few days (unpublished personal observations).

In chronic EAA/HP a variety of other forms of pneumonia have been reported: NSIP, UIP, and OP can be seen; however, in my experience a lymphocytic infiltration is usually present even in these late stages (Fig. 8.73). In contrast to acute HP/EAA, $CD4^+$ lymphocytes can dominate the infiltration, which might cause concerns about the differentiation from sarcoidosis. But the combination of epithelioid cell granulomas with fibrosing types of pneumonia such as UIP, NSIP, or OP rules out sarcoidosis. In sarcoidosis fibrosis starts from the granulomas in a concentric fashion and in my experience is never combined with fibrosing pneumonia.

Sarcoid-Like Reaction

Not infrequently an epithelioid cell granulomatous inflammation in the lung and hilar lymph nodes in the setting of a bronchial carcinoma or lymphoma is found. The granulomas are indistinguishable from those in sarcoidosis. The distribution of lymphocyte subsets is similar to sarcoidosis. Lymphocytes in the granulomas are predominantly $CD4^+$ helper cells, whereas $CD8^+$ and B lymphocytes are found in the surrounding areas (unpublished personal observations). Within the lungs sarcoid granulomas are found along the draining lymphatics, a pattern also seen in sarcoidosis. A careful examination of all available data is necessary to separate this reaction from sarcoidosis: (a) clinical data are in favor of

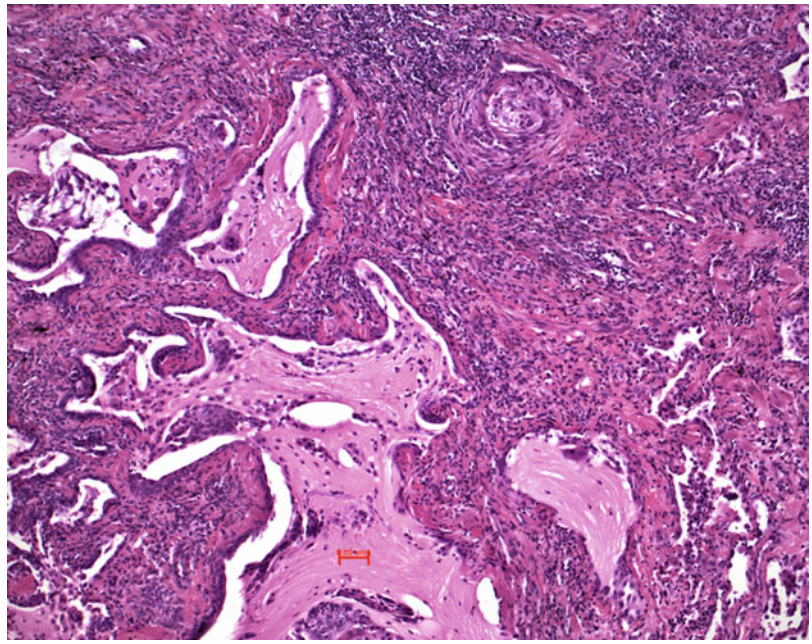

Fig. 8.73 Chronic EAA/HP, there is still intense lymphocytic infiltration; an epithelioid cell granuloma is seen in the upper part, fibrosis and cystic remodeling of lung has taken place. In another area fibroblastic foci were seen, giving the impression of UIP. H&E, bar 50 μm

a lung tumor, (b) no radiological features favoring sarcoidosis. If we are dealing with lymph nodes, we usually end up with a differential diagnosis of epithelioid cell granulomatous lymphadenitis, sarcoidosis vs. sarcoid reaction. The cause of these sarcoid granulomas has never been elucidated. The most reliable assumption is that cytokines released from lymphocytes and macrophages together with mediators liberated by tumor cell death induce this type of reaction.

Wegener's Granulomatosis/ Granulomatosis with Polyangiitis (GPA)

We will briefly mention GPA and parasitic granulomas. GPA besides other features is characterized by a granulocytic vasculitis and by necrosis (ischemic infarct). Epithelioid cell granulomas can be found in approximately 30 % of cases; however, since the changes in the vasculitis classification, those cases without granulomas might fall into microscopic polyangiitis.

Also parasitic infections can present with epithelioid cell granulomas. However, in parasitic infections eosinophils are the hallmark, not seen in this quantity in the diseases discussed above (this will be discussed in chapter on eosinophilic diseases).

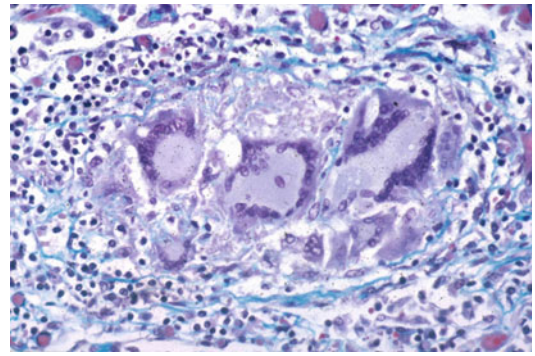

Fig. 8.74 Rheumatoid arthritis, with a rare epithelioid cell granuloma. Trichrome, ×400

Rheumatoid Arthritis

In cases of a negative AFS, GMS, and PAS stain, one should think of rheumatoid arthritis involving the lung and pleura. Although in the majority of cases lung involvement is usually associated with one of the variants of interstitial pneumonia, rarely a granulomatous reaction can be found. This might take the appearance of a classic rheumatoid granuloma with palisading histiocytes or an epithelioid cell granuloma without central necrosis, associated with seropositivity (Figs. 8.74 and 8.75). Both types of granulomas

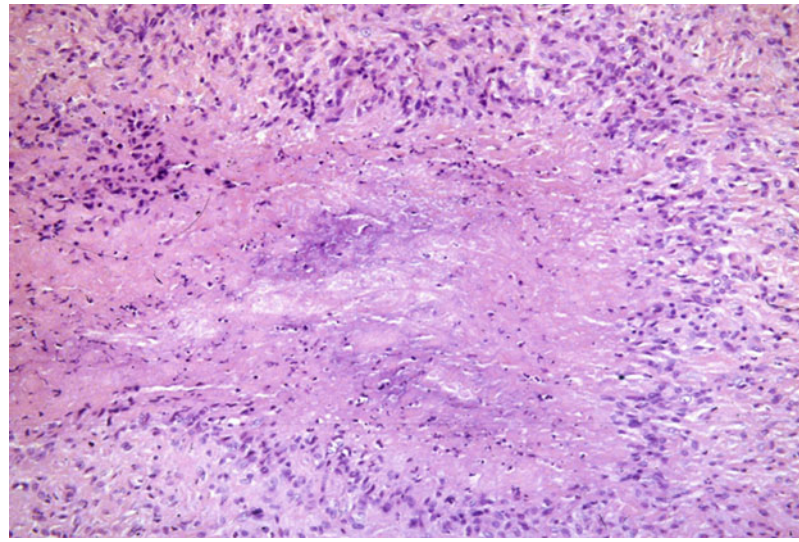

Fig. 8.75 Rheumatoid arthritis, with a classical histiocytic granuloma and palisading of the cells. Within the necrosis remnants of collagen fibers can be seen by polarization. This will help identifying the underlying disease. H&E, ×200

can be found side by side. For confirmation immunohistochemical stains for immunoglobulins and complement components can be used. Central necrosis very often contains remnants of destroyed collagen fibers (visible under polarized light), unusual in other variants of granulomatoses. It should be mentioned that rare cases of coincident rheumatoid arthritis and tuberculosis do exist; therefore mycobacteria should be excluded in these epithelioid cell granulomas. A more detailed discussion of common patterns in rheumatoid arthritis with lung involvement will follow in another chapter.

Bronchocentric Granulomatosis (BCG)

The hallmark is a necrotizing bronchiolitis with peribronchiolar extension of the inflammatory infiltrates. In the lumina necrotic debris can be seen, and remnants of fungi should be demonstrated. Within the bronchiolar walls, epithelioid cell granulomas and/or palisading histiocytic granulomas are found. In addition there is usually a dense infiltrate of eosinophils. In this classic variant, BCG is induced by an allergic reaction against different types of fungi, most often members of the *Aspergillus* family (Fig. 8.76). However, AFS and GMS stains should always be performed to exclude mycobacteria, especially when the inflammatory infiltrates contain many neutrophils (Fig. 8.76d). Another organism *Actinomyces* can present with bronchocentric granulomatosis, again with neutrophils in the necrotic center. In all these cases, BCG is an infectious disease, not allergic. If AFS is negative, fungal remnants are proven by GMS or PAS stains, and eosinophils are admixed to the granulomas, a diagnosis of bronchocentric granulomatosis as a variant of allergic bronchopulmonary mycosis/aspergillosis (ABPM/A) can be made. In my experience, it is often necessary to perform serial sections to demonstrate the fungus. The clinical information about positive allergy tests might be helpful. Combinations of type 1 and 4 immune reactions can be seen in this form of ABPM. In rare cases bronchocentric, necrotizing granulomatosis might also be seen in the setting of Wegener's disease. Therefore ANCA tests can be helpful in this differential diagnosis.

Lung Involvement in Chronic Inflammatory Bowel Disease

Both colitis ulcerosa and Crohn's disease can involve the lung (Fig. 8.77). In Crohn's disease a variety of patterns can be found; in most cases these are nonspecific. Without the knowledge of Crohn's disease, it might be impossible to make the correct association. Fortunately in about 84 % of cases, the bowel precedes lung involvement (Table 8.6).

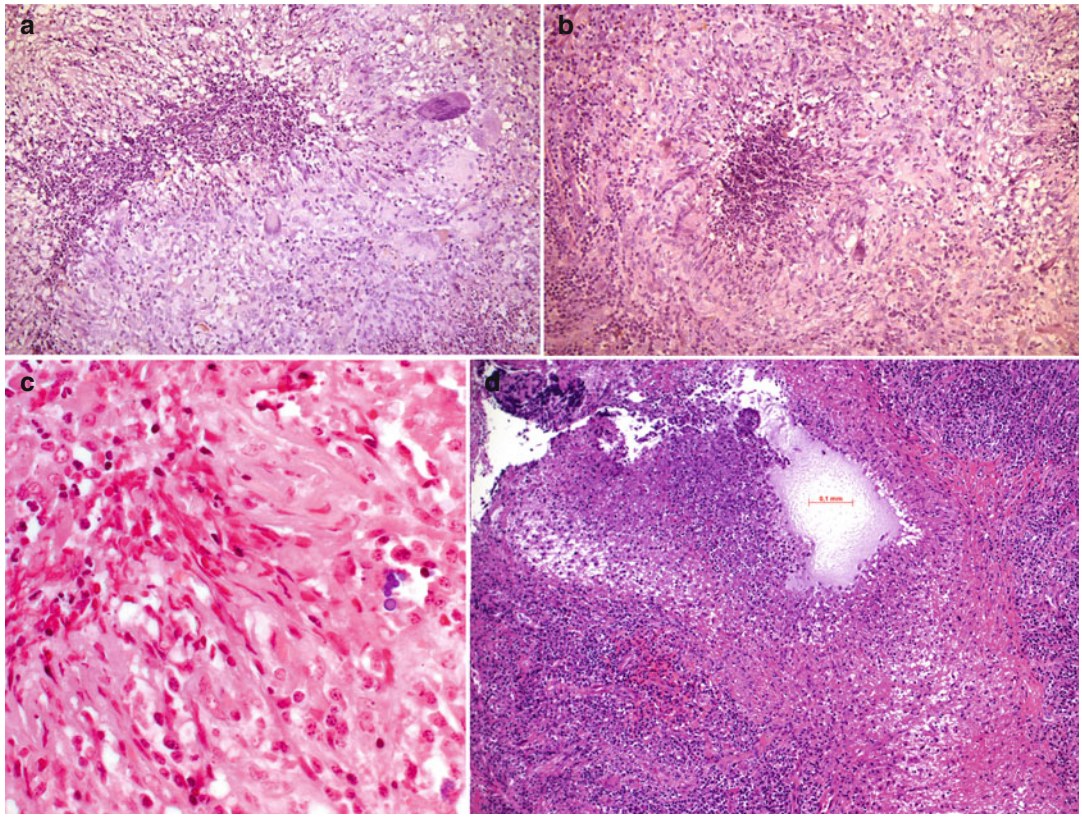

Fig. 8.76 Bronchocentric granulomatosis. (**a**–**c**) Allergic variant, characterized by necrosis along the airways with epithelioid cell granulomas along the bronchial mucosa and numerous eosinophils in the lumen. The granulomatous reaction almost replaces the wall. In (**c**) proof of fugal material within the granulomatous reaction. (**d**) The other form of BCG with epithelioid cell granulomas but with neutrophils in the lumen of the bronchus. Here a mycobacterial infection was proven. (**a**+**b**+**d**) H&E, ×160, ×160, ×100, respectively, (**c**) gram stain, ×400

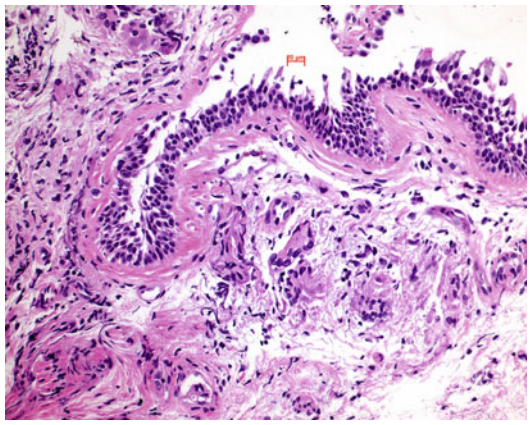

Fig. 8.77 Loose epithelioid granulomatous bronchitis in a case of Crohn's disease. In this case the lung reaction preceded the development of the classic bowel disease. In this case infection was ruled out, sarcoidosis was unlikely, because of these loose granulomas, HP/EAA was ruled out clinically. Finally a diagnosis of epithelioid reaction with unclear underlying pathology was stated. H&E, bar 20 µm

Table 8.6 Patterns in Crohn's disease with lung involvement according to Casey MB et al. [96]

Interstitial disease	35 %
Parenchymal nodules	5 %
Bronchiolitis with granulomas	46 %
OP ± granulomas or GC	25 %
NSIP ± giant cells	17 %
Acute bronchiolitis with suppuration	8 %
Eosinophilic pneumonia	4 %

In Colitis ulcerosa the pattern is more restricted. Acute bronchiolitis with ulceration, NSIP, and organizing pneumonia are most often found. The differential diagnosis is complicated by the fact that sulfasalazine can cause a drug-induced pneumonia, such as NSIP, DIP, eosinophilic pneumonia, and DAD [97–99].

Foreign Body Granuloma

Foreign body granulomatosis is a response of the innate immune system toward inhaled substances, which cannot be removed by macrophages or granulocytes. Most often this occur in aspiration of material from the digestive tract. Usually these are patients hospitalized because of CNS diseases or patients after an accident. The inhaled material can be identified in early granulomas, because the substances are not fully disintegrated by the giant cells. In later stages fibrosis can occur and the identification of the foreign material might be impossible (Fig. 8.78).

Although *lipid pneumonia* is not a granulomatous pneumonia, we will briefly discuss this here, because the cause is inhalation of lipid material, and a giant cell reaction can occur. This is a diffuse pneumonia sometimes involving several lobes. The reason in many instances is an inhalation of nasal droplets rich in paraffin oil or other substances as vitamin A dissolved in oil. A chronic use might result in inhalation and accumulation of significant amounts of these slowly degradable lipids, which ultimately results in lipid pneumonia. Another cause of lipid pneumonia is seen sometimes in the vicinity of squamous cell carcinomas. Most likely this lipids are derived from dying keratinized tumor cells. Lipid pneumonia is characterized by an accumulation of macrophages, which have ingested lipids and appear as foam or clear cells. These macrophages also can be seen in the interstitium; some foreign body giant cells are encountered within the alveoli (Fig. 8.79).

Hyaline granulomatosis is characterized by single or multiple nodules with a hyaline center surrounded by infiltrates composed of lymphocytes and plasma cells (Fig. 8.80). Many different diseases might result in such morphology. Infections can show such pictures, especially mycobacterial infections; however, there will be remnants of epithelioid cell granulomas, and the lymphocytic reaction is not as dense. Non-Hodgkin lymphomas especially plasmacytic variants should be excluded in cases with multiple nodules; finally IgG4-associated fibrosis and inflammatory myofibroblastic tumor need to be excluded. The latter ones will present with proliferating myofibroblasts or infiltrates of histiocytes; however, in old lesions the center can be hyalinized.

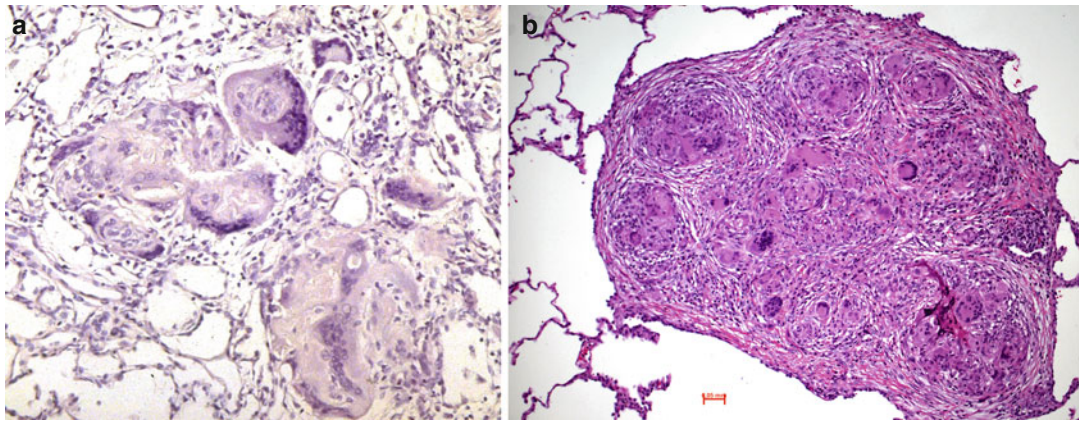

Fig. 8.78 Foreign body granulomas, in one case (*left side*) there was an aspiration of digested food, identified by polarization of remnants of vegetable, whereas in the other case (*right*) the cause could not be identified by the morphological analysis. H&E, ×400, bar 50 μm

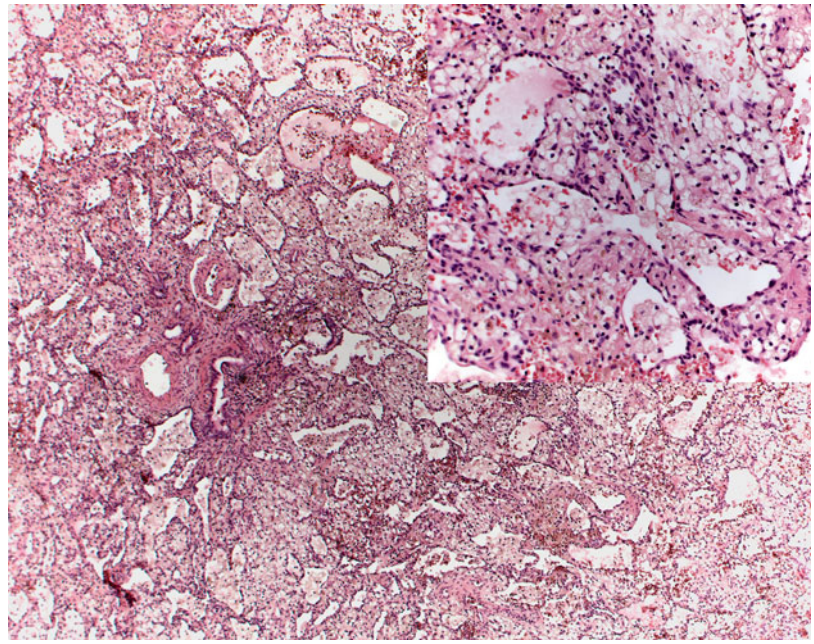

Fig. 8.79 Lipid pneumonia due to chronic inhalation of paraffin oil from nasal droplets. In the lung numerous macrophages have accumulated in the alveoli but also the interstitium. In the inset some brownish material is also seen in the cytoplasm of the macrophages, representing insoluble lipids not dissolved by the tissue processing. H&E, ×50 and 150

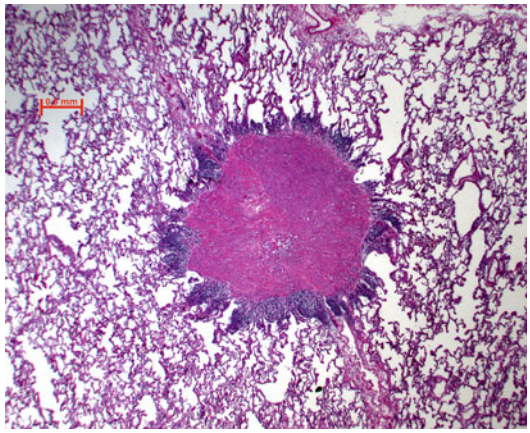

Fig. 8.80 Hyaline granulomatosis in an 11-year-old boy. Clinically there was a diagnosis of adrenogenitale syndrome established. If hyaline granulomatosis is associated with this disease cannot be answered. H&E, bar 500 µm

8.2.5 Methods to Be Used for a Definite Diagnosis of Infectious Organisms

All available materials (biopsies, BAL, sputum, secretions, etc.) from patients can be used for detection of infectious organisms. In most cases satisfactory results will be obtained. In our hands a combination of biopsy and BAL is superior. The organisms can be detected, either in BAL or biopsy, and the host's reaction can be evaluated. BAL and biopsy can predict even prognostic outcome. An identification of *M. tuberculosis* in an immunocompromised patient and non-necrotizing epithelioid cell granulomas as the reaction of the host can be interpreted as a good prognostic sign, because the host can mount an immune reaction against these mycobacteria. In sarcoidosis CD4/CD8 ratios >3.5 are usually good prognostic indicators. Fibrosis in the biopsy and mediators of fibroblast stimulation like PDGF in BAL fluid might predict end-stage lung disease (Popper, unpublished observations).

Special stains are necessary: First an acid-fast stain (AFS, either auramine-rhodamine fluorescence or Ziehl-Neelsen), a silver impregnation (GMS, methenamine silver impregnation according to Grocott), a Giemsa stain, and a periodic acid-Schiff stain (PAS) should be done simultaneously. We prefer the auramine-rhodamine stain, because in paucibacillary tuberculosis the mycobacteria are easier detected: they are orange fluorescent in a black background (Fig. 8.81). Based on these reactions, a differential diagnosis of tuberculosis or mycobacteriosis

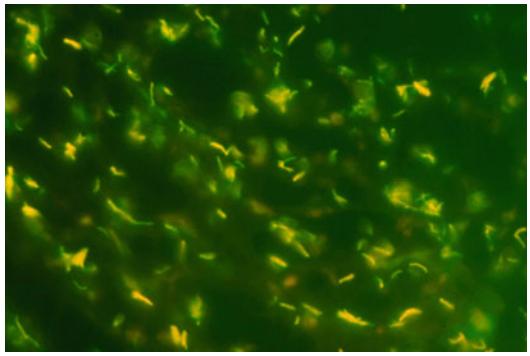

Fig. 8.81 *M. tuberculosis* stained by auramine-rhodamine. The slightly curved thin organisms are quite characteristic; only *M. fortuitum* can look similar. AR, ×630

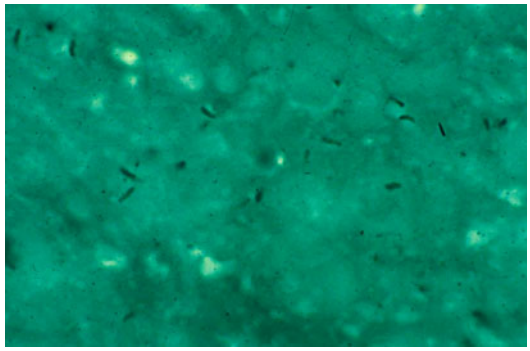

Fig. 8.82 *M. tuberculosis* stained by Grocott methenamine silver impregnation. GMS, ×630

can be made. It should be noted that mycobacteria can also be silver impregnated by the GMS stain (Fig. 8.82). The nontuberculous mycobacteria are sometimes described as having a shorter and thicker appearance in AFS; however, this should always be proven by PCR and culture. In every case of purulent pneumonia, a Gram stain should be added to the panel of special stains. Although an identification of a species is not possible, the information about gram-positive or gram-negative cocci or bacilli will already help the clinician to select possible antibiotics for treatment, until the organism has been identified by either culture or PCR. In all cases where a BAL is submitted together with the biopsy, this material is even better to find and identify the organisms, either bacteria, fungi, or parasites (Fig. 8.83).

Fungi can easily be identified by GMS and PAS stains. A tentative diagnosis can be made in many cases. However, in rare infections culture might be required to subtype the fungus. For many fungi also antibodies are available and can be used for immunohistochemical identification. In addition fungi can also be typed by PCR for specific gene sequences. Rare bacteria like *Treponema* can be stained by silver impregnation (Warthin-Starry stain) or immunohistochemically using specific antibodies. Unicellular parasites such as malaria, *Toxoplasma*, and *Trypanosoma* are usually difficult to identify in tissue section, but they are more easily identified in fluids either BAL or blood (Figs. 8.83 and 8.84).

A PCR-based characterization of slow-growing mycobacteria is recommended. For example, a culture of *M. avium* can be very time consuming (up to 11 weeks), whereas a PCR result can be reported within 2 days. We prefer a PCR for the mycobacterial chaperonin (65 kDa antigen coding gene), and for specific insertion sequences, unique for different mycobacteria. Other sequences, which characterize mycobacteria in general, are the DNA coding for the 16S rRNA and the 32 kDa protein. The insertion sequence IS 6110 can be used to demonstrate DNA of *M. tuberculosis*, *M. bovis*, *M. africanum*, and all members of the *M. tuberculosis* complex (Fig. 8.85). For the demonstration of MOTT, different strategies are available: either a multiplex PCR using unique sequences for different mycobacteria in one PCR run (Fig. 8.86) or the more time-consuming amplification of the 16S rRNA coding gene and sequencing of the amplicon can be done. The base exchanges characteristic for different mycobacteria can then be used for species typing. Alternatively amplicons can also be digested by restriction enzymes and the species identified by the length of the fragments [78, 100, 101].

The proof of chronic berylliosis and zirconiosis requires element analysis in tissue granulomas. This can be done under certain circumstances. The biopsy should be sent frozen to the pathology laboratory. The biopsy can be freeze dried, fixed in formalin vapor, and embedded in Epon. Ultrathin sections can be analyzed in the electron

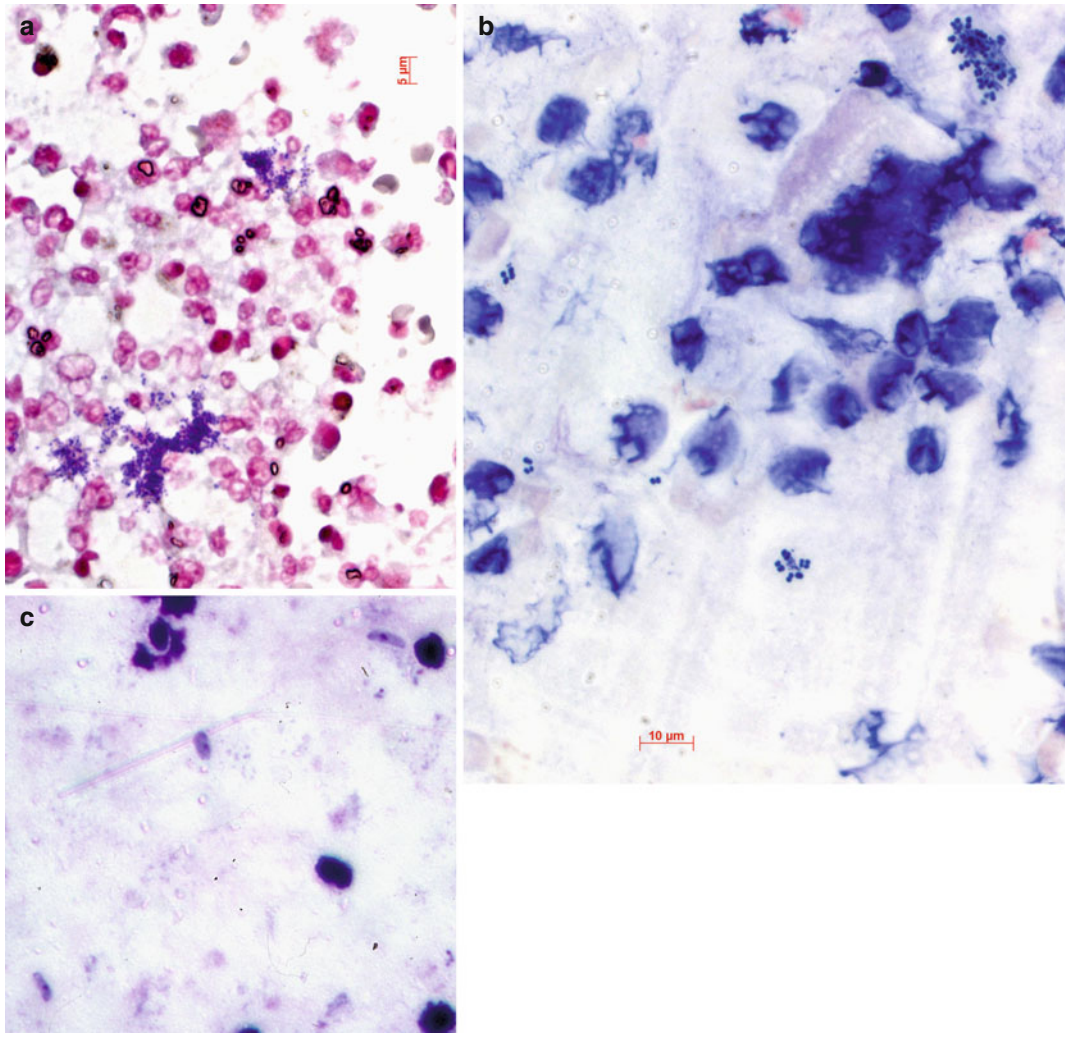

Fig. 8.83 Identification of organisms. (**a**) Gram stain identifying positive coccoid bacteria in a tissue section, (**b**) Giemsa stain in BAL identifying diplococcus species in lavage fluid, (**c**) May-Grunwald-Giemsa stain identifying *Toxoplasma gondii* in lavage fluid. Bar 5 µm and 10 µm, (**c**) ×1000

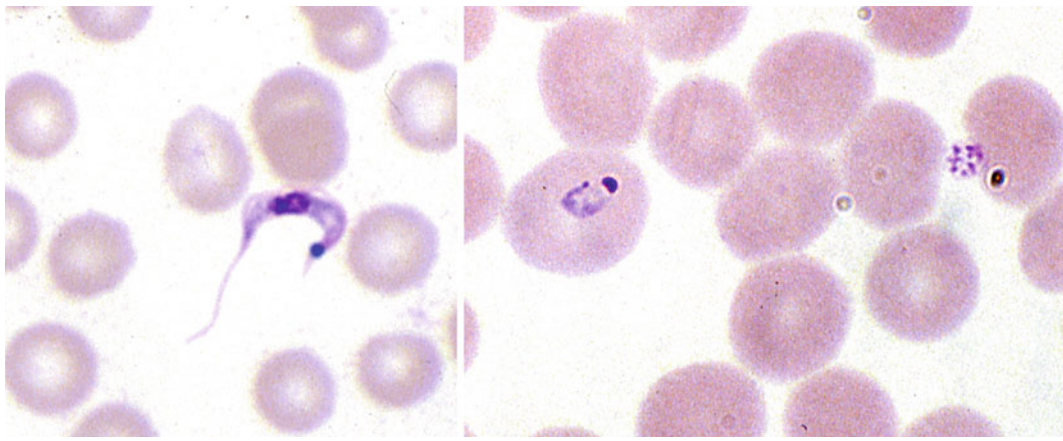

Fig. 8.84 Blood smear identifying *Trypanosoma cruzi* in a patient with Chagas disease (*left*) and *Plasmodium tertiana* in a patient with malaria (*right*). H&E, ×1200

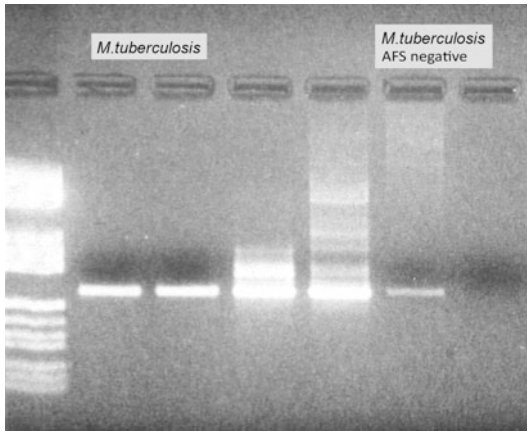

Fig. 8.85 Identification of *M. tuberculosis* using specific insertion sequence 6110 for members of the *M. tuberculosis* complex. PCR formalin-fixed, paraffin-embedded tissue sections

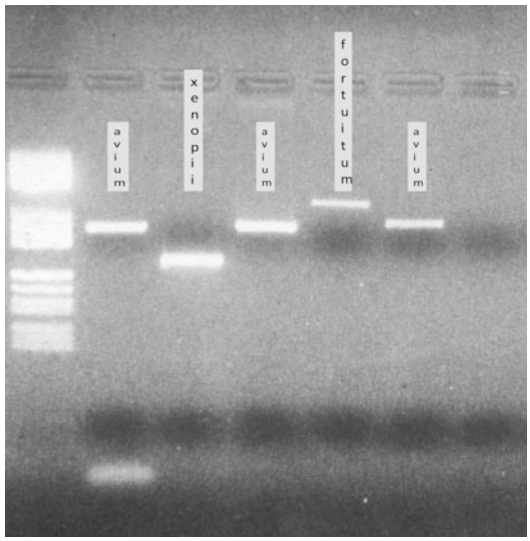

Fig. 8.86 Identification of different mycobacteria using specific insertion sequences for each of these (*M. avium*, *M. xenopi*, *M. fortuitum*). Multiplex PCR, formalin-fixed, paraffin-embedded tissue sections

microscope using EDAX, and the elements of interest can be identified. By this procedure leaching of BeO or ZrO can be reduced.

Culture of infectious organisms is still the ultimate proof and should always be done. But new methods are emerging, which might not only shorten the time until a specific organism is identified but also subtyping by strains will be possible. Next-generation sequencing or shotgun whole genome sequencing (WGS) can be used to simultaneously evaluate the microbiome in tissue sections and BAL [102, 103].

8.3 Fibrosing Pneumonias (Interstitial Pneumonias)

8.3.1 Historical Remarks on Interstitial Pneumonia Classification

Originally Liebow [104] proposed a classification based on morphological descriptions, with the following entities: UIP (usual interstitial pneumonia), BIP (bronchiolitis obliterans-interstitial pneumonia), diffuse alveolar damage (DAD, also acute interstitial pneumonia, clinically corresponding to acute respiratory distress syndrome (ARDS)), LIP (lymphocytic interstitial pneumonia), DIP (desquamative interstitial pneumonia), and GIP (giant cell interstitial pneumonia). He did not divide them into idiopathic or those with known etiology but recognized that there can be different etiology present behind each of these entities. Katzenstein's updates from 1993 to 1998 [105, 106] was the next major step, adding NSIP (nonspecific interstitial pneumonia) to the list of UIP, DIP, BIP, and AIP/DAD, and following the debate at that time structured the classification into idiopathic and non-idiopathic (=known etiology). Therefore she removed LIP and GIP, because an etiology could be assigned to them. The original BIP was renamed into bronchiolitis obliterans-organizing pneumonia (BOOP) [107], a term which was long before known as "pneumonia with carnification" (karnifizierende Pneumonie) in the German literature. Later on Mueller and Colby showed a radiologic-pathologic correlation and used the previously created name BOOP (bronchiolitis obliterans-organizing pneumonia) [108, 109] instead of BIP.

When these entities were combined with clinical data, it was apparent that there was a major difference between idiopathic UIP and the "rest": patients with UIP had a worse prognosis and most of them died within 5 years after diagnosis [110]. And there was no treatment for those patients: a hope of an effective treatment by interferon γ could not be proven [111]. At this time clinicians recognized that idiopathic pulmonary

fibrosis (IPF or cryptogenic fibrosing alveolitis (CFA)) was not a rare disease. Therefore it seemed logical to separate idiopathic interstitial pneumonias from those with known cause and thus to provide prognostic and therapeutic information for the clinicians: no response of patients with UIP/IPF toward corticosteroids and immunosuppressive drugs and dismal prognosis, whereas responsiveness of patients with NSIP to corticosteroids and immunosuppressive drugs and a better prognosis.

The next step happened when UIP and the fibrosing variant of NSIP were compared to each other showing that the initial difference vanished especially when evaluated for a 10-year survival [110]. But it became clear more and more that the underlying etiology largely predicts the outcome: autoimmune diseases would respond to immunosuppressive regimen, whereas idiopathic IPs would not. Following this aspect DIP and RBILD were next excluded from idiopathic interstitial pneumonias, because in both entities cigarette smoking was identified as the main cause of the disorder. LIP was also skipped, probably because of a clearly defined etiology in almost all cases, either lymphoma, allergic, or autoimmune diseases. GIP was skipped, since it either is induced by hard metal inhalation or viral infection (measles, respiratory syncytial virus, and others) [112, 113].

What makes the present-day classification complicated is the combination of radiology, pathology, and pulmonology resulting in provisional diagnoses or divergent names for pathology and clinics. And different views came into the classification: clinicians introduced symptoms, lung function data, and age of the patient, and radiologists introduced their terminology in what correlates to UIP. Finally the ATS/ERS/JRS/ALAT societies recommended that these three disciplines should together make the final diagnosis of IIPs [114].

There are examples which support such a perspective: organizing pneumonia has a wide variety of etiologic causes, and the idiopathic form COP needs exclusion of all other causes, which on several occasions can be done by pathologists, but in other cases only by combining morphology with clinical information. Furthermore radiology has gained a major impact on the diagnosis of IIPs, which resulted in decreasing numbers of patients for whom a pathologic diagnosis is required.

Table 8.7 Clinical-radiological-pathological (CRP) diagnoses and their morphologic counterparts

Clinico-radiologic-pathologic (CRP) diagnosis of idiopathic interstitial pneumonias	Morphologic pattern
Idiopathic pulmonary fibrosis (IPF)	Usual interstitial pneumonia (UIP)
Idiopathic nonspecific interstitial pneumonia (NSIP)	Nonspecific interstitial pneumonia (NSIP)
Cryptogenic organizing pneumonia (COP)	Organizing pneumonia (OP)
Acute interstitial pneumonia	Diffuse alveolar damage (DAD)*

*We will not discuss DAD within the fibrosing pneumonias, as this is an acute pneumonia, and in those cases with DAD undergoing organization, this is organizing pneumonia

Based on recommendations from a joint committee established by the ERS, ATS, JRS, and ALAT, pathologists, radiologists, and pulmonologists proposed a new classification and also a diagnostic algorithm for ILD and IPF [114, 115] (Tables 8.7 and 8.8).

8.3.2 Usual Interstitial Pneumonia (UIP)/Idiopathic Pulmonary Fibrosis (IPF)

UIP/IPF is a chronic progressive fibrosing disease of the lung, which leads to death of the patient usually within 3–5 years after the diagnosis is made [116]. It affects predominantly patients in their four to fifth decade of life; however, lesions may occur much earlier and remain undetected until they will cause impaired lung function by their increasing number. Due to increased awareness and increased resolution of CT scans, UIP/IPF might be seen more often in younger-aged patients. Characteristically lesions are found in both lower lobes with a predominance of subpleural regions. The involvement of both lobes is most often symmetrical.

8.3.2.1 Epidemiology and Incidence

UIP/IPF is the most common interstitial pneumonia, accounting for approximately 55 % [114,

Table 8.8 Diagnostic algorithm for idiopathic interstitial lung diseases excluding some of the diseases with known etiology

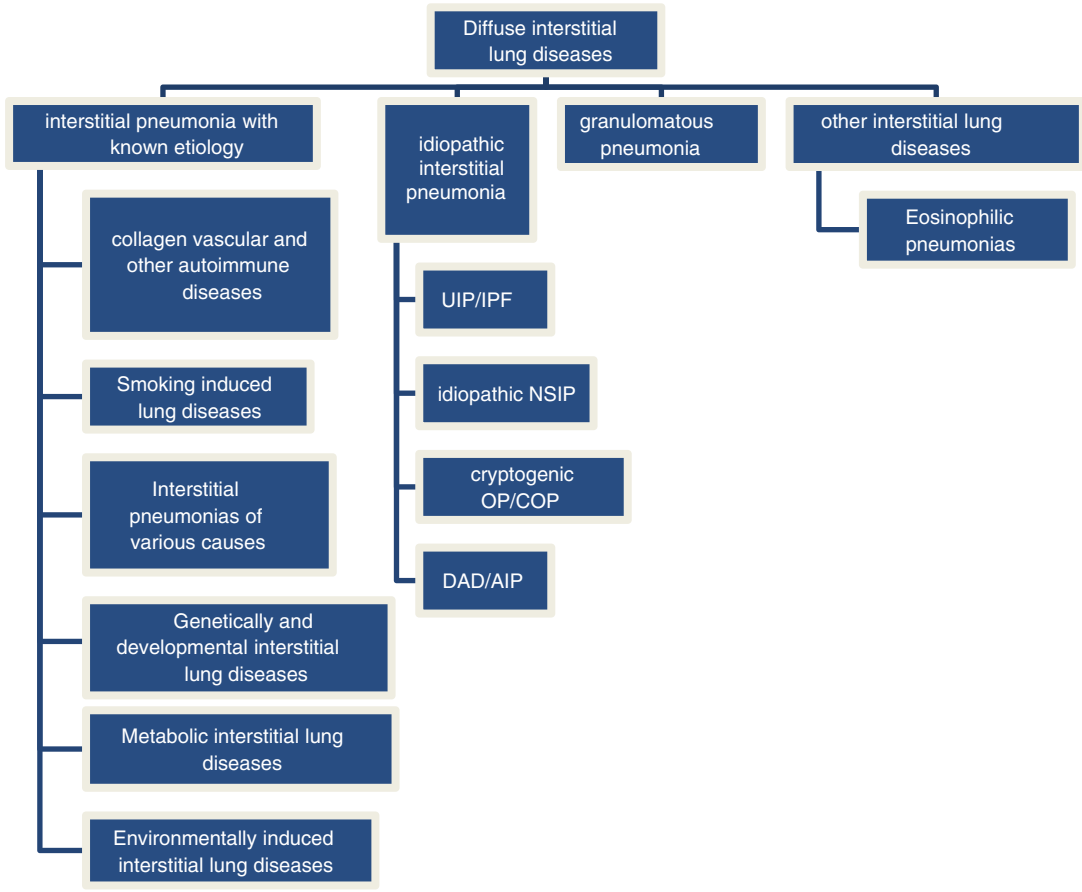

Modified from Travis et al. [115]
This schema includes also a stepwise algorithm for the diagnosis starting with the clinical examination, followed by the interpretation of the HRCT picture. If the clinical history and presentation, and the CT scan presents with classical features, a lung biopsy might not be required, as stated by the consensus conference. However, in my personal experience based on many consultation cases many so-called typical ones turned out to be other diseases as suspected

117]. The disease predominantly occurs in an older age group, usually >50 years [117]. Disease prevalence has been estimated for the EU to be around 1:120,000. However, this could change, because UIP/IPF most often is diagnosed at a late stage. If our diagnostic capabilities can be refined, it might be reasonable that the disease could be diagnosed in a younger-aged group, since we know from the pathogenesis that fibrosis starts much earlier.

8.3.2.2 Clinical Presentation and CT

The clinical symptoms are characterized by insidious onset of dyspnea on exertion, duration of disease ≥3 months, and bibasilar inspiratory dry crackles. These clinical symptoms are quite unspecific and therefore need a further confirmation by high-resolution computed tomography (HRCT). There should be subpleural predominantly basal abnormalities, reticular changes and scars, honeycombing with or without traction bronchiectasis (Fig. 8.87), and the absence of middle field predominance, micronodules, diffuse mosaic attenuation and air trapping, or consolidations in segments [118].

Macroscopically the pleura show multiple retractions giving the surface a cobblestone appearance, but pleuritis is not seen. On cut surface cystic lesions, consolidations and scars are found (Fig. 8.88).

Fig. 8.87 CT scan of a patient suffering from UIP/IPF. The characteristic patterns are symmetrical peripheral bibasilar accentuated abnormalities, honeycombing, reticular abnormalities, and traction bronchiectasis. Also tiny little scars are present

Fig. 8.88 VATS biopsy of a case with UIP/IPF. There are some consolidated areas associated with cystic lung remodeling (honeycomb lesions, *arrows*) and traction bronchiectasis (*double arrow*). Note the smooth surface of the pleura, which is unaffected

8.3.2.3 Pathogenesis and Etiology

The cause and the etiology of IPF/UIP are not well understood. There is a working hypothesis, which can explain some of the features. The disease starts with an as yet unidentified epithelial injury causing apoptosis of pneumocytes [119–122]. Inflammatory signals released by the dying pneumocytes cause transformation and proliferation of fibroblasts and myofibroblasts in a myxoid stroma and repair [123] (so-called fibroblastic focus). Genetic abnormalities may underlie these apoptotic response: in the recent years, research in familial forms of IPF has highlighted the importance of surfactant apoproteins in maintaining a homeostasis between injury and repair and that mutations in the surfactant apoprotein C gene might be causally related to the development of familial IPF [124]. In these familial IPF, mutations in genes encoding surfactant apoprotein C and A2 increase endoplasmic stress reactions in pneumocytes type II, and in addition mutations in the telomerase genes TERT and TERC are responsible for telomere shortening probably decreasing the pool of peripheral lung stem cells and thus impairing repair and regeneration [125]. This later defects are also found in sporadic IPF cases. Therefore inhalation of any kind of toxic material from the environment might cause an overwhelming oxidative stress reaction leading to increased apoptosis of pneumocytes and impaired regeneration [126]. This fits quite well into the epidemiology of IPF patients: the majority are smokers; some have a history of environmental dust exposure [127, 128]. There is also evidence of epithelial-mesenchymal transition (EMT) of pneumocytes into myofibroblasts, but also scattered bone marrow-derived mesenchymal stem cells seem to move into these foci [129–131] (Fig. 8.89). These foci undergo maturation with collagen deposition, and finally the process results in fibrosis of alveolar septa and bronchiolar walls [121]. This in turn causes obstruction of the terminal airways resulting in cystic destruction of the remaining peripheral lobules, giving rise to honeycombing and remodeling of the lung parenchyma [122, 132, 133]. Recently additional mutations have been identified in IPF: a mutation of MUC5B gene promoter was shown to be associated with risk for IPF and also fibrosing NSIP [134], and another gene mutation in dyskerin (DKC1) was associated with familial IPF [135]. Whereas the function of MUC5B is not explored, dyskerin cooperates with hTERT and thus may be another variant of this complex scenario. IPF develops stepwise, which means there are lung lobules not

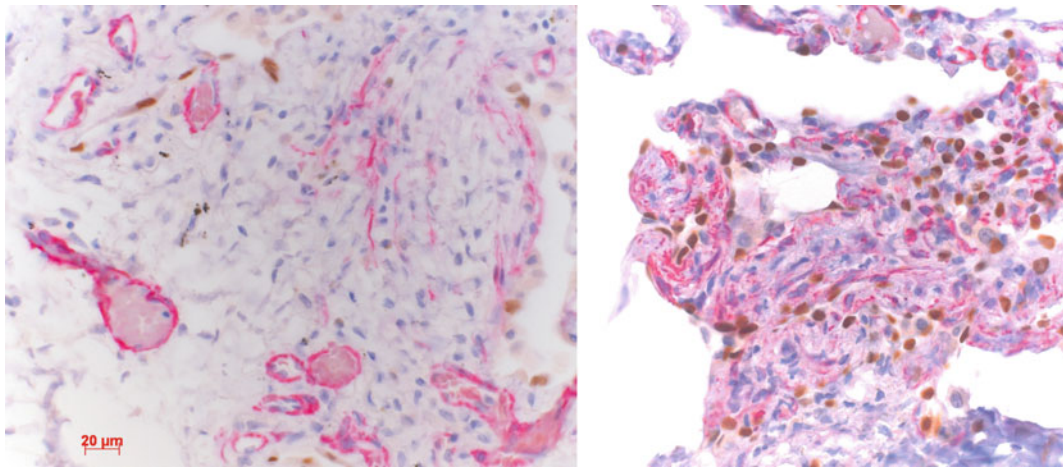

Fig. 8.89 Immunohistochemistry for smooth muscle actin (*red*) and TTF1 (*brown*). In the *left* figure, two spindle-shaped cells are shown, which still express TTF1 but are negative for SMA. In the *right* figure, there are cells within this myofibroblastic focus, which express SMA and TTF1 simultaneously. This demonstrates that myofibroblasts can undergo mesenchymal to epithelial transition, and vice versa; pneumocytes can undergo epithelial to mesenchymal transition. Immunohistochemistry for SMA and TTF1, bar 20 µm, and ×400

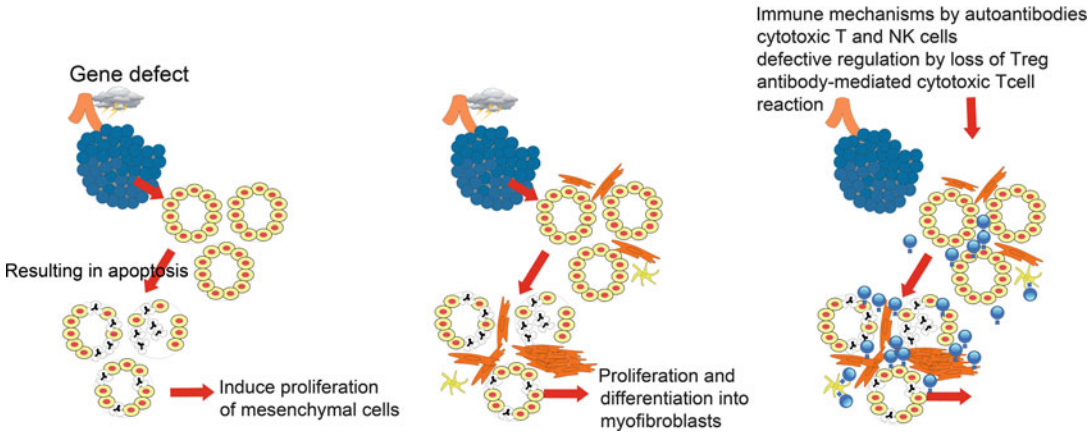

Fig. 8.90 Schematic diagram of the development of UIP/IPF. In familial and sporadic IPF, an underlying gene defect induces apoptosis of pneumocytes; this in turn elicits a release of cytokines and growth factors, which induce proliferation and differentiation of myofibroblasts. These causes fibrosis. There are still open questions, such as: how much EMT and MET contributes to the continuation of the myofibroblast proliferation and what is the role of bone marrow-derived stem cells? In chronic autoimmune and allergic diseases, the causing factors are autoimmune mechanisms and deregulation of the immune system, by which probably cytotoxic lymphocytes induce apoptosis and necrosis of pneumocytes, followed by the same downstream inflammatory mechanisms, leading to fibrosis

affected yet looking normal, whereas others are destroyed or even completely lost to fibrosis and scarring. This is meant by the term "timely heterogeneity" (Fig. 8.90).

8.3.2.4 Histology

The histological hallmarks are fibroblastic foci, scars and diffuse fibrosis, honeycomb areas, and uninvolved areas in between (heterogeneity). In the author's experience, a diagnosis of UIP/IPF can be established in some cases even without clinical information when the following features are given: fibroblastic foci, timely heterogeneity (involved and uninvolved peripheral lobules), cystic and fibrotic destruction resulting in honeycombing, and most important the absence of inflammatory infiltrates in areas of fibroblastic foci, absence of granulomas, or features of other interstitial inflammation.

Let us briefly characterize the main morphologic features, since this still causes confusion and misunderstanding:

The *fibroblastic focus* lies within the walls of alveolar and interlobular septa, as well as bronchioles. They do not project into the alveolar lumen. In early stages they are composed of myofibroblasts and fibroblasts in an immature myxoid matrix. This matrix will stain for immature collagen and reticulin fibers. The overlaying surface is either denuded (no pneumocytes) or can show pneumocyte regeneration with a lot of reactive changes of the nuclei, even epithelial giant cells can be present (Figs. 8.91, 8.92, and 8.93). When the focus get's older, mature collagen appears and the cells look more like fibrocytes. The overlaying epithelium looks reactive and usually has a type II or bronchiolar cell appearance.

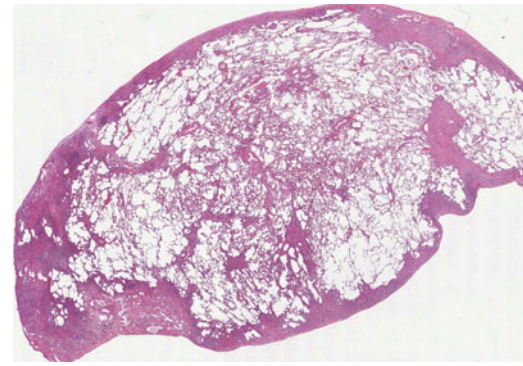

Fig. 8.91 VATS biopsy, overview of UIP/IPF. There is fibrosis, areas of cystic remodeling of the peripheral lung tissue associated with inflammation, normal lung. H&E, ×60

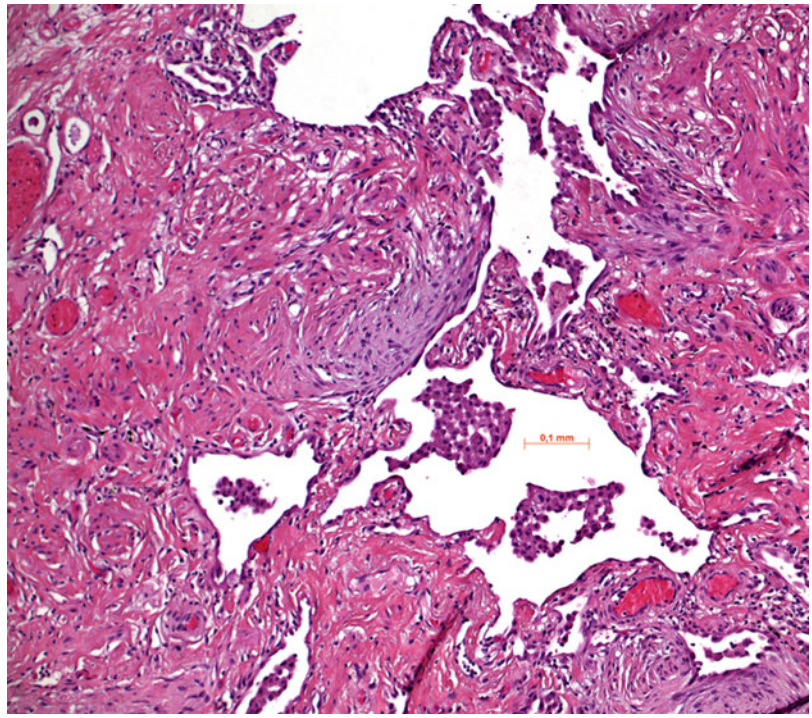

Fig. 8.92 Fibroblastic focus, i.e., a proliferation of myofibroblasts. There are no inflammatory infiltrates in these areas, and many pneumocytes type II show signs of apoptosis. Macrophages within the alveoli are usually signs of tobacco smoke exposure as many patients with IPF are smokers. H&E, bar 100 µm

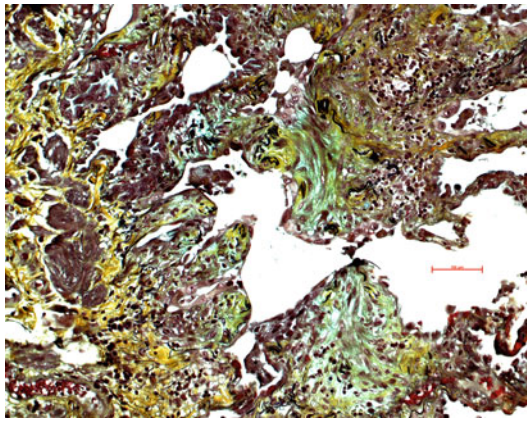

Fig. 8.93 The different ages of the fibroblast foci can be evaluated by Movat stain: immature collagen stains green, whereas mature collagen stains yellow. In this case two foci are shown and within both replacement of immature by mature collagen is taking place. Movat, bar 100 µm

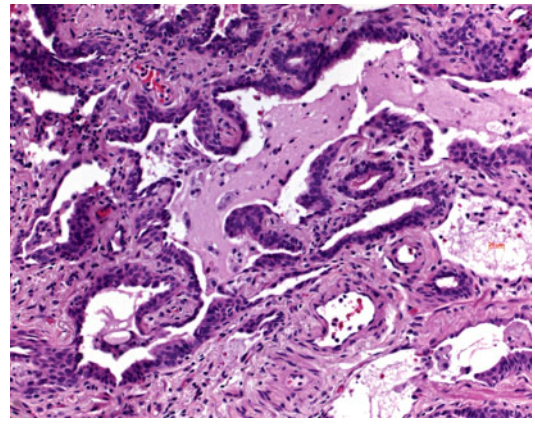

Fig. 8.94 Cystic remodeling of alveolar tissue. Terminal bronchioles are included, from the alveolar tissue only cystic spaces remained. The surface is covered by a reactive epithelium of bronchiolar type, some cell layers look pseudosquamous. H&E, bar 20 µm

The *honeycomb lesion* was originally defined by radiologists as a single or multicystic lesion within a fibrotic lung area [136]. Given the differences in resolution between HRCT and histology, there is a substantial difference in size between the two. Pathologically a so-called honeycomb lesion is a cystic lung lesion involving a secondary lobule. This lobule has lost most of the peripheral alveoli, shows a cystic central area composed of bronchioles and centroacinar structures, covered by a cuboidal and cylindrical epithelium, resembling bronchiolar epithelium and transformed pneumocytes type II (Fig. 8.94). In some cases a

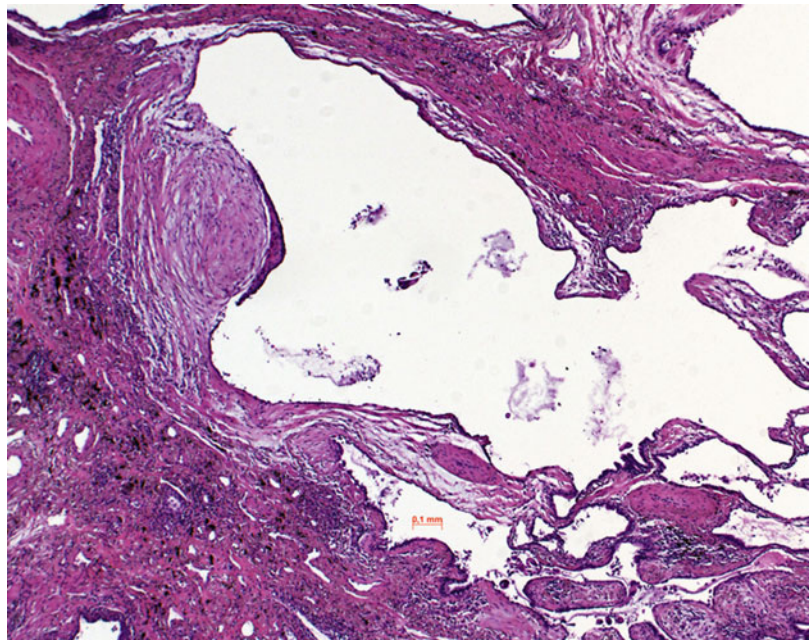

Fig. 8.95 Cystic remodeling of alveolar tissue, here in a case of UIP, but non-IPF due to the multifocal infiltrations of lymphocytes within the fibroblastic foci. H&E, bar 100 µm

pseudostratified squamous-looking epithelium can be present. The cyst walls are fibrotic and often merge with scarred lung tissue or large fibrotic areas involving sometimes a subsegment of the lung. Within the lumen mucus can accumulate, and in late stage this can be the starting point for secondary infection and bronchopneumonia causing death of the patient (Figs. 8.95 and 8.96). I prefer the term lobular cystic lung remodeling (LCR) instead of honeycombing, because of the size differences between HRCT and microscopy.

The areas of *fibrosis* and *scarring* and the uninvolved lung tissue (*heterogeneity*) do not need an explanation. But what about inflammation? From what we understand presently, IPF/UIP is not an immune-driven or classic inflammatory disease. Therefore we do not expect inflammatory cells within the myofibroblastic foci. If lymphocytes appear in numbers (>10/HPF) within a myofibroblast focus, this should raise the possibility of an underlying immune reaction (Figs. 8.97 and 8.98). The appearance of granulocytes within these foci should prompt the search of remnants of hyaline membranes, because this may represent organizing DAD.

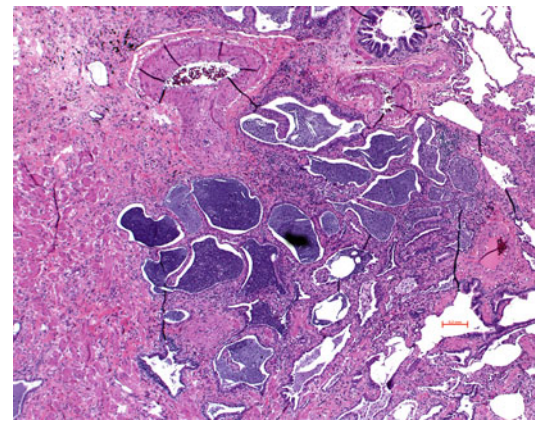

Fig. 8.96 Cystic remodeling of alveolar tissue, here the cysts are filled with cellular debris, macrophages, and scattered neutrophils. This reflects mucostasis, and out of these areas, infection and subsequent pneumonia can develop (exacerbation). H&E, bar 200 µm

8.3.2.5 Modes of Handling Diagnosis

The ATS/ERS recommends that a panel of experts composed of pulmonologists, radiologists, and pathologists (CRP) should make the diagnosis of IPF. The clinical presentation and course, the HRCT picture, and the pathologic pattern of UIP should be combined. Five categories of confidence of IPF diagnosis can be reached:

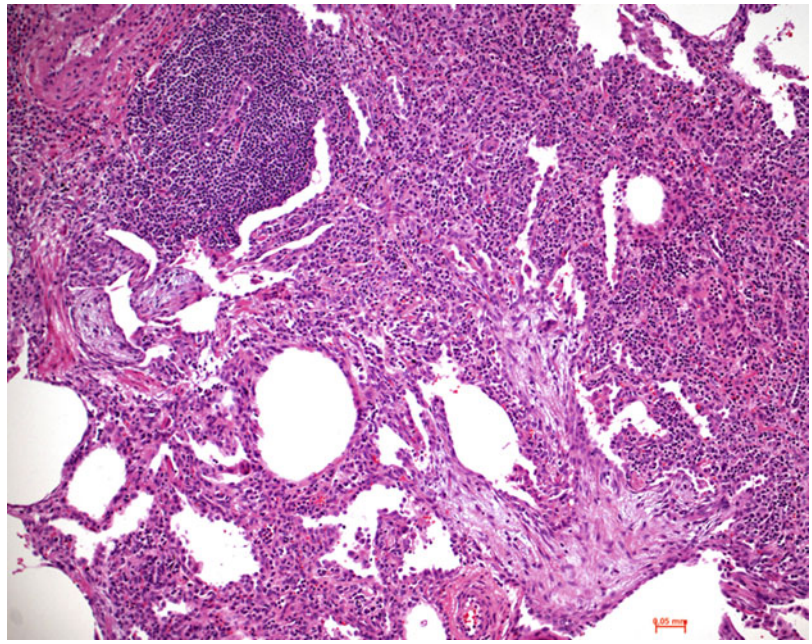

Fig. 8.97 Myofibroblastic focus in a patient with rheumatoid arthritis. In this case there is a dense lymphocytic infiltration extending into the foci and thus pointing to an underlying immune mechanism. H&E, bar 50 µm

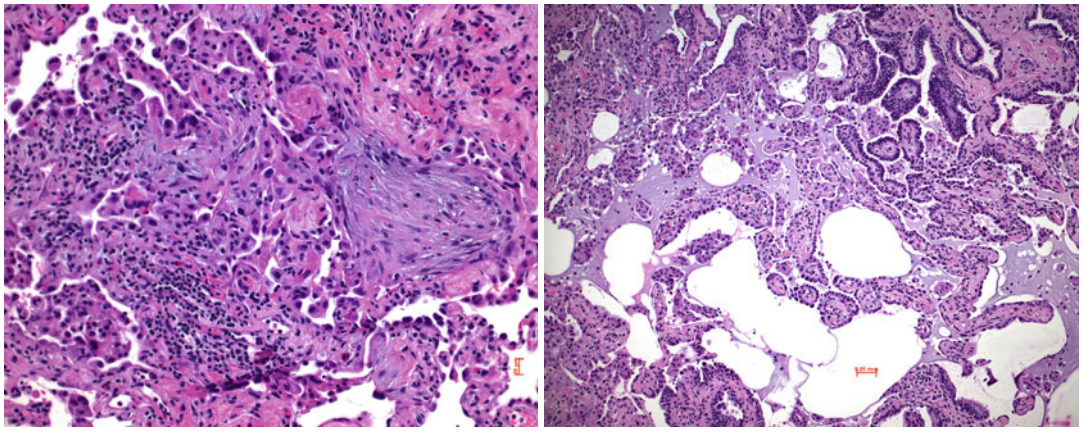

Fig. 8.98 UIP pattern in drug-induced disease (neuroleptic drug). In the *left panel*, there are myofibroblastic foci with mild lymphocytic infiltration; there are focal lymphocytic infiltrations and there is no apoptosis of pneumocytes; the *right panel* shows cystic remodeling of alveolar tissue. Both together points to a non-IPF etiology. H&E, bars 20 µm and 50 µm

- Definite IPF, when UIP with a classical HRCT and typical clinical presentation is present
- Probable IPF, when one of the classical features is not present (e.g., no definite UIP or no definite HRCT scan)
- Possible IPF, if several features from CT and histology are not conclusive
- Probable not IPF, when CT and pathology show features not compatible with IPF
- Definite not IPF, if there are features of other interstitial diseases [114]

In some cases the diagnosis of IPF can be based on clinical and CT findings alone. Whenever pathologic evaluation is involved, a diagnosis of UIP is mandatory for the diagnosis of IPF. However, it should be noted that even among specialists in interstitial lung diseases,

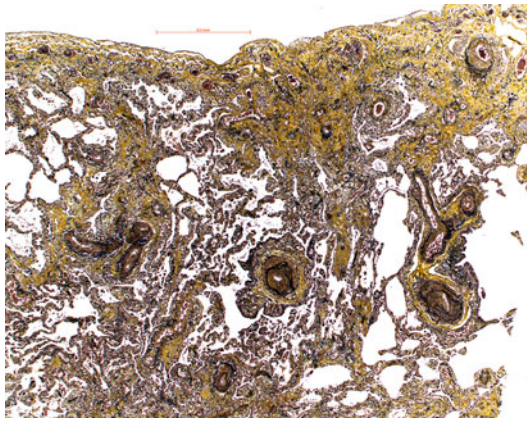

Fig. 8.99 Severe stenosis and sclerosis of pulmonary arteries clinically with hypertension in this patient with UIP/IPF. Movat, bar 500 µm

radiologists and pulmonologists had low kappa statistics, when evaluating UIP/IPF cases. It was always the pathologic diagnosis of UIP, which solved many cases [114, 137–139]. In addition in a study by Morell, many cases diagnosed as being IPF were retrospectively corrected as chronic hypersensitivity pneumonia [140]. This points to the importance of a pathological diagnosis.

Acute exacerbation of UIP/IPF is clinically characterized by rapid worsening of the patient's symptoms and severe hypoxia most often requiring mechanical ventilation and oxygen supply. Many patients will die under this condition. Histologically two types of acute exacerbations can be seen examining autopsy cases: secondary infection with infectious pneumonia in the background of UIP or multiple fibroblastic foci and severe fibrosis leaving not much lung parenchyma for ventilation. In these latter cases, there is usually severe lung edema present. If a viral infection is present, the histological pattern is diffuse alveolar damage (DAD) [20] overlaying UIP; if bacterial or fungal infection causes exacerbation, a purulent bronchopneumonia is found. Another complication is severe stenosis of pulmonary arteries and hypertension (Fig. 8.99).

Besides in IPF a UIP pattern can occur in many other diseases, such as autoimmune diseases, allergic diseases, toxic inhalation, drug-induced pneumonias, and many more. This still causes a lot of confusion, because the term UIP is not used uniformly: some authors use UIP strictly in the sense of IPF, others do not care about etiology and simply diagnose UIP as a pattern, and a third group discerns UIP and UIP-like tissue reactions. The same happens with clinicians: most think a UIP diagnosis already means IPF and are confused to learn that UIP can present in chronic EAA/HP as well as drug reactions, for example. We will discuss these in Chap. 9.

Diagnosis in Small Biopsies

Cryobiopsy is a new technology to evaluate cancer but is also used to provide tissues for interstitial lung disease diagnosis. The diagnosis of UIP by the pathologist is often possible but an etiology-based diagnosis most often not. So in those patients where the clinical and radiological diagnosis is in favor of UIP/IPF, cryobiopsy might add the missing piece in confirming the diagnosis (Fig. 8.100).

8.3.3 Familial IPF (FIPF)

The morphology of FIPF shows more heterogeneity than seen in sporadic IPF. Maybe this reflects the different underlying mechanisms such as defects in the telomere reconstruction or defects in the surfactant system. There are myofibroblastic foci, cystic remodeling of the alveolar tissue, fibrosis, and normal areas of alveolar tissue – all criteria like sporadic IPF. However, in some cases dense inflammatory infiltrates and even aggregates of lymphocytes can be seen (Figs. 8.101, 8.102, and 8.103). In cases under the age of 15, fibrosing NSIP might also be found [141]. In a case series by Leslie et al., UIP was found in less than 50 % of patients with FIPF. In the other cases, unclassifiable parenchymal fibrosis and smooth muscle proliferations in fibrosis was noted. The survival for the entire cohort was poor, with an estimated mortality of 93 % and a median age at death of 60.9 years [142].

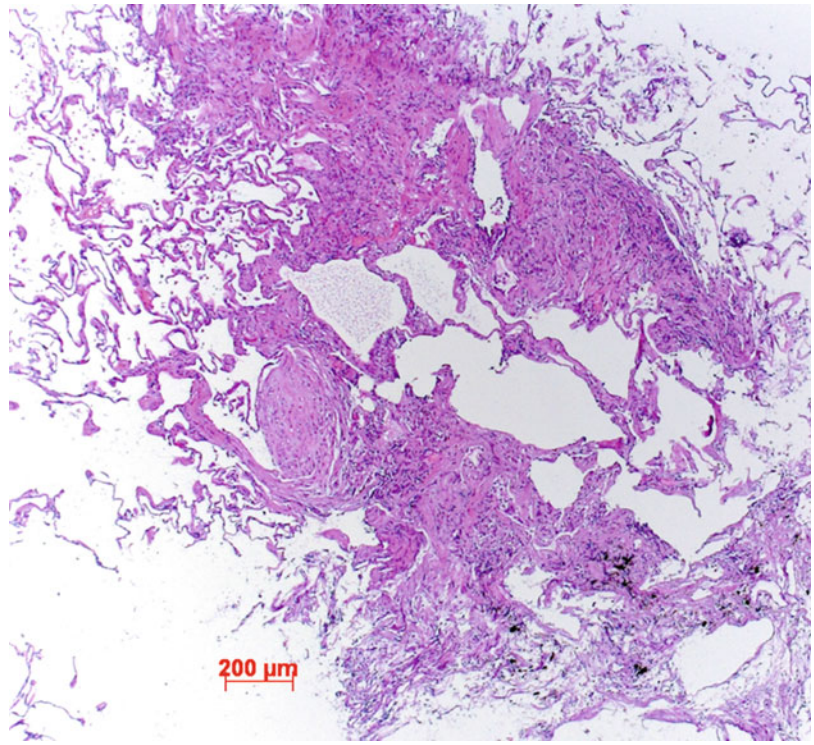

Fig. 8.100 Cryobiopsy of a patient clinically suspected of having IPF. Also the CT scan was in favor of UIP. In this biopsy fibroblastic foci were present together with cystic remodeling and normal alveolar tissue. So the diagnosis of UIP could be made. H&E, bar 200 µm

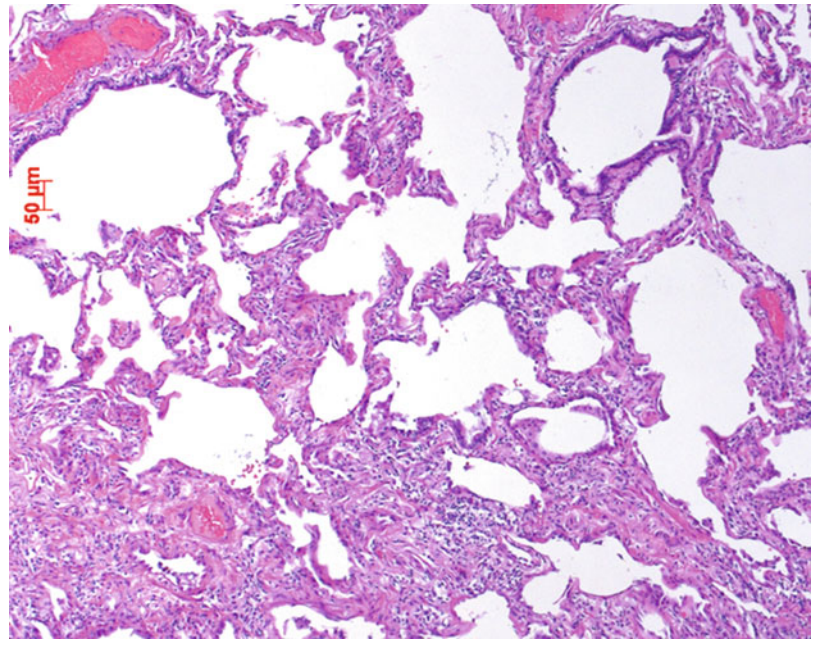

Fig. 8.101 Familial IPF. In this overview there are areas with myofibroblastic foci, cystic remodeling, and fibrosis. In a few areas there was also normal lung. H&E, bar 50 µm

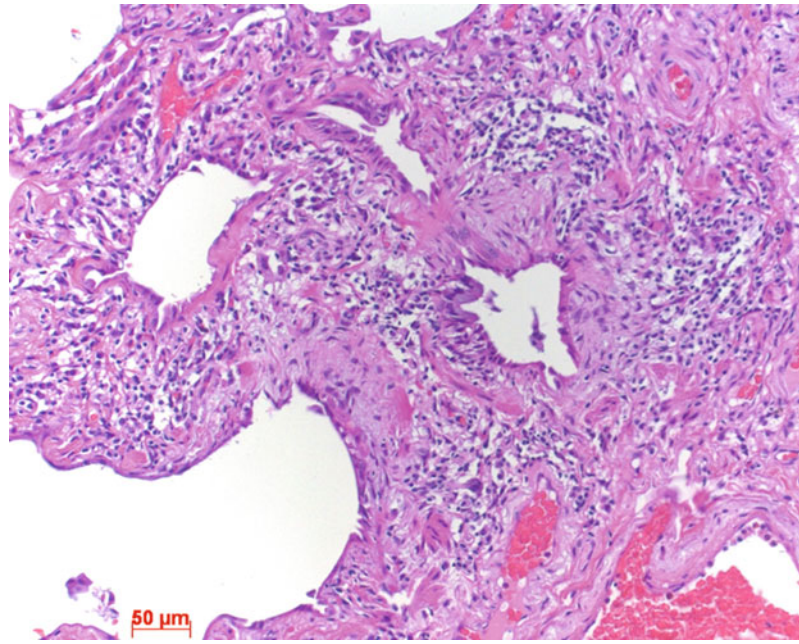

Fig. 8.102 Same case, showing a higher magnification of fibroblastic foci. Note also scattered lymphocytic infiltrations but also apoptosis and regeneration of pneumocytes. H&E, bar 50 µm

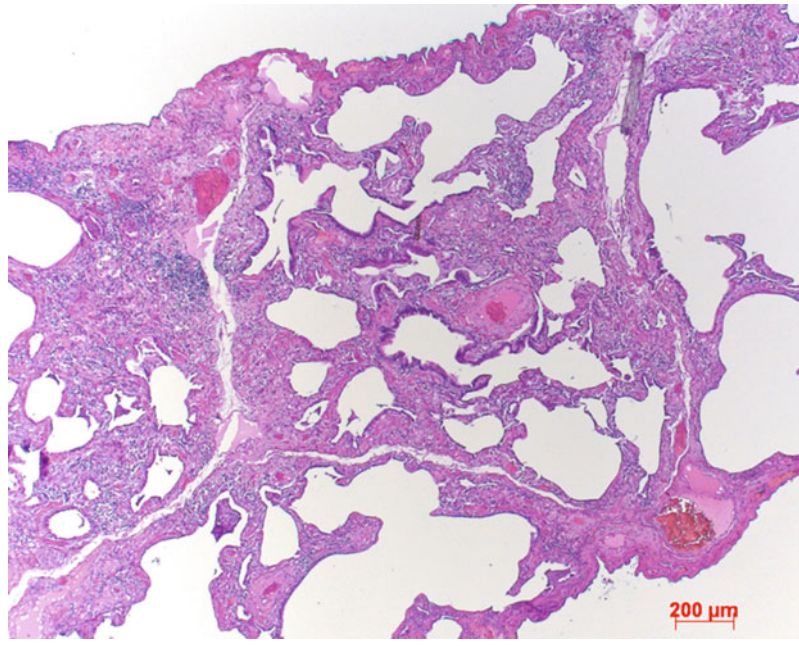

Fig. 8.103 Another area in these sections from familial IPF. Most of the lung was already destroyed by fibrosis and concomitant inflammation. Many remodeled cystic areas are present. The underlying defect was surfactant apoprotein C mutation. H&E, bar 200 µm

8.3.4 Nonspecific Interstitial Pneumonia (NSIP)

NSIP is a diffuse interstitial pneumonia, characterized by loose lymphocytic, macrophagocytic, and histiocytic cell infiltration within alveolar septa combined with mild fibrosis. There is no timely heterogeneity, meaning that the lesions seem to have appeared at the same time. Hyperplasia of the bronchus-associated lymphoid tissue (BALT) is usually not present [116, 143]. The lung architecture is preserved in

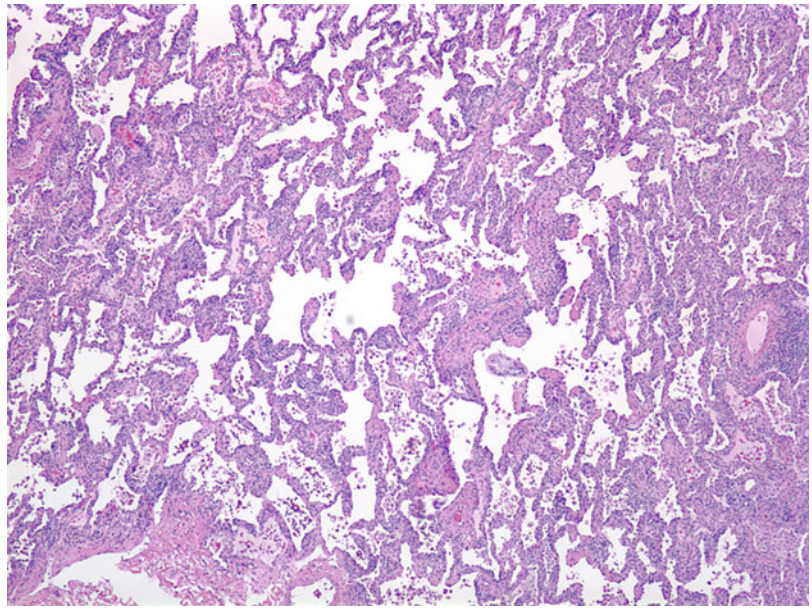

Fig. 8.104 Nonspecific interstitial pneumonia (NSIP), cellular form. Most important the morphology should be assessed primarily on low power magnification to appreciate the timely uniform pathology. The architecture of the alveolar septa is retained and round cells uniformly infiltrate the septa. H&E, ×50

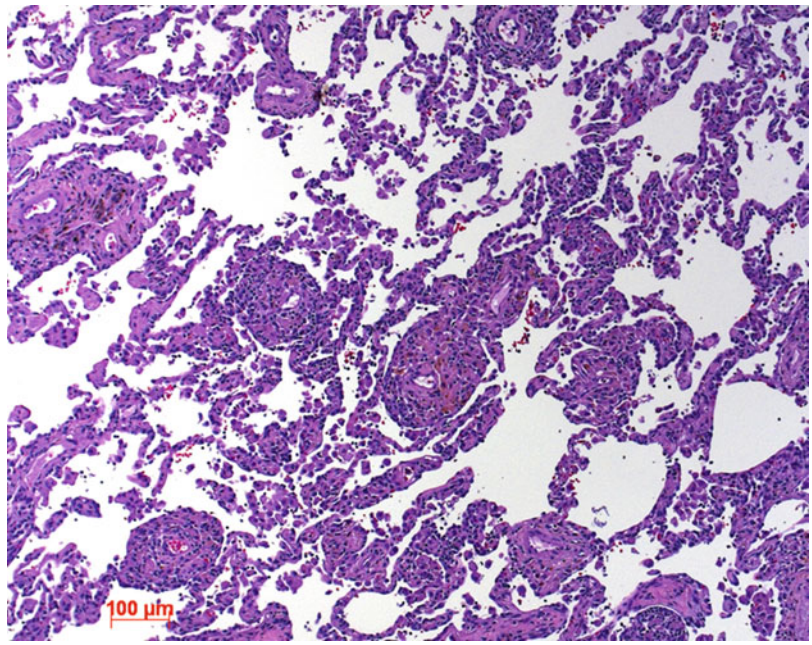

Fig. 8.105 NSIP, showing the different cell types: lymphocytes, histiocytes, and plasma cells. H&E, bar 100 µm

contrast to UIP, and cystic destruction is absent. Two forms are discerned, which in some cases might represent timely sequences of the disease: the cellular and fibrotic type (Figs. 8.104, 8.105, 8.106, and 8.107). Both behave different; the cellular type has a better prognosis, whereas the fibrotic variant is more close to UIP [110]. In the etiologic background, NSIP is most often associated with autoimmune diseases, especially with collagen vascular diseases [28, 144–147]. An association with drug-induced pneumonia and also with allergic diseases such as extrinsic allergic alveolitis/hypersensitivity pneumonia (EAA/HP) has also been reported [148, 149]. Only those cases without an identifiable etiology are labeled as idiopathic NSIP. However, the

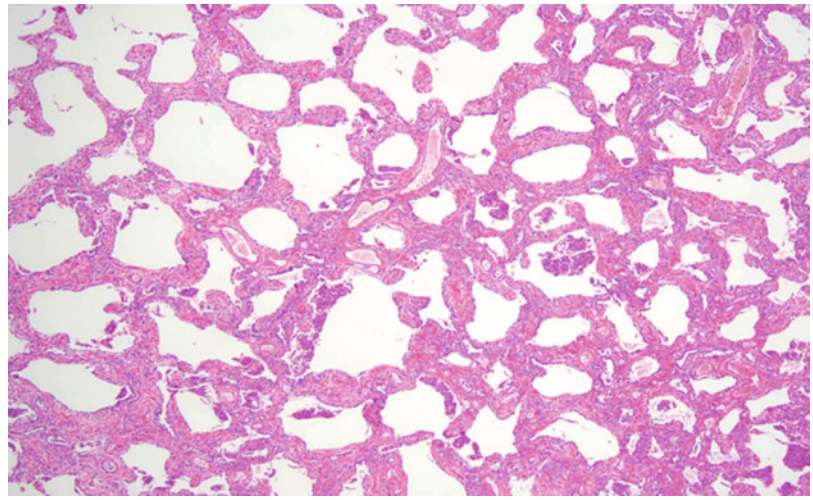

Fig. 8.106 Fibrosing NSIP, in this overview, there is not much inflammatory infiltration but uniform fibrosis of alveolar septa. H&E, ×50

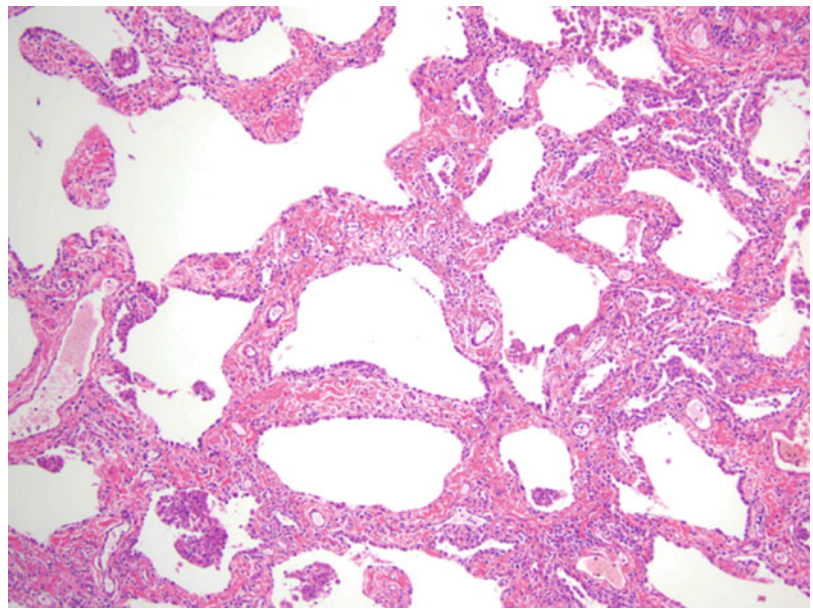

Fig. 8.107 Fibrosing NSIP. There are few scattered lymphocytes, fibroblasts and fibrocytes, and few histiocytes. H&E, ×100

morphologic pattern is identical; therefore in most instances, idiopathic NSIP remains a clinical diagnosis. There are some exceptions: in cases where additional features such as epithelioid cell granulomas are identified, this will favor EAA/HP; an additional pathology of endothelia could point to drug-induced disease. Clinically NSIP shows diffuse infiltrations, corresponding to ground glass opacities on HRCT. Symptoms as in the other interstitial lung diseases are quite unspecific. Many patients with NSIP will respond to corticosteroid and/or immunosuppressive drug treatment, but also spontaneous resolution of the disease has been reported [150, 151]. So far no genetic factors leading to NSIP have been identified.

So what makes this diagnosis?

- The lung architecture is preserved. On low power the alveolar walls, interlobular septa, and primary as well as secondary lobules can be outlined (draw lines along alveolar walls on a digitized photograph, this helps in understanding).

- Diffuse infiltrates composed of lymphocytes macrophages and histiocytic cells, usually few plasma cells.
- If fibrosis is present, this usually causes no distortion of the lung architecture.
- Fibrosis is diffuse, not merging with scars. Inflammatory infiltrates in cases of fibrosing NSIP are usually scarce.
- Non-necrotizing granulomas can be present in certain cases (EAA/HP); however they should not be encountered in idiopathic NSIP.
- Hyperplasia of BALT is absent.

8.3.5 Organizing and Cryptogenic Organizing Pneumonia (OP, COP)

Cryptogenic organizing pneumonia (COP) is a diagnosis of exclusion, based on the morphology of organizing pneumonia (OP, formerly bronchiolitis obliterans-organizing pneumonia (BOOP)). On HRCT OP/COP shows a pattern with combinations of ground glass opacities and consolidations and the almost diagnostic tree-in-bud pattern, sometimes also reticulonodular pattern [152] (Fig. 8.108). In rare cases the consolidation can mimic a tumor [153]. Histologically the hallmark of OP is an intra-alveolar granulation tissue, the so-called Masson body (Fig. 8.109). It consists of proliferating fibroblasts and myofibroblasts with inflammatory cells like neutrophils, lymphocytes, histiocytes, and macrophages. Hemosiderin-laden macrophages are often present. The granulation tissue can start from the wall of bronchi, bronchioles, and alveoli. There is usually a defect of the epithelial layer and also the basal lamina. Fibroblasts and myofibroblasts grow into the defect; however, in contrast to normal repair, the granulation tissue does not stop but continuously grows into the airspaces, filling these completely or incompletely. In later stages pneumocytes will grow over these granulation tissue plugs and therefore a slit-like airspace can be formed (Fig. 8.110) [153]. The amount of inflammatory cells within the granulation tissue depends on the cause of OP. The morphologic

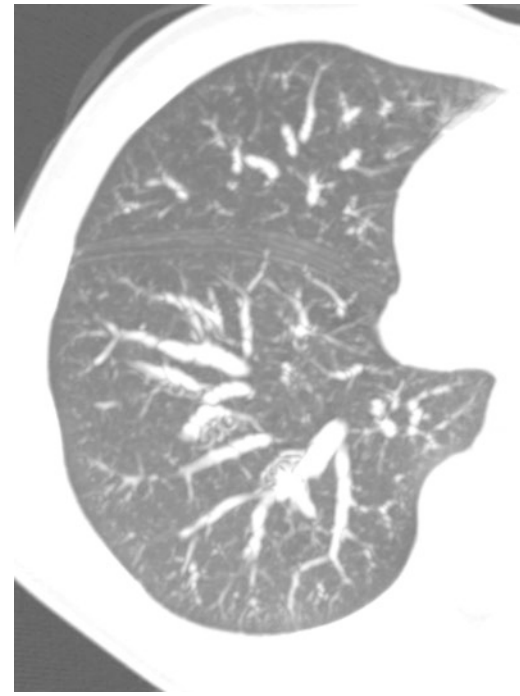

Fig. 8.108 CT scan of a patient with organizing pneumonia. The reticulonodular pattern and the tree-in-bud pattern are nicely shown. There are also some nodular densities in the peripheral lung and ground glass opacities

pattern of organizing pneumonia (OP) has a very wide range of etiologies (Table 8.9).

In some cases of OP, the etiologic cause can be determined, for example, by hyaline membranes in DAD or by viral inclusion bodies in post-viral OP or by endothelial cell reactions in drug-induced OP. In some cases an additional pathologic tissue reaction besides OP can also point to the underlying etiology. If looking for the etiology, one should also closely investigate the small blood vessels and the regenerating pneumocytes: viral inclusion bodies might be still visible, scattered neutrophilic granulocytes can be found in the granulation tissue in cases of bacterial or fungal infection, and eosinophils might be seen pointing to a previous drug-induced pneumonia. In virus-induced pneumonias another feature can be found, even after several months: single transformed pneumocytes showing atypical nuclei and a homogenously stained smudged chromatin pattern

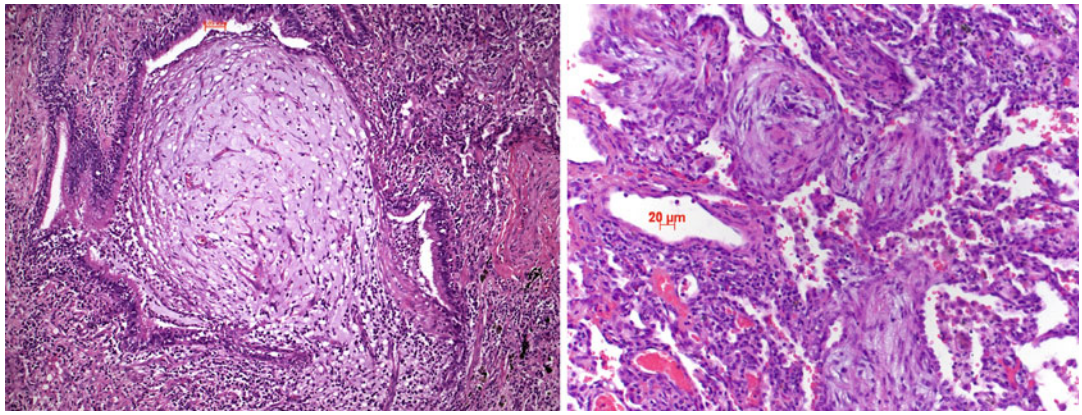

Fig. 8.109 Intra-alveolar granulation tissue (Masson body); left an early granulation tissue with newly formed capillaries and undifferentiated mesenchymal cells and scattered leukocytes. Right an older granulation tissue still containing remnants of hyaline membranes. H&E, bars 50 µm and 20 µm

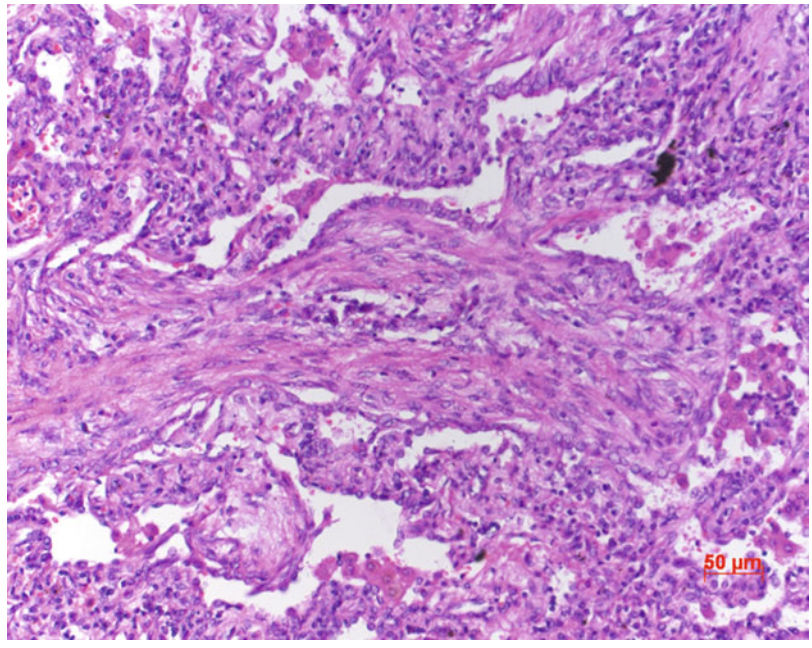

Fig. 8.110 OP the granulation tissue almost completely fills the alveolar spaces; only slit-like remnants are left

(Fig. 8.111). In drug-induced and metabolic as well as in autoimmune diseases, the vascular walls can show various structural changes making an etiology-based diagnosis probable: eccentric vasculopathy with scattered lymphocytes and without endothelial damage might point to deposition of idiotypic-anti-idiotypic immune complexes (without complement activation; Fig. 8.112) and endothelial damage with fibrosis and repair can point toward drug-induced damage (Fig. 8.113).

So what are the diagnostic features?

- Granulation tissue growing into bronchi, bronchioles, and alveoli, usually with remnants of inflammatory cells
- Fibrotic occlusion of whole lobules or remaining slit-like spaces covered by pneumocytes

Table 8.9 Etiology of organizing pneumonia [96, 97, 154, 155]

Organization of DAD
Organization of infectious pneumonias
Organization distal to bronchial obstruction
Organization of aspiration pneumonia
Organization of drug reactions, gas inhalation, and exposure to toxins
Autoimmune diseases including collagen vascular disease
EAA/HP
Eosinophilic lung diseases
Chronic inflammatory bowel disease
Secondary to chronic bronchiolitis
Repair at the border of other processes, such as abscess, Wegener's granulomatosis, tumors, etc.
As an idiopathic process = cryptogenic organizing pneumonia COP

- A mixture of inflammatory cells within these granulation tissue plugs depending on the cause of previous damage

COP as a CRP diagnosis is a diagnosis of exclusion: if all possible underlying diseases are excluded, COP can be diagnosed (Fig. 8.114). This has some importance, since COP responds well to corticosteroid treatment.

8.3.6 Airway-Centered Interstitial Fibrosis (ACIF)

ACIF has already been described in the airway chapter, so it is only mentioned briefly here. It affects patients with a history of environmental exposure to

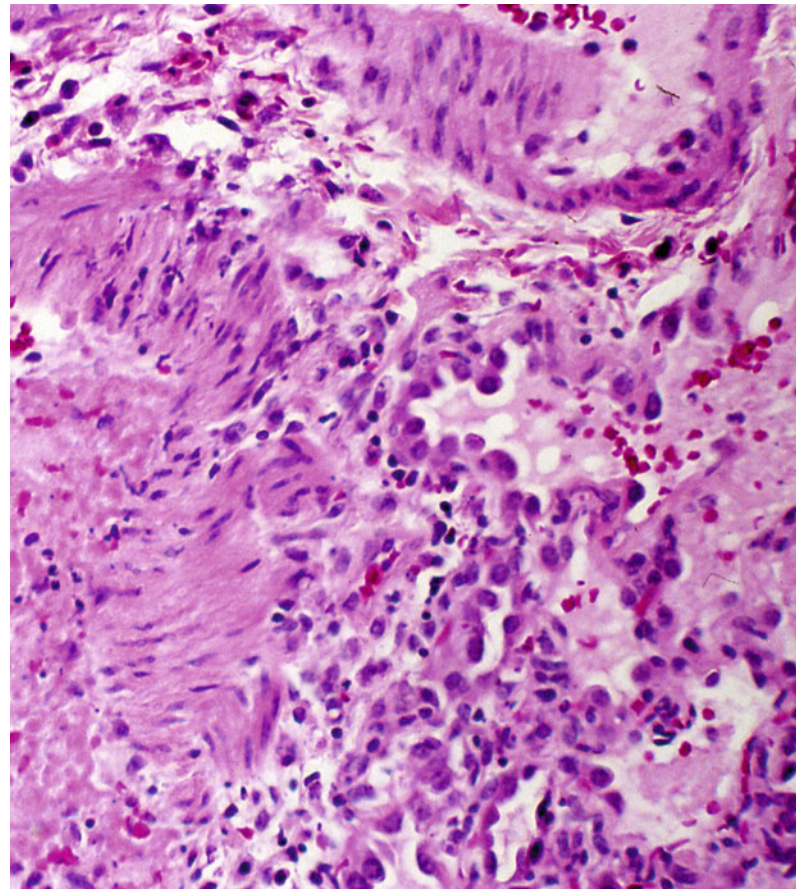

Fig. 8.111 OP in a case of viral infection. Although the acute phase has passed, there are still foci of atypical pneumocyte proliferation/regeneration, which point to the previous infection. H&E, ×400

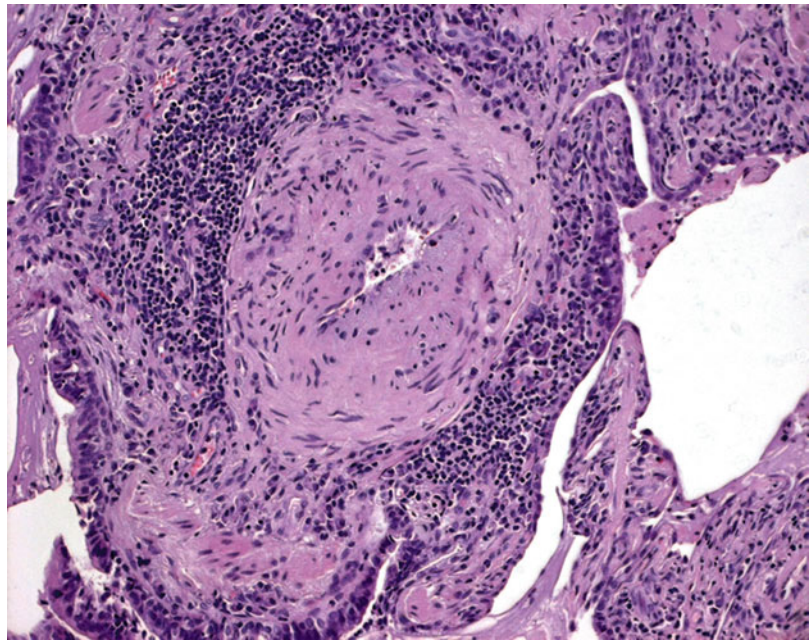

Fig. 8.112 Eccentric vasculopathy and dense lymphocytic infiltrations in this case of OP. These are features where one should look for previous endothelial damage, probably induced by immune reactions. H&E, ×250

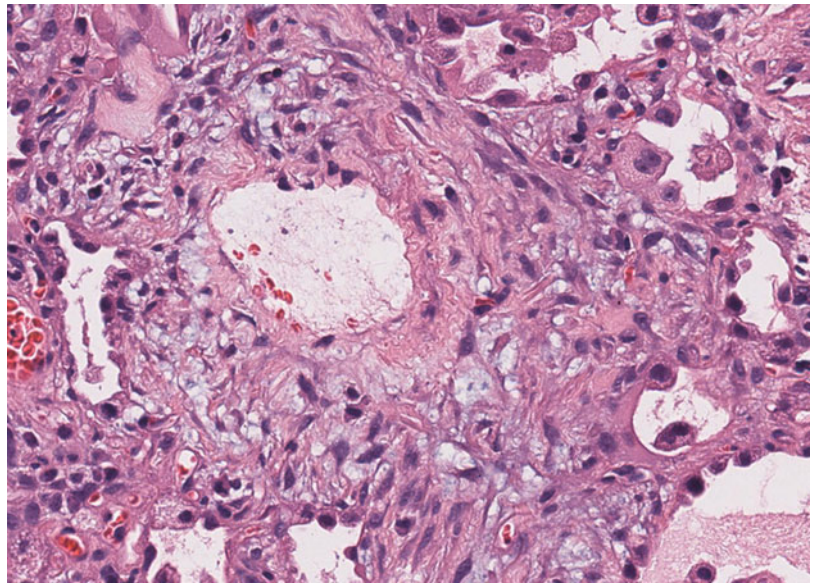

Fig. 8.113 In some areas of this case of OP, there was endothelial damage with fibrosis and repair, which points toward drug-induced damage. H&E, ×250

toxic or allergic substances. Also cocaine abuse was found in one [156]. The morphology is characterized by fibrosis along the small bronchi extending into the peripheral lung following a lobular distribution. In some cases fibroblastic foci can occur, however, always associated with this distribution pattern. Cystic lung remodeling is absent; instead a whole lobule or subsegment is destroyed by fibrosis. Metaplastic epithelium is common in the affected lobules and also hyperplasia of smooth muscle cells (muscular cirrhosis). The disease rapidly progresses and in the reported series almost half of the patients died of disease. Corticosteroid treatment was effective in some patients.

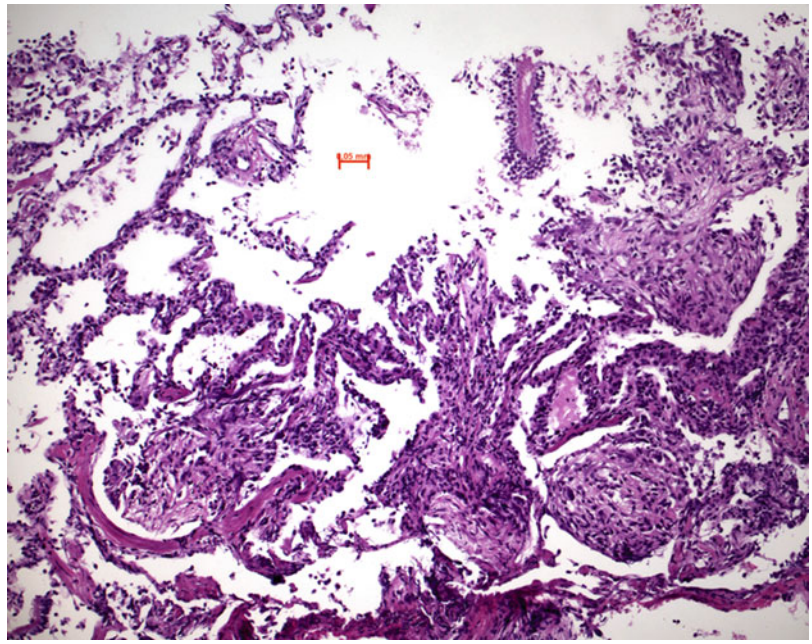

Fig. 8.114 OP in a transbronchial biopsy. No other causes could be identified neither by pathologic nor by clinical investigation, so finally this case was diagnosed as COP. H&E, bar 50 μm

References

1. Knapp S, Wieland CW, van't Veer C, Takeuchi O, Akira S, Florquin S, van der Poll T. Toll-like receptor 2 plays a role in the early inflammatory response to murine pneumococcal pneumonia but does not contribute to antibacterial defense. J Immunol. 2004;172:3132–8.
2. Popper H, Jakse R, Loidolt D. Problems in the differential diagnosis of Kartagener's syndrome and ATPase deficiency. Pathol Res Pract. 1985;180:481–5.
3. Rubin BK, Knowles MR, Boucher RC. Physiology of airway mucus clearance mucus clearance as a primary innate defense mechanism for mammalian airways. Respir Care. 2002;47:761–8.
4. Sharif O, Matt U, Saluzzo S, Lakovits K, Haslinger I, Furtner T, Doninger B, Knapp S. The scavenger receptor CD36 downmodulates the early inflammatory response while enhancing bacterial phagocytosis during pneumococcal pneumonia. J Immunol. 2013;190:5640–8.
5. Message SD, Johnston SL. The immunology of virus infection in asthma. Eur Respir J. 2001;18: 1013–25.
6. van Iwaarden F, Welmers B, Verhoef J, Haagsman HP, van Golde LM. Pulmonary surfactant protein A enhances the host-defense mechanism of rat alveolar macrophages. Am J Respir Cell Mol Biol. 1990;2:91–8.
7. Slater L, Bartlett NW, Haas JJ, Zhu J, Message SD, Walton RP, Sykes A, Dahdaleh S, Clarke DL, Belvisi MG, Kon OM, Fujita T, Jeffery PK, Johnston SL, Edwards MR. Co-ordinated role of TLR3, RIG-I and MDA5 in the innate response to rhinovirus in bronchial epithelium. PLoS Pathog. 2010;6:e1001178.
8. Liu PT, Stenger S, Li H, Wenzel L, Tan BH, Krutzik SR, Ochoa MT, Schauber J, Wu K, Meinken C, Kamen DL, Wagner M, Bals R, Steinmeyer A, Zugel U, Gallo RL, Eisenberg D, Hewison M, Hollis BW, Adams JS, Bloom BR, Modlin RL. Toll-like receptor triggering of a vitamin D-mediated human antimicrobial response. Science. 2006;311:1770–3.
9. Nitadori JI, Bograd AJ, Kadota K, Sima CS, Rizk NP, Morales EA, Rusch VW, Travis WD, Adusumilli PS. Impact of micropapillary histologic subtype in selecting limited resection vs lobectomy for lung adenocarcinoma of 2cm or smaller. J Natl Cancer Inst. 2013;105:1212–20.
10. Kim KJ, Malik AB. Protein transport across the lung epithelial barrier. Am J Physiol Lung Cell Mol Physiol. 2003;284:L247–59.
11. Rusznak C, Sapsford RJ, Devalia JL, Wang JH, Shah SS, Mills PR, Davies RJ, Lozewicz S. Cigarette smoke decreases the expression of secretory component in human bronchial epithelial cells, in vitro. Acta Microbiol Immunol Hung. 2001;48:81–94.
12. Message SD, Johnston SL. Host defense function of the airway epithelium in health and disease: clinical background. J Leukoc Biol. 2004;75:5–17.
13. Chiu BC, Freeman CM, Stolberg VR, Hu JS, Komuniecki E, Chensue SW. The innate pulmonary granuloma: characterization and demonstration of dendritic cell recruitment and function. Am J Pathol. 2004;164:1021–30.
14. Ito T, Schaller M, Hogaboam CM, Standiford TJ, Sandor M, Lukacs NW, Chensue SW, Kunkel SL.

TLR9 regulates the mycobacteria-elicited pulmonary granulomatous immune response in mice through DC-derived Notch ligand delta-like 4. J Clin Invest. 2009;119:33–46.
15. Kameda H, Okuyama A, Tamaru J, Itoyama S, Iizuka A, Takeuchi T. Lymphomatoid granulomatosis and diffuse alveolar damage associated with methotrexate therapy in a patient with rheumatoid arthritis. Clin Rheumatol. 2007;26:1585–9.
16. Parambil JG, Myers JL, Ryu JH. Diffuse alveolar damage: uncommon manifestation of pulmonary involvement in patients with connective tissue diseases. Chest. 2006;130:553–8.
17. Nicholson AG, Colby TV, Wells AU. Histopathological approach to patterns of interstitial pneumonia in patient with connective tissue disorders. Sarcoidosis Vasc Diffuse Lung Dis. 2002;19:10–7.
18. Hamman L, Rich AR. Fulminating diffuse interstitial fibrosis of the lungs. Trans Am Clin Climatol Assoc. 1935;51:154–63.
19. Popper H, Juettner F, Pinter J. The gastric juice aspiration syndrome (Mendelson syndrome). Aspects of pathogenesis and treatment in the pig. Virchows Arch A Pathol Anat Histopathol. 1986;409:105–17.
20. Wootton SC, Kim DS, Kondoh Y, Chen E, Lee JS, Song JW, Huh JW, Taniguchi H, Chiu C, Boushey H, Lancaster LH, Wolters PJ, DeRisi J, Ganem D, Collard HR. Viral infection in acute exacerbation of idiopathic pulmonary fibrosis. Am J Respir Crit Care Med. 2011;183:1698–702.
21. Beasley MB, Franks TJ, Galvin JR, Gochuico B, Travis WD. Acute fibrinous and organizing pneumonia: a histological pattern of lung injury and possible variant of diffuse alveolar damage. Arch Pathol Lab Med. 2002;126:1064–70.
22. Yazdy AM, Tomashefski Jr JF, Yagan R, Kleinerman J. Regional alveolar damage (RAD). A localized counterpart of diffuse alveolar damage. Am J Clin Pathol. 1989;92:10–5.
23. Hariri LP, Mino-Kenudson M, Shea B, Digumarthy S, Onozato M, Yagi Y, Fraire AE, Matsubara O, Mark EJ. Distinct histopathology of acute onset or abrupt exacerbation of hypersensitivity pneumonitis. Hum Pathol. 2012;43:660–8.
24. Poletti V, Kitaichi M. Facts and controversies in the classification of idiopathic interstitial pneumonias. Sarcoidosis Vasc Diffuse Lung Dis. 2000;17:229–38.
25. Liu QF, Fan ZP, Luo XD, Sun J, Zhang Y, Ding YQ. Epstein-Barr virus-associated pneumonia in patients with post-transplant lymphoproliferative disease after hematopoietic stem cell transplantation. Transpl Infect Dis. 2010;12:284–91.
26. Voulgarelis M, Moutsopoulos HM. Lymphoproliferation in autoimmunity and Sjogren's syndrome. Curr Rheumatol Rep. 2003;5:317–23.
27. Parambil JG, Myers JL, Lindell RM, Matteson EL, Ryu JH. Interstitial lung disease in primary Sjogren syndrome. Chest. 2006;130:1489–95.
28. Tansey D, Wells AU, Colby TV, Ip S, Nikolakoupolou A, du Bois RM, Hansell DM, Nicholson AG. Variations in histological patterns of interstitial pneumonia between connective tissue disorders and their relationship to prognosis. Histopathology. 2004;44:585–96.
29. Herschke F, Plumet S, Duhen T, Azocar O, Druelle J, Laine D, Wild TF, Rabourdin-Combe C, Gerlier D, Valentin H. Cell-cell fusion induced by measles virus amplifies the type I interferon response. J Virol. 2007;81:12859–71.
30. Delage G, Brochu P, Robillard L, Jasmin G, Joncas JH, Lapointe N. Giant cell pneumonia due to respiratory syncytial virus. Occurrence in severe combined immunodeficiency syndrome. Arch Pathol Lab Med. 1984;108:623–5.
31. Ramaswamy G, Jagadha V, Tchertkoff V. Diffuse alveolar damage and interstitial fibrosis in acquired immunodeficiency syndrome patients without concurrent pulmonary infection. Arch Pathol Lab Med. 1985;109:408–12.
32. Joshi VV, Oleske JM, Minnefor AB, Saad S, Klein KM, Singh R, Zabala M, Dadzie C, Simpser M, Rapkin RH. Pathologic pulmonary findings in children with the acquired immunodeficiency syndrome: a study of ten cases. Hum Pathol. 1985;16:241–6.
33. Nash G, Fligiel S. Pathologic features of the lung in the acquired immune deficiency syndrome (AIDS): an autopsy study of seventeen homosexual males. Am J Clin Pathol. 1984;81:6–12.
34. Sung TJ. Ureaplasma infections in pre-term infants: recent information regarding the role of ureaplasma species as neonatal pathogens. Kor J Pediatr. 2010;53:989–93.
35. Reiterer F, Dornbusch HJ, Urlesberger B, Reittner P, Fotter R, Zach M, Popper H, Muller W. Cytomegalovirus associated neonatal pneumonia and Wilson-Mikity syndrome: a causal relationship? Eur Respir J. 1999;13:460–2.
36. Harris VJ. Wilson-Mikity syndrome: a pulmonary disorder of premature infants. Chic Med Sch Q. 1970;30:50–8.
37. Hoepker A, Seear M, Petrocheilou A, Hayes Jr D, Nair A, Deodhar J, Kadam S, O'Toole J. Wilson-Mikity syndrome: updated diagnostic criteria based on nine cases and a review of the literature. Pediatr Pulmonol. 2008;43:1004–12.
38. Oetgen WJ. Chlamydial pneumonia of infancy vs Wilson-Mikity syndrome. Pediatrics. 1979;64:119–20.
39. Philip AG. Chronic lung disease of prematurity: a short history. Semin Fetal Neonatal Med. 2009;14:333–8.
40. Numazaki K, Chiba S, Kogawa K, Umetsu M, Motoya H, Nakao T. Chronic respiratory disease in premature infants caused by Chlamydia trachomatis. J Clin Pathol. 1986;39:84–8.
41. Bose CL, Dammann CE, Laughon MM. Bronchopulmonary dysplasia and inflammatory

biomarkers in the premature neonate. Arch Dis Child Fetal Neonatal Ed. 2008;93:F455–61.
42. Zhang H, Fang J, Su H, Chen M. Risk factors for bronchopulmonary dysplasia in neonates born at </= 1500 g (1999–2009). Pediatr Int. 2011;53:915–20.
43. Coclite E, Di Natale C, Nigro G. Congenital and perinatal cytomegalovirus lung infection. J Matern Fetal Neonatal Med. 2013;26:1671–5.
44. Hofer N, Jank K, Resch E, Urlesberger B, Reiterer F, Resch B. Meconium aspiration syndrome – a 21-years' experience from a tertiary care center and analysis of risk factors for predicting disease severity. Klin Padiatr. 2013;225:383–8.
45. Reuter S, Moser C, Baack M. Respiratory distress in the newborn. Pediatr Rev. 2014;35:417–28; quiz 429.
46. Mofenson LM, Brady MT, Danner SP, Dominguez KL, Hazra R, Handelsman E, Havens P, Nesheim S, Read JS, Serchuck L, Van Dyke R. Guidelines for the Prevention and Treatment of Opportunistic Infections among HIV-exposed and HIV-infected children: recommendations from CDC, the National Institutes of Health, the HIV Medicine Association of the Infectious Diseases Society of America, the Pediatric Infectious Diseases Society, and the American Academy of Pediatrics. MMWR Recomm Rep. 2009;58:1–166.
47. Popper HH. Differential diagnosis and etiology of epithelioid cell granulomatosis of the lung. Verh Dtsch Ges Pathol. 2000;84:118–28.
48. Boeck C. Multiple benign sarcoid of the skin. Norsk Mag Laegevid. 1899;14:1321–45.
49. Newman LS. Metals that cause sarcoidosis. Semin Respir Infect. 1998;13:212–20.
50. Werfel U, Schneider J, Rodelsperger K, Kotter J, Popp W, Woitowitz HJ, Zieger G. Sarcoid granulomatosis after zirconium exposure with multiple organ involvement. Eur Respir J. 1998;12:750.
51. Romeo L, Cazzadori A, Bontempini L, Martini S. Interstitial lung granulomas as a possible consequence of exposure to zirconium dust. Med Lav. 1994;85:219–22.
52. Liippo KK, Anttila SL, Taikina-Aho O, Ruokonen EL, Toivonen ST, Tuomi T. Hypersensitivity pneumonitis and exposure to zirconium silicate in a young ceramic tile worker. Am Rev Respir Dis. 1993;148:1089–92.
53. Itoh A, Yamaguchi E, Kuzumaki N, Okazaki N, Furuya K, Abe S, Kawakami Y. Expression of granulocyte-macrophage colony-stimulating factor mRNA by inflammatory cells in the sarcoid lung. Am J Respir Cell Mol Biol. 1990;3:245–9.
54. Spiteri MA, Poulter LW, Geraint-James D. The macrophage in sarcoid granuloma formation. Sarcoidosis. 1989;6 Suppl 1:12–4.
55. Naito M, Umeda S, Takahashi K, Shultz LD. Macrophage differentiation and granulomatous inflammation in osteopetrotic mice (op/op) defective in the production of CSF-1. Mol Reprod Dev. 1997;46:85–91.
56. Seitzer U, Scheel-Toellner D, Toellner KM, Reiling N, Haas H, Galle J, Flad HD, Gerdes J. Properties of multinucleated giant cells in a new in vitro model for human granuloma formation. J Pathol. 1997;182:99–105.
57. Popper HH. Epithelioid cell granulomatosis of the lung: new insights and concepts. Sarcoidosis Vasc Diffuse Lung Dis. 1999;16:32–46.
58. Perez RL, Rivera-Marrero CA, Roman J. Pulmonary granulomatous inflammation: from sarcoidosis to tuberculosis. Semin Respir Infect. 2003;18:23–32.
59. Ma J, Chen T, Mandelin J, Ceponis A, Miller NE, Hukkanen M, Ma GF, Konttinen YT. Regulation of macrophage activation. Cell Mol Life Sci. 2003;60:2334–46.
60. Segovia-Juarez JL, Ganguli S, Kirschner D. Identifying control mechanisms of granuloma formation during M. tuberculosis infection using an agent-based model. J Theor Biol. 2004;231:357–76.
61. Takimoto H, Maruyama H, Shimada KI, Yakabe R, Yano I, Kumazawa Y. Interferon-gamma independent formation of pulmonary granuloma in mice by injections with trehalose dimycolate (cord factor), lipoarabinomannan and phosphatidylinositol mannosides isolated from Mycobacterium tuberculosis. Clin Exp Immunol. 2006;144:134–41.
62. Puissegur MP, Lay G, Gilleron M, Botella L, Nigou J, Marrakchi H, Mari B, Duteyrat JL, Guerardel Y, Kremer L, Barbry P, Puzo G, Altare F. Mycobacterial lipomannan induces granuloma macrophage fusion via a TLR2-dependent, ADAM9- and beta1 integrin-mediated pathway. J Immunol. 2007;178:3161–9.
63. Lay G, Poquet Y, Salek-Peyron P, Puissegur MP, Botanch C, Bon H, Levillain F, Duteyrat JL, Emile JF, Altare F. Langhans giant cells from M. tuberculosis-induced human granulomas cannot mediate mycobacterial uptake. J Pathol. 2007;211:76–85.
64. Puissegur MP, Botanch C, Duteyrat JL, Delsol G, Caratero C, Altare F. An in vitro dual model of mycobacterial granulomas to investigate the molecular interactions between mycobacteria and human host cells. Cell Microbiol. 2004;6:423–33.
65. Yanagishita T, Watanabe D, Akita Y, Nakano A, Ohshima Y, Tamada Y, Matsumoto Y. Construction of novel in vitro epithelioid cell granuloma model from mouse macrophage cell line. Arch Dermatol Res. 2007;299:399–403.
66. Rickman OB, Ryu JH, Fidler ME, Kalra S. Hypersensitivity pneumonitis associated with mycobacterium avium complex and hot tub use. Mayo Clin Proc. 2002;77:1233–7.
67. Khoor A, Leslie KO, Tazelaar HD, Helmers RA, Colby TV. Diffuse pulmonary disease caused by nontuberculous mycobacteria in immunocompetent people (hot tub lung). Am J Clin Pathol. 2001;115:755–62.
68. Aly S, Mages J, Reiling N, Kalinke U, Decker T, Lang R, Ehlers S. Mycobacteria-induced granuloma necrosis depends on IRF-1. J Cell Mol Med. 2009;13:2069–82.

69. Goldman DL, Lee SC, Mednick AJ, Montella L, Casadevall A. Persistent Cryptococcus neoformans pulmonary infection in the rat is associated with intracellular parasitism, decreased inducible nitric oxide synthase expression, and altered antibody responsiveness to cryptococcal polysaccharide. Infect Immun. 2000;68:832–8.
70. Romer FK. Sarcoidosis with large nodular lesions simulating pulmonary metastases. An analysis of 126 cases of intrathoracic sarcoidosis. Scand J Respir Dis. 1977;58:11–6.
71. McCullough PC, McCullough AE. Images in clinical medicine. Nodular sarcoidosis. N Engl J Med. 2002;346:1970.
72. Liebow AA. The J. Burns Amberson lecture – pulmonary angiitis and granulomatosis. Am Rev Respir Dis. 1973;108:1–18.
73. Churg A, Carrington CB, Gupta R. Necrotizing sarcoid granulomatosis. Chest. 1979;76:406–13.
74. Popper HH, Klemen H, Colby TV, Churg A. Necrotizing sarcoid granulomatosis – is it different from nodular sarcoidosis? Pneumologie. 2003;57:268–71.
75. Mitchell IC, Turk JL, Mitchell DN. Detection of mycobacterial rRNA in sarcoidosis with liquid-phase hybridisation. Lancet. 1992;339:1015–7.
76. Saboor SA, Johnson NM, McFadden J. Detection of mycobacterial DNA in sarcoidosis and tuberculosis with polymerase chain reaction. Lancet. 1992;339:1012–5.
77. Fidler HM, Rook GA, Johnson NM, McFadden J. Mycobacterium tuberculosis DNA in tissue affected by sarcoidosis. BMJ. 1993;306:546–9.
78. Popper HH, Winter E, Hofler G. DNA of mycobacterium tuberculosis in formalin-fixed, paraffin-embedded tissue in tuberculosis and sarcoidosis detected by polymerase chain reaction. Am J Clin Pathol. 1994;101:738–41.
79. Ozcelik U, Ozkara HA, Gocmen A, Akcoren Z, Kocagoz T, Kiper N, Gogus S, Caglar M, Kale G, Kotiloglu E. Detection of mycobacterium tuberculosis DNA in tissue samples of children with sarcoidosis. Pediatr Pulmonol. 1997;24:122–4.
80. Ebe Y, Ikushima S, Yamaguchi T, Kohno K, Azuma A, Sato K, Ishige I, Usui Y, Takemura T, Eishi Y. Proliferative response of peripheral blood mononuclear cells and levels of antibody to recombinant protein from propionibacterium acnes DNA expression library in Japanese patients with sarcoidosis. Sarcoidosis Vasc Diffuse Lung Dis. 2000;17:256–65.
81. Ishige I, Usui Y, Takemura T, Eishi Y. Quantitative PCR of mycobacterial and propionibacterial DNA in lymph nodes of Japanese patients with sarcoidosis. Lancet. 1999;354:120–3.
82. Iwai K. Propionibacterium acnes in sarcoidosis. Sarcoidosis. 1989;6:73–5.
83. Nishiwaki T, Yoneyama H, Eishi Y, Matsuo N, Tatsumi K, Kimura H, Kuriyama T, Matsushima K. Indigenous pulmonary propionibacterium acnes primes the host in the development of sarcoid-like pulmonary granulomatosis in mice. Am J Pathol. 2004;165:631–9.
84. Klemen H, Husain AN, Cagle PT, Garrity ER, Popper HH. Mycobacterial DNA in recurrent sarcoidosis in the transplanted lung – a PCR-based study on four cases. Virchows Arch. 2000;436:365–9.
85. Song Z, Marzilli L, Greenlee BM, Chen ES, Silver RF, Askin FB, Teirstein AS, Zhang Y, Cotter RJ, Moller DR. Mycobacterial catalase-peroxidase is a tissue antigen and target of the adaptive immune response in systemic sarcoidosis. J Exp Med. 2005;201:755–67.
86. Hjalmarson O, Brynjarsson H, Nilsson S, Sandberg KL. Spectrum of chronic lung disease in a population of newborns with extremely low gestational age. Acta Paediatr. 2012;101:912–8.
87. Kang TJ, Lee SB, Chae GT. A polymorphism in the toll-like receptor 2 is associated with IL-12 production from monocyte in lepromatous leprosy. Cytokine. 2002;20:56–62.
88. Petzmann S, Maercker C, Markert E, Kern I, Osolnik K, Pohl W, Popper HH. Enhanced proliferation and decreased apoptosis in lung lavage cells of sarcoidosis patients. Sarcoidosis Vasc Diffuse Lung Dis. 2006;23:190–200.
89. Ishihara M, Ohno S, Ishida T, Mizuki N, Ando H, Naruse T, Ishihara H, Inoko H. Genetic polymorphisms of the TNFB and HSP70 genes located in the human major histocompatibility complex in sarcoidosis. Tissue Antigens. 1995;46:59–62.
90. Iannuzzi MC. Genetics of sarcoidosis. Semin Respir Crit Care Med. 2007;28:15–21.
91. Schurmann M, Kwiatkowski R, Albrecht M, Fischer A, Hampe J, Muller-Quernheim J, Schwinger E, Schreiber S. Study of toll-like receptor gene loci in sarcoidosis. Clin Exp Immunol. 2008;152:423–31.
92. Samuel G, Maier LA. Immunology of chronic beryllium disease. Curr Opin Allergy Clin Immunol. 2008;8:126–34.
93. McCleskey TM, Buchner V, Field RW, Scott BL. Recent advances in understanding the biomolecular basis of chronic beryllium disease: a review. Rev Environ Health. 2009;24:75–115.
94. Clayton GM, Wang Y, Crawford F, Novikov A, Wimberly BT, Kieft JS, Falta MT, Bowerman NA, Marrack P, Fontenot AP, Dai S, Kappler JW. Structural basis of chronic beryllium disease: linking allergic hypersensitivity and autoimmunity. Cell. 2014;158:132–42.
95. Falta MT, Pinilla C, Mack DG, Tinega AN, Crawford F, Giulianotti M, Santos R, Clayton GM, Wang Y, Zhang X, Maier LA, Marrack P, Kappler JW, Fontenot AP. Identification of beryllium-dependent peptides recognized by CD4+ T cells in chronic beryllium disease. J Exp Med. 2013;210:1403–18.
96. Casey MB, Tazelaar HD, Myers JL, Hunninghake GW, Kakar S, Kalra SX, Ashton R, Colby TV. Noninfectious lung pathology in patients with Crohn's disease. Am J Surg Pathol. 2003;27:213–9.

97. Camus P, Piard F, Ashcroft T, Gal AA, Colby TV. The lung in inflammatory bowel disease. Medicine (Baltimore). 1993;72:151–83.
98. Teague WG, Sutphen JL, Fechner RE. Desquamative interstitial pneumonitis complicating inflammatory bowel disease of childhood. J Pediatr Gastroenterol Nutr. 1985;4:663–7.
99. Fujita J, Ohtsuki Y, Yoshinouchi T, Yamadori I, Bandoh S, Tokuda M, Miyawaki H, Kishimoto N, Ishida T. Idiopathic non-specific interstitial pneumonia: as an 'autoimmune interstitial pneumonia'. Respir Med. 2005;99:234–40.
100. Klemen H, Bogiatzis A, Ghalibafian M, Popper HH. Multiplex polymerase chain reaction for rapid detection of atypical mycobacteria and mycobacterium tuberculosis complex. Diagn Mol Pathol. 1998;7:310–6.
101. Popper HH, Klemen H, Hoefler G, Winter E. Presence of mycobacterial DNA in sarcoidosis. Hum Pathol. 1997;28:796–800.
102. Goldberg B, Sichtig H, Geyer C, Ledeboer N, Weinstock GM. Making the leap from research laboratory to clinic: challenges and opportunities for next-generation sequencing in infectious disease diagnostics. MBio. 2015;6:e01888–15.
103. Ranjan R, Rani A, Metwally A, McGee HS, Perkins DL. Analysis of the microbiome: advantages of whole genome shotgun versus 16S amplicon sequencing. Biochem Biophys Res Commun. 2016;469:967–77.
104. Liebow A, Carrington C. In: Simon M, Potchen E, LeMay M, editors. The interstitial pneumonias. Orlando: Grune & Stratton; 1969.
105. Katzenstein AL. Idiopathic interstitial pneumonia: classification and diagnosis. Monogr Pathol. 1993;36:1–31.
106. Katzenstein AL, Myers JL. Idiopathic pulmonary fibrosis: clinical relevance of pathologic classification. Am J Respir Crit Care Med. 1998;157:1301–15.
107. Yousem SA, Colby TV, Carrington CB. Lung biopsy in rheumatoid arthritis. Am Rev Respir Dis. 1985;131:770–7.
108. Hunninghake GW, Lynch DA, Galvin JR, Gross BH, Muller N, Schwartz DA, King Jr TE, Lynch 3rd JP, Hegele R, Waldron J, Colby TV, Hogg JC. Radiologic findings are strongly associated with a pathologic diagnosis of usual interstitial pneumonia. Chest. 2003;124:1215–23.
109. Johkoh T, Muller NL, Colby TV, Ichikado K, Taniguchi H, Kondoh Y, Fujimoto K, Kinoshita M, Arakawa H, Yamada H, Suga M, Ando M, Koyama M, Nakamura H. Nonspecific interstitial pneumonia: correlation between thin-section CT findings and pathologic subgroups in 55 patients. Radiology. 2002;225:199–204.
110. Travis WD, Matsui K, Moss J, Ferrans VJ. Idiopathic nonspecific interstitial pneumonia: prognostic significance of cellular and fibrosing patterns: survival comparison with usual interstitial pneumonia and desquamative interstitial pneumonia. Am J Surg Pathol. 2000;24:19–33.
111. Ziesche R, Hofbauer E, Wittmann K, Petkov V, Block LH. A preliminary study of long-term treatment with interferon gamma-1b and low-dose prednisolone in patients with idiopathic pulmonary fibrosis. N Engl J Med. 1999;341:1264–9.
112. Abati A, Cajigas A, Holland SM, Solomon D. Chronic granulomatous disease of childhood: respiratory cytology. Diagn Cytopathol. 1996;15:98–102.
113. Tabatowski K, Roggli VL, Fulkerson WJ, Langley RL, Benning T, Johnston WW. Giant cell interstitial pneumonia in a hard-metal worker. Cytologic, histologic and analytical electron microscopic investigation. Acta Cytol. 1988;32:240–6.
114. Raghu G, Collard HR, Egan JJ, Martinez FJ, Behr J, Brown KK, Colby TV, Cordier JF, Flaherty KR, Lasky JA, Lynch DA, Ryu JH, Swigris JJ, Wells AU, Ancochea J, Bouros D, Carvalho C, Costabel U, Ebina M, Hansell DM, Johkoh T, Kim DS, King Jr TE, Kondoh Y, Myers J, Muller NL, Nicholson AG, Richeldi L, Selman M, Dudden RF, Griss BS, Protzko SL, Schunemann HJ. An official ATS/ERS/JRS/ALAT statement: idiopathic pulmonary fibrosis: evidence-based guidelines for diagnosis and management. Am J Respir Crit Care Med. 2011;183:788–824.
115. Travis W, King T, Bateman E, et al. American Thoracic Society/European International Multidisciplinary consensus classification of the idiopathic interstitial pneumonias. ATS/ERS joint statement adopted by the ATS board of directors, June 2001 and by the ERS Executive Committee, June 2001. Am J Respir Crit Care Med. 2002;165:277–304.
116. Bjoraker JA, Ryu JH, Edwin MK, Myers JL, Tazelaar HD, Schroeder DR, Offord KP. Prognostic significance of histopathologic subsets in idiopathic pulmonary fibrosis. Am J Respir Crit Care Med. 1998;157:199–203.
117. Meltzer EB, Noble PW. Idiopathic pulmonary fibrosis. Orphanet J Rare Dis. 2008;3:8.
118. Raghu G. Idiopathic pulmonary fibrosis: guidelines for diagnosis and clinical management have advanced from consensus-based in 2000 to evidence-based in 2011. Eur Respir J. 2011;37:743–6.
119. Coward WR, Saini G, Jenkins G. The pathogenesis of idiopathic pulmonary fibrosis. Ther Adv Respir Dis. 2010;4:367–88.
120. Cha SI, Groshong SD, Frankel SK, Edelman BL, Cosgrove GP, Terry-Powers JL, Remigio LK, Curran-Everett D, Brown KK, Cool CD, Riches DW. Compartmentalized expression of c-FLIP in lung tissues of patients with idiopathic pulmonary fibrosis. Am J Respir Cell Mol Biol. 2010;42:140–8.
121. Lynch 3rd JP, Wurfel M, Flaherty K, White E, Martinez F, Travis W, Raghu G. Usual interstitial pneumonia. Semin Respir Crit Care Med. 2001;22:357–86.

122. White ES, Lazar MH, Thannickal VJ. Pathogenetic mechanisms in usual interstitial pneumonia/idiopathic pulmonary fibrosis. J Pathol. 2003;201:343–54.
123. Lepparanta O, Pulkkinen V, Koli K, Vahatalo R, Salmenkivi K, Kinnula VL, Heikinheimo M, Myllarniemi M. Transcription factor GATA-6 is expressed in quiescent myofibroblasts in idiopathic pulmonary fibrosis. Am J Respir Cell Mol Biol. 2010;42:626–32.
124. Chibbar R, Shih F, Baga M, Torlakovic E, Ramlall K, Skomro R, Cockcroft DW, Lemire EG. Nonspecific interstitial pneumonia and usual interstitial pneumonia with mutation in surfactant protein C in familial pulmonary fibrosis. Mod Pathol. 2004;17:973–80.
125. Garcia CK. Idiopathic pulmonary fibrosis: update on genetic discoveries. Proc Am Thorac Soc. 2011;8:158–62.
126. Bocchino M, Agnese S, Fagone E, Svegliati S, Grieco D, Vancheri C, Gabrielli A, Sanduzzi A, Avvedimento EV. Reactive oxygen species are required for maintenance and differentiation of primary lung fibroblasts in idiopathic pulmonary fibrosis. PLoS ONE. 2010;5:e14003.
127. Lee SH, Shim HS, Cho SH, Kim SY, Lee SK, Son JY, Jung JY, Kim EY, Lim JE, Lee KJ, Park BH, Kang YA, Kim YS, Kim SK, Chang J, Park MS. Prognostic factors for idiopathic pulmonary fibrosis: clinical, physiologic, pathologic, and molecular aspects. Sarcoidosis Vasc Diffuse Lung Dis. 2011;28:102–12.
128. Taskar VS, Coultas DB. Is idiopathic pulmonary fibrosis an environmental disease? Proc Am Thorac Soc. 2006;3:293–8.
129. Moeller A, Gilpin SE, Ask K, Cox G, Cook D, Gauldie J, Margetts PJ, Farkas L, Dobranowski J, Boylan C, O'Byrne PM, Strieter RM, Kolb M. Circulating fibrocytes are an indicator of poor prognosis in idiopathic pulmonary fibrosis. Am J Respir Crit Care Med. 2009;179:588–94.
130. Chilosi M, Zamo A, Doglioni C, Reghellin D, Lestani M, Montagna L, Pedron S, Ennas MG, Cancellieri A, Murer B, Poletti V. Migratory marker expression in fibroblast foci of idiopathic pulmonary fibrosis. Respir Res. 2006;7:95.
131. Degryse AL, Tanjore H, Xu XC, Polosukhin VV, Jones BR, McMahon FB, Gleaves LA, Blackwell TS, Lawson WE. Repetitive intratracheal bleomycin models several features of idiopathic pulmonary fibrosis. Am J Physiol Lung Cell Mol Physiol. 2010;299(4):L442–52.
132. Frankel SK, Cosgrove GP, Cha SI, Cool CD, Wynes MW, Edelman BL, Brown KK, Riches DW. TNF-alpha sensitizes normal and fibrotic human lung fibroblasts to Fas-induced apoptosis. Am J Respir Cell Mol Biol. 2006;34:293–304.
133. Kinnula VL, Hodgson UA, Lakari EK, Tan RJ, Sormunen RT, Soini YM, Kakko SJ, Laitinen TH, Oury TD, Paakko PK. Extracellular superoxide dismutase has a highly specific localization in idiopathic pulmonary fibrosis/usual interstitial pneumonia. Histopathology. 2006;49:66–74.
134. Kumar A, Dougherty M, Findlay GM, Geisheker M, Klein J, Lazar J, Machkovech H, Resnick J, Resnick R, Salter AI, Talebi-Liasi F, Arakawa C, Baudin J, Bogaard A, Salesky R, Zhou Q, Smith K, Clark JI, Shendure J, Horwitz MS. Genome sequencing of idiopathic pulmonary fibrosis in conjunction with a medical school human anatomy course. PLoS ONE. 2014;9:e106744.
135. Kropski JA, Mitchell DB, Markin C, Polosukhin VV, Choi L, Johnson JE, Lawson WE, Phillips JA, Cogan JD, Blackwell TS, Loyd JE. A novel dyskerin (DKC1) mutation is associated with familial interstitial pneumonia. Chest. 2014;146:e1–7.
136. Schmidt SL, Sundaram B, Flaherty KR. Diagnosing fibrotic lung disease: when is high-resolution computed tomography sufficient to make a diagnosis of idiopathic pulmonary fibrosis? Respirology. 2009;14:934–9.
137. Flaherty KR, Thwaite EL, Kazerooni EA, Gross BH, Toews GB, Colby TV, Travis WD, Mumford JA, Murray S, Flint A, Lynch 3rd JP, Martinez FJ. Radiological versus histological diagnosis in UIP and NSIP: survival implications. Thorax. 2003;58:143–8.
138. Flaherty KR, Andrei AC, King Jr TE, Raghu G, Colby TV, Wells A, Bassily N, Brown K, du Bois R, Flint A, Gay SE, Gross BH, Kazerooni EA, Knapp R, Louvar E, Lynch D, Nicholson AG, Quick J, Thannickal VJ, Travis WD, Vyskocil J, Wadenstorer FA, Wilt J, Toews GB, Murray S, Martinez FJ. Idiopathic interstitial pneumonia: do community and academic physicians agree on diagnosis? Am J Respir Crit Care Med. 2007;175:1054–60.
139. Flaherty KR, King Jr TE, Raghu G, Lynch 3rd JP, Colby TV, Travis WD, Gross BH, Kazerooni EA, Toews GB, Long Q, Murray S, Lama VN, Gay SE, Martinez FJ. Idiopathic interstitial pneumonia: what is the effect of a multidisciplinary approach to diagnosis? Am J Respir Crit Care Med. 2004;170:904–10.
140. Morell F, Villar A, Montero MA, Munoz X, Colby TV, Pipvath S, Cruz MJ, Raghu G. Chronic hypersensitivity pneumonitis in patients diagnosed with idiopathic pulmonary fibrosis: a prospective case-cohort study. Lancet Respir Med. 2013;1:685–94.
141. Lee HL, Ryu JH, Wittmer MH, Hartman TE, Lymp JF, Tazelaar HD, Limper AH. Familial idiopathic pulmonary fibrosis: clinical features and outcome. Chest. 2005;127:2034–41.
142. Leslie KO, Cool CD, Sporn TA, Curran-Everett D, Steele MP, Brown KK, Wahidi MM, Schwartz DA. Familial idiopathic interstitial pneumonia: histopathology and survival in 30 patients. Arch Pathol Lab Med. 2012;136:1366–76.
143. Cottin V, Donsbeck AV, Revel D, Loire R, Cordier JF. Nonspecific interstitial pneumonia.

Individualization of a clinicopathologic entity in a series of 12 patients. Am J Respir Crit Care Med. 1998;158:1286–93.
144. Arakawa H, Yamada H, Kurihara Y, Nakajima Y, Takeda A, Fukushima Y, Fujioka M. Nonspecific interstitial pneumonia associated with polymyositis and dermatomyositis: serial high-resolution CT findings and functional correlation. Chest. 2003;123:1096–103.
145. Bouros D, Wells AU, Nicholson AG, Colby TV, Polychronopoulos V, Pantelidis P, Haslam PL, Vassilakis DA, Black CM, du Bois RM. Histopathologic subsets of fibrosing alveolitis in patients with systemic sclerosis and their relationship to outcome. Am J Respir Crit Care Med. 2002;165:1581–6.
146. Kim DS, Yoo B, Lee JS, Kim EK, Lim CM, Lee SD, Koh Y, Kim WS, Kim WD, Colby TV, Kitiaichi M. The major histopathologic pattern of pulmonary fibrosis in scleroderma is nonspecific interstitial pneumonia. Sarcoidosis Vasc Diffuse Lung Dis. 2002;19:121–7.
147. Yoshinouchi T, Ohtsuki Y, Fujita J, Yamadori I, Bandoh S, Ishida T, Ueda R. Nonspecific interstitial pneumonia pattern as pulmonary involvement of rheumatoid arthritis. Rheumatol Int. 2005;26:121–5.
148. Jinta T, Miyazaki Y, Kishi M, Akashi T, Takemura T, Inase N, Yoshizawa Y. The pathogenesis of chronic hypersensitivity pneumonitis in common with idiopathic pulmonary fibrosis: expression of apoptotic markers. Am J Clin Pathol. 2010;134:613–20.
149. Martin N, Innes JA, Lambert CM, Turnbull CM, Wallace WA. Hypersensitivity pneumonitis associated with leflunomide therapy. J Rheumatol. 2007;34:1934–7.
150. Daniil ZD, Gilchrist FC, Nicholson AG, Hansell DM, Harris J, Colby TV, du Bois RM. A histologic pattern of nonspecific interstitial pneumonia is associated with a better prognosis than usual interstitial pneumonia in patients with cryptogenic fibrosing alveolitis. Am J Respir Crit Care Med. 1999;160:899–905.
151. Fujisawa T, Suda T, Nakamura Y, Enomoto N, Ide K, Toyoshima M, Uchiyama H, Tamura R, Ida M, Yagi T, Yasuda K, Genma H, Hayakawa H, Chida K, Nakamura H. Differences in clinical features and prognosis of interstitial lung diseases between polymyositis and dermatomyositis. J Rheumatol. 2005;32:58–64.
152. Tanaka N, Newell JD, Brown KK, Cool CD, Lynch DA. Collagen vascular disease-related lung disease: high-resolution computed tomography findings based on the pathologic classification. J Comput Assist Tomogr. 2004;28:351–60.
153. Popper HH. Bronchiolitis obliterans. Organizing pneumonia. Verh Dtsch Ges Pathol. 2002;86:101–6.
154. Myers JL, Katzenstein AL. Ultrastructural evidence of alveolar epithelial injury in idiopathic bronchiolitis obliterans-organizing pneumonia. Am J Pathol. 1988;132:102–9.
155. Uner AH, Rozum-Slota B, Katzenstein AL. Bronchiolitis obliterans-organizing pneumonia (BOOP)-like variant of Wegener's granulomatosis. A clinicopathologic study of 16 cases. Am J Surg Pathol. 1996;20:794–801.
156. Churg A, Myers J, Suarez T, Gaxiola M, Estrada A, Mejia M, Selman M. Airway-centered interstitial fibrosis: a distinct form of aggressive diffuse lung disease. Am J Surg Pathol. 2004;28:62–8.

Immunological Lung Diseases

9

9.1 Introduction into Interstitial Lung Diseases

Most of the diseases discussed here present as interstitial lung diseases and thus are characterized by a diffuse infiltration of both lungs, usually evaluated by high-resolution CT scan (HRCT). The types of infiltrating cells are not predefined, so this can be inflammatory as well as tumorlike cells. Here we recapitulate the algorithm in evaluating ILDs (Table 9.1).

9.2 Autoimmune Diseases

In autoimmune-induced interstitial lung disease, many different factors come together: a wide variety of immune reactions can cause a wide variety of tissue reactions, for example, circulating autoantibodies either capable or devoid of complement activation, circulating immune complexes including large insoluble immune complexes formed by idiotypic-anti-idiotypic antibody networks, activation of coagulation, metabolism of pro-inflammatory substances, involvement of different types of leukocytes, and not the least drugs given for the relief of symptoms. These drugs themselves can cause toxic or inflammatory side effects. Another aspect in autoimmune diseases lies within its dynamic: an acute phase is changed into a phase with declining symptoms, going into a resolving stage, again starting acute, but also can progress into a subacute and chronic phase. Each of these phases will be accompanied by a different histology. This is why interpretation is difficult and will need a good understanding of immune mechanisms. Each of the different diseases will induce a different reaction pattern, and this pattern will be modified during the course of the disease. Therefore we cannot expect a single reaction or pattern, but a complex picture composed of new and old lesions, resolving lesions, and acute exacerbations of the disease. It will always be of help to know the mechanisms and underlying pathogenesis of each disease to interpret the histological picture in its presented form.

Since we have already extensively discussed the different interstitial pneumonias, we will focus now on the spectrum of lesions and combinations thereof induced by autoimmune diseases.

9.2.1 Rheumatoid Lung Disease

Interstitial pneumonia in rheumatoid arthritis (RhA) is not uncommon, but is often complicated by additional drug reactions, which can look like RhA-induced pneumonia. Most often NSIP is associated with this disease [2, 3], but these reported studies have in common a selection bias: they looked up the incidence of RhA in cases presenting with NSIP. The diversity of reaction patterns is much better reflected in studies looking up

© Springer-Verlag Berlin Heidelberg 2017
H. Popper, *Pathology of Lung Disease*, DOI 10.1007/978-3-662-50491-8_9

Table 9.1 Diagnostic algorithm for idiopathic interstitial lung diseases as already shown in fibrosing pneumonias Modified from Travis et al. [1]
Here the focus is on autoimmune diseases, genetically and developmental diseases, and some interstitial processes of various causes

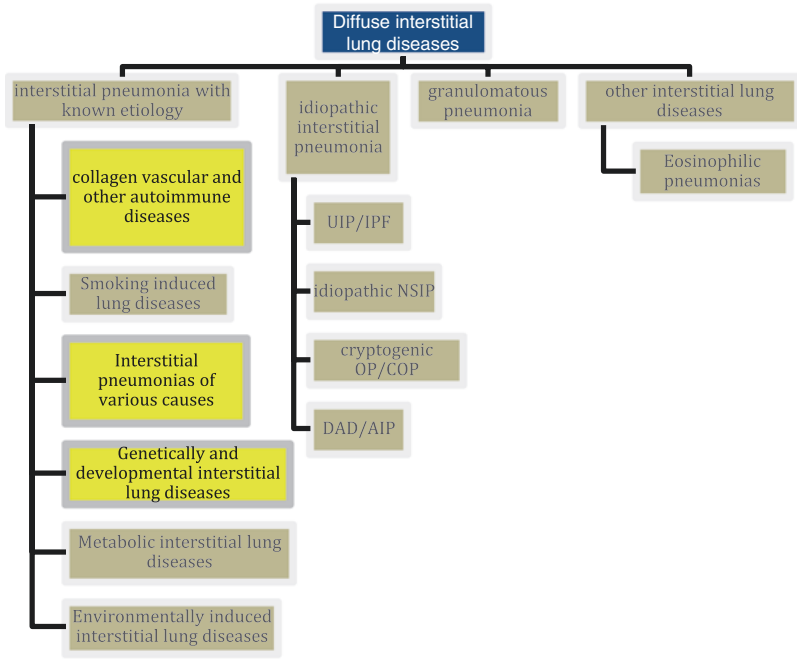

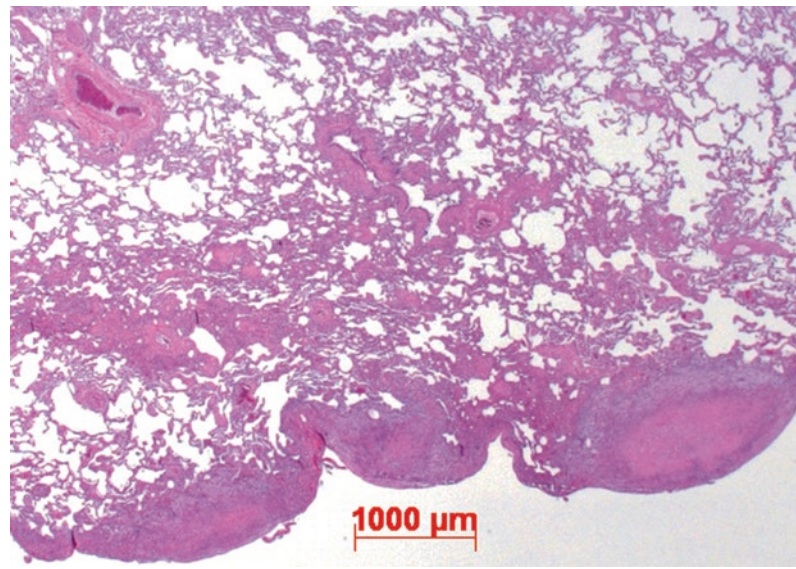

Fig. 9.1 Rheumatoid arthritis with numerous necrotizing histiocytic granulomas. In this case, many granulomas are involving the peripheral lung as well as the pleura. H&E, bar 1 mm

patients with RhA and lung involvement [4]. UIP was more common in this study. In my own experience, most often a mixture of reaction patterns occurred, such as UIP combined with dense lymphocytic infiltrates or LIP and UIP combined with OP or NSIP. If features of DAD occur, one should stress drug reactions with the clinicians, because many immunosuppressive drugs given in RhA and other collagen vascular diseases (CVD) can cause DAD [5–8]. Not uncommonly granulomas are present too. These are most often foreign body-type granulomas with giant cells, sometimes classical rheumatoid granulomas with palisading histiocytes, and rarely epithelioid cell granulomas [5] (Figs. 9.1, 9.2, 9.3, and 9.4). More common than granulomas is lymphocytic pneumonia

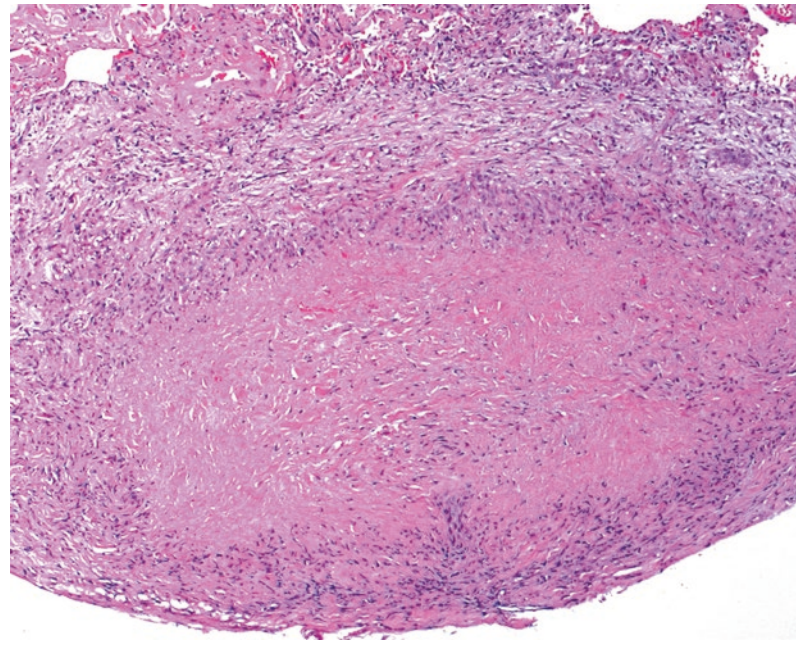

Fig. 9.2 Higher magnification of one granuloma from previous figure: the palisading of the histiocytes is seen; within the necrotic center, remnants of collagen fibers can be appreciated. H&E, ×100

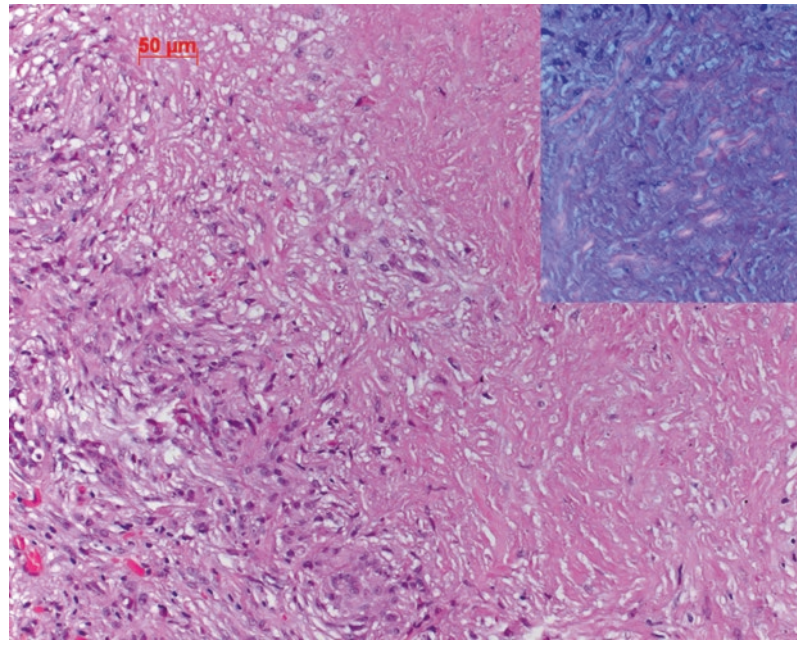

Fig. 9.3 Same granuloma in higher magnification. There is no nuclear debris as it would be seen in infectious granulomas, but collagen remnants are seen. In the *inset*, this was semi-polarized to highlight the collagen fibers. H&E, ×260

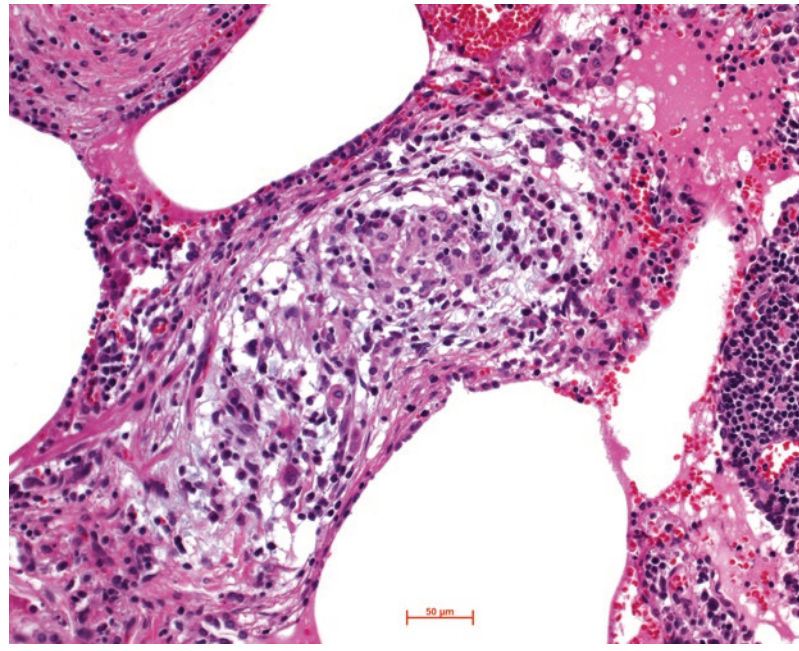

Fig. 9.4 Epithelioid cell granuloma in a case of rheumatoid arthritis

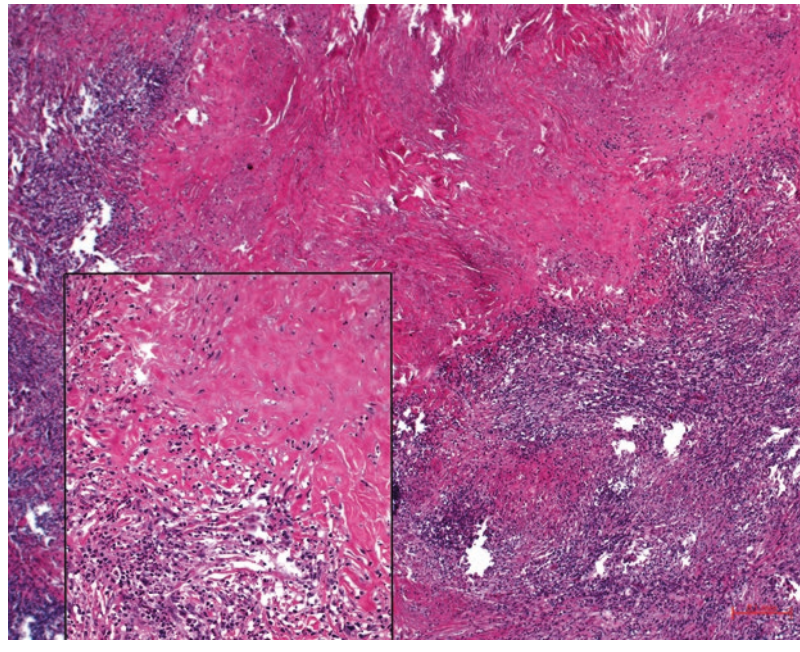

Fig. 9.5 LIP pattern combined with amyloid deposition in form of an amyloidoma (single nodule). The amyloid material stained positively for amyloid P and microglobulin and also showed green birefringence on polarization. The inset shows foreign body cells in higher magnification. H&E, ×50 and 100

combined with other patterns such as amyloid deposition (Fig. 9.5), LIP combined UIP (Figs. 9.6 and 9.7), and LIP combined OP (Fig. 9.8). Most often there is LIP pattern sometimes with fibrosis and ill-formed granulomas (Fig. 9.9). In classical rheumatoid granulomas, it is essential to exclude infectious organisms, since patients receiving immunosuppressive drugs like methotrexate and leflunomide are prone to acquire infections [8–10]. This is even more important with the new "biologicals." As these drugs can also induce pneumonias, it is important to know these reactions. Gold salts can induce LIP or granulomatous reactions, leflunomide can induce DAD [8] (Fig. 9.10), and methotrexate can induce NSIP, LIP, and OP in the resolving phase.

The etiology of rheumatoid arthritis is still an enigma. Genetic variants for several immune regulators such as Toll receptors and interleukins may form the basis for the susceptibility to adversely react against antigens and immune complexes trapped in cartilages and by that induce an inflammatory reaction resulting in cartilage damage [11, 12]. Regulatory T cells either deficient or functionally impaired might also play an important role in rheumatoid arthritis. In addition to the genetic basis for the disease, the autoimmune reaction might be triggered by streptococcal infections, and in that respect, probably mimicry of proteins of the organism might come into play.

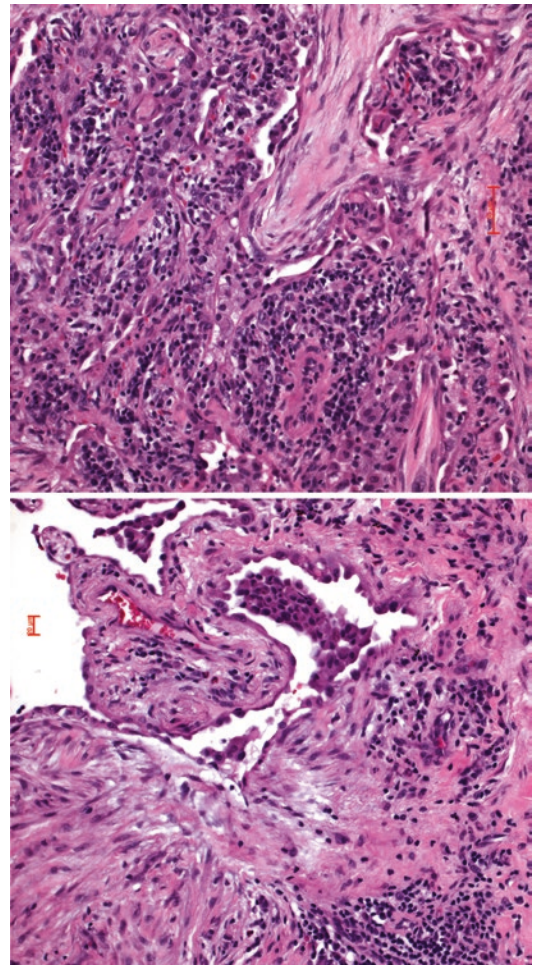

Fig. 9.6 LIP combined UIP in rheumatoid arthritis. Foci of myofibroblast proliferations are shown in both panels; in the upper one, this focus may raise the differential diagnosis of organizing pneumonia, whereas in the lower panel, the focus is clearly within the septum. In both a dense lymphocytic infiltration is present, extending into the fibroblast foci. H&E, bars 50 μm and 20 μm

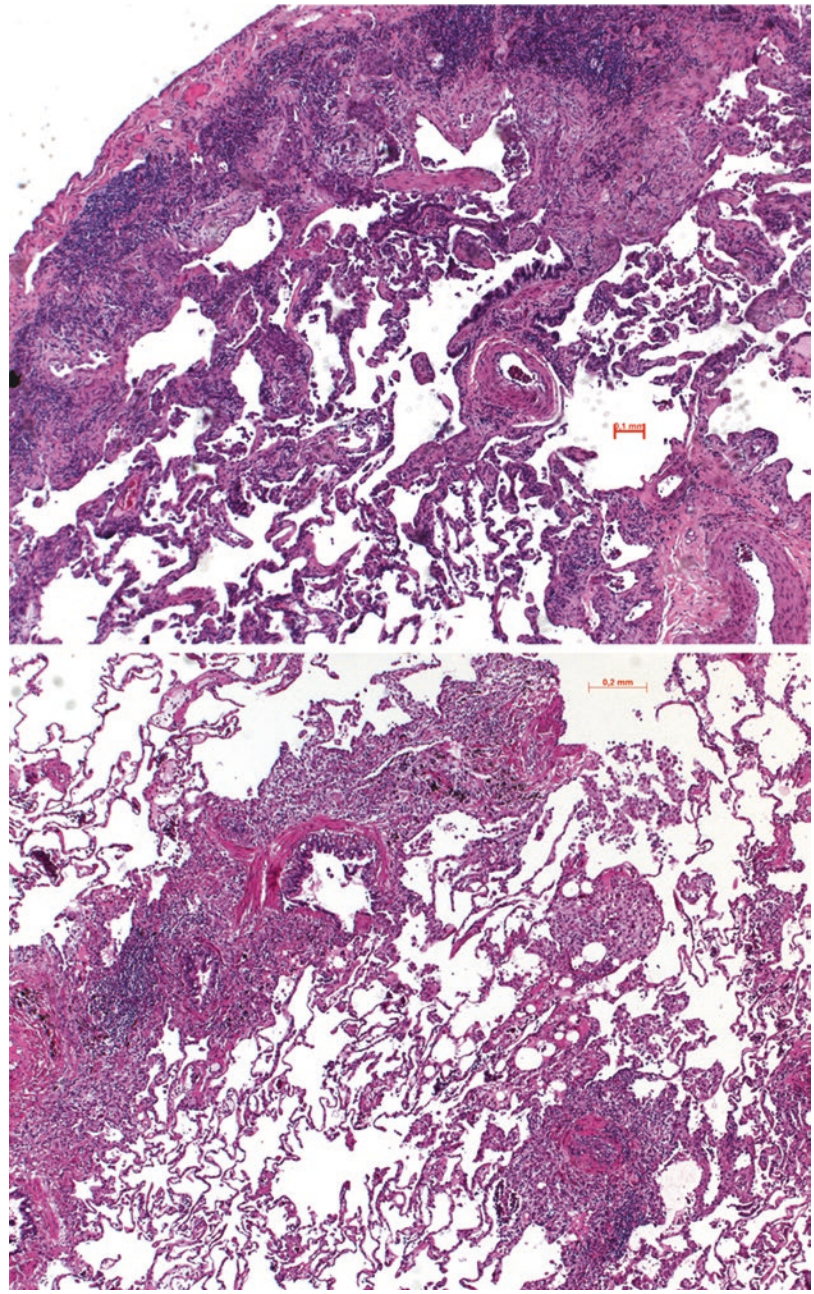

Fig. 9.7 Another case of RhA presenting with LIP combined UIP. The lesion is predominantly at the periphery, with dense lymphocytic infiltrations, some lymph follicles, fibroblast foci, and cystic remodeling of the lung (*upper panel*). Another focus (*lower panel*) showed LIP patterns and focal fibrosis, but also areas of uninvolved lung. On CT scan, this case was interpreted as UIP pattern. H&E, bars 100 μm and 200 μm

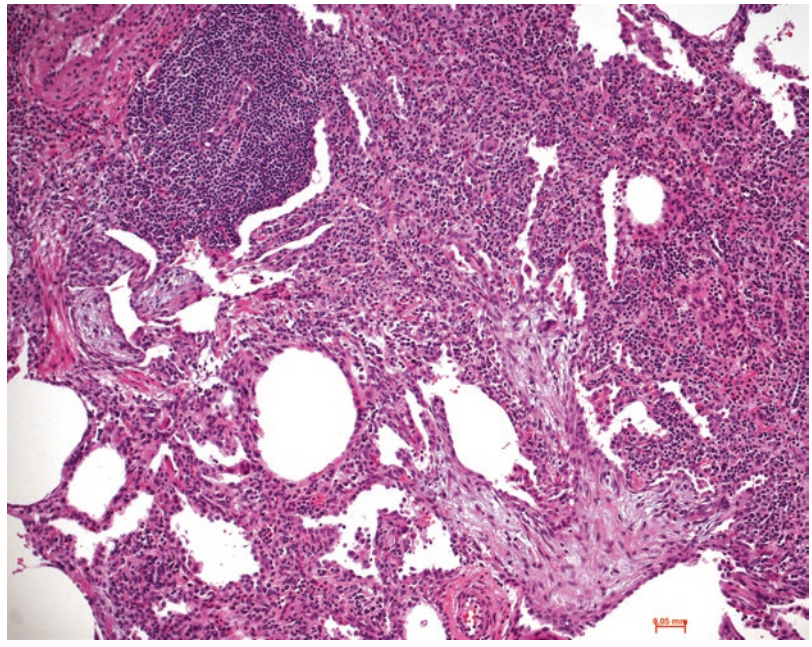

Fig. 9.8 LIP combined with OP in RhA. A lymph follicle is in the *upper left corner*. H&E, bar 50 μm

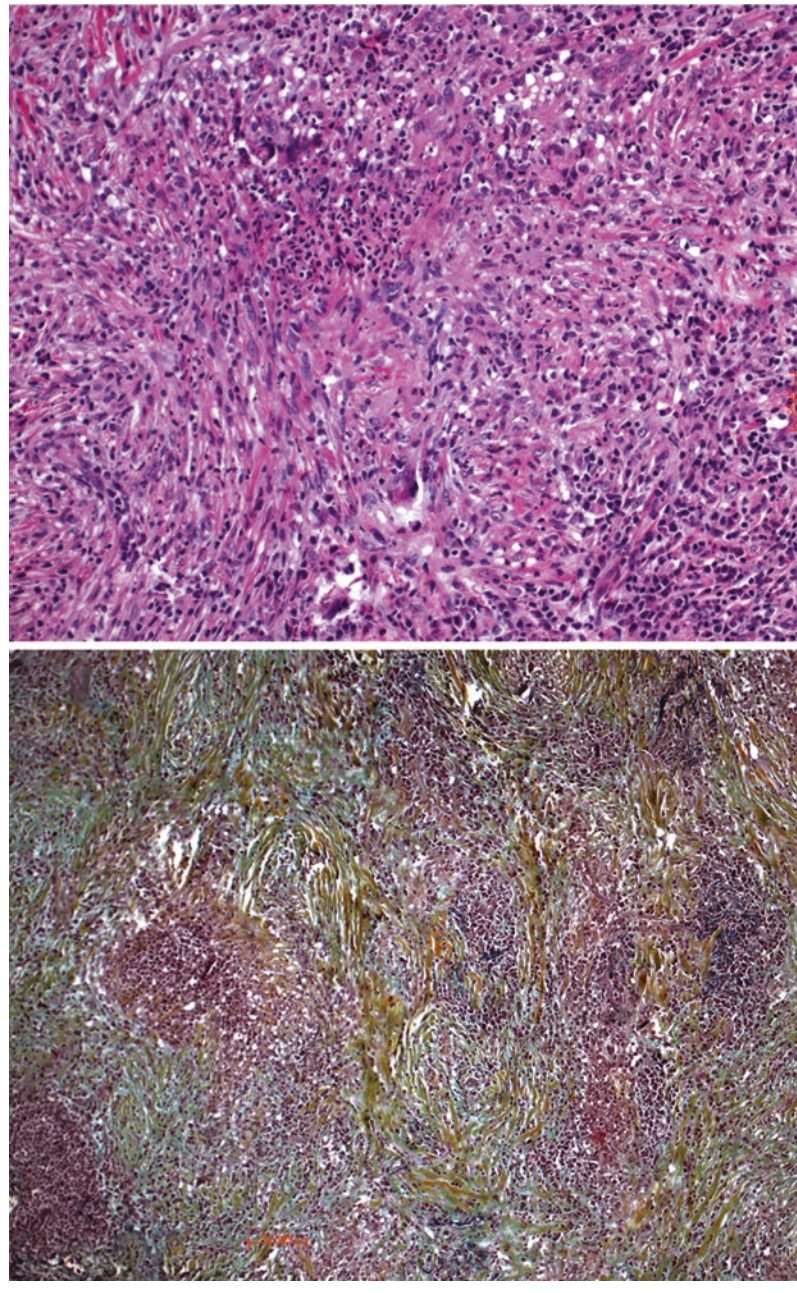

Fig. 9.9 Classical LIP in RhA, however, and also diffuse fibrosis. There was a dense lymphocytic infiltration throughout with many lymph follicles. Focally there were accumulations of neutrophils and histiocytic cells, a few multinucleated. In the *lower panel*, the same focus is shown in Movat stain highlighting mature (*yellow*) and immature (*green*) fibrosis. Clinically this was acute exacerbation of RhA. H&E, Movat, bars 50 μm

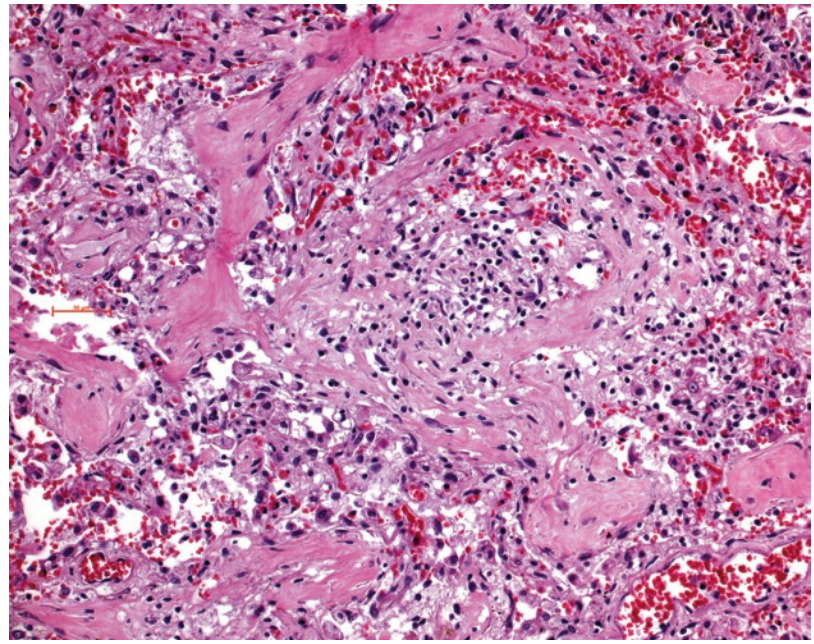

Fig. 9.10 DAD being organized by granulation tissue in a patient with RhA treated with leflunomide. This will later on develop into organizing pneumonia. H&E, bar 50 µm

9.2.2 Systemic Lupus Erythematosus

Localized lupus is usually seen in dermatology and rarely biopsied. Acute systemic lupus with lung manifestation is more often autopsied and rarely seen as surgical material. A variety of morphological patterns are found as hemorrhagic pneumonia, infarcts, or DAD or all mixed [13–15]. Most probably the extent of any of these reactions depends on the extent of intravascular death of neutrophils attacked by lupus autoantibodies: low numbers of dying neutrophils might release less toxic enzymes and therefore cause focal endothelial cell death and interstitial edema; proteins leak out into alveolar spaces and finally DAD with hyaline membrane formation occur (Fig. 9.11). In case of massive neutrophilic cell death, there might be massive leakage of vessel walls, and hemorrhage will occur (Fig. 9.12). In later stages, DAD will be organized, so OP is another feature found in systemic lupus (Fig. 9.13). Since the disease affects the coagulation cascade, lung infarction is a common feature of SLE. Perivascular amyloidosis is another feature in active SLE most often combined with other patterns (Fig. 9.14). Most likely amyloid deposition is associated with the deposition of immune complexes. These complexes can be large, as an immune complex may be additionally cause formation of idiopathic autoantibodies, followed by complex formation. So finally several orders of immune complex idiotypic-anti-idiotypic autoantibody complexes are formed, which are no longer soluble and therefore are deposited in the stroma. Another common finding is pleuritis. In these cases, a careful examination of the lesion is necessary as one might find LE phenomenon in the inflammatory infiltrate (Fig. 9.15). Lymphocytic infiltrations are less common in active SLE in contrast to RhA. Finally the occurrence of pulmonary hypertension with sclerosis and stenosis of pulmonary blood vessels is less well understood [16, 17] (Fig. 9.16).

The etiology of SLE is also not well understood. Autoantibodies directed against granulocytic enzymes have been shown to be secondary effects and not the cause of SLE. In a recent study in familial forms of SLE, a null mutation in the DNASE1L3 gene has been found. This finding confirms the critical role of impaired clearance of degraded DNA in SLE as a probable cause, a finding also seen in adult SLE [18]. However, given the wide range of autoantibodies found in SLE, there might be much more autoimmune mechanisms involved than anticipated [19–21].

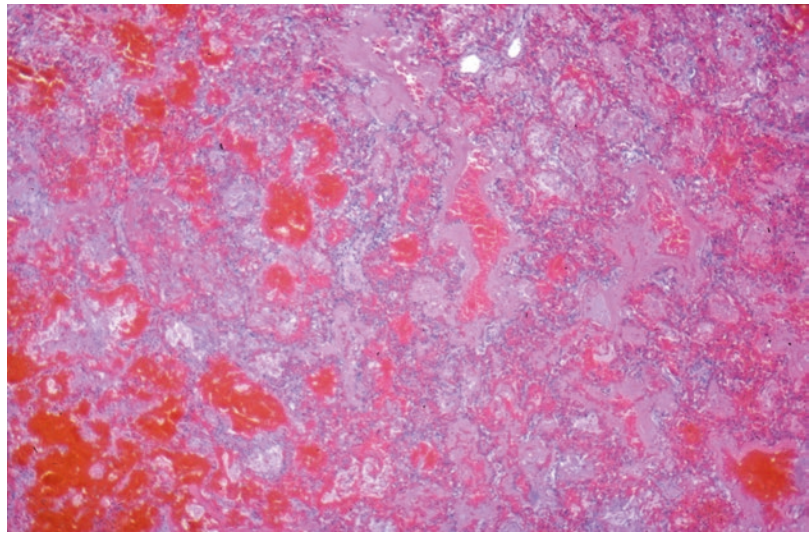

Fig. 9.11 Acute SLE with hemorrhage and hyaline membrane formation; autopsy case. H&E, ×50

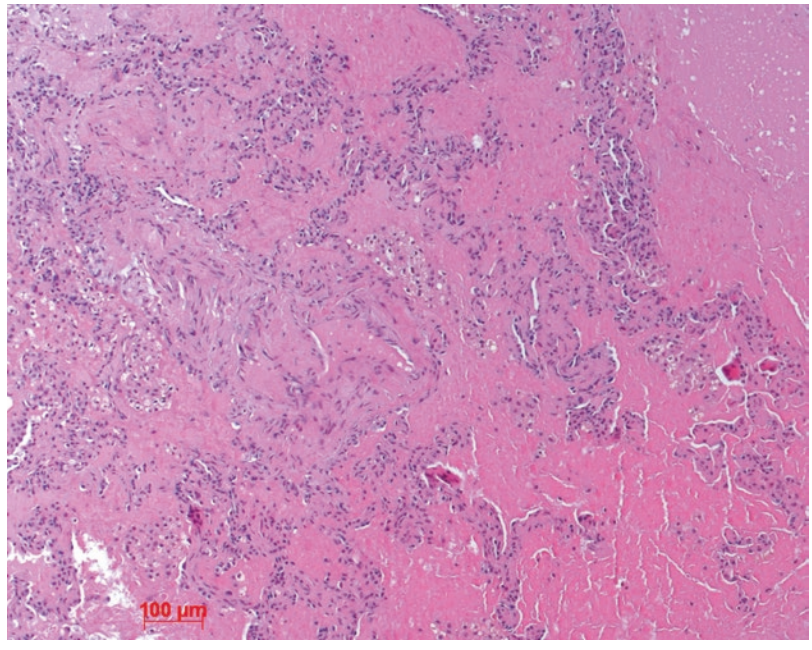

Fig. 9.12 Acute hemorrhage in SLE. Focal hemosiderin-laden macrophages are present pointing to previous hemorrhage. This also helps to sort out artificial bleeding from real hemorrhage. H&E, bar 100 µm

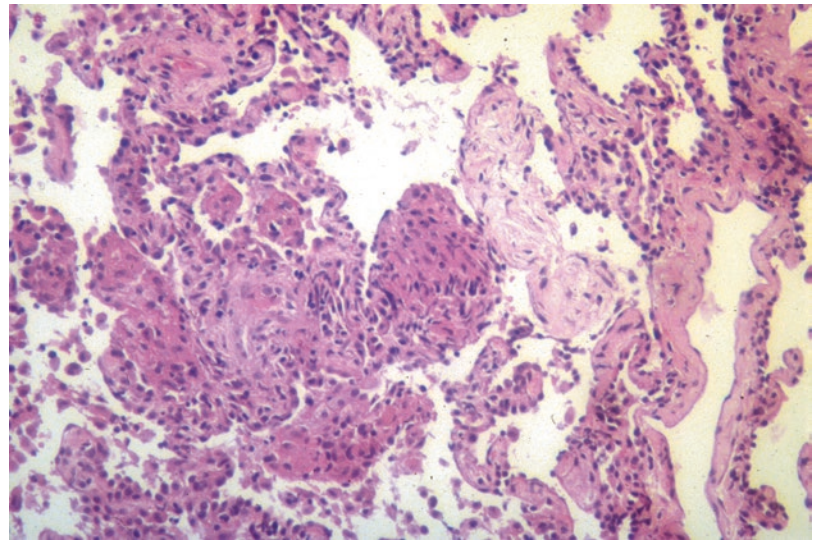

Fig. 9.13 Organizing pneumonia was the only finding in this transbronchial biopsy from a patient with SLE. Clinically the patient was in resolving phase and under immunosuppressive drugs. H&E, ×200

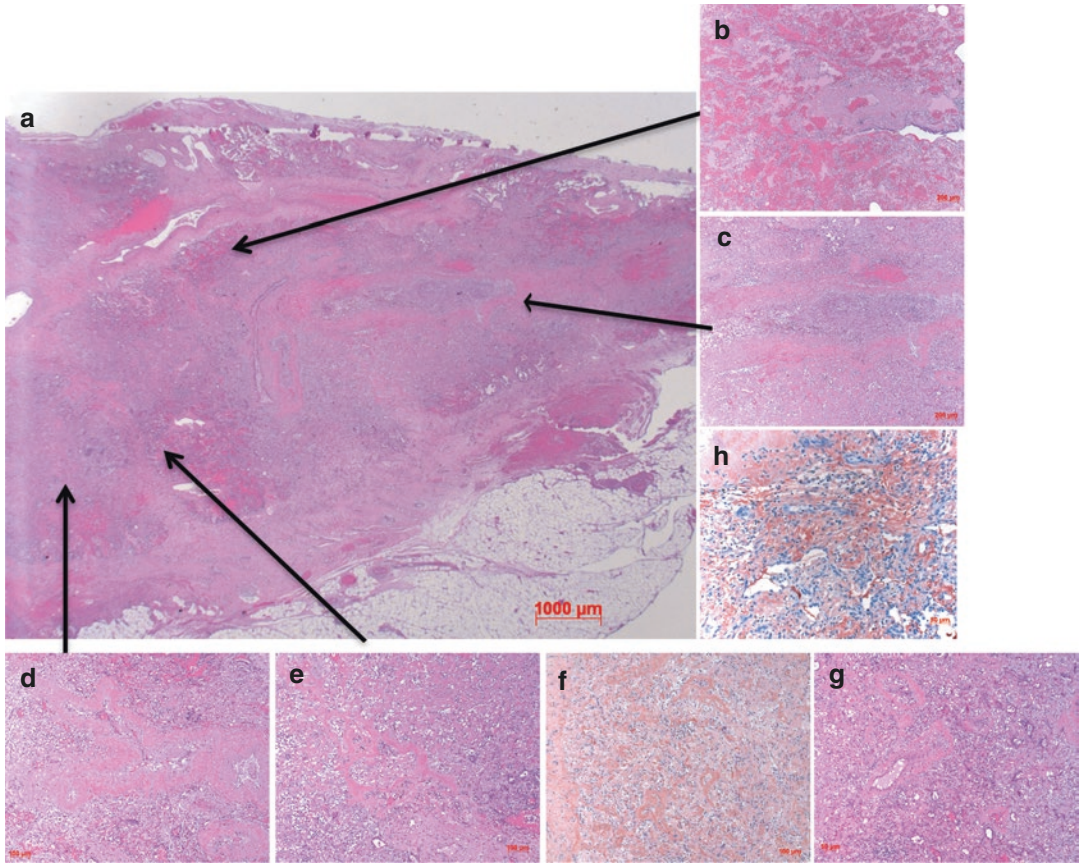

Fig. 9.14 Complex pattern in acute SLE: (**a**) shows the overview of the VATS biopsy. In (**b**) hemorrhage is the dominant pattern; in (**c**) there is occlusion of a pulmonary artery causing an infarct; in (**d**, **e**) there is amyloid deposition, within pulmonary arteries as well as interstitial. This is proven by Congo red stain in (**f**); on polarization this was green. In (**g**) there is already organization of hemorrhage and amyloid by unspecific granulation tissue. (**h**) By immunohistochemistry, deposition of immune complexes with IgG2 autoantibodies was proven, in which complexes also activated the classical complement cascade. (**a**–**h**): H&E, bars 1 mm, 100, and 50 µm, Congo red 100 µm, immunohistochemistry for IgG 50 µm

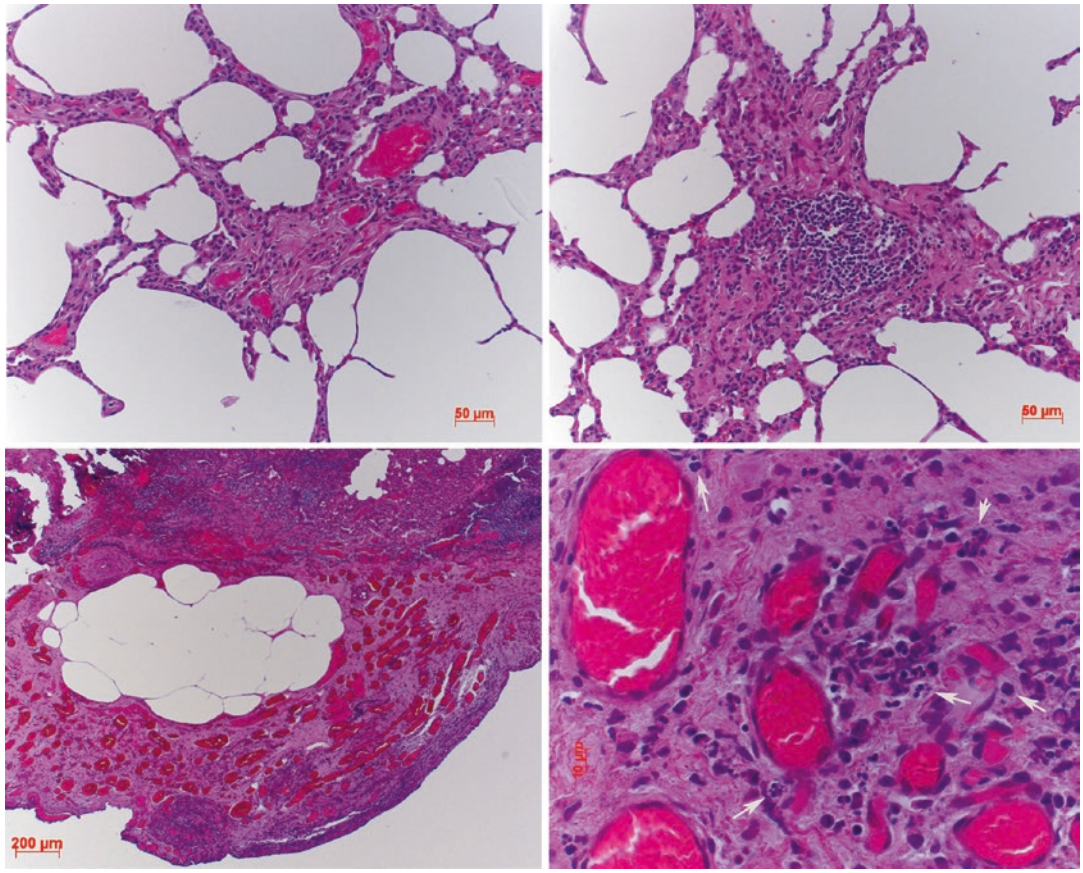

Fig. 9.15 SLE in a 15-year-old girl. Within the lung tissue, there was only focal and mild lymphocytic infiltration (*upper panels*). In the pleura (*lower panel left*), there was hemorrhage and dense granulocytic infiltration, which did not fit into the whole picture. On high power, the neutrophils showed the LE phenomenon. H&E, bars 50, 200 µm, 10 µm

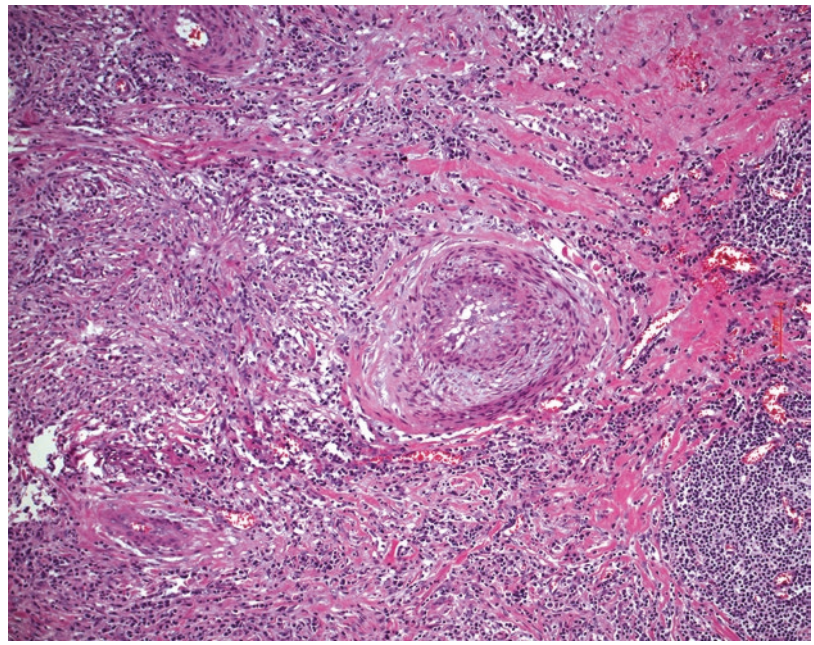

Fig. 9.16 Sclerosis and stenosis of pulmonary arteries in a case of SLE. In addition there is dense lymphocytic infiltration. H&E, bar 100 µm

9.2.3 Systemic Sclerosis

Systemic sclerosis (SSc) usually presents with a mixture of tissue reactions, dependent on the immune phenomena present at the time of biopsy. Most often an UIP or NSIP pattern is found; some cases present as LIP with hyperplasia of BALT (Figs. 9.17, 9.18, and 9.19). Germinal centers are less common compared to Sjøgren's syndrome. Ill-formed granulomas composed of histiocytic and/or epithelioid cells can be seen (Fig. 9.20). The distribution pattern of the interstitial pneumonia is irregular, involving peripheral as well as mid-zone areas of the lung. This is clinically helpful in separating it from UIP/IPF. Another feature helpful in the diagnosis is a vasculopathy. Medium- and small-sized arteries show a thickening of the intima and media. Within the thickened vessel wall, there is a myxoid change of the matrix. A few lymphocytes can be seen, however, no endothelial necrosis or any other sign of vasculitis. These changes can possibly be best interpreted as a consequence of immune complex deposition (Fig. 9.21). Functionally these vascular changes will cause pulmonary hypertension, which is common in systemic sclerosis [22, 23].

Genetic studies provided some new insights into SSc. Interleukins especially IL8 has an impact on lung fibrosis in SSc patients [24]. Also transforming growth factor-beta (TGF-β) and connective tissue growth factor (CTGF) received attention as essential factors in the pathogenesis of SSc. CTGF mRNA expression was observed in the fibrotic lesions; serum CTGF concentrations were significantly elevated and correlated with skin sclerosis and lung fibrosis. In an animal model, TGF-β-induced subcutaneous fibrosis and subsequent CTGF application caused persistent fibrosis. Based on these data, the authors of this study hypothesized that TGF-β induces fibrosis in the early stage, whereas CTGF acts to maintain tissue fibrosis [25]. In another study, fibrillin has been investigated. It has been demonstrated that caveolin-1 and fibrillin-1 influence storage and regulation of TGF-β and other cytokines and fibrillin-1 mutations might be responsible for a congenital form of scleroderma called stiff skin syndrome [26, 27]. In addition to tissue-resident fibroblasts, also bone marrow-derived fibroblasts and endothelial and epithelial cells undergoing epithelial-mesenchymal transition (EMT) are under the control of fibrillin. Gain-of-function and loss-of-function abnormalities of these mediators may account for the characteristic activated phenotype of SSc fibroblasts [27]. The impaired expression of the nuclear orphan receptor PPAR-γ in SSc seems to play an important role in causing uncontrolled progression of fibrosis through impaired control of fibroblast activation and differentiation [28].

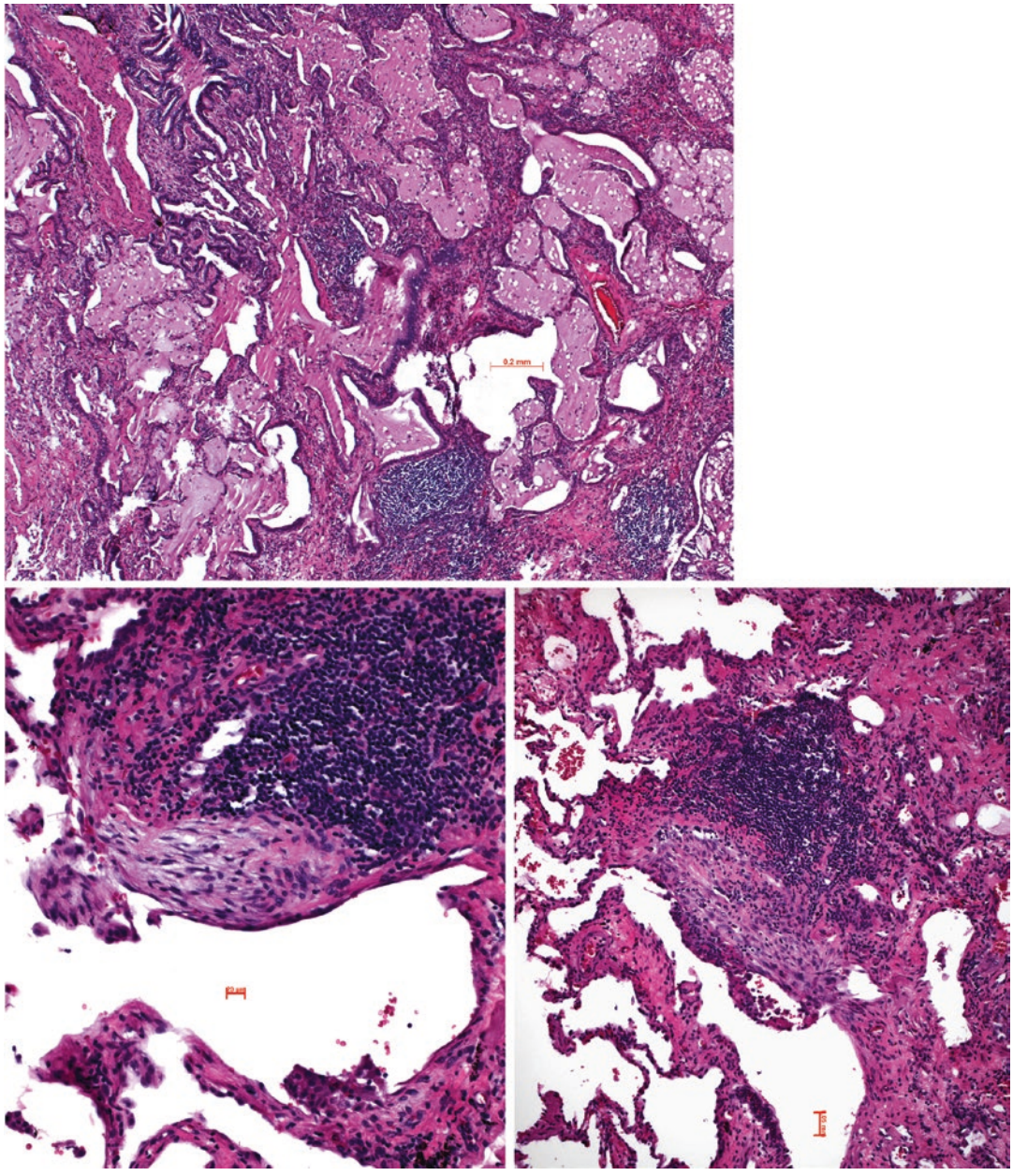

Fig. 9.17 Systemic sclerosis with a combination of UIP and LIP patterns. In the *upper panel*, there is cystic remodeling of alveolar tissue and dense lymphocytic infiltration with several lymph follicles; in the *lower panel*, myofibroblastic foci associated with lymphocytic infiltration are seen. H&E, bars 200, 20, and 50 μm

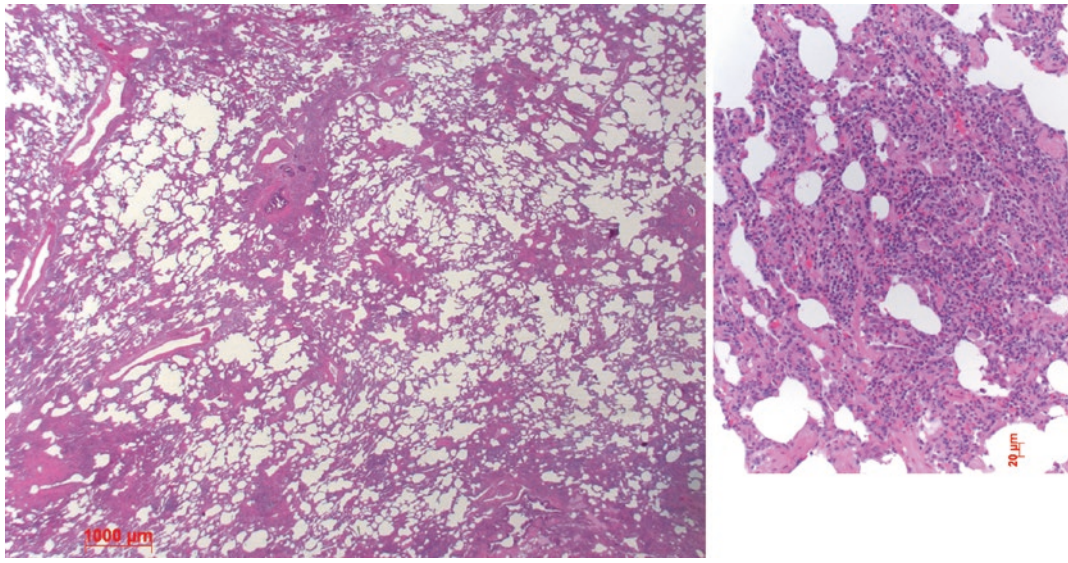

Fig. 9.18 Systemic sclerosis with NSIP pattern. Left overview, right magnification showing a mixed infiltrate of lymphocytes, plasma cells, and histiocytes. H&E, bars 1 mm and 20 µm

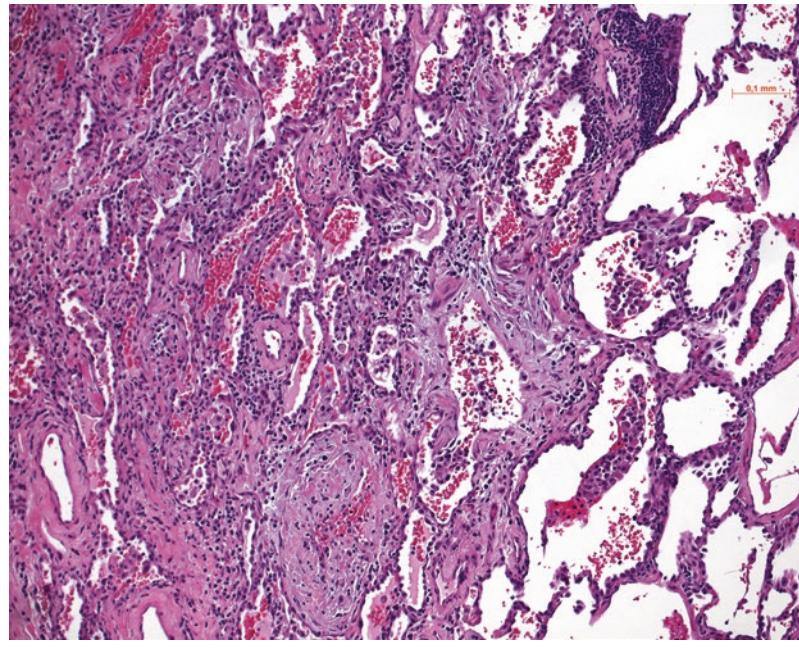

Fig. 9.19 Systemic sclerosis with fibrosing NSIP pattern. H&E, bar 100 µm

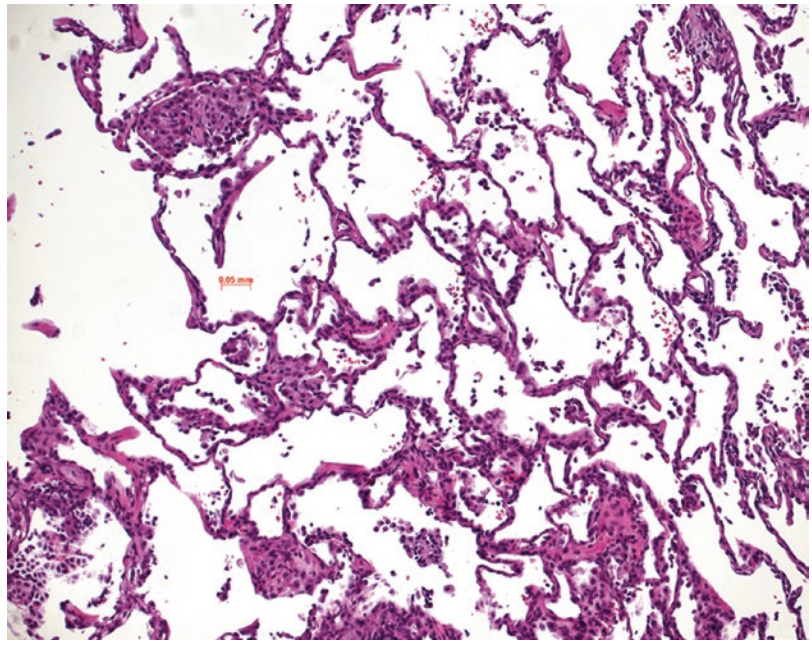

Fig. 9.20 Systemic sclerosis with an ill-formed histiocytic granuloma in the upper left corner. H&E, bar 50 µm

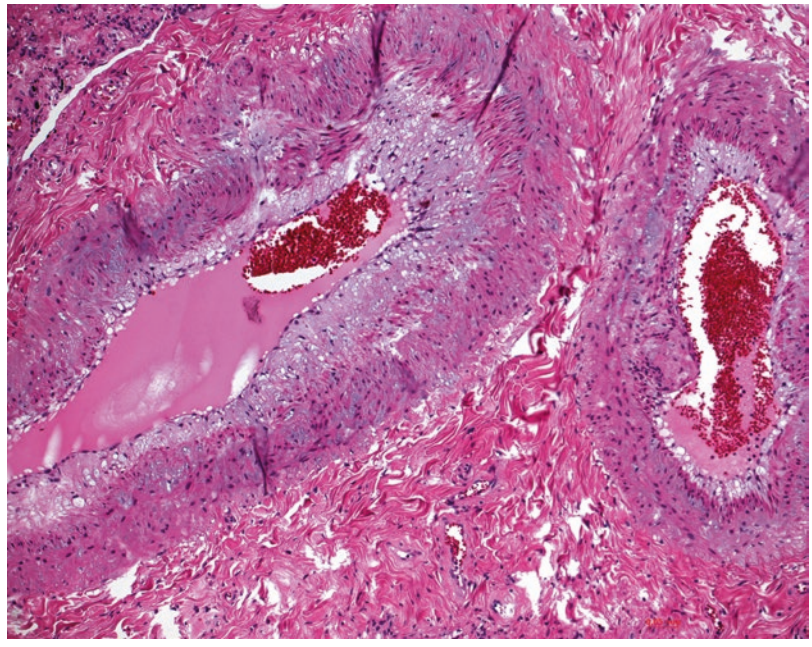

Fig. 9.21 Systemic sclerosis with vasculopathy. This is a common phenomenon in SSc not seen in other autoimmune diseases. Together with the mixed interstitial pneumonia pattern, it allows in some cases to directly suppose the diagnosis from the pathological report. H&E, ×250

9.2.4 Dermatomyositis/ Polyserositis

Dermatomyositis rarely affects the lung. If lung involvement is present, various forms and combinations of pneumonias can occur. UIP and NSIP are the most common alterations; however, histiocytic and ill-formed epithelioid cell granulomas can be encountered in some cases in my personal experience. Lymphocytic infiltrates are quite common, most often exceeding what is seen in NSIP and better matched by LIP (Figs. 9.22 and 9.23). Vasculopathy is rare. The serosa is usually involved too; this is common in other CVDs. Polyserositis in contrast to the other CVDs cannot be diagnosed on tissues, since these serosal infiltrations are unspecific and occur in a multitude of diseases (Fig. 9.24).

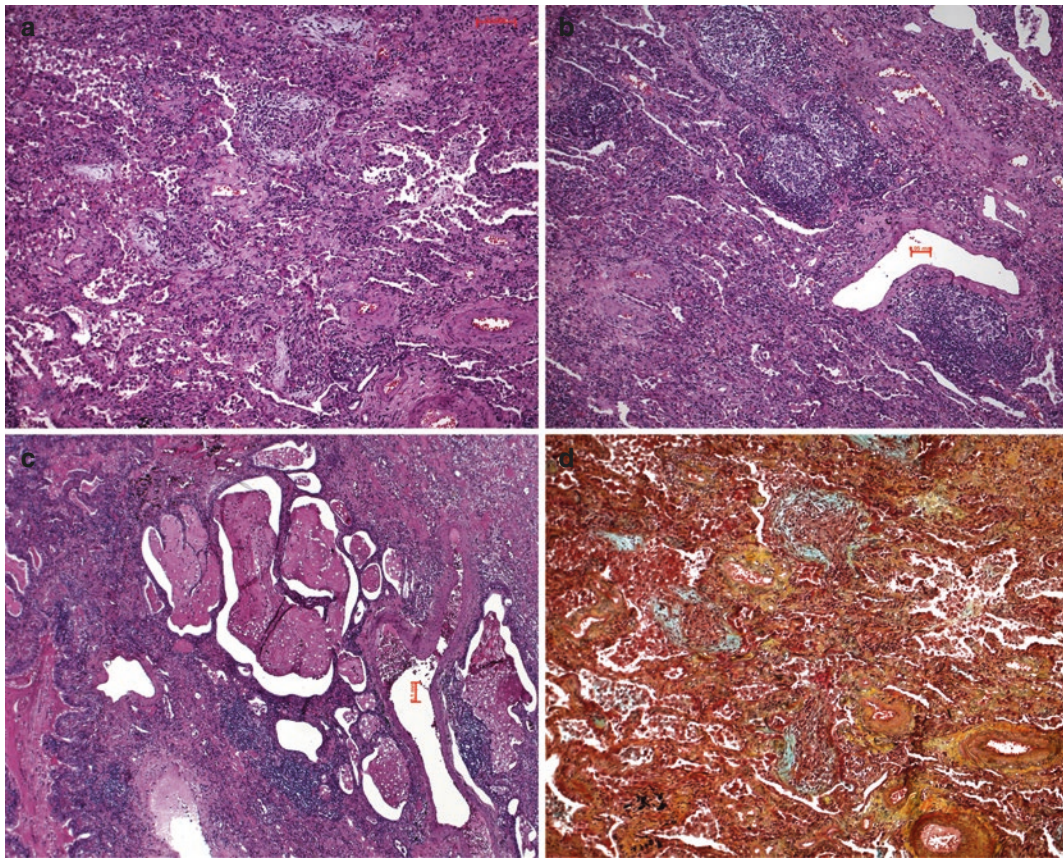

Fig. 9.22 Dermatomyositis with lung involvement. In this case, there is a mixed pattern, dominated by LIP with BALT hyperplasia (**a**+**b**). In addition there are fibroblastic foci, which are best seen with Movat stain (**a**, **d**). In some areas, there is cystic remodeling of alveolar tissue (**c**). In contrast to classical UIP, there is no temporal heterogeneity. H&E and Movat, bars 100 and 50 μm

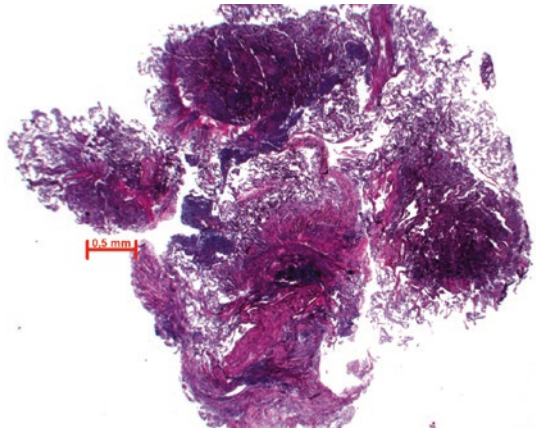

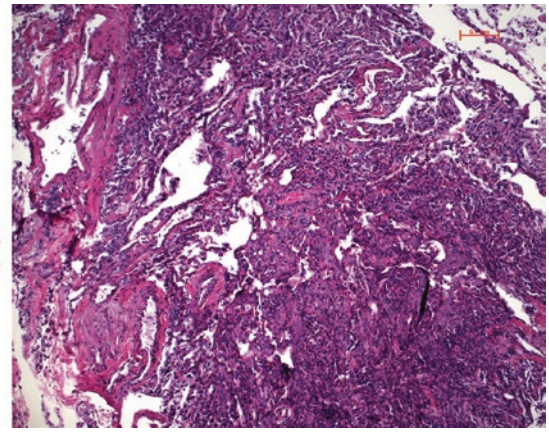

Fig. 9.23 Dermatomyositis in transbronchial lung biopsy: in this case, the clinical question was if pathology could confirm lung involvement in DM. Given the morphology, this case most likely is consistent with an autoimmune disease. H&E, bars 500 and 100 μm

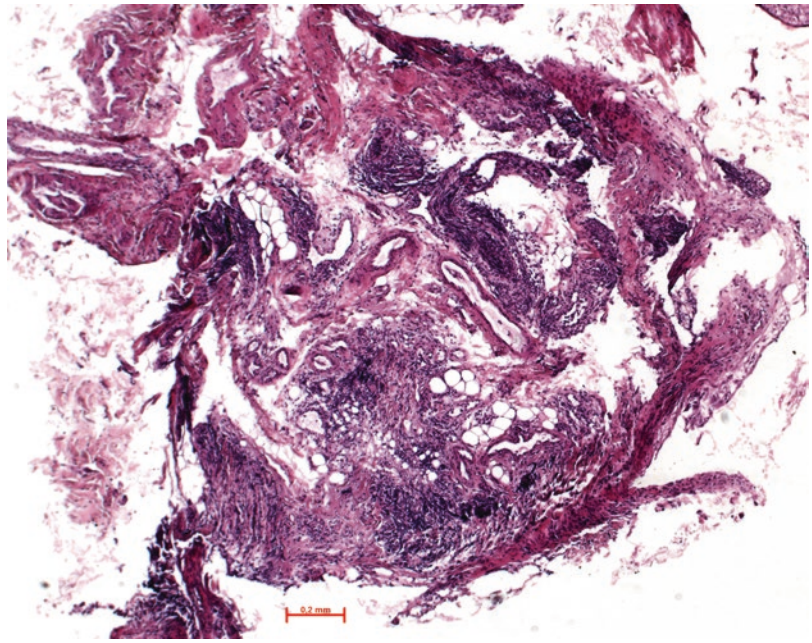

Fig. 9.24 Lymphocytic pleuritis with micronodular aggregates of small lymphocytes. This by itself is not diagnostic; however, in the clinical context of known dermatomyositis, this fits well with polyserositis, common in this disease. H&E, bar 200 μm

9.2.5 Sjøgren's Syndrome

Sjøgren's syndrome (SjS) is another multisystemic collagen vascular or autoimmune disease. It affects predominantly the mucosa of salivary and lacrimal glands, but can also similarly affect the lung. The main finding is an aggressive lymphocytic infiltration into the epithelial lining of bronchi and bronchioles and a diffuse infiltration of the alveolar walls, qualifying as LIP (Fig. 9.25). In the bronchi/bronchioles, lymphoepithelial lesions occur, similar to what is seen in marginal zone lymphomas. The epithelial layer is disrupted, which later on is repaired and can present as OP (Fig. 9.26). The lymphocytic infiltration is polyclonal and composed of T and B lymphocytes. Lymph follicles are well formed and will show activated germinal centers. Other types of interstitial pneumonias can be associated to LIP, even UIP can occur, usually in the form of UIP-LIP mixed pattern (Figs. 9.27 and 9.28).

As in SSc interleukins are playing an important role in Sjøgren's syndrome too. IL12 overexpressing transgenic mice developed bronchial and alveolar abnormalities such as lymphocytic infiltrates around the bronchi, cell proliferation in the alveolar septa, and increased interstitial and alveolar macrophages, strikingly similar to those found in the lungs of Sjøgren's patients. There were also fourfold higher numbers of natural killer cells. A new mouse model highlights the role of IL12 in the initiation of Sjøgren's syndrome [29]. Rangel-Moreno studied the hyperplasia of BALT in patients with pulmonary involvement in rheumatoid arthritis and Sjøgren's syndrome. Increased expression of CXCL13 and CCL21, as well as B-cell activating factor of the TNF family (BAFF), ICOS ligand, and lymphotoxin, correlated with BALT hyperplasia. The presence of BALT hyperplasia correlated also with tissue damage in the lungs of these patients [30]. In a recent investigation, genes have been identified related to one of the major symptoms of Sjøgren's syndrome, namely, the immunological attack of salivary and lacrimal glands resulting in the loss of acinar cell tissue and function, leading to stomatitis sicca and keratoconjunctivitis sicca. One gene lying on chromosome 1 (autoimmune exocrinopathy 2, Aec2) and the second on chromosome 3 (autoimmune exocrinopathy 1, Aec1) have been shown to be necessary and sufficient to replicate SjS-like disease in C57BL/6 mice. Aec2 lies distal to the centromere. This chromosomal region contains several sets of genes known to correlate with various immunopathological features of SjS. One gene in particular, tumor necrosis factor (ligand) superfamily member 4 (or Ox40 ligand), encoding a product whose biological functions correlate with both physiological homeostasis and immune regulations, could be a potential candidate SjS susceptibility gene [31]. Although many open questions remain, this mouse model opens the way to better understand this autoimmune disease and also will serve to study the mechanisms, which are responsible for the common development into MALT lymphomas.

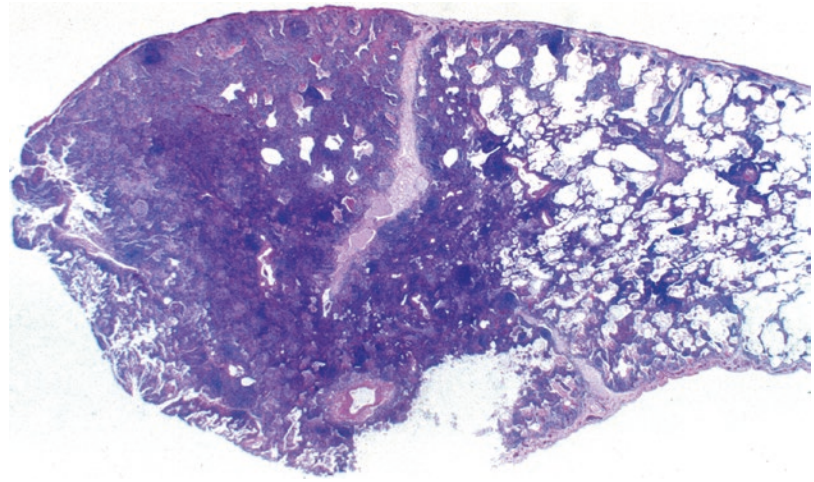

Fig. 9.25 Classical picture of Sjøgren's syndrome (SjS) with lung involvement. Together with the finding shown in Fig.9.26, this is almost diagnostic, if monoclonality of the lymphocytic infiltration is excluded. H&E, ×12

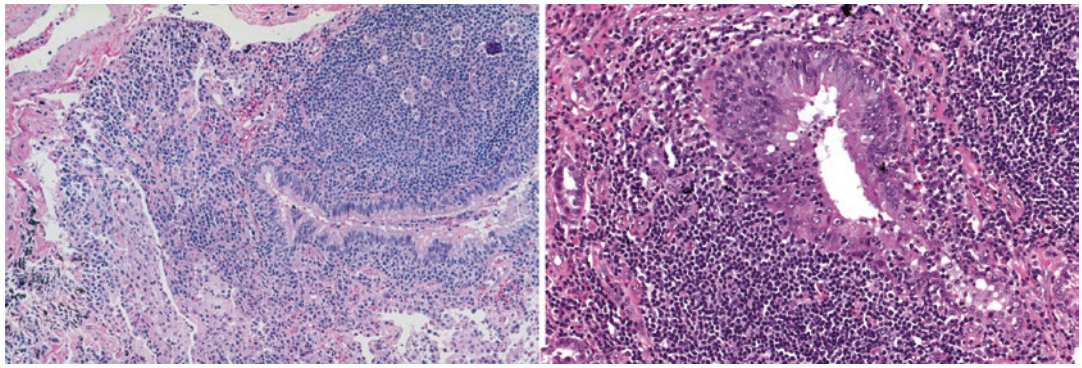

Fig. 9.26 Two examples of aggressive lymphocytic infiltration of the bronchial mucosa. The lymphocytes destroy the epithelium similar to what is seen in MALT lymphoma (lymphoepithelial lesion). This feature points to the underlying pathology of autoaggression toward epithelia. H&E, ×100 and 200

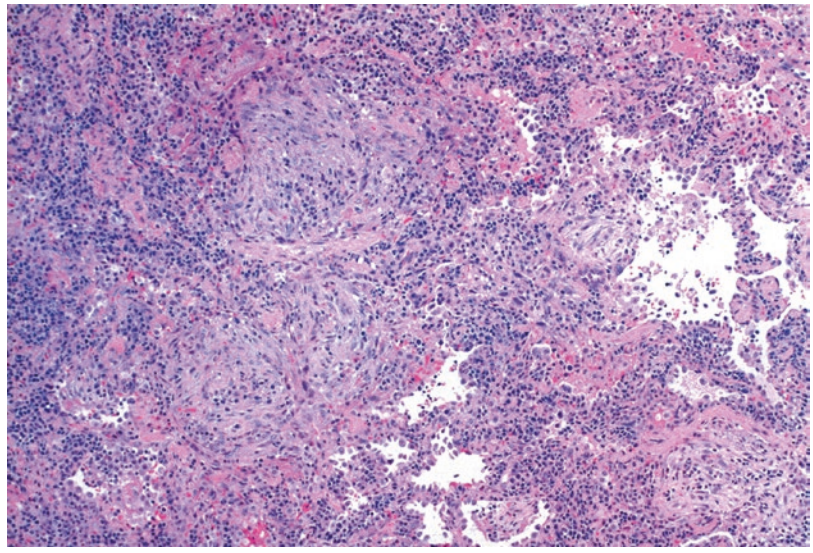

Fig. 9.27 Combination of LIP and organizing pneumonia in SjS. In this case, the clinical picture was in favor of resolving disease. H&E, ×200

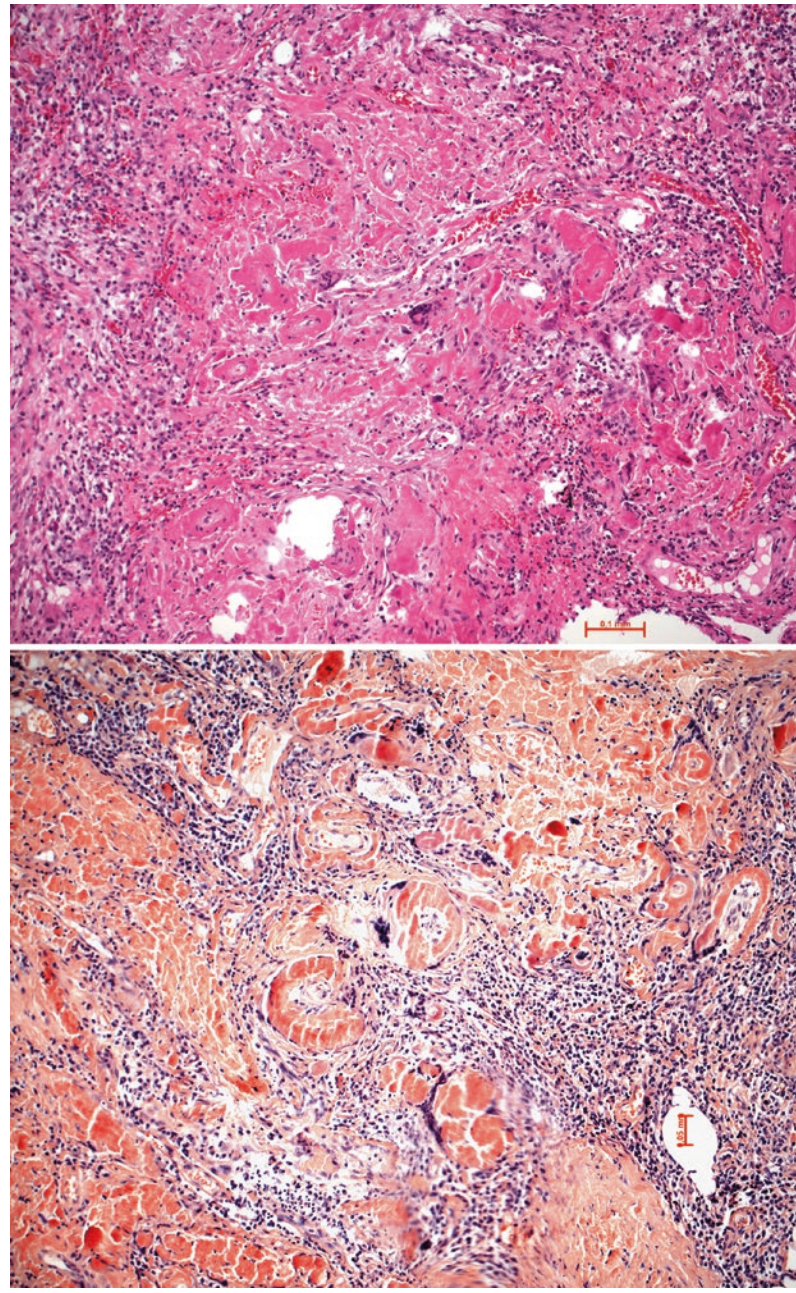

Fig. 9.28 Amyloid deposition in a case of SjS. There is only mild lymphocytic infiltration. Deposition of hyaline material is shown in the *upper panel* and proven by Congo red stain, green polarization (*lower panel*). In addition also immunohistochemistry for amyloid components confirmed the diagnosis. H&E and Congo red, bars 100 and 50 μm

9.2.6 Mixed Collagen Vascular Diseases (CVD)

Mixed CVD cannot be diagnosed with certainty. The combination of features of two different CVD makes it almost impossible to come up with an etiologic suggestion or proposal. Depending on the features of the single CVD, morphologic mixtures can be found. For example, mixed Sjøgren's-lupus CVD can either have dominant features of Sjøgren's syndrome or systemic lupus [32]. However, general features suggestive of CVD are usually present: a combination of different features of interstitial pneumonias with lymphocytic infiltrations, hemorrhage, etc. (Fig. 9.29).

So when to think about lung affected by autoimmune diseases?

- Any combination of LIP and fibrosing pneumonias
- Any kind of interstitial fibrosing pneumonia with a high proportion of lymphocytes
- Any combination of an interstitial pneumonia with other inflammatory reactions not fitting within IPs, such as combination of UIP/NSIP/LIP with epithelioid or histiocytic granulomas
- Any kind of interstitial pneumonia with unusual vasculopathy (not arteriosclerosis!) and/or alveolar hemorrhage

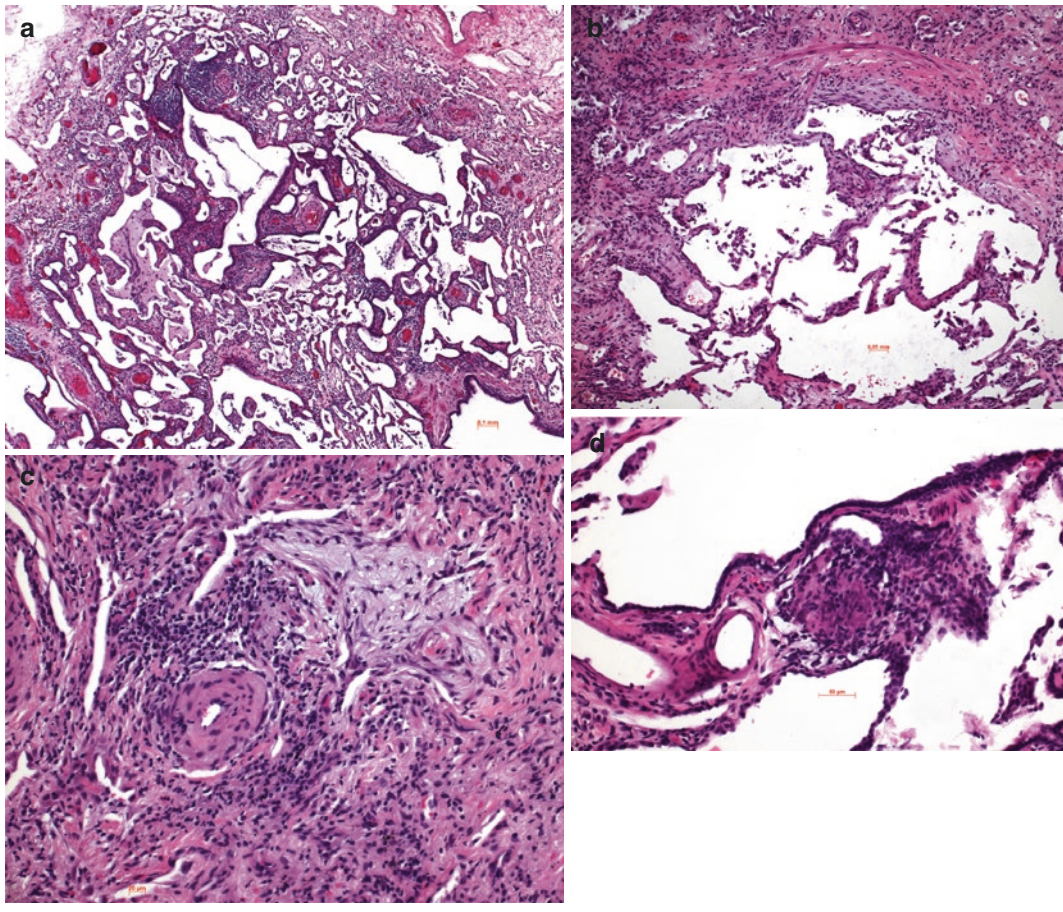

Fig. 9.29 Mixed collagen vascular disease. Overview in (**a**) showing cystic remodeling of alveolar tissue. In (**b**) fibroblastic foci are seen, in (**c**) there is a focus of organizing pneumonia and also concentric sclerosis of a small pulmonary artery, and in (**d**) a tiny epithelioid cell granuloma is visible. H&E, bars 1 mm, 50, and 20 µm

9.2.7 Goodpasture Syndrome

Goodpasture syndrome is an autoimmune disease not related to CVD. The cause has been identified recently: by a mimicry against bacterial proteins, cross-reacting autoantibodies are formed, which bind to the α-3-chain of collagen IV causing disruption and hemorrhage by complement activation (most often the alternate pathway) [33, 34]. There are still unexplained features such as why collagen IV in glomerular, alveolar, and alveolar capillary basement membranes is attacked, but not those in other organs.

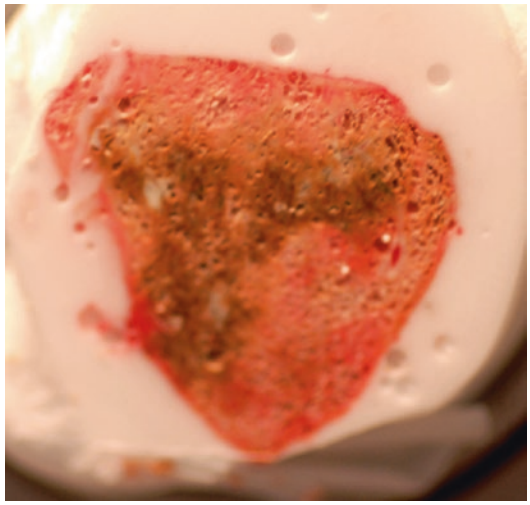

Fig. 9.30 Goodpasture syndrome (GPS): macroscopic features are scattered areas of hemorrhage as in this specimen ready for frozen section diagnosis

Macroscopically there are scattered areas of hemorrhage corresponding to the clinical picture of alveolar hemorrhage (Fig. 9.30). The major histologic finding is alveolar hemorrhage without infiltrating leukocytes (Figs. 9.31 and 9.32). Most important is the finding of hemosiderin-laden alveolar macrophages in alveoli and in the interstitium, pointing to previous episodes of hemorrhage. In rare cases with massive hemorrhage, hyaline membranes may be focally encountered (Fig. 9.33), which will undergo organization and result in focal scars. Depending on the duration of the disease, finally septal fibrosis results [35]. In all cases, the deposition of autoantibodies to the constituents of the basal lamina needs to be proven. These cytotoxic autoantibodies (immune reaction type II) can be demonstrated as linear deposits along the alveolar basement membrane as well as that of capillaries (Fig. 9.34). These autoantibodies activate the complement cascade without any additional help from leukocytes; in my experience, most often the alternative complement pathway is activated.

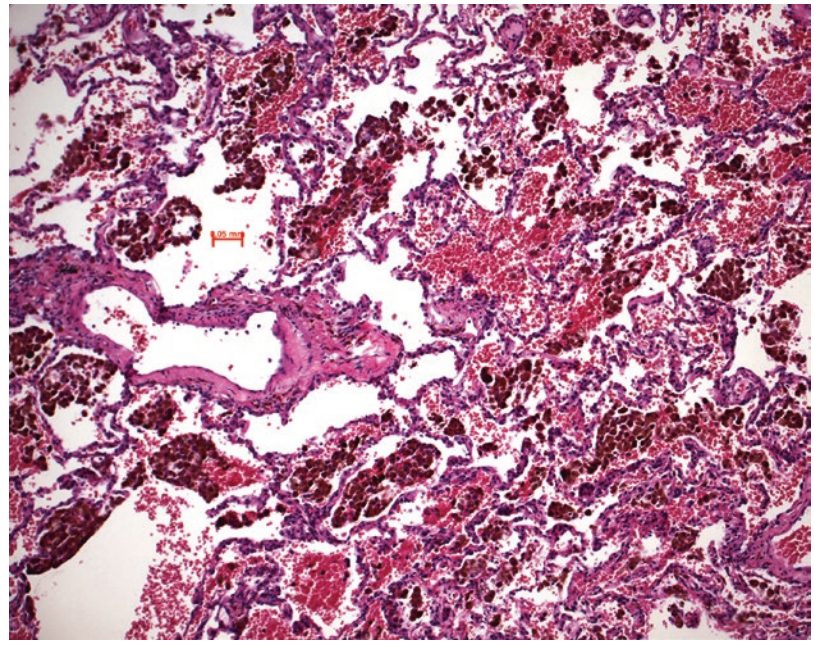

Fig. 9.31 Classical feature of GPS: fresh and old alveolar hemorrhage. The latter represented by alveolar macrophages laden with hemosiderin. H&E, bar 50 µm

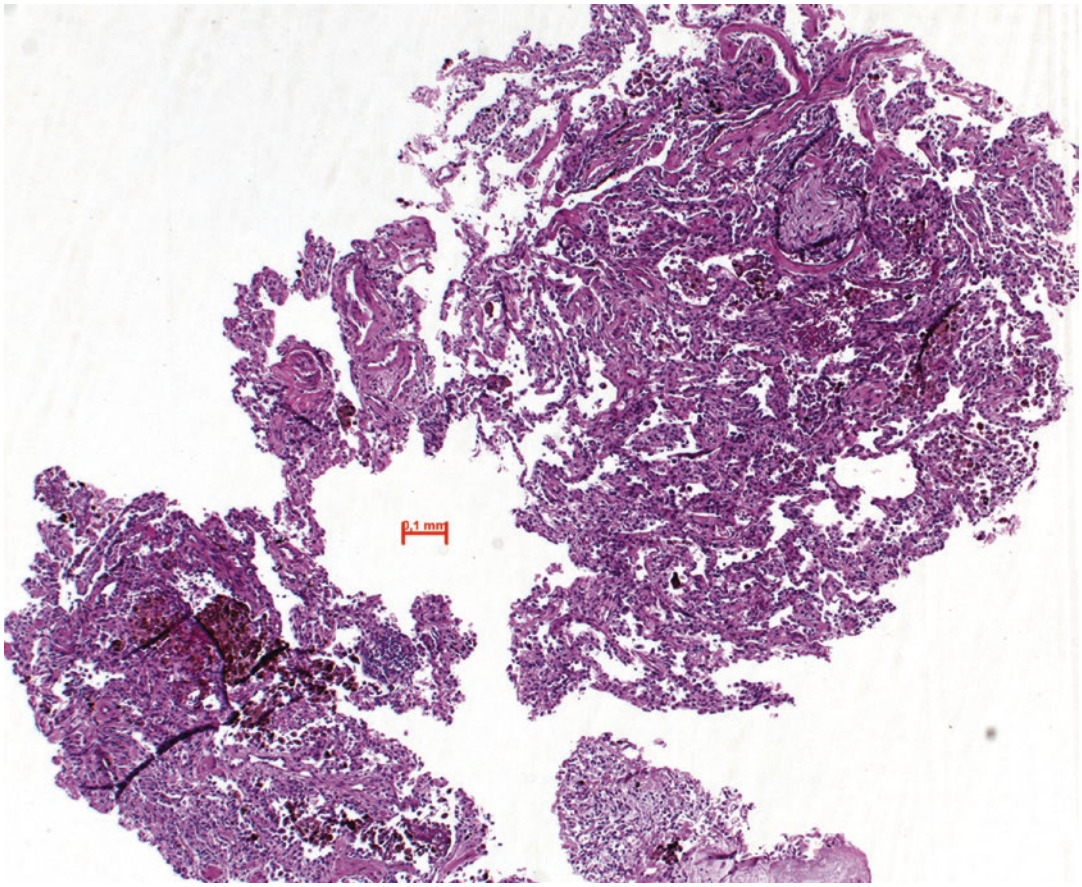

Fig. 9.32 A diagnosis of GPS can also be made on transbronchial biopsies as in this case. H&E, bar 100 µm

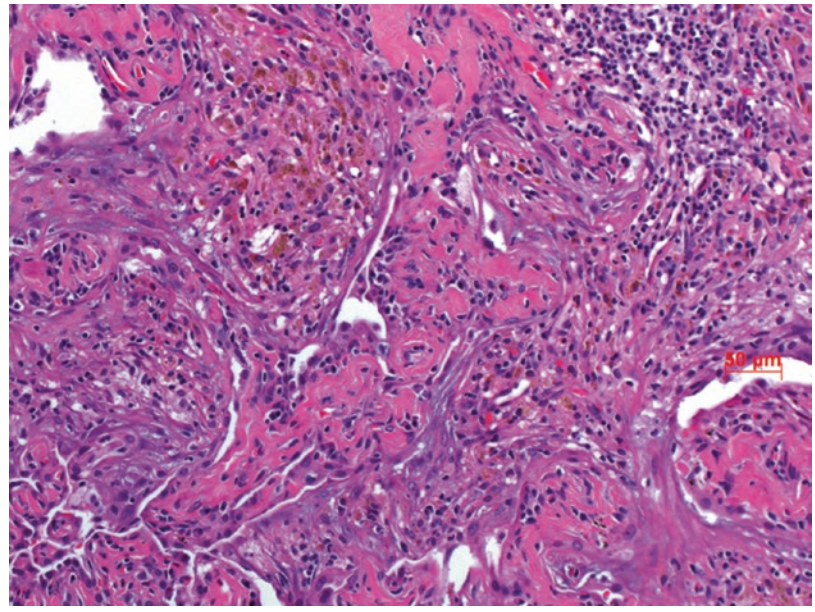

Fig. 9.33 In later stages of GPS, and especially if hyaline membranes have developed (massive bleeding), organization and fibrosis can occur. However, these are small nodules of fibrosis. H&E, bar 50 µm

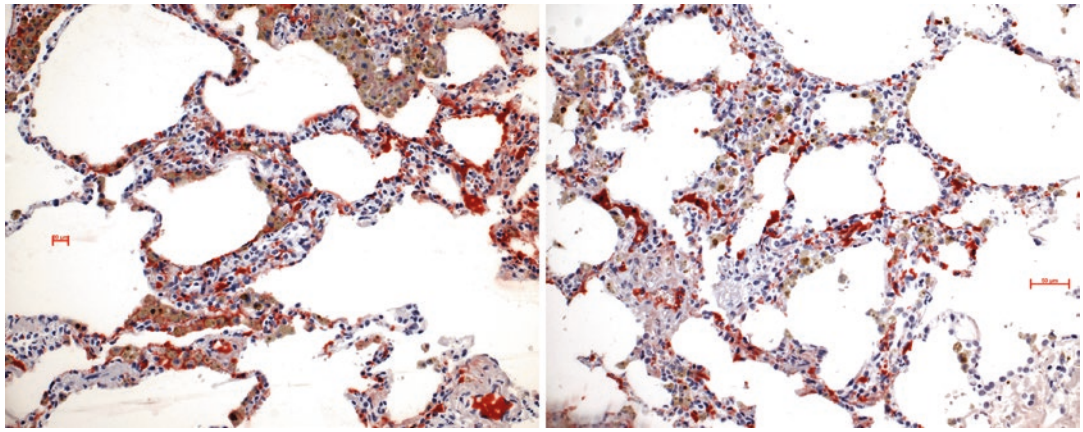

Fig. 9.34 Proof of GPS by immunohistochemistry for linear immunoglobulin deposition and activation of complement, here the alternative complement pathway. Immunohistochemistry for IgG showing linear deposition, *left*, bar 20 μm, and complement component C3c, *right*, bar 50 μm

9.2.8 Other Autoimmune Diseases Affecting the Lung

Interstitial pneumonias can be encountered in Behcet's disease and Kikuchi disease, whereas in Whipple's disease, granulomatous pneumonia with histiocytes and macrophages is the prominent feature, similar to what is seen in the small bowel [36]. There are other autoimmune diseases for which lung involvement has not been well documented. Single case reports have discussed lung involvement in autoimmune thyroiditis, autoimmune hemolytic anemia, and autoimmune cholangitis. However, as the mechanisms how lung might be affected by these diseases are not clear, a meaningfull discussion is not possible and thus avoided here.

IgG4-related sclerosis is an autoimmune disease involving many organs such as the pancreas, mediastinum, and retroperitoneal space. Hypergammaglobulinemia and deposition of IgG4 are seen in affected tissues. In the lung the disease usually present with extensive lymphoplasmacytic infiltration (Fig. 9.35), very often simulating inflammatory pseudotumor (plasmacytic variant); however, in this disease increased numbers of IgG4-positive plasma cells are found (≥25 % of IgG-positive cells), not seen in inflammatory pseudotumor (myofibroblastic tumor) [37]. This inflammation typically results in sclerosis of the lung tissue [38].

Phospholipid autoantibody-mediated lung disease is another rare disease affecting the lung but also other organs [39]. In the affected lung, the major finding is alveolar hemorrhage or hemorrhagic pneumonia and DAD, followed by an organizing pneumonia in a later stage. Lymphocytic infiltration is rare (Fig. 9.36). The cause is unknown; the morphologic findings are not specific. The disease needs the proof of phospholipid autoantibodies in the serum.

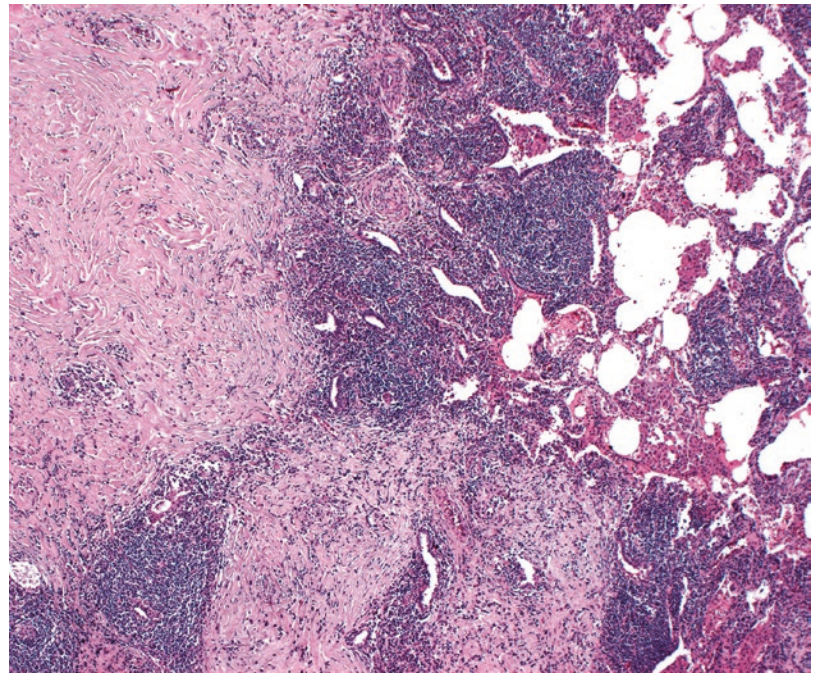

Fig. 9.35 IgG4-related fibrosis of the lung. There is multinodular fibrosis surrounded by dense lymphoplasmacytic infiltration. The differential diagnosis is inflammatory pseudotumor (myofibroblastic tumor) versus lymphoma versus IgG4 disease. Polyclonality excludes the lymphoma; IgG4 dominated staining of lymphocytes confirmed IgG4 disease. H&E, ×100

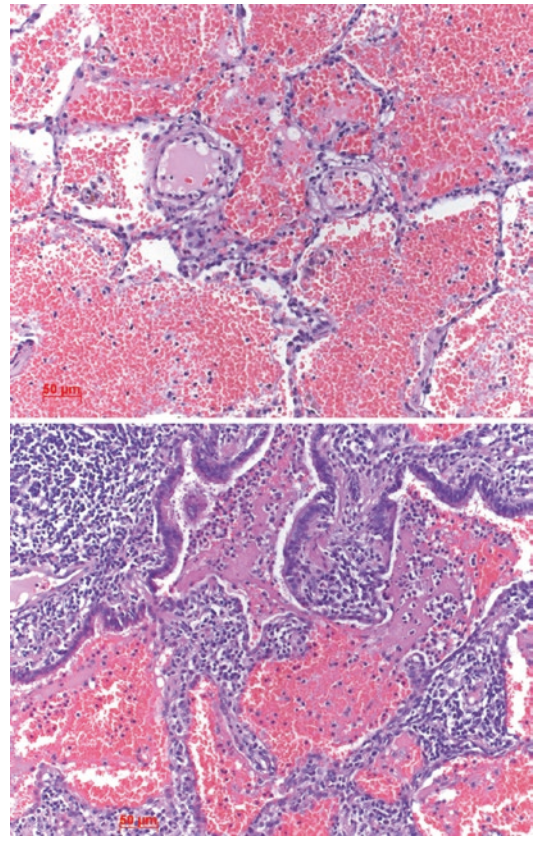

Fig. 9.36 Antiphospholipid autoantibody-mediated lung disease. The histologic picture is dominated by alveolar hemorrhage (*upper panel*). In this case, there was also focal lymphocytic infiltration (*lower panel*). H&E, bars 50 µm

9.2.9 Surfactant-Related Interstitial Pneumonias: Alveolar Proteinosis

Alveolar proteinosis occurs in two forms, either as a genetically inherited disease or as an acquired disease of adults [40–44]. It is characterized by an accumulation of surfactant lipids and proteins within the alveoli, in severe cases completely obstructing the peripheral parenchyma and causing severe dyspnea. Morphologically there is eosinophilic material within the alveoli sometimes mixed with debris and in some cases accompanied by an inflammatory infiltration of the alveolar walls.

We have already discussed the inherited form under the childhood diseases, so we have to focus on the adult form. In the acquired form (predominantly adults), different defects of the degradation cascade of surfactant do occur. The most common is a deficiency of GM-CSF caused by autoantibodies against this protein [40, 42, 43, 45]. GM-CSF is necessary for the uptake and subsequent degradation of surfactant by alveolar macrophages. The hallmark is an accumulation of surfactant material within the alveoli. There is usually no inflammatory infiltrate present (Fig. 9.37). The diagnosis can even easily be made by bronchoalveolar lavage (BAL): the recovered fluid looks milky (Fig. 9.38). In later stages, the disease can get chronic. In addition to the accumulation of surfactant lipids and proteins, there is a diffuse interstitial fibrosis, which can cause death of the patient. Sometimes alveolar proteinosis can be induced by tuberculosis, acute silicosis, and other diseases; the mechanisms in these are still unclear (Fig. 9.39). We will come back to this disease in the chapter on metabolic diseases.

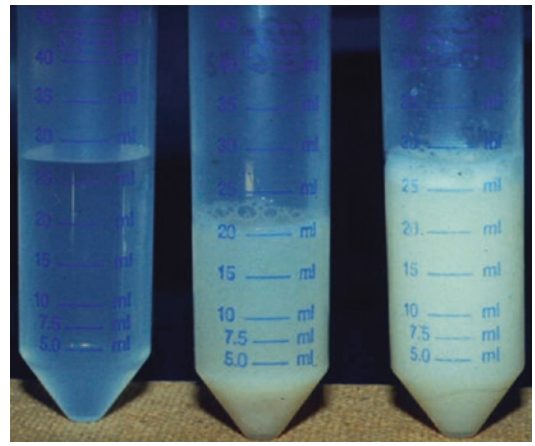

Fig. 9.38 Bronchoalveolar lavage in a case of alveolar proteinosis. These are washings from the patient's lungs. To the right is the initial sample washed out. It shows a milky fluid, characteristic for the disease

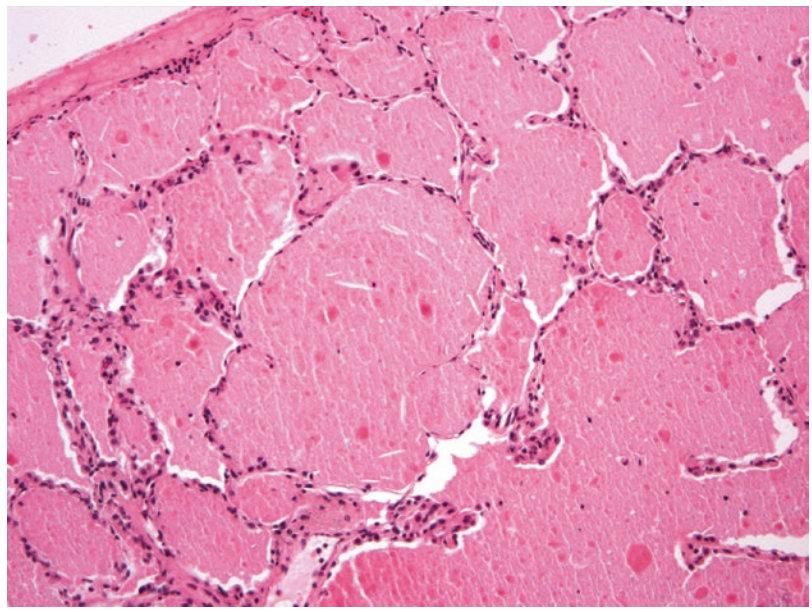

Fig. 9.37 Alveolar proteinosis in an adult. Autoantibodies against GM-CSF were clinically identified. H&E, ×200

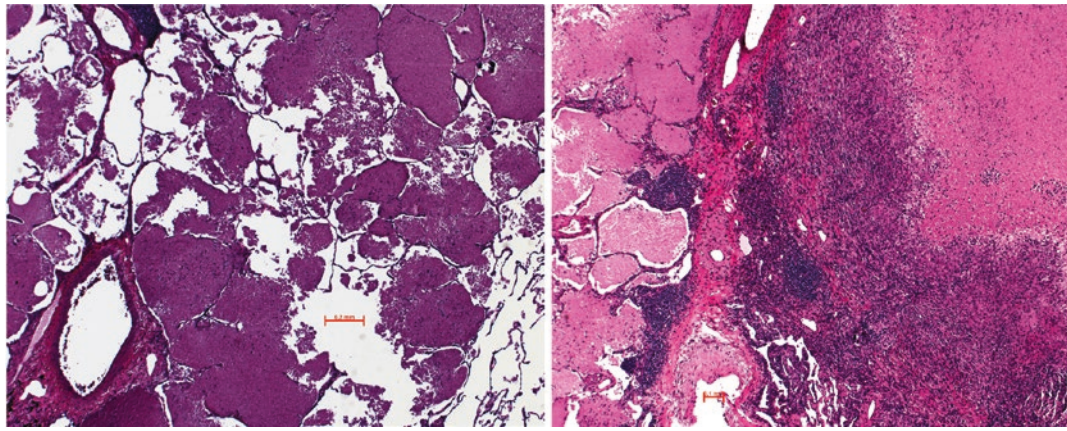

Fig. 9.39 Alveolar proteinosis in a case of tuberculosis. (*Left*) There is proteinaceous material filling the alveoli; (*Right*) besides the proteinosis, there is a large epithelioid cell granuloma with necrosis. *M. tuberculosis* was identified. H&E, bars 200 and 100 μm

9.2.9.1 Autoimmune Diseases in Childhood

Many of the discussed diseases can occur in children, usually at an age above 5 years. The presentation is most often similar to that in adults, but severity might be much more pronounced. SLE and rheumatoid arthritis are the most often seen autoimmune diseases in children. Also sarcoidosis can present at an early age.

9.3 Diseases of the Innate Immune System Based in Genetic Abnormalities

At a first glance, it looks as these diseases do not fit into immune disorders. But when we look more closely, we encounter abnormalities of the immune reaction as a consequence of a genetic abnormality. TSC mutations result in a proliferation of PEC and immature smooth muscle cells, mutations of the HPS genes result in a blockade of maturation of lysosomes, giant cells phagocytose elastin fibers based on an unidentified genetic abnormality, and mutations in genes related to the RAS pathway result in proliferation of dendritic/histiocytic cells in ECD. All these genetic abnormalities affect cells of the innate immune system, and this is the link to group these diseases in this chapter.

9.3.1 Idiopathic Pulmonary Hemosiderosis

Idiopathic pulmonary hemosiderosis is an interstitial disease usually found in children, but also young adults. The characteristic clinical feature is recurrent alveolar hemorrhage and morphologically diffuse lymphocytic and histiocytic/macrophage infiltrations in both lungs. The etiology is largely unknown. Many patients develop iron deficiency anemia due to recurrent bleeding. There is usually a high mortality rate. A degradation of elastic fibers followed by an incrustation by iron-containing proteins (Prussian blue positive) can be seen on histologic examination and is a diagnostic feature. Usually foreign body giant cells are found in the areas of ongoing destruction of the elastic fibers ingesting the fibers together with the iron coat [46] (Fig. 9.40). In later stages, interstitial fibrosis results. Vasculitis, granulomatous inflammation, or immunoglobulin deposits are absent. Corticosteroids alone or in combination with other immunosuppressive agents may be effective for either exacerbations or maintenance therapy of idiopathic pulmonary hemosiderosis [46, 47].

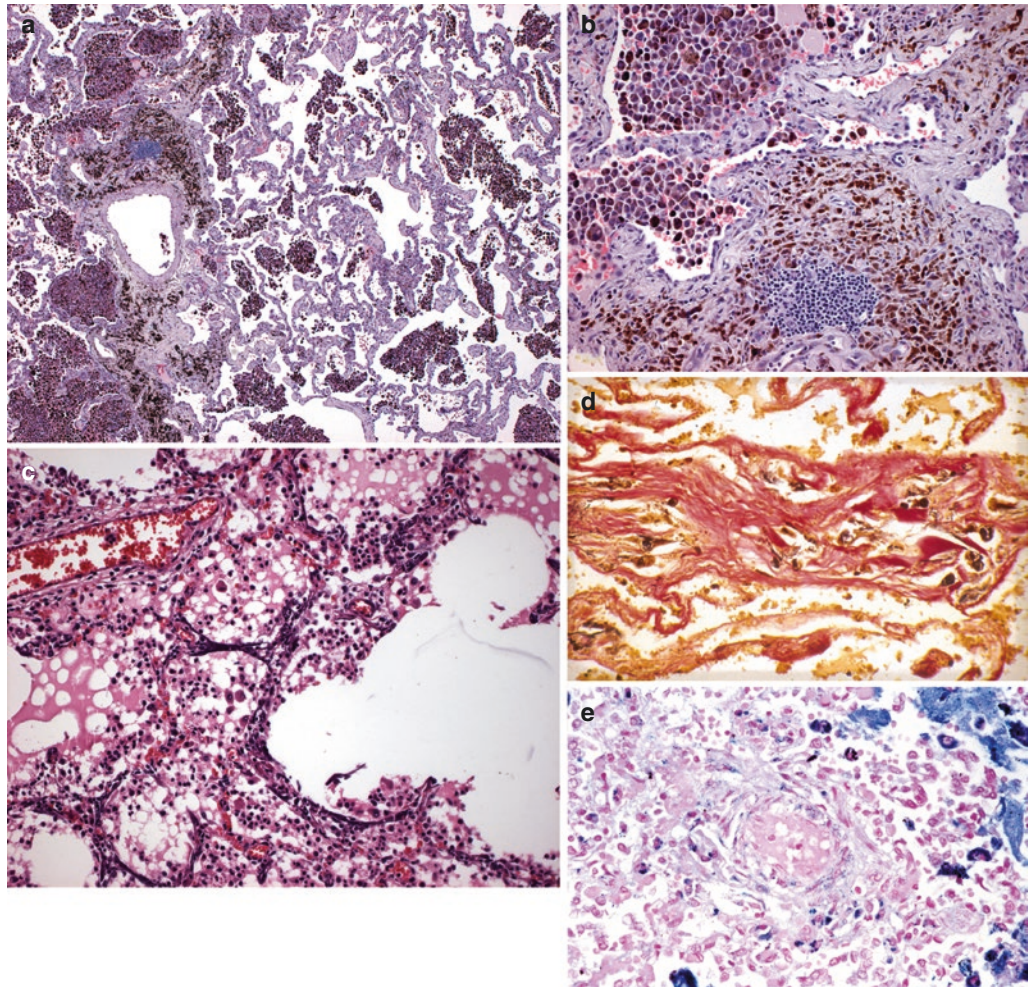

Fig. 9.40 Idiopathic pulmonary hemosiderosis. (**a**) Overview with numerous hemosiderin-laden macrophages in the alveoli and septa. (**b**) Within the septa, there is fibrosis and a few foreign body giant cells. (**c**) Elastic fibers are encrusted by hemosiderin-containing substances. (**d**) Foreign body giant cells phagocytosing elastic and collagen fibers. (**e**) Prussian blue staining showing the amount of hemosiderin. (**a**–**b**), H&E ×12, ×200, ×100, Elastica v. Gieson, ×200, Prussian blue, ×200

9.3.2 Lymphangioleiomyomatosis (LAM)

LAM is an inherited disease, based on the dysfunction of tuberous sclerosis genes (TSC genes). TSC1 coding for hamartin and TSC2 coding for tuberin are both required controlling the expression and regulation of mTOR and the mTOR complexes TORC1/2. Both proteins form a complex, which activates cAMP-kinase, which subsequently inactivates mTOR. In LAM TSC2 is more often mutated then TSC1 [48–51]. Tuberin is thus not functional and does not form heterodimers with hamartin, and TORC1/2 is constantly activated (Fig. 9.41). TSC mutation can be a germline mutation as in tuberous sclerosis syndrome or is mutated somatically, by some authors called "form fruste" [52]. The second allele is most often mutated somatically. The type of mutation also dictates the extent of syndromes and tumors associated with this mutation. Patients carrying the germline mutation present with genetic instability causing several somatic mutations and therefore in addition to LAM can present with different other benign tumors. Previously lung

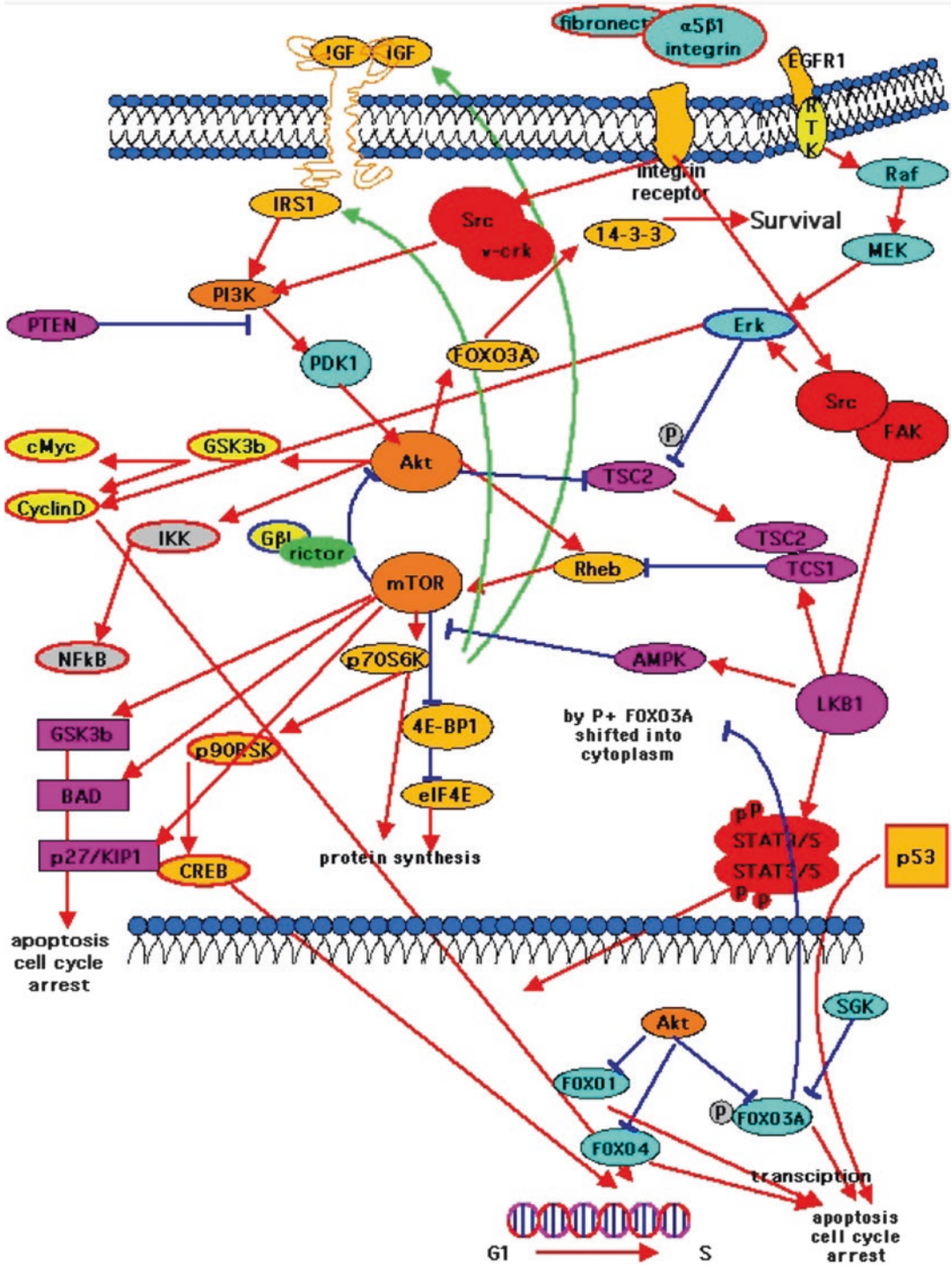

Fig. 9.41 Schema demonstrating the important pathway position of TSC genes. cAMP-kinase interacts with TSC1 and TSC2 to inhibit mTOR via Rheb. This functions as an autoregulatory pathway: when mTOR is activated, TSC1/TSC2 complex deactivates. In case of mutation of either TSC1 or TSC2, the inhibition of mTOR does not work and the molecule is constantly upregulated. New therapeutic approaches interact here by inhibiting mTOR

transplantation was one of the few choices of treatment. Since the discovery of the function of both TSC proteins, a clinical trial with anti-mTOR therapy has been started and seems to be effective [53–55]. Interestingly in rare cases with lung transplantation, a recurrence of the disease occurred from circulating LAM cells, repopulating the transplanted lungs [56–60]. This raises the question if LAM should be considered a systemic tumor or still classified under interstitial diseases; this question is unanswered up to now.

Macroscopically as well as by CT scan, LAM is characterized as a cystic disease (Figs. 9.42 and 9.43). Histologically LAM is characterized by a proliferation of immature myoblasts in the periphery of the lung and in lymph nodes. Some cases present predominantly with cysts and few proliferation foci; others have numerous foci (Figs. 9.43 and 9.44). There are cases where in addition also perivascular epithelioid cells proliferate (probably derived from pericytic stem cells). The proportion of myoblasts and perivascular epithelioid cells (PEC) can vary considerably: in some cases of LAM, PEC are numerous, in other cases scarce (Fig. 9.44). The cells together form microscopic nodules in the bronchiolar mucosa, along lymphatics and arteries, and in alveolar septa, causing lymphatic obstruction and rupture (chylothorax), but also bronchial obstruction and cystic lung destruction (Fig. 9.45). These myoblasts show immature myofilaments and are not ordered in parallel as normal smooth muscle cells, and they also have a more epithelioid appearance. Nuclei are round and larger than in regular smooth muscle cells. Most importantly these cells proliferate in locations where no muscle cell proliferation does occur (Figs. 9.44 and 9.45). By immunohistochemistry, the myoblasts express smooth muscle actin and a few also desmin, whereas the PEC express HMB45 [52, 61].

Treatment options have increased recently as mTOR inhibition has been shown to successfully suppress the proliferation of the muscle cells and PEC [53]. In former times, double lung transplantation was the ultimate goal. Many years ago, also hormonal treatment was applied as some of the LAM cases showed response to antiestrogen therapy [62].

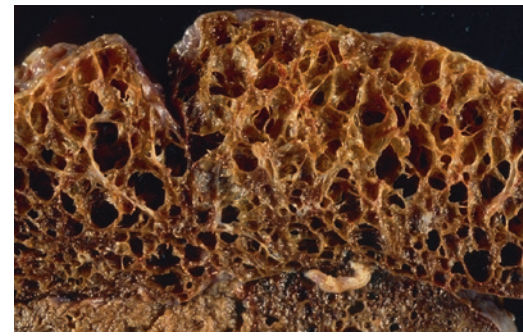

Fig. 9.42 Macroscopic picture of an explanted lung of a patient with lymphangioleiomyomatosis (LAM). Multiple cysts of different diameters destroy the whole lung

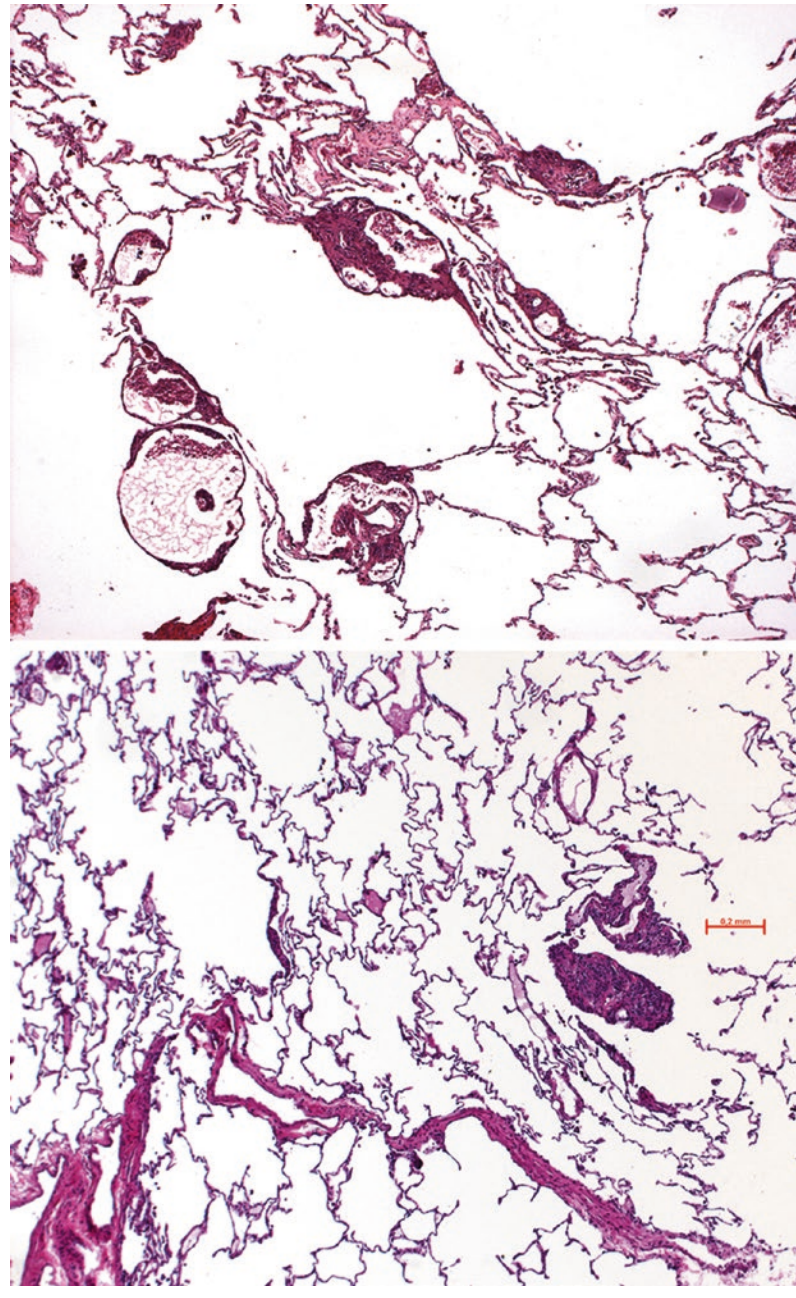

Fig. 9.43 LAM, showing two different types of infiltrations, a patient with multiple foci of smooth muscle proliferations (*upper panel*) and another one with only few foci (*lower panel*). H&E and Movat, bar 200 µm

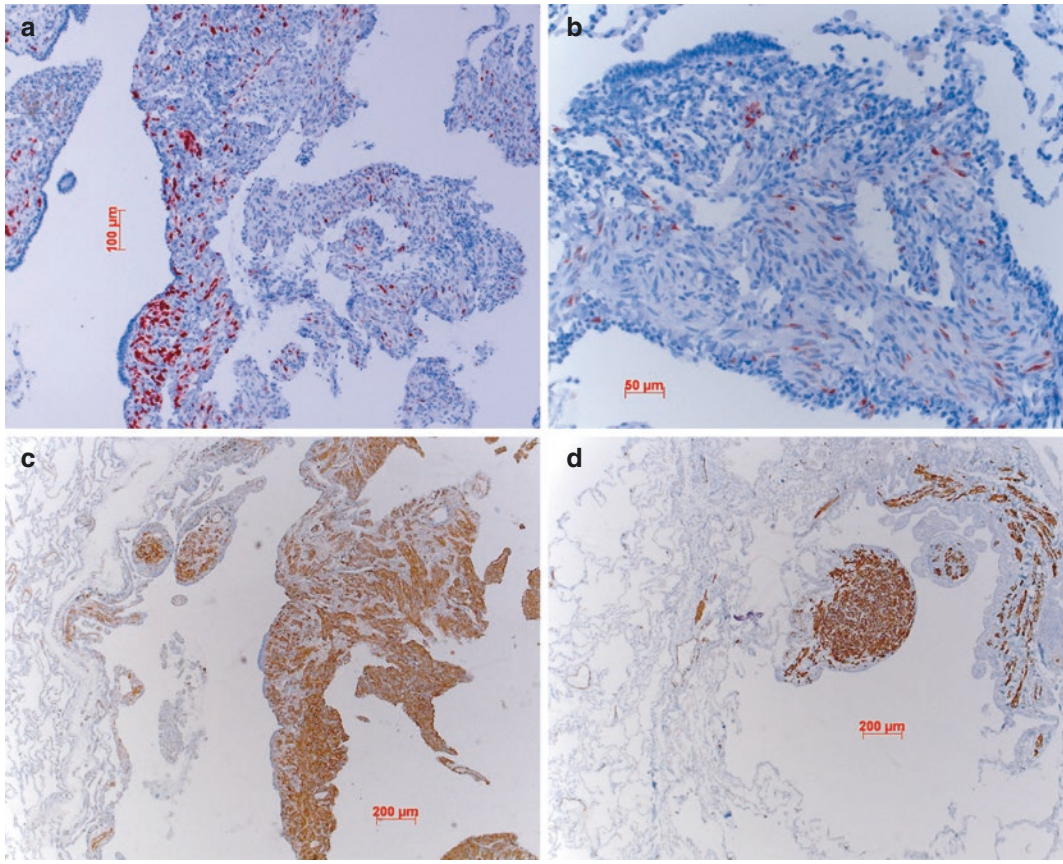

Fig. 9.44 LAM immunohistochemistry for HMB45 demonstrating perivascular epithelioid cells (PEC); in (**a**) numerous positive cells are seen, whereas in (**b**) only few scattered PEC are encountered. In rare instances especially in a transbronchial biopsy, not a single cell might be seen. In (**c**) smooth muscle cells are stained by a-actin antibodies, whereas in (**d**) the cells are stained by desmin antibodies. Immunohistochemistry, bars 100, 50, and 200 µm

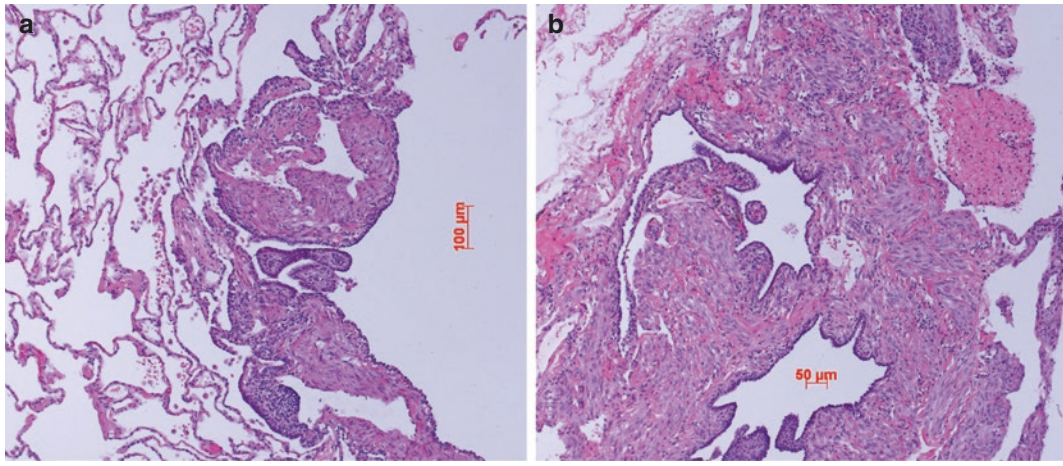

Fig. 9.45 LAM showing obstruction of lymphatics (**a**), which in a subpleural position might cause chylothorax, whereas in (**b**) there is also an obstruction of bronchioles. H&E, bars 100 and 50 µm

9.3.3 Hermansky-Pudlak Syndrome

Hermansky-Pudlak syndrome is an autosomal recessive disease, which results in the inability of several cells to form intracellular vesicles. This can affect the ability to form melanosomes (resulting in albinism), platelet granules (inducing bleeding diathesis), but also phagolysosomes in macrophages and lamellar bodies in type II pneumocytes [63] (Fig. 9.46). To date seven forms are known, but only two of them (type I and IV) constantly affect the lung, causing phagocytosis defects with accumulation of macrophages, lamellar body defects in type II pneumocytes with disturbed surfactant release and macrophage foam cell changes, inflammation, and finally lung fibrosis [64–67]. The characteristic morphologic changes are hyperplasia of pneumocytes type II, giant lamellar bodies (large PAS-positive cytoplasmic granules), accumulation of foamy macrophages within the alveoli, lymphocytic interstitial infiltration, and lung fibrosis, sometimes as organizing pneumonia with intra-alveolar granulation tissue, but also as interstitial fibrosis with myofibroblastic foci, identical to those in UIP (Fig. 9.47). Even both types of fibrosis OP and UIP can be present concomitantly in one patient. In contrast to UIP/IPF, honeycomb lesions are scarce, and usually the lung is diffusely involved leaving not much uninvolved tissue in between (no timely heterogeneity). In contrast to UIP/IPF, the involvement of the lung is not symmetric; fibrosis can occur peripherally as well as centrally and is always patchy. Ultrastructurally there are no well-formed lamellar bodies within pneumocytes type II. Within macrophages, lysosomes are enlarged and irregular contoured; phagolysosomes are absent (no fusion of lysosomes with phagosomes).

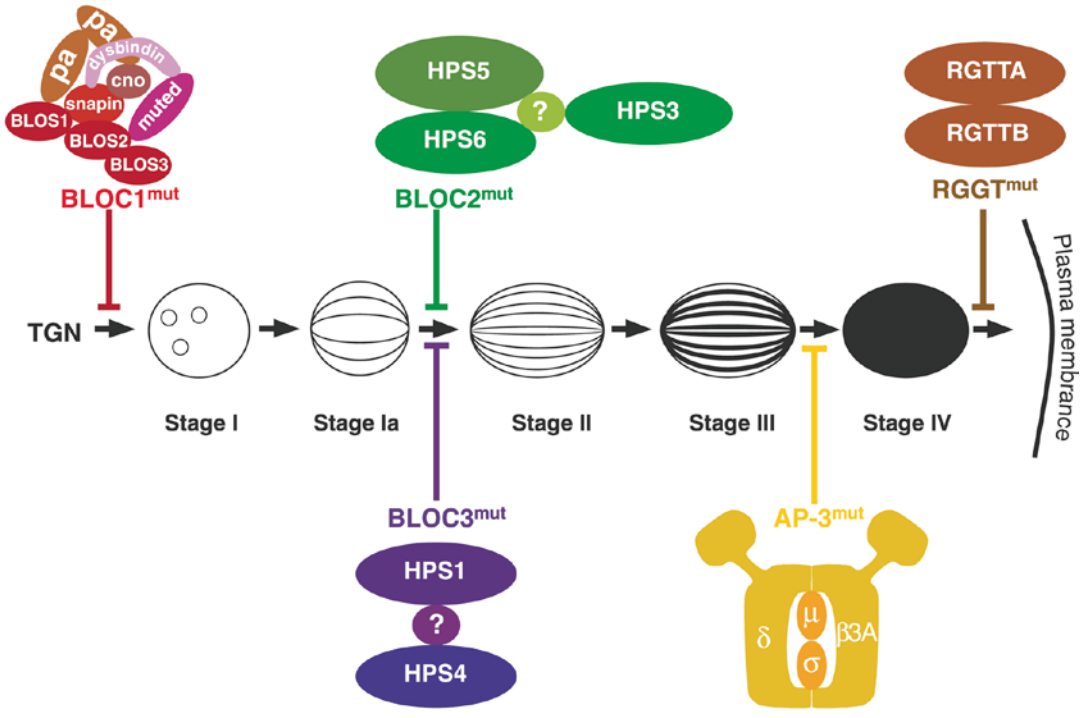

Fig. 9.46 Phases of formation of melanosomes and the genes responsible for the maturation. Similarly also lysosomes and phagosomes are under the control of HPS genes. In case of mutation, no mature and functioning phagolysosomes can be formed

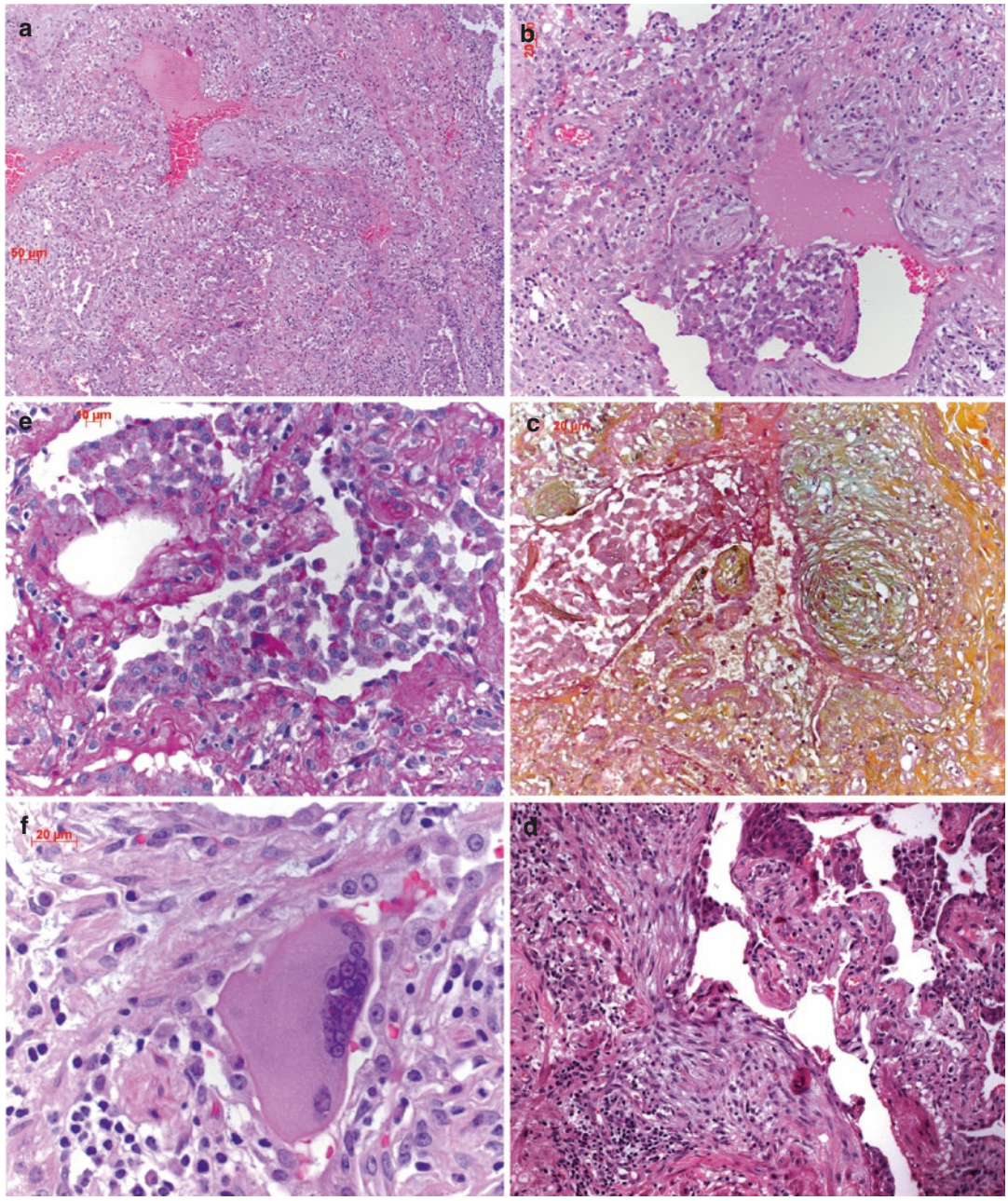

Fig. 9.47 Hermansky-Pudlak syndrome. (**a**) Overview of areas with dense infiltration by inflammatory cells and consolidation of the lung tissue. (**b**) Shows fibroblast foci, which are highlighted by Movat stain (**c**). In (**d**) another case with UIP pattern is shown; to the right, also foamy macrophages are seen. (**e**) Shows the PAS-positive granular material in the cytoplasm of macrophages, corresponding to giant lysosomes. In (**f**) a multinucleated giant cell is shown, a common feature in this disease. (**a**, **b**, **d**) H&E, (**c**) Movat, (**e**, **f**) PAS stain; bars 50, 20, and 10 µm

9.3.4 Erdheim-Chester Disease

Erdheim-Chester disease is a rare systemic histiocytosis (non-Langerhans dendritic cells) that may present with pulmonary symptoms. Mutation within the BRAF gene has been found in few cases; other rare mutations have been reported for MAP2K1, RAS, and PI3K. ECD should be now regarded as a systemic hematologic tumor and will be discussed in the tumor chapter.

9.4 Allergic Diseases

Extrinsic allergic alveolitis/hypersensitivity pneumonia has already been discussed in the pneumonia chapter under the granulomatosis; asthma has been discussed in bronchitis.

9.4.1 Allergic Bronchopulmonary Mycosis

Allergic bronchopulmonary mycosis (ABPM, formerly ABPA because it was assumed that only aspergillus species cause the disease).

9.4.1.1 Etiology

ABPM is induced by different fungi causing an immune reaction. Most often fungi colonize the upper respiratory airways, preferentially the nasal sinuses. Fungi cause a chronic inflammation; invasion into deeper layers is usually absent. The fungal mycelia are destroyed by granulocytes, and a balance between fungal growth and destruction is achieved. Fungal fragments are inhaled into the lower airways and cause an allergic reaction.

ABPM can present with different patterns depending on the type of immune reaction. The most common is a bronchial-related disease called *mucoid impaction*. Here an acute immune reaction of type I is mounted. This most likely is the reason why mucoid impaction looks like asthma.

9.4.1.2 Clinical and Radiological Findings

Patients present with asthma-like symptoms; however, hyperreactivity of the bronchial system is less pronounced. Patients usually suffer from hypoxia. On CT scan the bronchi are widened, whereas the peripheral lung tissue looks normal. By bronchoscopy the most striking feature is the thick compact mucus, which can be extracted from the bronchial tree in one piece. It looks like a negative cast of the bronchial tree.

9.4.1.3 Histology

On bronchial biopsies, a chronic eosinophilic bronchitis is the main finding (Fig. 9.48). Within the epithelium and in bronchial glands, the number of goblet cells is increased (hyperplasia). Epithelial shedding common in asthma is rarely seen. There is also a thickening of the basal lamina. The infiltration is composed of numerous eosinophils, lymphocytes, and plasma cells (Fig. 9.49). Within the mucus, remnants of fungi might be demonstrated by Grocott silver stain.

Two other patterns are seen in ABPM: bronchocentric granulomatosis, allergic variant, and eosinophilic pneumonia. BCG has been discussed in granulomatous pneumonias; eosinophilic pneumonia will be discussed in the next chapter. There are certain modifications in the immune reactions associated with these patterns. BCG has the same cause as mucoid impaction, namely, inhalation of fragments of mycelia from fungi. However, in this subacute to chronic disease are combined type I and type IV immune reactions. Therefore there is eosinophilic infiltration in the wall of the bronchi induced by IgE antibodies, but in addition a granulomatous reaction with epithelioid cells induced by a delayed type IV reaction. Eosinophilic pneumonia is the most rare form of ABPM. The immune mechanisms underlying this pattern are not fully understood. There are IgE antibodies present in these patients, but why the reaction is in the alveolar periphery has not been evaluated.

9.5 Drug Allergy

Allergic reaction against a wide variety of drugs is encountered. Whereas the skin most often is the affected organ, the lungs can be involved

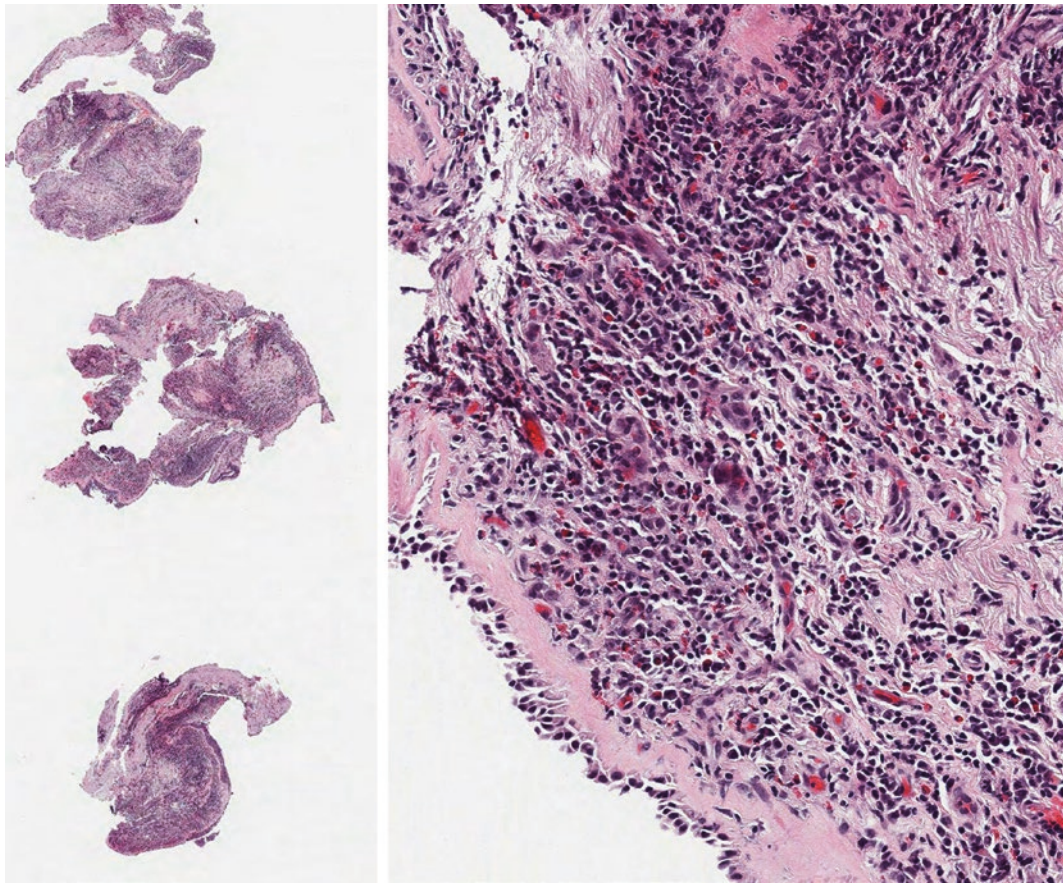

Fig. 9.48 Allergic bronchopulmonary mycosis, mucoid impaction type. There is shedding of columnar cells and thickening of basal lamina as in asthma and also dense infiltration by lymphocytes, plasma cells, and eosinophils. Left overview of bronchial biopsies, right higher magnification. H&E, ×12 and 100

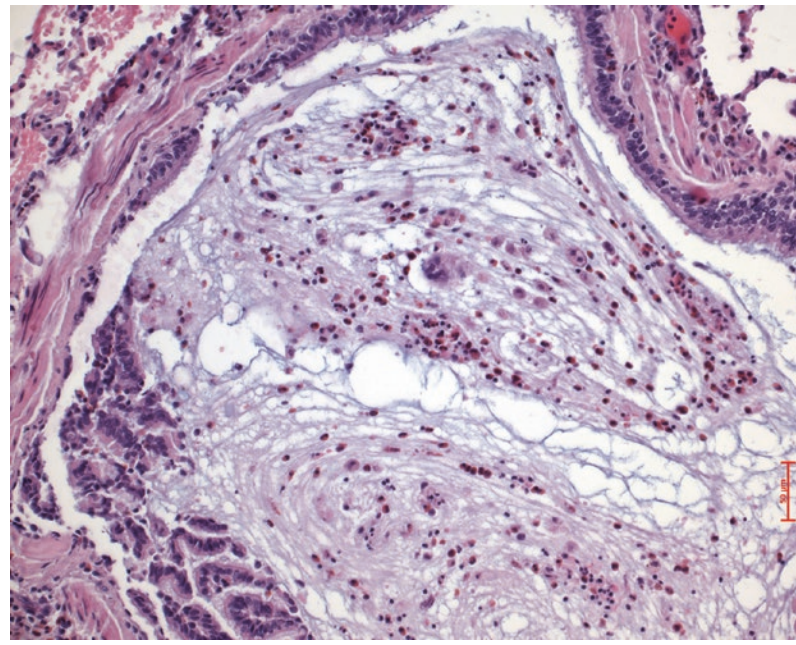

Fig. 9.49 Numerous eosinophils are seen within the mucus, less in the bronchial mucosa in this case. The columnar cell look normal; goblet cells are slightly increased. H&E, bar 50 µm

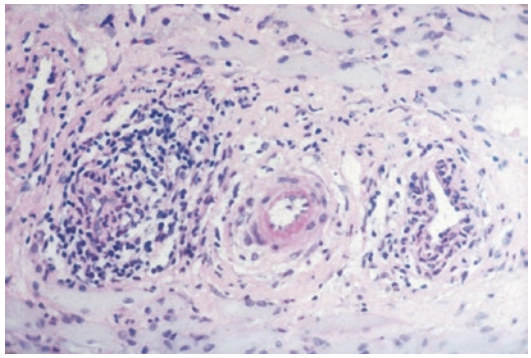

Fig. 9.50 Drug-induced allergic vasculitis in a patient with penicillin allergy. Note the dense vascular and perivascular infiltration by lymphocytes and eosinophils. There is also endothelial necrosis in the small artery and the vein. PAS stain, ×200

too. The patterns to be seen in drug allergies vary depending on how drugs or their metabolites interact with the organ and the cells of the immune system. Drug allergies can induce an IgE-mediated reaction, if the drug acts like a hapten (an example is penicillin allergy), which associates with a regular protein of the host to form an antigen. This type usually presents with blood eosinophilia, in the tissues with mixed lymphocytic and eosinophilic infiltration, and small vessel eosinophilic vasculitis (Fig. 9.50). This vasculitis is most often formed by deposition of complexes within the walls of capillaries, venules, and small veins; the inflammatory infiltrate is concentrated around the vessels and endothelial necrosis is always present. If the drug is inhaled, an eosinophilic bronchitis/bronchiolitis but also pneumonia can be the resulting morphology (salbutamol, capsaicin). Mucus accumulation is not seen in these cases, so it can be easily separated from mucoid impaction. In chronic forms, fibrosis and proliferation of myofibroblasts can also be seen, which are strictly confined to the septa and do not extend into the alveolar lumina. Thrombosis can occur, again predominantly in small blood vessels. Without clinical information, diagnosis can only be assumed. The final diagnosis will need a multidisciplinary discussion (see also next chapter).

References

1. Travis W, King T, Bateman E, et al. American Thoracic Society/European International Multidisciplinary Consensus Classification of the Idiopathic Interstitial Pneumonias. ATS/ERS joint statement adopted by the ATS board of directors and by the ERS Executive Committee, June 2001. Am J Respir Crit Care Med. 2002;165:277–304.
2. Fujita J, Ohtsuki Y, Yoshinouchi T, Yamadori I, Bandoh S, Tokuda M, Miyawaki H, Kishimoto N, Ishida T. Idiopathic non-specific interstitial pneumonia: as an "autoimmune interstitial pneumonia". Respir Med. 2005;99:234–40.
3. Yoshinouchi T, Ohtsuki Y, Fujita J, Yamadori I, Bandoh S, Ishida T, Ueda R. Nonspecific interstitial pneumonia pattern as pulmonary involvement of rheumatoid arthritis. Rheumatol Int. 2005;26:121–5.
4. Lee HK, Kim DS, Yoo B, Seo JB, Rho JY, Colby TV, Kitaichi M. Histopathologic pattern and clinical features of rheumatoid arthritis-associated interstitial lung disease. Chest. 2005;127:2019–27.
5. Fellbaum C, Domej W, Popper H. Rheumatoid arthritis with extensive lung lesions. Thorax. 1989;44:70–1.
6. Kameda H, Okuyama A, Tamaru J, Itoyama S, Iizuka A, Takeuchi T. Lymphomatoid granulomatosis and diffuse alveolar damage associated with methotrexate therapy in a patient with rheumatoid arthritis. Clin Rheumatol. 2007;26:1585–9.
7. Parambil JG, Myers JL, Ryu JH. Diffuse alveolar damage: uncommon manifestation of pulmonary involvement in patients with connective tissue diseases. Chest. 2006;130:553–8.
8. Vallbracht II, Popper HH, Rieber J, Nowak F, Gallenberger S, Piper B, Helmke K. Lethal pneumonitis under leflunomide therapy. Rheumatology (Oxford). 2005;44:1580–1.
9. Kinder AJ, Hassell AB, Brand J, Brownfield A, Grove M, Shadforth MF. The treatment of inflammatory arthritis with methotrexate in clinical practice: treatment duration and incidence of adverse drug reactions. Rheumatology (Oxford). 2005;44:61–6.
10. Zimmer C, Beiderlinden M, Peters J. Lethal acute respiratory distress syndrome during anti-TNF-alpha therapy for rheumatoid arthritis. Clin Rheumatol. 2006;25:430–2.
11. Garcia Campelo MR, Alonso Curbera G, Aparicio Gallego G, Grande Pulido E, Anton Aparicio LM. Stem cell and lung cancer development: blaming the Wnt, Hh and Notch signalling pathway. Clin Transl Oncol. 2011;13:77–83.
12. Koch AE. The pathogenesis of rheumatoid arthritis. Am J Orthop (Belle Mead NJ). 2007;36:5–8.
13. Haupt HM, Moore GW, Hutchins GM. The lung in systemic lupus erythematosus. Analysis of the pathologic changes in 120 patients. Am J Med. 1981;71:791–8.
14. Lee JG, Joo KW, Chung WK, Jung YC, Zheung SH, Yoon HJ, Kim YS, Ahn C, Han JS, Kim S,

Lee JS. Diffuse alveolar hemorrhage in lupus nephritis. Clin Nephrol. 2001;55:282–8.
15. Quadrelli SA, Alvarez C, Arce SC, Paz L, Sarano J, Sobrino EM, Manni J. Pulmonary involvement of systemic lupus erythematosus: analysis of 90 necropsies. Lupus. 2009;18:1053–60.
16. Dorfmuller P, Humbert M, Perros F, Sanchez O, Simonneau G, Muller KM, Capron F. Fibrous remodeling of the pulmonary venous system in pulmonary arterial hypertension associated with connective tissue diseases. Hum Pathol. 2007;38:893–902.
17. Weng CT, Chung TJ, Liu MF, Weng MY, Lee CH, Chen JY, Wu AB, Lin BW, Luo CY, Hsu SC, Lee BF, Tsai HM, Chao SC, Wang JY, Chen TY, Chen CW, Chang HY, Wang CR. A retrospective study of pulmonary infarction in patients with systemic lupus erythematosus from southern Taiwan. Lupus. 2011;20:876–85.
18. Tsukumo S, Yasutomo K. DNaseI in pathogenesis of systemic lupus erythematosus. Clin Immunol. 2004;113:14–8.
19. Sherer Y, Gorstein A, Fritzler MJ, Shoenfeld Y. Autoantibody explosion in systemic lupus erythematosus: more than 100 different antibodies found in SLE patients. Semin Arthritis Rheum. 2004;34:501–37.
20. Dall'Era M, Davis J. CTLA4Ig: a novel inhibitor of costimulation. Lupus. 2004;13:372–6.
21. Yang CA, Chiang BL. Inflammasomes and human autoimmunity: a comprehensive review. J Autoimmun. 2015;61:1–8.
22. Hassoun PM. Pulmonary arterial hypertension complicating connective tissue diseases. Semin Respir Crit Care Med. 2009;30:429–39.
23. Renzoni EA, Walsh DA, Salmon M, Wells AU, Sestini P, Nicholson AG, Veeraraghavan S, Bishop AE, Romanska HM, Pantelidis P, Black CM, Du Bois RM. Interstitial vascularity in fibrosing alveolitis. Am J Respir Crit Care Med. 2003;167:438–43.
24. Southcott AM, Jones KP, Li D, Majumdar S, Cambrey AD, Pantelidis P, Black CM, Laurent GJ, Davies BH, Jeffery PK, et al. Interleukin-8. Differential expression in lone fibrosing alveolitis and systemic sclerosis. Am J Respir Crit Care Med. 1995;151:1604–12.
25. Takehara K. Hypothesis: pathogenesis of systemic sclerosis. J Rheumatol. 2003;30:755–9.
26. Castello-Cros R, Whitaker-Menezes D, Molchansky A, Purkins G, Soslowsky LJ, Beason DP, Sotgia F, Iozzo RV, Lisanti MP. Scleroderma-like properties of skin from caveolin-1-deficient mice: implications for new treatment strategies in patients with fibrosis and systemic sclerosis. Cell Cycle. 2011;10:2140–50.
27. Wei J, Bhattacharyya S, Tourtellotte WG, Varga J. Fibrosis in systemic sclerosis: emerging concepts and implications for targeted therapy. Autoimmun Rev. 2011;10:267–75.
28. Wei J, Bhattacharyya S, Tourtellotte WG, Varga J. Fibrosis in systemic sclerosis: emerging concepts and implications for targeted therapy. Autoimmun Rev. 2011;10:267–75.
29. McGrath-Morrow S, Laube B, Tzou SC, Cho C, Cleary J, Kimura H, Rose NR, Caturegli P. IL-12 overexpression in mice as a model for Sjogren lung disease. Am J Physiol Lung Cell Mol Physiol. 2006;291:L837–46.
30. Rangel-Moreno J, Hartson L, Navarro C, Gaxiola M, Selman M, Randall TD. Inducible bronchus-associated lymphoid tissue (iBALT) in patients with pulmonary complications of rheumatoid arthritis. J Clin Invest. 2006;116:3183–94.
31. Nguyen CQ, Cornelius JG, Cooper L, Neff J, Tao J, Lee BH, Peck AB. Identification of possible candidate genes regulating Sjogren's syndrome-associated autoimmunity: a potential role for TNFSF4 in autoimmune exocrinopathy. Arthritis Res Ther. 2008;10:R137.
32. Crestani B. The respiratory system in connective tissue disorders. Allergy. 2005;60:715–34.
33. Arends J, Wu J, Borillo J, Troung L, Zhou C, Vigneswaran N, Lou YH. T cell epitope mimicry in antiglomerular basement membrane disease. J Immunol. 2006;176:1252–8.
34. MacDonald BA, Sund M, Grant MA, Pfaff KL, Holthaus K, Zon LI, Kalluri R. Zebrafish to humans: evolution of the alpha3-chain of type IV collagen and emergence of the autoimmune epitopes associated with Goodpasture syndrome. Blood. 2006;107:1908–15.
35. Specks U. Diffuse alveolar hemorrhage syndromes. Curr Opin Rheumatol. 2001;13:12–7.
36. Sharma OP. Unusual systemic disorders associated with interstitial lung disease. Curr Opin Pulm Med. 2001;7:291–4.
37. Zen Y, Kitagawa S, Minato H, Kurumaya H, Katayanagi K, Masuda S, Niwa H, Fujimura M, Nakanuma Y. IgG4-positive plasma cells in inflammatory pseudotumor (plasma cell granuloma) of the lung. Hum Pathol. 2005;36:710–7.
38. Dhobale S, Bedetti C, Killian P, Ilyas M, Liput J, Jasnosz K, Giclas P. IgG4 related sclerosing disease with multiple organ involvements and response to corticosteroid treatment. J Clin Rheumatol. 2009;15:354–7.
39. Hughson MD, McCarty GA, Brumback RA. Spectrum of vascular pathology affecting patients with the antiphospholipid syndrome. Hum Pathol. 1995;26:716–24.
40. Bonfield TL, Russell D, Burgess S, Malur A, Kavuru MS, Thomassen MJ. Autoantibodies against granulocyte macrophage colony-stimulating factor are diagnostic for pulmonary alveolar proteinosis. Am J Respir Cell Mol Biol. 2002;27:481–6.
41. Ioachimescu OC, Kavuru MS. Pulmonary alveolar proteinosis. Chron Respir Dis. 2006;3:149–59.
42. Reed JA, Ikegami M, Cianciolo ER, Lu W, Cho PS, Hull W, Jobe AH, Whitsett JA. Aerosolized GM-CSF ameliorates pulmonary alveolar proteinosis in GM-CSF-deficient mice. Am J Physiol. 1999;276:L556–63.
43. Trapnell BC, Whitsett JA. Gm-CSF regulates pulmonary surfactant homeostasis and alveolar macrophage-mediated innate host defense. Annu Rev Physiol. 2002;64:775–802.
44. Tredano M, Griese M, Brasch F, Schumacher S, de Blic J, Marque S, Houdayer C, Elion J, Couderc R,

Bahuau M. Mutation of SFTPC in infantile pulmonary alveolar proteinosis with or without fibrosing lung disease. Am J Med Genet. 2004;126A: 18–26.
45. Thomassen MJ, Raychaudhuri B, Bonfield TL, Malur A, Abraham S, Barna BP, Kavuru MS. Elevated IL-10 inhibits GM-CSF synthesis in pulmonary alveolar proteinosis. Autoimmunity. 2003;36:285–90.
46. Ioachimescu OC, Sieber S, Kotch A. Idiopathic pulmonary haemosiderosis revisited. Eur Respir J. 2004;24:162–70.
47. Kahraman H, Koksal N, Ozkan F. Eight years follow-up of a case with idiopathic pulmonary hemosiderosis after corticosteroid therapy. N Am J Med Sci. 2012;4:49–51.
48. Astrinidis A, Khare L, Carsillo T, Smolarek T, Au KS, Northrup H, Henske EP. Mutational analysis of the tuberous sclerosis gene TSC2 in patients with pulmonary lymphangioleiomyomatosis. J Med Genet. 2000;37:55–7.
49. Carsillo T, Astrinidis A, Henske EP. Mutations in the tuberous sclerosis complex gene TSC2 are a cause of sporadic pulmonary lymphangioleiomyomatosis. Proc Natl Acad Sci U S A. 2000;97:6085–90.
50. Popper HH, Gamperl R, Pongratz MG, Kullnig P, Juttner-Smolle FM, Pfragner R. Chromosome typing in lymphangioleiomyomatosis of the lung with and without tuberous sclerosis. Eur Respir J. 1993;6:753–9.
51. Smolarek TA, Wessner LL, McCormack FX, Mylet JC, Menon AG, Henske EP. Evidence that lymphangiomyomatosis is caused by TSC2 mutations: chromosome 16p13 loss of heterozygosity in angiomyolipomas and lymph nodes from women with lymphangiomyomatosis. Am J Hum Genet. 1998; 62:810–5.
52. Johnson SR, Cordier JF, Lazor R, Cottin V, Costabel U, Harari S, Reynaud-Gaubert M, Boehler A, Brauner M, Popper H, Bonetti F, Kingswood C. European Respiratory Society guidelines for the diagnosis and management of lymphangioleiomyomatosis. Eur Respir J. 2010;35:14–26.
53. Dabora SL, Franz DN, Ashwal S, Sagalowsky A, DiMario Jr FJ, Miles D, Cutler D, Krueger D, Uppot RN, Rabenou R, Camposano S, Paolini J, Fennessy F, Lee N, Woodrum C, Manola J, Garber J, Thiele EA. Multicenter phase 2 trial of sirolimus for tuberous sclerosis: kidney angiomyolipomas and other tumors regress and VEGF- D levels decrease. PLoS ONE. 2011;6, e23379.
54. Davies DM, de Vries PJ, Johnson SR, McCartney DL, Cox JA, Serra AL, Watson PC, Howe CJ, Doyle T, Pointon K, Cross JJ, Tattersfield AE, Kingswood JC, Sampson JR. Sirolimus therapy for angiomyolipoma in tuberous sclerosis and sporadic lymphangioleiomyomatosis: a phase 2 trial. Clin Cancer Res. 2011;17:4071–81.
55. McCormack FX, Inoue Y, Moss J, Singer LG, Strange C, Nakata K, Barker AF, Chapman JT, Brantly ML, Stocks JM, Brown KK, Lynch 3rd JP, Goldberg HJ, Young LR, Kinder BW, Downey GP, Sullivan EJ, Colby TV, McKay RT, Cohen MM, Korbee L, Taveira-DaSilva AM, Lee HS, Krischer JP, Trapnell BC. Efficacy and safety of sirolimus in lymphangioleiomyomatosis. N Engl J Med. 2011;364: 1595–606.
56. Bittmann I, Rolf B, Amann G, Lohrs U. Recurrence of lymphangioleiomyomatosis after single lung transplantation: new insights into pathogenesis. Hum Pathol. 2003;34:95–8.
57. Bittmann I, Dose TB, Muller C, Dienemann H, Vogelmeier C, Lohrs U. Lymphangioleiomyomatosis: recurrence after single lung transplantation. Hum Pathol. 1997;28:1420–3.
58. Crooks DM, Pacheco-Rodriguez G, DeCastro RM, McCoy Jr JP, Wang JA, Kumaki F, Darling T, Moss J. Molecular and genetic analysis of disseminated neoplastic cells in lymphangioleiomyomatosis. Proc Natl Acad Sci U S A. 2004;101:17462–7.
59. Nine JS, Yousem SA, Paradis IL, Keenan R, Griffith BP. Lymphangioleiomyomatosis: recurrence after lung transplantation. J Heart Lung Transplant. 1994;13:714–9.
60. O'Brien JD, Lium JH, Parosa JF, Deyoung BR, Wick MR, Trulock EP. Lymphangiomyomatosis recurrence in the allograft after single-lung transplantation. Am J Respir Crit Care Med. 1995;151:2033–6.
61. Bonetti F, Chiodera PL, Pea M, Martignoni G, Bosi F, Zamboni G, Mariuzzi GM. Transbronchial biopsy in lymphangiomyomatosis of the lung. HMB45 for diagnosis. Am J Surg Pathol. 1993;17:1092–102.
62. Matsui K, Takeda K, Yu ZX, Valencia J, Travis WD, Moss J, Ferrans VJ. Downregulation of estrogen and progesterone receptors in the abnormal smooth muscle cells in pulmonary lymphangioleiomyomatosis following therapy. An immunohistochemical study. Am J Respir Crit Care Med. 2000; 161:1002–9.
63. Spritz RA. Molecular genetics of the Hermansky-Pudlak and Chediak-Higashi syndromes. Platelets. 1998;9:21–9.
64. Anderson PD, Huizing M, Claassen DA, White J, Gahl WA. Hermansky-Pudlak syndrome type 4 (HPS-4): clinical and molecular characteristics. Hum Genet. 2003;113:10–7.
65. Hermos CR, Huizing M, Kaiser-Kupfer MI, Gahl WA. Hermansky-Pudlak syndrome type 1: gene organization, novel mutations, and clinical-molecular review of non-Puerto Rican cases. Hum Mutat. 2002;20:482.
66. Starcevic M, Nazarian R, Dell'Angelica EC. The molecular machinery for the biogenesis of lysosome-related organelles: lessons from Hermansky-Pudlak syndrome. Semin Cell Dev Biol. 2002;13:271–8.
67. Wei ML. Hermansky-Pudlak syndrome: a disease of protein trafficking and organelle function. Pigment Cell Res. 2006;19:19–42.

Eosinophilic Lung Diseases 10

10.1 Introduction

Eosinophilic lung diseases are discussed in a separate chapter, due to the variation of etiologies and similarities of the morphologic appearance. However, some eosinophilic diseases such as bronchial asthma and Langerhans cell histiocytosis are not included here, because they have been discussed in previous chapters; eosinophilic granulomatosis with polyangiitis (EGPA, previously Churg-Strauss syndrome/vasculitis) will be discussed in the chapter on vascular diseases.

Eosinophilic granulocytes (eosinophil) are the main defense cells against parasitic infection. Why these cells also play a major role in allergic diseases and in drug reactions is still not solved. However there is some knowledge, which might explain their role in such diverse inflammatory reactions.

The eosinophil can react pro-inflammatory as well as anti-inflammatory. The cells contain toxic proteins such as major basic (cationic) protein, exotoxin, which are stored in their large secondary granules, but also contain anti-inflammatory proteins, such as a leucine-aminodipeptidase and histaminase [1, 2]. Depending on the presence of substances in the microenvironment, large granules are released together with their content and cause tissue necrosis or paralysis of parasites and holes in the parasitic cuticle, the latter especially using enzymes which can dissolve the cuticle as arylsulfatase. In resolving inflammation, constituents from small granules are released resulting in deactivation of leukotrienes by aminopeptidase, histamine by histaminase, and glycolipids/glycosaminoglycans by arylsulfatase B [1, 3]. It might well be that similar microenvironmental conditions are present in allergen-induced diseases as in parasitic infections. In experimental work, a similarity was shown on the amino acid sequences between some pollens and cuticles of worms [4]. So probably a molecular mimicry might be one of the reasons for eosinophils to infiltrate in allergic reactions including asthma [5].

10.2 Allergic or Hyperreactive Diseases

10.2.1 Allergic Bronchopulmonary Mycosis (Aspergillosis)

We have discussed allergic bronchopulmonary mycosis already in the previous chapter; therefore, we will briefly recall the main aspects, as this is necessary for differential diagnosis.

In most patients, a type I immune reaction with IgE antibodies is produced, causing a similar clinical presentation as in allergic asthma. Patients cannot cough up mucus; however, hyperreactivity of the airways is much less pronounced as in asthma. Dyspnea in

© Springer-Verlag Berlin Heidelberg 2017
H. Popper, *Pathology of Lung Disease*, DOI 10.1007/978-3-662-50491-8_10

mucoid impaction is predominantly induced by obstruction of the airways by thick mucus plugs [6]. The disease presents as an eosinophilic bronchitis with extreme hyperplasia of goblet cells in the mucosa and the bronchial glands. Hyperplasia of the smooth muscle layer is common (Fig. 10.1). Silver impregnation stains, such as Grocott methenamine, can highlight the causing fungal remnants. On bronchoscopy these mucus casts can be completely removed from the bronchial tree by sucking up with the bronchoscope. This is almost diagnostic for mucoid impaction and in addition relives symptoms of the patient.

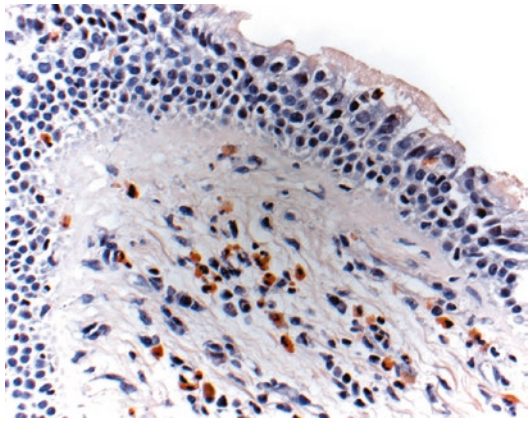

Fig. 10.1 Eosinophilic bronchitis in mucoid impaction type of ABPM. Congo red stain highlights eosinophilic cationic proteins. Congo red, ×250

The second form of ABPM is *bronchocentric granulomatosis*. This is a combined immune reaction toward fungal proteins with an IgE-based antibody reaction and a granulomatous type IV reaction. The disease presents with necrotizing bronchitis/bronchiolitis with peribronchiolar extension of the inflammatory infiltrates. Within the bronchiolar walls, epithelioid cell granulomas and/or palisading his-

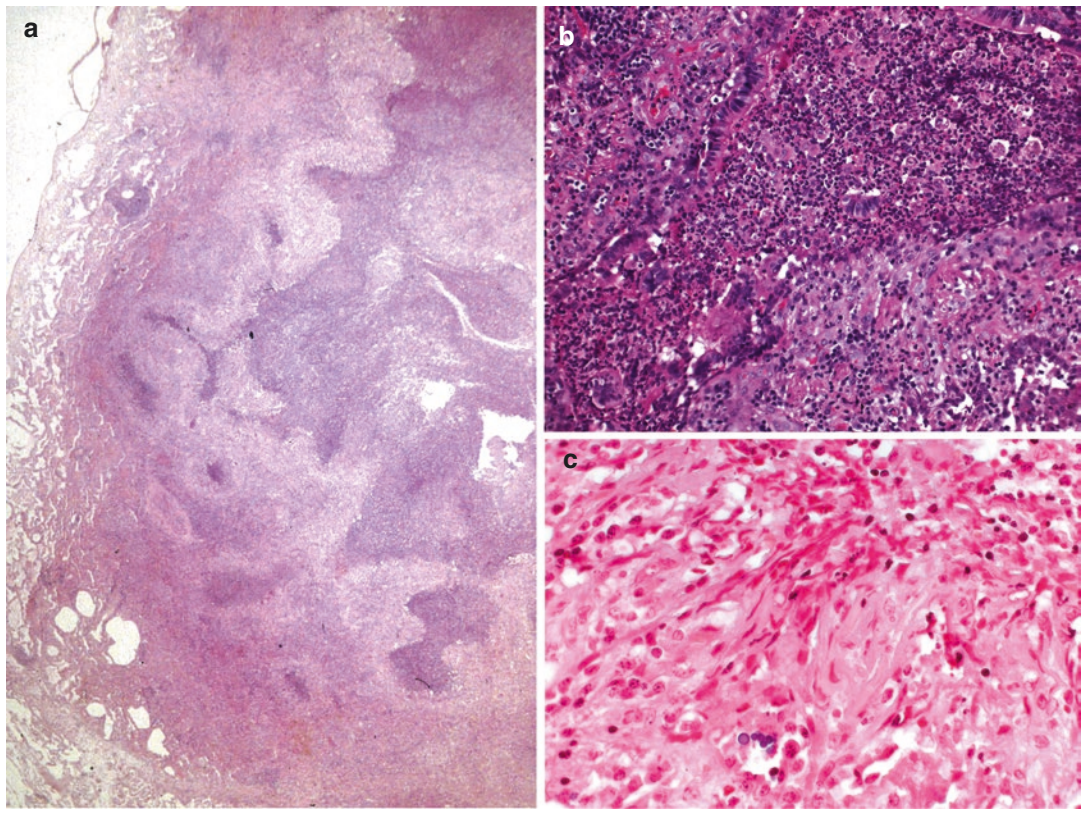

Fig. 10.2 Bronchocentric granulomatosis. (**a**) Shown in an overview how the dark stained necrosis follows or outlines the airways. In (**b**) the necrosis of a bronchus is seen; in (**c**) by Gram stain remnants of fungi are demonstrated. H&E, ×12 and 100, Gram, ×400

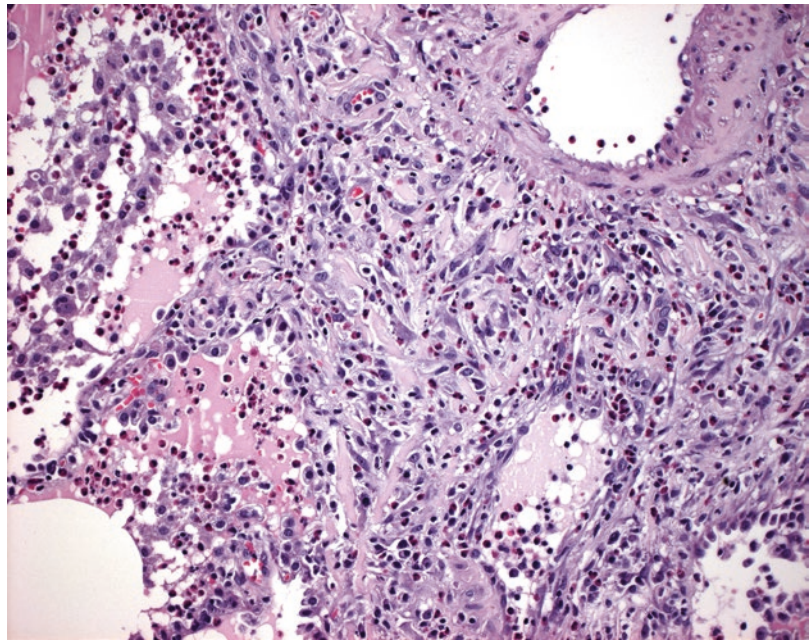

Fig. 10.3 Eosinophilic pneumonia here in a patient with an allergic reaction for fungal proteins, thus representing the rare variant of eosinophilic pneumonia in ABPM. H&E, ×200

tiocytic granulomas are found. In addition there is usually a dense infiltrate of eosinophils (Fig. 10.2). In full-blown disease, the necrosis might outline the bronchial tree like a cast formed by necrotic debris. In the lumina remnants of organisms might be demonstrated using silver impregnation or other special stains. In this classic variant, BCG is induced by an allergic reaction against different types of fungi, most often members of the *Aspergillus* family. However, AFS and GMS stains should always be performed to exclude mycobacteria, especially when the inflammatory infiltrates contain predominantly neutrophils. The clinical information about positive allergy tests might be helpful. In rare cases bronchocentric, necrotizing granulomatosis might also be seen in the setting of Wegener's disease [7]. Therefore ANCA tests can be helpful in this differential diagnosis.

In rare cases ABPM can present as *eosinophilic pneumonia* (Fig. 10.3). This is very similar to chronic eosinophilic pneumonia, which will be discussed below.

Bronchial asthma has already been discussed in airway diseases so the reader is referred to Chap. 6; drug allergies have been discussed in the previous chapter.

10.3 Eosinophilic Pneumonias (EP)

10.3.1 Epidemiology and Incidence

Eosinophilic pneumonias can present as acute or chronic eosinophilic pneumonia.

10.3.2 Clinical Presentation and CT

On CT/HRCT EP present focal densities, sometimes with ground-glass pattern; in other cases, there might be densities fluctuating over time within different lung lobes (Fig. 10.4).

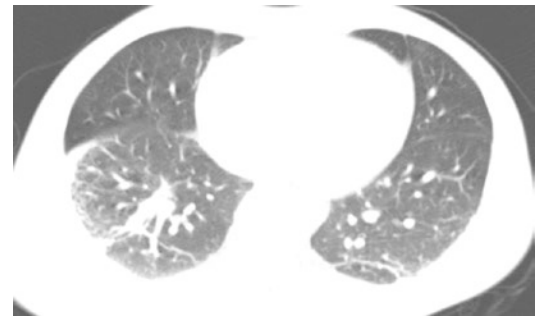

Fig. 10.4 CT scan of eosinophilic pneumonia with ground-glass opacities in both lower lobes in addition to bronchiectasis

There is no specific feature, which might differentiate EP from other pneumonias. Clinically EP present with a sudden onset of cough, fever usually of 1 week duration, myalgia and chest pain, and dyspnea. Spontaneous resolution does occur in some cases; in others clinical symptoms worsen rapidly. Most often patients present without blood eosinophilia. In some progressive cases, patients can die with respiratory failure.

10.3.3 Pathogenesis and Etiology

In acute as well as chronic eosinophilic pneumonia, parasitic infection is the most common cause. Eosinophilic pneumonia can also be seen in vasculitis, especially eosinophilic granulomatosis with polyangiitis (Churg-Strauss syndrome), in drug reactions, in exogenous vapor inhalation, in hypereosinophilic syndrome, and in allergic fungal reactions; finally in some cases, no underlying etiology can be detected, leaving this EP as idiopathic.

Macroscopically on gross sections, there are grayish-red consolidations, not otherwise specific.

The most prominent feature is a dense infiltration of the lung by eosinophils, although macrophages can sometimes be present in substantial number (Fig. 10.5). Eosinophilia can be also seen in bronchoalveolar lavage; the percentage is usu-

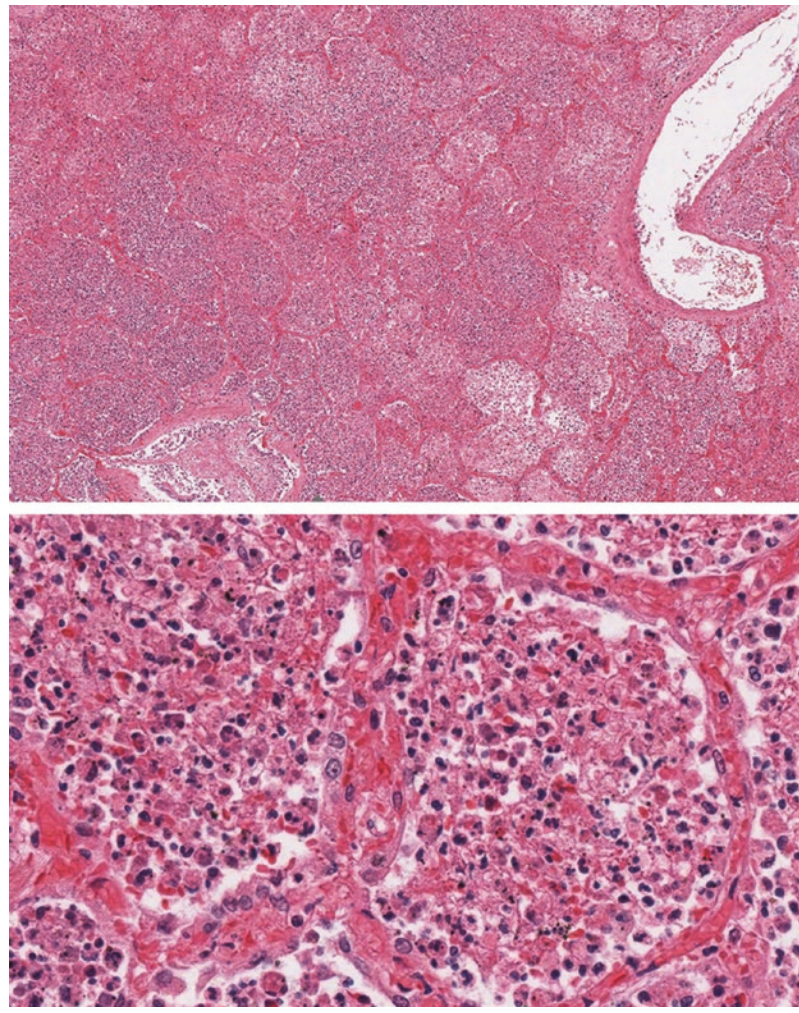

Fig. 10.5 Acute eosinophilic pneumonia of unknown cause. Overview showing diffuse dense infiltrations in all alveoli and respiratory bronchioles (*upper panel*); by higher magnification the cells are predominantly eosinophils (*lower panel*). H&E, ×12 and 200

ally above 25 %. Fibrosis, sometimes presenting as organizing pneumonia, can be seen in chronic eosinophilic pneumonia (Figs. 10.6 and 10.7).

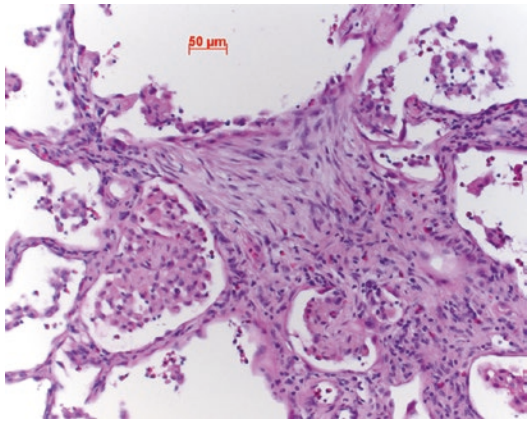

Fig. 10.6 Organizing pneumonia as a fibrosing process in eosinophilic pneumonia. There are still many eosinophils present, but also macrophages. H&E, bar 50 µm

Peripheral blood eosinophilia may or may not be present. Eosinophils are directly responsible of tissue damage or at least are part of the process.

10.3.3.1 Acute Eosinophilic Pneumonia

Acute eosinophilic pneumonia (AEP) is characterized by an acute onset with dyspnea and diffuse infiltrations by eosinophils in both lungs. Blood eosinophilia can be present, especially in Loffler's syndrome and in parasitic infections. On histology the alveoli and alveolar and bronchiolar walls are stuffed by eosinophils and macrophages (Fig. 10.5). Etiologically parasitic infection and hypersensitivity reaction for drugs are the cause; however, also an idiopathic form does exist. An infection by helminthes will usually cause mild symptoms, whereas in filarial infections (tropic eosinophilia), the symptoms can be severe (high fever, cough, wheezing,

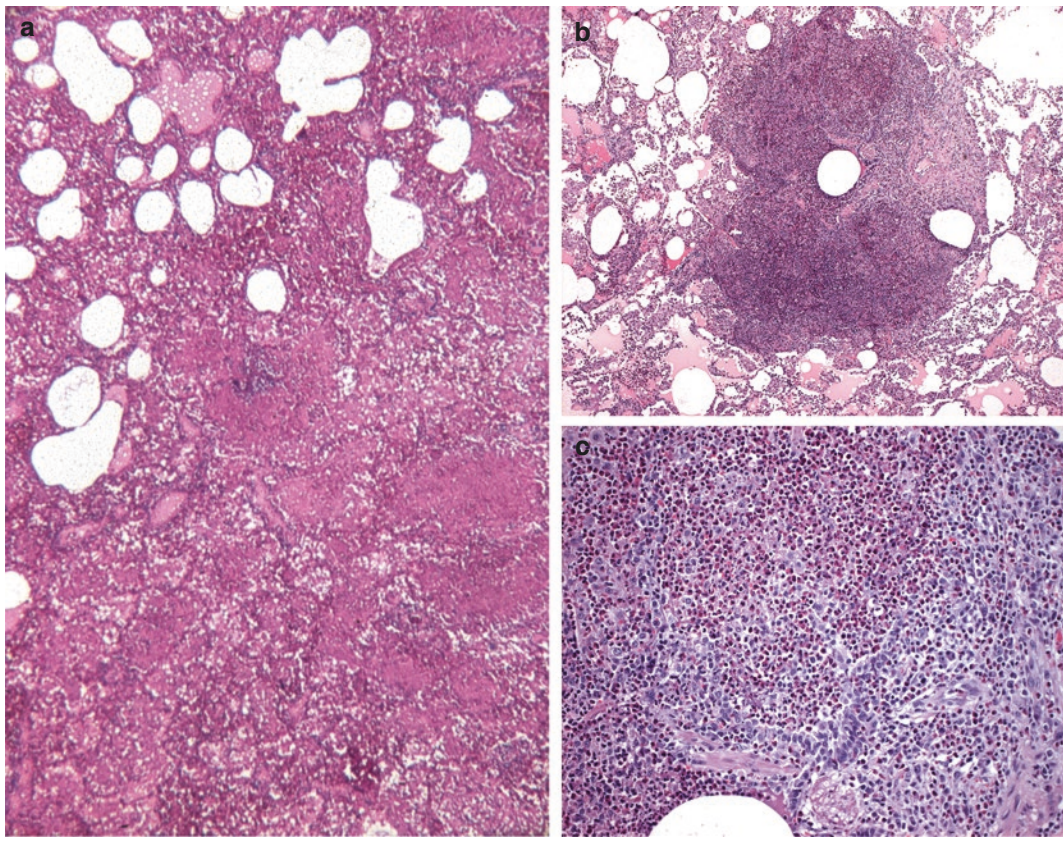

Fig. 10.7 Chronic eosinophilic pneumonia with abscess formation. (**a**) Overview with many pink necrotic areas. (**b**) Higher magnification of such necrotic areas and abscess formation in (**c**). H&E, ×12, 25, and 100

peripheral eosinophilia) [8, 9]. Evaluation of parasitosis can be time-consuming. Parasites or eggs from parasites can be hidden in some areas, whereas the eosinophilic infiltrate is diffusely distributed. In case of parasitic larva, their movement can also cause a long search for the causing organisms (Table 10.1).

Several drugs can cause an eosinophilic pneumonia. Many of these are antibiotics, where they form haptens and associate with body proteins to form an antigen. A classical example is penicillin and beta-lactam allergy [10, 11]. However, many more drugs can cause EP (see Table 10.2). In some drugs, not only chronic eosinophilic pneumonia but moreover acute eosinophilic pneumonia can be seen such as in amoxicillin, amphetamines, chloroquine, cocaine, E-cigarettes, gemcitabine, tacrolimus, waterproofing agents/sprays, and household cleaning compounds (see also www.pneumotox.com).

A proper investigation of treatment protocols is advised (more details are found on www.pneumotox.com). In addition other inhaled toxins can cause EP such as cocaine, nickel carbonyl, and constituents of fire extinguisher foams [12].

Allergic reaction for fungal hyphae can in rare cases also cause EP (see above). In primary vasculitis such as Churg-Strauss vasculitis, this can be accompanied by an eosinophilic pneumonia [13, 14] (this vasculitis will be discussed in Chap. 11 on vascular diseases).

Loffler's syndrome is a self-limited condition, resolving usually within 1 month. On CT scan migratory pulmonary infiltrates can be seen, accompanied by a peripheral blood eosinophilia. In some cases specific causes such as chronic eosinophilic leukemia but also parasitic infections can be identified; however, in other cases no underlying etiology can be identified [15, 16].

In acute idiopathic eosinophilic pneumonia, there is acute febrile illness usually of 1-week duration, with myalgia, chest pain, and hypoxemic respiratory failure. On CT scan alveolar and interstitial infiltrates are seen; in BAL eosinophils increase over 25 %; however, there is no blood eosinophilia. Patients rapidly respond to steroid therapy without relapse after suspension of steroids. No cause can be identified.

Chronic eosinophilic pneumonia is a serious disease that requires a specific treatment. Most often affected are middle-aged patients sometimes

Table 10.1 Parasites causing eosinophilic pneumonia

Ascaris lumbricoides (Fig. 10.8)
Strongyloides stercoralis and *venezuelensis* (Fig. 10.9)
Toxocara canis
Necator americanus
Echinococcus hydatidosis
Paragonimus westermani, *miyazaki*, and *kellicotti* (Fig. 10.10)
Toxoplasma gondii
Schistosoma mansoni
Angiostrongylus cantonensis
Clonorchis sinensis
Dirofilaria species (Fig. 10.11)
Wuchereria bancrofti and other filarial species
Taenia saginata, *Taenia solium* (Fig. 10.12)

Table 10.2 Drugs and causing eosinophilic pneumonia

Drugs	Vapors/inhalants
Ampicillin	Cocaine
Penicillin	Nickel carbonyl
Streptomycin	Fire extinguisher foam
Tetracycline	Arsenic trioxide
Sulfonamide	
Clarithromycin	
Carbamazepine	
Beclorobethasone	
Nitrofurantoin	
Bleomycin	
Chlorpromazine	
Chlorpropamide	
Cromolyn	
Dilantin	
Gold salts	
Naproxen	
Nitrofurantoin	
Propylthiouracil	
Phenylbutazone	
Phenothiazine	

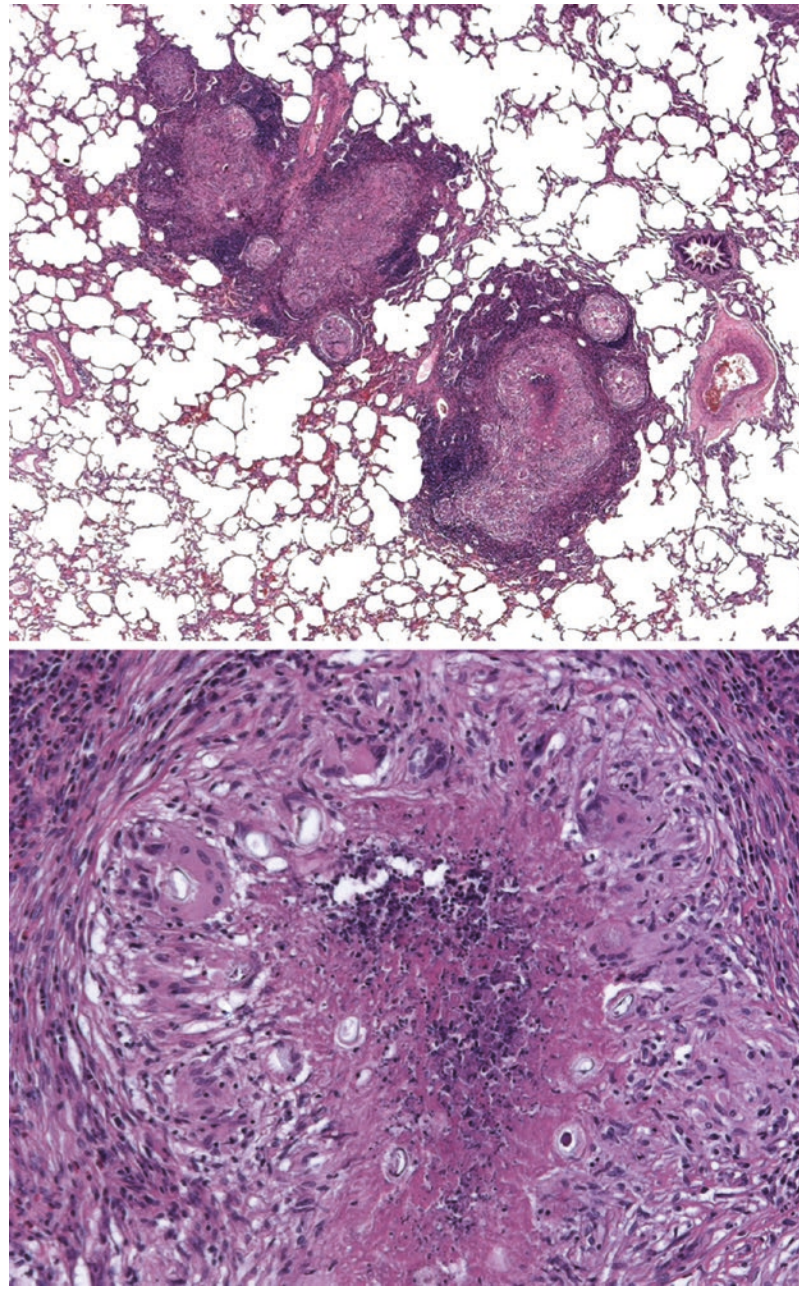

Fig. 10.8 Eosinophilic pneumonia with granuloma formation in a case of *Ascaris lumbricoides* infection. Overview and high magnification of a granuloma. H&E, ×25 and 250 (Courtesy of Dr. U. Gruber-Moesenbacher, Feldkirch)

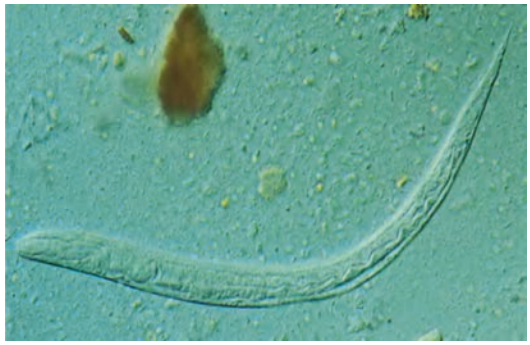

Fig. 10.9 Strongyloides species in BAL. H&E, ×50

also young atopic women. The disease starts with an insidious onset with progressive respiratory symptoms, as febrile illness, myalgia, chest pain, and hypoxia. A history of asthma is present in 50–60 % cases. Some cases can be attributed to drug toxicity (ampicillin, bleomycin, nitrofurantoin, penicillin, streptomycin, tetracycline, others); in others hypersensitivity to fungi has been shown. Some cases represent chronic infection with parasites. Single cases have been described where chronic eosinophilic pneumonia was associated with cocaine or nickel carbonyl vapor inhalation. On CT scan alveolar and interstitial infiltrates are seen in both lungs. The characteristic histologic picture shows dense eosinophilic infiltrations accompanied by macrophages and lymphocytes. There can be eosinophilic abscesses. Fibroblast proliferations can be seen focally, which finally results in interstitial fibrosis (Figs. 10.6 and 10.7).

In all cases of eosinophilic pneumonia, a careful research for parasitic infections or drugs should be done before labeling it as idiopathic. This is especially important, because also chronic EP can respond to corticosteroid treatment.

Hypereosinophilic syndrome is a rare disease of unknown cause [17]. It is characterized by increased eosinophilic infiltrations in multiple

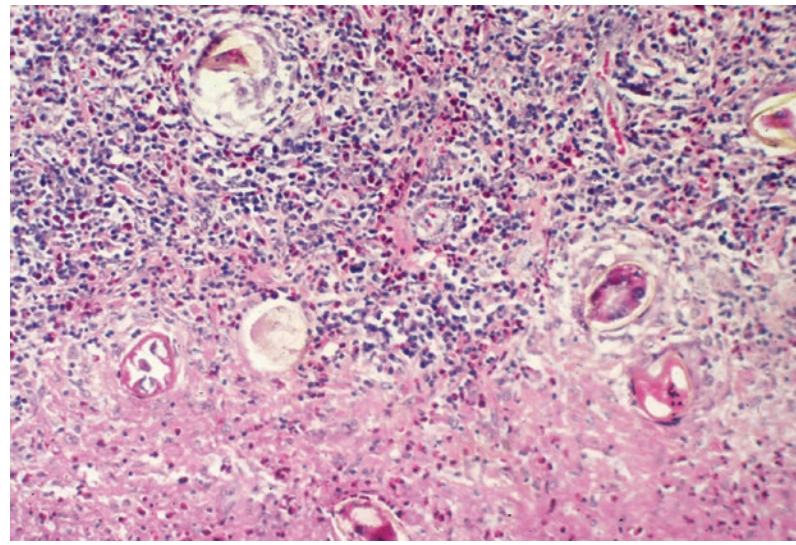

Fig. 10.10 Eosinophilic pneumonia in infection with eggs from *Paragonimus brasiliensis*. H&E, ×100

organs (mainly the heart and CNS, rarely the lungs). Fatal cases have been reported mainly caused by restrictive cardiomyopathy.

10.3.4 Immunohistochemistry, Genetics, and Immunology

Eosinophilia is most often induced by the release of interleukins 4 and 5 [18, 19]. It can vary quite remarkably in the different diseases, less pronounced in Langerhans cell histiocytosis, whereas massive in eosinophilic pneumonias. By bronchoalveolar lavage, a tentative diagnosis can be made: eosinophil counts in BAL usually are between 5 % and 20 % in Langerhans cell histiocytosis, whereas in the eosinophilic pneumonias, it usually exceeds 30 %. In parasitic diseases, sometimes the parasites (larvae) might be seen in BAL (Fig. 10.9).

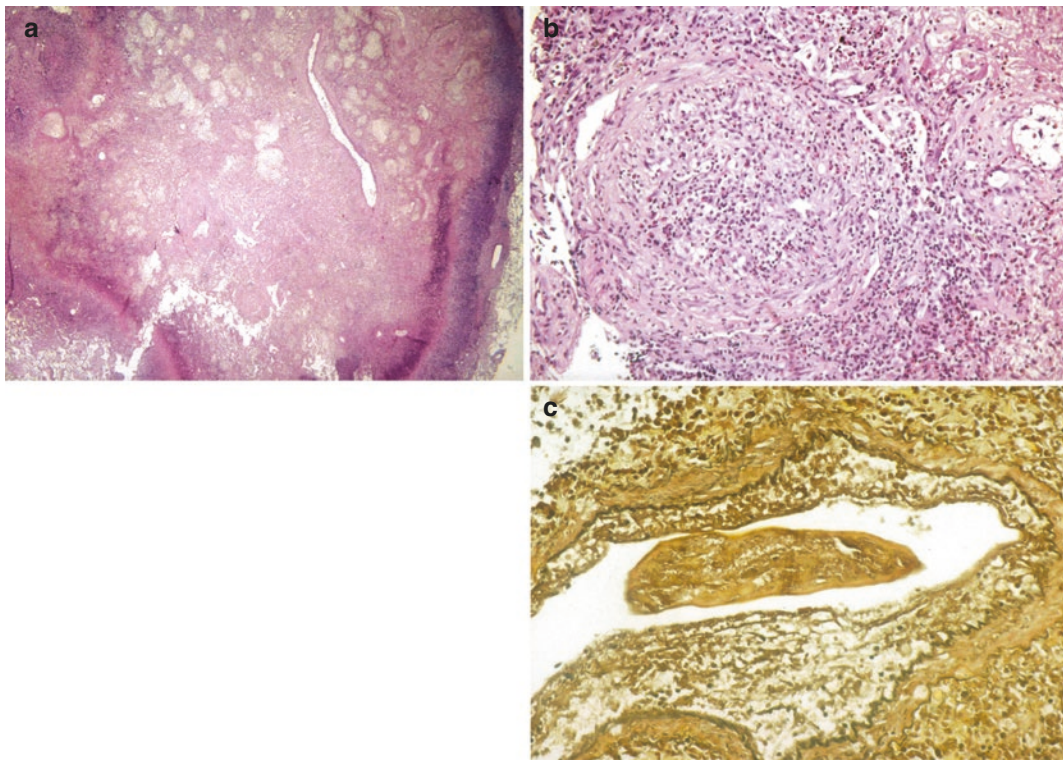

Fig. 10.11 *Dirofilaria* infection. Due to multiple nodules in both lungs, metastatic tumor was suspected in this patient. (**a**) A large ischemic infarct is seen; (**b**) eosinophilic vasculitis has caused this infarct; (**c**) *Dirofilaria* species was identified in one of the pulmonary arteries. H&E, ×12 and 100, Elastica v. Gieson, 200

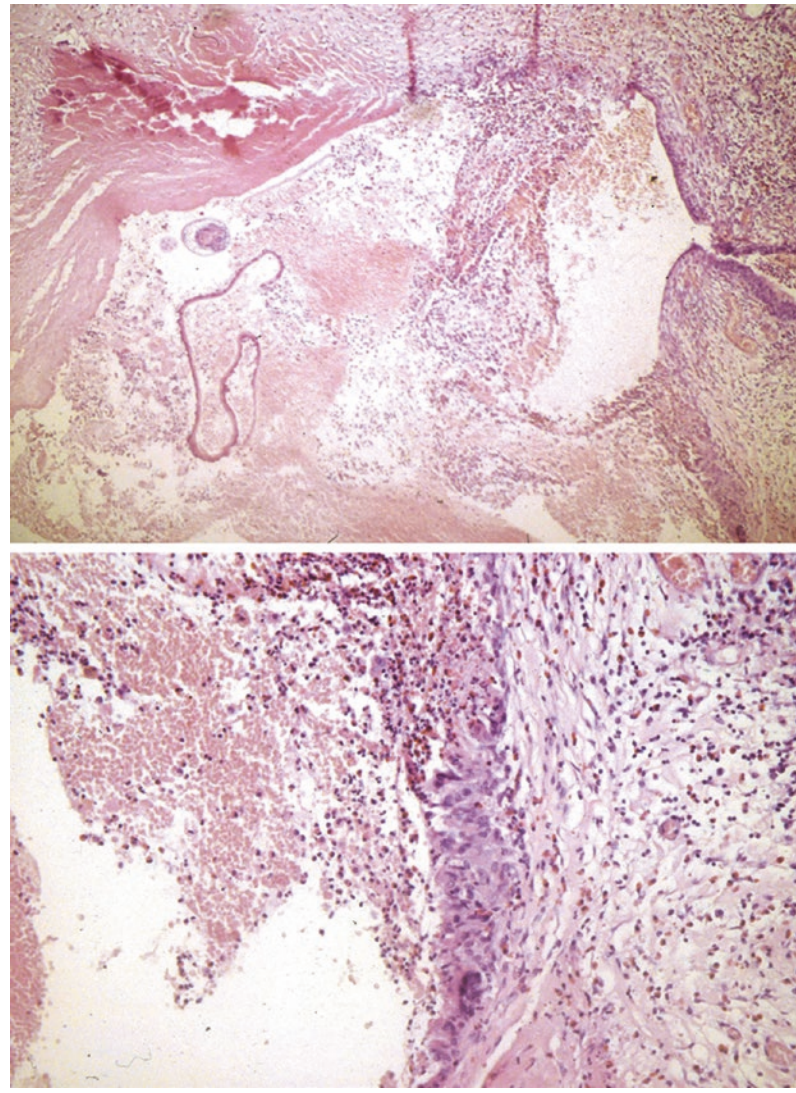

Fig. 10.12 Infection by *Taenia saginata* (cysticercosis). In the upper panel, the cyst is shown with fragments of the parasite including parts of the head. In the lower panel, the tissue reaction with epithelioid granuloma formation and eosinophilic pneumonia is seen. H&E, ×12 and 100

References

1. Popper H, Knipping G, Czarnetzki BM, Steiner R, Helleis G, Auer H. Activation and release of enzymes and major basic protein from guinea pig eosinophil granulocytes induced by different inflammatory stimuli and other substances. A histochemical, biochemical, and electron microscopic study. Inflammation. 1989;13:147–62.
2. Acharya KR, Ackerman SJ. Eosinophil granule proteins: form and function. J Biol Chem. 2014;289:17406–15.
3. Fechter M, Egger D, Auer H, Popper H. Experimental eosinophilia and inflammation – the effect of various inflammatory mediators and chemoattractants. Exp Pathol. 1986;29:153–8.
4. Platts-Mills TA, Woodfolk JA. Allergens and their role in the allergic immune response. Immunol Rev. 2011;242:51–68.
5. Garon EB, Rizvi NA, Hui R, Leighl N, Balmanoukian AS, Eder JP, Patnaik A, Aggarwal C, Gubens M, Horn L, Carcereny E, Ahn MJ, Felip E, Lee JS, Hellmann MD, Hamid O, Goldman JW, Soria JC, Dolled-Filhart M, Rutledge RZ, Zhang J, Lunceford JK, Rangwala R, Lubiniecki GM, Roach C, Emancipator K, Gandhi L. Pembrolizumab for the treatment of non-small-cell lung cancer. N Engl J Med. 2015;372:2018–28.
6. Katzenstein AL, Liebow AA, Friedman PJ. Bronchocentric granulomatosis, mucoid impaction, and hypersensitivity reactions to fungi. Am Rev Respir Dis. 1975;111:497–537.

7. Uner AH, Rozum-Slota B, Katzenstein AL. Bronchiolitis obliterans-organizing pneumonia (BOOP)-like variant of Wegener's granulomatosis. A clinicopathologic study of 16 cases. Am J Surg Pathol. 1996;20:794–801.
8. Janz DR, O'Neal Jr HR, Ely EW. Acute eosinophilic pneumonia: a case report and review of the literature. Crit Care Med. 2009;37:1470–4.
9. Chitkara RK, Krishna G. Parasitic pulmonary eosinophilia. Semin Respir Crit Care Med. 2006;27: 171–84.
10. Macy E. Penicillin allergy: optimizing diagnostic protocols, public health implications, and future research needs. Curr Opin Allergy Clin Immunol. 2015;15: 308–13.
11. Ariza A, Mayorga C, Fernandez TD, Barbero N, Martin-Serrano A, Perez-Sala D, Sanchez-Gomez FJ, Blanca M, Torres MJ, Montanez MI. Hypersensitivity reactions to beta-lactams: relevance of hapten-protein conjugates. J Investig Allergol Clin Immunol. 2015; 25:12–25.
12. Laitinen JA, Koponen J, Koikkalainen J, Kiviranta H. Firefighters' exposure to perfluoroalkyl acids and 2-butoxyethanol present in firefighting foams. Toxicol Lett. 2014;231:227–32.
13. Marchand E, Cordier JF. Idiopathic chronic eosinophilic pneumonia. Semin Respir Crit Care Med. 2006;27:134–41.
14. Abril A. Churg-Strauss syndrome: an update. Curr Rheumatol Rep. 2011;13:489–95.
15. Acar A, Oncul O, Cavuslu S, Okutan O, Kartaloglu Z. Case report: Loffler's syndrome due to Ascaris lumbricoides mimicking acute bacterial community – acquired pneumonia. Turkiye Parazitol Derg. 2009;33:239–41.
16. Song G, Liu H, Sun F, Gu L, Wang S. Acute lymphocytic leukemia with eosinophilia: a case report and review of the literature. Aging Clin Exp Res. 2012; 24:555–8.
17. Bunc M, Remskar Z, Brucan A. The idiopathic hypereosinophilic syndrome. Eur J Emerg Med. 2001;8:325–30.
18. Popper HH, Pailer S, Wurzinger G, Feldner H, Hesse C, Eber E. Expression of adhesion molecules in allergic lung diseases. Virchows Arch. 2002;440:172–80.
19. Takatsu K, Nakajima H. IL-5 and eosinophilia. Curr Opin Immunol. 2008;20:288.

Vascular Lung Diseases 11

Here we will discuss infarct and thromboembolic disease, vasculitis, vascular malformations, and pulmonary hypertension. Vascular tumors have already been discussed.

11.1 Infarct and Thromboembolic Disease

Thromboembolism is a frequent event in older patients. Often the underlying disease is chronic heart failure with venous congestion. Thrombi are formed in the lower extremities but also in the pelvic region and give rise to emboli. Large emboli will get stuck in the large pulmonary arteries and cause sudden death with the symptoms similar to cardiac infarct. Smaller emboli might be pressed into smaller arteries and get stuck there. These emboli will cause a hemorrhagic infarct by occlusion of a pulmonary artery and retrograde influx of blood from the venous side as well as from bronchial arteries. Since the lung has a double system of blood flow, bronchial and pulmonary system ischemic infarcts do not occur – there is one exception, ischemic infarct in vasculitis.

11.1.1 Gross Examination and Histology

An infarct has a cuneiform appearance, the broad side is at the periphery, and the tip is where the artery is occluded. On cut surface the infarct is dark red with a hemorrhagic dark blue-red border. The consistency is firm.

On histology, the center of the infarct has lost staining of the cells (no nuclei visible), and the cells appear like ghost cells; however, the alveolar structure is still visible (Fig. 11.1). If the infarct is older, an inflammatory granulation tissue develops (usually a type of organizing pneumonia), which slowly will organize the infarct and replace it with scar tissue. Even as scar the cuneiform figure will remain. At the border of the infarct, numerous hemosiderin-laden macrophages will appear. Elastic stains can easily highlight obstructed arteries. Typically there are thick-walled arteries in the vicinity of the infarct, probably reflecting increased vascular pressure.

11.2 Vasculitis

11.2.1 Classification of Vasculitis

According to the Chapel Hill classification, there is primary systemic vasculitis and secondary (most often infection associated) vasculitis, and there is large medium and small vessel vasculitis [1]; the affection of arteries and veins is not further acknowledged. In this last update of the primary 1994 classification, changes were made such as granulomatosis with polyangiitis instead of Wegener's granulomatosis and eosinophilic granulomatosis with polyangiitis instead of

© Springer-Verlag Berlin Heidelberg 2017
H. Popper, *Pathology of Lung Disease*, DOI 10.1007/978-3-662-50491-8_11

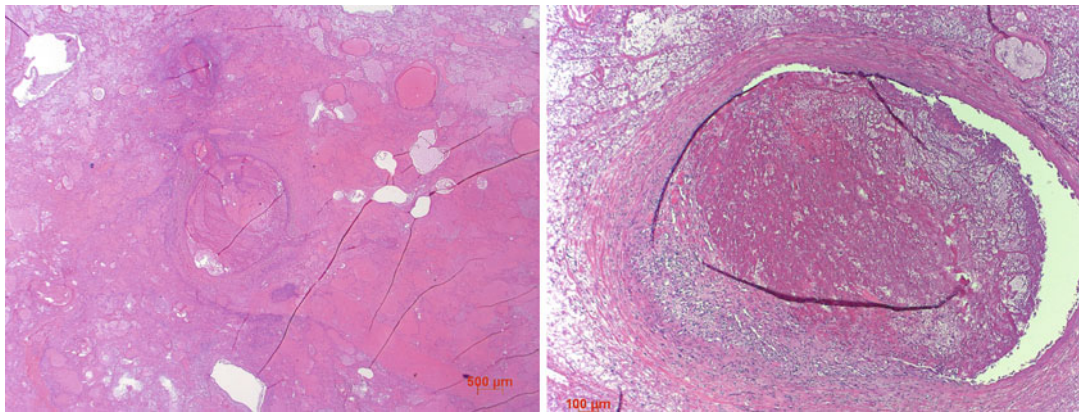

Fig. 11.1 Hemorrhagic infarct, left the infarct is seen with hemorrhage and the occluded artery, to the right an artery with a thromboembolus is shown, the embolus is already undergoing organization by granulation tissue. H&E, bars 500 and 100 µm

Churg-Strauss vasculitis. In addition, categories for variable vessel vasculitis and secondary forms of vasculitis were added. The lung is affected by a few variants of primary systemic vasculitis, which are discussed here. Secondary vasculitis will not extensively be discussed.

Schema of the classification of vasculitides according to the 1994 Chapel Hill classification: Vasculitides are grouped according to the size of the affected vessels; this classification was modified in 2012; however, the involvement of vessels is still the basis of the updated classification.

Jennette, Falk, et al., *Arthritis & Rheumatism*

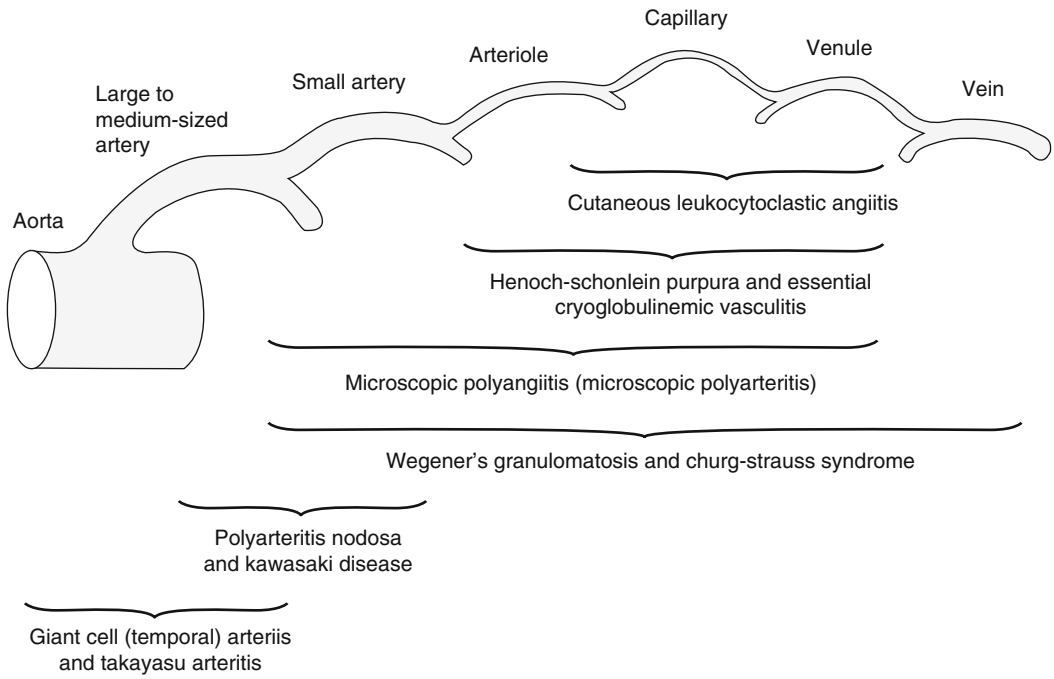

11.2.2 Granulomatosis with Polyangiitis

Granulomatosis with polyangiitis (GPA), formerly called *Wegener's granulomatosis*, affects medium to small arteries, arterioles, capillaries, venules, and small- to medium-sized veins. There are three main organ systems involved: mucosa of the upper airways, lungs, and kidneys. In some patients, only one organ system, in other patients two organ systems, and in some patients all three systems can be affected.

The vasculitis will cause vascular obstruction followed by occlusion, which finally will cause ischemic infarct if the vessel is large enough.

11.2.2.1 Clinical and Radiological Findings

Patients present with hemoptysis, fever may be seen, on serum examination antineutrophil cytoplasmic antibodies (ANCA) may be present; antibodies are a sign of the underlying vasculitis. Examination of ANCA antibodies will show more common anti-proteinase 3 (PR3) [2]. On X-ray and CT scan, classical GPA will show infarct with less dense center parts (Fig. 11.2). Several infarcts can be present. If only small vessels are affected, the CT scan is less characteristic with diffuse interstitial infiltrates. Usually both lungs are involved. In these cases hemoptysis will be more pronounced, and on BAL alveolar hemorrhage will be diagnosed.

For a clinical diagnosis, the following features are required: histopathological evidence of granulomatous inflammation, upper airway involvement, laryngo-tracheo-bronchial involvement, pulmonary involvement (X-ray/CT), antineutrophilic cytoplasmic antibody positivity, and renal involvement [3].

11.2.2.2 Gross Examination

If infarcts are present, these will have a similar cuneiform appearance as in hemorrhagic infarct; however, the cut surface is yellowish white with a hemorrhagic border. If only small vessels are involved, the cut surface shows hemorrhage without any further characteristics (Fig. 11.3).

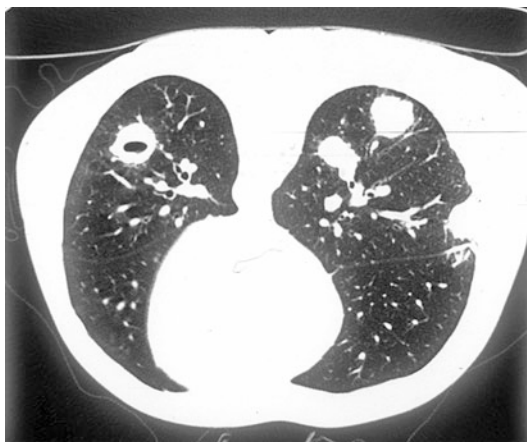

Fig. 11.2 Granulomatosis with polyangiitis (GPA, Wegener's granulomatosis), in this CT scan there are nodular densities one of them with central necrosis, a typical finding in this disease

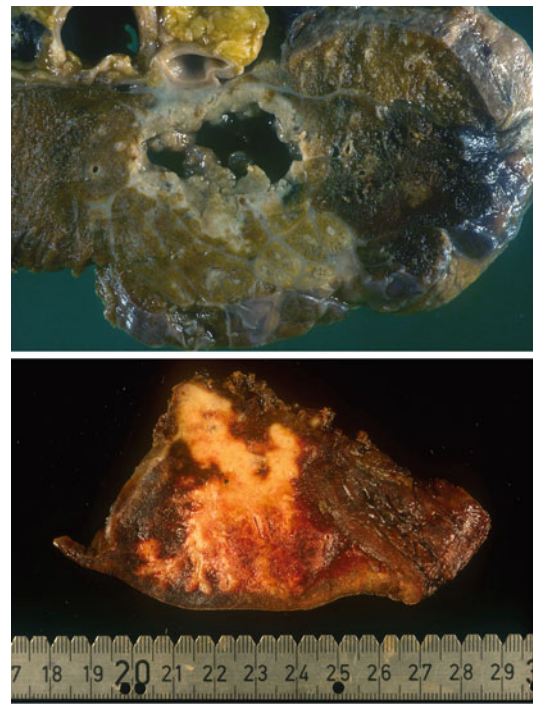

Fig. 11.3 GPA, macroscopic features of a case with large central necrosis (*upper panel*) and another case with ischemic infarct (*lower panel*)

11.2.2.3 Histology

The vasculitis is characterized by a destructive infiltration of the vessel wall by neutrophils, rarely also by eosinophils (Fig. 11.4). The vasculitis causes fibrinoid necrosis of the endothelium and bleeding, which depending on the size of the vessels can be focal or massive. The necrosis of endothelia is the most important sign of vasculitis, because in the differential diagnosis, transmigration of neutrophils in infections can be very prominent and therefore cannot be regarded as the proof of vasculitis. More often vasculitis causes thrombosis and vascular occlusion, which consequently lead to infarction and necrosis of the parenchyma. Since most often there is arterial occlusion, the infarcts are ischemic.

Epithelioid cell granulomas should be present in this new classification, as granulomatosis is now a requisite of the diagnosis (Fig. 11.5). Cases which present exclusively with vasculitis including those with capillaritis are now included into microscopic polyangiitis (see below).

In later stages, and under therapy, the neutrophils might be replaced by lymphocytes. In these cases, one has to exclude an infectious, mainly viral-induced secondary vasculitis (Fig. 11.6).

GPA usually presents with PR3 antibodies. ANCA testing nowadays is a routine in clinical practice. But be aware that ANCA can be negative in early stages of GPA, and ANCA can be positive in some infectious secondary vasculitis.

GPA can start with unspecific syndromes, even organizing pneumonia without vasculitis [4]; in these cases the patients should be observed until specific features will be present.

GPA patients will be treated primarily with corticosteroids; if non-responding, an immunosuppressive treatment with drugs like cyclophosphamide is the second choice.

11.2.2.4 Molecular Biology

GPA can be regarded as an autoimmune disease. ANCA directed against proteinase 3 (PR3) are preferentially associated with GPA. Anti-PR3 antibodies can activate neutrophils in vitro. A significant association of PR3-ANCA and HLA-DP and the genes encoding alpha-1 antitrypsin and PR3 have been found [2]. How these are associated with the production of autoantibodies is not understood. Lymphocytes are also involved in GPA, mainly lesional T cells, which exhibit pro-inflammatory properties and promote granuloma formation. Apart from T cells,

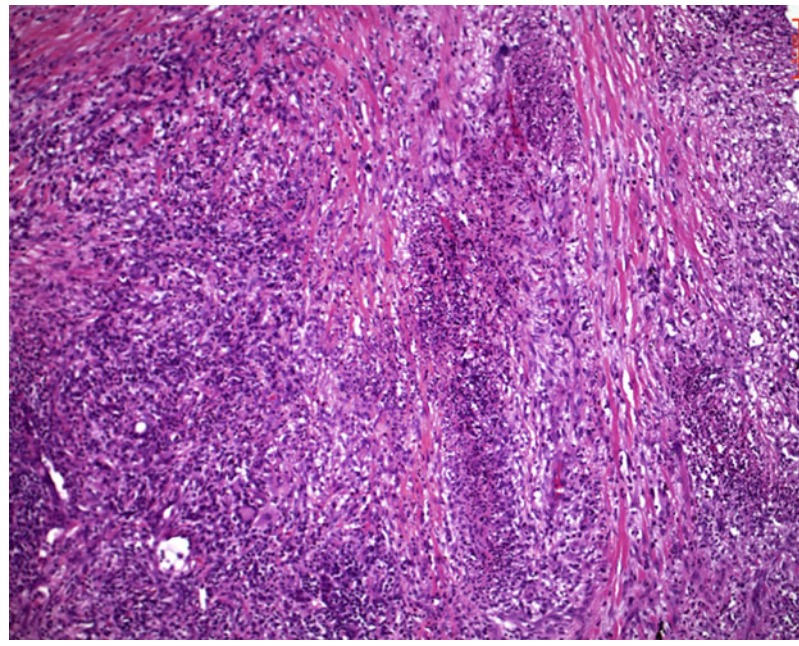

Fig. 11.4 Neutrophilic vasculitis in GPA. In the center a middle-sized artery is shown, which is completely destroyed by the infiltrating neutrophils. Some smaller arteries are seen right and lower left. On the left also an ill-formed epithelioid cell granuloma is visible. H&E, bar 100 µm

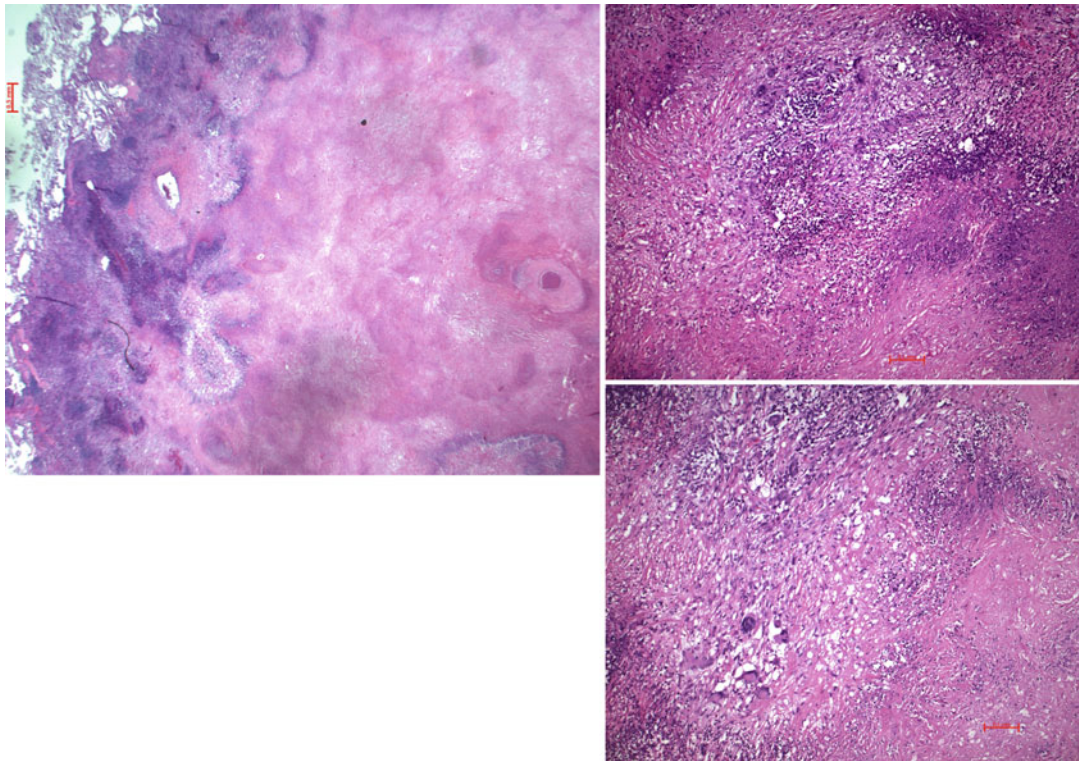

Fig. 11.5 GPA with a large ischemic infarct (*left*) and vasculitis with neutrophils as well as some epithelioid cell granulomas (*upper and lower right*). In both pictures also the edge of the infarct is visible. Granulomas in GPA are more loose, not as compact as in sarcoidosis or necrotizing sarcoid granulomatosis. H&E, bars 500 and 100 µm

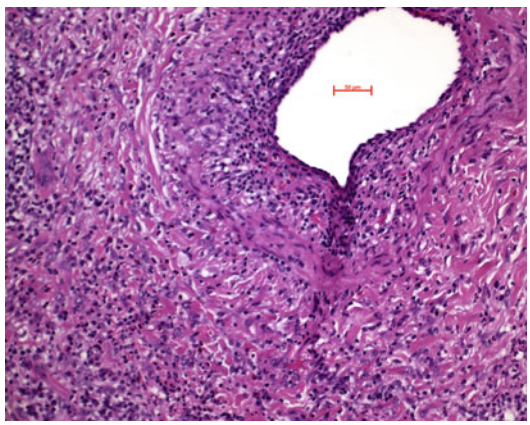

Fig. 11.6 Lymphocytic vasculitis in a case of GPA, the patient was already treated with high-dose corticosteroids. A few epithelioid cells and one giant cell can still be seen on the left. H&E, bar 50 µm

dendritic cells are abundantly present at the sites of inflammation and locally orchestrate the immune response [5].

11.2.3 Eosinophilic Granulomatosis with Polyangiitis (EGPA, Formerly Called Churg-Strauss Vasculitis)

11.2.3.1 Clinical Presentation

EGPA was first described in 1951 as a small- and medium-sized vessel vasculitis, characterized by an almost constant association with asthma and eosinophilia. Vasculitis typically develops in a previously asthmatic middle-aged patient. Asthma is severe, associated with eosinophilia and extrapulmonary symptoms. Some patients report allergic rhinitis without asthma. Most frequently EGPA involves the peripheral nerves and skin (allergic superficial eosinophilic vasculitis). Other organs such as the heart, kidney, and gastrointestinal tract, if affected, confer a poorer prognosis. In about 30–40 % of the patients, anti-myeloperoxidase (MPO) antineutrophil cytoplasm antibodies (ANCA) are present [2].

EGPA patients with anti-MPO ANCA suffered more, albeit not exclusively, from vasculitis symptoms, such as glomerulonephritis, mononeuritis multiplex, and alveolar hemorrhage, whereas ANCA-negative patients more frequently develop heart involvement [6, 7]. In recent time *EGPA* has been linked to new antiasthmatic drugs such as montelukast. However, new investigations have ruled out this as a possible cause of the disease [8].

Elevated IgG4 levels were found in active EGPA patients compared to controls. Serum IgG4 correlated with the number of eosinophils. During treatment and in disease remission, both IgG4 level and IgG4/IgG ratio dropped [9].

11.2.3.2 Radiology

The major findings at X-ray and CT scan are diffuse interstitial infiltrates; hemorrhage will be seen on CT scans (Fig. 11.7). If eosinophilic pneumonia is present, this will cause more density and focally also ground glass changes.

11.2.3.3 Gross Morphology

On cut surface, pneumonia (consolidations) and hemorrhage are the major, however, unspecific findings.

11.2.3.4 Histology

The hallmark is an eosinophilic vasculitis, again with destruction of the vessel wall and fibrinoid necrosis of the endothelium. Besides numerous eosinophils, also macrophages and histiocytes can be seen within these infiltrations. This causes focal bleeding if capillaries are affected and hemorrhage if larger vessels are involved. In older lesions or in patients under therapy, an eosinophilic infiltrate can persist up to 1 month, and hemosiderin-laden macrophages tell the story about previous bleeding. In florid cases there might be also an eosinophilic pneumonia with parenchymal necrosis. Granulomas are not associated with the vasculitis. In areas with parenchymal necrosis, a foreign body giant cell granulomatous reaction can be seen around the necrosis (Fig. 11.8).

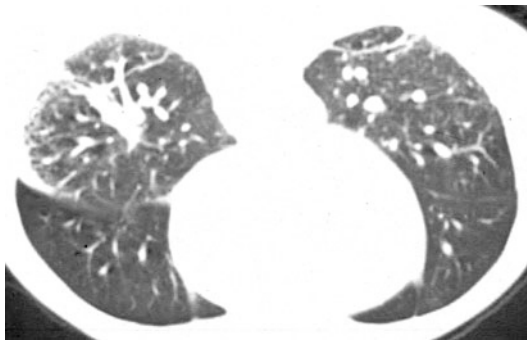

Fig. 11.7 CT scan of a case with eosinophilic granulomatosis with polyangiitis (EGPA). Note similar nodular densities, but usually there is no cavitation

11.2.3.5 Molecular Biology

A strong association with IL10 promoter polymorphisms was detected in EGPA. Other associations, including CTLA4, CD226, and copy number polymorphisms of FCGR3B need to be validated in further investigations [10].

11.2.3.6 Therapy

In most cases patients will respond to corticosteroid treatment, rarely an immunosuppressive therapy might be necessary. Encouraging results have been reported for the treatment of EGPA with rituximab or with the eosinophil-targeted antiinterleukin-5 agent mepolizumab [11].

The nomenclature remains a source of confusion: (1) Is vessel inflammation or the presence of ANCAs essential for the diagnosis of EGPA? (2) Are granulomas required for the diagnosis, and what type of granulomas should be seen? (3) Is eosinophilic pneumonia in EGPA another disease or just a variant? (4) Is hypereosinophilic syndrome a variant of EGPA?

As the understanding of the relation between the vasculitis and the eosinophilic proliferation is profoundly lacking, these questions so far cannot be answered.

11.2.4 Microscopic Polyangiitis

Microscopic polyangiitis (MPA) is a small vessel vasculitis, sometimes indistinguishable from GPA. Epithelioid cell granulomas and infarct-like necrosis are absent. In contrast to GPA, MPA is often limited to the lungs; however, it may

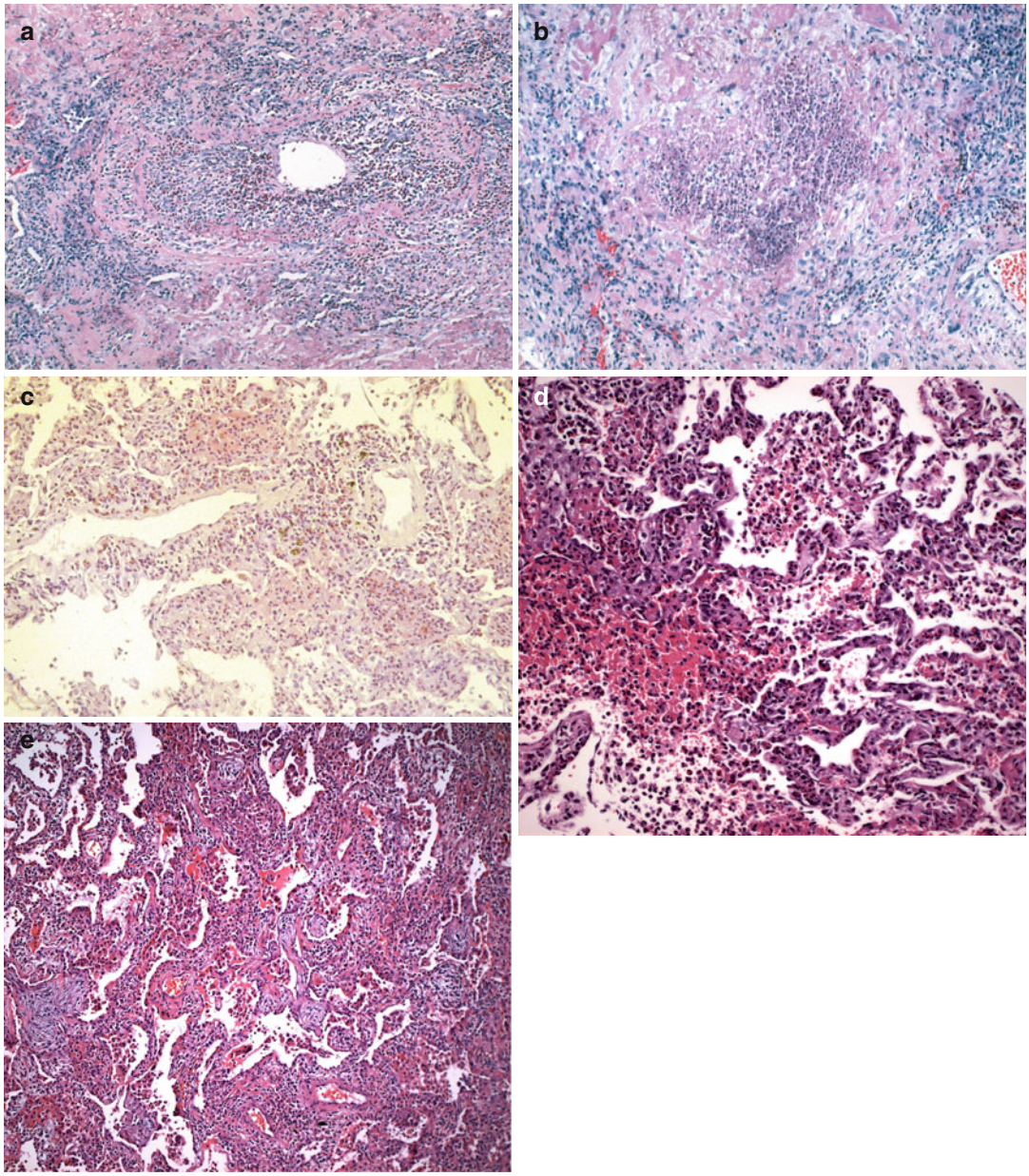

Fig. 11.8 EGPA illustrated with three cases. In (**a**) and (**b**) eosinophilic vasculitis is shown with a small necrotic focus and few scattered epithelioid and giant cells. In (**c**) a patient with EGPA was treated with corticosteroids for 2 weeks before the transbronchial biopsy was taken. This resulted that the vasculitis was no longer present (no endothelial necrosis, no infiltration of the vascular wall), but the eosinophilia could still be evaluated. In (**d**–**e**) an eosinophilic vasculitis is present, here predominantly as capillaritis. But there is also organizing pneumonia as a sign of a long-standing process with repair. H&E, ×50 and 100

involve the kidneys. Diffuse alveolar hemorrhage is most commonly seen in small vessel vasculitides, specifically MPA [12]. There is a wide variation of possible underlying diseases, but some might also be coincidentally associated with MPA. The most common are chronic airway diseases (CAD), where MPO-ANCA tended to be lower than in the non-CAD group. None of the patients in the CAD group had pulmonary hemorrhage or interstitial pneumonia. Also the outcome in the CAD group was better than in the non-CAD group [13].

There is also a geographic variance as MPA and MPO-ANCA were more common in Japan, whereas granulomatosis with polyangiitis and PR3-ANCA were more common in the UK [14]. This difference may at least in part derive from the difference in genetic background. In Japanese patients with MPA, HLA-DRB1*09:01 was increased as well as in MPO-ANCA-positive vasculitis. HLA-DRB1*09:01 is one of the most common HLA-DRB1 alleles in Asians but is rare in Caucasian populations [15]. In an attempt to identify autoantigens within the ANCAs, Regent et al. identified antibodies targeting lamin A, vimentin, alpha-enolase, and FUBP2 in patients with MPA. IgG from patients with microscopic polyangiitis reacted stronger against culture endothelial cells and induced a strong ERK phosphorylation in these cells [16].

In a European study on GPA and MPA patients, HLA-DP, SERPINA1, PRTN3, and HLA-DQ SNPs were more significantly associated with ANCA specificities (PR3 vs. MPO) than with the clinical syndromes [17]. In the study by Rahmatulla, these genetic variants were tested in GPA and MPA: CD226, CTLA-4, FCGR2A, HLA-B, HLA-DP, HLA-DQ, HLA-DR, HSD17B8, IRF5, PTPN22, RING1/RXRB, RXRB, STAT4, SERPINA1, and TLR9. Subdivision based on ANCA serotype matched better with these gene variants compared to clinical diagnosis. Within the identified 33 genetic variants, alpha-1 antitrypsin, the major histocompatibility complex system, and several distinct inflammatory processes play a major role [18].

11.2.4.1 Gross Morphology

In a VATS biopsy, there is hemorrhage without any specific morphology other than bleeding. The specimen should be sectioned in a 90° angle to the axis of the blood vessels to get the best cross sections of the larger vessels.

11.2.4.2 Histology

In MPA small vessels are involved. There is a neutrophilic rarely eosinophilic granulocytic infiltration within capillary walls, also arterioles and venules can be affected. Since necrosis of the endothelial cells will cause disruption of the vessel walls, focal bleeding (alveolar hemorrhage) will result. As this process recurs, macrophages are following and ingest the blood. The histological picture is not easy to interpret; however, a strictly to the capillary wall-associated granulocytic infiltration, and no outside accumulation within alveoli, as well as the scattered hemosiderin-laden macrophages will guide to the correct diagnosis (Fig. 11.9). Granulomas as well as infarct are absent.

11.2.4.3 Prognosis

A higher mortality is seen in patients with MPA-associated fibrosing interstitial lung disease (ILD) compared to those with peripheral nervous system involvement [19]. This was also confirmed in the study by Katsumata et al [20].

11.2.5 Panarteritis Nodosa

Panarteritis nodosa is a large, medium, and small vessel vasculitis, which very rarely affects the lungs. Within the Armed Forces Institute collection, there are only a few cases recorded involving the lungs. Organs most commonly affected are the gastrointestinal tract, arteries at the base of the

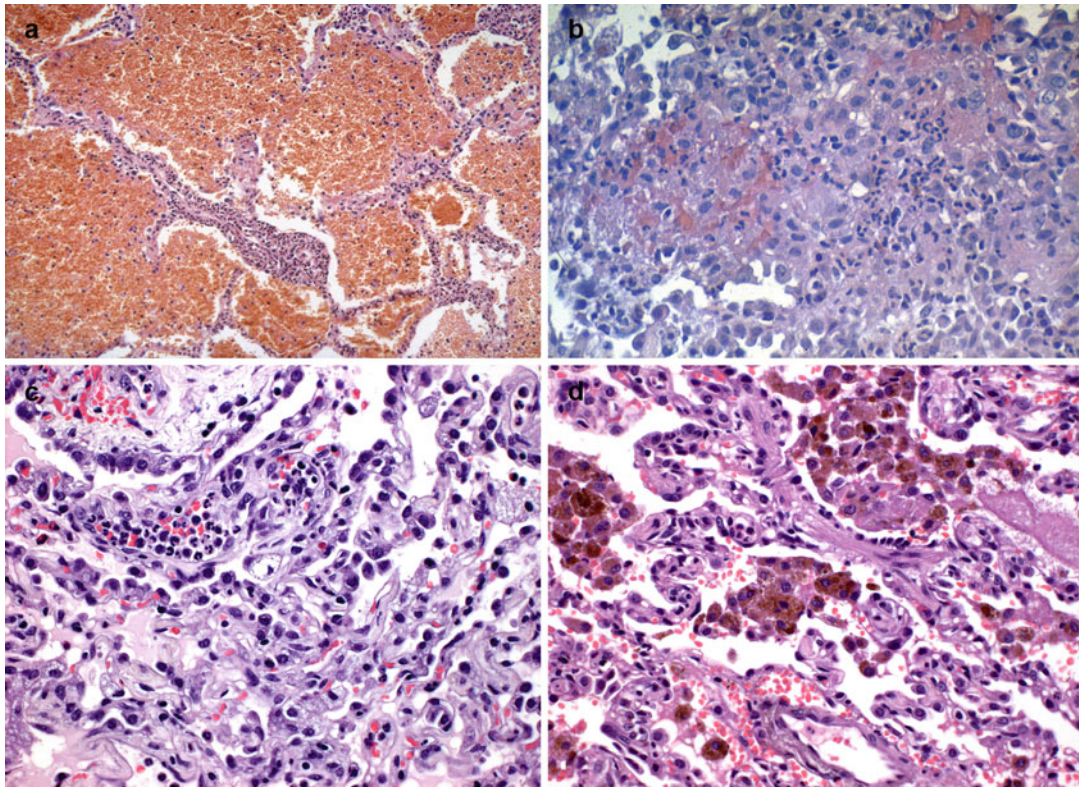

Fig. 11.9 Microscopic polyangiitis (MPA) illustrated by four cases. (**a**) A classical picture with capillaritis and alveolar hemorrhage. Due to the hemorrhage, the vascular pathology is almost highlighted. (**b**) The vasculitis is obscured by the hemorrhage; however, if one follows the alveolar septum, it becomes clear that the granulocytes are within and around the blood vessels, and the hemosiderin-laden macrophages represent former bleeding. (**c**) In this case the vasculitis is nicely shown and also the necrosis of endothelial cells. (**d**) Here hemorrhage is the only feature; the few scattered granulocytes within the capillaries are not diagnostic, because they are not associated with endothelial damage. Only clinical history and CT scan together with morphology could establish the correct diagnosis. H&E, Trichrome, ×50 and 100

brain, heart, liver, and spleen. To my knowledge only one definitely proven case has been published in the literature, which involved the lungs [12]. It is a neutrophilic granulocytic vasculitis, but during the course of the disease, also histiocytes are present too; the vasculitis is nodular and granulomatous, causing either stenosis with ischemic infarcts or dilation with aneurysm formation, rupture, and bleeding (Fig. 11.10).

The relevance of the classification system of vasculitides, relying on affected vessel size as the primary discriminator, is still questionable. Classification on ANCA-positive and negative vasculitis is a first step to get a better separation, and also the type of ANCA is clinically important. However, some entities remain ill defined: polyarteritis nodosa, microscopic polyangiitis, and adult immunoglobulin A vasculitis [21] (Table 11.1).

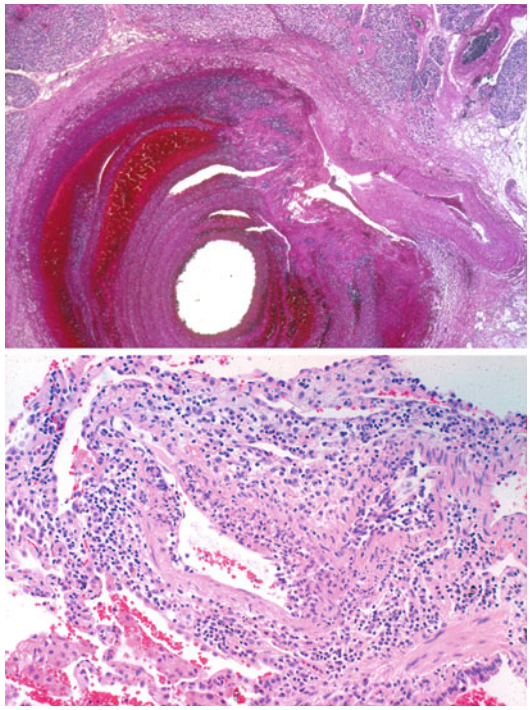

Fig. 11.10 Panarteritis nodosa involving the lung, an exceptional rare organ affection. *Top panel* shows a large artery with vasculitis and thrombosis. In the *lower panel*, a middle-sized artery is involved by a neutrophilic vasculitis with endothelial cell damage. H&E, ×12 and 200 (Case photographed at the AFIP during my stay there)

Table 11.1 ANCA and other autoantibodies in vasculitis and autoimmune diseases

GPA initial	PR3	50 %	MPO	<5 %
Generalized	PR3	90 %	MPO	<5 %
EGPA	PR3	20 %	MPO	20 %
MPA	PR3	10 %	MPO	60 %
PanA	PR3	<5 %	MPO	<5 %
SLE	PR3	–	LF/HLE/LZ	25 %
Sjøgren	PR3	–	LF/HLE/LZ	25 %
Polymyositis	PR3	–	LF/HLE/LZ	<10 %
Rheumatoid	PR3	–	LF/HLE/LZ	20–50 %

As a rule, infections should always be ruled out in cases with vasculitis before a systemic vasculitis is diagnosed.

11.3 Secondary Vasculitis with Infection

Most infections can cause a secondary vasculitis; in case of bacterial and fungal infections, these are usually granulocytic (neutrophilic) vasculitis, whereas viral infections cause lymphocytic vasculitis (Figs. 11.11 and 11.12). Parasitic infections come as eosinophilic vasculitis, similar to allergic reaction.

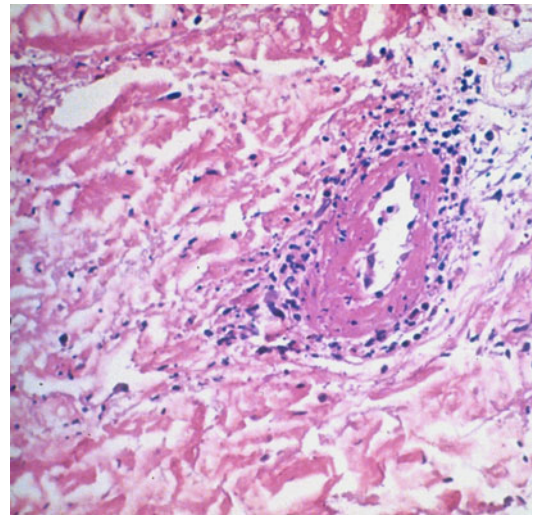

Fig. 11.11 Secondary vasculitis due to infection with herpesvirus, H&E, ×100

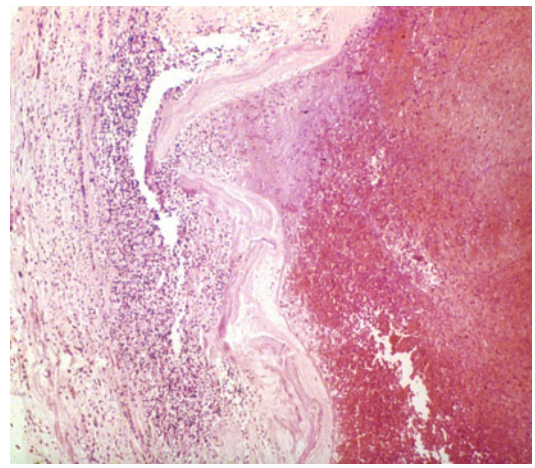

Fig. 11.12 Secondary vasculitis due to infection with *Staphylococcus aureus* infection and sepsis. H&E

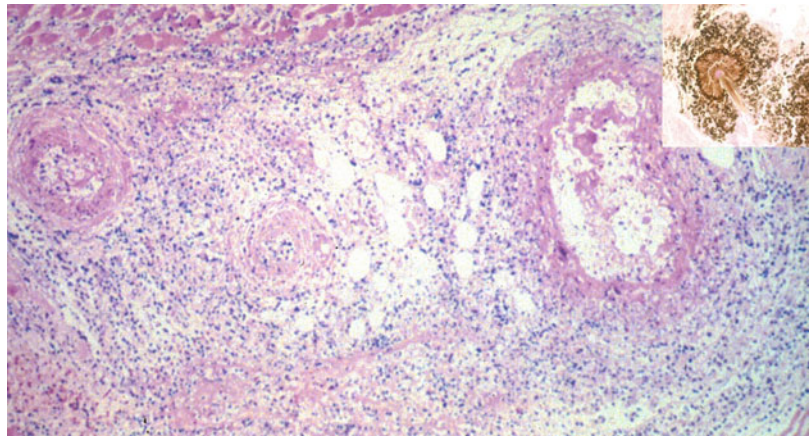

Fig. 11.13 Secondary vasculitis due to sepsis with an *Aspergillus* species in a child after chemotherapy for leukemia. *Inset*: a fruiting body of the fungus allowed a more specific diagnosis. H&E, Grocott, ×100 and 400

Most common secondary infectious vasculitides occur in tuberculosis, mycobacteriosis, almost all forms of fungal infections, and many viral infections. Of note some infectious vasculitides can also be ANCA positive, as we have seen in a case of infectious vasculitis caused by *Treponema pallidum*.

In children mycotic infections are seen in patients treated for leukemia and in bone marrow transplant (Fig. 11.13). In these cases processing of the tissue and diagnosis by the pathologist should be done as quick as possible, because these children are on a high risk of developing sepsis: all fungi grow toward high oxygen tension and therefore can invade the pulmonary vascular system within hours, resulting in bacteremia and sepsis.

11.4 Secondary Vasculitis Without Infection

These forms of vasculitis have been discussed in other chapters. Examples are vasculitis in sarcoidosis, necrotizing sarcoid granulomatosis, and hypersensitivity pneumonia. An unusual form of eosinophilic vasculitis has been described in a newborn with congenital chylothorax [22]. The vasculitis vanished after correction of the ductus thoracicus within a week (Fig. 11.14). Other forms of noninfectious vasculitis can occur in drug abuse, for example, in methadone abuse, where the filling material from the drugs is injected together with the drug into a vein. The filling material often contains talcum, which will cause a granulomatous vasculitis with foreign body giant cells. Another vasculitis can be induced by material from dialysis membranes. If used several times, polyhydrocarbon fragments

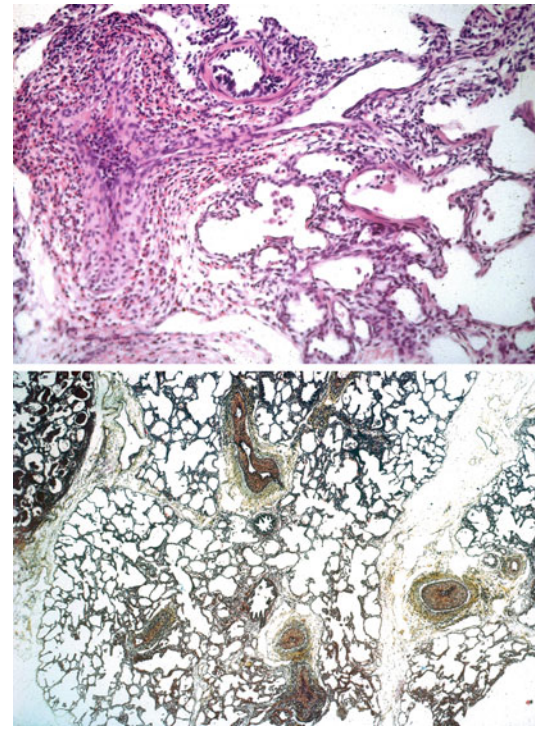

Fig. 11.14 Eosinophilic vasculitis due to chylothorax in a 2-day-old child. Note the dense eosinophilic infiltration confined to the blood vessels, whereas the alveolar tissue is normal. H&E and Movat stain, ×200 and 50

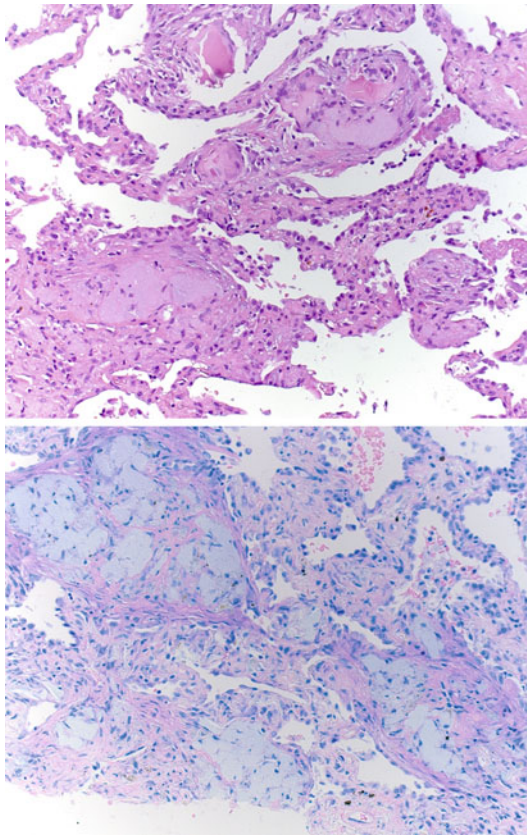

Fig. 11.15 Foreign body vasculitis caused by material dissolved from medical devices. The material looks amorphous eosinophilic and is surrounded by a macrophage reaction (*upper panel*). On PAS stain the material is negative (*lower panel*). H&E and PAS, ×200

can be dissolved and will circulate via the venous system, reaching the lung and will cause a macrophage vasculitis (Fig. 11.15).

11.5 Vascular Diseases and Malformation

Pulmonary arteries and veins can be affected by different malformations, which are at present ill defined. Usually patients present with alveolar hemorrhage, which sometimes can be life threatening. The underlying pathology can be capillary or cavernous hemangiomas, arteriovenous malformations, or angiomas but also rare diseases such as Marfan syndrome and Ehlers-Danlos disease type IV. Usually a careful examination is necessary to find the underlying cause of bleeding. This requires extensive sectioning. In my experience one should select those areas, where massive hemorrhage is present. Take many sections and start searching for malformations. In *Marfan disease* clinical information, if provided, might help a lot, so one can immediately focus on the large arteries and investigate the elastic laminae (Fig. 11.16). The formation of elastin is disabled, causing thin-walled large blood vessels, which easily rupture; in the lung mainly the large pulmonary arteries are affected; however, in these patients the symptoms are mainly due to aortic problems (rupture). In *Ehlers-Danlos disease IV*, the most important finding is thin-walled large arteries and ill-developed collagen in the adventitia. The synthesis of different types of collagen is blocked. In the lungs large pulmonary arteries are affected. Most important both diseases will manifest in a young-aged population.

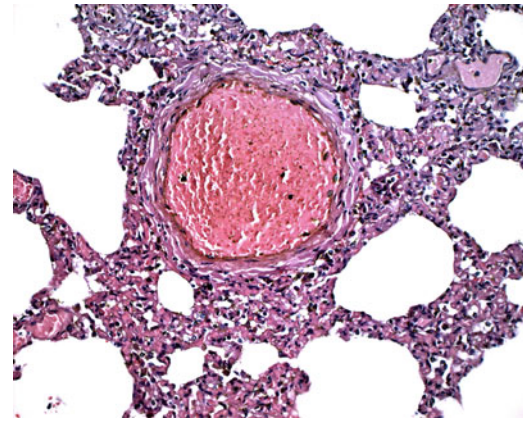

Fig. 11.16 Pulmonary involvement in Marfan disease. Note the thin-walled artery without a visible elastic lamina. Trichrome stain, ×200

Clinical symptoms are massive hemorrhage in young patients, which tend to be fatal. As this is a systemic disease, there is no option for treatment.

11.5.1 Histology

On low power examination, no abnormalities are seen. The bronchovascular bundles are well

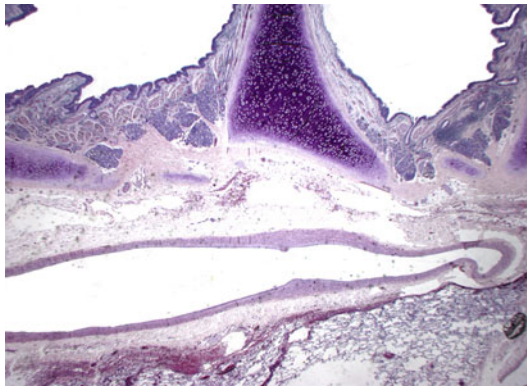

Fig. 11.17 Lung involvement in Ehlers-Danlos disease type IV. Here again a thin-walled artery is seen, but here the collagen fibers are reduced in number and they are functional impaired. H&E, ×12

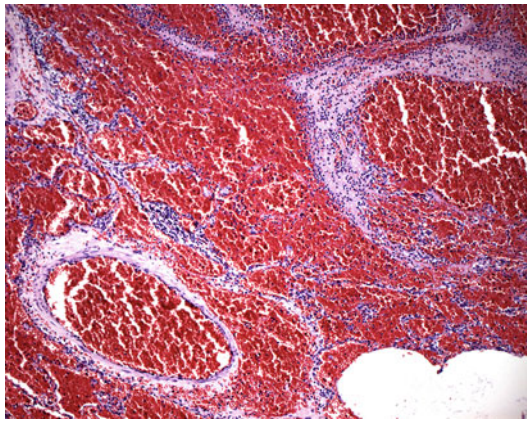

Fig. 11.18 Lung involvement in Ehlers-Danlos disease type IV. Here rupture of a small blood vessel is seen, which caused massive bleeding. H&E, ×50

structured; within the lung parenchyma, massive hemorrhage is the only finding. The abnormality, which will lead to further chemical investigation, is the thin wall of large pulmonary arteries seen on mesenchymal tissue stains such as Movat pentachrome. The intima is normal and the elastic laminae are normal, but the collagen is abnormally thin (Figs. 11.17 and 11.18). This combination together with the age of the patient and the rapid deterioration should cause chemical investigation for the underlying enzyme defect.

Mutation within the COL3AI gene results in the disorder of type III procollagen. The diagnosis is confirmed by demonstrating the synthesis of abnormal type III procollagen molecules from cultured dermal fibroblasts or by identifying the mutation in the COL3A1 gene [23]. Biallelic sequence variants have a significantly worse outcome than heterozygous variants for either null mutations or missense mutations, and frontoparietal polymicrogyria may be an added phenotype feature. This genetic constellation provides a very rare explanation for marked intrafamilial clinical variation due to sequence variants in COL3A1 [24].

11.6 Malformation and Systemic (Inborn) Vascular Diseases in Children

This has been already discussed in the chapter on childhood and will not further be treated here.

11.7 Pulmonary Hypertension

Pulmonary hypertensive diseases will not often be subjected to pathological analysis; however, the pathologist might be questioned in autopsy cases or in rare diseases with hypertension. Therefore we will describe the morphological changes to be seen in histological specimen to enable the pathologist to make the diagnosis of pulmonary hypertension and some variants. In some cases such as in systemic diseases or in autopsy cases with heart diseases, the pathologist can arrive at a diagnosis, which includes also the etiology of hypertension, but in biopsies the final diagnosis has to be established by a multidisciplinary team led by the clinician.

Pulmonary hypertension is defined as an arterial pressure of $\geq$25 mmHg under resting condition. There are also definitions for pre- and postcapillary hypertension, where >15 mmHg defines a postcapillary hypertension whereas precapillary hypertension is defined by $\leq$15 mmHg.

The severity of changes within the walls of pulmonary arteries can be graded, and to my experience the grading system by Heath and Edwards is most useful (Table 11.2).

Table 11.2 Grading of sclerosis according to Heath and Edwards [25]

Grade 1: medial hypertrophy and muscularization of arterioles
Grade 2: medial hypertrophy and intimal proliferation in small arteries
Grade 3: medial hypertrophy, intimal proliferation, and concentric laminar fibrosis
Grade 4: medial hypertrophy, intimal proliferation, and concentric laminar fibrosis and plexiform lesions
Grade 5: prominent plexiform and angiomatoid lesions, + hemosiderin deposition
Grade 6: as grade 5, + necrotizing arteritis

Primary pulmonary hypertension, veno-occlusive syndrome (diseases), and pulmonary capillary hemangiomatosis were originally considered separate diseases, although D. Dail many years ago pointed to a connection of these three in his thesis work. Primary pulmonary hypertension is caused by a vascular obstruction of medium to small blood vessels. As a reaction a secondary proliferation of small capillaries with a glomerulum-like appearance is started – the so-called plexiform lesion (Fig. 11.19). The driving forces are vascular factors such as VEGF, endothelin, endostatin, and their receptors (Fig. 11.19d). Small areas of necrosis can occur, and a hemangioma-like dilation of veins is typically found around these proliferations (Fig. 11.19e). Small areas of necrosis can occur. Larger arteries will show vessel wall thickening and stenosis. Bleeding and hemosiderin deposits can be found; however, no large hemorrhage will be seen.

Veno-occlusive disease is characterized by an occlusion of pulmonary veins, which are found along interlobular septa. Sometimes an elastic stain is necessary, to highlight remnants of these vessels (Fig. 11.20). Pulmonary capillary hemangiomatosis often can be found associated with the former two diseases. PCH is characterized by a proliferation of pulmonary capillaries typically in septa. There are at least doubled capillary beds (Fig. 11.21). The disease occurs in children and young adults and causes alveolar hemorrhage syndrome. To my experience and according to case reports in the literature, there are two probably separated forms: PCH associated with PAH ± VOD and PCH as an isolated tumorlike form.

PAH in collagen vascular disease, most often systemic sclerosis, is characterized by vessel wall thickening (grades 2–4). In some cases this thickening resembles sclerosis as in chronic vascular transplant rejection due to antigen-antibody complex deposition. Also vasculitis can occur.

PAH in intravenous drug abuse comes usually as foreign body giant cell vasculitis with obstruction of small arteries and capillaries. Plexiform lesions can be present in rare cases. The reason is embolization of tablet filling substances such as talcum. Another drug *Sauropus androgynus* inducing PAH was reported in Korea and Japan. This starts with myxoid changes in arteries and bronchioles, followed by eosinophilic vasculitis and bronchiolitis, and finally occlusion of bronchioles and blood vessels.

Signs of pulmonary hypertension including elastosis of the arteries are characteristically found in lung sequestration with and without CPAM. Elastosis (multiplicity of elastic layers), which is also present in other types of pulmonary hypertension, is most severe in sequestration and can be used as another aid in making the correct diagnosis.

PAH is also found in thromboembolic disease, even with plexiform lesions, but venous dilations associated with these lesions do not occur (Fig. 11.22) (Table 11.3).

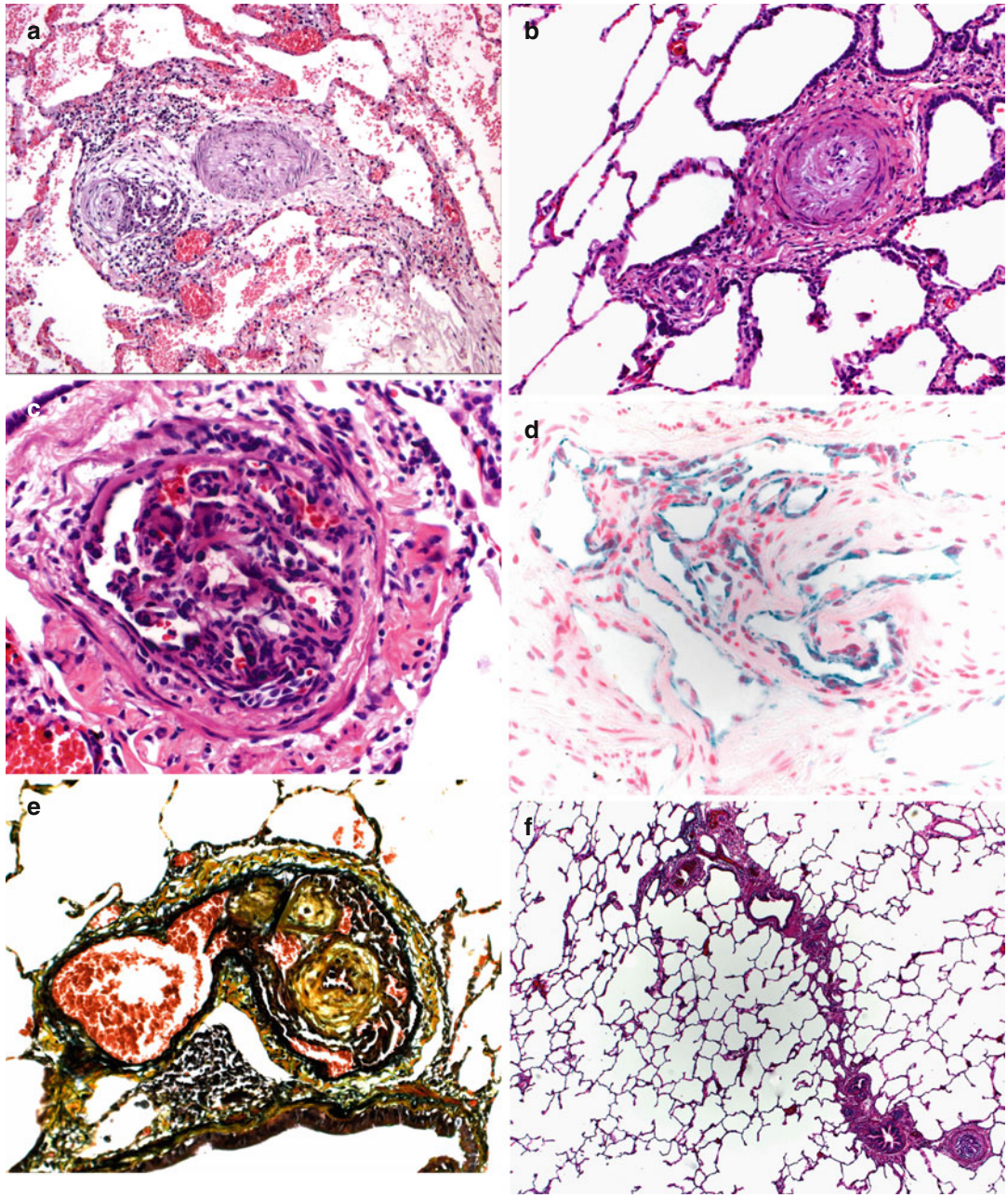

Fig. 11.19 Idiopathic arterial pulmonary hypertension. (**a**) Shows an occluded artery and adjacent a plexiform proliferation of primitive endothelial tubules and capillaries. (**b**) Another case of IPH with stenosis of the artery and early plexiform lesion. (**c**) Plexiform lesion within an artery, and (**d**) expression of VEGF in the endothelia of this plexiform proliferation. (**e**) A typical and diagnostic finding in PAH is a dilated vein adjacent to the obstructed artery. (**f**) Opening of arteriovenous anastomoses, probably "reuse of preexisting anastomoses from the fetal period." H&E, immunohistochemistry for VEGF, and Movat, ×50, 100, and 200

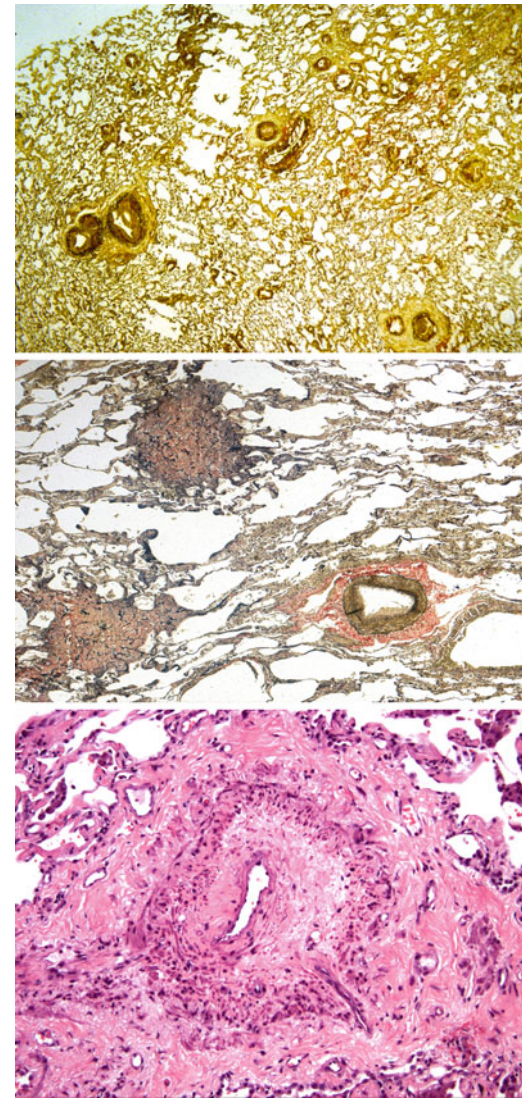

Fig. 11.20 Veno-occlusive disease: the overview in *top panel* shows an almost normal peripheral lung; however, the thickened and obstructed veins stick out. In the middle one artery with thickened wall is shown and two veins, which are occluded and therefore lost to circulation. In the *lower panel*, another vein is shown, which is severely obstructed. H&E, Movat, ×12, 50, 100

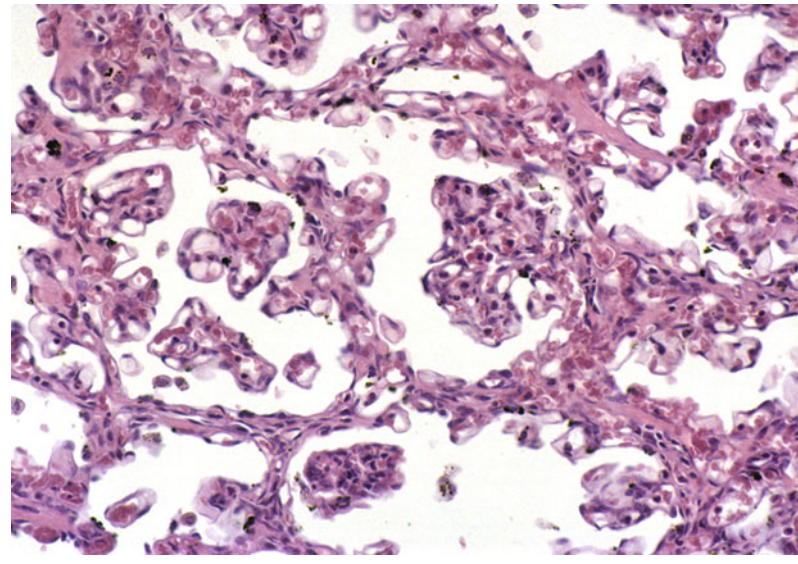

Fig. 11.21 Pulmonary capillary hemangiomatosis in a case of idiopathic arterial hypertension. There are many capillaries within an alveolar septum, best seen at cross sections in the middle of the picture. H&E, ×200

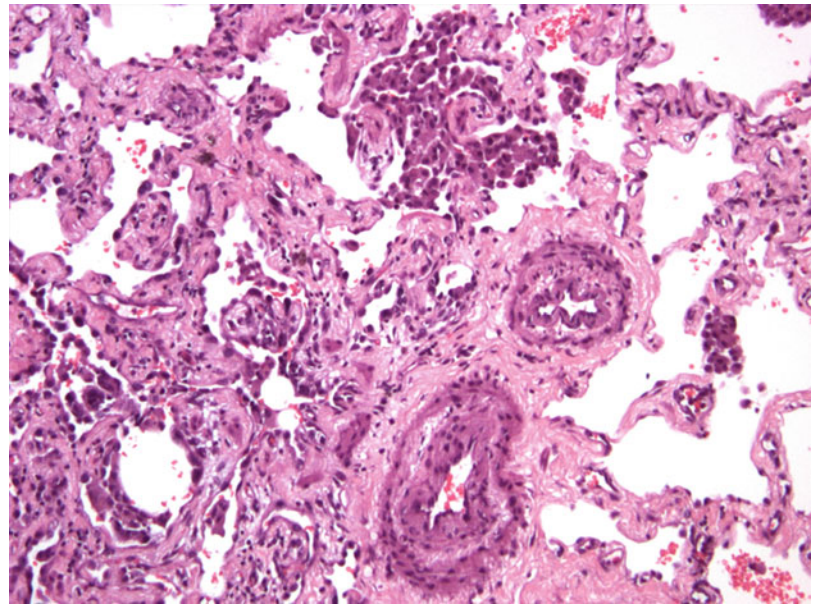

Fig. 11.22 Chronic thromboembolic disease and thickened arteries are seen and within the vessel wall some primitive endothelial proliferations, which will give raise to plexiform lesion later on. Note that there are no dilated veins. H&E, ×200

Table 11.3 The updated Venice classification 2012–2015 [26–29]

A1. Pulmonary arterial hypertension (PAH)
A1.1. idiopathic (iPAH)
A1.2. heritable
A1.2.1. BMPR2
A1.2.2. ALK1, endoglin ± hereditary hemorrhagic telangiectasia
A1.2.3. unknown
A1.3. drug and toxin induced
A.1.4. associated with
A1.4.1. connective tissue disease
A1.4.2. HIV infection
A1.4.3. portal hypertension
A1.4.4. congenital heart disease
A1.4.5. schistosomiasis
A1.4.6. chronic hemolytic anemia
A1.5. persistent pulmonary hypertension of the newborn
A1.6. pulmonary veno-occlusive disease (PVOD) ± pulmonary capillary hemangiomatosis (PCH)
A2. pulmonary hypertension in left heart diseases
A2.1. systolic dysfunction
A2.2. diastolic dysfunction
A2.3. valvular disease (Fig. 11.23)
A3. pulmonary hypertension associated with chronic obstructive pulmonary disease
A3.1. COPD
A3.2. ILD
A3.3. other pulmonary diseases with mixed restrictive and obstructive patterns
A3.4. sleep apnea syndrome
A3.5. alveolar hypoventilation
A3.6. high altitude sickness
A3.7. developmental abnormalities
A4. chronic thromboembolic pulmonary hypertension (CTEPH; Fig. 11.22)
There is no longer a differentiation into thromboembolic obstruction of proximal or distal pulmonary arteries

Table 11.3 (continued)

A5. pulmonary hypertension with unclear multifactorial mechanisms
A5.1. hematologic disorders as myeloproliferative diseases, splenectomia
A5.2. systemic disorders: sarcoidosis, Langerhans cell histiocytosis, LAM, neurofibromatosis, vasculitis
A5.3. metabolic disorders: glycogen storage diseases, Gaucher, others, thyroid diseases
A5.4. others: tumoral obstruction, fibrosing mediastinitis, and chronic renal failure on dialysis

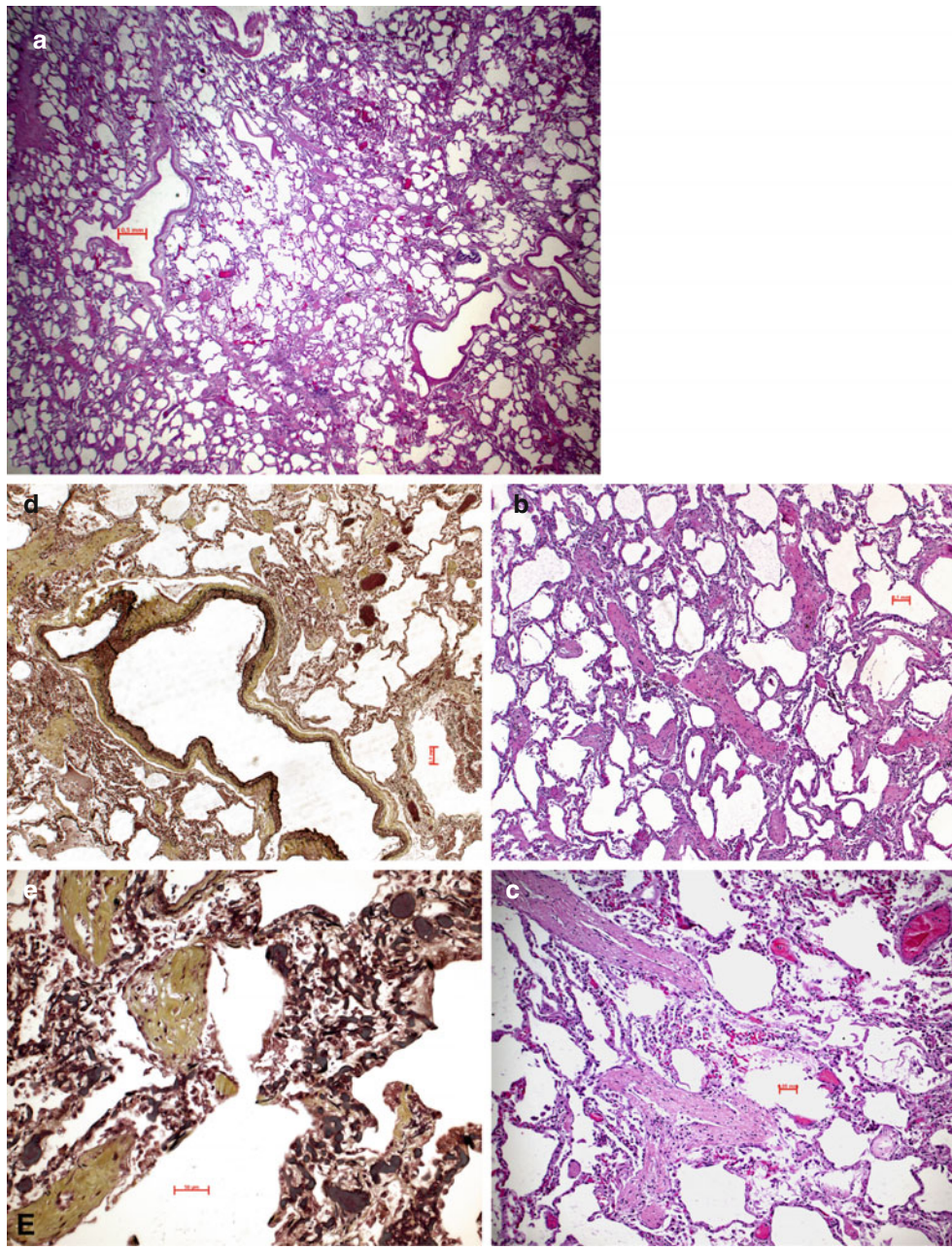

Fig. 11.23 Pulmonary hypertension in valvular disease. (**a**) Overview showing large dilated veins whereas everything else looks normal. (**b**, **c**) On higher magnification there are strands of fibrosed tissue, which show narrow lumina and represent severely stenosed veins. This morphology is also illustrated by Movat stain in (**d**, **e**) where also the dilation of the capillary bed is clearly seen. H&E, Movat, bars 500, 100, 50 μm

11.7.1 Mechanisms of PAH

Some reports have shed light to the mechanisms, but a final cause has not been discovered. Mutations in bone morphogenic protein receptor type II (BMPR2) have been discovered, and it has been shown that BMPR2 mutations in different exons result in altered function. However, BMPR2 mutations are found in only a minority of PAH patients [30, 31]. So it is speculated that disease modifier genes might exist. Activin-like kinase type I (ALK1) was found altered in hereditary hemorrhagic telangiectasia. Since both genes belong to the TGFβ family, this pathway might be most probably affected [31]. BMP receptors 1 and 2 associate to form homo- or heterodimers. BMP4, a ligand for BMPR2, inhibits the proliferation of arterial muscle cells from proximal pulmonary arteries but stimulates proliferation of peripheral arteries. In iPAH hypoxia induces production of endothelium-derived BMP4, associated with increased proliferation and migration of vascular smooth muscle cells.

The serotonin transporter (5-HTT) was found to be overexpressed in PAH [32]. Functional polymorphism of the 5-HTT gene promoter has been demonstrated in some patients, an increase of the expression of the 5-HT transporter (5-HTT) in others. This all result in an abnormally strong proliferative response to serotonin. Interestingly appetite-suppressant drugs are potent inhibitors of neuronal 5-HT uptake and inhibit 5-HTT.

In the downstream pathway, VEGF and VEGF receptors play an essential role in PAH. Also an increase of TXA_2 synthesis was shown in patients with iPAH, pointing to the involvement of thrombotic and inflammatory mechanisms [33].

PAH caused by antiphospholipid autoantibodies most likely is caused by fibrin thrombi causing widespread obstruction of small pulmonary arteries with concentric cellular and fibrous intimal hyperplasia (Fig. 11.24) [34].

In children the group of Fukushima studied the mechanisms of PAH with PVOD in left-to-right shunt of the heart. There was a predominant biosynthesis of TXA_2 over PGI_2, which might cause vasoconstriction in these infants [33]. Finally in a study on PCH, the authors reported on mutations in the eukaryotic translation initiation factor 2α kinase 4 (EIF2AK4) gene. EIF2AK4 potentially connects with BMPR2 to cause PCH. Mutant EIF2AK4 could promote proliferation of small pulmonary arteries by cross talk with mammalian targets of the rapamycin signaling pathway [35] (Table 11.4).

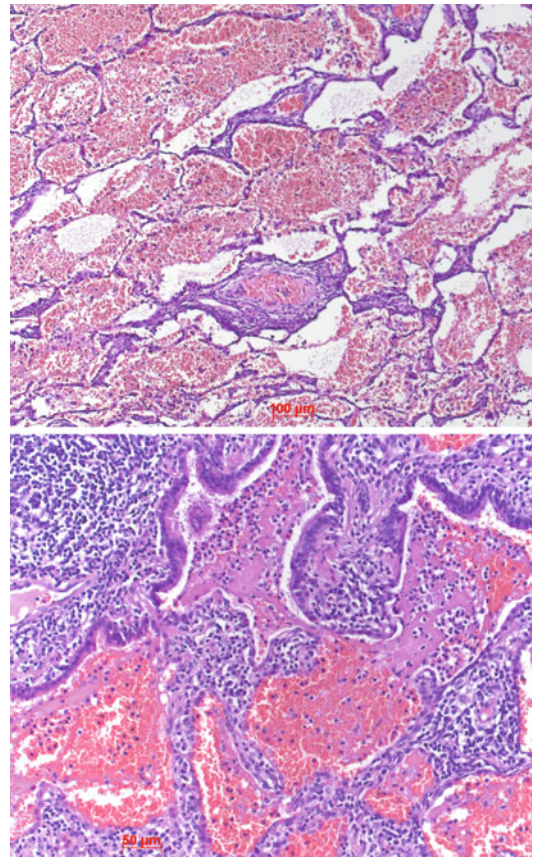

Fig. 11.24 Two cases of antiphospholipid antibody syndrome presenting with alveolar hemorrhage. In the case at the *top panel*, there is only hemorrhage and no other morphological feature. In the second case (*lower panel*), there is an additional lymphocytic pneumonia (LIP), which at least point to an immunological disorder. H&E, bars 50 and 100 µm

Table 11.4 How to diagnose vasculopathy

Pulmonary arteriopathy (pre- and intra-acinar arteries)
Subsets:
Pulmonary arteriopathy with isolated medial hypertrophy
Pulmonary arteriopathy with medial hypertrophy and intimal thickening (cellular, fibrotic)
Concentric laminar or eccentric, concentric non-laminar
Pulmonary arteriopathy with plexiform and/or dilation lesions or arteriitis
Pulmonary arteriopathy with isolated arteriitis
As above but with coexisting venous-venular changes (cellular and/or fibrotic intimal thickening, muscularization)
The presence of the following changes should be noted:
Adventitial thickening; thrombotic lesions (fresh, organized, recanalized, colander lesion); necrotizing or lympho-monocytic arteriitis; elastic artery changes (fibrotic or atheromatous intimal plaques, elastic laminae degeneration); bronchial vessel changes, ferruginous incrustation, calcifications, foreign body emboli, organized infarct; perivascular lymphocytic infiltrates
Pulmonary occlusive venopathy (veins of various size and venules) with or without coexisting arteriopathy
Histopathologic features:
Venous changes: intimal thickening/obstruction (cellular, fibrotic); obstructive fibrous luminal septa (recanalization)
Adventitial thickening (fibrotic); muscularization; iron and calcium incrustation with foreign body reaction:
Capillary changes: dilated, congested capillaries; angioma-like lesions
Interstitial changes: edema; fibrosis; hemosiderosis; lymphocytic infiltrates
Others: dilated lymphatic, alveoli with hemosiderin-laden macrophages, type II cell hyperplasia
Pulmonary microvasculopathy with or without coexisting arteriopathy and/or venopathy
Histopathologic features:
Microvessel changes: localized capillary proliferations within pulmonary interstitium; obstructive capillary proliferation in veins and venular walls
Venous-venular intimal fibrosis
Interstitial changes: edema, fibrosis, and hemosiderosis
Others: dilated lymphatics: alveoli with hemosiderin-laden macrophages; type II cell hyperplasia

11.8 Alveolar Hemorrhage

Alveolar hemorrhage syndrome (AHS) presents with bleeding in the lung parenchyma. In some patients, AHS will cause hemoptysis; in other patients, there is only sometimes blood found in expectorations. In BAL specimen there are red blood cells as well as hemosiderin-laden macrophages – this is essential to differentiate AHS from artificial bleeding induced by bronchoscopy or biopsy, as well as from aspiration from the upper respiratory tract. There are several underlying diseases, which can present with AHS. Within the differential diagnosis, they are vasculitis, primary systemic as well as secondary; pulmonary hypertension; autoimmune diseases including collagen vascular diseases; Goodpasture syndrome; antiphospolipid autoantibody syndrome (Fig. 11.24); infections such as tuberculosis, influenza virus, *Hantavirus*, SARS, dengue fever, and Nile virus fever; inhalation of herbicides and pesticides; and drug reactions, especially cytostatics.

11.9 Diseases of the Lymphatics (Adult and Childhood)

Tumors of the lymphatic system have been covered in tumors. Here we have to discuss malformation, obstruction, and inflammation.

11.10 Malformation

Malformation of the ductus thoracicus will cause obstruction of the lymphatic flow resulting in leakage of the fluid into the alveoli. The

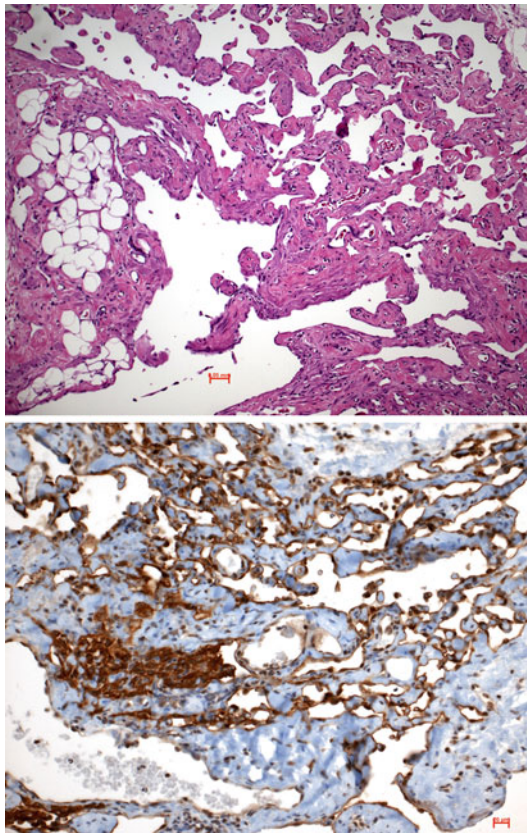

Fig. 11.25 Systemic lymphangiomatosis (Gorham-Stout syndrome) here presented in a resection from a cystic tumor of the mediastinum. In this 22-year-old male patient, there was bone disease and also lung involvement. *Upper* panel shows the lymphangioma-like histology. In the *lower* panel, the endothelia all express VEGFR3. Bars 50 and 20 μm

histological picture will resemble edema; however red blood cells are missing, whereas scattered leukocytes are encountered. The septa are widened by this fluid. Leakage can also affect the pleura causing chylothorax. This malformation can be focal, involving the lung and mediastinum, but exists also as a systemic form, Gorham-Stout syndrome [36, 37]. In this case also the bones and many other organs are affected too (Fig. 11.25). These patients present with symptoms related to loss of electrolytes and small peptides/proteins. Most prominent is albuminemia. Patients are of young age or children. The diagnosis can be made by CT scan, because the multitude of cystic-dilated lymphatics within the

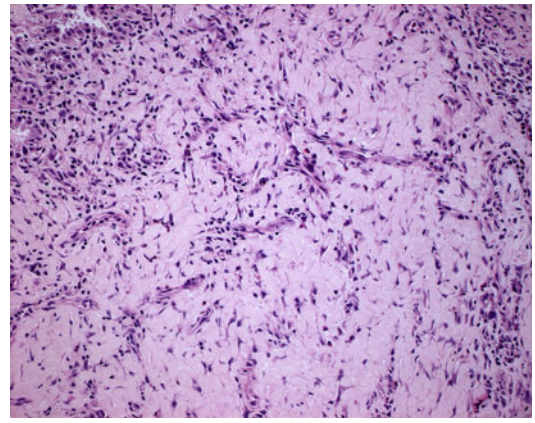

Fig. 11.26 Diffuse capillary lymphangiomatosis with many proliferating lymphatic vessels within a fibrotic tissue. The diagnosis will require immunohistochemical positivity for podoplanin and/or VEGF-C or VEGFR3. H&E, ×200

mediastinum will simulate a cystic tumor. The local form will present as lymphangiosis, with the characteristic proliferation of lymphatic vessels (Fig. 11.26). As an aid in the diagnosis, antibodies against podoplanin and VEGFR can highlight the lymphatics[3].

11.11 Obstruction

Several diseases can cause lymphatic obstruction. Here we will give a list of common and rare causes.

Lymphangioleiomyomatosis: The obstruction is caused by the proliferation of smooth muscle cells.

Tumors: Central tumors might directly compress lymphatics, or tumor cell clusters might obstruct lymphatics.

Parasites: Larvae as well as eggs can obstruct lymphatics. This is very common in tropical parasitic infection such as filariasis.

11.12 Inflammation

Lymphatics are always involved in any kind of infection. However, in common bacterial and viral infections lymphatics are usually not seen

due to their small size. An exception is granulomatous pneumonias such as tuberculosis and sarcoidosis, where the granulomas can be more easily seen centered on lymphatics.

References

1. McInnis EA, Badhwar AK, Muthigi A, Lardinois OM, Allred SC, Yang J, Free ME, Jennette JC, Preston GA, Falk RJ, Ciavatta DJ. Dysregulation of autoantigen genes in ANCA-associated vasculitis involves alternative transcripts and new protein synthesis. J Am Soc Nephrol. 2015;26:390–9.
2. Alberici F, Martorana D, Bonatti F, Gioffredi A, Lyons PA, Vaglio A. Genetics of ANCA-associated vasculitides: HLA and beyond. Clin Exp Rheumatol. 2014;32:S90–7.
3. Ozen S, Pistorio A, Iusan SM, Bakkaloglu A, Herlin T, Brik R, Buoncompagni A, Lazar C, Bilge I, Uziel Y, Rigante D, Cantarini L, Hilario MO, Silva CA, Alegria M, Norambuena X, Belot A, Berkun Y, Estrella AI, Olivieri AN, Alpigiani MG, Rumba I, Sztajnbok F, Tambic-Bukovac L, Breda L, Al-Mayouf S, Mihaylova D, Chasnyk V, Sengler C, Klein-Gitelman M, Djeddi D, Nuno L, Pruunsild C, Brunner J, Kondi A, Pagava K, Pederzoli S, Martini A, Ruperto N. EULAR/PRINTO/PRES criteria for Henoch-Schonlein purpura, childhood polyarteritis nodosa, childhood Wegener granulomatosis and childhood Takayasu arteritis: Ankara 2008. Part II: final classification criteria. Ann Rheum Dis. 2010;69:798–806.
4. Uner AH, Rozum-Slota B, Katzenstein AL. Bronchiolitis obliterans-organizing pneumonia (BOOP)-like variant of Wegener's granulomatosis. A clinicopathologic study of 16 cases. Am J Surg Pathol. 1996;20:794–801.
5. Wilde B, Thewissen M, Damoiseaux J, van Paassen P, Witzke O, Tervaert JW. T cells in ANCA-associated vasculitis: what can we learn from lesional versus circulating T cells? Arthritis Res Ther. 2010;12:204.
6. Chanseaud Y, Tamby MC, Guilpain P, Reinbolt J, Kambouchner M, Boyer N, Noel LH, Guillevin L, Boissier MC, Mouthon L. Analysis of autoantibody repertoires in small- and medium-sized vessels vasculitides. Evidence for specific perturbations in polyarteritis nodosa, microscopic polyangiitis, Churg-Strauss syndrome and Wegener's granulomatosis. J Autoimmun. 2005;24:169–79.
7. Pagnoux C, Guillevin L. Churg-Strauss syndrome: evidence for disease subtypes? Curr Opin Rheumatol. 2010;22:21–8.
8. Frankel SK, Sullivan EJ, Brown KK. Vasculitis: Wegener granulomatosis, Churg-Strauss syndrome, microscopic polyangiitis, polyarteritis nodosa, and Takayasu arteritis. Crit Care Clin. 2002;18:855–79.
9. Vaglio A, Strehl JD, Manger B, Maritati F, Alberici F, Beyer C, Rech J, Sinico RA, Bonatti F, Battistelli L, Distler JH, Schett G, Zwerina J. IgG4 immune response in Churg-Strauss syndrome. Ann Rheum Dis. 2012;71:390–3.
10. Wieczorek S, Holle JU, Epplen JT. Recent progress in the genetics of Wegener's granulomatosis and Churg-Strauss syndrome. Curr Opin Rheumatol. 2010;22:8–14.
11. Grayson PC, Carmona-Rivera C, Xu L, Lim N, Gao Z, Asare AL, Specks U, Stone JH, Seo P, Spiera RF, Langford CA, Hoffman GS, Kallenberg CG, St Clair EW, Tchao NK, Ytterberg SR, Phippard DJ, Merkel PA, Kaplan MJ, Monach PA. Neutrophil-related gene expression and low-density granulocytes associated with disease activity and response to treatment in antineutrophil cytoplasmic antibody-associated vasculitis. Arthritis Rheum. 2015;67:1922–32.
12. Fishbein GA, Fishbein MC. Lung vasculitis and alveolar hemorrhage: pathology. Semin Respir Crit Care Med. 2011;32:254–63.
13. Safdar Z, Tamez E, Chan W, Arya B, Ge Y, Deswal A, Bozkurt B, Frost A, Entman M. Circulating collagen biomarkers as indicators of disease severity in pulmonary arterial hypertension. JACC Heart Fail. 2014;2:412–21.
14. Wong KM, Noonan S, O'Bryant C, Jimeno A. Alectinib for the treatment of ALK-positive stage IV non-small cell lung cancer. Drugs Today (Barc). 2015;51:161–70.
15. Toyokawa G, Hirai F, Inamasu E, Yoshida T, Nosaki K, Takenaka T, Yamaguchi M, Seto T, Takenoyama M, Ichinose Y. Secondary mutations at I1171 in the ALK gene confer resistance to both Crizotinib and Alectinib. J Thorac Oncol. 2014;9:e86–7.
16. Hoeper MM. Definition, classification, and epidemiology of pulmonary arterial hypertension. Semin Respir Crit Care Med. 2009;30:369–75.
17. Gomberg-Maitland M. Naming and understanding rare diseases: international classification of Diseases coding and the epidemiologic designations of idiopathic pulmonary arterial hypertension. Chest. 2011;139:482–3.
18. van den Hoogen F, Khanna D, Fransen J, Johnson SR, Baron M, Tyndall A, Matucci-Cerinic M, Naden RP, Medsger Jr TA, Carreira PE, Riemekasten G, Clements PJ, Denton CP, Distler O, Allanore Y, Furst DE, Gabrielli A, Mayes MD, van Laar JM, Seibold JR, Czirjak L, Steen VD, Inanc M, Kowal-Bielecka O, Muller-Ladner U, Valentini G, Veale DJ, Vonk MC, Walker UA, Chung L, Collier DH, Csuka ME, Fessler BJ, Guiducci S, Herrick A, Hsu VM, Jimenez S, Kahaleh B, Merkel PA, Sierakowski S, Silver RM, Simms RW, Varga J, Pope JE. Classification criteria for systemic sclerosis: an American College of Rheumatology/European League against Rheumatism collaborative initiative. Arthritis Rheum. 2013;65:2737–47.
19. Kantari C, Millet A, Gabillet J, Hajjar E, Broemstrup T, Pluta P, Reuter N, Witko-Sarsat V. Molecular analysis of the membrane insertion domain of proteinase 3, the Wegener's autoantigen, in RBL cells: implication for its

pathogenic activity. J Leukoc Biol. 2011;90: 941–50.
20. Kelley JM, Monach PA, Ji C, Zhou Y, Wu J, Tanaka S, Mahr AD, Johnson S, McAlear C, Cuthbertson D, Carette S, Davis Jr JC, Dellaripa PF, Hoffman GS, Khalidi N, Langford CA, Seo P, St Clair EW, Specks U, Stone JH, Spiera RF, Ytterberg SR, Merkel PA, Edberg JC, Kimberly RP. IgA and IgG antineutrophil cytoplasmic antibody engagement of Fc receptor genetic variants influences granulomatosis with polyangiitis. Proc Natl Acad Sci U S A. 2011;108:20736–41.
21. Kitaura K, Miyagawa T, Asano K, Oouchi S, Miki T, Fujisawa T, Ishida K. Mixed connective tissue disease associated with MPO-ANCA-positive polyangiitis. Intern Med. 2006;45:1177–82.
22. Resch B, Popper HH, Urlesberger B, Muller WD. Pulmonary eosinophilic vasculitis in a neonate with congenital chylothorax. Pediatr Pulmonol. 2002;33:501–4.
23. Watanabe A, Kawabata Y, Okada O, Tanabe N, Kimura H, Hatamochi A, Shinkai H, Sakai N, Shimada T, Hiroshima K, Kuriyama T. Ehlers-Danlos syndrome type IV with few extrathoracic findings: a newly recognized point mutation in the COL3A1 gene. Eur Respir J. 2002;19:195–8.
24. Jorgensen A, Fagerheim T, Rand-Hendriksen S, Lunde PI, Vorren TO, Pepin MG, Leistritz DF, Byers PH. Vascular Ehlers-Danlos Syndrome in siblings with biallelic COL3A1 sequence variants and marked clinical variability in the extended family. Eur J Hum Genet. 2015;23:796–802.
25. Lee JK, Bae JA, Sun EG, Kim HD, Yoon TM, Kim K, Lee JH, Lim SC, Kim KK. KITENIN increases invasion and migration of mouse squamous cancer cells and promotes pulmonary metastasis in a mouse squamous tumor model. FEBS Lett. 2009;583:711–7.
26. Ryan JJ, Thenappan T, Luo N, Ha T, Patel AR, Rich S, Archer SL. The WHO classification of pulmonary hypertension: a case-based imaging compendium. Pulm Circ. 2012;2:107–21.
27. Millet A, Pederzoli-Ribeil M, Guillevin L, Witko-Sarsat V, Mouthon L. Antineutrophil cytoplasmic antibody-associated vasculitides: is it time to split up the group? Ann Rheum Dis. 2013;72:1273–9.
28. Kang JH, Lee EH, Park SW, Chung IY. MUC5AC expression through bidirectional communication of Notch and epidermal growth factor receptor pathways. J Immunol. 2011;187:222–9.
29. Capaccione KM, Hong X, Morgan KM, Liu W, Bishop JM, Liu L, Markert E, Deen M, Minerowicz C, Bertino JR, Allen T, Pine SR. Sox9 mediates Notch1-induced mesenchymal features in lung adenocarcinoma. Oncotarget. 2014;5:3636–50.
30. Feng YX, Liu D, Sun ML, Jiang X, Sun N, Mao YM, Jing ZC. BMPR2 germline mutation in chronic thromboembolic pulmonary hypertension. Lung. 2014;192:625–7.
31. Eleftheriou D, Dillon MJ, Tullus K, Marks SD, Pilkington CA, Roebuck DJ, Klein NJ, Brogan PA. Systemic polyarteritis nodosa in the young: a single-center experience over thirty-two years. Arthritis Rheum. 2013;65:2476–85.
32. Demirkaya E, Ozen S, Pistorio A, Galasso R, Ravelli A, Hasija R, Baskin E, Dressler F, Fischbach M, Garcia Consuegra J, Iagaru N, Pasic S, Scarpato S, van Rossum MA, Apaz MT, Barash J, Calcagno G, Gonzalez B, Hoppenreijs E, Ioseliani M, Mazur-Zielinska H, Vougiouka O, Wulffraat N, Luqmani R, Martini A, Ruperto N, Dolezalova P. Performance of Birmingham vasculitis activity score and disease extent index in childhood vasculitides. Clin Exp Rheumatol. 2012;30:S162–8.
33. Fukushima H, Kosaki K, Sato R, Yagihashi T, Gatayama R, Kodo K, Hayashi T, Nakazawa M, Tsuchihashi T, Maeda J, Kojima Y, Yamagishi H, Takahashi T. Mechanisms underlying early development of pulmonary vascular obstructive disease in Down syndrome: an imbalance in biosynthesis of thromboxane A2 and prostacyclin. Am J Med Genet A. 2010;152A:1919–24.
34. Hughson MD, McCarty GA, Brumback RA. Spectrum of vascular pathology affecting patients with the antiphospholipid syndrome. Hum Pathol. 1995;26: 716–24.
35. Ma L, Bao R. Pulmonary capillary hemangiomatosis: a focus on the EIF2AK4 mutation in onset and pathogenesis. Appl Clin Genet. 2015;8:181–8.
36. Scalzetti EM, Heitzman ER, Groskin SA, Randall PA, Katzenstein AL. Developmental lymphatic disorders of the thorax. Radiographics. 1991;11:1069–85.
37. Dupond JL, Bermont L, Runge M, de Billy M. Plasma VEGF determination in disseminated lymphangiomatosis-Gorham-Stout syndrome: a marker of activity? A case report with a 5-year follow-up. Bone. 2010;46:873–6.

Metabolic Lung Diseases

12

12.1 Amyloidosis

Amyloidosis is a metabolic disease characterized by the deposition of amyloid in lung tissues. Amyloidosis is presently regarded as a protein-misfolding disease [1, 2]. Normally four proteins are folded into a complex with the help of chaperones. Many different forms of amyloid proteins have been identified. Misfolding can occur in several different compositions of amyloid [3]. Most common are amyloid A and P; however, microglobulin 2β, transthyretin, and others can also be seen in pulmonary amyloidosis. These misfolded proteins are much less soluble and therefore are deposited along blood vessels in different organs, among them also the lung.

The reason for amyloid deposition can be a tumor; one of the best-known examples is plasmocytoma. In this case, amyloid is formed out of misfolded immunoglobulins secreted by the tumor cells. Chronic inflammation such as collagen vascular diseases can also cause amyloid deposition [4, 5]. Amyloid deposition can occur as a tumorlike deposit, either along the bronchial tree or within the lung periphery (nodular form), or it can be diffuse perivascular and interstitial (Figs. 12.1 and 12.2). Nodular amyloidosis most often is associated with primary amyloidosis. Peribronchial amyloidosis most often imitates a tumorlike pattern on X-ray and HRCT pattern (Fig. 12.3), parenchymal deposits, if nodular, also imitates a tumor; diffuse deposition can be peribronchial or parenchymal and is

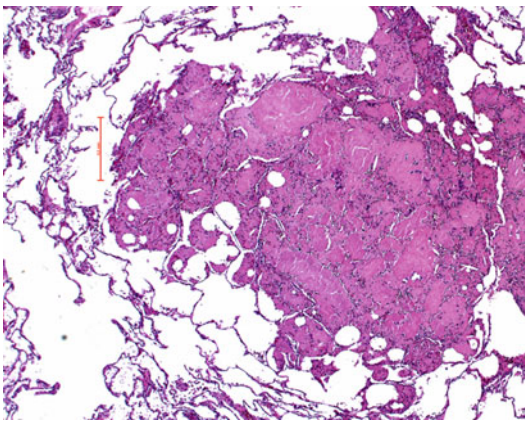

Fig. 12.1 Nodular amyloidosis showing an isolated nodule within an otherwise normal lung background. H&E, bar 500 μm

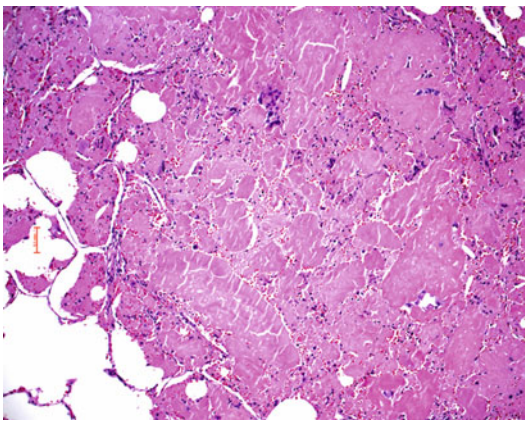

Fig. 12.2 Diffuse amyloidosis with abundant deposition in alveoli and alveolar walls. H&E, bar 100 μm

© Springer-Verlag Berlin Heidelberg 2017
H. Popper, *Pathology of Lung Disease*, DOI 10.1007/978-3-662-50491-8_12

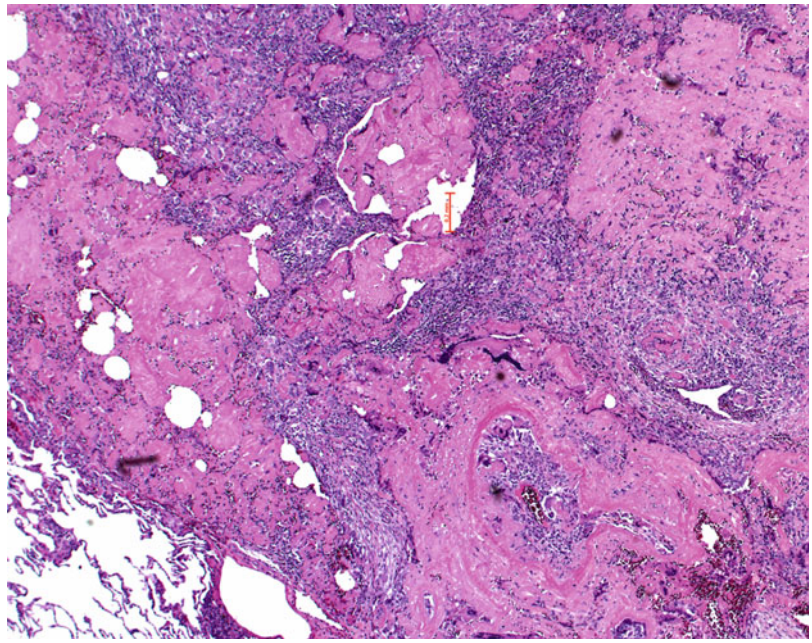

Fig. 12.3 Nodular amyloidosis with an additional dense lymphocytic background. This case presented as amyloidoma. In the lower center, obstruction of a large blood vessel by amyloid is seen. H&E, bar 200 μm

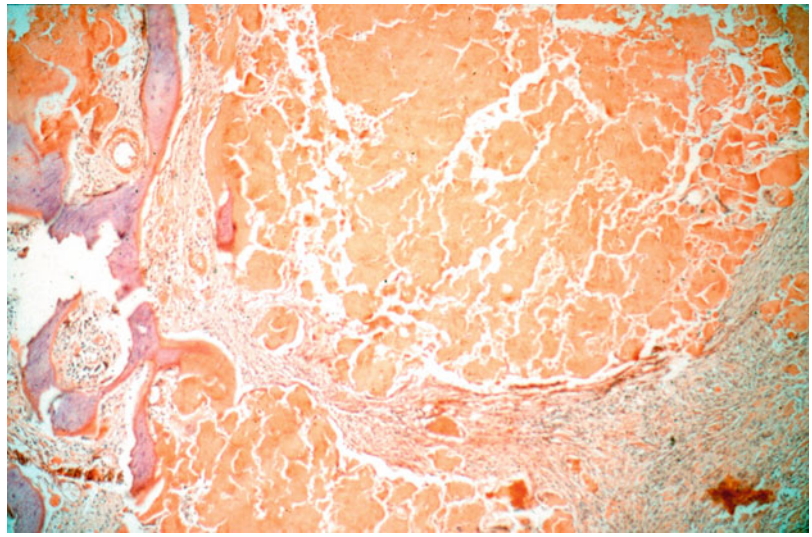

Fig. 12.4 Amyloidosis, *Congo red* stain shows orange staining. ×100

most often caused by systemic amyloidosis [6–8]. Amyloid stains eosin red and orange by the Congo red stain; it can be demonstrated by immunohistochemistry using specific antibodies for the different components [9]. If a Congo red stain is applied, the tissue section should be examined under polarized light, where the stain exhibits a green birefringence – this is essential because immune complexes might show an identical staining pattern, but do not polarize light (Figs. 12.4 and 12.5). Amyloid deposits very often will cause a tissue reaction with lymphoplasmacytic infiltrates and foreign body giant cells forming granulomas at the border of the deposits; in addition calcification and metaplastic bone formation do occur (Fig. 12.6). The major differential diagnosis to amyloidosis is IgG4-mediated fibrosis and hyalinosis; however, the dense lymphoplasmacytic infiltrations will lead to the correct diagnosis.

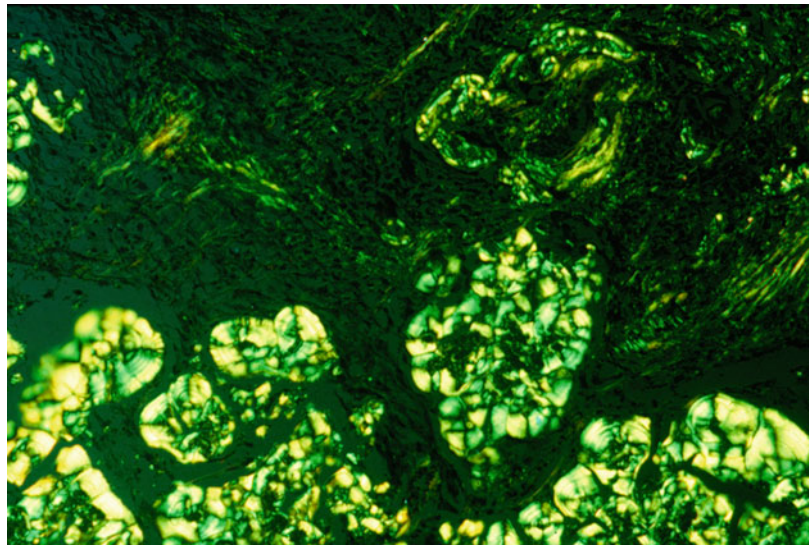

Fig. 12.5 Amyloidosis, *Congo red* stain polarized. Note the change of the color into *green*. ×50

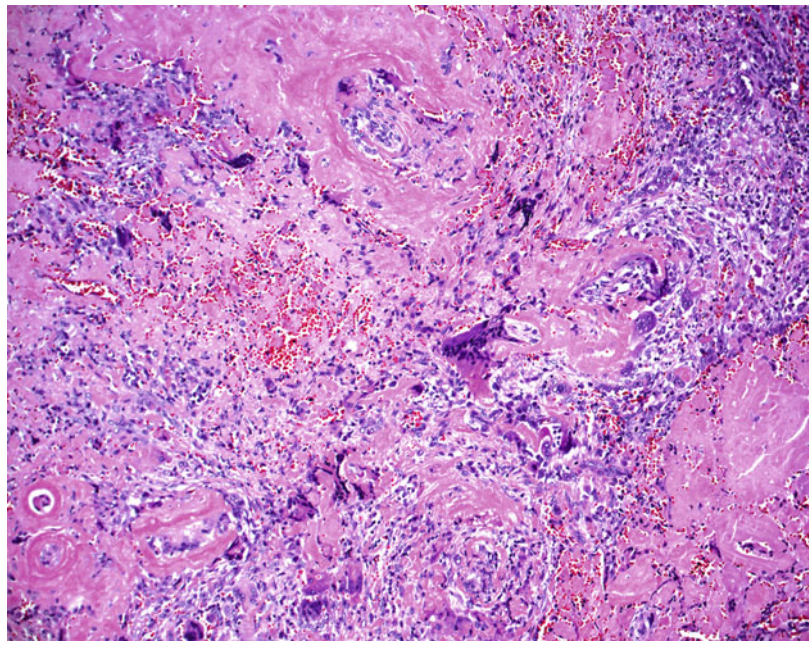

Fig. 12.6 Foreign body giant cell reaction in amyloidosis. Many giant cells try to ingest the deposited amyloid. H&E

12.2 Disturbed Calcium Metabolism

Calcification and Osseous Metaplasia

Tracheobronchopathia chondro-osteoplastica is characterized by an osseous metaplasia outside preexisting cartilages. It occurs only in large bronchi. Calcification can occur and even the bone marrow can be formed within the bones (Figs. 12.7 and 12.8). The border to the surrounding soft tissue is respected. In cases of irregular ossification, think of either amyloidosis, which quite often can show osseous metaplasia within the amyloid deposits, or osseous metaplasia in the peripheral lung, which is different (see below).

The cause is unknown, but a link to genes regulating bronchial maturation and differentiation is likely; it can occur in young-aged patients. It has also been described in dogs [10]. The major symp-

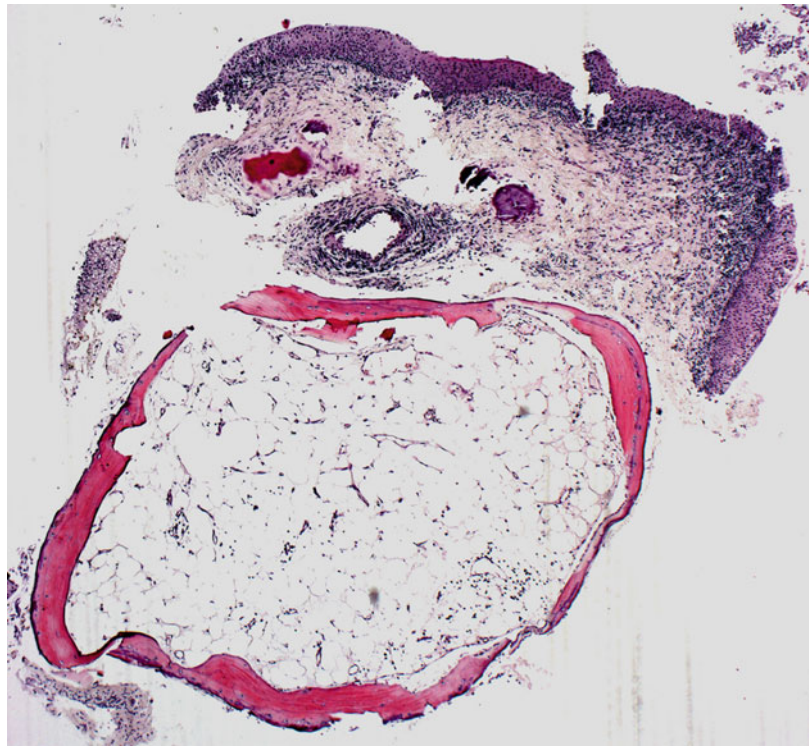

Fig. 12.7 Tracheobronchopathia chondro-osteoplastica. Note the newly formed bone with some bone marrow structures inside. There is no association with the cartilage. H&E, ×50

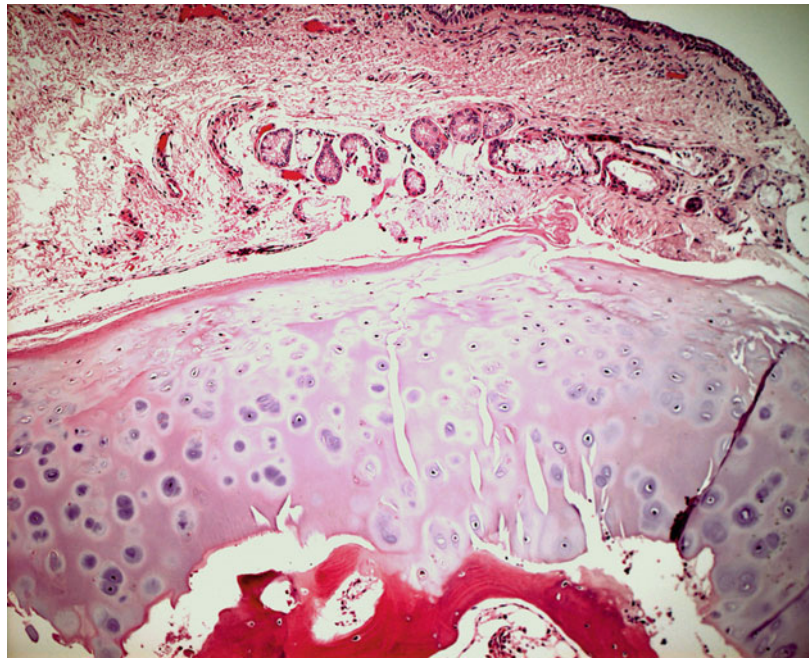

Fig. 12.8 For comparison a calcified cartilage is shown, which is not a tracheobronchopathia. H&E, ×100

tom is airflow obstruction sometimes followed by purulent bronchitis and pneumonia of the affected lobe/segment. It should be clearly differentiated from degeneration of the cartilage in the elderly with subsequent calcification and ossification – this has nothing to do with tracheobronchopathia.

Dendriform pulmonary ossification is characterized by bone formation within the alveolar

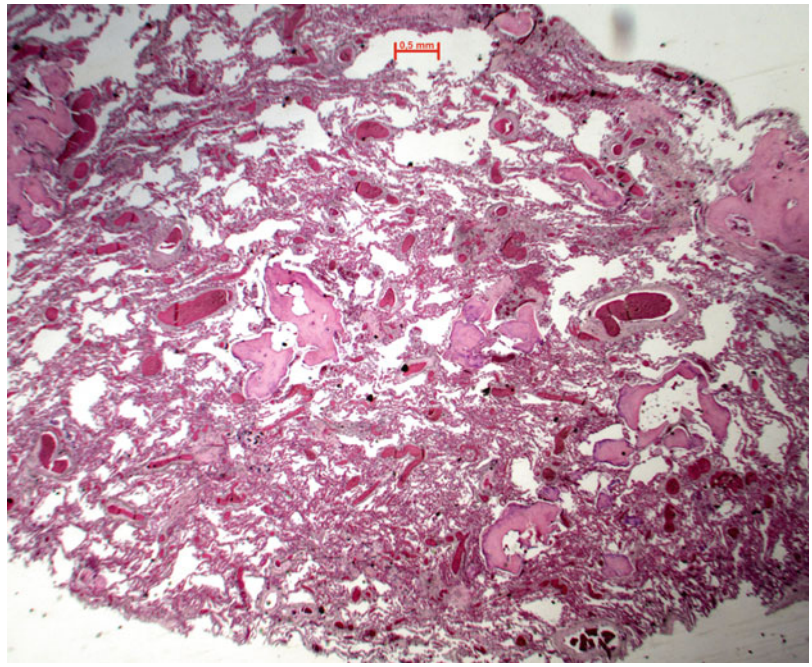

Fig. 12.9 Dendriform pulmonary ossification showing normal bone spicules within the otherwise regular lung tissue. H&E, 500 µm

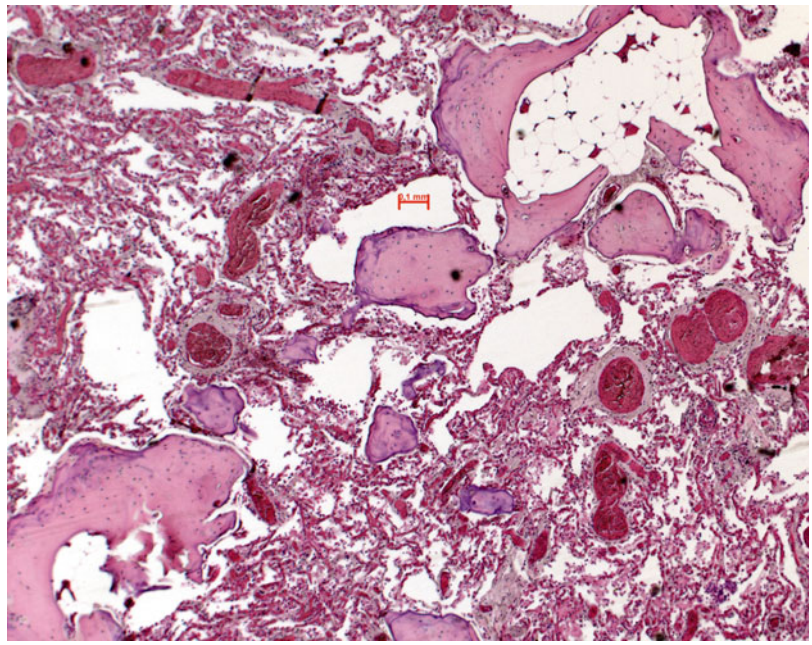

Fig. 12.10 Dendriform pulmonary ossification on higher magnification showing regular lamellar bone formation. H&E, 100 µm

septa, most often localized within one lobe and the upper lobes preferentially involved (Figs. 12.9 and 12.10). There is often fibrosis of the alveolar septa, out of which bone metaplasia evolves. The bone marrow can develop within these bones. The cause is unclear. In some instances, hypoxia might be the cause as in fibrosing pneumonia; in other cases, it is found in patients with kidney insufficiency [11–13]; however, there are other cases described in the literature and in my experience in some of them no underlying diseases could be identified. There is usually no disturbance of the calcium metabolism. Parenchymal ossification (osseous metaplasia) does not interfere with lung function.

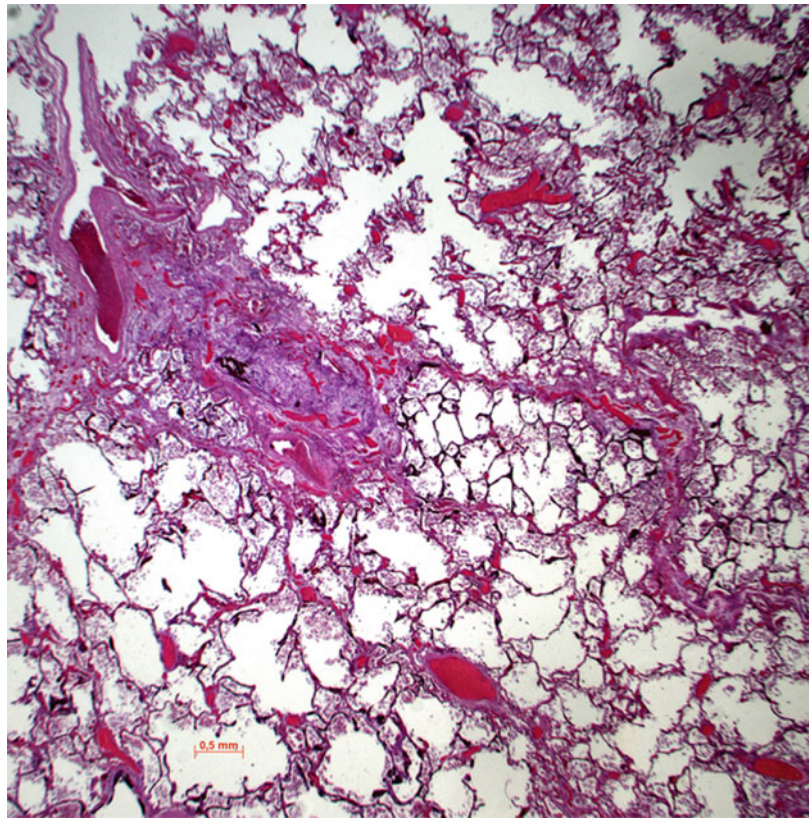

Fig. 12.11 Diffuse metabolic calcification in a patient with primary hyperthyroidism. Note the fine calcium compound deposition outlining the alveolar septa. H&E, bar 500 μm

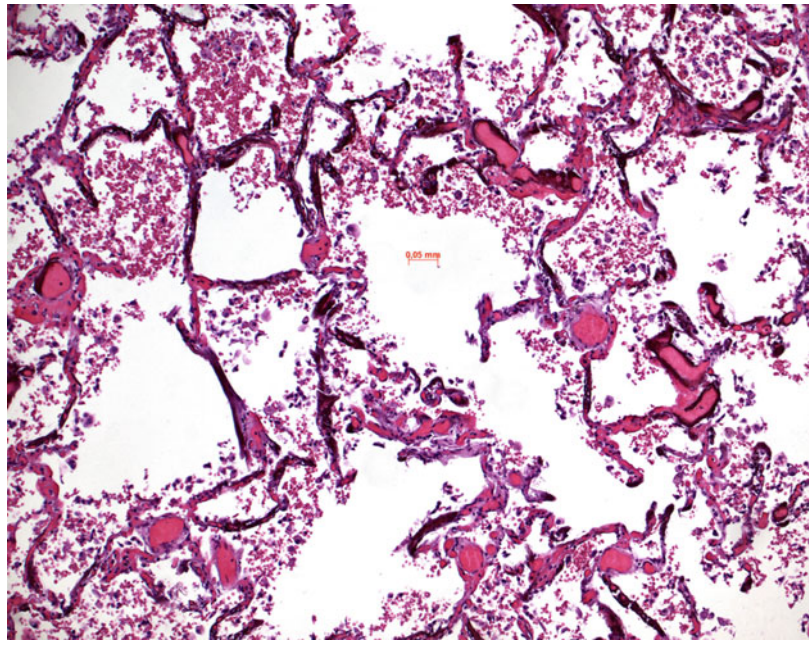

Fig. 12.12 Diffuse metabolic calcification in a patient with primary hyperthyroidism, higher magnification of the same case. H&E, bar 50 μm

Metabolic/metastatic pulmonary calcification of the alveolar septa can occur in patients with hyperparathyroidism and hypercalcemia [14–17]. Most often the kidneys and the stomach, which functionally are involved in ion exchange, are additionally affected. A loss of anions (CO_3^-) will lead to the deposition of insoluble calcium compounds. The deposition is usually diffuse and forms a network completely outlining the septa (Figs. 12.11 and 12.12). There is no inflammatory reaction toward the calcium deposits in contrast to microlithiasis and no ossification. Primary and secondary hyperthyroidism equally can induce diffuse lung calcification. Therapy is mainly focused on the treatment of the underlying disease. In addition rare cases without endocrine disorders have been described [14, 18].

Microlithiasis is a diffuse lung disease characterized by a deposition of microliths in the alveolar septa and lumina with a foreign body giant cell reaction. The giant cells phagocytose the microliths. Large foreign body cell granulomas can be formed. The microliths show usually a center, which can be calcified, and several layers of different minerals usually also containing calcium deposited in an appositional cockleshell-like growth (Fig. 12.13). Microlithiasis can be a

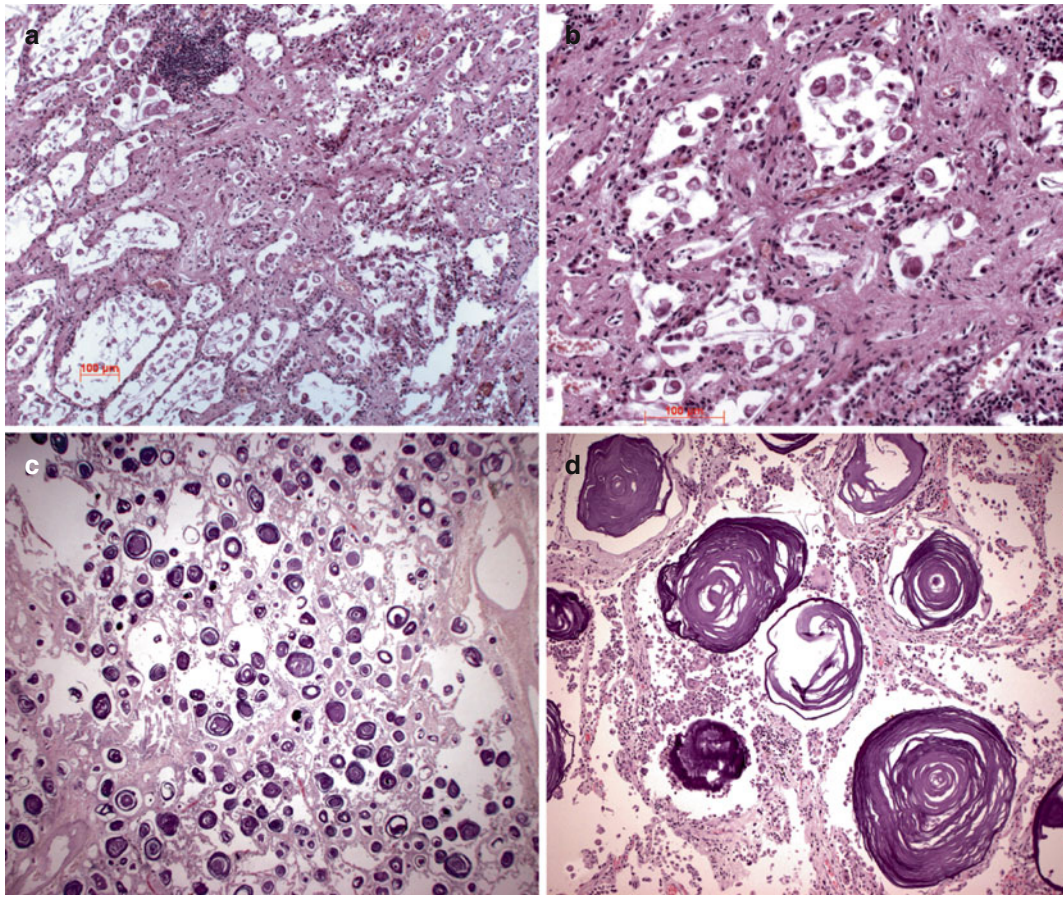

Fig. 12.13 Microlithiasis of the lung, three different cases are shown. (**a**, **b**) Microlithiasis with pronounced fibrosis of the lung. The small stones are most often within cystic remnants of lung lobules, only few are also in the stroma. (**c**, **d**) Another case with numerous stones, which show an appositional growth, again most stones are in remnants of lung lobules. (**e**–**g**) In the final case, here the classical picture is seen with the stones within the fibrosed tissue and also with pronounced foreign body giant cell reaction. In addition there is intense inflammation and some fibroblast foci. (**h**) A case with alveoliths. This material is a waste product of pneumocytes and has nothing to do with microlithiasis. The corpuscles are lying within the alveoli without any reaction from the tissue. Alveoliths can be seen in bronchoalveolar lavage. H&E, bars 100, 50 µm

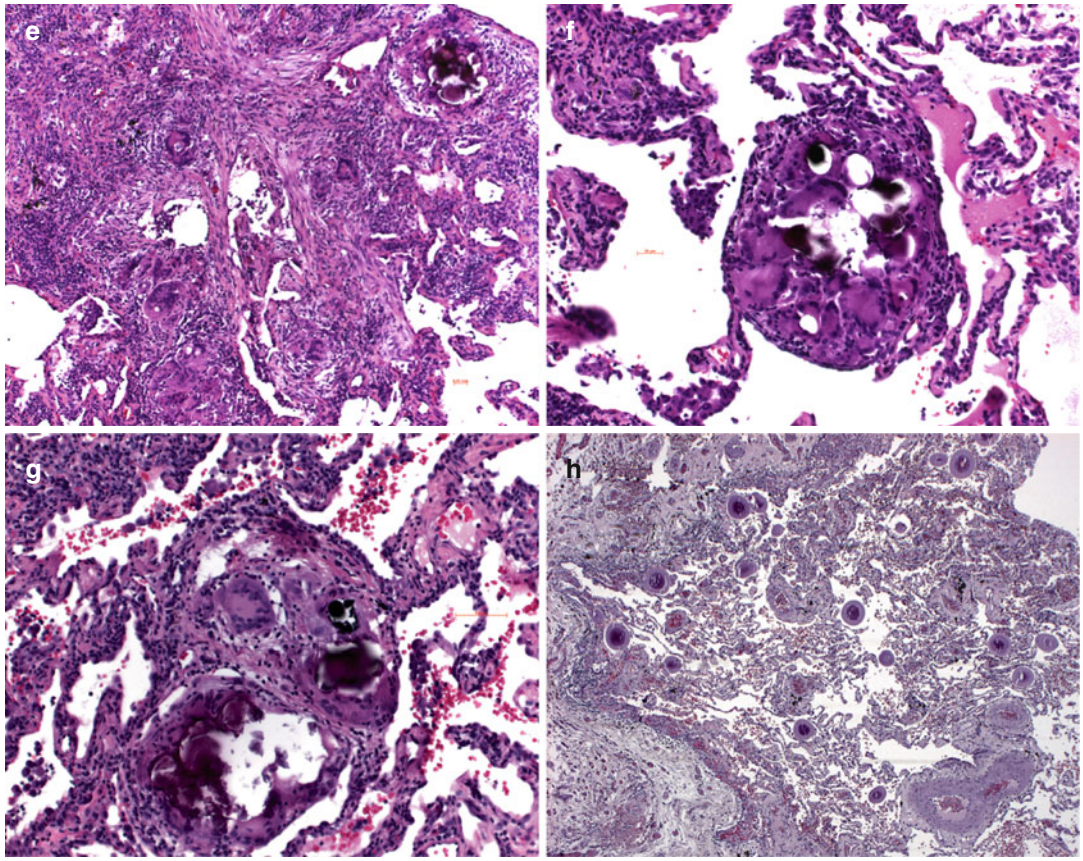

Fig. 12.13 (continued)

focal or a diffuse lung disease. The etiology was unknown until recently: first familial cases were described [19], and finally a candidate gene, SLC34A2, which encodes a type IIb sodium phosphate cotransporter was found to be mutated in all six patients being investigated. SLC34A2 is specifically expressed in type II pneumocytes, and the mutation abolishes the normal protein function, finally resulting in calcium compound deposition [20, 21]. There exists no specific therapy. In most instances, patients will die within several years, because the disease is slowly progressive and will impair lung function. In severe cases, lung transplantation can be considered [22, 23]. Microlithiasis should be clearly separated from lung tissue with alveoliths (Fig. 12.13h), i.e., concentric lamellae of proteins around a crystalline center, lying within the alveolar lumina without any tissue reaction.

12.3 Lipid and Surfactant Metabolism

Specific metabolic surfactant disturbances due to genetic defects/disorders are seen in children and adults. In some instances, these are based on defects in surfactant apoprotein or transporter genes (congenital type), namely, surfactant protein B and C (SP-B, SP-C), and ATP-binding cassette transporter family member mutations (ABCA3) [24–28]. Other factors causing alveolar proteinosis are associated with the metabolic degradation pathway as GM-CSF, GM receptor gene, located on chromosomes 2, 5, and 22, respectively [29]. In these cases, most often autoantibodies against GM-CSF or the receptor has been found [30–32]. Also the downregulation of GM-CSF synthesis might induce alveolar proteinosis [33]. Whereas in children alveolar

proteinosis is most often inherited and based on gene function loss, in adults, it is most often acquired. The etiology in the adult form in many cases is based on autoantibodies for GM-CSF; mutations of surfactant genes and transporter genes are absent. In addition exposure to dusts or chemicals, insecticides, silica, aluminum, or titanium dust, as well as infections such as tuberculosis, HIV infection in immunosuppressed patients, and finally hematological malignancies may cause alveolar proteinosis [30, 34]. There exists a rare autosomal recessive multisystem disorder called lysinuric protein intolerance that occurs in Finland and Italy, which also produces alveolar proteinosis [35–37]. The mechanisms on how these diverse diseases cause alveolar proteinosis are still to be discovered. The histology of alveolar proteinosis can present with different morphology depending on the underlying abnormality.

Alveolar proteinosis is characterized by a deposition of proteinaceous material usually within the alveoli, but sometimes also in alveolar walls. The material is composed of proteins, lipids, and surfactant components (Fig. 12.14). In adults usually no inflammatory infiltrations are seen. A bronchoalveolar lavage is almost diagnostic: on recovery a milky fluid is seen with high lipid content. On cytology there are few cells, but a proteinaceous material, positively stained by PAS. High-resolution CT shows a panlobular distribution of increased alveolar density and a superimposed reticular pattern, called "crazy paving." Chronic alveolar proteinosis is rarely seen in young patients suffering from idiopathic alveolar proteinosis. After several years of treatment, there is mild, however, functionally important diffuse fibrosis of the alveolar walls (Fig. 12.15).

In childhood alveolar lipoproteinosis, the alveoli are again filled by a proteinaceous material, but in addition cellular debris can be seen and a mild inflammatory infiltration of the alveolar septa. Whereas in SP-B deficiency and ABCA3 mutation, the symptoms of acute respiratory failure are immediately present at birth, the presentation of SP-C can develop more slowly. On histology ABCA3 and SP-B are characterized by lot of debris, whereas in SP-C there is less inflammation and less debris in the alveoli (Fig. 12.16). The histological picture

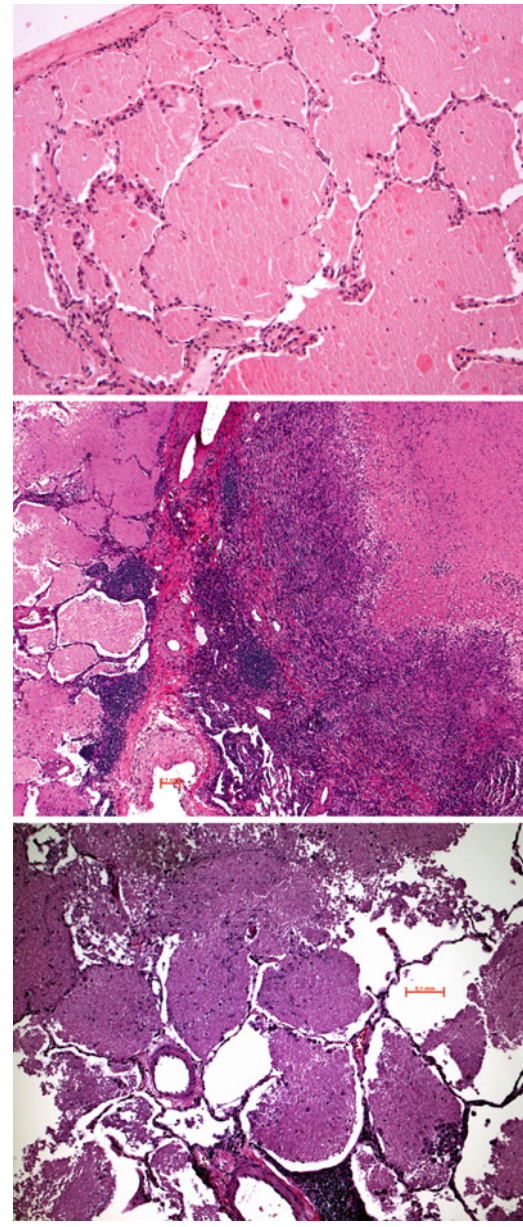

Fig. 12.14 Alveolar proteinosis with two different etiologies. *Upper panel* is alveolar proteinosis from a young male with autoantibodies against GM-CSF with classical accumulation of lipids and proteins in the alveoli. *Middle* and *lower panels* are alveolar proteinosis in a case with tuberculosis. A large granuloma is seen at the right side of the figure in the middle; the alveolar proteinosis pattern is seen to the left and higher magnified in the lower panel figure. H&E, ×100, bars 100 μm

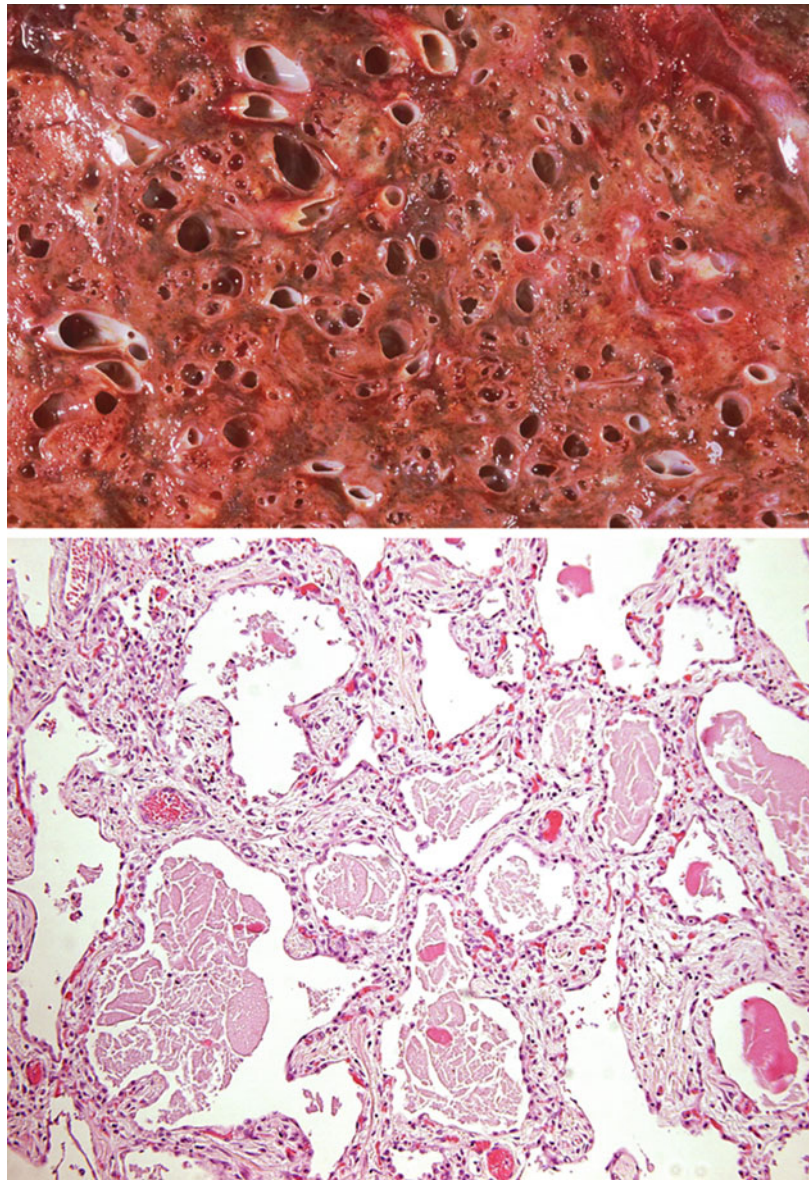

Fig. 12.15 Chronic alveolar proteinosis in a 19-year-old male. The patient was diagnosed with surfactant apoprotein C mutation and was treated by BAL for years. He finally developed diffuse fibrosis and died with acute alveolar proteinosis. *Top*: autopsy lung showing cystic remodeling of the lung. *Middle*: diffuse fibrosis of alveolar walls, the lumina are filled with proteinaceous material. *Bottom*: electron microscopy showing the abnormal lamellar bodies. ×100 and 6,000 (Courtesy Abida Haque, Galveston)

Fig. 12.16 Alveolar proteinosis based on defects of the surfactant regulatory genes. (**a**, **b**) surfactant apoprotein B gene defect, (**c**) surfactant apoprotein C gene defect, and (**d**) ABCA3 gene defect. In all these gene defects, the resulting picture is alveolar proteinosis, very intense in apoprotein B and ABCA3 defects, less pronounced in apoprotein C defect. Within the alveoli, there is this characteristic accumulation of proteins and lipids. On electron microscopy, different forms of atypical lamellar bodies can be seen. There is always also a mild lymphocytic infiltration within the alveolar septa. Bars 500 and 50 μm

Fig. 12.15 (continued)

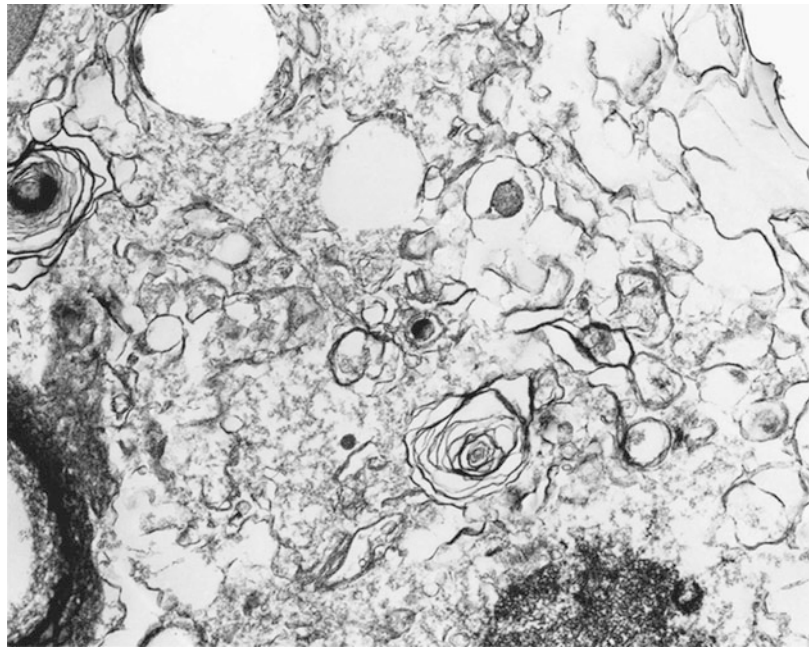

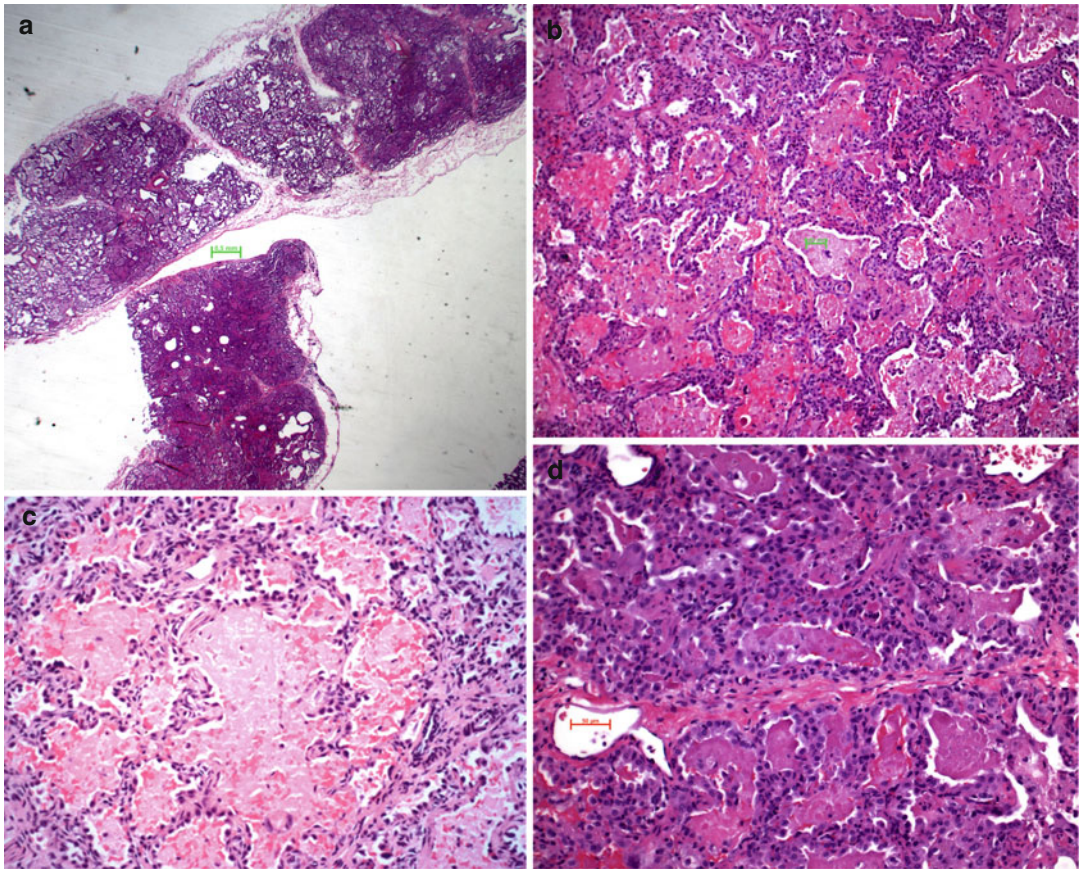

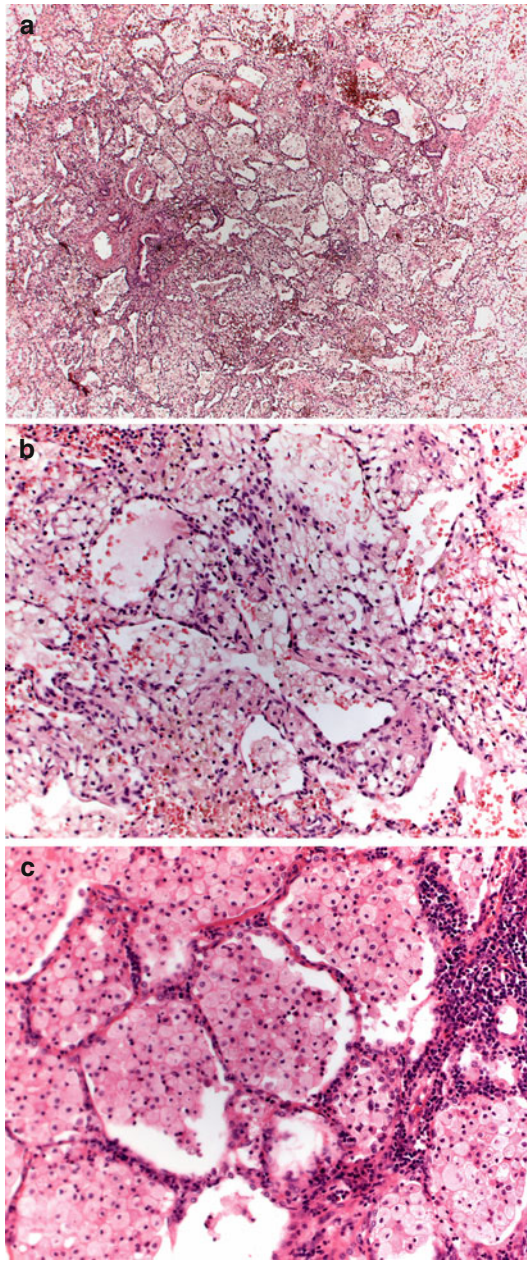

Fig. 12.17 (**a**, **b**) A 79-year-old female presented with diffuse chest X-ray abnormalities and on VATS biopsy lipid pneumonia was diagnosed. The alveoli and also in part within the septa lipid-laden macrophages were seen. In the follow-up, chronic abuse of nasal oil drops for rhinitis was the cause of this pneumonia. In (**c**) a lipid pneumonia was seen adjacent to a squamous cell carcinoma. In these cases, most likely dying tumor cells release lipids, which are taken up by macrophages and cause this morphology. H&E, ×12, 100

was formerly also called chronic interstitial pneumonia of infancy (CIP), but since there is a defined underlying genetic defect, it has been separated from CIP. Using electron microscopy, the morphology of the lamellar bodies within type II pneumocytes can help in the distinction of the different forms of deficiencies: in SP-B deficiency, there are numerous pleomorphic inclusions with membranous and vesicular structures in the cytoplasm, whereas in ABCA3 deficiency, a mixture of cytoplasmic electron dense inclusions with concentric membranes and distinctive electron dense aggregates are seen [38].

Lipid Accumulation Syndromes

Lipid pneumonia is caused by inhalation of lipids. Most often this occurs in patients chronically applying lipid-rich liquids for chronic rhinitis. Most of these drugs contain paraffin oil and this is inhaled as small droplets. Within the lung, foam cell reaction and pneumonia develop over the years (Fig. 12.17). The macrophage infiltration is seen within alveoli as well as in the septa. The infiltration can be so dense that the lung architecture is obscured. Sometimes a similar reaction is found in the vicinity of tumors. Most probably this reaction is also caused by a liberation of lipids from tumor necrosis or secretions of lipid-rich material from tumor cells.

A giant cell granulomatous reaction is often seen in patients suffering from rheumatoid arthritis and treated with corticosteroids. The giant cells contain an abundant amount of cholesterol clefts. It is unclear if this represents a reaction against lipids, derived from corticosteroids, or is a reaction against idiosyncratic antigen-antibody-complexes, usually formed in seropositive rheumatoid arthritis patients. A similar reaction was also described in patients on gold therapy (see chapter on "Autoimmune Diseases").

Lipid storage diseases are absolutely rare diseases (see Chap. 3). Fabry's and Gaucher's

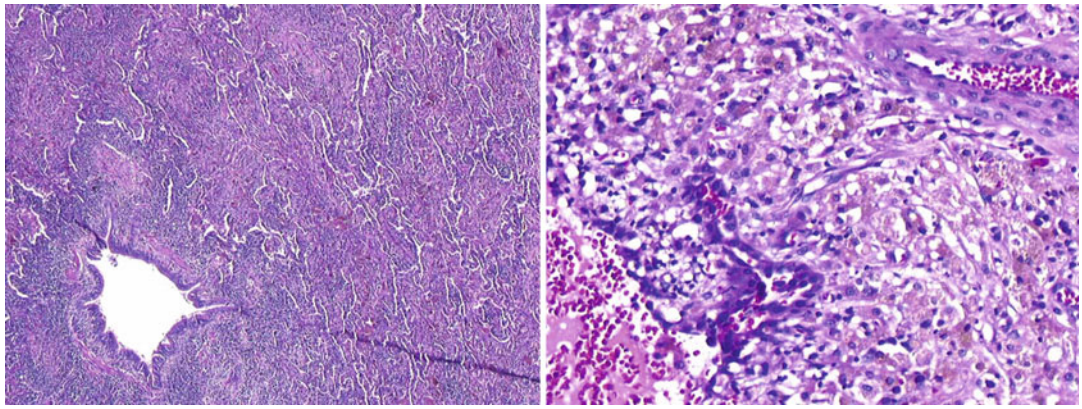

Fig. 12.18 Niemann-Pick type A disease in a child. There is a dense infiltration of the lung leaving not much parenchyma for respiration (*left*); on higher magnification, a dense infiltration of macrophages is seen, which contain brownish granular material in their cytoplasm, corresponding to sphingomyelin. H&E, 12, 200

diseases usually do not affect the lungs. However, Niemann-Pick disease can involve the lungs. In full-blown Niemann-Pick disease, children usually die. But there exists a rare "mild" form in adults, which presents with lung infiltrations. Characteristically this comes as macrophage infiltrations within bronchial, bronchiolar, and alveolar walls (Fig. 12.18). The macrophages contain lipids. This accumulation is followed by bronchial obstruction, which secondarily gives rise to bronchitis and bronchopneumonia.

Niemann-Pick disease is divided into four main types: type A, type B, type C1, and type C2 [39]. These types are classified on the basis of genetic cause and the signs and symptoms of the condition. In Niemann-Pick type A, there is hepatosplenomegaly, failure to gain weight, and growth. There is widespread lung damage that can cause recurrent lung infections and eventually lead to respiratory failure. Other abnormalities are not discussed here. Children with Niemann-Pick disease type A generally do not survive past early childhood. Type B usually presents in mid-childhood. The signs and symptoms are similar to A, but not as severe. There is often hepatosplenomegaly, recurrent lung infections, and thrombocytopenia. The prognosis is better compared to A. Types C1 and C2 are very similar; these types differ only by their genetic cause. Children also develop severe liver and interstitial lung disease.

Niemann-Pick disease types A and B are caused by mutations in the *SMPD1* gene, which codes for the enzyme acid sphingomyelinase. This enzyme is located in lysosomes. Acid sphingomyelinase is responsible for the conversion of sphingomyelin into ceramide. Mutations in *SMPD1* result in reduced breakdown of sphingomyelin and accumulation in cells. Mutations in either the *NPC1* or *NPC2* gene cause Niemann-Pick disease type C. The NPC coded proteins are involved in the transport of lipids within cells. Mutations prevent transport of cholesterol and other lipids, leading to their accumulation in cells. As a consequence, cell membrane formation is impaired.

A similar reaction is seen in chronic tungsten inhalation. Probably other rare metals can cause a similar reaction (see in "Pneumoconiosis" chapter).

Gaucher's disease is another lysosomal storage disorder with a high penetrance in Ashkenazi descendants [40]. The disease is autosomal recessive. The disease is caused by a

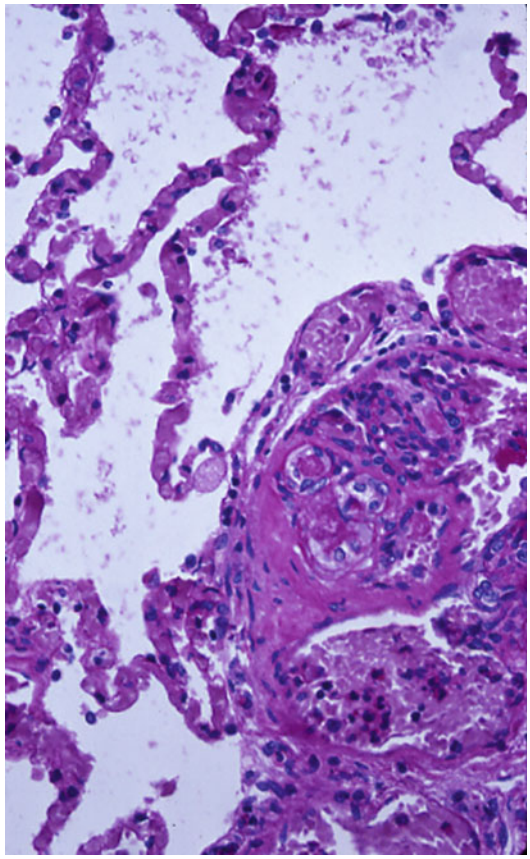

Fig. 12.19 Gaucher's disease involving the lung in a child (autopsy). There is accumulation of glucosylceramide in the interstitium, predominantly around small blood vessels. In addition there is also thrombosis with fibrin clots in the small blood vessels, a common finding in this disease. PAS, ×200

gene defect in GBA, which codes for β-glucocerebrosidase, which converts glucocerebroside into glucose and ceramide. Its defect causes accumulation of glucosylceramide in the bone marrow, lung, spleen, liver, and sometimes brain [41]. The disease has been subdivided in three subtypes according to the presence or absence of neurological involvement. In the lung accumulation of glucocerebroside is the main feature (Fig. 12.19).

12.4 Iron and Elastin Metabolism

Idiopathic pulmonary hemosiderosis can be regarded as metabolic lung disease, because it affects elastin metabolism [42, 43]. Elastin is destroyed, encrusted with hemosiderin, and finally digested by multinucleated giant cells of foreign body type (Fig. 12.20). On bronchoalveolar lavage, many hemosiderin-laden macrophages are seen. The differential diagnosis is within the spectrum of alveolar hemorrhage. In children especially, vasculitis has to be considered. Affected are children and young adults. The symptoms are variable from hemoptysis to anemia [44]. So far immunosuppressive therapy has improved the outcome [42, 44–46], which points to some underlying abnormal immune reaction causing this disease.

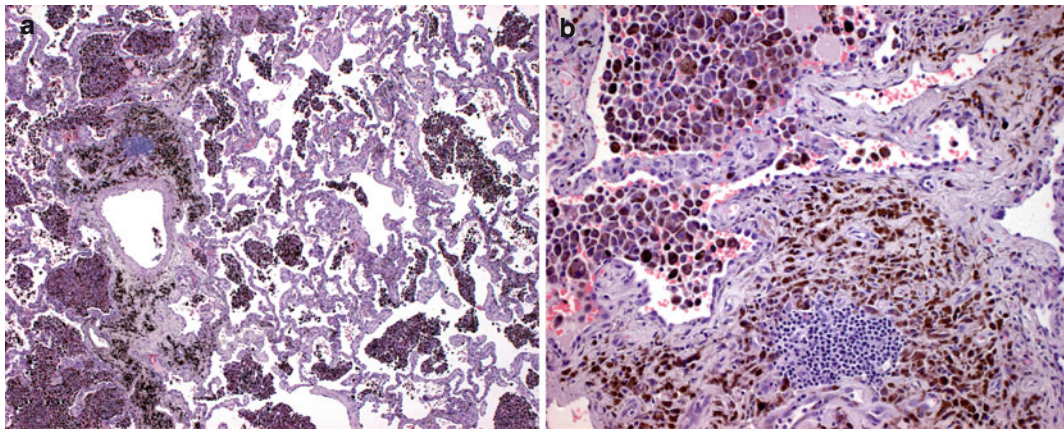

Fig. 12.20 Idiopathic pulmonary hemosiderosis illustrated by two cases. (**a**–**c**) shows a patient with massive infiltration of the alveolar septa and alveoli by hemosiderin-laden macrophages; only minimal fresh bleeding is focally present. In the interstitium sometimes foreign body giant cells are encountered, in one area with phagocytosed elastin and collagen fibers (**c**). (**d**–**e**) another case shows hemosiderin-encrusted elastic fibers in the alveolar septa and again fresh bleeding as well as macrophage accumulation in the alveoli. Some macrophages contain hemosiderin-encrusted elastic fibers in their cytoplasm (**e**). H&E, Elastica v. Gieson, ×25, 100, 200

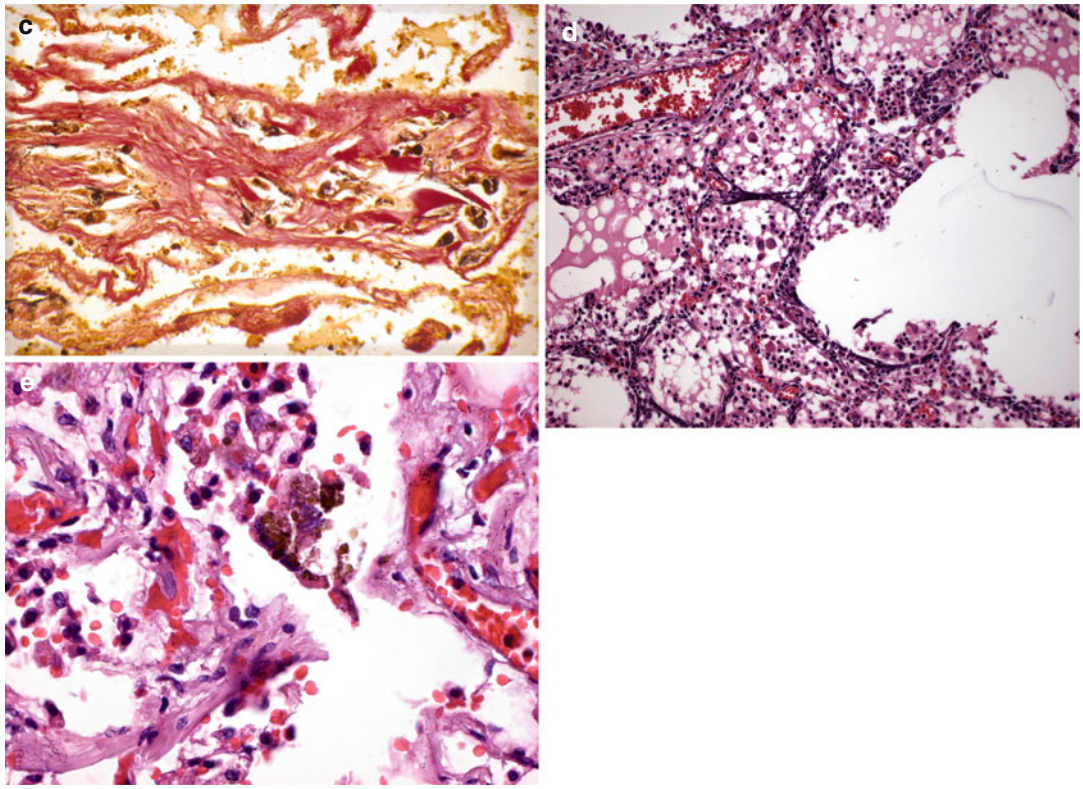

Fig. 12.20 (continued)

References

1. Glabe CG, Kayed R. Common structure and toxic function of amyloid oligomers implies a common mechanism of pathogenesis. Neurology. 2006;66:S74–8.
2. Stefani M, Dobson CM. Protein aggregation and aggregate toxicity: new insights into protein folding, misfolding diseases and biological evolution. J Mol Med. 2003;81:678–99.
3. Westermark P. Aspects on human amyloid forms and their fibril polypeptides. FEBS J. 2005;272:5942–9.
4. Kobayashi H, Matsuoka R, Kitamura S, Tsunoda N, Saito K. Sjogren's syndrome with multiple bullae and pulmonary nodular amyloidosis. Chest. 1988;94:438–40.
5. Marenco JL, Sanchez-Burson J, Ruiz Campos J, Jimenez MD, Garcia-Bragado F. Pulmonary amyloidosis and unusual lung involvement in SLE. Clin Rheumatol. 1994;13:525–7.
6. Sharma OP. Unusual systemic disorders associated with interstitial lung disease. Curr Opin Pulm Med. 2001;7:291–4.
7. Lachmann HJ, Hawkins PN. Systemic amyloidosis. Curr Opin Pharmacol. 2006;6:214–20.
8. Linke RP, Oos R, Wiegel NM, Nathrath WB. Classification of amyloidosis: misdiagnosing by way of incomplete immunohistochemistry and how to prevent it. Acta Histochem. 2006;108:197–208.
9. Kebbel A, Rocken C. Immunohistochemical classification of amyloid in surgical pathology revisited. Am J Surg Pathol. 2006;30:673–83.
10. Xiang R, Luo Y, Niethammer AG, Reisfeld RA. Oral DNA vaccines target the tumor vasculature and microenvironment and suppress tumor growth and metastasis. Immunol Rev. 2008;222:117–28.
11. Lara JF, Catroppo JF, Kim DU, da Costa D. Dendriform pulmonary ossification, a form of diffuse pulmonary ossification: report of a 26-year autopsy experience. Arch Pathol Lab Med. 2005;129:348–53.
12. Yoon HK, Moon HS, Park SH, Song JS, Lim Y, Kohyama N. Dendriform pulmonary ossification in patient with rare earth pneumoconiosis. Thorax. 2005;60:701–3.
13. Rajwani NA, Puttagunta L, Barrie J, Kalluri M. Pulmonary ossification syndrome in a patient with chronic thromboembolic pulmonary hypertension. Can Respir J. 2014;21:83–5.
14. Chan ED, Morales DV, Welsh CH, McDermott MT, Schwarz MI. Calcium deposition with or without bone formation in the lung. Am J Respir Crit Care Med. 2002;165:1654–69.
15. Chung MJ, Lee KS, Franquet T, Muller NL, Han J, Kwon OJ. Metabolic lung disease: imaging and histopathologic findings. Eur J Radiol. 2005;54:233–45.
16. Madhusudhan KS, Shad PS, Sharma S, Goel A, Mahajan H. Metastatic pulmonary calcification in chronic renal failure. Int Urol Nephrol. 2012;44:1285–7.

17. Eggert CH, Albright RC. Metastatic pulmonary calcification in a dialysis patient: case report and a review. Hemodial Int. 2006;10 Suppl 2:S51–5.
18. Marchiori E, Muller NL, Souza Jr AS, Escuissato DL, Gasparetto EL, de Cerqueira EM. Unusual manifestations of metastatic pulmonary calcification: high-resolution CT and pathological findings. J Thorac Imaging. 2005;20:66–70.
19. Al-Alawi AS. Familial occurrence of pulmonary alveolar microlithiasis in 3 siblings. Saudi Med J. 2006; 27:238–40.
20. Corut A, Senyigit A, Ugur SA, Altin S, Ozcelik U, Calisir H, Yildirim Z, Gocmen A, Tolun A. Mutations in SLC34A2 cause pulmonary alveolar microlithiasis and are possibly associated with testicular microlithiasis. Am J Hum Genet. 2006;79:650–6.
21. Huqun, Izumi S, Miyazawa H, Ishii K, Uchiyama B, Ishida T, Tanaka S, Tazawa R, Fukuyama S, Tanaka T, Nagai Y, Yokote A, Takahashi H, Fukushima T, Kobayashi K, Chiba H, Nagata M, Sakamoto S, Nakata K, Takebayashi Y, Shimizu Y, Kaneko K, Shimizu M, Kanazawa M, Abe S, Inoue Y, Takenoshita S, Yoshimura K, Kudo K, Tachibana T, Nukiwa T, Hagiwara K. Mutations in the SLC34A2 gene are associated with pulmonary alveolar microlithiasis. Am J Respir Crit Care Med. 2007;175:263–8.
22. Mariotta S, Ricci A, Papale M, De Clementi F, Sposato B, Guidi L, Mannino F. Pulmonary alveolar microlithiasis: report on 576 cases published in the literature. Sarcoidosis Vasc Diff Lung Dis. 2004;21:173–81.
23. Prakash UB. Pulmonary alveolar microlithiasis. Semin Respir Crit Care Med. 2002;23:103–13.
24. Hamvas A, Nogee LM, White FV, Schuler P, Hackett BP, Huddleston CB, Mendeloff EN, Hsu FF, Wert SE, Gonzales LW, Beers MF, Ballard PL. Progressive lung disease and surfactant dysfunction with a deletion in surfactant protein C gene. Am J Respir Cell Mol Biol. 2004;30:771–6.
25. Whitsett JA, Wert SE, Trapnell BC. Genetic disorders influencing lung formation and function at birth. Hum Mol Genet. 2004;13(Spec No 2):R207–15.
26. Tredano M, Griese M, Brasch F, Schumacher S, de Blic J, Marque S, Houdayer C, Elion J, Couderc R, Bahuau M. Mutation of SFTPC in infantile pulmonary alveolar proteinosis with or without fibrosing lung disease. Am J Med Genet. 2004;126A:18–26.
27. Bruder E, Hofmeister J, Aslanidis C, Hammer J, Bubendorf L, Schmitz G, Rufle A, Buhrer C. Ultrastructural and molecular analysis in fatal neonatal interstitial pneumonia caused by a novel ABCA3 mutation. Mod Pathol. 2007;20:1009–18.
28. Wert SE, Whitsett JA, Nogee LM. Genetic disorders of surfactant dysfunction. Pediatr Dev Pathol. 2009; 12:253–74.
29. Trapnell BC, Whitsett JA. Gm-CSF regulates pulmonary surfactant homeostasis and alveolar macrophage-mediated innate host defense. Annu Rev Physiol. 2002;64:775–802.
30. Bonfield TL, Russell D, Burgess S, Malur A, Kavuru MS, Thomassen MJ. Autoantibodies against granulocyte macrophage colony-stimulating factor are diagnostic for pulmonary alveolar proteinosis. Am J Respir Cell Mol Biol. 2002;27:481–6.
31. Latzin P, Tredano M, Wust Y, de Blic J, Nicolai T, Bewig B, Stanzel F, Kohler D, Bahuau M, Griese M. Anti-GM-CSF antibodies in paediatric pulmonary alveolar proteinosis. Thorax. 2005;60:39–44.
32. Ioachimescu OC, Kavuru MS. Pulmonary alveolar proteinosis. Chron Respir Dis. 2006;3:149–59.
33. Thomassen MJ, Raychaudhuri B, Bonfield TL, Malur A, Abraham S, Barna BP, Kavuru MS. Elevated IL-10 inhibits GM-CSF synthesis in pulmonary alveolar proteinosis. Autoimmunity. 2003;36:285–90.
34. Brasch F, Birzele J, Ochs M, Guttentag SH, Schoch OD, Boehler A, Beers MF, Muller KM, Hawgood S, Johnen G. Surfactant proteins in pulmonary alveolar proteinosis in adults. Eur Respir J. 2004;24:426–35.
35. Parto K, Svedstrom E, Majurin ML, Harkonen R, Simell O. Pulmonary manifestations in lysinuric protein intolerance. Chest. 1993;104:1176–82.
36. Douda DN, Farmakovski N, Dell S, Grasemann H, Palaniyar N. SP-D counteracts GM-CSF-mediated increase of granuloma formation by alveolar macrophages in lysinuric protein intolerance. Orphanet J Rare Dis. 2009;4:29.
37. Barilli A, Rotoli BM, Visigalli R, Bussolati O, Gazzola GC, Kadija Z, Rodi G, Mariani F, Ruzza ML, Luisetti M, Dall'asta V. In lysinuric protein intolerance system y+L activity is defective in monocytes and in GM-CSF-differentiated macrophages. Orphanet J Rare Dis. 2010;5:32.
38. Edwards V, Cutz E, Viero S, Moore AM, Nogee L. Ultrastructure of lamellar bodies in congenital surfactant deficiency. Ultrastruct Pathol. 2005;29:503–9.
39. Guillemot N, Troadec C, de Villemeur TB, Clement A, Fauroux B. Lung disease in Niemann-Pick disease. Pediatr Pulmonol. 2007;42:1207–14.
40. Dinwiddie R, Sonnappa S. Systemic diseases and the lung. Paediatr Respir Rev. 2005;6:181–9.
41. Miller A, Brown LK, Pastores GM, Desnick RJ. Pulmonary involvement in type 1 Gaucher disease: functional and exercise findings in patients with and without clinical interstitial lung disease. Clin Genet. 2003;63:368–76.
42. Ioachimescu OC, Sieber S, Kotch A. Idiopathic pulmonary haemosiderosis revisited. Eur Respir J. 2004; 24:162–70.
43. Nuesslein TG, Teig N, Rieger CH. Pulmonary haemosiderosis in infants and children. Paediatr Respir Rev. 2006;7:45–8.
44. Zhang X, Wang L, Lu A, Zhang M. Clinical study of 28 cases of paediatric idiopathic pulmonary haemosiderosis. J Trop Pediatr. 2010;56:386–90.
45. Airaghi L, Ciceri L, Giannini S, Ferrero S, Meroni PL, Tedeschi A. Idiopathic pulmonary hemosiderosis in an adult. Favourable response to azathioprine. Monaldi Arch Chest Dis. 2001;56:211–3.
46. Kahraman H, Koksal N, Ozkan F. Eight years follow-up of a case with idiopathic pulmonary hemosiderosis after corticosteroid therapy. N Am J Med Sci. 2012;4:49–51.

Pneumoconiosis and Environmentally Induced Lung Diseases

13

13.1 Introduction

Pneumoconiosis is characterized by an inhalation of foreign nonliving material in the widest sense but is usually restricted to inorganic matter. Inhalation causes a tissue reaction, which can be any kind of pneumonia, granulomatosis, or similar. Primarily when thinking about pneumoconiosis, silicosis and asbestosis will immediately come into one's mind; however, there are many more agents causing pulmonary diseases. As in many other diseases in all kinds of pneumoconiosis, there is a dose-effect relationship: this means there is a threshold dose required to induce disease (amount of a mineral) and duration of exposure. In addition, the dimension of the particles is important too: particles larger than 10 μm are deposited in the larger airways; particles below 2–5 μm will reach the alveolar periphery. But there is another factor, aerodynamic diameter: particles are within the airstream and will orient themselves along the axis of the airflow; therefore, asbestos fibers although 100–200 μm in length are less than 5 μm thick, which means they are oriented within the airstream and might reach small bronchioles before being trapped at bifurcations. Another quality of inhaled mineral dust is durability: some metals are easily dissolved in extracellular fluids and can be absorbed and removed by macrophages. Other minerals such as quartz and asbestos fibers are long lasting and resist degradation by macrophages for months. Finally also the chemical composition plays a role: highly toxic compounds will cause acute injury to the lung, whereas other minerals cause injury only in huge quantities, as example for both is chromates versus titanium oxides. On the other hand, our lung has developed many clearance and defense mechanisms during evolution. We all inhale some amount of quartz, but usually do not develop silicosis, because quartz is cleared. There are several mechanisms: The evolutionary oldest mechanism is the mucus escalator system; mucus is produced by goblet cells and moved toward the larynx. Particles deposited within the mucus are transported with it and expectorated or coughed out. Another evolutionary old mechanism is clearance by macrophages; these cells of the innate immune system patrol through the lungs, phagocytose, and degrade foreign particles, thus preventing toxic injury. Finally there is also a chemical defense system. The epithelial cells of the airways and the pneumocytes produce two different enzyme systems: oxidizing enzymes such as the cytochromes and detoxifying enzymes such as the (de)aminidases, glutathione synthases and glutathione transferases, etc. [1–5]. All these form together an efficient defense against inhaled mineral particles.

There are several tissue reactions in those cases when the amount of inhaled particles and their toxicity and durability overcome the clearance mechanisms (Table 13.1).

© Springer-Verlag Berlin Heidelberg 2017
H. Popper, *Pathology of Lung Disease*, DOI 10.1007/978-3-662-50491-8_13

13.2 Silicosis

Quartz oxides induce silicosis, the major component being SiO_2. The mechanism on how silica oxides cause silicosis is not entirely clear; however, most probably inflammation is started by depolarization of biological membranes caused by quartz. Quartz crystals phagocytosed by macrophages act by their piezoelectric effect and cause depolarization of the phagolysosomes and thus release toxic enzymes into the cytoplasm, subsequently causing cell death [6]. These enzymes then will cause oxygen radical production and activation of NFκB, TNFα, and cyclooxygenase II and contribute to the destruction of pneumocytes and alveolar walls including basement membranes [7–9]. The first tissue reaction in silicosis is a granulomatous reaction with histiocytes, in very early stages even foreign body giant cells. In acute silicosis with high-dose inhalation, a simple macrophage reaction is also seen (Fig. 13.1). In rare cases, silicoproteinosis can be caused by high-dose inhalation, especially if amorphous silica is inhaled (Fig. 13.2). TGF-β seems to be the major mediator of fibrosis and is produced by hyperplastic pneumocytes type II as well as by fibroblasts and macrophages at the periphery of silicotic granulomas. The hyperplastic pneumocytes appear to be the predominant sites of production and secretion of TGF-β1 and mediate the production of extracellular matrix [10]. These granulomas represent the early stages of silicosis and fulfill the criteria for compensation by state agencies. Later on these granulomas undergo hyalinization and form the typical hyaline granulomas of full-blown silicosis (Fig. 13.3). By polarized light quartz is seen as white birefringent crystals, usually 7 μm in length and less 1 μm in diameter (Fig. 13.4). Usually nodules coalesce and form large aggregates. In the center necrosis can occur, most probably by ischemia.

Silica degradation takes several months, and usually silica crystals are constantly released from the granuloma border and subsequently will start the destructive process again. So even if the

Table 13.1 Examples of tissue reactions and their most common agents

Asthma	Isocyanates, metals
Bronchiolitis	Nitrogen oxides
Nodular pneumoconiosis	Coal, silica, silicates
Diffuse interstitial fibrosis	Asbestos
Granulomatous pneumonia	Beryllium
Diffuse alveolar damage	Toxic fumes, hard metal, beryllium oxide
Hypersensitivity pneumonia	Isocyanates, chromium, nickel
Giant cell interstitial pneumonia GIP	Hard metal, cobalt
Alveolar proteinosis	Silica
Emphysema	Coal, cadmium, chromium
Pleural plaque/fibrosis	Asbestos
Lung cancer	Asbestos, nickel, arsenic
Mesothelioma	Asbestos

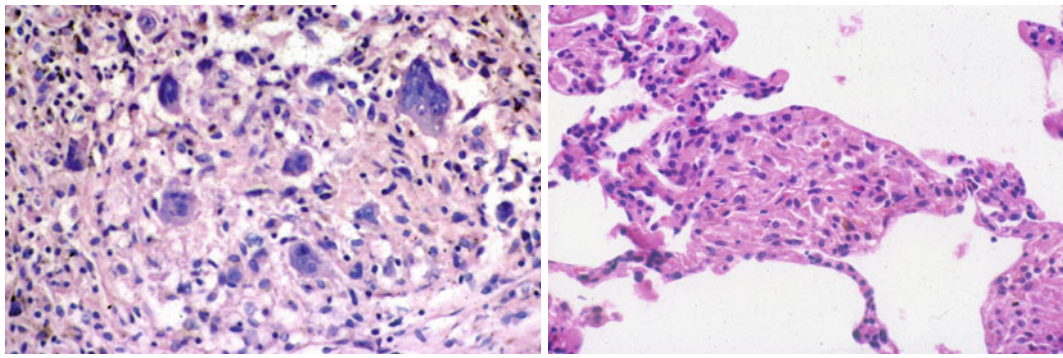

Fig. 13.1 Silicosis with two different types of early reaction: in the *left panel*, a granulomatous reaction with foreign body giant cells and histiocytes is seen and in the *right panel*, a macrophage accumulation is the only reaction in this high-dose inhalation by a patient working with sand blasting. H&E, ×200

patient is withdrawn from the exposure, silicosis will progress although less rapidly. Over time the granulomas undergo fibrosis, forming large scars. This in turn will cause tractions of the bronchi and bronchiectasis. If bronchi are within the fibrotic area, they can even be obliterated.

The upper lobes are usually more severely affected by silicosis, and the hilar lymph nodes can appear black, firm, and packed together. The distribution pattern of silicosis can be best demonstrated by HRCT scan or by whole lung sections on paper mounts (Fig. 13.5).

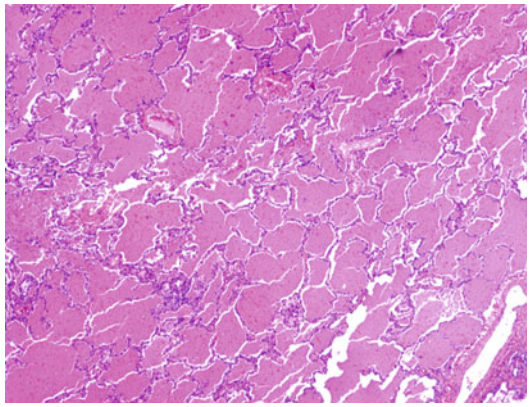

Fig. 13.2 Alveolar proteinosis in acute silicosis. The alveoli are diffusely filled with eosinophilic material without cells. By polarization numerous silica crystals can be seen. H&E, ×50

Occupational exposure: In former days, the majority of patients presenting with silicosis were found within coal mines (e.g., the Rhine-Ruhr area in Germany and the coal mines in Poland) due to the contamination of hard coal with high proportion of silicates (up to 35 %). Other exposures occurred in tunnel construction, brick production, sandblasting, masonry, founding, ceramic fabrication, gold mining (South African mines), and dental laboratories [11–13]. Silicon oxides come in two forms, crystalline (quartz, tridymite, cristobalite) and amorphous (diatomite). For many years, amorphous silica was regarded as non-fibrogenic. However, experimental work has shown that amorphous silica is as dangerous as crystalline [14].

Outcome and secondary changes: Bronchiectasis and bronchial obstruction will cause severe emphysema; pulmonary blood vessels usually undergo fibrosis and obliteration. Especially the small arteries and capillaries are lost. The whole diameter of the peripheral capillary system can be reduced by

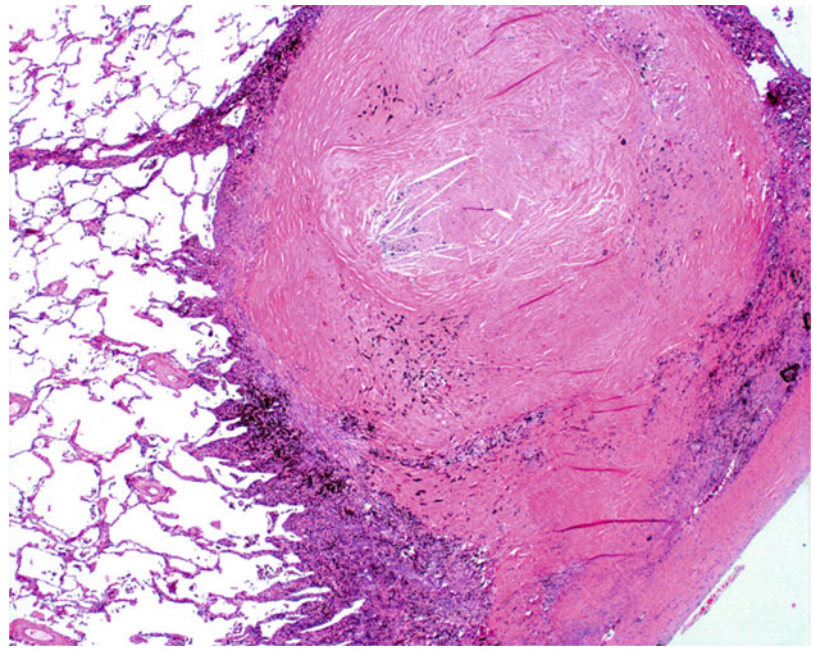

Fig. 13.3 Hyaline granuloma in silicosis. This is the typical reaction in silicosis. The center of the granuloma is built by concentric depositions of collagen fibers, which may undergo purification as in this example. The outer wall is built by macrophages with dark pigment and numerous silica particles. H&E, ×25

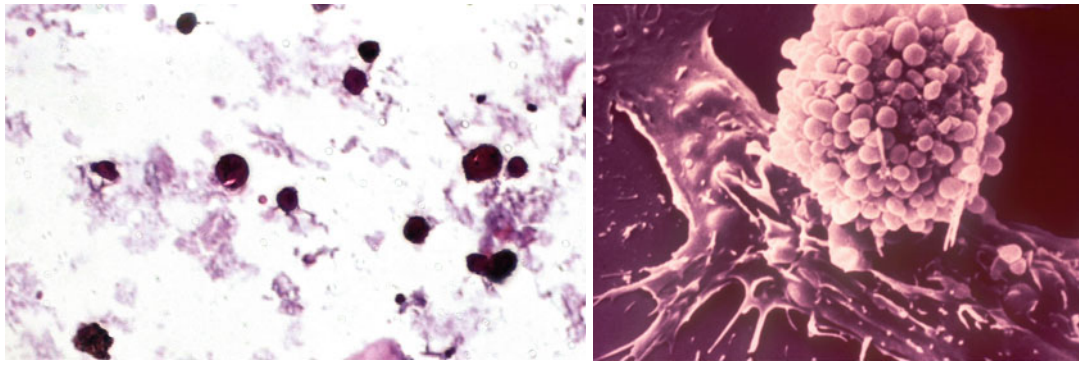

Fig. 13.4 Silica crystal as seen in bronchoalveolar lavage specimen (semi-polarized light), H&E, ×400. Right a scanning electron microscopic picture with two macrophages, the upper one is going to die, because of the ingested silica crystals, and the lower one is just approaching the crystalline material. Numerous blebs characterize the toxic injury. ×4,000

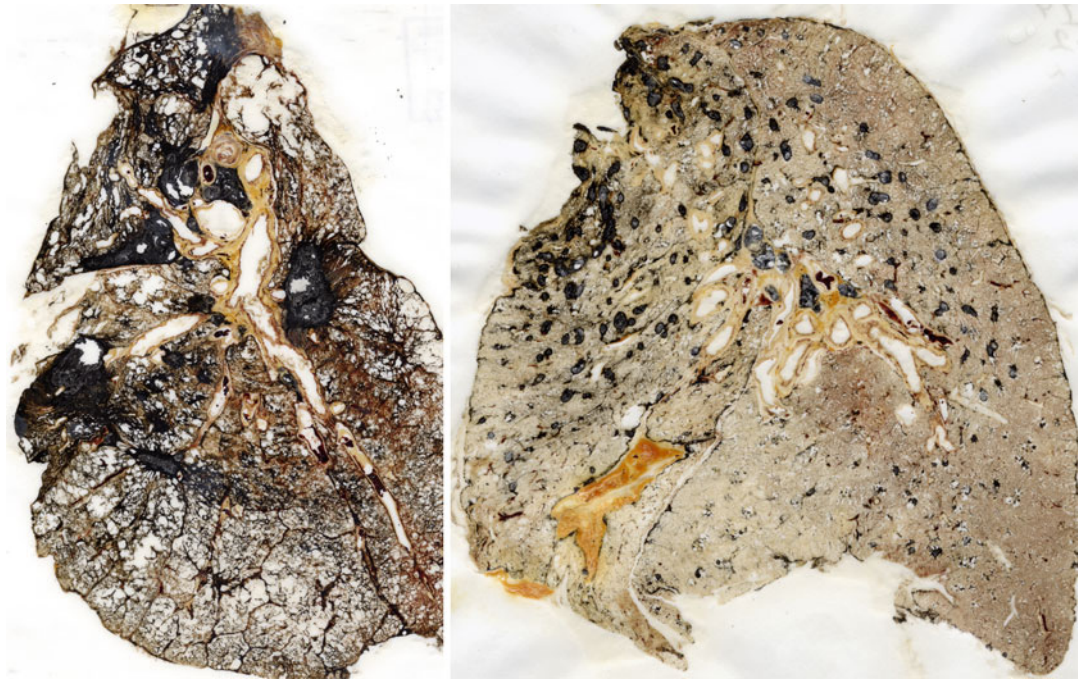

Fig. 13.5 Silicosis, whole lobe section mounted on paper (unstained). This type of section can evaluate several aspects of silicosis: it is clear that the left case has caused much more symptoms compared to right side case. The hilar lymph nodes are scarred in both but much more severe in the left. Whereas emphysema is mild on the right specimen, it is severe in the left specimen

more than one third. Emphysema formation results in hypoxia, sclerosis of pulmonary arteries will cause pulmonary arterial hypertension, and both will together act on right ventricular hypertrophy followed by right ventricular failure.

Silica/quartz has been regarded as fibrogenic but not cancerous. This dogma has also been refuted by several studies [11, 15–18].

13.3 Silicatosis

All complex Silica compounds, causing pneumoconiosis, are called *silicatosis*. There is non-asbestos silicatosis, such as mica, talc, kaolin, vermiculite, and wollastonite, and there is asbestosis. Non-asbestos silicatosis usually causes the same tissue reactions as silica; however, the gran-

ulomatous reaction might be missed. Sometimes a more diffuse fibrosis develops, such as in talcosis. The most important silicatosis is asbestosis.

13.3.1 Asbestosis

Asbestosis is defined as an interstitial fibrosis of the lung induced by asbestos fiber inhalation. It does occur in heavily exposed persons with >25 fibers/ml/year [19]. The disease develops slowly and the latency period can be up to 30 years. Asbestos exposure can manifest itself with different clinical presentations at the pleura: pleural effusion, pleural plaques, diffuse pleural fibrosis, and mesothelioma. Lung features are interstitial fibrosis but also lung carcinomas. The diagnosis of pulmonary asbestosis requires the proof of asbestos bodies and the presence of interstitial fibrosis (Figs. 13.6 and 13.7). There should be more than two asbestos bodies per 1 cm^2 tissue area. Alternatively a similar number of uncoated asbestos fibers that falls into the range recorded for asbestosis are sufficient [19].

In asbestosis the tissue reaction primarily starts as acute bronchiolitis and progress into fibrosing bronchiolitis [20–22]. In the periphery, DIP-like and UIP-like reactions can be seen, which progress into lung fibrosis [19]. Importantly, fibrosis in asbestosis is usually paucicellular and collagenous rather than fibroblastic and inflammatory. Also fibrosis is focal and asymmetric in distribution and early on can involve central portions of the lung. In the pleura, chronic pleuritis progresses into fibrosis and hyalinosis, resulting in the classical pleural plaque.

Asbestosis is graded into four grades:

Grade 0: No fibrosis
Grade 1: Peribronchiolar fibrosis, less 50 % bronchioles involved
Grade 2: Peribronchiolar fibrosis, >50 % bronchioles involved, focal interstitial fibrosis
Grade 3: “Bridging” interstitial fibrosis
Grade 4: Honeycomb lung

Besides diffuse lung fibrosis, the hallmarks of asbestosis are asbestos bodies. These are asbestos fibers covered or encrusted by a proteinaceous, iron-containing core. The asbestos fiber can be seen in the center. Macrophages can break down asbestos fibers, which can easily be found in BAL (Fig. 13.7). However, be aware: asbestos bodies are a sign of exposure, not the proof of disease! The tissue reaction is mandatory! Asbestos bodies can be highlighted by an iron stain (Prussian blue).

It should be mentioned that other manmade mineral fibers could undergo the same changes and look like asbestos bodies. Therefore, unless an exposure anamnesis is submitted, these bodies should be called asbestos-like bodies and be analyzed by electron microscopy and EDAX or chemically from wet tissue or BAL samples.

It is important to know that only approximately 1 % asbestos fibers form asbestos bodies. Therefore a mineral analysis is necessary. This can be done by electron microscopy using EDAX for the element analysis, by digesting 1 cm^3 of tissue (KOH) filtering the fibers and counting them either by electron or light microscopy. Another method is to centrifuge 1 ml of BAL and count the fibers on a glass slide (Fig. 13.7).

Important factors for the diagnosis of asbestosis are in addition an exposure anamnesis, irregular opacities on CT scan, a lung function test with combined obstructive and restrictive changes, and clinical symptoms.

Asbestosis can sometimes present with unusual features, like rapid clinical progression within 3–5 years in patients with collagen vascular disease, in patients with UIP-like pathology.

Different kinds of asbestos fibers do exist: chrysotile and the amphiboles amosite, crocidolite, tremolite, actinolite, and anthophyllite (Table 13.2 and Fig. 13.8).

Erionite, sheet silicates, carbon, metal oxides, manmade minerals, and elastin can form pseudoasbestos bodies.

Asbestos fibers in addition to asbestosis and pleura fibrosis can induce malignant tumors, especially malignant mesothelioma and lung carcinomas (NSCLC). Smoking in asbestos-exposed patients is a cofounding factor much enhancing the development of malignancy [23–28]. With respect to fiber type, amphiboles are more potent than chrysotile.

Erionite, a fibrous non-asbestos mineral of the zeolite family, is found in Turkey, Sicily, Greece, Cyprus, Corsica, Mexico, North Dakota, and New Caledonia, the best-known areas are in Cappadocia, Turkey [29–34]. Erionite causes mesotheliomas

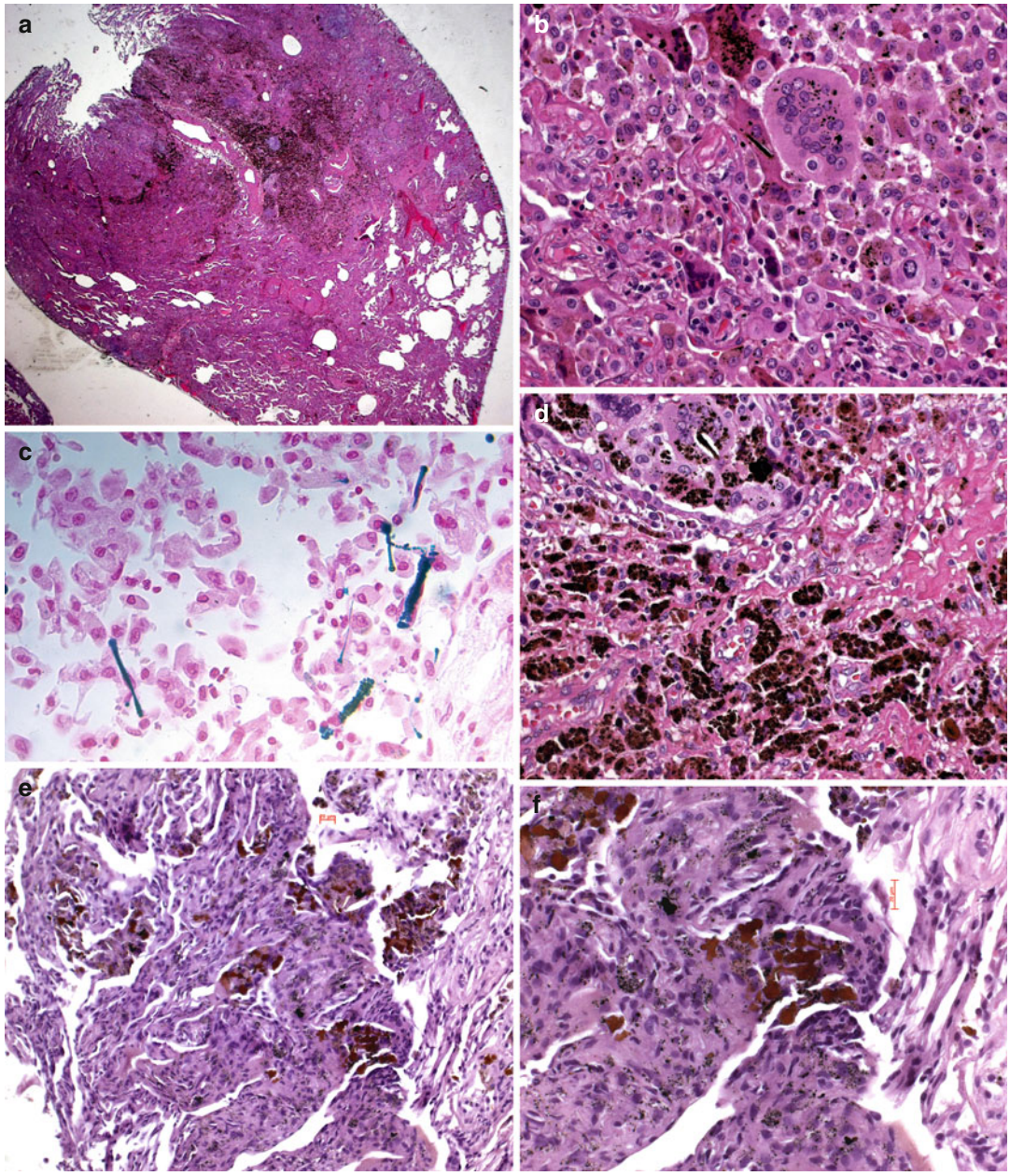

Fig. 13.6 Asbestosis, in (**a**) overview of a VATS biopsy showing consolidation of the peripheral lung tissue and deposition of brownish material. (**b**) Shows a macrophage accumulation with some giant cells. There is *brown* pigment deposited, in the center a needlelike structure, possibly an asbestos fiber. (**c**) Shows asbestos fibers highlighted by a *Prussian blue* stain, in (**d**) again massive deposition of *brown* coarse granular material including some asbestos-like fibers. The deposition or coarse granular foreign material should prompt a search for asbestos fibers, which will be seen in even in a transbronchial biopsy (**e**, **f**). H&E, *Prussian blue*, ×12, 200, 400, bars 20 μm

with a high incidence; however, genetic predisposition seems to play a minor but additional role [35]. There are no reports about lung fibrosis in these populations caused by erionite; therefore, this topic will be discussed in the chapter on pleural diseases.

13.3.2 Other Silicatoses

Different complex silicates can also cause lung fibrosis. The most common minerals are mica, talcum, kaolin, vermiculite, and wollastonite

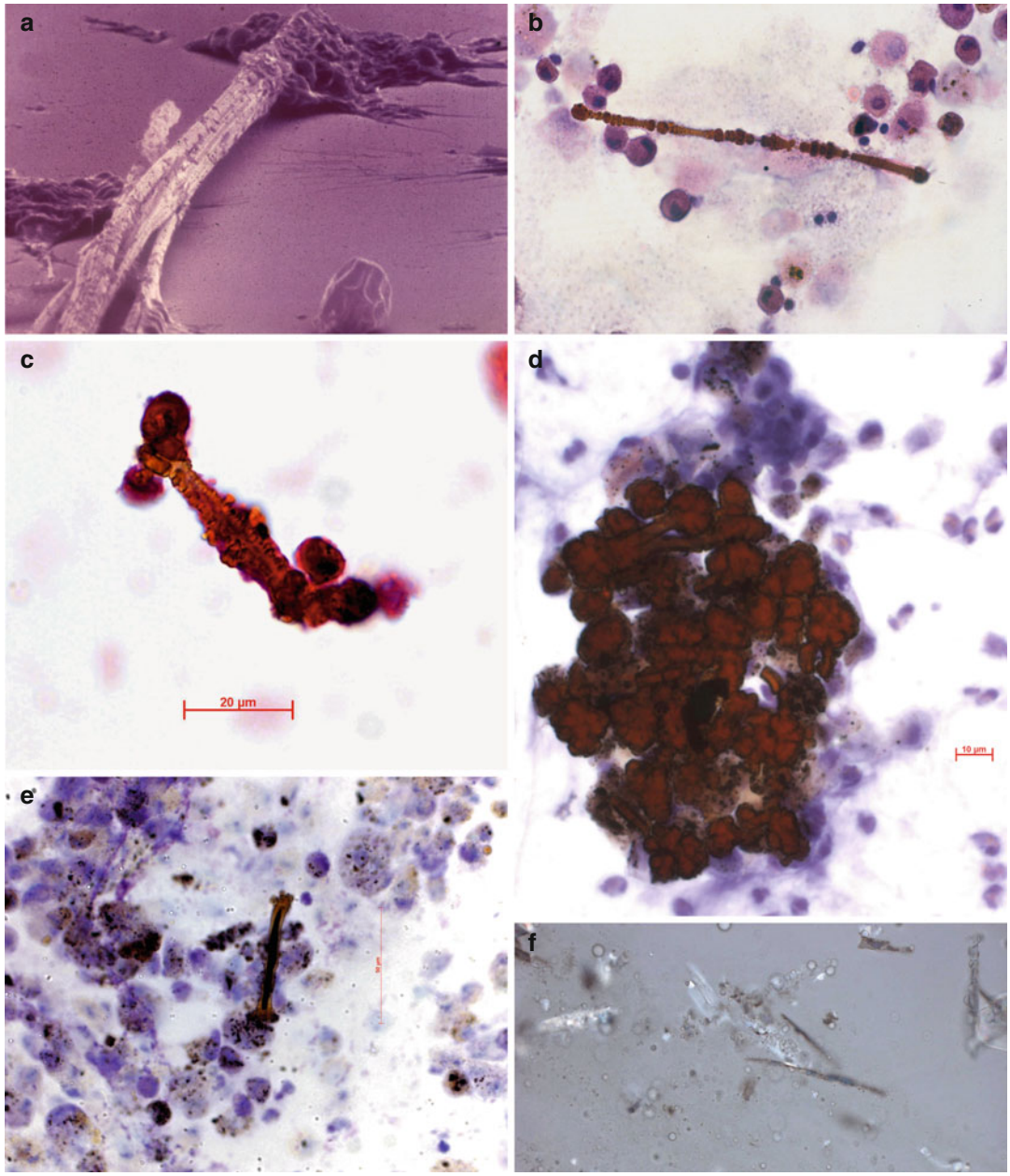

Fig. 13.7 Asbestos bodies/fibers can be demonstrated by electron microscopy (scanning mode, **a**), but also in BAL specimen (**b**–**e**); in lavage fluid different forms of asbestos bodies can be seen, sometimes with macrophages engulfing the fibers. The measurement of asbestos fiber burden can also be assessed using BAL: 1 ML native fluid is filtered and the fibers can be counted by light microscopy. The number of fibers is almost equivalent to the number in 1 MM^3 of tissue. In (**f**) asbestos fibers are demonstrated after KOH digestion of a tissue block. H&E, Giemsa, ElMi, ×4,000, 400, bars 50, 20, 10 µm

[36–46]. These minerals most often cause diffuse fibrosis and much less often granulomas (Fig. 13.9). Some minerals can be easily diagnosed, because of their characteristic pattern on polarized light microscopy (talcum crystals); others are less characteristic and will need element analysis (kaolin, vermiculite; Fig. 13.10). Most important: in several of these minerals, a mixture with other mineral dusts can occur. Silicosis and silicatosis can be mixed in some

Table 13.2 Asbestos minerals and definitions

Silicates	Formula	Fibrous form
Serpentines		
Serpentine	$Mg_3Si_2O_5(OH)_4$	Chrysotile
Amphiboles	$X_7Si_8O_{22}(OH)_2$	
Anthophyllite	$Mg_7Si_8O_{22}(OH)_2$	Anthophyllite
Grunerite	$Fe_2Mg_5Si_8O_{22}(OH)_2$	Amosite
Riebeckite	$NaMgFe_5Si_8O_{22}(OH)_2$	Crocidolite
Tremolite	$Ca_2Mg_5Si_8O_{22}(OH)_2$	Tremolite

For further information and figures on how asbestos fibers look like, see [19, 27]

patients, so a combination of diffuse fibrosis and hyaline granulomas should prompt a search for silica and asbestos bodies. Also muscovite and kaolinite can be found mixed, causing mixed dust fibrosis with no silicotic nodules [47].

Manmade fibers have been accused to cause asbestos-like diseases, especially mesothelioma. However, there are still discussions about the potential to be carcinogenic. The carcinogenic potency of a fiber is dependent on length and on the diameter, more precisely the length-to-diameter ratio; their piezoelectric potency might play a role and not to forget the chemical structure and the ability to form oxygen radicals. The carcinogenic potency of short fibers may be weak, but many short fibers may induce a tumor as easily as a few long fibers [48].

Coal worker's pneumoconiosis is induced by massive coal inhalation. Simple coal worker's pneumoconiosis (SCWP) is usually without any symptoms, and also lung function tests are almost normal. Macroscopically in SCWP the lungs present dark gray to black. On cut surface and also microscopically, SCWP is characterized by multiple coal dust macules (Fig. 13.11). SCWP is seen in coal mining [49–52]. The deposition of coal dust is increased over the clearance mechanisms, causing accumulation of the dust in the interstitium. Normally this causes no functional disturbance [53]. Rarely accumulation of macrophages and release of enzymes can induce lung lesions; similar to what is seen in overload reaction in laboratory animals, also genetic factors might contribute [54–56]. Complex coal worker's pneumoconiosis (CCWP) is seen in coal mines with a silica content of less than 10 % (often around 7 %). In complex coal worker's pneumoconiosis, there is fibrosis of bronchioles and adjacent lung tissue, causing functional impairment of the lungs (Fig. 13.12). Nodular structures or granulomas are not encountered, but in the fibrotic areas, accumulation of dust-laden macrophages, which also contain few silica crystals; in addition, also iron was accused to be a component for the fibrogenic response [57–59].

New pneumoconioses are emerging. Graphitosis or toner pneumoconiosis is based on the inhalation of graphite (toner for laser printer) combined with O_3 toxicity in minimally ventilated small rooms (Fig. 13.13). Manmade mineral fibers are another source of new types of pneumoconiosis.

Diesel exhaust consists of coal particles covered by many different hydrocarbon compounds. Initially diesel exhaust was claimed to be nontoxic. There exist several arguments, which are against this initial hypothesis: diesel exhaust carbon particle (DECP) are ultrafine particles, less than 1 μm in diameter – many of them are part of so-called nanoparticles, which means these particles can easily cross epithelial and endothelial barriers. Both the organic and the particulate components cause oxidant lung injury. The particulate components induce alveolar epithelial damage, alter thiol levels in alveolar macrophages and lymphocytes, and induce production and release of oxygen radicals and pro-inflammatory cytokines by macrophages. The organic components generate intracellular oxygen radicals, leading to a variety of cellular responses including apoptosis. There are a number of differences between the biological actions exerted by these two components. The organic component is

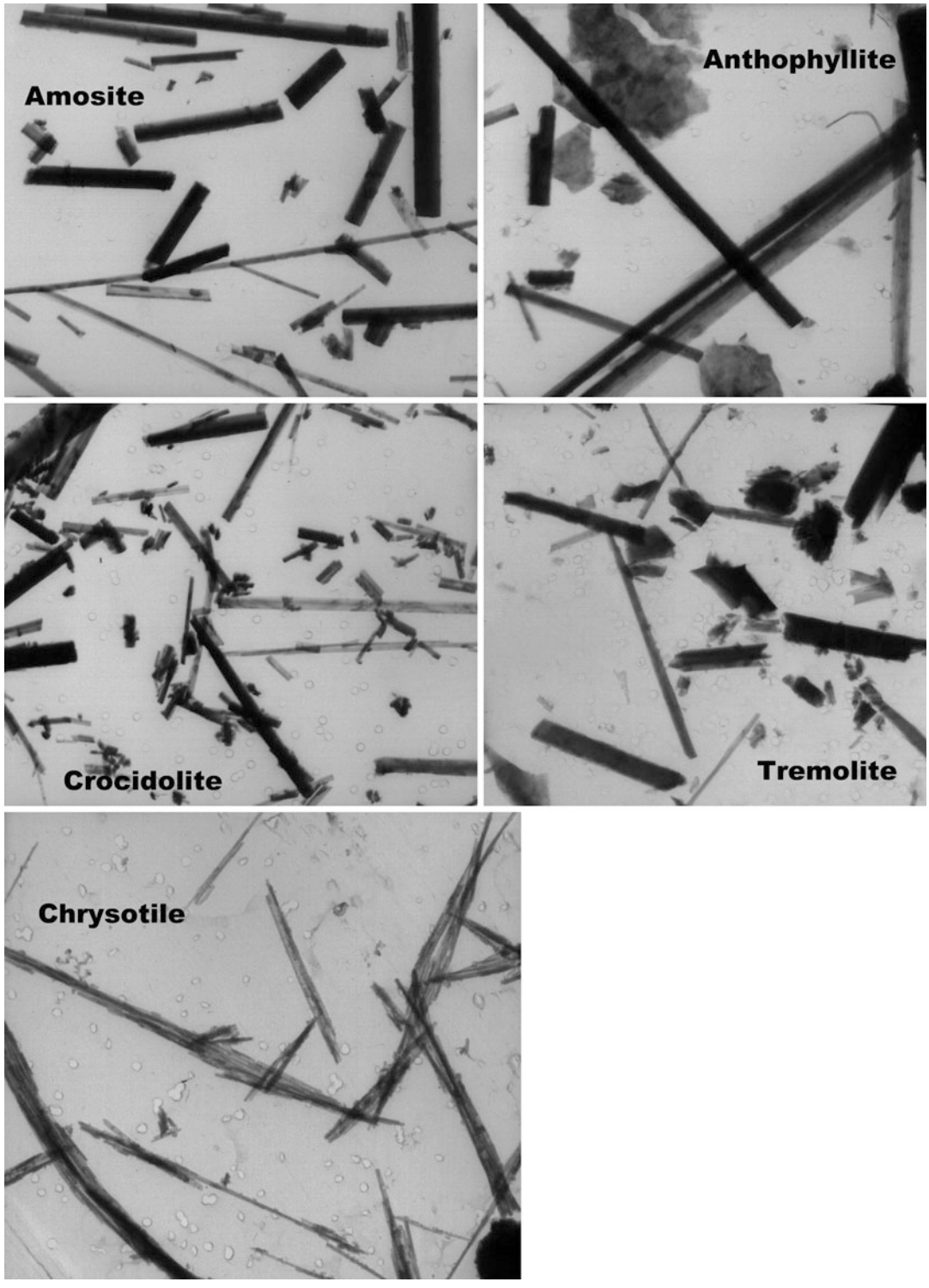

Fig. 13.8 Different types of asbestos fibers, standardized preparations as used for research. Compare the rigid fibers of amosite, anthophyllite, crocidolite, and tremolite versus the thin flexible fibers of chrysotile. Electron microscopy

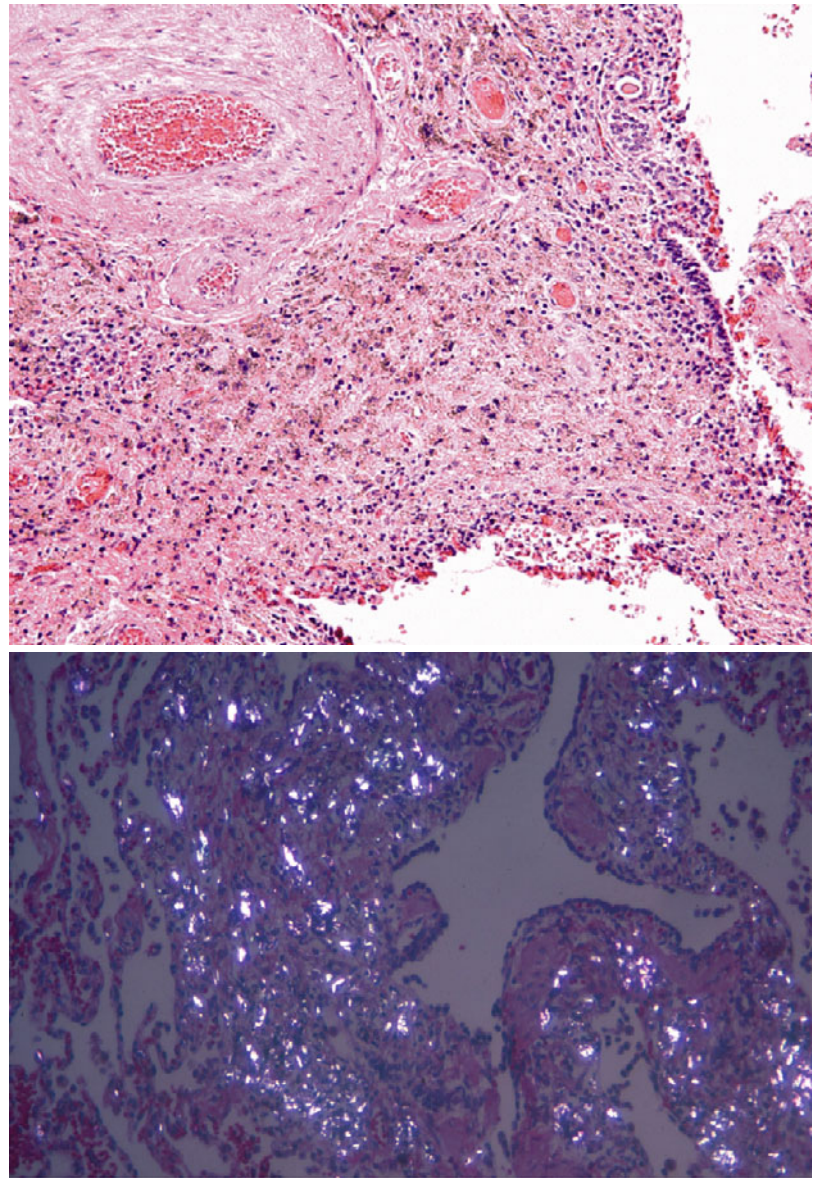

Fig. 13.9 Talcosis, in the top morphology is shown with macrophages containing a light brown-tinged foreign granular material. In the bottom picture the typical plates of talcum are shown under polarized light. H&E, ×100

responsible for DECP induction of cytochrome P450 family 1 enzymes that are critical to the polycyclic aromatic hydrocarbons (PAH) and nitro-PAH metabolism in the lung [60]. High concentrations of DEP (125 μg/ml) modulate the tight junction occludin mRNA in the cells of the defense system and thus decrease epithelial integrity following exposure to particulate antigens in lung cells [61]. DECP posses a physical property of binding hydrocarbons quite firmly on their surface, making them an ideal tracer for carcinogenic and inflammation-inducing compounds. Recent work has uncovered an association with asthma, COPD, and lung cancer [62–68].

13.4 Metal-Induced Pneumoconiosis and Disease

Different metals can cause lung diseases. Some of these we will not discuss here, as chronic allergic metal disease, which is characterized by

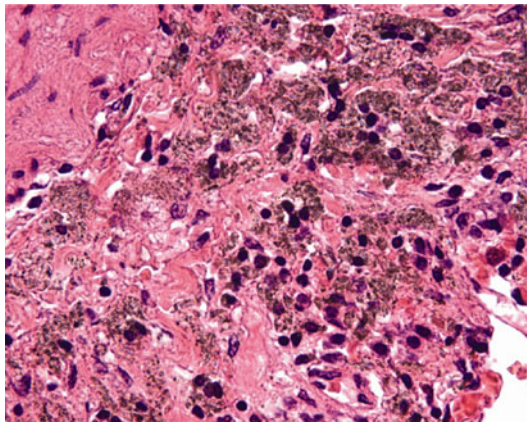

Fig. 13.10 Kaolinosis in a female worker in a ceramic industry. Her job was polishing and she did not use any protection. Macrophages have ingested grayish-brown granular material, corresponding to kaolin. H&E, ×400

Fig. 13.11 Coal worker's pneumoconiosis shown in an autopsy specimen, whole lung section on paper mount. The numerous black-pigmented macules are see in this case of simple coal worker's pneumoconiosis

non-necrotizing epithelioid cell granulomas (beryllium, zirconium). Others cause a classical pneumoconiosis, such as hard metal, aluminum,

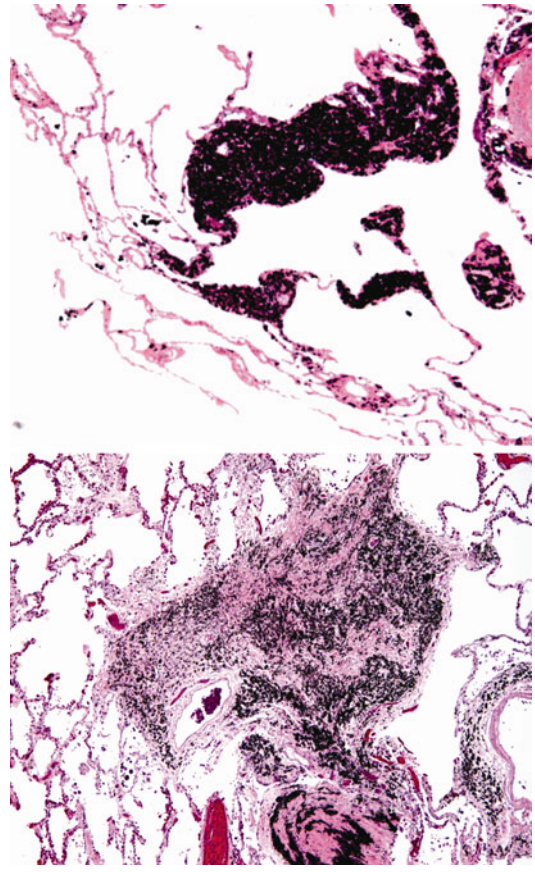

Fig. 13.12 Coal worker's pneumoconiosis, top panel simple CWP, is shown, corresponding to the dust macules seen in Fig. 13.11. Below is complex CWP with fibrosis in addition to the coal dust deposit. H&E, ×50

and zinc. Different types of metals can be detected by electron microscopy using devices for element detection. One problem in these investigations is that several of these metals are easily dissolved by the fixation and dehydration in fluid and leach out of the tissue. Another option is using "old-style" chemical reactions used for the analysis of complex compounds. This can be done using solvents to leach out the materials of interest followed by a chemical reaction with dyes, which turn color, if the element is present. Many of these chemical reactions can also be performed on tissue sections. However, this all is only possible for elements, which normally do not occur within human tissues.

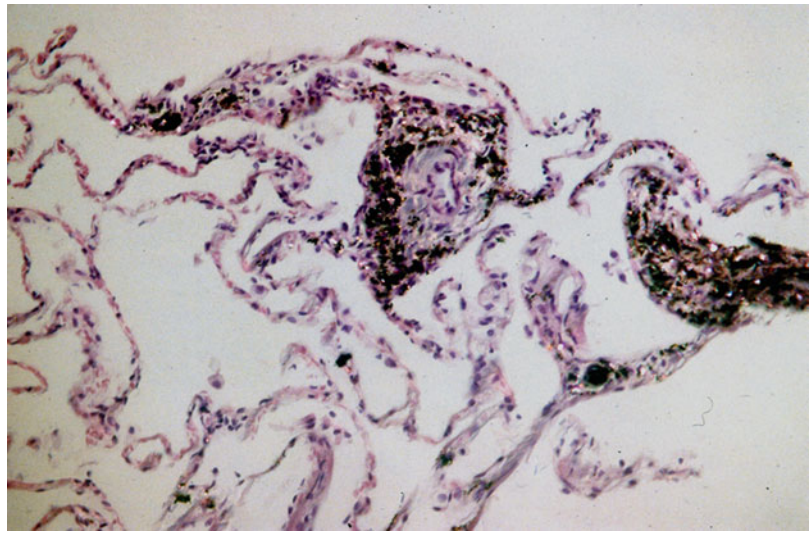

Fig. 13.13 Graphitosis in a male patient involved in service of multiple laser printers in an ill-ventilated office. H&E, semi-polarized, ×100

13.4.1 Hard Metal Lung Disease

Hard metal lung disease is caused by the inhalation of dust from hard metal. Hard metal is an alloy composed of several metals, usually chromium, titanium, cobalt, nickel, iron, tungsten, and others. Due to its hardness, it can be used to sharpen instruments made from steel. By the process of sharpening, dust is released from the hard metal and can be inhaled.

The clinical symptoms are like an acute respiratory distress syndrome with hypoxia, shortness of breath, chest pain, and edema. By HRCT scan, ground-glass opacities are seen in both lungs, predominantly in mid and lower zones.

Macroscopically the lung weight and consistency is increased, the color is dark red, and the cut surface is edematous. Histologically in early development and in heavy exposure, there is an accumulation of macrophages in the alveolar lumina, fibrin clots are present, and hyaline membranes can be seen (diffuse alveolar damage; Fig. 13.14a). In less severe exposure, respiratory bronchiolitis can be seen early on. This later on develops into a giant cell interstitial pneumonia (GIP). Numerous macrophages and multinucleated foreign body giant cells are within alveoli and in the interstitium, sometimes with ingested brown-black material (Fig. 13.14b). Besides a mild lymphocytic infiltration might be encountered. The main elements causing this reaction are cobalt, nickel, and tungsten. Especially cobalt is highly toxic. In experiments, it has been shown that cobalt is the most toxic compound within this alloy, can easily dissolve out, and will subsequently induce giant cell formation of macrophages [69–71]. If the patient survives the acute onset, peribronchial/peribronchiolar fibrosis and fibrosis of the alveolar septa result [71–73]. Large scars are usually absent.

In BAL, the diagnosis can be suspected, because one of the elements titanium oxide persists in the tissues in contrast to the other easily dissolvable metal compounds. TiO_2 gives a red-orange birefringence on polarized light (Fig. 13.14c–e).

GIP seen in tissue sections is almost diagnostic of hard metal lung disease: there is only one differential to be considered, which is viral-induced GIP, commonly seen in measles and RSV infections.

13.4.2 Aluminosis

Aluminosis is caused by inhalation of aluminum dust. The disease predominantly is seen in workers in mining, welding, as well as in the processing of aluminum although rarely in those processes where electrolysis is used [74]. Workers exposed to aluminum dust present acute

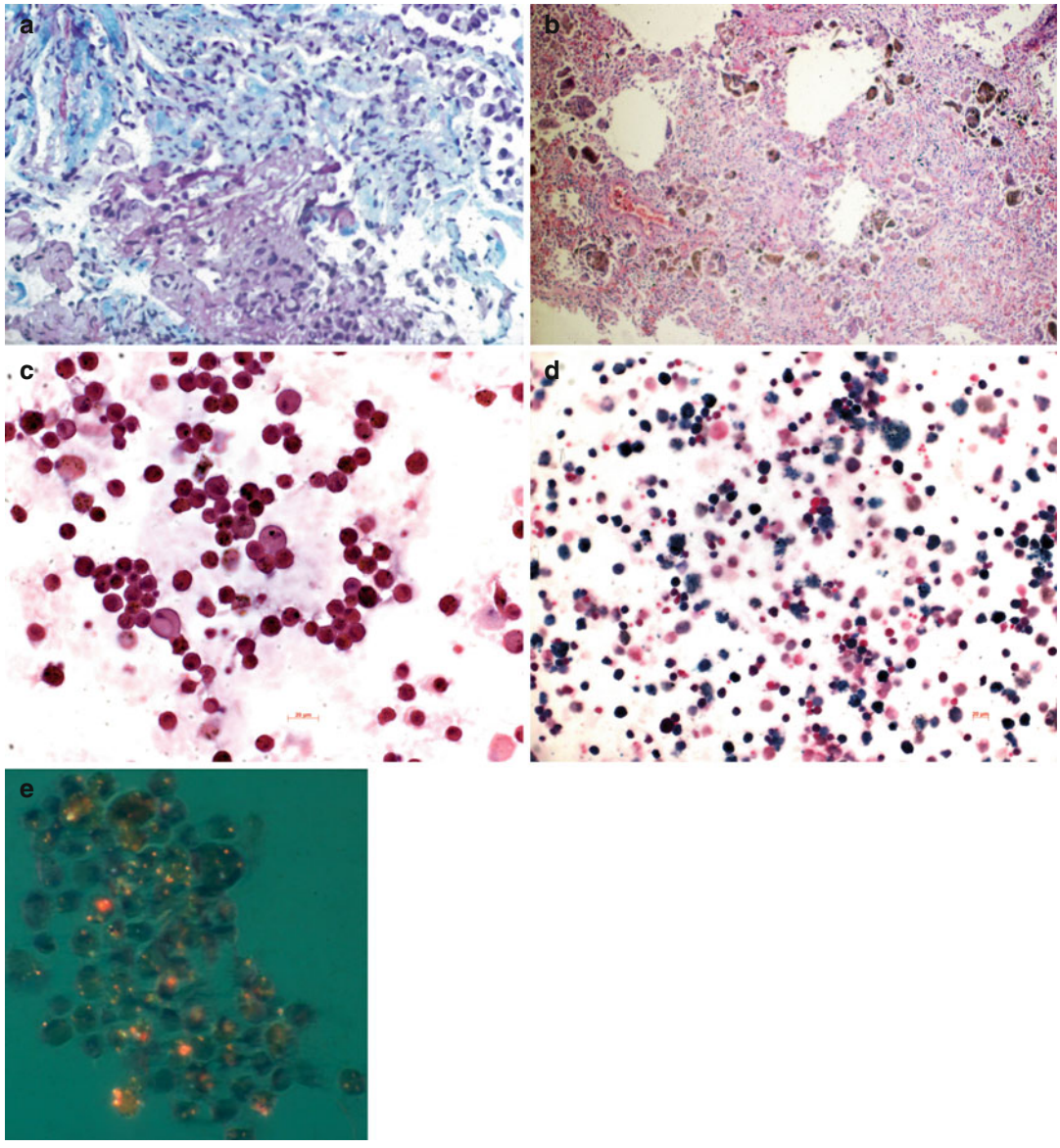

Fig. 13.14 Hard metal lung disease: in (**a**) an acute reaction is seen with DAD and macrophages but also areas with necrosis of the lung parenchyma. In (**b**) the chronic form is illustrated with the morphology of giant cell interstitial pneumonia. By BAL a macrophage reaction is seen (**c**), which is positive for *Prussian blue* stain (**d**) and is *bright orange* on polarized light due to the birefringence of TiO_2 (**e**)

onset of shortness of breath. On CT scan, ground-glass opacities are seen scattered in both lungs. In lung tissues, the dominant picture is a DIP-like accumulation of macrophages, which contain finely granular brown to black material (Fig. 13.15a–f). Foreign body granulomas can be present; sometimes histiocytic granulomas can be formed. In later stages, peribronchiolar fibrosis will develop [75–77]. Van Kossa reaction stains aluminum grayish (Fig. 13.15c). In the disease pathogenesis, an allergic reaction is discussed and some experimental studies support this assumption [78]. In these cases, a granulomatous reaction is seen, usually with epithelioid cell granulomas [79]. In BAL sometimes an eosinophilic reaction was reported [77].

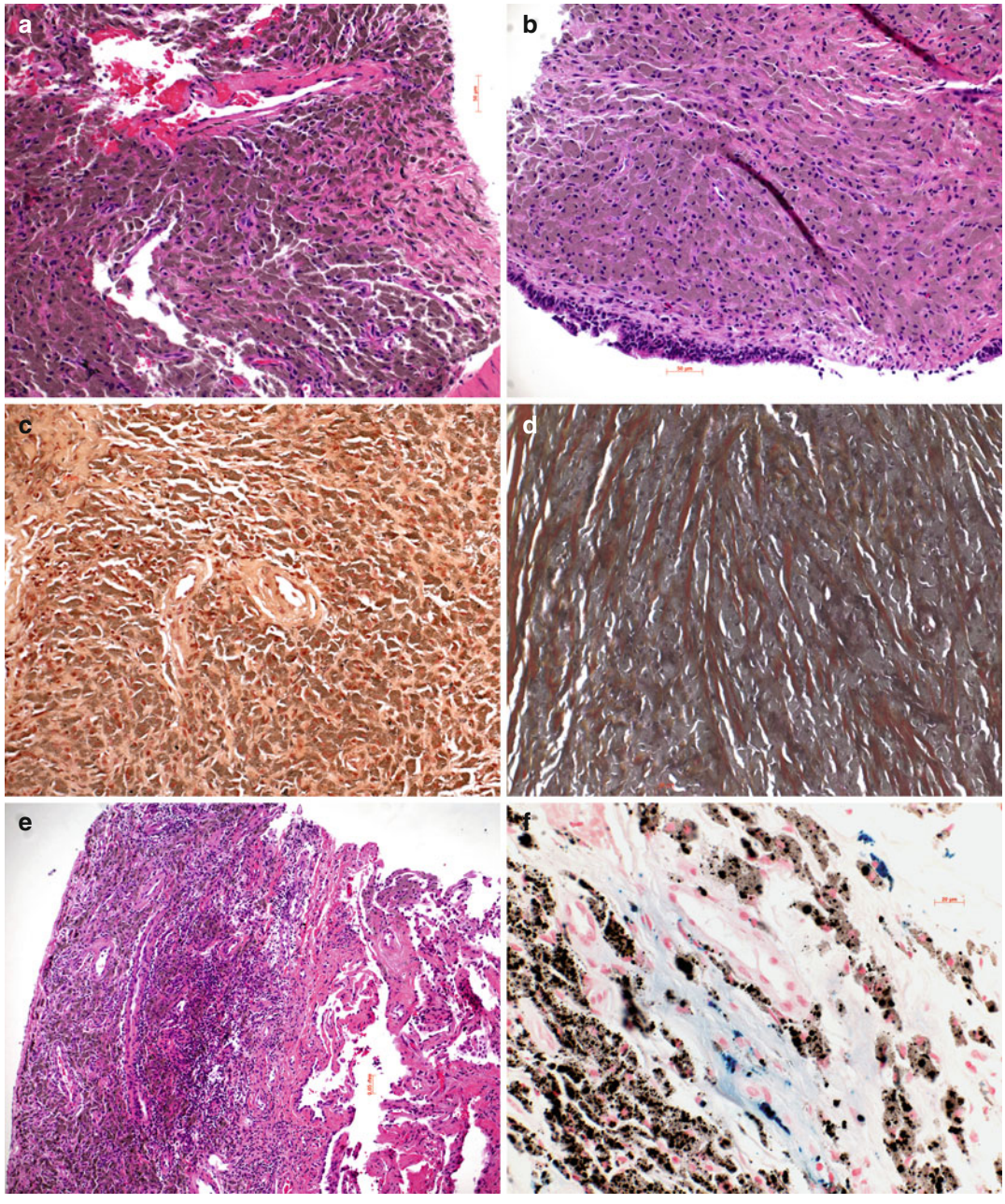

Fig. 13.15 Aluminosis illustrated by two cases. (**a**–**d**) Case 1 was diagnosed in a transthoracic core needle biopsy. In (**a**, **b**) the morphology is shown with macrophages having ingested a grayish material, finely granular. By Kossa stain (**c**) the material changed the color to *grayish-yellow*, which is a hint to aluminum. In (**d**) focal fibrosis is seen by the Movat stain. Case 2 is represented by a transbronchial biopsy, again showing macrophages with the phagocytosed material (**e**). In this case an additional compound out of an aluminum alloy is present in the *Prussian blue* stain as *black* coarse particles and iron-positive iron-containing compound (**f**). H&E, Kossa, Movat, *Prussian blue* stains, bars 50 and 20 μm

13.4.3 Chromium and Vanadium

Inhalation of chromium and vanadium is predominantly found in mining and welding [80]. The clinical symptoms are flu-like with tracheobronchitis and pneumonia. Fever may be present. Both metals when inhaled in larger quantities will cause alveolar hemorrhage, edema, and DIP-like reactions sometimes accompanied by neutrophils due to the toxicity of the oxides. Due to the high chemical reactivity of both metals being able to form different oxides (CrO_3, instable Cr_2O_4, Cr_2O_5; VO_3, V_2O_4, V_2O_5), they can induce toxicity by releasing oxygen radicals [81–83]. In contrast to the upper airways, where chromates and vanadates are carcinogenic, in the lower airways, no tumors could be induced experimentally by chronic chromate inhalation; however, mice as well as rats developed chronic bronchitis, bronchiectasis, and emphysema, histologically very similar to human COPD [82] (Fig. 13.16). Bronchial asthma may be caused by complex chromium compounds, presumably on the basis of allergic sensitization [84]. In rare cases, chromium compounds used in dentistry may cause chronic hypersensitivity pneumonia with UIP pattern and granulomas (Fig. 13.17) [13, 85].

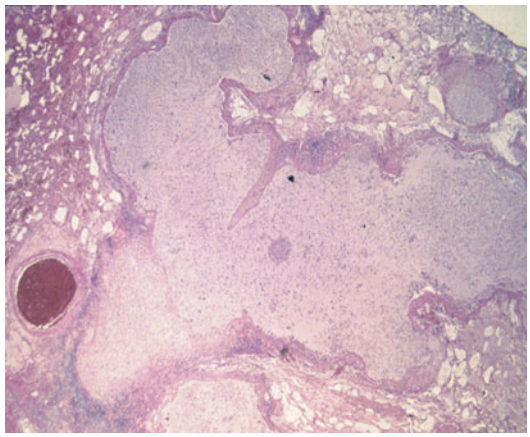

Fig. 13.16 Experimental bronchiectasis induced by chronic chromate inhalation in mice. Within the bronchus, accumulation of mucus and debris from leukocytes is seen. H&E, ×12

13.4.4 Tungsten

Tungsten as a component of hard metal has been discussed. Tungsten alone does not cause severe symptoms; however, if inhaled in large quantities, it causes lipid pneumonia and accumulation of lipid-laden macrophages in the mucosa of the upper and lower airways (Fig. 13.18). This might morphologically simulate the rare lipid storage disease Niemann-Pick. Hemorrhage can occur, but more often nasal bleeding from the involvement of the mucosa of the upper airways. How

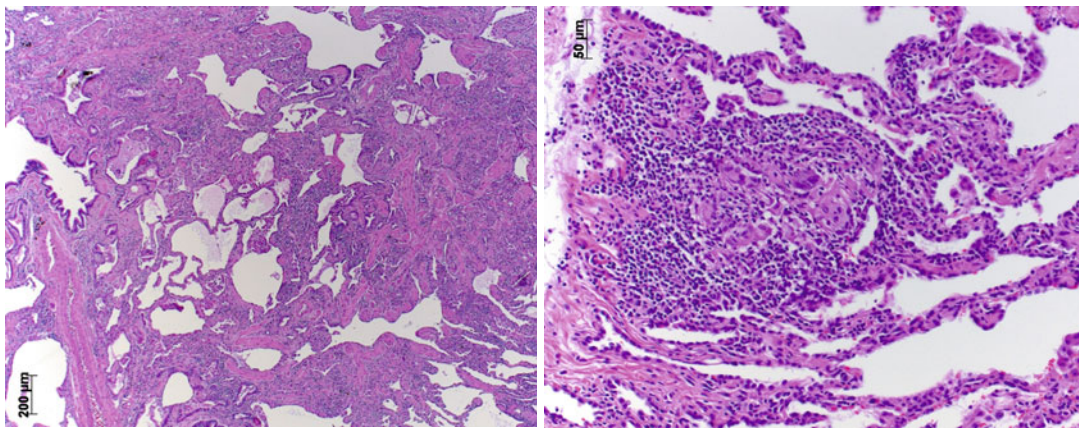

Fig. 13.17 Chronic hypersensitivity pneumonia with epithelioid cell granuloma, LIP, and UIP pattern in a case of hypersensitivity for an alloy containing different metals, including chromium. In the *left panel*, there is dense lymphocytic infiltration, but also cystic remodeling of the lung with many fibroblastic foci. In the *right panel*, an epithelioid cell granuloma with accompanying lymphocytes is shown. H&E, 50 and 200 µm

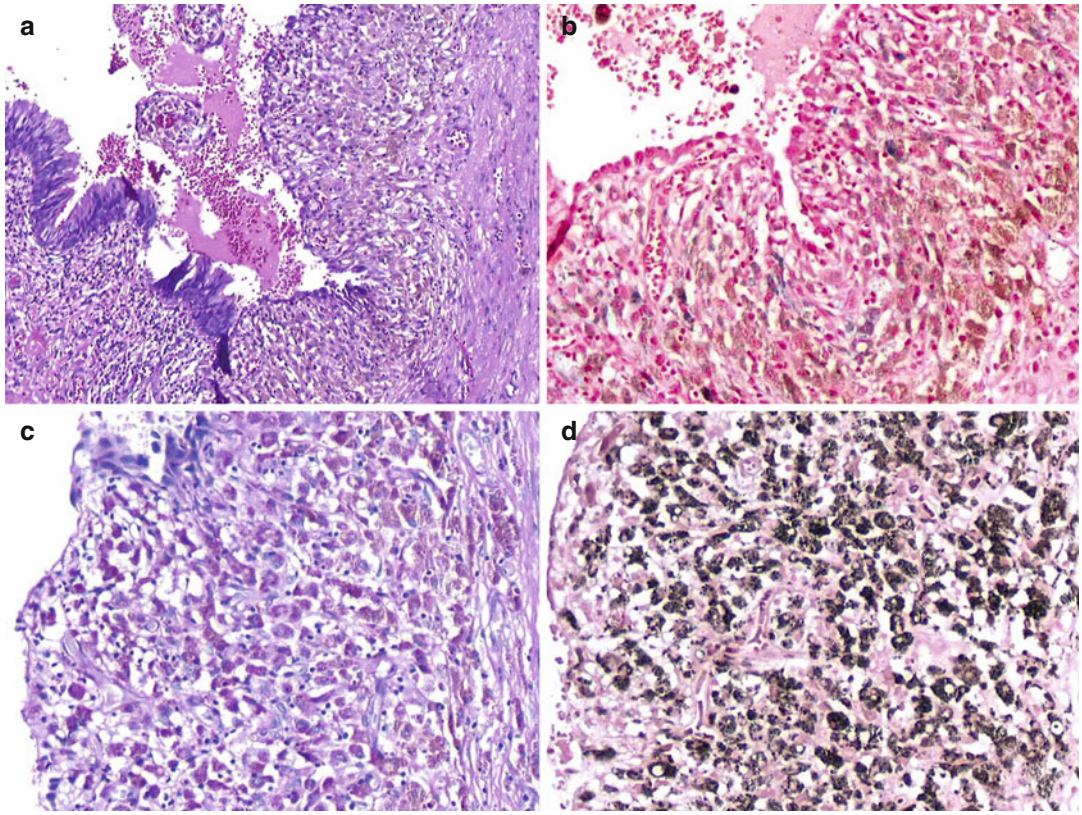

Fig. 13.18 Chronic tungsten inhalation in a young student who worked in a small company shipping tungsten into containers. He realized black material in his nose as well as in expectorations. Bronchial biopsies show an accumulation of macrophages in the mucosa (**a**), which was negative for iron (**b**), negative for PAS (**c**), but positive for Sudan *black* B (**d**). Analysis showed tungsten associated with several lipids. This case very much resembled Niemann-Pick storage disease. ×100 and 200

tungsten interfere with the metabolism of lipids has not been investigated, but so far fibrosis reported in tungsten workers/miners is most likely induced by contamination with cobalt compounds [69, 86–88]. Tungsten when administered via nose-only inhalation to rats was absorbed systemically, and blood tungsten levels increased as inhaled concentration increased. Increased lung weight was attributed to deposition of TBO in the lungs, inducing a macrophage influx. There was a dose-related increase in alveolar pigmented macrophages, alveolar foreign material, and individual alveolar foamy macrophages recorded in the lung. Microscopic findings were interpreted as non-adverse response to exposure and were not considered a specific reaction to TBO [89].

13.4.5 Cobalt

Exposure to cobalt dust may induce giant cell interstitial pneumonitis similar to hard metal lung disease. In contrast to hard metal lung disease, exposure cessation and corticosteroid treatment improved the disease [90].

The reactivity of the tungsten carbide-cobalt mixture toward alveolar macrophages is quite different from that of cobalt metal powder. The ground tungsten carbide-cobalt mixture prepared is almost as toxic as crystalline silica, whereas tungsten carbide has no effect, and pure cobalt metal powder slightly impairs cell viability [91]. Tungsten carbide (WC) alone behaves as an inert dust producing only a mild accumulation of macrophages in the alveolar duct walls.

Co particles alone cause a moderate inflammatory response. An identical amount of cobalt given as WC-Co mixture produces a severe alveolitis and fatal pulmonary edema. The acute lung toxicity of tungsten carbide-cobalt mixture is much higher than that of each individual component and may explain why lung fibrosis is rare if ever induced by exposure to pure cobalt dust [69, 92].

With respect to the sensitivity for cobalt, it was shown that pneumocytes type II are twice as sensitive than alveolar macrophages. The presence of WC almost doubled the toxic effects, but this synergy between Co and WC only occurred if the particles were in close contact with the cells. $CoCl_2$ showed a similar toxicity for pneumocytes and macrophages [93].

Exposure to cobalt and tungsten is highest in areas handling powders and lowest in areas handling finished product. Inhalable cobalt and tungsten exposures were observed in all work areas. All sizes of cobalt-containing particles that deposit in the lung and airways have the potential to cause asthma. Cobalt-tungsten mixtures that deposit in the alveolar region of the lung may potentially cause asthma and lung cancer [88].

Instilled haptenic metal oxide NiO, Co_3O_4, Cr_2O_3, and CuO induced chronic interstitial inflammation. Neither Cr_2O_3 nor CuO NPs elicited immunoinflammatory reactions. Pulmonary alveolar proteinosis (PAP) was induced by both NiO and Co_3O_4 during the chronic phase. PAP was associated with overproduction of surfactant by proliferation of type II cells and impaired clearance of surfactant by macrophages [94].

13.4.6 Other Metals

Other metals such as *cadmium* and *mercury* induce nonspecific damage, probably by initiating production of reactive oxygen species [76]. Cadmium does occur in tobacco plants, especially in areas with heavy traffic pollution, as cadmium is present in trace amounts in gasoline. Cadmium is taken up by tobacco plants in exchange for calcium. Therefore the route into the airways is by cigarette smoking [95]. Cadmium has been proven to be carcinogenic [96–102]. There are possible mechanisms explored on how cadmium might induce carcinogenesis. One aspect is generation of radical oxygen species by acute Cd overload. This leads to acute cell damage. By chronic Cd exposure, ROS production is reduced but results in aberrant gene expression and finally carcinoma development [103]. In another experiment, cadmium treatment induced inflammatory and growth responses in transformed A549 cells with an activation of EGFR and its downstream modulators [104]. In addition Cd induced HIF-1 expression via ROS/ERK/AKT signaling pathway and furthermore vascular endothelial growth factor expression and transcriptional activation through ROS, ERK, and AKT pathways. Finally, cadmium transformed human bronchial epithelial cells in culture; the transformed cells induced tube formation in vitro, angiogenesis on chicken chorioallantoic membrane, and formed tumors in nude mice [105]. Cd induced global DNA methylation and overexpression of the DNA methyltransferase genes DNMT1 and DNMT3a. Expression of mRNA and proteins of the repair genes hMSH2, ERCC1, XRCC1, and hOGG1 were reduced by methylation of promoters for hMSH2, ERCC1, XRCC1, and hOGG1. The DNMT1 and DNMT3a overexpression induced by Cd can result in global DNA hypermethylation and silencing of the hMSH2, ERCC1, XRCC1, and hOGG1 genes [106].

Chronically cadmium-treated lung cells showed marked increases in secreted MMP-2 activity, invasion, and colony formation in soft agar. The cells also showed decreased expression of the tumor suppressor genes p16 and SLC38A3. Also cells showed increased expression of the oncoproteins K-RAS and N-RAS as well as the epithelial-to-mesenchymal transition marker protein vimentin. Metallothionein (MT) expression was increased by cadmium. Oxidant adaptive response genes HO-1 and HIF-1A were also activated. These data suggest that exposure of human lung epithelial cells to cadmium causes acquisition of cancer cell characteristics [107].

13.4.7 Mercury

Exposure to mercury is most often seen in gold miners who used elemental mercury to amalgamate and extract gold. Among individuals exposed occupationally, concentrations of mercury in their hair, urine, blood, and other tissues significantly exceeded all criteria proposed by various national and international regulatory agencies for protection of human health [108]. An investigation of postmortem patients showed diffuse alveolar damage and variable amounts of fibrosis, depending on various stages of organization. Additional findings included acute proximal renal tubular necrosis, vacuolar hepatoxicity, and a spectrum of central nervous system alterations including multifocal ischemic necrosis, gliosis, and vasculitis [109]. Probable mechanisms behind this tissue reaction increased the expression of tumor necrosis factor-alpha (TNFα), TNF-receptor-1, interleukin 2 (IL2), IL7, prostaglandin E2 receptor, and heat-shock proteins induced by HgO vapor. Interestingly chronic exposure induced adaptive responses, such as glutathione S-transferases, metallothionein, and thioredoxin peroxidase [110].

13.4.8 Nickel

The lung and the skin are the principal target organs upon occupational nickel and nickel compound exposure. Inhalation exposure is a primary route for nickel-induced toxicity in the workplace. The most important adverse health effects due to occupational exposure to nickel and its compounds are skin allergies, lung fibrosis, and lung cancer. The exact mechanisms of nickel-induced carcinogenesis are not clear [111].

Nickel compounds can cause different types of reaction when inhaled. Nickel carbonyl inhalation causes acute pneumonia, and inhalation of nickel aerosols causes chronic rhinitis and sinusitis, whereas cutaneous and parenteral exposures to nickel alloys might induce cancers of the nasal cavities and lungs and dermatitis and other hypersensitive reactions [112]. In addition nickel compounds may produce pulmonary alveolar proteinosis [113].

In experimental settings, $NiSO_4$, Ni_3S_2, and NiO caused interstitial phagocytic cell infiltrates in rats and mice. A toxicity ranking of $NiSO_4$ greater than Ni_3S_2 greater than NiO was recorded [114, 115]. The carcinogenic effect of nickel was related to its lipid peroxidation properties with induction of DNA strand gaps and breaks and DNA-protein cross-links [116]. NADPH oxidase-derived reactive oxygen species production by Ni(II)compounds induces apoptosis. Increased apoptosis mediated by nickel may disrupt the physiological activities of neutrophils, with potential impact in its immunological and antimicrobial role [117].

13.4.9 Arsenic, Tin

Dimethylarsinic acid (DMA) has been used as herbicide (cacodylic acid) and is the major metabolite formed after exposure to tri-arsenite or pentavalent arsenate and inorganic arsenic (iAs) via ingestion or inhalation in both humans and rodents. DMA induces an organ-specific lesion – single-strand breaks in DNA – in the lungs of both mice and rats and in human lung cells in vitro, due to the peroxyl radical of DMA and production of active oxygen species by pulmonary tissues. DMA acts as a promoter of urinary bladder, kidney, liver, and thyroid gland cancers in rats and as a promoter of lung tumors in mice [118].

Employees at a tin smelter cohort presented with excess mortality from lung cancer associated with occupational exposure to tin, arsenic, lead, antimony, and polonium-210. The excess of lung cancer mortality in this tin smelter cohort was most probably due to arsenic as the principal occupational carcinogen acting together with tobacco smoking [119].

13.4.10 Indium, Tin

Indium tin oxide (ITO) is a sintered mixture of indium oxide (In_2O_3) and tin oxide (SnO_2) used

for the manufacture of LCD screens. Interstitial pulmonary diseases have been reported in workers [120]. By a single pharyngeal administration, ITO particles induced a strong inflammatory reaction. The inflammatory reaction appeared more marked with ITO particles than with each oxide separately. This inflammatory reaction persisted and even worsened. No significant fibrotic response was observed. While ITO particles did not affect epithelial cell integrity, a strong cytotoxic response was found in macrophages exposed to ITO. ITO particles also induced a secondary genotoxic mechanism, especially by liberating radical oxygen species. The sintering process through which SnO_2 molecules are introduced within the crystal structure of In_2O_3 appears critical to explain the unique toxicological properties of ITO [121].

13.4.11 Siderosis

Siderosis normally is not a disease. In ironworkers the inhalation of iron dust does not harm the lungs. The dust is deposited in the interstitium and gradually transported into the lymph nodes. Iron is metabolized and either deposited in the reticuloendothelial system or excreted. The dust can be seen without staining but is highlighted by iron stain. Within the differentials, all types of alveolar hemorrhage have to be considered. However, when hemosiderin is predominantly deposited beneath the alveolar surface and within the alveoli, an exogenic source is most probable (Fig. 13.19). Besides siderosis, other metal diseases can present in this manner. One of those is zinc welder's disease. It is assumed that zinc causes a combined toxic and allergic reaction, with only mild lymphocytic infiltration in the alveolar septa (Fig. 13.20). In BAL there is mild lymphocytosis. Most likely, other components in the electrodes are involved too, such as organic compounds, for example, different aldehydes, hydrocarbons including benzene, etc. Another disease is arc welder's pneumoconiosis. Here siderosis is often combined with asbestosis.

13.4.12 Rare Metals and Chronic Allergic Metal Diseases

Some metals and their oxides can cause acute toxic reactions with diffuse alveolar damage, but also chronic allergic reactions. Two examples are *beryllium* and *zirconium* [122–125]. Beryllium was used in the fabrication of fluorescent lamps in the 1940s, but is still used in the rocket and airplane industry. Within an alloy, it transmits high resistance against heat – these alloys can withstand temperatures up to 1,600 °C. Workers in these industries if exposed to high concentrations of beryllium can develop acute lung disease, but this is rare. More commonly found is chronic exposure and the development of allergic metal disease. Zirconium is used as a metal reactor component, which is hand finished, but also exposure occurs in mining of zirconium silicates [126, 127].

Whereas in acute high-dose inhalation both metals and their oxides cause an acute interstitial pneumonia and edema, chronic inhalation (usually also at lower doses) will cause allergic metal disease. Chronic inhalation causes a formation of an antigen with body proteins – the metal or metal oxide reacts like a hapten [128]. Against this antigen, a type IV immune reaction is mounted with lymphocytic infiltration and the production of epithelioid cell granulomas (Fig. 13.21). In the granulomas as well as in BAL, CD4+ lymphocytes predominate, almost identical to sarcoidosis, for which chronic berylliosis was often misdiagnosed [129–132]. Similar findings were reported for chronic zirconiosis, again with epithelioid cell granulomas almost identical to sarcoidosis [133].

The diagnosis of chronic berylliosis and zirconiosis can be established by an exposure anamnesis, a sarcoid-like granulomatous reaction with $CD4^+$dominance in tissue as well as BAL, by electron microscopy with EDAX, or simply by a lymphocyte proliferation test [134]. Lymphocytes derived from BAL are short term cultivated in cell culture medium. After 2–3 days, BeO or ZO is added to the cell culture. In case of chronic allergic metal disease, the lymphocytes will proliferate and form cell clusters.

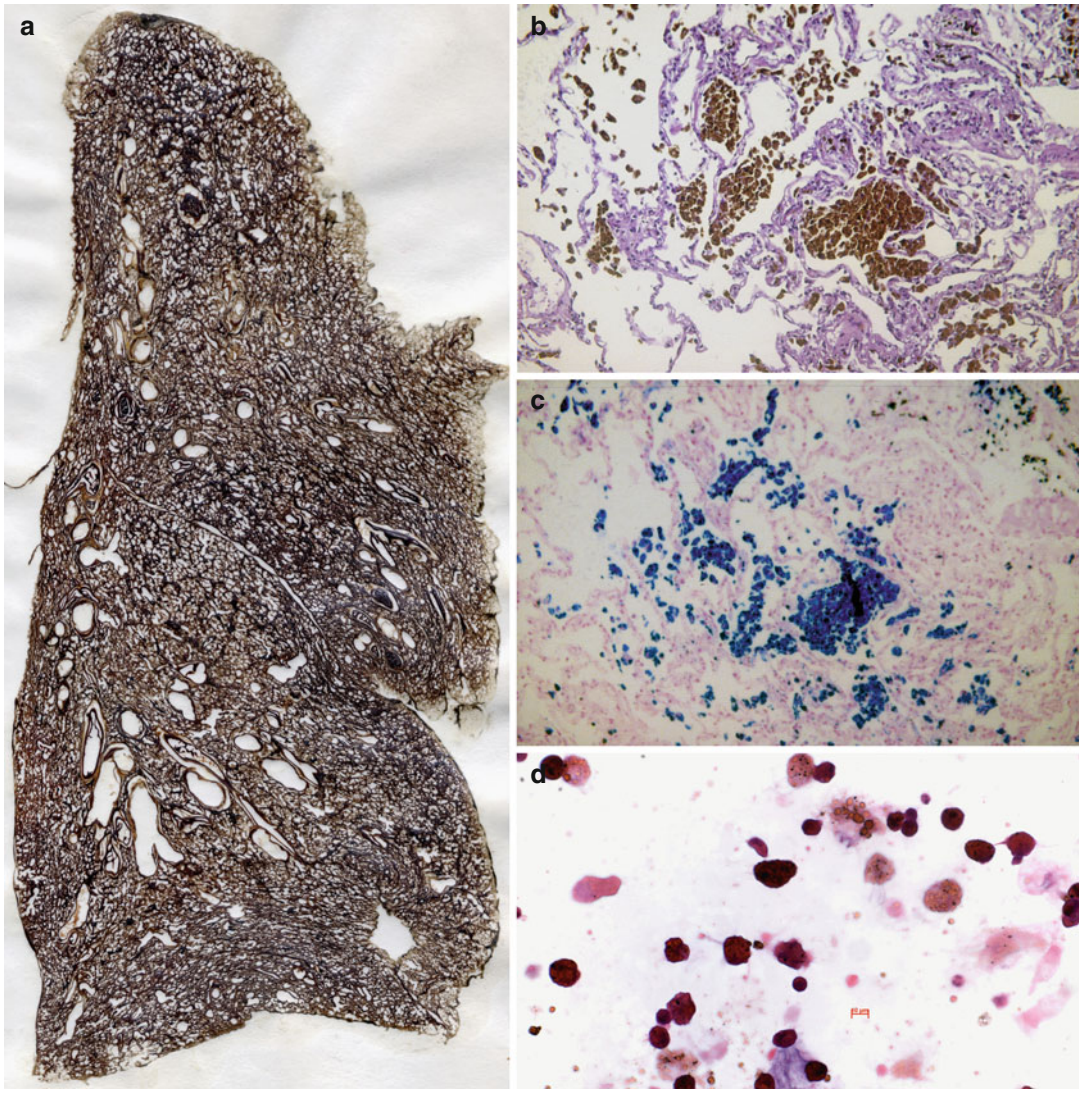

Fig. 13.19 Siderosis in a steel worker. (**a**) Is from an autopsy lung showing the impregnation of the lung by iron; especially the elastic fibers are intensely impregnated. Whole lung section, paper mount. (**b**–**c**) Siderosis diagnosed in transbronchial biopsies, showing the accumulation of hemosiderin-laden macrophages predominantly within the alveoli (H&E, *Prussian blue* stain). In (**d**) a BAL from a patient with siderosis is shown. In the upper middle, extracellular iron particles are seen. ×100, bar 10 μm

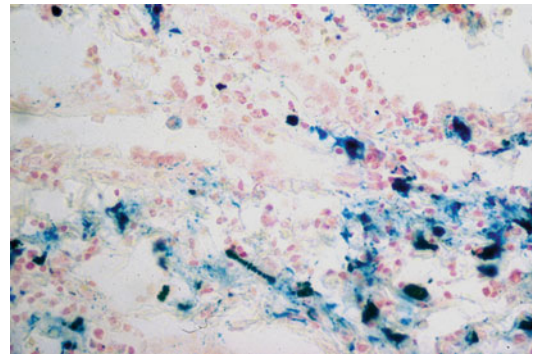

Fig. 13.20 Siderosis in a zinc welder, BAL specimen showing besides many hemosiderin-containing macrophages also an asbestos body. This is a common finding as the electrodes can contain asbestos fibers in older days. *Prussian blue*, ×200

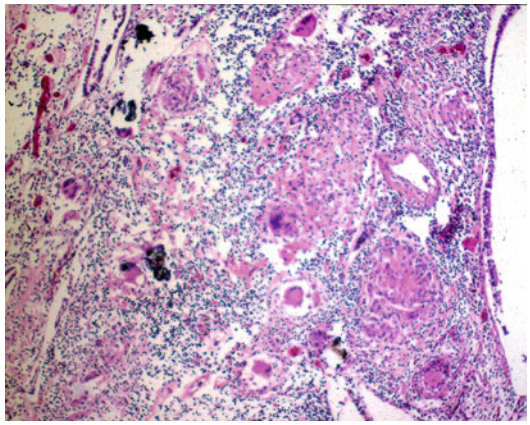

Fig. 13.21 Chronic berylliosis with epithelioid cell granulomas in the bronchial mucosa. This pattern is indistinguishable from sarcoidosis and can only separated from this disease by the proof of beryllium oxide in the granulomas. H&E, ×150

Nickel compounds are well-known allergens in the skin. Less well it is known that nickel can also cause an allergic reaction in dentistry workers chronically exposed to nickel compounds. The lung presents with lymphocytic infiltration in florid stages like a LIP; also hyperplasia of BALT is seen. Usually histiocytic foreign body but also epithelioid cell granulomas are encountered. Around the granulomas but also at alveolar septa, immunoglobulin deposits can be seen, which progress into fibrosis. Organizing pneumonia most often is focally seen. Besides nickel also palladium and metal alloys used for crown and bridges can cause a similar reaction [85, 135–137] (and personal experiences).

Metal might be sometimes be inhaled together with other minerals such as silicon oxides, which results in a more complex morphologic picture (Fig. 13.22).

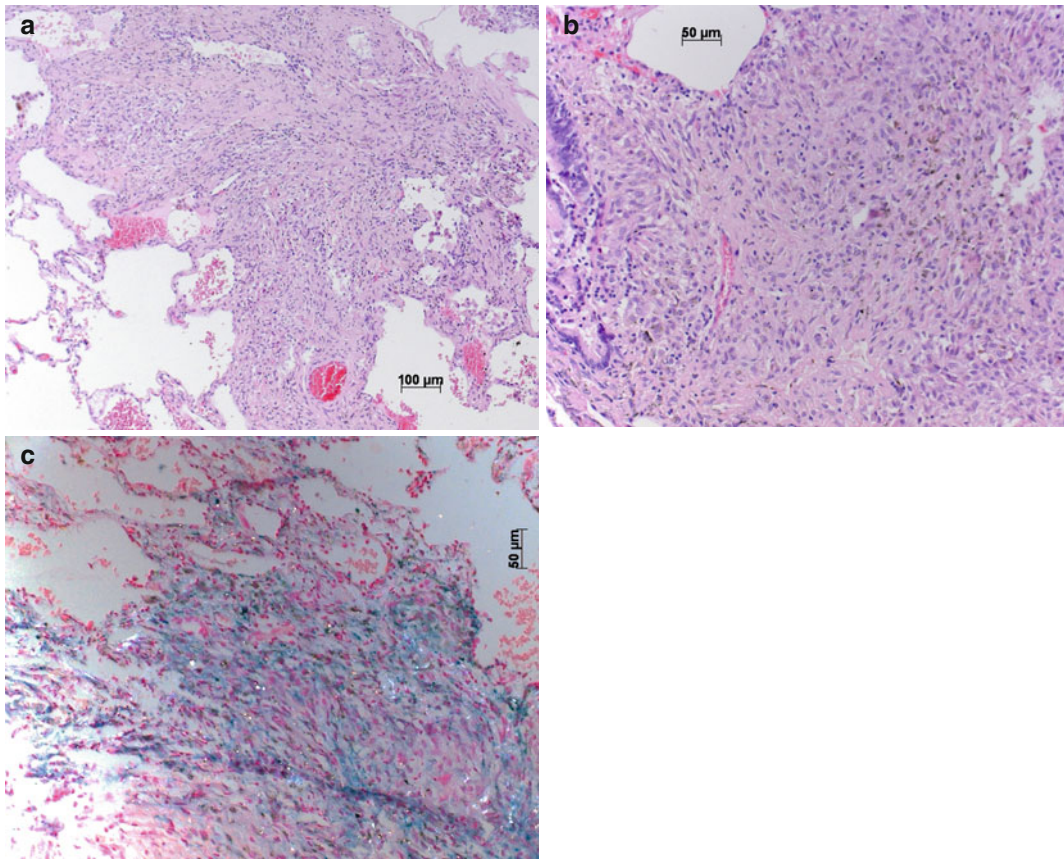

Fig. 13.22 Combined silicosis and metal dust pneumoconiosis. There is fibrosis with many macrophages, which contain brown to black pigment (**a**). Focal there is also formation of a histiocytic granuloma (**b**). On *Prussian blue* (**c**) stain the macrophages contain hemosiderin, on polarization there is also crystalline material of quartz type. Bars, 100 and 50 µm

13.5 Cotton Dust, Flock Workers' Lung, and Byssinosis

Extracts of cotton plants are toxic to alveolar, tracheal, and bronchial epithelium and that 5,7,3′,4′-tetrahydroxy-flavan 3,4-diol (THF) or other tannins may be the responsible agents [138]. Tannins present in inhaled cotton mill dust significantly decrease the ability of alveolar macrophages to phagocytize and clear inhaled dust particles. Exposed macrophages produce blebs on the surface of the cells and loss of most of the cellular organelle structure. This inhibition of macrophage function may therefore contribute to the pathogenesis of byssinosis [139]. Airway-centered interstitial fibrosis is one of the pathological presentations of chronic cotton dust inhalation [140]. Airway hyperreactivity and chronic bronchitis is another form of presentation [141]. Summarizing the pathologic findings in another form of byssinosis (flock workers' lung), Kern and Boag listed nonspecific interstitial pneumonia, lymphoid nodules, and lymphocytic bronchiolitis and added finally also desquamative interstitial pneumonia to the pathological reaction spectrum [142, 143].

13.6 Manmade Fibers, Hydrocarbon Compounds, and Polyvinyls

Fibrous hydrocarbon and polyvinyl fibers can cause toxic injury to the lung. In experimental setting, an intrapleural inoculation caused fibrous adhesions and nodular lesions. By inhalation chronic inflammation, fibrosis, and foreign body reaction were found in rats. Later on rats developed mesothelial hyperplasia and dysplasia and finally malignant mesothelioma [144]. Inhaled polyhydrocarbon fibers can also be detected in BAL; however, the analysis of its compounds requires a chemical investigation (Fig. 13.23).

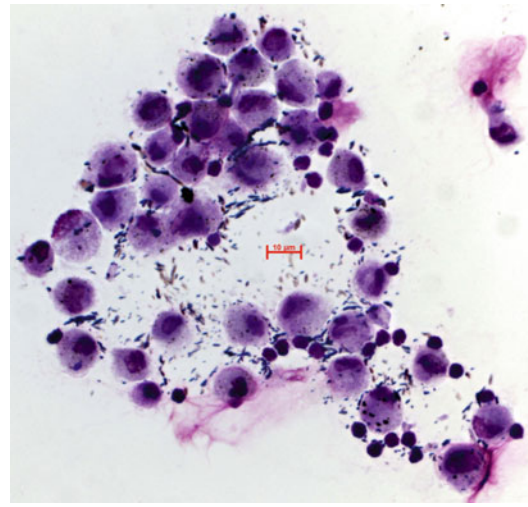

Fig. 13.23 Bronchoalveolar lavage in a female worker in a chemical industry. She had to fill bags with polyhydrocarbon fibers without any protection and developed diffuse lung disease. By BAL this organic fiber type material was identified. Bar 10 µm

13.7 Pesticides and Insecticides

Although pesticides and insecticides are not mineral particles and moreover are organic in chemical structure, we will shortly describe their toxicity and the tissue reaction. This is especially important, because many companies are using these chemicals in less-developed countries, where safety regulations are not present or not consequently followed, and pathologists are sometimes faced with poisoning, even at autopsy.

However, there are limitations, as not only the organic compound itself can cause injury but also the formula in which these compounds are used may influence the toxic property. Irritant combustion gases, volatile and semi-volatile organic substances, particulates (soot), condensation aerosols, and recondensed substances onto particulates may act independently, synergistically, or mixture specific. This

needs to be investigated independently in inhalation and toxicological test systems [145]. In addition some chemical might act specifically in one laboratory animal but not in another. As an example 1,3-dichloropropene inhalation caused benign tumors in the lungs of male mice, while ingestion of similar test material by rats and mice resulted in a low incidence of benign liver tumors in rats [146]. Deltamethrin an insecticide in the pyrethroid class caused heavy congestion, marked perivascular edema, and lymphoplasmacytic infiltration with focal nonspecific interstitial pneumonia, foamy macrophage accumulation, emphysema, peribronchial lymphoid tissue hyperplasia, and focal hemorrhage. Pneumocytes revealed mild degeneration and a slight hyperplasia in type II cells. Increases in the number of collagen bundles and edema in the alveolar septa were also seen [147].

Some information is available on the herbicide/pesticide paraquat. In experimental tests after severe incidents with humans using this herbicide in agriculture, it was found that there is a selective damage of pneumocytes with basement membrane destruction. Type II cells show damage to mitochondria. The edema in the lung caused by paraquat in rats is caused by damage to endothelial cells. But the main compartment into which paraquat is accumulated is the alveolar epithelial cell [148]. Initial necrosis and sloughing of the bronchiolar and alveolar epithelia with intact endothelium were followed by type 2 pneumocyte hyperplasia, fibroblast proliferation, and increased synthesis of collagen [149]. Since that time, paraquat is no longer used in agriculture in developed countries, but used experimentally to reproduce lung fibrosis, especially to simulate UIP/IPF. However, important: the sequence of morphological damage is DAD followed by organizing pneumonia, quite different from UIP/IPF.

13.8 Inhalation of Combustibles

Inhalation of combustibles will cause severe injury of the mucosa of the airways as well as the alveolar tissue, especially if these combustibles are burning as in a fire-eater. The injury starts with edema and DAD, which is replaced by organizing pneumonia and fibrosis. A hallmark is the accumulation of macrophages, which ingest the lipids and can form giant cells (Fig. 13.24).

13.9 Cocaine and Marijuana

Cocaine is well known for its fibrogenic effect. In a study on airway-centered interstitial lung fibrosis, cocaine use was identified in few of these patients [140]. In addition when compared for molecular abnormalities, there were more often alterations in Ki-67, epidermal growth factor receptor, globular actin, and DNA ploidy compared to tobacco smokers. Smoking marijuana and/or cocaine, like tobacco smoking, exerts field cancerization effects on the bronchial epithelium, which may place smokers of these substances at increased risk for the subsequent development of lung cancer [150]. Other pathologic findings in cocaine abusers were hemorrhage, interstitial pneumonia with fibrosis, congestion, and intra-alveolar edema. Pulmonary hemorrhage is the most frequent finding, whereas interstitial fibrosis is seen in long-term users [151].

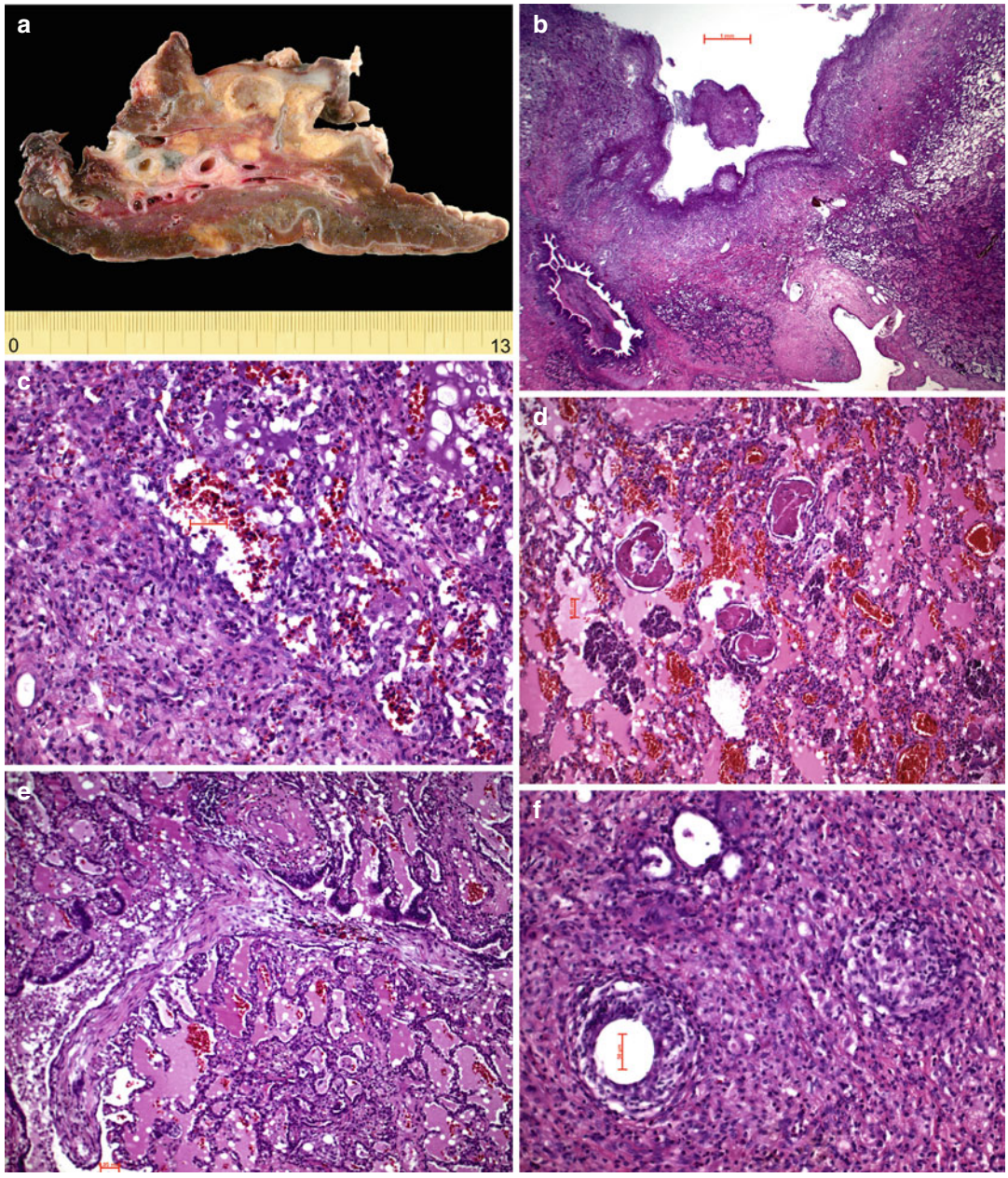

Fig. 13.24 Inhalation of combustibles by an artist (fire-eater). The patient burned down into his lung, a lobe resection had to be performed. (**a**) Macroscopic picture of the resected lobe showing necrosis surrounded by *yellow* lipid pneumonia. (**b**) The bronchial mucosa is completely destroyed. (**c**) Granulation tissue and fibrosis are seen together with macrophages, some of them with lipids stored in the cytoplasm (few pseudo-signet ring cells). (**d**) Fibrin engulfed by giant cells, edema, and macrophage accumulation are seen in areas with ongoing inflammation. (**e**) Edema, organizing pneumonia, and regeneration of bronchial mucosa are seen in this area. (**f**) Macrophage reaction with lipids and some foreign body giant cells having engulfed lipid fluid. H&E, bars 1 mm and 50 μm

References

1. Cohen GM. Pulmonary metabolism of foreign compounds: its role in metabolic activation. Environ Health Perspect. 1990;85:31–41.
2. Beckmann JD, Spurzem JR, Rennard SI. Phenol sulfotransferase expression in the airways: enzymological and immunohistochemical demonstration. Cell Tissue Res. 1993;274:475–85.
3. Wright DT, Cohn LA, Li H, Fischer B, Li CM, Adler KB. Interactions of oxygen radicals with airway epithelium. Environ Health Perspect. 1994;102 Suppl 10:85–90.
4. Ibanez-Tallon I, Heintz N, Omran H, Salathe M, Forteza R, Conner GE, Lillehoj ER, Kim KC, Foster WM, Rubin BK. To beat or not to beat: roles of cilia in development and disease post-secretory fate of host defence components in mucus airway mucus: its components and function mucociliary transport and cough in humans physiology of airway mucus clearance. Hum Mol Genet. 2003;12(Spec No 1):R27–35.
5. Baulig A, Garlatti M, Bonvallot V, Marchand A, Barouki R, Marano F, Baeza-Squiban A. Involvement of reactive oxygen species in the metabolic pathways triggered by diesel exhaust particles in human airway epithelial cells. Am J Physiol Lung Cell Mol Physiol. 2003;285:L671–9.
6. Allison AC. Pathogenic effects of inhaled particles and antigens. Ann N Y Acad Sci. 1974;221: 299–308.
7. Ghio AJ, Kennedy TP, Schapira RM, Crumbliss AL, Hoidal JR. Hypothesis: is lung disease after silicate inhalation caused by oxidant generation? Lancet. 1990;336:967–9.
8. Mossman BT, Churg A. Mechanisms in the pathogenesis of asbestosis and silicosis. Am J Respir Crit Care Med. 1998;157:1666–80.
9. Ding M, Chen F, Shi X, Yucesoy B, Mossman B, Vallyathan V. Diseases caused by silica: mechanisms of injury and disease development. Int Immunopharmacol. 2002;2:173–82.
10. Williams AO, Flanders KC, Saffiotti U. Immunohistochemical localization of transforming growth factor-beta 1 in rats with experimental silicosis, alveolar type II hyperplasia, and lung cancer. Am J Pathol. 1993;142:1831–40.
11. Hnizdo E, Murray J, Klempman S. Lung cancer in relation to exposure to silica dust, silicosis and uranium production in South African gold miners. Thorax. 1997;52:271–5.
12. Tsuda T, Mino Y, Babazono A, Shigemi J, Otsu T, Yamamoto E, Kanazawa S. A case-control study of lung cancer in relation to silica exposure and silicosis in a rural area in Japan. Ann Epidemiol. 2002;12:288–94.
13. Centers for Disease Control and Prevention (CDC). Silicosis in dental laboratory technicians – five states, 1994–2000. MMWR Morb Mortal Wkly Rep. 2004;53:195–97.
14. Reuzel PG, Bruijntjes JP, Feron VJ, Woutersen RA. Subchronic inhalation toxicity of amorphous silicas and quartz dust in rats. Food Chem Toxicol. 1991;29:341–54.
15. Heppleston AG. Silica, pneumoconiosis, and carcinoma of the lung. Am J Ind Med. 1985;7:285–94.
16. Saffiotti U. Lung cancer induction by crystalline silica. Prog Clin Biol Res. 1992;374:51–69.
17. Honma K, Chiyotani K, Kimura K. Silicosis, mixed dust pneumoconiosis, and lung cancer. Am J Ind Med. 1997;32:595–9.
18. Umemura S, Fujimoto N, Hiraki A, Gemba K, Takigawa N, Fujiwara K, Fujii M, Umemura H, Satoh M, Tabata M, Ueoka H, Kiura K, Kishimoto T, Tanimoto M. Aberrant promoter hypermethylation in serum DNA from patients with silicosis. Carcinogenesis. 2008;29:1845–9.
19. Roggli VL, Gibbs AR, Attanoos R, Churg A, Popper H, Cagle P, Corrin B, Franks TJ, Galateau-Salle F, Galvin J, Hasleton PS, Henderson DW, Honma K. Pathology of asbestosis- an update of the diagnostic criteria: report of the asbestosis committee of the college of American pathologists and pulmonary pathology society. Arch Pathol Lab Med. 2010;134:462–80.
20. Churg A, Wright JL. Small airways disease and mineral dust exposure. Pathol Annu. 1983;18(Pt 2):233–51.
21. Filipenko D, Wright JL, Churg A. Pathologic changes in the small airways of the guinea pig after amosite asbestos exposure. Am J Pathol. 1985;119:273–8.
22. Wright JL, Churg A. Morphology of small-airway lesions in patients with asbestos exposure. Hum Pathol. 1984;15:68–74.
23. Selikoff IJ, Hammond EC, Churg J. Carcinogenicity of amosite asbestos. Arch Environ Health. 1972;25: 183–6.
24. Kannerstein M, Churg J, McCaughey WT. Asbestos and mesothelioma: a review. Pathol Annu. 1978;13(Pt 1):81–129.
25. Churg A, Vedal S. Fiber burden and patterns of asbestos-related disease in workers with heavy mixed amosite and chrysotile exposure. Am J Respir Crit Care Med. 1994;150:663–9.
26. Jaurand MC, Fleury-Feith J. Pathogenesis of malignant pleural mesothelioma. Respirology. 2005;10:2–8.
27. Gibbs GW, Berry G. Mesothelioma and asbestos. Regul Toxicol Pharmacol. 2008;52:S223–31.
28. Hobson J, Gilks B, Wright J, Churg A. Direct enhancement by cigarette smoke of asbestos fiber penetration and asbestos-induced epithelial proliferation in rat tracheal explants. J Natl Cancer Inst. 1988;80:518–21.
29. Baris YI, Saracci R, Simonato L, Skidmore JW, Artvinli M. Malignant mesothelioma and radiological chest abnormalities in two villages in Central Turkey. An epidemiological and environmental investigation. Lancet. 1981;1:984–7.
30. Baris B, Demir AU, Shehu V, Karakoca Y, Kisacik G, Baris YI. Environmental fibrous zeolite

(erionite) exposure and malignant tumors other than mesothelioma. J Environ Pathol Toxicol Oncol. 1996;15:183–9.
31. Comba P, Gianfagna A, Paoletti L. Pleural mesothelioma cases in Biancavilla are related to a new fluoro-edenite fibrous amphibole. Arch Environ Health. 2003;58:229–32.
32. Constantopoulos SH. Environmental mesothelioma associated with tremolite asbestos: lessons from the experiences of Turkey, Greece, Corsica, New Caledonia and Cyprus. Regul Toxicol Pharmacol. 2008;52:S110–5.
33. Carbone M, Baris YI, Bertino P, Brass B, Comertpay S, Dogan AU, Gaudino G, Jube S, Kanodia S, Partridge CR, Pass HI, Rivera ZS, Steele I, Tuncer M, Way S, Yang H, Miller A. Erionite exposure in North Dakota and Turkish villages with mesothelioma. Proc Natl Acad Sci U S A. 2011;108:13618–23.
34. Ortega-Guerrero MA, Carrasco-Nunez G. Environmental occurrence, origin, physical and geochemical properties, and carcinogenic potential of erionite near San Miguel de Allende, Mexico. Environ Geochem Health. 2014;36:517–29.
35. Roushdy-Hammady I, Siegel J, Emri S, Testa JR, Carbone M. Genetic-susceptibility factor and malignant mesothelioma in the Cappadocian region of Turkey. Lancet. 2001;357:444–5.
36. Cortex Pimentel J, Peixoto Menezes A. Pulmonary and hepatic granulomatous disorders due to the inhalation of cement and mica dusts. Thorax. 1978;33:219–27.
37. Sahu AP, Shanker R, Zaidi SH. Pulmonary response to kaolin, mica and talc in mice. Exp Pathol (Jena). 1978;16:276–82.
38. Zinman C, Richards GA, Murray J, Phillips JI, Rees DJ, Glyn-Thomas R. Mica dust as a cause of severe pneumoconiosis. Am J Ind Med. 2002;41:139–44.
39. Gibbs AE, Pooley FD, Griffiths DM, Mitha R, Craighead JE, Ruttner JR. Talc pneumoconiosis: a pathologic and mineralogic study. Hum Pathol. 1992;23:1344–54.
40. Morgan WK, Donner A, Higgins IT, Pearson MG, Rawlings Jr W. The effects of kaolin on the lung. Am Rev Respir Dis. 1988;138:813–20.
41. Wagner JC, Pooley FD, Gibbs A, Lyons J, Sheers G, Moncrieff CB. Inhalation of china stone and china clay dusts: relationship between the mineralogy of dust retained in the lungs and pathological changes. Thorax. 1986;41:190–6.
42. Altekruse EB, Chaudhary BA, Pearson MG, Morgan WK. Kaolin dust concentrations and pneumoconiosis at a kaolin mine. Thorax. 1984;39:436–41.
43. Al-Ghimlas F, Hoffstein V. Pleuroparenchymal lung disease secondary to nonoccupational exposure to vermiculite. Can Respir J. 2007;14:164–6.
44. McDonald JC, Sebastien P, Armstrong B. Radiological survey of past and present vermiculite miners exposed to tremolite. Br J Ind Med. 1986;43:445–9.
45. Huuskonen MS, Tossavainen A, Koskinen H, Zitting A, Korhonen O, Nickels J, Korhonen K, Vaaranen V. Wollastonite exposure and lung fibrosis. Environ Res. 1983;30:291–304.
46. McConnell EE. Fibrogenic effect of wollastonite compared with asbestos dust and dusts containing quartz. Occup Environ Med. 1995;52:621.
47. Algranti E, Handar AM, Dumortier P, Mendonca EM, Rodrigues GL, Santos AM, Mauad T, Dolhnikoff M, De Vuyst P, Saldiva PH, Bussacos MA. Pneumoconiosis after sericite inhalation. Occup Environ Med. 2005;62, e2.
48. Pott F. Animal experiments on biological effects of mineral fibres. IARC Sci Publ. 1980;30:261–72.
49. Laney AS, Weissman DN. Respiratory diseases caused by coal mine dust. J Occup Environ Med. 2014;56 Suppl 10:S18–22.
50. Mo J, Wang L, Au W, Su M. Prevalence of coal workers' pneumoconiosis in China: a systematic analysis of 2001–2011 studies. Int J Hyg Environ Health. 2014;217:46–51.
51. Petsonk EL, Rose C, Cohen R. Coal mine dust lung disease. New lessons from old exposure. Am J Respir Crit Care Med. 2013;187:1178–85.
52. Vallyathan V, Landsittel DP, Petsonk EL, Kahn J, Parker JE, Osiowy KT, Green FH. The influence of dust standards on the prevalence and severity of coal worker's pneumoconiosis at autopsy in the United States of America. Arch Pathol Lab Med. 2011;135:1550–6.
53. Liebow AA. Pathology of coal workers' pneumoconiosis. IMS Ind Med Surg. 1970;39:118–9.
54. Oberdorster G. Lung particle overload: implications for occupational exposures to particles. Regul Toxicol Pharmacol. 1995;21:123–35.
55. Kim KA, Cho YY, Cho JS, Yang KH, Lee WK, Lee KH, Kim YS, Lim Y. Tumor necrosis factor-alpha gene promoter polymorphism in coal workers' pneumoconiosis. Mol Cell Biochem. 2002;234–235:205–9.
56. Nadif R, Jedlicka A, Mintz M, Bertrand JP, Kleeberger S, Kauffmann F. Effect of TNF and LTA polymorphisms on biological markers of response to oxidative stimuli in coal miners: a model of gene-environment interaction. Tumour necrosis factor and lymphotoxin alpha. J Med Genet. 2003;40:96–103.
57. Miller BG, MacCalman L. Cause-specific mortality in British coal workers and exposure to respirable dust and quartz. Occup Environ Med. 2010;67:270–6.
58. Laney AS, Attfield MD. Quartz exposure can cause pneumoconiosis in coal workers. J Occup Environ Med. 2009;51:867. author reply 868.
59. McCunney RJ, Morfeld P, Payne S. What component of coal causes coal workers' pneumoconiosis? J Occup Environ Med. 2009;51:462–71.

60. Ma JY, Ma JK. The dual effect of the particulate and organic components of diesel exhaust particles on the alteration of pulmonary immune/inflammatory responses and metabolic enzymes. J Environ Sci Health Part C Environ Carcinog Ecotoxicol Rev. 2002;20:117–47.
61. Lehmann AD, Blank F, Baum O, Gehr P, Rothen-Rutishauser BM. Diesel exhaust particles modulate the tight junction protein occludin in lung cells in vitro. Part Fibre Toxicol. 2009;6:26.
62. Hannigan MP, Busby Jr WF, Cass GR. Source contributions to the mutagenicity of urban particulate air pollution. J Air Waste Manag Assoc. 2005;55:399–410.
63. Alexis NE, Carlsten C. Interplay of air pollution and asthma immunopathogenesis: a focused review of diesel exhaust and ozone. Int Immunopharmacol. 2014;23:347–55.
64. Moller W, Hofer T, Ziesenis A, Karg E, Heyder J. Ultrafine particles cause cytoskeletal dysfunctions in macrophages. Toxicol Appl Pharmacol. 2002;182:197–207.
65. Rengasamy A, Barger MW, Kane E, Ma JK, Castranova V, Ma JY. Diesel exhaust particle-induced alterations of pulmonary phase I and phase II enzymes of rats. J Toxicol Environ Health A. 2003;66:153–67.
66. Zhou F, Li S, Jia W, Lv G, Song C, Kang C, Zhang Q. Effects of diesel exhaust particles on microRNA-21 in human bronchial epithelial cells and potential carcinogenic mechanisms. Mol Med Rep. 2015;12:2329–35.
67. Jaguin M, Fardel O, Lecureur V. AhR-dependent secretion of PDGF-BB by human classically activated macrophages exposed to DEP extracts stimulates lung fibroblast proliferation. Toxicol Appl Pharmacol. 2015;285:170–8.
68. Koh DH, Kong HJ, Oh CM, Jung KW, Park D, Won YJ. Lung cancer risk in professional drivers in Korea: a population-based proportionate cancer incidence ratio study. J Occup Health. 2015;57:324–30.
69. Lasfargues G, Lison D, Maldague P, Lauwerys R. Comparative study of the acute lung toxicity of pure cobalt powder and cobalt-tungsten carbide mixture in rat. Toxicol Appl Pharmacol. 1992;112:41–50.
70. Lison D, Lauwerys R, Demedts M, Nemery B. Experimental research into the pathogenesis of cobalt/hard metal lung disease. Eur Respir J. 1996;9:1024–8.
71. Naqvi AH, Hunt A, Burnett BR, Abraham JL. Pathologic spectrum and lung dust burden in giant cell interstitial pneumonia (hard metal disease/cobalt pneumonitis): review of 100 cases. Arch Environ Occup Health. 2008;63:51–70.
72. Fontenot AP, Amicosante M. Metal-induced diffuse lung disease. Semin Respir Crit Care Med. 2008;29:662–9.
73. Blanc PD. Is giant cell interstitial pneumonitis synonymous with hard metal lung disease? Am J Respir Crit Care Med. 2007;176:834. author reply 834–835.
74. Herbert A, Sterling G, Abraham J, Corrin B. Desquamative interstitial pneumonia in an aluminum welder. Hum Pathol. 1982;13:694–9.
75. Hull MJ, Abraham JL. Aluminum welding fume-induced pneumoconiosis. Hum Pathol. 2002;33:819–25.
76. Kelleher P, Pacheco K, Newman LS. Inorganic dust pneumonias: the metal-related parenchymal disorders. Environ Health Perspect. 2000;108 Suppl 4:685–96.
77. Schwarz Y, Kivity S, Fischbein A, Abraham JL, Fireman E, Moshe S, Dannon Y, Topilsky M, Greif J. Evaluation of workers exposed to dust containing hard metals and aluminum oxide. Am J Ind Med. 1998;34:177–82.
78. Kang KY, Bice D, Hoffman E, D'Amato R, Salvaggio J. Experimental studies of sensitization to beryllium, zirconium, and aluminum compounds in the rabbit. J Allergy Clin Immunol. 1977;59:425–36.
79. Newman LS. Metals that cause sarcoidosis. Semin Respir Infect. 1998;13:212–20.
80. Nemery B. Metal toxicity and the respiratory tract. Eur Respir J. 1990;3:202–19.
81. Popper HH, Woldrich A. Oxygen radical formation a probable mechanism for chromate toxicity. Prog Histochem Cytochem. 1991;23:220–6.
82. Popper HH, Wiespainer G, Leingartner E, Weybora W, Ratschek M. Short term chromate inhalation in a computer-assisted inhalation chamber: immediate toxicity and late cancer development. Environ Hyg. 1992;3:127–31.
83. Popper H, Grygar E, Ingolic E, Wawschinek O. Cytotoxicity of chromium-III and -VI compounds. I. In vitro studies using different cell culture systems. Inhal Toxicol. 1993;5:345–70.
84. Kolarzyk E, Stepniewski M, Zapolska I. Occurrence of pulmonary diseases in steel mill workers. Int J Occup Med Environ Health. 2000;13:103–12.
85. Kim YH, Chung YK, Kim C, Nam ES, Kim HJ, Joo Y. A case of hypersensitivity pneumonitis with giant cells in a female dental technician. Ann Occup Environ Med. 2013;25:19.
86. Kitamura H, Yoshimura Y, Tozawa T, Koshi K. Effects of cemented tungsten carbide dust on rat lungs following intratracheal injection of saline suspension. Acta Pathol Jpn. 1980;30:241–53.
87. Bastian S, Busch W, Kuhnel D, Springer A, Meissner T, Holke R, Scholz S, Iwe M, Pompe W, Gelinsky M, Potthoff A, Richter V, Ikonomidou C, Schirmer K. Toxicity of tungsten carbide and cobalt-doped tungsten carbide nanoparticles in mammalian cells in vitro. Environ Health Perspect. 2009;117:530–6.

88. Stefaniak AB, Virji MA, Day GA. Characterization of exposures among cemented tungsten carbide workers. Part I: size-fractionated exposures to airborne cobalt and tungsten particles. J Expo Sci Environ Epidemiol. 2009;19:475–91.
89. Rajendran N, Hu SC, Sullivan D, Muzzio M, Detrisac CJ, Venezia C. Toxicologic evaluation of tungsten: 28-day inhalation study of tungsten blue oxide in rats. Inhal Toxicol. 2012;24:985–94.
90. Sundaram P, Agrawal K, Mandke JV, Joshi JM. Giant cell pneumonitis induced by cobalt. Indian J Chest Dis Allied Sci. 2001;43:47–9.
91. Lison D, Lauwerys R. In vitro cytotoxic effects of cobalt-containing dusts on mouse peritoneal and rat alveolar macrophages. Environ Res. 1990;52: 187–98.
92. Lison D. Human toxicity of cobalt-containing dust and experimental studies on the mechanism of interstitial lung disease (hard metal disease). Crit Rev Toxicol. 1996;26:585–616.
93. Roesems G, Hoet PH, Dinsdale D, Demedts M, Nemery B. In vitro cytotoxicity of various forms of cobalt for rat alveolar macrophages and type II pneumocytes. Toxicol Appl Pharmacol. 2000; 162:2–9.
94. Cho WS, Duffin R, Bradley M, Megson IL, Macnee W, Howie SE, Donaldson K. NiO and Co3O4 nanoparticles induce lung DTH-like responses and alveolar lipoproteinosis. Eur Respir J. 2012;39:546–57.
95. Kazantzis G. Cadmium: sources, exposure and possible carcinogenicity. IARC Sci Publ. 1986;71:93–101.
96. Oberdorster G, Cherian MG, Baggs RB. Importance of species differences in experimental pulmonary carcinogenicity of inhaled cadmium for extrapolation to humans. Toxicol Lett. 1994;72:339–43.
97. Boffetta P. Methodological aspects of the epidemiological association between cadmium and cancer in humans. IARC Sci Publ. 1992;118:425–34.
98. Bachelet M, Pinot F, Polla RI, Francois D, Richard MJ, Vayssier-Taussat M, Polla BS. Toxicity of cadmium in tobacco smoke: protection by antioxidants and chelating resins. Free Radic Res. 2002;36:99–106.
99. Verougstraete V, Lison D, Hotz P. A systematic review of cytogenetic studies conducted in human populations exposed to cadmium compounds. Mutat Res. 2002;511:15–43.
100. Waalkes MP. Cadmium carcinogenesis. Mutat Res. 2003;533:107–20.
101. Garcia-Esquinas E, Pollan M, Tellez-Plaza M, Francesconi KA, Goessler W, Guallar E, Umans JG, Yeh J, Best LG, Navas-Acien A. Cadmium exposure and cancer mortality in a prospective cohort: the strong heart study. Environ Health Perspect. 2014;122:363–70.
102. Luevano J, Damodaran C. A review of molecular events of cadmium-induced carcinogenesis. J Environ Pathol Toxicol Oncol. 2014;33: 183–94.
103. Liu J, Qu W, Kadiiska MB. Role of oxidative stress in cadmium toxicity and carcinogenesis. Toxicol Appl Pharmacol. 2009;238:209–14.
104. Kundu S, Sengupta S, Bhattacharyya A. EGFR upregulates inflammatory and proliferative responses in human lung adenocarcinoma cell line (A549), induced by lower dose of cadmium chloride. Inhal Toxicol. 2011;23:339–48.
105. Jing Y, Liu LZ, Jiang Y, Zhu Y, Guo NL, Barnett J, Rojanasakul Y, Agani F, Jiang BH. Cadmium increases HIF-1 and VEGF expression through ROS, ERK, and AKT signaling pathways and induces malignant transformation of human bronchial epithelial cells. Toxicol Sci. 2012;125:10–9.
106. Zhou Z, Wang C, Liu H, Huang Q, Wang M, Lei Y. Cadmium induced cell apoptosis, DNA damage, decreased DNA repair capacity, and genomic instability during malignant transformation of human bronchial epithelial cells. Int J Med Sci. 2013;10:1485–96.
107. Person RJ, Tokar EJ, Xu Y, Orihuela R, Ngalame NN, Waalkes MP. Chronic cadmium exposure in vitro induces cancer cell characteristics in human lung cells. Toxicol Appl Pharmacol. 2013;273:281–8.
108. Eisler R. Health risks of gold miners: a synoptic review. Environ Geochem Health. 2003;25:325–45.
109. Kanluen S, Gottlieb CA. A clinical pathologic study of four adult cases of acute mercury inhalation toxicity. Arch Pathol Lab Med. 1991;115:56–60.
110. Liu J, Lei D, Waalkes MP, Beliles RP, Morgan DL. Genomic analysis of the rat lung following elemental mercury vapor exposure. Toxicol Sci. 2003;74:174–81.
111. Zhao J, Shi X, Castranova V, Ding M. Occupational toxicology of nickel and nickel compounds. J Environ Pathol Toxicol Oncol. 2009;28:177–208.
112. Sunderman Jr FW. A review of the metabolism and toxicology of nickel. Ann Clin Lab Sci. 1977;7:377–98.
113. Johansson A, Curstedt T, Robertson B, Camner P. Rabbit lung after inhalation of soluble nickel. II. Effects on lung tissue and phospholipids. Environ Res. 1983;31:399–412.
114. Benson JM, Burt DG, Cheng YS, Hahan FF, Haley PJ, Henderson RF, Hobbs CH, Pickrell JA, Dunnick JK. Biochemical responses of rat and mouse lung to inhaled nickel compounds. Toxicology. 1989;57:255–66.
115. Dunnick JK, Elwell MR, Benson JM, Hobbs CH, Hahn FF, Haly PJ, Cheng YS, Eidson AF. Lung toxicity after 13-week inhalation exposure to nickel oxide, nickel subsulfide, or nickel sulfate hexahydrate in F344/N rats and B6C3F1 mice. Fundam Appl Toxicol. 1989;12:584–94.
116. Savolainen H. Biochemical and clinical aspects of nickel toxicity. Rev Environ Health. 1996;11: 167–73.
117. Freitas M, Barcellos-de-Souza P, Barja-Fidalgo C, Fernandes E. Nickel induces apoptosis in human neutrophils. Biometals. 2013;26:13–21.

118. Kenyon EM, Hughes MF. A concise review of the toxicity and carcinogenicity of dimethylarsinic acid. Toxicology. 2001;160:227–36.
119. Jones SR, Atkin P, Holroyd C, Lutman E, Batlle JV, Wakeford R, Walker P. Lung cancer mortality at a UK tin smelter. Occup Med (Lond). 2007;57: 238–45.
120. Homma S, Miyamoto A, Sakamoto S, Kishi K, Motoi N, Yoshimura K. Pulmonary fibrosis in an individual occupationally exposed to inhaled indium-tin oxide. Eur Respir J. 2005;25:200–4.
121. Lison D, Laloy J, Corazzari I, Muller J, Rabolli V, Panin N, Huaux F, Fenoglio I, Fubini B. Sintered indium-tin-oxide (ITO) particles: a new pneumotoxic entity. Toxicol Sci. 2009;108:472–81.
122. Hazard JB. Pathologic changes of beryllium disease; the acute disease. AMA Arch Ind Health. 1959;19:179–83.
123. Machle W, Beyer E, Gregorious F. Berylliosis; acute pneumonitis and pulmonary granulomatosis of beryllium workers. Occup Med (Chic Ill). 1948;5:671–83.
124. Jones Williams W. Beryllium disease. Postgrad Med J. 1988;64:511–6.
125. Leininger JR, Farrell RL, Johnson GR. Acute lung lesions due to zirconium and aluminum compounds in hamsters. Arch Pathol Lab Med. 1977;101:545–9.
126. Hadjimichael OC, Brubaker RE. Evaluation of an occupational respiratory exposure to a zirconium-containing dust. J Occup Med. 1981;23:543–7.
127. Elmore AR. Final report on the safety assessment of aluminum silicate, calcium silicate, magnesium aluminum silicate, magnesium silicate, magnesium trisilicate, sodium magnesium silicate, zirconium silicate, attapulgite, bentonite, Fuller's earth, hectorite, kaolin, lithium magnesium silicate, lithium magnesium sodium silicate, montmorillonite, pyrophyllite, and zeolite. Int J Toxicol. 2003;22 Suppl 1: 37–102.
128. McCleskey TM, Buchner V, Field RW, Scott BL. Recent advances in understanding the biomolecular basis of chronic beryllium disease: a review. Rev Environ Health. 2009;24:75–115.
129. Freiman DG, Hardy HL. Beryllium disease. The relation of pulmonary pathology to clinical course and prognosis based on a study of 130 cases from the U.S. beryllium case registry. Hum Pathol. 1970;1:25–44.
130. Fontenot AP, Torres M, Marshall WH, Newman LS, Kotzin BL. Beryllium presentation to CD4+ T cells underlies disease-susceptibility HLA-DP alleles in chronic beryllium disease. Proc Natl Acad Sci U S A. 2000;97:12717–22.
131. Fireman E, Haimsky E, Noiderfer M, Priel I, Lerman Y. Misdiagnosis of sarcoidosis in patients with chronic beryllium disease. Sarcoidosis Vasc Diffus Lung Dis. 2003;20:144–8.
132. Silveira LJ, McCanlies EC, Fingerlin TE, Van Dyke MV, Mroz MM, Strand M, Fontenot AP, Bowerman N, Dabelea DM, Schuler CR, Weston A, Maier LA. Chronic beryllium disease, HLA-DPB1, and the DP peptide binding groove. J Immunol. 2012;189:4014–23.
133. Werfel U, Schneider J, Rodelsperger K, Kotter J, Popp W, Woitowitz HJ, Zieger G. Sarcoid granulomatosis after zirconium exposure with multiple organ involvement. Eur Respir J. 1998;12:750.
134. Rossman MD, Kern JA, Elias JA, Cullen MR, Epstein PE, Preuss OP, Markham TN, Daniele RP. Proliferative response of bronchoalveolar lymphocytes to beryllium. A test for chronic beryllium disease. Ann Intern Med. 1988;108:687–93.
135. Report on base metal alloys for crown and bridge applications: benefits and risks. Council on dental materials, instruments, and equipment. J Am Dent Assoc. 1985;111:479–83.
136. Kielhorn J, Melber C, Keller D, Mangelsdorf I. Palladium – a review of exposure and effects to human health. Int J Hyg Environ Health. 2002;205: 417–32.
137. Hu SW, Lin YY, Wu TC, Hong CC, Chan CC, Lung SC. Workplace air quality and lung function among dental laboratory technicians. Am J Ind Med. 2006;49:85–92.
138. Ayars GH, Altman LC, O'Neil CE, Butcher BT, Chi EY. Cotton dust-mediated lung epithelial injury. J Clin Invest. 1986;78:1579–88.
139. Kreofsky TJ, Russell JA, Rohrbach MS. Inhibition of alveolar macrophage spreading and phagocytosis by cotton bract tannin. A potential mechanism in the pathogenesis of byssinosis. Am J Pathol. 1990;137:263–74.
140. Churg A, Myers J, Suarez T, Gaxiola M, Estrada A, Mejia M, Selman M. Airway-centered interstitial fibrosis: a distinct form of aggressive diffuse lung disease. Am J Surg Pathol. 2004;28:62–8.
141. Wang XR, Pan LD, Zhang HX, Sun BX, Dai HL, Christiani DC. A longitudinal observation of early pulmonary responses to cotton dust. Occup Environ Med. 2003;60:115–21.
142. Kern DG, Kuhn 3rd C, Ely EW, Pransky GS, Mello CJ, Fraire AE, Muller J. Flock worker's lung: broadening the spectrum of clinicopathology, narrowing the spectrum of suspected etiologies. Chest. 2000;117:251–9.
143. Boag AH, Colby TV, Fraire AE, Kuhn 3rd C, Roggli VL, Travis WD, Vallyathan V. The pathology of interstitial lung disease in nylon flock workers. Am J Surg Pathol. 1999;23:1539–45.
144. Fraire AE, Greenberg SD, Spjut HJ, Roggli VL, Dodson RF, Cartwright J, Williams G, Baker S. Effect of fibrous glass on rat pleural mesothelium. Histopathologic observations. Am J Respir Crit Care Med. 1994;150:521–7.
145. Achmadi UF, Pauluhn J. Household insecticides: evaluation and assessment of inhalation toxicity: a workshop summary. Exp Toxicol Pathol. 1998; 50:67–72.
146. Stott WT, Gollapudi BB, Rao KS. Mammalian toxicity of 1,3-dichloropropene. Rev Environ Contam Toxicol. 2001;168:1–42.

147. Erdogan S, Zeren EH, Emre M, Aydin O, Gumurdulu D. Pulmonary effects of deltamethrin inhalation: an experimental study in rats. Ecotoxicol Environ Saf. 2006;63:318–23.
148. Sykes BI, Purchase IF, Smith LL. Pulmonary ultrastructure after oral and intravenous dosage of paraquat to rats. J Pathol. 1977;121:233–41.
149. Popenoe D. Effects of paraquat aerosol on mouse lung. Arch Pathol Lab Med. 1979;103:331–4.
150. Barsky SH, Roth MD, Kleerup EC, Simmons M, Tashkin DP. Histopathologic and molecular alterations in bronchial epithelium in habitual smokers of marijuana, cocaine, and/or tobacco. J Natl Cancer Inst. 1998;90:1198–205.
151. Bailey ME, Fraire AE, Greenberg SD, Barnard J, Cagle PT. Pulmonary histopathology in cocaine abusers. Hum Pathol. 1994;25:203–7.

Iatrogenic Lung Diseases

14

14.1 Drug-Induced Interstitial Lung Diseases

Drug-induced interstitial lung diseases present with a variety of tissue reaction, most of them already discussed in previous chapters. A common presentation is diffuse alveolar damage as an acute reaction, often followed by organizing DAD, where hyaline membranes can still be recognized, and finally ending as organizing pneumonia and lung fibrosis. Other drugs induce NSIP-like tissue reactions. The major problem in interpreting drug reaction in the lung is our limited understanding of drug metabolism. Some drugs will induce toxic injury of endothelial cells, thus the blood barrier is leaking, and proteins can enter the interstitium and finally the alveolar lumen. Here these proteins will form complexes and by the action of respiration hyaline membranes will form. In addition the exudate from the capillaries will cause a transient edema and this is followed by hypoxia affecting the pneumocytes. This damage will contribute to DAD development (Fig. 14.1). Later on organizing pneumonia can result. Other drugs act on the immune system, forming immune complexes either because they are immunogenic by themselves or by complexing with endogenous proteins like a hapten. In these cases a NSIP or LIP pattern can result. In these cases scattered eosinophils are regularly found. Rarely granulomas are formed, usually pointing to an underlying immune mechanism. Since our understanding is so limited and no systematic experimental investigation has been performed, we still need to rely on databases, summarizing all described drug reactions in a systematic way (www.pneumotox.com; [1–8]).

14.2 Action of Drugs and Morphologic Changes Associated with Drug Metabolism

There are different mechanisms a drug can act with:

1. Drugs taken up parenterally are moving through the liver, might be metabolized, and reach the lung. At this first passage, the concentration is high. This can induce early lesions of the pulmonary endothelia, followed by edema, hemorrhage, and vasculitis and DAD. Biological mechanisms behind this reaction can be formation of oxygen radicals and lipid peroxides.
2. Drugs or their metabolites can be poisonous for mitotic spindle proteins and thus inhibit mitosis and regeneration.
3. Drugs and their metabolites can interfere with normal metabolism, for example, the glucose metabolism.
4. An interaction with lipid metabolism can result in lipoproteinosis, but also the formation of lipid peroxides, or an interference with surfactant lipids and proteins.

© Springer-Verlag Berlin Heidelberg 2017
H. Popper, *Pathology of Lung Disease*, DOI 10.1007/978-3-662-50491-8_14

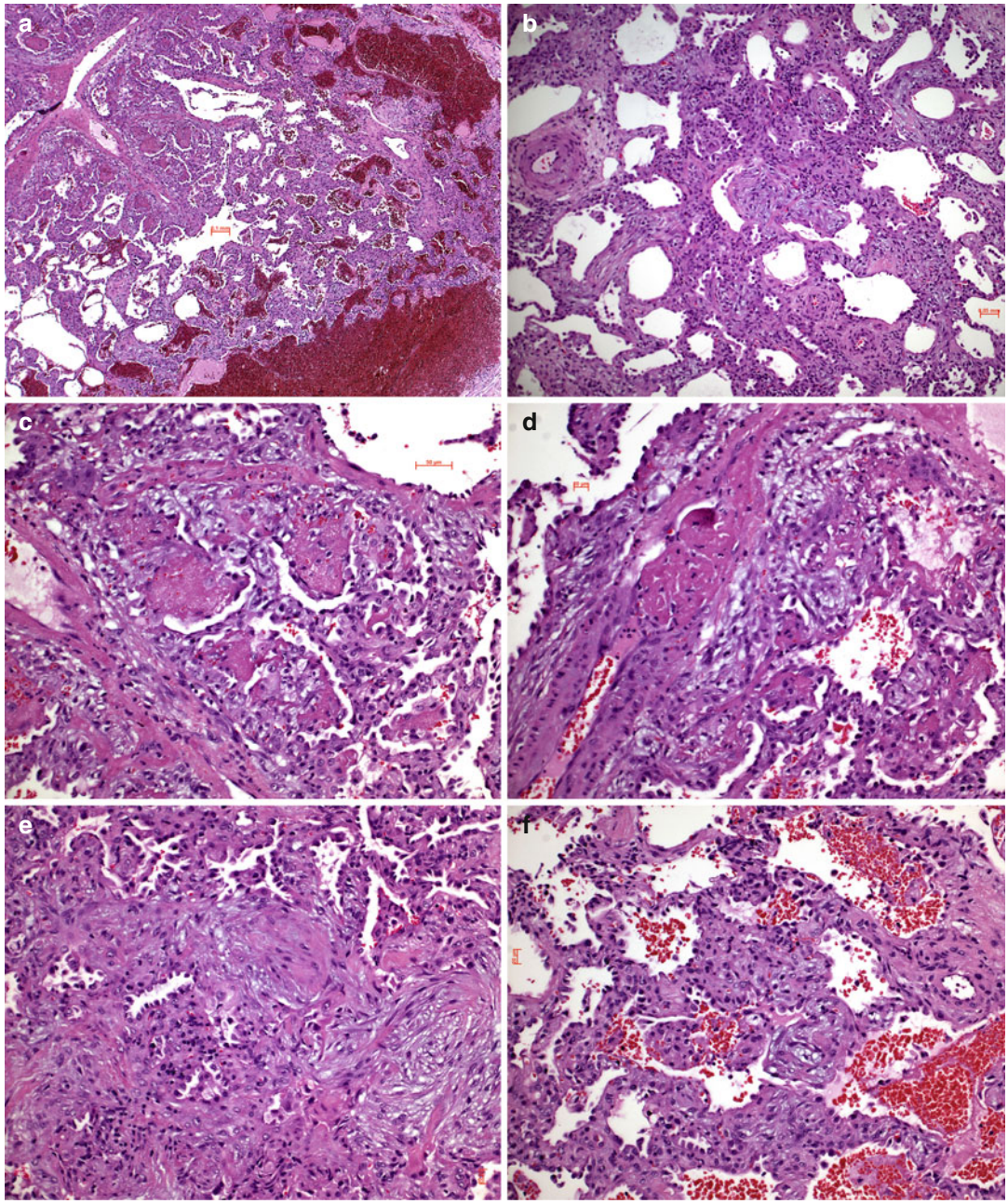

Fig. 14.1 Lung disease induced by a neuroleptic is a good example how to analyze such a drug reaction. (**a**) In this overview there is acute bleeding, intra-alveolar fibrin, thickening of alveolar septa, and some organization. (**b**) Shows organizing pneumonia associated with pink material corresponding to hyaline membranes in organization, but some of these granulation processes are within the alveolar septa and look almost like fibroblast foci. The arteries have thickened walls. (**c**) Here fibrin is organized by granulation tissue out of the wall; this granulation tissue appears myxoid; in (**d**) there is a fibrin cloth within the blood vessel. This points to an injury coming from the blood stream! In (**e**) the interstitial granulation tissue is shown, and with this magnification one can see that this fibrosis is associated with blood vessels, which are lost. Also remnants of hyaline membranes are there. In (**f**) the fibrosis follows the capillaries, which are shifted into the center of the septum. In (**g**) this association with the blood vessels is highlighted by the Movat stain, which shows immature collagen and destroyed elastic fibers from blood vessels and alveolar septa. H&E, Movat, bars 100, 50, 20 μm

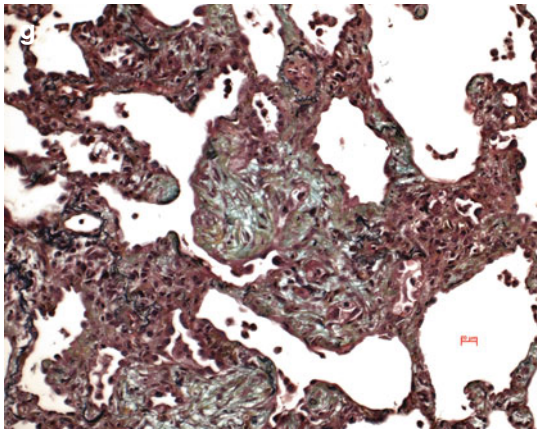

Fig. 14.1 (continued)

5. A vasculopathy can be induced by drugs most likely by deposition of immune complexes, which do not activate the complement system and therefore do not elicit an infiltration of leukocytes.

Morphologic patterns drugs can cause:

14.2.1 Granulomatous Reactions

In this case the drug associates with some endogenous protein(s) and forms immunogenic complexes, which are deposited in the lung stroma. These complexes are either too large to be dissolved by leukocytes or their chemical property does prohibit the uptake and digestion by these cells. The reaction can be a simple foreign body granuloma, when the complex is just too large, or it can be a histiocytic or epithelioid cell granuloma, when the complex has immunogenic properties (Fig. 14.2).

14.2.2 DAD Pattern

If a drug is toxic by itself or metabolites derived from the drug, a DAD reaction can be caused. In these cases the first action of the drug is on endothelial cells causing necrosis. This is followed by edema and extravasation of proteins from the circulation. These proteins enter the alveolar lumina, coagulate, and will be compressed by breathing and finally form hyaline membranes. Since edema and protein extravasation will result in hypoxia, also pneumocytes will die and thus contribute to the development of DAD (Figs. 14.3 and 14.4).

14.2.3 Organizing Pneumonia Pattern

Organizing pneumonia in drug-induced lung diseases usually is the subacute to chronic phase of DAD, i.e., organizing DAD (Figs. 14.5 and 14.6).

14.2.4 NSIP and LIP Patterns

In cases of allergic reactions for drugs, NSIP and LIP reactions can be seen (Fig. 14.7). Sometimes this is also associated with small vessel vasculitis. The drug or its metabolites act as an allergen and will cause the formation of antibodies. Antigen/allergen and antibodies will form immune complexes, which are deposited in the wall of small blood vessels and cause a lymphocytic infiltration. The ratio of allergen to antibody will be responsible for the number of infiltrating lymphocytes and also dictate which other antigen-presenting cells will take part in this immune reaction. Whereas LIP usually points to an acute immune reaction with large amounts of deposited immune complexes, NSIP will predominate in those cases, where the amount of immune complexes is low, and these complexes are still soluble, thus mounting a reaction with numerous dendritic cells infiltrating the lesion.

14.2.5 UIP Pattern

UIP in drug-induced lung diseases is not well understood. As the drugs cause apoptosis of pneumocytes followed by repair in the form of fibroblastic foci, the drugs most likely are cytotoxic for the pneumocytes. This view is supported by the fact that many cytotoxic drugs used in cancer therapy are among those causing UIP (Fig. 14.8). However, why these drugs also perpetuate the reaction even when withdrawn is unclear.

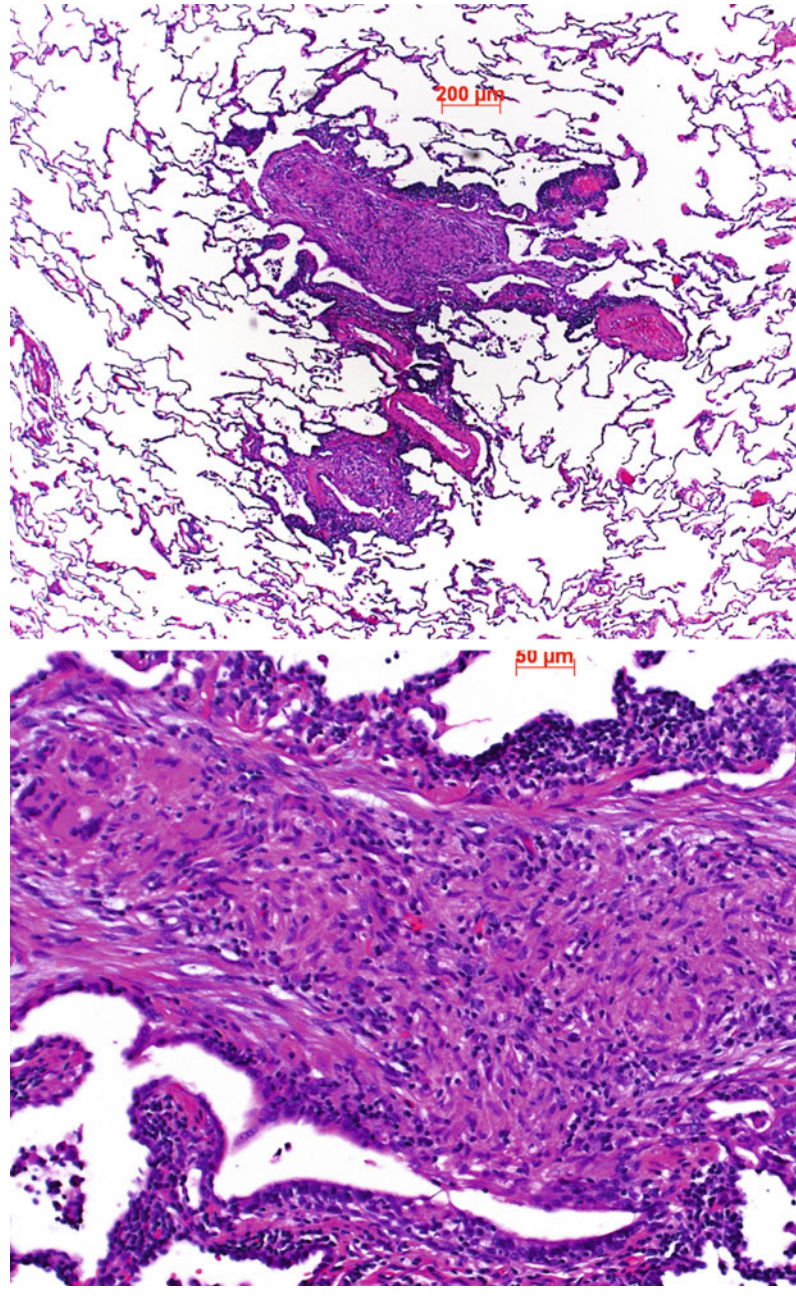

Fig. 14.2 Drug reaction with intravascular and bronchial epithelioid cell granulomas, pointing to an allergic mechanism. The drug could not be identified. H&E, bars 200 and 50 µm

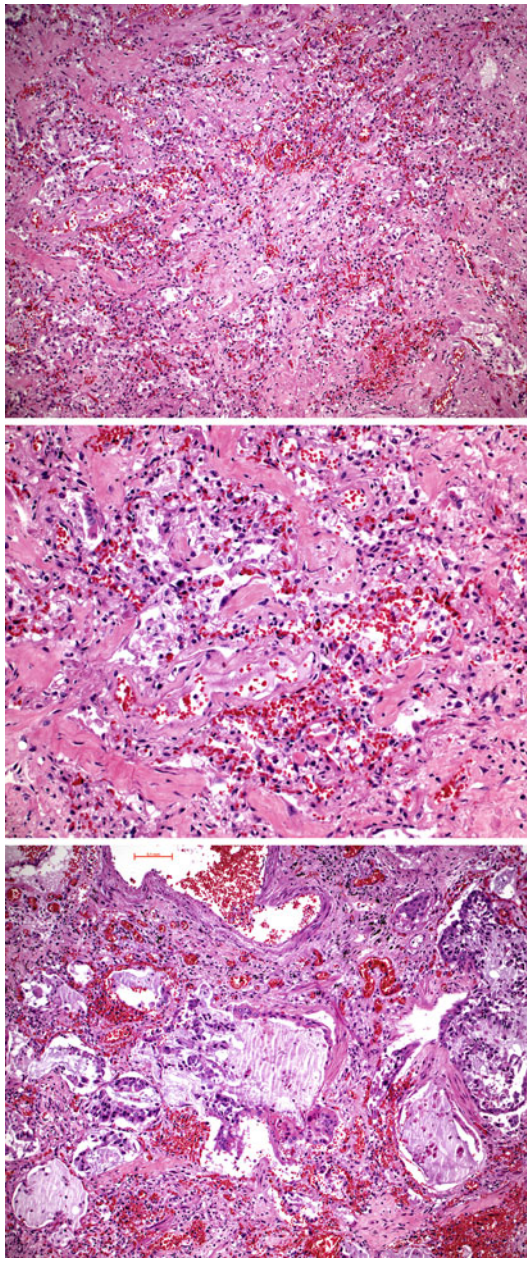

Fig. 14.3 Drug reaction of leflunomide, a basic medication for rheumatoid arthritis. In a small fraction of patients, this drug will cause DAD, followed by organizing pneumonia and fibrosis, and can cause death of the patient. Here organizing pneumonia is shown at an early stage of development still with many hyaline membranes (*top and middle panels*). In the *lower panel*, there is cystic remodeling of the lung architecture with prominent bronchiolar cell metaplasia in the remaining alveoli. Some of the fibrotic foci resemble fibroblast foci. Note also atypia of single cells (*middle panel*). H&E, bars 100 μm, and ×100 and 200

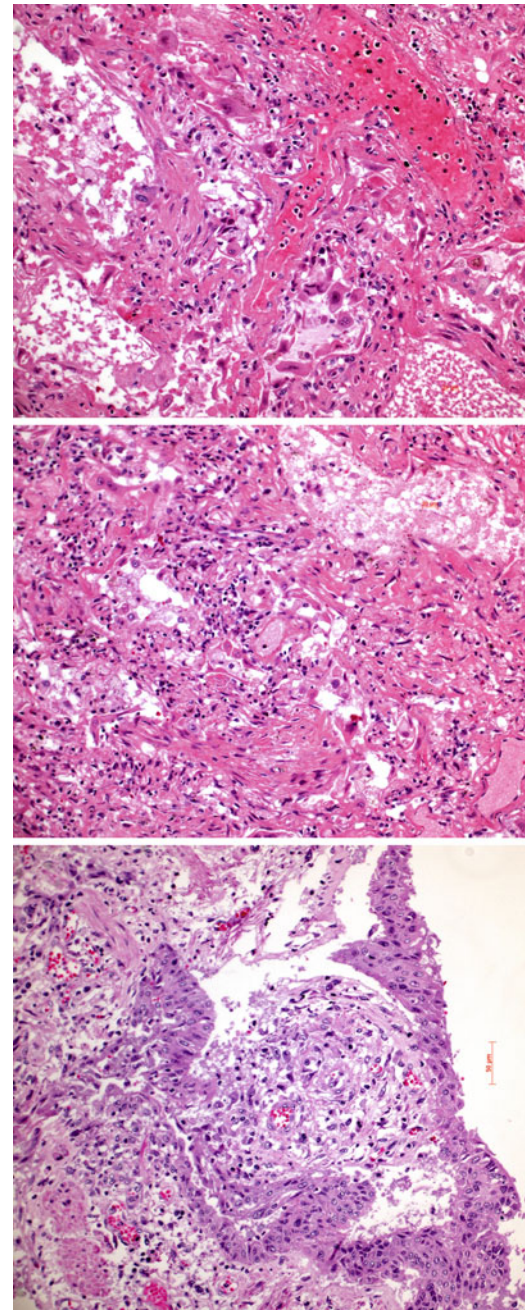

Fig. 14.4 Another drug, which can present with DAD is methotrexate. In this case there is fibrin in the alveoli, fibroblast proliferation into the alveoli with organization of debris and hyaline membranes (*top and middle panels*). There is marked atypia of regenerating pneumocytes, which can result in peripheral squamous cell metaplasia, quite characteristic for this drug. H&E, bars 50 and 20 μm

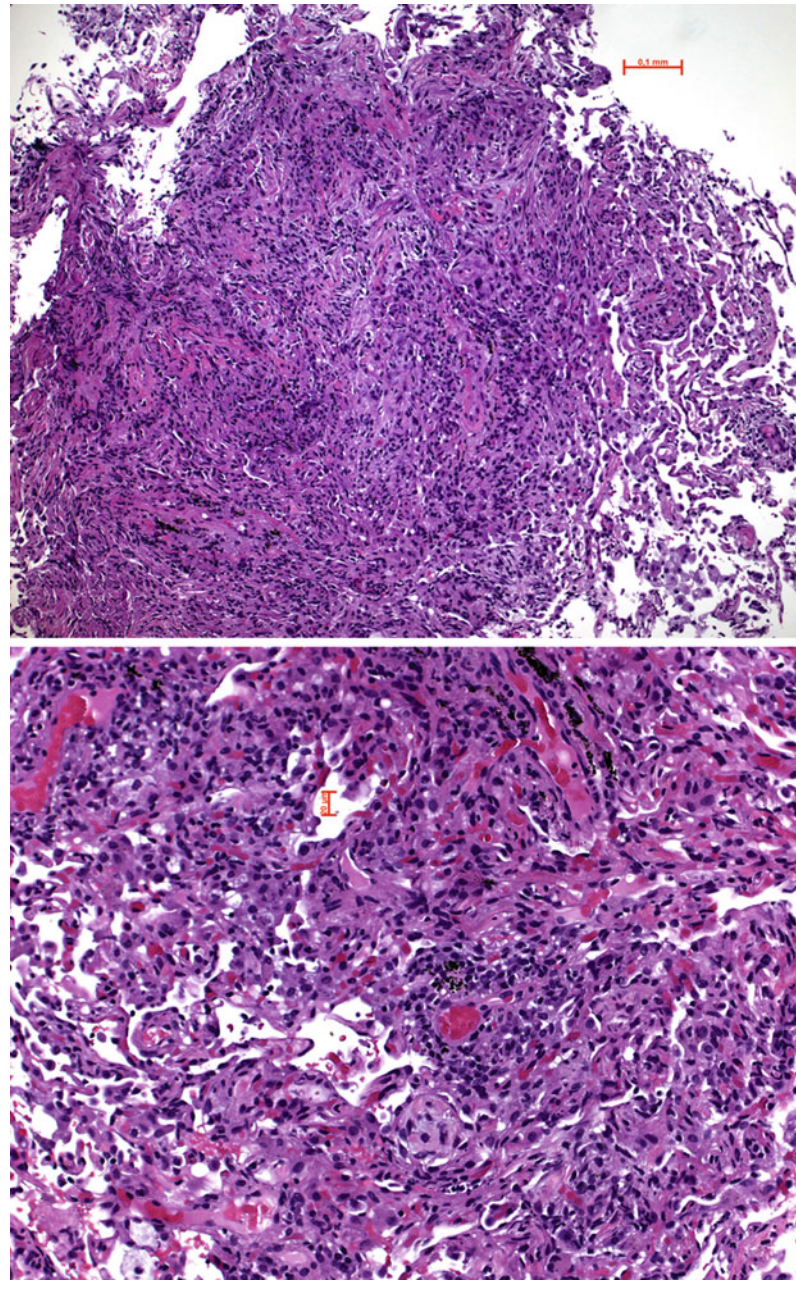

Fig. 14.5 Organizing pneumonia in amiodarone-induced lung injury. In the *upper panel*, the granulation tissue has completely obscured the alveolar structure, but the single atypical reactive pneumocytes help in getting an orientation within this transbronchial biopsy. Around the veins there is also lymphocytic reaction; some venous lumina are obstructed. In less affected alveoli, there is an accumulation of macrophages. The granulation tissue is shown at higher magnification in the *lower panel*; here also the lymphocytic perivascular accumulation is easier seen. H&E, bars 100 and 20 μm

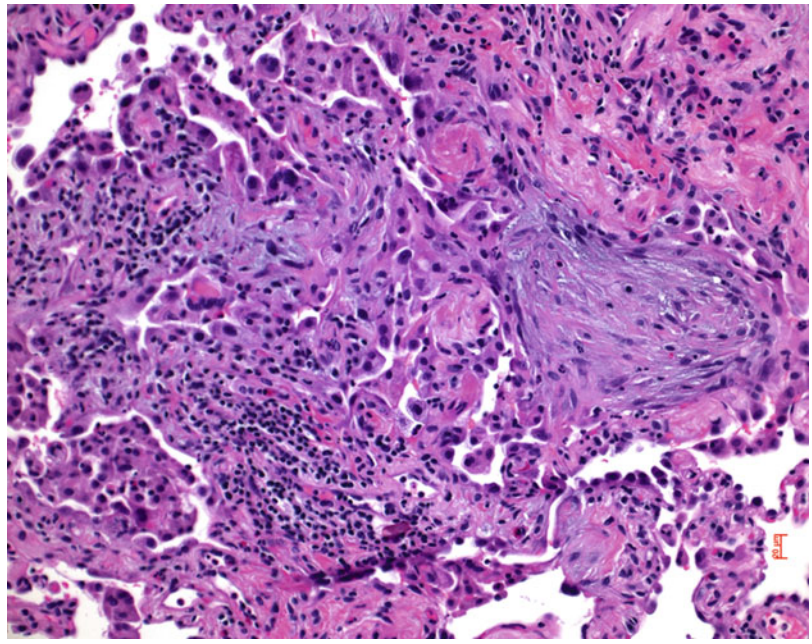

Fig. 14.6 Organizing pneumonia in BCNU chemotherapy. Here a classical OP pattern is seen accompanied by a mild lymphocytic infiltration. Note the reactive changes of the pneumocytes pointing to some interference with their metabolism. H&E, bar 20 µm

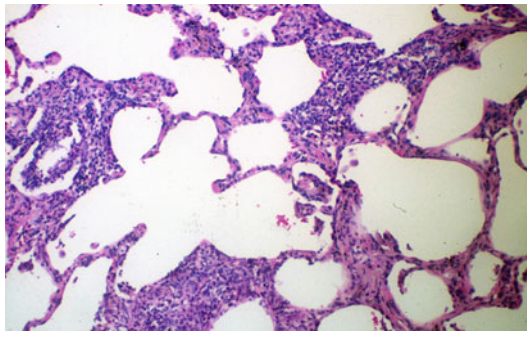

Fig. 14.7 Lymphocytic interstitial pneumonia (LIP) in a case under Cytoxan therapy. One of the known mechanisms this drug can induce. H&E, ×150

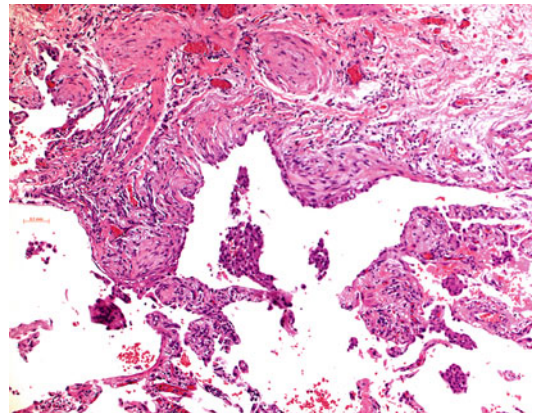

Fig. 14.8 Usual interstitial pneumonia pattern in a patient under therapy with cytostatics. He presented with numerous fibroblastic foci, focally with cystic remodeling of the lung architecture, and had areas of uninvolved lung. H&E, bar 100 µm

14.2.6 Vasculitis

Drugs acting like an allergen can cause small vessel vasculitis. This hypersensitivity vasculitis is characterized by numerous eosinophils infiltrating the vessel wall and causing necrosis of endothelia. Most often capillaries and venules of the skin are affected, but also pulmonary small vessels can be involved.

14.2.7 Edema

Edema in drug-induced reaction points usually to a mild cytotoxic action of the drug or to low-dose effect.

14.2.8 Fibrinous Pneumonia

In some cases fibrinous pneumonia and organizing pneumonia can be combined, very much as in organizing pneumonia of other causes. However, there are no granulocytes and also lymphocytes are rarely seen. If there is fibrin also within the septa and around the blood vessels, a drug reaction might be suspected (Fig. 14.9).

In many drug reactions, eosinophils are involved. Eosinophilic infiltrations are most often hallmarks of cytotoxic drug reactions. Usually these infiltrations are mixed with cytotoxic lymphocytes.

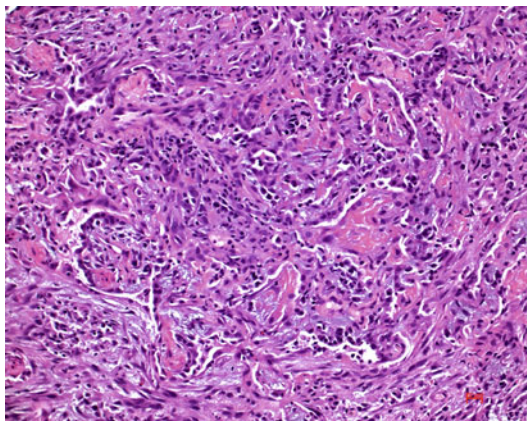

Fig. 14.9 Combined fibrinous and organizing pneumonia in methotrexate therapy. Fibrin is seen in alveoli but also in the interstitium and is being organized by granulation tissue. H&E, bar 20 μm

Therefore this type of inflammation should prompt the differential diagnosis of parasitic infection, allergic reaction, and drug reactions.

In the differential diagnosis of drug reactions, many other diseases are to be listed. We have discussed this already in several other chapters. As a rule the following should be considered: primary lesions of the endothelia most often point to drug-induced reactions, although pathologists do not often see these early lesions in their practice. Lists of different drugs and their reaction pattern can be found in the chapter on this subject written by J. Myers [8].

14.3 Iatrogenic Pathology by Radiation

Radiation therapy can cause many different reactions in the lung. The most dramatic effect is widespread necrosis of lung parenchyma, so-called acute radiation pneumonitis, which can lead ultimately to death of the patient [9]. However, more common are late-onset changes occurring after radiation therapy has been finished.

The changes seen are epithelial lesions such as atrophy, necrosis, followed by regeneration with cellular atypia, metaplasia, and preneoplastic proliferations [9, 10]. More commonly seen in routine evaluation is fibrinous exudation, necrosis, and fibrosis – not only the tumor but also lung stroma. Included in these fibrotic reactions are also blood vessels. These will show endothelial necrosis, thrombosis, and capillary rupture. Predominantly affected are small vessels. In medium-sized blood vessels, neointimal proliferation, fibrinoid necrosis, thrombosis, or acute arteritis can be seen (Fig. 14.10). Damage in large vessels is less common. Some other organ lesions are veno-occlusive liver disease and permanent bone marrow hypoplasia or aplasia.

Within the fibrotic changes seen in the lung are diffuse fibrosis involving the whole irradiated area and scar-like fibrosis [10, 11]. Pulmonary damage after radiotherapy is typically characterized by an initial alveolar inflammation followed by chronic fibrosis. In an experimental study, changes in lung architecture were the earliest

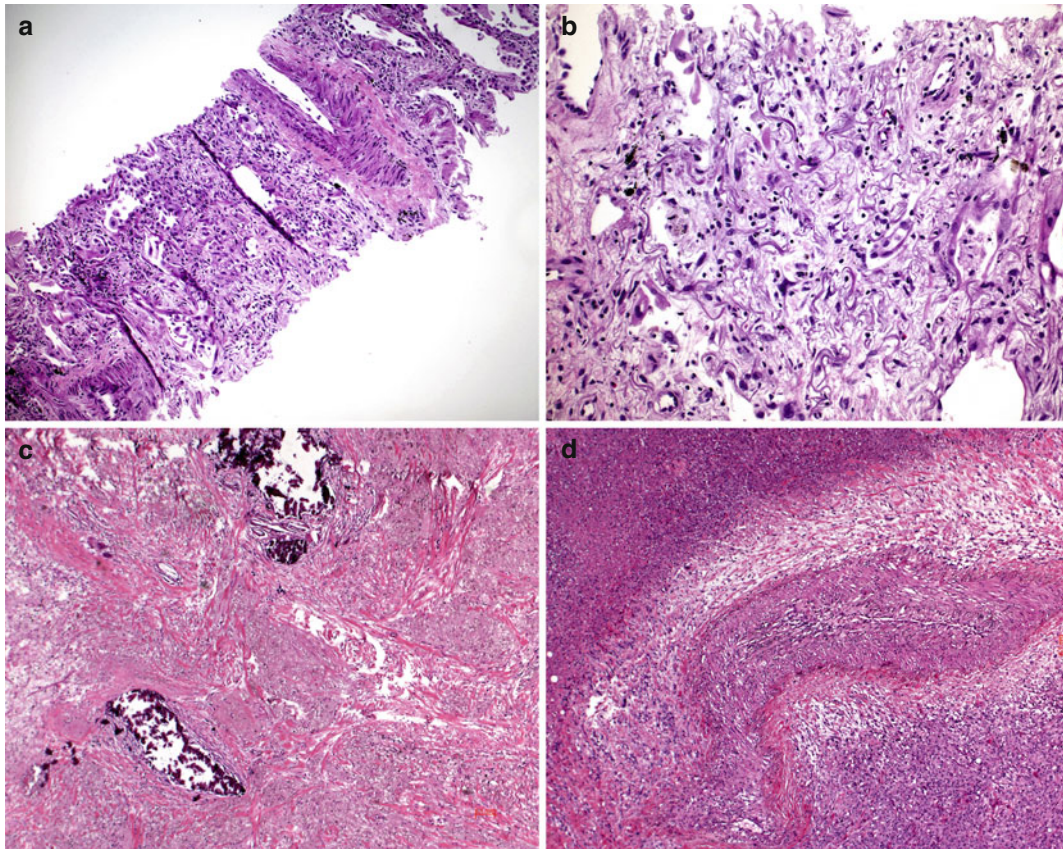

Fig. 14.10 Radiation-induced lung injury. In (**a**, **b**) a transthoracic core needle biopsy showed loose fibrosis with many broken elastic fibers, dilated small blood vessels, and few bizarre mesenchymal cells. In (**c**, **d**) calcification, necrosis, and a vasculopathy is seen, which is quite typical for radiation: the lumina of arteries are occluded or extremely narrowed with degeneration of elastic fibers, loose fibrosis, and almost no cellular infiltration. H&E, ×50 and 100

findings in this experimental irradiation in mice [10]. Another constant finding after radiation therapy is organizing pneumonia with intra-alveolar granulation tissue [12].

References

1. Beinert T, Binder D, Stuschke M, Jorres RA, Oehm C, Fleischhacker M, Sezer O, Mergenthaler HG, Werner T, Possinger K. Oxidant-induced lung injury in anticancer therapy. Eur J Med Res. 1999;4:43–53.
2. Buckpitt A, Boland B, Isbell M, Morin D, Shultz M, Baldwin R, Chan K, Karlsson A, Lin C, Taff A, West J, Fanucchi M, Van Winkle L, Plopper C. Naphthalene-induced respiratory tract toxicity: metabolic mechanisms of toxicity. Drug Metab Rev. 2002;34:791–820.
3. Cohen GM. Pulmonary metabolism of foreign compounds: its role in metabolic activation. Environ Health Perspect. 1990;85:31–41.
4. Dinsdale D. Lung injury: cell-specific bioactivation/deactivation of circulating pneumotoxins. Int J Exp Pathol. 1995;76:393–401.
5. Garrido M, O'Brien A, Gonzalez S, Clavero JM, Orellana E. Cryptogenic organizing pneumonitis during oxaliplatin chemotherapy for colorectal cancer: case report. Chest. 2007;132:1997–9.
6. Gupta S, Mahipal A. Fatal pulmonary toxicity after a single dose of cyclophosphamide. Pharmacotherapy. 2007;27:616–8.
7. Kameda H, Okuyama A, Tamaru J, Itoyama S, Iizuka A, Takeuchi T. Lymphomatoid granulomatosis and diffuse alveolar damage associated with methotrexate therapy in a patient with rheumatoid arthritis. Clin Rheumatol. 2007;26:1585–9.
8. Myers J, El-Zammar O. Pathology of drug-induced lung disease; In: Katzenstein AL. Surgical pathology of non-neoplastic lung disease. Philadelphia, London,

Toronto, Montreal, Sydney, Tokyo: Saunders Elsevier; 2006. pp 81–111.
9. Fajardo LF. The pathology of ionizing radiation as defined by morphologic patterns. Acta Oncol. 2005;44:13–22.
10. Downing L, Sawarynski KE, Li J, McGonagle M, Sims MD, Marples B. A simple quantitative method for assessing pulmonary damage after x irradiation. Radiat Res. 2010;173:536–44.
11. Faruqi S, Giuliani ME, Raziee H, Yap ML, Roberts H, Le LW, Brade A, Cho J, Sun A, Bezjak A, Hope AJ. Interrater reliability of the categorization of late radiographic changes after lung stereotactic body radiation therapy. Int J Radiat Oncol Biol Phys. 2014;89:1076–83.
12. Crestani B, Kambouchner M, Soler P, Crequit J, Brauner M, Battesti JP, Valeyre D. Migratory bronchiolitis obliterans organizing pneumonia after unilateral radiation therapy for breast carcinoma. Eur Respir J. 1995;8:318–21.

Bronchoalveolar Lavage as a Diagnostic and Research Tool

15

By bronchoalveolar lavage (BAL) a proportion of inflammatory cells are washed out from the lung. The mechanism is still poorly understood. The normal composition of BAL cells is 80–85 % macrophages, up to 15 % lymphocytes, predominantly of T lineage with a balanced helper-suppressor ratio of 1:1, 1–3 % neutrophils, <1 % eosinophils, and <0,1 % mast cells. In children BAL composition is slightly different: normal lymphocyte count is around 10 %, mast cells can be higher (0.5 %), and the other cells are similar in number to adults [1]. Since there exists a macrophage alveolitis, it is necessary to study the phenotype of macrophages. Normally there will be a mixture of small, monocyte-like, and mature larger macrophages; multinucleated and giant cells are absent. In case of macrophage alveolitis, there will be a mixture of immature monocytoid, mature and large reactive cells, as well as multinucleated giant cells – as a response to different diseases, for example, respiratory bronchiolitis. In this chapter, we will not add figures, because BAL examples from different diseases have been added in the respective chapters.

15.1 Where and When Doing BAL?

BAL should be done in all interstitial lung diseases, in infectious pneumonias, and in pneumoconiosis. The method is, however, not very useful to diagnose malignancies, except in situ adenocarcinomas. BAL should be done in the affected segments. A routine BAL from the lingula is most often not diagnostic, unless the lingula is affected too – which is rarely the case!

BAL is a very useful tool to diagnose infectious organisms, as well as foreign substances in case of pneumoconiosis. Organisms can easily be identified on Giemsa stains, and if positive, additional stains such as Gram, Grocott methenamine silver, and Fite can be added; immunostains and in situ hybridization can be performed if necessary. Foreign substances can be seen in H&E stains, can be polarized for a refractile crystalline structure, or can be evaluated for an iron-protein incrustation as in asbestos fibers using Prussian blue stain. With respect to interstitial lung diseases, some show a characteristic pattern, whereas in others the pattern changes with disease activity or resolution.

A lymphocytic "alveolitis" is usually found in sarcoidosis, EAA, and tuberculosis. Whereas sarcoidosis and tuberculosis present as T-helper-dominated alveolitis, in EAA cytotoxic T lymphocytes predominate. But, there are exceptions: under therapy the composition of lymphocytes may change in EAA as well as in sarcoidosis and tuberculosis [2]. Antigen withdrawal in EAA changes the composition as well. And, when a patient with EAA inhales the antigen, the primary response is granulocytic. Especially in the pediatric population, a lymphocytic alveolitis is suggestive for a viral pneumonia [3, 4]. If hemorrhage is additionally present, and atypical looking

© Springer-Verlag Berlin Heidelberg 2017
H. Popper, *Pathology of Lung Disease*, DOI 10.1007/978-3-662-50491-8_15

pneumocytes are seen, viral pneumonia is nearly a firm diagnosis (adenovirus might be suspected).

Granulocytic "alveolitis" is found in UIP, neutrophils predominate, but up to 4 % eosinophils can be present. Eosinophilic alveolitis is seen in Langerhans cell histiocytosis (up to 15 %) and eosinophilic pneumonias, including chronic eosinophilic pneumonia, hypereosinophilic syndrome, and Churg-Strauss syndrome/eosinophilic granulomatosis with polyangiitis (usually >30 %). In allergic asthma and allergic bronchopulmonary mycosis, mucoid impaction type and bronchocentric granulomatosis also eosinophils predominate; however, they will show a more specific pattern, namely, degranulation. This can be highlighted by a Congo red stain, which picks up major basic protein, a granule constituent [2, 5, 6].

At the moment there is no specific pattern known for NSIP, collagen vascular diseases, and most pneumoconiosis. The latter, however, can be diagnosed by the proof of foreign substances [1, 7–10]. But there is a caveat: finding asbestos bodies makes not asbestosis. For the diagnosis you will need the tissue reaction. Human usually inhale foreign substances, which then will show up in BAL. Only the tissue response will clarify, if these inhaled substances act toxic within the lung and causes inflammation with or without fibrosis. In most cases BAL is most useful in combination with histology. Therefore a strong recommendation is to insist on histology. BAL can also assist in evaluating disease activity, response to therapy, etc.

Alveolar proteinosis can be diagnosed in BAL without biopsy (one of the very few diseases!) by the proteinaceous "milky" fluid. By PAS the proteins are heavily stained. The remainder is paucicellular or even devoid of cells [11] (Table 15.1).

15.2 Processing of BAL

Ovoid the first 30–40 ML portions, since they usually contain mucus and bronchial cells. These portions are suitable for culture of microbes. The third and fourth portion is rich in cells from the terminal bronchioles and alveoli.

The first step is assessment of cell types, exclusion of carcinoma cells, and exclusion of infections. Then a BAL cell count has to be performed. At least 300 cells should be counted. This will result in macrophagocytic, granulocytic, eosinophilic, or lymphocytic alveolitis, respectively. In case of a lymphocyte count over 18 % (adults) or 15 % (children), these lymphocytes are immunotyped (Fig. 15.1). The minimal investigation should differentiate between B and T lymphocytes and natural killer cells and CD4+ and CD8+ lymphocytes. Additional investigations might focus on subsets of CD4+ and CD8+ cells as well as regulatory T cells.

Table 15.1 Differential cell counts in BAL and diagnostic considerations; this is not a complete list, only the most frequent diseases are listed

Lymphocytosis	Consider epithelioid granulomatosis, lymphoma, interstitial pneumonias, such as LIP, NSIP, etc.	CD4/8 ratio >1.5	Sarcoidosis, tuberculosis
Lymphocytosis	Consider viral or rickettsia pneumonia, epithelioid granulomatosis, lymphoma, interstitial pneumonias, such as LIP, NSIP, etc.	CD4/8 ratio <0.8	EAA, viral infection
Granulocytosis	Bacterial pneumonia, systemic vasculitis		
Eosinophilia	Eosinophils >5 %		Consider Langerhans cell histiocytosis
Eosinophilia	Eosinophils >20 %		Parasitosis, eosinophilic vasculitis (Wegener, Churg-Strauss), ABPA
Eosinophilia	Eosinophils >30 %		Acute and chronic eosinophilic pneumonia, hypereosinophilic syndrome, eosinophilic leukemia, eosinophilic vasculitis, acute parasitic pneumonia
Macrophagocytosis	The following features are required: immature macrophages with monocytoid features, large cells, often multinucleated		RBILD, DIP
Siderophages	Alveolar hemorrhage syndrome	Granulocytes	Consider vasculitis
Siderophages	Alveolar hemorrhage syndrome	No granulocytes	Consider Goodpasture, SLE, and other collagen vascular diseases, hemorrhagic pneumonia (viral), idiopathic hemosiderosis
Lymphocytosis and granulocytosis[a]	Consider interstitial pneumonia (UIP, NSIP, OP), vasculitis (Wegener/GPA)	Either type of T lymphocytes can occur	
Lymphocytosis and eosinophilia	Allergic diseases, systemic vasculitis, Langerhans cell histiocytosis, drug reactions		

[a]Granulocytic "alveolitis" is found in several interstitial pneumonias, for example, also UIP; however, most data on BAL in UIP dates back to a period, when the differentiation of UIP, NSIP, and others was not clear. Up to 4 % eosinophils can be present and are regarded as a worse prognostic sign. Most probably neutrophils in UIP might be a sign of exacerbation, such as infectious pneumonia overlaying UIP in late stages. At the moment there is no specific pattern known for NSIP, collagen vascular diseases, and most pneumoconiosis. The latter, however, can be diagnosed by the proof of foreign substances. But there is a caveat: finding asbestos bodies makes not asbestosis. For the diagnosis you will need the tissue reaction. We all inhale foreign substances, which than will show up in BAL

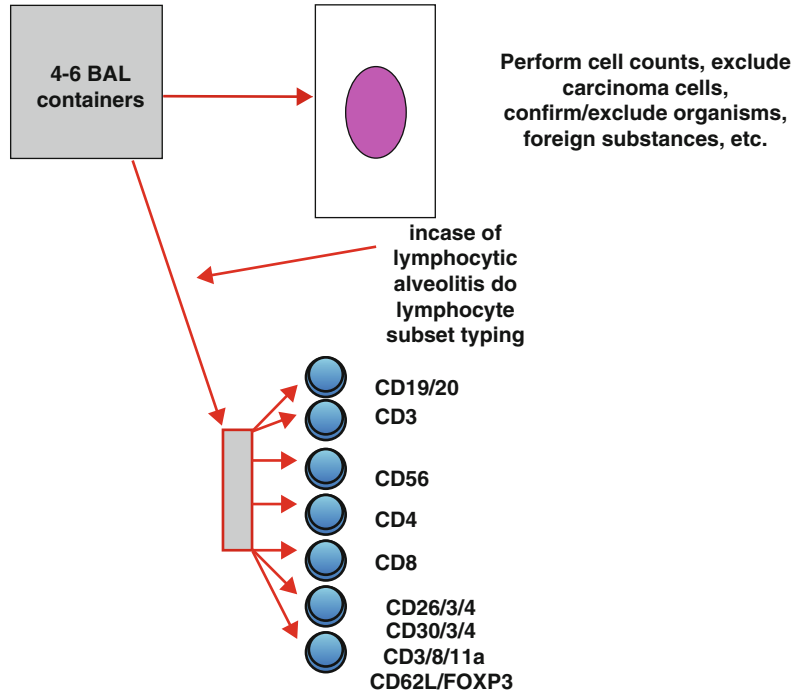

Fig. 15.1 Schema how to process BAL specimen. After performing cell counts and evaluating the stained slides, a decision is made, if a lymphocyte subtyping is necessary; immunotyping for T and B lymphocytes as well as NK cells, followed by subtyping T cells into CD4+ and CD8+ lymphocytes, are required. Additional profiles as shown here are not required for diagnostic purposes but may be done for further insight into a lymphocyte-dominated inflammatory process

References

1. Popper H, Pongratz M. Value and indications for bronchoalveolar lavage combined with transbronchial lung biopsy. Wien Klin Wochenschr. 1987;99:848–55.
2. Wells AU. The clinical utility of bronchoalveolar lavage in diffuse parenchymal lung disease. Eur Respir Rev. 2010;19:237–41.
3. Message SD, Johnston SL. The immunology of virus infection in asthma. Eur Respir J. 2001;18:1013–25.
4. Conron M, Bondeson J, Pantelidis P, Beynon HL, Feldmann M, DuBois RM, Foxwell BM. Alveolar macrophages and T cells from sarcoid, but not normal lung, are permissive to adenovirus infection and allow analysis of NF-kappa b-dependent signaling pathways. Am J Respir Cell Mol Biol. 2001;25:141–9.
5. Schnabel A, Reuter M, Biederer J, Richter C, Gross WL. Interstitial lung disease in polymyositis and dermatomyositis: clinical course and response to treatment. Semin Arthritis Rheum. 2003;32:273–84.
6. Meloni F, Caporali R, Marone Bianco A, Paschetto E, Morosini M, Fietta AM, Patrizio V, Bobbio-Pallavicini F, Pozzi E, Montecucco C. BAL cytokine profile in different interstitial lung diseases: a focus on systemic sclerosis. Sarcoidosis Vasc Diffuse Lung Dis. 2004;21:111–8.
7. Forni A. Bronchoalveolar lavage in the diagnosis of hard metal disease. Sci Total Environ. 1994;150:69–76.
8. Michetti G, Mosconi G, Zanelli R, Migliori M, Gaffuri G, Villa R, Michetti L. Bronchoalveolar lavage and its role in diagnosing cobalt lung disease. Sci Total Environ. 1994;150:173–8.
9. Kelleher P, Pacheco K, Newman LS. Inorganic dust pneumonias: the metal-related parenchymal disorders. Environ Health Perspect. 2000;108 Suppl 4:685–96.
10. Ameen M, Ahmad I, Rahman Q. Pulmonary toxicity of dust generated during weaving of carpets. Hum Exp Toxicol. 2002;21:667–74.
11. Honda Y, Kuroki Y, Matsuura E, Nagae H, Takahashi H, Akino T, Abe S. Pulmonary surfactant protein D in sera and bronchoalveolar lavage fluids. Am J Respir Crit Care Med. 1995;152:1860–6.

Lung Transplantation-Related Pathology

16

Fiorella Calabrese

Lung transplantation-related pathology includes a large box of disorders such as (a) explant pathology, (b) perioperative allograft pathology, (d) rejection (acute and chronic), (e) infections, and (f) tumors.

In all these settings, the pathologist plays a key role for final diagnostic characterization.

16.1 Explant Pathology

Lung transplantation has become an accepted modality of treatment for several end-stage pulmonary diseases that can be categorized in three main groups. These are *obstructive*, *restrictive*, and *vascular diseases*, the latter including both primary and secondary causes. The study of native lungs represents a unique opportunity to carefully study whole lungs without the superimposed agonal complications seen in autopsy specimens. The availability of fresh lung samples allowed a lung biobank to be set up, a valuable source for research into a range of pulmonary diseases [1]. Diagnostic characterization of lung diseases prior to transplantation has often been made on clinical and radiological data. Examination of the explanted lungs often permits a more accurate diagnosis and represents an audit of thoracic medical practice. A review of explanted lungs over a long period (10 years and 12 years) performed by two European lung transplant centers (Papworth, UK, and Padova, IT) reported important findings [2, 3]. Both centers reported significant discrepancies between referral and pathologic diagnoses, some of them with significant impact on recipient management. In the Padova experience, the rate of major discrepancies was mainly detected in the group of interstitial lung diseases (ILDs), mainly in those cases without a pretransplant biopsy diagnosis. Incorrect histological pretransplant diagnoses could be due to a truly difficult morphologic characterization of ILDs, performed late in the course of the disease often obtaining insufficient samples with frequently fading histopathologic markers. Another important reason is that some patients with ILDs were not investigated in the transplant unit but in hospitals without specific experience in this field. A multidisciplinary specialist approach and experience in the diagnosis of ILDs are considered mandatory for accurate diagnosis [4]. An important step to improve the accuracy of referral diagnosis is that every lung biopsy should be reviewed by skilled pathologists of transplant centers at the time of assessment. If necessary an additional biopsy should be planned if permitted by the patient's clinical conditions [2, 3].

16.1.1 Obstructive Diseases

The principal end-stage lung diseases of this group include *cystic fibrosis*, *bronchiectasis*, and *emphysema*.

Cystic fibrosis: Life expectancy in cystic fibrosis (CF) has improved substantially over the last

© Springer-Verlag Berlin Heidelberg 2017
H. Popper, *Pathology of Lung Disease*, DOI 10.1007/978-3-662-50491-8_16

75 years, with a median predicted survival now approaching 40 years; however CF and non-CF bronchiectasis are the most important chronic suppurative diseases requiring lung transplantation, usually bilateral lung transplantation. The availability of stored explanted CF lungs has significantly supported research into pathogenesis, providing also detailed histopathological reports. CF is caused by mutations in the gene encoding the CF transmembrane conductance regulator (CFTR) protein [5]; however, the pathophysiology of CF lung disease remains incompletely understood. In particular the contribution of inflammation, airway remodeling, and other factors remain undefined. A better knowledge of the disease in particular the true onset (usually it begins before symptoms) is extremely important for suggesting new preventions and treatments. The lack of an animal model that mirrors CF in humans has delayed progress in discovering the origins of the lung disease [6]. Lung disease such as that in humans does not develop in mice with *cftr* mutations, even if new animal models have recently been successfully generated [7]. Interesting findings coming from the study of explanted lungs are now changing the pathogenetic view. Fibro-obliterative processes either isolated to the airways, i.e., obliterative bronchiolitis, or as a part of organizing pneumonia of a bronchiolitis obliterans-organizing pneumonia pattern are frequently detected. This has renewed the pathogenesis of the disease with more interest in the small airways instead of large airways, which has been the main area of clinical and pathologic interest. Other important data frequently detected from careful morphological studies is the presence of emphysema, until recently considered minimal [8, 9]. Mets et al. assessing by morphometry explanted lungs of 20 CF patients and found that emphysema is common and age related [10]. Emphysema might become an increasingly important disease component in the aging CF population. This finding appears of particular importance due to the fact that life expectancy of CF patients has dramatically increased in the last decades.

Other associated pathologic lesions that can be detected in end-stage CF and *non*-CF *bronchiectasis* lungs are *Aspergillus* or mycobacterial infections and neuroendocrine lesions (i.e., carcinoids and tumorlet); both lesions are important and should be described in the diagnostic report for more careful monitoring of recipients.

16.1.1.1 Emphysema

Emphysema/chronic bronchitis with or without alpha-1-antitrypsin (AAT) deficiency is a common indication for lung transplantation. Unexpected findings have been found in explanted lungs such as asthma lesions and infective complications, the latter with important implications in the remaining native lung when a single lung procedure is used [2, 3]. New discoveries have recently changed the pathogenesis of the disease: the importance of inflammatory response has been highlighted, inviting a broader look at the possible involvement of the immune system in the pathogenetic events of chronic obstructive pulmonary disease [11]. Emerging evidence has emphasized the role of adaptive immune responses, possibly with an autoimmune component. The study of emphysematous native lungs detected many stigmata of autoimmune disease such as the consistent presence of B-cell infiltration sometimes aggregate in follicular patterns and the presence of BAFF pathway and cytokines such as interleukin 32 that play a key role in various autoimmune diseases [12–14]. Inflammation is also evident in AAT deficiency-related emphysematous lung. The disease appears far from "burnt out," and the interstitial space, both in irreversibly damaged and less affected areas, shows extensive inflammatory infiltration [12, 15]. The presence of complex cell infiltration even in end-stage disease promotes the development of new treatment strategies for a more effective control of inflammation.

16.1.2 Restrictive Diseases

Among restrictive forms idiopathic pulmonary fibrosis (IPF) represents the most frequent referral end-stage lung disease. IPF, the most common form of idiopathic interstitial pneumonias, is a chronic, progressive, irreversible, and

usually lethal lung disease often occurring in middle-aged and elderly adults (median age at diagnosis 66 years, range 55–75 years) [16]. The annual incidence of IPF is rising and is estimated to be between 4·6 and 16·3 per 100,000 people, and the prevalence is 13–20 cases per 100,000 [17–19]. The main histopathological features of IPF, named usual interstitial pneumonia, is characterized by a heterogeneous appearance with areas of subpleural/paraseptal fibrosis and honeycombing alternating with areas of less affected or normal parenchyma (spatial heterogeneity). Small areas of active fibrosis called fibroblast foci are present in the background of collagen deposition, and they reflect the temporal heterogeneity of the process. Inflammation is usually mild and consists of a patchy lymphoplasmacytic interstitial infiltrate. All these pathologic changes can be also detected in end-stage disease of explant lungs. More inflammation and moreover a temporally uniform distribution of the lesions are present in other interstitial lung diseases (desquamative interstitial pneumonia, nonspecific interstitial pneumonia, acute interstitial pneumonia, hypersensitivity pneumonia, collagen vascular diseases) which should be distinguished from UIP/IPF due to a better responsiveness to steroid treatment, better prognosis, and rarely indication for lung transplantation [19]. Multidisciplinary teams with high expertise and experience have been recommended by several authors to obtain a more correct final diagnosis [5, 18]. In our internal audit, both minor and major discrepancies were found in explanted lungs with a clinical diagnosis of IPF [3]. One of the most important lesions detected in our IPF explanted lungs was the presence of lung cancer; all our recipients with unsuspected neoplasia had a poor posttransplant follow-up (death or disease recurrence).

Today the increased diagnostic sensitivity of noninvasive techniques (such as high-resolution computed tomography scan) particularly if performed in referral centers have significantly reduced the use of lung biopsy [19]. Thus explanted lungs now represent an important tissue source available for any type of research. Many recent views about the IPF/UIP pathogenesis have just come from the study of native lungs. The recent hypothesis of IPF pathogenesis indicates that injured and hyperplastic alveolar epithelial cells are able to release cytokines causing proliferation of fibroblasts/myofibroblasts and deposition of extracellular matrix. Among profibrogenetic cytokines, transforming growth factor β (TGF β) represents the key growth factor which leads to mesenchymal differentiation, myofibroblast infiltration, and proliferation. Interestingly, the molecular pathways aberrantly activated in IPF seem to be the same involved in epithelial-mesenchymal communications occurring in lung development and differentiation [20].

Our experience, studying a large number of IPF native lungs, demonstrated that there is an abnormal epithelial renewal with diffuse signs of morphological changes through variegated cellular alterations, such as hyperplasia, atypia, squamous metaplasia, and various degrees of dysplasia [21, 22]. In particular, hyperplasic lesions and epithelial atypia have often been detected in highly remodeled lung areas as honeycomb.

This area represents a site of high instability at risk of neoplastic transformation, which are more frequently of squamous type [23–30]. Serpin B3/B4, a clade B serpin involved in several pathways including apoptosis/proliferation imbalance, has been found overexpressed in patients with squamous cell carcinoma type of different organs [31–38] and in metaplastic/dysplastic area of IPF lungs. Different works, in vitro and in vivo (both human and animal), have demonstrated a strict influence between serpin B3 and TGF-ß [39, 40]. Apoptosis/proliferation imbalance with a significant gain of epithelial proliferation has recently been demonstrated in bleomycin-induced lung damage using serpin B3 transgenic mice [40]. The overexpression of serpin B3/B4, particularly the isoform B4, in IPF patients may be an important factor in the resistance of injured epithelial cells to apoptosis, thus leading to progressive lesions at high risk of malignant transformation. Interestingly our group found a direct relationship between serpin B3/B4 and TGF-β expression [22, 39]. The ov-serpins have been shown to render cells more resistant to apoptotic cell death, and pro-apoptotic effect of TGF-β might represent a

counterbalancing mechanism leading to accumulation of fibrosis as a secondary effect. Epithelial mesenchymal transition, typically ascribed to TGF-ß [41], has also been related to serpin B3 [42]. The study has provided evidence that the antiprotease activity of serpin could be implicated in the TGF-ß induction.

Another important aspect extensively explored in lung tissue sampled from IPF native lungs concerns the investigation of viral infection as a contributing etiological factor [43]. Several studies have implicated viral infection as a cause of epithelial injury and therefore an important factor in its pathogenesis [44–61]. Among viral agents herpes viruses, in particular Epstein-Barr virus (EBV), have been suggested as principal cofactors (as initiating or exacerbating agents) of fibrotic lung disease, and treatment with ganciclovir has been shown to attenuate disease progression in a subgroup of patients [62]. Our experience demonstrated a different phenotype of virus-positive IPF patients. In particular virus-positive IPF cases showed more pronounced vessel remodeling and a higher mean pulmonary arterial pressure (mPAP) and significantly higher primary graft dysfunction after transplantation. While there is large mechanistic evidence of epithelial herpesvirus-associated alveolar injury, the effect of these viruses on the pulmonary vasculature in IPF merits investigation. A deeper knowledge of viral-induced pathways in endothelial cells could give new insights for a targeted therapeutic approach to pulmonary hypertension, one of the most important IPF complications.

16.1.3 Vascular Disease (Pulmonary Hypertension)

Pulmonary hypertension, either primary or secondary origin, is considered an important indication for lung transplantation (with and without the heart). Patients with pulmonary hypertension secondary congenital heart disease and patients with end-stage thromboembolic pulmonary hypertension are usually diagnosed on native lungs at transplantation. However chronic thromboembolic pulmonary hypertension is now rarely considered an indication for transplantation being treated surgically by pulmonary thrombectomy. There is an increasing focus on the cellular and molecular pathogenesis of idiopathic pulmonary hypertension. Animal models do not reproduce the morphological features of human pulmonary hypertension, thus it is mandatory that the human tissue available through transplantation is adequately studied. Many studies have given significant improvement in the understanding of pathogenesis and evolution of plexiform lesions leading to better clinical staging and more effective treatment strategies [63]. Explanted lungs were also successfully used for several studies focusing on key biomarkers such as the expression of genes for bone morphogenetic protein receptor type II (BMPR2) and TGF-β type I and II receptors [64]. The group of Papworth studying explanted lungs with primary pulmonary hypertension demonstrated that TGF-β R1 and RII co-localized to vascular endothelium in the normal pulmonary circulation, with reduced expression of TGF-β RII subtype in plexiform and intimal lesions of primary pulmonary hypertension [64]. Evidence is emerging that germline and/or somatic mutations in key cell growth regulatory genes play a role in the development of idiopathic sporadic and familial pulmonary hypertension [65]. Our group studied lungs with pulmonary hypertension (primary and secondary forms) and demonstrated increased intrapulmonary endothelial progenitor cells (EPC), suggesting that these cells may contribute to vascular remodeling [66]. The localization of specific cell markers and the identification of EPC are very likely to have an impact on therapy for both pre- and posttransplant conditions.

16.2 Perioperative Complications

These include surgical complications (anastomotic airway and vascular complications) and ischemia reperfusion injury. The most recent International Society of Heart-Lung Transplantation (ISHLT) registy, reports early

graft failure in 2,3 % of recipients with a significant high 30-day rate mortality mainly due to perioperative complication [67]. Anastomotic airway complications may be characterized by formation of granulation tissue which sometimes may appear as exuberant polypoid granulation tissue. Superimposed infection, including fungi and bacteria, can often complicate the healing. Ischemia/reperfusion injury occurs in 10–20 % of patients. Transbronchial biopsies of the recently implanted lung may show a number of minor morphological changes such as peribronchiolar and perivascular edema, lymphatic dilatation, and neutrophil infiltration. In cases with important ischemia/reperfusion injury, the biopsy shows diffuse alveolar damage and organizing pneumonia whose features should be distinct by hyperacute lung rejection. The absence of perivascular and airway mononuclear cell infiltrates distinguishes it from acute rejection.

16.3 Lung Allograft Rejection

In the ISHLT 2012 report, lung transplantation-related pathology, specifically acute rejection, was reported to affect 34 % of lung transplant recipients within the first postoperative year. In the revised working formulation for the standardization of nomenclature in the diagnosis of rejection, the key role of biopsy for final diagnosis of rejection was again emphasized, while the most sensitive tool for infection is bronchoalveolar lavage usually collected at the same time of biopsy [68]. Adequacy of specimens (at least five slices of well-expanded alveolated lung parenchyma) and histological processing (three-level serial section of paraffin block and additional special stains for microorganism and collagen deposition) have been reported in the revised international grading scheme as general recommendations to reach a more sensitive diagnosis.

Lung allograft rejection is classified as hyperacute, acute, and chronic and affects the vasculature and the airways. The rejection process may involve humoral/antibody-mediated and cell-mediated immune mechanisms.

16.3.1 Hyperacute Lung Rejection

Hyperacute rejection is an early complication of transplantation, caused by the presence in the recipient of preformed donor-directed antibodies. It occurs within 24–48 h of graft implantation and should be suspected when the lungs become markedly congested and edematous with the production of copious frothy bloodstained sputum from the bronchial orifice of the graft. The histologic features of hyperacute rejection include diffuse alveolar damage, alveolar hemorrhage, interstitial pneumonia, and vasculitis. As only a few well-documented cases of hyperacute rejection of the lung have recently been reported in the literature [69, 70], it was not included in the working formulation. Ancillary techniques are useful for the final diagnosis: immunofluorescence may show IgG and complement (C3d and C4d) deposition in the alveolar septa. Immunohistochemistry for C4d should be interpreted as positive only when strongly stained deposition are detected.

16.3.2 Acute Rejection (Grade A, B)

The diagnosis is based on the presence of perivascular or airway inflammatory infiltrates that are composed mainly of activated lymphocytes, few eosinophils, neutrophils, and plasma cells (grade A). Lymphocytic bronchiolitis can also be observed and is characterized by bronchiolar inflammatory cell infiltrates with epithelial cell ulceration in severe forms (grade B). The histologic grade is based on the intensity and distribution of the infiltrate (Table 16.1; Fig. 16.1a–d).

16.3.3 Chronic Rejection (Grade C and D)

Chronic rejection is primarily manifested as bronchiolitis obliterans (grade C). It is the most significant complication limiting long-term survival, affecting up to 50 % of patients 3 years after transplantation. Previous episodes of acute

Table 16.1 Revised working formulation for the classification of pulmonary allograft rejection [68]

Rejection	Grading	Histological features
Acute rejection	*Grade AX* Ungradable	No alveolated lung tissue or no arteriole/venule
	Grade A0 No acute rejection	Parenchyma without perivascular inflammation
	Grade A1 Minimal acute rejection	Perivascular infiltrates forming an incomplete or a 2-or 3-cell-layer-thick cuff. Rare eosinophils; endothelialitis usually absent
	Grade A2 Mild acute rejection	More frequent perivascular infiltrates consisting of lymphocytes, macrophages, eosinophils, and endothelialitis
	Grade A3 Moderate acute rejection	Dense perivascular mononuclear cell infiltrates with frequent foci of endothelialitis and extension into alveolar walls; eosinophils and neutrophils often present
	Grade A4 Severe acute rejection	Diffuse perivascular, interstitial and alveolar infiltrates; pneumocyte damage, endothelialitis, intra-alveolar necrotic epithelial cells, hyaline membrane hemorrhage, and neutrophils
Lymphocytic bronchiolitis	*Grade BX* Ungradable	Insufficient sample, artifact, infection
	Grade B0 No lymphocytic bronchiolitis	No evidence of airway inflammation
	Grade B1R Low-grade small airway inflammation	Few lymphocytes and plasma cells within submucosa, rare eosinophils
	Grade B2R High-grade small airway inflammation	More inflammation with greater numbers of eosinophils and plasmacytoid cells. Epithelial damage and marked intraepithelial lymphocytes
Chronic airway rejection	*Grade C0* No airway rejection	No evidence of obliterative bronchiolitis
	Grade C1 Airway rejection	Asymmetric or concentric/partial or complete airway obstruction
Chronic vascular rejection	*Grade D* Vascular rejection	Presence of fibrointimal thickening with/without inflammation
	Grade D0 No vascular rejection	No evidence of vascular thickening (atherosclerosis)

rejections are the most well-recognized risk factor. Since bronchiolitis obliterans (BO) is a patchy process and diagnostic yield of transbronchial biopsy is low, pulmonary functional tests are considered as more sensitive tools: when the decline is greater than 10 % of baseline, a clinical diagnosis of BO syndrome is made (without pathologic confirmation) and graded from 1 to 3 based on the degree of loss of lung function [71] (Table 16.1; Fig. 16.2a).

Chronic vascular rejection (grade D) is characterized by fibrointimal thickening of arteries and veins, with or without inflammatory infiltrates (Table 16.1; Fig. 16.2b).

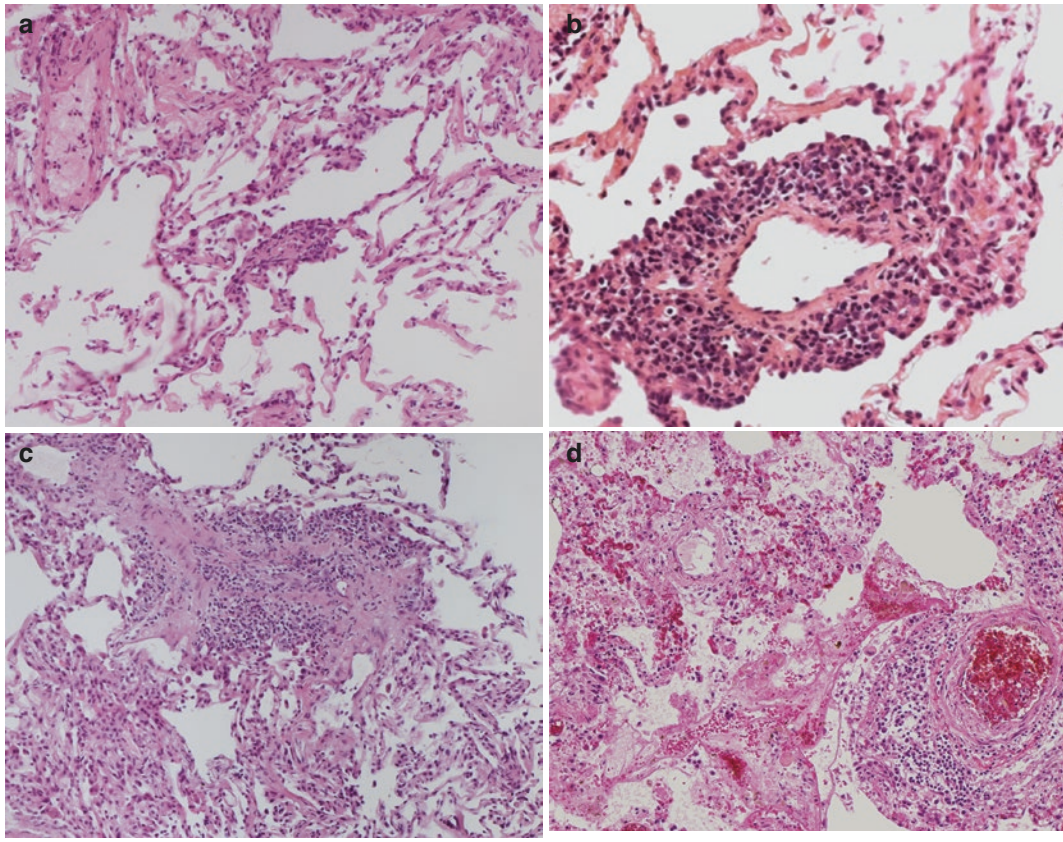

Fig. 16.1 (**a**) Grade A1 minimal acute rejection: a high power view reveals a minimum perivascular mononuclear cell infiltrate with no evidence of endotheliitis, usually occurring in a background of entirely normal lung parenchyma. (**b**) Grade A2 mild acute rejection: a dense perivascular infiltrate with expansion of the adventitial space is seen, but no involvement of alveolar walls. (**c**) Grade A3 moderate acute rejection: a dense perivascular infiltrate with endothelial involvement and extension into adjacent airspaces is well visible. The inflammatory infiltrate consists of small and large lymphocytes, macrophages, and polymorphs. (**d**) Grade A4 severe acute rejection: a section from an autopsy case demonstrating perivascular infiltrate associated with hemorrhage and edema with alveolar capillary congestion and hyaline membrane formation. Perivascular distribution is not a feature of diffuse alveolar damage due to reimplantation/perfusion injury, infection, hypovolemic shock, or other causes of posttransplantation diffuse alveolar damage.

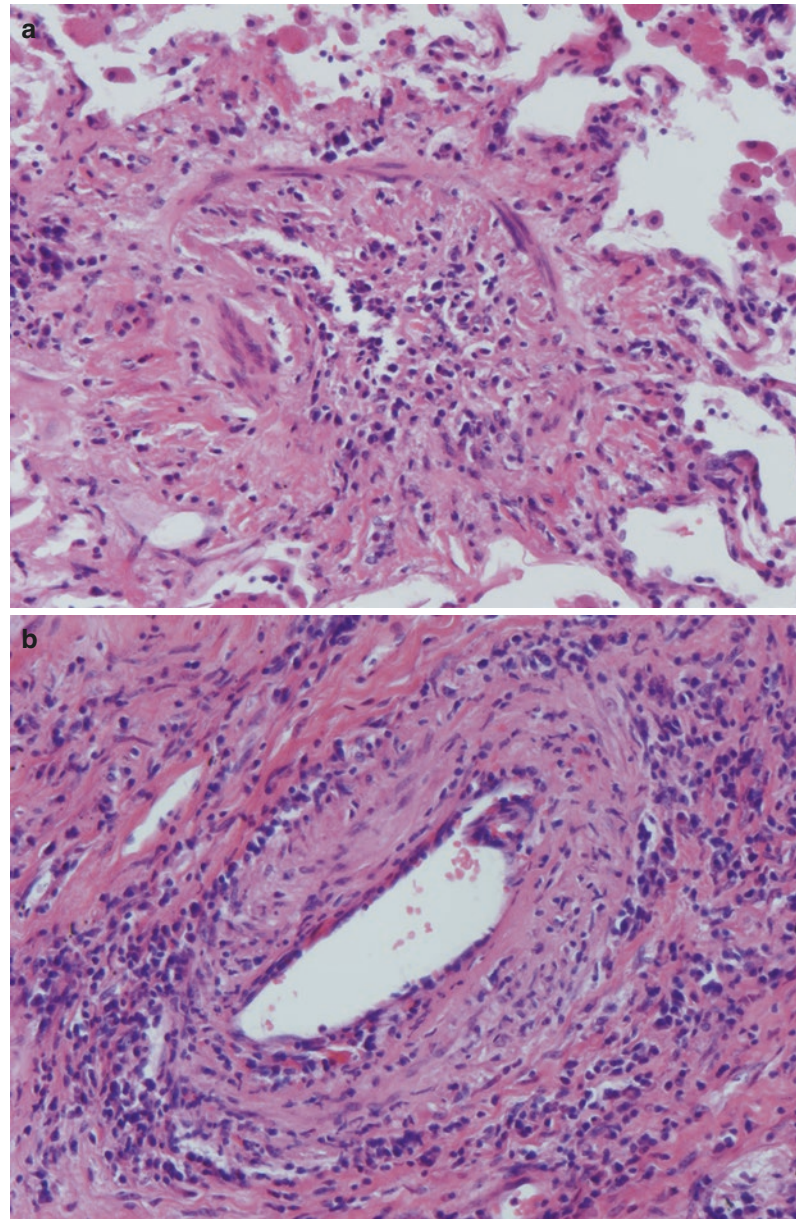

Fig. 16.2 (**a**) Grade C1 obliterative bronchiolitis: little cellular infiltrate and marked concentric fibrotic narrowing of the bronchiolar lumen is seen. The smooth muscle in the wall is interrupted by the bronchiolar fibrosis. (**b**) Grade D chronic vascular rejection: a section from an autopsy case of chronic lung allograft dysfunction showing a thickened vessel with massive fibrointimal fibrosis

16.3.4 Emerging Immunological Lesions

16.3.4.1 Antibody-Mediated (Humoral) Rejection

Emerging data suggest that humoral immunity plays an important and previously underestimated role in lung rejection and chronic allograft dysfunction. Antibody-mediated rejection (AMR) is believed to be triggered by the binding of donor-specific antibodies to the lung microvasculature. Currently AMR is a widely accepted and well-defined form of rejection in the fields of kidney and heart transplantation. A summary statement on the pathology of AMR following lung transplantation has recently been proposed [72]. However, the morphological aspect, including histology and immunohistochemistry in the lung,

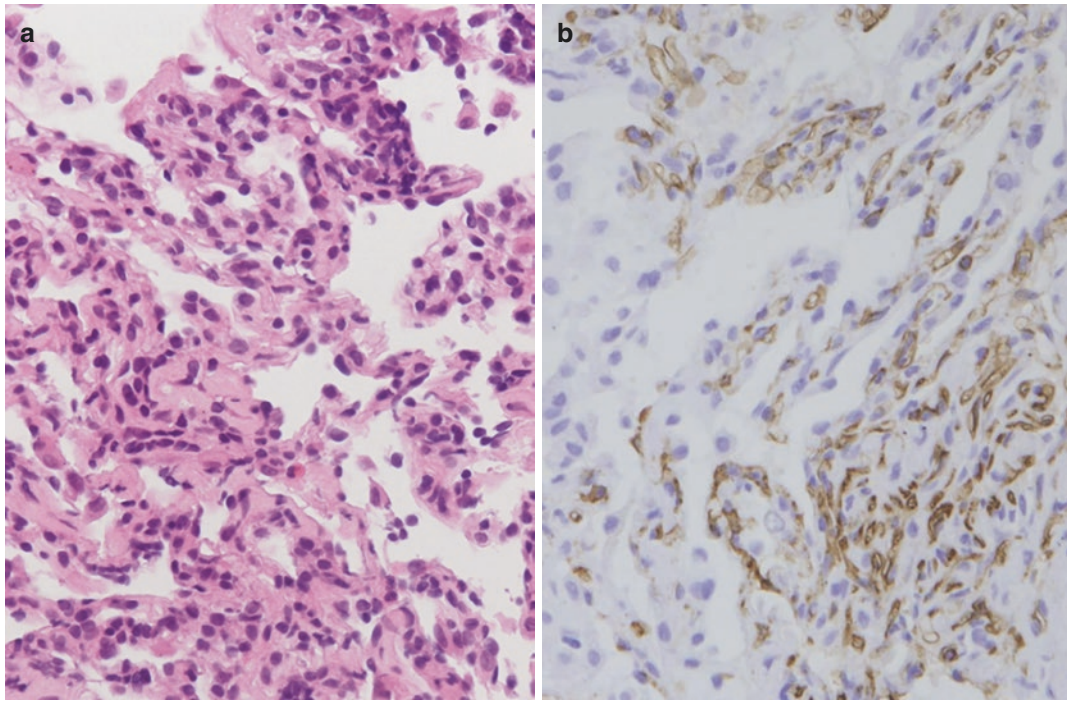

Fig. 16.3 (**a**, **b**) Antibody-mediated rejection: histological section showed widening of interstitial spaces with mixed inflammatory cell infiltration (**a**), immunohistochemistry shows a crisp lining of C4d deposition along the endothelial cells of capillaries and small vessels (**b**). The patient had high level of donor-specific antibody

defies accurate characterization. The histopathology criteria of lung AMR were not addressed in the 1990 and 1996 ISHLT classifications of lung allograft rejection and were not clearly defined in the revised 2007 ISHLT classification [68]. The 2012 statement from the Pathology Council reported "Non-specific patterns of injury that can also be seen in disorders such as severe acute cellular rejection, infection (especially bacterial and viral), graft preservation injury and drug reaction." Reported AMR histological findings such as neutrophilic capillaritis, arteritis, and diffuse alveolar damage are so broad that it is difficult to diagnose AMR. The significance of complement 4d (C4d) deposition in the diagnosis of AMR in lung allografts is controversial. A potential cause may be the problematic reproducibility of immunostaining. A multidisciplinary approach seems to be the best way to diagnose AMR in lung allograft biopsies (Fig. 16.3a, b).

2) Restrictive allograft syndrome (RAS): RAS is a novel form of chronic lung allograft dysfunction after lung transplantation. Although BO syndrome, characterized clinically by irreversible obstructive deficits in pulmonary function tests, remains the major cause of late mortality, recently a distinct form of chronic lung allograft dysfunction demonstrating restrictive pulmonary function decline has been reported with an estimated frequency of 25–35 % of chronic lung allograft dysfunction [73, 74]. Pleuroparenchymal fibroelastosis is a major histopathologic correlate of restrictive allograft syndrome. Idiopathic pleuroparenchymal fibroelastosis as a distinct entity was first proposed by Frankel et al. in 2004 [75]. It is characterized radiologically by features suggestive of a chronic interstitial pneumonia with upper lobe predominance. From histological aspects it is characterized by pleural fibrosis and parenchymal fibroelastosis in a predominantly subpleural distribution, with a sharp demarcation between fibroelastotic and unaffected lung parenchyma, and with the presence of fibroblastic foci at this interface (Fig. 16.4).

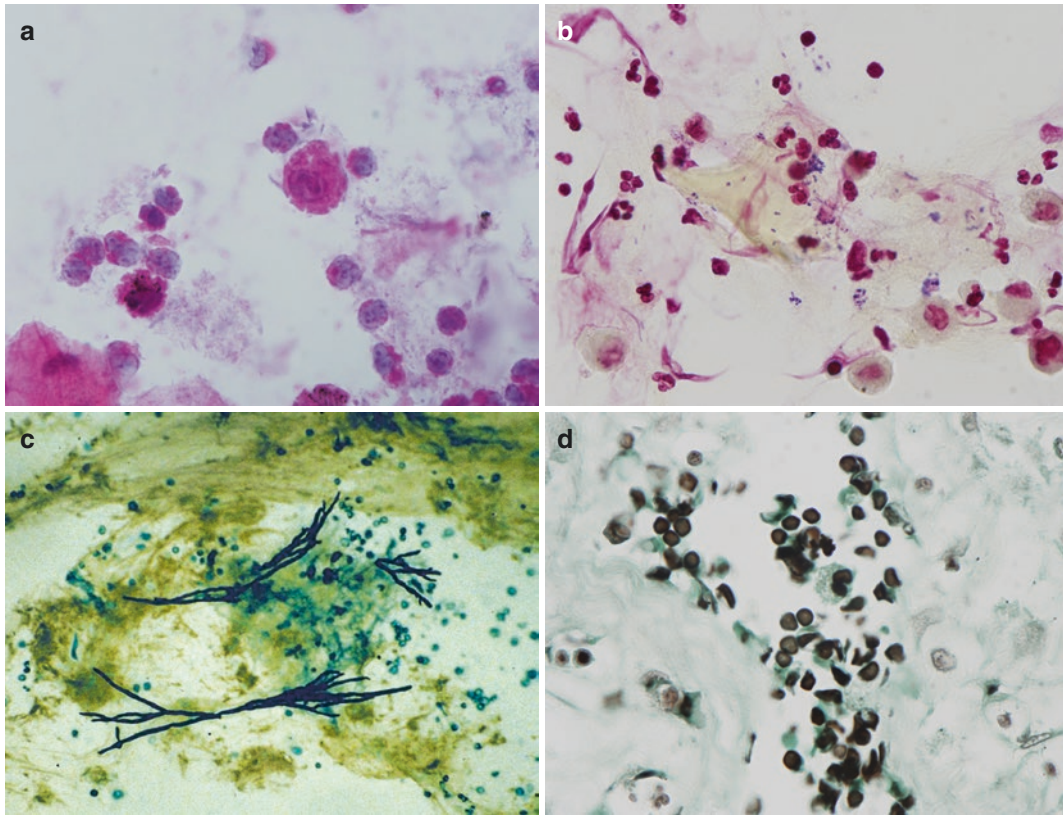

Fig. 16.4 (**a**) *Cytomegalovirus* infection: bronchoalveolar lavage demonstrates viral inclusion of CMV in the center of field. (**b**) Bacterial infection: the lavage shows necrotic debris and polymorphs in the background. Gram staining reveals numerous gram-positive bacteria. (**c**) *Aspergillus* infection: Grocott silver stain shows the pathognomonic features characterized by dichotomous branching and septate, broad, and regular hyphae. (**d**) *Pneumocystis carinii* infection: bronchoalveolar lavage shows cluster of microorganism cysts

Pleuroparenchymal fibroelastosis in restrictive allograft syndrome patients is often present concurrently with features of diffuse alveolar damage as well as BO [76]. The etiologic factors underlying restrictive allograft syndrome and pleuroparenchymal fibroelastosis remain uncertain. Immunological mechanism (autoantibodies) and/or infections have been suggested to play a contributing role in the development and progression of the lesion [77, 78].

16.4 Infections

Lung transplant recipients are at risk of developing infections that can be bacterial, viral, or fungal. In the context of infection, the pathologist should take into consideration several aspects, the most important include (1) differentiation of acute rejection from viral infection; (2) differentiation between colonization, subclinical infection, and significant clinical disease; and (3) identification of infections with histological patterns that may differ from those observed in the non-transplanted, immunocompetent patient. Bronchoalveolar lavage is the best tool for more sensitive diagnosis of various forms of infections (Fig. 16.4a–d).

16.4.1 Viral Infection

Cytomegalovirus (CMV) infection is the most important cause of pneumonia. Primary infec-

tion, through blood transfusion or transmitted in the graft, may cause very severe disease in the allograft with systemic spread. Reactivation in a seropositive recipient may cause clinical disease that is less severe than in seronegative recipients. A prophylactic regimen has significantly reduced the severity and the frequency of CMV pneumonia [79–81]. CMV pneumonia is diagnosed in transbronchial biopsies by finding the classical single intranuclear and multiple small cytoplasmic inclusions in an enlarged cell. Treated patients may show more frequently smudged eosinophilic inclusions which may be difficult to identify as CMV. In these cases the use of in situ hybridization or immunohistochemistry against immediate-early antigen could be extremely useful [82, 83]. Routine histology with immunohistochemistry and/or in situ hybridization shows however low sensitivity in CMV detection often leading to underdiagnosis and/or delayed diagnosis of CMV pneumonitis. Increasing interest has focused on more sensitive molecular detection techniques both applied to transbronchial biopsy and overall to bronchoalveolar lavage. Although the critical threshold of viral load (4.6×10^4 and 5.0×10^5) is not yet completely validated, several works have proposed CMV quantification in bronchoalveolar lavage to have a higher sensitivity in the differentiation of patients with active CMV disease from latently infected patients, and they suggested that molecular quantitative assay on bronchoalveolar lavage should replace traditional culture and also CMV DNA assay in the blood [84–86]. The use of these ancillary techniques is overall useful to differentiate histological changes from acute rejection particularly when both diseases coexist and inclusions are sparse. Indeed CMV is known to be associated with an increased incidence of allograft dysfunction, possibly through upregulation of MHC class I and class II antigens in alveolar cells [87, 88]. In severe infection, diffuse alveolar damage is the prevalent histological finding. Adenovirus infection is more common in children, and scattered adults and pediatric patients develop serious pneumonias due to other respiratory viruses (e.g., respiratory syncytial virus, rhinovirus, parainfluenza, influenza).

16.4.2 Bacterial Infection

Bacterial infections may manifest as acute bronchitis or bronchopneumonia. Gram-negative infections, in particular those caused by *Pseudomonas* spp., account for about 75 % of bacterial forms. In acute bronchitis there is an important neutrophilic infiltration with mucosal ulceration. As in the normal host, acute pneumonia is recognized by the presence of neutrophils within the alveolar spaces.

16.4.3 Fungal Infections

Fungal infections are less frequent than other infections but may cause serious morbidity, including colonization of bronchiectatic airways, cavitating pneumonia, bronchocentric granulomatosis, invasive infection with mediastinitis, and infection of the airway anastomosis. The fungal species most commonly encountered in lung transplant biopsies are *Aspergillus* and *Candida*. The histopathological findings range from aspergillomas to suppuration with abscess formation, to granulomatous inflammation which may be suppurative. The pathologist should always have a high index of suspicion for fungal infection when these patterns are present. Special stains such as Gomori's methenamine silver can significantly help to highlight the yeast forms.

Pneumocystis carinii infection: *Pneumocystis jirovecii* is now considered a fungus and causes peculiar histological lesions. Pneumonia is now rare in lung transplantation due to chemoprophylaxis. The typical intra-alveolar foamy exudate containing numerous cysts and a mild lymphohistiocytic pneumonitis is rarely found, perhaps due to the fact that immunosuppression in a solid organ transplant recipient is not as profound as in the human immunodeficiency virus (HIV)-positive patient with acquired immune deficiency syndrome (AIDS). The most frequent pattern is characterized by lymphoplasmacytic interstitial pneumonia with scanty exudate and/or granulomatous reaction with no exudate: the cysts are sparse. When a lymphoplasmacytic pattern is present, the perivascular component mimics

acute rejection, and differentiation depends on the identification of microorganisms by using ancillary techniques (special stains, immunohistochemistry, or molecular analysis).

16.5 Tumors

After chronic allograft dysfunction, malignant tumors are the most significant limiting factor for long-term survival [89, 90]. The most frequently observed are squamous carcinoma of the skin and lips, posttransplant lymphoproliferative diseases (PTLD), lymphomas, Kaposi's sarcoma, and genitourinary carcinomas. Predisposing factors include immunosuppressive treatment, ultraviolet irradiation in skin tumors, and activation/infection of oncogenic viruses such as Epstein-Barr virus (EBV) human papilloma virus (HPV), and human herpesvirus.

PTLDs: occur in 3–5 % of lung transplant recipients with frequent involvement of the allograft, as one or multiple nodules [91]. The majority are associated with primary or reactivated EBV infection and appear to represent EBV-induced B-cell or rarely T-cell proliferations. Approximately 20 % of PTLDs are EBV negative. The classification by the World Health Organization (WHO) is now widely accepted and applied in this setting [92] (Table 16.2).

Table 16.2 PTLD (WHO classification 2012)

Early lesion
Reactive plasmacytic hyperplasia
Infectious mononucleosis-like lesion
PTLD – polymorphic
Polyclonal (rare)
Monoclonal
PTLD – monomorphic
B-cell neoplasms
Diffuse large B-cell lymphoma
Burkitt lymphoma; plasma cell myeloma
Plasmacytoma-like lesion
Other
T-cell neoplasms
Peripheral T-cell lymphoma, not otherwise cathegorized
Hepatosplenic T-cell lymphoma
Other
Classic Hodgkin lymphoma-type PTLD

The final diagnosis should include routine morphology, immunophenotyping, and overall molecular analysis both for EBV detection (mRNA EBER) and for lymphocyte clonal gene rearrangement. A complete investigation and final diagnosis may be difficult on small biopsy due to the frequent crush artifact in small-sized biopsy and the frequent necrosis of pulmonary PTLD due to angioinvasion. Thus surgical biopsy is strongly suggested for a more correct diagnosis [93].

16.5.1 Other Tumors

After PTLD the most frequently detected tumors are cutaneous in origin as squamous cell carcinomas and premalignant skin lesions often associated to HPV [94, 95]. More recently several authors have suggested that long-term use of voriconazole may be associated with the development of cutaneous squamous cell carcinoma in patients after lung transplant who showed a greater clinical aggressiveness [96]. Other tumors that develop more frequently than in the general population are renal tumors [97, 98] and lung carcinoma [99] which are often discovered in advanced stage. Kaposi's sarcoma (KS) accounts for 5.7 % of these malignancies [100], with the skin being the most commonly affected organ. It primarily affects the skin and can also cause disseminated diseases in different organs. Human herpesvirus 8 (HHV8) and other cofactors (e.g., cytokine-induced growth factors) play an important role in the development of the disease. Although rare, involvement of the allograft can occur [101]. In transplanted patients KS can be often due to reactivation of a latent virus during immunosuppression even though the virus can be transmitted also from donor to recipient [102]. A multicenter longitudinal Italian study performed in a 4,767 recipients demonstrated that the primary predictors of increased risk of KS were male sex, older age, and lung transplantation. Recipients born in southern Italy compared with northern Italy demonstrated a significant 2.2-fold increased risk [103]. From a

histological point of view, the neoplasia appears as a low-grade mesenchymal tumor that involves blood and lymphatic vessels. HHV8 can be often detected both with immunohistochemistry and molecular analysis. The histology is surely the gold standard for the final diagnosis of Kaposi's sarcoma, but when there is graft involvement, there is a considerable risk of major bleeding after biopsy. Open lung biopsy and video-assisted thoracoscopic surgery to obtain large tissue samples are invasive procedures and rarely performed for this indication. The detection of HHV8 DNA in bronchoalveolar lavage may be considered a very useful noninvasive test to confirm suggested Kaposi's sarcoma. The identification of the virus within pathologic tissue is extremely important in lung recipients whose treatment should be changed with tapering of standard immunosuppression and/or switching to other immunosuppressive drugs and overall association of specific antiviral therapy.

16.6 Other Complications

16.6.1 Graft-Versus-Host Disease (GVHD)

GVHD is a rare complication after lung transplantation [104–106]. The transplanted lung contains a significant amount of lymphoid tissue, and a rash, colitis, pancytopenia, and liver dysfunction may suggest that GVHD has developed. The identification of donor lymphocytes both in the blood and in the bronchoalveolar lavage of patients support this possibility. GVHD usually develops early after lung transplantation and usually shows a good response to increased immunosuppression. The GVHD of bone marrow transplantation may cause constrictive bronchiolitis similar to that seen in lung rejection, but in lung transplantation the donor is spared by this complication. Biopsy diagnosis is not easy because the morphological appearance of the skin, the most frequently biopsied site, looks like that of lichenoid drug reaction. The final diagnosis requires the detection of donor and recipient chimerism on HLA typing of peripheral blood lymphocytes.

16.6.2 Disease Recurrence in the Graft

Lung transplantation is performed for a wide range of lung diseases, some of which are associated with extrapulmonary disease and may recur in the allograft. Up to 60 % of recipients transplanted for sarcoidosis have recurrence without clinical impact [107, 108]. Other diseases that can recur in the graft include idiopathic pulmonary hemosiderosis [109], Langerhans cell histiocytosis [110–113], lymphangioleiomyomatosis, desquamative interstitial pneumonia [16, 114], pan bronchiolitis [115], and in an α1-antitrypsin-deficient recipient [116].

16.6.3 Drug Injury

Some immunosuppressive drugs can cause side effect in different organs. Cyclosporine can cause renal damage and rhabdomyolysis, while azathioprine may damage the liver and bone marrow. Sirolimus can cause lung injury, and the principal lesions are lymphocytic interstitial pneumonia, organizing pneumonia, diffuse alveolar hemorrhage, and pulmonary hemorrhage [117–119].

References

1. Calabrese F, Lunardi F, Nannini N. In: Caenazzo L, editor. The role of biobanking in rare diseases. New insights on biobanks. Padova: CLEUP; 2013. p. 67.
2. Stewart S, McNeil K, Nashef SA, Wells FC, Higenbottam TW, Wallwork J. Audit of referral and explant diagnoses in lung transplantation: a pathologic study of lungs removed for parenchymal disease. J Heart Lung Transplant. 1995;14:1173–86.
3. Calabrese F, Alessandrini L, Loy M, Marulli G, Balestro E, Perissinotto E, Valente M, Rea F. Comparison between referral diagnosis of patients requiring transplantation and pathologic diagnosis of native lungs. J Heart Lung Transplant. 2009;28:1135–40.
4. Travis WD, Costabel U, Hansell DM, King Jr TE, Lynch DA, Nicholson AG, Ryerson CJ, Ryu JH, Selman M, Wells AU, Behr J, Bouros D, Brown KK, Colby TV, Collard HR, Cordeiro CR, Cottin V, Crestani B, Drent M, Dudden RF, Egan J, Flaherty K, Hogaboam C, Inoue Y, Johkoh T, Kim DS, Kitaichi M, Loyd J, Martinez FJ, Myers J, Protzko S, Raghu G, Richeldi L, Sverzellati N, Swigris J,

Valeyre D. ATS/ERS committee on idiopathic interstitial pneumonias: an official American Thoracic Society/European Respiratory Society statement: update of the international multidisciplinary classification of the idiopathic interstitial pneumonias. Am J Respir Crit Care Med. 2013;188:733–48.
5. Rommens JM, Iannuzzi MC, Kerem B, Drumm ML, Melmer G, Dean M, Rozmahel R, Cole JL, Kennedy D, Hidaka N. Identification of the cystic fibrosis gene: chromosome walking and jumping. Science. 1989;245:1059–65.
6. Grubb BR, Boucher RC. Pathophysiology of gene-targeted mouse models for cystic fibrosis. Physiol Rev. 1999;79:S193–214.
7. Stoltz DA, Meyerholz DK, Welsh MJ. Origins of cystic fibrosis lung disease. N Engl J Med. 2015;372:351–62.
8. Tomashefski Jr JF, Bruce M, Stern RC, Dearborn DG, Dahms B. Pulmonary air cysts in cystic fibrosis: relation of pathologic features to radiologic findings and history of pneumothorax. Hum Pathol. 1985;16:253–61.
9. Tomashefski Jr JF, Bruce M, Goldberg HI, Dearborn DG. Regional distribution of macroscopic lung disease in cystic fibrosis. Am Rev Respir Dis. 1986;133:535–40.
10. Mets OM, Roothaan SM, Bronsveld I, Luijk B, van de Graaf EA, Vink A, de Jong PA. Emphysema is common in lungs of cystic fibrosis lung transplantation patients: a histopathological and computed tomography study. PLoS One. 2015;10:e0128062.
11. Cosio MG, Saetta M, Agusti A. Immunologic aspects of chronic obstructive pulmonary disease. N Engl J Med. 2009;360:2445–54.
12. Calabrese F, Giacometti C, Beghe B, Rea F, Loy M, Zuin R, Marulli G, Baraldo S, Saetta M, Valente M. Marked alveolar apoptosis/proliferation imbalance in end-stage emphysema. Respir Res. 2005;6:14.
13. Calabrese F, Baraldo S, Bazzan E, Lunardi F, Rea F, Maestrelli P, Turato G, Lokar-Oliani K, Papi A, Zuin R, Sfriso P, Balestro E, Dinarello CA, Saetta M. IL-32, a novel proinflammatory cytokine in chronic obstructive pulmonary disease. Am J Respir Crit Care Med. 2008;178:894–901.
14. Polverino F, Baraldo S, Bazzan E, Agostini S, Turato G, Lunardi F, Balestro E, Damin M, Papi A, Maestrelli P, Calabrese F, Saetta M. A novel insight into adaptive immunity in chronic obstructive pulmonary disease: B cell activating factor belonging to the tumor necrosis factor family. Am J Respir Crit Care Med. 2010;182:1011–9.
15. Baraldo S, Turato G, Lunardi F, Bazzan E, Schiavon M, Ferrarotti I, Molena B, Cazzuffi R, Damin M, Balestro E, Luisetti M, Rea F, Calabrese F, Cosio MG, Saetta M. Immune activation in alpha1-antitrypsin-deficiency emphysema. Beyond the protease-antiprotease paradigm. Am J Respir Crit Care Med. 2015;191:402–9.
16. King Jr TE, Pardo A, Selman M. Idiopathic pulmonary fibrosis. Lancet. 2011;378:1949–61.
17. Hodgson U, Laitinen T, Tukiainen P. Nationwide prevalence of sporadic and familial idiopathic pulmonary fibrosis: evidence of founder effect among multiplex families in Finland. Thorax. 2002;57:338–42.
18. Gribbin J, Hubbard RB, Le Jeune I, Smith CJ, West J, Tata LJ. Incidence and mortality of idiopathic pulmonary fibrosis and sarcoidosis in the UK. Thorax. 2006;61:980–5.
19. Raghu G, Collard HR, Egan JJ, Martinez FJ, Behr J, Brown KK, Colby TV, Cordier JF, Flaherty KR, Lasky JA, Lynch DA, Ryu JH, Swigris JJ, Wells AU, Ancochea J, Bouros D, Carvalho C, Costabel U, Ebina M, Hansell DM, Johkoh T, Kim DS, King Jr TE, Kondoh Y, Myers J, Muller NL, Nicholson AG, Richeldi L, Selman M, Dudden RF, Griss BS, Protzko SL, Schunemann HJ. ATS/ERS/JRS/ALAT committee on idiopathic pulmonary fibrosis: an official ATS/ERS/JRS/ALAT statement: idiopathic pulmonary fibrosis: evidence-based guidelines for diagnosis and management. Am J Respir Crit Care Med. 2011;183:788–824.
20. Selman M, Pardo A, Kaminski N. Idiopathic pulmonary fibrosis: aberrant recapitulation of developmental programs? PLoS Med. 2008;5:e62.
21. Calabrese F, Giacometti C, Rea F, Loy M, Valente M. Idiopathic interstitial pneumonias: primum movens: epithelial, endothelial or whatever. Sarcoidosis Vasc Diffuse Lung Dis. 2005;22 Suppl 1:S15–23.
22. Calabrese F, Lunardi F, Balestro E, Marulli G, Perissinotto E, Loy M, Nannini N, Valente M, Saetta M, Agostini C, Rea F. Serpin B4 isoform overexpression is associated with aberrant epithelial proliferation and lung cancer in idiopathic pulmonary fibrosis. Pathology. 2012;44:192–8.
23. Meyer EC, Liebow AA. Relationship of interstitial pneumonia honeycombing and atypical epithelial proliferation to cancer of the lung. Cancer. 1965;18:322–51.
24. Kato H. Expression and function of squamous cell carcinoma antigen. Anticancer Res. 1996;16:2149–53.
25. Belinsky SA, Nikula KJ, Palmisano WA, Michels R, Saccomanno G, Gabrielson E, Baylin SB, Herman JG. Aberrant methylation of p16(INK4a) is an early event in lung cancer and a potential biomarker for early diagnosis. Proc Natl Acad Sci U S A. 1998;95:11891–6.
26. Hironaka M, Fukayama M. Pulmonary fibrosis and lung carcinoma: a comparative study of metaplastic epithelia in honeycombed areas of usual interstitial pneumonia with or without lung carcinoma. Pathol Int. 1999;49:1060–6.
27. Kawasaki H, Ogura T, Yokose T, Nagai K, Nishiwaki Y, Esumi H. P53 gene alteration in atypical epithelial lesions and carcinoma in patients with idiopathic pulmonary fibrosis. Hum Pathol. 2001;32:1043–9.
28. Aubry MC, Myers JL, Douglas WW, Tazelaar HD, Washington Stephens TL, Hartman TE, Deschamps C, Pankratz VS. Primary pulmonary carcinoma in patients with idiopathic pulmonary fibrosis. Mayo Clin Proc. 2002;77:763–70.

29. Murata K, Ota S, Niki T, Goto A, Li CP, Ruriko UM, Ishikawa S, Aburatani H, Kuriyama T, Fukayama M. p63 - key molecule in the early phase of epithelial abnormality in idiopathic pulmonary fibrosis. Exp Mol Pathol. 2007;83:367–76.
30. Li CP, Goto A, Watanabe A, Murata K, Ota S, Niki T, Aburatani H, Fukayama M. AKR1B10 in usual interstitial pneumonia: expression in squamous metaplasia in association with smoking and lung cancer. Pathol Res Pract. 2008;204:295–304.
31. Zhou Q, Salvesen GS. Activation of pro-caspase-7 by serine proteases includes a non-canonical specificity. Biochem J. 1997;324(Pt 2):361–4.
32. Schick C, Pemberton PA, Shi GP, Kamachi Y, Cataltepe S, Bartuski AJ, Gornstein ER, Bromme D, Chapman HA, Silverman GA. Cross-class inhibition of the cysteine proteinases cathepsins K, L, and S by the serpin squamous cell carcinoma antigen 1: a kinetic analysis. Biochemistry. 1998;37:5258–66.
33. Yamazaki T, Aoki Y. Cathepsin G enhances human natural killer cytotoxicity. Immunology. 1998;93: 115–21.
34. Cataltepe S, Gornstein ER, Schick C, Kamachi Y, Chatson K, Fries J, Silverman GA, Upton MP. Co-expression of the squamous cell carcinoma antigens 1 and 2 in normal adult human tissues and squamous cell carcinomas. J Histochem Cytochem. 2000;48:113–22.
35. Stenman J, Hedstrom J, Grenman R, Leivo I, Finne P, Palotie A, Orpana A. Relative levels of SCCA2 and SCCA1 mRNA in primary tumors predicts recurrent disease in squamous cell cancer of the head and neck. Int J Cancer. 2001;95:39–43.
36. McGettrick AF, Barnes RC, Worrall DM. SCCA2 inhibits TNF-mediated apoptosis in transfected HeLa cells. The reactive centre loop sequence is essential for this function and TNF-induced cathepsin G is a candidate target. Eur J Biochem. 2001;268: 5868–75.
37. Biggs JR, Yang J, Gullberg U, Muchardt C, Yaniv M, Kraft AS. The human brm protein is cleaved during apoptosis: the role of cathepsin G. Proc Natl Acad Sci U S A. 2001;98:3814–9.
38. Hsu KF, Huang SC, Shiau AL, Cheng YM, Shen MR, Chen YF, Lin CY, Lee BH, Chou CY. Increased expression level of squamous cell carcinoma antigen 2 and 1 ratio is associated with poor prognosis in early-stage uterine cervical cancer. Int J Gynecol Cancer. 2007;17:174–81.
39. Calabrese F, Lunardi F, Giacometti C, Marulli G, Gnoato M, Pontisso P, Saetta M, Valente M, Rea F, Perissinotto E, Agostini C. Overexpression of squamous cell carcinoma antigen in idiopathic pulmonary fibrosis: clinicopathological correlations. Thorax. 2008;63:795–802.
40. Lunardi F, Villano G, Perissinotto E, Agostini C, Rea F, Gnoato M, Bradaschia A, Valente M, Pontisso P, Calabrese F. Overexpression of SERPIN B3 promotes epithelial proliferation and lung fibrosis in mice. Lab Invest. 2011;91:945–54.
41. Xu J, Lamouille S, Derynck R. TGF-beta-induced epithelial to mesenchymal transition. Cell Res. 2009;19:156–72.
42. Quarta S, Vidalino L, Turato C, Ruvoletto M, Calabrese F, Valente M, Cannito S, Fassina G, Parola M, Gatta A, Pontisso P. SERPINB3 induces epithelial-mesenchymal transition. J Pathol. 2010;221:343–56.
43. Calabrese F, Kipar A, Lunardi F, Balestro E, Perissinotto E, Rossi E, Nannini N, Marulli G, Stewart JP, Rea F. Herpes virus infection is associated with vascular remodeling and pulmonary hypertension in idiopathic pulmonary fibrosis. PLoS One. 2013;8:e55715.
44. Egan JJ, Stewart JP, Hasleton PS, Arrand JR, Carroll KB, Woodcock AA. Epstein-Barr virus replication within pulmonary epithelial cells in cryptogenic fibrosing alveolitis. Thorax. 1995;50:1234–9.
45. Kuwano K, Nomoto Y, Kunitake R, Hagimoto N, Matsuba T, Nakanishi Y, Hara N. Detection of adenovirus E1A DNA in pulmonary fibrosis using nested polymerase chain reaction. Eur Respir J. 1997;10:1445–9.
46. Stewart JP, Egan JJ, Ross AJ, Kelly BG, Lok SS, Hasleton PS, Woodcock AA. The detection of Epstein-Barr virus DNA in lung tissue from patients with idiopathic pulmonary fibrosis. Am J Respir Crit Care Med. 1999;159:1336–41.
47. Kelly BG, Lok SS, Hasleton PS, Egan JJ, Stewart JP. A rearranged form of Epstein-Barr virus DNA is associated with idiopathic pulmonary fibrosis. Am J Respir Crit Care Med. 2002;166:510–3.
48. Lok SS, Haider Y, Howell D, Stewart JP, Hasleton PS, Egan JJ. Murine gammaherpesvirus as a cofactor in the development of pulmonary fibrosis in bleomycin resistant mice. Eur Respir J. 2002;20: 1228–32.
49. Tang YW, Johnson JE, Browning PJ, Cruz-Gervis RA, Davis A, Graham BS, Brigham KL, Oates Jr JA, Loyd JE, Stecenko AA. Herpesvirus DNA is consistently detected in lungs of patients with idiopathic pulmonary fibrosis. J Clin Microbiol. 2003;41:2633–40.
50. Zamo A, Poletti V, Reghellin D, Montagna L, Pedron S, Piccoli P, Chilosi M. HHV-8 and EBV are not commonly found in idiopathic pulmonary fibrosis. Sarcoidosis Vasc Diffuse Lung Dis. 2005;22:123–8.
51. Mora AL, Woods CR, Garcia A, Xu J, Rojas M, Speck SH, Roman J, Brigham KL, Stecenko AA. Lung infection with gamma-herpesvirus induces progressive pulmonary fibrosis in Th2-biased mice. Am J Physiol Lung Cell Mol Physiol. 2005;289: L711–21.
52. Mora AL, Torres-Gonzalez E, Rojas M, Xu J, Ritzenthaler J, Speck SH, Roman J, Brigham K, Stecenko A. Control of virus reactivation arrests pulmonary herpesvirus-induced fibrosis in IFN-gamma receptor-deficient mice. Am J Respir Crit Care Med. 2007;175:1139–50.
53. McMillan TR, Moore BB, Weinberg JB, Vannella KM, Fields WB, Christensen PJ, van Dyk LF, Toews GB. Exacerbation of established pulmonary fibrosis

in a murine model by gammaherpesvirus. Am J Respir Crit Care Med. 2008;177:771–80.
54. Arase Y, Suzuki F, Suzuki Y, Akuta N, Kobayashi M, Kawamura Y, Yatsuji H, Sezaki H, Hosaka T, Hirakawa M, Saito S, Ikeda K, Kumada H. Hepatitis C virus enhances incidence of idiopathic pulmonary fibrosis. World J Gastroenterol. 2008;14:5880–6.
55. Malizia AP, Keating DT, Smith SM, Walls D, Doran PP, Egan JJ. Alveolar epithelial cell injury with Epstein-Barr virus upregulates TGFbeta1 expression. Am J Physiol Lung Cell Mol Physiol. 2008;295:L451–60.
56. Malizia AP, Lacey N, Walls D, Egan JJ, Doran PP. CUX1/Wnt signaling regulates epithelial mesenchymal transition in EBV infected epithelial cells. Exp Cell Res. 2009;315:1819–31.
57. Malizia AP, Egan JJ, Doran PP. IL-4 increases CD21-dependent infection of pulmonary alveolar epithelial type II cells by EBV. Mol Immunol. 2009;46:1905–10.
58. Pozharskaya V, Torres-Gonzalez E, Rojas M, Gal A, Amin M, Dollard S, Roman J, Stecenko AA, Mora AL. Twist: a regulator of epithelial-mesenchymal transition in lung fibrosis. PLoS One. 2009;4:e7559.
59. Pulkkinen V, Salmenkivi K, Kinnula VL, Sutinen E, Halme M, Hodgson U, Lehto J, Jaaskelainen A, Piiparinen H, Kere J, Lautenschlager I, Lappalainen M, Myllarniemi M. A novel screening method detects herpesviral DNA in the idiopathic pulmonary fibrosis lung. Ann Med. 2012;44:178–86.
60. Vannella KM, Luckhardt TR, Wilke CA, van Dyk LF, Toews GB, Moore BB. Latent herpesvirus infection augments experimental pulmonary fibrosis. Am J Respir Crit Care Med. 2010;181:465–77.
61. Sides MD, Klingsberg RC, Shan B, Gordon KA, Nguyen HT, Lin Z, Takahashi T, Flemington EK, Lasky JA. The Epstein-Barr virus latent membrane protein 1 and transforming growth factor-beta1 synergistically induce epithelial-mesenchymal transition in lung epithelial cells. Am J Respir Cell Mol Biol. 2011;44:852–62.
62. Egan JJ, Adamali HI, Lok SS, Stewart JP, Woodcock AA. Ganciclovir antiviral therapy in advanced idiopathic pulmonary fibrosis: an open pilot study. Pulm Med. 2011;2011:240805.
63. Tuder RM, Lee SD, Cool CC. Histopathology of pulmonary hypertension. Chest. 1998;114:1S–6.
64. Atkinson C, Stewart S, Upton PD, Machado R, Thomson JR, Trembath RC, Morrell NW. Primary pulmonary hypertension is associated with reduced pulmonary vascular expression of type II bone morphogenetic protein receptor. Circulation. 2002;105:1672–8.
65. Rabinovitch M. Molecular pathogenesis of pulmonary arterial hypertension. J Clin Invest. 2012;122:4306–13.
66. Schiavon M, Fadini GP, Lunardi F, Agostini C, Boscaro E, Calabrese F, Marulli G, Rea F. Increased tissue endothelial progenitor cells in end-stage lung diseases with pulmonary hypertension. J Heart Lung Transplant. 2012;31:1025–30.
67. Yusen RD, Edwards LB, Kucheryavaya AY, Benden C, Dipchand AI, Goldfarb SB, Levvey BJ, Lund LH, Meiser B, Rossano JW, Stehlik J. The Registry of the International Society for heart and lung transplantation: thirty-second official adult lung and heart-lung transplantation report–2015; Focus Theme: Early Graft Failure. J Heart Lung Transplant. 2015;34(10):1264–77.
68. Stewart S, Fishbein MC, Snell GI, Berry GJ, Boehler A, Burke MM, Glanville A, Gould FK, Magro C, Marboe CC, McNeil KD, Reed EF, Reinsmoen NL, Scott JP, Studer SM, Tazelaar HD, Wallwork JL, Westall G, Zamora MR, Zeevi A, Yousem SA. Revision of the 1996 working formulation for the standardization of nomenclature in the diagnosis of lung rejection. J Heart Lung Transplant. 2007;26:1229–42.
69. Masson E, Stern M, Chabod J, Thevenin C, Gonin F, Rebibou JM, Tiberghien P. Hyperacute rejection after lung transplantation caused by undetected low-titer anti-HLA antibodies. J Heart Lung Transplant. 2007;26:642–5.
70. Dawson KL, Parulekar A, Seethamraju H. Treatment of hyperacute antibody-mediated lung allograft rejection with eculizumab. J Heart Lung Transplant. 2012;31:1325–6.
71. Estenne M, Maurer JR, Boehler A, Egan JJ, Frost A, Hertz M, Mallory GB, Snell GI, Yousem S. Bronchiolitis obliterans syndrome 2001: an update of the diagnostic criteria. J Heart Lung Transplant. 2002;21:297–310.
72. Berry G, Burke M, Andersen C, Angelini A, Bruneval P, Calabrese F, Fishbein MC, Goddard M, Leone O, Maleszewski J, Marboe C, Miller D, Neil D, Padera R, Rassl D, Revello M, Rice A, Stewart S, Yousem SA. Pathology of pulmonary antibody-mediated rejection: 2012 update from the pathology council of the ISHLT. J Heart Lung Transplant. 2013;32:14–21.
73. Sato M, Waddell TK, Wagnetz U, Roberts HC, Hwang DM, Haroon A, Wagnetz D, Chaparro C, Singer LG, Hutcheon MA, Keshavjee S. Restrictive allograft syndrome (RAS): a novel form of chronic lung allograft dysfunction. J Heart Lung Transplant. 2011;30:735–42.
74. Verleden GM, Vos R, Verleden SE, De Wever W, De Vleeschauwer SI, Willems-Widyastuti A, Scheers H, Dupont LJ, Van Raemdonck DE, Vanaudenaerde BM. Survival determinants in lung transplant patients with chronic allograft dysfunction. Transplantation. 2011;92:703–8.
75. Frankel SK, Cool CD, Lynch DA, Brown KK. Idiopathic pleuroparenchymal fibroelastosis: description of a novel clinicopathologic entity. Chest. 2004;126:2007–13.
76. Ofek E, Sato M, Saito T, Wagnetz U, Roberts HC, Chaparro C, Waddell TK, Singer LG, Hutcheon MA, Keshavjee S, Hwang DM. Restrictive allograft syndrome post lung transplantation is characterized by pleuroparenchymal fibroelastosis. Mod Pathol. 2013;26:350–6.

77. von der Thusen JH, Hansell DM, Tominaga M, Veys PA, Ashworth MT, Owens CM, Nicholson AG. Pleuroparenchymal fibroelastosis in patients with pulmonary disease secondary to bone marrow transplantation. Mod Pathol. 2011;24:1633–9.
78. Reddy TL, Tominaga M, Hansell DM, von der Thusen J, Rassl D, Parfrey H, Guy S, Twentyman O, Rice A, Maher TM, Renzoni EA, Wells AU, Nicholson AG. Pleuroparenchymal fibroelastosis: a spectrum of histopathological and imaging phenotypes. Eur Respir J. 2012;40:377–85.
79. Valantine HA, Luikart H, Doyle R, Theodore J, Hunt S, Oyer P, Robbins R, Berry G, Reitz B. Impact of cytomegalovirus hyperimmune globulin on outcome after cardiothoracic transplantation: a comparative study of combined prophylaxis with CMV hyperimmune globulin plus ganciclovir versus ganciclovir alone. Transplantation. 2001;72:1647–52.
80. Weill D, Lock BJ, Wewers DL, Young KR, Zorn GL, Early L, Kirklin JK, McGiffin DC. Combination prophylaxis with ganciclovir and cytomegalovirus (CMV) immune globulin after lung transplantation: effective CMV prevention following daclizumab induction. Am J Transplant. 2003;3:492–6.
81. Palmer SM, Limaye AP, Banks M, Gallup D, Chapman J, Lawrence EC, Dunitz J, Milstone A, Reynolds J, Yung GL, Chan KM, Aris R, Garrity E, Valentine V, McCall J, Chow SC, Davis RD, Avery R. Extended valganciclovir prophylaxis to prevent cytomegalovirus after lung transplantation: a randomized, controlled trial. Ann Intern Med. 2010;152:761–9.
82. Arbustini E, Grasso M, Diegoli M, Percivalle E, Grossi P, Bramerio M, Campana C, Goggi C, Gavazzi A, Vigano M. Histopathologic and molecular profile of human cytomegalovirus infections in patients with heart transplants. Am J Clin Pathol. 1992;98:205–13.
83. Lu DY, Qian J, Easley KA, Waldrop SM, Cohen C. Automated in situ hybridization and immunohistochemistry for cytomegalovirus detection in paraffin-embedded tissue sections. Appl Immunohistochem Mol Morphol. 2009;17:158–64.
84. Riise GC, Andersson R, Bergstrom T, Lundmark A, Nilsson FN, Olofsson S. Quantification of cytomegalovirus DNA in BAL fluid: a longitudinal study in lung transplant recipients. Chest. 2000;118:1653–60.
85. Westall GP, Michaelides A, Williams TJ, Snell GI, Kotsimbos TC. Human cytomegalovirus load in plasma and bronchoalveolar lavage fluid: a longitudinal study of lung transplant recipients. J Infect Dis. 2004;190:1076–83.
86. Calabrese F, Lunardi F, Popper H. Molecular diagnosis in lung diseases. Front Biosci (Landmark Ed). 2015;20:644–88.
87. You XM, Steinmuller C, Wagner TO, Bruggeman CA, Haverich A, Steinhoff G. Enhancement of cytomegalovirus infection and acute rejection after allogeneic lung transplantation in the rat: virus-induced expression of major histocompatibility complex class II antigens. J Heart Lung Transplant. 1996;15:1108–19.
88. Halenius A, Gerke C, Hengel H. Classical and non-classical MHC I molecule manipulation by human cytomegalovirus: so many targets-but how many arrows in the quiver? Cell Mol Immunol. 2015;12:139–53.
89. Penn I. Occurrence of cancers in immunosuppressed organ transplant recipients. Clin Transpl. 1998;12:147–58.
90. Gutierrez-Dalmau A, Campistol JM. Immunosuppressive therapy and malignancy in organ transplant recipients: a systematic review. Drugs. 2007;67:1167–98.
91. Calabrese F, Loy M, Lunardi F, Marino D, Aversa SM, Rea F. Acute cellular rejection and Epstein-Barr virus-related post-transplant lymphoproliferative disorder in a pediatric lung transplant with low viral load. Transpl Infect Dis. 2010;12:342–6.
92. Glotz D, Chapman JR, Dharnidharka VR, Hanto DW, Castro MC, Hirsch HH, Leblond V, Mehta AK, Moulin B, Pagliuca A, Pascual J, Rickinson AB, Russo FP, Trappe RU, Webster AC, Zuckermann AO, Gross TG. The Seville expert workshop for progress in posttransplant lymphoproliferative disorders. Transplantation. 2012;94:784–93.
93. Paya CV. Indirect effects of CMV in the solid organ transplant patient. Transpl Infect Dis. 1999;1 Suppl 1:8–12.
94. Rashtak S, Dierkhising RA, Kremers WK, Peters SG, Cassivi SD, Otley CC. Incidence and risk factors for skin cancer following lung transplantation. J Am Acad Dermatol. 2015;72:92–8.
95. Harwood CA, Surentheran T, McGregor JM, Spink PJ, Leigh IM, Breuer J, Proby CM. Human papillomavirus infection and non-melanoma skin cancer in immunosuppressed and immunocompetent individuals. J Med Virol. 2000;61:289–97.
96. Feist A, Lee R, Osborne S, Lane J, Yung G. Increased incidence of cutaneous squamous cell carcinoma in lung transplant recipients taking long-term voriconazole. J Heart Lung Transplant. 2012;31:1177–81.
97. Dufek S, Haitel A, Muller-Sacherer T, Aufricht C. Duct Bellini carcinoma in association with BK virus nephropathy after lung transplantation. J Heart Lung Transplant. 2013;32:378–9.
98. Torbenson M, Wang J, Nichols L, Randhawa P, Nalesnik MA. Renal cortical neoplasms in long term survivors of solid organ transplantation. Transplantation. 2000;69:864–8.
99. Collins J, Kazerooni EA, Lacomis J, McAdams HP, Leung AN, Shiau M, Semenkovich J, Love RB. Bronchogenic carcinoma after lung transplantation: frequency, clinical characteristics, and imaging findings. Radiology. 2002;224:131–8.
100. Penn I. Kaposi's sarcoma in transplant recipients. Transplantation. 1997;64:669–73.
101. Nannini N, Rebusso A, Lunardi F, Loy M, Calabrese F, Battistella L, Schiavon M, Rea F, Calabrese F. A symptomatic pulmonary allograft Kaposi's sarcoma: a case report. Exp Clin Transplant. 2016 Jan 14. [Epub ahead of print].

102. Regamey N, Tamm M, Wernli M, Witschi A, Thiel G, Cathomas G, Erb P. Transmission of human herpesvirus 8 infection from renal-transplant donors to recipients. N Engl J Med. 1998;339: 1358–63.
103. Piselli P, Busnach G, Citterio F, Frigerio M, Arbustini E, Burra P, Pinna AD, Bresadola V, Ettorre GM, Baccarani U, Buda A, Lauro A, Zanus G, Cimaglia C, Spagnoletti G, Lenardon A, Agozzino M, Gambato M, Zanfi C, Miglioresi L, Di Gioia P, Mei L, Ippolito G, Serraino D, Immunosuppression and Cancer Study Group. Risk of Kaposi sarcoma after solid-organ transplantation: multicenter study in 4,767 recipients in Italy, 1970–2006. Transplant Proc. 2009;41:1227–30.
104. Smith DM, Agura ED, Ausloos K, Ring WS, Domiati-Saad R, Klintmalm GB. Graft-vs-host disease as a complication of lung transplantation. J Heart Lung Transplant. 2006;25:1175–7.
105. Assi MA, Pulido JS, Peters SG, McCannel CA, Razonable RR. Graft-vs.-host disease in lung and other solid organ transplant recipients. Clin Transplant. 2007;21:1–6.
106. Worel N, Bojic A, Binder M, Jaksch P, Mitterbauer G, Streubel B, Thalhammer F, Staudinger T, Laczika KF, Locker GJ. Catastrophic graft-versus-host disease after lung transplantation proven by PCR-based chimerism analysis. Transpl Int. 2008;21:1098–101.
107. Kazerooni EA, Jackson C, Cascade PN. Sarcoidosis: recurrence of primary disease in transplanted lungs. Radiology. 1994;192:461–4.
108. Martinez FJ, Orens JB, Deeb M, Brunsting LA, Flint A, Lynch 3rd JP. Recurrence of sarcoidosis following bilateral allogeneic lung transplantation. Chest. 1994;106:1597–9.
109. Calabrese F, Giacometti C, Rea F, Loy M, Sartori F, Di Vittorio G, Abudureheman A, Thiene G, Valente M. Recurrence of idiopathic pulmonary hemosiderosis in a young adult patient after bilateral single-lung transplantation. Transplantation. 2002;74:1643–5.
110. Gabbay E, Dark JH, Ashcroft T, Milne D, Gibson GJ, Healy M, Corris PA. Recurrence of Langerhans' cell granulomatosis following lung transplantation. Thorax. 1998;53:326–7.
111. Habib SB, Congleton J, Carr D, Partridge J, Corrin B, Geddes DM, Banner N, Yacoub M, Burke M. Recurrence of recipient Langerhans' cell histiocytosis following bilateral lung transplantation. Thorax. 1998;53:323–5.
112. O'Brien JD, Lium JH, Parosa JF, Deyoung BR, Wick MR, Trulock EP. Lymphangiomyomatosis recurrence in the allograft after single-lung transplantation. Am J Respir Crit Care Med. 1995;151:2033–6.
113. Bittmann I, Dose TB, Muller C, Dienemann H, Vogelmeier C, Lohrs U. Lymphangioleiomyomatosis: recurrence after single lung transplantation. Hum Pathol. 1997;28:1420–3.
114. Verleden GM, Sels F, Van Raemdonck D, Verbeken EK, Lerut T, Demedts M. Possible recurrence of desquamative interstitial pneumonitis in a single lung transplant recipient. Eur Respir J. 1998;11:971–4.
115. Baz MA, Kussin PS, Van Trigt P, Davis RD, Roggli VL, Tapson VF. Recurrence of diffuse panbronchiolitis after lung transplantation. Am J Respir Crit Care Med. 1995;151:895–8.
116. Mal H, Guignabert C, Thabut G, d'Ortho MP, Brugiere O, Dauriat G, Marrash-Chahla R, Rangheard AS, Leseche G, Fournier M. Recurrence of pulmonary emphysema in an alpha-1 proteinase inhibitor-deficient lung transplant recipient. Am J Respir Crit Care Med. 2004;170:811–4.
117. Pham PT, Pham PC, Danovitch GM, Ross DJ, Gritsch HA, Kendrick EA, Singer J, Shah T, Wilkinson AH. Sirolimus-associated pulmonary toxicity. Transplantation. 2004;77:1215–20.
118. Garrean S, Massad MG, Tshibaka M, Hanhan Z, Caines AE, Benedetti E. Sirolimus-associated interstitial pneumonitis in solid organ transplant recipients. Clin Transplant. 2005;19:698–703.
119. Hamour IM, Mittal TK, Bell AD, Banner NR. Reversible sirolimus-associated pneumonitis after heart transplantation. J Heart Lung Transplant. 2006;25:241–4.

Lung Tumors

17

In this chapter, we will provide a short overview on carcinogenesis and epidemiology, as far as it is necessary to understand the resulting morphology. The aim is not to extensively discuss these aspects, because there are many articles, reviews, and books out, which can be used for a more in-depth understanding. Molecular biology and genetics are discussed in the chapters on Molecular Pathology and Metastasis. In these chapters, molecular abnormalities in the different tumors are discussed, and moreover, mechanisms of invasion, migration, and metastasis are described. So here we have only to focus on mechanisms of carcinogenesis to that moment an in situ carcinoma has been formed, and the primary tumor is established. Not much knowledge is available on the genetic mechanisms of benign epithelial tumors, whereas some data are available for mesenchymal tumors. These aspects will be discussed with the respective tumor entity, because it seems to be unique for each entity.

Since the lung is composed of many different epithelial and mesenchymal cell types at different locations (approximately 56 different cell types), from the large bronchi via the different generations of bronchi and bronchioles, down to the alveoli and along the septa to the pleura, it is not surprising that so many different tumors exist. Some tumors are strictly structure related, such as glandular adenomas, which occur only in large bronchi, or alveolar adenoma occurring only peripheral. Other tumors can occur either peripherally or centrally. Some tumors are confined to the pleura, others spread along the interlobular septa into the lung.

17.1 Epithelial Tumors

17.1.1 Benign Epithelial Tumors

Within the group of benign epithelial tumors, there are centrally located bronchial gland adenomas, cystadenoma, pleomorphic adenoma, as well as the peripheral located papillary adenoma and sclerosing hemangioma.

17.1.1.1 Bronchial Mucous Gland Adenoma (Salivary Gland-Type Adenoma)

Definition and Incidence

These are tumors similar to their salivary gland counterparts. The tumors outgrow from and replace mucous glands of the bronchus. They all arise in the central portion of the large bronchi in areas where bronchial glands are normally found. As their salivary cousins, they can have different cell compositions, which will give rise to the different names used. Tumors comprise many cystic spaces or glands filled with mucus. Lining cells are cylindrical or cuboidal. Mitoses and atypia are absent. Sometimes the surface of the tumor is covered by metaplastic squamous epithelium. In the stroma there are inflammatory cells. Myoepithelial cells might occur in specific entities.

© Springer-Verlag Berlin Heidelberg 2017
H. Popper, *Pathology of Lung Disease*, DOI 10.1007/978-3-662-50491-8_17

Symptoms

These centrally located tumors most often present with symptoms of bronchial obstruction and are often found in the young-aged population; even children might be affected.

Mucous Gland Adenoma

This is the "common" type of these adenomas. It can occur in both sexes and at any age. Cases have been described in peripheral locations but these need to be separated from papillary adenoma [1]. The major symptom is bronchial obstruction causing cough and purulent inflammation.

Gross Appearance

The tumor grows endobronchial and usually induces bronchial obstruction (Fig. 17.1). The size can be from a few millimeters up to few centimeters in diameter. The tumor is grayish red to white; the cut surface is glistening due to mucous production. The tumors most often grow out from the bronchial mucosa with a broad basis.

Microscopy

Histologically mucous gland adenomas are composed of numerous tubules and papillae, often cystic dilated, filled with mucous (PAS positive) and lined by cuboidal or columnar cells, which are either of the goblet or the secretory cell type [2–4] (Fig. 17.2). Rarely oxyphilic cell may be present; exceptionally rare the entire tumor can be composed of oxyphilic cells; some authors have called these variants of bronchial gland adenomas oncocytoma [5–8] (Fig. 17.2a). Clear cells can also be seen, usually admixed with the other mucous-producing cells.

Immunohistochemistry

The epithelial cells showed strong and diffuse cytoplasmic staining for high molecular weight cytokeratins (cytokeratin 5/cytokeratin 6) and may also be positive for cytokeratin 20 and often lack TTF1 expression [9]. Scattered myoepithelial cells may stain with S100 protein antibodies.

In the differential diagnosis, low-grade mucoepidermoid carcinoma can closely mimic mucous gland adenoma. However, the mixture of squamous and transitional cell complexes in mucoepidermoid carcinoma will immediately guide to the correct diagnosis.

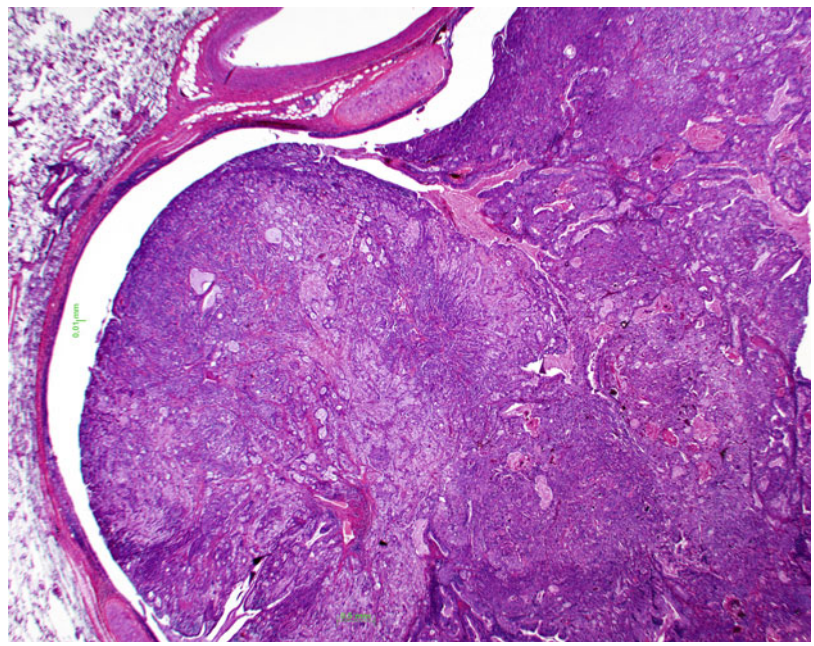

Fig. 17.1 Bronchial mucus gland adenoma with typical endobronchial growth and obstruction of the bronchial lumen. H&E, bar 500 µm

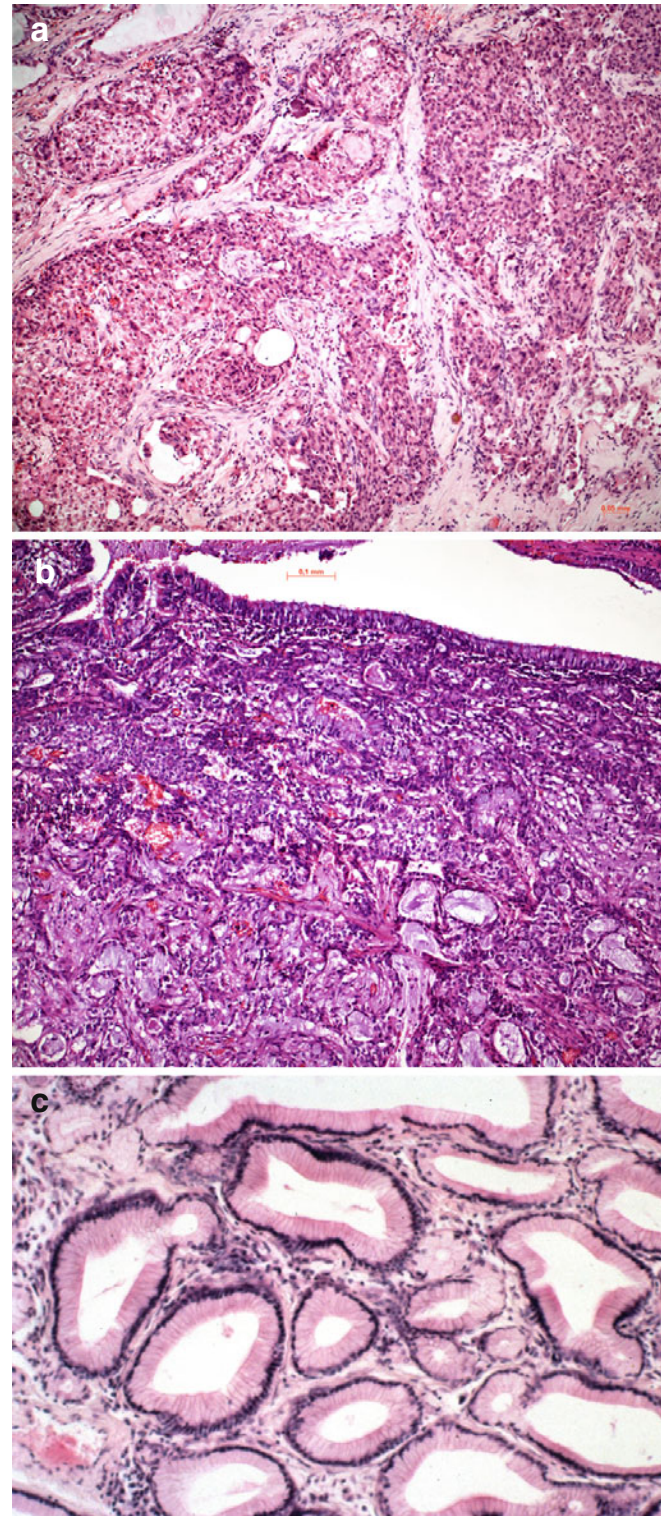

Fig. 17.2 Three different examples of mucus gland adenomas of the bronchus. (**a**) Is dominated by oxyphilic cells, (**b**) shows a mixture of serous and goblet cells, (**c**) is entirely composed of high columnar cells. H&E, bars 50 and 100 μm, and ×260

Molecular Biology

There is only one report, which analyzed a bronchial gland adenoma for genetic aberrations. Pfragner et al. reported trisomy for several chromosomes in a tubular adenoma out of cell cultures from the tumor [10].

Serous and Mucinous Cystadenoma Including Borderline Variants

Gross Pathology

These cystic tumors arise most often in central bronchi but may be found peripheral. The tumor is most often asymptomatic [5, 11]. On gross examination the tumor will present as a cystic mass, which easily rupture when prepared or resected surgically. The tumor is usually encapsulated and separated by a thin fibrous band from the adjacent lung. On cut surface the mucus-filled cysts are easily visible (Fig. 17.3).

Fig. 17.3 Mucinous cystadenoma, resection specimen. The tumor is composed of numerous cysts filled with mucus. At the border there is macrophage reaction with many macrophages filled with mucus but also lipids (*yellow* areas)

Microscopy

They resemble ovarian cystadenoma. However, they present with unilocular or multilocular cysts lined by one layer of tall columnar or cuboidal cells either producing a serous fluid (Fig. 17.4) or mucus (Figs. 17.5 and 17.6). The nuclei are bland, often in a basal orientation; nucleoli if present are small and inconspicuous. Papillary projections may be found. In these areas stratification of cells and nuclei can be seen. A correct diagnosis is only possible on whole resection specimen, although a diagnosis might be suspected on biopsy (Fig. 17.7).

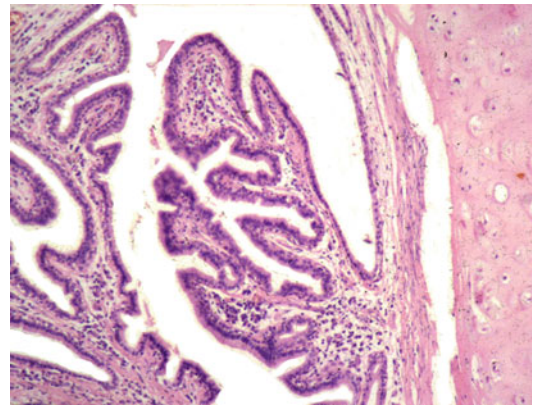

Fig. 17.4 Papillary cystadenoma in a main bronchus, obstructing the lumen. This type of tumor very closely mimics its ovarian cousin. H&E, ×100

Differential Diagnosis

Within the differential diagnosis, adenocarcinoma in situ (AIS), colloid or mucinous carcinoma, and congenital pulmonary adenomatoid malformation (CPAM) have to be considered. Well-differentiated mucinous AIS cannot be separated from mucinous cystadenoma on small biopsies, the same applies to colloid carcinoma. The sharp demarcation and the lack of atypia in mucinous cystadenoma will be the main criterion. In contrast to mucinous cystadenoma, colloid carcinoma will present with discontinuous growth along alveolar septa. In cystadenoma, the cells form a continuous line along preexisting structures, either bronchi or alveoli. From CPAM types I and II, the cystadenoma can usually be separated more easily: the CPAM cysts (types I and II) are covered by normal bronchial-type epithelium, show mesenchymal cells within their cyst wall, and if present will exhibit atypical goblet cell hyperplasia,

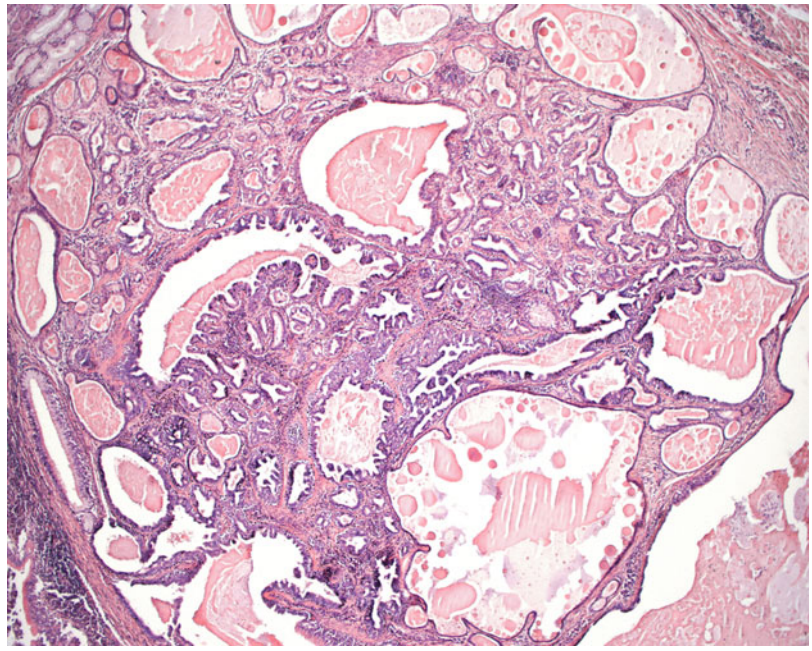

Fig. 17.5 Mucinous cystadenoma in a main bronchus. H&E, ×12 (Case kindly provided by Dr. B. Papla, Krakow)

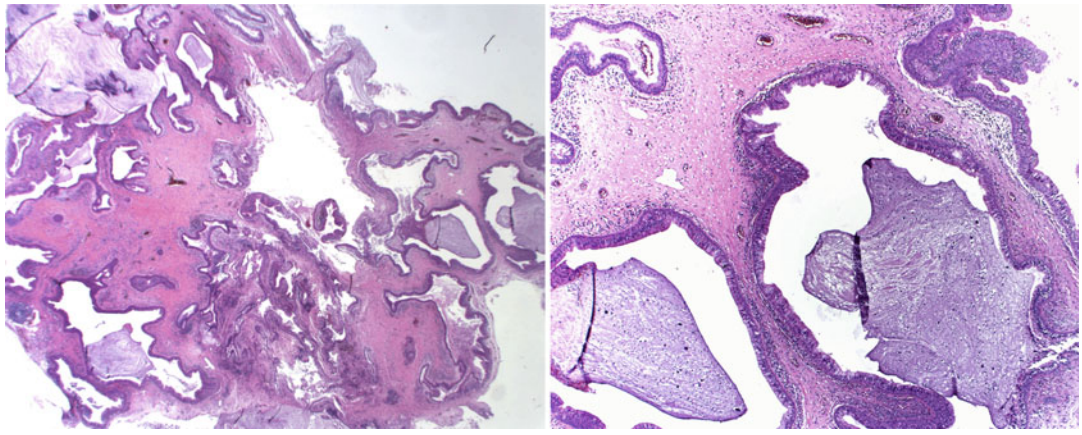

Fig. 17.6 Mucinous cystadenoma of the bronchus. Another case shows predominantly large acini filled with mucus. Overview *left*, and higher magnification *right*, showing bland cytology and a mixture of columnar cells including goblet cells. H&E, ×12 and 100

which is a focal goblet cell proliferation within the cyst epithelium [12].

Borderline Variant

In cystadenomas atypia can be present and similar to the tumors of the ovary have been called borderline tumors or variants of serous or mucinous cystadenoma (Fig. 17.8). The borderline variants are still encapsulated, but extensive sampling has to be done to exclude invasion. In these cases there is atypia of the nuclei, enlarged nucleoli, formation of cell papillae, and few mitoses including atypical mitosis [13–15].

No data exist in the literature about genetic aberrations or specific markers, associated with the development of these adenomas.

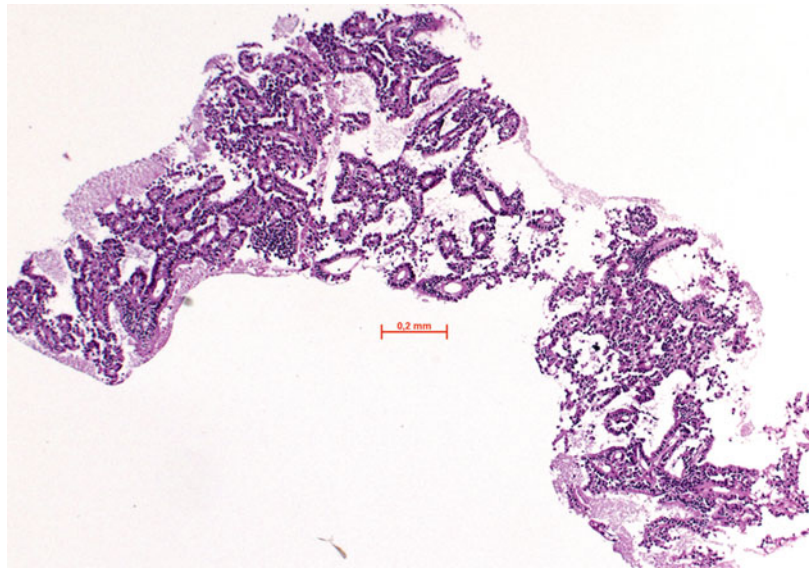

Fig. 17.7 Bronchial biopsy of a serous type of bronchial gland adenoma. On this biopsy the diagnosis can be suspected, because the glands are close together, too large for normal glands, and the cytology of the cells is bland. H&E, bar 200 µm

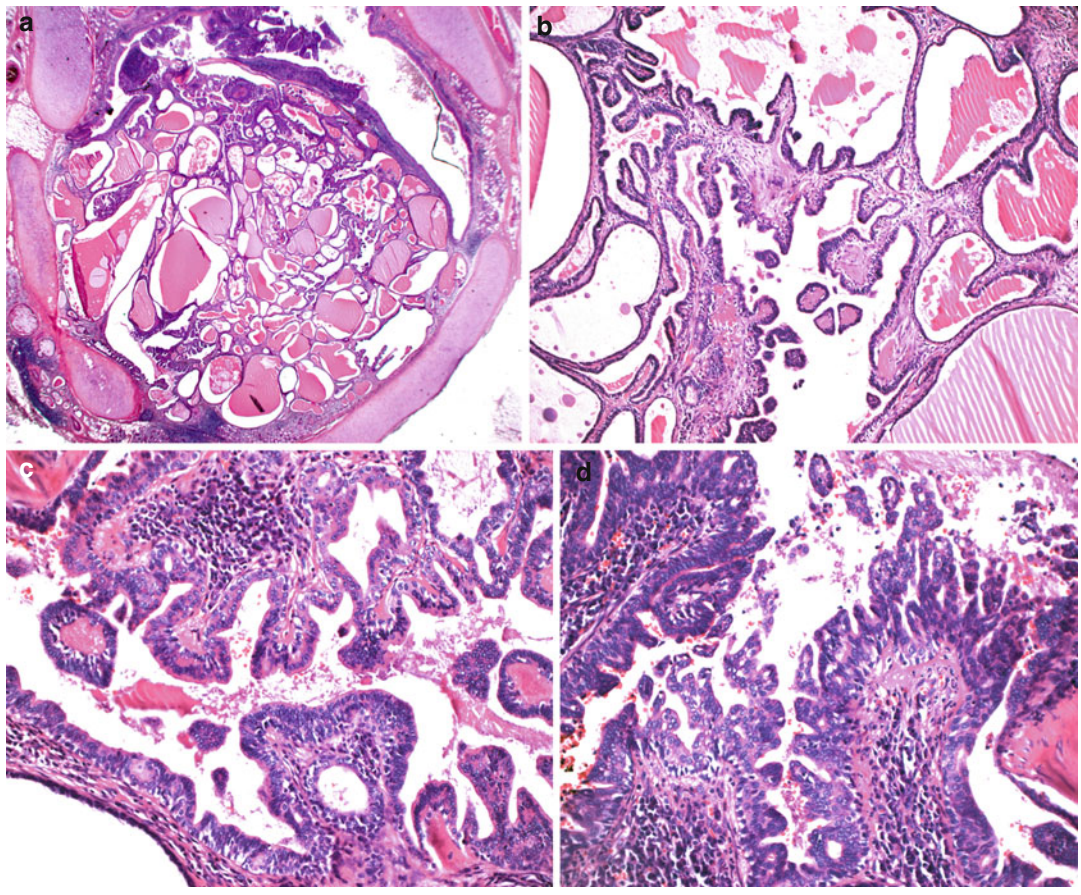

Fig. 17.8 Mucinous papillary cystadenoma in a large bronchus. In this case a borderline variant. In (**a**) overview of the tumor with many cystic spaces filled by mucin. Already areas with higher cellularity are seen. (**b**) Area with bland cytology but already papillary projections. (**c**, **d**) show areas with cellular atypia, crowding, epithelial papillae, and nuclear atypia. H&E, ×12, 100, and 200 (Case kindly provided by Dr. B. Papla)

Prognosis and Treatment

Prognosis is usually excellent, if these tumors are completely removed. In mucinous cystadenomas the removal might sometimes be complicated by rupture of the tumor, releasing mucus and within the mucus also tumor cells. This might give rise to recurrence. In case of a borderline variant of cystadenoma, a careful workup of the entire tumor is essential. There might be areas of invasion, which immediately change the diagnosis and also shifts this tumor into the group of mucinous adenocarcinomas.

17.1.1.2 Pleomorphic Adenoma

Pleomorphic adenoma of the lung is a rare tumor but otherwise resembles its counterpart in the large salivary glands [16]. It affects man and woman in almost all ages, except childhood, but most often older patients. There is no gender predominance.

Gross Pathology

Most cases reported so far arise from the large bronchi and may grow with an endobronchial portion into the lumen, causing obstruction. The size may vary from one up to several cm in diameter. On cut surface pleomorphic adenoma are well circumscribed but lack a well-defined capsule. The color is grayish red to myxoid white glistening, depending on the amount of myxoid and glandular areas.

Histology

Pleomorphic adenoma is composed of ducts and glands, resembling bronchial glands. A spindle cell component is usually present, whereas in contrast to the salivary glands chondroid metaplasia is rare; however, myxoid and hyaline changes of the matrix proteins can be seen. Myoepithelial cells are usually present and in some cases may form a major portion [5, 16–18] (Fig. 17.9).

Differential Diagnosis

Pleomorphic adenoma is usually not difficult to diagnose correctly because of its benign cytological features and the biphasic nature. However, in cases with a prominent spindle or myoepithelial component, the differential diagnosis toward myoepithelioma or inflammatory myofibroblastic tumor might be rendered. Important features to correctly diagnose this entity include also positivity for pan-cytokeratin, S100 protein, smooth muscle actin, vimentin, and glial fibrillary acidic protein (GFAP) [1, 17, 19]. In rare instances within a pleomorphic adenoma carcinomas can arise [1, 19].

Immunohistochemistry

Pleomorphic adenoma will stain positively for pan-cytokeratin and high molecular weight cytokeratins (CK 5/CK 6); the myoepithelial component will be positive for S100 protein and smooth muscle actin; some epithelia and myoepithelial cells might coexpress vimentin together with cytokeratin and GFAP.

Prognosis and Therapy

Pleomorphic adenoma in most instances can be regarded as a benign tumor, which is cured by complete surgical resection. Benign pleomorphic adenomas are usually well circumscribed. There are a few cases, which have been reported to behave as low malignant tumors [19, 20].

17.1.1.3 Myoepithelioma

Myoepithelioma is an exceptionally rare benign tumor arising in the central portion of the lung [21].

Macroscopy

Myoepithelioma usually presents as an endobronchial nodule obstructing the lumen. Myoepitheliomas can reach a size of 2 cm before causing symptoms. On gross sections this will be a grayish-white nodule, the cut surface being soft and fleshy.

Microscopy

Microscopically the tumor is composed of small glands and ducts, presenting with an inner cuboidal and an outer spindle or flat cell layer (Fig. 17.10). The inner cells are stained by cytokeratins, the outer layer in addition also by S100 protein antibodies. Mitoses are absent, and the nuclei are small and round, the chromatin is finely distributed, and nucleoli are inconspicuous. In a few cases spindle cell may predominate [22]. The mitotic rate is usually low with approximately 1 in 20 high-power fields.

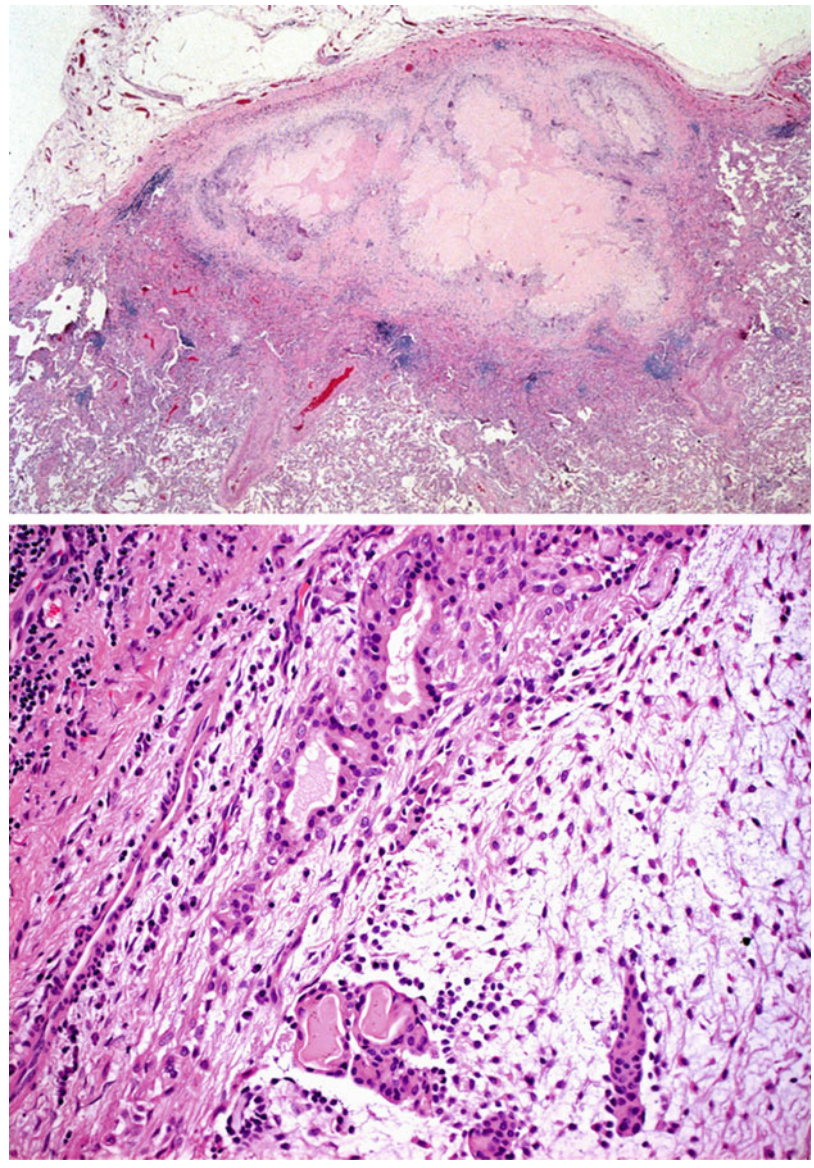

Fig. 17.9 Pleomorphic adenoma of the bronchus. In the *upper* panel, an overview is shown; in the *lower* panel, there are ducts and acini embedded in a myxoid stroma with stellate cells. H&E, ×12 and 100

Immunohistochemistry and Molecular Biology

The inner layer of the glands stains for cytokeratin, TTF1, and epithelial membrane antigen and the outer layer for S100 and smooth muscle actin. In one case the spindle cells stained for CD34. P27/kip-1 protein plays a fundamental role in the development of these neoplasms. It shows an aberrant cytoplasmic location [23]. In another investigation p63 expression was demonstrated in this tumor [21]. So TP63 might have an impact on the development of this tumor.

In the differential diagnosis, only myoepithelial carcinoma has to be considered. A proper sampling is essential, especially the basis of the tumor needs to be examined at multiple levels to exclude invasion, which is the only reliable criterion to separate these two entities. Myoepithelial carcinoma will usually show nuclear polymorphism and a few mitoses. Due to the fact that epithelial-myoepithelial tumor is difficult to separate from epithelial-myoepithelial carcinoma, some authors prefer to group these entities

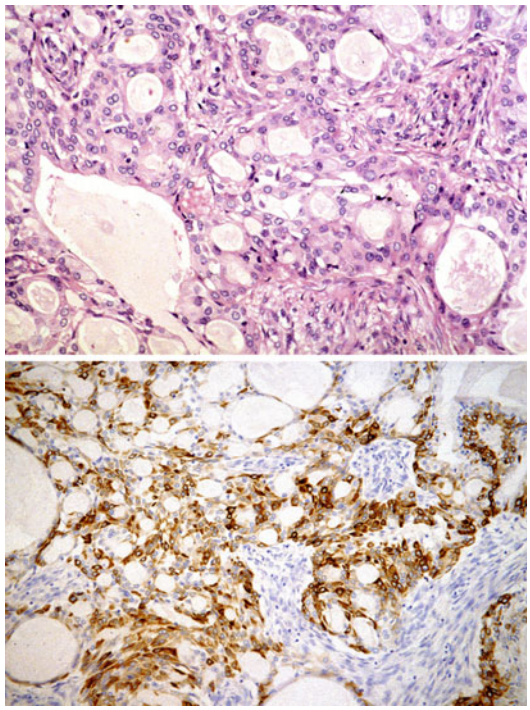

Fig. 17.10 Myoepithelioma arising from a large bronchus. The tumor is composed of glandular epithelium surrounded by myoepithelial cells, which usually have a spindle cell appearance (*upper* panel). There are no mitoses and no nuclear atypia. The myoepithelial cells stain positively for S100 protein (*lower* panel). H&E, immunohistochemistry, ×200

together. But a high mitotic rate, tumoral necrosis, and nuclear pleomorphism favor the carcinoma diagnosis [22].

17.1.1.4 Papilloma in Adult and Childhood

Epidemiology and Incidence

Pulmonary papillomas are rare epithelial neoplasms, often an incidental finding on bronchoscopy, for which no incidence is available. The incidence in children is somewhat higher; however, there are also no data on papilloma and papillomatosis in the literature. In our own experience, a papilloma diagnosis was rendered in 210 cases out of 48,676 cases within the lung and pleura collection. In only 25 cases, the diagnosis was confirmed by proving one of the HPV types. Out of these 25 cases, there were 7 cases with a proof of HPV 16 or 18, respectively, whereas in 18 cases, one of the non-oncogenic or facultative oncogenic types was identified. In children bronchial papillomas are often seen together with papillomas in the upper respiratory tract (tracheal, laryngeal, sinonasal papillomas) [24–26]. Papillomas are caused by human papilloma viruses, mainly by types 6b, 11, 16, 18, 31, 33, and 35 [27]. There are data pointing that infection especially in children do occur during delivery via an infected mother [28]. Adult patients are usually younger compared to carcinoma patients. In our experience it occurs always in smokers with a male predominance. There are no specific symptoms. Sometimes papillomas are associated with invasive squamous cell carcinoma [29].

Symptoms

Patients with papillomas present with hoarseness, cough, hemoptysis, wheezing, chest tightness, and non-purulent expectoration. Some patients have no symptoms and therefore papillomas are also found incidentally. Large papillomas might cause obstruction and poststenotic pneumonia. On bronchoscopy papillomas present as small round polyps, usually pedunculated with a broad stalk.

Radiographic Findings

Usually papillomas present as solitary nodules obstructing a large bronchus. Some papillomas will also have a cystic appearance on X-ray and CT scans [24, 30]. In addition atelectasis and poststenotic pneumonia might obscure the picture.

Gross Findings

Papilloma can occur as solitary or multiple nodules or as diffuse proliferation. It projects into the lumen of bronchi like any other endobronchial tumor. Usually it presents as a small tan-white tumor (Fig. 17.11) with a small branching stalk and a smooth or verrucoid surface. However, the gyrated surface with a similar appearance as a colonic adenoma may guide the pathologist into the right direction. In cases of a papillomatosis, the gross appearance is less typical and might

simulate features of other tumors (Fig. 17.12). On a closer look, one may appreciate the endobronchial growth and the composition of different nodular structures.

Fig. 17.11 Bronchial papilloma at the resection margin of an upper lobe resected because of squamous cell carcinoma. The papilloma shows the characteristic stromal tree structure and is covered by squamous epithelium. H&E, ×25

Histopathology

Papillomas are benign epithelial tumors, characterized by a treelike branching of the stroma, composed of thin-walled capillaries or veins with a hyalinized wall and few mesenchymal cells, covered by an epithelium, which can be either entirely composed of squamous cells or a mixture of cuboidal, cylindrical, and/or transitional cells. On surgical resection specimen, the diagnosis is apparent already on low-power magnification: the treelike structure of the mesenchymal stalk covered by multilayered epithelium, most often of the squamous nonkeratinized type, sometimes with certain degrees of dysplasia (Figs. 17.11, 17.13, and 17.14). Other types of epithelia such as columnar, transitional, and mixed type are found and will be acknowledged in the name [31–33]. Especially in the squamous cell papillomas, koilocytes are seen (Fig. 17.15), and by immunohistochemistry, by in situ hybridization, or by PCR, human papillomavirus can be detected [29, 34]. Koilocytes are characterized by

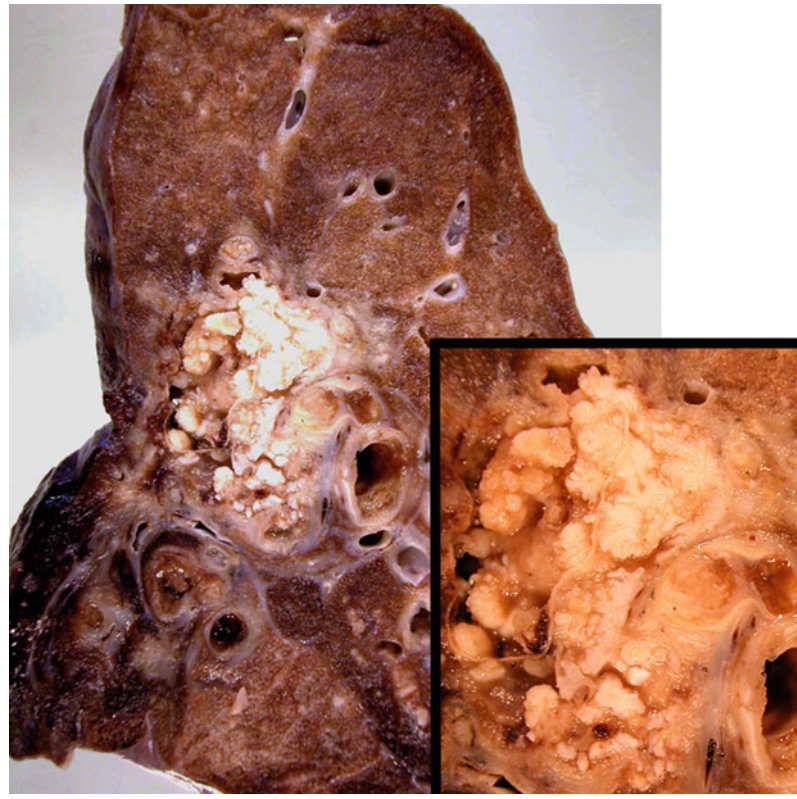

Fig. 17.12 Papillomatosis of the lung. Numerous papillary proliferations are seen in the large bronchi. *Inset*: enlarged view of the lesion (kindly provided by Dr. A. Moresi-Hauff, Gauting)

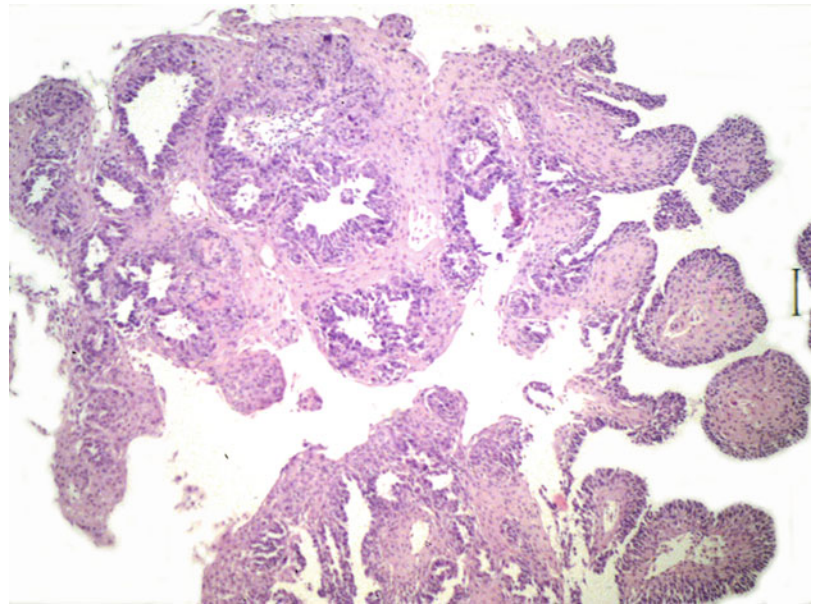

Fig. 17.13 Bronchial biopsy showing fragments of a squamous cell papilloma. H&E, bar 100 µm

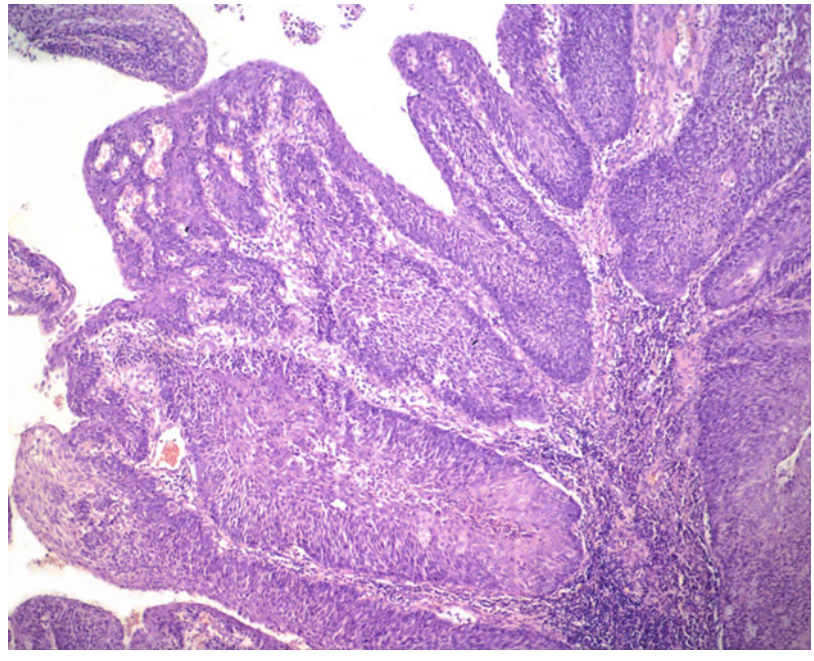

Fig. 17.14 Squamous cell papilloma with severe dysplasia. Nuclei are increased, epithelial layering and maturation of cells is lost, focal areas show already dyskeratosis of cells. H&E, ×100

halos close to the nuclei; in addition a bizarre outline of nuclei is usually detected in cases of HPV 16- or HPV 18-positive cases. Also "nuclear rupture" might be seen: nuclear membrane is vanishing and chromatin loses its staining intensity. When dealing with bronchial biopsies, the diagnosis might be not as easy. The papilloma is broken into parts; the treelike structure of the stalk is not seen in its entire length. Therefore one needs clearly defined criteria. The stroma should be branching, usually there is not much inflammatory infiltrate present, the capillaries or veins are thin-walled, the basement membrane is thickened, and there are only a few other mesenchy-

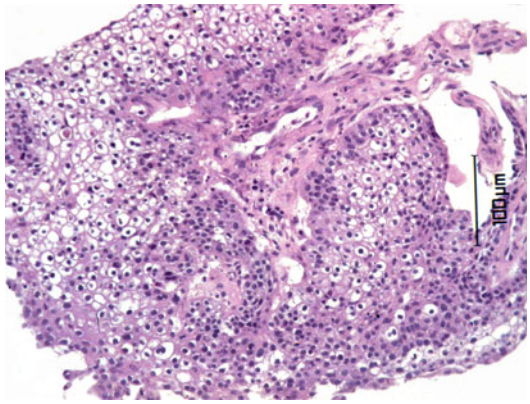

Fig. 17.15 Koilocytes in a squamous cell papilloma. Around nuclei a halo is seen. The more the nuclei show bizarre configuration, the more likely they are infected by an oncogenic type of HPV. H&E, bar 100 µm

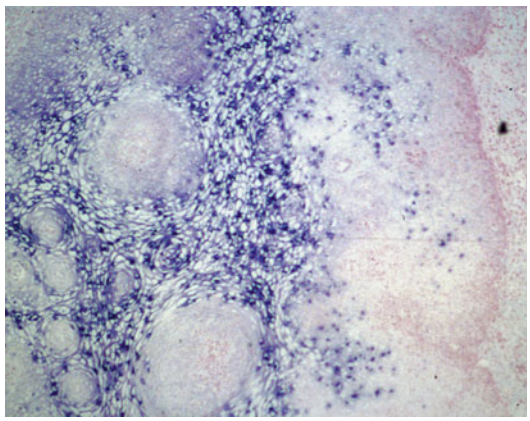

Fig. 17.16 In situ hybridization for human papilloma virus type 6b. There are dense signals in many of the squamous cells. ISH, ×100

mal cells present. The epithelium is composed of layers of squamous cells, focally showing koilocytic features (Fig. 17.13). In rare cases the epithelium might be of a transitional or even columnar type, in this case with or without goblet cells. In these cases koilocytes are usually not encountered. Dysplasia might be present; some may have carcinoma in situ [35] (Fig. 17.14).

Immunohistochemistry

In all cases human papilloma virus (HPV) typing should be done. In the author's experience, immunohistochemistry for low- and high-risk types is sufficient. HPV typing by in situ hybridization or by PCR might be done instead (Figs. 17.16 and 17.17) [27, 36].

Cytology

The diagnosis of a papilloma cannot be made on cytological specimen, although koilocytes might be correctly diagnosed. The diagnosis requires the structural features. However, by molecular investigation HPV can be detected, which together with koilocytes might be used to make a tentative diagnosis of papilloma.

Molecular Biology

HPV types are oncogenic due to their interference with cell cycle proteins [36, 37]. They can interact with p53 as well as with retinoblastoma gene protein. The most common HPV types in the upper and lower respiratory tract are types 6b, 11, 16, 18, 31, 33, and 35. Whereas types 16 and 18 are regarded as oncogenic types and infer a

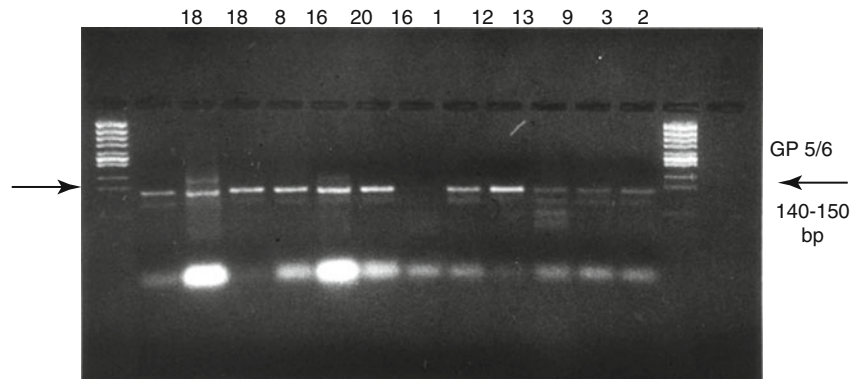

Fig. 17.17 PCR for common sequence in human papilloma virus GP5/GP6. A series of cases have been tested

risk for progression of papillomas to invasive carcinoma, 6 and 11 are associated with recurrent papillomas/papillomatosis but rarely with carcinomas [38]. There is an exception to the rule: within the HPV genome, there are segments designated E1 through E7, which code for different functions. Within E2 there is a regulatory gene controlling the expression of the oncogenic E6 and E7 genes. If E2 is mutated in HPV 11, the virus will show an uncontrolled expression of E6 and/or E7 and thus behaves similar to the oncogenic HPV 16 and 18. This might be an explanation for case reports on HPV 11 in papillomas progressing to invasive squamous cell carcinomas [37, 39–45]. The oncogenic E6 and E7 sequences induce inactivation of p53 and rb1 proteins, respectively, and therefore these control mechanisms for DNA integrity are lost. In addition to an increased expression of p53 and Rb proteins, HPV also reduced the expression of p21 (WAF1) protein [46]. HPV-E6 protein also increases the activity of cyclin A-dependent kinase 2 (CDK2). Malanchi and coworkers also confirmed the downregulation of p21(WAF1/CIP1) and enabled cells to overcome the G1 arrest upregulating oncogenic RAS [36].

Cell of Origin

Detection of HPV by in situ hybridization will show a low amount of viral gene in the basal cells and increased reactivity in the middle and upper part of the epithelium. However, this most probably reflects expansion and multiplication of the viral genome or parts thereof. Most probably reserve cells of the bronchial mucosa are the target of HPV, which then will undergo transformation and expansion, giving rise to the papilloma [47].

Differential Diagnosis

There is no differential diagnosis to be considered in solitary papillomas. In papillomatosis the major differential diagnosis is squamous cell carcinoma. If papillomatosis is seen in children, then squamous cell carcinoma is most unlikely. In adults the differential diagnosis might be difficult or even impossible. Immunohistochemical stains for p63 proteins might be of help, as well as a positive stain for carboanhydrase IX and increased staining for the proliferation marker MiB1(Ki67).

Prognosis and Therapy

Papillomas are cured by surgical resection or laser abrogation. However, recurrence is common. The pathologist should insist that primarily a biopsy is taken, to make the proper diagnosis including HPV typing. Cases with proven oncogenic HPV are at high risk for development of recurrence and progression into squamous cell carcinoma [27]. These patients need to be closely monitored and controlled by bronchoscopy. Since in older age HPV genomic integration is most often accompanied by smoking habits, the risk of developing a squamous cell carcinoma is increased. The proportion of squamous cell carcinomas arising from papillomas is rare. However, a papilloma remnant can sometimes be seen in squamous cell carcinomas, usually in the exophytic part.

If a treatment with antiviral drugs has any effect, it is not clear; HPV vaccination in children might not prevent infection in all cases, since infection can occur during delivery by the infected mother. If vaccination has a protective effect of already infected children will be seen in follow-up observation studies [48].

Variants

Transitional Cell Papilloma

Transitional papillomas are characterized by their transitional epithelium covering an otherwise identical branching stroma stalk. Transitional papilloma often present as a mixed type with squamous cell papilloma (Fig. 17.18).

Columnar Cell Papilloma

Columnar cell papilloma is extremely rare. A few cases have been reported. Columnar cell might be mucin-producing goblet cells or secretory columnar cells (Fig. 17.18). HPV might be detected in this type of papilloma, similar to columnar cell proliferations in the cervix, but might also be negative for HPV. Sometimes cellular atypia can be seen as in the case presented here. So far HPV testing was not reported.

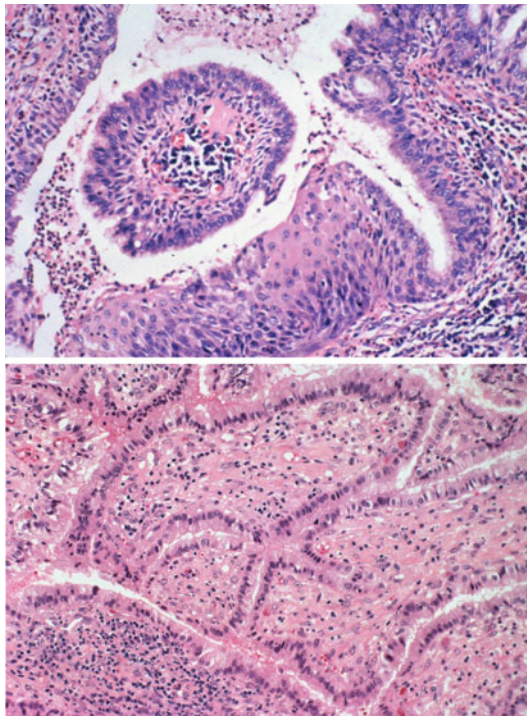

Fig. 17.18 Variants of HPV-induced papilloma, a mixed squamous and columnar type of papilloma (*upper* panel), and a columnar cell papilloma (*lower* panel; this one kindly supplied by B. Papla). H&E, ×150

Squamous Cell Intrabronchial Papillomatosis

There exists a rare diffuse form of *papillomatosis* [25, 49]. A whole lung lobe can be affected. Papillomatosis is characterized by an intrabronchial growth of papillomas, which all together form a multinodular lesion (Figs.17.12, 17.19, 17.20, and 17.21). In papillomatosis the normal columnar epithelium is replaced by metaplastic often dysplastic squamous epithelium, and there is an ingrowth of mesenchymal stalks into the bronchial lumen. Many of these papilloma projections grow and spread intrabronchially, completely filling the lumina. They may grow down into the bronchioles and alveolar ducts and reach the centrilobular portion of the alveoli (Figs. 17.20 and 17.21). This entity is different from what some authors call recurrent papillomatosis, namely, using the term for multiple papillomas spreading within the upper and lower airways [50]. This should instead be called multifocal papilloma but not papillomatosis. Papillomatosis can occur in children as well as in adults. In the newborn the disease is probably a result of infection with papilloma viruses during delivery. Recurrent upper respiratory tract papillomatosis in children younger than 10 years of age will more likely spread to the lower respiratory tract [24, 26, 49]. These tumors undergo spontaneous regression in puberty and usually do not progress to a malignant form. HPV is present in all cases. The oncogenic types 16 or 18 prevail in adults, whereas HPV 6 or 11 in children. In 5 % of the cases it involves lower airways and presents with the symptoms of pneumonia, hemoptysis, and asthma. The dignity of papillomatosis is difficult to assess: due to the fact that the papillomatosis fills the airways completely and may exhibit some nuclear atypia because of the presence of the viral genome, malignant transformation is hard to prove and invasion hard to rule out. The differentiation from microinvasive squamous cell carcinoma developing from papillomatosis can in some cases be impossible (Fig. 17.19c). Radical surgical resection is recommended and the only choice for treatment.

Glandular papillomatosis has never been described, but in the European rare pulmonary disease collection, a case of intrabronchial papillomatosis has been collected. This proliferation is characterized by an intrabronchial growth of benign-looking papillary structures, covering a delicate mesenchymal stalk. The nuclei of the epithelial proliferation are small and round, chromatin is evenly distributed and fine, and nucleoli are inconspicuous or absent. The lesion is characterized by a bronchiolar columnar and cuboidal cell proliferation forming a single row without mitosis, which extends into the alveolar region replacing normal pneumocytes (Fig. 17.22). This lesion resembles intraductal papillomatosis of the breast. The biological behavior is uncertain, and no follow-up data are available.

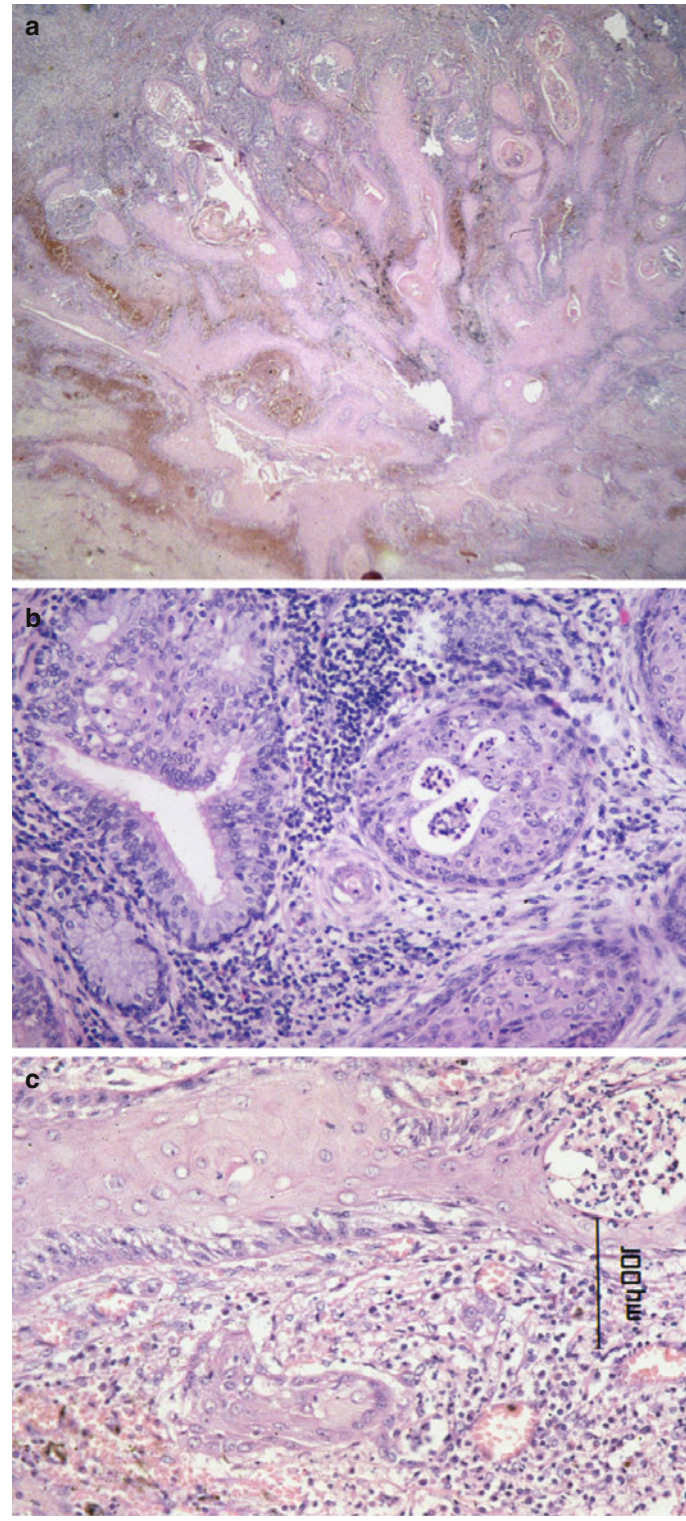

Fig. 17.19 Squamous cell papillomatosis, positive for HPV16. (**a**) Overview of the papillomatosis, the growth along the bronchial tree is evident; however, squamous cell carcinoma can be suspected. (**b**) Area of squamous cell metaplasia, the epithelium replaces the original columnar epithelium. (**c**) Another area suspected as representing invasive squamous cell carcinoma arising in papilloma. H&E, ×12 and 200, bar 100 µm

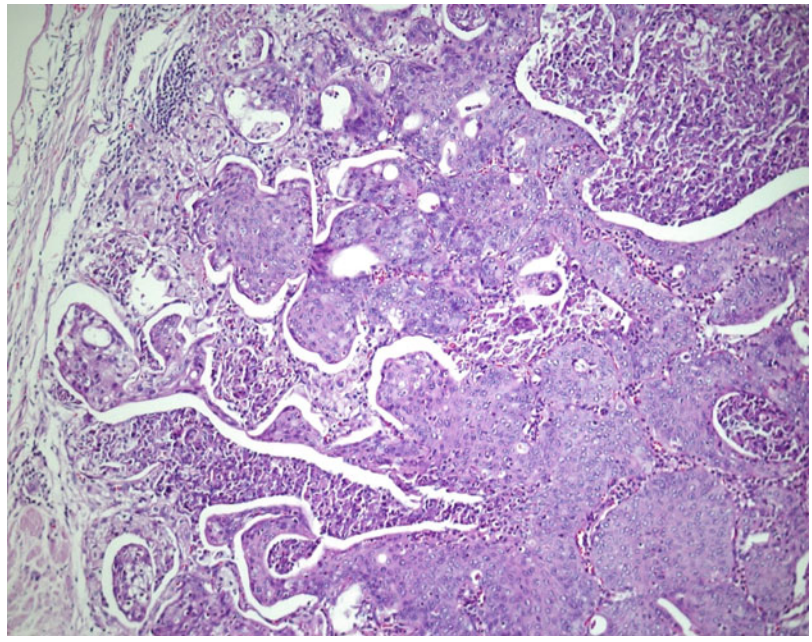

Fig. 17.20 Squamous cell papillomatosis in a 10-year-old girl, positive for HPV11. H&E, ×150

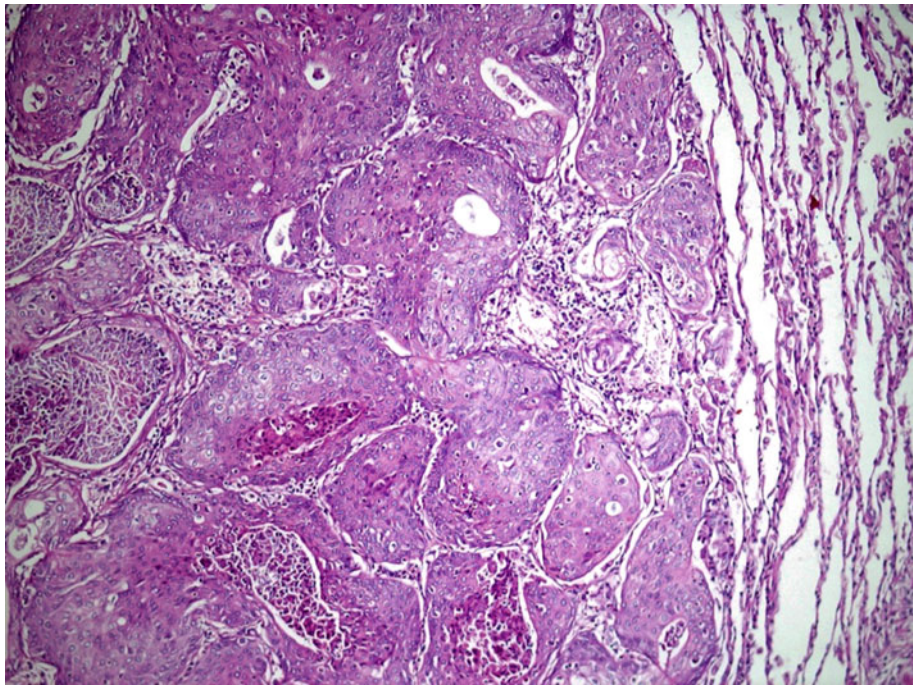

Fig. 17.21 Same case of papillomatosis, here the koilocytes can be seen. There is some nuclear atypia with polymorphism. H&E, ×200

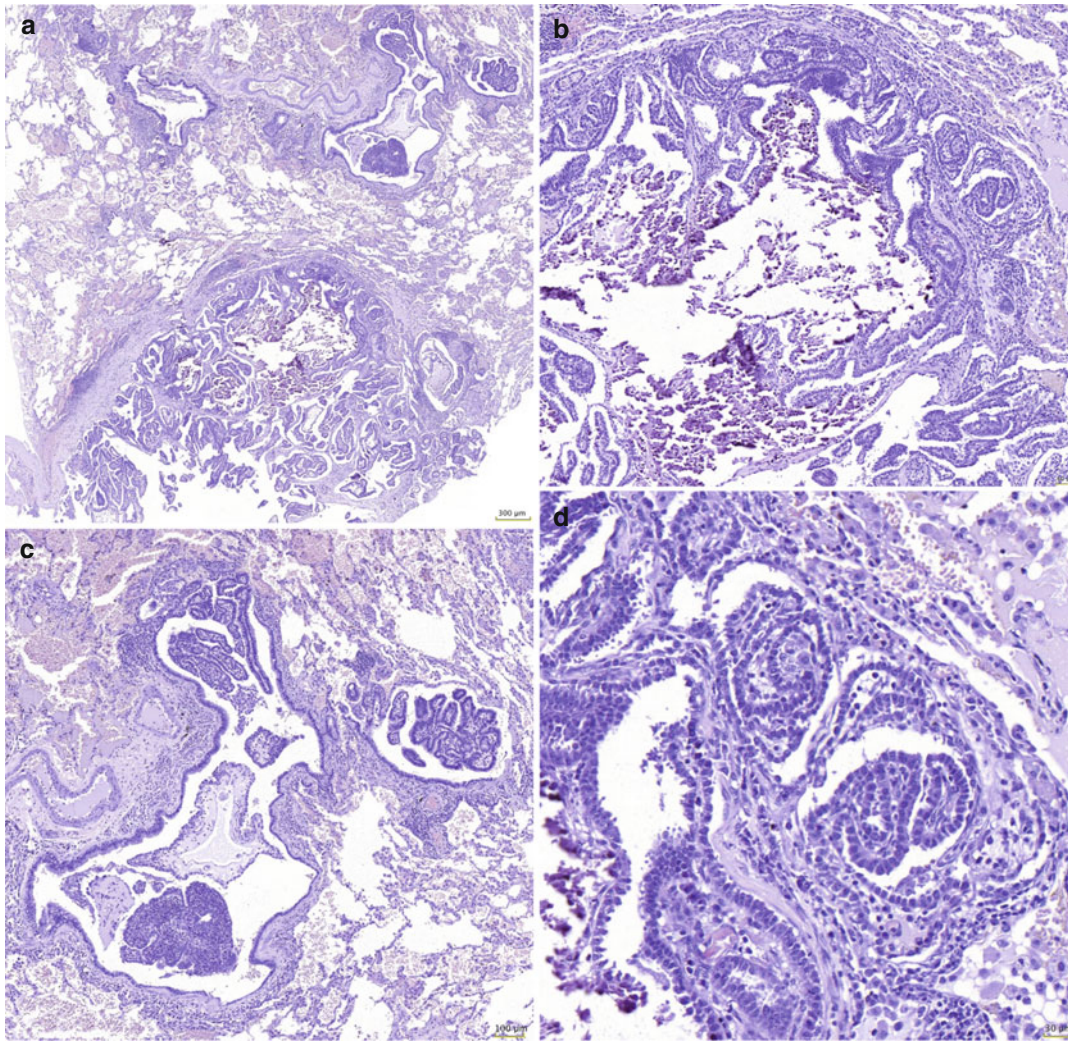

Fig. 17.22 Glandular papillomatosis, a lesion so far unknown to the literature. (**a**) Overview showing an adenoma-like lesion, however, not encapsulated. (**b**) Higher magnification, some calcifications are within the central area. (**c**) shows the extension of the papillomatosis into adjacent bronchi and bronchioles. The tumor grows in a similar fashion as intraductal papillomatosis of the breast. (**d**) High-power view shows a bland tumor epithelium without atypia and organized in a single row of columnar cells, some cells with signs of apocrine secretion. H&E, bars 300, 60, 100, and 30 μm

17.1.1.5 Papillary Adenoma

Definition and Incidence

Papillary adenoma is a very rare peripheral pulmonary tumor. It is more common in males; the average age at presentation is around 32 years. Clinically the tumor is asymptomatic. Only single case reports are available [44–46].

Radiographic Findings

The tumor presents as a well-circumscribed small peripheral solitary nodule on CT scans.

Gross Pathology

These tumors present as solitary, rarely as multinodular lesion. The nodules are usually small and well circumscribed, measuring from a few mm

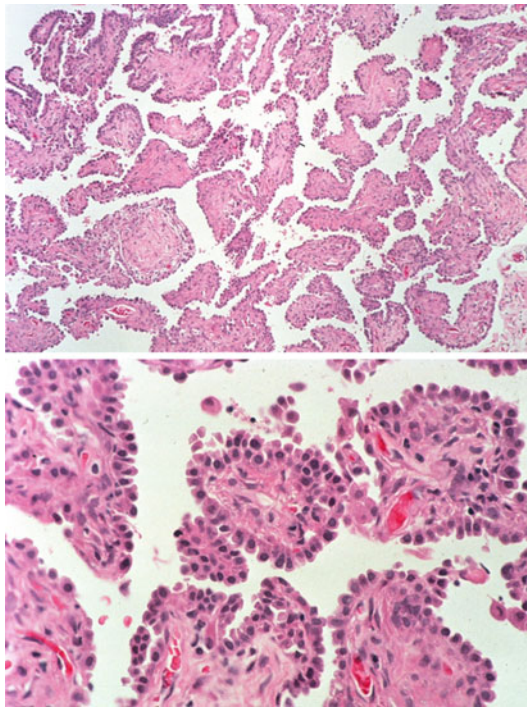

Fig. 17.23 Papillary adenoma, a rare tumor arising in the peripheral lung. *Upper* panel shows the many papillary projections; in the *lower* panel, details of the papillae are seen. The bland-looking stroma is covered by a single row of columnar or cuboidal cells, some of them resembling Clara cells. Note the bland morphology, without mitosis or nuclear atypia. H&E, ×50 and 200

up to 3 cm in diameter. Cut surface is grayish red and soft and can show a variety of features, such as hemorrhage and sclerosis/scaring. The tumor does not contain a capsule but compresses the adjacent lung parenchyma.

Histopathology

Microscopically the tumor is well circumscribed and shows papillary structures composed of fibrovascular stroma covered by uniform cuboidal to columnar cells, which resemble type II pneumocytes. Clara cells and ciliated cells are present, but also solid areas can be found (Figs. 17.23 and 17.24). Nuclei of cells have typical cytoplasmatic invaginations. Surrounding lung parenchyma can show features of organizing pneumonia, fibrosis, or simple pneumonia due to bronchial obstruction and mucostasis.

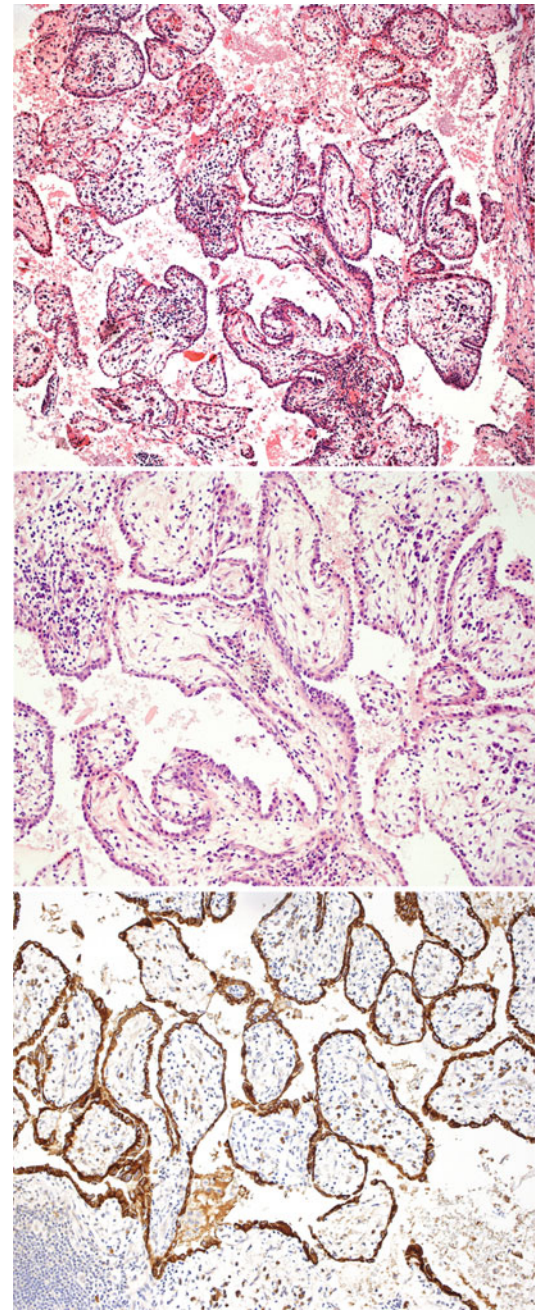

Fig. 17.24 Papillary adenoma, other case. (**a**) Low-power overview of the tumor with papillae covered by bland-looking epithelium. In (**b**) the epithelial cells are cuboidal, some with features of Clara cells. (**c**) Immunohistochemistry for cytokeratin 7 shows positivity of the single epithelial layer. H&E, ×50, 100, immunohistochemistry ×100

Immunohistochemistry and Molecular Biology

Immunohistochemically, the tumor cells react positively with antibodies for surfactant apoproteins, carcinoembryonic antigen, cytochrome oxidases P-450 1A1/A2 and 2B1/B2, surfactant apoproteins, and Clara cell proteins. Also a positive reaction for TTF1 can be demonstrated. Tumor cells have microvilli but also may develop lamellar bodies. Papillary adenoma is a benign, and morphologically distinctive tumor, which may develop from Clara cells or pneumocyte type II precursors [51–53]. Ultrastructurally many osmiophilic lamellar bodies and electron-dense granules can be demonstrated [51–55]. No mitotic figures, no necrosis, and no mucin can be found.

In experimental mouse model papillary and lepidic pulmonary adenomas could be induced by fibroblast growth factor 10 expression. FGF10 might induce a differentiation of cells to a pneumocyte type II phenotype. Withdrawal from FGF10 expression caused regression of the tumors and loss of the differentiation markers TTF1, SP-B, and proSP-C [56].

Prognosis and Treatment

Radical surgery is curative in almost all cases described so far. However, as stated above atypia and invasion has to be ruled out.

The main differential diagnoses are sclerosing hemangioma/pneumocytoma and carcinomas (primary and metastatic). The absence of atypia, mitosis, and necrosis are features of this tumor. Invasion should be ruled out. However, in two reports the dignity of papillary adenoma have been questioned: Mori et al. [55] described a case, which showed vascular invasion and also dissemination into the surrounding lung. Invasion of the lung and pleura was reported by Dessy and colleagues in their papillary adenoma [53]. The papillary adenoma can be differentiated from intrabronchial glandular papillomatosis because it is a solitary tumor, does not grow intrabronchially, and compresses the adjacent lung.

Biphasic Papillary Adenoma and Myomatous Hamartoma

This tumor was excised with the clinical diagnosis of a benign-looking cystic tumor.

Histologically it was composed of a papillary adenoma with cuboidal and columnar cells, some containing cilia. In addition there were smooth muscle cells in the walls of the cysts, and in the center of the tumor was a myomatous variant of hamartoma embedded. The tumor stained for low molecular weight cytokeratin 7, apoprotein A and B antibodies, and the mesenchymal cells were positive for HHF35, smooth muscle actin; in addition there was an increase of ACTH-positive neuroendocrine cells within the papillary cysts. Similar tumors have been reported. Matsumoto reported on a mixed tumor of the salivary gland type with chondromyxoid stroma. In the glandular wall, myoepithelial components and cartilage formation were embedded. The glandular component was positive for TTF1 and the surface lining cells were positive for surfactant apoprotein A [57]. The five cases reported by Chang showed glandular and spindle cell differentiation. The inner, cuboidal epithelial cell layer (positive for panCK, EMA, and TTF1; some glands also positive for surfactant apoprotein A) was surrounded by an outer layer of myoepithelial cells (high molecular weight CK, S100, SMA, calponin, caldesmon, and p63 positive) [58].

17.1.1.6 Sclerosing Pneumocytoma (Formerly Sclerosing Hemangioma)

Clinical Symptoms and Epidemiology

The tumor is more common in middle-aged women (more than 80 %; mean age 40–45 years) and is rare in Europe and North America but frequent in Asia (Japan and China). The tumor is asymptomatic and usually incidentally detected by chest X-ray. Most often there is a single tumor nodule, but also multiple tumors have been reported [59–61]. The tumor grows slowly and is expansive, but few cases of malignant metastasizing sclerosing pneumocytoma have been reported [62–65].

Misnomers

The name hemangioma is misleading and originally was selected because the first cases presented with massive bleeding and central sclerosis

[66]. The epithelial proliferations at the border were erroneously interpreted as reactive [67]. Other terms used for these tumors were pneumocytoma, papillary pneumocytoma, benign sclerosing pneumocytoma, and post-inflammatory pseudotumor. At that time immunohistochemistry was not available and the hemorrhagic part of the tumor was interpreted as hemangioma. In consecutive reports the epithelial nature of the tumor was finally proven [68, 69]. Therefore in the last WHO classification, the name was changed back to sclerosing pneumocytoma [70].

Radiographic Findings

An inhomogenous enhancement is frequently present in sclerosing hemangioma, especially in sclerotic and predominantly papillary types. The presence of a tail sign, intra-tumoral cystic areas, and a prominent artery sign are the most frequent features [71]. In one case also positron emission tomography (PET) was performed, and an increased accumulation of 18F-fluorodeoxyglucose (FDG) was demonstrated [72].

Macroscopy

The tumor can present as an endobronchial mass [73], but more often the tumor is embedded within the lung parenchyma forming a solitary nodule of less than 3 cm [74–76]. There are usually no clinical symptoms except in the rare endobronchial variant, which will cause bronchial obstruction. On cut surface they are grayish red to white in color; the different parts may stick out by their different color composition (Fig. 17.25a). They can be located peripheral as well as central endobronchial [62–64].

Histopathology

SP can present with a variety of morphological features: there might be central hyalinization, areas of thin-walled veins with extensive hemorrhage (therefore the original name), and areas of papillary epithelial proliferations (Fig. 17.25). Sometimes parts with hyalinization, hemorrhagic areas with hemosiderin-laden macrophages, xanthoma cells, calcification, or chronic inflammation can be quite large [76]. There are two different cell populations: the one at the surface is mature and of a pneumocyte phenotype positive for TTF1, surfactant apoproteins, and low molecular cytokeratins, whereas the cells within the stroma are immature pneumocytes, epithelioid, and round to polygonal with eosinophilic sometimes clear cytoplasm (Fig. 17.25). The tumor cells are large cuboidal epithelial cells forming sheets but also can present as single cells, embedded in a hyalinized stroma. Nuclei are round to oval with inconspicuous nucleoli. Cells lining the papillary structures are cuboidal with prominent nucleoli and cytoplasmatic invaginations. Mitotic figures are very rare, but some tumors will present with atypia and with multinucleated tumor cells. Both types of cells seem to belong to the tumor, based on findings of their monoclonality [77].

Immunohistochemistry and Electron Microscopy

Immunohistochemically the tumor cells at the surface will positively stain for EMA, pan-cytokeratin, surfactant apoproteins, carcinoembryonic antigen, and Clara cell proteins. Epithelioid cells within the alveolar walls are positive for surfactant apoproteins [74], TTF1, and EMA (Fig. 17.26) but negative for cytokeratins and thus may be transformed pneumocytes [68, 78, 79]. Ultrastructural investigations confirmed that the tumor cells are of epithelial origin, most probably pneumocyte precursor cells [80], because they present with whorled bodies and lamellae, which resemble those of type 2 pneumocytes. However, differences were also found, namely, the loss of the apico-lateral and a restricted surface differentiation in the stroma cells, whereas the surface cells form small lumina, microvilli, and multivesicular or multilamellar bodies. It was concluded that sclerosing hemangioma is a proliferation of rather fetal type II pneumocytes [80]. The higher frequency of in women prompted the search for hormonal determinants: these tumors are positively stained by progesterone and estrogen receptor antibodies [81].

Molecular Biology

Sclerosing hemangioma has been extensively investigated for their cells of origin and for

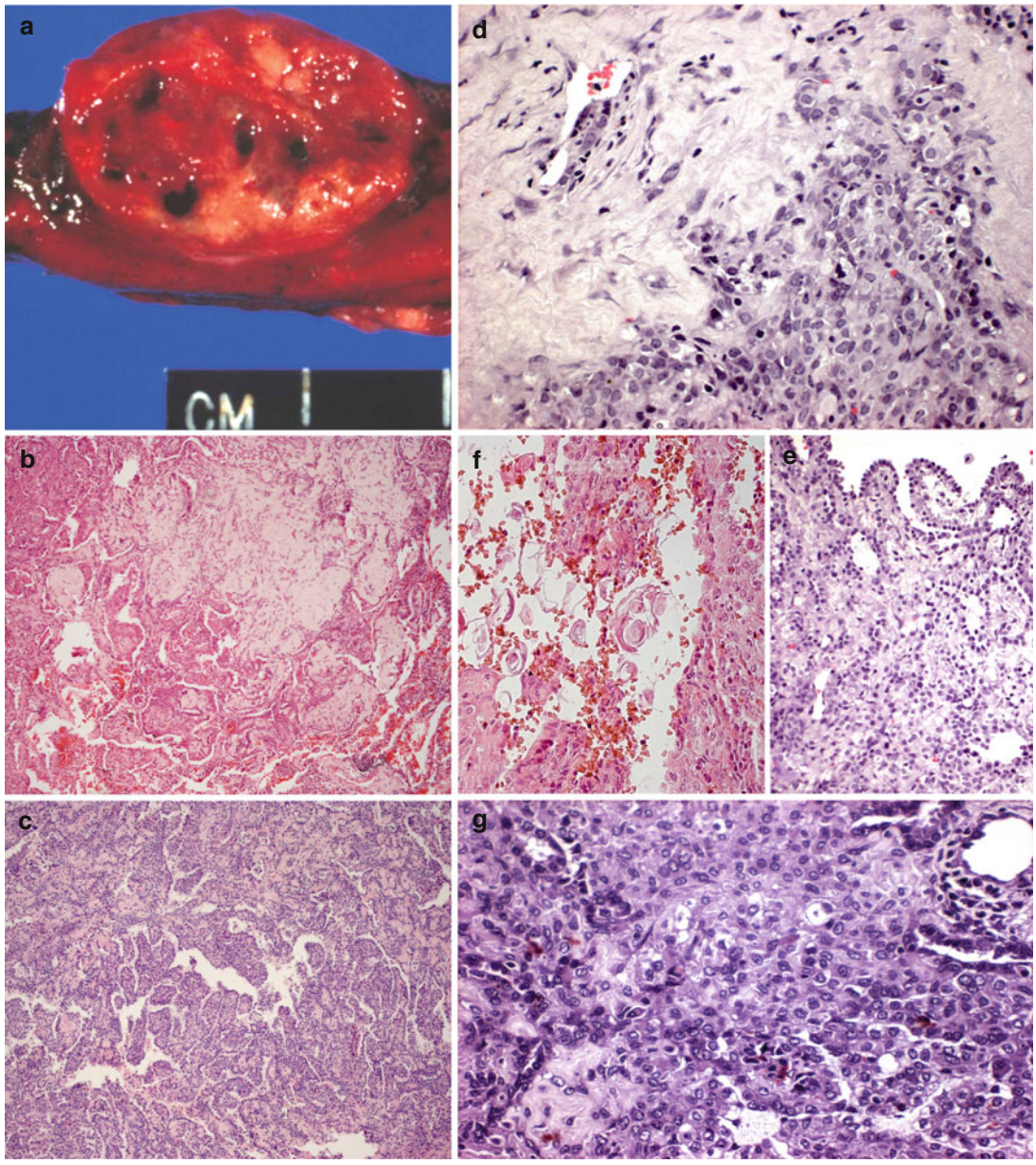

Fig. 17.25 Sclerosing pneumocytoma (formerly sclerosing hemangioma). (**a**) Resected tumor with hemorrhage, one of the reasons for the old name. (**b**) Tumor with sclerosis in the center. (**c**) Other case with mild fibrosis. (**d**) Border between tumor and sclerotic center. (**e**) Tumor front shows mature-type pneumocytes and immature cells. (**f**) In rare cases as this one giant lamellar bodies released from pneumocytes can be seen. (**g**) High power showing the two types of pneumocytes, mature at the surface and immature at the stroma of the tumor. H&E, ×12, 100, and 250

other factors related to their occurrence. In a loss of heterozygosity study, Dacic and coworkers studied sclerosing hemangioma at a few microsatellite markers and found frequent allelic loss on chromosomal arms 5q and 10q. When compared with bronchioloalveolar carcinoma, the microsatellite marker D5S615 was significantly more frequently affected than in BAC. The authors concluded that a putative tumor suppressor gene located on the chromo-

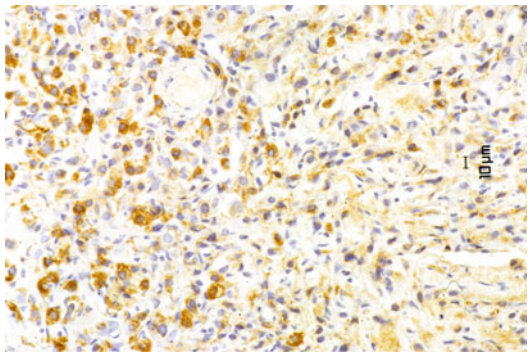

Fig. 17.26 Sclerosing pneumocytoma, positivity of many tumor cells for surfactant apoprotein A. This demonstrates that these tumors are derived from primitive pneumocytes. Bar 10 µm

somal arm 5q might play a role in tumorigenesis of sclerosing hemangioma [82]. In an immunohistochemical investigation, the surface as well as the polygonal stroma cells of sclerosing hemangioma expressed MUC1, thyroid transcription factor 1 (TTF1), and EMA. Thomsen-Friedenreich antigen and cytokeratin were positive only in the surface cells. It was concluded that the two types of cells in sclerosing hemangioma might derive from a common precursor cell through divergent differentiation toward the type II pneumocyte during tumorigenesis [83]. Expression of EGFR but not Her2 was observed in the several cases of sclerosing pneumocytoma. Analysis of gene mutations in EGFR and HER2 and also KRAS sequencing did not reveal molecular alterations, whereas allelic losses at p16 and Rb loci were observed in few cases [84]. Both cell types of SP are positive TTF1, EMA, β-catenin, E-cadherin, and VEGF. In SP no CpG island methylation was seen for p16(INK4a) but low for RASSF1A gene methylation was seen for HOX D9, D11, and D13 in approximately one third of cases, respectively [85]. In several cases of sclerosing pneumocytoma, the tuberous sclerosis complex (TSC) pathways were investigated. The mammalian target of rapamycin (phospho-mTOR), phospho-Akt, hamartin, and tuberin, as well as hyperoxide inducible factor (HIF-) 1alpha and VEGF showed a positive reaction implying that aberrant mTOR signaling may play a role in the development of sclerosing pneumocytoma [86]. The finding of metalloproteinase 9 (MMP-9) in sclerosing pneumocytoma was discussed in relation to the locally invasive growth pattern, whereas the proof of tubulin-alpha was discussed as being responsible for sclerosis [87].

Differential Diagnosis

Inflammatory pseudotumor, clear cell "sugar" tumor (PECOMA), some primary and metastatic carcinomas, and low-grade epithelioid hemangioendothelioma have been considered as probable differentials. Inflammatory pseudotumor usually can easily be separated, because of the mixture of plasma cells, myofibroblasts, smooth muscle cells, as well as histiocytes. Even pure histiocytic variants will morphologically look differently. The clear cell tumor might look similar but will not present with the two cell types mentioned above. Epithelioid hemangioendothelioma might give problems in the differential diagnosis: the sclerotic areas can look similar, hemorrhage is sometimes present, but the pseudo-signet ring cell appearance of the tumor cells within sclerotic areas will usually guide one toward the correct diagnosis. A positive reaction for surfactant apoprotein A and a negative one for endothelial markers will help in making the right diagnosis. Primary and metastatic carcinomas can look similar to sclerosing pneumocytoma – this is especially true for metastatic lobular breast and prostate carcinomas. Since nuclear atypia and mitotic counts are not immediately apparent, immunohistochemical stains might be necessary.

Prognosis and Natural History: Treatment

Unusual associations of sclerosing pneumocytoma were reported for familial adenomatous polyposis [88] and also for Cowden syndrome [89]. If this association is incidental or not cannot be answered yet. SP is a benign tumor. However, malignant variants have been reported. Chan reported lymph node metastasis in one case [62], Iyoda and Wei each recurrences in two other cases [75, 90]. Komatsu and coworkers reported intrapulmonary metastasis [63]; however, this

might be questioned, since in another report multifocality was seen with several sclerosing pneumocytomas in both lungs [60]. So sclerosing pneumocytoma might be locally invasive but still has to be regarded as benign – a death due to tumor burden has not been seen in any patient.

17.1.1.7 Alveolar Adenoma (Pneumocytoma)

Epidemiology and Incidence

Alveolar adenoma/pneumocytoma is a rare tumor or tumorlike lesion. It was first described by Yousem and Hochholzer [91]. There are no data about epidemiology, and the incidence has never been assessed. Alveolar adenoma can be regarded as either a developmental disease or a tumor. It is formed by numerous alveoli without any connection to bronchioles or bronchi. Since there is no connection with the bronchial tree other then the channels of Lambert and the pores of Kohn, alveolar adenoma usually present with enlarged and cystic dilated alveoli. These will steadily increase, because lipids and proteins produced by the epithelia are drained insufficiently.

Special Clinical Features

Patients are of older age and equal sex. Alveolar adenoma is incidentally detected, because it will cause compression and thus atelectasis of the adjacent normal lung and consequently causes hypoxia, if large enough. Clinically alveolar adenomas are usually asymptomatic and detected accidentally in routine chest X-ray.

Radiographic Findings

On X-ray only large alveolar adenomas will be detected because of its translucent feature. On HRCT it presents as a cystic translucent well-circumscribed emphysema-like lesion. If the adjacent parenchyma is compressed, the more likely radiologists will be able to correctly diagnose this tumor.

Macroscopy

Alveolar adenoma present as a multicystic structure surrounded by normal lung parenchyma, the latter might be atelectatic. Macroscopically, tumor is solitary tan or grayish white and 1–2 cm in diameter. The mucus-filled cystic structures are easily identified. Secondary bleeding into the cysts can occasionally obscure the tumor and make the diagnosis difficult.

Histopathology

The adenoma is composed of cystic structures lined by flat or cuboidal pneumocytes (Fig. 17.27). Within the lumen PAS-positive material (surfactant proteins) is usually found. Foamy macrophages can be seen with ingested PAS-positive material. There are no bronchi or bronchioles and consequently also no medium-sized blood vessels. The entire tumor is composed of enlarged alveoli. Ultrastructurally the epithelial cells contain lamellar bodies and blunt surface microvilli and other features of type 2 pneumocytes. The interstitium between the cysts varies in thickness and contains myxoid collagenous matrix and myofibroblasts.

Immunohistochemistry

In case of uncertainties, immunohistochemical stains using surfactant apoprotein antibodies will highlight the alveolar lining cells. These cells are also positive for TTF1.

Differential Diagnosis

Other cysts within the lung are the main differentials: in emphysema bronchioles can be seen, and thus this will be not a complicated differential diagnosis. Bronchogenic cyst will present with a bronchial epithelium, a wall with smooth muscle cells, and rarely also cartilage. Congenital pulmonary adenomatoid malformation (CPAM) of type I and II can be separated, because the epithelium again is of bronchial type and within the cyst wall elements of normal bronchi can be found. In addition CPAM is a disease most often found in children, whereas alveolar adenoma is most often detected in older patients of both sexes. Atypical adenomatous hyperplasia (AAH) might be occasionally difficult to differentiate from alveolar adenoma if there are a lot of inflammatory changes in the adenoma. In these adenomas the pneumocytes are enlarged and show reactive changes. However, atypia is not as prominent as in AAH. In addition in AAH, respiratory

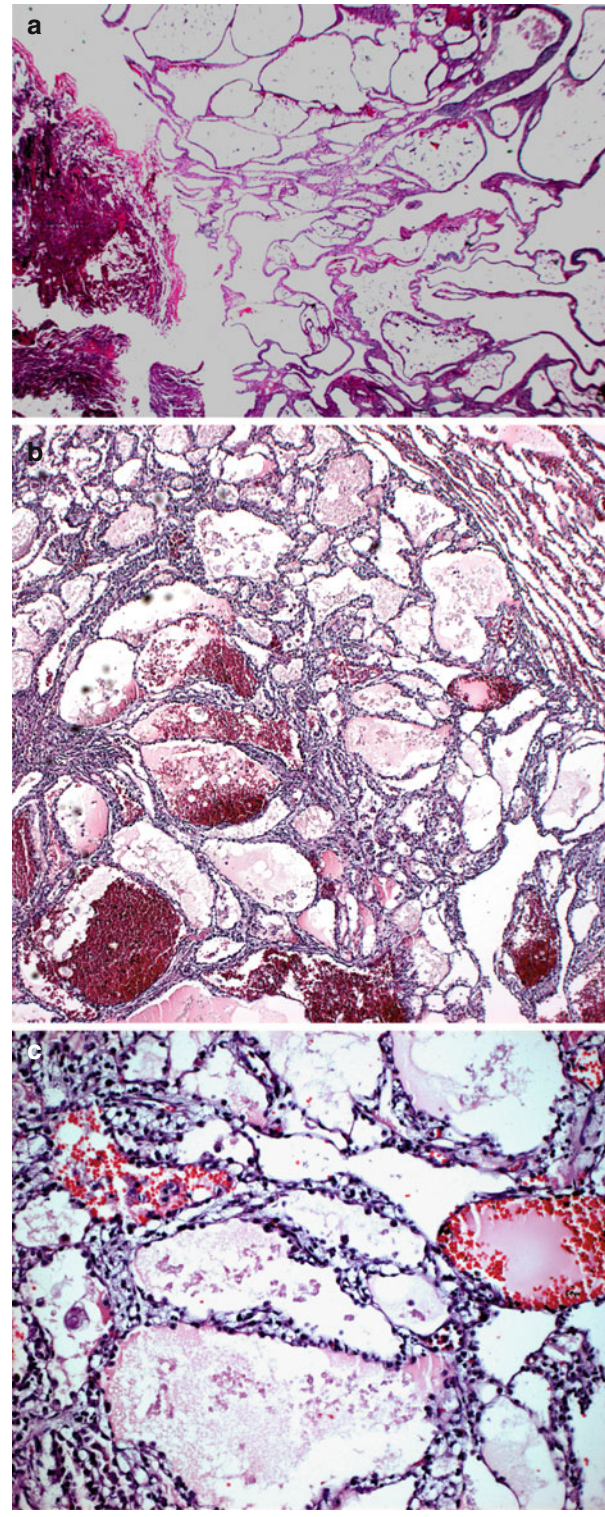

Fig. 17.27 Alveolar adenoma, (**a**) a case with large cystic spaces without a connection to bronchioles. (**b**) Alveolar adenoma with bleeding and compressed adjacent lung. Again no bronchioles are seen. Higher magnification of second case, showing flat pneumocytes covering the surface of the cystic dilated alveoli. H&E, ×12, 25, 100

bronchioles and alveolar ducts can be found in the vicinity, which would be not seen in the adenoma. Lymphangiomatosis and lymphangioleiomyomatosis might be other problematic lesions to differentiate. Lymphangiomatosis presents with cystic spaces, but the endothelial cells are usually flat. The cyst walls are usually fibrosed. Immunohistochemical stains for cytokeratins or podoplanin (D2-40) will unequivocally enable the correct diagnosis. Lymphangioleiomyomatosis also can present with multiple cysts. However, the cyst epithelium is flat, and usually at some foci areas of myoblast, proliferations will be seen, which enable the correct diagnosis.

Prognosis and Natural History

The etiology of alveolar adenoma is unknown. The process represents most probably a neoplastic epithelial proliferation predominantly of type II pneumocytes. Alveolar adenoma grows slowly, there are no mitoses, and only isolated nuclear staining for Ki-67 can be found in pneumocytes at the peripheral part of the tumor. These tumors do not infiltrate, recur if resected, and do not metastasize.

Molecular Biology

Roque et al. showed a clonal chromosomal aberration of der(16)t(10;16)(q23;q24) in 19 % of the cases. This may serve as an argument of a neoplastic character [92].

17.1.1.8 Multifocal Nodular Pneumocyte Hyperplasia (MNPH)

Epidemiology and Incidence

Micronodular pneumocyte hyperplasia is a tumorlike lesion associated with tuberous sclerosis and lymphangioleiomyomatosis [93]. Its incidence is unknown, but it is more rare than lymphangioleiomyomatosis (LAM). In contrast to LAM, MNPH is not restricted to females but can also occur in men. No clinical symptoms are recorded.

Radiology

MNPH might present with subtle cystic changes, if many nodules are present. However, cystic changes are not as pronounced as in LAM.

Macroscopy

This lesion is composed of multiple small nodules within the peripheral lung. The nodules are clinically silent and are therefore detected incidentally on HRCT. Their size can be between 2 and 8 mm. The nodules are tan white well demarcated from the lung. Small cysts are always present but macroscopically are inconspicuous.

Microscopy

Histologically the nodules are composed of tumor cells, which form nests and groups on the surface of alveoli but also within alveolar septa (Fig. 17.28). The cells resemble immature and mature pneumocytes without atypia, which will stain for low molecular weight cytokeratins, EMA, and surfactant apoproteins [93, 94]. The cells proliferate within alveolar septa. There is no progression into malignant tumors known and even no progression of these lesions into larger tumors.

Molecular Biology

A germline mutation of TSC2 and an immunohistochemical staining for tuberin have been demonstrated in LAM as well as in MNPH [94–96]. In another investigation mutations have been found in TSC1 and TSC2 [97]; therefore, MNPH is associated with tuberous sclerosis complex. Mutation of the TSC1 and TSC2 genes induces genetic instability, a reason for the occurrence of several benign tumors [98, 99].

Differential Diagnosis

The differential diagnosis is meningothelial nodules and chemodectomas (negative for cytokeratin and surfactant ApoA) and AAH (no growth within alveolar septa). Morphologically MNPH resembles cells of sclerosing pneumocytomas (both are based on a proliferation of cells differentiated into pneumocytes). So it was speculated

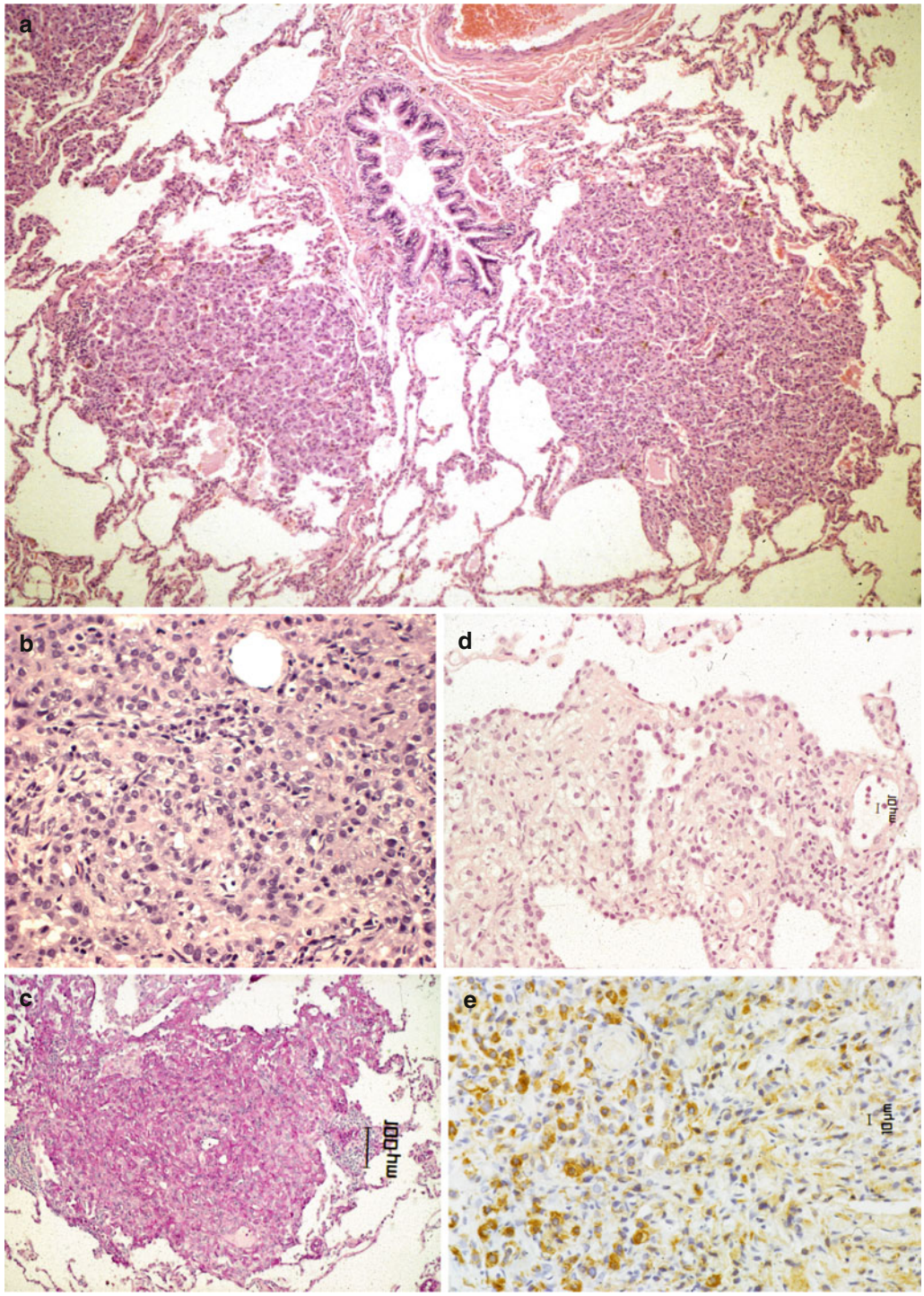

Fig. 17.28 Multifocal nodular pneumocyte hyperplasia (MNPH). (**a**) A case with several nodules without a capsule. (**b**) High magnification of the cells, which clearly resemble pneumocytes type II. (**c**) Many of the cells are positive for glycogen. (**d**) A small MNPH focus with predominantly immature pneumocytes. (**e**) Immunohistochemistry for surfactant apoprotein A. H&E, ×50, 250, 100, PAS, ×100, immunohistochemistry, bar 10 µm

that MNPH might be a precursor lesion of sclerosing pneumocytoma. However, this has never been proven. Even more, no case of sclerosing pneumocytoma was reported with adjacent MNPH lesions, and in addition sclerosing pneumocytoma does no exhibit mutations in the TSC genes but alterations of the mTOR pathway [86]. In other investigations some similarities were found between sclerosing pneumocytoma and pulmonary in situ adenocarcinomas [84, 85]. Based on these studies, MNPH and sclerosing pneumocytoma are most probably initiated by two different pathway activations but resulting in tumors of pneumocyte lineage, the former without, the latter with malignant potential.

Prognosis and Therapy

This proliferation is benign; all cases so far reported never developed into larger tumors or malignant neoplasms. No therapy other than resection has ever been applied. Resection, however, in all instances was done on the basis of a suspicious clinico-radiological diagnosis of either early malignancy or LAM.

17.1.1.9 Endometriosis

Although endometriosis is not a tumor, it most often presents as a tumor. In cases with pleural location, it causes pain and effusion, usually hemorrhagic. In addition it presents with multiple small nodules and is therefore mistaken as metastasis on X-ray and CT scan examinations. Intrapulmonary endometriosis is mistaken as a tumor for two reasons: by CT scan, it appears either as a single nodule or with multiple small nodular densities, again suspected as malignant tumor. Histologically misdiagnosis is also not uncommon; the proliferation is regarded as mixed epithelial-mesenchymal tumor.

Endometriosis can occur in the lung as well as in the pleura. Endometrial glands are surrounded by stroma cells. Fresh and old hemorrhage are present within this lesion. Cytokeratin antibodies can stain the epithelium, whereas the stroma cells will express estrogen and progesterone receptors (Fig. 17.29). The most important aspect is to not overdiagnose this lesion for a metastatic carcinoma or worse a carcinosarcoma.

17.1.1.10 Intrapulmonary Thymoma

Epidemiology and Incidence

Intrapulmonary thymoma is an extremely rare primary tumor within the lung. There are no data about the incidence of these tumors, only single case reports. More common are metastatic thymomas or thymomas infiltrating the lung directly from the mediastinum. The pathogenesis of these tumors is subject of speculation; an embryonal displacement of thymic "anlagen" is suspected or its development from germ cells [100].

Clinical Presentation

Some intrapulmonary thymomas present with myasthenia gravis, similar to their mediastinal counterparts [72], but most of them will not cause symptoms, other than due to enlargement and obstruction.

Radiographic Findings

Radiologically thymomas will present as solitary nodules up to 10 cm in diameter, usually well circumscribed.

Macroscopic Pathology

Macroscopically tumors are up to 10 cm and are located in the hilum, in the peripheral lung, or subpleuraly [101]. These will show a thin fibrous capsule and are clearly demarcated from the surrounding lung parenchyma.

Histopathology

Histologically primary pulmonary thymomas present most often as thymomas type A or AB, rarely other types are seen (Fig. 17.30). Malignant variants, such as type B3, are exceedingly rare among these rare tumors. Most often the spindle cell component (type A) will predominate; type B1 areas are usually restricted to small foci within the tumor [102, 103]. Consequently the lymphocytic compartment is not as prominent as it is seen in the mediastinal AB thymomas. The nuclei are small, chromatin is finely dispersed, and nucleoli are either absent or inconspicuous. Fibrous septa usually separate the spindle cell clusters. The diagnosis might be achieved by fine needle aspiration cytology, but enough material

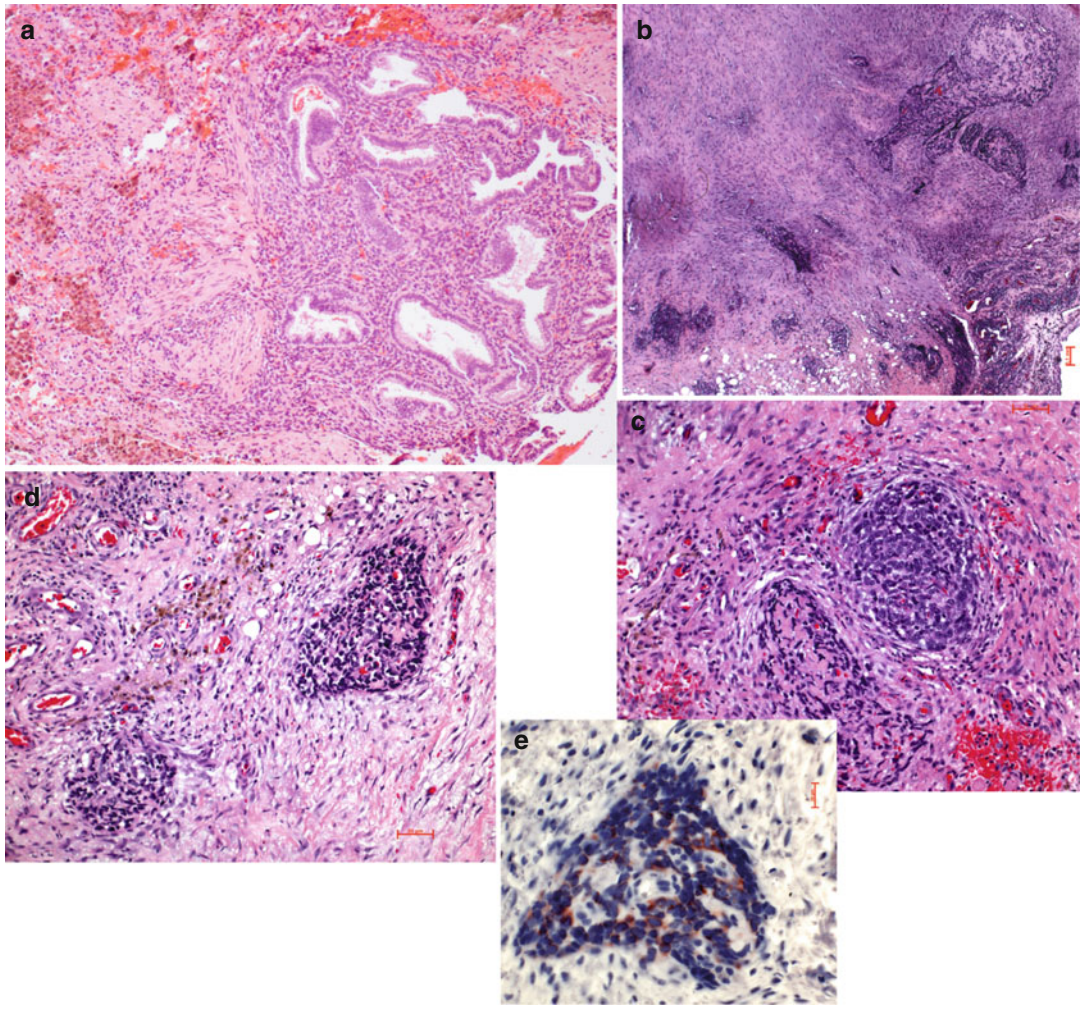

Fig. 17.29 (**a**) Intrapulmonary and pleural endometriosis. The pulmonary lesion is composed of bland endometrial glands, some of them with Arias-Stella phenomenon. Between the glands typical endometrium-type stroma cells as seen, many of them transformed. Note fresh and remnants of old hemorrhage. B-E another case of endometriosis in the pleura. (**b**) Overview with thickened stroma of the pleura and lymphocytic infiltrations (*right lower* corner). (**c**, **d**) Shows two endometriosis foci, in **c** the epithelial nature is obvious, whereas the focus in **d** might be taken as mesenchymal proliferation. By immunohistochemistry using cytokeratin 14 antibodies, the epithelial nature of this focus is confirmed, but also negative stroma cells are seen. H&E, ×150, bars 100, 50, and 20 μm

is necessary, to perform the necessary immunocytochemical stains. A rare type A3 malignant variant of the A-type thymomas has also been seen, but in these cases a metastasis from the mediastinum has to be excluded.

Immunohistochemistry

The tumor cells are positive for cytokeratin (cytokeratin 19) and EMA; the lymphocytes stain for CD45RO, CD4, CD8, CD99, and Tdt.

Prognosis and Treatment

Tumors are benign, and they are best removed by complete excision. Cases which present with myasthenia gravis will behave worse than cases without clinical syndromes [102]. There are rarely malignant variants of thymomas reported [101]; however, when dealing with a thymoma of types B2 or B3, one should primarily exclude metastasis from a mediastinal primary.

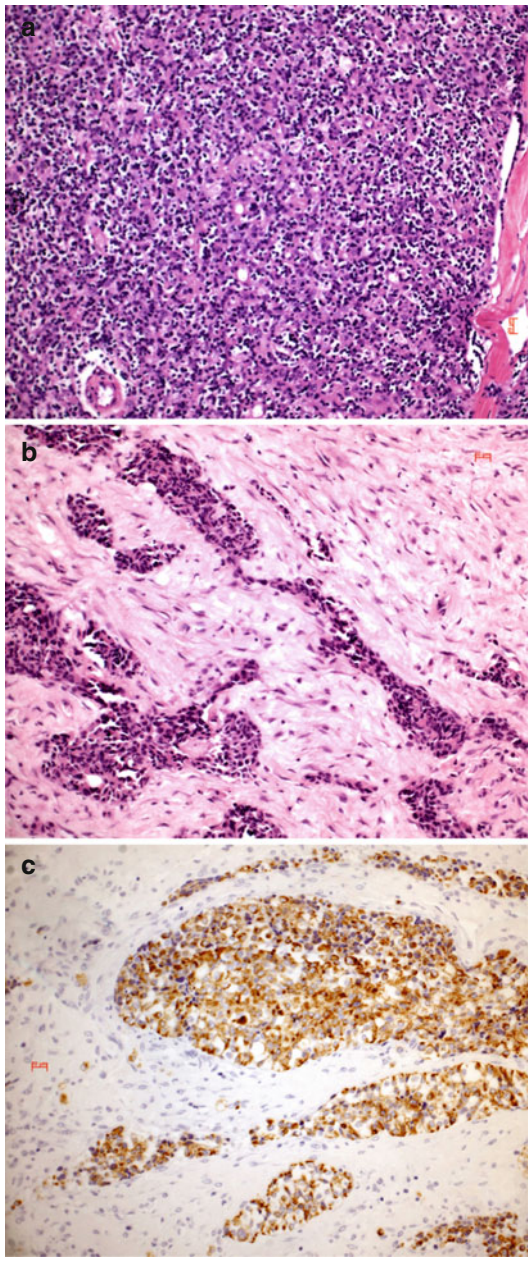

Fig. 17.30 Intrapulmonary thymoma, (**a**) shows an area of B1 type, in (**b**) there are infiltrating tumor cells with dense desmoplastic reaction, in (**c**) immunohistochemistry for pan-cytokeratin, staining the epithelial tumor cells. H&E and immunohistochemistry, bars 20 μm

Differential Diagnosis

There are many different tumors to be considered in the differential diagnosis of intrapulmonary thymomas: spindle cell carcinoid, metastasizing leiomyoma, inflammatory pseudotumor (myofibroblastic tumor), pleomorphic carcinoma, and malignant lymphoma.

Spindle cell carcinoids will show a rich vascular network and stain for neuroendocrine general markers (chromogranin A, synaptophysin); metastasizing leiomyoma on high-power magnification will clearly show myofilaments in their cytoplasm, which can be highlighted by smooth muscle markers (e.g., smooth muscle actin). In both tumors there is no lymphocytic focus, where spindle cells are intermingled with immature lymphocytes. Inflammatory pseudotumor, especially the mixed variant, can be problematic to differentiate on H&E stains alone. The infiltrative growth of IPT will be one clue to the correct diagnosis, and a positive cytokeratin or EMA stain will definitely exclude IPT.

Pleomorphic carcinomas of the lung, especially the pure spindle cell carcinoma, might be problematic too. But, nuclear polymorphism, frequent mitosis, and again an invasive growth into the surrounding lung will easily separate these two spindle cell neoplasms. Malignant lymphoma is not a problematic differential diagnosis in this setting. High-grade non-Hodgkin lymphomas are easily separated due to their nuclear polymorphism, large nuclear and nucleoli size, and coarse chromatin. This differential diagnosis might only be considered, if dealing with a B3 thymoma. In this case an immunohistochemical stain for cytokeratin 19 will clearly rule out the lymphoma. Low-grade lymphomas, such as marginal zone lymphomas of MALT/BALT type on the other end of the spectrum, are rarely a differential diagnosis, because of their rich lymphoid cell infiltration and the absence of spindle cells or thymoma cells of the type B1. Again cytokeratin 19 will highlight the thymoma cells, whereas the lymphoma will be negative.

A rare differential diagnosis, which might create considerable problems, is a metastasis from a biphasic endometrial stroma tumor/sarcoma. Morphologically the epithelial components will be clearly separated from the spindle cell component, the lymphocytic background infiltration will be more scarce, and these lymphocytes will express mature lymphocyte markers, such as CD20 and CD3. The tumor cells will express cytokeratins and also CD5 and CD10.

Molecular Biology

There are no genetic data for intrapulmonary thymomas and also only scarce data for those arising in the mediastinum. Comparative genomic hybridization has been performed on mediastinal thymomas and also some markers have been evaluated, but if these data can be transferred, also intrapulmonary thymomas has to be confirmed [104–106].

17.2 In Situ Carcinoma and Precursor Lesions

17.2.1 Preneoplastic Lesions – Squamous Cell Dysplasia

Actually our knowledge on preneoplastic lung lesions is limited: for a few carcinomas, the preneoplastic lesion is known, for most carcinomas not. In addition there is no good knowledge about driving genes, which induce progression into carcinoma. We still do not know the factors responsible for progression, invasion, etc. Molecular biology of these preneoplasias is mentioned where necessary; otherwise, these will be discussed in the next subchapter on malignant epithelial tumors.

For squamous cell carcinomas, the preneoplastic lesion is known for a while [107]. In the large bronchi, there exists a protection program for toxin/carcinogen exposure, which goes from goblet cell hyperplasia to squamous cell metaplasia and on to *squamous cell dysplasia or intraepithelial neoplasia* [108]. So far only a few factors influencing this progress have been identified, such as TP53 mutations, allelic loss and/or inactivating mutations of FHIT on 3p14, and inactivation of genes on 5p like AP1. VEGF seems to play a role in progression, since it is upregulated in rapid progressive squamous cell dysplasia with prominent vascular intraepithelial growth pattern. However, the interrelation of genes upregulated and downregulated has not been elucidated, so we are presently limited to single gene abnormalities, which do not allow understanding the process fully.

The grading of squamous cell dysplasia is quite subjective. In analogy to the cervix, also in the bronchus grading of dysplasia is done by the presence of cytological atypia, mitosis, and pattern. Whereas grade 3 does not cause a problem for most pathologists, the differentiation of grades 1 and 2 from reactive or regenerative proliferation in squamous cell metaplasia will cause disagreement between different experienced observers. Below are given the official definitions of grading of squamous dysplasia. It should be noted that there are discussions to reduce grading to low- and high-grade dysplasia, where high grade corresponds to grade 3 whereas low grade includes grade 1 and 2. We will follow this two-tiered graduation.

Low grade (G1+G2): expanded basal cell layer into the lower two thirds of the epithelium, mild to moderate atypia (anisocytosis, pleomorphism), maturation in the upper third, and rare mitosis.

High grade (G3): expansion of the basal cell layer up to the surface, complete loss of orientation, atypia present in all layers, which results in an epithelium looking the same in the basal and apical site, mitosis in all layers (Figs. 17.31 and 17.32).

The vascular variant of dysplasia is characterized by an ingrowth of capillaries into the squamous epithelium (Fig. 17.33). Atypia and mitosis might be mild or even absent; however these are rapid progressive lesions due to the expression and release of VEGF [109].

Squamous cell in situ carcinoma cannot always be separated from high-grade dysplasia especially in nonkeratinizing carcinoma; however, it can be done in cases with focal "maturation," which means keratinization/dyskeratosis

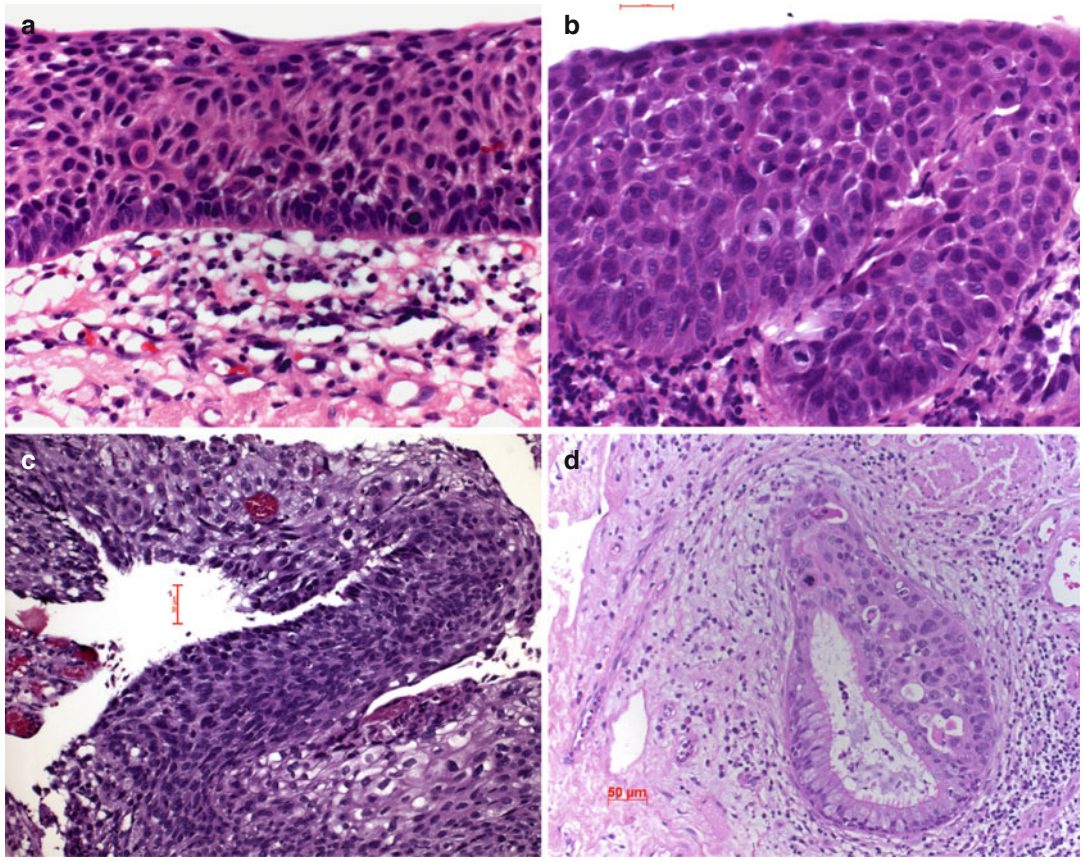

Fig. 17.31 Squamous cell dysplasia (intraepithelial neoplasia). (**a**) Low-grade dysplasia with expansion of basal cells into the middle of the epithelium; a few atypical cells are seen, one with dyskeratosis. (**b**, **c**) High-grade dysplasia, the atypical basal cells have replaced the normal epithelium throughout the whole thickness; atypia and mitosis is seen until the surface. (**d**) High-grade dysplasia with transition into in situ squamous cell carcinoma within a bronchial gland; there is dyskeratosis, apoptosis of single cells, and high-grade nuclear atypia. H&E, bars, 50 µm

of single cells or small groups or formation of squamous pearls. The separation of dysplasia from regeneration and squamous metaplasia is another sometimes difficult decision. Nuclei in regeneration can be large and polymorphic, intranuclear vacuoles might suggest atypia and inflammation, and bleeding might add in a suspicious morphology (Fig. 17.34). In difficult cases immunohistochemistry for p63 and p53 proteins can help. P63 protein stains basal cells of the bronchial epithelium, and in case of metaplasia and dysplasia, these cells expand into the upper layers of the epithelium. P53 can also be used, as squamous dysplasia usually occurs in cigarette smokers and most of them carry a TP53 mutation in their epithelia (Fig. 17.35).

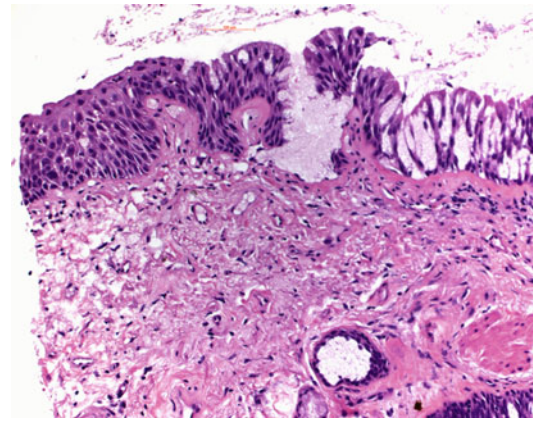

Fig. 17.32 Squamous cell dysplasia (low grade) with sharp transition from the adjacent goblet cell hyperplasia. This sharp demarcation is helpful when deciding on dysplasia. H&E, 100 µm

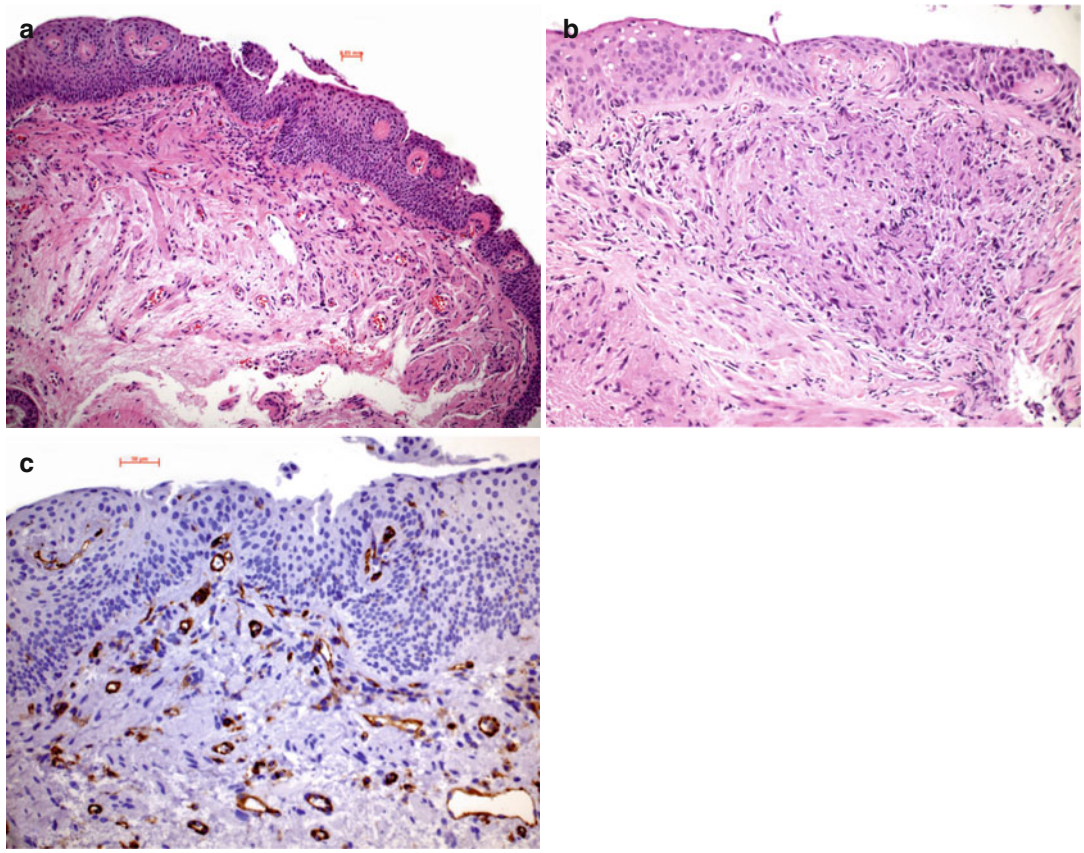

Fig. 17.33 Vascular variant of squamous cell dysplasia. (**a**, **b**) Show two cases of this type of dysplasia. The cellular features as well as nuclear atypia are mild. (**c**) Shows the ingrowth of ill-formed capillaries into the epithelium. H&E, bar 50 µm, ×100, immunohistochemistry for CD31, bar 50 µm

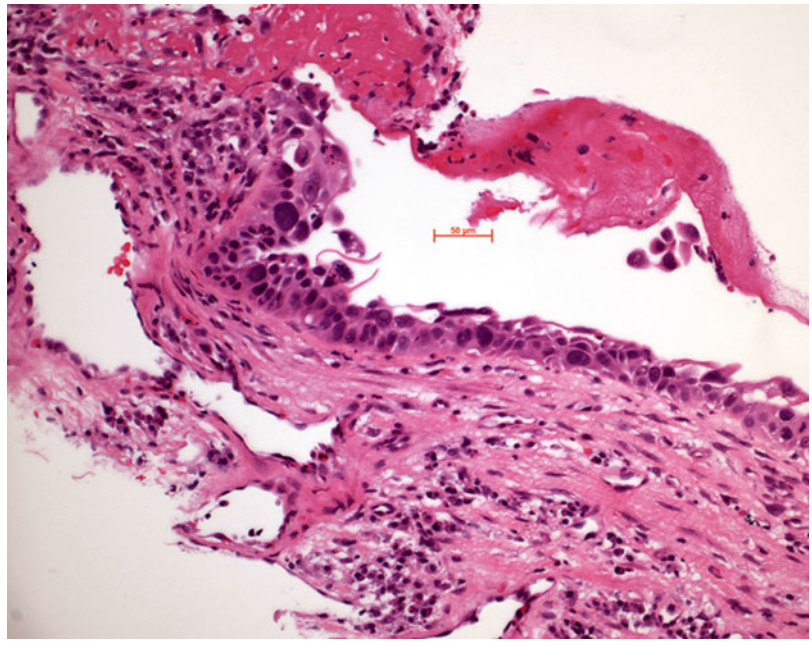

Fig. 17.34 Atypia in regenerating epithelium. There was a previous biopsy resulting in bleeding and necrosis with fibrin on top. At the border a squamous metaplasia has developed, which shows polymorphism of nuclei, some with dense chromatin. Inflammation and fibrin should prevent here to render a diagnosis of dysplasia. H&E, bar 50 µm

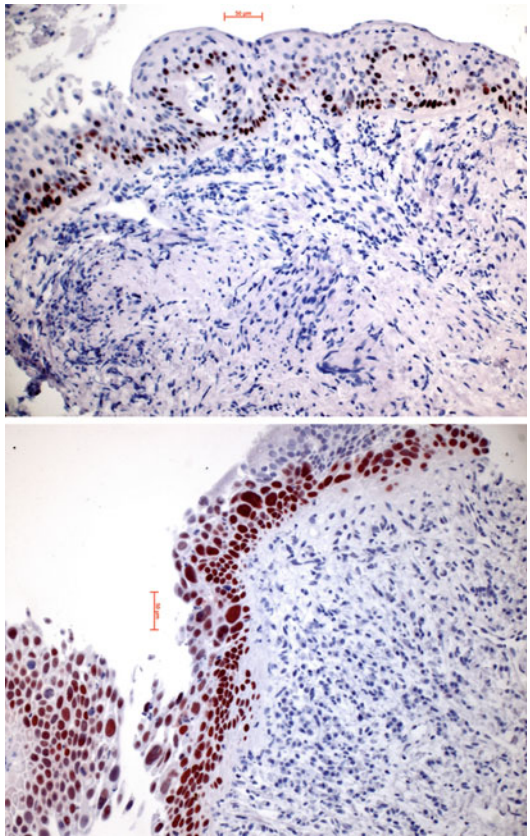

Fig. 17.35 Immunohistochemistry for p63 (*upper* panel) and p53 (*lower* panel). In the *upper* panel, there is squamous metaplasia; the basal cells still form a single or double row stained by p63. Staining with p53 antibodies in the *lower* panel shows a high-grade dysplasia, where the cells with TP53 mutations have expanded into the surface of the epithelium. Immunohistochemistry, bars 50 µm

17.2.2 Atypical Adenomatous Hyperplasia

Atypical adenomatous hyperplasia and bronchiolar columnar cell dysplasia are two preneoplastic lesions confined to the alveolar and bronchiolar periphery, respectively. Atypical alveolar hyperplasia (AAH) [110–112] is visible already at low-power magnification (Fig. 17.36a).

If the resected lung is fixed in an expanded way and thin tissue slices expanded under water are examined under light, the tiny spots with grayish thickened septa can be seen.

Histologically the normal epithelium is replaced by either pneumocyte type II-like atypical cuboidal cells or by columnar cells. The nuclear and nucleolar size is increased; nuclei are usually round to oval, nucleoli are polygonal, and intranuclear inclusion bodies are frequently seen, representing entrapped surfactant apoprotein. Between the cells, lined up as a single row, there are gaps (Fig. 17.36). When these gaps are lost, usually also higher grades of atypia are seen, mitotic rate increases, and focally epithelial papillae are formed; the diagnosis changes to in situ adenocarcinoma (AIS, Fig. 17.36h). The WHO classification [70] draws a line of 5 mm size between AIS and AAH, which, however, does not make sense. The problem of distinction of AIS and AAH can only be solved by cytomorphology and structure: in AAH there is no alveolar collapse, no atelectasis, and no desmoplasia, and the alveolar structure is rigid. The cytomorphology of the cells is uniform, most often pneumocyte-like, nuclei are slightly enlarged, nucleoli are either invisible or inconspicuous, and mitosis is absent. In AIS there can be alveolar collapse and atelectasis and no desmoplasia, the nuclei are larger compared to AAH, and nucleoli are increased and can be polymorphic [113]. A few mitotic figures can be seen, usually 0–2/HPF. Size is not a reliable criterion for distinguishing AAH and AIS: cases of AIS as small as 2 mm have been seen by the author and AAH cases with up to 8 mm too (Fig. 17.36). As in other organ systems, size is not reliable. In addition as we usually examine tissues after formalin fixation, shrinkage is another problem changing the real size.

17.2.3 Bronchiolar Columnar Cell Dysplasia

In contrast to AAH, *bronchiolar columnar cell dysplasia* (BCCD) can only be seen at the microscope under high magnification [114]. In BCCD atypical cells, gradually replace normal bronchiolar/bronchial epithelium. Normally bronchial/bronchiolar epithelium is composed of different cell types, as ciliated, secretory, goblet, Clara, and reserve cells. All these cells look different and have differently sized and shaped nuclei. In early stages of BCCD, a monomorphous proliferation of cells replace these differentiated cells and gradually expand within the epithelium (Fig. 17.37). Atypia can be low as well as high

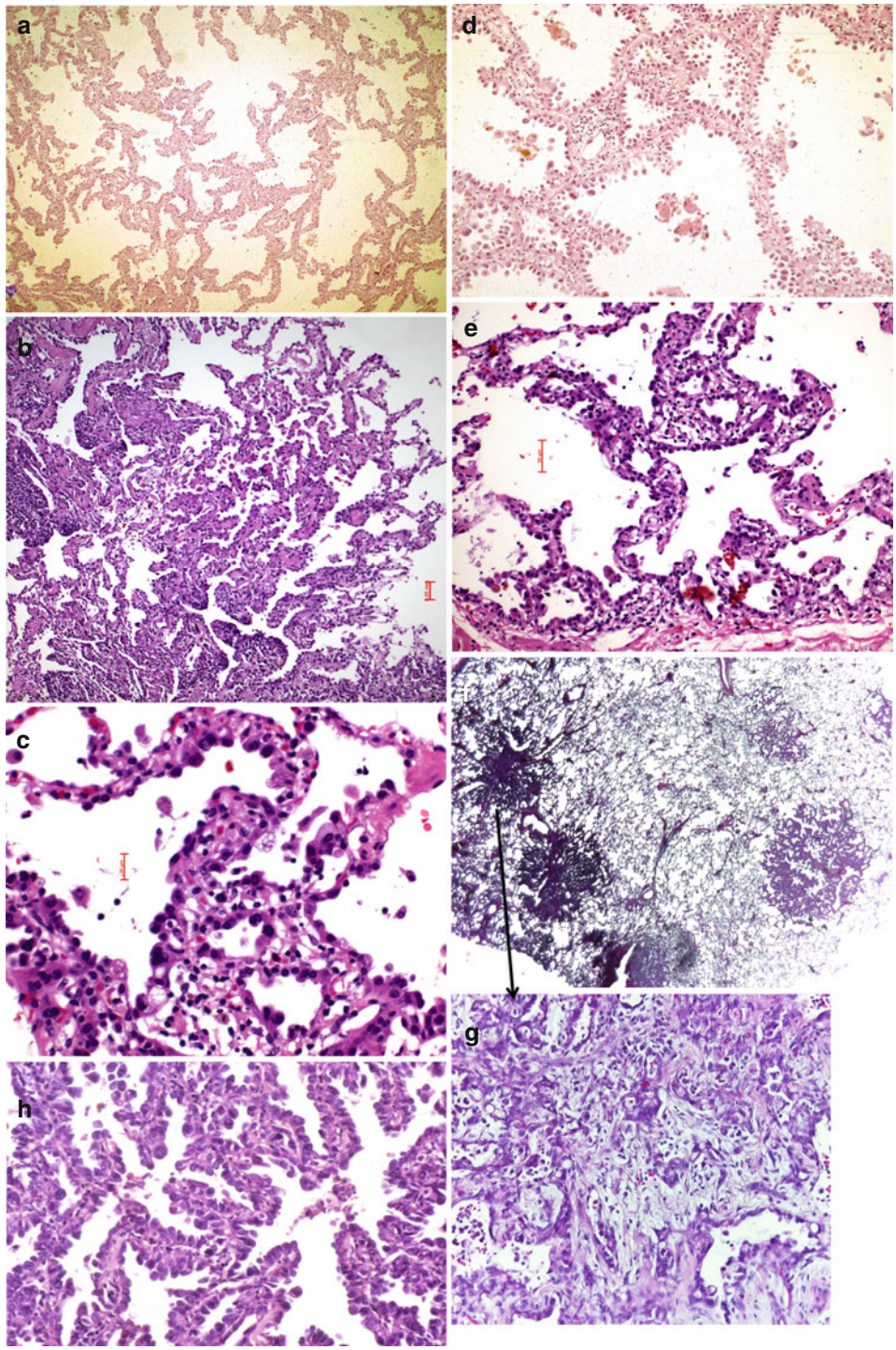

Fig. 17.36 Atypical adenomatous hyperplasia (AAH). Several cases are shown. In cases from Southeast Asia, most often there is no inflammation in AAH (**a**; case provided by Y. Shimosato), whereas in European cases most often there is considerable inflammation and in some cases also fibrosis of the septa present (**b**, **c**). The major criterion and difference to in situ adenocarcinoma is less nuclear atypia and the presence of intercellular gaps between the tumor cells (**d**, **e**). Multiple AHH can be seen in a lung but rarely close by as in (**f**). Here several AAH lesions are present, but one of them already associated with an invasive adenocarcinoma (**f**, **g**, *arrow* shows the lesion). For comparison in (**h**), an in situ adenocarcinoma is shown. Here the tumor cells form a tight layer of cells, the gaps are no longer present, and nuclear polymorphism and atypia is increased. H&E, ×25, 100, 12, and 250, bars 50 and 20 μm

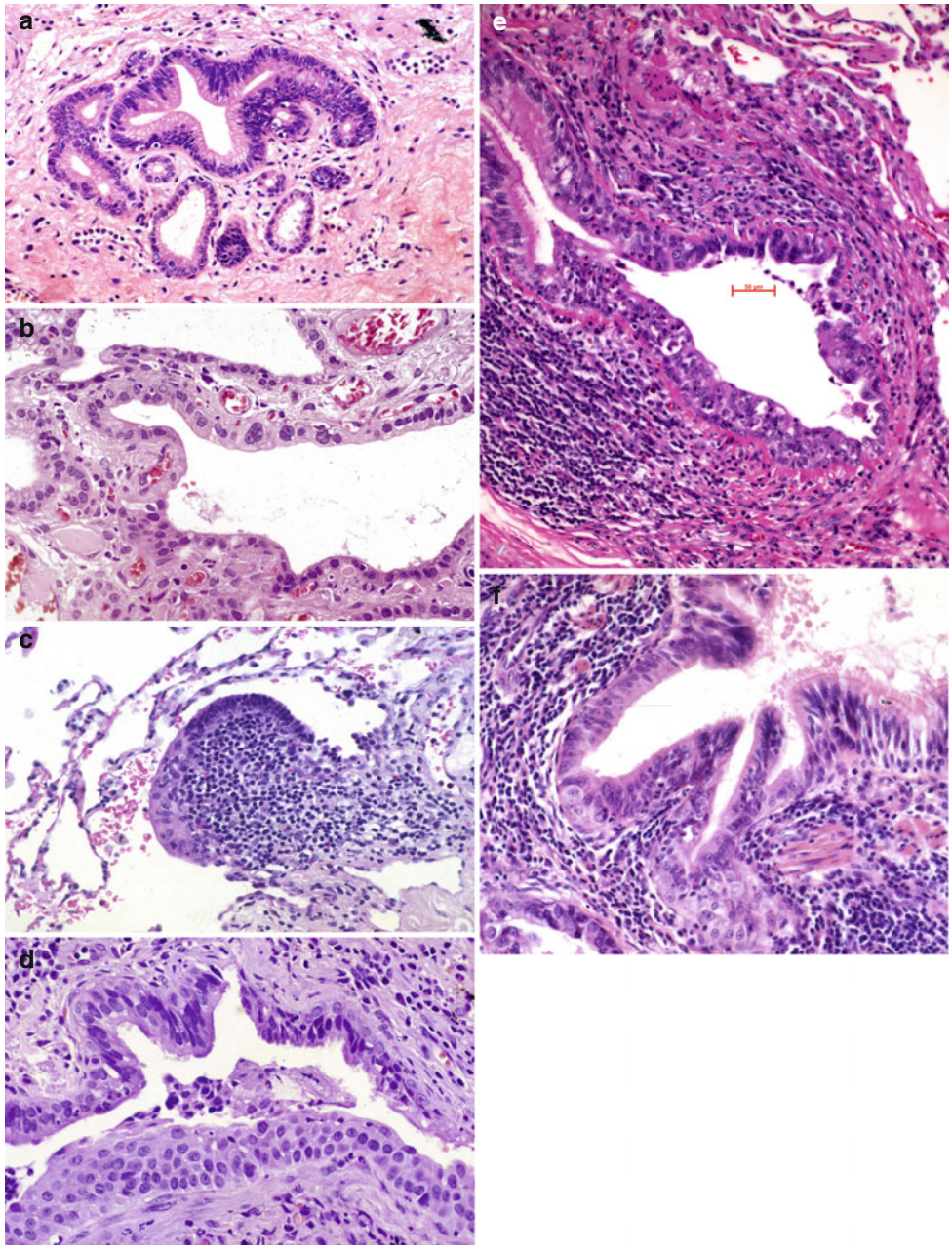

Fig. 17.37 Bronchiolar columnar cell dysplasia (BCCD). In A, B, and C, BCCD is shown at three different levels of bronchioles. In (**a**) BCCD is seen in small bronchioles. The bronchiolar layer of differentiated cells is replaced by uniform cells with enlarged nuclei with increased nucleoli. Also chromatin abnormalities are seen. In (**b**) BCCD is within a terminal respiratory bronchiole. The layer of Clara cells (*right*) is replaced by atypical cells, a few multinucleated. The nuclei of these cells are enlarged, nucleoli are increased, and nuclear membrane is accentuated. In (**c**) BCCD is seen in a terminal bronchiole at the opening into an alveolar duct. Note the abrupt transition from the normal cuboidal to an atypical epithelium. In (**d**) in the upper side of this bronchiole, scattered atypical cells are seen; on the lower side, the epithelium is replaced by squamous cell metaplasia. In (**e**) regeneration of the epithelium is shown. In regeneration the different types of cells are retained, and although there is some atypia, this is not the uniform proliferation of dysplastic cells. In (**f**) another example of BCCD is shown, and the difference of dysplasia to regeneration is evident. H&E, ×100, 200, bar 50 μm

grade. In contrast to regeneration, BCCD appears monomorphic. As in AAH the important molecular events driving this preneoplasia into adenocarcinoma is unknown. However, BCCD can give rise to adenocarcinomas arising in small bronchi and bronchioli, in contrast to AAH, which is the precursor for non-mucinous adenocarcinomas arising from the bronchiolar-alveolar junction zone.

17.2.4 Atypical Goblet Cell Hyperplasia

Atypical goblet cell hyperplasia (AGCH) is difficult to recognize: the nuclei are compressed at the basal cell border, and the chromatin structure is invisible. As in BCCD the growth pattern of the cells is more important: atypical, goblet, or signet ring cells are replacing the normal epithelium, resulting in a monotonous pattern. In contrast to goblet cell hyperplasia in dysplasia, the atypical cells replace the normal epithelium completely (Fig. 17.38). Atypical goblet cell hyperplasia might give rise to the different mucinous adenocarcinomas of the lung [115]. AGCH is often found in CPAM types I and II. From our study it seems obvious that this represents the preneoplastic lesion for the rare adenocarcinomas of childhood [12].

17.2.5 Neuroendocrine Cell Hyperplasia

Neuroendocrine cell hyperplasia (NEH) is divided into NEH associated with fibrosis, bronchiectasis, carcinoid, and diffuse NEH of unknown cause; in addition there is tumorlet and nodular NEH. At present it is unclear, to what extent NEH is associated with neoplasia, and the factors influencing neoplastic progression are unknown. However, NEH is most probably a preneoplasia for carcinoids but not for the high-grade neuroendocrine carcinomas!

Neuroendocrine cells in the lung can be found in two places: as single dispersed neuroendocrine cells within the bronchial tree and as neuroepithelial bodies in the peripheral lung. Neuroendocrine markers, such as chromogranin A (CGA), Bombesin the frog analog of gastrin-releasing peptide (GRP), synaptophysin, PGP 9.5, and γγ-enolase (neuron-specific enolase (NSE)) can identify the cells [116–118]. They are part of Feyerter's diffuse neuroendocrine system of the body [119, 120] and play a role in fetal lung development. Genes regulate growth and differentiation of the bronchial buds and the joining with the coelomic structure, but neuroendocrine cells act locally in fine tuning of the development in response to a variety of stimuli, as in hypoxia [121]. Two of the growth hormones expressed during fetal lung development act later on in neuroendocrine carcinomas as autocrine growth factor loop: GRP and adrenocorticotropin (ACTH) [122, 123].

NEH can be a reactive process, such as in bronchiectasis. The proliferation of the NE cells is the answer for obstruction. By this proliferation repair mechanisms are stimulated to restore normal lung structure as it did work in fetal lung. This question was addressed in publications by J. Polak's group: in children dying from respiratory distress syndrome, bombesin content was lowered [121]. In an experimental model, CGRP was increased after 7 days of hypoxia [124].

A similar process might be the basis of NEH in UIP and other idiopathic interstitial pneumonias, this time starting from peripheral NE cells and neuroepithelial bodies. NE hyperplasia in the vicinity of carcinoids might be stimulated by growth factors released from the tumor, but this has not been proven so far.

Whereas single neuroendocrine cells are usually not identifiable on H&E-stained sections, NEH can be diagnosed when clear cell clusters are seen within the mucosa (Fig. 17.39). Nodular NEH can be characterized by an increase of these cells into clusters. A *tumorlet* is an aggregation of several nodular clusters of neuroendocrine cells separated by bundles of stroma but all together appearing as a small tumorlike lesion (Fig. 17.40). The major feature differentiating tumorlet from carcinoid is the presence of these dissecting fibrous bands between the neuroendocrine nodules. Tumorlets are usually less than 5 mm in diameter. They most likely represent early carcinoids. They are incidentally found in the

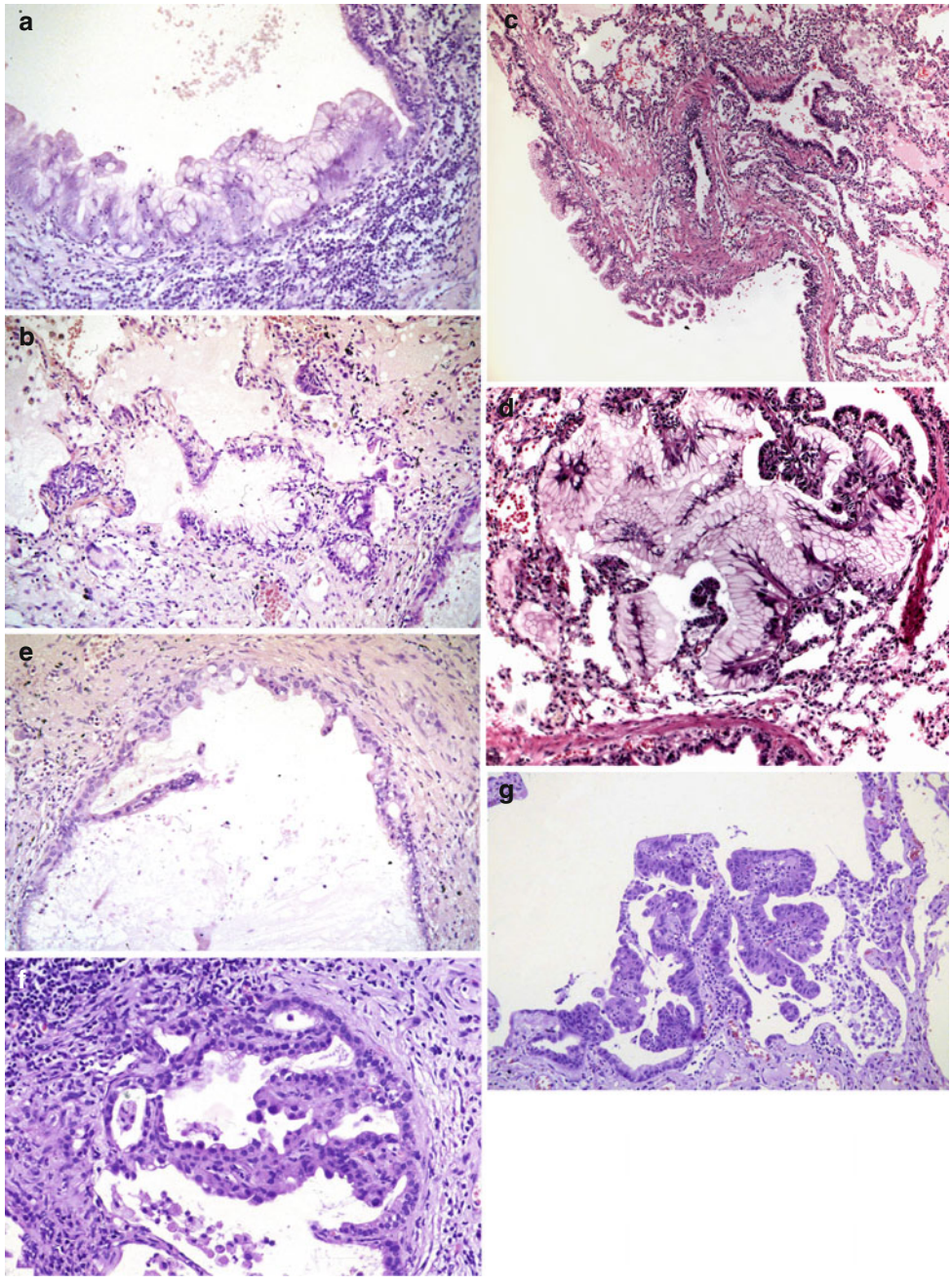

Fig. 17.38 Goblet cell dysplasia. (**a**, **b**) Shows two examples of goblet cell dysplasia. These might be precursor lesions for mucinous adenocarcinomas. In (**c**, **d**) atypical goblet cell hyperplasia within congenital pulmonary adenomatoid malformation type I and II is shown. In C the atypical proliferation is in the cyst epithelium, whereas in (**d**) the proliferation is growing into adjacent lung tissue. In contrast (**e**–**g**) show already lesions, which are regarded as in situ adenocarcinoma. (**e**) Is an intraepithelial growth of adenocarcinoma forming bridges similar what is seen in breast carcinomas. In (**f**) the proliferation forms roman type of bridges, again similar to what is seen in breast carcinoma. In (**g**) finally there is papillary growth pattern, which might give rise of a papillary adenocarcinoma. H&E, ×150, 100, 60, 200

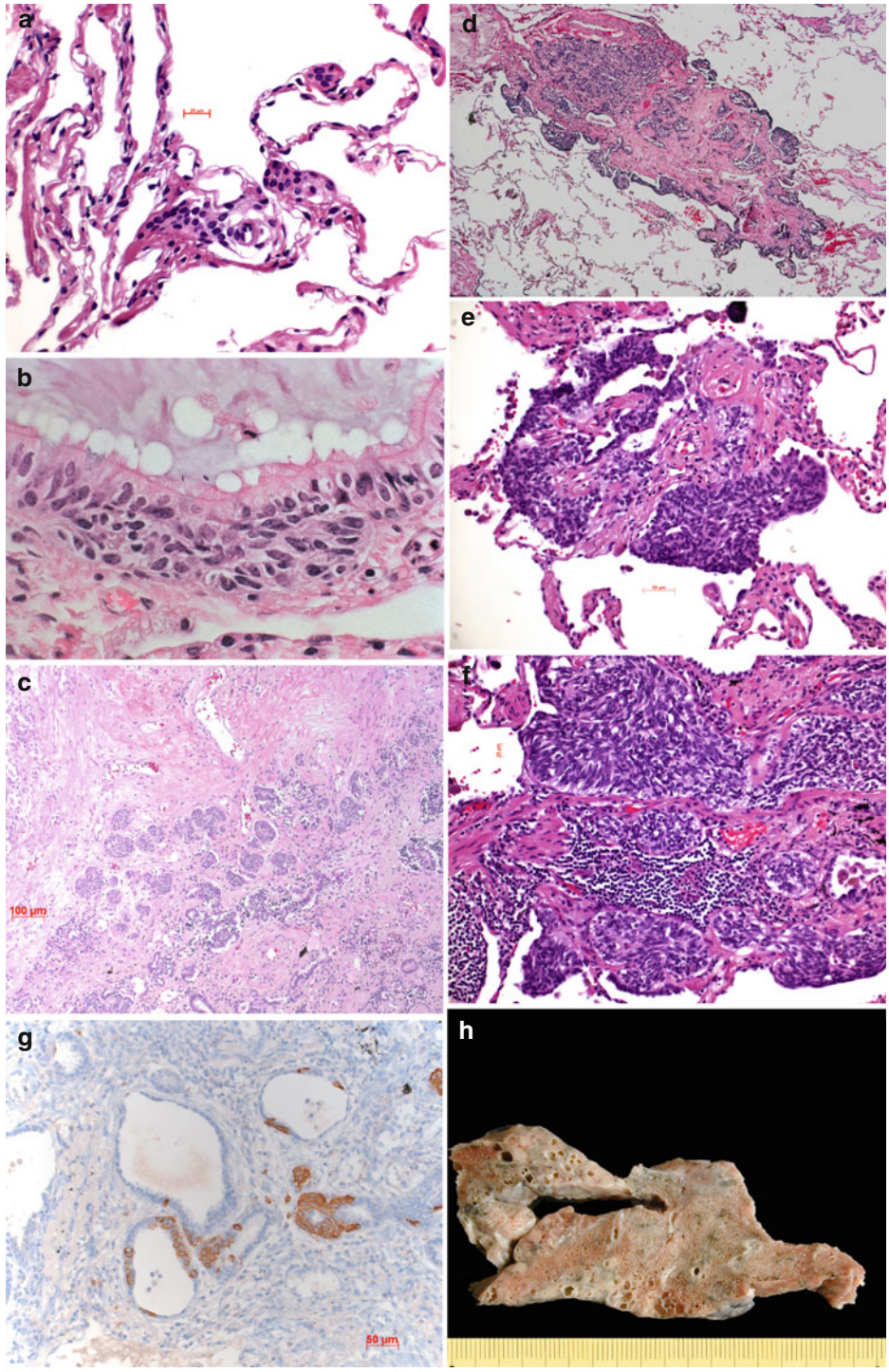

Fig. 17.39 Neuroendocrine hyperplasia (NEH). In (**a**) a neuroepithelial body is shown, a normal but rare finding in an adult lung. (**b**) Shows NEH within a bronchus, the cells have clear- or pale-stained cytoplasm. (**c**) Shows small nodular proliferations of neuroendocrine cells in the wall of an already obstructed bronchus. (**d**) Is from another case with obstructive bronchitis and consecutive NEH. (**e**) Is NEH in the wall of small bronchi in a case of diffuse idiopathic neuroendocrine hyperplasia (DIPNEC). (**g**) Shows NEH in small bronchi and bronchioles highlighted by an immunostain for chromogranin A. (**h**) Is a resection specimen resected because of purulent bronchiectasis and pneumonia. In this case many small grayish-white nodules are seen, representing NE hyperplasia and tumorlets. H&E, bars 20, 50, 100 µm, ×50

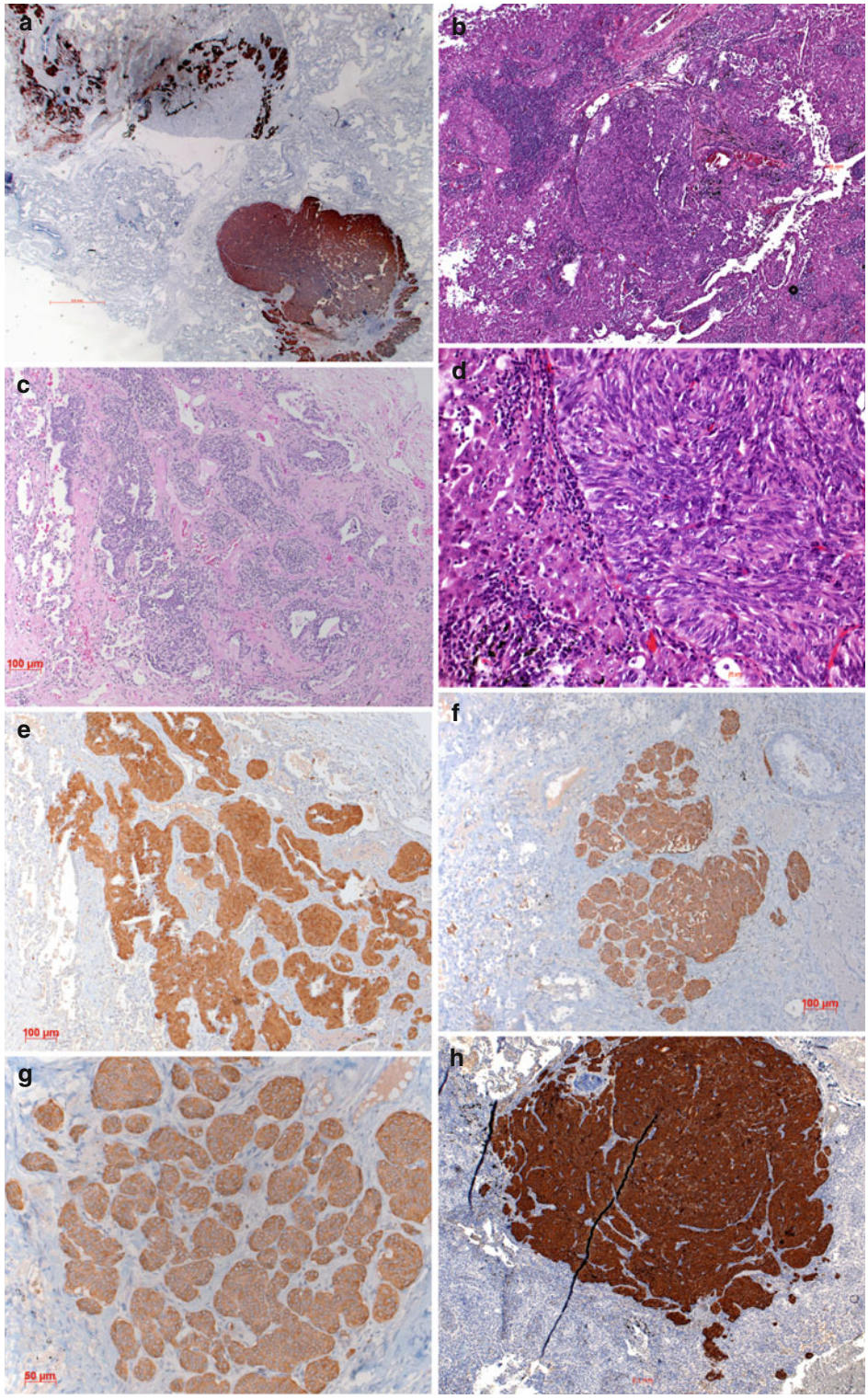

Fig. 17.40 Tumorlet and carcinoid. In (**a**) there is a carcinoid and scattered foci of NEH, demonstrated by chromogranin A immunohistochemistry. (**b**) Shows a tumorlet in the vicinity of an adenocarcinomas, the transition zone between the two tumors is seen magnified in (**d**). (**c**) Shows another tumorlet. Here the nodules are joined together by fibrous bands. (**e**–**g**) Shows tumorlets, the neuroendocrine cells highlighted by chromogranin A immunohistochemistry, and a large tumorlet is seen in (**h**) here demonstrated by immunohistochemistry for PGP9.5. H&E, ×50, bars 100, 20 µm, immunohistochemistry, bars 0.5 mm, 100 or 50 µm

same setting as NEH, i.e., close to carcinoids, and in fibrosis or obstructive lung disease.

If there is no known cause found for a diffuse NE hyperplasia, these are regarded as idiopathic.

17.3 Malignant Epithelial Tumors

17.3.1 Epidemiology

In contrast to many other organs in the lung, the vast majority of tumors are belonging to the malignant epithelial category. In the early 1900s, lung cancer was a rare tumor, but around the 1920s an increase of lung cancer was recorded in central European Pathology Institutes [125–127]. This has mainly to do with exposure to cigarette smoke. Whereas cigar smoking was common in the upper classes in the nineteenth century, but too expensive for the lower class population, this changed completely when cheap manufactured cigarettes appeared. Approximately some 15–20 years after introducing the cheap cigarette at the turn of the nineteenth century, lung cancer appeared on the scene and since then has not stopped rising until recently reaching the number one tumor worldwide [128–130]. The following decades saw an uprise of squamous and small-cell carcinomas until the 1950s. These were called the smoking-related carcinomas, whereas adenocarcinomas were regarded as not cigarette smoking associated [128, 131]. This view was also "confirmed" by experimental cigarette smoke inhalation studies in mice, rats, and hamsters, which resulted in adenomas and adenocarcinomas. The tobacco industry used these findings as arguments that cigarette smoking at all is not carcinogenic.

Within tobacco smoke, side- as well as mainstream, approximately 600 different chemical compounds are identified, from which roughly 10 % are carcinogenic on their own; however, many others act together and are carcinogenic too, for example, by chemical interaction [132–141]. Also within the respiratory tract, several enzymes act as modifiers, which can transform precarcinogens into carcinogens, for example, by oxidation at specific CH_3 or NH sites. In addition specific polymorphisms within the P450 cytochrome oxidases might also be important [142]. Most carcinogens belong to carbohydrates and nitrosocomponents, amines, and more complex chemicals. Several chemical side chains have been identified as being responsible for their carcinogenic action, such as instable C=O, HN=NH, and C=NH binding sites. Of note are especially HN=NH and C=NH binding sites as these can directly interact with DNA nucleotides and result in point mutations.

Many tobacco carcinogens induce strand breaks on the double-stranded DNA. It has become clear that this follows exact rules: normally DNA is in a coiled or supercoiled state, and oxygen radicals, for example, cannot act on the coding nucleotides. So strand breaks can occur only when the DNA is uncoiled and opened for transcription. This is the reason why cells (especially different kinds of stem cells) undergoing mitosis are more prone to acquire genetic hits, whereas differentiated cells divide rarely and therefore are protected from injury. DNA repair mechanisms have been less studied; however, the few reports showed a contribution to the development of lung cancer. In the study by Park et al., a polymorphism at the 8-oxoguanine DNA N-glycosylase 1 gene involved in base excision repair showed increased dose-dependent risk for lung cancer in smokers [143]. The DNA damage repair genes, mutY and mutM, prevent G to T mutations caused by reactive oxygen species. In mice deficiencies of both genes resulted in lung and ovarian tumors. G to T mutations were identified in 75 % of the lung tumors at codon 12 of KRAS [144] and it seems that this is gene specific. ERCC1 if highly expressed in tumors was able to counteract chemotherapy-induced DNA strand breaks resulting in shorter survival of patients with NSCLC, whereas patients with tumors negative for ERCC1 showed a prolonged survival [145]. So more in-depth studies on the different repair mechanisms are necessary to see how much these enzyme systems are involved in carcinogenesis. Another enigma is that mutations often occur on specific genes. One explanation might

be that first of all mutations can occur only at sites of an uncoiled DNA, i.e., a DNA area which is to access, which is common for cell cyle associated genes. Oxygen radicals cannot approach coiled and supercoiled DNA.

Besides tobacco smoke as a collection of major carcinogens, some other causes are emerging especially from China. There is indoor cooking, where many carcinogens are released and due to ill ventilation are inhaled in high concentrations [146, 147]. Other possible causes are toxic and carcinogenic waste in industrial areas (this will be discussed in detail in the pneumoconiosis chapter).

However, the story is not complete, if we do not also see the action of cancer prevention systems. As the lung is exposed to outside air, it is also exposed to many natural carcinogens present in the environment. Therefore during evolution the organ has developed several defense mechanisms to protect it from injury. These mechanisms have evolved over millions of years starting with old mucociliary and macrophage clearance, followed by enzymatic defense, and finally also by the action of the immune system.

The mucociliary escalator system is composed of the mucus-producing cells and the ciliated cells. Mucus is produced by the goblet cells along the bronchial surface epithelium and the bronchial glands. Mucus forms a fine liquid surface layer, into which particles as well as chemical substances are impacted and diluted. The ciliated cells move the mucus constantly toward the larynx, and therefore many inhaled substances either do not contact the surface epithelium or only for a short time period. Therefore the action of toxic substances is limited. In the alveolar periphery including the small bronchioles, macrophages constantly patrol through the airspaces and remove any harmful substances by phagocytosis, again preventing toxic injury.

The anatomy of human airways is characterized by asymmetric branching of bronchi/bronchioli. One bronchus divides into a main branch with approximately two thirds of the diameter, whereas the minor bronchus has a diameter of one third. This branching results in a disturbed airflow with turbulences at the bifurcations. Large particles >10 μm impact at the bifurcations of the larger bronchi, and only small particles of <2 μm can reach the alveolar periphery. Thus the inhalation of larger particles is prevented and the air is cleared.

Less well known is the protective enzymatic system of the airways. There are two major systems: class one and two; class one consists of the cytochrome P450 oxidases, microsomal epoxide hydrolase, and myeloperoxidase and the antioxidases superoxide dismutase, catalase, and glutathione peroxidase [142, 148]. In class two there are several enzymes such as the glutathione S-transferases family enzymes capable of protecting from oxygen radical injury by a redox mechanism [148, 149].

In addition to enzymes, also pro- and anti-inflammatory proteins/lipoproteins are involved in maintaining homeostasis of the airway system. How these interact with inhaled toxicants/carcinogens is not known. Immunoglobulins especially from the A class protect against inhaled bacteria by opsonization. Surfactant apoproteins and other substances such as Clara cell proteins also are involved in a protective manner but can even be produced and secreted by adenocarcinomas – so their function in health and disease is still not understood.

17.3.2 Carcinogenesis: Our Current Sight on the Development of Cancer

In these paragraphs we will focus on the development of carcinomas from normal epithelium to dysplasia to in situ carcinoma. Invasion, migration, and metastasis will be discussed in the metastasis chapter.

Several conditions need to be functioning for carcinoma development from the early changes in the epithelium to preneoplastic lesions and finally to in situ carcinoma. Some of these factors are general, working in different carcinoma types, whereas other factors are subtype specific, and even individual settings do occur. Generally each preneoplastic cell needs appropriate nutri-

tion, especially supply of amino acids for the synthesis of nucleotides to be used for each round of DNA replication, and oxygen as well as glucose as a provider of energy since each cell division consumes energy in the form of ATP. These early events of carcinogenesis are less explored than the development of genetic abnormalities. Preneoplastic cells also acquire genetic aberrations, which will result in cell cycle stop at one or both cell cycle checkpoints where DNA integrity is proven, repaired in case of failure, or cells are sent into apoptosis, if the gene defect is irreparable. So these checkpoints as well as apoptosis need to be inactivated. In addition genes harboring DNA defects (deletion, mutation, amplification, rearrangements/translocations) will translate into proteins, which are detected by immune cells. This might be recognized by immune cells, which will immediately attack the neoplastic cells. So preneoplastic cells need to develop mechanisms to avoid immune cell attack. Stem cells are another factor, which can play a role in some tumors, but this is not a general rule. Finally once a tumor has formed an in situ lesion, tumor cells need to transverse the basal lamina, interact with the stroma, and migrate. Within the primary tumor due to accelerated growth, hypoxia develops, as new blood vessel formation do not keep with tumor growth. So tumor cells have to change their metabolism into anaerobic glycolysis.

17.3.2.1 Changes in Metabolism: Access to Nutrition and Oxygen

It has been shown that many enzymes as ATP synthase subunit D, beta1,4-galactosyltransferase, cytosolic inorganic pyrophosphatase, glutathione-S-transferase M4, prolyl 4-hydroxylase β-triosephosphate isomerase, and ubiquitin thiolesterase (UCHL1) are overexpressed in adenocarcinomas and most likely also in preneoplastic lesions such as AAH [150]. Tumor cells express exclusively the embryonic M2 isoform of pyruvate kinase, which is necessary for aerobic glycolysis and thus provides a selective growth advantage [151]. Glycolytic ATP supports growth under hypoxic conditions. Glutamine conversion into the tricarboxylic acid cycle by glutaminase and alanine aminotransferase is essential for KRAS-induced anchorage-independent growth. Changes in the mitochondrial complex III metabolism generate reactive oxygen species, which is also required for KRAS-induced anchorage-independent growth through ERK-MAPK signaling [152]. This finding was further explored in the study of Beuster, who showed that L-alanine aminotransferase (ALAT) promote mitochondrial metabolism by L-alanine production and enhanced D-glucose uptake. ALAT enhanced anchorage-dependent and anchorage-independent growth and enhanced ATP production via the Warburg effect [153]. The Warburg effect is characterized by glucose uptake and breakdown through the process of aerobic glycolysis. The importance of the glutamine (Gln) in cancer development and progression has been studied by van den Heuvel and coworkers. A variety of essential products to sustain cell proliferation, such as ATP and macromolecules, are provided. GLS1 is the key enzyme. NSCLC cell lines depend on Gln for glutaminolysis to a varying degree, in which the GLS1 splice variant GAC plays an essential role [154]. Glyceraldehyde 3-phosphate dehydrogenase (GAPDH) overexpression induces progression in NSCLC, again pointing to the importance of the glucose metabolism in cancer development [155]. GLUT1 another enzyme in the glucose metabolic cycle is overexpressed in smoking-associated carcinomas preferentially in squamous cell type. GLUT1 overexpression was also correlated with EGFR-negative and KRAS mutation-positive carcinomas [156].

The second most important factor is oxygen supply by increase in vascular density. In experimental carcinogenesis induced by N-nitrosobis(2-hydroxypropyl)amine in rats, VEGF, VEGFR-1, and VEGFR-2 were upregulated in malignant and premalignant lung lesions. In addition, VEGF mRNA and VEGFR mRNAs were overexpressed in adenocarcinomas and squamous cell carcinomas [157]. In the study by Fontanini and coworkers, increased microvascular density (MVD),

accompanied by overexpression of VEGF and p53, was seen in normal bronchial epithelium, moderate dysplasia, in situ carcinoma, and invasive cancer. The association between MVD, VEGF expression, p53 mutations, and preinvasive lesions of the bronchial tree suggests that neoangiogenesis is an early event in NSCLC [158].

17.3.2.2 Mutations in Mitochondrial Genes

Mitochondria are the energy-producing factories of the cell. Therefore it seems logical that cancer cells also use enzymes to suit their higher energy consumption. Increase in the rate of glycolysis is one of the metabolic alterations in most cancer cells. In the study by Pelosi et al., mutations in the D-loop of mitochondrial DNA (mtDNA) were found in 22 % of lung cancers and mutations in the mtDNA in 57 %; there were changes in the mononucleotide or dinucleotide repeats, deletions, or multiple insertions. Instability in the D-loop region of mtDNA and decrease in mtDNA copy number seems to be involved in carcinogenesis [159]. MtDNA copy number changes are a biologic response to mtDNA damage and dysfunction. Polycyclic aromatic hydrocarbons (PAHs) may cause mitochondrial toxicity. Workers with high PAH exposure showed higher mtDNA copy number changes, as well as higher levels of genetic and chromosomal DNA adducts, micronuclei, telomere length, and epigenetic p53 gene-specific promoter methylation alterations [152]. In the study by Kadota, missense mtDNA mutations were found in 9 of 13 mtDNA coding genes. They found a variety of mtDNA mutations and mtDNA polymorphisms in human lung cancer, some of them involved in human lung carcinogenesis [160].

Mutations of TP53 are frequently in lung cancers. Synthesis of cytochrome c oxidase 2 (SCO2) is one of the genes' downstream of TP53 and regulated by it. In p53-deficient cells SCO2 gene is disrupted and this leads to a metabolic switch toward glycolysis. So via SCO2 p53 is coupled to mitochondrial respiration and shows another function of mutated p53 explaining the Warburg effect in cancer cells [161]. Two other genes coding for the enzymes ATPase6 and NADH dehydrogenase 3 are mutated in 86 % of lung cancer cases. It seems both are cooperating during cancer development [162].

17.3.2.3 Proliferation, Cell Cycle, and Chromosomal Strand Breaks

Once the supply of oxygen and nutrition is solved, the preneoplastic cells need to high check the cell cycle machinery. Here a variety of mechanisms can be used to overcome the cell cycle controls. Stimulatory factors USF-1 and USF-2 dimerize to regulate transcription through E-box motifs in target genes. In phenotypically normal bronchial tissues, USF-2 was highly expressed at 1 cm distance from the tumor. USF-2 was restricted to ciliated cells in normal bronchial epithelium but more strongly expressed in dysplastic epithelium as well as in small- and large-cell neuroendocrine carcinoma and squamous cell carcinoma. USF-2 represents an early molecular marker for the development of bronchial dysplasia and non-adenocarcinoma lung cancer and may also play a role in bronchial carcinogenesis by promoting cell proliferation [163].

Oxygen radicals (reactive oxygen species (ROS)) play a major role in carcinogenesis, as many tobacco carcinogens act via this mechanism. ROS induce DNA strand breaks and point mutations but also interfere with cell cycle checkpoint function [164]. Also the inactivation of protective enzymes plays a role in the initial process of cell transformation. MTH1, MUTYH, and OGG1 play important roles in mammalian cells to avoid an accumulation of oxidative DNA damage, both in the nuclear and mitochondrial genomes, thereby suppressing carcinogenesis and cell death. But in carcinogenesis one or several of these enzymes can be inactivated by mutation, which will ultimately lead to carcinoma formation [165]. The tumor suppressor gene RASSF1A regulates the stability of mitotic cyclins and the timing of mitotic progression. RASSF1A localizes to microtubules during interphase and to centrosomes and the spindle during mitosis. The

overexpression of RASSF1A induced stabilization of mitotic cyclins and mitotic arrest at prometaphase. RASSF1A is frequently silenced by hypermethylation of its promoter. Depletion of RASSF1A by RNA interference accelerated the mitotic cyclin degradation and mitotic progression. It also caused a cell division defect characterized by centrosome abnormalities and multipolar spindles [166]. Thus silencing might be another cause of increase of mutations, deletions, and other kind of chromosomal aberrations during early carcinogenesis.

MicroRNAs (miR) are involved in many cell cycle processes. How much they are involved in early carcinogenesis has not been extensively explored. Mascaux and colleagues showed that miR-32 and miR-34c expression decreased from normal bronchial tissues of nonsmokers to squamous cell carcinomas. Others behaved differently at successive stages, such as miR-142-3p or miR-9, or are only altered from a specific stage, such as miR-199a or miR-139. miR follows a two-step evolution, first decreasing during the earliest morphological modifications of bronchial epithelium and thereafter increasing at later stages of lung carcinogenesis [167]. In this respect the regulation of the tumor progression locus 2 (TPL2) by miR fits well into this concept: TPL2 acts as a suppressor of lung carcinogenesis and is genetically altered in lung cancer patients. Upregulation of miR-370 downregulate TPL2 and activates RAS signaling. Low TPL2 levels correlate with accelerated onset and multiplicity of urethane-induced lung tumors in mice. TPL2 antagonize oncogene-induced cell transformation and survival through a pathway involving p53 downstream of JNK and be required for optimal p53 response to genotoxic stress [168].

17.3.2.4 Apoptosis

The more tumor cells acquire genetic aberrations, the more important is control of apoptosis checkpoints for these cells. Otherwise tumor cells would be sent to apoptosis due to irreparability of their genome. To overcome apoptosis tumor cells can inhibit the checkpoint control by several mechanisms: mutation of TP53 results in its inability to recognize DNA damage. Since p53 protein cooperates with p16 in regulating apoptosis, and as p16 is also often mutated/deleted, the overall effect is apoptosis escape of the tumor cell [169–171]. Another mechanism to escape apoptosis is facilitated via the PTEN NFkB pathway. The promoter of PTEN can be downregulated by NFkB. Restoration of PTEN expression inhibited NFkB transcriptional activity and augmented TNF-induced apoptosis, indicating a negative regulatory loop involving PTEN and NFkB. PTEN is, thus, a novel target whose suppression is critical for antiapoptosis by NFkB [172]. In small-cell carcinoma, another mechanism of antiapoptosis is used: suppression of aurora kinase A (AURKA) increased apoptosis of SCLC cells. An activation of AURKA resulted in upregulation of Bcl-2 and downregulation of Bax, thus preventing apoptosis [173].

17.3.2.5 Stem Cell Theory

The debate on lung cancer stem cells is still ongoing. One of the problems in research is the misunderstanding of researchers about the organogenesis of the lung. From fetal lung development, it is well known that the bronchial buds are proliferating toward the coelom structure and finally merge with it. Lung stem cells are not a homogenous cell population, as there are stems cells within the central portion with a capability to give rise to many different cell types, stem cells along the bronchial tree, and finally stem cells in the bronchioloalveolar junction zone with much less differentiation capabilities. Since peripheral adenocarcinomas arise from this junction zone, stem cells in these carcinomas are quite different from stem cells in the central area where SCLC arises. SCLC seems to be close to central stem cells with a capability to move within the epithelium, easily invade the stroma early on, and differentiate into SCC upon chemo- or radiation therapy (transdifferentiation).

Inhibition of EGFR, Src, and Akt signaling suppressed SOX2 and the self-renewal growth and expansion of stem cells in NSCLC. In contrast other stem cell factors like Oct4 and Nanog played a lesser role in regulating self-renewal [174]. In a subsequent study, Li and colleagues studied the stem cell markers Bmi1, CD133,

CD44, SOX2, Nanog, OCT4, and Msi2 in lung cancer. Bmi1, CD133, CD44, SOX2, Nanog, and Msi2 mRNA and protein were abundantly expressed in lung cancer. Nanog expression was exclusively upregulated in lung cancer tissues [175].

In a study focusing on brain metastases, CD15 and CD133 were identified as possible markers of a stemlike cell population [176]. Furthermore CD133 expression correlated with chemoresistance and increased tumorigenicity in vitro and in vivo accompanied by increased expression of Akt and Bcl-2. CD133 expressing small-cell neuroendocrine cancer cells had also an increased expression of the mitogenic neuropeptide receptors for gastrin-releasing peptide and arginine vasopressin [177]. However, to make the story a bit more complicated, in another study, cells surviving radiation therapy showed upregulation of CD44, SNAIL, and PDGFRβ and showed features of EMT pointing to the possibility that there are more than one factor related to stem cell morphology [178]. This leads one to the fact that stem cells but probably also other cancer cells can move liberally within the epithelial layer. Most of us have seen or will see SCLC cases, where the primary tumor is 5 mm in diameter, whereas the patient present with brain metastasis as large as 3 cm. There is only one explanation: carcinoma cells start to invade the stroma early on, long before a radiologically visible tumor is formed. In the case of multiple AAH, we found an almost identical genotype in all the lesions and in only one focus an invasive adenocarcinoma [179]. The only logical explanation is that cells out of the initial precursor stem cells move out and create other foci from where similar precursor lesions start to evolve. Multifocal carcinomas seen in different organs might be explained by this phenomenon. There are no studies in pulmonary carcinogenesis, which had this in focus. However, in urinary bladder intraepithelial neoplasia, it has been shown that a reduction in integrin β4 plays a role in migration of carcinoma in situ cells along laminin [180]. Similarly another adhesion molecule E-cadherin, when downregulated, was associated with circumferential non-muscle-type βactin organization, increased motility, and random cell migration [181]. Again in another organ preneoplasia PanIN, it was shown that MUC5AC, upregulated by GLI1, interfered with the membrane localization of E-cadherin, leading to decreased E-cadherin-dependent cell-cell adhesion and promoted migration and invasion. GLI1 induced the nuclear accumulation of βcatenin in a MUC5AC-dependent manner [182].

17.3.2.6 Driver Genes and Bystander Genes: Better to Be Called Cooperators

With all these many genes involved in carcinogenesis, one might be totally confused, as it seems that there is no general rule, which gene induces what. However, we have learned through the findings of EGFR- and KRAS-mutated lung adenocarcinomas that we have to discern driver genes from bystander genes. In mouse models KRAS-mutated gene constructs induced a proliferation of stemlike cells at the bronchioloalveolar junction zone, which via hyperplasia and AAH-like lesions progressed into adenocarcinoma in situ [183]. However, KRAS needs a cooperation of mutated TP53 and deletion of PTEN to progress further into an invasive adenocarcinoma. So KRAS functions as a driver gene. Similar findings are seen in mutated EGFR adenocarcinomas. Cooperator genes are either cooperation partners of the driver or have other important functions for the maintenance of the developing carcinoma. This is nicely addressed by the work of Chitale: in KRAS-mutated adenocarcinomas, growth is upregulated by the mutated driver KRAS itself, no other passenger mutation is necessary for this function. In EGFR-mutated adenocarcinomas a passenger mutation is required: DUSP4 is involved in negative feedback control of EGFR signaling. DUSP4 is underexpressed due to a single-copy loss on 8p. DUSP4 functions as a growth suppressor in EGFR-mutant lung adenocarcinoma, and furthermore DUSP4 loss is associated with p16/CDKN2A deletion, which acts as a G2-S checkpoint control and might send cells to apoptosis, in case of ROS-induced DNA alteration [184]. Another gene TWIST1 collaborates with the EGF pathway in promoting EMT in EGFR-mutated

lung adenocarcinoma [185]. So these genes are not bystanders but cooperating genes fulfilling specific functions, which the driver cannot do. Similarly in KRAS-mutated adenocarcinoma, exclusive gene fusions were found for CD74-NRG1, SLC3A2-NRG1, EZR-ERBB4, TRIM24-BRAF, and KIAA1468-RET. The CD74-NRG1 fusion activated HER2-HER3 signaling, whereas the EZR-ERBB4 and TRIM24-BRAF fusions constitutively activated the ERBB4 and BRAF kinases, respectively [186].

As of the end of 2015, these driver genes were identified in pulmonary carcinomas, with some variations among different races: mutations in EGFR, KRAS, NRAS, BRAF, PIK3CA, MET, and CTNNB1. Novel driver mutations were identified in LMTK2, ARID1A, NOTCH2, and SMARCA4. Furthermore there are rearrangements in ALK, RET, ROS1, FGFR2, AXL, and PDGFRA. Among recurrent alternative splicing events, exon 14 skipping in the proto-oncogene MET identified it as another cancer driver. For several genes there was a strong association with smoking history of patients [187]. Similar finding were reported for Asian patients; however, the frequency for each gene alteration was different [182]. In African Americans again a similar genetic profile was seen for NSCLC [188]. In a Chinese study involving never-smokers 75 % harbored EGFR mutations, 6 % had HER2 mutations, 5 % had ALK fusions all involving EML4 as the 5′ partner, 2 % had KRAS mutations, and 1 % harbored ROS1 fusions. BRAF mutation was absent [189]. Independent from race EGFR mutations were highly associated with female sex, Asian race, and never-smoking status; ALK rearrangements were strongly associated with never-smoking status and more weakly associated with the presence of liver metastases. ERBB2 mutations were strongly associated with Asian race and never-smoking status; single mutations were seen for PIK3CA, ALK, or MET [190]. When looking up adenocarcinomas in smokers, EGFR, STK11, and KRAS were most common; in squamous cell carcinomas, the following driver genes were identified: PTEN (16.1 %), STK11 (8.3 %), and PIK3CA (7.2 %) were the three most frequently enriched genes in smokers with SCC. DDR2 and FGFR2 were exclusively present in smokers with SCC, whereas EGFR, c-Met, and PIK3CA alterations were found in the non-smoker population with SCC [191].

17.3.3 Common Carcinomas

Adenocarcinoma has replaced squamous cell carcinoma as the leading carcinoma, comprising 40–60 % of all pulmonary carcinomas. The percentage of small-cell carcinoma is decreasing to the range of 8–12 % in Austria, Germany, and other Western and Central European countries; however it is still high in eastern parts of Europe. Squamous cell carcinoma in Austria decreased from 35 % to 18 % but increased again within the last 5 years to 27 %, probably due to immigrants from southeastern Europe. Squamous cell carcinoma is still high in Eastern European countries. The number of large-cell carcinomas for a long time remained stable at 12 % but since 2005 decreased to 4 % due to the use of immunohistochemical markers for the differentiation of NSCLC, which shifted almost two thirds of them into the adenocarcinoma and a smaller fraction into squamous cell carcinoma.

By X-ray and CT scan, carcinomas present as a tumor mass with ill-defined border. Spicule radiating from the tumor center represents outgrowth of the tumor into the periphery. In situ carcinoma, especially adenocarcinoma, is characterized by ground-glass densities, whereas invasive portions will show higher densities.

Due to the invention of ultrasound-guided biopsy in bronchology, the size of biopsies decreased considerably during the last few years. For that reason the WHO classification now also included a new classification for small biopsies and cytology specimen [70].

The previous editions of the WHO classification of lung tumors were mainly based on the experience from resected tumors. This is especially true for lung carcinomas. This means the classification is based on the experience from less than 30 %, whereas more than 70 % of lung carcinomas are diagnosed on small tissue samples or on cell preparations. In the past this was not important, because there were not much therapy options available for patients with non-resectable

lung carcinomas. In these periods oncologists asked for the differentiation of small-cell (SCLC) versus non-small-cell carcinomas (NSCLC); everything else was unimportant.

This has changed dramatically! New chemotherapeutics have been introduced, which are efficient under certain circumstances and in defined tumor entities; targeted therapy has finally also found its way into lung cancer treatment.

Several of these therapies were especially suitable for adenocarcinomas, or even squamous histology had to be excluded before this therapy was applied. Cisplatin-based chemotherapy showed better outcome in adenocarcinomas; nucleotide excision repair enzyme (ERCC1) is more prevalent in squamous cell carcinomas, which result in repair of DNA damage induced by platinum compounds, thus explaining why adenocarcinomas responded better. The thymidylate synthase blocker pemetrexed is efficient in most adenocarcinomas and not in squamous cell carcinomas.

Finally activating mutations of the epidermal growth factor receptor (EGFR) are most often found in never-smokers, in females, and in patients with adenocarcinoma histology. Other molecular targets such as ALK kinase gene fusion with the EML4 gene (and others) has been recently shown in patients with adenocarcinomas. ROS1 rearrangement followed again in adenocarcinomas.

Angiogenesis is essential for the primary tumor as well as for metastasis. The secretion of VEGFs facilitates most often neoangiogenesis. Tumor blood vessels are fragile and are prone to rupture. Using antibodies against VEGF (bevacizumab) and more recently by FGF receptor inhibitors, the vascularization can be inhibited and regression of the tumor is induced.

17.3.3.1 Squamous Cell Carcinoma (SCC)

Clinical Symptoms

SCC usually presents with weight loss, hemoptysis, hoarseness, cough, mucopurulent expectations, and due to frequent bronchial obstruction by an endobronchial component also purulent pneumonia. On X-ray as well as on CT scan, it presents as a central mass, which often also involves regional lymph nodes.

Gross Morphology

SCC is most often a tumor mass located in the central bronchial tree. Regional lymph nodes are often directly involved by an ingrowth of the carcinoma (Fig. 17.41). On cut surface the tumor can look coarse granular in keratinized forms – the granules correspond to sheets of keratinized cells. Necrosis is common and can be widespread. There is a rare form of SCC occurring in the peripheral lung (Fig. 17.42). In most of these cases, a previous inflammatory lesion is reported,

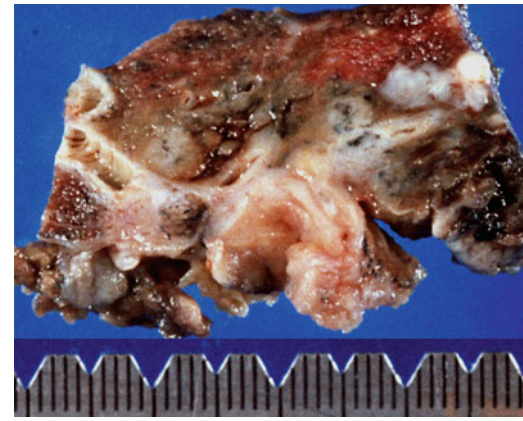

Fig. 17.41 Gross morphology of a squamous cell carcinoma (SCC), located in an upper lobe bronchus. The endobronchial growth is seen as well as some lymph node metastasis in N1 nodes

Fig. 17.42 Unusual variant of a SCC arising in peripheral location. In addition to the carcinoma (*white* nodules), there is also bronchiectasis and emphysema

most often previous treatment with cytotoxic drugs.

Histology

SCC is defined by a platelike layering of cells, keratinization of groups or single cells, intercellular spaces or gaps, and bridges (represented by desmosomes and hemidesmosomes) (Figs. 17.43, 17.44, and 17.45). Squamous cell carcinomas can be keratinizing or nonkeratinizing; however, they are not different with respect to prognosis. Similar to the cervix, there exists a rare small-cell variant of SCC, which might cause diagnostic problems because of simulating small-cell

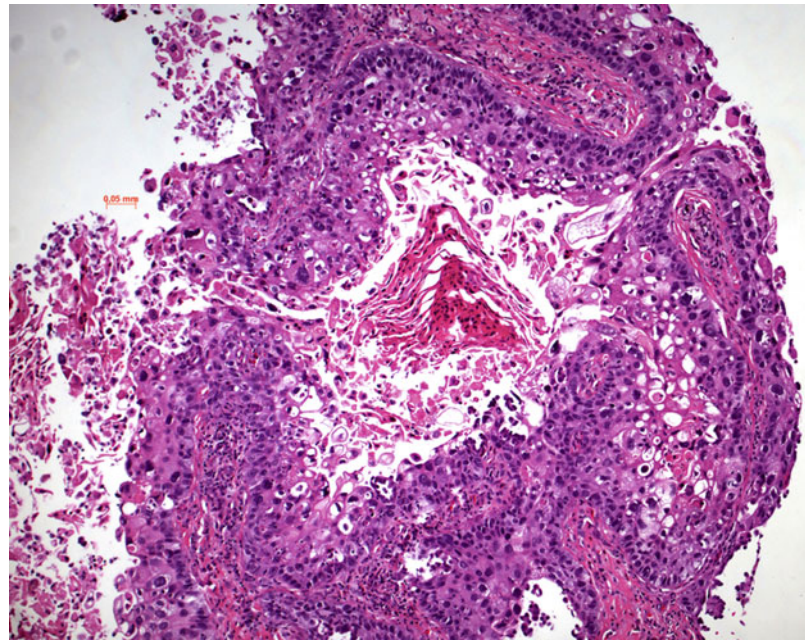

Fig. 17.43 Bronchial biopsy of a SCC. This case shows sheets of keratinized tumor cells. The cell borders are clearly visible by the intercellular gaps. There is a lot of apoptotic cells and infiltration by neutrophils, which point to autophagy. H&E, bar 50 µm

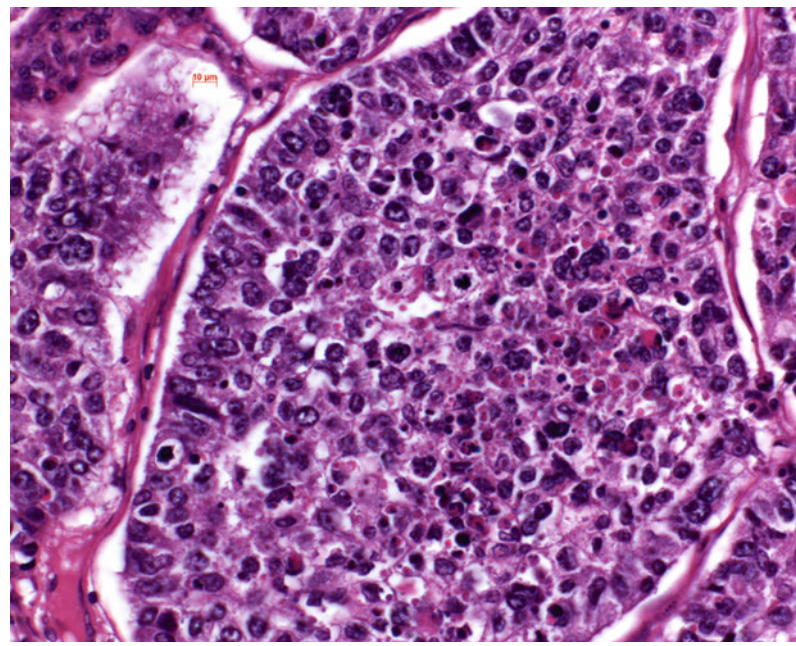

Fig. 17.44 Another case of SCC. The intercellular gaps/bridges are clearly seen; in addition there is a row of palisading cells on the *left side*, a feature not uncommon in SCC. There is single cell keratinization and considerable nuclear atypia, placing this case more into the high-grade type. H&E, bar 10 µm

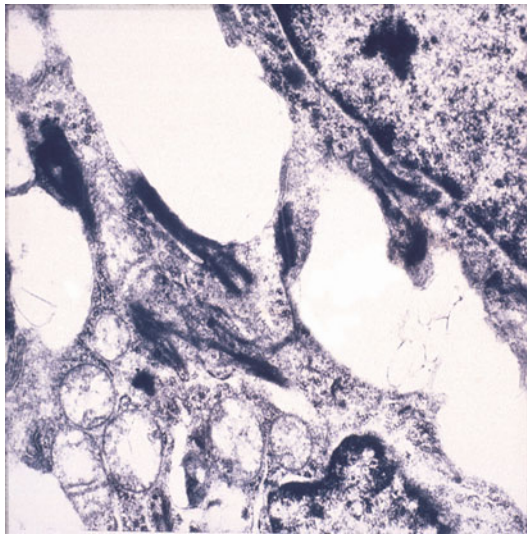

Fig. 17.45 Electron microscopy of an SCC. The intercellular gap between two tumor cells is shown. The cell connection in the middle is closed by a desmosome. There are other desmosomes and hemidesmosomes present (densely stained structures). Different filaments such as cytokeratin filaments insert in these structures. ×6,000

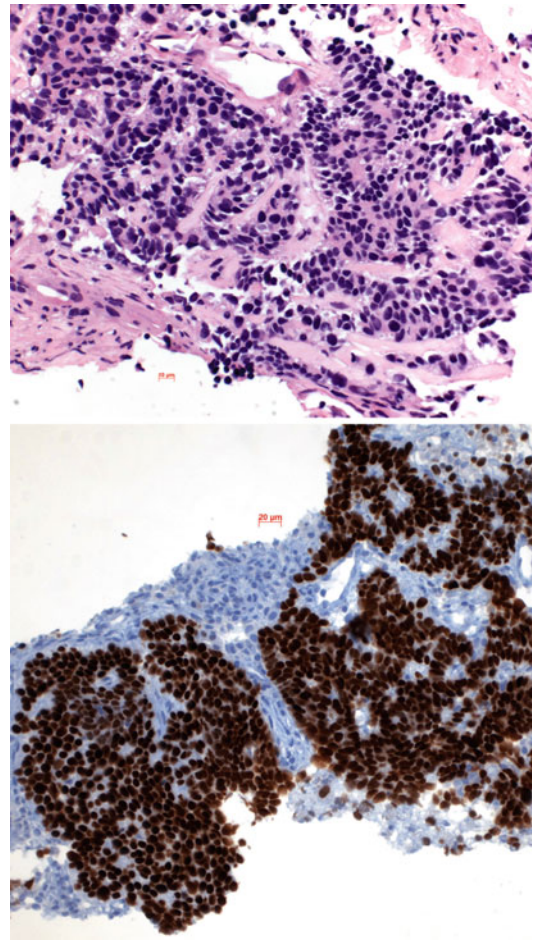

Fig. 17.46 Small-cell variant of SCC. In the *upper panel*, the infiltrating tumor is seen in a transcutaneous needle biopsy. The nuclei are dense and dark stained; however, there is ample cytoplasm. In some foci a peripheral palisading was seen. In the *lower panel*, an immunohistochemical stain for p63 protein confirmed the diagnosis of SCC. H&E, bar 10 µm, immunohistochemistry, bar 20 µm

neuroendocrine carcinoma. However, the former has visible nucleoli, and also intercellular gaps are focally seen (Figs. 17.46 and 17.47). In addition this variant also expresses high molecular weight cytokeratins.

There exist no general accepted grading system for squamous cell carcinoma. In the AFIP fascicles, keratinization was proposed for grading: a SCC with more than 20 % keratinized tumor cells was graded as G1, less as G2, and if there are only single keratinized cells or no keratinization at all, this was graded as G3.

In my opinion this grading is not accurate, as it does not reflect biological behavior. In some SCC keratinized carcinoma cells are exclusively found in lymph node metastasis, whereas the nonkeratinized component is seen in the primary tumor. In addition as the classification changed into keratinizing and nonkeratinizing SCC, keratinization cannot be used anymore. In many malignancies mitosis is used for grading, and I adapted this for SCC and other lung carcinomas. It proved to be very useful. These are the recommended features:

G1 = mitotic counts 0–3/HPF (×400), minor nuclear polymorphism, small nucleoli (Fig. 17.48).

G2 = mitotic counts 4–8/HPF, nuclear polymorphism clearly visible, medium-sized nucleoli (Fig. 17.49).

G3 = mitotic counts >8/HPF, nuclear polymorphism clearly visible, a few scattered multinucleated cells might be encountered; nucleoli are enlarged and irregularly shaped (Fig. 17.50).

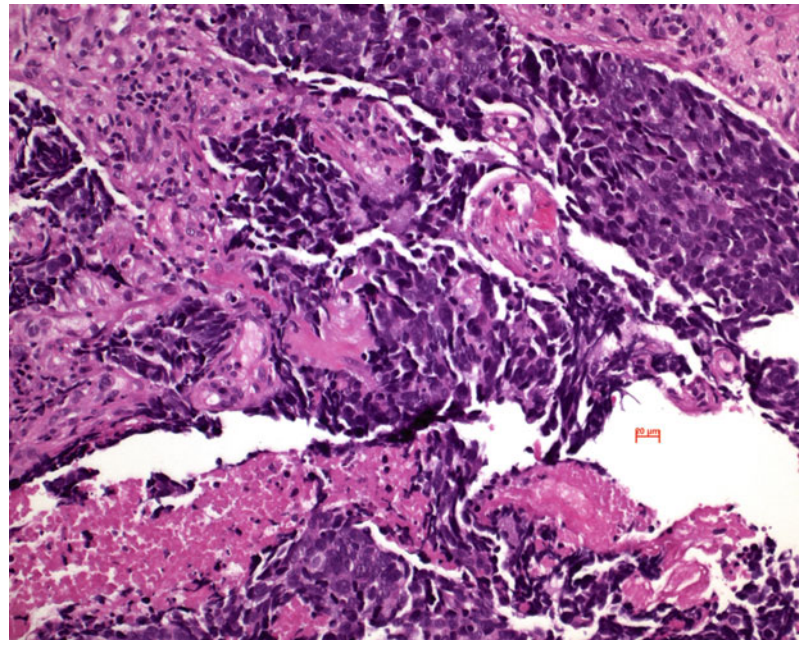

Fig. 17.47 Other case of small-cell variant of SCC, which in addition showed positivity for NCAM in about 10 % of tumor cells but also stained for p40. H&E, bar 20 μm

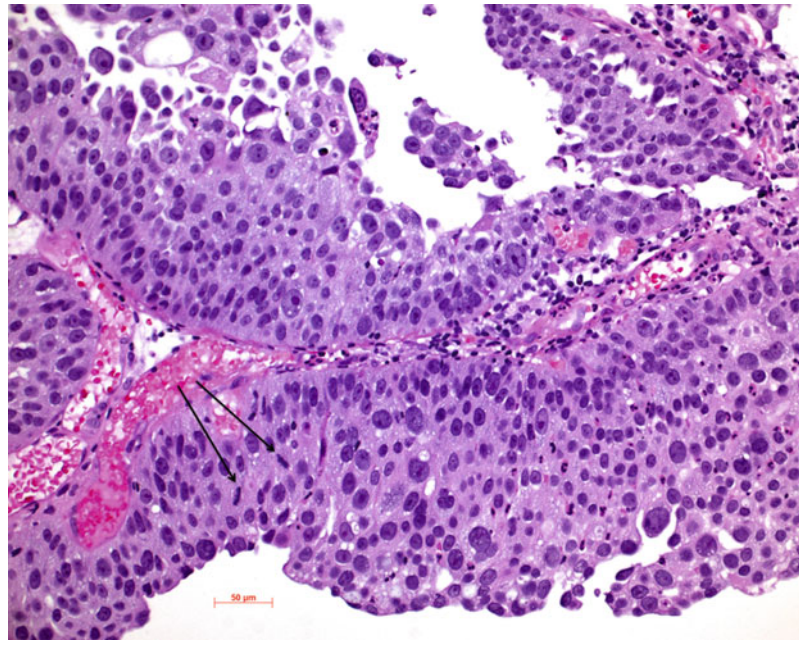

Fig. 17.48 SCC well differentiated with some nuclear polymorphism but only two mitoses (*arrow*)

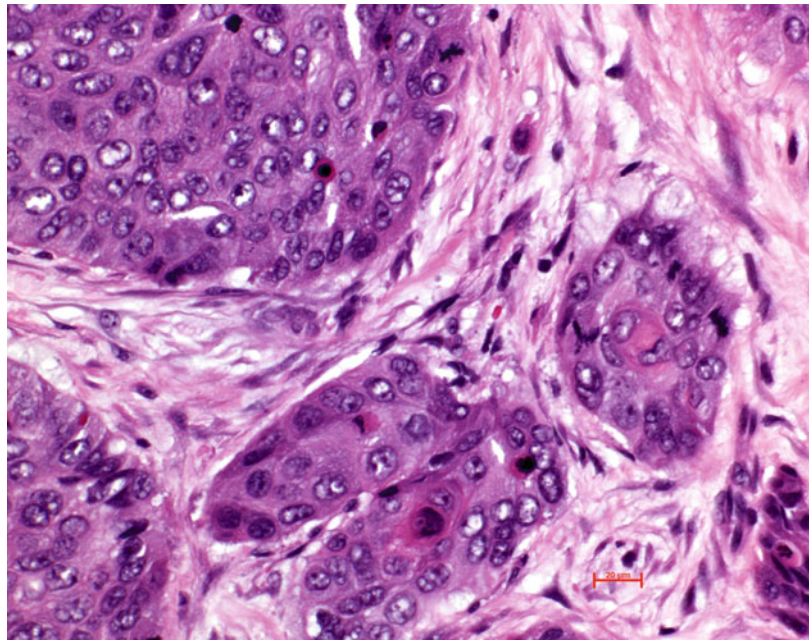

Fig. 17.49 SCC, G2 type. Keratinization of single cells is present; five mitotic counts are present. There are still good visible intercellular gaps. H&E, bar 20 µm

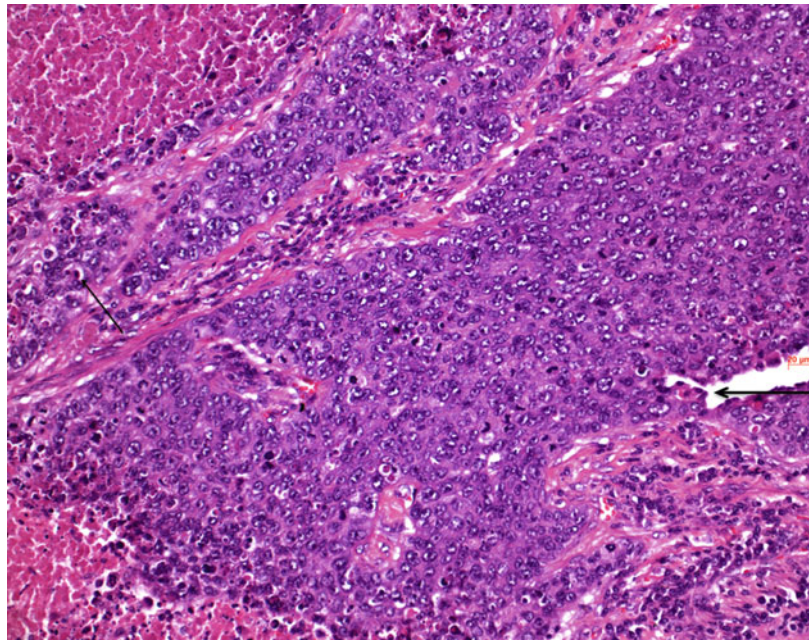

Fig. 17.50 High-grade SCC with more than eight mitoses per HPF. Here intercellular gaps are hardly seen; the carcinoma looks almost undifferentiated. However, there are areas with single keratinized cells (*arrows*), and also this carcinoma expressed SCC markers. H&E, bar 20 µm

In looking for markers predictive for survival, Kadota and coworkers compared keratinizing, nonkeratinizing, basaloid, and clear cell subtypes, as well as single cell invasion, nuclear diameter, and tumor budding, and found that only these later factors were independent prognostic factors [192].

The etiology of squamous cell carcinomas is to almost 100 % linked to cigarette smoking, especially to filterless cigarettes. Some other agents inducing SCC are metals such as cadmium and arsenic, but also radon and uranium exposure has been linked to SCC [193–197]. Additional to these chemicals also HPV similarly to the cervix

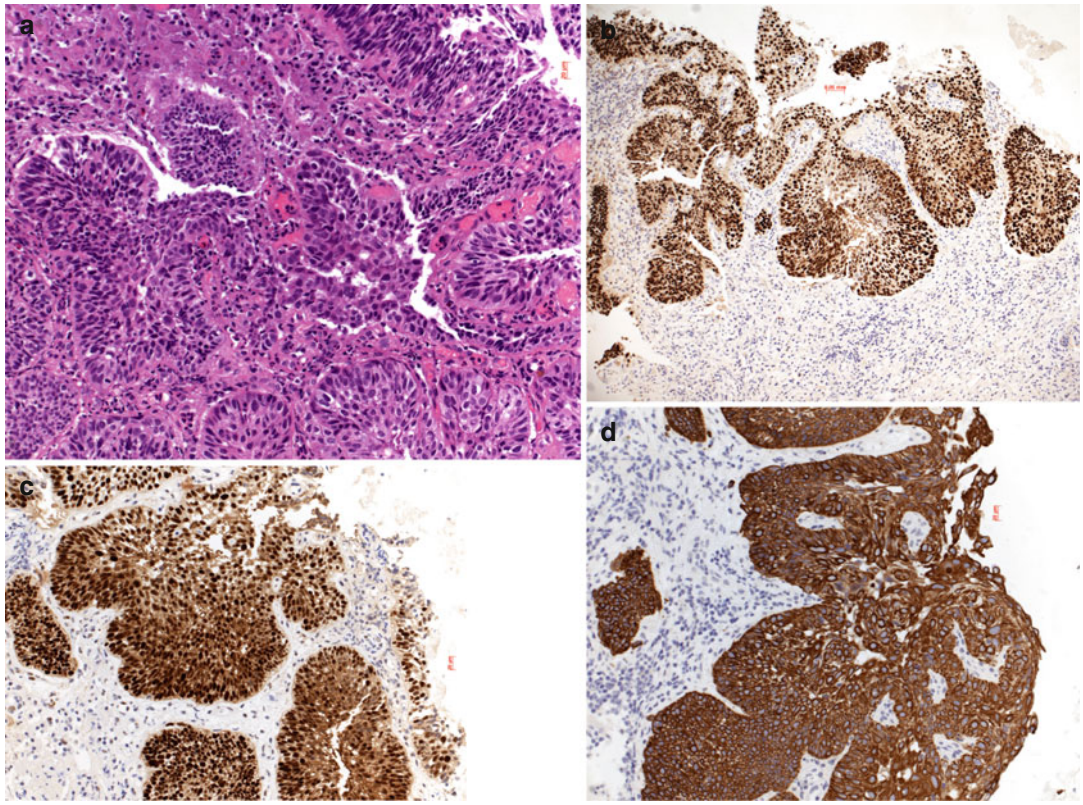

Fig. 17.51 Immunohistochemical markers in SCC. (**a**) Histology of an SCC, (**b**) shows reactivity for p40 with stained almost all tumor cells. (**c**) A staining for p53 can sometimes be used, as almost all patients with SCC are smokers, and therefore have mutations of TP53 gene. (**d**) Staining for cytokeratin 5/cytokeratin 6, a high molecular cytokeratin present in SCC. Bars 20 and 50 μm

might be involved in SCC development. HPV-induced papillomas exist in the airways, from the upper respiratory tract to the bronchi. In most cases non-oncogenic HPV types have been demonstrated in these papillomas. However, in rare instances oncogenic types have been proven, which subsequently developed into SCC [27, 29, 43]. While HPV 16 and 18 directly interfere with the mitosis checkpoint controls RB1 and TP53, HPV11 by itself is not oncogenic, unless there is a mutation in the E2 sequence, which controls the oncogenic E6 and E7 sequences [37, 38]. All patients reported so far had HPV gene sequences in their tumors but also were heavy smokers. So the final clue if HPV alone is able to induce SCC is still missing. It is more likely that HPV infection together with smoking accelerate the development of the carcinoma, as most of these patients are of much younger age.

Immunohistochemistry

SCC expresses several differentiation markers, which can be used for diagnostic purpose. High molecular weight cytokeratins such as acidic CK3, CK5, and CK6 and basic CK13 and CK14 stain SCC, and also desmocollin3 and the basal cell marker p63 or its splice variant p40 are useful, especially in small biopsies or cytologic specimen [198–201]. Helpful is also a cell membrane-accentuated staining with cytokeratin antibodies (Figs. 17.51 and 17.52). To differentiate primary pulmonary squamous cell carcinomas from those of other locations within the upper respiratory tract, this is not always possible. SCC from the esophagus can be differentiated by the positivity for CK4, which is not expressed by pulmonary SCC. Laryngeal SCC cannot be differentiated, because this shares the same immunoprofile, whereas SCC from the oral cavity

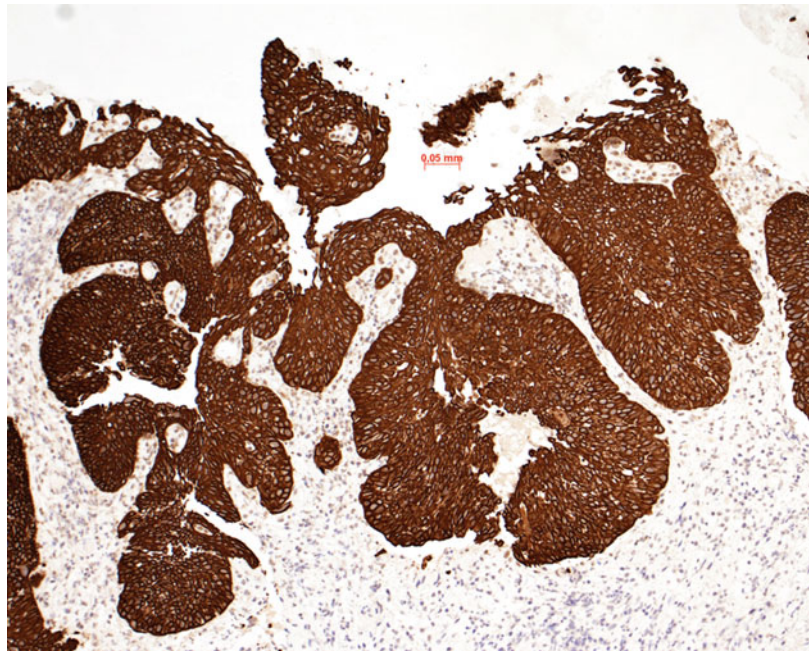

Fig. 17.52 Immunohistochemistry for cytokeratin 5/cytokeratin 6, showing the cell membrane-accentuated staining pattern. Bar 50 µm

might express CK1 and CK2, which is not expressed by the pulmonary SCC [202].

Genetic Abnormalities in SCC and Targets for Therapy

Gene aberrations are common in SCC. Gains are found on chromosomes 2, 3q, 5p, and 8q, whereas deletions are common on 3p, 5q, and 8p. The most specific aberrations are gain of 7p and 8q, whereas the most specific deletions are on 13q and 19p when compared to adenocarcinomas and small-cell neuroendocrine carcinomas [203–206] (and unpublished data by CGH and array CGH). Several targetable genes have been identified in SCC so far: amplifications and activating mutations of FGFR1 [207]; inactivating mutations or deletions of PTEN [208]; amplifications of PDGFRα [209], MCV1, SOX2 [210], EGFR [211, 212], and HER2NEU [213]; and mutations of CDKN2A [214], NOTCH1 [215], FGFR2 [191], and DDR2 [191, 216]. TP53 is frequently either mutated, deleted, or has a truncation mutation [217, 218], whereas PI3K and AKT1 are mutated or amplified in many cases [216, 219–222]. For some of these genes, therapeutic drugs are available as dasatinib for DDR2 mutation and FGFR kinase inhibitors for FGFR1 amplifications (Fig. 17.53). However, as SCC carries concomitant genetic aberrations, inhibition as in adenocarcinomas might not work: a good example is FGFR1 amplification, which can be accompanied by PI3KCA activating mutations – FGFR1 TKI inhibition therefore will not work.

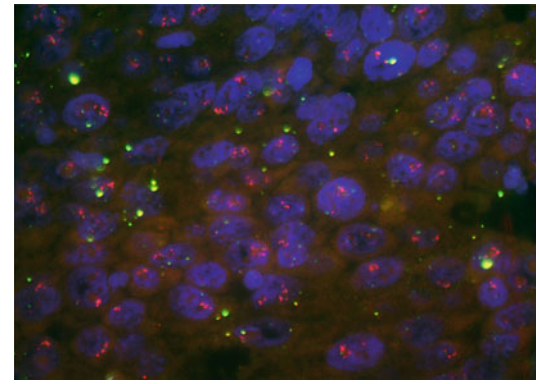

Fig. 17.53 FISH analysis for amplification of FGFR1. The FGFR1 probe is labeled in *red*; the centromere probe in *green*. There are many cells of this SCC, which show clusters of FGFR1 gene signals. Such a case would need further analysis for concomitant genetic abnormalities before applying FGFR1 inhibitor therapy. ×630

A basal cell variant of SCC does exist, and in the previous WHO edition, basaloid cell

carcinoma was listed as a variant of large-cell carcinoma [223]. In the new WHO classification [70], both are now unified into the variant *basaloid squamous cell carcinoma* (Figs. 17.54 and 17.55). In basaloid squamous cell carcinoma (BSCC), there might be either regular SCC elements even with keratinization or cases which are entirely basaloid without any differentiation. Immunohistochemical markers such as p40, p63, cytokeratins 5/cytokeratins 6, and desmocollin-3 will help in confirming the diagnosis [224]. This marker expression was the main reason for reclassification. p40 was also proven in BSCC in another study [225]. In basaloid carcinoma there is a uniform population of large cells with vesicular large nuclei, nucleoli are not prominent, but good visible. The cells form sheets and nests. On low-power magnification, the basaloid pattern is easily seen. It resembles basalioma of the skin: there is an outer layer of cells forming a palisading ring and an inner portion, where the cells are totally disoriented, i.e., cells lie in any direction. On higher magnification numerous mitoses are seen. Sometimes the organoid pattern may resemble a neuroendocrine morphology, but this vanishes on closer examination. Basaloid carcinoma is a highly aggressive carcinoma with a poor prognosis despite aggressive chemotherapy. This might be due to a specific mRNA expression profile, with upregulated factors for cell cycle progression, and some genes related to maintenance of stem cell-like features, while genes related to squamous differentiation are repressed. Among the genes specific for BSCC, SOX4 and IVL discriminate it from regular SCC [226].

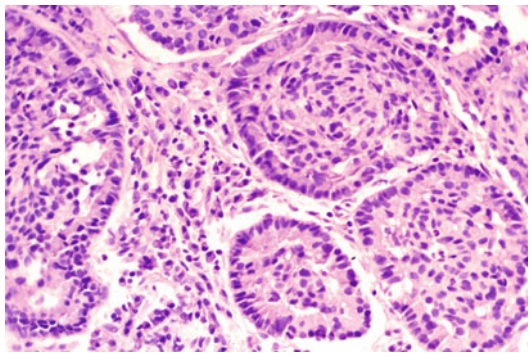

Fig. 17.54 Basaloid variant of SCC, here the classical type with features reminiscent of basalioma of the skin. There is an outer row of tumor cells with palisading, whereas the other cells are totally disoriented. H&E, ×200

Cytology and small biopsy classification for SCC: nuclei usually with coarse chromatin,

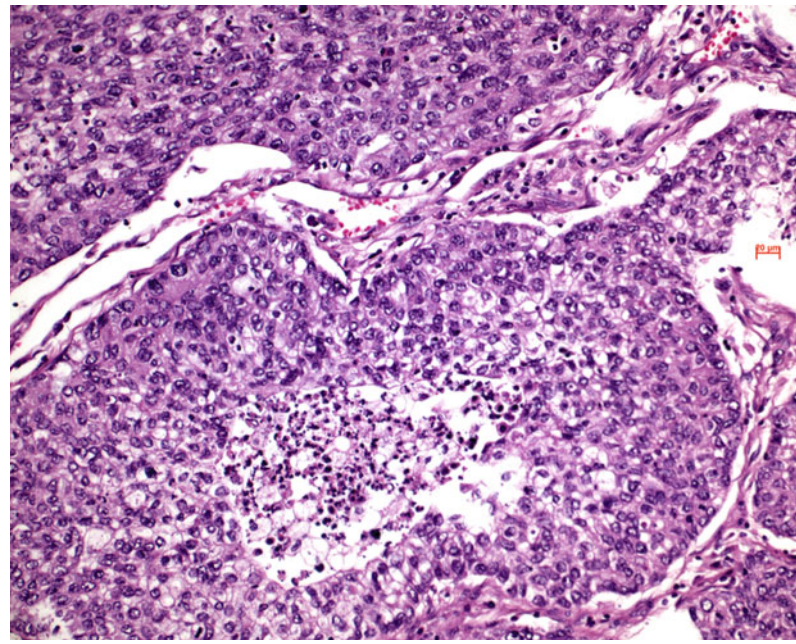

Fig. 17.55 Basaloid variant of SCC, here a case in the previous WHO classification placed in the large-cell carcinoma group, now regrouped in SCC because of expression of SCC markers. There is still some kind of palisading of tumor cells, but otherwise no clear differentiation is seen. Cell borders are visible, in few cells intercellular gaps are seen. H&E, bar 20 µm

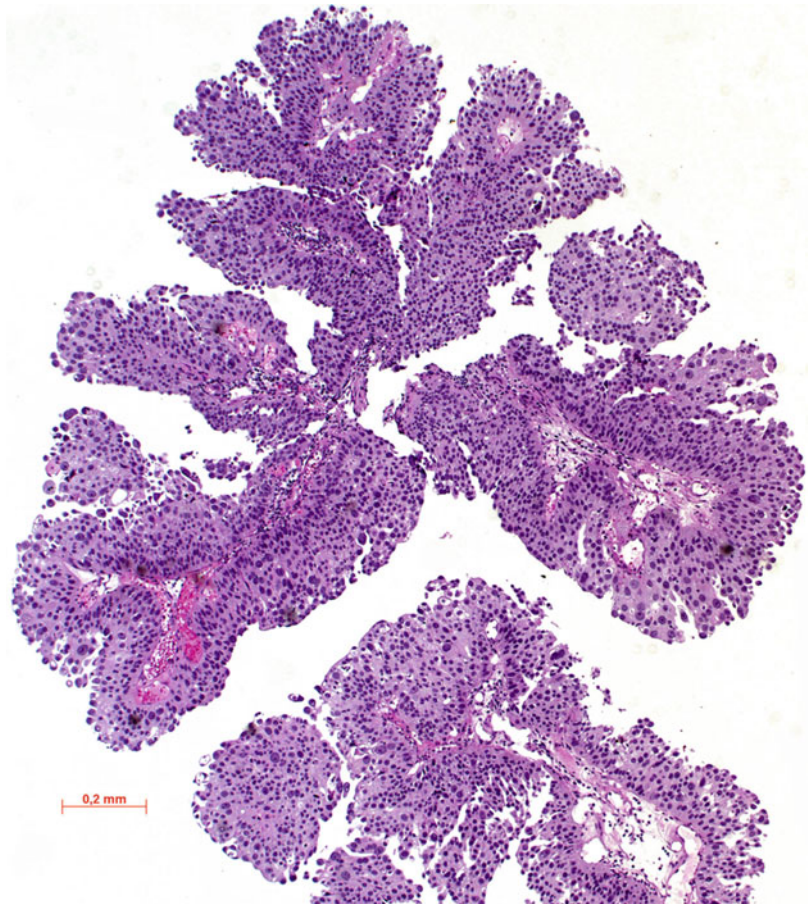

Fig. 17.56 Biopsies of SCC, where only surface parts of the carcinoma has been taken. Invasion is not present. The morphology however confirms SCC. H&E, bar 200 µm

nucleoli middle sized, keratinization of single cells or groups, and intercellular gaps visible on small-cell groups (Fig. 17.56), layering of cells if there are large sheets of cells (in well-differentiated SCC); in addition in biopsies – layering of cells and basal cell layer. Keratinization is highlighted in PAP stain or similar (Fig. 17.57).

17.3.3.2 Adenocarcinoma

Clinical Findings

The clinical symptoms are usually very unspecific including weight loss, fatigue, and less often cough. Hemoptysis is usually not a feature, but blood-tinged mucus expectorations might be seen. On X-ray and CT scan, this is usually a peripheral lesion, sometimes close to the pleura. Some small carcinomas present entirely as ground-glass opacities – these correspond most often to adenocarcinoma in situ.

Gross Morphology

Non-mucinous adenocarcinomas present as grayish-white solitary nodule or mass. Mucinous adenocarcinomas appear with a grayish-white cut surface and abundant gelatinous material. Colloid adenocarcinomas also look gelatinous; however, whitish small foci are scattered within these mucin lakes, like speckles. AIS appears grayish with a finely cystic structure, representing rigid extended alveoli. There are rare adenocarcinomas in central portions, most often histologically of the bronchial gland type again with some mucin seen on cut surface, and adenocarcinomas arising from small bronchi and bronchioli, which do not present with specific features, just solid whitish-grayish nodule (Fig. 17.58).

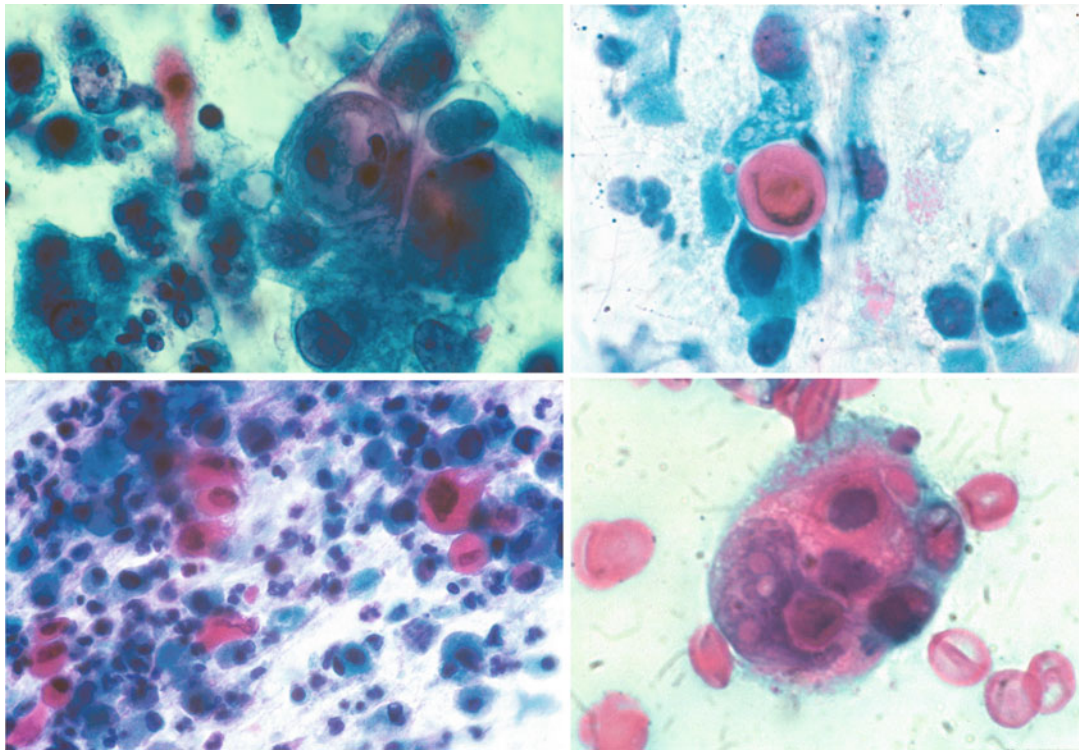

Fig. 17.57 Cytology of SCC, clockwise from *upper left*: the tumor cells show intercellular gaps, a keratinized cell is also present; in this photograph a keratinized tumor cell is surrounded by other carcinoma cells; in the third graph, emperipolesis of red blood cells by a carcinoma cell. In addition another SCC cell has also been phagocytosed (cannibalism); in the last graph, several keratinized carcinoma cells are seen (tadlepol cells). PAP stain, ×400 and 630

Histology

Adenocarcinomas can present with different morphological pattern, such as lepidic, acinar, papillary, micropapillary, solid, and cribriform. In most ACs different patterns are mixed; acinar and papillary are the most common combinations. The pure forms are quite rare. Lepidic AC is characterized by a tumor cell growth along preexisting alveolar septa (Fig. 17.59a). In contrast to adenocarcinoma in situ, lepidic AC will always have an invasive focus, which should be >5 mm. In *acinar* AC the tumor forms well-defined gland-like acini, surrounded by a small rim of stroma, but sometimes the stroma might be thin (Fig. 17.59b, c). In *papillary* AC the tumor forms papillae projecting into a widened lumen. The papillae have stoma stalks, which are formed by newly formed blood vessels and some myofibroblasts (Fig. 17.59e). The tumor cells grow along these papillae. In *micropapillary* AC the tumor cells form micropapillae, which in contrast to the papillary form have no stroma, but consist of epithelial proliferations, projecting into the lumen (Fig. 17.59d). This type of AC is characterized by downregulated cellular adherence, the reason why these tumor cells easily disconnect from the septa and form small-cell clusters. This structure is also seen in lymph node metastasis, where the tumor cells lie within some liquid secretions. *Solid* AC is defined by a solid growth pattern (Fig. 17.59f) and can present with a small amount of mucin-producing cells: a minimum is two times five cells in two different fields. By the use of immunohistochemistry, another form of solid AC has arrived, characterized by solid growth pattern and TTF1 positivity.

Cribriform AC has not been included in the new WHO classification, but this subtype does

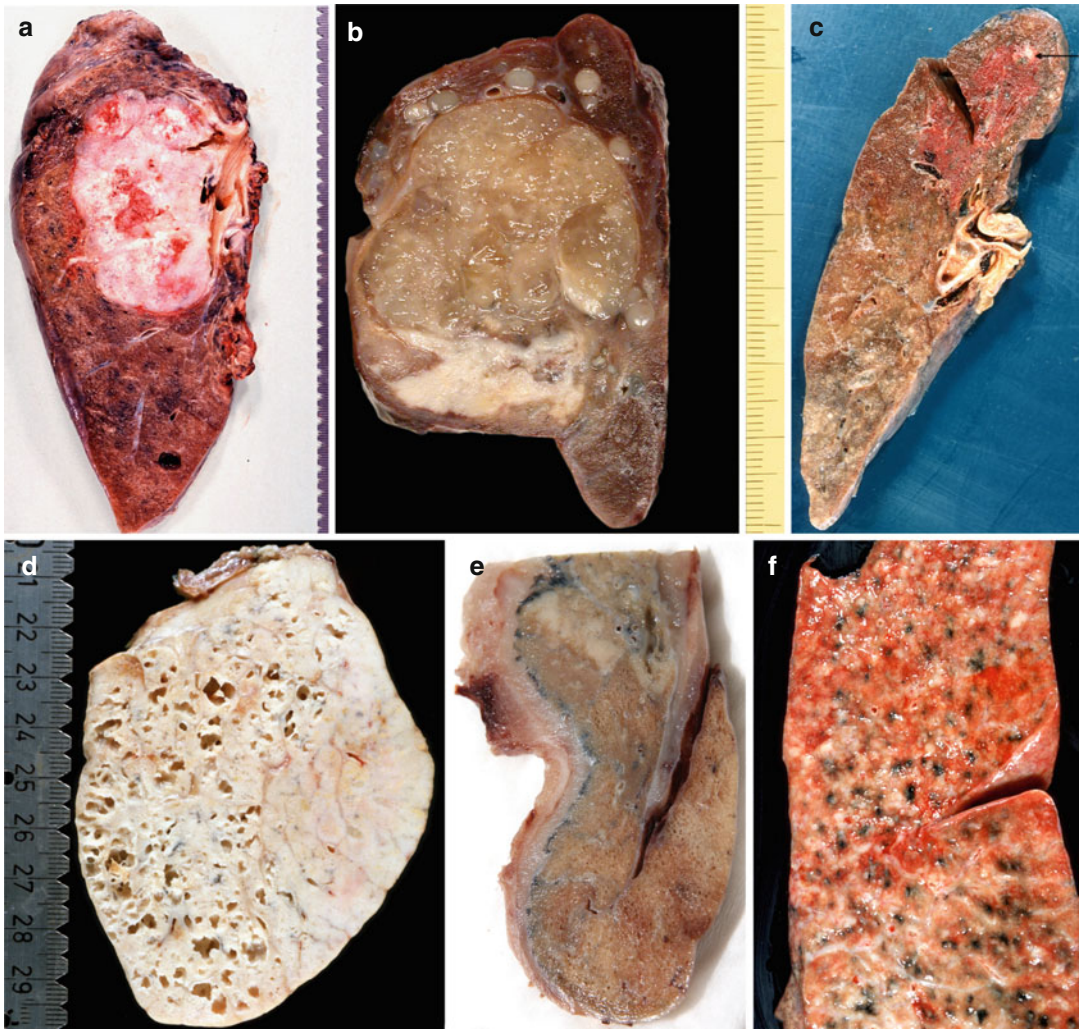

Fig. 17.58 Examples of adenocarcinomas of the lung, (**a**) large adenocarcinoma of central type (bronchial gland type), (**b**) mucinous adenocarcinoma, (**c**) small peripheral adenocarcinoma arising in lung fibrosis, (**d**) diffuse mucinous adenocarcinoma (pneumonia type), (**e**) adenocarcinoma with extensive pleura involvement (pseudomesothelioma type), (**f**) adenocarcinoma with massive intrapulmonary metastasis

exist. It resembles metastasis of colon carcinoma. The tumor presents with complex acinar structures, which have formed secondary and tertiary lumina out of a primary acinus (Fig. 17.59g).

Adenocarcinomas usually have large vesicular nuclei and prominent nucleoli; the chromatin is most often lightly stained or unstained (euchromatin more abundant than heterochromatin). Nucleoli tend to be larger and more bizarre, the less the AC is differentiated. Nuclear membrane is accentuated by chromatin; the cytoplasm can be finely vacuolated or present with larger vacuoles. The content of these vacuoles is not always mucin but may also contain some proteins, lipo-, and glycoproteins, if the cells are differentiating toward secretory columnar cells.

As the lung is a 3D structure, where alveoli fill up all spaces, and our sections just confront us with a 2D picture, some uncertainties remain: Are acini and papillary structures real different? Or are these only different views and section planes of the same acinar structure. This might be resolved by applying new techniques producing

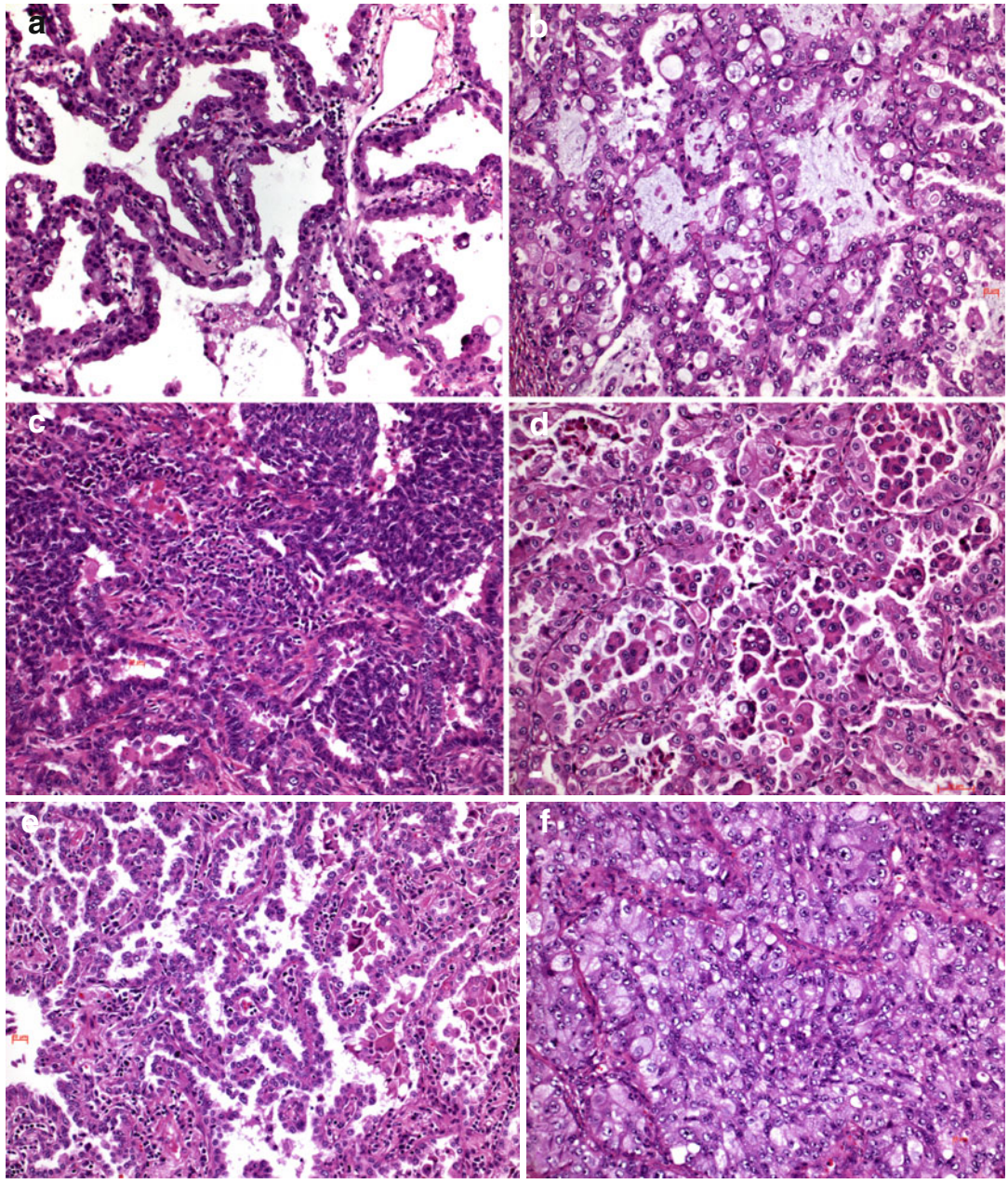

Fig. 17.59 Patterns in adenocarcinomas: (**a**) lepidic, the tumor cells grow along preexisting alveolar septa; (**b**) acinar, the tumor cells form an acinar glandular structure; (**c**) acinar with morula formation, in this cases within acini solid structures called morules are formed, similar to what is seen in some endometrial adenocarcinomas; (**d**) acinar mixed with micropapillary, the micropapillary component is composed of groups of tumor cells without a stroma stalk; (**e**) papillary, the tumor cells cover a stroma stalk, which is a newly formed mesenchymal structure with mesenchymal cells and new blood vessels; (**f**) solid, the tumor cells form solid cell complexes, the basal orientation of the nucleus is seen, and the cytoplasm shows fine vacuolation; (**g**) cribriform, the tumor cells form primary, secondary, and tertiary acini; (**h**) bronchial gland type, the tumor cells simulate serous cells of the bronchial glands. H&E, bars, 20 and 50 μm

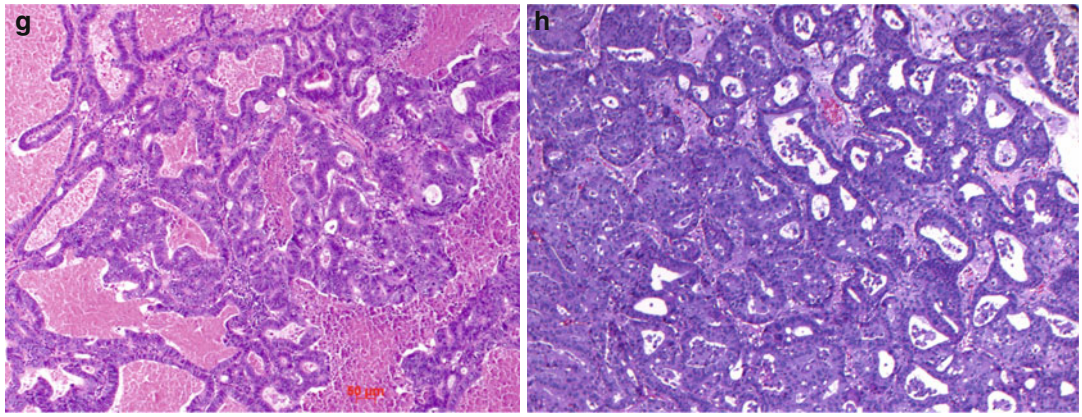

Fig. 17.59 (continued)

3D views of the acini using step sections and 3D reconstruction.

Invasion in adenocarcinomas can be difficult to assess, because in contrast to SCC adenocarcinomas show often less prominent desmoplastic stroma formation, especially in the well-differentiated forms. Invasion in AC can be diagnosed, if a desmoplastic stroma is present, if lymphatic or blood vessel invasion is seen, and if pleural invasion is present. Another help in the assessment of invasion is alveolar collapse (atelectasis). This is the area where one should look for desmoplastic stroma cells (Fig. 17.60). Invasion also implicates a change in morphology: When adenocarcinoma cells invade, the nice arrangement along alveolar surface structures as in lepidic type is impossible. Instead the tumor cells usually arrange themselves into small acinar or tubular, papillary, or solid structures or invade as single cells (Figs. 17.60 and 17.61).

In the WHO classification, *airspace spreading* is mentioned. In this condition tumor cells are free floating or moving within the alveoli and are separated from the primary tumor. This can be difficult to assess: small complexes of carcinoma cells lying within airspaces might be well attached at an alveolar septum, which will be seen on serial sections. So a freely floating tumor cell complex especially if these are close to the tumor will require step sections and/or 3D reconstruction to prove. In addition airspace spreading might be an extension or outgrowth of tumor cells or just reflect tumor cells moving along alveolar septa, as precursor cells already do. Another aspect is artifact: sectioning of the tissue block might transfer tumor cells. Airspace spreading has no impact on metastasis; however, it is important as a resection margin, because from these cells recurrence can occur. Airspace spreading is not invasion and not intrapulmonary metastasis: invasive tumor cells have access to vessels, move within the stroma, and interact with it, and metastasis means establishment of tumor cells at a different area of the lung clearly separated from the primary tumor. In intrapulmonary metastasis usually there will be areas of tumor cells within lymphatics.

In situ AC (AIS) is a rare form of AC. AIS is defined as a proliferation of carcinoma cells along alveolar septa, completely covering the surface (Fig. 17.62). They can produce epithelial papillae; *invasion or desmoplasia should be excluded*. Different cell types are involved: Clara-like cells, pneumocyte II-like cells, columnar cells, and goblet cells (Fig. 17.63). Most often AIS presents with a mixture of these cellular differentiations; however, pure Clara cell- or pneumocyte-like AIS does occur. AIS is a precursor of peripheral adenocarcinomas arising at the bronchioloalveolar junction zone. AIS can be non-mucinous or mucinous; however, in cases of multiple nodules of mucinous AIS, a careful examination and step sections are required to rule

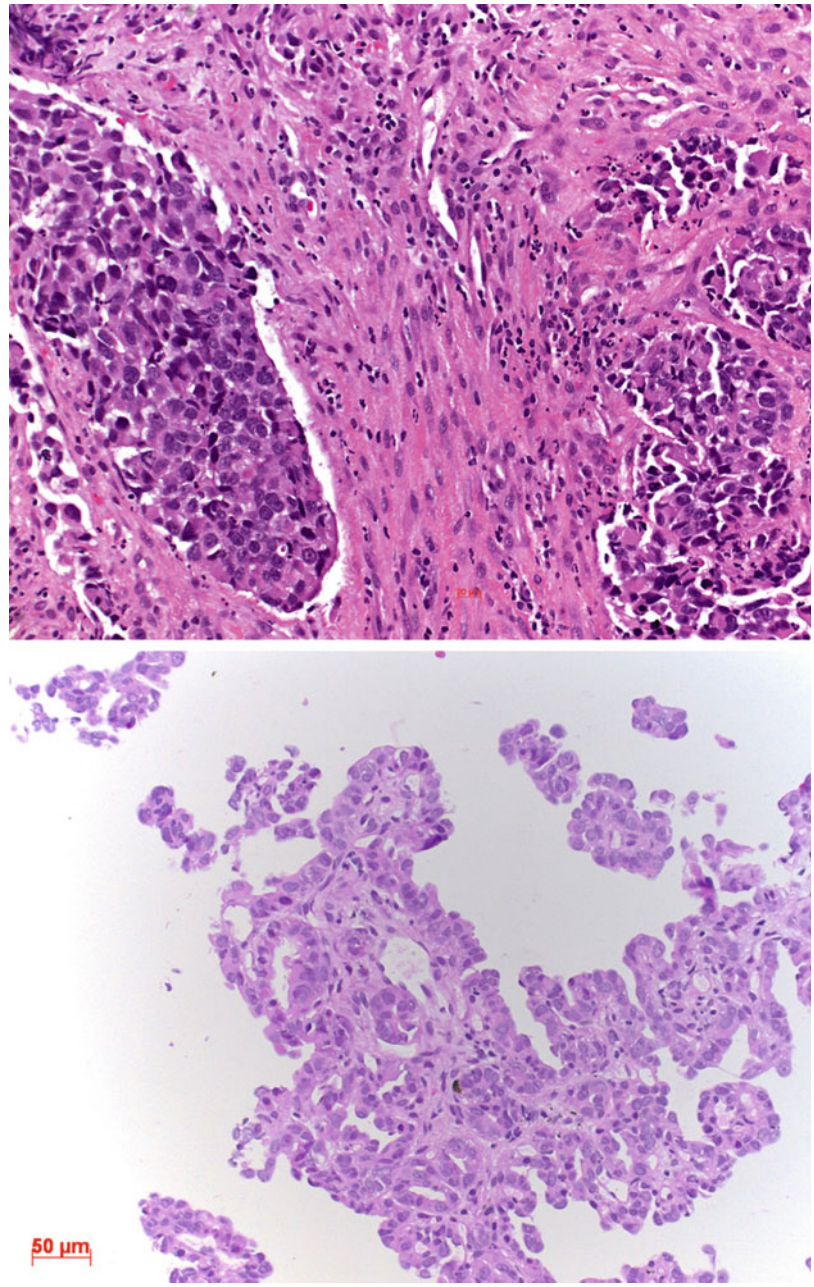

Fig. 17.60 Assessment of invasion in adenocarcinomas; in the *upper* panel, solid adenocarcinomas invade the stroma causing proliferation of myofibroblastic stroma cells and a granulocytic infiltration as part of desmoplastic stroma formation. In the *lower* panel, there is only mild desmoplastic reaction with few stroma cells, but single cells and small groups are within the septum and reactive endothelia and few myofibroblasts are seen. H&E, bars 20 and 50 µm

out invasion. In mid- and central portions of the lung, AIS has not been identified so far.

Microinvasive adenocarcinoma (MIA) is another entity based on histology and CT scan. On CT this type of AC is characterized by ground-glass opacity as in AIS. On histology a small invasive focus is seen, whereas the AC is lepidic in the majority. The invasive focus should be ≤5 mm in diameter (Fig. 17.64). The reason for creating a separate entity, different from AIS and lepidic AC, is that MIA confers the same good prognosis as AIS, i.e., a 100% survival after surgical removal [227, 228]. The term microinvasive or minimally invasive AC was already proposed for the 1999 WHO classification by Y. Shimosato, based on his experiences with small size adenocarcinomas [229,

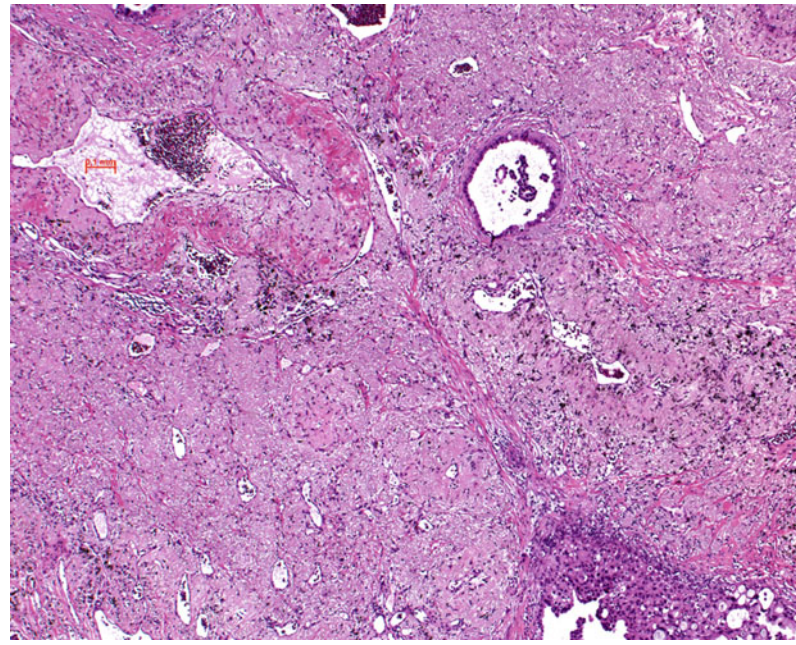

Fig. 17.61 Central scar in an adenocarcinoma. Tumor cells are within the scar and also in dilated lymphatics, a sign of worse prognosis. H&E, bar 100 µm

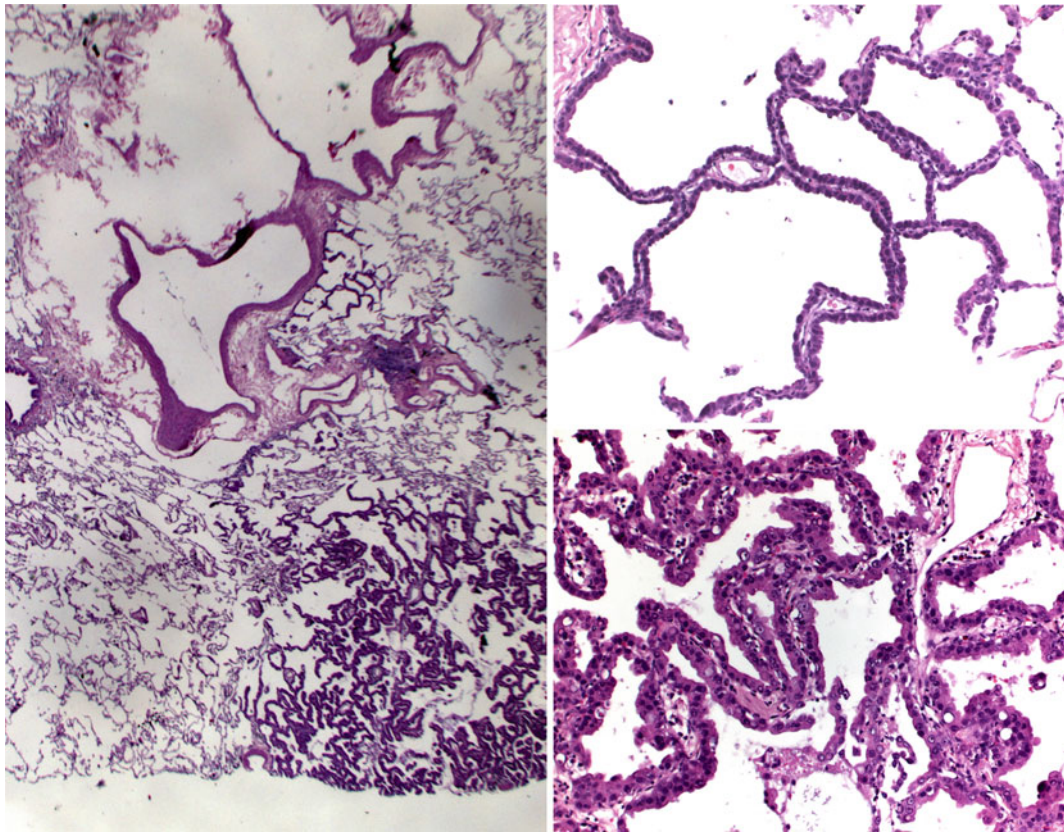

Fig. 17.62 In situ adenocarcinoma (AIS), the tumor has been incidentally detected and removed. On the *left side*, the tumor is shown, consisting of lepidic growth pattern without invasion. In the *right side*, two different differentiation grades are seen: above a single cell row with hardly any mitosis, a grade 1, and below cells with larger nuclei, some epithelial papillae, and a few mitotic counts, graded as 2. Also surfactant nuclear pseudoinclusions are seen. H&E, ×12, 60, and 100

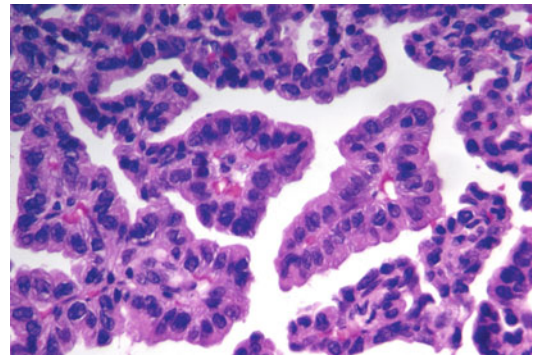

Fig. 17.63 Adenocarcinoma entirely composed of Clara cell-like tumor cells, a rare finding as most adenocarcinomas are composed of a mixture of cells of the bronchioloalveolar junction zone. H&E, ×400

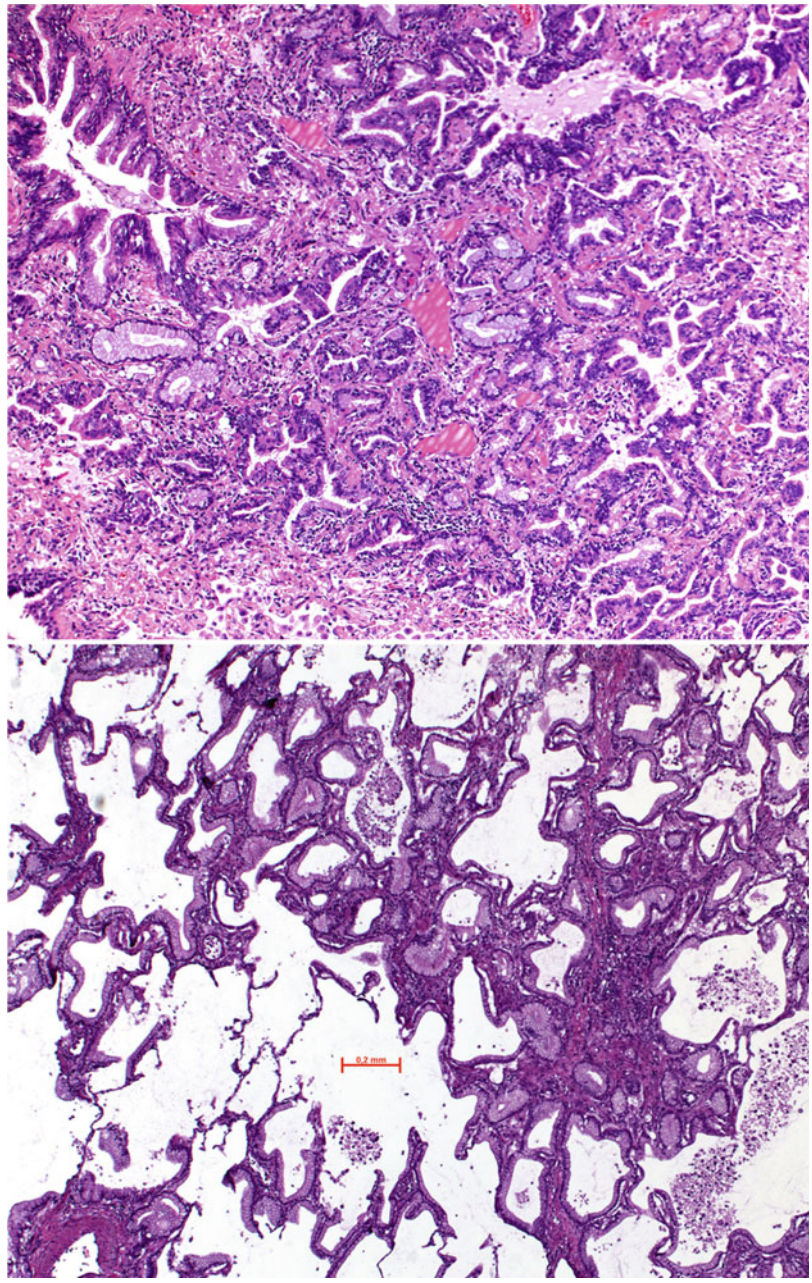

Fig. 17.64 Microinvasive adenocarcinoma (MIA); two examples are shown. At the *top* adenocarcinoma shows a small focus of invasion into the bronchial wall – the only focus in this case. In the *middle* another small adenocarcinoma is shown, differentiated in a mucinous type, again with a small focus of invasion into a bronchial wall, shown in higher magnification at the *bottom*. H&E, bars 200 and 50 µm

Fig. 17.64 (continued)

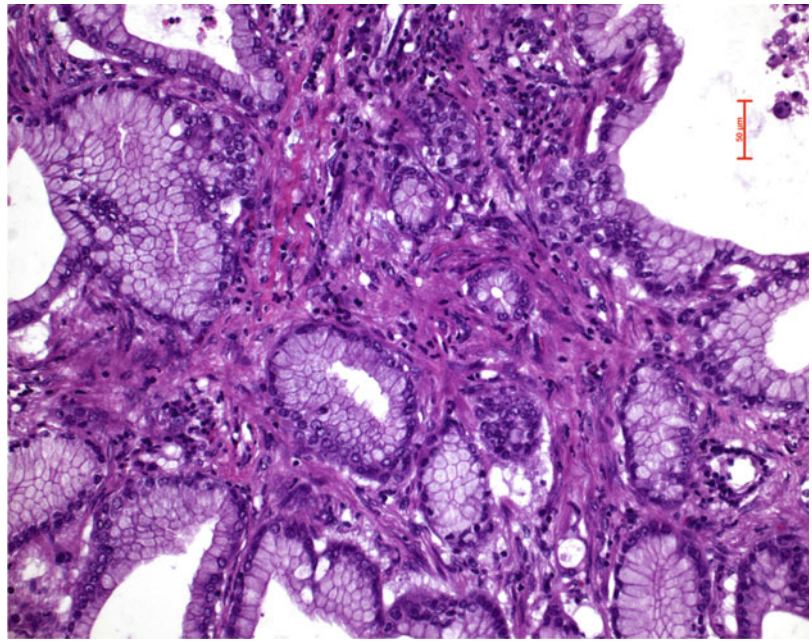

230] (and personal communication). In his proposal invasion should be less than 10% of the whole tumor diameter. However, this proposal was rejected by the majority of the WHO panel members.

Adenocarcinoma Variants

Invasive Mucinous AC (IMAC)

This is a newly created entity, defined by invasion, abundant mucin production, and a columnar or goblet cell morphology [70]. There is an additional sentence, which will create confusion: "This entity should replace mucinous bronchioloalveolar carcinoma." Mucinous bronchioloalveolar carcinoma was defined in the 1999 and 2004 WHO classification as noninvasive adenocarcinoma, so it is the same entity, which we now call either mucinous or non-mucinous AIS. So a carcinoma, which already was defined as AIS now, is placed into invasive mucinous AC. Abundant mucin is another imprecise term: how much is abundant? This will open individualized IMAC diagnoses according to what each pathologist regards as abundant.

In two recent investigations, large series of invasive mucinous AC have been presented. In both outcome was not different from non-mucinous AC, pointing that TNM staging is important, but differentiation into mucinous AC has no impact on prognosis [147, 231]. However, in both studies KRAS mutations are the most frequent driver mutations (over 50% of cases); some other cooperating genes were identified such as deletion of p16, mutations of BRAF and PI3KCA, as well as gene fusions of CD74-NRG1, VAMP2-NRG1, TRIM4-BRAF, and TPM3-NTRK1. ALK1 rearrangements were seen in a similar frequency as in non-mucinous AC; surprisingly mutations of TP53 were rare, although in this type of AC, smoking is common.

So how IMAC can be more precisely classified: mucin production is seen in more than 70% of tumor cells. Tumor cells can present as columnar cells where mucin is stored in small vacuoles and secreted toward the apical cell portion. Secretion can be simple release of the mucin or can be facilitated by holocrine secretion, i.e., a portion of the apical cytoplasm is extruded together with the mucin. In other cases mucin is stored in large vacuoles apical of the nucleus, which results in a goblet cell morphology. Mucin secretion is also apical. Since mucin production is not synchronized in AC, the cells are usually in

different stages of synthesis. This can result that some cells do not show mucin, others show small amounts, and others show signs of release. In case of uncertainty, a stain for any of the MUC proteins (MUC1, MUC2, MUC5AC) will help to solve this problem. Mucins synthesized and secreted by IMACs are all acidic, so they will stain by Alcian blue stain at pH <2.5.

As in non-mucinous AC, also the mucinous AC can present with a lepidic (rare), acinar (frequent), papillary (frequent), micropapillary (less common), and solid pattern (Fig. 17.65). As in non-mucinous AC also in mucinous AC, solid and micropapillary patterns confer a worse prognosis [147, 232].

There are two rare variants of invasive mucinous adenocarcinoma, the multifocal and the pneumonia type (Fig. 17.58b, d). The multifocal mucinous invasive adenocarcinoma is usually composed of more than five nodules separated from each other but usually within the same lobe, more rarely within different lobes but on the same side. Some of the nodules are in situ AC, others are clearly invasive. There is no lymphangiosis carcinomatosa, so these nodules seem to arise from a precursor clone, which spread early on and created several independent tumors, but if genetically analyzed they will show a similar genetic profile. The other variant is the pneumonia type. This was long ago recognized as pneumonia carcinomatosa in the old German literature. Here the tumor cells float within the mucus as small clusters of cells, usually mixed with mucophages. There is no visible nodule, often both lungs can be involved, and airspace spreading is common. Very often this type of carcinoma cannot be surgically removed, despite lymph node metastasis is uncommon. On small biopsies this type cannot be differentiated from colloid carcinoma. The patients are often of young age. If there is any relationship to CPAM has never been explored.

Colloid Adenocarcinoma

Colloid AC has been lumped with mucinous cystadenocarcinoma, although there is some difference: mucinous cystadenocarcinoma is usually a centrally located carcinoma, whereas colloid adenocarcinoma most often is a peripherally located carcinoma. In colloid AC, there is no capsule, the tumor grows diffusely into adjacent lung tissue, whereas in mucinous cystadenocarcinoma, there is a fibrous pseudocapsule (Fig. 17.65a, b). In addition for mucinous cystadenocarcinoma, there is an cystadenoma-carcinoma sequence, with mucinous cystadenoma, borderline mucinous cystadenoma, and mucinous cystadenocarcinoma.

Colloid AC shows huge amount of mucin secretion, which is already visible at gross inspection: the cut surface is glistening with gelatinous material. The tumor cells are focally at alveolar septa, forming strands of cells firmly attached to the wall. Some cells may float within the mucus. It seems they have developed a special metabolism, as these floating cells look well and viable, so their nutrition might involve also secreted material. In some cases one needs to make several sections until tumor cells are encountered. The cells can present with goblet or columnar cell morphology or a mixture of both. Also some cells with Clara cell morphology might be encountered between the columnar cells. Nuclei are usually round, smaller than the average AC cell nucleus, chromatin is finely dispersed, and nucleoli are small.

In *mucinous cystadenocarcinoma* the cells are tall columnar, goblet cells can be seen, but they are usually not numerous. In contrast to colloid, AC lymph node metastasis is most often present. The nuclei are much more pleomorphic, chromatin is coarse granular, and nucleoli are enlarged and sometimes bizarre. Mitosis is more frequent compared to colloid AC. At the invasion a desmoplastic stroma reaction is seen.

Enteric Adenocarcinoma

Enteric adenocarcinoma is a rare form of AC resembling a colonic AC. The structure is acinar, sometimes cribriform, otherwise the cytomorphologic features are similar to the other non-mucinous AC (Fig. 17.66). The most important and helpful finding is the brush-border formation seen at the top of the cells. This carcinoma does not produce mucin. Enteric adenocarcinomas are usually positive for cytokeratin 20 but usually express TTF1.

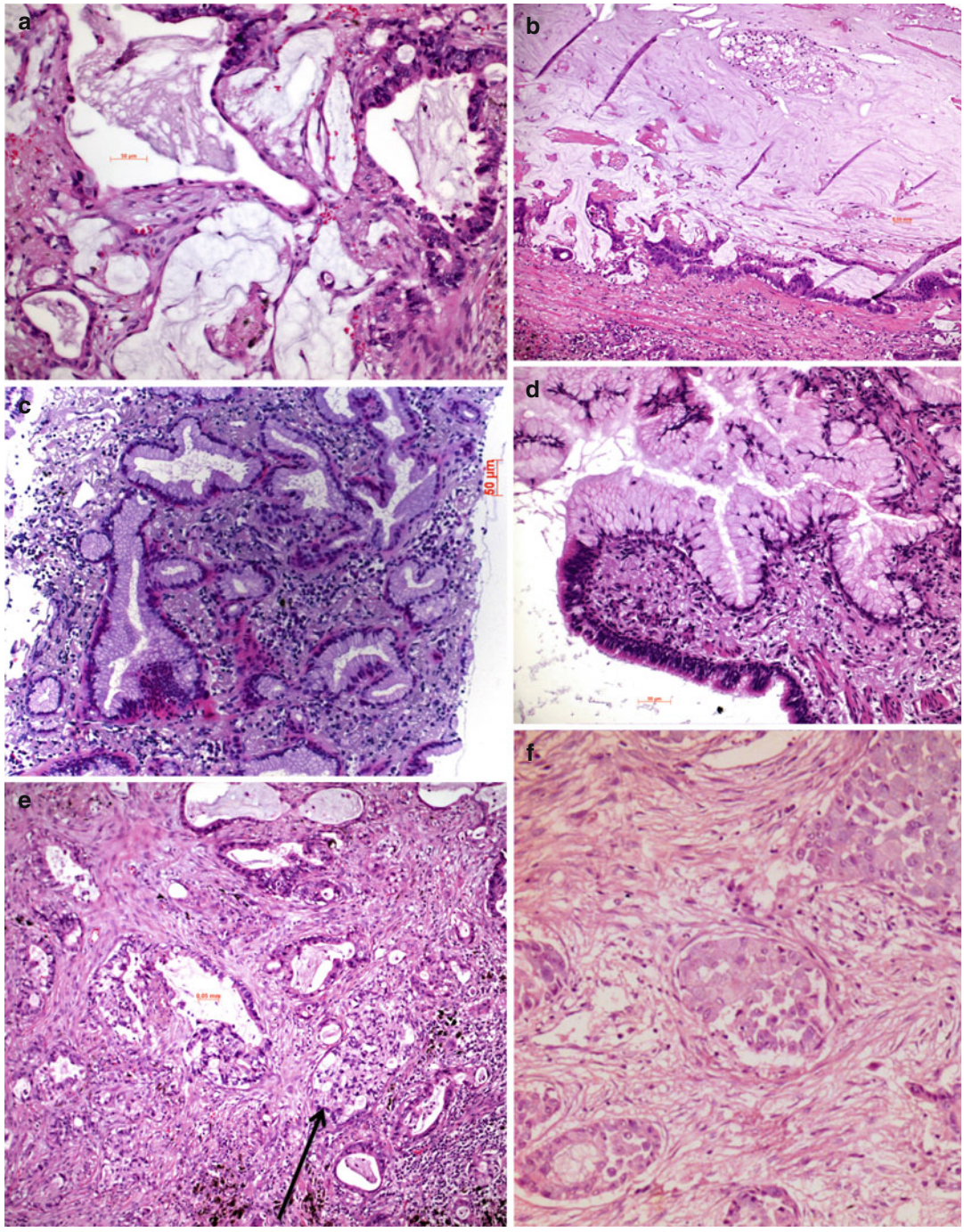

Fig. 17.65 Invasive mucinous adenocarcinomas. (**a**) Colloid mucinous adenocarcinoma, (**b**) mucinous cystadenocarcinoma with a pseudocapsule, (**c**, **d**) are mucinous adenocarcinomas with acinar and papillary pattern, and goblet cell differentiation; (**e**) mucinous adenocarcinoma with signet ring cell component (*arrow*), (**f**) is a mucinous adenocarcinoma with predominant signet ring cell pattern. (**a**–**f**), H&E, bars 50 µm, (**f**) ×150

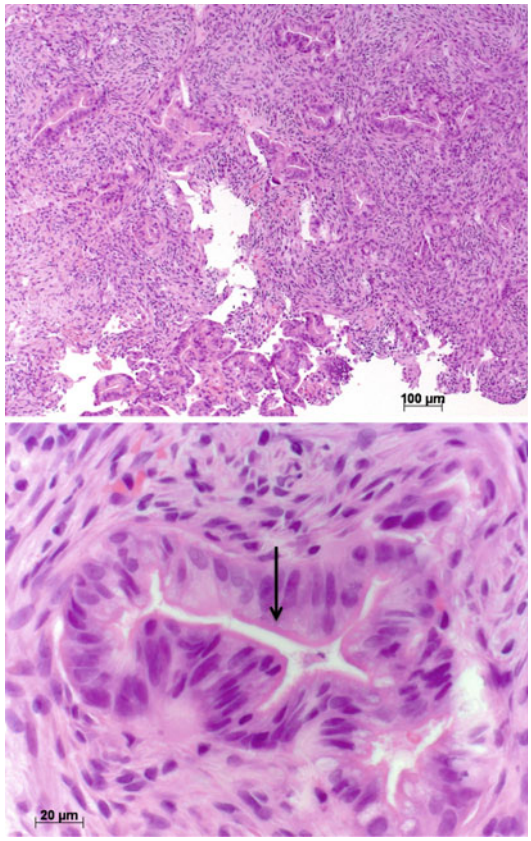

Fig. 17.66 Enteric adenocarcinoma, a rare entity; in the *upper* panel, an overview is shown, the carcinoma is acinar, and an extensive desmoplastic stroma reaction is present. In the *lower* panel, the characteristic features are shown: enteric brush border with microvilli as in colonic adenocarcinomas. This case was positive for CK20; some cells expressed CDX2, other TTF1. H&E, bars 100 and 20 µm

Fetal Adenocarcinoma

Fetal type of adenocarcinoma was described in 1995. It resembles a fetal developmental stage of around the 12th week of gestation. At that time the bronchial buds are branching, the cells are full of glycogen, and the nuclei are at an apical position within the cytoplasm. In this type of carcinoma, again the cells might look like clear cells, because glycogen is removed by tissue processing. The nuclei are also at the apical top of the cell. In contrast to pulmonary blastoma, which we discuss later, morules are either not present or exceptionally rare (Fig. 17.67). When considering the apical nuclear position, one has to consider what also happens during fetal maturation: initially all nuclei are apical, but with every week passing, more and more nuclei shift down to the middle of the cells and finally to the basal position. This can be seen also in fetal AC: so this carcinoma reflects the maturation of the bronchial bud in every respect. Nuclei at mid position and even same basal-oriented nuclei do not abolish the other diagnostic criteria. Most fetal ACs are well differentiated with round nuclei, chromatin is often finely distributed within the nucleus, and nucleoli are small. Mitosis is rare, less than 3/HPF. However, there is a rare high-grade form; the architecture is the same, but the cytomorphological features are different: nuclei are enlarged and pleomorphic, nucleoli are enlarged, and mitosis can be up to 8/HPF (Fig. 17.67c, d).

Signet Ring Cell Adenocarcinoma (SRC-AC)

Signet ring cells are most often scattered within mucinous AC; however, they rarely can occur as a carcinoma entirely composed of these cells, which has to be called SRC-AC. In a series of mucinous AC, few cases have been identified (Fig. 17.65e, f). The pulmonary SRC-ACs in contrast to the SRC-ACs of the gastrointestinal tract behave not like high-grade carcinomas but instead behave as other mucinous AC. So biologically they are different from their GI tract cousins [147].

Immunohistochemistry of AC

Non-mucinous ACs are predominantly arising from the bronchioloalveolar junction zone, where precursor cells for Clara cells and pneumocyte II are located in niches (niches where several alveoli and their alveolar duct join). These cells express TTF1, are positive for napsin A, and most often also for one or several of the surfactant apoproteins (Fig. 17.68). With respect to cytokeratins, these carcinomas express CK7 and CK18/CK19. They are usually negative for basal cell markers such as p63. In adenocarcinomas arising in small bronchioles and bronchi, there is a tendency to lose TTF1 staining and also to express focally p63. If the AC arises further proximal, TTF1 is negative, CK7 might be only focal positive, and AC can express CK20. This is especially true in AC of bronchial gland type (Fig. 17.59h). They are usually also positive for CEA and secretory component but negative for CDX2 (Fig. 17.69).

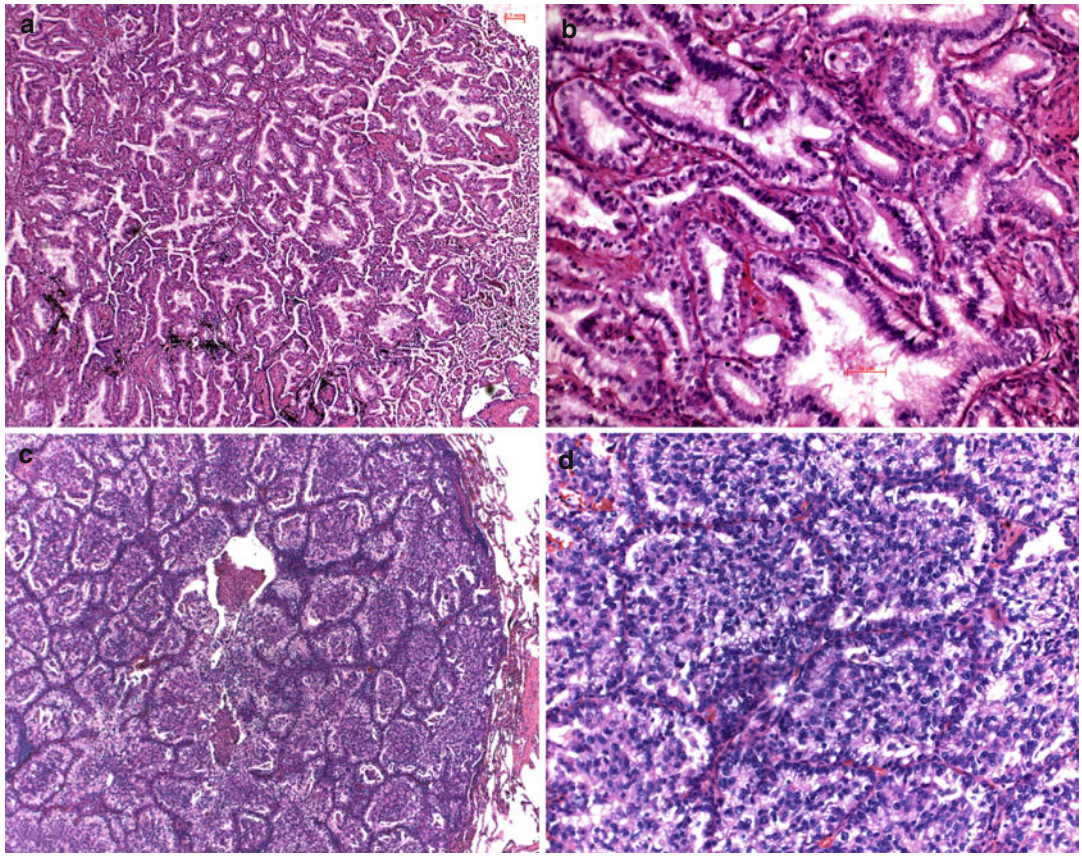

Fig. 17.67 Fetal adenocarcinoma, two cases are shown. (**a**, **b**) Represent a well-differentiated form, which is the most common one. The tumor presents with an acinar pattern, the tumor cell cytoplasm is clear, and the nuclei are in part apical but also in mid portion and in other cells already at the final bottom side of the cell. The clear cytoplasm is a result of dissolving glycogen by tissue processing. The lower case (**c**, **d**) is a high-grade fetal adenocarcinoma with cell crowding, more atypia, and frequent mitosis. H&E. bars 100 and 50 μm

Mucinous AC are most often positive for TTF1 and CK7, but a minority will show positivity for CK20 and few also for CDX2, a marker for enteric differentiation. Even two cell populations might be encountered, one staining for TTF1 and the other for CDX2 [147]. CDX2 as well as CK20 is positive in enteric AC, although in different case series, also positivity for TTF1 and CK7 was reported [233–235]. MUC1, MUC2, and 5 AC proteins are positive in all types of mucinous AC. Colloid AC is usually positive for CK7, sometimes CK20; however they are all positive for TTF1. In addition all colloid AC harbor KRAS mutation. Fetal AC is positive for TTF1, surfactant apoprotein antibodies, especially SApoB, and CK7. Signet ring cells are again positive for CK7and TTF1.

Another remarkable variant does exist, which is psammomatous adenocarcinoma. Usually this is an acinar or papillary structured AC with many psammoma bodies, at least 3–5/HPF. This type of AC is not different from acinar or papillary AC with respect of biological behavior, but since this type of AC is most frequent in AC from the ovary and thyroid, it needs to be mentioned. In these cases an immunohistochemical investigation is necessary, and TTF1 is not helpful in differentiating this from thyroid AC (Fig. 17.70). Here immunohistochemistry for surfactant apoproteins is the only way of sorting metastasis out. Clear cell changes occur in almost every non-small-cell carcinoma type, so this should be described but is of no diagnostic or prognostic value (Fig. 17.71).

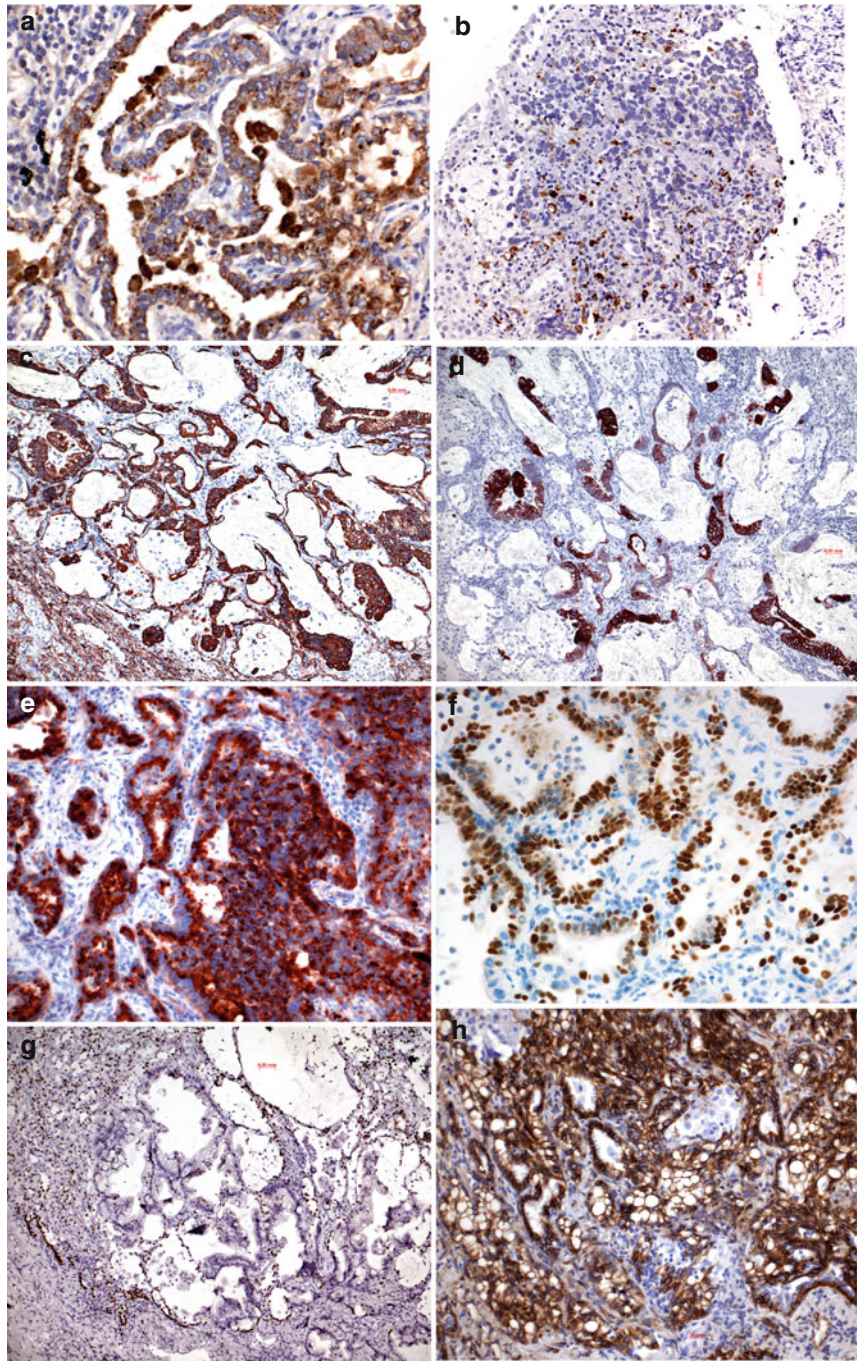

Fig. 17.68 Immunohistochemical markers in adenocarcinoma. (**a**, **b**) Staining for Napsin A, the papillary adenocarcinoma is positive with granular reaction in the cytoplasm, whereas in the solid adenocarcinoma only few cells are positive. Staining for cytokeratins are helpful in establishing the diagnosis of an adenocarcinoma, but there might be some exceptions: in (**c**) most of the cells from mucinous adenocarcinoma stain for CK7, however, a minority also for CK20 (**d**). An aid in the diagnosis of primary pulmonary adenocarcinoma is antibodies for surfactant apoprotein B (**e**) and TTF1 (**f**). However, TTF1 might be negative in some colloid adenocarcinomas (**g**). Not a diagnostic marker but an aid in separating primary lung versus gastric metastasis is b-catenin (**h**). Bars

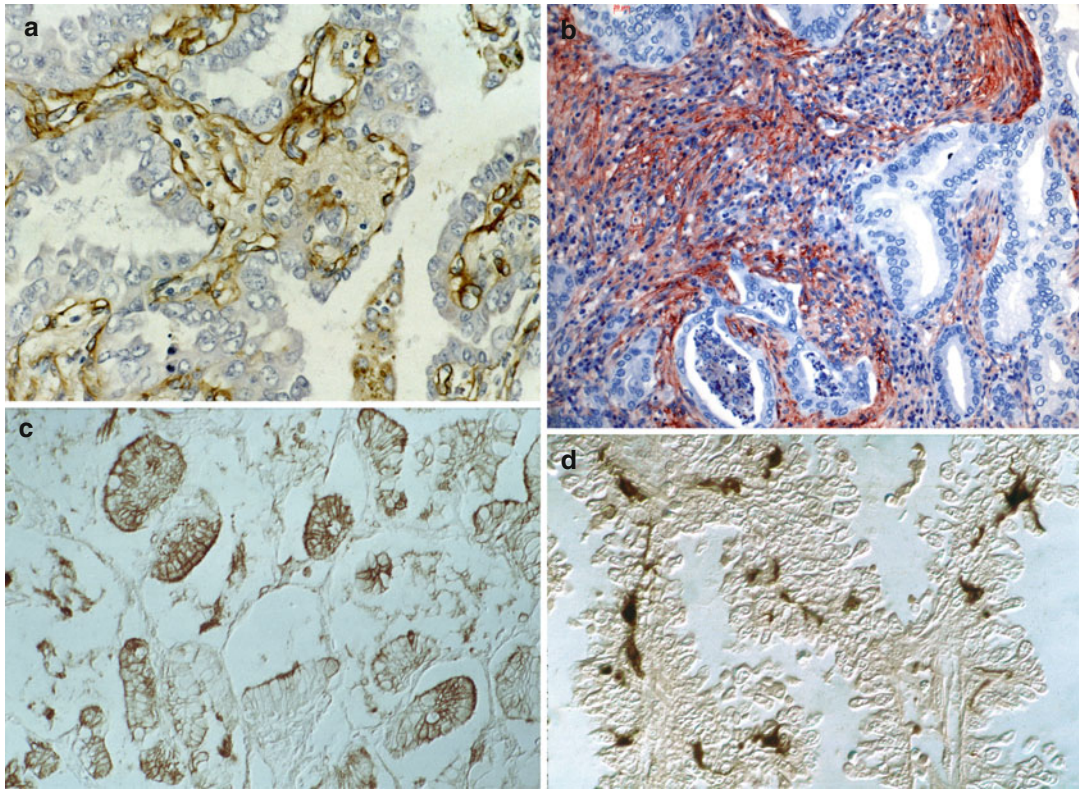

Fig. 17.69 Immunohistochemistry for laminin (**a**) and fibronectin (**b**) can be used in those cases where invasion cannot be decided on H&E morphology. Staining for CEA and secretory component (**c**) can be used for adenocarcinomas arising in central bronchi. Staining for S100 protein will highlight dendritic cells, which are preferentially seen in papillary adenocarcinomas (**d**). ×200 and 100

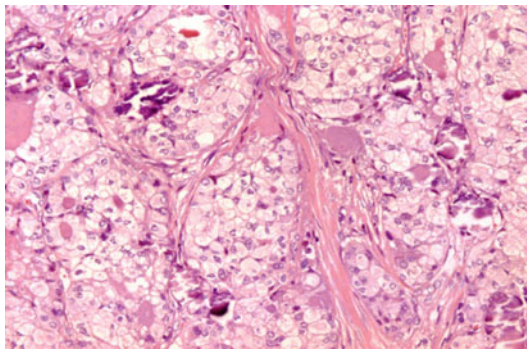

Fig. 17.70 Psammomatous variant of adenocarcinoma. The tumor presents with clear cell pattern; some cells contain eosinophilic material, which is also found outside the cells. In addition numerous psammomatous bodies are encountered. The differentiation from thyroid carcinomas will need additional immunohistochemical investigation. H&E, ×200

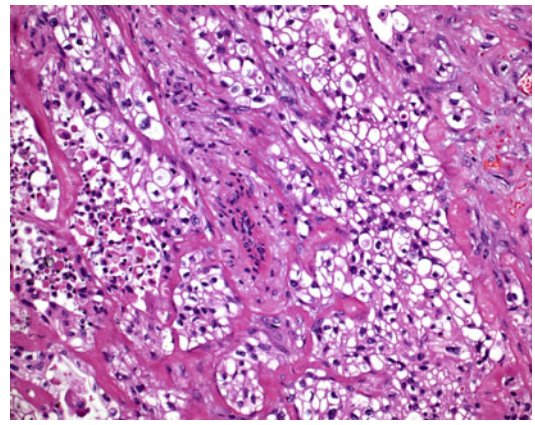

Fig. 17.71 Clear cell pattern in adenocarcinoma; this is nonspecific; the adenocarcinomas will behave as any other type. H&E, bar 20 μm

Prognostic Factors

TNM staging is the most important factor for behavior of AC. The higher the stage, the worse the prognosis. Within AC there are some cases, which are so far not investigated: AC with low T but high N, and AC with high T and low N. Some of these cases can be explained, for example, by a micropapillary component, but not all of them. Architecture has been included now into grading; however, I still prefer cytomorphology over architecture. I also do not accept AIS or MIA as low grade, because this reflects staging.

Grading in Adenocarcinomas

G1 = mitotic counts 0–2/HPF, minor nuclear polymorphism, well-formed acinar or papillar structures, and important a single row of carcinoma cells

G2 = mitotic counts 3–7/HPF, nuclear polymorphism clearly visible, nucleoli enlarged, acinar, papillary pattern, but cells form double layers and also few cell papillae

G3 = mitotic counts >8/HPF, nuclear polymorphism clearly visible, prominent irregular formed nucleoli, solid, micropapillary, and also cribriform patterns

There are exceptions within the variants: fetal adenocarcinoma with regular nuclei, few mitoses, and no polymorphism is a slowly progressing AC G1, whereas there exists also a high-grade form, G3.

Another prognostic factor is invasion of the adenocarcinoma cells into lymphatics within a central scar predicts worse behavior. In most cases lymphatics can be easily identified by their thin wall and their endothelial cells; in a few cases, staining using antibodies against podoplanin might be necessary. In addition invasion into blood vessels and into the pleura is a sign of worse prognosis, whereas lymphatic invasion outside scar does not change prognosis (Fig. 17.72) [236, 237].

Cytology and Small Biopsies in AC Diagnosis

Almost 80 % of ACs are in stage IV when diagnosed. This means that most often, the diagnosis is established on small biopsies (bronchial, transbronchial, transthoracic/transcutaneous) or cytological material (EBUS-/EUS-guided fine needle aspiration, transthoracic needle aspiration, bronchial brush cytology, bronchial washings, and BAL). Due to the possibility of specific treatable driver gene mutations in the tumors, a significant portion of this already tiny material has to be pre-

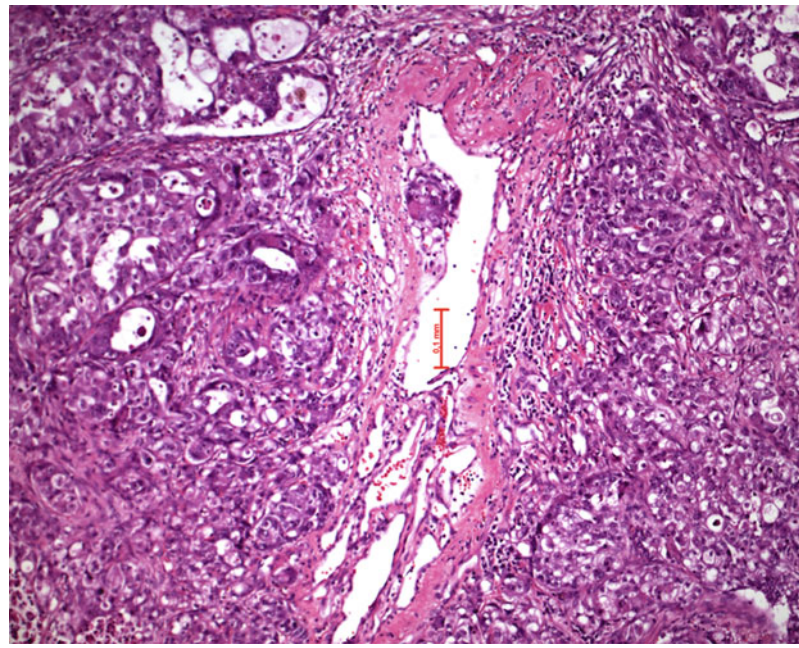

Fig. 17.72 Invasion of adenocarcinomas into blood vessels (*upper* panel), lymphatic vessels (*middle*), and into the pleura (*lower* panel). H&E, bars 100 and 50 µm

Fig. 17.72 (continued)

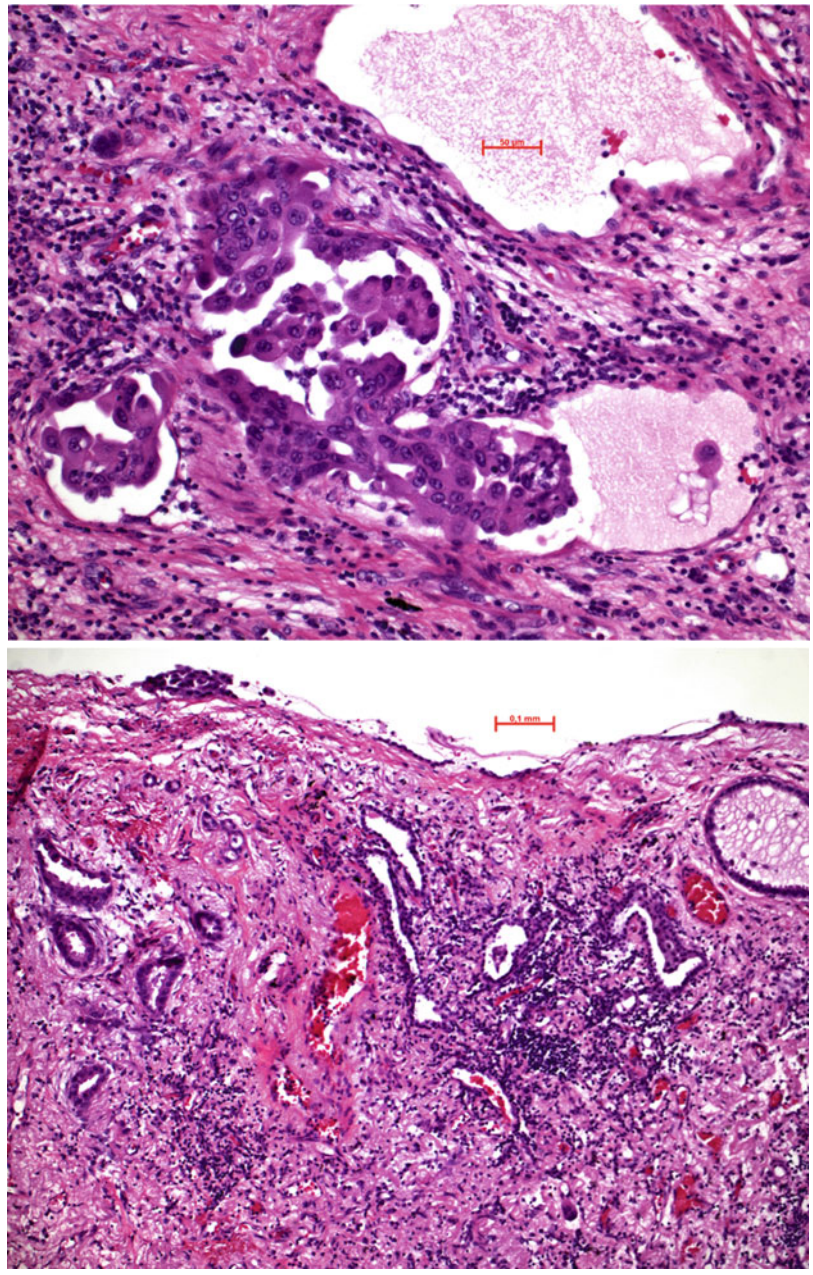

served for molecular analysis. Therefore less is available for immunohistochemistry. This has led to a restrictive use of differentiation markers.

There are classical features which enable the diagnosis of adenocarcinomas in cytological specimen and small biopsies: polar orientation of nuclei, vesicular chromatin, large nuclei in high-grade adenocarcinoma, intranuclear inclusions (surfactant proteins), papillary complexes often in 3D spheres, mucin secretion, and goblet cell differentiation in mucinous adenocarcinomas (Fig. 17.73), and in addition in biopsies, acinar, papillary, micropapillary structures, solid with intracellular mucin, and solid with cytomorphological features suggestive of AC. In any case of uncertainty, immunohistochemistry is applied. However, only the two-marker approach is recommended: TTF1 for AC and p40/p63 for

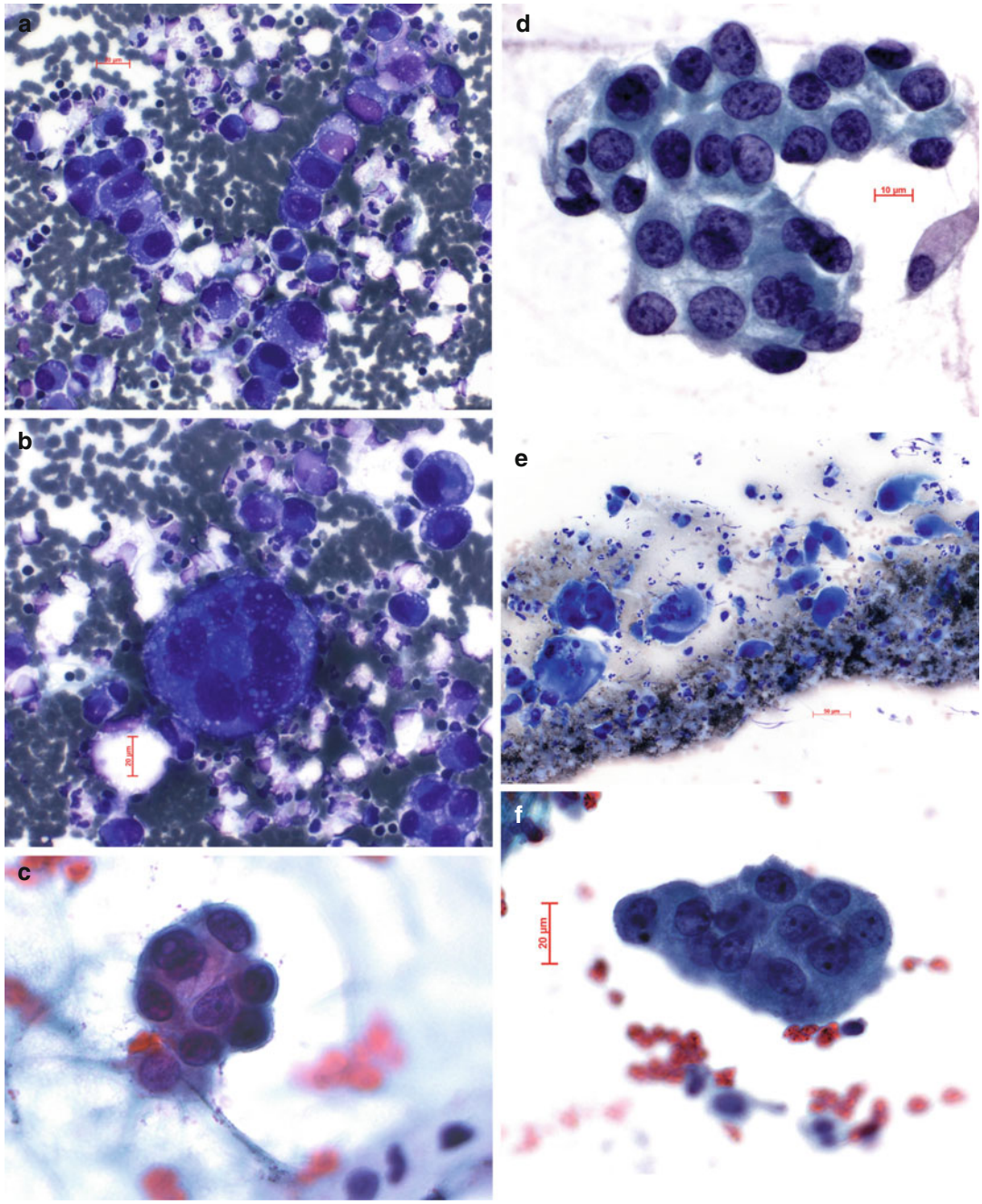

Fig. 17.73 Cytology of adenocarcinomas; the tumor cells show basal orientation of nuclei (**a**), clustering of cells into papillae (**c**, **d**, **f**), cytoplasmic vacuoles (**a**, **b**), ill-defined cell borders (**d**). Some tiny microvilli can be seen (**c**), multinuclear cells (**b**), and coarse chromatin pattern (**d**) best seen on H&E or PAP stains. Some tumor cells can mimic tadlepool cells characteristic for squamous cell carcinomas, but the basal located nucleus will help (**e**). Giemsa, H&E, PAP stains, bars 10, 20, 50 µm

SCC. With classical cytomorphology and these two markers, almost 95 % of AC (and also SCC) can be correctly diagnosed (Fig. 17.74). There remains a small portion of so-called *n*ot *o*therwise *s*pecified carcinomas.

This tendency of submitting less tissues and requesting more tests has led to the invention of the cellblock technique for cytology. Aspirated cells are transferred into liquids and submitted to pathology. Cells are centrifuged directly into warm liquid agarose forming a cell pellet at the bottom, or aspirates are transferred into a clotting substance. The so formed cell pellet is fixed in formalin and can be embedded in paraffin as a tissue biopsy. With this technology serial sections can be performed and immunohistochemistry is possible for different markers, if necessary.

Classification and Classification Problems

A new 2015 WHO adenocarcinoma classification has been published and should replace the 2004 WHO classification. This new classification also includes statements on the diagnosis of carcinomas in biopsies, which is becoming a major issue due to new treatment options (targeted therapy, see above).

What Are the Major Changes? (Table 17.1)

We have tried to solve these problems based on our own experience and literature data with invasive mucinous AC type. This results in a modification of the classification of invasive mucinous AC (Table 17.2):

More problems in the present classification: AAH as the precursor lesion is not well separated from AIS. AAH is defined as an atypical proliferation of alveolar cells along the alveolar septa, without invasion. The lower degree of atypia and a size less than 5 mm are regarded as the main difference from AIS. However, grading of nuclear and cellular atypia is very subjective and thus not really helpful – no practicing pathologist would do morphometry. The most important feature of gaps between the neoplastic cells in AAH and the close of AIS cells should be more clearly stated. This feature points to the biology of tumor

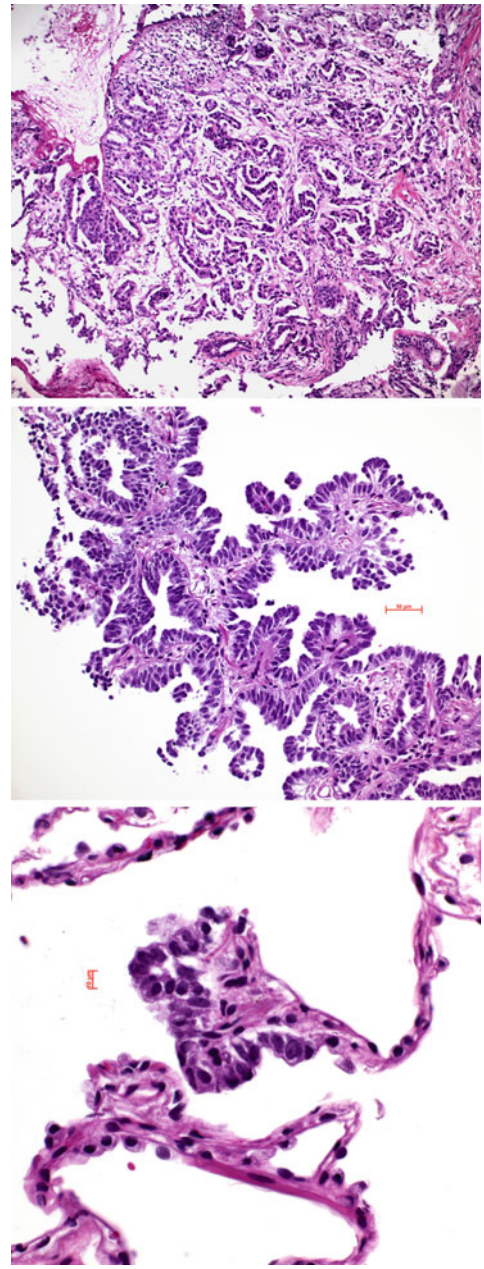

Fig. 17.74 Small biopsies in adenocarcinomas: top a bronchial biopsy showing nicely arranged acini; a papillary pattern is seen in the transthoracic needle biopsy (*middle*). No invasion was encountered, however in a biopsy one can only state that invasion is not present. A tiny little transbronchial biopsy shows a cluster of cells from an adenocarcinoma. Not much information can be retrieved from such a biopsy, and even molecular analysis is not possible. H&E, bars 10, 50, 100 µm

Table 17.1 Comparison of changes in the WHO classification of adenocarcinomas

WHO classification 2004	WHO classification 2015
BAC with variants as mucinous, non-mucinous, and mixed mucinous-non-mucinous BAC	Replaced by in situ adenocarcinoma (this makes sense, because BAC was already classified as an noninvasive, i.e., in situ adenocarcinoma with variants as mucinous, non-mucinous, mixed mucinous-non-mucinous AIS)
Minimal invasive adenocarcinoma was proposed by Y. Shimosato in 1999; the invasive focus should be less than 10 % of the tumor diameter, i.e., in a carcinoma of 15 mm diameter, invasion should not exceed 1.5 mm (but this was rejected by the majority of pathologists from the USA)	Minimal invasive adenocarcinoma (invasive portion less 5 mm[a]) Mucinous, non-mucinous, mixed mucinous-non-mucinous MIA
Mixed adenocarcinoma	Predominant acinar Predominant papillary Predominant micropapillary Predominant solid[b] Adenocarcinoma[c] Invasive mucinous adenocarcinoma[d]
Mucinous (colloid) adenocarcinoma	Mucinous (colloid) adenocarcinoma
Mucinous cystadenocarcinoma	Now merged with colloid adenocarcinoma
Fetal adenocarcinoma	Fetal adenocarcinoma
Signet ring adenocarcinoma	This entity was skipped, but signet ring cells should be mentioned in the description[e]
Clear cell adenocarcinoma	This entity was skipped; clear cells might be mentioned in the description Enteric adenocarcinoma; this is a newly accepted variant, which is characterized by a morphology mimicking colonic adenocarcinoma and by the expression of markers of colonic adenocarcinomas

[a]This can give rise to problems: invasion can only be measured on H&E-stained glass slides, i.e., after shrinkage due to formalin fixation; therefore, the 5 mm cutoff point on the section might be 8–9 mm in reality

[b]Very useful, because in the era of targeted therapy, we might be able to assign specific mutations to one of these adenocarcinoma types, for example, the frequency of EGFR mutation is 27 % in acinar and papillary AC

[c]Another problem is that there are two types of solid AC: one is defined by mucin production (more than ten mucin-producing cells in 2 high-power fields), but listed under non-mucinous AC; the other is defined by solid pattern and expression of TTF1, which means no mucin production is necessary. These are issues to be solved in future classifications. Probably those with mucin-producing cells should be shifted to invasive mucinous AC, whereas the non-mucin-producing solid AC with TTF1 expression should remain in the non-mucinous group

[d]The problem with invasive mucinous AC: there are mucinous acinar ACs and non-mucinous acinar ACs; for the non-mucinous types we have now an architectural component, whereas all mucinous are lumped together. Another problem exists in invasive mucinous adenocarcinoma definition: invasive mucinous adenocarcinoma is said to replace mucinous BAC; however, since the 1999 WHO classification, BAC was defined as noninvasive adenocarcinoma and now correctly has been replaced by mucinous AIS; so what is invasive mucinous adenocarcinoma replacing mucinous BAC? Another point is mucinous adenocarcinomas have abundant mucin, whereas non-mucinous adenocarcinomas can show some mucin – this is very vague and will create diagnostic problems

[e]Signet ring adenocarcinoma although skipped from the classification does exist (has not read the books!); there are even cases which are composed entirely of signet ring cells; so probably this AC type should be included in the next update on AC classification

Table 17.2 Classification of mucinous adenocarcinomas in comparison to non-mucinous types – the way I classify these tumors

Invasive non-mucinous AC	Invasive mucinous AC
Predominant acinar	Predominant mucinous acinar
Predominant papillary	Predominant mucinous papillary
Predominant micropapillary	Predominant mucinous micropapillary
Predominant solid (mucin producing and/or TTF1+)	Predominant mucinous solid
Predominant cribriform	Predominant mucinous cribriform
	With predominant or focal signet ring cell component

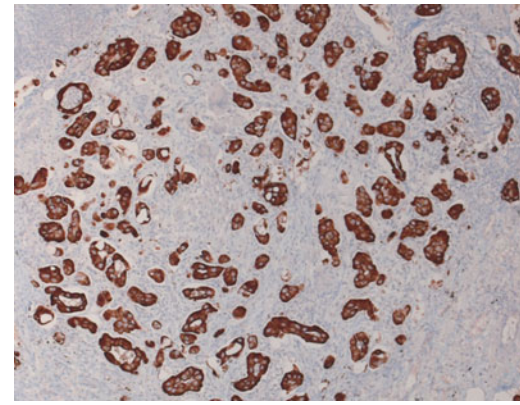

Fig. 17.75 Immunohistochemistry for ALK1, all tumor cells are strongly stained (3+). These will be positive by FISH in almost every case, and even in FISH-negative cases, treatment by ALK inhibitor will improve the patient's condition. ×100

growth: a slow-growing lesion as AAH will leave a space between the tumor cells, whereas in the rapid-growing carcinoma, the cells use all spaces for their developing daughter cells. This has been proposed by the group of Shimosato [230]. In this classification AAH is characterized by a single row of atypical pneumocyte-like cells, proliferating along the alveolar surface, with intercellular gaps. As a caveat atypical cells must completely replace the alveolar epithelium; otherwise this is regeneration or reactive hyperplasia! The former high-grade AAH was transferred to AIS. AIS was characterized as an atypical proliferation along the alveolar surface, without invasion, and without alveolar collapse. The involved part of the lung is rigid and entirely covered by this proliferation. Epithelial papillae might be present. There are no longer gaps between the atypical cells.

Genes and Targets for Treatment in Adenocarcinoma

Although this will be more in deep discussed in the molecular pathology chapter, here a list of targetable driver genes are listed:

EGFR mutations in exon 18, 19, 20, 21, and few rare ones in exons 22–24. The best responders are with deletions within exon 19, followed by point mutations in exon 21. These also account for approximately 90 % of all mutations. The frequency of mutations is highest in Southeastern Asian patients (up to 65 %), less in Caucasians (12 %), and low in African Americans (6–8 %).

AKL1 gene rearrangement: The most common fusion partner is EML4, which also resides on chromosome 2 (inversion). This is seen in approximately 4–8 % of patients. Immunohistochemistry can serve to sort out negative cases; those with 3+ intensity staining by immunohistochemistry will almost always be positive by FISH analysis (Fig. 17.75).

ROS1 translocation is another gene fusion type of genetic aberrations found in AC. It accounts for approximately 2–4 % of patients. Also in these cases, immunohistochemistry should be used to sort out the negative cases.

KIF5B is one of the fusion partners for either ALK1 or RET. The KIF5B-RET fusion gene is caused by a pericentric inversion of 10p11.22-q11.21. This fusion gene overexpresses chimeric RET receptor tyrosine kinase, which can spontaneously induce cellular transformation. Besides KIF5B, CCDC6 and NCOA4 can form fusion genes with RET. Patients with lung adenocarcinomas with RET fusion gene had more poorly differentiated tumors, are younger, and more often never-smokers.

MET is another receptor tyrosine kinase bound to cell membranes in NSCLC. The ligand for MET is HGF, originally found in hepatic

carcinomas. This receptor came into consideration in lung carcinomas, because amplification of MET or alternatively upregulation of HGF was identified as a mechanism of the resistance in EGFR-mutated adenocarcinomas. MET amplification was rare in NSCLC but upregulation of MET is approximately 20 % in NSCLC including adenocarcinomas and squamous cell carcinomas (Fig. 17.76).

KRAS mutations are found in 25 % of all adenocarcinomas but in >50 % of mucinous AC. At this time there are only phase I and II trials targeting the downstream proteins ERK and mTOR.

Some rare genetic aberrations are in amplifications and mutations in ERBB2 (HER2Neu) and BRAF, which can be targeted by drugs available for other malignancies.

A marker for response to chemotherapy of platinum compounds has been reported. ERCC1 is a member of the DNA repair enzyme machinery. In those cases, where ERCC1 is highly expressed, this type of chemotherapy is ineffective (Fig. 17.77) [145].

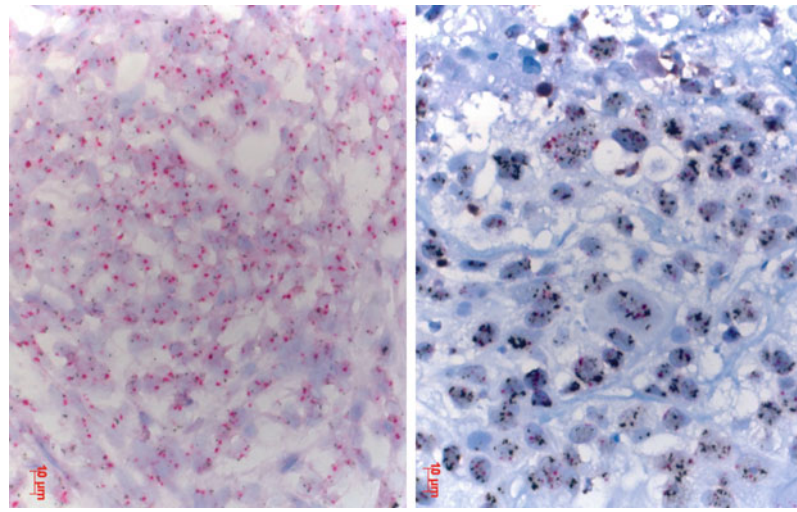

Fig. 17.76 FISH for cMET, *left* a negative case with two signals for MET and centromere probes; *right* a positive case with clusters of MET amplicons. CISH, bars 10 µm

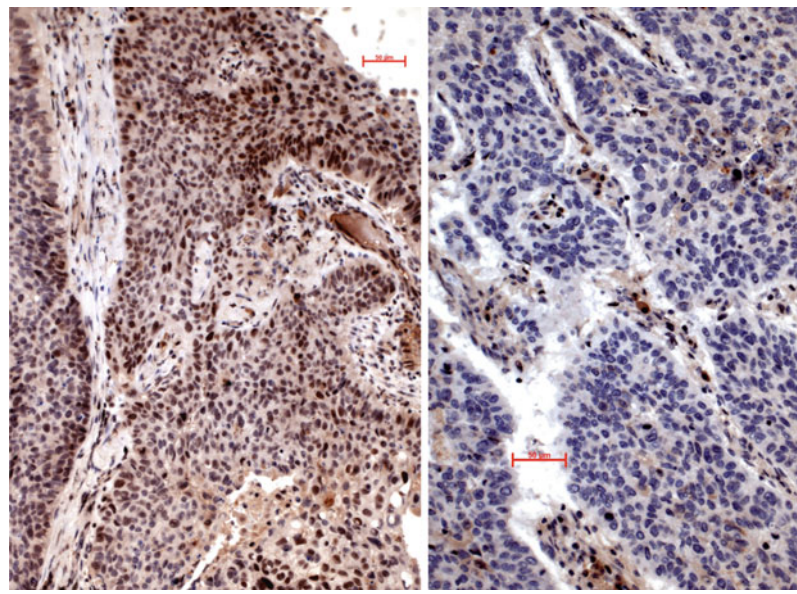

Fig. 17.77 Immunohistochemistry for ERCC1, *left* a case with strong nuclear expression (SCC); *right* a case with almost negative staining (adenocarcinoma). Bars 50 µm

17.3.3.3 Large-Cell Carcinoma (LC)

Gross Morphology and Clinical Picture

LC is usually a large tumor, which will present with unspecific clinical findings such as weight loss, cough, and sometimes hemoptysis. Since LC is most often peripheral in location, symptoms due to bronchial obstruction are rare (Fig. 17.78). On X-ray and CT scan, the tumor presents as a mass lesion, which on PET-CT will also show tracer uptake.

Histology

LC is defined by large cells devoid of any cytoplasmic differentiation and large vesicular nuclei (>26 mμ). Nucleoli are sometimes as prominent as in AC. They have a well-ordered solid structure but no palisading, no rosettes, or any other characteristics (Fig. 17.79). By electron microscopy differentiation structures can be seen such as hemidesmosomes, tight junctions, intracytoplasmic vacuoles with microvilli, and ill-formed cilia. This fits clearly into the concept of a carcinoma, at the doorstep of adenocarcinoma and squamous cell carcinoma differentiation. Mitotic counts can be numerous or scarce; despite this carcinoma is a grade 3. LC numbers have dramatically decreased due to the use of immunohistochemistry, because many of them are either solid undifferentiated AC or SCC. Those cases expressing TTF1 and CK7 are now regarded as undifferentiated AC; those with positivity for p63/p40 and CK5/CK6 are now undifferentiated SCC. Therefore only few cases remain in LC. In addition as this is a diagnosis of exclusion, this diagnosis can only be made after careful analysis of a resected tumor specimen (Fig. 17.80). In biopsies this carcinoma will fall under NSCLC NOS.

Fig. 17.78 Macroscopic picture of a large-cell carcinoma with typical peripheral location

By cytology the cells looks like any undifferentiated carcinoma. Nuclei are large centrally positioned, diameter >26 μm, chromatin is coarse, nucleoli are middle sized, cytoplasm basophilic without any differentiation, and cells form small and large clusters.

17.3.3.4 Neuroendocrine Carcinomas

Within this group, typical, atypical carcinoid, and small and large-cell neuroendocrine carcinoma is placed. Each of these tumors show infiltrative growth as any other carcinoma; each can set metastasis and might kill the patient, if not treated properly. However, there are also differences. Typical carcinoid is a slow-growing tumor, which rarely set metastasis. Atypical carcinoid is of intermediate malignancy, with a higher frequency of metastasis. Both carcinoids behave biologically different from the two high-grade carcinomas: metastasis after surgical removal does not occur before 7 years, and the risk of dying from recurrence and metastasis peaks around 12 years after surgery [238]. This was also a reason for Masson-Hamperl (Virchows Arch [Pathol Anat] 266:509–548, 1927) to name these tumors carcinoids, i.e., carcinoma-like but not identical. In addition by the name carcinoid, it was also implicated that this is an epithelial tumor. In the last decade, several attempts were made by non-pulmonary pathologists to change the classification according to their classification in the gastrointestinal tract, using neuroendocrine tumor, well-differentiated neuroendocrine carcinoma, and high-grade carcinomas [239]. However, in contrast to GI tract tumors, the lung tumors are different in several aspects: there is no common genetic alterations among them, they do not evolve from each other, and the low grade arise from neuroendocrine cells and share precursor

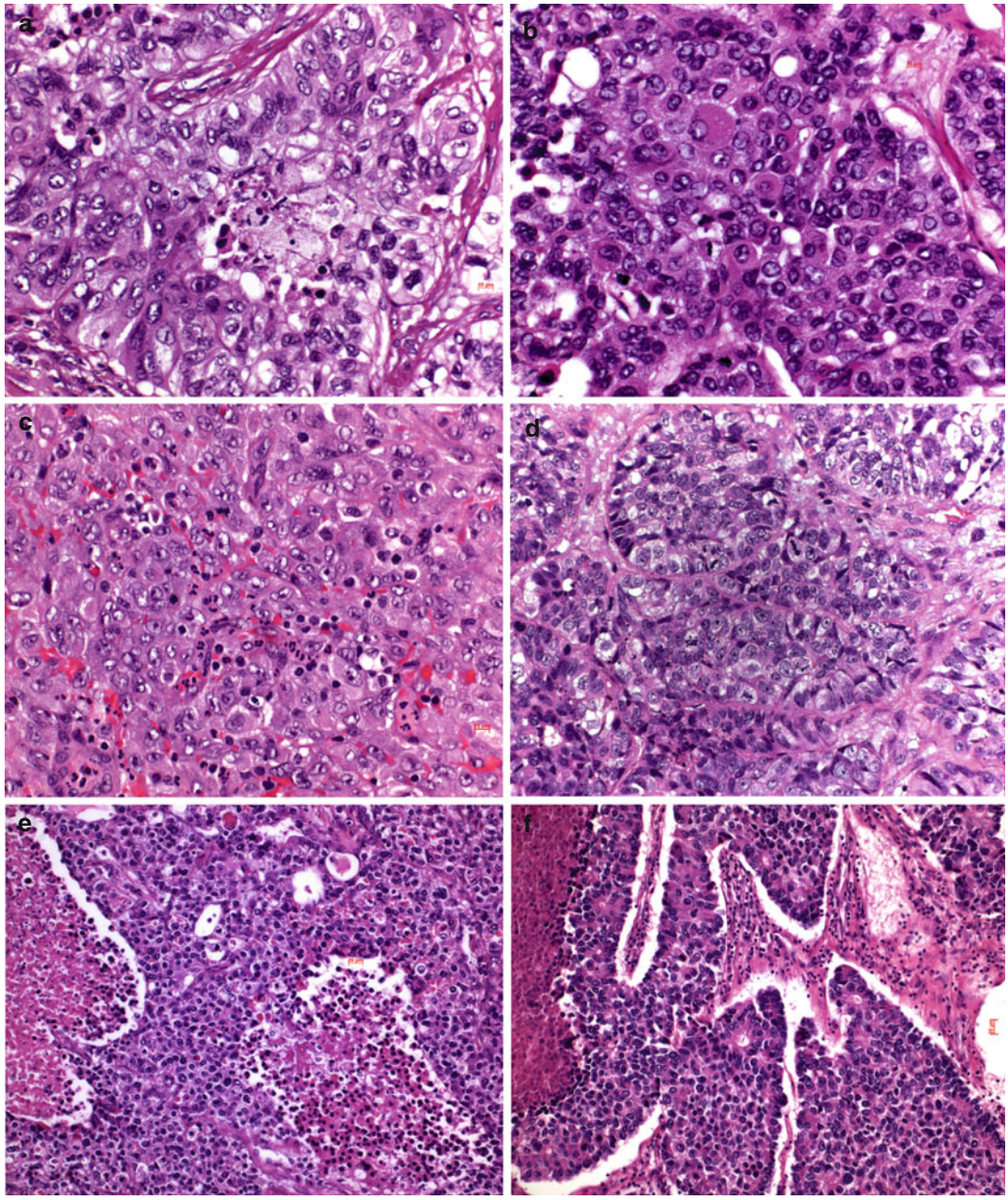

Fig. 17.79 (**a**–**f**) Examples of large-cell carcinomas. In most of them, nuclei show coarse chromatin, enlarged middle-sized nucleoli, and accentuated nuclear membrane. The cytoplasm can be vacuolated or clear, nuclear size is >26 μm, and cell borders are most often vague. (**e**, **f**) Represent a case, which at a first glance resemble large-cell neuroendocrine carcinoma with rosette-like structures, but as the other cases was negative for neuroendocrine markers, TTF1, and p40. H&E, bars 10 and 20 μm

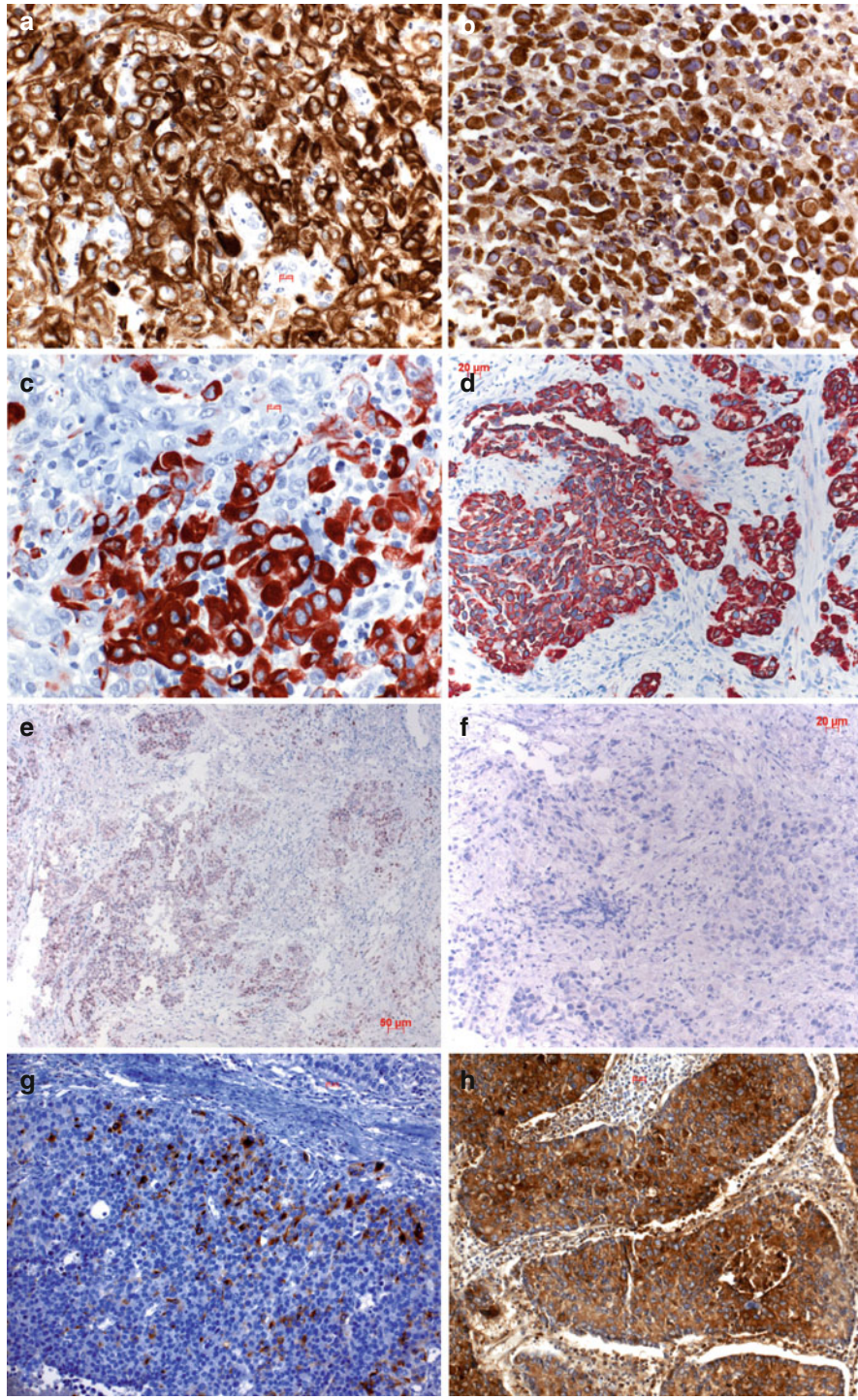

Fig. 17.80 Immunohistochemistry in large-cell carcinomas: (**a**) pan-cytokeratin staining; (**b**) vimentin can be expressed in some cases, but usually a coexpression with cytokeratins; (**c**, **d**) CK7 with different intensities; (**e**) focal and only weak staining for p63; (**f**) absence of TTF1; and (**g**) in rare cases a few cells can stain for neuroendocrine markers; here chromogranin A (**h**) and in rare instances LC might be positive for CEA but is negative for markers of germ cell tumors. Bars 10, 20, 50 µm

lesions such as tumorlets, whereas the high grades are from undifferentiated probably stem cell-like precursor cells. Three of them are associated with cigarette smoking, whereas typical carcinoid is not [240, 241]. So a change of the name without having new definitions at hand would be like changing the emperor's clothes (he is naked: in the fairy tale of *The Emperor's New Clothes*).

Small-Cell Neuroendocrine Carcinoma (SCLC)

Epidemiology

SCLC together with SCC formed the major part of pulmonary carcinomas from the early twentieth century until the early 1990s in Austria. During the 1990s this changed, adenocarcinoma became the number one, SCC dropped dramatically, whereas SCLC remained with about 25 % of lung carcinomas stable. In the early 2000, SCLC started to drop also and is seen today in about 8 % of pulmonary carcinomas. One of the reasons are the changes of smoking behavior 20 years back: filter cigarette has completely replaced the filterless one; due to lowered nicotine content, smokers more frequently and more deeply inhaled tobacco smoke to reach the desired nicotine level. Due to the latency period of 15–30 years after starting with smoking (for females the latency period is shorter, for males longer), this fits well with our observation.

Gross Morphology and Clinical Symptoms

SCLC will show symptoms such as hemoptysis, cough, and rapid weight loss; SCLC can present as a small tumor with large metastasis at detection. Hormonal symptoms can be found in some cases, most often due to production and release of corticotropin, serotonin, calcitonin, and parathyroid hormone [242].

Small-cell carcinoma is defined by nuclear size of 16–23 mμ (not so small!), dark-stained nuclei (mainly composed of heterochromatin), inconspicuous or lacking nucleoli, small cytoplasmic rim, often invisible in light microscopy, and fragile nuclei. On frozen sections the cytoplasm can be quite broad, and so these carcinomas can be misdiagnosed as non-SCLC. In frozen sections carefully investigate the nuclear details! To assess the nuclear size, just look for adjacent lymphocytes or granulocytes: those have diameters of 7 and 14–16 mμ, respectively. The fragility of the nuclei gives rise to chromatin encrustation of veins, where the chromatin gets trapped at the basal lamina (Fig. 17.81).

SCLC is regularly positive for the neuroendocrine marker NCAM, often for synaptophysin and NSE but most often negative for chromogranin A. The best marker is NCAM with a strong membranous staining. SCLC is usually positive for low molecular weight cytokeratins (CK18) and will show a capping-like reaction, i.e., the positive staining is like a cap on one side of the cell (this is the area where intermediate filaments are concentrated together with neurosecretory granules). SCLC produces hormones, such as adrenocorticotropin (ACTH), but also substances interfering with the blood coagulation system (Fig. 17.82). In contrast to carcinoids, SCLC more often are positive for heterotopic hormones (i.e., hormones usually not found in adult lung). If SCLC is combined with any other type of carcinoma, it is defined as SCLC, combined form. There is one exception: carcinosarcoma that can have an SCLC component. In these cases the diagnosis is carcinosarcoma. In these cases I personally list all the components present in the tumor.

SCLC is defined by high mitotic counts; rarely visible organoid pattern; round, ovoid, or spindle-shaped nuclei between 16 and 23 mμ in diameter; dense heterochromatin; invisible nucleoli; and small or even invisible cytoplasm. By electron microscopy usually neurosecretory granules can be found. By immunohistochemistry SCLC are positive for low molecular weight cytokeratins (CK 7/CK 8, CK 18/CK 19), neuroendocrine markers (NCAM, synaptophysin, NSE, rarely CGA), and also for some hormones (Figs. 17.81 and 17.82). TTF1 is positive in most SCLC with a high percentage of stained nuclei - the function of TTF1 in SCLC is not known. In our experience a positive reaction for gastrin-releasing hormone and ACTH is most often seen. The secretion of ACTH can cause Cushing's syndrome.

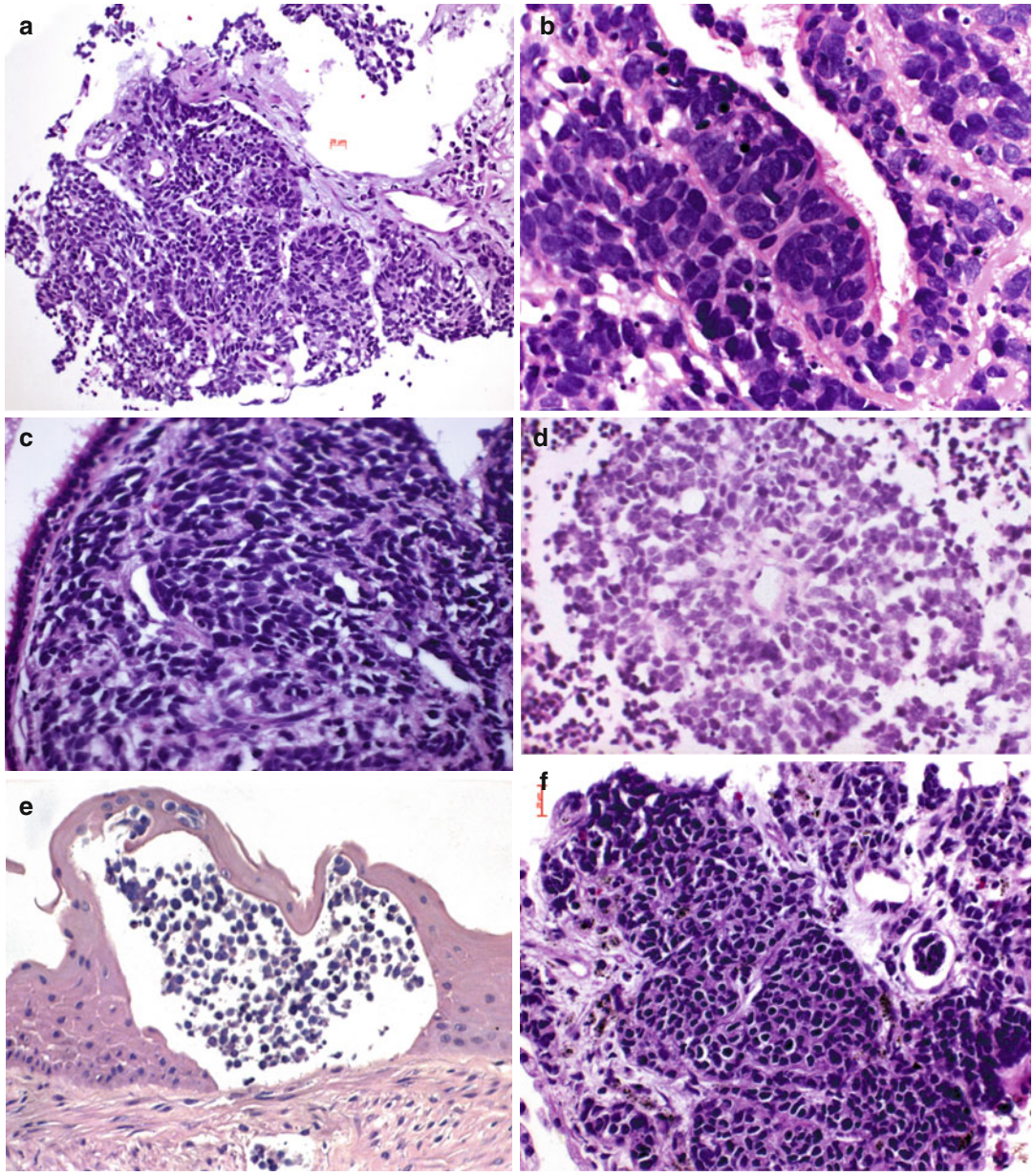

Fig. 17.81 (**a**–**c**) Different examples of SCLC. In (**a**) a well-preserved bronchial biopsy, an organoid structure is visible, even some ill-formed rosettes. The nuclear characteristics are most important: nuclear size 18–23 µm, dense chromatin, invisible nucleoli, and nuclear crowding. The amount of cytoplasm can vary, depending on fixation time. In frozen section SCLC will look essentially as here. (**b**) Surface area of a bronchial biopsy. The tumor cells are spreading within the epithelium. It is very likely that SCLC arise from stem cell-like precursors in this area. The carcinoma cells from the very first beginning can move within the epithelium and across the basement membrane like stem cells do. (**c**) Another case with less well-preserved tumor cells. However the nuclear features are visible, and lymphocytes (7 µm) or granulocytes (14–16 µm) will serve as measurement standards for the size of the tumor cell nuclei. (**d**) Ill-formed rosette in a SCLC, not very common in biopsies. (**e**) Carcinoma cells invading the squamous metaplasia. (**f**) Transthoracic biopsy, not properly fixed, which causes this dense nuclear picture. In such a case, one might be forced to search for better preserved areas. (**g**, **h**) Crush artifacts in bronchial biopsies. In (**g**) there is a characteristic finding of encrustation of small veins by tumor DNA. This is common in SCLC due to the high rate of apoptosis and the rapid growth. Such a finding is suggestive but not diagnostic. (**h**) A biopsy where SCLC might be suspected. Immunohistochemistry can help in some cases. H&E, bars 50, 20, 10 µm

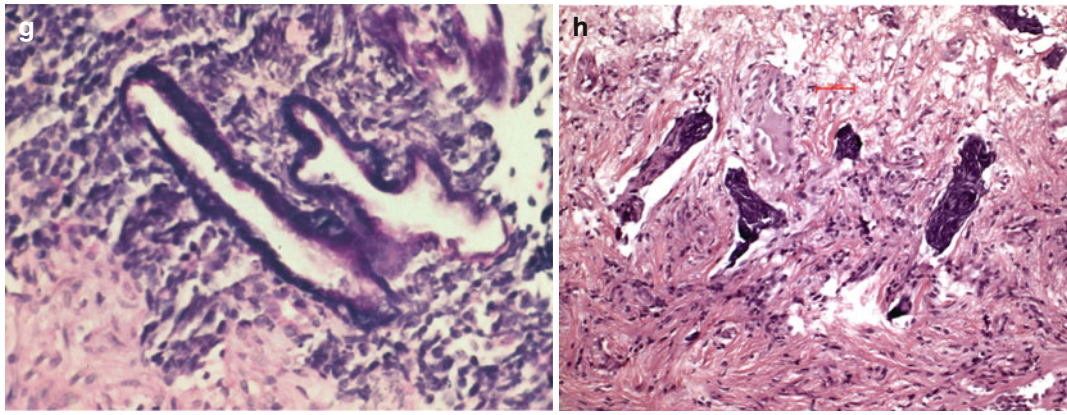

Fig. 17.81 (continued)

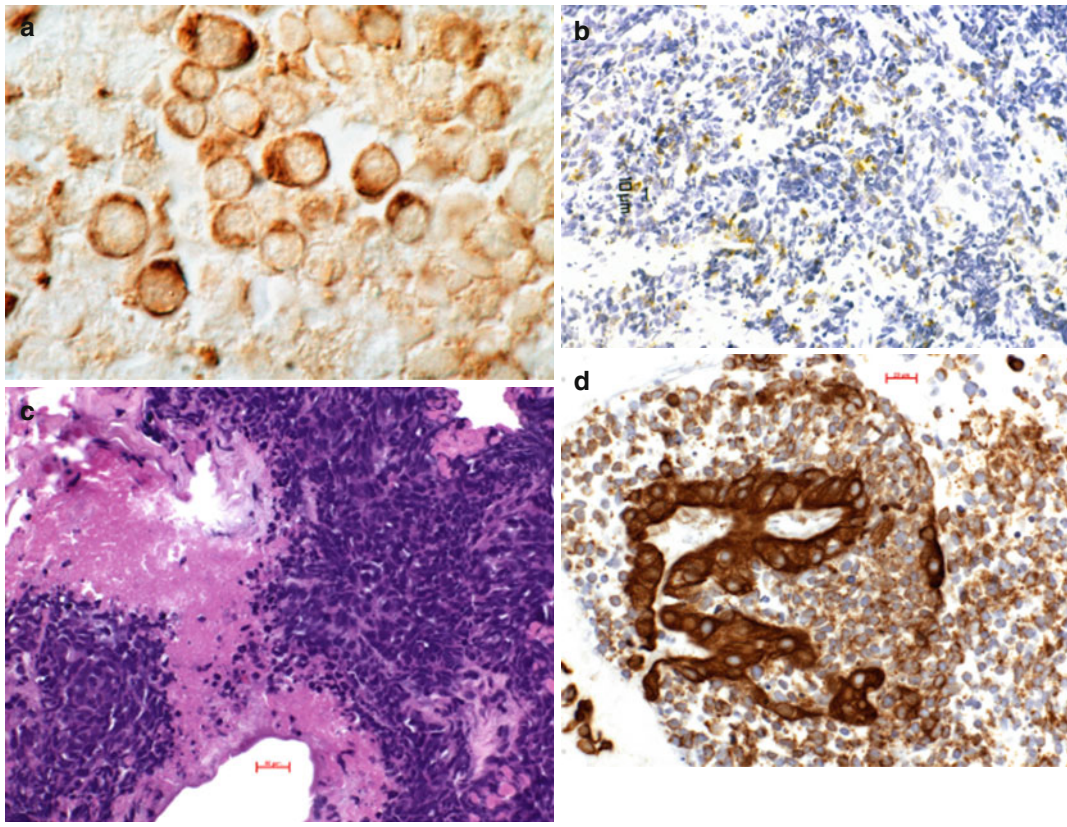

Fig. 17.82 Immunohistochemistry and electron microscopy of SCLC. (**a**) Staining with cytokeratin shows a cup-like pattern, due to an uneven distribution of intermediate filaments (see **g**). (**b**) This case of SCLC was detected because of Cushing syndrome. Immunohistochemistry with antibodies for corticotropin (*yellow*) showed the reason for high cortisol levels in the blood. Upon chemotherapy the hormone levels dropped down to normal. (**c**–**e**) A case of SCLC where in (**d**) the typical cytokeratin staining pattern is nicely seen and contrasts well with the staining of normal epithelial remnants. The membranous staining for NCAM (**e**) is one of the most helpful aids in SCLC diagnosis. (**f**) SCLC in contrast to carcinoid has usually few neurosecretory granules (small *dark dots* in the cytoplasm), which explains why staining for chromogranin A is often negative (below threshold). The cytoplasmic rim in the tumor cells points to the shrinkage normally seen in formalin-fixed specimen. (**g**) Two neighboring tumor cells. The cell border is not well delineated but the concentration of intermediate filaments is evident. Among these proteins are cytokeratins, explaining the cuplike reaction. (**a**, **b**), ×600, 100, (**f**, **g**), ×3,000, 7,000, bars 20 µm

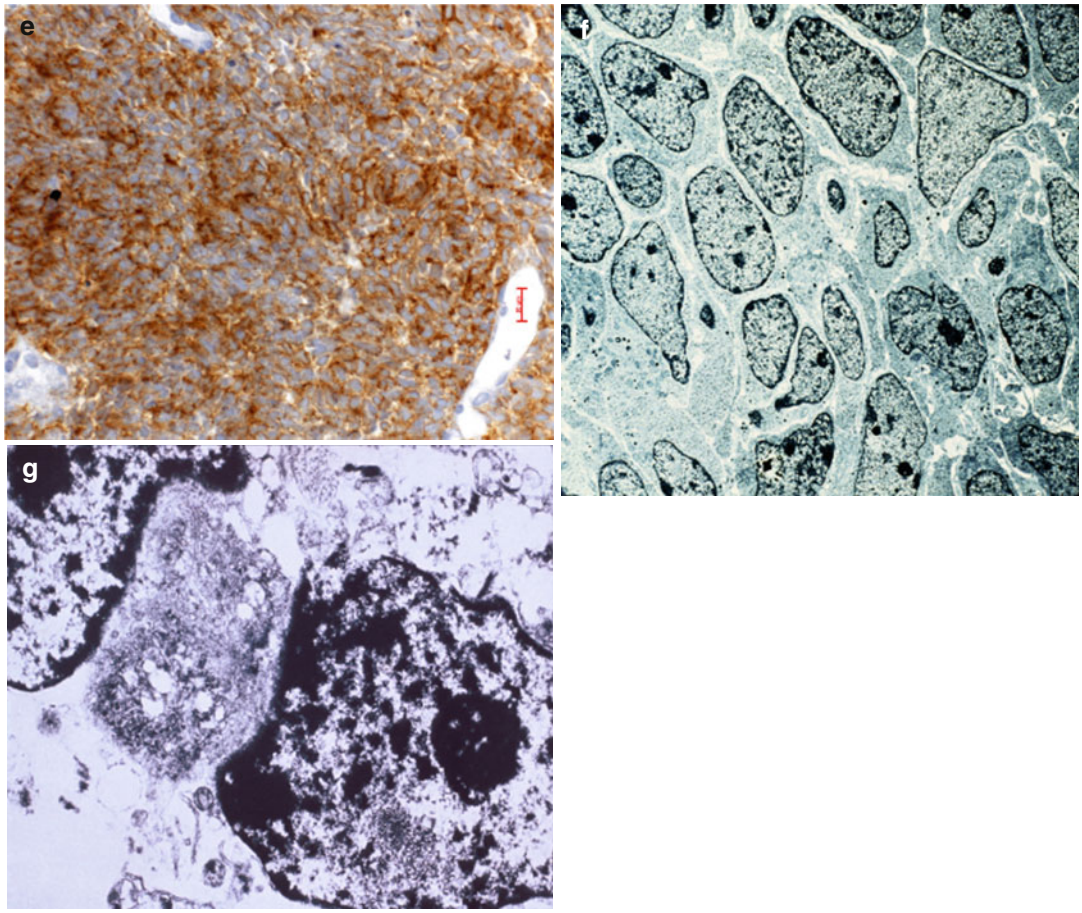

Fig. 17.82 (continued)

High copy number gains are detected in SCLC encoding JAK2, FGFR1, and MYC family members. Most common losses are seen in RB1 and 59 microRNAs of which 51 locate in the DLK1-DIO3 domain. Alterations of the TP53 gene and the MYC family members were predominantly observed in SCLC. Potential drug targets might be the AKT-mTOR and apoptosis pathways in SCLC [243]. In array CGH unbalanced aberrations are in almost every chromosome; a specific gain on chromosome 3q was however seen in two thirds of SCLC discerning it from LCNEC [244] (Fig. 17.83). A further analysis of the area might disclose some markers suitable for this differential diagnosis.

SCLC can occur combined with other non-endocrine carcinomas, which is then acknowledged as combined SCLC. SCLC was previously staged as either limited or extensive disease. A change to TNM is now mandatory.

SCLC is sensitive for chemotherapy and radiotherapy in almost 100 %. However, the prognosis is still pure. Recurrence does occur in most cases, and metastasis is most often present, even when the primary tumor is small. Less than 20 % of patients survive more than 5 years. New therapy might be available within the next years, interfering with the regulation of cell proliferation (inhibitors of tyrosine kinases such as the Src kinase family members, etc.). Another feature of

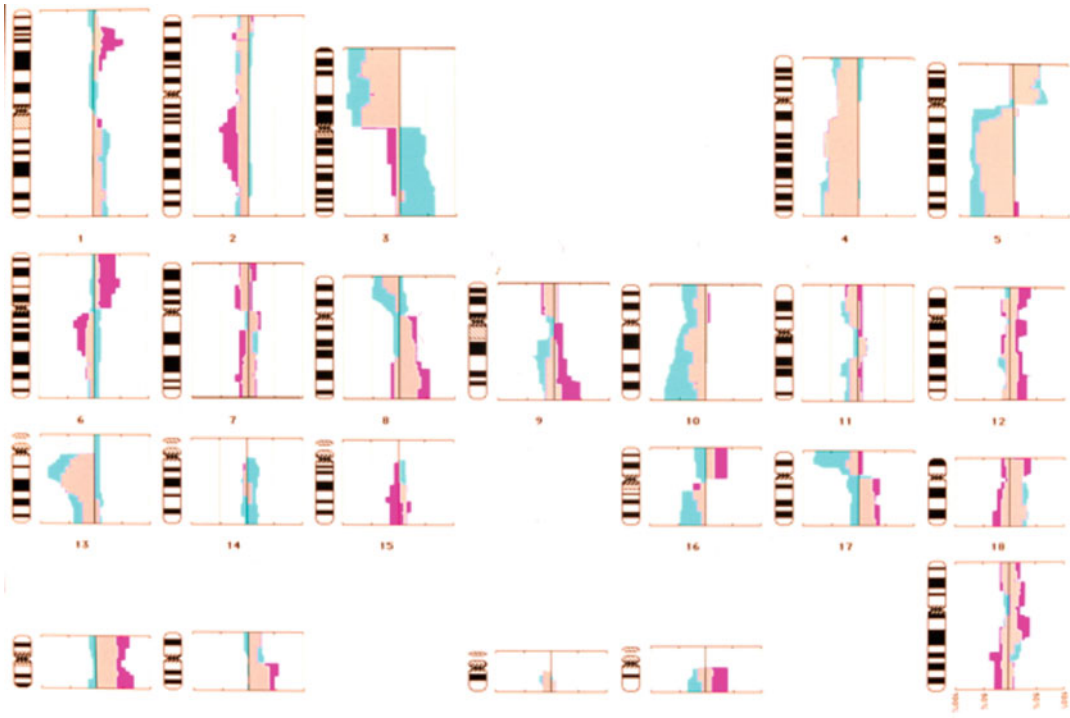

Fig. 17.83 Comparative genomic hybridization of small-cell and large-cell neuroendocrine carcinomas. SCLC in *blue*, LCNEC in *violet*, overlaps of both are in orange. There are some characteristic numeric aberrations: in chromosome 3q SCLC have gains, whereas LCNEC is normal, in chr.10q: SCLC has losses toward the telomeric end, LCNEC no; chr.9q LCNEC has gains, SCLC not; chro.16q SCLC has losses, LCNEC no, but LCNEC has gains in chr.16p; and finally SCLC has losses on chr.17p, LCNEC not. All these aberrations will need further investigation for specific genes within these regions

SCLC is a change of the phenotype in recurrent disease: there might be a predominant squamous cell component and even no SCLC. There are two explanations for this phenomenon, and both have been proven: within the SCLC there are hidden non-SCLC tumor cells, which have a growth advantage, when the SCLC tumor is destroyed by chemotherapy and, second, SCLC cells themselves might react to chemotherapy by differentiating into non-SCLC variants, which are more resistant to chemotherapy (transdifferentiation; Fig. 17.84).

In small biopsies and cytology, SCLC is characterized by a nuclear size of 18–23 µm in diameter (3× lymphocyte, 1.5× granulocyte), dense chromatin, invisible or tiny nucleoli, and small

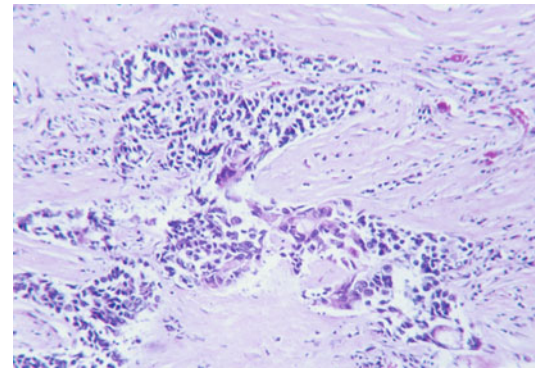

Fig. 17.84 SCLC resection after primary chemotherapy with clinical and radiological response. Within the scars there were small remnants of the carcinoma, focally showing transdifferentiation into squamous cell carcinoma. H&E, ×150

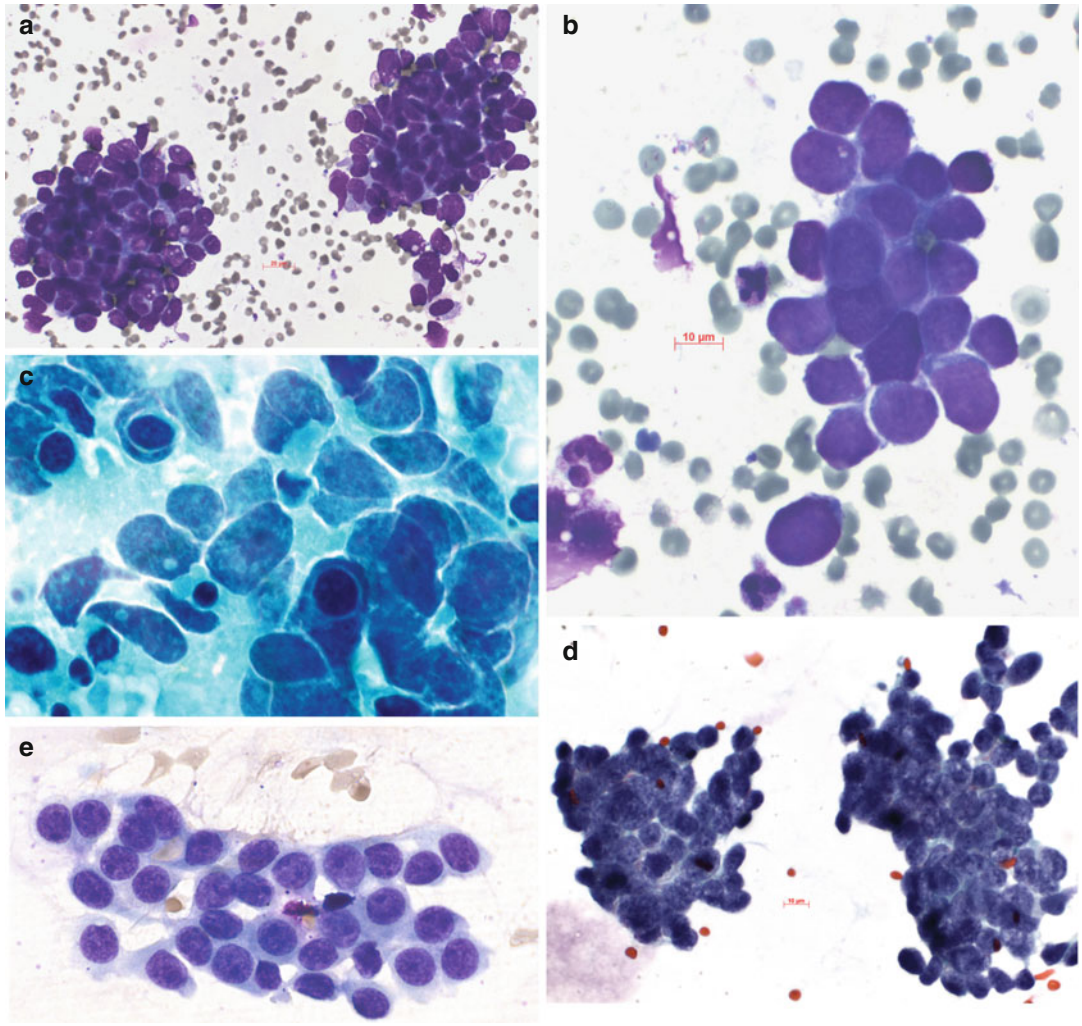

Fig. 17.85 Cytology of SCLC, (**a**–**d**), and comparison to carcinoid (**e**). Clustering of the tumor cells (crowding) is common in this tumor (**a**, **d**); the nuclear features are best seen in (**b**, **c**): dense chromatin, no visible nucleoli, small cytoplasmic rim, and cell cannibalism. In contrast carcinoids (**e**) present with epithelial clusters, well-organized nuclei have coarse chromatin, nucleoli are visible and enlarged, and abundant cytoplasm is present. Mitosis is rarely seen in cytological preparations of carcinoids. Giemsa (**a**, **b**, **e**), PAP (**d**), and modified Giemsa-azure blue (**c**); bars 10 and 20 µm, in (**c**) ×630, in (**e**) ×400

rim of cytoplasm; the comparison with internal size markers is useful, as shrinkage due to formalin fixation affects also lymphocytes and granulocytes. Typically the carcinoma forms minimal cohesive cell groups but rarely rosettes (Fig. 17.85). By immunohistochemistry positivity for NCAM (CD56) and for low molecular weight cytokeratin is helpful. In cytokeratin immunohistochemistry the important feature is a focal cuplike staining, which corresponds to a concentration of intermediate filaments on one side of the cells, usually where also neurosecretory granules are found. By NCAM the staining is membrane based and even retained in necrotic areas. Chromogranin A is most often less helpful, because the small numbers of neurosecretory

granules present in SCLC very often results in low protein concentration below the detection rate of the CGA antibody. NSE and synaptophysin are the two other markers, which can be used; however, it should be noted that these are less sensitive and can stain tumors within the differential diagnosis of SCLC such as PNET.

Large-Cell Neuroendocrine Carcinoma (LCNEC)

On gross examination the only feature that might point to LCNEC are large areas of necrosis, which by themselves are not specific. Clinically LCNEC present as a tumor mass on CT scan and X-ray. There are no specific clinical symptoms.

Large-cell neuroendocrine carcinoma is defined by a neuroendocrine pattern, i.e., rosettes, trabeculas, and solid cell nests. On low-power LCNEC looks organoid, similar to a carcinoid, but on higher magnification abundant mitoses are obvious. By counting the number of mitoses, one can easily reach 20 per high-power field, making a total of up to 200 per 2 mm^2, which is never reached by atypical carcinoid. LCNEC is defined by large polymorphic nuclei 25–35 mμ, a coarse granular chromatin, and large, landscape-like necrosis (Fig. 17.86) [245, 246]. To confirm the diagnosis, a staining for neuroendocrine markers is recommended, such as NCAM, synaptophysin, chromogranin A, and also NSE. LCNEC can produce hormones as SCLC. LCNEC is also positive for low molecular weight cytokeratin. LCNEC can occur combined with other pulmonary carcinomas; if combined with non-SCLC, the diagnosis is combined LCNEC; if combined with SCLC, the diagnosis is combined SCLC.

The prognosis in LCNEC is similar to SCLC. Surgery is recommended for LCNEC in stages I–IIIA. In recent time also a similar chemotherapy regimen is favored, similar to SCLC. A majority of patients respond to these treatments; however, recurrence and metastasis are as high as in SCLC. Recent investigations have found some genes specifically altered in LCNEC: FGFR2 mutation was detected exclusively in LCNEC [247], and in another study, mutations in TP53, and STK11, were seen frequently, whereas mutations of PTEN rarely in LCNECs [248]. As tyrosine kinase inhibitors do exist for FGFRs, this finding might open potentially a new treatment strategy. Another finding useful for the differentiation of SCLC and LCNEC is the finding that CDX2 and VIL1 in combination showed sensitivity and specificity of 81 % for LCNEC, while BAI3 showed 89 % sensitivity and 75 % specificity for SCLC [249].

In small biopsies LCNEC can be diagnosed, if rosettes and trabeculas are present, and the nuclei are large (diameter >26 μm), the chromatin is coarse, and the nucleoli are middle sized. High mitotic counts might be encountered, whereas the large necrotic areas might not be seen (Fig. 17.87). Immunohistochemistry will be an aid. In cytological preparations the diagnosis is more difficult. If the nuclear features are present and numerous mitoses are seen, an immunocytochemistry for neuroendocrine markers should be performed.

Carcinoid, Typical, and Atypical

Clinically carcinoids present by symptoms of obstruction due to the endobronchial part of the tumor. This results in productive cough and recurrent infections in the tumor-bearing lobe. On X-ray and CT scan, a most often centrally located tumor is seen (Figs. 17.88 and 17.89). On bronchoscopy an almost characteristic bleeding is reported, whenever the tumor is touched by the bronchoscope. Symptoms by the release of hormones are rare; Cushing's syndrome can be seen due to the release of corticotropin.

Typical carcinoid is defined by neuroendocrine structures, such as rosettes, trabecules, and solid nests, 0 or 1 mitosis per 2 mm^2, and absence of necrosis. You will usually find central capillaries or veins in the rosettes. In general carcinoids are well vascularized, which is the cause why they tend to bleed when touched by the endoscope during bronchoscopy. The rosette is the functional structure where carcinoid cells release their hormones and biogenic amines into the local circulation. The nuclei of typical carcinoids are uniform, round, with finely dispersed chromatin,

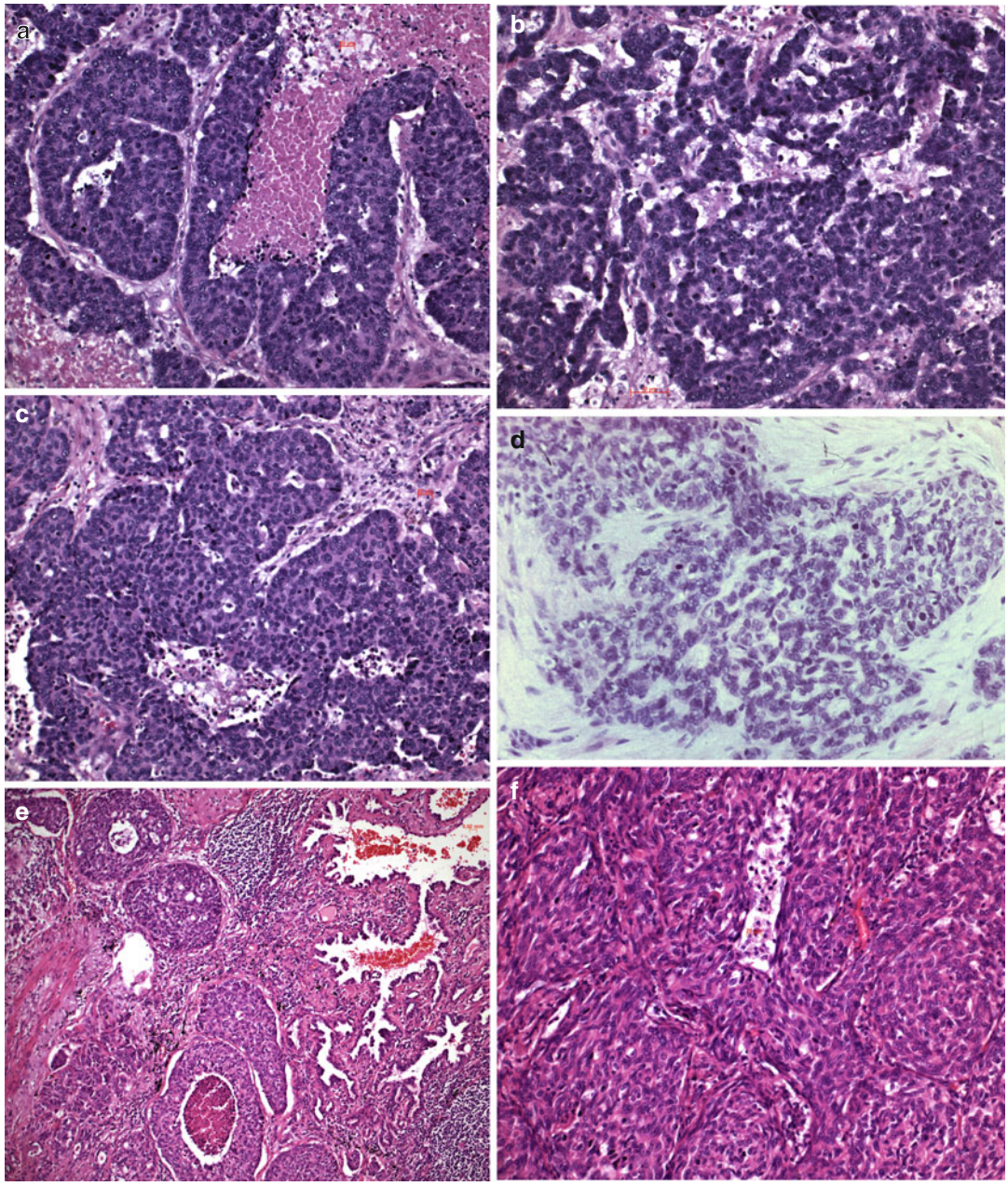

Fig. 17.86 Examples of large-cell neuroendocrine carcinomas (LCNEC) in (**a**–**d**), and a mixed LCNEC with adenocarcinoma as well as a spindle cell carcinoma in (**e**, **f**). In (**a**) large necrosis is seen, rosettes are ill formed. Rosettes are better seen in (**b**–**d**); in addition the nuclear features show enlarged nuclei, coarse chromatin, enlarged nucleoli, and frequent mitosis (can be up to 25/HPF). (**e**) A mixed LCNEC (*left*) with adenocarcinoma (*right*) and spindle cell carcinoma (**f**) is presented. Immunohistochemistry for chromogranin A (**g**), synaptophysin (**h**), and NCAM (**i**). In contrast to SCLC, this high-grade neuroendocrine carcinoma is less often intensely stained for NCAM but more common for CGA and synaptophysin. H&E, bars 20 and 50 μm

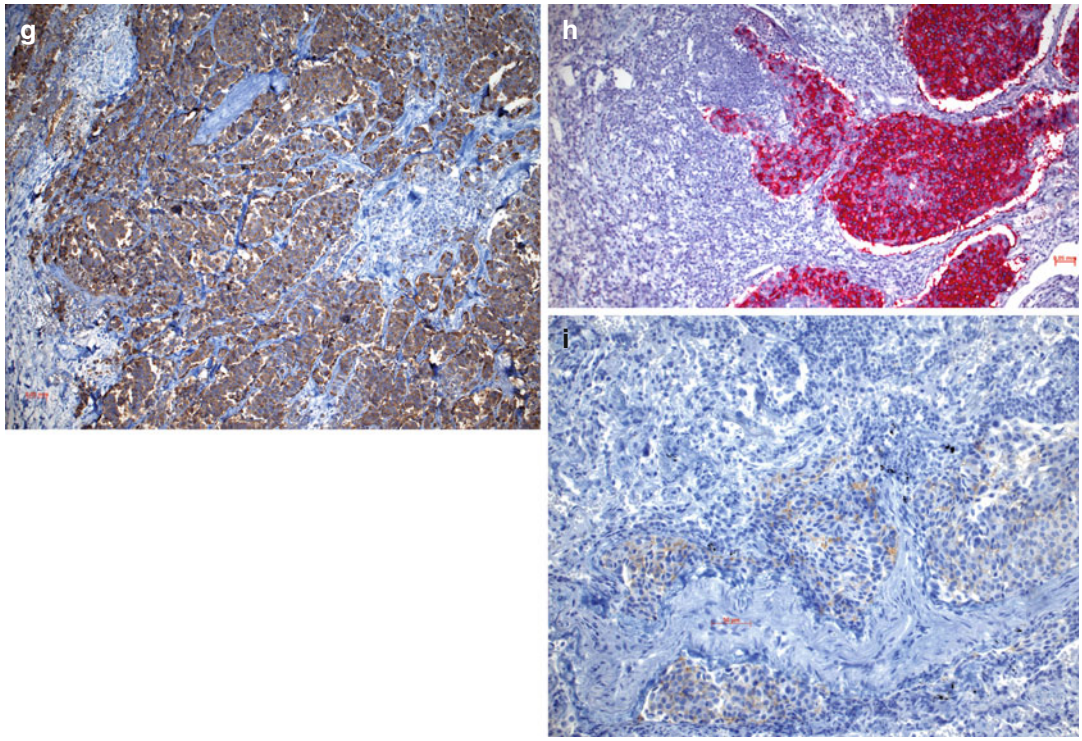

Fig. 17.86 (continued)

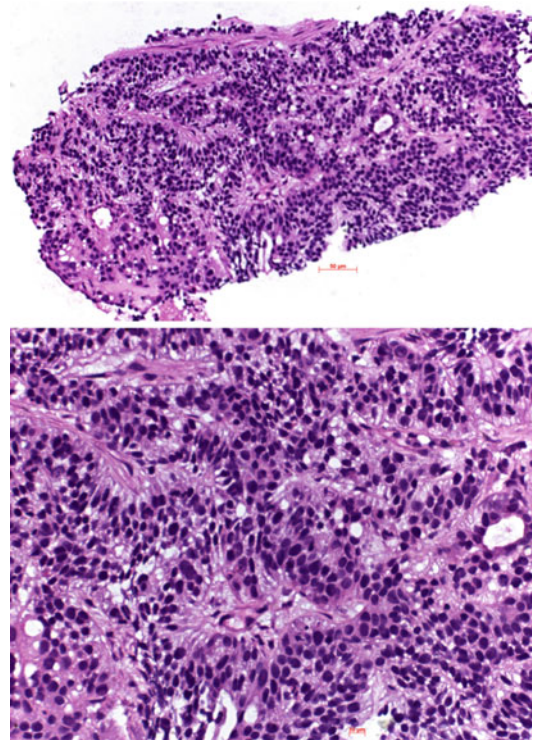

Fig. 17.87 LCNEC can sometimes easily be diagnosed on transthoracic core needle biopsies if the rosette pattern is clearly visible. A stain for one of the neuroendocrine markers will confirm this diagnosis. H&E, bars 50 and 10 µm

Fig. 17.88 CT scan of a carcinoid. The tumor is visible at the *lower left side*, located within a bronchus with obstruction of the peripheral branches

and inconspicuous nucleoli (Fig. 17.90). There are some variants, which can create problems in diagnosis, such as spindle cell carcinoid and oncocytic carcinoid. The spindle cell carcinoid cannot be diagnosed without immunohistochemistry. The entire tumor or large parts of it is composed by spindle cells arranged in whorls without stroma in between them. A few capillaries might be seen. This rare variant behave the same as any other typical carcinoid. Also carcinoids, which synthesize and secrete some hormones such as parathyroid hormone and calcitonin, can present with bone or amyloid formation.

Atypical carcinoid is defined by two to ten mitoses per 2 mm^2, and/or presence of necrosis, and again neuroendocrine structures. The nuclei of ATC are usually larger; enlarged nucleoli are seen more frequently (Fig. 17.91a, b). In both carcinoids there is an invasive/infiltrative growth into the lung, and lymphatic and blood vessel invasion can be found in some cases. Some carcinoids can metastasize, but so far there are uniform predictive markers for the biological behavior. In general atypical carcinoids with mitotic counts >5/2 mm^2 or carcinoids with lymphatic or blood vessel invasion will behave more aggressively, will metastasize, and will ultimately kill the patient (Fig. 17.91c). This group comprises 25 % of atypical carcinoids and single cases of typical ones.

Fig. 17.89 Typical carcinoid (*upper* and *middle panel* and atypical carcinoid (*lower* panel). The resection specimen is shown, from the resection margin a polypoid tumor is visible, obstructing both *upper* and *lower left* bronchus (17-years old boy). In the middle the tumor is seen (after frozen section margin analysis), and the mucus accumulation is visible behind the tumor. In the atypical carcinoid, an intrapulmonary metastasis was already present

In addition those carcinoids, which have more than two losses on distal chromosome 11q (LOH), and those with multiple chromosomal losses (<5), also show a pure outcome [240, 241, 250]. There is an overlap of chromosomal losses and higher mitotic counts, however, not a 100 % concordance. On the other hand, typical carcinoids with 0–1 mitotic counts per 2 mm^2

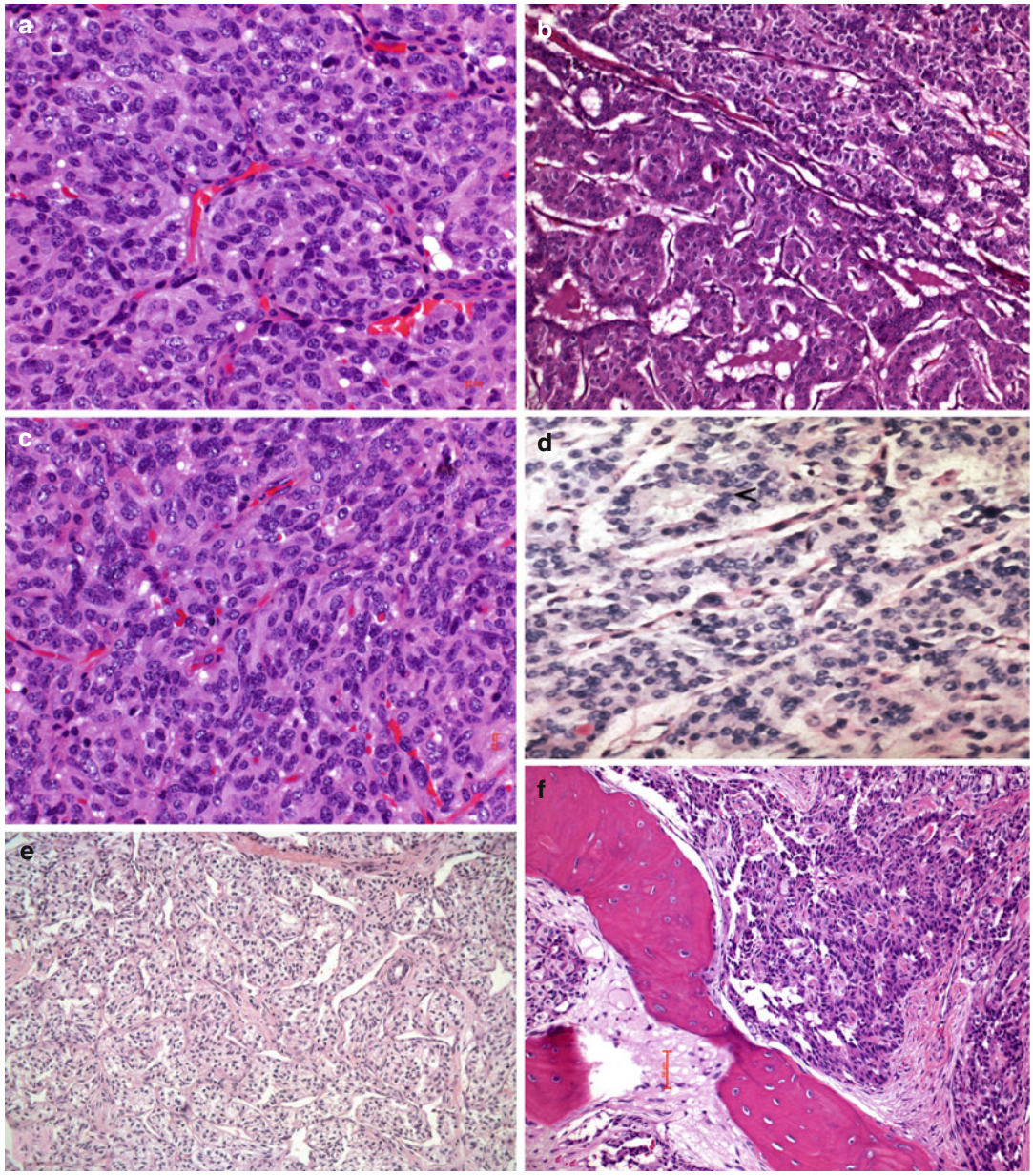

Fig. 17.90 Typical carcinoid and variants. In (**a**, **c**) a more solid and nesting pattern dominates in this case; the typical rich capillary network is nicely demonstrated. (**b**) This carcinoid shows rosettes and trabecules. In (**d**) rosettes dominate the pattern. (**e**) This is an unusual oxyphilic carcinoid with giant mitochondria on electron microscopy. (**f**) shows bone formation and (**g**) amyloid deposition in carcinoids. In carcinoids with bone formation, usually parathyroid hormone and/or calcitonin secretion is found in the tumor cells, whereas amyloid is based on calcitonin production and secretion. (**h**) A spindle cell carcinoid is a rare variant where the diagnosis can only be made with the aid of immunohistochemistry. H&E, bars 10, 20, 50 μm, ×200, 100, 150

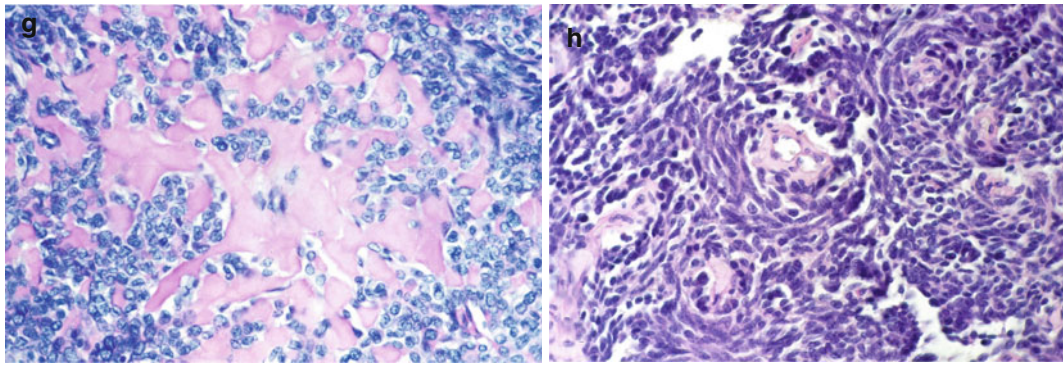

Fig. 17.90 (continued)

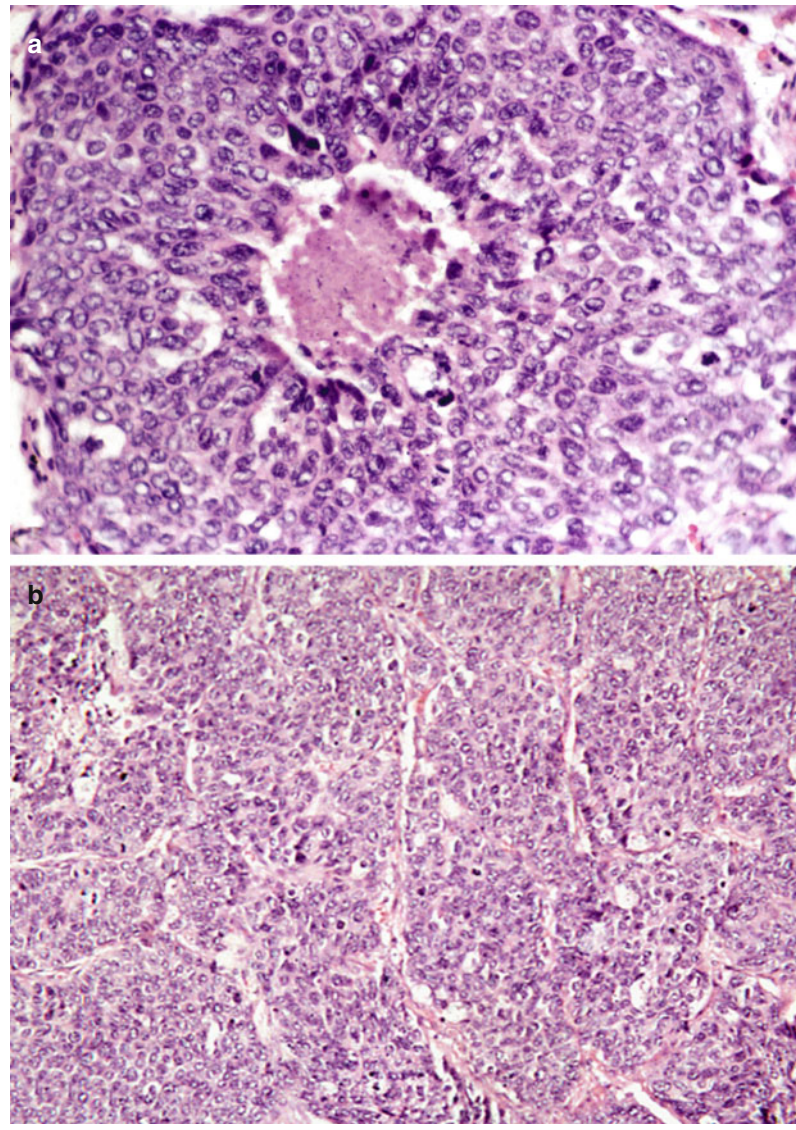

Fig. 17.91 (**a**) Small necrotic foci are one of the hallmarks of atypical carcinoid; another feature is increased mitosis (**b**); (**c**) lymphatic invasion can be found in both carcinoids, but more frequently in atypical ones. Lymphatic invasion should be investigated in the border zone of carcinoids especially around blood vessels. They cannot be seen in the tumor center. H&E, ×250, 150, 100

Fig. 17.91 (continued)

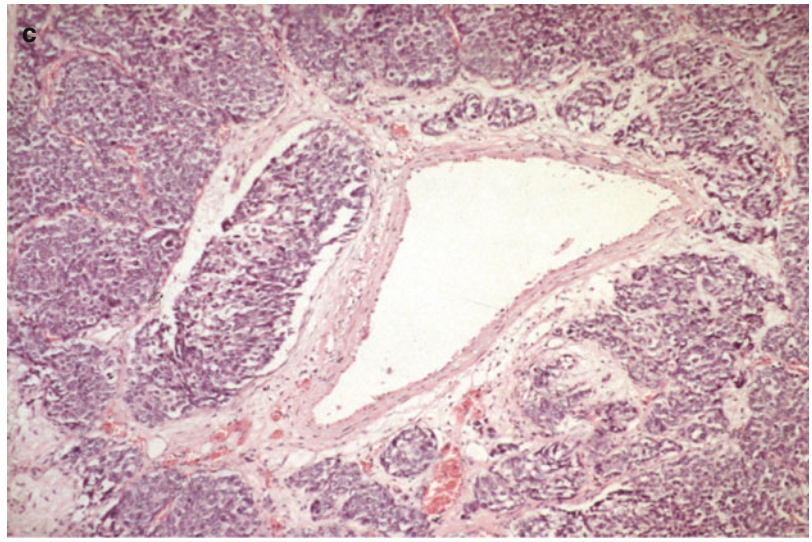

and without lymphatic or blood vessel invasion have a good prognosis, when completely resected – in our experience a 100 % survival, no recurrence, and no metastasis (L0, V0, N0) [238]. But there remain a group of carcinoids, most atypical ones, for which the prognosis cannot be predicted.

Diagnosis of carcinoids can be made on biopsies and cytology. However, it is recommended to produce Cytoblock from cytological material for additional immunocytochemistry (Fig. 17.92). However, a differentiation into typical or atypical carcinoid is often impossible, unless there are two mitoses within the specimen.

Carcinoids can produce multiple hormones and neurotransmitters. The synthesis and secretion are not coordinated as in normal neuroendocrine cells. So the production can be seen by immunohistochemistry, but there might be no secretion. The production of hormones has no correlation with the biological behavior. In rare cases there is no detectable hormone production but instead an increase of mitochondria (oncocytic carcinoid); this is easily visible on H&E stain, because the mitochondria stick out as tiny eosinophilic granules (Fig. 17.93).

Carcinoids can be found as central tumors or peripheral. Central carcinoids usually show an iceberg phenomenon: a small part of the tumor produces bronchial stenosis by an endobronchial component (tip of the iceberg), whereas the major part lies within the lung parenchyma. Therefore carcinoids should never be locally excised like hamartomas. There is no preferred location; all lobes can be affected equally.

Based on genetic studies, it can be speculated that NCAM, its 140 kDa isoform precursor (NCAM 140), Zinc finger protein-like 1, and sorting Nexin 15 might be involved in the genesis of carcinoids [250].

Staging: staging of large-cell neuroendocrine carcinomas is done as usual. The IASCL and UICC new staging manual recommends staging of all neuroendocrine tumors including SCLC and carcinoids. We have staged carcinoids since the 1980s and have found this to be a very useful prognostic marker.

There is an ongoing discussion since decades that neuroendocrine tumors share a common precursor cell and even that the highly aggressive ones might develop from the low malignant ones. This hypothesis is based on the behavior of all four tumors to express general neuroendocrine markers, to synthesize hormones, and to form neuroendocrine structures. So these tumors share some phenotypic features. When looking at the

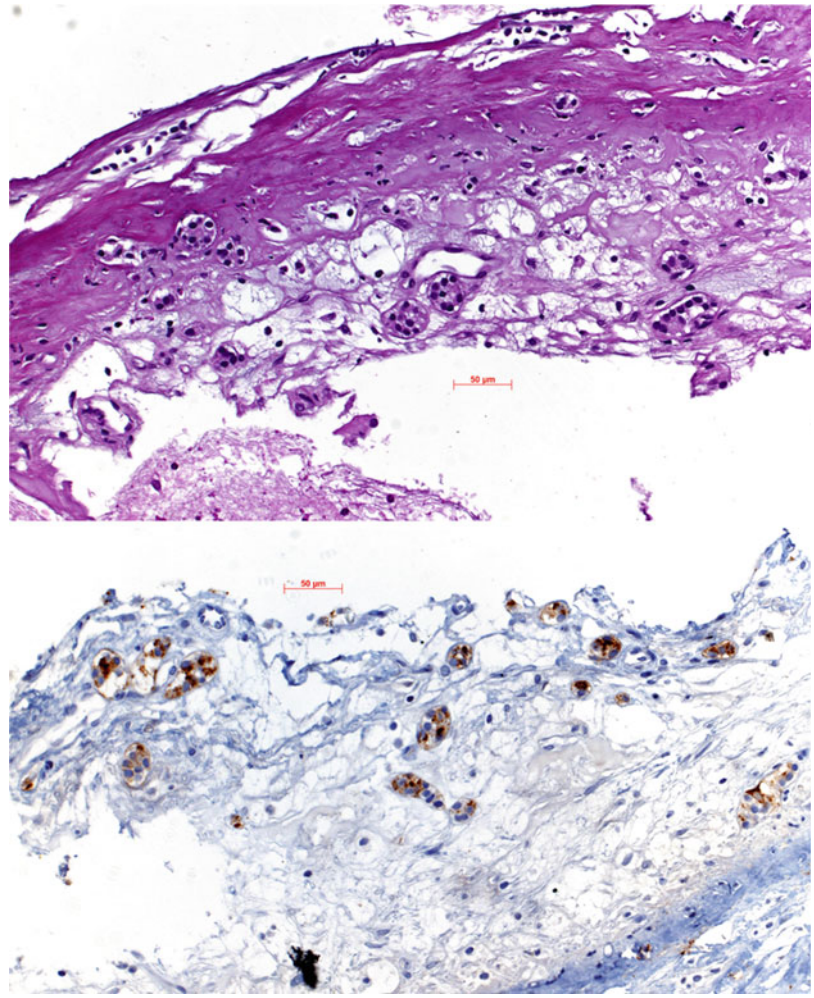

Fig. 17.92 Cells from a carcinoid derived from fine needle aspiration. A Cytoblock was prepared, which enables to cut serial sections for H&E and immunocytochemistry, here chromogranin A. Small rosettes are visible in these clusters of cells. Bars 50 µm

genotype, it is obvious: these tumors have not much in common. Whereas SCLC and LCNEC have typical chromosomal aberrations at chromosomes 3, carcinoids have a few aberrations, and at chromosomal locations, uncommon in the high-grade forms – except chromosome 11q where LCNEC and atypical carcinoids share similar losses. If a high-grade tumor could develop out of a low-grade one, then chromosomal aberrations, such as gains and losses, should be retained in the high-grade carcinoma, and other aberrations should be seen on top of those [241, 244]. In the development of SCLC and LCNEC, tobacco carcinogens are the main factors, whereas in carcinoids not much is known about the inducing factors. In atypical carcinoids approximately 50 % are smokers and the other half never-smokers, and only in smokers also TP53 gene mutations do occur [251]. It has become clear that carcinoids can develop from neuroendocrine cell hyperplasia and also from tumorlets, whereas SCLC and LCNEC do not. Some new information point to the fact that primitive stem cells of the lung posses' neuroendocrine features, and in organogenesis of the lung, neuroendocrine cells are probably the first differentiated cells within the epithelium, which we have proven in a study using fetal lung from different gestational ages. SCLC in our

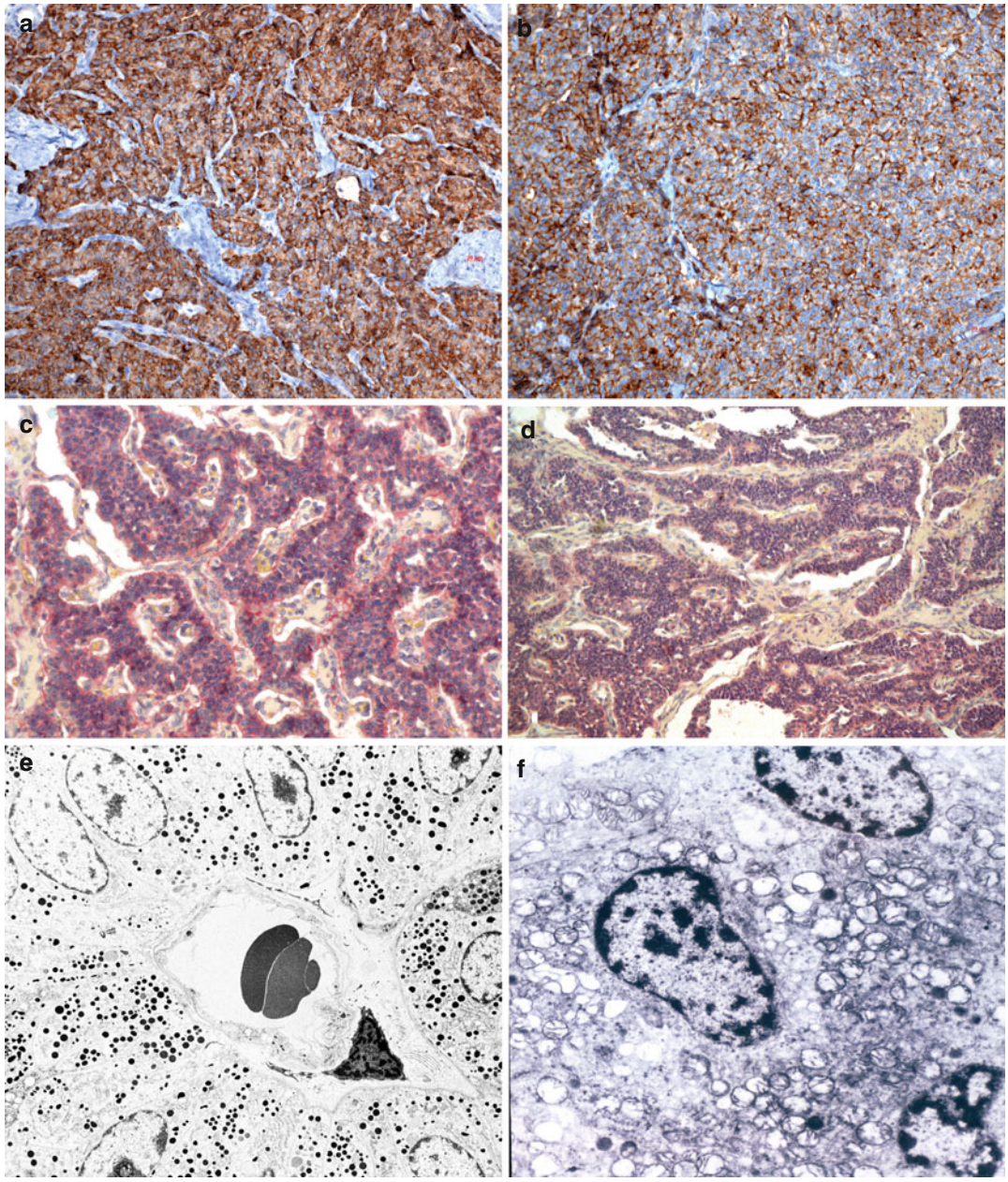

Fig. 17.93 Immunohistochemistry and electron microscopy of carcinoids. (**a**) Staining for chromogranin (**b**) staining for NCAM, (**c**) synthesis of vasointestinal peptide in a typical carcinoid, (**d**) synthesis of parathyroid hormone in a carcinoid. (**e**) Electron microscopy of a typical carcinoid shows multiple neurosecretory granules, and also the intimate association of the tumor cells with the capillary in the center. This structure corresponds to the rosette, seen on light microscopy. (**f**) Oncocytic carcinoid, here only single neurosecretory granules are found, but multiple mitochondria, some giant forms. ×100; ×2,500 and 3,000

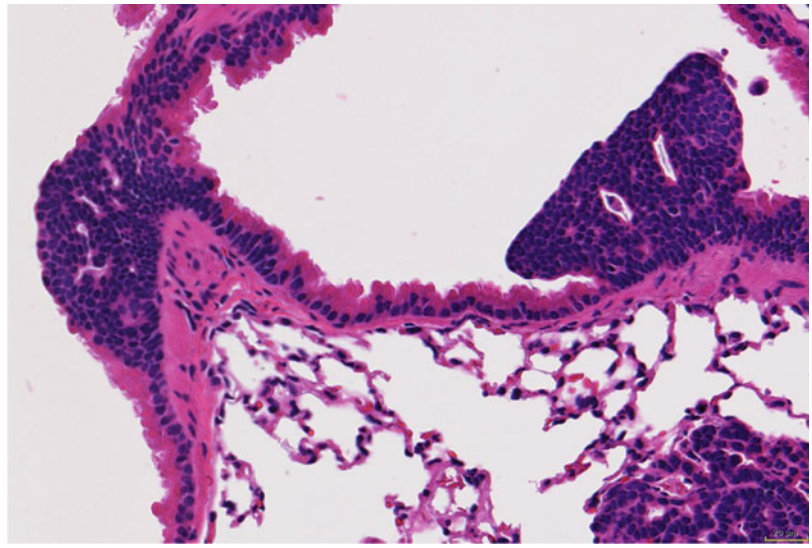

Fig. 17.94 Genetically engineered mouse model with SCLC in an early stage. In this stage the carcinoma cells can be seen replacing the normal epithelium, and the cells are indistinguishable from the basal cells. A few cells have started to move into the stroma. H&E, bar 20 µm (Courtesy of Adi Gazdar)

present understanding develops from primitive stem cells of the central lung, which exhibit a neuroendocrine phenotype. Therefore the primary expansion of carcinoma cells within the epithelium is not visible, because the cells look like undifferentiated stem cells (Fig. 17.94) [252]. And most probably these tumor cells are capable of immediately invading the stroma. In surgical resection specimen carcinoma cells can be recognized within the epithelium as sheets but also as single cells interspersed between normal bronchial epithelium, probably representing the precursor lesion.

There are different signaling cascades, driving neuroendocrine differentiation in high-grade carcinomas. Human achaete-scute homolog-1 (hASH1) was identified as responsible for inducing a neuroendocrine phenotype in SCLC, also proven in mouse models [252–255]. However, ASH1 does not induce small-cell carcinoma by itself but can induce a neuroendocrine phenotype in other cell types as well, for example, in Clara cells in a mouse model of undifferentiated lung carcinoma with expression of neuroendocrine features, but not reproducing the SCLC morphology [256]. Loss of RB1 and p130, mutation of TP53, and probably alterations of other genes are responsible for the induction of SCLC [257]. ASH1 is an important regulator of neuroendocrine differentiation in normal and fetal lung but also plays an important role in neuroendocrine differentiation of high-grade carcinomas, whereas seems less important in carcinoids [258, 259]. Some other genes within the Achaete-scute complex-like1 such as ASCL1, hASH1, and Mash1; atonal homolog 1 genes as ATOH1, hATH1, MATH1, and NEUROD4 genes (ATH-3, Atoh3, MATH-3); and neurogenic differentiation factor 1 (NEUROD1, NEUROD, BETA2) might be candidates as well, because they also show differential expression among lung tumors. Tumors with high levels of ASCL1 also express neuroendocrine markers, and this is accompanied by increased levels of NEUROD1. ATOH1 expression was found in adenocarcinomas with neuroendocrine features. Aberrant activation of ATOH1 leads to a neuroendocrine phenotype similar to what is observed for ASCL1 and might be another mechanism for NSCLC with neuroendocrine phenotype [260]. Interestingly hASH1 is not only responsible for the neuroendocrine phenotype in SCLC and LCNEC but has also other much broader function. Knockdown of hASH1 gene in human lung cancer cells in vitro suppressed growth by increasing apoptosis, whereas forced expression of hASH1 in human bronchial epithelial cells decreases apoptosis. This can be interpreted that hASH1 promotes remodeling in lung epithelium through multiple pathways [261].

ASH1 is placed within the Notch signaling pathway and seems to be antagonized by HES1. By overexpression of NOTCH-1, NOTCH-2, or the Notch effector protein, human hairy enhancer of split-1 (HES1) in SCLC cell cultures and Notch proteins but not HES1 caused a profound growth arrest. Active Notch proteins led to marked reduction in hASH1 expression and activation of phosphorylated ERK1 and ERK2. So in contrary to the oncogenic function of Notch in other tumors, Notch in the setting of highly proliferative hASH1-dependent neuroendocrine carcinomas causes growth arrest and thus acts like a suppressor [262]. This findings fit well with the observation on Notch-inactivating mutations in EGFR-mutated adenocarcinomas under tyrosine kinase inhibitor therapy. In EGFR-mutated and tyrosine kinase inhibitor-resistant adenocarcinomas, mutations in the Notch genes seem to regulate the transdifferentiation into a carcinoma of small-cell neuroendocrine phenotype [263].

Differential Diagnosis of Neuroendocrine Tumors

High grade can be easily differentiated from the low-grade ones by their number of mitoses. The differentiation of LCNEC from SCLC is not always easy: there are rare overlapping cases, which do not fit well into one of these categories. Helpful features are nuclear size >25 µm favors LCNEC, almost 100 % positivity for TTF1 favors SCLC. By cytokeratin stain SCLC shows a cup-like reaction, whereas in LCNEC the cell membrane and cytoplasm is circumferentially stained. LCNEC can be differentiated from other undifferentiated carcinomas by the staining for neuroendocrine markers (>30 % of cells for either NCAM, CGA, synaptophysin). In SCLC almost 100 % of tumor cells stain for NCAM; the staining for the other neuroendocrine markers is variable.

SCLC cannot be differentiated from small-cell carcinomas of other location, because the staining pattern is identical. Also LCNEC can occur outside the lung and a metastasis from the upper respiratory tract within the lung can be hard to differentiate from a lung primary. Within the differential diagnosis of SCLC, other blue small round cell tumors need to be discussed. A cytokeratin positivity differentiates SCLC from PNET and the tumors of the Ewing sarcoma group. Synovial sarcoma presents with larger cells if epithelioid, and in case of the sarcomatoid variant, the cell nuclei are all spindle type, whereas in SCLC there are always two types of nuclei present, a polygonal one and a plump spindle type.

In our current understanding of carcinogenesis, we have learned that different phenotypic features in carcinoma cells are not always related to each other. Capability of invasion, metastatic potential, lymphatic invasion, are capabilities, which some carcinoma cells acquire, others not. The ability to produce hormones can be an advantage for some carcinoma cells, because they can produce their own growth hormone, synthesize receptors for these factors, and so get independent for growth stimuli (autocrine growth stimulatory loop). But this by no means can be taken as a proof of a common ancestry. In SCLC such loops exist: gastrin-releasing peptide or corticotropin is synthesized by the tumor cells; they express receptors for these hormones. The receptor-hormone ligand interaction activates the RAS signaling system either directly or indirectly by stimulating synthesis of ligands for tyrosine receptor kinases; this results in proliferation. SCLC in cell cultures can double their cells within 30 days [264–267].

NSCLC with NE features is defined as a non-small-cell carcinoma (SQCC, AC, LC) with positivity for at least one neuroendocrine marker, such as NCAM, CGA, and synaptophysin in up to 25 % of tumor cells. Since there is no prognostic difference among non-SCLC with and without neuroendocrine features, this diagnosis is clinically of no importance. The diagnosis can only be made by immunohistochemical stains, because these carcinomas do not show neuroendocrine structures (Fig. 17.95) [268].

17.3.4 Carcinomas with Clear Cells

Carcinomas with clear cells: This was a separate entity, but as clear cells can occur in almost every carcinoma, this is now mentioned in the description. Take care on frozen sections: these cytoplasms are by no means clear but are well stained. There is another caveat: clear cell carcinomas in

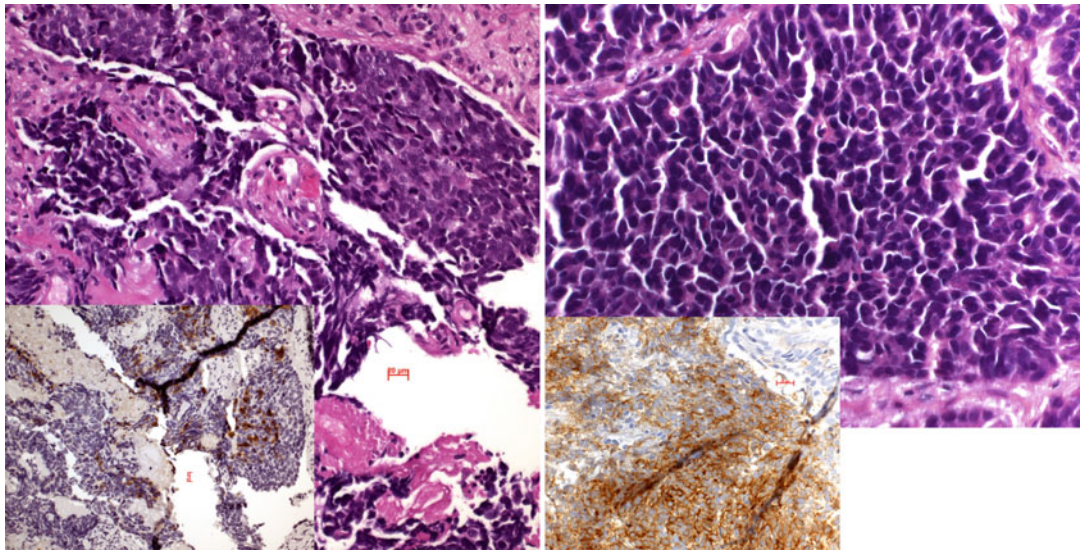

Fig. 17.95 Comparison of non-small-cell carcinoma with neuroendocrine features and SCLC. Left a small-cell variant of SCC, the inset shows scattered tumor cells which express NCAM, whereas to the right a SCLC is shown and in the *inset* more than 60 % of tumor cells expressing NCAM. H&E, bars 20 µm

the lung are most often metastases of renal clear cell carcinomas and rarely lung primaries. Primary pulmonary carcinomas entirely composed of clear cells are vimentin negative and cytokeratin positive (renal will often show coexpression of cytokeratins and vimentin; Fig. 17.96a, b). In addition renal carcinoma metastases are usually centered along pulmonary arteries and show large infarct-like necrosis.

17.3.5 Rhabdoid Carcinoma

Rhabdoid carcinoma is characterized by a solid growth pattern, often overlaid by a reactive proliferation of pneumocytes, which can give these tumors a pseudoalveolar pattern and a pseudocomposition of two cell populations. Within the cytoplasm of the tumor cells, eosinophilic inclusion bodies can be found, similar to those seen in rhabdomyosarcomas. These inclusion bodies are stained by eosin and are negative for striated muscle markers but positive for vimentin. The nuclei are large with a diameter >26 µm, chromatin is coarse, and nucleoli are middle sized. Rhabdoid carcinoma can be diagnosed on small biopsies or cytology (Fig. 17.96e–g).

17.3.6 LC of Hepatoid Phenotype

LC of hepatoid phenotype is characterized by large cells which resemble hepatocytic carcinoma. The cells form sheets of cells, the nuclei are large, chromatin is coarse, and nucleoli are enlarged. The cytoplasm is eosinophilic; some inclusions can be seen in a few cells, which resemble Mallory corpuscles (Fig. 17.96c, d).

17.3.7 Lymphoepithelioma-like Carcinoma

Sheets of undifferentiated tumor cells embedded in a lymphocyte-rich stroma characterize *lymphoepithelioma-like carcinoma*. On frozen sections it might be difficult to encounter the tumor cells. The carcinoma cells are positive for cytokeratin 7 and cytokeratins 13/14; the lymphocytes in most cases are B cells (Figs. 17.97 and 17.98). A diagnostic feature is the intense intermingle of tumor cells and lymphocytes, i.e., lymphocytes are everywhere in between the tumor cells, and seem to be associated with the carcinoma, similar to what is seen in thymomas. In cases from Southeast Asia, most

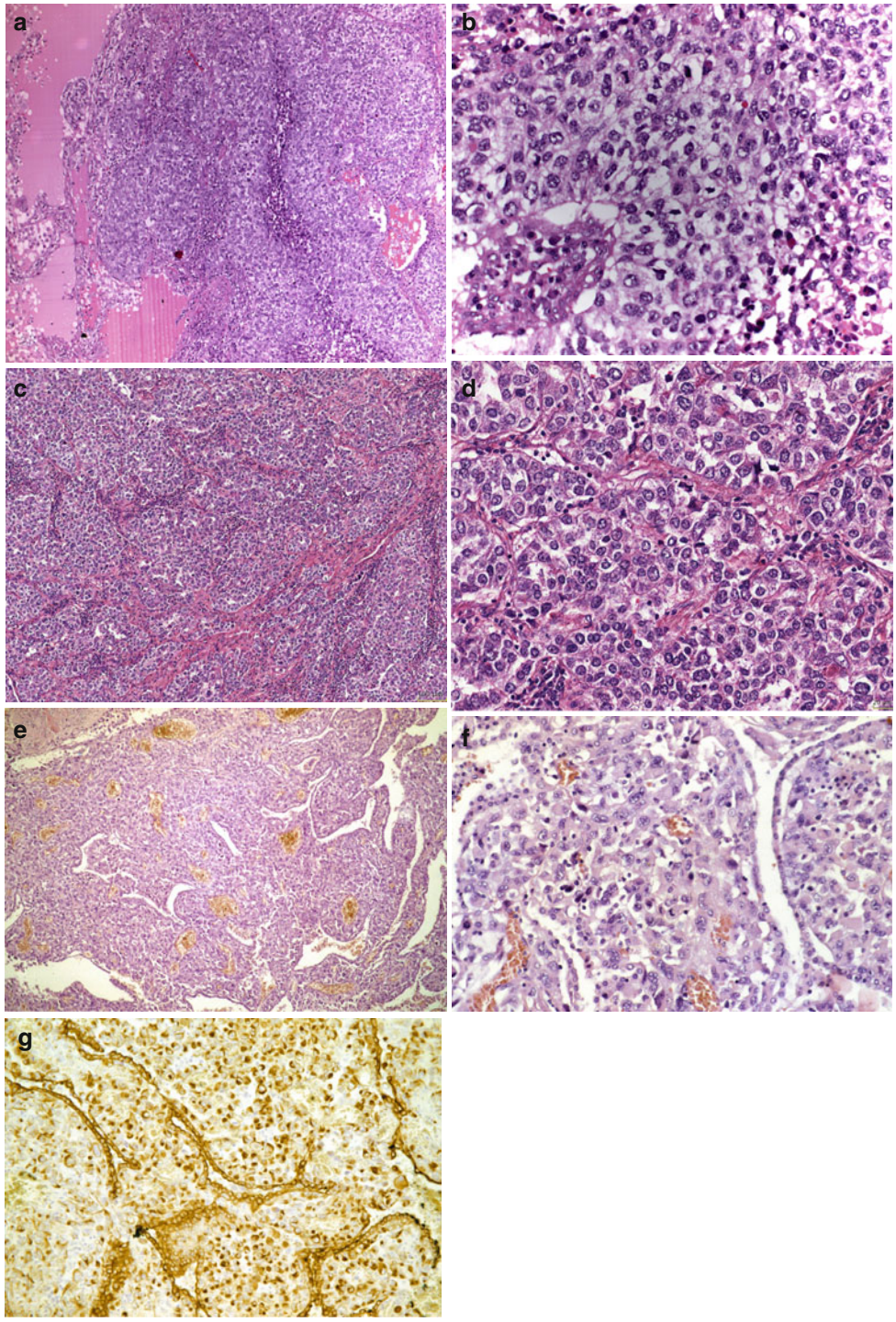

Fig. 17.96 (**a**, **b**) Undifferentiated primary pulmonary carcinoma entirely composed of clear cells. This would have corresponded to the former clear cell variant of large-cell carcinoma. (**c**, **d**) Hepatoid carcinoma showing strands of tumor cells, which on higher magnification resemble hepatocytic carcinomas. There are some inclusions, which look like Mallory bodies (**d**). (**e**–**g**) Carcinoma with rhabdoid morphology; especially in F the growth pattern is interesting, as the tumor cells grow underneath the pneumocytes and thus might simulate an epithelioid angiosarcoma or any other epithelioid sarcoma. The eosinophilic inclusion bodies are quite good seen in (**f**); the cytokeratin stain in (**g**) highlights the less intense staining of the tumor cells compared to the normal epithelium. The inclusion bodies are even better seen as negative corpuscles in the cytokeratin stain. H&E, ×25, 150, and 200

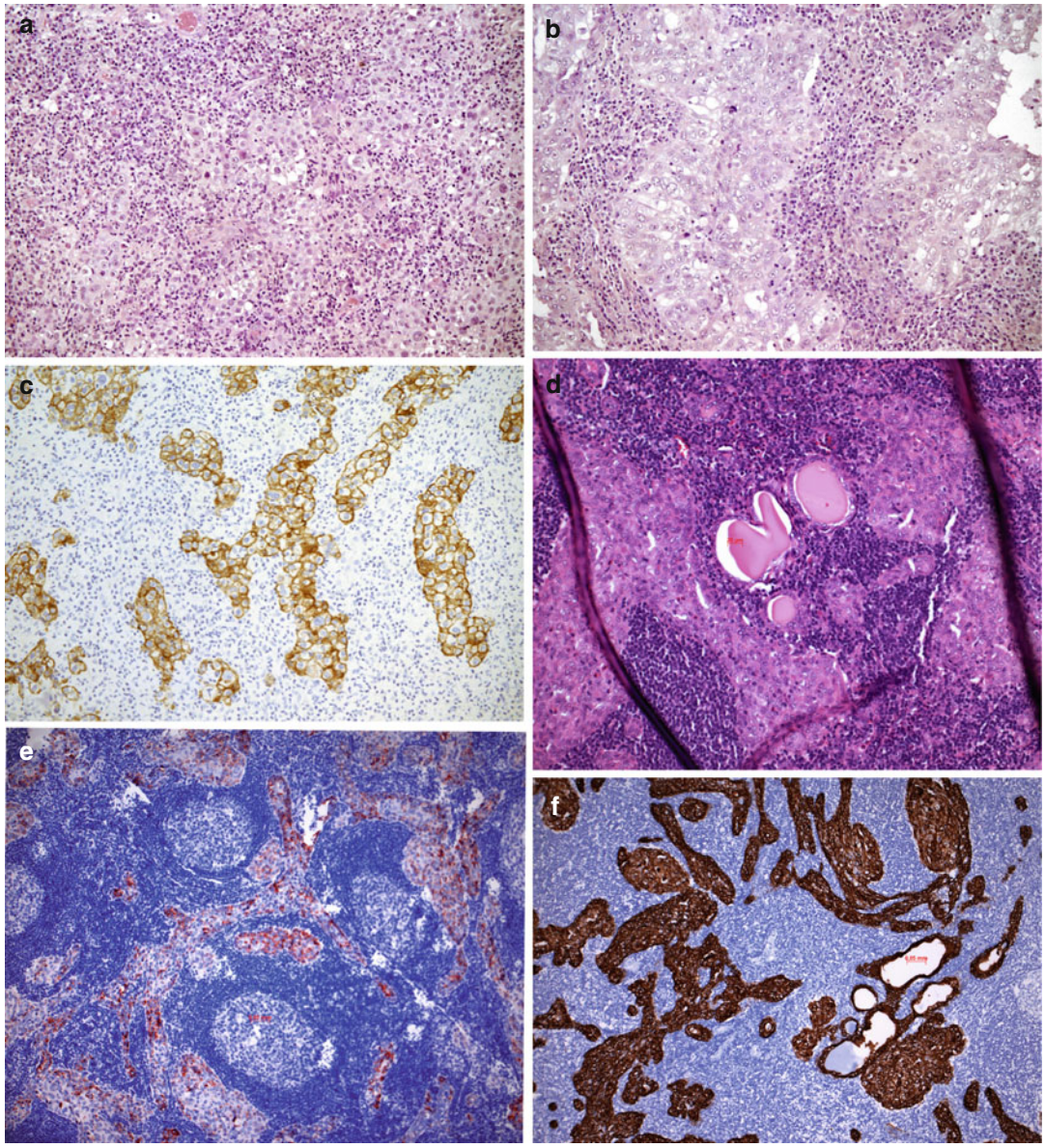

Fig. 17.97 Lymphoepithelioma-like carcinoma. In (**a**, **b**) two cases are shown, where the tumor cells are hardly to discern in the dense lymphocytic background infiltration. By pan-cytokeratin stain in (**c**), the infiltrating tumor cells are highlighted. The tumor cells are large; the nuclei are enlarged as well as the nucleoli. Chromatin is coarse granular and the nuclear membrane often are dark stained to the high traffic of nucleic acids between nucleus and cytoplasm. The cytoplasm is usually pale stained by H&E. In (**d**–**f**) another case is shown. Here the initial decision of primary tumor and lymph node metastasis was hard, because the clinical information was scarce. The tumor cells formed large strands in a dense lymphocytic stroma. The extent of tumor infiltration is best seen on pan-cytokeratin stain (**f**); however of diagnostic help is the staining for cytokeratin 14 (**e**), which is characteristic in many of the tumor cells. H&E, ×200, immunohistochemistry bars 50 μm

lymphoepithelial-like LCs are positive for EBV, and EBV seems to play a role in carcinogenesis, whereas in Caucasians these carcinomas are negative for EBV.

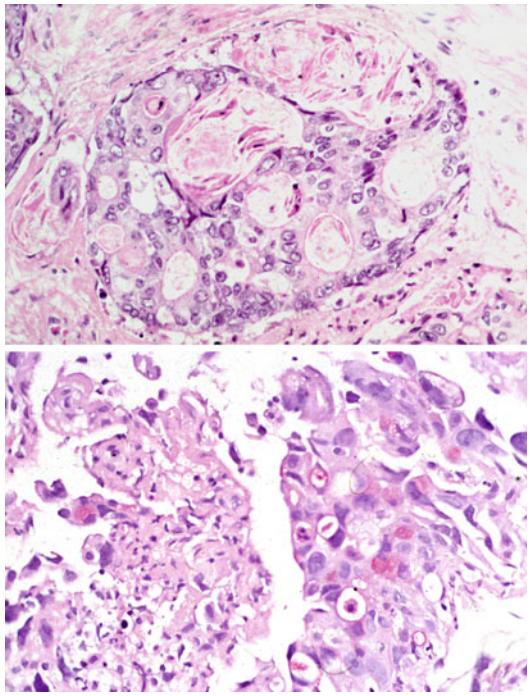

Fig. 17.98 Two cases of adenosquamous carcinomas, both are of mixed type; in the *upper panel*, there are cells with keratinization as well as cells forming acinar structures (H&E). In the *lower panel*, another case is shown, again some single cells with keratinization but a majority of cells producing mucin (PAS stain). ×400

17.3.8 Adenosquamous Carcinoma

Adenosquamous carcinoma, although not regarded as a major type of pulmonary carcinomas, will be discussed here. A mixture of squamous and adenocarcinoma cells characterize it; each component should be represented by at least 10%. Adenosquamous cell carcinoma can present as a collision tumor, i.e., an adenocarcinoma and a squamous cell carcinoma merges. But there are also true mixed adenosquamous carcinomas. In these cases within cell clusters, both differentiations are seen. In contrast to high-grade mucoepidermoid carcinoma, keratinization does occur in adenosquamous ones. In addition mucoepidermoid carcinoma is a centrally located carcinoma with an endobronchial component, whereas adenosquamous carcinoma is usually peripherally located. Studies on these carcinomas have shown that despite the two phenotypes, these carcinomas represent a clonal proliferation [269], which has also an impact for molecular testing: these carcinomas can harbor a mutation for EGFR and also for EML4-ALK and ROS1 [270–272] (Table 17.3).

17.3.9 Diagnosis on Small Biopsies and Cytology Preparations

Most pulmonary carcinomas are detected at a late stage when metastasis already had occurred. Therefore in approximately 75% of NSCLC and

Table 17.3 Useful immunohistochemical markers for differentiation; ApoA: surfactant apoprotein A

	LMW CK	HMW CK	P40	TTF1	ApoA	CK20	S100	NE markers
Squamous cell	+	+	+	±	–	–	–	–
Small cell	+	–	±	+	–	–	–	+
Adenocarcinoma	+	–	–	+[a]	+	±[c]	+[d]	–
Large cell	+	±	±	±	–	–		–
LCNEC	+	–	±	–	–	–	–	+
Adenosquamous	+	Focal +	+	+[b]	±	–		–
Mucoepidermoid	+	Focal +	–	+[b]	–	Focal+	Focal+	–

[a]Mucinous adenocarcinomas can be negative for TTF1
[b]Most often only the adenocarcinoma component is positive for TTF1
[c]CK 20 can be positive in central adenocarcinomas of the bronchial gland type
[d]S100 will stain Langerhans and dendritic reticulum cells, which are increased in papillary AC and IS-AC, and thus can help in the differentiation from metastatic AC

90 % of SCLC, no resection is possible and instead small biopsy samples or fine needle aspirates have to be used for diagnosis. Therefore most of the time, pulmonary carcinomas are diagnosed with these small samples. In the 2015 WHO classification, this has been taken into account, and diagnostic criteria were adapted also to cytology preparations and small biopsies. The criteria for diagnosis have been included in the respective entity, but some general remarks are discussed here.

(a) Cytology

Cytological material comes as smears from fine needle aspirations and from brush. The cell preparations can be of various qualities depending on the experience of the clinician performing the smears. Tumor cell may be well preserved and easy to diagnose. Sometimes the accurate diagnosis might be impossible, especially in high-grade and undifferentiated carcinomas.

Immunocytochemistry is possible on smears but requires distaining of the smears followed by immunocytochemical procedures. This is time consuming and usually allows not more than two antibodies to be evaluated.

Cellblock technique is a good alternative. Cells from aspiration or brushes are not smeared on glass slides but dissolved in physiological solutions. The cells are centrifuged and coated in agarose or fibrinogen. After fixation in formalin, the cell pellet can be embedded in paraffin and sectioned. With this preparation immunohistochemical investigations can be done as usual. Molecular and genetic investigations can be done on cytological material; however, it is limited to a few investigations (sample size limitations). EGFR mutation testing can be done, if enough tumor cells are present (at least 200 cells).

(b) Biopsies

Biopsies are obtained from bronchial mucosa (usually in centrally located carcinomas), from the peripheral lung via bronchi (transbronchial biopsies), and transthoracic with a core needle from peripheral tumors. Three to five biopsies and two to three needle biopsies from different sites are usually sufficient and will allow immunohistochemical investigations, mutation analysis, FISH, or CISH/SISH. Up to 30 sections can be done with good biopsies. It is advised to perform up to 15 unstained sections together with the H&E-stained sections for any additional investigations.

(c) Diagnostic criteria in cytological preparations and biopsies

Tumors can be diagnosed most often with the same accuracy as in resected specimen. Immunohistochemistry will assist in the diagnosis of undifferentiated carcinomas. In the few remaining cases, which do not show any differentiation either histologically nor expressing any differentiation, marker should be diagnosed as carcinoma not otherwise specified (NOS). These cases should be transferred to molecular investigation for driver gene mutations as adenocarcinomas or squamous cell carcinomas.

(d) Ancillary techniques for the subtyping of lung carcinomas

Some special stains can still be used for subtyping of carcinomas. PAS and other mucin stains can be used to diagnose mucinous adenocarcinomas. Immunohistochemical stains can be used to help differentiate squamous cell, large cell, and adenocarcinomas. Squamous cell carcinomas express high molecular cytokeratins, most useful is CK5/CK6, and almost all cells are also positive for the basal cell marker p63 or better for the truncated version p40. Adenocarcinomas are negative for CK5/CK6 and positive for CK7; a few single cells can be stained for p63 rarely for p40. In addition non-mucinous adenocarcinomas will express NapsinA and surfactant apoproteins A and B. Mucinous adenocarcinomas will express CK7 a few also CK20, but most are negative for CDX2. Large-cell carcinomas are negative for CK5/CK6 and positive for CK7; several cells are positive for p63. Neuroendocrine carcinomas will stain for NCAM (CD56), chromogranin A, and synaptophysin. NCAM (140 kDa

Table 17.4 Useful markers for the differentiation of common lung carcinomas in biopsies, cytology, and resection specimen

Tumor type	Negative	Positive
SCLC	p63, p40	NCAM[b], CK7, TTF1
LCNEC	p63, p40	NCAM, CK7, TTF1±
Adeno	CK20[a], NEmarkers[b]	TTF1, CK7[c], SurfApoA/B, NapsinA
SCC	TTF1, NEmarkers[b]	CK5/6, p63, p40
LC	p63±, CK5/6	TTF1±, CK7, CK14±

[a]CK20 can be positive and CK7 negative in centrally located and mucinous AC
[b]Neuroendocrine markers: most useful NCAM, less chromogranin A, synaptophysin; NE makers can be focally positive in NSCLC, usually less than 25 % of cells are stained; in this case the diagnosis is NSCLC with neuroendocrine features
[c]CK7 is positive in most adenocarcinomas, but a few can be negative

variant) is most useful, because the intensity of the stain increases in high-grade carcinomas and is faintly positive in carcinoids (Table 17.4).

(e) Primary versus metastasis

The success in chemotherapy in general has resulted in an increase of secondary tumors. Patients survive breast, prostate, and colon carcinomas and suffer from secondary tumors like lung carcinomas. Our clinical colleagues nowadays often ask if a patient suffers from metastasis of a known carcinoma or a secondary lung carcinoma. Can we answer this question on small biopsies or even cytology? Here lies the main strength of immunohistochemistry. Using panels of differentiation marker, we can in most instances provide the most likely primary site of the carcinoma.

However, there are caveats to mention: there are mucinous pulmonary adenocarcinomas, which express CK20, negative for CK7. Some of these are centrally located adenocarcinomas probably arising from stem cells at the bronchial glands. Also an enteric type of adenocarcinoma has been described, which might express the same markers as colonic adenocarcinomas. However, also classical cytokeratin and MUC gene expression has been observed (Table 17.5).

Table 17.5 Markers to separate primary lung carcinomas from metastasis

Origin	Positive	Negative
Colon	CK20, CDX2[a]	CK7, TTF1, NapsinA
Breast	MFG1, MFG2, ER[b], PR, CK7	NapsinA, SurfApoAB
Pancreas	Pancreatic stone protein, CK7	SurfApoB, NapsinA±
Prostate	PSA	CK5/6
Ovary	CK7	TTF1, SurfApoAB
Larynx	CK5/6	CK7
Esophagus	CK4, CK5/6	CK7
Stomach	CK7, ß-catenin, E-cadherin	TTF1, SurfApoA/B, NapsinA

[a]CDX2 can be positive in some mucinous adenocarcinomas of the lung, and CK20 can be expressed by mucinous and enteric adenocarcinomas
[b]Less useful because of positivity in the lung; milk fat globulin 1 and 2 are usually coexpressed in breast carcinomas, whereas only one of them can be expressed in carcinomas of the ovary and lung. PR in contrast to ER is rarely expressed in pulmonary adenocarcinoma

17.3.10 Salivary Gland-Type Carcinomas

Salivary gland tumors can occur in the lung, always in a central location. These are rare carcinomas with a wide range of affected ages, from children as early as 3 years of age and also in old patients.

17.3.10.1 Mucoepidermoid Carcinoma (MEC)

Previously mucoepidermoid tumor and carcinoma were discerned, the former a slow-growing well-differentiated variant, the latter a poorly differentiated aggressive carcinoma. In the new WHO classification, low-grade and high-grade carcinomas are the adequate terms.

Clinical Symptoms and Gross Appearance

Due to the central location, MEC grows as a polypoid mass occluding large bronchi and thus causing obstruction (Fig. 17.99a) – this is often the cause for the main clinical symptoms poststenotic bronchopneumonia and productive cough. On X-ray and CT scan, a central mass is seen, and on bronchoscopy, the endobronchial part of the tumor is recognized.

Morphology

In low-grade carcinomas, cystic and solid areas found in both mucin-producing columnar cells form glands, tubules, and cysts. Within the glandular areas, squamous epithelium is interspersed; the tumor cells are usually nonkeratinizing. In addition tumor cells with transitional cell morphology can also be seen (Fig. 17.99b–d). Necrosis is usually absent; mitoses are rarely found. The stroma is very often edematous, focal hyalinized; sometimes an amyloid-like material can be seen. Invasion is seen at the basis of the polypoid tumor: tumor cells invade the submucosal tissue, the bronchial cartilage, preexisting glands, and sometimes also nerves. This variant is a slowly growing carcinoma with infrequent or late lymph node involvement; distant organ metastasis can occur late in the course [273–276].

In high-grade carcinomas the distinction from adenosquamous carcinoma might sometimes be impossible, due to overlapping features. The proof is the mixture of squamous and mucin-producing columnar cells within a gland, endobronchial growth, and absence

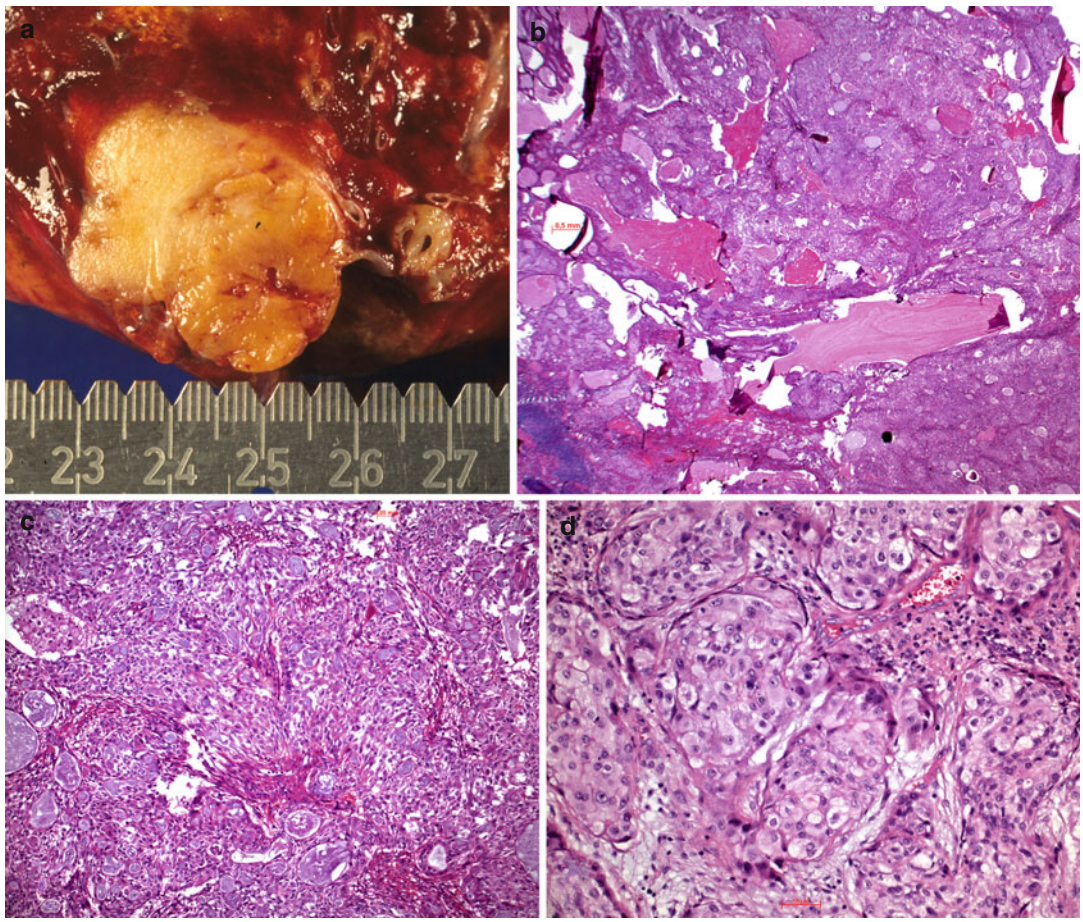

Fig. 17.99 Mucoepidermoid carcinoma. (**a**) A low-grade carcinoma resected in a 12-year-old girl. Note the central location in a main lobar bronchus. (**b**) Overview of the tumor with some glandular and cystic spaces, filled with mucus. (**c**) shows the glandular component and also the squamous epithelium. The amount of each component can vary, as shown in case (**d**); here the cells are predominantly of a nonkeratinizing squamous type. In these tumors the EGFR-PI3K-mTOR pathway is often activated but on a posttranslational level – mutations of the EGFR gene does not occur: (**e**) PI3K predominantly in squamous cells, (**f**) mTOR again much more intense in the squamous component. (**g**) MIB1 staining shows the low percentage of positively stained tumor cells. (**h**) High-grade mucoepidermoid carcinoma. There is a dominance of nonkeratinized squamous cells. H&E, bars 500, 50, and 20 µm

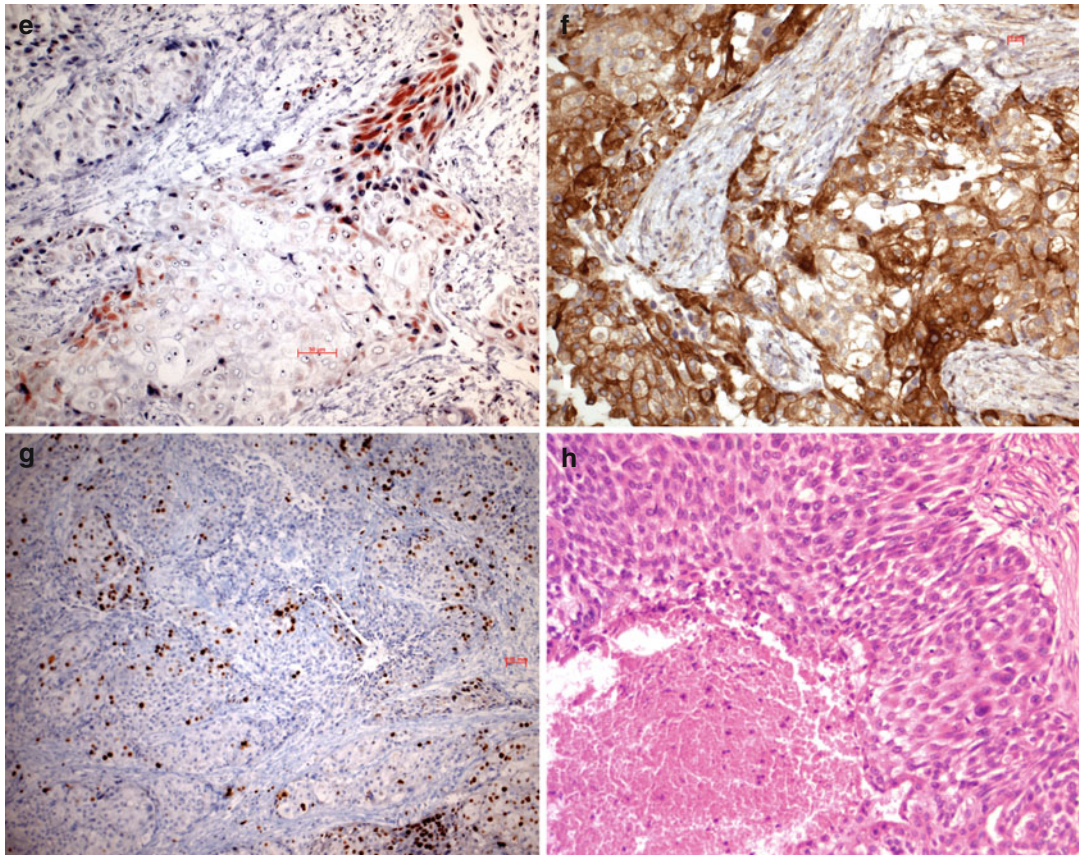

Fig. 17.99 (continued)

of keratin pearls and an in situ component. A centrally located tumor is usually a MEC, whereas adenosquamous carcinomas most often arise in peripheral location. In high-grade carcinomas, cystic areas are absent, the tumor grows in solid sheets and nests, squamous and transitional cells predominate with few intermingled mucin-producing cells, necrosis is frequent, as well as many mitotic figures (Fig. 17.99h). High-grade variants are diffusely infiltrating and set frequent metastasis. The prognosis of high-grade mucoepidermoid carcinomas is similar to adenosquamous carcinoma or other NSCLC. MEC can be diagnosed on biopsies as well as cytology preparations if both elements are present. The diagnosis is easier on well-differentiated MEC, whereas much more difficult in high-grade MEC. Activation of the EGFR pathway with activation of phosphoinositol-3-kinase and mTOR downstream is common but on a protein level (posttranslational; Fig. 17.99e, f) [276].

Chromosomal alterations have been described in these tumors, and two fusion genes with mammalian mastermind-like 2 (MAML2) have been found. The balanced translocation t(11;19) (q21; p12~p13.11) is known for a while; a MAML2 fusion transcript with MECT1 was found in a child with mucoepidermoid lung carcinoma. This fusion gene can lead to an altered cyclic adenosine monophosphate signaling. The MECT1-MAML2 fusion gene is associated with a better prognosis in MEC tumors [277]. Another fusion oncogene CRTC1-MAML2 has been demonstrated in salivary gland MEC. Interestingly MEC cell lines with t(11;19) are sensitive to gefitinib. As CRTC1-MAML2 fusion gene upregulates amphiregulin, this could confer sensitivity to EGFR tyrosine kinase inhibition with gefitinib [278].

17.3.10.2 Adenoid-Cystic Carcinoma (ACC)

Clinical Symptoms and Gross Morphol ogy

Similar to the salivary counterpart, adenoid-cystic carcinoma of the bronchus is a slowly growing tumor with late lymph node and distant organ involvement. However, recurrence is frequent. They occur in the trachea and the large bronchi as far as normal bronchial glands are found. ACC usually infiltrate the bronchial or tracheal mucosa and spread into the submucosa and the surrounding soft tissues. Thus the tumor compresses the bronchus, which will result in obstructive symptoms. Due to the common infiltration of large nerves, also symptoms from this side can occur. On CT scan a centrally located tumor is seen, usually not much above 3 cm in diameter (Fig. 17.100).

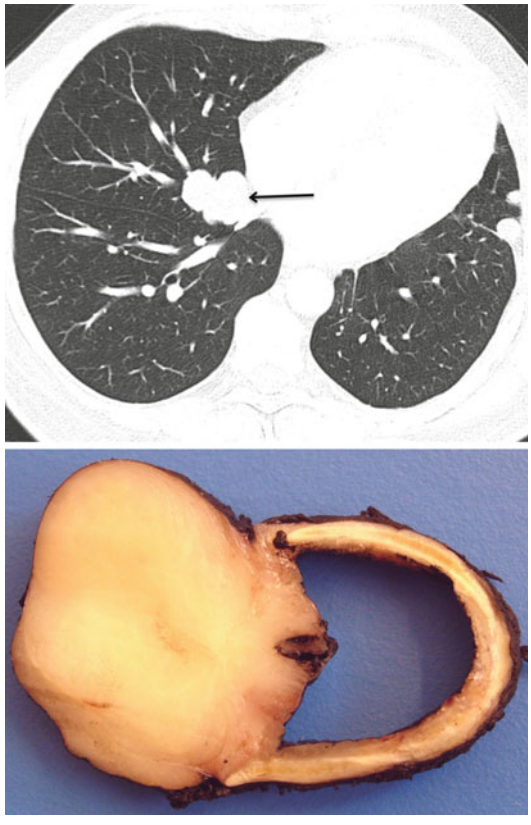

Fig. 17.100 Adenoid-cystic carcinoma, *upper panel* CT scan, *arrow point* to the central tumor. Obstruction of the lobar and segmental bronchi can be seen (widening); they are filled with mucus. *Lower panel* cut surface of an adenoid-cystic carcinoma, here resected from the trachea close to the bifurcation

On resection some special care is to be taken: tumor cells can surround the cartilage and spread into adjacent tissues. The so-called skip lesions are common, i.e., between tumor cell nests there can be a larger area of uninvolved normal tissue. Therefore on the evaluation of resection margins, a good sampling is important, and for frozen section, diagnosis of resection margins step sections are recommended.

The tumor forms pseudotubules filled with mucin-like material but also solid nests and sheets. These structures are lined by cuboidal cells with round bland-looking nuclei; most important there is no "lumen-oriented" cell polarity. Necrosis is absent and mitoses are infrequent (Fig. 17.101a–d). The mucin-like material is composed of matrix proteins of the basal lamina and thus will stain for collagen type 4, fibronectin, and alike (Fig. 17.101e, f). The tumor cells express epithelial markers, such as cytokeratins, but in part may also be positive for mesenchymal markers (SMA, S100 protein, vimentin). ACC can be easily diagnosed on small biopsies and cytology due to the tubular and sheet structure. On cytology metachromasia is seen on Giemsa, azure blue, or toluidine blue stain (the matrix proteins stain violet; Fig. 17.102).

17.3.10.3 Epithelial-Myoepithelial Carcinoma (EMEC)

EMEC is a rare salivary gland-type carcinoma; usually single case reports are found in the literature. As the other carcinomas, this is also a centrally located carcinoma, and endobronchial component can be present. It forms a solid mass, which can be detected on CT scan. The clinical symptoms are unspecific. EMEC is a slowly growing tumor.

EMEC consists of two components: one element is composed of tubular ducts similar to adenocarcinoma, but an additional component exists with spindle and/or plasmacytoid cells, positive for myoepithelial markers (SMA, S100 protein). Usually the inner epithelial layer of the duct-like structures is positive for epithelial markers (EMA, cytokeratins), whereas the outer layer is positive for S100 and SMA. The nuclei are round, the chromatin is finely distributed, and nucleoli are small. Mitosis is infrequent; there is rarely more than one mitosis per HPF (Figs. 17.103 and 17.104). Rarely the tumor

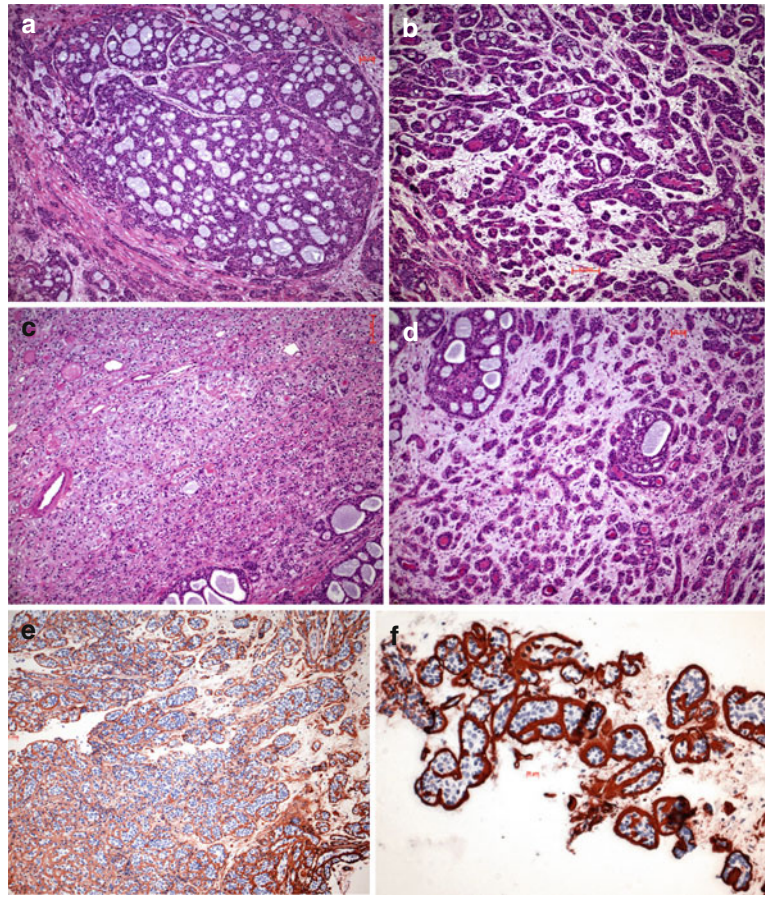

Fig. 17.101 Adenoid-cystic carcinoma; (**a**–**d**) different morphological patterns, the classical cystic pattern is seen in (**a**), in (**b**) there are small tubules and many solid and nesting structure, in (**c**) the solid strand pattern dominates, and in (**d**) a mixture of cystic and solid and small tubular pattern is present (H&E). (**e**) Shows the reaction for collagen IV here most often deposited around the strands of cells. In (**f**) a needle biopsy is shown, where immunohistochemistry for collagen IV was done to confirm the diagnosis. Bars, 500, 100, 50, and 20 µm

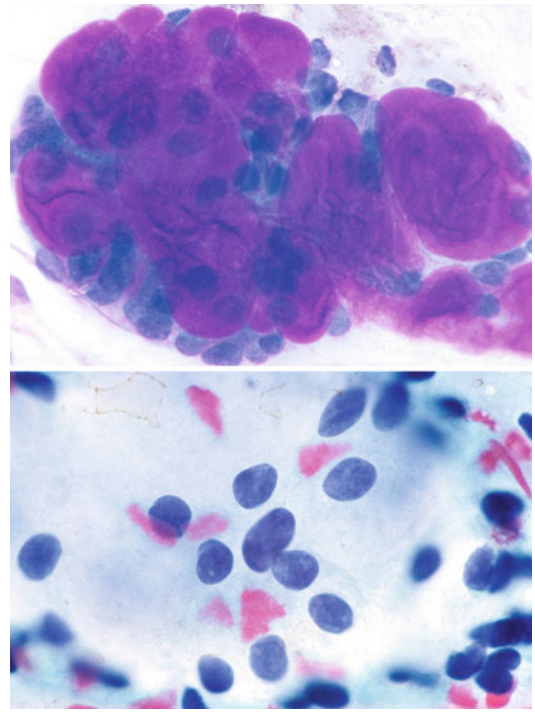

Fig. 17.102 Cytology of adenoid-cystic carcinoma. In the *upper panel*, the characteristic metachromasia of the proteinaceous material produced by the tumor cells is seen. In such a case, the diagnosis can be made right away. In the *lower panel*, the cytologic picture shows tumor cells with finely dispersed chromatin and enlarged nuclei. Here several differential diagnoses have to be considered. Giemsa, ×630

might be composed of myoepithelial cells only. In these cases the term myoepithelioma is used. There can be recurrences, but surgical removal usually cures the patient. The diagnosis might be approached in cytological and bioptic material, if the dual cell pattern is present in the sample.

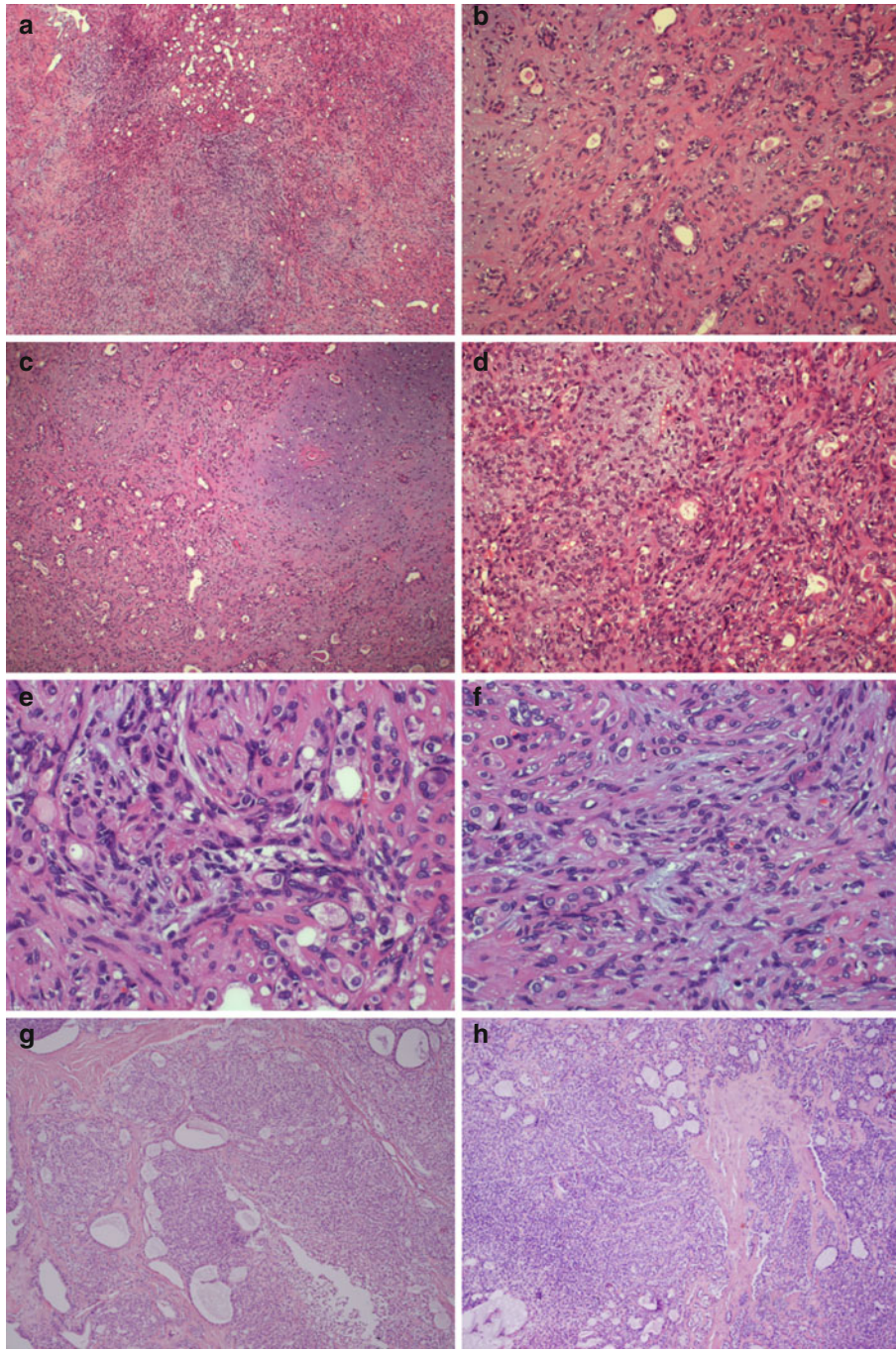

Fig. 17.103 Epithelial myoepithelial carcinoma, two cases are shown. (**a**–**f**), case 1, shows in the overview (**a**) bluish myxoid areas and also eosinophilic areas corresponding to matrix protein deposition. In (**b**) a mixture of tubular structures and diffuse myoepithelial cell proliferation is seen; (**c**) highlights the myxoid areas with spindle cells, surrounded by tubular epithelial proliferations. In (**d**–**f**) the mixture of tubular proliferations and myoepithelial cells including the myxoid areas (**f**) are demonstrated in higher magnification. Case 2 (**g**, **h**) is a case with dominant epithelial tubular structures; the myoepithelial component is less visible. H&E, ×12, 50, 100, 200

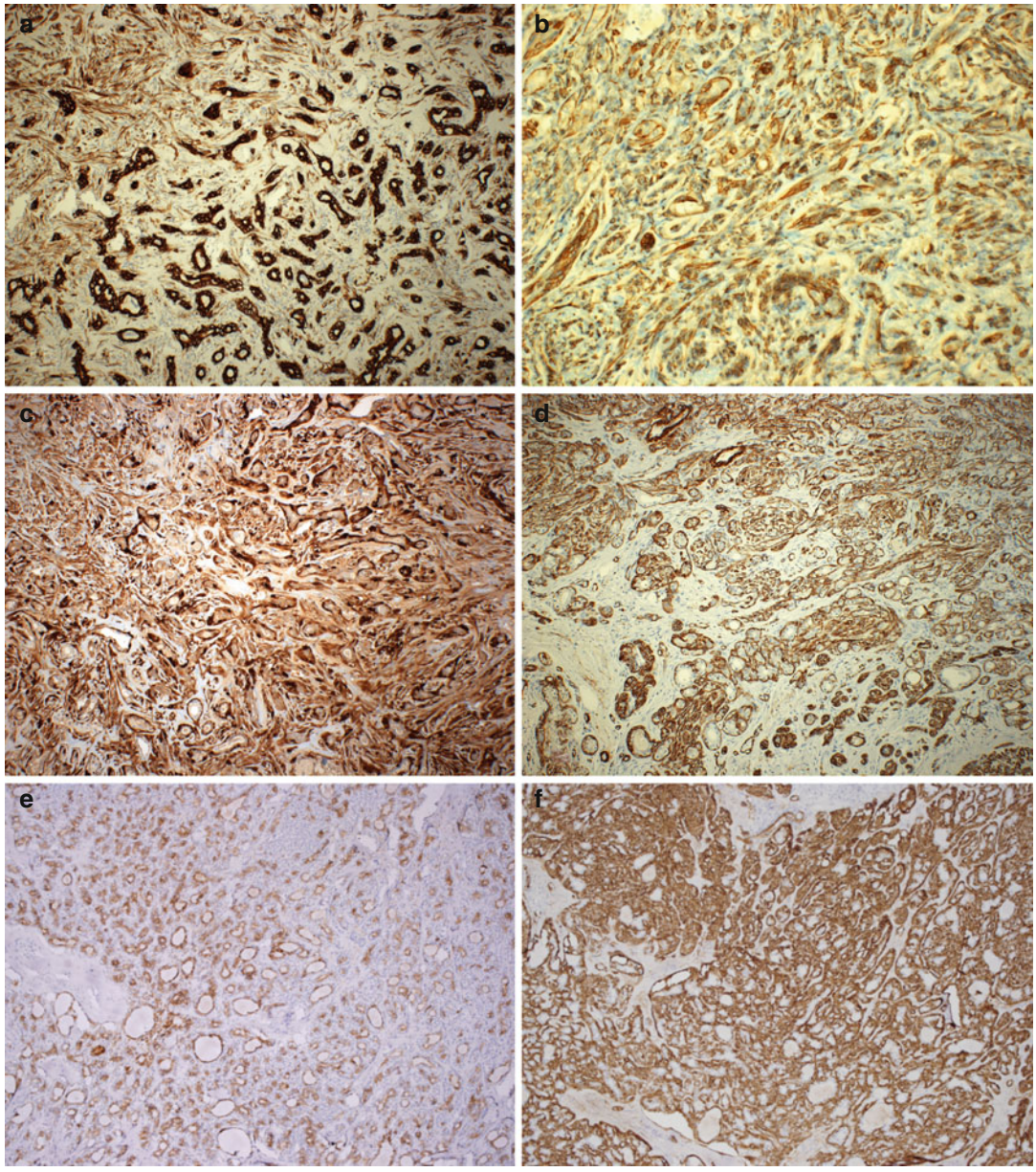

Fig. 17.104 Immunohistochemistry of EMEC, A-D case 1, E-F case 2. (**a**) Staining for cytokeratin 7 shows strong staining of the tubular epithelia, whereas the myoepithelial cells are weakly stained. (**b**) By cytokeratin 14 the myoepithelial cells are strongly stained, whereas the tubular component is weakly stained or remain even unstained. (**c**) Epithelial and myoepithelial components are stained by S100 protein antibodies; by antibodies for smooth muscle actin (**d**), the myoepithelial component of the tumor is seen. In case 2 the epithelial component is stained by cytokeratin 7 (**e**), and both component are positive for S100 protein (**f**). ×100, 60

17.3.10.4 Acinic Cell Carcinoma

This is another rare salivary gland carcinoma. The tumor is also slowly growing and forms a central mass. Endobronchial growth is uncommon. The tumor cells show round nuclei, chromatin is finely dispersed, and nucleoli are small. Usually few mitoses are seen. The characteristic features are the acidophilic/azurophilic granules in the tumor cell cytoplasm. These carcinoma cells are positive for zymogen and will

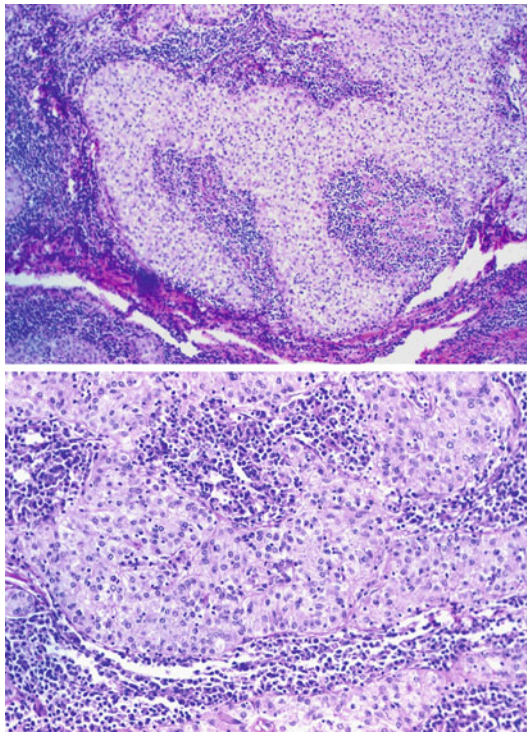

Fig. 17.105 Acinic cell carcinoma of the lung. In the *upper panel*, an overview is given; the carcinoma is surrounded by numerous plasma cells and small lymphocytes; in the *lower panel*, the morphology of the tumor cells is better seen. The cells are middle sized, nuclei are slightly enlarged, nucleoli are visible, and the nuclear membrane is accentuated by the H&E stain. Within the cytoplasm fine granular pink material is dispersed, corresponding to the characteristic granules, which on zymogen stains will be positive. PAS, ×100, 200

also positively be stained by PAS (Fig. 17.105). Resection is recommended in this slowly growing salivary-type carcinoma. Metastasis can occur but usually late in the course.

17.3.11 The Sarcomatoid Carcinomas

The sarcomatoid carcinomas are a group of carcinomas with sarcomatoid features. Within this group there is pleomorphic carcinoma, spindle and giant cell carcinoma, pulmonary blastoma, and carcinosarcoma. Whereas almost all these carcinomas share something in common, either morphology or genetic features, pulmonary blastoma does not fit into this group: morphology is different and no similar changes are seen in the others from this group, and also molecular biology is different [279].

Clinical Symptoms

These are all high-grade carcinomas, rapidly progressing and with a dismal outcome. They form large tumor masses within the lung parenchyma and can present as a central or peripheral tumor. The symptoms are unspecific with weight loss, cough, and chest pain in case of thoracic wall and pleura infiltration and hemoptysis.

On CT scan a large tumor is seen; lymph nodes are often involved and enlarged.

17.3.11.1 Spindle Cell Carcinoma

On gross morphology this carcinoma resembles a sarcoma with fleshy appearance, whitish grayish, and sometimes with necrosis and hemorrhage. On histology the carcinoma is composed of spindle cells arranged in cords and strands. The nuclei are enlarged and round to ovoid or fusiform; chromatin is coarse granular and irregularly distributed. Nucleoli are enlarged and middle sized. Mitoses are frequent, often >5/HPF (Fig. 17.106a, b).

By immunohistochemistry the tumor cells are positive for pan-cytokeratin but also may show expression of smooth muscle actin (SMA). In few cases the tumor cell lose their cytokeratin expression – this should not prompt a change in the diagnosis. Epithelial to mesenchymal transition (EMT) is very common in this carcinoma. This is also seen in single cell infiltration or small tumor cell complexes invading the lung.

17.3.11.2 Giant Cell Carcinoma

This is the most aggressive carcinoma of the lung. The few cases diagnosed in our center all died within 4 months after diagnosis despite aggressive chemotherapy. On gross the tumor is whitish grayish with many necroses. On histology giant cells are the main component: there are multinucleated giant cells but also cells with large single nucleus. Nuclear size is usually larger than 40–50 μm in diameter; multinucleated tumor cell can measure 200 μm. Nucleoli are bizarre and large. Chromatin is coarse granular

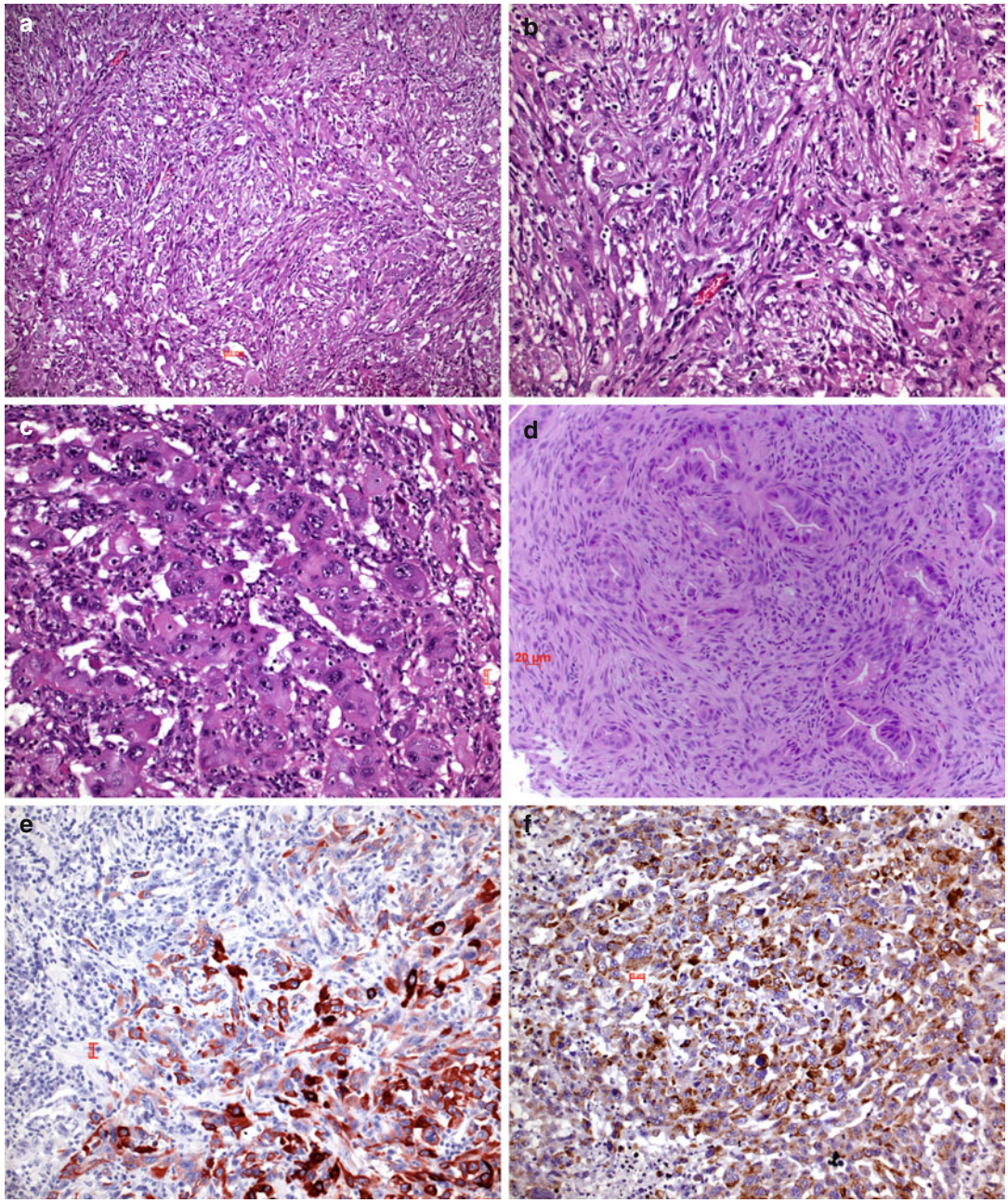

Fig. 17.106 Spindle cell carcinoma (pure form **a**, **b**), the tumor is entirely composed of spindle cells, which are positive for either cytokeratin or smooth muscle actin. This is a sign of epithelial to mesenchymal transition, also an explanation why these carcinomas are so aggressive. (**c**) Shows a pleomorphic carcinoma composed of giant cells and undifferentiated carcinoma, in (**d**) another pleomorphic carcinoma is shown here combined with an enteric variant of adenocarcinoma. (**e**, **f**) shows immunohistochemical stains for cytokeratin (**e**), and vimentin (**f**) in a pleomorphic carcinoma with spindle cell and large-cell carcinoma. H&E, bars 50, 20 µm

and unevenly distributed; nuclear membrane is intense stained due to high traffic of nucleic acids between cytoplasm and nucleus. There should be at least 10 % giant cells per HPF for the diagnosis of a giant cell carcinoma (Fig. 17.107). The tumor is loosely cohesive, similar to SCLC. The tumor cells usually coexpress low molecular weight cytokeratins and vimentin.

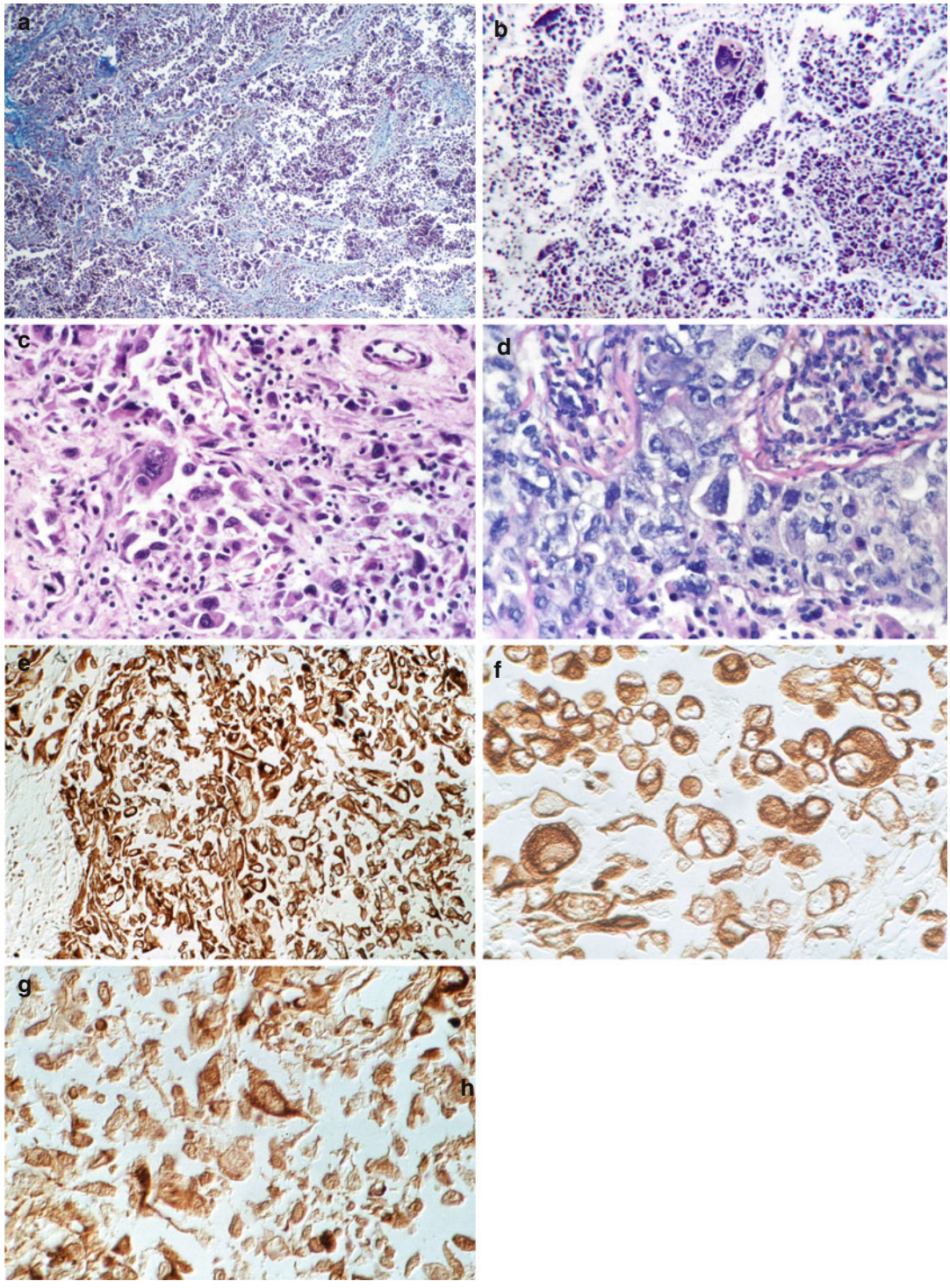

Fig. 17.107 Giant cell carcinoma of the lung. In (**a**, **b**) even in low magnification, the giant cells already stick out. (**c**, **d**) Higher magnification show multinucleated as well as large tumor cells with enlarged nuclei. Many of these nuclei are >50 µm; a few may even reach 200 µm. (**e**, **f**) Immunohistochemistry for cytokeratin showing positivity of the tumor cells; however, most of them coexpress vimentin (**g**). ×12, 25, 200, 100, 200

17.3.11.3 Pleomorphic Carcinoma

Pleomorphic carcinoma is defined as a carcinoma with either a spindle or giant cell component and any of the NSCLC components. This can be a squamous cell, large cell, or adenocarcinoma. However, there is an exception to the rule: a small-cell carcinoma with spindle cell component should be called mixed or combined SCLC, but I recommend to list the other components in the diagnosis too (Fig. 17.106d, e, f). On small biopsies the second component of the carcinoma might be missing (Fig. 17.106d). On cytology the diagnosis depends on what cell types are harvested: if spindle or giant cells are present, the diagnosis will go into the right direction (Fig. 17.108); otherwise any other NSCLC might be diagnosed.

Pleomorphic carcinomas are highly aggressive carcinomas, have a worse prognosis, and are less responsive toward chemotherapy. Thus the diagnosis of pleomorphic carcinoma by itself is already a worse prognostic "marker" [280]. EGFR tyrosine kinase inhibitor therapy might be an option in a few cases, usually those with an adenocarcinoma component, although less effective; an antiangiogenic treatment is another hope as these carcinomas express VEGF and HIF1 [271, 281, 282] (Table 17.6).

17.3.11.4 Pulmonary Blastoma

Pulmonary blastoma was placed into the group of sarcomatoid carcinomas, because of the combination of epithelial and mesenchymal tumor components. In pulmonary blastoma the major and characteristic element is an adenocarcinoma of fetal type; in addition, morules, similar to that seen in endometrioid carcinomas, can be found within the acini. As in fetal type of adenocarcinoma, the nuclei are round to ovoid, and nucleoli are small. Chromatin is granular and irregularly distributed. Mitosis is frequent. Between the epithelial tubules and acini, a primitive mesenchymal stroma is seen, which resembles a fetal lung at the tubular stage. The mesenchymal component is composed of smooth muscle cells, fibroblasts, primitive vascular channels, and rarely nests of primitive chondroid tissue (Fig. 17.109). In most cases the mesenchymal component is

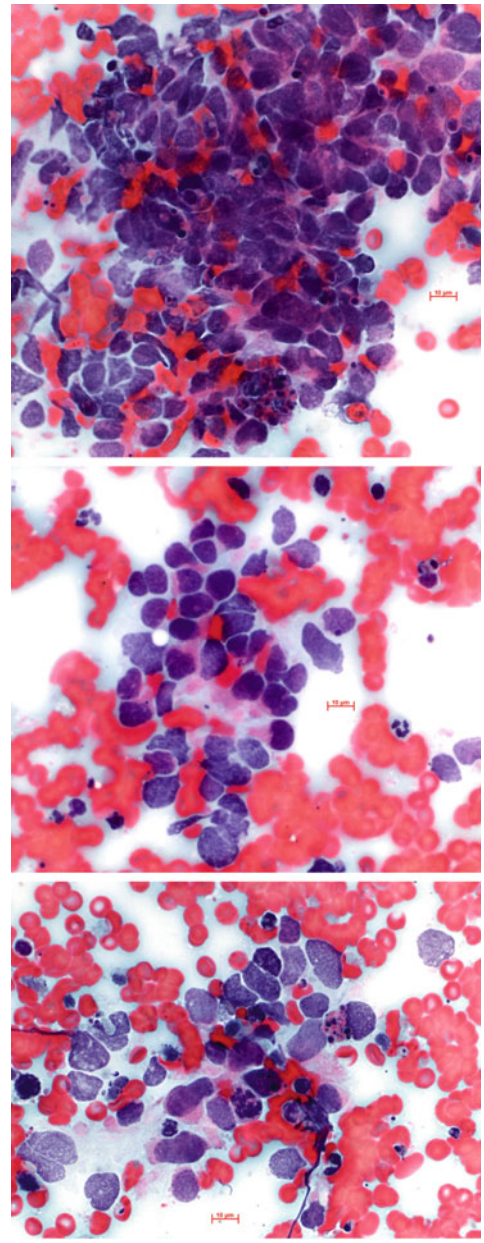

Fig. 17.108 Cytology of pleomorphic carcinoma, here only undifferentiated carcinoma cell are seen; a diagnosis of one of the sarcomatoid carcinomas is impossible. Three different examples are shown. In the upper example, nuclear crowding is evident, nuclei are large polymorphic in all three cases, the chromatin is fine granular, and nucleoli cannot be seen in this preparation but were seen in H&E-stained smears. Cytoplasm is small. A few atypical mitoses are present. Compare the size of the nuclei with neutrophils: they are most often double the size of a neutrophil (28 μm), thus ruling out SCLC. Giemsa, bars 10 μm

Table 17.6 Diagnostic flow chart for sarcomatoid carcinomas

	Pleomorphic CA	Spindle cell CA	Giant cell CA
Spindle cells	Yes[a]	Yes	No
Giant cells	Yes[a]	No	Yes
NSCLC components	Yes	No	No
Cytokeratin	Yes[b]	Yes, may be only focal or even few cells	Yes
Vimentin coexpression	No	No	Yes

[a]Either one of these or both
[b]A part of the carcinoma might be negative for cytokeratins

benign; however, in rare cases it can be malignant. In contrast to carcinosarcoma, the malignant mesenchymal component is a leiomyosarcoma. In metastasis only the epithelial component will be seen in most cases.

It should be reminded that pulmonary blastoma is a mixed epithelial and mesenchymal (biphasic) tumor, whereas pleuropulmonary blastoma (discussed below) is a primitive childhood tumor, devoid of an epithelial differentiation.

17.3.11.5 Carcinosarcoma

Carcinosarcoma is defined as a combination of carcinoma and sarcoma arising within the lung (Fig. 17.110). The carcinoma can be a mixture of all known variants of pulmonary carcinomas, including SCLC and LCNEC, whereas the sarcoma should be composed of heterologous elements: these are osteo-, chondro-, or rhabdomyosarcoma components. The nuclei of both components are large, chromatin is coarse granular, and nucleoli are large. The nuclei are polymorphic often bizarre. Many mitoses are seen (Figs. 17.111 and 17.112).

A carcinosarcoma with an SCLC component in contrast to all other carcinomas is not called combined SCLC but carcinosarcoma with SCLC component. Again to avoid any misinterpretation, after starting with the main diagnosis of a carcinosarcoma, I give a summary of all the component of the carcinosarcoma in my report. So the best treatment can be discussed at the tumor board. Carcinosarcomas as well as pulmonary blastomas are aggressive tumors. There is some primary response to aggressive chemotherapy, but the overall outcome is poor [280]. Immunotherapy might be a new option in carcinosarcomas and the other sarcomatoid carcinomas, because due to their large amount of synthesized neoantigens, they express PDL1 [283].

The diagnosis of carcinosarcoma can be made sometimes on biopsies and cytology preparations if cells from the sarcoma component are present. A blastoma cannot be diagnosed, because the stroma will be either not seen or misinterpreted as normal background lung tissue. Giant cell and spindle cell carcinomas can be diagnosed in cytopathology and biopsies; however, immunohistochemistry will be required.

17.3.12 Primary Intrapulmonary Germ Cell Neoplasms

Germ cell tumors can arise but rarely within the lung. More likely these tumors are derived from a mediastinal primary. Therefore a mediastinal mass and metastasis from a gonadal primary tumor have to be ruled out before the diagnosis of a primary germ cell tumor in the lung can be made. Especially nonseminomatous germ cell tumors follow a predictable pattern of mediastinal dissemination, primarily following the course of the thoracic duct and its major tributaries [284]. Intrapulmonary germ cell tumors may develop from ectopic tissues [100].

17.3.12.1 Embryonal Carcinoma

As in the gonads, this carcinoma is characterized by solid strands of tumor cells; sometimes small tubules, pseudoalveolar, and papillary patterns can be present (Fig. 17.113). It can contain giant cells, which will be positive for βHCG; other cells may express AFP. The tumor cells will express low molecular weight cytokeratins, PLAP, CD30, SOX2, and Oct3/Oct4.

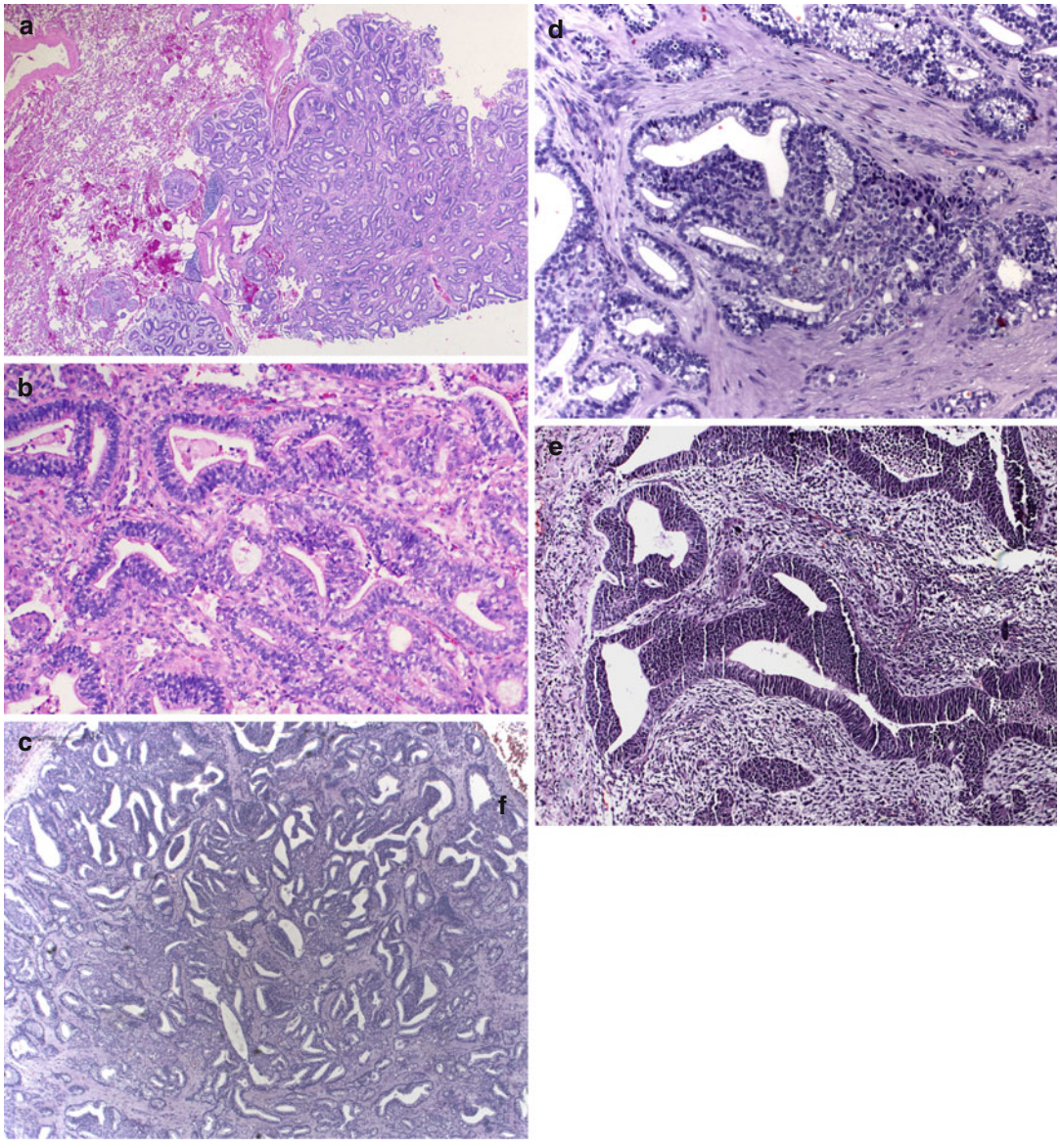

Fig. 17.109 Pulmonary blastoma; an overview of a resection specimen, where the acinar structure of the adenocarcinoma is visible. On higher magnification (**b**) the primitive stroma between the acini of the carcinoma is composed of smooth muscle cells and primitive vascular channels. In (**c**, **d**) the fetal adenocarcinoma shows morules, but the characteristic features of the fetal adenocarcinoma with the clear cells and the apical position of the nuclei is well retained in many cells. The stroma in this case is predominantly composed of smooth muscle cells. In E the blastoma shows primitive mesenchymal cells embedded in a primitive myxoid stroma. The fetal adenocarcinoma does not have much clear cytoplasm, but still the nuclei are often in the apical position. PAS stain demonstrated glycogen in a small percentage of the carcinoma cells. The mesenchymal cells show some atypia; therefore this case was labeled as pulmonary blastoma with mesenchymal component of intermediate dignity. H&E, ×25, 100, 200

Fig. 17.110 Resection specimen of a carcinosarcoma. Note the different colors of the components; however, it can only be stated as a malignant tumor

17.3.12.2 Choriocarcinoma

So far this tumor has only been found in female patients. As in the gonads, this tumor usually presents with hemorrhage and necrosis. Polygonal round cytotrophoblast with distinct cell borders, clear cytoplasm, and single bland nucleus are mixed with large multinuclear syncytiotrophoblast cell with eosinophilic and vacuolated cytoplasm (Fig. 17.114). βHCG, HPL, EMA, cytokeratin 7, PLAP, and CEA are the helpful positive markers.

17.3.12.3 Yolk Sac Tumor

As in the testis, this tumor can present with different patterns such as reticular, papillary, or cord-like pattern of cuboidal cells. Cells have bland nuclei; in almost half of the cases,

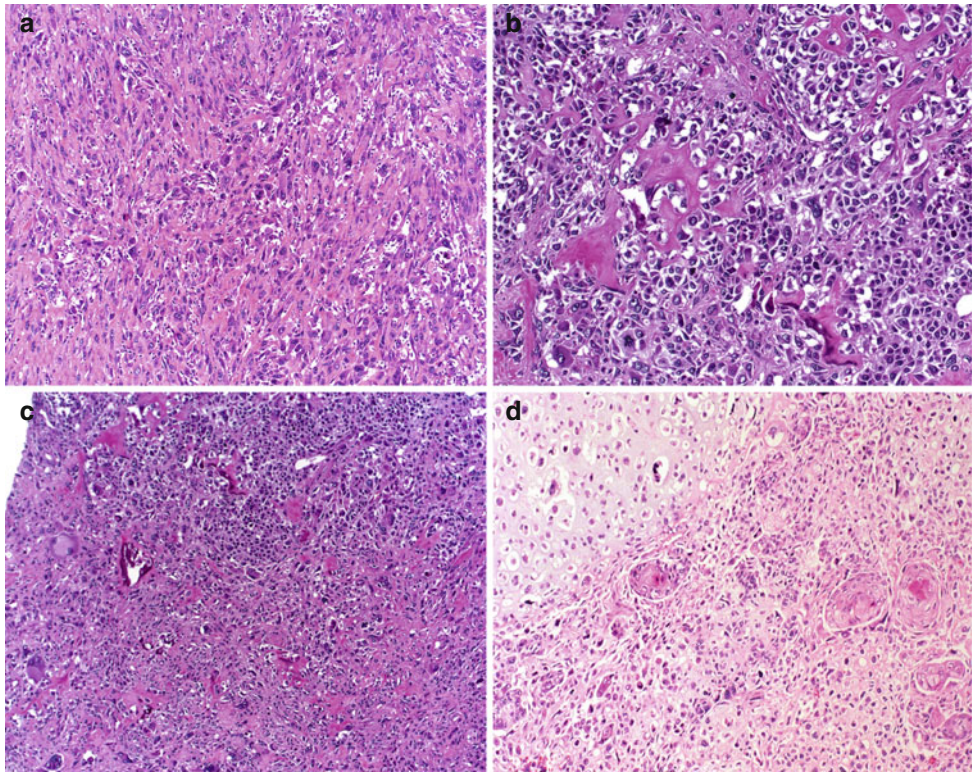

Fig. 17.111 Carcinosarcoma examples; (**a**–**c**) a carcinosarcoma composed of a solid adenocarcinoma (**c** upper half) and a pleomorphic sarcoma (**a**), and finally an osteosarcoma component (**b**). In (**d**) a squamous cell carcinoma with a chondrosarcoma is shown. (**e**–**h**) is another carcinosarcoma with an adenocarcinoma (**e**), an osteosarcoma with osteoid deposition (**f**), and two undifferentiated cellular compartment (**g**, **h**), which did only express vimentin, no other marker. H&E, 50, 100, 200

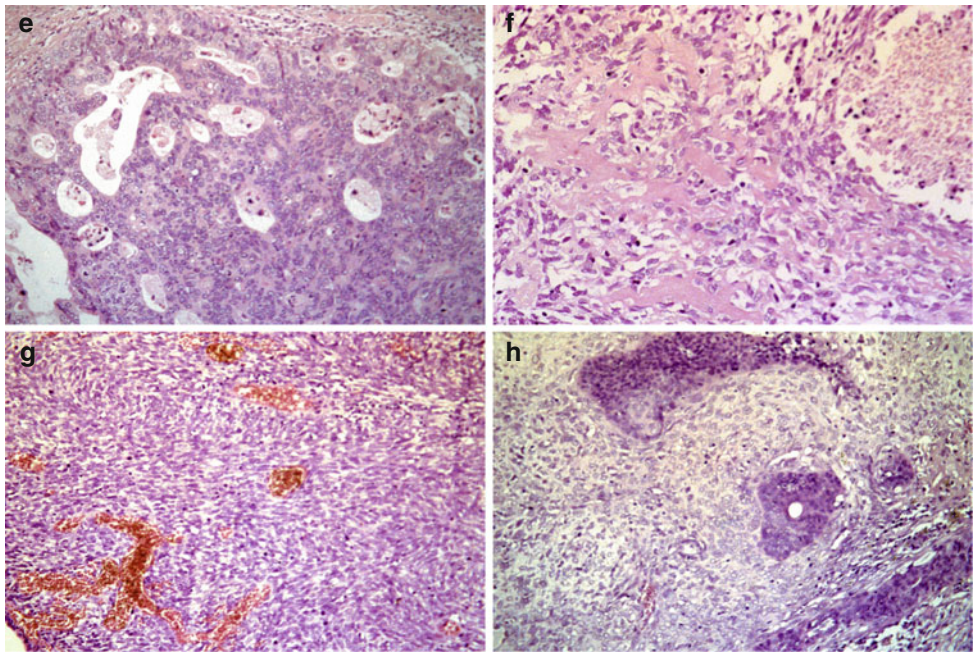

Fig. 17.111 (continued)

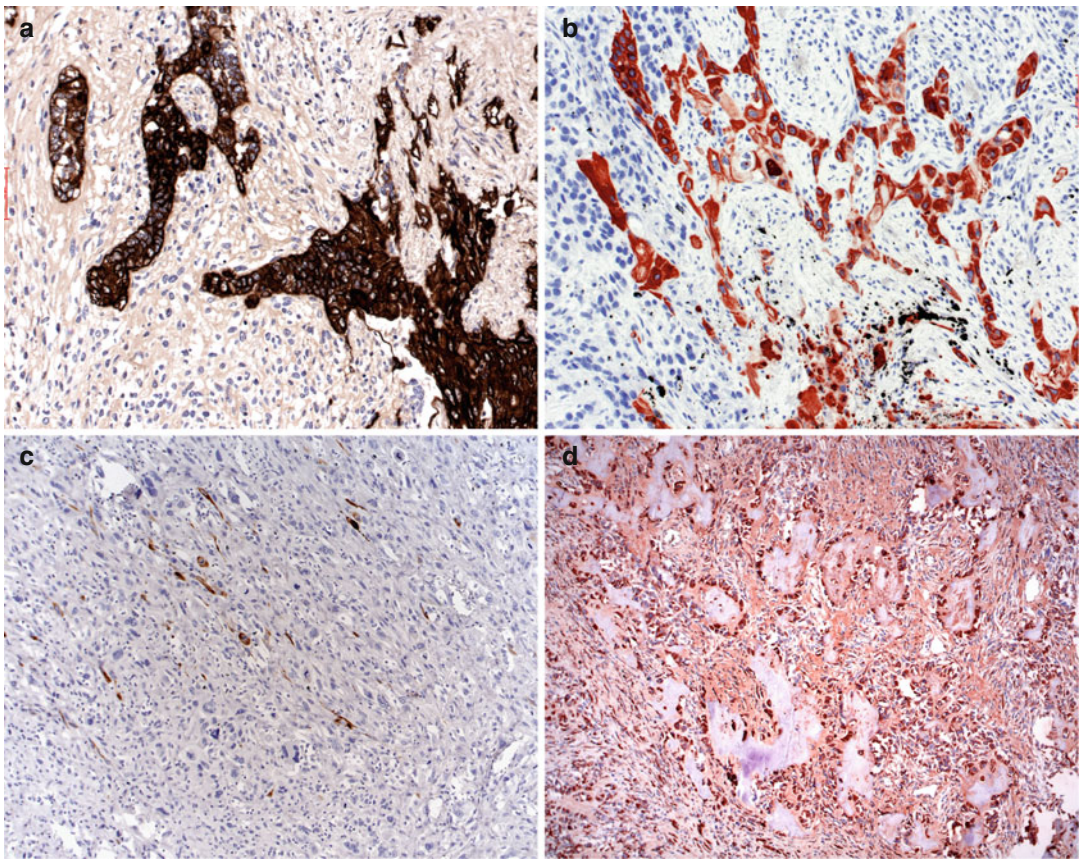

Fig. 17.112 Immunohistochemistry of a carcinosarcoma with squamous cell carcinoma, leiomyosarcoma and osteosarcoma components; (**a**) pan-cytokeratin, (**b**) cytokeratin 5/cytokeratin 6, (**c**) desmin, (**d**) osteonectin in the osteosarcoma component. ×100 and 200

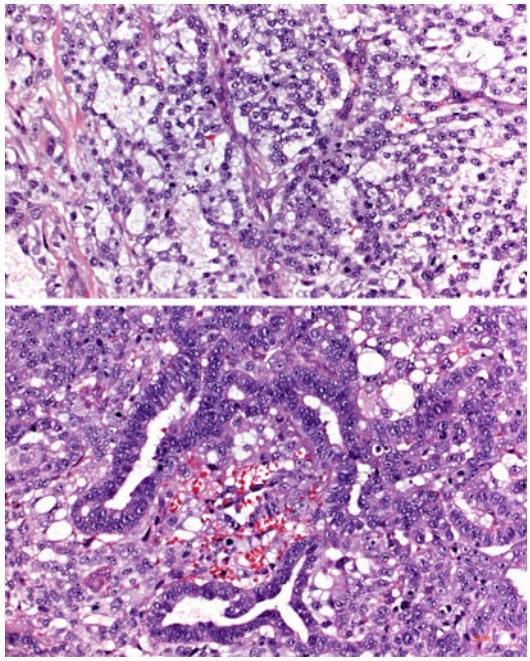

Fig. 17.113 Embryonic carcinoma; in this case it could never be clarified if the tumor invaded the lung from the mediastinum or arose primarily within the lung

Schiller-Duval bodies are present. Tumor cells have eosinophilic hyaline globules that are alpha-1-antitrypsin and diastase PAS positive. The tumor cells are positive for AFP, cytokeratin, SALL4, Glypican3, PLAP, and CD117.

17.3.13 NUT Carcinoma

NUT carcinoma of the lung is another rare carcinoma, preferentially found in young adults, median age 30 (range 21–68). It corresponds to the older term midline carcinoma and is often located in the midline structures such as the mediastinum, larynx, and nasopharynx. It is characterized by chromosomal translocation between chromosomes 15 and 19 with the formation of a chimeric gene BRD-NUT (nuclear protein in testis).

Symptoms are nonspecific as in most carcinomas with dyspnea, nonproductive cough, and pain. A smoking history might be absent.

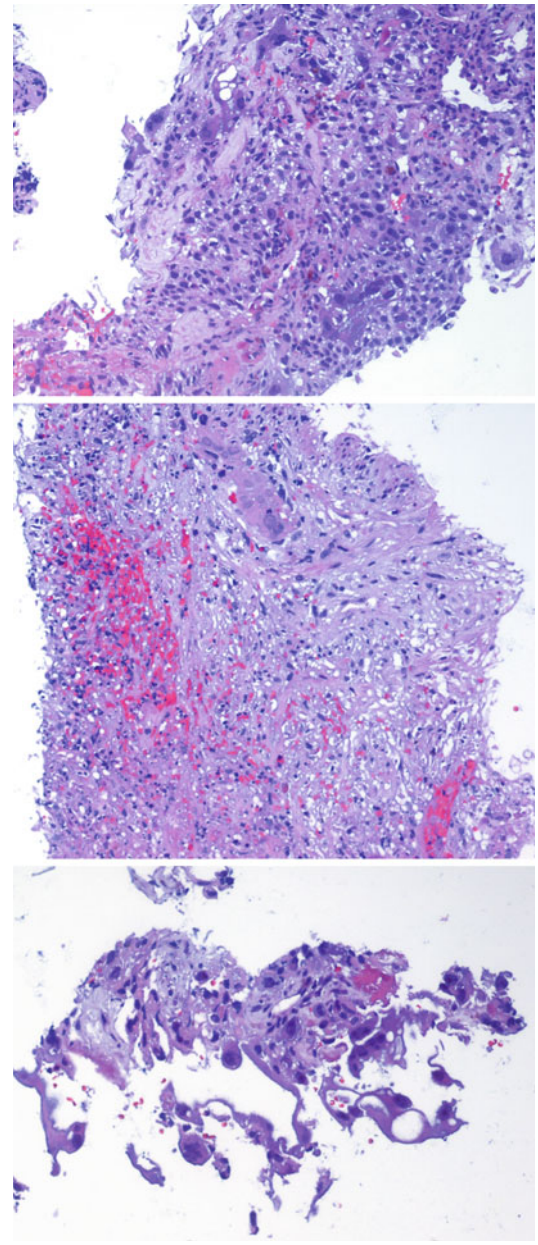

Fig. 17.114 Choriocarcinoma arising in the lung. The *upper* and *middle panel* shows two different areas of a transthoracic core needle biopsy of the tumor. Note the two cell populations, large sometimes multinucleated syncytiotrophoblasts and the small cytotrophoblasts. In the lower panes, material from the aspiration cytology of the same case shows nicely the syncytiotrophoblasts of the tumor. H&E, ×200 and 400

On chest CT scan, a hilar mass and often mediastinal adenopathy are seen.

Histology

The tumor cells appearing as round to epithelioid cells, growing in nests and sheets, focally pseudoglandular, nuclei show fine to coarse chromatin pattern, irregular nuclear contour, and prominent nucleoli. Karyorrhexis and mitosis are rare. Squamous or glandular differentiations are absent. By electron microscopy prominent bundles of tonofilaments, occasional clusters of pleomorphic granules, small numbers of lipid inclusions, and rare glycogen deposits are seen. The cells exhibited microvillous projections and were enveloped by a basal lamina. There are also numerous well-formed desmosomal-type junctions and occasional junctional complexes [285–287].

Immunohistochemistry

The carcinoma is positive for p63 and p40 and for NUT immunohistochemistry. Staining for Ki-67/MIB1 is high (around 80%). The tumor cells are negative for keratin, lymphoid, myeloid, neuroendocrine markers, and S100. By FISH analysis BRD4-NUT or BRD3-NUT rearrangement should be confirmed.

A median overall survival was reported within 2.2 months; lytic bone metastases are common, but brain metastases were absent.

17.3.14 Staging of Pulmonary Carcinomas

In all cases the TNM staging system has to be applied [288, 289]. The tumor size is staged as:

T1a ≤1 cm
T1b >1 ≤2 cm
T1c >2 ≤3 cm
T2a >3 ≤4 cm
T2b >4 ≤5 cm
T3 >5 ≤7 cm
T4 >7 cm and also diaphragm and thoracic wall invasion (for more details on T and M descriptors, see references above; the N staging will not be changed in the upcoming eighth TNM system).

17.4 Benign and Malignant Mesenchymal Tumors

Mesenchymal tumors of the lung are in general rare. Most probably the pulmonary stroma is protected from all kinds of stress, either toxic or oncogenic by an effective epithelial barrier. Lung epithelia can detoxify most harmful substances by their unique composition of oxidizing, deaminizing enzymes, and their high amount of oxygen radical scavengers. However, most of these mechanisms have not been studied in conjunction with mesenchymal tumors of the lung. Instead of grouping the mesenchymal tumors into benign and malignant, they will be grouped according to their cell of origin or differentiation, respectively. This enables much better to place also tumors with intermediate malignancy in place without recapitulating too much on histogenesis.

17.4.1 Hamartoma

Clinical Features

Hamartomas can present clinically by causing obstructive lung disease or recurrent pneumonia in those cases, which arise in large bronchi, but they also can present symptomless and are detected incidentally.

Radiological Features

Radiologically hamartomas are well-circumscribed nodular lesions. The CT scan-based diagnosis most often is benign well-circumscribed tumor; rarely adjacent pneumonia infiltration can obscure the nodule and cause the misinterpretation of a malignant lesion. In those cases, which have a substantial chondroid or osseous, component with calcification are often correctly diagnosed by the radiologist.

Pathologic Features

Gross Findings

Hamartomas are well-circumscribed nodules, ranging from a few mm to several cm in diameter. Most often cartilaginous areas predominate within the hamartoma, which is easily recognized

by its characteristic cartilage features and will immediately result in the correct diagnosis (Fig. 17.115).

Microscopic Findings

Hamartomas are composed of primitive epithelial tubules, sometimes traversing the whole tumor, in other cases concentrated at the borders. They are lined by a single row of cuboidal cells, reminiscent of embryonic bronchial buds. These tubules are devoid of a muscular coat. A few undifferentiated mesenchymal cells form the wall. The mesenchymal component can be a mixture of cartilaginous, myxoid, leiomyomatous, and fat tissues. Sometimes one element predominates [290, 291]. In these cases the hamartoma should be subtypes into, for example, myxoid variant of hamartoma (Fig. 17.116). Ancillary studies are not necessary.

Fine Needle Aspiration Biopsy

A correct diagnosis can be made on fine needle aspiration biopsy when the mesenchymal elements as well as fragments of the tubules are present; however, since the tumor should be excised, a surgical intervention will be necessary.

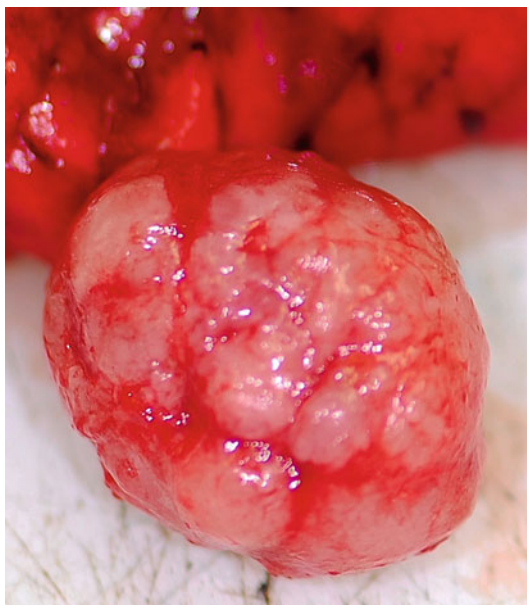

Fig. 17.115 Hamartoma resected. The tumor slipped out during VATS preparation

Differential Diagnosis

These differential diagnoses should be considered: lipoma, leiomyoma, and chondroma. In all instances these tumors are entirely mesenchymal without epithelial tubules. Entrapped bronchioles should not be confused with epithelial tubules, because the former contain smooth muscle cells in their wall.

Molecular Pathology and Genetics

For some time the nature of hamartomas was questioned. There were controversies of a real tumor versus a malformation. Since the proof of genetic aberrations in these tumors, these discussions are gone. There are characteristic rearrangements between chromosomes 6p21 and 12q14–15, and finally the proof that HMGIC genes rearrangement is the major factor involved in the development of chondromatous hamartomas [292–296]. One partner of this fusion gene was identified as LPP. Another gene fusion found in chondroid hamartomas was the RAD51L1 protein kinase [297].

Prognosis and Therapy

Hamartomas are benign tumors. They tend to grow slowly over the years. No malignant transformation was reported. Surgical excision is the treatment of choice.

17.4.2 Smooth Muscle Tumors

Leiomyoma

Incidence and Clinical Presentation

Leiomyoma of the lung is a rare tumor. It is slightly more often seen in females (ratio 1.5:1). They are more often localized peripheral as bronchial. Leiomyoma occur more often in patients at 20–40 years of age. The tumor is rarely seen in children [298]. Especially the endobronchial origin is extremely rare [299]. Pulmonary leiomyoma most commonly presents as an asymptomatic solitary lung nodule. The endobronchial variety may cause cough, hemoptysis, or shortness of breath, whereas the peripheral form is usually symptomless. The tumor can also occur in the trachea [300, 301].

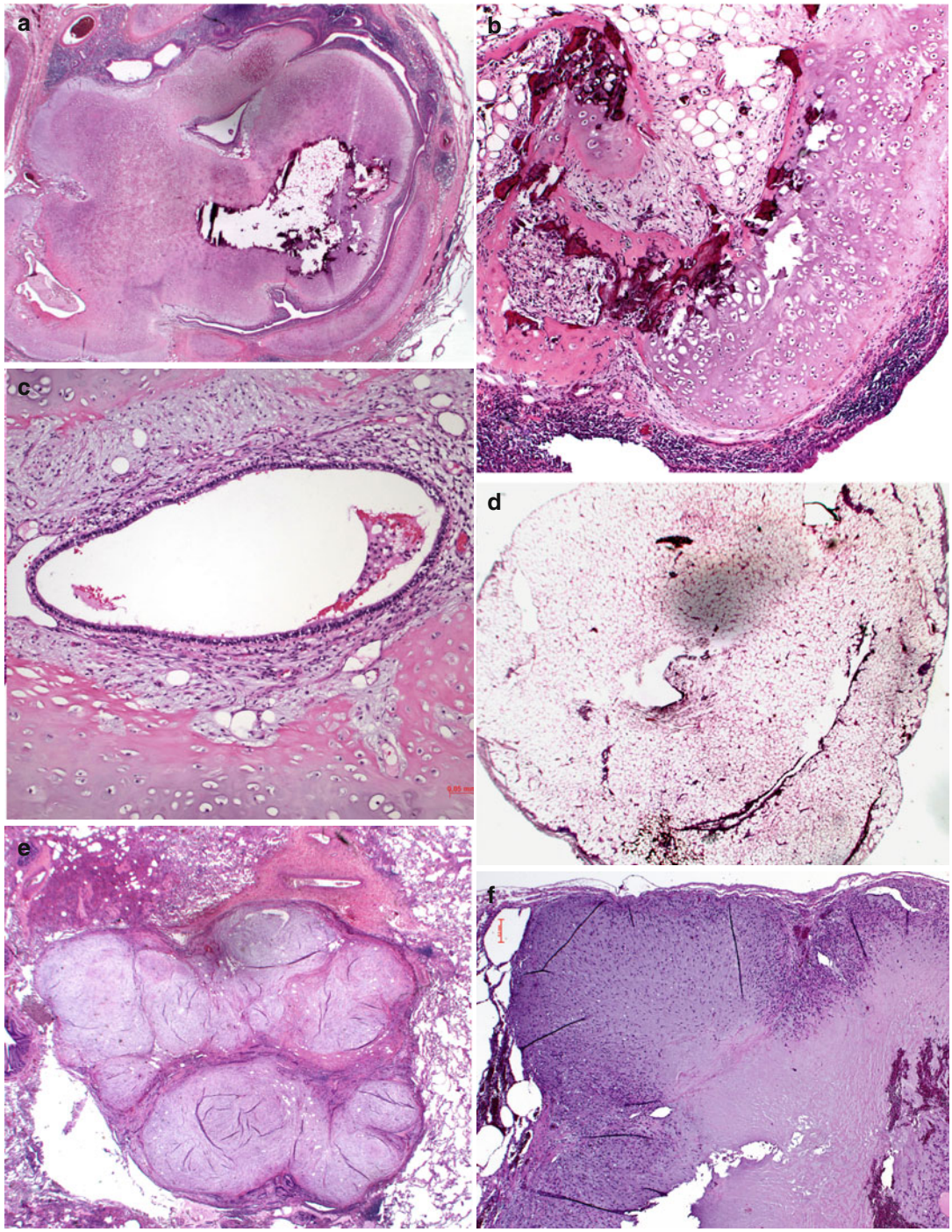

Fig. 17.116 Different variants of hamartomas. In all besides the major mesenchymal component, there are small epithelial tubules, composed of primitive or already differentiated bronchiolar epithelium. (**a**) Shows the classical chondroid variant, in (**b**) focal ossification has started, (**c**) shows the epithelial tubules; (**d**) is an example of lipomatous hamartoma, whereas in (**e**) myxoid mesenchyme dominates, higher magnified in (**f**); (**g**) is a case of myomatous hamartoma. H&E, ×12 and 25

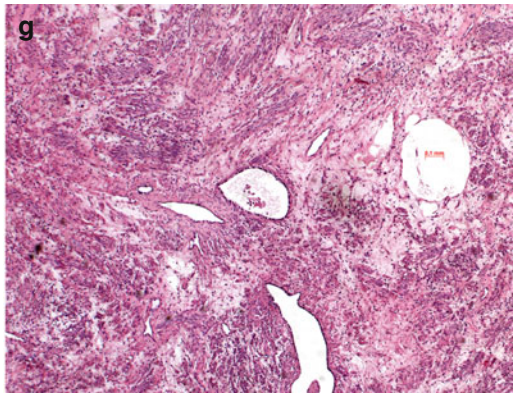

Fig. 17.116 (continued)

Radiology

There are no specific features on X-ray or CT scan. The lesion is usually described as malignancy. Most often leiomyomas are incidental findings.

Gross Pathology

Leiomyoma presents as a soft fleshy grayish-white nodule. On cut surface the myomatous bands might be seen occasionally. A single case was described with giant cyst formation [302].

Histopathology

On low magnification the tumor cells form bundles of mesenchymal cells, which on higher magnification will clearly show smooth muscle cells with elongated nuclei. There are usually perinuclear vacuoles, which are positive by PAS stain. Myofilaments can be seen. There is no nuclear atypia, no mitosis.

Immunohistochemistry

Usually immunohistochemical stains are not necessary, because of the clear histology. Of course markers of smooth muscle differentiation are all positive (SMA, HHF35, myoglobin).

Treatment and Prognosis

The tumor has to be treated by pulmonary resection, although a lesser resection would have sufficed [300]. Treatment could be conservative surgery, but 65 % of reported cases have been managed by lobectomy or pneumonectomy, because a malignant tumor was anticipated [301].

17.4.2.1 Leiomyosarcoma and Metastasizing Leiomyoma

Clinical Features

Leiomyosarcomas are usually found as endobronchial growing tumors, obstructing the lumen. This explains the symptoms they are causing, if any at all. However, in another series of cases, some were also seen within the lung parenchyma as well [300, 303]. In contrast, metastasizing leiomyoma of the lung is exclusively located in the periphery and rarely produces symptoms [304, 305].

Radiologic Features

There is no specific radiological feature for leiomyosarcoma. Metastasizing leiomyoma is usually diagnosed as metastatic disease [305, 306].

Gross Findings

Leiomyosarcoma is a well-circumscribed tumor located in the bronchial wall, with a predominant endobronchial growth or found in the peripheral lung tissue. Metastasizing leiomyoma is located in the pulmonary periphery and can present as multiple or single nodule but is otherwise not different from other mesenchymal tumors. The cut surface of both is grayish whitish and glistening; a whorled structure can be discerned. In high-grade leiomyosarcoma there can be necrosis and hemorrhage within the tumor.

Microscopic Findings

Both tumors are composed of plump elongated cells with typically elongated, cigar-shaped nuclei. Nucleoli are slightly enlarged in well differentiated but prominent in high-grade leiomyosarcomas. Chromatin is granular in metastasizing leiomyomas and coarse in leiomyosarcoma. Perinuclear glycogen vacuoles are usually present and can be highlighted by a PAS stain. Myofilaments can be seen in the cytoplasm of the tumor cells. Collagen fibers are scarce. Mitotic figures can be found; at least $\geq$5 mitotic counts per 10 mm^2 in leiomyosarcomas. Leiomyosarcomas will show blood vessel invasion. Metastasizing leiomyomas can have focal collagen deposition in their matrix.

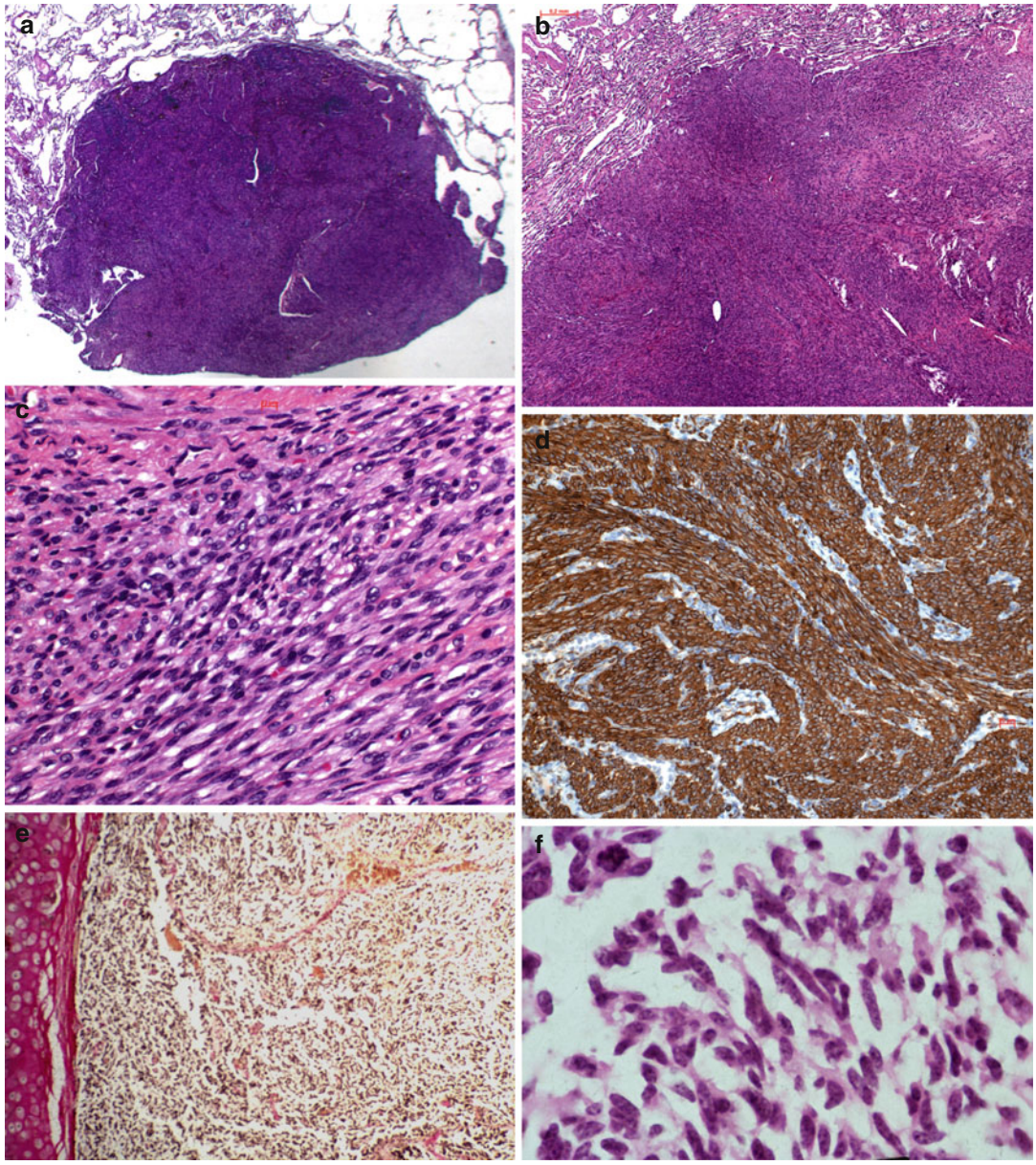

Fig. 17.117 Metastasizing leiomyoma (**a**–**d**); (**a**) shows one nodule, in (**b**) the infiltrative pattern as well as some compression of the adjacent lung is seen. (**c**) Shows the plump spindly tumor cells with characteristic perinuclear halos and the round "cigar-shaped" nuclei. Chromatin is finely dispersed; mitosis is absent. By MIB1 staining only few cells are stained. (**d**) Shows the positivity of the tumor cells for SMA. (**e**, **f**) Is a case of leiomyosarcoma of the lung. This was an incidental finding at autopsy. A 1.5 cm nodule was obstructing a lobar bronchus. (**e**) Shows the tumor nodule arising from the bronchial wall, in (**f**) higher magnification shows nuclear atypia and one atypical mitosis (*upper left*). H&E, ×12, 200, bars 10, 200 μm, Elastica v. Gieson, ×25, IHC bar 20 μm

Myofilaments are present in the tumor cell cytoplasm as well. Mitoses are rare in metastasizing leiomyomas, usually less than 1 per 2 mm^2 (Fig. 17.117).

Immunohistochemistry

The nature of the smooth muscle proliferation can be confirmed by immunohistochemical stains for smooth muscle actin (SMA) and other

myogenic markers (myoglobin, myogenin, HHF35). Immunohistochemistry will be necessary in assisting the diagnosis of high-grade leiomyosarcomas [307, 308].

Molecular Biology

Structural abnormalities are found in leiomyosarcomas such as gains on chromosomes 2 and 11 and loss on chromosomes 9, 19, 20, and 22, along with the presence of multiple marker chromosomes [309–312]. To differentiate leiomyosarcomas from metastasizing leiomyomas, in situ hybridization for miR-221 can be used, which is selectively upregulated in leiomyosarcomas but not in leiomyomas or metastasizing leiomyomas [313]. There is some evidence that pulmonary metastasizing leiomyoma might represent metastases from low-grade uterine leiomyosarcomas [310, 314, 315]; analysis of allelic inactivation of the human androgen receptor gene might prove their clonal origin from low-grade uterine leiomyosarcoma [316].

Differential Diagnosis

Fibrosarcoma/myofibroblastic sarcoma, MPNST, and monophasic synovial sarcoma enter the differential diagnosis of leiomyomatous tumors. Myofibroblastic sarcoma and fibrosarcoma are characterized by abundant collagen fiber deposition. This can be seen at a first glance by just looking under polarized light, which will highlight birefringent collagen fibers. In addition fibrosarcomas have a more monomorphic appearance and usually the typical herringbone pattern. MPNST can usually be differentiated from leiomyomatous tumors by their typical comma-shaped nuclei and immunohistochemically by their negativity for myogenic proteins. Monophasic synovial sarcoma has a high nuclear to cytoplasmic ratio and the nuclei are monomorphic granular and hyperchromatic. For leiomyosarcoma another primary outside the lung has to be excluded; however, in case of an endobronchial growth, this should not be difficult.

Metastasizing leiomyomas have provoked a debate about their origin for decades: in a third of cases, they represent metastasis from well-differentiated leiomyosarcomas of the uterus. There is usually a history of hysterectomy years ago. The time elapsed between the primary tumor in the uterus and metastasizing leiomyomas in the lung can be up to 20 years. In certain cases the primary uterine tumor has been missed, due to sampling errors, in others a diagnosis of cellular myoma has been made, which on reevaluation might turn into well-differentiated leiomyosarcoma. However, in up to two thirds, no other primary tumor can be found. So a primary pulmonary origin has to be accepted, unless better data are available (see also genetics above as a possibility for separation). The differential diagnosis might be inflammatory pseudotumor, also called myofibroblastic tumor (although not in all myofibroblasts are present). However, a mixture of histiocytes, lymphocytes, and plasma cells characterizes the latter, which is not seen in metastasizing leiomyoma. In addition a typical feature in inflammatory pseudotumor is a persistent inflammation at the border.

Prognosis and Therapy

Metastasizing leiomyoma is a slowly growing tumor with a benign course, usually in elderly women, rarely men. A surgical removal is the adequate treatment.

Leiomyosarcoma of the lung has to be treated by surgical resection. Depending on the grade of differentiation, chemotherapy and/or radiotherapy has to be added although leiomyosarcomas seem resistant to chemotherapy or radiotherapy, and therefore radical resection is best, resulting in a 45 % 5-year survival rate [300]. Otherwise, the prognosis for leiomyosarcomas is similar to those in other locations. Important prognostic factors are the grade of differentiation, presence or absence of metastasis and/or necrosis, and the tumor size.

17.4.2.2 Lymphangioleiomyomatosis

Clinical Features

Lymphangioleiomyomatosis (LAM) is a rare disease associated with tuberous sclerosis, which can affect the lungs, the pulmonary lymph nodes, and the mediastinum. LAM presents with chylo- and pneumothorax, shortening of breath, and dyspnea on exertion. Up to a 100 % young women in their

reproductive age are affected. There can be an association with angiomyolipoma of the kidneys and clear cell tumor of the lung. Other features of the tuberous sclerosis complex can be present as well, such as benign tumors of the skin, rhabdomyoma of the heart, and Bourneville-Pringles disease of the CNS. Patients present usually with exertional dyspnea and pneumothorax. Common abnormalities on pulmonary function tests were decreased diffusing capacity of carbon monoxide, hypoxemia, and airway obstruction [317–319].

Radiologic Features

On high-resolution CT scan, LAM presents as a cystic disease with a peripheral accentuated distribution [320]. There are some similarities with emphysema; however, the cystic spaces will show a typical distribution and not much size variation.

Gross Findings

A surgical specimen will show a cystic lung tissue, with only thin walls remaining. The extent of the cystic destruction depends on the severity and the duration of the disease (Fig. 17.118).

Microscopic Findings

A smooth muscle cell proliferation confined to vascular walls and bronchioles. The proliferating smooth muscle cells look mature, but sometimes they can look like embryonic myoblasts with larger nuclei, finely distributed chromatin, and enlarged nucleoli. The cystic lumina represent dilated lymphatics; sometimes also dilated bronchioles and alveoli can be seen.

Fig. 17.118 Lymphangioleiomyomatosis (LAM), gross morphology of an explanted lung. The multiple cysts are impressively shown here

Two different types of LAM can be separated: a more solid and a predominantly cystic variant. There is no correlation to biological behavior; however, the number of muscular and of cystic lesions present in a biopsy has an impact on the prognosis; hemorrhage in addition is another worse prognostic feature (Figs. 17.119 and 17.120a–c) [321, 322]. In a subsequent study, Kumasaka and coworkers demonstrated that increased lymphangiogenesis in LAM or VEGF-C expression on LAM cells and LAM histologic score together have a prognostic significance [323].

FNA and Small Biopsies

LAM diagnosis might be difficult in FNA and small biopsies. Especially HMB45-positive PECells might be missed. However, if the smooth muscle proliferation is present, the diagnosis can be made even when no HMB45 cells are in the biopsy.

Immunohistochemistry

The muscular proliferation stains for smooth muscle actin, sometimes groups of cell are also positively stained for desmin and cathepsin K. The most important stain is HMB45. This melanocytic marker will stain parts of the smooth muscle cell proliferation (Fig. 17.120e–h). By electron microscopy in these cells, premelanosomes can be found, which is the cause of this reaction. These cells have been identified as perivascular epithelioid cells (PECells) [324]. These cells are part of the proliferation in LAM but give also rise to clear cell tumor (PECOMA) and angiomyolipoma of the kidney [325].

Molecular Biology

Genetically LAM is related to the tuberous sclerosis complex. Mutations of the TSC1 and TSC2 have been demonstrated in most cases evaluated [99, 326, 327]. The proteins hamartin and tuberin transcribed from TSC1/TSC2 normally associate to form a complex, which activate cAMP cyclase, and this enzyme inhibits and regulates mTOR complex expression (Fig. 17.121). If one of the genes is mutated, no functional protein is synthesized; therefore, mTOR inhibition does not function [328–331]. In addition mutations of the TSC

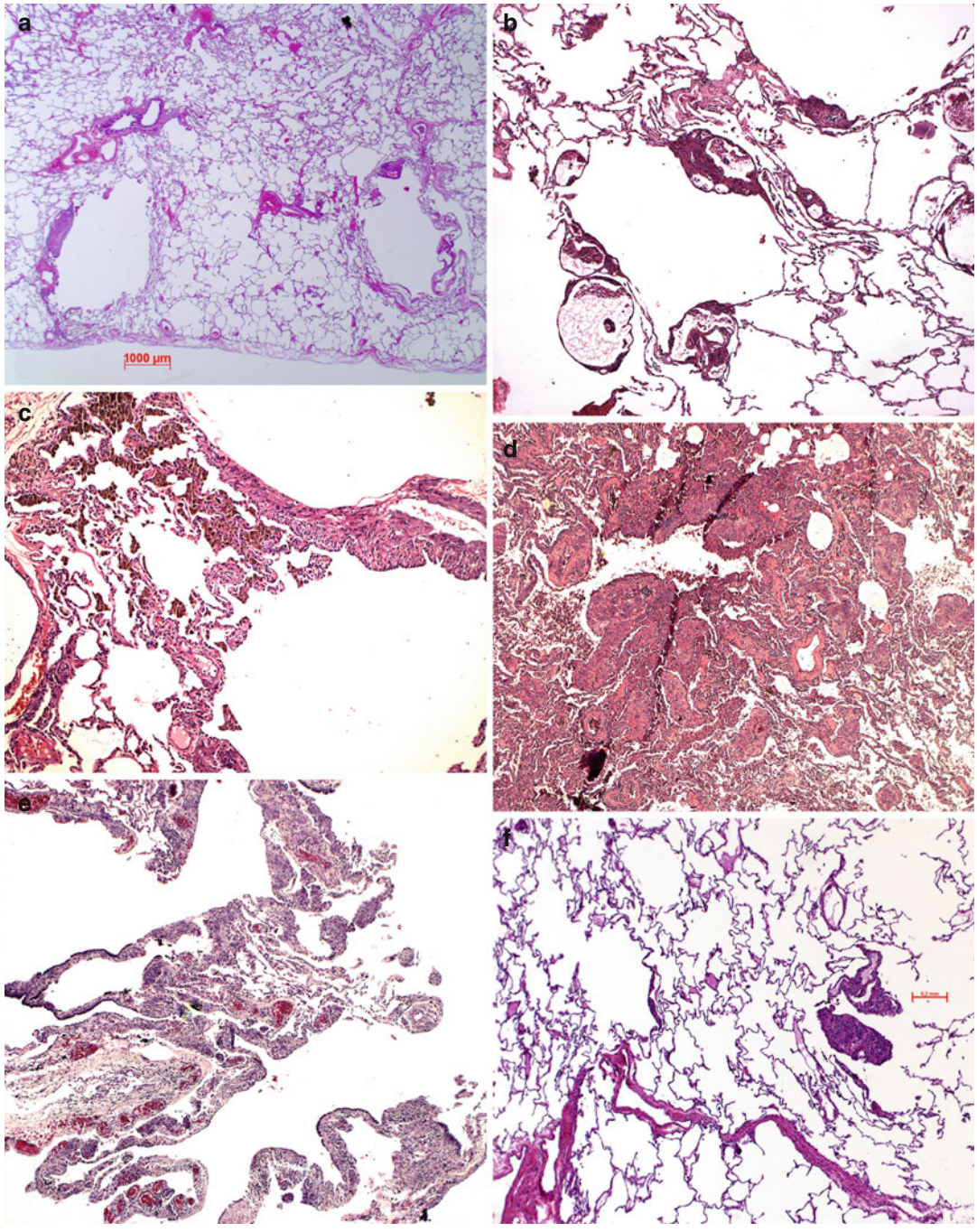

Fig. 17.119 LAM can present with few proliferation foci and large cysts as in (**a**, **f**) or can have many myoblastic foci as in (**b**, **d**, **e**). LAM can sometimes be obscured by acute and old hemorrhage as in (**c**, **d**). In cases of pleural involvement, rupture and chylothorax can result. H&E, bars 1 mm and 200 µm, or ×12 and 25

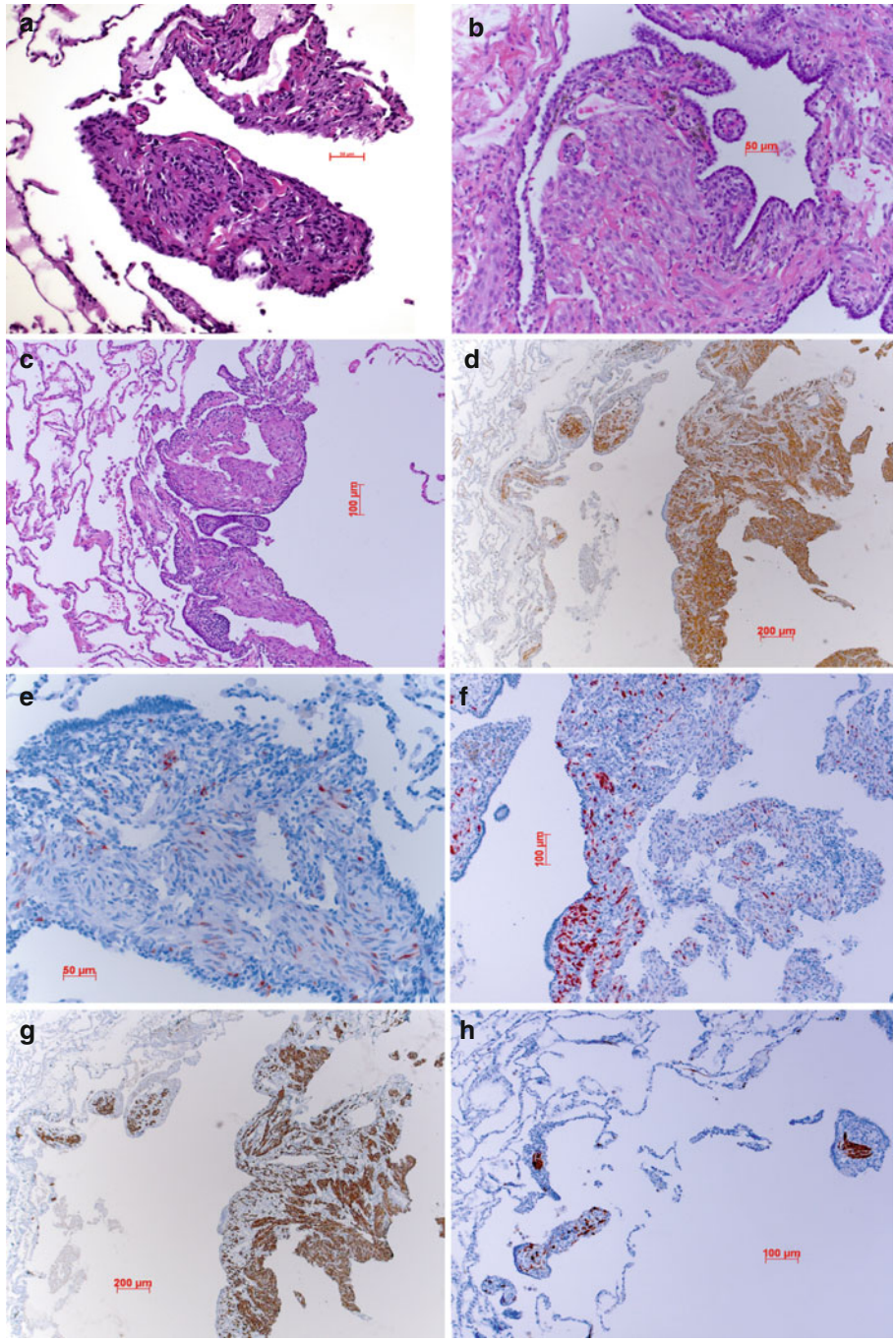

Fig. 17.120 LAM proliferations and immunohistochemistry: (**a**–**c**) shows the myoblasts with ovoid nuclei, finely dispersed chromatin and small nucleoli (can be invisible), and pale-stained cytoplasm. PEC cells cannot be discerned by H&E stains. Bars, 50, 100 µm. Note the widening of lymphatics in (**a**, **c**) but also the obstruction of airways in (**b**). (**d**) shows the smooth muscle cells by antibodies for SMA. (**e**, **f**) Illustrated the variable amounts of perivascular epithelioid cells, scarce in (**e**) and numerous in (**f**). The myoblasts will also stain for desmin (**g**, **h**), but again the number of positive cells can vary. Bars 200, 100, 50 µm

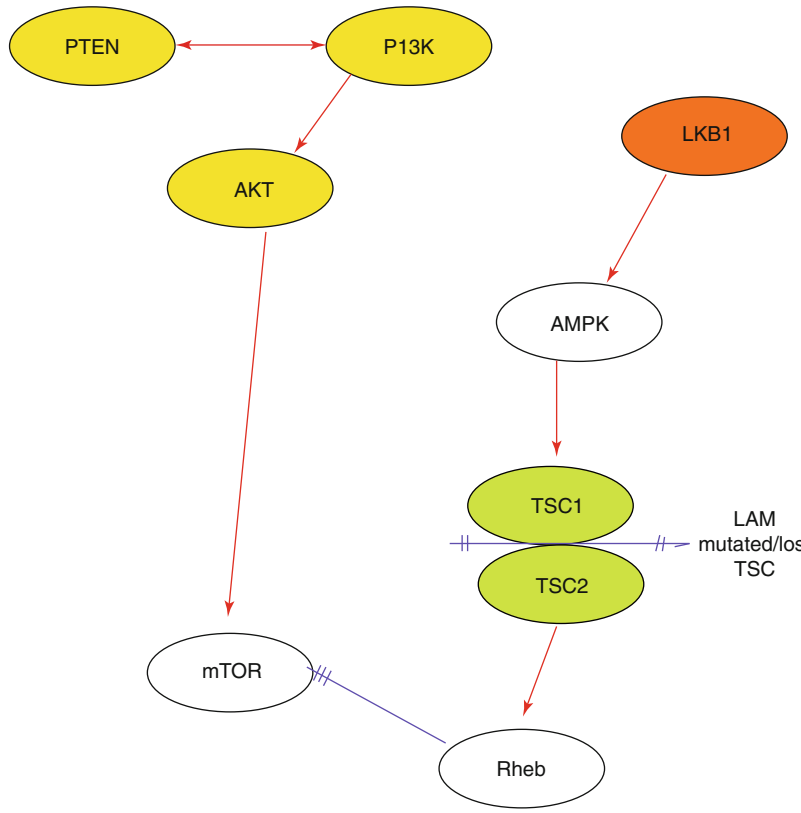

Fig. 17.121 Schema of the signaling pathway in LAM with indication of the new treatment option. Due to mutations of one of the TSC genes, the association of both proteins (tuberin and hamartin) does not happen and therefore no signal to mTOR inactivation is sent – thus mTOR stimulation by AKT remains active. The new treatment option is an inhibition of mTOR by drugs

genes result in genetic instability. LAM is one of the "benign" tumors associated with somatic mutations found in this disease.

Differential Diagnosis

Centrilobular emphysema is characterized by destroyed alveolar septa, widened cystic lobules, and enlarged dilated bronchioli usually with some inflammatory infiltrates. A smooth muscle cell proliferation, the so-called muscular cirrhosis, can be found in severe grade emphysema and in interstitial pneumonias and end-stage fibrosis. Muscular cirrhosis always arises from smooth muscle cell layers of pulmonary arteries and bronchi or bronchioles. In LAM the muscular proliferations are de novo lesions without a connection to the preexisting muscular coat.

Prognosis and Therapy

Prognosis of LAM cannot be predicted. There are slow progressing as well as rapid progressing variants. Histology scoring as explained above will assist. Over the time the lung parenchyma is destroyed and replaced by cystic structures.

Because some cases are positive for estrogen receptors, antiestrogen therapy and oophorectomy have been done in the past [332–334]. Lung transplantation is another option and has been performed in many patients [335]. However, recurrence of the disease has been seen in patients [336–338]. Recently it was shown that LAM cells from the transplant recipient repopulate the transplanted lungs [339]. Therefore it can and should be questioned, if LAM is really a benign disease. LAM cells migrate due to the missing

inhibition of tuberin [340]. Based on the findings by Bittmann [339], LAM cells might circulate within the circulation like malignant cells in systemic tumors. At least this shows an association to organ-specific metastasis, and thus LAM might be considered to be a low-grade malignant systemic tumor.

Based on the discovery of TSC1/TSC2 mutations and their role in regulating mTOR complex, a new therapeutic option resulted: treatment with inhibitors of the mTOR system has resulted in improvement and control of the disease [341–343].

17.4.3 Fibromatous Tumors

17.4.3.1 Intrapulmonary Solitary Fibrous Tumor (Fibroma): Benign and Malignant

Clinical Features

Solitary fibrous tumor (SFT) usually occurs in the pleura; however, sometimes it can arise from the interlobular septa and thus presents as an intrapulmonary tumor. Most SFTs are benign; however, malignant variants have been described. One of the most prominent clinical features is hyperinsulinism. Patients usually present with severe hypoglycemia. The reason is the hormonal effect of insulin-like growth factor. If tumors are large, they produce significant amounts of ILG1/ILG2 and release the hormone into the circulation [344, 345].

Radiologic Features

Radiologically SFT presents as a well-circumscribed mass lesion; often the pleura-based tumor is located in the recessus costodiaphragmaticus and is pedunculated. In these cases a radiological diagnosis might be done. The intrapulmonary variant is not pedunculated and therefore is usually diagnosed as an intrapulmonary tumor.

Gross Findings

SFT is a well-circumscribed mesenchymal tumor with a pseudo capsule. The cut surface is whitish and glistening; interweaving bundles are recognized (Fig. 17.122). Rarely hemorrhage but regularly myxoid areas are seen. Some patients might present with a giant tumor, which can compress the whole lung.

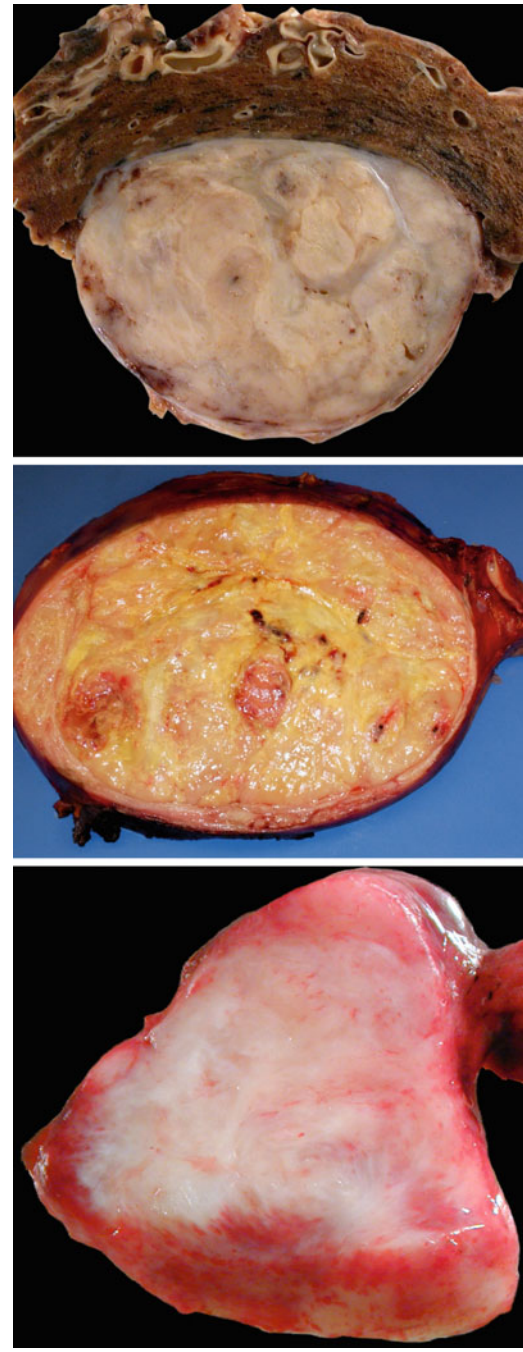

Fig. 17.122 Examples of gross sections of solitary fibrous tumors (SFT), *top* a giant SFT, *middle* a malignant SFT, and *bottom* a benign classical SFT from the right costodiaphragmatic angle

Microscopic Findings: Benign and Malignant

SFT is characterized by massive amounts of collagen bundles arranged in an unorganized fashion (patternless pattern). In between fibrocytes are seen. The tumor cells are small; nuclei are elongated with blunt end on one and sharp end on the other side of the nucleus. Chromatin is finely dispersed; nucleoli are inconspicuous. Mitosis is not encountered. In malignant SFT there are cellular areas and less collagen bundles. The collagen is organized into short bundles, sometimes hyalinized. The cells are still elongated fibroblast-like or oval histiocyte-like. Nucleoli are invisible; however, chromatin is granular, more than four mitoses per 2 mm^2 indicate aggressive behavior, and necrosis can be present. There can be a prominent vascular network composed of dilated veins (Fig. 17.123). The decision about malignancy in SFT is still not solved. Although the above criteria have been proposed for malignancy, these criteria do not reliably sort malignant and benign cases: in a series of SFTs, recurrence in malignant variants was not increased over the benign cases, and further more metastasis were not observed in any malignant case [344, 346, 347]. But there are few case reports on metastasis in malignant SFT [348–351]. In the series reported by Rao, additional features of malignancy were included, such as pleomorphism of tumor cells, multinucleated tumor cells, higher mitotic rate, and appearance similar to pleomorphic sarcoma adjacent to classical SFT areas. So a refinement of morphological features might be necessary to clearly separate benign from malignant SFT.

Immunohistochemistry

SFT will be stained by antibodies for CD34 (Fig. 17.123h), vimentin, and insulin-like growth factors 1 and 2. The cells also express the respective receptors for these growth factors (autocrine loop). Immunohistochemistry for the receptors can also be used to confirm the diagnosis in uncertain cases. A new marker helpful for the diagnosis in difficult cases is nuclear staining for STAT6 [345, 352–355].

Molecular Biology

A fusion gene composed of NAB2 and STAT6 has been found in SFT, which acts as a driver mutation. However, other mutations were found in TP53, and immunohistochemical staining for p53 has been discussed as a helpful feature for predicting malignant behavior [347, 349, 356]. The relationship of STAT6 and insulin-like growth factor receptors has not been studied in SFT, but in hematopoietic cells it was shown that IL4 synergizes with IGF-I for cell proliferation through cross talk between SHC/Grb2/MAPK and STAT6 pathways and through c-myc gene upregulation [357]. This mitogenic effect was confirmed in a study using hepatocellular carcinoma cells [358] and might therefore also act in SFT similarly.

Differential Diagnosis

There are not many differentials to be considered. Leiomyomas and schwannomas do not have this amount of collagen, although myxoid changes are usually also present. Angiomatoid fibrous histiocytoma, if arising in the lung, presents usually either as a pure pleomorphic type or at least has pleomorphic areas, and thus have much more atypical cells and many mitoses. MPNST have characteristic comma-shaped nuclei, higher mitotic counts, and less collagen. Monophasic synovial sarcoma can be excluded by the expression of epithelial immunohistochemical markers and also does not possess such amounts of collagen.

Prognosis and Therapy

SFT is a slowly growing tumor; most of them are benign. A few are of low malignant potential. It causes compression of adjacent lung lobes, segments, or the whole lung in cases of giant SFT [359, 360]. The most severe complication is hypoglycemia, caused by the release of ILGF, which can cause death of the patient. Surgical excision is the therapy of choice. Recurrence is quite common in benign as well as malignant SFT, whereas metastatic disease is rare.

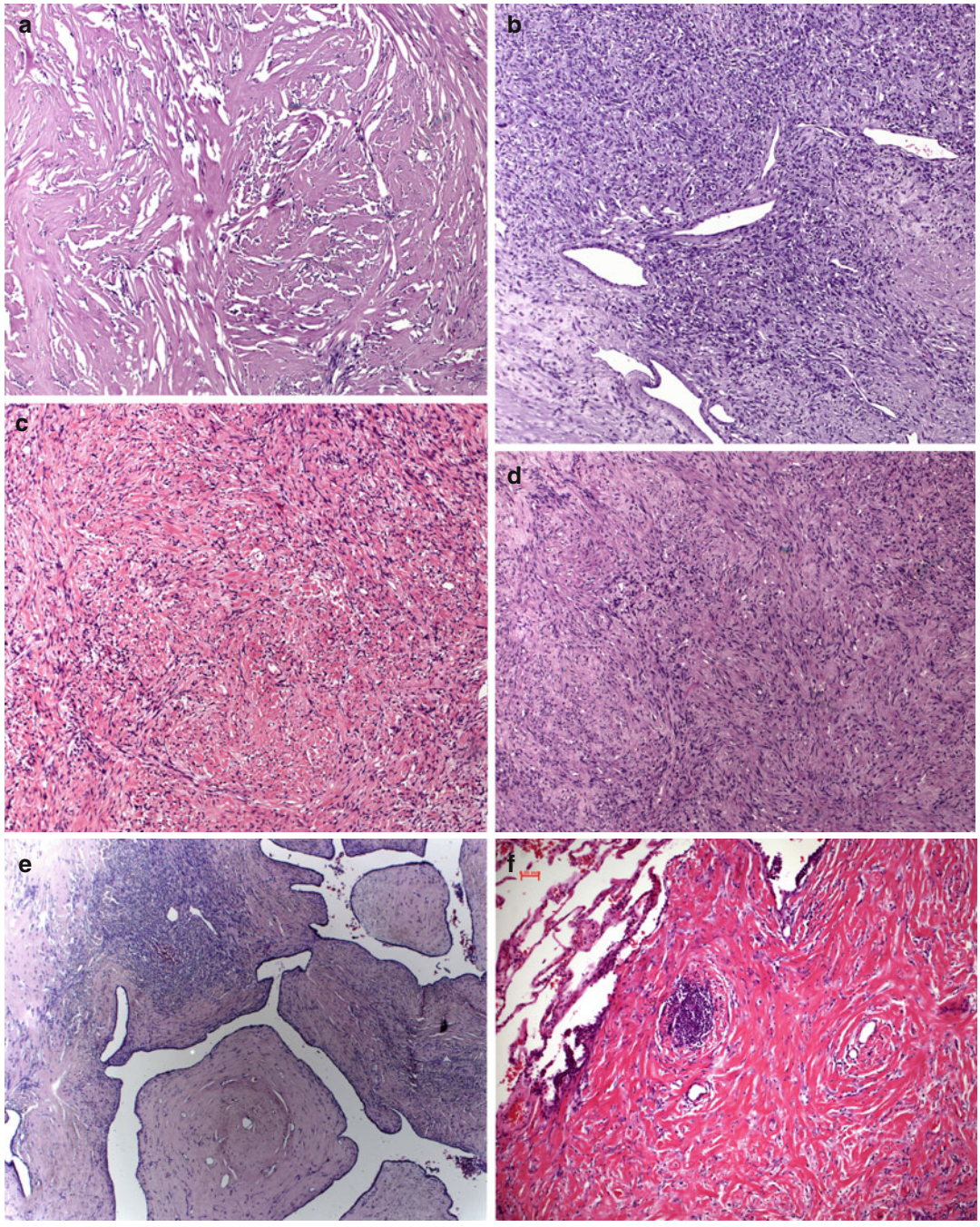

Fig. 17.123 SFT different patterns: (**a**) classical patternless pattern; there are not many tumor cells, the collagen deposition is unstructured, and bundles are in every direction. (**b**) Is an SFT with hemangiopericytoma pattern; note the dilated vascular channels. (**c**) Another classical SFT but more cellular; (**d**) this SFT resembles a neurofibroma; (**e**) an SFT pattern resembling a phyllodes tumor of the breast; on top the tumor is covered by normal mesothelial cells. (**f**) is an example of an intrapulmonary SFT; in (**g**) a malignant SFT is shown. The malignant form is characterized by high cellularity and >5 mitoses per 10 HPF. To prove the diagnosis, an immunohistochemical stain for CD34 or STAT6 can be done, here CD34

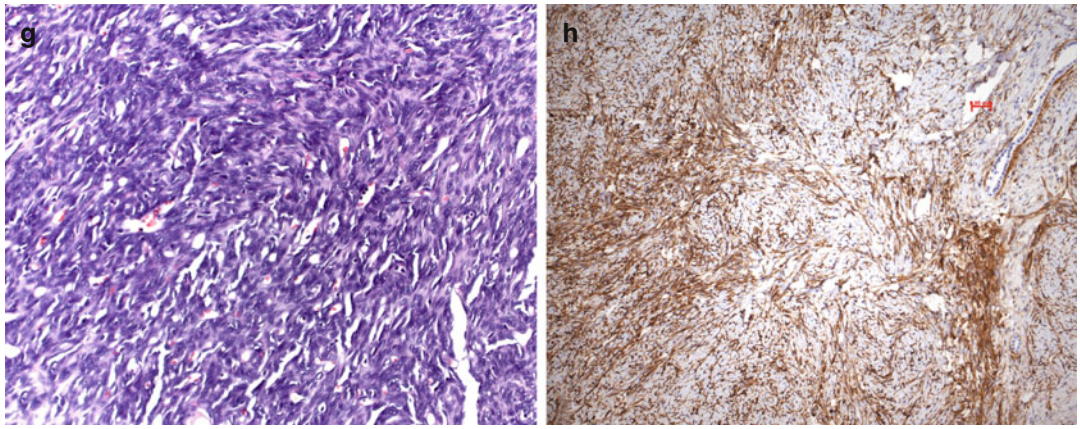

Fig. 17.123 (continued)

17.4.3.2 Inflammatory Pseudotumor (IPT) or Inflammatory Myofibroblastic Tumor (IMT)

Clinics

IPT has a variety of names: plasma cell granuloma, inflammatory myofibrohistiocytic proliferation, myofibroblastic tumor (MFT), and inflammatory fibrosarcoma. There were some controversies about IPT or MFT, and some authors claimed the tumor should be renamed as MFT [361, 362]. However, Farris and coworkers nicely showed that myofibroblastic cells do occur in some of the tumors but not all [363]. When looking up IPTs from our own collection, there are cases with myofibroblasts and dense plasmacytic infiltrates, cases with histiocytic cells and no myofibroblasts, and cases with a mixture of all cells. For this reason we will stick with the name of IPT.

Patients present with IPT with a median age of 47 years (range, 5–77 years). Symptoms are cough, weight loss, fever, and fatigue.

Radiology

The radiological findings are unspecific. Tumor masses are from 1 to 15 cm in diameter.

Gross Pathology

On gross inspection the tumor presents usually with ill-defined borders. Cut surface will show hemorrhage, consistency varies from soft to firm, and color is grayish to red.

Histopathology

Inflammatory pseudotumor is a benign mesenchymal tumor composed of histiocytic cells admixed with plasma cells and myofibroblasts. Three variants do exist: IPT with a predominance of plasma cells; now plasmacytic variant (formerly called plasma cell granuloma) where the histiocytic cells are scarce; IPT with equally mixed histiocytic, myofibroblastic, and plasmacytic cells, which is the classic and most frequent form; and the histiocytic variant, where histiocytic cells predominate (Fig. 17.124). The cells show a variety of nuclei from fibrocytic spindle form to polygonal histiocytic and to oval plasmacytic. Mitosis is not encountered, chromatin is finely distributed, and nucleoli are small. Organizing pneumonia is a common feature at the edges of the tumor, and this is also the cause of the ill-defined tumor border.

Molecular Biology

A translocation involving 12q15 have been described in IPT but also other benign tumors. But this translocation has been further specified as affecting the HMGIC gene. This showed an intragenic rearrangement of HMGIC, resulting in an aberrant transcript of that gene [364]. A more frequent genetic aberration was shown for ALK and p80, both on chromosome 2p23. This was associated with a higher frequency of recurrence [365]. In contrast Chan et al. showed a favorable outcome in ALK-positive IPT but confirmed the rearrangement and immunohistochemical

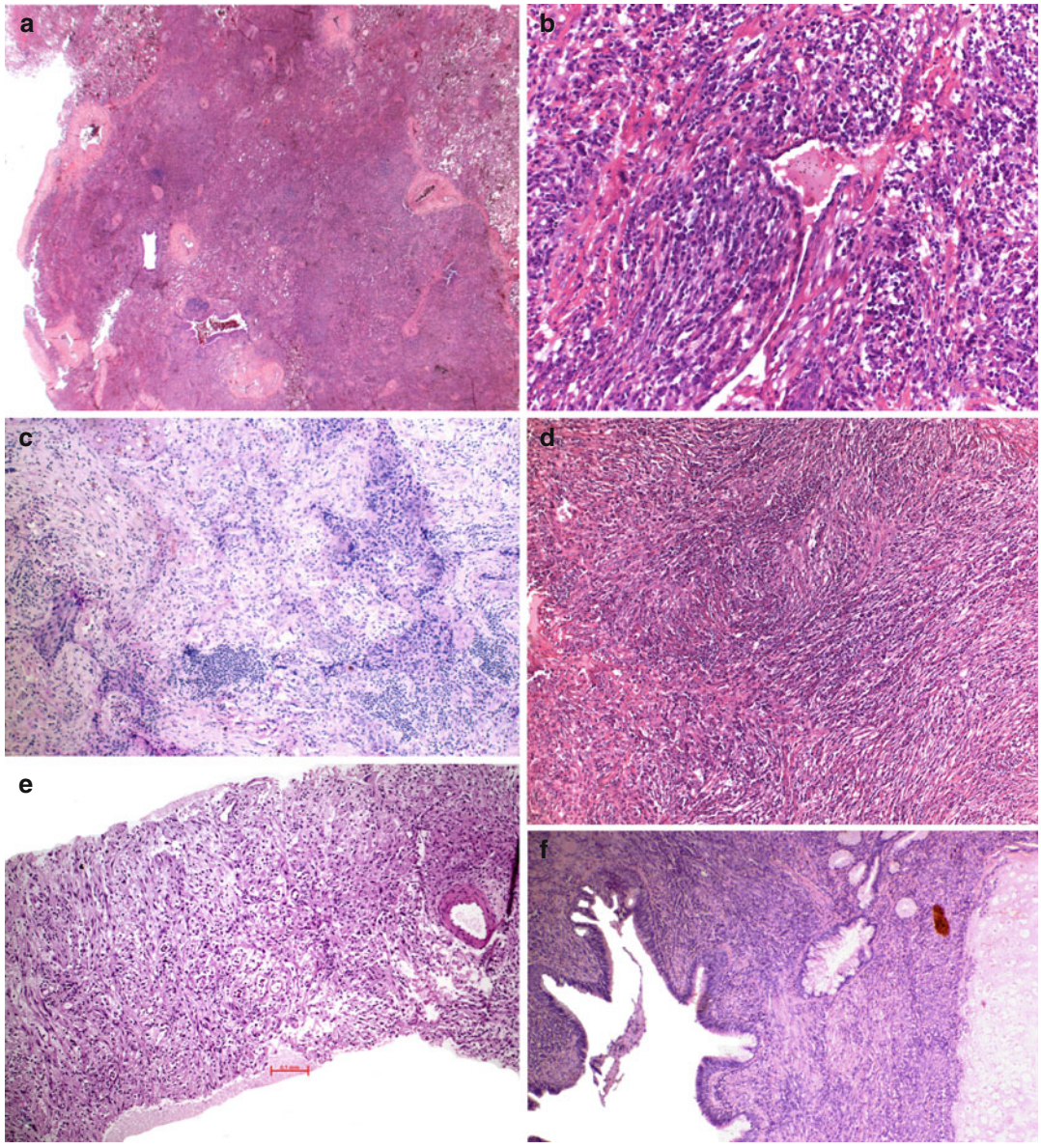

Fig. 17.124 Inflammatory pseudotumor (IPT/IMT); in (**a**) low magnification demonstrates a tumor with ill-defined borders. In (**b**) the classical form with plasma cells and myofibroblasts is shown in (**c**) the rare form dominated by histiocytes with plasma cells but without myofibroblasts. In (**d**) the myofibroblast-rich form is demonstrated. The diagnosis can be made on small biopsies, here a transthoracic core needle biopsy, (**e**). In (**f**) the local aggressive biology of the tumor is shown: tumor cells infiltrate the bronchial wall and destroy it as well as the adjacent cartilage. H&E, ×12, 25, 60, 100

expression of ALK in a high proportion of inflammatory pseudotumors [366]. Antonescu and coworkers confirmed ALK gene rearrangement in IPT and defined more closely the fusion partners, such as EML4-ALK, ROS1 rearrangement as TFG-ROS1 fusions, and a RET gene rearrangement. In 68 % of their IPTs, a kinase fusion was found. Fusion-negative IPTs were seen predominantly in adults, whereas pediatric IPTs showed gene rearrangements [367].

Differential Diagnosis

The most important differential diagnosis is IgG4-related fibrosis. IgG4 dysregulation and inflammatory pseudotumor (IPT) were first reported in sclerosing pancreatitis, followed by reports in liver and breast. By examining IPT of the lung, cases with dense lymphoplasmacytic infiltrates intermixed with fibrosis showed many IgG4-positive plasma cells diffusely distributed within nodules, with a high ratio of IgG4 to IgG-positive plasma cells [368]. Therefore IPT should always be investigated for IgG/IgG4 in order to separate IPT from IgG4-related fibrosis [369]. ALK positivity favors IPT, whereas high amounts of IgG4-positive plasma cells and obstructive phlebitis are characteristics for IgG4-related fibrosis.

Prognosis and Therapy

Complete resection is the most important procedure and will cure the patient. Overall 5-year survival is usually high [370]. However, the tumor can behave biologically "malignant," when arising centrally, because it usually invades the surrounding structures and cause bronchial obstruction. In one of our cases, the patient responded to irradiation. A new treatment option is treatment using ALK inhibitor similar to the protocol in ALK-positive adenocarcinomas.

17.4.3.3 IgG4-Related Fibrosis/Tumor

An association between IgG4 deregulation and inflammatory pseudotumor was reported in sclerosing pancreatitis as well as in IPTs of the liver and breast. Also in lung cases of IPT with numerous IgG4-positive plasma cells and previously diagnosed as IPT were shown to belong to the category of IgG4-related fibrosis or tumors [368, 369].

Clinical Features

The clinicopathologic similarities between IPT of the lung and sclerosing pancreatitis suggest that IgG4-related immune processes might be involved in the pathogenesis of the disease.

Radiologic Features

On X-ray nodular lesions can be seen; however, a more precise evaluation by CT scan showed four different types of patterns: solid nodular type with a solitary nodular lesion; round-shaped ground-glass opacity (GGO) characterized by multiple GGOs; alveolar interstitial type showing honeycombing, bronchiectasis, and diffuse GGO; and bronchovascular type showing thickening of bronchovascular bundles and interlobular septa [371]. Also an NSIP-like pattern has been described [372]. In FDG-PET/CT FDG accumulation without evidence of an associated inflammatory reaction can be seen [373].

Gross Findings

On gross examination the same types of patterns can be seen. The nodular pattern is the one, which will be recognized as a tumor, whereas interstitial patterns will enter a wide range of differential diagnoses.

Histopathology

The main characteristics are dense lymphoplasmacytic infiltrates intermixed with fibrosis. In the nodular variant, the diagnosis will most often be an IPT and plasmacytic variant and will need immunohistochemistry to sort out IPT versus IgG4-related tumor (Fig. 17.125). In some cases prominent eosinophilic infiltration can be seen, which might open the differential diagnosis of Langerhans cell histiocytosis. Narrowing of bronchioles within the nodules and interstitial pneumonia at the boundaries of nodules are also frequent findings. Almost diagnostic is obliterative phlebitis and sometimes in addition obliterative arteritis. The nodular lesions correspond to the IPT-type lesion with lymphoplasmacytic infiltration and fibrosis, whereas the GGO on CT images corresponded to lymphoplasmacytic infiltration and fibrosis with irregular and ill-defined boundaries, respectively. In case of honeycombing, disrupted alveolar structures and dilated peripleural airspaces are correlated.

Immunohistochemistry

In any case of suspected IgG4-related tumor, the plasma cells need to be stained by IgG and IgG4 antibodies. There should be a ratio of IgG/IgG4 of 4:1 (≥25 % of IgG-positive cell should be also IgG4 positive). In contrast IgG4-related tumor is negative for ALK1.

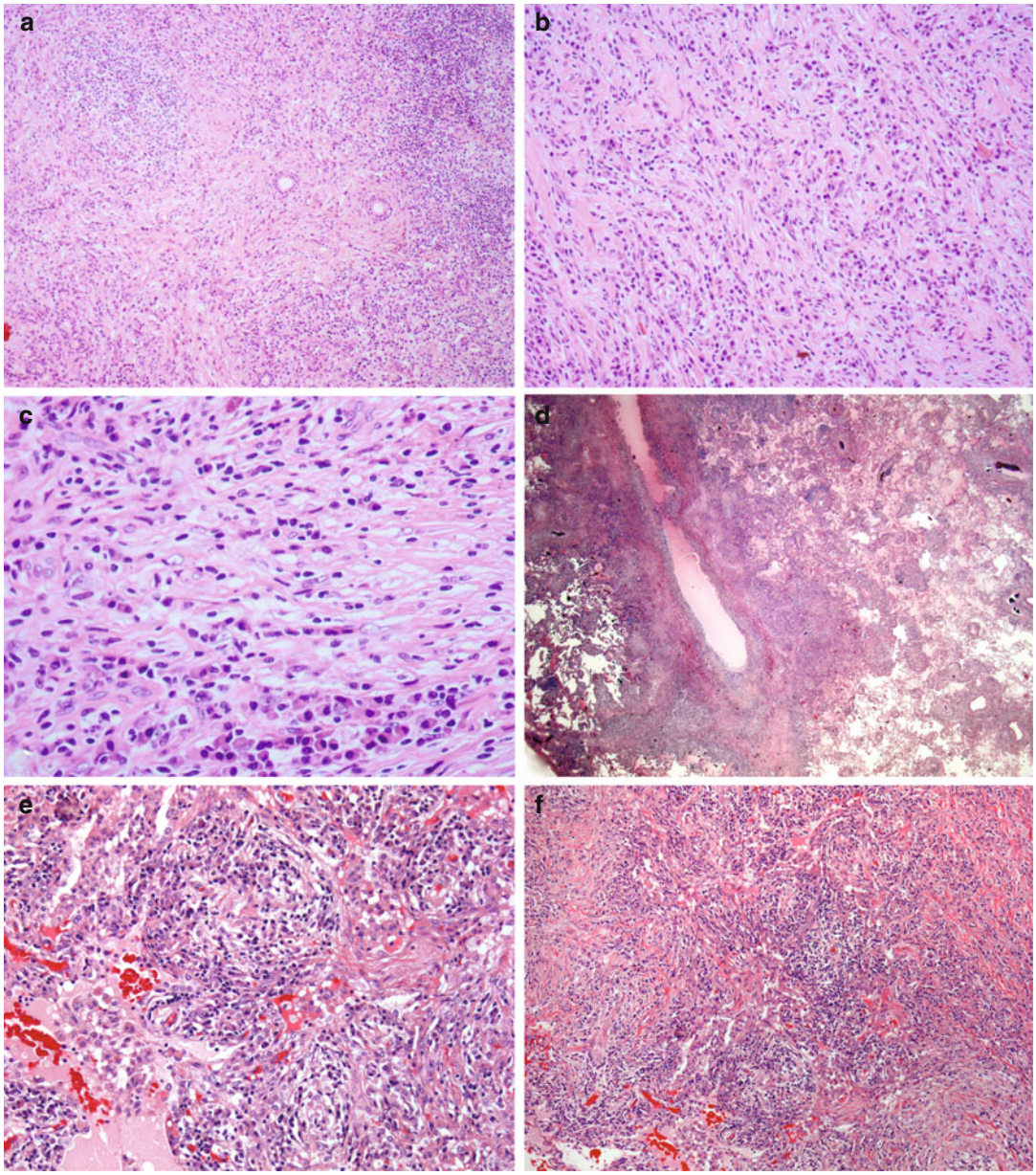

Fig. 17.125 IgG4-related fibrosis/tumor; in the first case there is a nodular pattern with areas of dense lymphoplasmocytic infiltration and aggregate formation (**a**); in (**b**) there is a mixture of plasma cells, myofibroblasts, and small lymphocytes very similar to IPT; in (**c**) the dense infiltration by plasma cells should cause one to investigate staining for IgG and IgG4. (**d**–**f**) Is another case with more diffuse infiltration and small nodules. (**d**) Shows an overview, in (**e**, **f**) the infiltration by plasma cells and myofibroblasts is shown. H&E, ×12, 25, 100, 200 (Case (**a**–**c**) courtesy of Ulrike Gruber-Moesenbacher, Feldkirch, (**d**–**f**) courtesy of Bruno Murer, Mestre)

Molecular Biology

Recently a methylation of the promoter region of Mst1, a serine/threonine kinase, has been identified in patients with IgG4-related fibrosis/tumors in the pancreas with additional involvement of extrapancreatic sites. Mst1 controls immune cell trafficking, proliferation, and differentiation and also thymocyte selection and regulatory T-cell

functions, preventing autoimmunity. There was also a decreased expression of MST1 in regulatory T cells suggesting that this contributes to the pathogenesis of IgG4-related tumors [374]. In patients with IgG4-related dacryoadenitis and sialoadenitis, the association between M2 macrophages and fibrosis was studied. The authors found an association of IL10 and CCL18 secreted by M2 macrophages and suggested that these macrophages play a key role in the development of fibrosis [375]. However, the causing agent(s) in IgG4-related tumor is still an enigma.

Differential Diagnosis

The main differential diagnosis is IPT as explained above; the main differences are IgG4-positive plasma cells and negativity for ALK1 [376]. In some cases with abundant plasma cells, the differential diagnosis of a plasmacytic variant of MALT lymphoma might be raised. Polyclonality of plasma cells will immediately rule this type of lymphoma.

Prognosis and Therapy

In many cases the multiorgan involvement in IgG4-related tumor/disease already helps in sorting out other tumors; however, in some patients, it may present as an exclusive pulmonary disorder [377–379]. In those cases surgical treatment with excision of the lesion is the treatment of choice. In systemic disease the patients can be treated with corticosteroid [368, 380, 381]. In other cases refractory for steroid treatment, a more aggressive immunosuppressive therapy needs to be applied [379, 382].

17.4.3.4 Undifferentiated Soft Tissue Sarcoma (Formerly Malignant Fibrous Histiocytoma, Also Epithelioid Sarcoma)

Clinical Features

Undifferentiated pleomorphic sarcoma (pleomorphic malignant fibrous histiocytoma) and undifferentiated spindle cell sarcoma present as a fast-growing mass lesion. Hypoglycemia can be present in rare cases, most probably related to the production and release of insulin-like growth factors, but is usually not a characteristic feature (see discussion below). No other specific symptoms are known.

Radiologic Features

Undifferentiated soft tissue sarcoma (USTS) is a mass lesion with ill-defined borders. Due to its enormous fast growth, many necrotic areas are seen on CT scan. However, it cannot be differentiated from any other malignant lung tumor or metastatic disease.

Gross Findings

On cut surface this tumor presents with many differently colored areas: collagen-rich white yellowish, dark grayish red due to hemorrhage, yellow corresponding to necrosis, and soft grayish yellowish reddish corresponding to cell-rich areas, most often corresponding to pleomorphic areas (Fig. 17.126). The tumor can grow quite large; in some cases tumors with a diameter of 17 cm have been seen. In these cases the tumor can replace almost totally a whole lung, which is seen as a small rim of compressed tissue [383].

Microscopic Findings

The sarcoma presents as fibromatous-storiform (spindle cell) and pleomorphic variants, whereas other variants have not been described in the lung. In storiform areas the cells look like fibroblasts, but more polymorphic, and mitoses are abundant. Collagen is deposited in short interweaving bundles. In pleomorphic areas there are many giant tumor cells, sometimes multinucleated and scarce structured matrix between the cells. The cells are most often isolated single epithelioid cells but lack an epithelial-like coherence and formation of tumor cell complexes. Chromatin is coarse, nucleoli are enlarged, and intranuclear vacuoles are frequent (Figs. 17.127 and 17.128). Mitoses as well as atypical mitotic figures are numerous, usually >10 per HPF. Invasion into blood vessels can be seen [384].

Immunohistochemistry

By immunohistochemistry the tumor is negative for epithelial and lymphocytic markers and negative for neuroendocrine markers. The mesenchymal marker vimentin is positive in all cells, desmin positivity can be seen in giant cells,

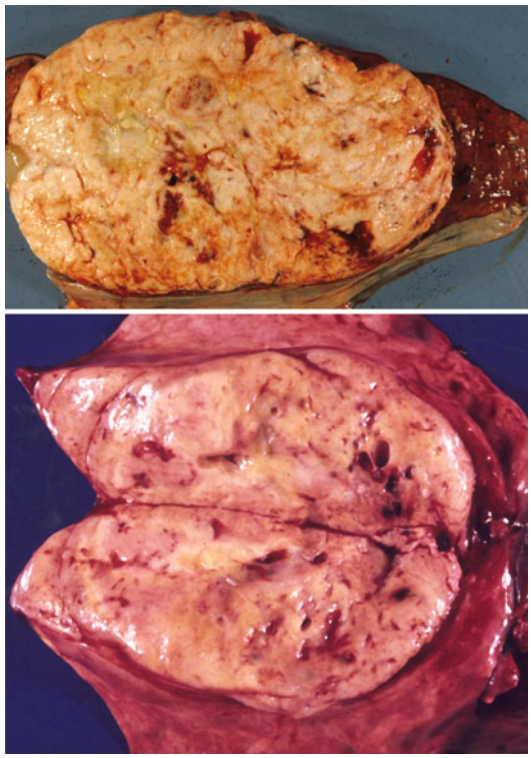

Fig. 17.126 Gross morphology of two cases of undifferentiated soft tissue sarcoma (USTS). In the *top* an autopsy specimen is shown; the tumor has replaced almost the entire lung tissue of the left lung. The patient died with respiratory failure. Of note, there was no metastasis outside the lung. The second case (*bottom*) is a lobar resection; similar the tumor has replaced almost the whole lung tissue in this lower lobe. In both *yellow* necrosis is seen, hemorrhage, and fleshy tissue, which already point to a mesenchymal tumor

smooth muscle markers as actin will highlight a few tumor cells, and neurofilament antibodies have been described in tumor cells but were negative in those cases we have seen. Rarely single cells can show a weak reaction for pan-cytokeratin antibodies or EMA, as well as CD99. S100 protein is always and CD34 is most often negative (Figs. 17.127e and 17.128c, e, f).

Molecular Biology

So far USTS has not been studied extensively. In one series of SFT, a case of USTS has been investigated and a week staining for STAT6 was noted [385]. In another study genomic hybridization showed some similarities between leiomyosarcomas and USTS [386]. However much more work is necessary, because USTS in soft tissues might not be the same entity as primary pulmonary USTS.

Differential Diagnosis

In the differential diagnosis, giant cell carcinoma, fibrosarcoma, MPNST, sarcomatoid mesothelioma, malignant solitary fibrous tumor, and metastatic disease have to be considered. Giant cell carcinoma of the lung will show a loose cohesive growth pattern; the cells usually coexpress cytokeratins and vimentin. There are no collagen deposits. Fibrosarcoma of the pleura may invade the lung and thus can mimic undifferentiated spindle cell sarcoma. However, fibrosarcoma cells and collagen are arranged into long bundles. MPNST does not produce this amount of collagen and usually has no pleomorphic areas. Tumor cells stain positively for S100 protein. Sarcomatoid mesothelioma might be hard to differentiate from MFH on H&E stain, but it expresses some of the mesothelioma markers, such as thrombomodulin, calretinin, and cytokeratin 5/cytokeratin 6, which have not been described in USTS. However, the cell polymorphism of USTS is quite characteristic compared to the "relative" monotony in sarcomatoid mesothelioma. The aberrant differentiation within undifferentiated pleomorphic sarcoma with cells positive for muscle markers will help in making the correct diagnosis [387–389]. Malignant SFT should not cause a problem in the differential diagnosis due to the low number of mitosis and the absent cell polymorphism. Even pure storiform undifferentiated spindle cell sarcoma is much more polymorphic than malignant SFT. However, in a single case of SFT, there were areas of malignant SFT together with a second area of undifferentiated pleomorphic sarcoma raising the possibility that pulmonary USTS might be the high malignant variant of SFT. Metastatic epithelioid and pleomorphic sarcomas might be very difficult to sort out, but there are additional markers (e.g., S100 protein for pleomorphic liposarcoma), which assist in that respect.

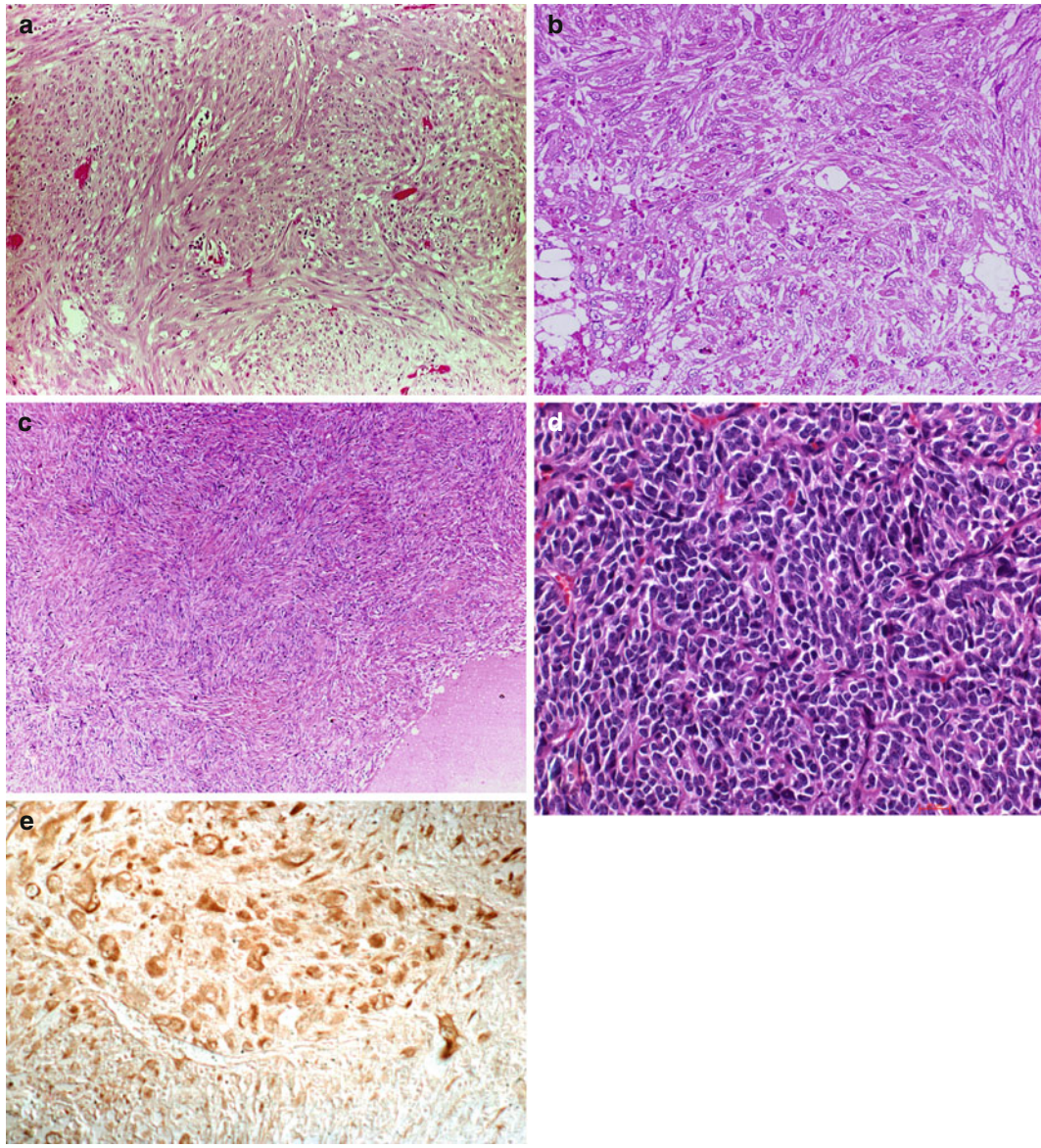

Fig. 17.127 Undifferentiated soft tissue sarcoma (USTS); in (**a**) the typical storiform pattern is seen; in (**b**) a predominant pleomorphic pattern is present, (**c**) shows the spindle cell pattern, and (**d**) a totally undifferentiated sarcoma. In (**e**) immunohistochemistry for vimentin is shown, one of the few markers constantly positive in these tumors. H&E, ×100, 60, 200 (Cases (**b**, **c**) courtesy of Bruno Murer)

Prognosis and Therapy

The prognosis of USTS is usually dismal. It grows fast, recurrences are seen, whereas metastasis is variable [383, 390]. Due to the high recurrence rate, aggressive chemotherapy and radical resection should be applied; however, the tumor cells in recurrent disease are most often chemoresistant. In contrast to USTS from soft parts, which is highly metastatic, pulmonary USTS in some cases does not metastasize at all or very late. This could support the theory of dedifferentiation of a more differentiated pulmonary soft tissue tumor, for example, SFT. As an alternative a tumor arising from primitive,

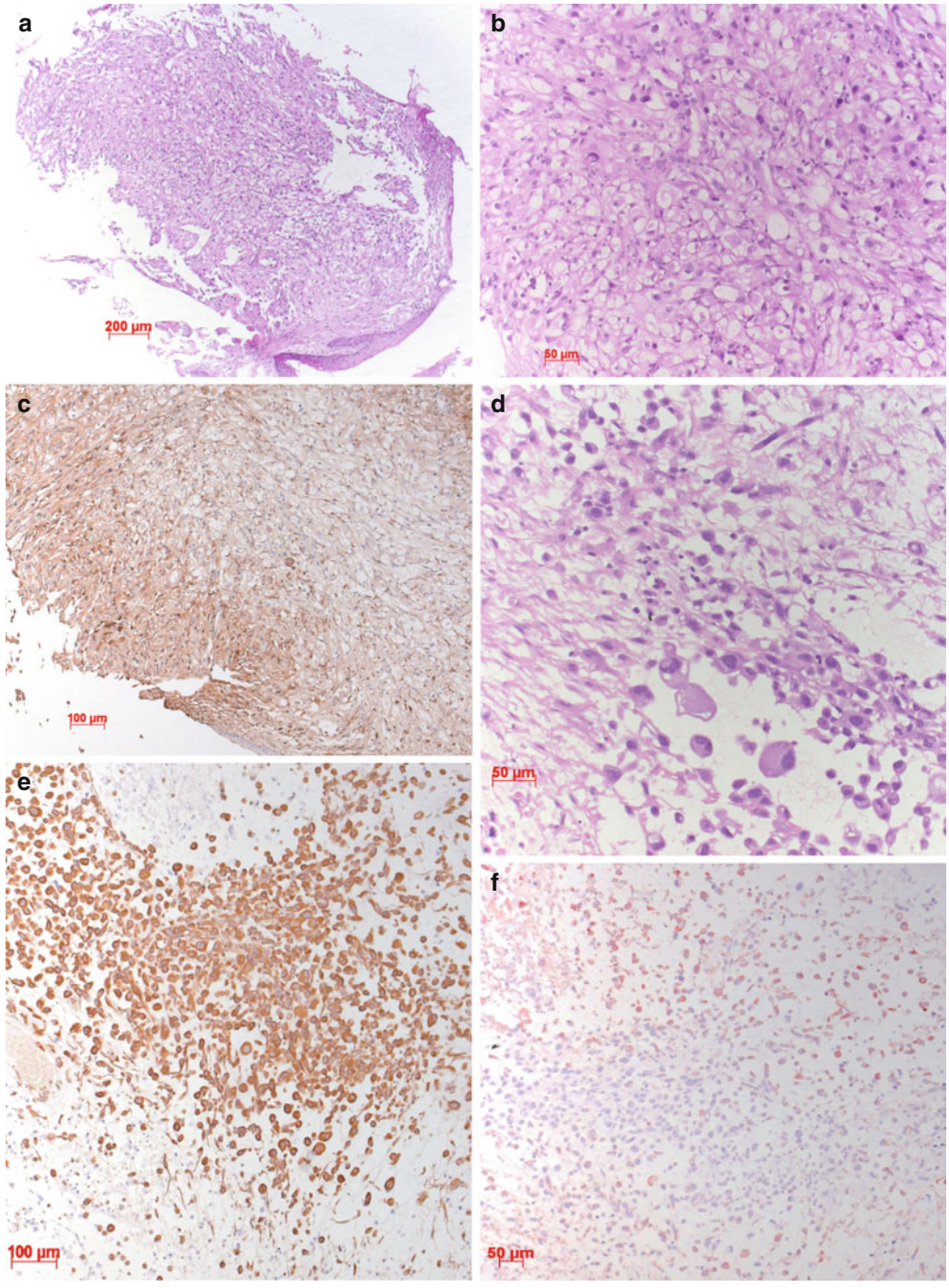

Fig. 17.128 USTS in small biopsies, shown are two different cases; (**a**–**c**), bronchial biopsy with an undifferentiated tumor in overview, and at higher magnification in (**b**). There are many clear cells, a marked polymorphism of tumor cells and nuclei with some large cells. By immunohistochemistry an undifferentiated carcinoma and several other entities could be excluded. In C a stain for lysozyme is shown. Case two (**d**–**f**) shows another USTS, here a pleomorphic type with many large tumor cells, by immunohistochemistry expressing vimentin (**e**) and α1-antitrypsin. Bars 200, 100, 50 µm

undifferentiated mesenchymal stem cells could also be considered. In those cases presenting with the clinical picture of hypoglycemia [391], the origin from a SFT is even more appealing. So the question remains if USTS is the same entity as in soft tissues or if pulmonary USTS is a different tumor.

17.4.4 PEComa (Clear Cell Tumor and Sugar Tumor)

History

This tumor was initially called sugar tumor, due to the abundant glycogen stored in the cytoplasm of the tumor cells. Later on the name changed into clear cell tumor, which reflects the dilution of the glycogen during fixation resulting in an empty-looking cytoplasm.

Origin of the Tumor Cells

PEComa arises from precursor cells within the vascular wall and differentiate along the perivascular epithelioid cell lineage (PECells). They are part of the pericytic cell complex, which can differentiate into smooth muscle cells, PEC, and pericytes. There are some features, which can also be seen in LAM and PEComas of other organ systems, especially angiomyolipomas of the kidney. In addition pulmonary PEComas can occur in the setting of tuberous sclerosis [324, 392].

Clinical Features

PEComa is most often an incidental finding in patients evaluated by X-ray due to an operation. There are no specific clinical symptoms, because the tumor is usually located deep in the lung parenchyma and does not cause symptoms. PEComa can be accompanied by angiomyolipoma of the kidney or can precede it. So whenever a PEComa is diagnosed in the lung, the clinician should be advised to carefully examine the kidneys.

Radiology

There are no specific findings in radiology, either X-ray or CT scan. A tumor mass is described.

Gross Findings

A solid tumor grayish-white well circumscribed, sometimes with clearly visible vascular spaces

Microscopic Findings

The tumor is composed of large polygonal tumor cells with small inconspicuous nuclei and usually invisible nucleoli. Chromatin is finely distributed, and the nuclear membrane smooth. On formalin-fixed paraffin-embedded material, the cytoplasm is clear. By PAS stain there is abundant glycogen demonstrated, which is best seen on frozen sections. Another characteristic feature is the prominent vascular network. Between the tumor nests, large dilated veins can be seen, often extensively branching, which gives the tumor a hemangiopericytoma-like appearance (Fig. 17.129). Most of these tumors will be benign, with small inconspicuous nuclei and invisible nucleoli. The chromatin is finely dispersed. However, there is a rare malignant variant with marked nuclear atypia, prominent nucleoli, and coarse chromatin pattern (Fig. 17.129c–f). Vascular invasion might be seen but is usually difficult to prove due to the dense vascular network.

Immunohistochemistry and Molecular Biology

The tumor is negative for cytokeratins and lymphocytic markers but positively stained by vimentin and HMB45 antibodies (Fig. 17.129d). A strong granular immunostaining in the tumor cell cytoplasm with the anti-MyoD1 antibody was reported in PEComas but may correspond to cross-reactivity with an undetermined cytoplasmic protein [393]. The gene TFE3 is closely related to microphthalmia-associated transcription factor (MiTF) and is overexpressed in PEComa showing a nuclear staining in most of them [394]. Positivity is seen most often in young age, absence of an association with tuberous sclerosis, predominant alveolar architecture, and epithelioid cytology. The authors concluded that PEComas harboring TFE3 gene fusions may represent a distinctive entity [395]. Overexpression of MITF also causes the expression of the cysteine protease cathepsin K, which was constantly and strongly expressed in renal PEComas. Cathepsin K might therefore

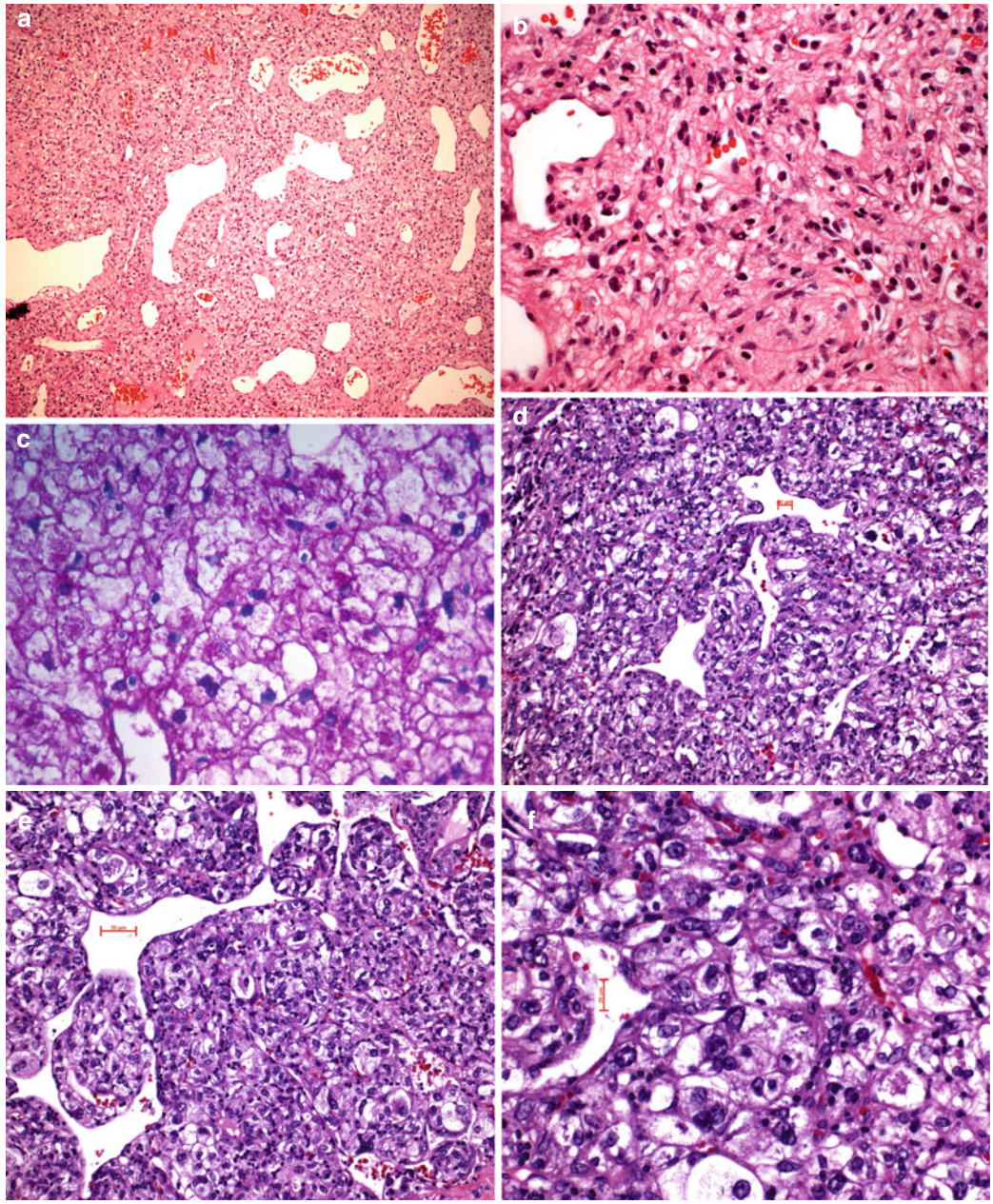

Fig. 17.129 Examples of PECOMA (clear cell tumor), in (**a**) classical case with many clear cells and bland nuclei (**b**). By PAS stain (**c**) the positivity corresponds to glycogen in the cytoplasm. The second case (**c**–**f**) shows a case with pronounced nuclear polymorphism, but again the clear cytoplasm stains for glycogen (PAS). The nuclei have coarse granular chromatin, nucleoli are visible, and the nuclear membrane is accentuated (**d**). This case might be called of intermediate dignity, and a close follow-up of the patients is recommended. Only blood vessel invasion is a definite proof of malignancy, which could not be proven in this case. In (**g**) immunohistochemical stain for HMB45 and in (**h**) a stain for Melan A is shown; both markers used to confirm the diagnosis. Bars 50, 20, 10 µm, and ×25, 200

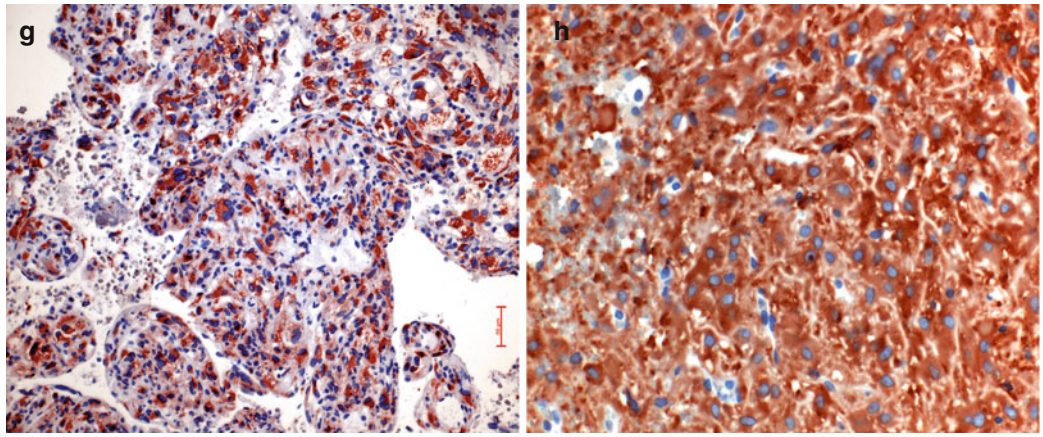

Fig. 17.129 (continued)

be a useful marker [396]. A mutation in the tuberous sclerosis complex, and possible deregulation of the RHEB/MTOR/RPS6KB2 pathway, has been observed in some PEComas, and regression was achieved under sirolimus therapy (mTOR inhibitor).

Differential Diagnosis

Metastases of renal and primary pulmonary clear cell carcinomas are the most important differentials. Both are positive for cytokeratins; in addition they usually show much more nuclear atypia than benign clear cell tumor. In the malignant variant, the nuclear features might not help in this respect. Another rare tumor coming into the differential diagnosis might be metastasis from melanoma and clear cell sarcoma. MUM1 positivity can be demonstrated in primary and metastatic melanomas and clear cell sarcomas, whereas MUM1 was only weakly positive in few PEComas [397].

Prognosis and Therapy

Clear cell tumor in almost all cases is a benign lung tumor. Surgical excision is the treatment of choice. No recurrence has been reported. It is a slow-growing tumor. For the exceedingly rare malignant variant, there are no data available. In addition clear cell tumor is part of the spectrum of the tuberous sclerosis complex. Thus it can be associated with angiomyolipoma of the kidney and LAM. In those cases with a mutation in one of the TSC genes, mTOR inhibitor therapy might be used, if surgical resection is not possible.

17.4.5 Chondroma, Osteoma, and Lipoma

Clinical Features

These are all benign tumors with unspecific clinical presentation, usually symptomless. All three tumors are extremely rare and are incidental findings [398, 399].

Radiologic Features

Chondroma as well as osteoma present with typical radiological features; however, they are usually mistaken for a hamartoma, because osseous and chondromatous areas are well known in these more common neoplasms. Lipoma can be correctly diagnosed by CT scan due to the low density of the tumor. However, this can also be erroneously being misidentified as mediastinal fat.

Gross Findings

Both tumors present with a specific gross pattern, either chondromatous or osseous. Chondroma usually is composed of hyaline cartilage and thus has a glistening smooth cut surface, bluish white. Osteoma will present as a well-circumscribed tumor composed of bone trabeculas and fatty bone marrow in between. Lipoma will be a soft

yellow, homogenous, well-encapsulated, and circumscribed tumor as in soft tissue location. Few cases are intraparenchymal, whereas most cases present as endobronchial tumors causing obstruction [400–402].

Microscopic Findings

Chondroma is a well-circumscribed tumor entirely composed of cartilage. In the lung this is the hyaline cartilage. Chondrocytes are embedded as single cells within the hyaline matrix. They do not exhibit nuclear atypia. Nuclei are small; chromatin is finely dispersed. There are no epithelial structures, especially no primitive tubules as in hamartoma.

Osteoma is a well-circumscribed benign tumor composed of mature lamellar bone trabeculas with mature osteocytes and a few osteoclasts. Between the trabeculas bone marrow or fatty tissue can be seen, usually also lacunar structures, such as in mature long bones. At the border spicules can be found, which is interpreted as the matrix from which bone formation starts (Fig. 17.130) [403].

A lipoma is composed of mature lipocytes with inconspicuous nuclei, finely dispersed chromatin, and univacuolated cytoplasm. In contrast to hamartoma, there are no epithelial tubules within the tumor (Fig. 17.131).

There is a rare lipoblastoma recognized in children presenting with opacification and in case of large size with mediastinal shift on chest radiograph [404]. Histologically the tumor is composed of immature lipoblasts. Prognosis is good; surgical excision is recommended [405].

Differential Diagnosis

Hamartoma is the major differential diagnosis in all three tumors. Hamartomas can be composed of different mesenchymal elements and primitive epithelial tubules, reminiscent of primitive bronchiolar sprouts in embryogenesis. These tubules are absent in chondroma, lipoma, and osteoma. However, in hamartomas the mesenchymal components can be dominated by either lipomatous or chondromatous elements, whereas osteoma-like areas are usually scarce in hamartomas. The major problem are entrapped bronchioles within the tumors usually around the border; these can easily be separated from the primitive tubules seen in hamartoma by the presence of a smooth muscle layer in the former. Metastasis of well-differentiated chondrosarcoma or osteosarcoma should be considered. Osteosarcoma is characterized by osteoid, no mature bone; in both tumors metastasis and nuclear atypia is present. Mitosis is usually found in the sarcomas, and clumping cells and binucleated chondroblasts are typically found in chondrosarcomas. Peripheral pulmonary ossification might be misdiagnosed for osteoma: the main difference is that an osteoma is well circumscribed without pulmonary tissue within the tumor. Well-differentiated liposarcomas do not metastasize, and the intermediate and high-grade variants cannot be mistaken for a lipoma.

Prognosis and Therapy

All of them are benign mesenchymal tumors, slowly growing, without a potential of metastasis. Surgical excision is the treatment of choice.

17.4.6 Tumors with Nervous Differentiation

17.4.6.1 Schwannoma and Malignant Peripheral Nerve Sheet Tumor (MNPST)

Granular Cell Schwannoma and Myxoid Schwannoma

Clinical Features

Benign schwannoma is a rare tumor of the lung. There are no clinical features, which could lead to a tentative diagnosis. The granular cell variant might be suspected on bronchoscopy, because it causes flat polypous projections or a cobblestone appearance of the mucosa (Fig. 17.132). All other schwannomas including the malignant peripheral nerve sheet tumor (MNPST) just present as a mass lesion not different from many other tumors.

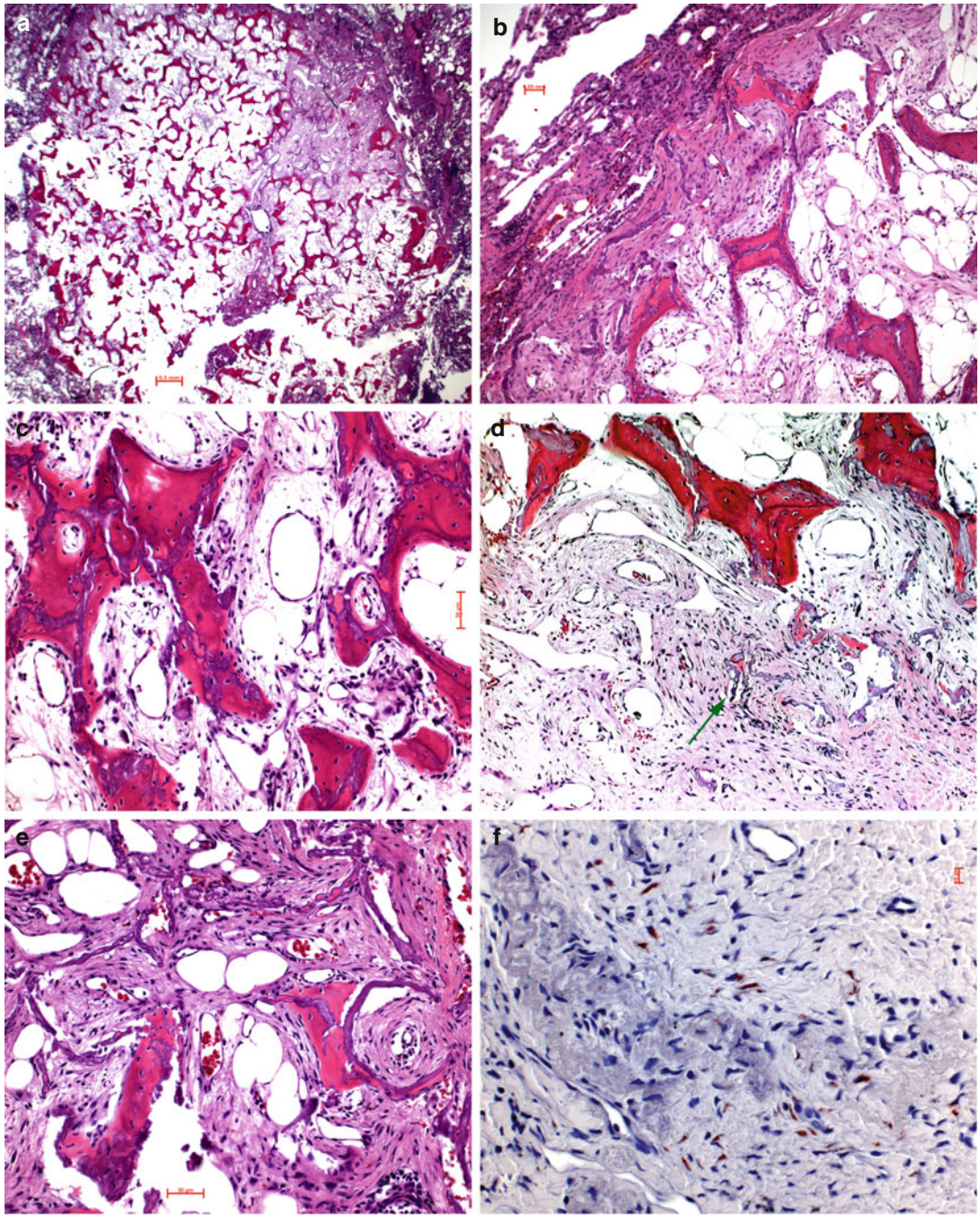

Fig. 17.130 Osteoma of the lung is shown in an overview in (**a**); the tumor is separated from the lung by a fibrous pseudocapsule. In contrast to a hamartoma, the tumor has no primitive bronchiolar tubules. In (**b**) the border to normal lung shows how this tumor might be formed: small calcified spicules are formed around which a mature bone synthesis starts. Even if fully formed lamellar bone trabeculas the calcified nucleus is retained (**b**–**e**). Around the calcium deposits a fibrous tissue is visible (**d** see *arrow*), fat tissue is focally present, and sinusoids are formed (**c**–**e**). In (**f**) some of the spindle cells express osteonectin. H&E, Movat, and immunohistochemistry, bars 500, 50, 10 µm

Radiology

On X-ray schwannomas are usually detected and described as lung mass. Granular cell schwannoma escapes the detection. MNPST is taken as a malignant tumor. FDG uptake is seen in many schwannomas and in MNPST too [406, 407].

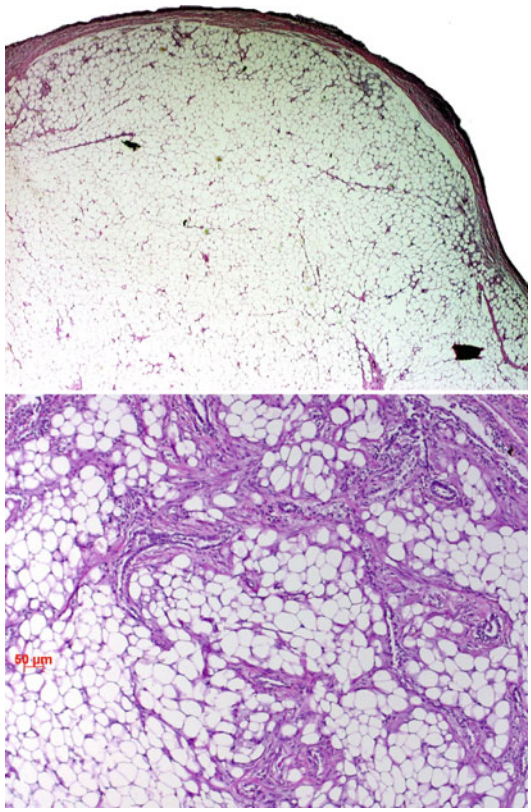

Fig. 17.131 Lipoma of the lung, overview in the *upper panel*, and detailed morphology in the *lower panel*. No epithelial tubules as in the lipomatous variant of hamartoma are present. H&E, ×12 and bar 50 µm

Gross Findings

Benign schwannoma presents as a solitary well-circumscribed tumor within the lung but more often arise in the posterior mediastinum, growing into the lung. These are well-circumscribed tumors, with a grayish-white cut surface and fascicular structures. Occasionally schwannomas can be very large and may cause lung collapse [408].

Granular cell schwannoma (granular cell tumor, Abrikosov tumor) is different in as far as it grows as small multinodular lesion within and under the bronchial mucosa. It causes a nodular or cobble stone appearance of the mucosa at bronchoscopy.

MNPST in contrast is macroscopically not different from any other malignant tumor. However, in most instances it arises from the posterior mediastinum and continuously invades the lung; rarely this tumor arises within the lung.

Microscopic Findings

Spindle cells with comma-shaped nuclei at one end and a blunt end on the other side characterize schwannomas. The classical picture of nuclear rows or palisades is not always clearly visible. The ill-defined cytoplasm usually shows wavy filament bundles. By polarization these filaments are not birefringent in contrast to collagen and are not stretched as myofilaments. If stained by Gieson stain, they are pale yellow. In myxoid schwannoma the matrix formed by myxoid glycoproteins and glycolipids (Fig. 17.133a–c). In ancient schwan-

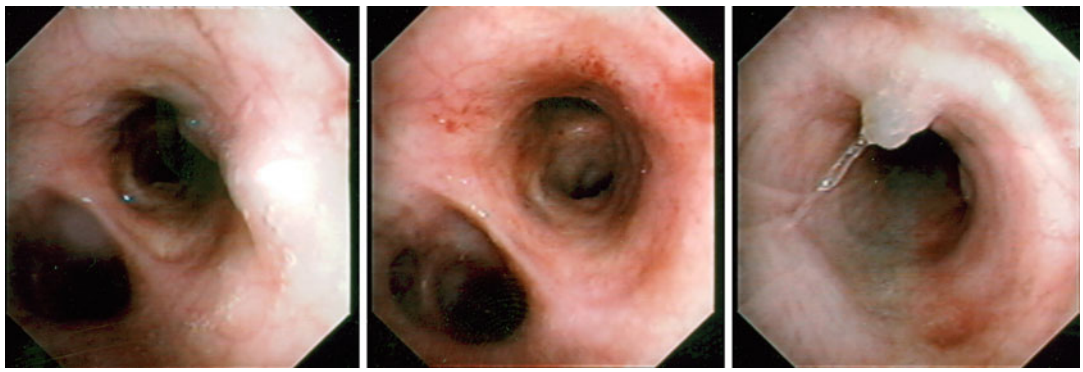

Fig. 17.132 Bronchoscopic appearance of granular cell schwannoma with the typical multinodular pattern on the mucosa surface

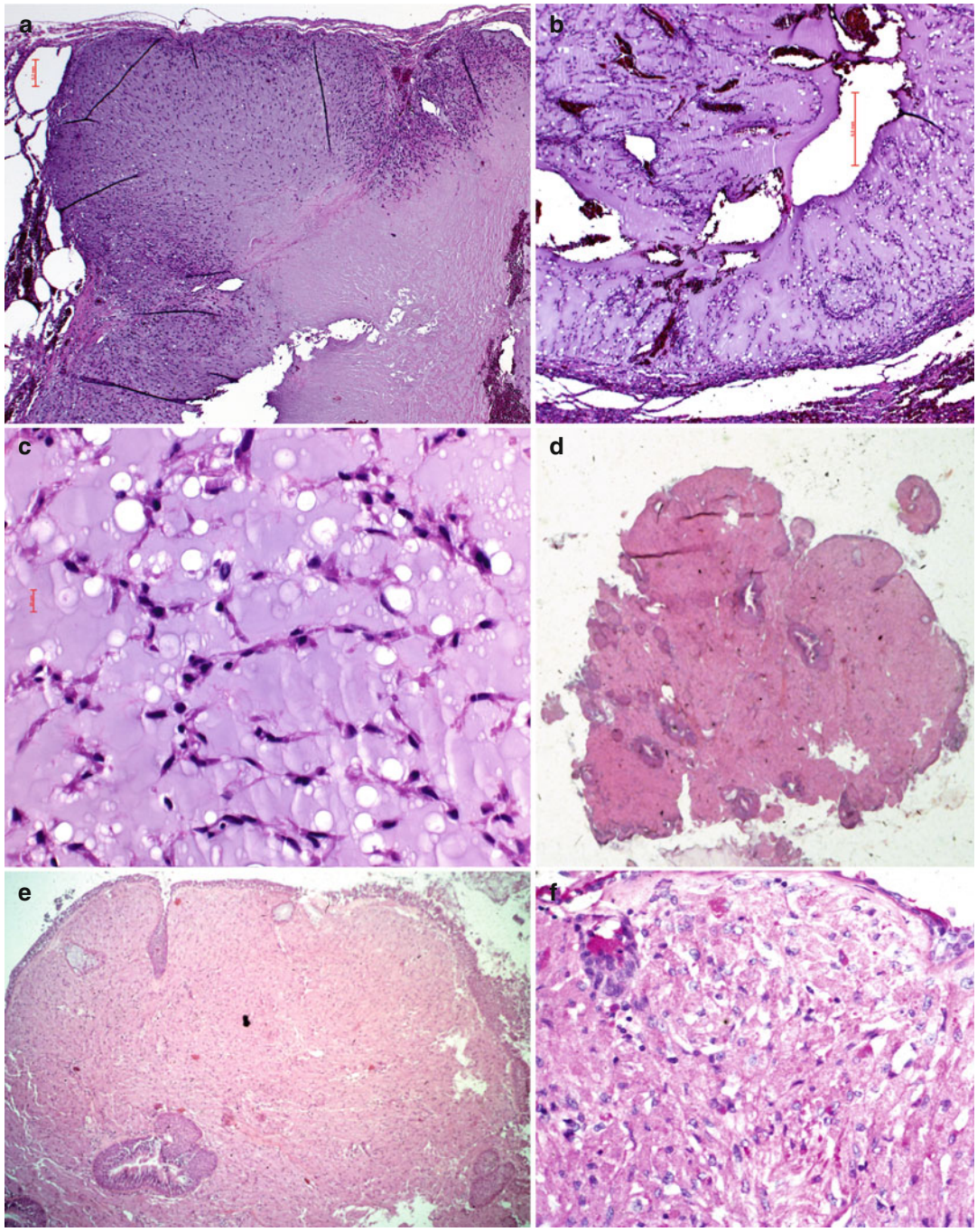

Fig. 17.133 Schwannomas of the lung; (**a**–**c**) a case of myxoid schwannoma arising within the lung. An overview is shown in (**a**); detailed morphology is seen in (**b**, **c**). There is abundant myxoid stroma; the tumor cells form a net within this matrix. The nuclei are typically comma shaped. The chromatin is finely dispersed, no atypia, and no mitosis is seen. (**d**–**f**) Shows a granular cell schwannoma. This tumor forms small nodules confined to the bronchial mucosa (**d**). The tumor cells have a broad cytoplasm and small inconspicuous nuclei. The cytoplasm is eosinophilic and granular (**e**), positive on PAS stain (**f**). Bars 500, 200, 20 μm, ×12, 50, 100

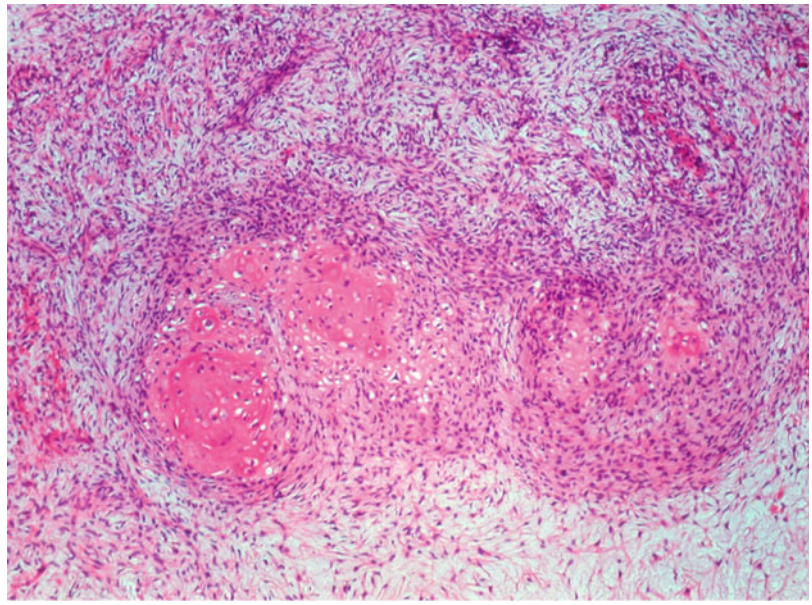

Fig. 17.134 Malignant peripheral nerve sheet tumor (MPNST) with high cellularity. The cells have the characteristic comma-shaped nuclei as in schwannoma, but here is nuclear polymorphism and mitotic activity. In the center are two areas, which simulate a chondroid differentiation. The stroma between the tumor cells does not show any collagen deposition and the matrix pale blue. In the cytoplasm of some tumor cells, neurofilaments can be seen. H&E, 200

noma there are usually extensive regressive changes but also small preserved areas composed of Antoni A and B areas. A rare case of psammomatous melanotic schwannoma was also described arising within the lung, characterized by melanin pigment in the Schwann cells. Neurofibromas do also occur in the lung but usually in patients with generalized neurofibromatosis. In these tumors there is more abundant collagen fiber deposition, but otherwise the cells are similar. Ganglioneuromas are exceedingly rare in the lung but have been seen, whereas these are more common in the posterior mediastinum [409–413].

Large polygonal cells with small round nuclei, usually located centrally within the cell, characterize granular cell schwannoma. The cytoplasm has a granular eosinophilic appearance, positively highlighted by the PAS stain. A characteristic feature is the growth pattern: the tumor cells can be found close up to the basal lamina. Also these tumors usually form several small nodules (Fig. 17.133d–f). Bulging into the lumen of the bronchus or trachea, very rare these tumors are within the parenchyma [414–416]. Granular cell schwannoma is in almost all cases a benign tumor; however, few malignant cases have been described. These are characterized by nuclear polymorphism and mitotic figures usually 1 per high-power field, whereas in the benign cases, mitoses are not seen, and nuclei are monomorphous [417].

In MNPST

In MNPST the typical features are focally nuclear palisading and areas of cellular crowding. Nuclei are spindle shaped; chromatin is dense with large irregular-shaped nucleoli. The nuclei are most often also comma shaped. Nuclear atypia and polymorphism is prominent. In the epithelioid variant, the cells are larger and polygonal, and nuclei are more round but also show polymorphism (Fig. 17.134). There are >5 mitosis/10 HPF [413, 418–420].

A diagnosis might be possible by fine needle aspiration biopsy due to the characteristic nuclei of schwannomas.

Ancillary Studies

By immunohistochemistry all these tumors stain positively for S100 and vimentin antibodies but are negative for epithelial markers. In the epithelioid variant of MNPST, positivity for cytokeratin can be focally found.

Differential Diagnosis

For granular cell schwannoma, there is no differential diagnosis. The typical pale cytoplasm,

positive on PAS stains, the fine granularity, and the growth pattern approaching the basal lamina are quite characteristic. For classical schwannomas other benign mesenchymal tumors enter the differential diagnosis, such as fibromas and leiomyomas. The Gieson stain will help in excluding fibromas and a stain for smooth muscle marker leiomyomas. For MNPST other malignant mesenchymal tumors enter the differential diagnosis, such as undifferentiated sarcoma and leiomyosarcoma. Also the rare dendritic cell tumors can mimic MNPST. An immunohistochemical investigation for S100, smooth muscle actin (SMA), and neurofilament antibodies will assist in differentiating between MNPST and leiomyosarcoma and also undifferentiated sarcoma, which might show focally single cytokeratin-positive tumor cells. Dendritic cell tumor will also be S100 positive; therefore, markers for dendritic cells (CD35, CD83, HLADR) have to be added to come up with the correct diagnosis. Malignant synovialoma can sometimes mimic MNPST, but in the biphasic type, the epithelioid cell will be focally positive for cytokeratin, and both components are negative for S100.

Molecular Biology

Merlin (moesin-ezrin-radixin-like protein) is a gene product of NF2 and serves as a linker between transmembrane proteins and the actin cytoskeleton. Merlin is involved in integrating and regulating the extracellular cues and intracellular signaling pathways for cell fate, shape, proliferation, survival, and motility. Merlin also functions as a negative regulator of growth and progression of several non-NF2-associated cancer types [421]. In some schwannomas merlin expression is lost. This is associated with loss of SOX10 protein, which is vital for normal Schwann cell development, and is key to the pathology of Merlin-null schwannoma tumors [422]. LZTR1 germline mutations were identified in multiple schwannoma syndrome. Loss of heterozygosity with retention of an LZTR1 mutation was present in all schwannomas. LZTR1 was identified as a gene predisposing to an autosomal dominant inherited disorder of multiple schwannomas [423]. In another study mutation of LATS1 and loss of function was found in inherited schwannomas, but only exceptionally in sporadic schwannomas. These familial cases had also an associated germline MSH4 mutation [424]. Neurofibromatosis is an autosomal dominant genetic disorder with mutations in NF1 and NF2 and can be associated with multiple schwannomas. In some of these schwannomas, mutations in SMARCB1 were identified [425]. However, there are many neurogenic tumors with unknown genetic abnormalities.

Prognosis and Therapy

Granular cell schwannoma is almost ever a benign tumor, which is cured by surgical excision sometimes even by simple bronchial biopsies. Even a regression might occur, since we personally know of cases, where the nodular lesions have been removed by laser surgery and did not recur. Classical schwannomas and neurofibromas are usually surgically removed and again have an excellent prognosis without recurrence. MNPST are highly malignant tumors, which behave similar to those in other location and metastasize regularly via the blood vessels. Surgical excision and postoperative chemotherapy might be necessary. In some cases a treatment with kinase inhibitors has been successfully done [426].

17.4.7 Triton Tumor

Triton tumor is a tumor with multifaceted differentiation. Malignant as well as benign variants do exist. Almost all organ systems can be involved, and incidental case reports have described Triton tumors in the lung [407, 427]. Triton tumor is seen predominantly in children but also in young adults [428]. Patients often also present with neurofibromatosis.

Clinical Presentation

Shortness of breath and dyspnea are common but unspecific symptoms.

Radiology

A tumor mass is seen by X-ray and CT scan in the lung.

Gross Morphology

The tumor presents as a large, soft, and gelatinous mass; size can be from a few cm to large tumors of >10 cm in diameter.

Histology

The tumor cells are spindle shaped, embedded in abundant myxoid stroma. Atypia of nuclei and enlarged nucleoli are present in the malignant variant. Areas of rhabdomyoblastic differentiation characterized by large cells with abundant eosinophilic cytoplasm and occasional cytoplasmic striated muscle fibers could be seen. Within the tumor both elements are mixed. In benign Triton tumor skeletal muscle, fibrous tissue, and nerve tissue are arranged in a disorganized way [429].

Immunohistochemistry

The tumor cells are positive for S100 protein in the atypical spindle cells, whereas a strong positive reaction for desmin and myoglobin is seen in the rhabdomyoblastic areas. In one case a focal positive reactivity for cytokeratins was reported [430].

Molecular Biology

In a molecular analysis of a single case, translocations were found in 49,XY, der(14;15)(q10;q10),+i(8)(q10)×4 and by FISH an additional i(8)(q10) in all tumor cells. The analysis of TP53 revealed a polymorphism in exon 9 [124]. In another study loss of one Patched gene allele was found. On recurrence Patched expression was lowered suggesting a haploinsufficiency [431].

Differential Diagnosis

Given the two elements within the tumor, not much differentials do exist. Synovial sarcoma might be one of them. A biphasic synovial sarcoma will show cytokeratin expression in the epithelial component, whereas in the monophasic variant, only spindle cells are seen in the entire tumor. Synovial sarcoma present with a characteristic translocation not present in Triton tumor, and Triton tumor is negative for CD99 and TLE1, which are markers for synovial sarcoma.

Prognosis and Therapy

The prognosis of malignant Triton tumor is worse compared to malignant peripheral nerve sheath tumors; the status of NF1 mutation has no impact on the prognosis [432]. Most patients die within months. Factors that correlate with worse outcome are mitotic rate >4 mitoses/50 HPF and increased cellularity [433]. Complete tumor resection is the treatment of choice; adjuvant radiation and chemotherapy may also improve survival [122].

17.4.8 Paraganglioma

Clinical Features

Primary paragangliomas of the lung are extremely rare. Most often they are metastatic to the lung. I have seen four cases of pulmonary paragangliomas out of approximately 9,000 cases of lung tumors, three of them primary paragangliomas, and one a metastasis from a pheochromocytoma, preceding the primary tumor for several months. As in many endocrine neoplasms, there are no clear-cut features for predicting biological behavior. Paragangliomas might induce clinical symptoms, such as paroxysmal blood pressure increase (most often this should induce a careful examination of the adrenal medulla for pheochromocytoma) or crisis, palpitations, headache, and diaphoresis, but more often they are symptomless [434, 435]. In patients with abnormal blood pressure symptoms, determination of catecholamine metabolites in urine should be done.

Radiology

Paragangliomas are detected incidentally and are described a single nodule within the lung by CT scan.

Gross Findings

Paragangliomas are grayish-reddish tumors of different size, usually not above 2 cm, are embedded in peripheral lung tissue, and have no specific appearance.

Microscopic Findings

As in any other location, they are characterized by a "cell-ballen" structure: chief cells form epithelioid cohesive cell aggregates, the so-called

cell ballen, and are surrounded by sustentacular spindle cells. Chief cells have finely granular cytoplasm, round nuclei with finely dispersed chromatin, and inconspicuous nucleoli, whereas the chromatin of the nuclei of sustentacular cells is darker, also equally dispersed, and nucleoli are invisible or unremarkable. Within the tumor dilated blood vessels are prominent, forming a sinusoidal venous network (Fig. 17.135). On low magnification paragangliomas are often mistaken as carcinoid. In metastasizing paraganglioma mitosis is more frequent as well as nuclear atypia. In addition in metastasis, the sustentacular cells are missing.

Immunohistochemistry

Paragangliomas are negative for cytokeratin antibodies, positive for neuroendocrine markers, especially chromogranin A, synaptophysin, and NSE, whereas the sustentacular cells are positive for S100 protein antibodies.

Molecular Biology

Succinate dehydrogenase B (SDHB) was the earliest molecular abnormality reported in paragangliomas. However many more genetic abnormalities have been added to date, such as VHL (von Hippel-Lindau), RET (multiple endocrine neoplasia type 2), NF1, SDHA, SDHB, SDHC, SDHD, SDHAF2, TMEM127, MAX, EGLN1, HIF2A, and KIF1B. Germline mutations in one of these genes occur in about 35 % of the paragangliomas. Furthermore, somatic mutations of RET, VHL, NF1, MAX, HIF2A, and H-RAS can also be detected [436]. Fortunately immunochemistry has been shown to be an excellent indicator of germline mutations in the SDH genes [437]. Based on signaling pathways, paragangliomas can be divided into a pseudohypoxic cluster and a cluster rich in kinase receptor signaling and protein translation pathways. Interestingly both clusters are interconnected via somatic and germline mutations in HIF2α gene [438]. An additional mutation was found for MDH2 patient with multiple malignant paragangliomas. MDH2 encodes a Krebs cycle enzyme. MDH2 protein expression was downregulated in MDH2-mutated tumors [439].

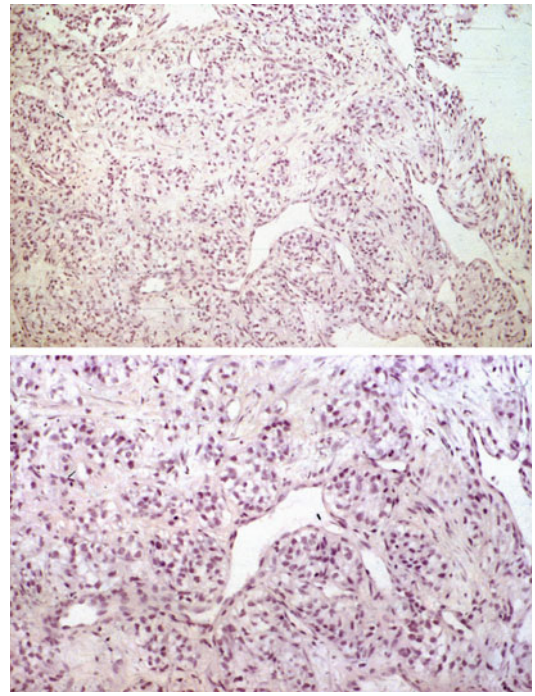

Fig. 17.135 Primary paraganglioma of the lung. The tumor shows the characteristic pattern of nests of chief cells surrounded by satellite cells in the *upper* and *lower panels*. Immunohistochemistry is not required in such a case, but metastasis from outside the lung has to be ruled out. H&E, 100, 200

Different syndromes are associated with paraganglioma and pheochromocytomas, such as the MEN syndromes, hereditary cancer syndromes, etc. An overview is given by the Baysal and O'Toole reports; in addition a recommendation for testing was also published [440–442].

Differential Diagnosis

The major differential diagnoses are pulmonary carcinoids. These are positive for neuroendocrine markers and cytokeratin. Scattered S100 protein-positive Langerhans cells are sometimes seen in carcinoids, whereas sustentacular cells in paragangliomas surround the chief cell clusters. Morphologically there is no possibility to differentiate primary versus secondary paraganglioma so far. It can happen that metastasis precede the primary tumor. So careful investigation for and exclusion of an unknown primary is the only way to diagnose a primary pulmonary paraganglioma.

Prognosis and Therapy

The biological behavior of primary paraganglioma of the lung cannot be predicted. At present factors such as genetic background, tumor size, and tumor location are associated with higher rates of metastatic disease. Surgery is the only curative treatment [443].

17.4.9 Pulmonary Meningioma

Pulmonary meningioma is a rare benign mesenchymal lung tumor. It is proposed that these tumors arise from precursor cells in the deeper pleural layer. Tumors are usually within the lungs, probably growing out from the interlobular septa [100]. Rare cases have been reported with NF2 germline mutation presenting with anaplastic biparietal falx meningioma, tentorium meningioma multiple cranial and spinal tumors, and recurrent pulmonary benign meningiomas and single neurinoma [444].

Clinical Features

No specific clinical symptoms are recorded. The tumors are usually incidental findings.

Gross Findings

Either one of multiple small grayish-white well-circumscribed nodules are seen. There is no capsule. Cut surface is smooth; a fine lobular structure might be visible.

Microscopic Findings

The tumor is composed of nests and cords of meningothelial bland-looking cells, not different from those in the meninges. Pulmonary meningiomas are usually of the meningothelial, rarely of the transitional type (Fig. 17.136). In one report a chordoid variant has been described [445].

Immunohistochemistry

There is no need of immunohistochemistry, because the structure and the cells are typical and cannot be misdiagnosed once the fact is known that these tumors do exist. Immunohistochemistry with positivity for glial fibrillary acidic protein (GFAP), anti-collagen IV, CD44, EMA, and vimentin and negativity for cytokeratin might be used for confirmation and in those cases with unusual morphology.

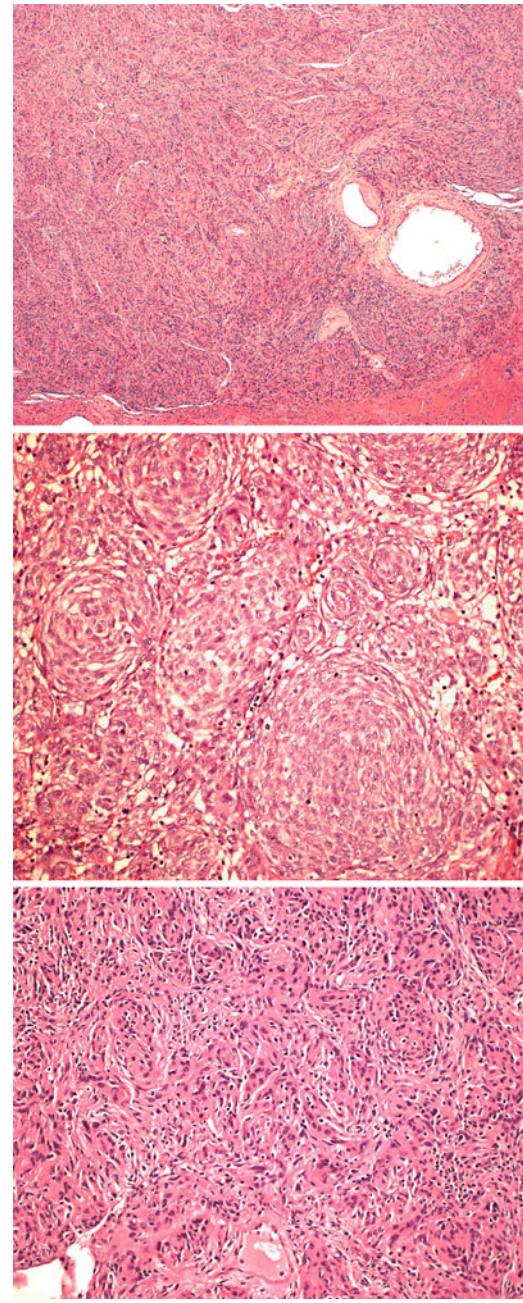

Fig. 17.136 Pulmonary meningiomas, one of them a classical meningothelial type shown in an overview (*top*) and more close (*middle*) with the classical meningothelial whorls. A transitional type is shown at the *bottom*, with many more fibroblast-like cells. H&E, ×50 and 160

Differential Diagnosis

There is no differential diagnosis to be considered. Diagnosis can be made on H&E-stained sections.

Prognosis and Therapy

This is in almost all cases a benign tumor. On rare occasion a concomitant meningioma of the meninges can occur [446]. Surgical resection is the treatment of choice. There are rare cases of malignant meningiomas in the lung, some proven to be primary other retrospectively identified as being metastasis of atypical grade III CNS meningiomas or meningiosarcomas [447–451].

17.4.10 Vascular Tumors

17.4.10.1 Hemangioma

Clinical Features

Recurrent hemoptoe and hemoptysis might be the only symptom. Unexpected life-threatening bleeding usually in a young-aged population can result. Patients may require urgent lung surgery, and in our experience most often a lobe or even a whole lung has to be removed, because intraoperatively the source of the bleeding cannot be located. Hemangioma can be centrally localized in large bronchi [452, 453] or can occur as arteriovenous or cavernous hemangiomas [454–457] within the lung parenchyma (Fig. 17.137). The main affected populations are children or young adults. In small children, the occurrence of hemangiomas, especially if these are multiple, should cause the search into other malformations, as these can occur in the setting of partial trisomy [458].

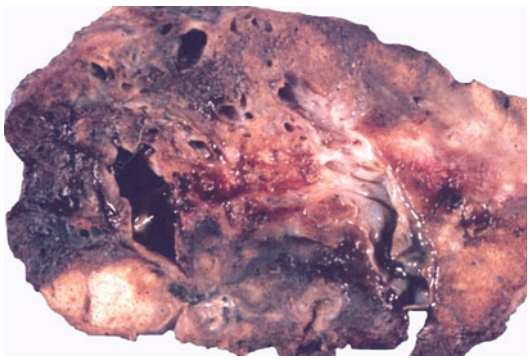

Fig. 17.137 Cavernous hemangioma in a 7-year-old girl. The large dilated blood vessels are easily seen accompanied by hemorrhage, which was the leading symptom in the patient

Radiologic Findings

Centrally located hemangiomas are usually small nodular lesions, which are detected by bronchoscopy but not by radiology (X-ray or CT scan). Peripheral hemangiomas are detected due to hemorrhage, which is seen on CT scan. Cavernous hemangiomas might be detected on CT scan when tracers are used.

Gross Findings

Bronchial hemangioma presents as a small bluish-red nodule on cut surface. Peripheral hemangioma cannot be detected on gross sections due to large areas of hemorrhage. No specific features can be seen. In cases where there was no acute bleeding, an area with localized hemorrhage and dilated blood vessels might be recognized.

Microscopic Findings

Bronchial hemangiomas are usually capillary hemangiomas with many small capillary loops underneath the bronchial mucosa. Ulceration of the mucosa is common, which sometimes makes it impossible to separate hemangioma from granulation tissue (Fig. 17.138). In these cases fibroblasts and inflammatory cells will help to come up with the correct diagnosis of repair tissue. The peripheral hemangiomas are most often cavernous type, composed of large dilated, thin-walled blood vessels, forming a convolute (Fig. 17.139) and also hemangiomas of arteriovenous type (Fig. 17.140). A rupture is often the reason why these lesions have been removed. To prove the rupture requires usually multiple serial sections.

Immunohistochemistry

Immunohistochemical stains are usually not necessary to make the diagnosis but can assist in detecting ruptures in the peripheral hemangiomas. Factor VIII-associated antigen, factor XIII, CD31, or any other endothelial marker can be used.

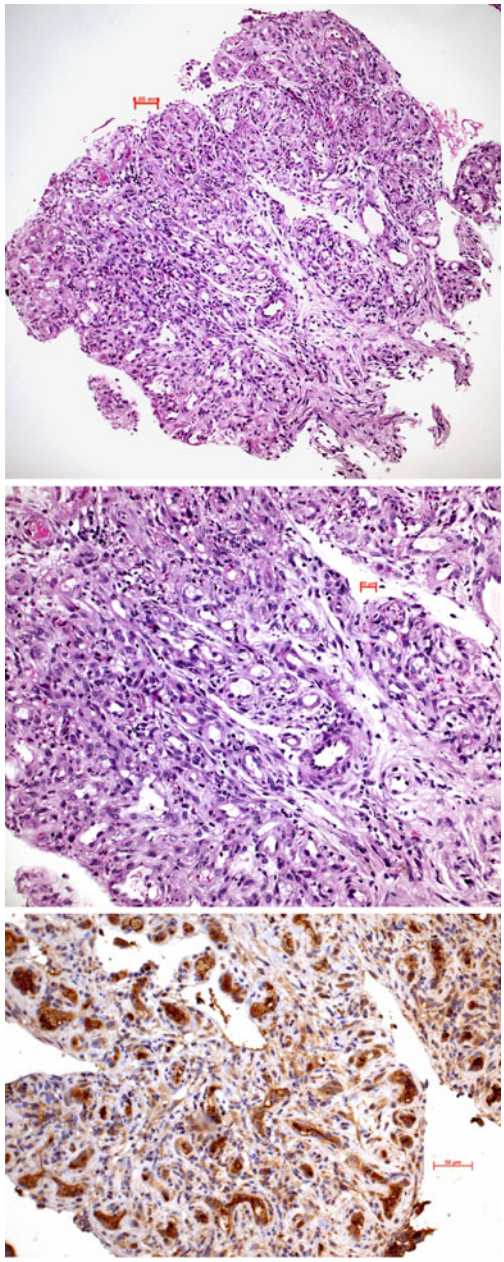

Fig. 17.138 Bronchial hemangioma, showing the many thin-walled capillaries and dilated veins. One of the supplying arteries is in the center (*top*). Higher magnification is seen in the middle; a major feature differentiating hemangioma from granulation tissue is the absence of a pronounced inflammation and stroma cell proliferation. By immunohistochemistry for VEGF-C, the vascular proliferation is highlighted, and also several cells within the stroma are shown to be primitive endothelial precursor cells. Bars 50 and 20 μm

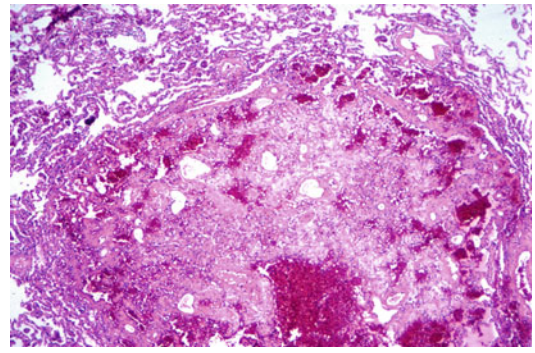

Fig. 17.139 Cavernous hemangioma, same case as in Fig. 17.138. The large dilated venous blood vessels are seen, in addition some hyalinization and hemorrhage. H&E ×25

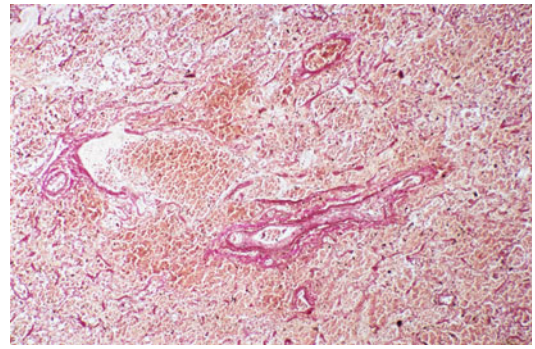

Fig. 17.140 AV angiomatosis in a 19-year-old male patient. The patient presents with sudden hemoptysis, and because the source of bleeding was not found by bronchoscopy, a lobe resection had to be performed. The picture shows the rupture of an AV angioma. However, more such areas were found within the resected lung. Elastica v. Gieson, ×50

Differential Diagnosis

Other diseases associated with alveolar hemorrhage have to be separated. Vasculitis is easily diagnosed; congenital malformation of blood vessels, however, might be indistinguishable from hemangioma. Especially Scimitar syndrome can look like peripheral hemangioma. Osler's disease of the lung is characterized by arteriovenous anastomosis, and in these areas dilated veins are usually seen. In addition in Osler's disease, there might be pulmonary hypertension with plexiform lesions, which will help in making the right diagnosis.

Prognosis and Therapy

Surgical excision is the treatment of choice. If diagnosed early the prognosis is excellent. There is no recurrence.

17.4.10.2 Pulmonary Capillary Hemangiomatosis

Clinical Features

Pulmonary capillary hemangiomatosis (PCH) can present as a reactive proliferation of capillary blood vessels, usually associated with primary pulmonary hypertension or veno-occlusive disease, or as a tumor. The clinical symptoms are rather unspecific such as hemoptoe or hemoptysis. Whereas the reactive form can occur at any age, the tumor form is exclusively found in children of older age [459–461]. In one case report, PCH was associated with hereditary hemorrhagic telangiectasia or Osler-Weber-Rendu syndrome [462].

Radiological Features

The radiological features are uncharacteristic as well: a ground-glass pattern can prevail, which represents alveolar hemorrhage. A thickening of alveolar septa and diffuse bilateral reticulonodular pattern associated with enlarged central pulmonary arteries can sometimes be seen on high-resolution CT scan [463].

Gross Findings

Hemangiomatosis will show focal hemorrhage, usually confined to lobules or segments. Several areas can be involved.

Microscopic Findings

Hemangiomatosis is characterized by a capillary proliferation within the alveolar septa. Instead of a single capillary loop, two or three loops can be seen. They can be arranged side by side or can be localized at both sides of the septum. Acute bleeding might obscure the lesion. Hemorrhage usually compresses the capillaries; therefore, the evaluation should focus on areas where there is no hemorrhage. The endothelial cells look normal. Illustrations are shown in the vascular chapter.

Ancillary Studies

Usually there is no need of immunohistochemistry, but in case of uncertainty, a stain for factor 8-associated antigen or any other endothelial marker can assist the diagnosis.

Molecular Biology

PCH expresses markers for proliferation and angiogenesis such as vascular endothelial growth factor and MiB1. In contrast to plexiform lesions in arterial hypertension, PCH retains peroxisome proliferator-activated receptor-γ (PPARγ) and caveolin-1, which also suppress growth [464]. PCH in addition expresses platelet-derived growth factor (PDGF)-B and PDGF-receptor β (PDGFRβ). PDGFB was found in type 2 pneumocytes and endothelial cells, whereas PDGFRβ localized to pericytic and vascular smooth muscle cells [465]. Recently another molecular abnormality was found in PCH: mutations in EIF2AK4, a kinase regulating angiogenesis in response to cellular stress, might cause autosomal-recessive PCH in familial and some nonfamilial cases [466]. In a subsequent report by Tenorio and colleagues, this mutation was attributed to familial pulmonary arterial hypertension, which questions the finding in respect to isolated PCH [467].

Differential Diagnosis

There is no differential diagnosis for hemangiomatosis. For a differential diagnosis of tumor or reactive the other features of primary pulmonary hypertension or veno-occlusive disease have to be excluded.

Prognosis and Therapy

This is a progressive disease, which will ultimately cause death of the patient. Lung transplantation is the recommended treatment at present, although hemangiomatosis might recur in the transplanted lung. Imatinib a PDGFR inhibitor may be beneficial in the treatment due to its potent antiproliferative effect. Two patients with pulmonary arterial hypertension and PCH have been treated safely and efficiently [468].

17.4.10.3 Epithelioid Hemangioendothelioma and Angiosarcoma

Clinical Features

Epithelioid hemangioendothelioma (EHE) presents as either solitary or in 60 % as multinodular mass; in a few cases, two organs usually the liver and lung can be involved [469, 470]. The multinodular form is usually mistaken as metastatic disease; in the combined liver and lung form, it is impossible to designate the location of the primary site. There are no specific clinical features; pain can be a symptom. Epithelioid angiosarcoma (EAS) presents as a solitary tumor either centrally or peripherally located. Metastasis in EAS is far more common than primary pulmonary EAS. Epidemiologically EAS was initially seen in patients exposed to vinyl chloride, arsenic compounds, and thorotrast [471–474].

Radiologic Features

The diagnosis of epithelioid hemangioendothelioma and angiosarcoma is rarely made. Most often the diagnosis will be metastatic disease due to multifocality and angiocentric pattern, which can be seen on CT scan [475].

Gross Findings

Epithelioid hemangioendothelioma (EHE) as well as angiosarcoma (EAS) presents as ill-circumscribed tumors of any size. If properly sectioned, the relationship to pulmonary blood vessels might be evident. The cut surface is grayish red to dark red, depending on the amount of hemorrhage. In EHE a hyalinized center can be seen by its white-grayish color and chondroid consistency. Hyalinization is usually not seen in EAS, which presents more often with extensive hemorrhage. In multinodular and bilateral cases, the individual nodules are <2 cm per nodule.

Microscopic Findings

EHE can present with a variety of features. There is hyalinization with few cells in the tumor center, but especially in these areas, endothelial cells with well-formed intracytoplasmic capillary lumina (pseudo-signet ring cells) are easily found. Hyalinization is sometimes preceded by myxoid stroma changes. This hyaline center is not a necrotic area of the tumor but a reactive hyalinization due to changes in the matrix protein composition and tertiary structure remodeling. In areas with hemorrhage, the tumor cells are usually obscured. At the borders there is a reactive proliferation of pneumocytes type II, which initially was misinterpreted as the tumor cell. Nuclei in EHE are round and vesicular with finely distributed chromatin and small inconspicuous nucleoli. Mitosis is absent. An infiltrative growth into alveolar septa along preexisting capillaries and even growth within the wall of blood vessels, sometimes narrowing the lumen, is quite characteristic (Fig. 17.141) [476–478].

In EAS the tumor cells look similar as in EHE, but there is higher cellularity and nuclear as well as cytoplasmic atypia. Mitosis is regularly seen. Mitotic counts are in the range of 2–8 per 10 HPF. Nucleoli are more prominent. In EAS the tumor forms many vascular channels and sinusoids, which are filled with red blood cells (Fig. 17.142). Necrosis does occur. Hyalinosis or scarring is absent. As EHE also EAS cells invade preexisting blood vessels, however, they destroy the vascular wall and therefore usually cause bleeding. In cases where the sarcoma is located near central arteries, massive lethal hemorrhage can occur due to the invasion of the sarcoma into the arterial wall. The sinusoids formed by the sarcoma connect with the larger arteries and veins, which is the reason why red blood cells are present within the lumina [453, 477–479].

Immunohistochemistry

The tumor cells express endothelial markers such as CD31, factor VIII-associated antigen, coagulation factor XIII, and vimentin. Up to 30 % of tumors can focally express cytokeratins, especially EAS. Low-grade EHE expresses vascular endothelial growth factor receptors 2 and 3 at the cell membrane, whereas EAS shows a nuclear and cytoplasmic expression of VEGFR2 and VEGFR3 (Figs. 17.143 and 17.144). This seems to be due to a translocation of the kinase domain into the nucleus [478]. Immunohistochemistry usually is not necessary, because of the unique location of the tumor and the growth pattern along and within blood vessels.

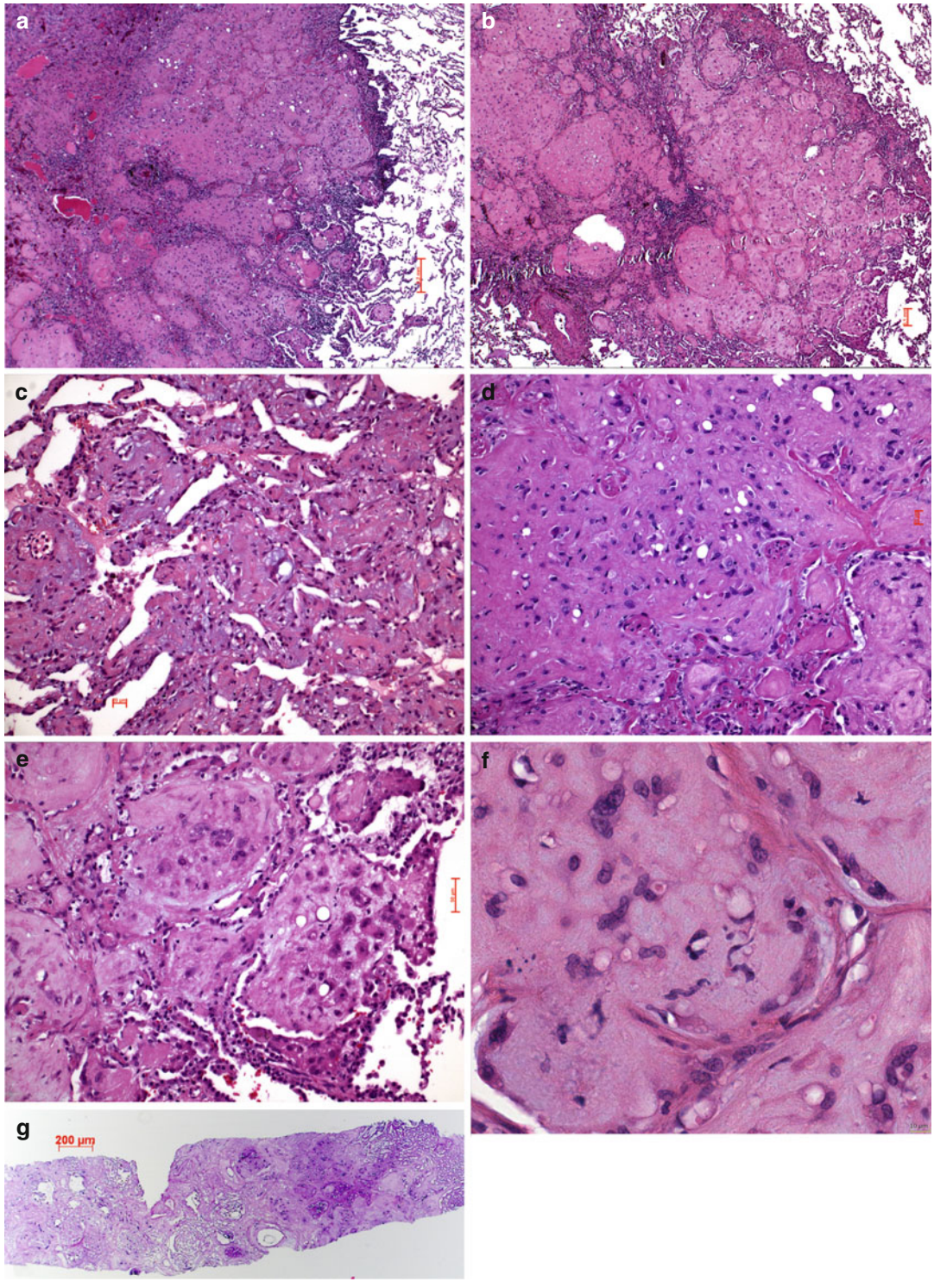

Fig. 17.141 Epithelioid hemangioendothelioma; three different cases are shown. (**a**, **b**) Show the classical nodular pattern, whereas in **c** a diffuse infiltration is seen. In the central areas, sclerosis is prevalent, whereas in the periphery the more cellular proliferation components are seen (**a**–**d**). The tumor cells are embedded in a myxoid matrix; they characteristically form small clusters or are as single cells. Signet ring cell-like vacuoles are present in many areas, which on high magnification are identified as primitive endothelial tubules; sometimes single red blood cells can be encountered in the lumen (**e**, **f**). The diagnosis can be made on small biopsies as shown in G. H&E, bars 200, 100, 50, 20, 10 µm

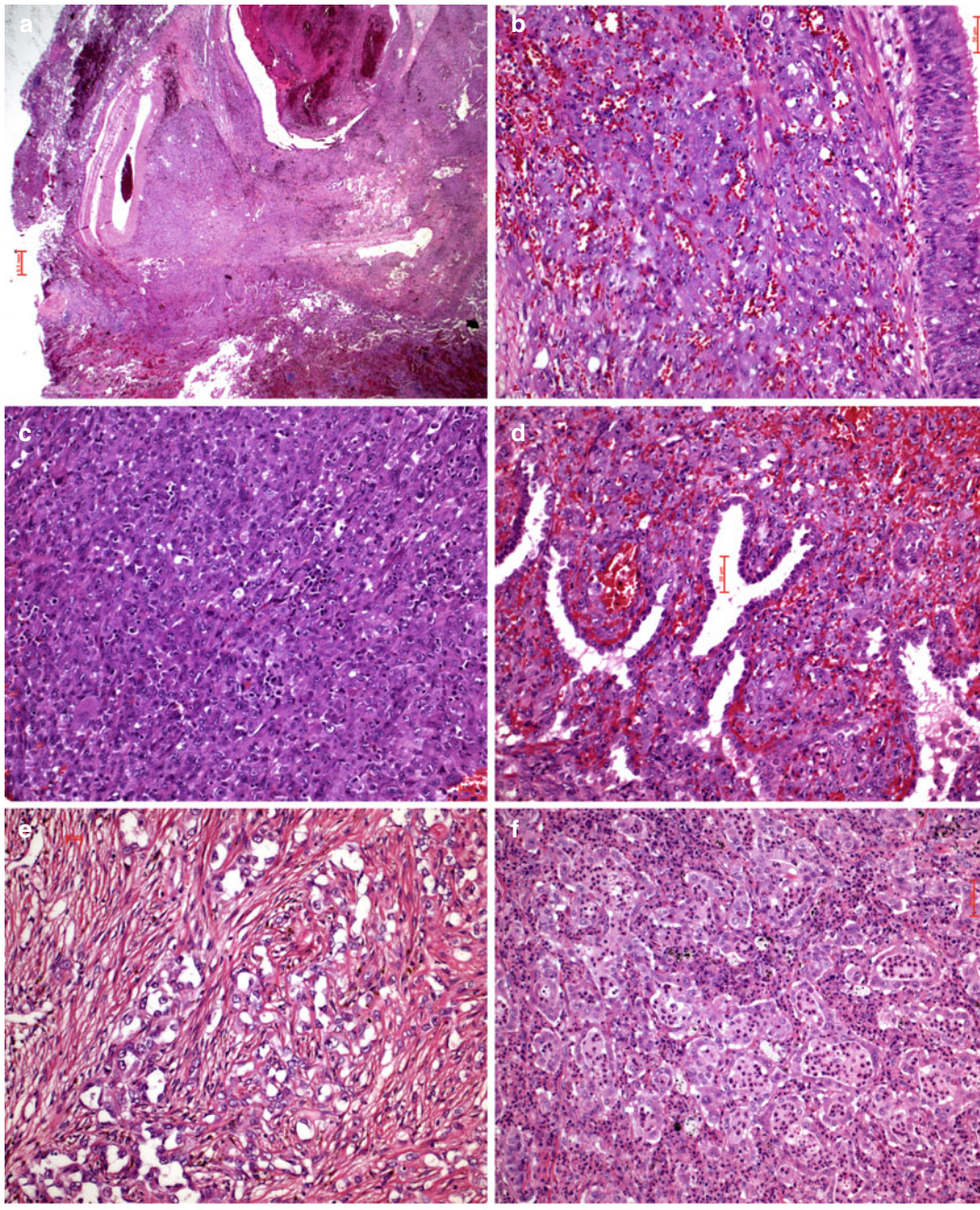

Fig. 17.142 Epithelioid angiosarcoma cases, in (**a**) an overview is presented, which shows the proximity of the sarcoma to a large lobar artery with thrombosis and hemorrhage. (**b**) Shows the infiltration underneath the bronchial epithelium, one of the reasons for hemoptysis, when the sarcoma breaks into the mucosa. (**c**–**f**) Shows examples of patterns epithelioid angiosarcoma can present with: a solid pattern (**c**), an infiltrative pattern within the alveolar septa without disrupting the epithelium (**d**), a pattern with extensive desmoplastic stroma formation (**e**), and a pattern with cord of tumor cells and dense granulocytic infiltration (**f**). The tumor cells have large nuclei, irregular distributed coarse granular chromatin, and large prominent nucleoli, often in eccentric position. Mitosis is frequent. The cytoplasm is most often basophilic faintly stained but can be clear (**e**). The tumor cells form primitive vascular channels, which are usually filled with red blood cells. H&E, bars 500, 50, 20 μm

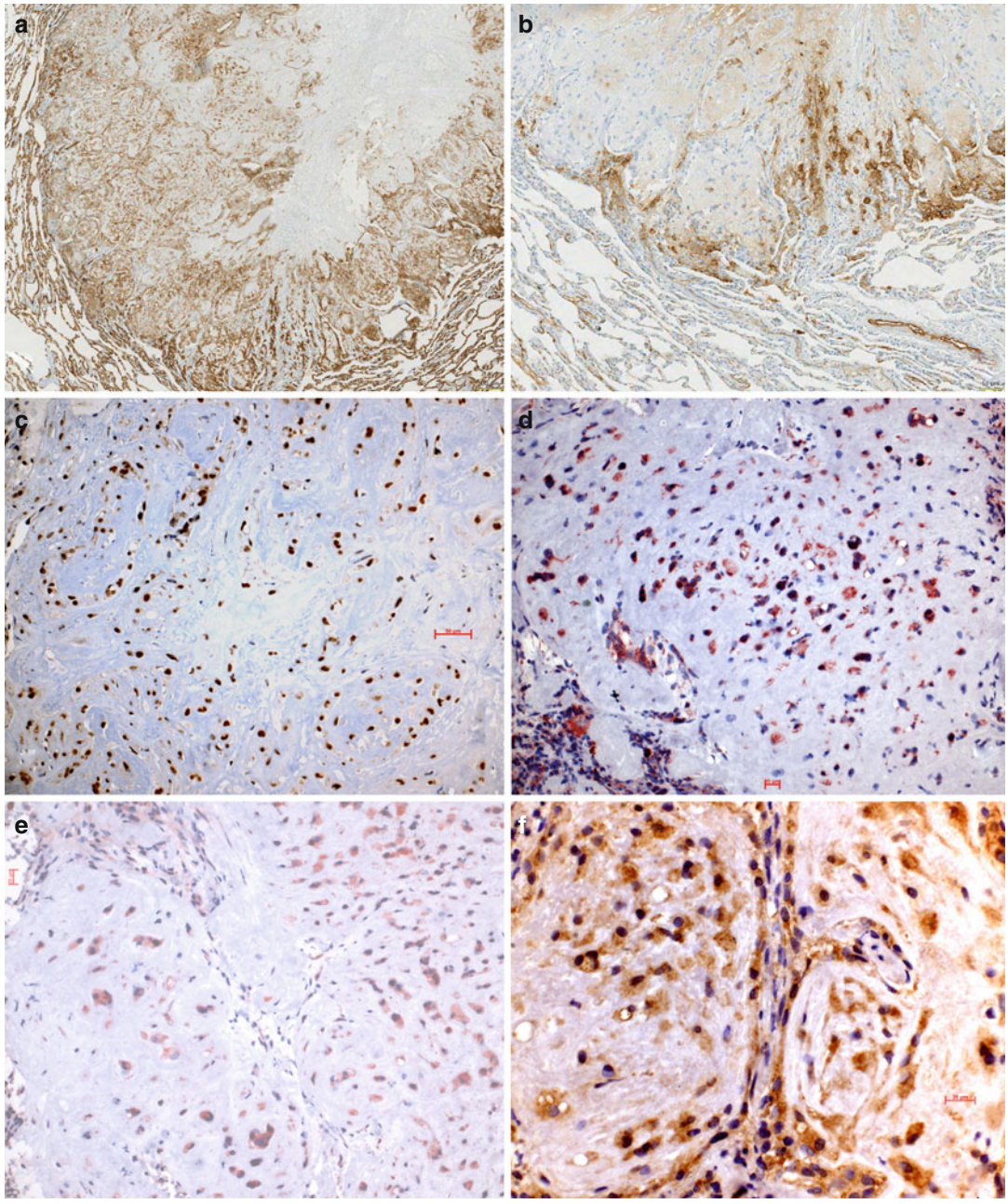

Fig. 17.143 Immunohistochemistry of epithelioid hemangioendothelioma showing CD31 (**a**), factor 8-associated antigen (**b**), vascular endothelial growth factor receptor 3 (**c**), VEGFR2 (**d**), endothelial receptor tyrosine kinase Tie2 (**e**), and VEGF-C (**f**). Note the nuclear staining of VEGFR3, which is common in the malignant angiogenic tumors. Bars 50, 20 μm, ×5

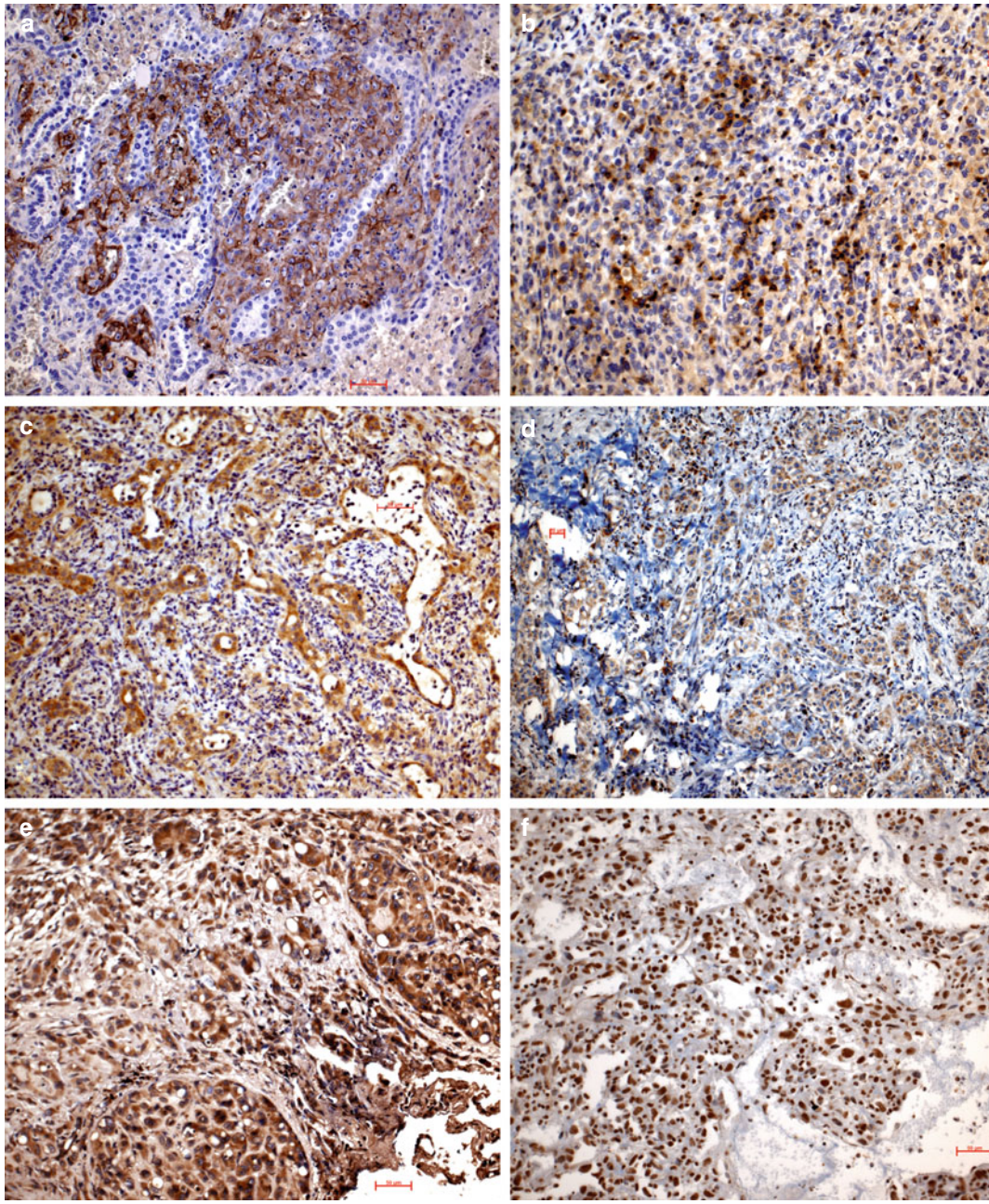

Fig. 17.144 Immunohistochemistry of epithelioid angiosarcoma, showing reactions for CD31 (**a**), Tie2 (**b**), VEGF-C (**c**), VEGFR2 (**d**), and two reaction patterns for VEGFR3, one with classical membranous and cytoplasmic (**e**) and the other with exclusive nuclear staining (**f**). Bars, 50, 20 μm

Differential Diagnosis

There are some differential diagnoses to be discussed: sclerosing pneumocytoma and EHE; epithelioid sarcomas, mesothelioma, and undifferentiated carcinomas and EAS; and metastatic disease.

Sclerosing pneumocytoma shows similar hyalinized centers as EHE but is positive for EMA and surfactant apoproteins and negative for endothelial markers. Organizing infarcts and other reactive processes can also sometimes mimic EHE – again the

positive reaction for endothelial markers and the presence of primitive endothelial tubules will help in the correct diagnosis. Metastasis from EHE might be difficult to differentiate; however, the central hyalinized area of primary EHE is not seen in metastasis. EAS can be differentiated from epithelioid sarcomas by the presence of sinusoids and capillaries and by the positivity for endothelial markers. The growth of tumor cells within the intima of pulmonary blood vessels is almost characteristic for EHE as well as EAS. With respect to mesothelioma, the ingrowth into the lung along interlobar and interlobular septa is in contrast to the expansion of EHE and EAS out of the lung following pulmonary blood vessels. Also some of the mesothelioma markers such as calretinin and cytokeratin 5/cytokeratin 6 are negative in EAS. Epithelioid sarcomas might be difficult to differentiate, especially in small biopsies. However, the vascular structures are absent in these sarcomas, and endothelial markers are not expressed. Metastasis from other primary epithelioid angiosarcoma is sometimes impossible to separate from primary pulmonary angiosarcoma: multiple foci within the lung are in favor of metastasis; otherwise the radiological and clinical information are the only source to rule out metastasis.

Molecular Biology

There are not many investigations in these rare tumors. In the report by Cao, they found small chromosomal gains in EHE but gains and deletions in EAS. In EAS gains in chromosomes 19q and 19p and deletions in chromosomes 9p and 13q were seen [480]. By FISH analysis Anderson et al. found CAMTA1-WWTR1 fusions in low-grade and intermediate-grade EHE whereas this was not seen in EAS. On the contrary a WWTR1 complex abnormality in one case of EAS has been described [477]. Tyrosine kinases are key factors for the proliferation of angiosarcomas in general, but for EHE and EAS in the lung are still not solved. Some reports on treatment with multikinase inhibitors show either limited or transient response [481, 482].

Prognosis and Therapy

Surgical removal is the best treatment in localized forms of these tumors. Systemic chemotherapy might be applied. Prognosis for EAS is usually dismal with a 5-year survival rate of 20 %. For EHE there are several risk factors: single tumor within the lung has the least bad prognosis, whereas multinodular or double organ involvement is associated with worse prognosis. Low-risk EHE slowly progresses and sometimes can be cured by surgical removal. Weight loss, anemia, and hemorrhagic pleural effusions are other negative prognostic features. Anderson et al. have divided EHE into low and intermediate grade based on the presence of necrosis, increased mitotic activity, and increased atypia [477]. In my experience increased mitosis (>1 per HPF) and nuclear atypia are seen in multinodular variants but not in singular tumors. Therefore I do not recommend grading. In cases with necrosis, these cases are more likely EAS.

17.4.10.4 Pulmonary Artery Intimal Sarcoma (PAIS; Giant Cell Sarcoma of Large Pulmonary Blood Vessels; Vascular Leiomyosarcoma of Large Pulmonary Blood Vessels)

Clinical Features

The diagnosis of pulmonary artery intimal sarcoma (PAIS) is most often made at autopsy. They present with symptoms of acute pulmonary embolism or cardiac infarction. PAIS is confined to the truncus pulmonalis or the main arteries. It arises from the vessel walls and obstructs the lumen like a thromboembolus, for which it is usually misdiagnosed [483]. A rare case of myxoid leiomyosarcoma originating from a pulmonary vein and extending into the left atrium was reported in a middle-aged woman [484]. The predominant clinical presentation is dyspnea and febrile pulmonary disease. Signs of embolic lung disease is a leading symptom in all patients [485]. There is no sex predilection.

Radiologic Features

If ever seen by radiologists, the diagnosis of sarcoma of the large pulmonary arteries is prone to be mistaken for thromboembolism.

Gross Findings

Pulmonary artery intimal sarcoma of the elastic pulmonary arteries is confined to the truncus pulmonalis or the main arteries, rarely to pulmonary veins. It arises from the vessel wall (intima) and obstructs the lumen like a thromboembolus. Therefore the gross morphology looks like a thromboembolus; however, it adheres firmly to the vascular wall and cannot be removed from it. Some cases replace the inner half of the vessel wall on cut surface and almost all of them obstruct or occlude the lumen.

Microscopic Findings

In pulmonary artery sarcoma, the main pattern is a discoherent proliferation of highly polymorphic cells, multinucleated giant cells, large spindle cells, and cells with polygonal shape. The nuclei are enlarged, irregularly shaped, the chromatin is coarse, and the nuclear membrane is accentuated by condensed chromatin. The cell border is ill defined. The tumor arises from the blood vessel wall (intima and media). Areas of necrosis are commonly seen (Fig. 17.145). There are variations in the morphology of these tumors, which caused the change of the name from leiomyosarcoma to intimal sarcoma. The tumor can be a poorly differentiated angiosarcoma or leiomyosarcoma. However there are also types composed of fibroblastic or myofibroblastic cells; others have storiform or pleomorphic-fascicular areas similar to malignant fibrous histiocytoma. Myxoid and osteo- and chondrosarcomatous differentiation can be present [486]. Follow-up revealed that low-grade myofibroblastic sarcomas could be cured. The other tumor subtypes, which represented intermediate and high-grade sarcomas, have a dismal prognosis [487].

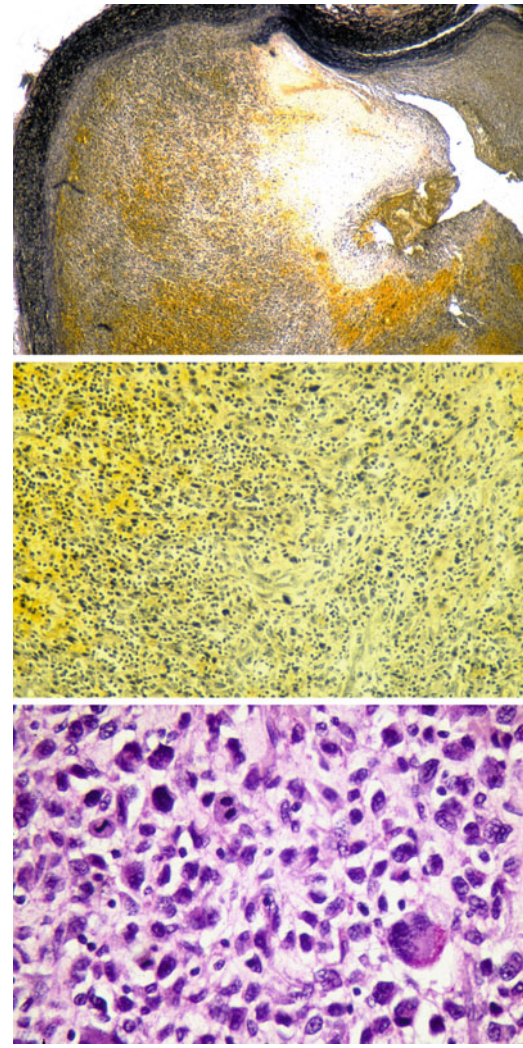

Fig. 17.145 Pulmonary artery intimal sarcoma (formerly giant cell sarcoma of large pulmonary vessels). In the *upper panel*, overview of such a tumor almost completely obstructing the left pulmonary artery; the patient died with symptoms of thromboembolism. In the *middle* the different cells are shown, spindle cells and giant cells, in between lymphocytic infiltration. In the *lower panel*, a high magnification of an area with giant cells. Elastica v. Gieson and H&E, ×12, 100, 400

Immunohistochemistry

Immunohistochemistry usually is not necessary, because of the unique location of the tumor and the embolus-like appearance. Intimal sarcomas are negative for desmin, factor VIII-related antigen, S100 protein, and CD34; all were positive for vimentin. Focal positivity was observed for alpha smooth muscle actin, CD117, CD68, p53, and bcl2. The proliferation index Ki-67 was between 5 % and 80 %. Another positive immunohistochemical stain is for MDM2, which is usually amplified.

Differential Diagnosis

Metastasis from pleomorphic sarcomas is the only differential to be considered, but due to the

unique location of intimal sarcoma, most cases can be diagnosed easily.

Molecular Biology

By chromosomal CGH, gains and amplifications were found in 12q13–14; less consistent alterations were losses on 3p, 3q, 4q, 9p, 11q, 13q, Xp, and Xq; gains on 7p, 17p, and 17q; and amplifications on 4q, 5p, 6p, and 11q. Intimal sarcomas show consistent amplifications and overexpression of MDM2, implicating the MDM2/p53 pathway [485]. In addition activated PDGFRα and EGFR frequently coexist with amplification and overexpression of the MDM2 oncogene. Due to cross talk between the PDGFRA and EGFR signaling pathways, a targeted therapy using a multiple multi-tyrosine kinase inhibitor might improve the outcome for patients [488].

Prognosis and Therapy

Pulmonary artery intimal sarcoma is a deadly disease. It can set metastasis into the lung, pleura, and skull. In most cases the diagnosis is made at autopsy. Patients, who had surgical intervention [483], can survive more than 3 years, especially in the low-grade myofibroblastic variant. In the other variants, patients die either postoperatively or within months after presentation [485]. The mean survival of intimal SA is around 23 months. Ex vivo immunoassays on primary IS cells from one case showed the potency of dasatinib to inhibit PDGFRα and downstream signaling pathways.

17.4.10.5 Kaposi Sarcoma

Clinical Presentation

Kaposi sarcoma involves the lung only in the setting of systemic disease. Therefore the diagnosis is often made in the skin or other easily accessible organ sites. The clinical question is therefore often for lung involvement. This tumor is usually found in patients suffering from AIDS [489]. A causal relationship has been found with HHV8. Disease starts as a reactive polyclonal angioproliferative response toward this virus, in which polyclonal cells change to form oligoclonal cell populations that expand and undergo malignant transformation.

Radiology

Chest high-resolution computed tomography scans commonly reveal peribronchovascular and interlobular septal thickening, bilateral and symmetric ill-defined nodules in a peribronchovascular distribution, fissural nodularity, mediastinal adenopathies, and pleural effusions.

Gross Morphology

Kaposi sarcoma appears as an ill-defined bluish-gray lesion. Small nodules can be found as well as a diffuse infiltration, which often does not look like a tumor.

Histology

Kaposi sarcoma is a vascular tumor composed of spindle cells forming small capillary blood vessels and slit-like spaces. The nuclei of Kaposi sarcoma look very bland and monomorphic. Chromatin is finely dispersed; nucleoli are inconspicuous. The cytoplasm is pale eosinophilic; the borders are invisible. Within the slit-like spaces, red blood cells are present, which helps in making the correct diagnosis. The tumor grows along bronchovascular bundles, with nodules corresponding to proliferations of neoplastic cells within the pulmonary parenchyma (Fig. 17.146). Septal thickening may represent edema or tumor infiltration, whereas ground-glass attenuation correspond to edema [490].

Immunohistochemistry

Kaposi sarcoma cells are positive for HHV8 antibodies. Another recently described useful marker is Prox1 which is consistently expressed in lymphangiomas, hemangiomas, Kaposi sarcoma, and some other vascular tumors [491].

Molecular Biology

HIF-1α and HIF-2α are expressed in KS. In cell culture IGF-I induced accumulation of both HIFα subunits. IGF-I-induced HIF alpha accumulation induced expression of VEGF-A. Specific blockade of IGF-I receptor might open new ways for targeted therapy [492].

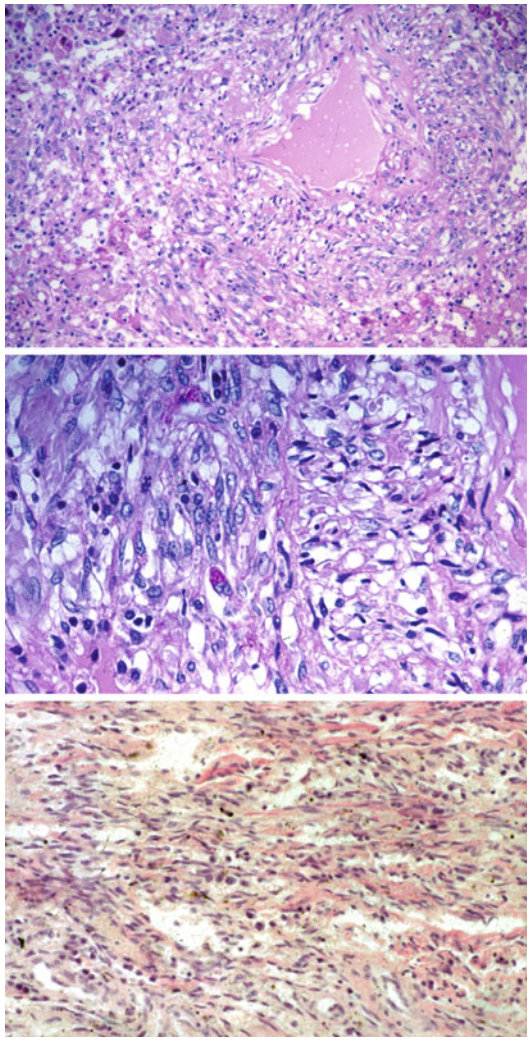

Fig. 17.146 Kaposi sarcoma, two different cases; *top panel* shows the spindle cell infiltration in the wall of a pulmonary vein and into the surrounding area. In the *middle* a higher magnification of the same case shows the spindle cells with elongated nuclei with sharp or blunt ends. Chromatin is slightly coarse, nucleoli are inconspicuous. The tumor cells form small slit-like spaces. In the *lower panel*, another case is illustrated, which shows again a spindle cell proliferation with slit-like spaces and bland nuclear features. H&E, Gieson, ×50, 100, 200

17.4.10.6 Lymphangioma and Lymphangiomatosis (Pulmonary and Systemic)

Lymphangioma can be regarded as a benign tumor or a localized malformation of lymphatics. With respect to lymphangiomatosis, it is not clear if this is a systemic tumor, a tumorlike lesion, or a malformation. In isolated cases such as in the mediastinum, a defect (atresia, obstruction) in the formation of the ductus thoracicus might cause lymphangiectasis, which over time increases and forms lymphangiomatosis. However, when considering systemic lymphangiomatosis with involvement of bones, lungs, mediastinum, and other organs, a malformation might be unlikely. These uncertainties resulted in numerous clinical presentations of congenital abnormalities of the lymphatic system in children and the confusing terminology and have provoked a clinical classification based on the actual symptoms [493].

Clinical Features

Lymphangioma most often occurs in children and is described as a solitary cystic lesion with mass-like proliferations of lymph vessels [494, 495]. A rare case was reported in a middle-aged man [496]. *Lymphangiectasis* is characterized by congenital anomalous dilatation of pulmonary lymph vessels. *Lymphangiomatosis* is a proliferation of vascular, mainly lymphatic spaces with visceral and skeletal involvement [497]. The systemic form involving bones has also been called Gorham-Stout or vanishing bone syndrome. Patients with lymphangiomatosis usually present with wheezing or asthma, dyspnea, and chylothorax or chylopericardium with pleuropulmonary lesions or generalized skeletal lesions [498].

Radiologic Features

Solitary lymphangioma is detected by CT scan and described as a cystic lesion with many differential diagnoses included. In pulmonary lymphangiomatosis thickening of pulmonary peribronchovascular bundles and interlobular septa has been reported using spiral and high-resolution computed tomography and ultrasonography [499]. In rare cases "honeycomb lung" was seen [500]. Pleural or pericardial effusions are present in almost all patients.

Gross Findings

Grossly lymphangioma presents as a cystic solitary mass usually with adjacent lung parenchyma.

Lymphangiomatosis in contrast shows ill-circumscribed cystic spaces throughout the lung tissue. In both a diagnosis includes several similar conditions.

Microscopic Findings

A lymphangioma presents with multiple endothelial-lined spaces forming a convolute. The lesion can be separated histologically from the adjacent lung tissue by a tiny fibrous capsule. In lymphangiomatosis anastomosing endothelial-lined spaces along the pleural and interlobular septa are seen. Asymmetrically spaced bundles of spindle cells can be prominent. Hemosiderin deposition is present in the spindle cell areas and in the adjacent lung. In some cases the adjacent pulmonary arteries and veins show thickened walls; in other cases the lung parenchyma is completely replaced by the lymphatic proliferation (Fig. 17.147). In contrast to lymphangiectasis, lymphomatosis usually involves a lung lobe or even a whole or both lungs (Fig. 17.148).

Immunohistochemistry

In lymphangioma as well as in lymphangiomatosis, the endothelial cells are positive for factor VIII-related antigen, CD31, and CD34; the spindle cells react for antibodies to vimentin, desmin, and actin and can be positive for progesterone receptor. The cells are negative for estrogen receptor, keratin, and HMB45 [501, 502]. Lymphangiomatosis showed low percentages of MIB1 and topoisomerase IIa positivity [503]. Podoplanin positivity is seen in the endothelial cells as well as the expression of VEGFR3 and VEGF-C, which might be the responsible factors for this proliferation (Fig. 17.148c–f).

Differential Diagnosis

The main differential diagnosis for lymphangioma is pneumocytoma and hemangioma. All three present as cystic lesions. In pneumocytoma the cysts are lined by pneumocytes and are therefore positive for cytokeratin and TTF1, whereas in hemangioma similar positive reactions as in lymphangioma can be seen. The main differential feature are red blood cells in hemangioma, whereas only few scattered red blood cells might be seen occasionally in lymphangioma. For lymphangiomatosis the main differentials are LAM and Kaposi sarcoma. In LAM there are clusters of proliferating smooth muscle cells and focal groups of perivascular HMB45-positive epithelioid cells – all of them not present in lymphangiomatosis. In Kaposi sarcoma there are similar spindle cells forming slit-like spaces; however within these spaces, red blood cells can be seen. Pulmonary capillary hemangiomatosis can be easily separated from lymphangiomatosis because PCH presents with well-structured capillaries not seen in lymphangiomatosis [501].

So far no genetic abnormalities have been recognized in lymphangioma or lymphangiomatosis.

Prognosis and Therapy

Lymphangioma should be surgically excised. No recurrence has been noted. The prognosis is good. In lymphangiomatosis patients can die from disease within 6–33 months especially in multiorgan involvement [502]. Radiotherapy has been successfully applied in lymphangiomatosis patients [504]. In patients with lung and pleural involvement, parietal pleurectomy, excision of lymphatic lakes, and ligation of lymphatics have been applied [498]. Also bilateral lung transplantation has been reported in pulmonary lymphangiomatosis [505]. A new line of treatment has been opened with recombinant interferon α-2b [506, 507] and recently with bevacizumab application [508].

17.4.10.7 Lymphangiosarcoma

Lymphangiosarcomas are exceedingly rare tumors, usually arising in soft tissues and metastasizing into almost all organs, including the lung [470, 509]. Lymphangiosarcoma has been described in patients with chronic lymphedema, especially in females after breast cancer treated by radical mastectomy [510]. If a lymphangiosarcoma can primarily arise within the lung can be questioned although a case report exists [511]. However, due to predominant pulmonary symptoms, the diagnosis has to be made in a lung biopsy or resection. The description is based on a single case seen here and few reported cases in the literature.

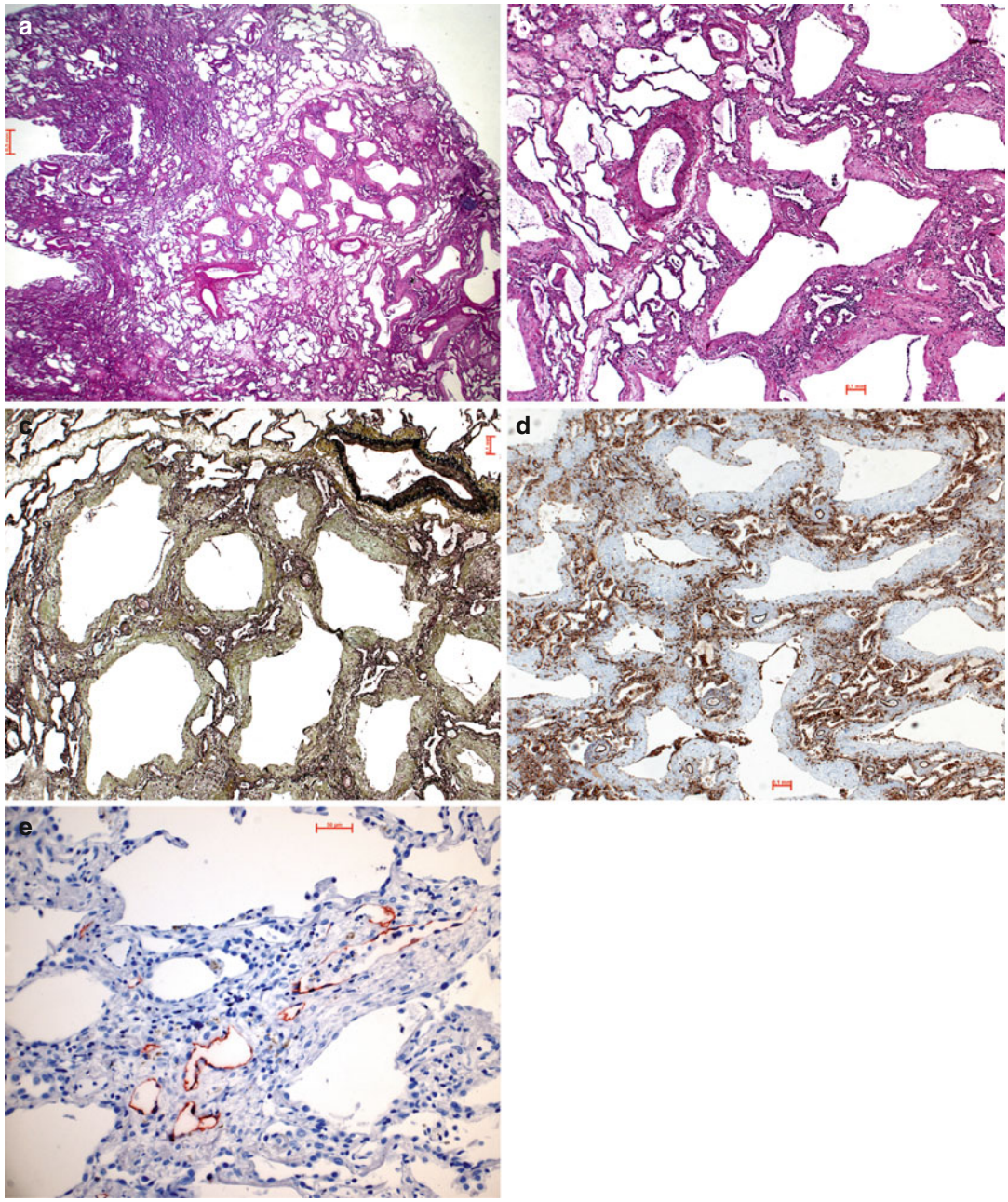

Fig. 17.147 Lymphangioma, in the overview a solitary lesion is seen (**a**), on higher magnification (**b**) dilated cystic angiomatous spaces are seen, and the wall is thickened and hyalinized, which is highlighted in the Movat stain (**c**). Immunohistochemical stains for CD31 show positivity of the lining endothelium; however, the true nature is best seen by antibodies for podoplanin (**e**). Bars, 500, 100, 50 μm

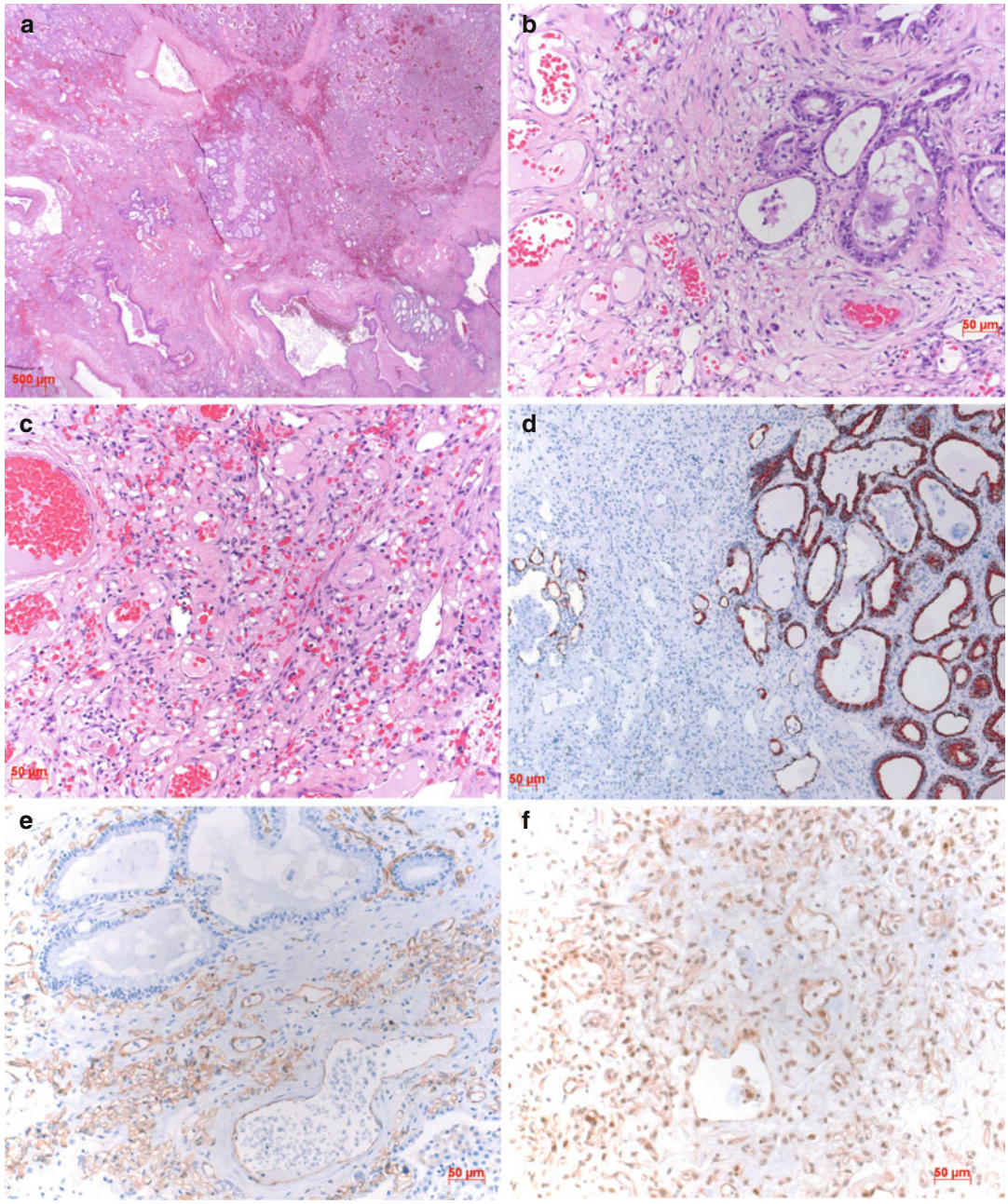

Fig. 17.148 Lymphangiomatosis in a 17-year-old male. On low power the lung looks malformed, because many peripheral lung lobules are missing, whereas the central areas with the bronchi seem to be intact (**a**). This is confirmed, when looking at a higher power (**b**, **c**), where only the central airways are seen and the alveolar periphery is completely lost. The small mesenchymal proliferation might be easily overlooked, although this is the important feature. Using immunohistochemistry for cytokeratin (**d**), one appreciates that there are remnants of alveolar tissue in this mesenchymal structures. By antibodies for CD31 (**e**), multiple small capillary proliferations are visible, representing lymphatic capillaries and tubules, which is also confirmed by staining for VEGFR3 (**f**)

Clinical Symptoms

Chylothorax and abnormal dilation of lymphatics within the lung and mediastinum are symptoms seen in patients. Long-standing asthma and shortness of breath were the main findings in our 19-year-old male patient.

Radiology

Lymphangiosarcoma in the lung most likely will present with an interstitial infiltration pattern such as widening of septa and focal densities. However, since this is such an unusual tumor, no studies have been performed.

Gross Morphology

On cut surface there are focal tiny densities, which are suspicious for an inflammatory interstitial pneumonia. No grossly visible nodules are seen.

Histology

Under low power a vascular malformation might be suspected, because of focal infiltrations with dark-stained cells. On higher-power examination the nuclear polymorphism and atypia are immediately recognized. Nuclei and nucleoli are enlarged, nuclei are polygonal, chromatin is coarse granular, nuclear membrane is accentuated, and some nuclei present with eosinophilic inclusions. Mitosis is occasionally seen, usually around 1/HPF. The most striking feature is the growth pattern: the tumor forms small bands of cells growing within alveolar septa adjacent to capillaries but without blood vessel invasion (Fig. 17.149). There is a small rim of cytoplasm, sometimes invisible; no filaments are encountered.

Immunohistochemistry

The tumor cells are negative for epithelial markers, smooth muscle cell markers, as well as for endothelial markers as factor VIII-associated antigen and factor XIII. The tumor cells are positive for podoplanin, CD31, VEGF-C and VEGF-D, and VEGFR3.

Differential Diagnosis

In the differential diagnosis, epithelioid angiosarcoma, Kaposi sarcoma, and high-grade lymphoma have to be considered. Undifferentiated carcinoma and sarcoma can easily be ruled out, because lymphangiosarcoma does not show compact cell clusters or nodules. Hemorrhage is common in both lymphangiosarcoma and angiosarcoma: however, there are no vascular channels or sinusoids in lymphangiosarcoma and the mitotic rate is much lower. Kaposi sarcoma presents with spindle cells, which are not seen in lymphangiosarcoma. And no slit-like spaces or vascular channels are formed. The infiltrative pattern seen in lymphangiosarcoma is unusual in large-cell lymphomas; only the intravascular variant might enter the differential diagnosis. But intravascular diffuse large B-cell lymphoma presents with less dense nuclei, and the tumor cells are within the pulmonary blood vessels, not perivascular. Immunohistochemistry will be of help, especially the positivity for podoplanin and VEGFR3.

Molecular Biology

No investigations on this rare tumor do exist in the literature.

Prognosis and Therapy

The outcome in this type of tumor is dismal. The reported patient died few days after the diagnosis was made. There were several organs involved including the heart. The major problems are disturbances with loss of electrolytes and low molecular weight proteins similar to systemic lymphangiomatosis. This might cause heart failure as the ultimate cause of death.

17.4.10.8 Meningothelial Nodules (Chemodectoma)

In the literature there is a mix-up of chemodectoma and paraganglioma, which has been discussed by Aubertine [434]. The author came across cases labeled as chemodectomas, which essentially were meningoendothelial nodules, just larger in size and more tumorlike. So the term chemodectoma should not be used any longer. Paraganglioma has been discussed in a previous paragraph; therefore here the focus is on meningothelial nodule. Another question has been raised about a connection of meningothelial

nodules and meningioma: Mukhopadhyay in his study based the assumption of meningothelial nodules as a precursor lesion for meningioma on the finding of NCAM (CD56) positivity in both [512]. But it should be mentioned that meningothelial nodules are positive for neuron-specific enolase γ, whereas meningiomas are not. In addition meningothelial nodules are not uncommon although most often found incidentally at autopsy whereas meningioma is a rare tumor. Also whereas meningothelial nodules are intimately associated with pulmonary small blood vessels and seem to be related to the regulation of local blood flow, meningiomas are not.

Clinical Features

Meningothelial nodules are incidental finding either at autopsy or in lung specimen resected for carcinoma. There are no special features or symptoms. Radiologically they cannot be detected due to their small size. Minute pulmonary meningothelial-like nodules are seen more often in females and more often in patients with malignant pulmonary tumors than in those with benign disease [513].

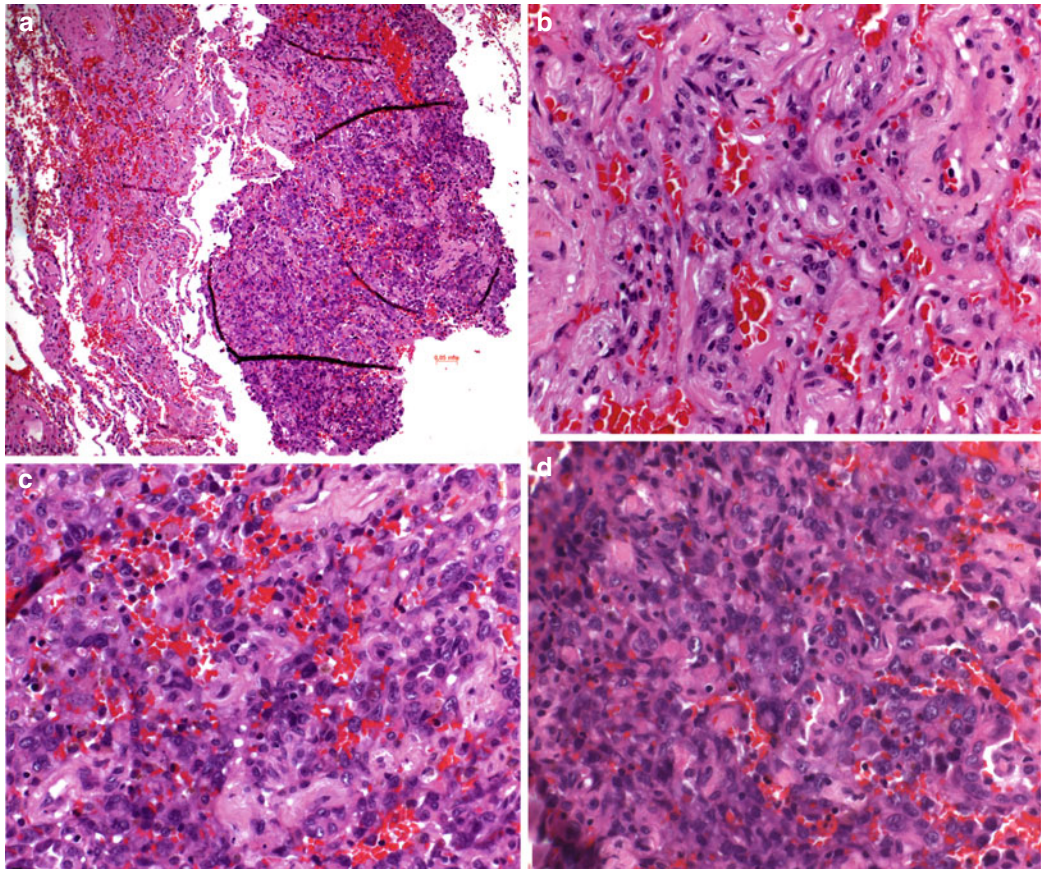

Fig. 17.149 Lymphangiosarcoma in a young 19-year-old male patient. A VATS biopsy was taken because of unclear pulmonary symptoms. On examination a tiny area was recognized, which looked abnormal (**a**). Examining this area closely, there were single large atypical cells (**b**), and in an area close by, strands of abnormal cells were recognized (**c**, **d**). These cells are large, with enlarged nuclei, chromatin is coarse granular, 1–3 nucleoli are visible, and the nuclear membrane is accentuated. These cells seem to follow pulmonary capillaries but are not part of them; best seen in C. By immunohistochemistry the cells did not stain for CD31 (**e**, *lower right corner*) but stained for podoplanin (**f**) and expressed VEGFR3 (**g**), thus confirming their nature as lymphatic endothelia. The patient died 4 days after the diagnosis was transmitted over phone. If this is a primary lymphangiosarcoma of the lung could not be evaluated, because autopsy was not performed

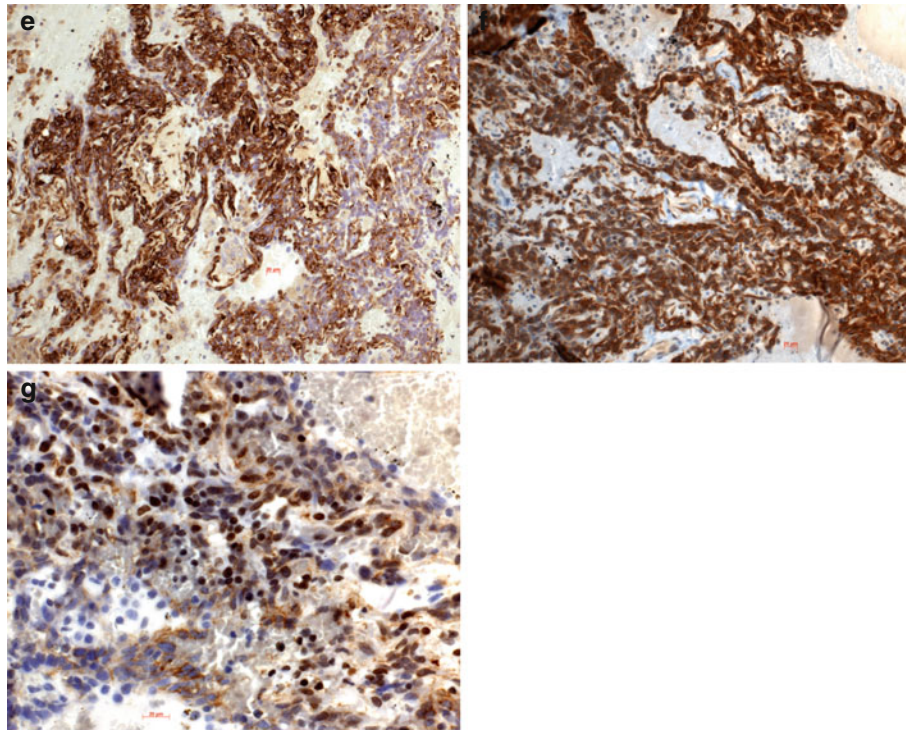

Fig. 17.149 (continued)

Gross Findings

Meningothelial nodules are single or multifocal small lesions, usually less than 1 cm in diameter. Some fibrosis can occur in the center of the lesion. On cut surface the nodules are grayish white.

Microscopic Findings

Meningothelial nodules are perivenular nodular aggregates of small regular cells that are entirely interstitial and have no contact with the airspaces (previously known as *multiple minute chemodectomas*). The tumor cells are small epithelioid or spindle cells with ill-defined cell borders. Nuclei are small, nucleoli are invisible, and chromatin is finely dispersed. Small groups of tumor cells are embedded in a network of veins and capillaries; sometimes the cells are within the vessel wall (Fig. 17.150).

Immunohistochemistry

The tumor cells are positive for vimentin and epithelial membrane antigen, focally positive for neuroendocrine markers, especially NSE and NCAM, but negative for cytokeratins, chromogranin A, synaptophysin, S100 protein, lysozyme, myosin, melanoma-associated antigens, and endothelial and smooth muscle markers. Positivity for CD68 might be seen in few cases.

Molecular Biology

The human androgen receptor gene (HUMARA) was amplified in half of the cases with monoclonal expansion, confirming the hypothesis that pulmonary meningothelial nodules have meningothelial-like and phagocytic characteristics [514]. On the contrary when LOH was investigated for meningothelial nodules and meningiomas, the latter showed major events at 22q and 14q and 1p not shared by meningothelial nodules [515]. Interestingly deletion of the NF2 gene and chromosomal gains of 22q were identified in meningothelial nodules and meningiomas, however, with much higher frequency in meningiomas. This may indicate that pleuropulmonary meningothelial lesions may arise from the same precursor cell [516].

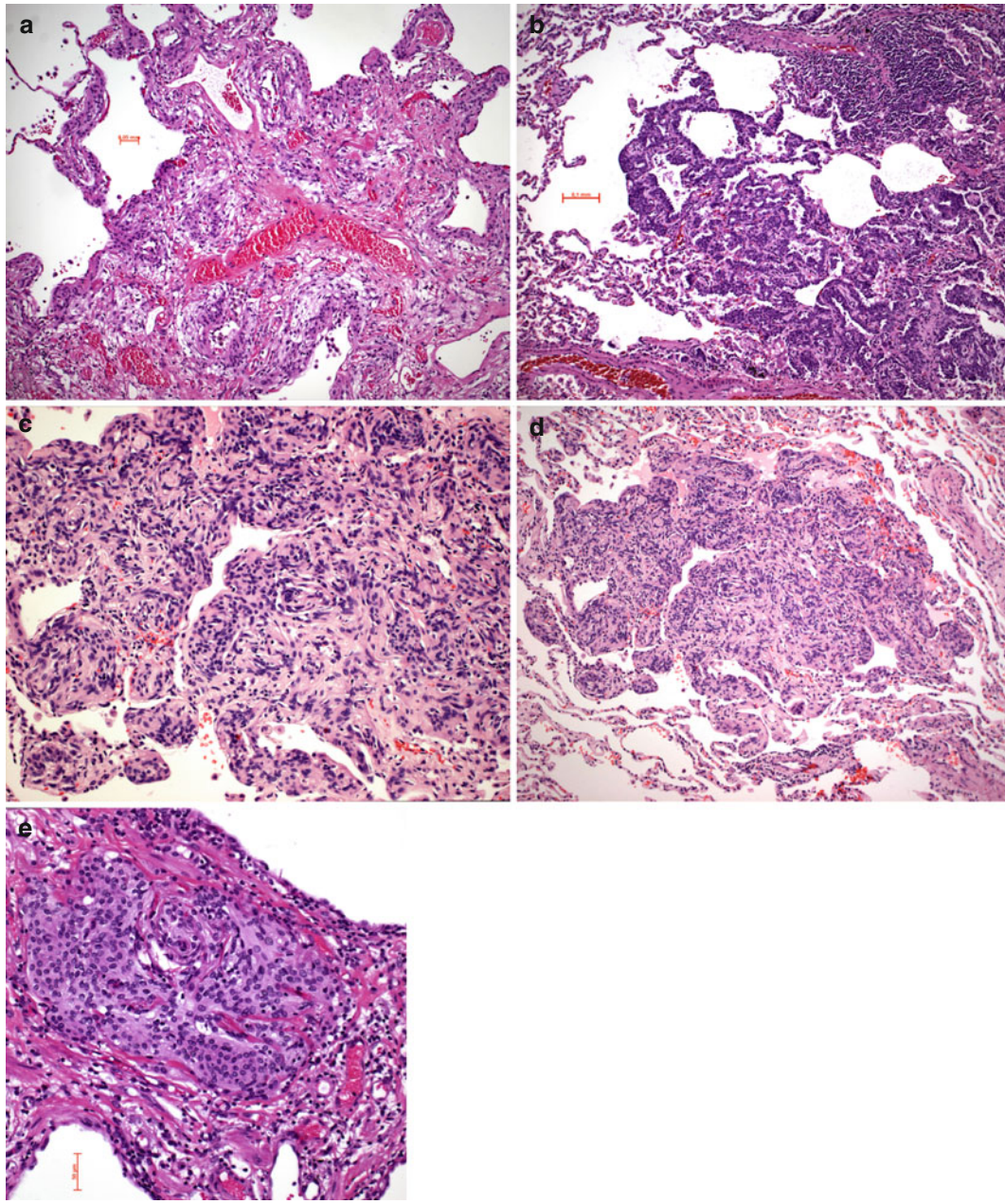

Fig. 17.150 Meningothelial nodules, four different cases are illustrated. In (**a**) the proliferation is predominantly around larger veins; in (**b**) there are several scattered nodules around a convolute of small blood vessels. (**c**, **d**) show classical nodules, which in former times would have been called chemothecoma, which essentially is the same entity. In (**e**) a higher magnification illustrates the cells. The nuclei are round and look normal, chromatin is finely dispersed, and nucleoli are invisible. The cells form clusters around blood vessels and most likely have a role in fine regulating blood flow, as they are usually encountered in areas of disturbed blood flow. H&E, bars 100, 50 µm

Differential Diagnosis

There are only few differential diagnoses to be considered: paraganglioma is positive for S100 protein, tumorlet and carcinoid are positive for cytokeratin, and glomus tumor is positive for CD31, VEGF, and VEGFR3 – all these markers are not shared by meningothelial nodules.

Prognosis and Therapy

The normal precursor cell is not known so far. Meningothelial nodules might have a regulatory function for local blood flow, as they usually occur in areas where normal blood flow is impaired: a good example is obstruction of small blood vessels by massive congestion by adenocarcinoma cells (intravascular dissemination). Meningothelial nodules are benign tumors or tumorlike lesions. No progression or recurrence is known, and no malignant transformation. There is no need for therapeutic intervention.

17.4.10.9 Tumors of Pericytic Lineage

Pericytic tumors have been described in soft tissues and in the lung as hemangiopericytoma [517–519]. This entity vanished but reappeared during the last decades. The major problem in defining this type of tumor lies in the origin of different cellular elements from stem cells and pericytes within the outer vascular wall: smooth muscle cells, perivascular epithelioid cells (PEC), glomus cells, and pericytes all differentiate from the precursor cells. Therefore tumors from these precursor cells can differentiate along all these different cell types, creating differently named tumors. Tumors that only occasionally display hemangiopericytoma-like features but otherwise are undifferentiated are synovial sarcoma. Tumors with myoid/pericytic differentiation correspond to true hemangiopericytoma. Within this spectrum glomangiopericytoma and myopericytoma can be placed. If solitary fibrous tumor should be placed into this category might be questioned [520]. Glomangiopericytoma presents in the lung most often as metastasis from a glomangiosarcoma of the extremities. However few cases of glomangiomas and one glomangiosarcoma primarily arising in the lung have been described [521]. Katabami and colleagues reported on a glomangiomyoma, again pointing to the differentiation capability of cells from the pericytic lineage [522]. A case seen by us demonstrated this capability most impressive: the tumor started with a diffuse and nodular proliferation, followed 4 years later by a large tumor with pericytes, cells with smooth muscle cell differentiation, and few clear cells (perivascular epithelioid cells).

Clinical Presentation

Patients present with unspecific symptoms, most often shortness of breath.

Radiology

Patients can present with solitary tumors but also with diffuse and reticular nodular densities on CT scan.

Gross Morphology

Diffuse thickening of alveolar septa, multiple small nodules, as well as large tumor can be present. The proliferations are grayish, and the large tumors are grayish to dark red, depending on the amount of hemorrhage.

Histology

The diffuse proliferations are confined to the thickened alveolar septa. There are round and spindle cells, nuclei are small with dark chromatin, and nucleoli are invisible. The cytoplasm is focally vacuolated; the cell borders are invisible. The proliferation follows and surrounds the capillaries, veins, and arterioles but without vascular invasion. In the nodular lesions, predominantly round cells are seen but also cells with clear cytoplasm. There is slightly more nuclear polymorphism with some large and even few giant cells. The large cells present with enlarged atypical nucleoli, the chromatin in these cells is coarse granular, and the nuclear membrane is accentuated by chromatin. Within the nodules a meshwork of capillaries and dilated veins is seen. In the large tumors, nuclear polymorphism is extensive, chromatin is coarse granular in all cells, and nucleoli are enlarged and irregular contoured. The tumor cells can show differentiation into PEComa cells, smooth muscle cells, primitive pericytic cells, and glomus cells. The vascular network can show large interconnected sinusoid as in hemangiopericytoma (Fig. 17.151).

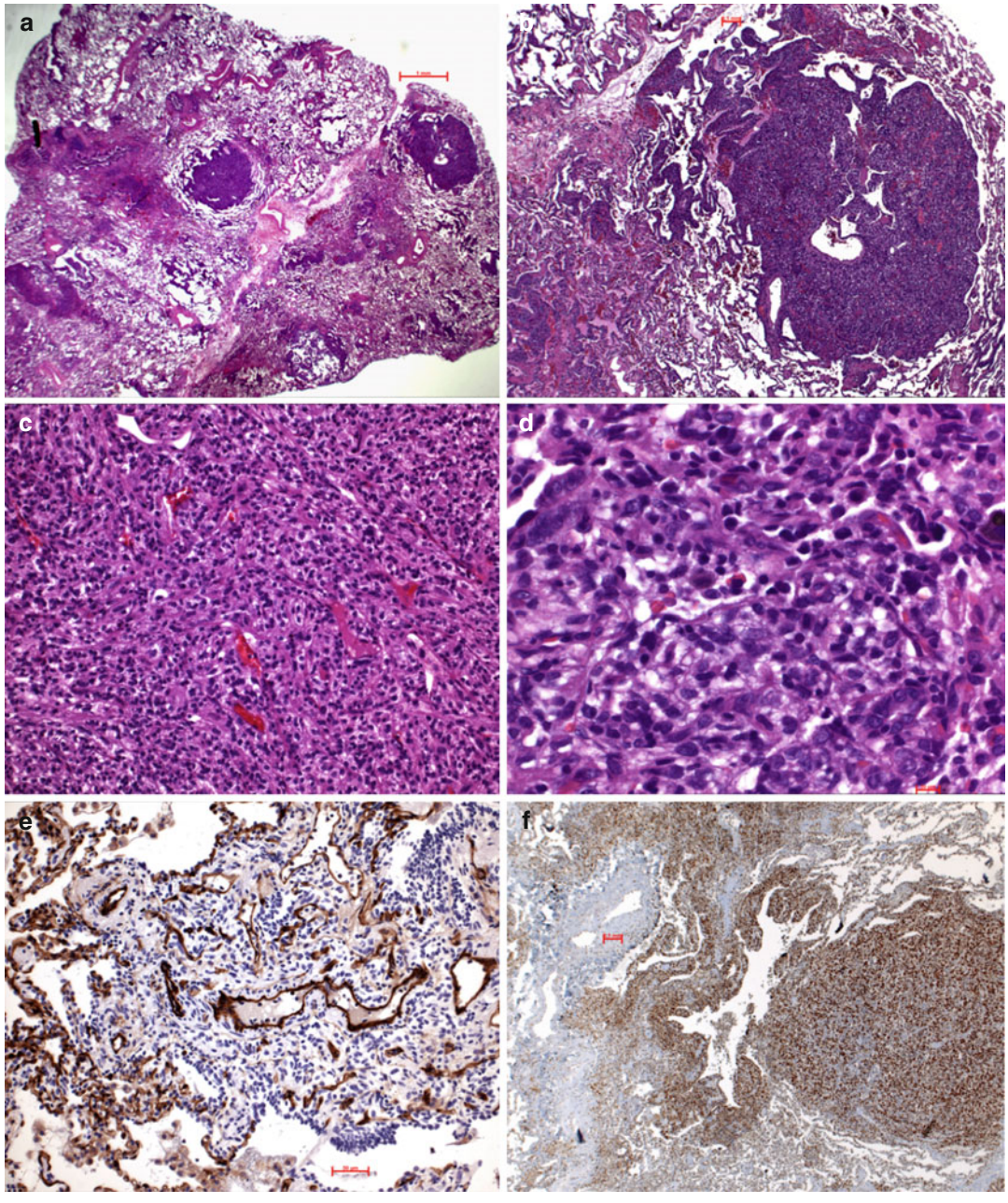

Fig. 17.151 Diffuse and nodular pericytosis combined with myopericytoma in a 54-year-old female patient. A diffuse and nodular proliferation was initially detected (**a**–**d**), which reacted with vimentin and VEGFR3 only. Four years later a large tumor developed, which showed additional differentiations with myogenic markers (SMA in I) and occasional HMB45 positive PECells. (**a**) shows the diffuse and nodular tumors, dark stained; in (**b**) one nodule is magnified; the diffuse proliferation is also visible. The cells are undifferentiated with nuclear atypia, dark-stained chromatin, basophilic, and in some cells clear cytoplasm. The cells follow the wall of capillaries (**e**, CD31). The tumor cells are positive for VEGFR3, however, similar to angiosarcomas again with a nuclear stain (**f**). In (**g**, **h**) areas of the 7 cm large tumor are shown, there are the same pericytic cells as in the nodular proliferation (**g**), but also cells with myofilaments (**h**) and large PECells (**g**). Immunohistochemistry demonstrates the focal myogenic differentiation (I, SMA stain). Bars, 1 mm, 100, 50, 20, 10 µm

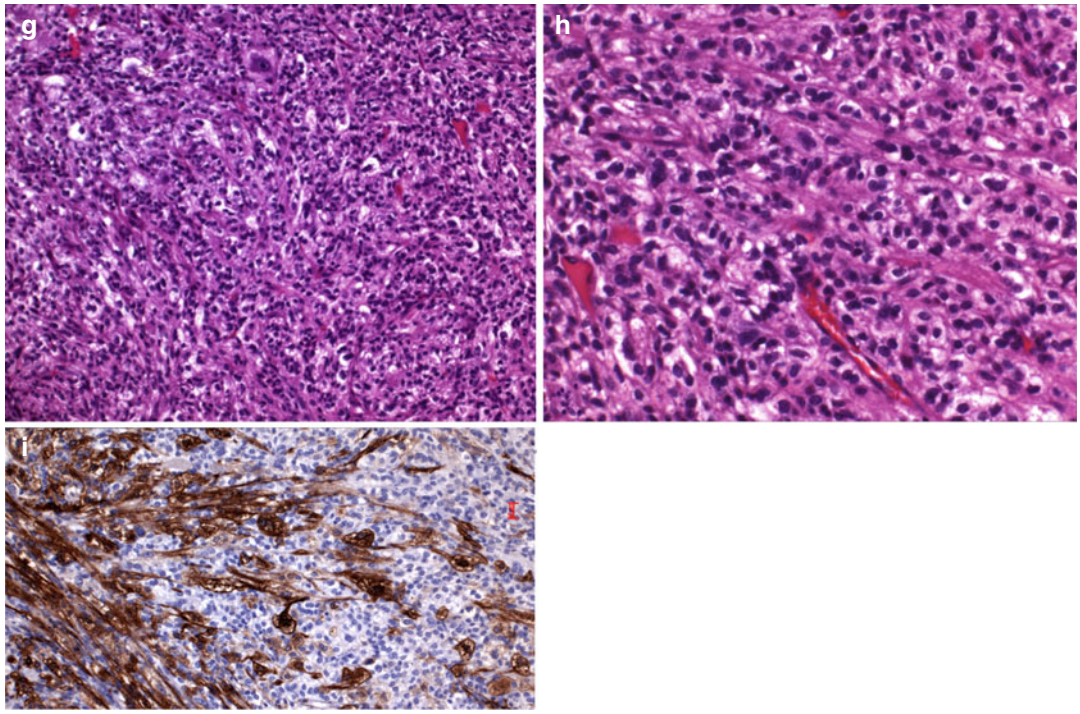

Fig. 17.151 (continued)

Besides this unusual tumor, there exist also the classical pericytoma, which similar to the one above can differentiate into the cells of the outer blood vessel wall (Fig. 17.152).

Immunohistochemistry

The tumor cells can react with HMB45 (PEC), smooth muscle actin (myogenic cell), or vimentin. The tumor cells are constantly negative for epithelial and endothelial markers, dendritic, and lymphoma cell markers. However, there is a nuclear reactivity for VEGFR3 (kinase domain).

Differential Diagnosis

All kinds of undifferentiated tumors have to be ruled out. Undifferentiated carcinomas are ruled out by negativity for cytokeratins and lymphomas by negativity for lymphocyte markers. Undifferentiated sarcomas may react for desmin and focally for cytokeratin, negative in these pericytic tumors. A PEComa can be ruled out, because in these pericytic tumors there are only focally PECells present. Leiomyosarcoma can be ruled out because myogenic differentiation is present in only small clusters of cells.

Prognosis and Therapy

Usually these tumors do not respond to conventional chemotherapy for sarcomas. Surgical removal of a solitary tumor is the best treatment option. In multinodular and diffuse tumors, other options have to be selected. Antiangiogenic therapy with bevacizumab has been successfully applied in our patient. Due to the positivity for VEGFR3, a treatment with a specific kinase inhibitor might be tried.

17.4.11 Primary Melanoma of the Bronchus

Clinical Features

No specific clinical features are known. Patients usually present with cough, hemoptysis, and lobar collapse. Hemoptysis may be a symptom in large tumors [523]. In addition to the pigmented tumor, the surrounding mucosa can show multiple melanin-pigmented freckles. In some patients hyperpigmentation is also seen in the mucosa of the nasal cavity, the paranasal sinuses, the esophagus, and the trachea and main bronchi.

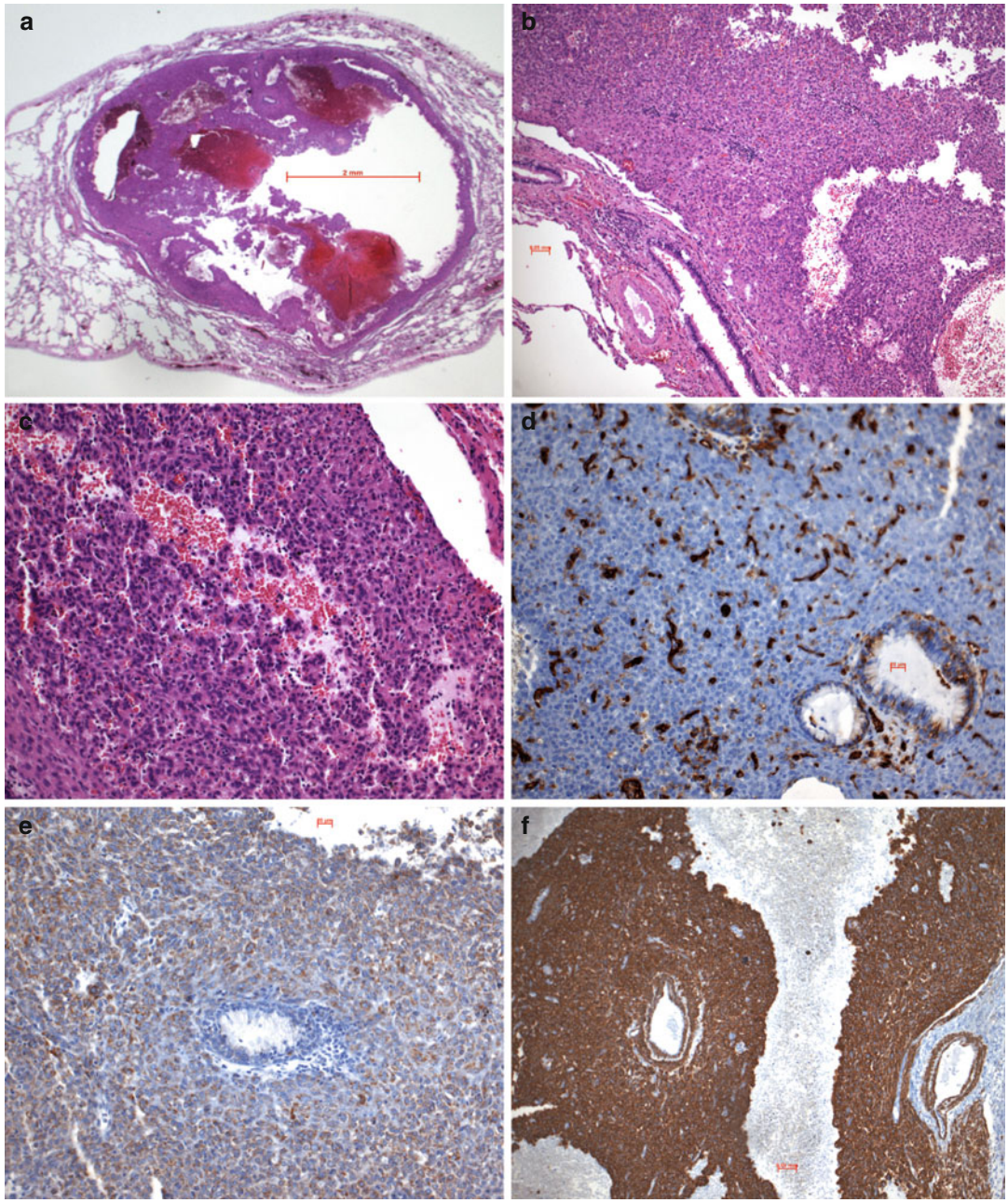

Fig. 17.152 Pericytoma of the lung. In (**a**) an overview of a tumor nodule is shown, approximately 3 mm in diameter. (**b**, **c**) Show the undifferentiated tumor cells forming large sheets. The tumor cells have small dark nuclei, no visible nucleoli, no mitosis, and a fine granular slightly eosinophilic cytoplasm. Staining for endothelial markers (CD31) is negative but shows the intimate association of the cells with the capillaries (**d**). The tumor cells express VEGFR3 (**e**) and also smooth muscle actin (**f**). Bars, 2 mm, 50, 20 μm

Radiology

A central tumor mass is described by X-ray and CT scan.

Gross Findings

These are centrally located tumors arising from the bronchial mucosa. The tumor is soft, grayish white to brown, on cut surface homogenous, and with or without brown pigmentation. Adjacent to the tumor, a hyperpigmentation with freckles of brown pigment in the mucosa is seen [398, 524, 525].

Microscopic Findings

As in other locations, the tumor is composed of epithelioid and/or spindle cells. Nuclei are enlarged, chromatin is coarse, and nucleoli are large and irregularly contoured (Fig. 17.153). Melanin pigment is usually found in the tumor cells, sometimes focally, and in other cases abundant. However, nonpigmented melanomas do occur.

Immunohistochemistry

A definite diagnosis can be made on fine needle aspiration biopsy; however, the differentiation of primary versus metastatic melanoma cannot be reached. By immunohistochemistry the diagnosis can be confirmed by a positive stain for HMB45, S100 protein, Melan A, as well as other melanoma markers. Cytokeratin is negative, except a few single cells in some rare cases; staining for vimentin is usually positive. As in all mucosal melanomas, BRAF and KIT mutation analysis has to be done.

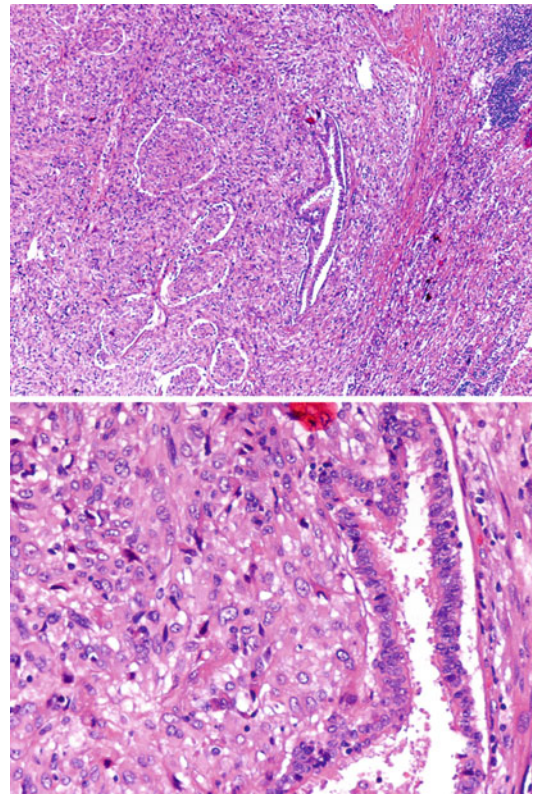

Fig. 17.153 Malignant melanoma primarily arising in the bronchus. This is an unusual rare tumor, most often associated with melanosis of the upper and lower respiratory airways. In the *upper panel*, a combined spindle and epithelioid cell melanoma is seen; in the *lower panel*, the epithelioid type dominates and grows already underneath the epithelium. The nuclei are enlarged, chromatin is coarse, and nucleoli are large and irregularly contoured. In this case no melanin synthesis was found, but melanoma markers were positive. H&E, ×50, 200

Differential Diagnosis

The major differential diagnosis is metastatic melanoma. This might be achieved in cases, when there are multiple nodules in the lung periphery, centered on pulmonary arteries, or when a primary melanoma is already known. A single nodule confined to the bronchial mucosa with the presence of freckles of melanin pigment within the bronchial mucosa is essential findings to establish the diagnosis of primary pulmonary malignant melanoma.

Prognosis and Therapy

Prognosis of primary bronchial malignant melanoma is usually dismal. Many reported cases are based on autopsy findings. As any other mucosal melanomas, these are detected late, sometimes after metastatic disease has been diagnosed. Patients are usually treated by chemotherapy. Immunostimulatory therapy might be installed in some patients. In those cases positive for BRAF or KIT mutations tyrosine kinase inhibitor therapy should be done.

17.5 Hematologic Tumors Primarily Arising in the Lung

Pseudolymphoma is a nodular, polyclonal proliferation and hyperplasia of the BALT system. On H&E-stained sections, it is indistinguishable from low-grade lymphoma. Well-formed germinal centers, however, should guide one into the correct diagnosis. LIP has already been discussed.

Posttransplant lymphoproliferative disease should be regarded as a pre-lymphoma. It is caused by EBV infection in transplant patients. EBV causes a proliferation of lymphocytes of the B-lineage. Usually there are large B-lymphoblastic cells, scattered within a dense lymphoid infiltrate (Fig. 17.154). The lymphocytes are polyclonal, but the large B cells are EBV positive and in addition will show a high proliferation index (or staining by MIB1). PTLD can progress into overt lymphoma within a short time. So this diagnosis should prompt a change in the immunosuppressive therapy.

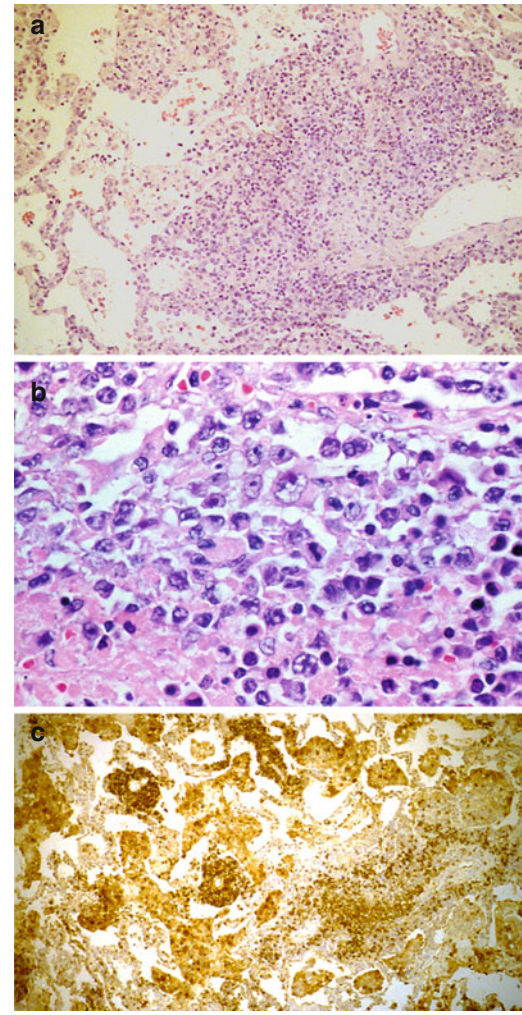

Fig. 17.154 Posttransplant lymphoproliferative disease. There is still a polyclonal infiltration in the lung (**a**), but focally blasts are encountered, which will stain positive for EBV (**b**). Most cells are B-lymphocytes as shown here with CD20 (**c**). H&E ×50, 200, Immunohistochemistry ×50

17.5.1 Lymphomas

17.5.1.1 Extranodal Marginal Zone Lymphoma of BALT Type (BALT Lymphoma)

Extranodal marginal zone lymphoma of BALT type (*BALT lymphoma*) is a low-grade non-Hodgkin lymphoma (NHL). It is characterized by an infiltration of lymphoid cells into the epithelia of the lung (bronchi, bronchioles, alveoli), so-called lymphoepithelial lesion. The lymphoid cells are larger than mature peripheral lymphocytes, which are usually of T-phenotype. By immunohistochemistry these cells are positive for CD20 and negative for T-cell markers and cytokeratin. A cytokeratin stain does highlight the lymphoepithelial lesions nicely (Fig. 17.155). For the differential diagnosis, monoclonality has to be demonstrated by kappa and lambda staining of the lymphocytes. In addition the tumor cells are positive for CD20, CD79a, Bcl2, and MUM1.

17.5.1.2 Chronic Lymphocytic Leukemia (CLL)

CLL cells can infiltrate the lung. The histology is similar to BALT/MALT lymphoma, but the lymphoepithelial lesions are absent. The size of the lymphocytes is similar. The cells express CD5, CD20, and CD23; CD38 might be expressed; a light chain restriction is common.

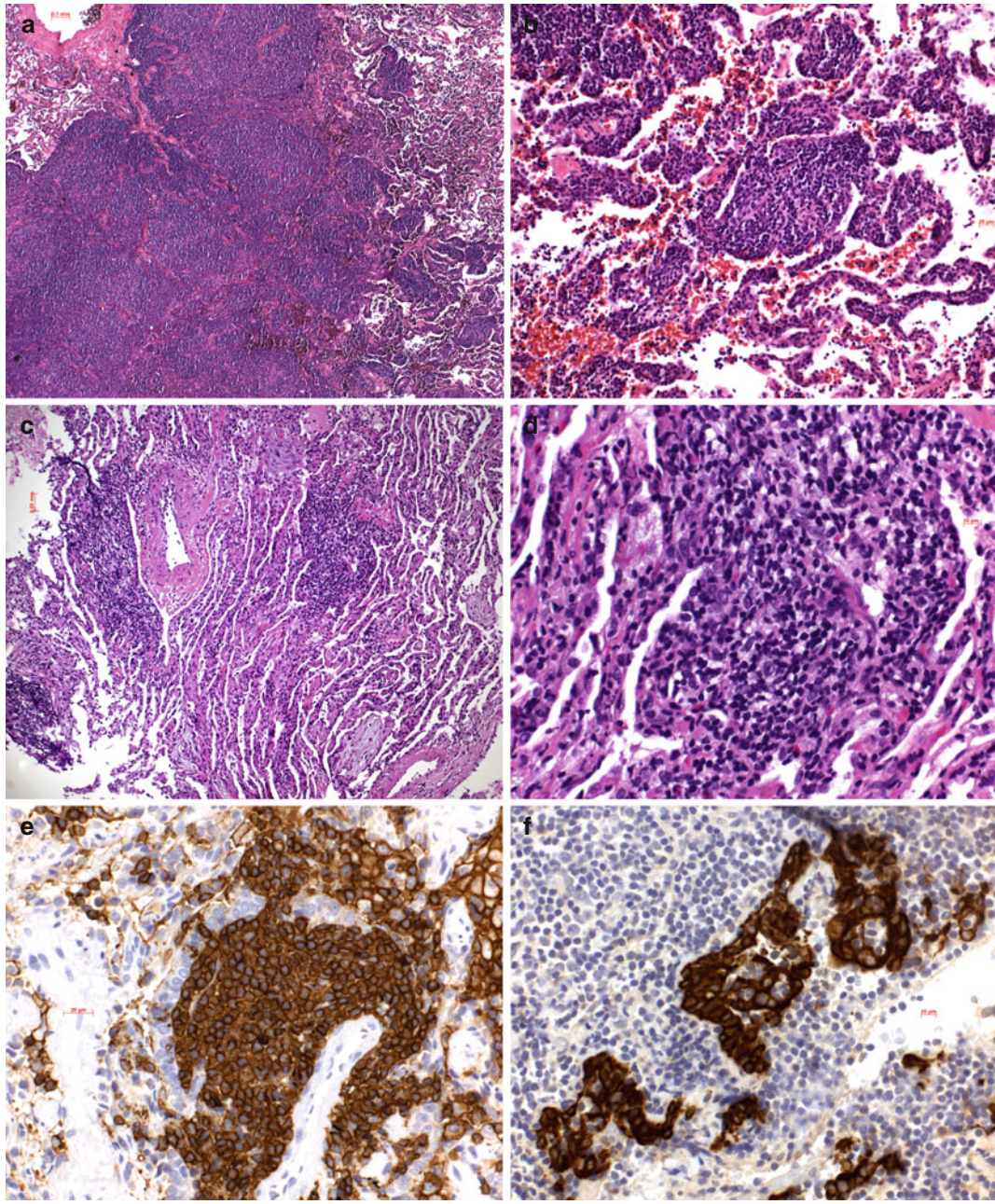

Fig. 17.155 Extranodal marginal zone lymphoma of MALT/BALT type. (**a**) Shows a resection specimen with large amounts of lymphocytic infiltration focally also with LIP pattern (**b**). In (**c**) a transbronchial biopsy is shown again with this lymphoma, magnified in (**d**). In (**e**) a lymphoepithelial lesion is shown by CD20 immunohistochemistry, a negative staining pattern, also useful for diagnosis is by cytokeratin stain in (**f**)

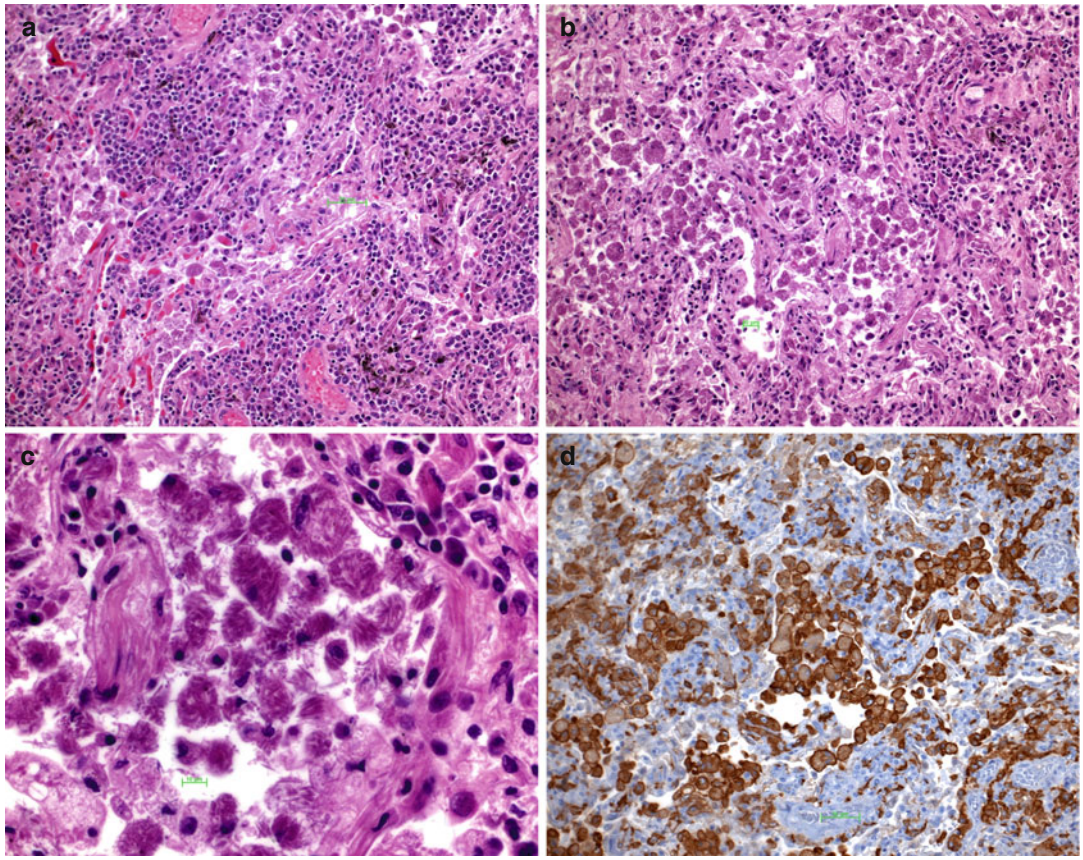

Fig. 17.156 Lymphoplasmocytic lymphoma with crystal storing macrophages is an uncommon rare lymphoma. In (**a**) overview with infiltrating lymphoid cells, predominantly plasma cells. In (**b**) the macrophages are shown, which have crystalline material in their cytoplasm. (**c**) shows a higher magnification of the macrophages with PAS positivity of the crystals. (**d**) Immunohistochemistry with CD163, a macrophage marker Bars 50, 20, 10 µm

17.5.1.3 Lymphoplasmocytic Lymphoma

This is another low-grade lymphoma, which can infiltrate the lung. There exists a variant, which is lymphoplasmocytic lymphoma with crystal storing macrophages, characterized with numerous macrophages containing PAS-positive crystalline material in their cytoplasm (Fig. 17.156). A similar pattern was observed also in a marginal zone lymphoma of MALT type. In this case also the nature of these crystals was detected as immunoglobulin crystals. Crystal storing histiocytosis is a rare phenomenon in which macrophages accumulate light chain or immunoglobulin crystalline inclusions [526].

17.5.1.4 Diffuse Large-Cell Lymphoma

Diffuse large-cell lymphoma can occur in the lung, as it is quite frequent in the mediastinum. Large pleomorphic cells, more or less mixed with small mature lymphocytes, characterize it. These lymphocytic infiltrations in my experience are quite helpful in guiding one into the right diagnosis (Fig. 17.157). On cytology the diagnosis of a large-cell lymphoma can be made; however, subtyping is most often impossible due to limitations of the material (Fig. 17.158). Using cellblocks some progress can be made. A variant, which is systemic but due to severe pulmonary symptoms might be first diagnosed in the lung, is the intravascular variant of diffuse large B-cell lymphoma.

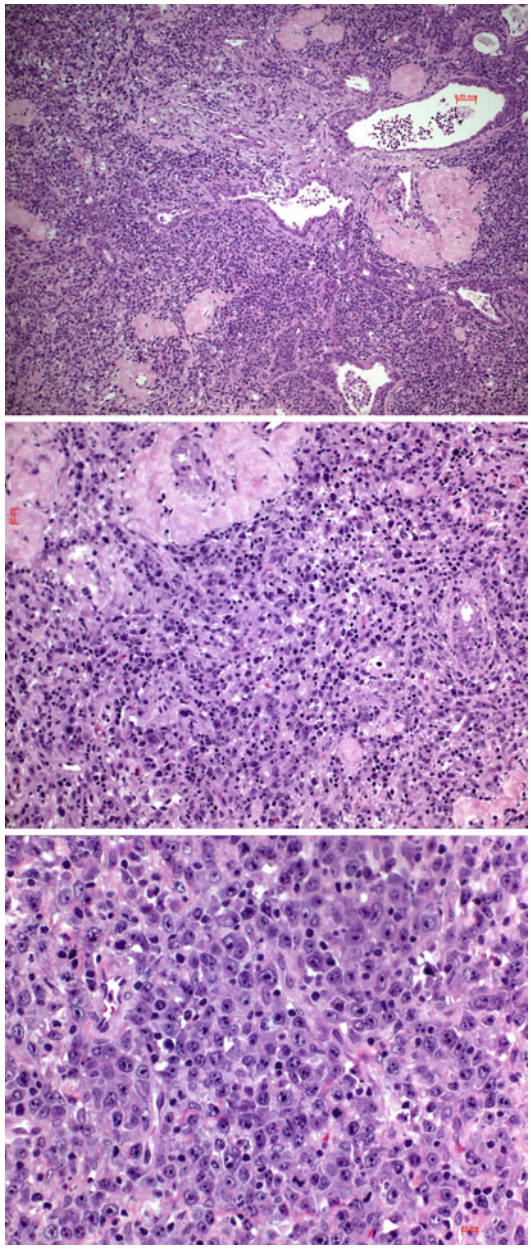

Fig. 17.157 Diffuse large B-cell lymphoma, a regular form is shown with an overview in the *top panel*, a higher magnification in the *middle*, and a high magnification at the *bottom*. The tumor cells form sheets and strands, accompanied by small lymphocytes in between them. The cells are large with increased nuclear size and large irregular contoured nucleoli. In some areas small lymphocytes are almost absent. The tumor cells are isolated and do not form epithelial-like complexes or nests. H&E, bars 50, 20, 10 μm

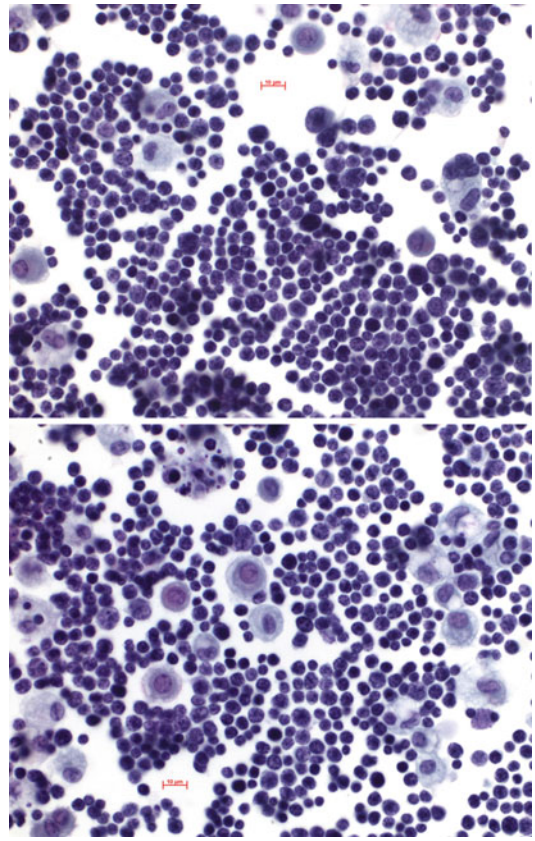

Fig. 17.158 Effusion cytology from the pleura showing large reactive mesothelial cells and numerous atypical lymphoid cells and scarce small lymphocytes. The nuclei of the larger cells show coarse granular chromatin, some enlarged nucleoli, and a small cytoplasmic rim. A tentative diagnosis of a high-grade lymphoma with blasts can be made. PAP, bars 10 μm

The tumor cells are positive for CD20, CD79a, Bcl6, MUM1, CD10, and PAX5; light chain restriction can be seen (Fig. 17.159). Another variant usually seen in the mediastinum can also arise within the lung, which is mediastinal diffuse large B-cell lymphoma. This entity has a slightly different immunophenotypic profile (Fig. 17.160).

17.5.1.5 Lymphomatoid Granulomatosis

Lymphomatoid granulomatosis is another large B-cell lymphoma, characterized by a prominent perivascular infiltration. The infiltrates are

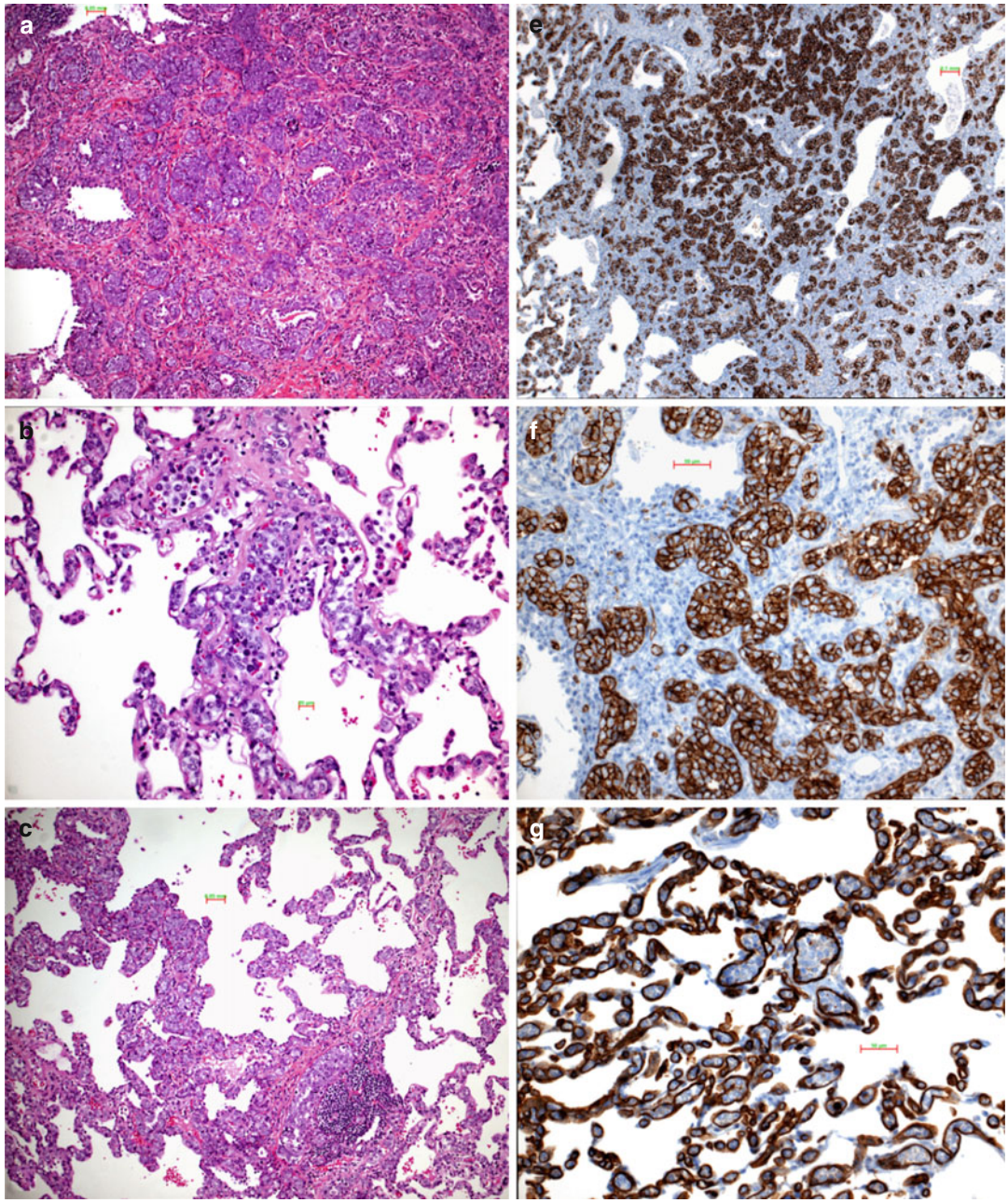

Fig. 17.159 Intravascular variant of diffuse large B-cell lymphoma diagnosed in a young woman presenting with pneumonia-like symptoms. Treatment with antibiotics and corticoids induced transient improvement, followed by rapid worsening. The blood vessels were stuffed with atypical large cells showing features of large B-cell lymphoma as described above (**a**–**d**). Immunostain for CD20 showed all tumor cells positive for this marker (**e**, **f**), in (**g**) the intravascular distribution is highlighted by CD31 staining the endothelia. The tumor cells were further positive for PAX5 (**h**), bcl2 (**j**), and MUM1 (**k**). Bars, 100, 50, 20, 10 μm

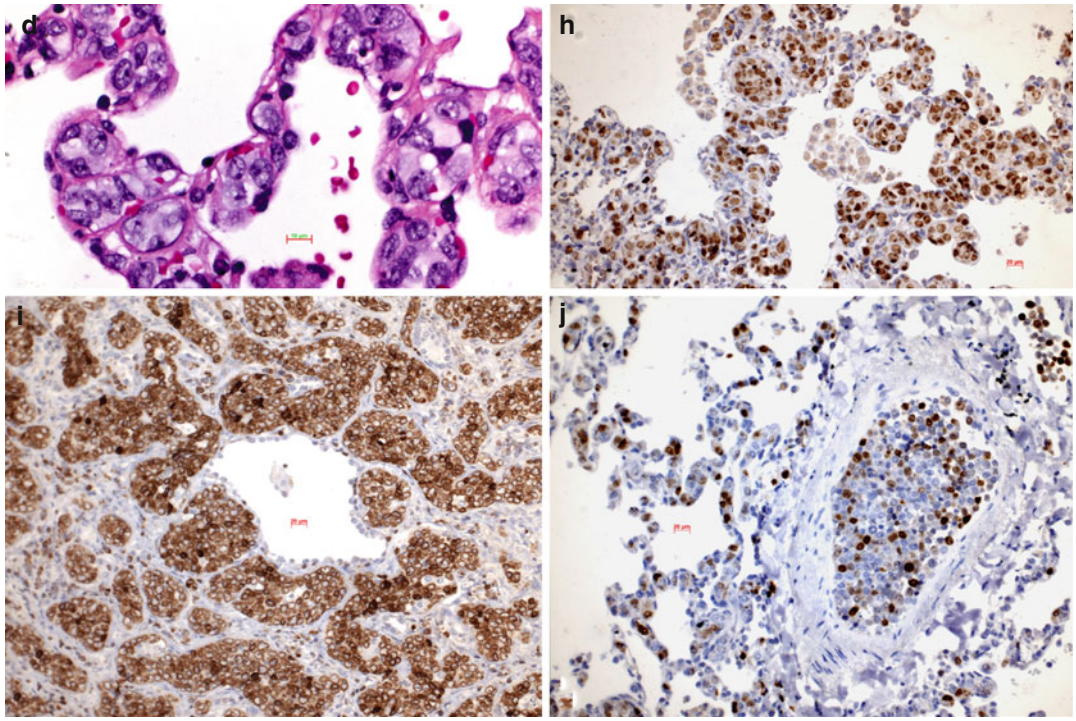

Fig. 17.159 (continued)

arranged in a granulomatous fashion, therefore the name. Previously it was renamed as angiocentric lymphoma, which is much more appropriate than lymphomatoid granulomatosis (Fig. 17.161). The lymphoma belongs to the B-cell lineage and therefore will be stained by B-cell markers, such as CD 79a and CD20. Most important is the presence of EBV: in situ hybridization using a probe for EBER1 will highlight the tumor cells. There are three grades, which also are associated with the prognosis, grade 3 being a high-grade lymphoma (Fig. 17.162).

Grade 1: less or equal 5 EBV-positive tumor cells per HPF
Grade 2: 5–15 EBV-positive tumor cells per HPF
Grade 3: >15 EBV-positive tumor cells per HPF

The diagnosis in grade 1 might be difficult as the large B cells can easily be overlooked. In many cases there are some epithelioid cell granulomas at the border of the tumor; this in addition might mislead the diagnosis. Grade 2 and 3 are more easily diagnosed as the large atypical B cells are better visible.

17.5.1.6 Castleman's and Waldenstrom's Disease

Finally two rare diseases with lung involvement will be mentioned briefly, which is **Castleman's and Waldenstrom's disease.** Both are exceedingly rare in the lung [527–533]. Castleman's disease can present a solitary nodule arising directly within the lung or from an intrapulmonary lymph node (Fig. 17.163); Morbus Waldenström can present as a diffuse lung disease, as amyloidosis, or can be associated with one of the low-grade lymphomas (Fig. 17.164).

There are other lymphomas infiltrating the lung, but in most instances these lymphomas have been diagnosed in other tissues, so in these only a confirmation is required. We will not discuss these other lymphomas, because they are only rarely seen in lung tissues. The reader is referred to the hematopathologic literature.

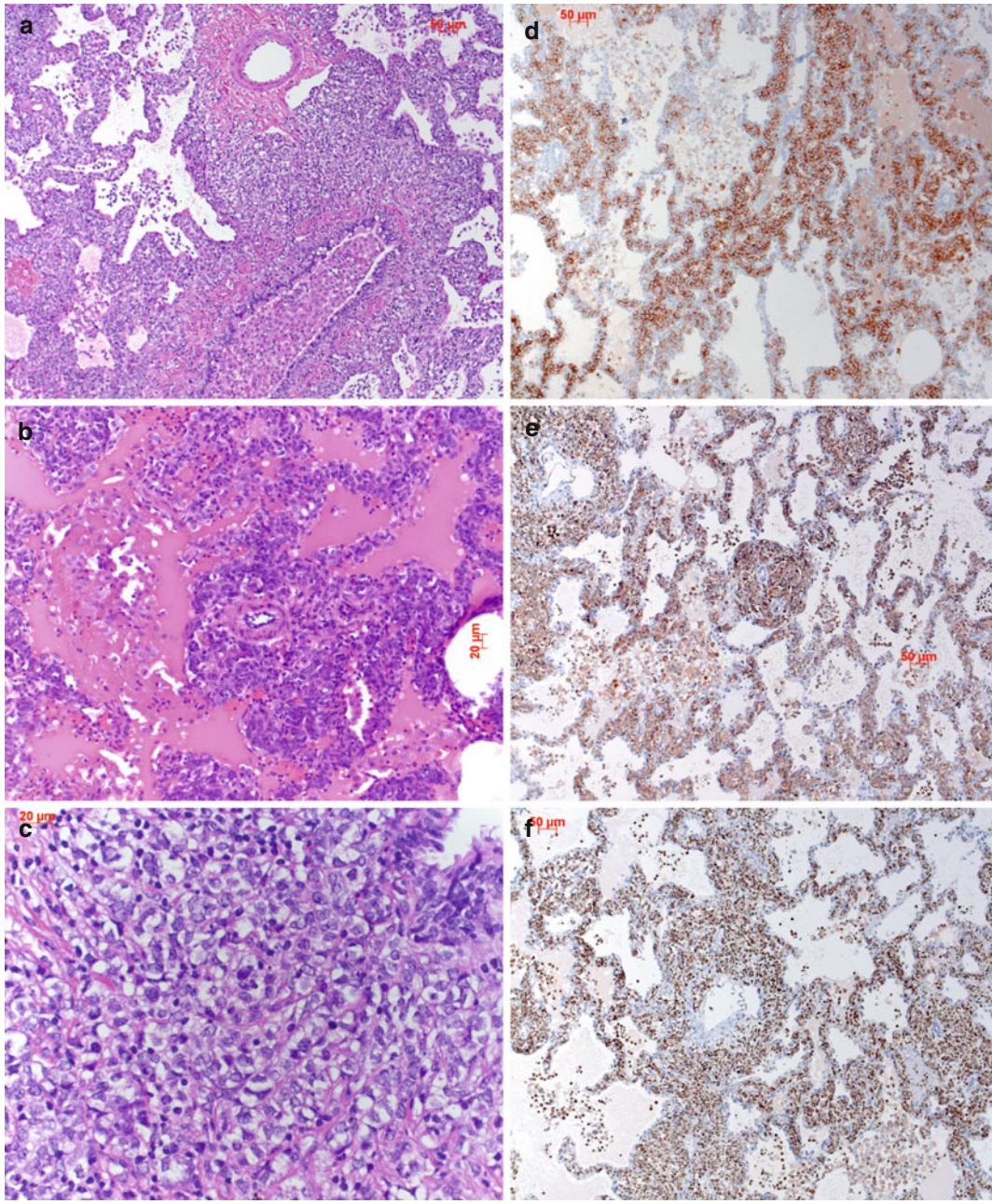

Fig. 17.160 Diffuse large B-cell lymphoma in a 17-year-old woman with lung infiltration. There was no DLBCL in the mediastinum, but instead she had classical Hodgkin lymphoma in mediastinal lymph nodes. Histology shows an infiltration by large lymphoid cells some with clear cytoplasm. Nuclei are atypical, irregular contoured, nucleoli are only slightly increased (**a**–**c**). Positivity for immunostains was seen with CD20 (**d**), CD10 (**e**), PAX5 (**f**), and bcl6 antibodies (**h**). The tumor showed a high proliferation rate by MIB1 stain (**g**). Bars, 50, 20 µm

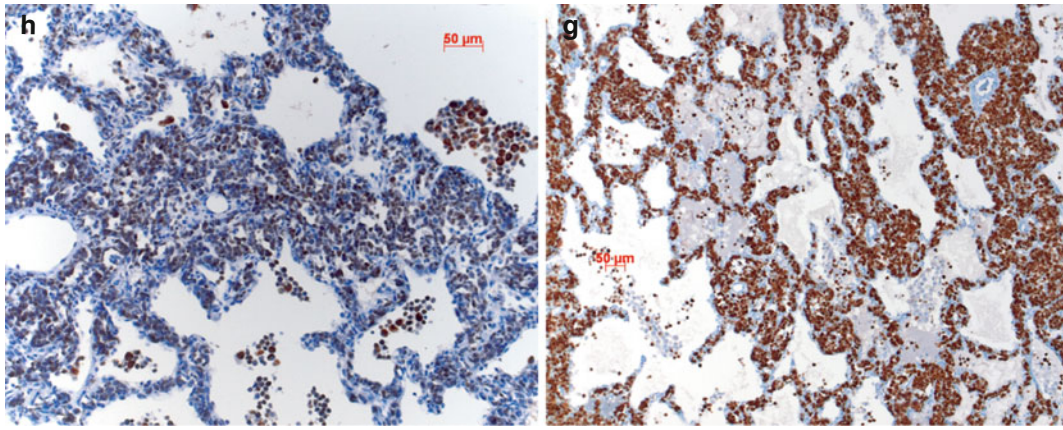

Fig. 17.160 (continued)

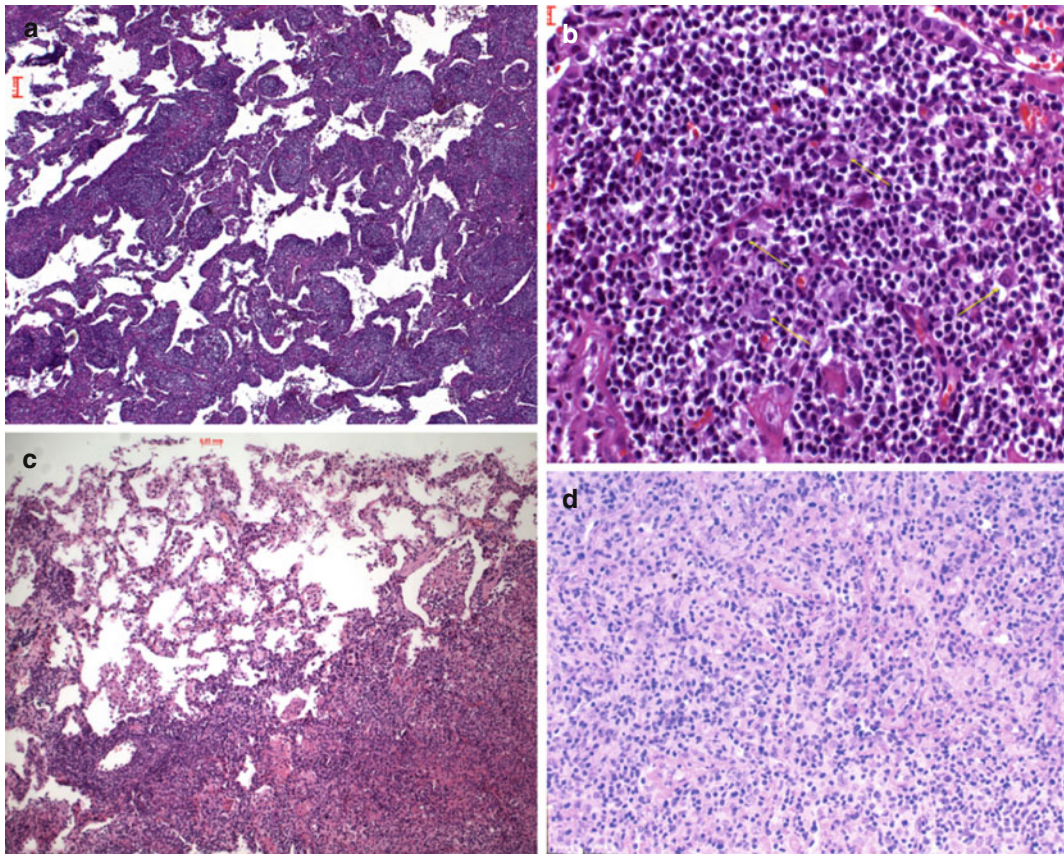

Fig. 17.161 Lymphomatoid granulomatosis (LYG) with different grades. (**a**, **b**) Grade 1 shows a dense reactive lymphoid infiltration reminiscent of lymphocytic pneumonia pattern. On higher magnification a few atypical large blasts are seen (*arrows*). Grade 2 shows a similar pattern (**c**), but the blasts are more numerous (**d**). In grade 3 there is almost in every case necrosis (**e**), the blasts are numerous (**f**), and the typical infiltration of blood vessels by the lymphoma cells causing these infarct-like necrosis (**g**). The diagnosis can be made on small transthoracic biopsies, if the characteristic vascular infiltration is present (**h**). H&E, bars 100, 50, 10 µm

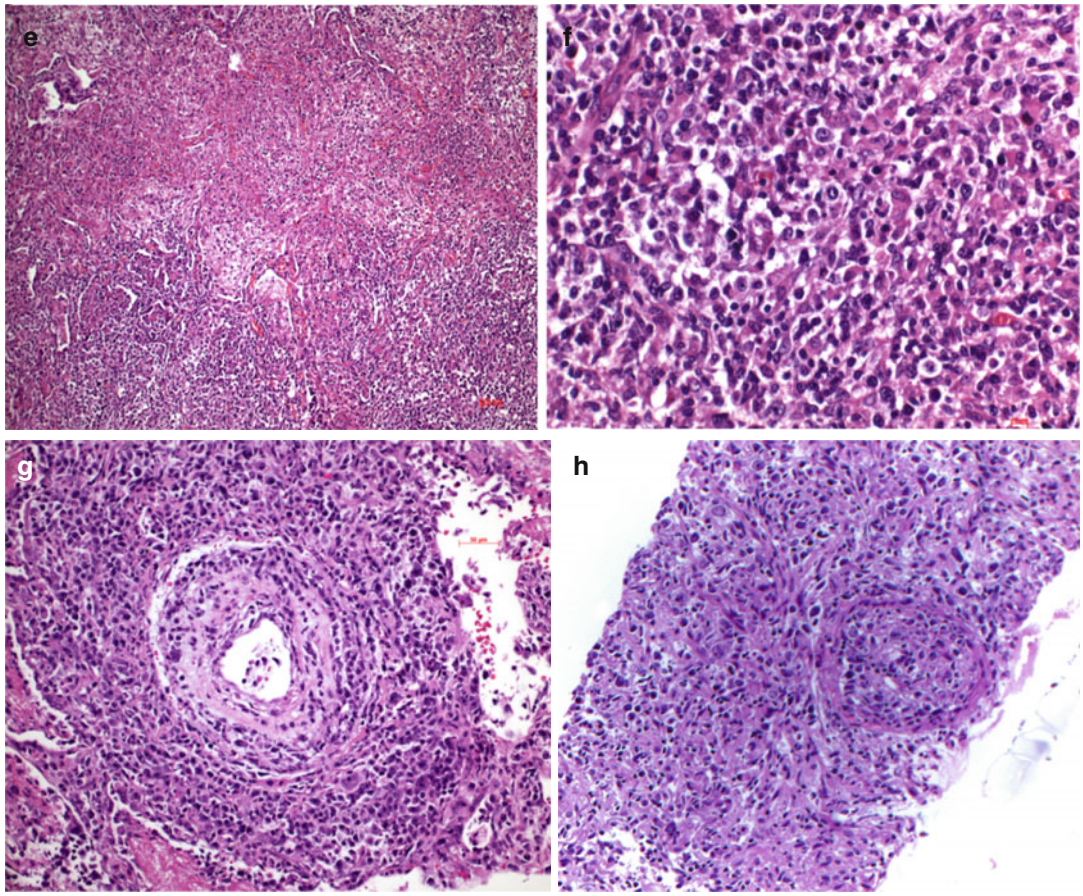

Fig. 17.161 (continued)

17.5.2 Dendritic Cell and Histiocytic Tumors

17.5.2.1 Interdigitating and Follicular Dendritic (Reticulum) Cell Tumor

Clinical Features

No specific clinical symptoms are found. By X-ray and CT scan, a malignant tumor mass will be diagnosed.

Gross Findings

A solitary tumor with ill-defined borders, a grayish-reddish smooth cut surface, and a lobular architecture will be encountered.

Microscopic Findings

The tumor is composed of epithelioid and spindle cells. The tumor grows invasive into the lung parenchyma and destroys the lung. Invasion of the blood vessels can occur. Nuclei are large, chromatin is coarse, and nucleoli are enlarged in some but not all tumor cells. Cell borders are ill defined, especially in the spindle cells, better visible in the epithelioid cells. Mitosis can be rare or easily visible (Figs. 17.165 and 17.166).

Immunohistochemistry

Immunohistochemistry is necessary to arrive at the correct diagnosis. The tumor cells are positive for S100 protein, CD68, lysozyme, vimentin and negative for HMB45, cytokeratins, and

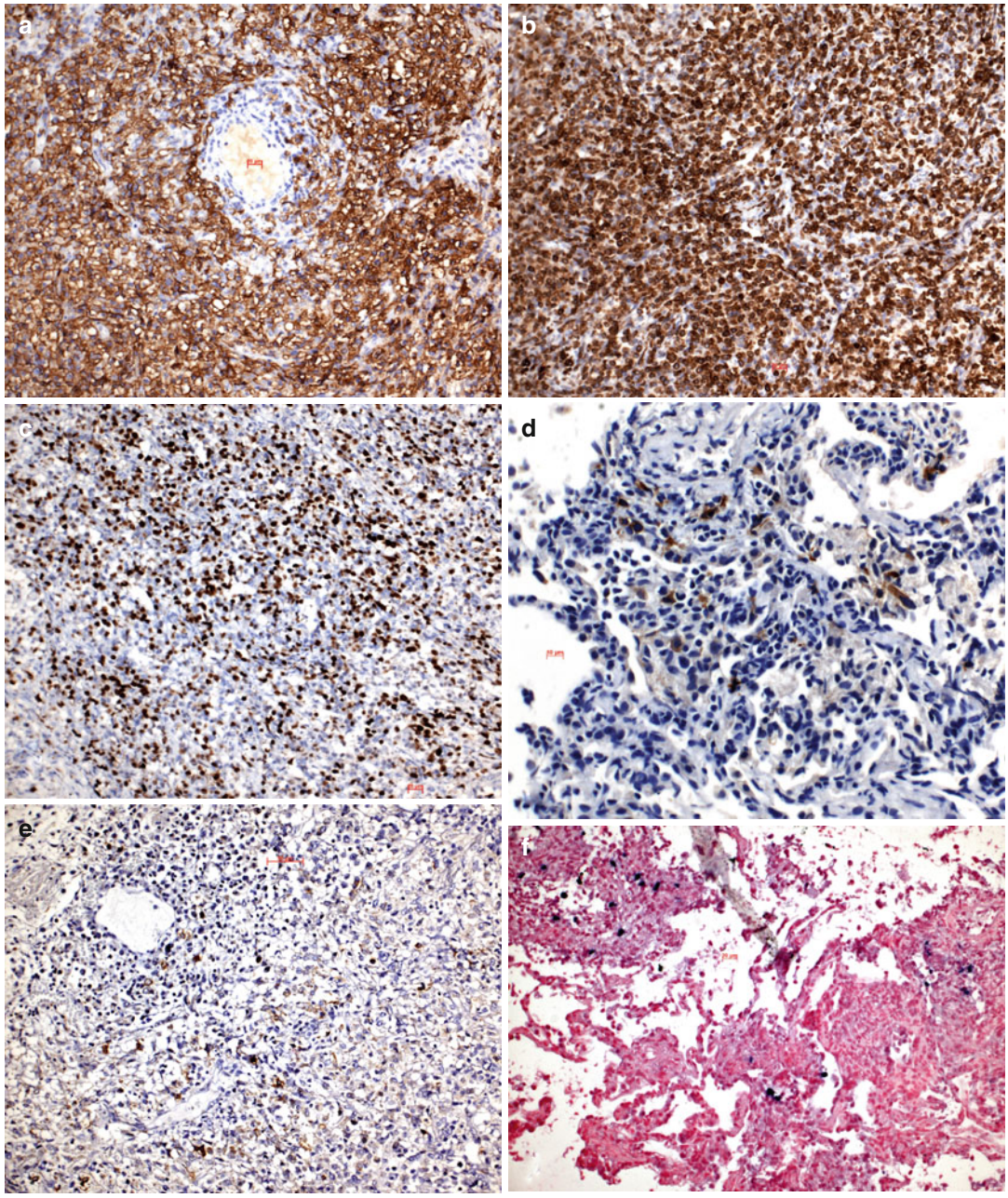

Fig. 17.162 Immunohistochemistry for LYG: the tumor cells stain positive for CD20 (**a**), MUM1 (**b**), bcl2 (**c**), and CD30 (**d**). A comparison for EBV immunohistochemistry (**e**) and in situ hybridization for EBER1 (**f**) is shown. In situ hybridization is much more sensitive compared to immunohistochemistry, and since it is important for grading, it is recommended. Bars, 50, 20, 10 μm

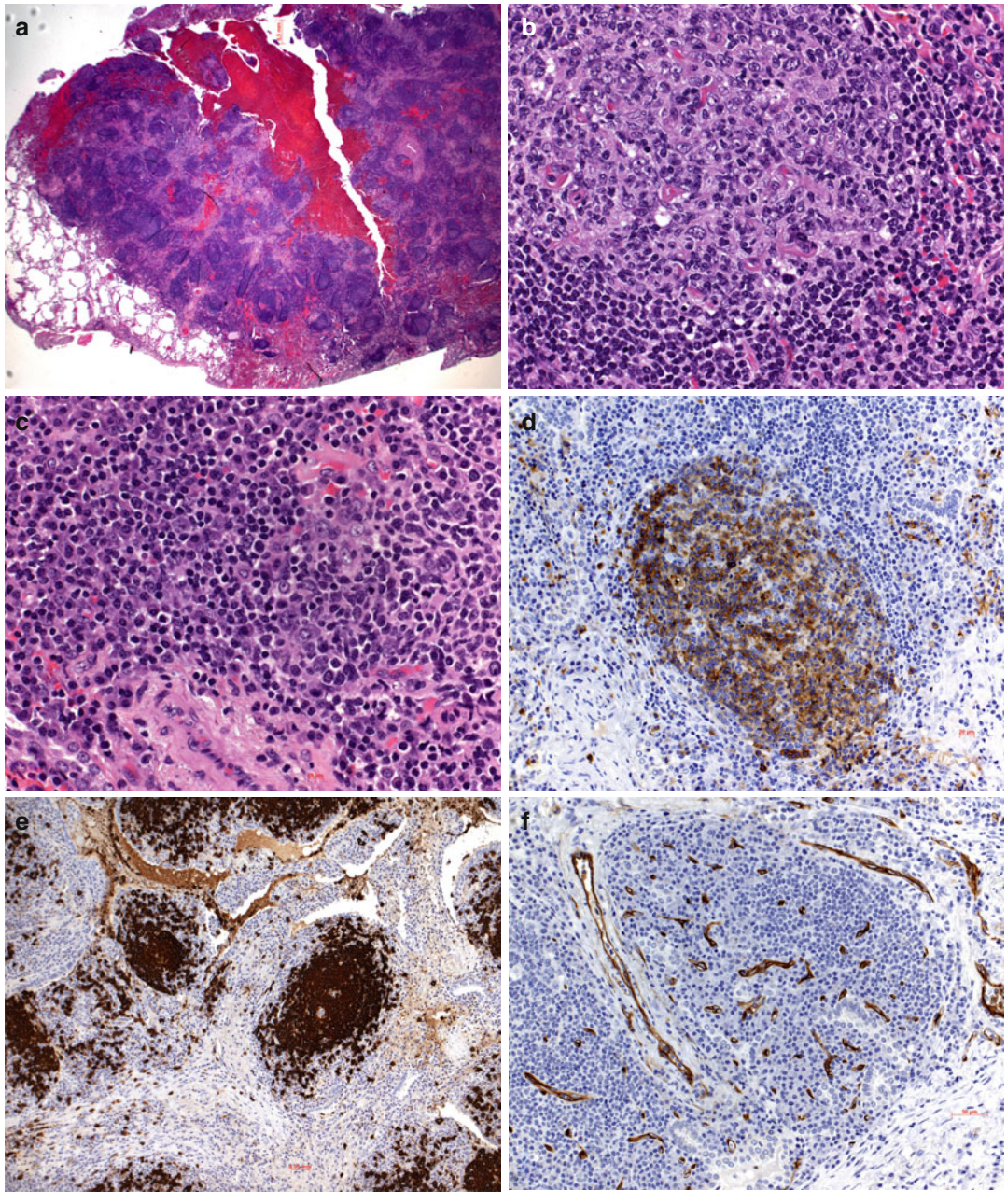

Fig. 17.163 Nodular form of Cattleman's disease. (**a**–**c**) Shows overview of a lymph node-like intrapulmonary structure; in (**b**) germinal centers are seen, however, also the many venules with high endothelial cells; the endothelial proliferation is also seen in (**c**). By immunohistochemistry CD10 (**d**), CD20 (**e**), and CD31 (**f**) are shown. Bars, 500, 50, 20, 10 μm

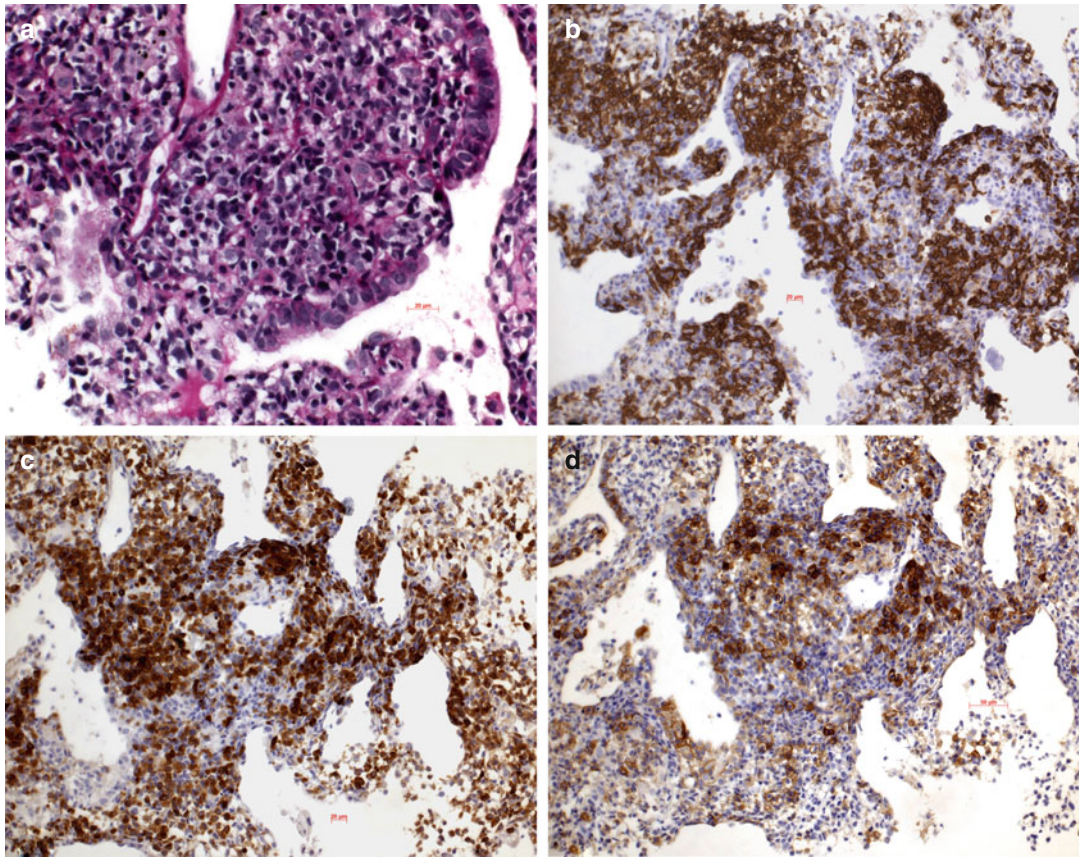

Fig. 17.164 A diffuse infiltrating form of Morbus Waldenström is presented. In (**a**) the diffuse lymphocytic polyclonal infiltration is seen; (**b**) shows the reaction for CD20, (**c**) for CD79a; and (**d**) highlights the amount of plasma cells (CD38). There was a light chain restriction for lambda. Bars 50, 20 µm

CD1a; the reaction for CD83 is positive in interdigitating DCT (Fig. 17.165), whereas CD35 is positive in the follicular DCT (Fig. 17.166). Usually only a minority of tumor cells express the specific markers CD83 and CD35, respectively. Occasionally tumor cells can express CD45RO, CD4, and CD8.

Differential Diagnosis

All types of epithelioid tumors have to be considered for a differential diagnosis. The most important ones are malignant melanoma (excluded by negative staining for HMB45), epithelioid hemangioendothelioma and angiosarcoma (excluded by negativity for endothelial markers), Langerhans cell histiocytosis (excluded by negativity for CD1a), sclerosing pneumocytoma (excluded by negativity for cytokeratins), and large-cell lymphomas (excluded by negativity for other lymphoma markers).

Prognosis and Therapy

Prognosis for interdigitating and follicular dendritic cells tumors is unpredictable. This group of tumors is characterized by invasive growth, some may recur several times; however, distant metastasis is rare. Therapy is excision. In some cases amplified genes might make the tumor sensitive for neoadjuvant therapy such as Herceptin treatment.

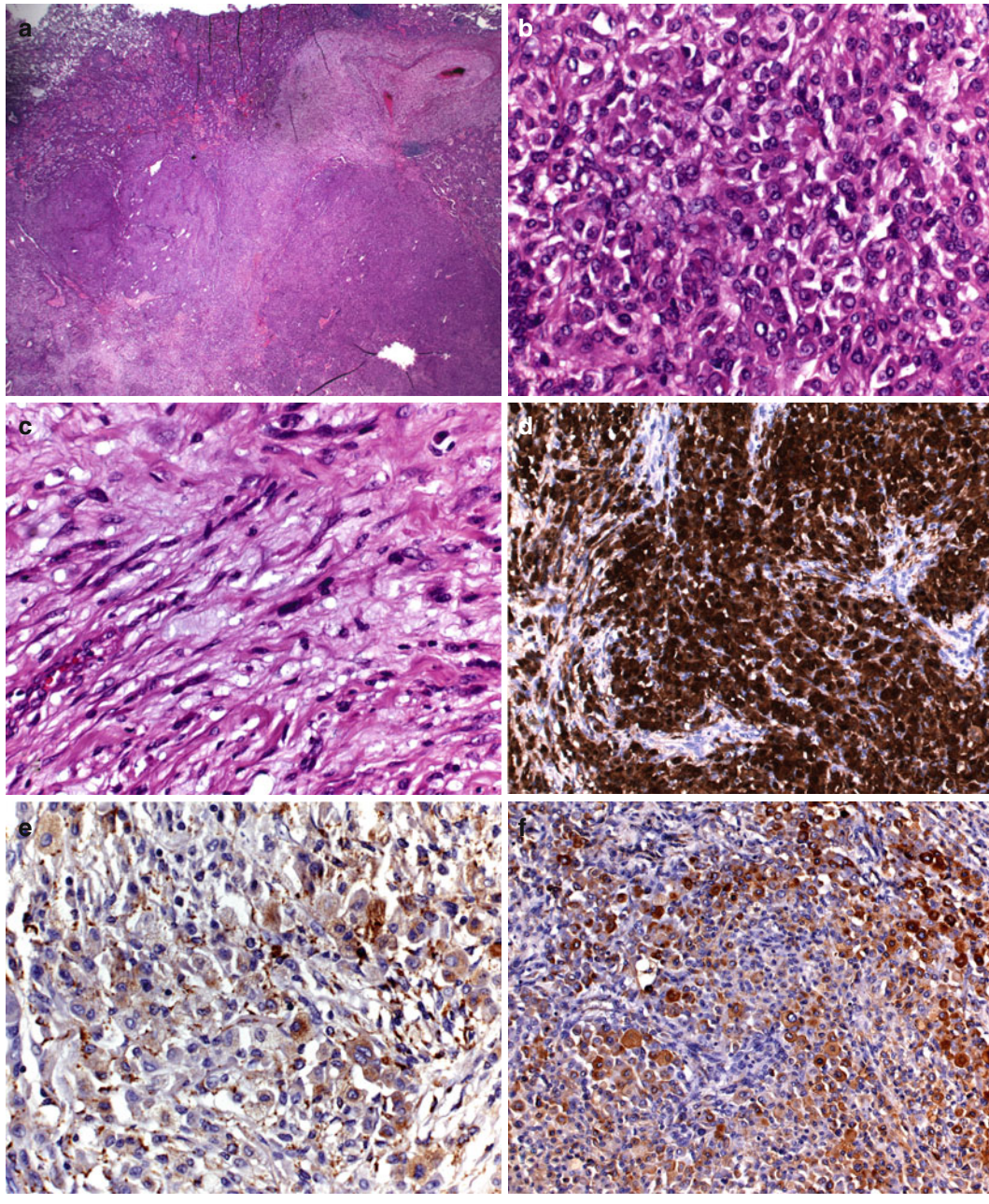

Fig. 17.165 Interdigitating dendritic reticulum cell tumor/sarcoma; a large tumor was detected in the lung (**a**); it is composed of large cells with abundant eosinophilic cytoplasm, nuclei are enlarged, nuclear membrane is accentuated, and nucleoli are middle sized and abnormal configured (**b**); in one area there is a transition into a phenotype with more spindle cells, which have a more dense chromatin (**c**); the tumor cells express S100 protein (**d**); a few are positive for CD68 but with a faint stain (**e**), vimentin (**f**), lysozyme (**g**), and CD83 (**h**). CD35 was negative thus the diagnosis was established. ×12, 100, 200, 400

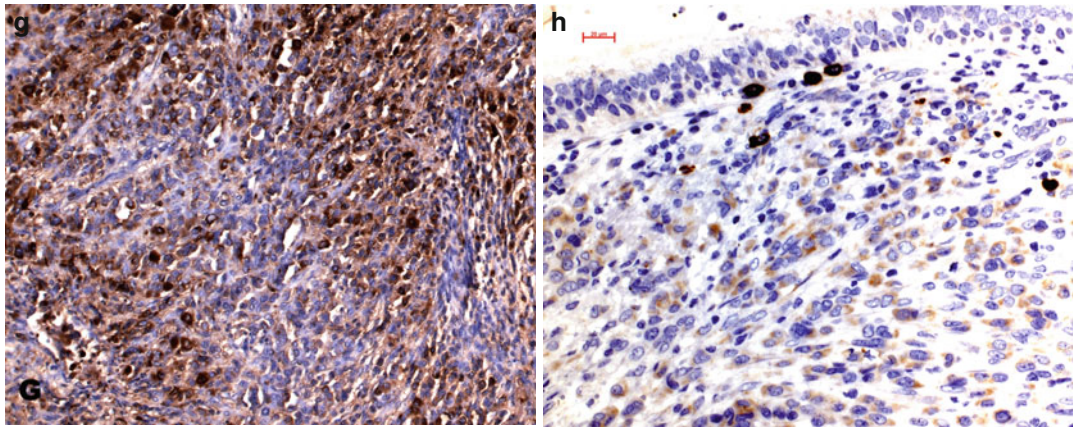

Fig. 17.165 (continued)

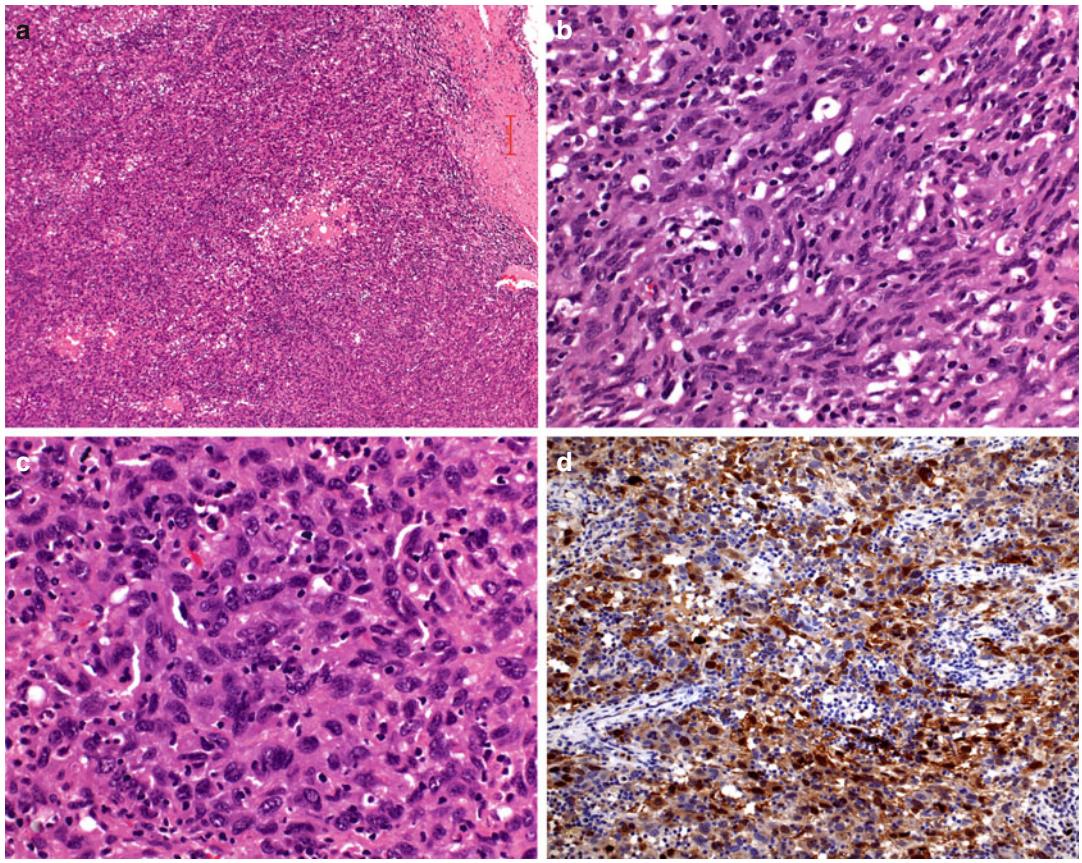

Fig. 17.166 Follicular dendritic reticulum cell tumor/sarcoma; this case as well presented as a solitary lung mass (**a**), suspected to be an early lung carcinoma. The tumor cells are either more spindly (**b**) or epithelioid (**c**); nuclei are large, the cytoplasm is eosinophilic, and cells present with a single cell pattern without any arrangement; chromatins is coarse granular; nucleoli are slightly enlarged. Immunohistochemical staining for S100 protein was pronounced (**d**). ×50, 200, 400

17.5.2.2 Malignant Langerhans Cell Histiocytosis (Abt-Letterer-Siwe)

Malignant Langerhans cell histiocytosis (Abt-Letterer-Siwe) is an extremely rare disease in childhood but also in young adults. It is now regarded as a proliferation of immature and sometimes malignant Langerhans cells. The LH cells can show all degrees of maturation; even within the infiltration, the population is not homogenous. In some cases the disease is self-limiting, in others it runs a fatal course. Infiltration is always systemic, most often affecting the lungs, bones, thymus, spleen, liver, kidney, and skin. In lungs it forms small and large aggregates around blood vessels and rarely infiltrates the alveoli. Birbeck granules can be found by electron microscopy in the tumor cells. The typical immunophenotype is S100 protein positive [534]. The tumor cells also express CD1a but only focally Langerin (Fig. 17.167).

17.5.2.3 Malignant Histiocytic Sarcoma

This is a rare neoplasm in humans but common in different mammals such as dogs and cats. The tumor is composed of sheets of large epithelioid

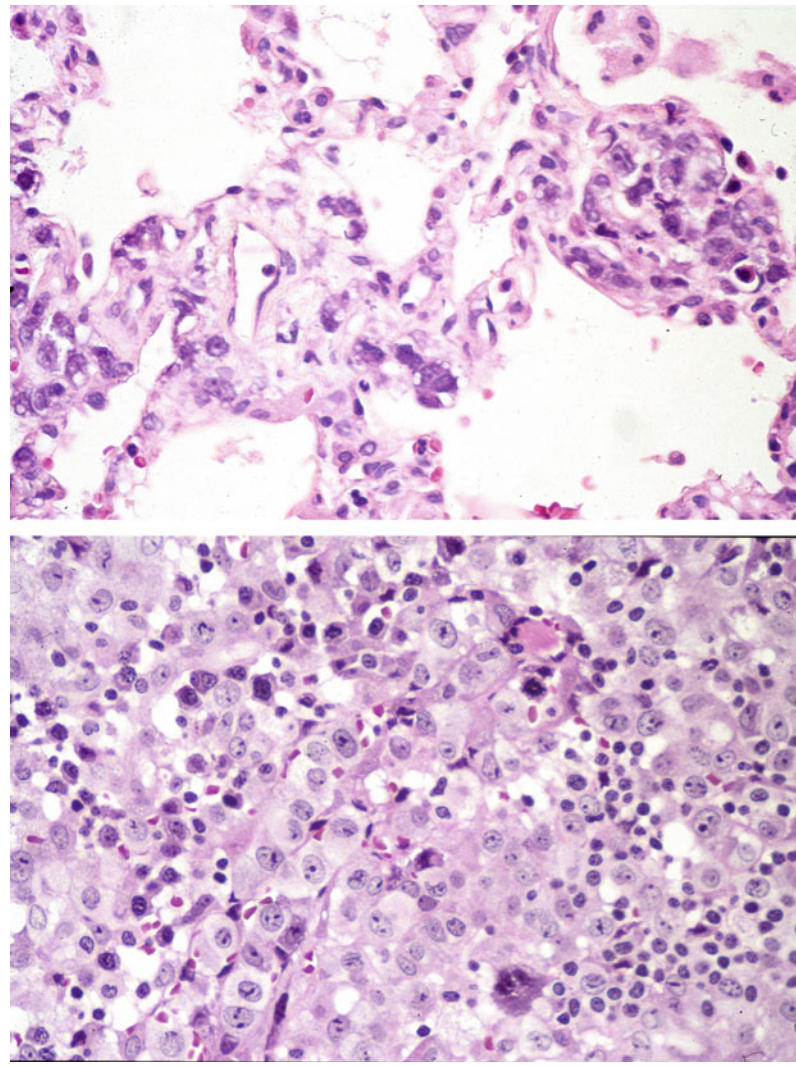

Fig. 17.167 Malignant Langerhans cell histiocytosis; the tumor was detected in a 2-year-old child at autopsy. It was already systemic involving several organs, but the main cause of death was respiratory insufficiency. In the lung a diffuse and a multinodular infiltration pattern was seen; the *upper panel* shows diffuse, and the *lower panel* the nodular pattern. H&E, ×400

cells with abundant eosinophilic cytoplasm, oval to irregular nuclei, vesicular chromatin, and large nucleoli. Binucleated cells and sometimes tumor giant cells can be seen. The mitotic range is wide from 1 to 64 per 10 HPF. Necrosis is usually present. In many tumors an inflammatory infiltrate composed of neutrophils or lymphocytes is seen. The tumor cells express LCA, CD45RO, and CD68; lysozyme and S100 protein is positive in most cases, whereas CD1a or Langerin is negative [535]. In some tumors spindle cells are noted, and hemophagocytosis was identified. A new specific marker CD163 was identified in the study by Vos (Fig. 17.168) [536]. In some cases the distinction from Langerhans cell histiocytosis might be difficult, but using the appropriate immunohistochemical markers, the diagnosis can be solved [537].

17.5.2.4 Erdheim-Chester Disease

Erdheim-Chester disease is a rare systemic histiocytosis (non-Langerhans dendritic cells) that may present with pulmonary symptoms. The condition seems to be nonfamilial and typically affects middle-aged adults. Radiographic and pathologic changes in the long bones are diagnostic but may mimic multisystemic Langerhans cell histiocytosis [538, 539]. Patients often present with extraskeletal manifestations. Advanced pulmonary lesions are associated with extensive fibrosis that may lead to cardiorespiratory failure [540]. In rare instances there are diffuse dense infiltrations by histiocytes accompanied by lymphocytes and plasma cells. These histiocytes are negative for Langerhans cell markers (CD1a, Langerin) and markers for follicular and interdigitating dendritic cells (CD35, CD83) but can be positive for S100 protein (much less intensive staining compare to interdigitating dendritic cells) and are usually positive for CD68, CD163, and lysozyme (Figs. 17.169 and 17.170). Histiocytes can express PDGFRα and PDGFRβ, which might be used as therapeutic targets. PDL1 expression has been found in this tumor and might make it suitable for immunotherapy with anti-PD1 antibodies [541]. The proof of mutations in BRAF, RAS, MAPK, and PI3K genes in the histiocytic cells [542–544] has changed the view of ECD as a tumor instead of an inflammatory disease. BRAF inhibition might be another therapeutic option.

17.6 Childhood Tumors

17.6.1 Congenital Peribronchial Myofibroblastic Tumor

Clinical Features

This is a congenital tumor usually presenting as a mass lesion at or shortly after birth [545, 546]. Polyhydramnion and hydrops fetalis may be present [547].

Gross Findings

A well-circumscribed tumor without a capsule. On cut surface the tumor is grayish red to grayish yellow; dark-red hemorrhage and yellow necrosis may be present. The tumor shows a peribronchial growth pattern; occlusion of the bronchus is common.

Microscopic Findings

The tumor cells are uniform and spindle shaped; a herringbone pattern can occur. Collagen deposition is seen; however, the fascicles are shorter compared to adult fibrosarcoma. Nuclei are elongated or round, sometimes fibroblast-like, chromatin is finely dispersed, nucleoli are absent, and mitosis is rare. The tumor invades and destroys the structures of the bronchovascular bundle and causes obstruction or occlusion (Fig. 17.171). An invasion of septa and pleural surface can occur.

Immunohistochemistry

By immunohistochemistry the tumor cells are positive for vimentin, whereas the reactivity for smooth muscle actin, desmin, and other muscle markers is usually confined to single or groups of cells. Other markers, which will stain few cells, are S100 protein, CD34, and CD68. On genetic analysis an unbalanced whole-arm translocation between chromosomes 9 and 16 has been found, which might provide a specific treatment in the future [548, 549].

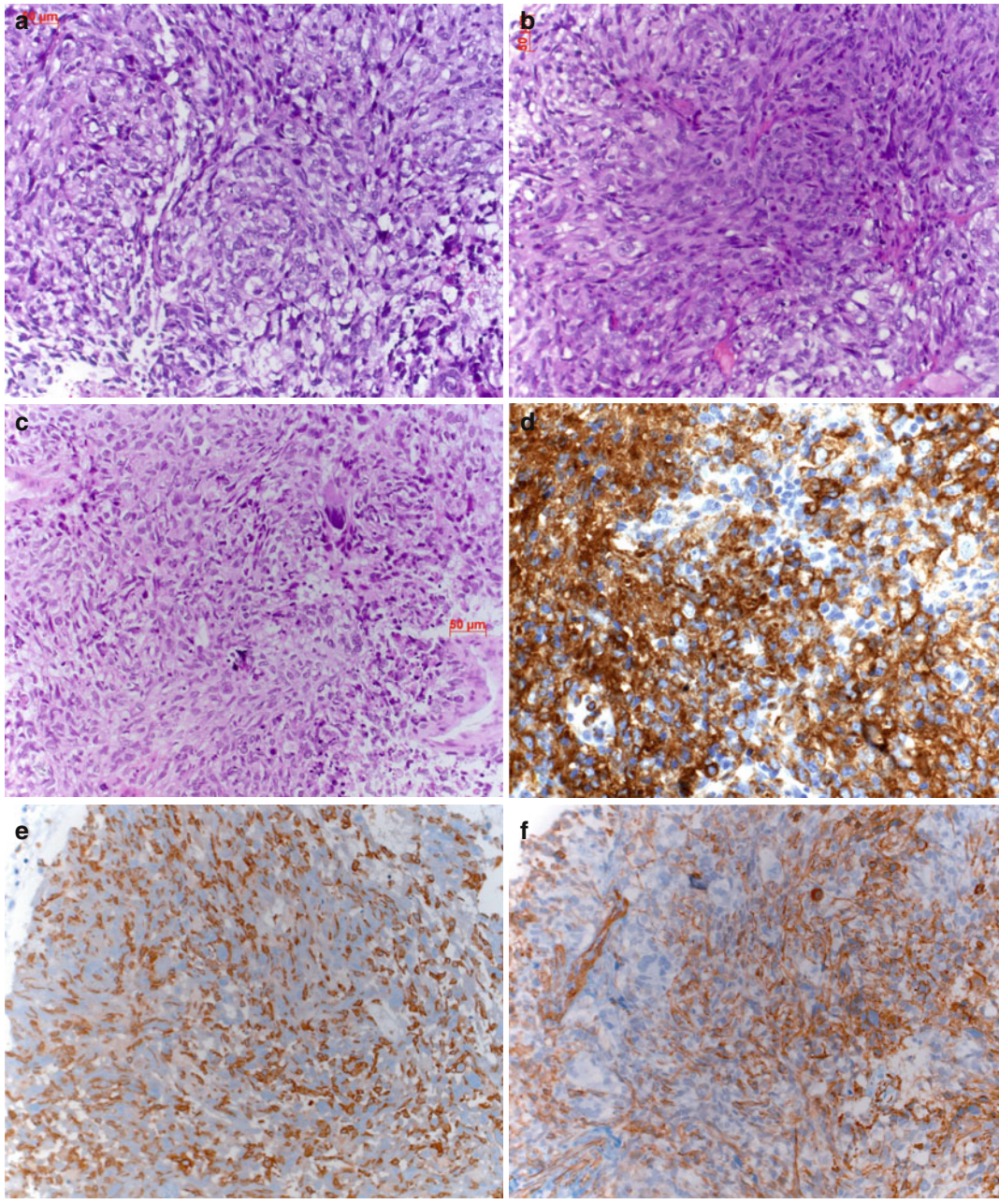

Fig. 17.168 Malignant histiocytic sarcoma shows areas with plump spindle cells mixed with epithelioid cells (**a**, **b**); in some areas also giant tumor cells can be seen (**c**). Nuclei are middle sized with basophilic cytoplasm, mitosis is frequent, and nucleoli are middle sized. Chromatin is vesicular and often seen at the nuclear membrane. Tumor cells are positive for CD14 (**d**), CD163 (**e**), SMA (**f**), and lysozyme but negative for S100 protein. Bars, 50 µm

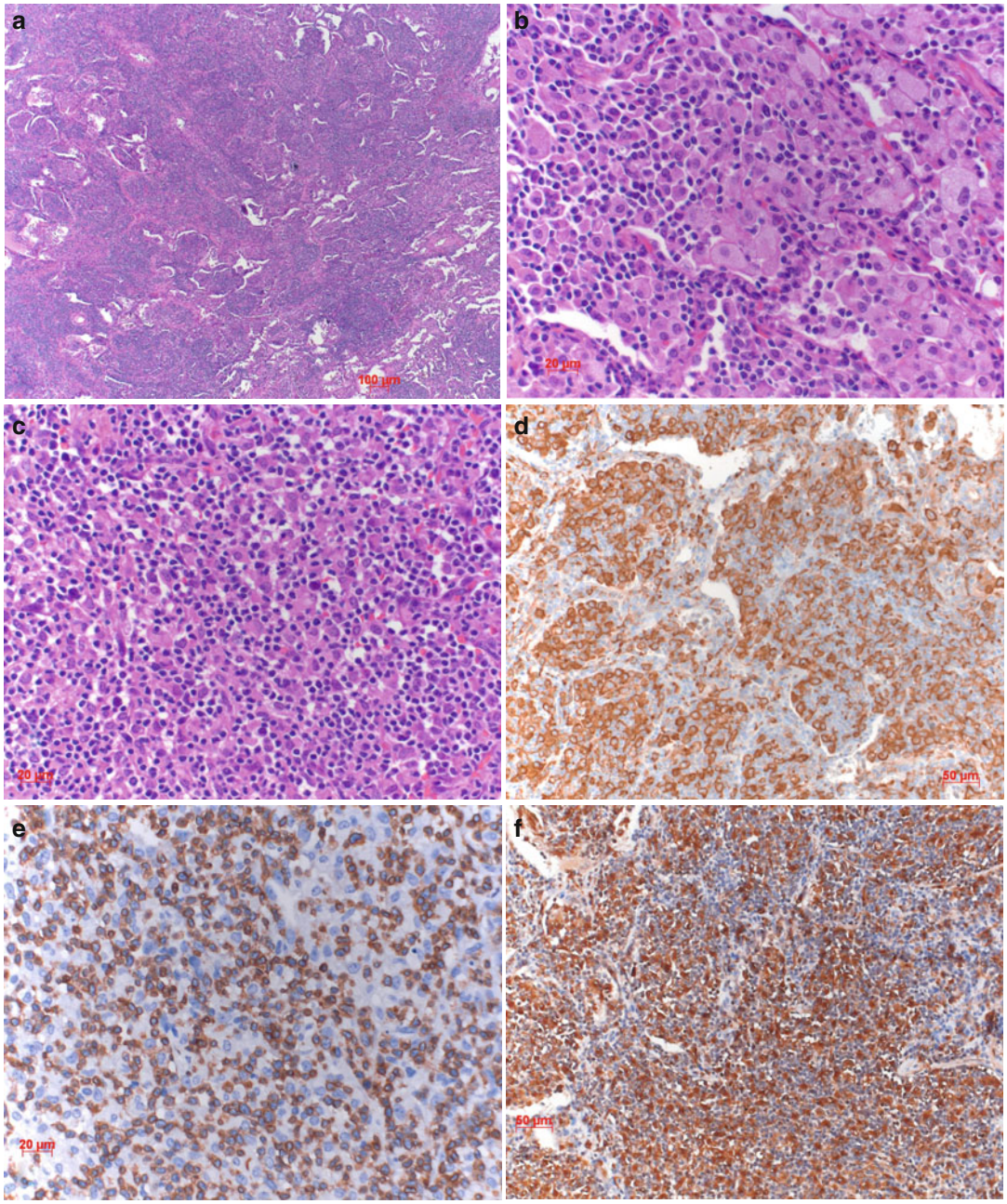

Fig. 17.169 Erdheim-Chester disease is another tumor of the histiocytic lineage. In (**a**) a diffuse infiltrating tumor is seen, which showed besides the tumor cells numerous lymphocytes (**b**, **c**). A lymphoma was excluded by immunohistochemistry and molecular investigation, before it was realized that the large histiocytic cells/macrophages are the tumor cells. By immunohistochemistry the tumor cells express CD163 (**d**), lysozyme (**f**), and CD68 (**g**); numerous CD3-positive lymphocytes are within the tumor (**e**). In addition the tumor cells show an upregulation of platelet-derived growth factor receptor β (PDGFRβ, (**h**). Bars, 100, 50, 20 µm

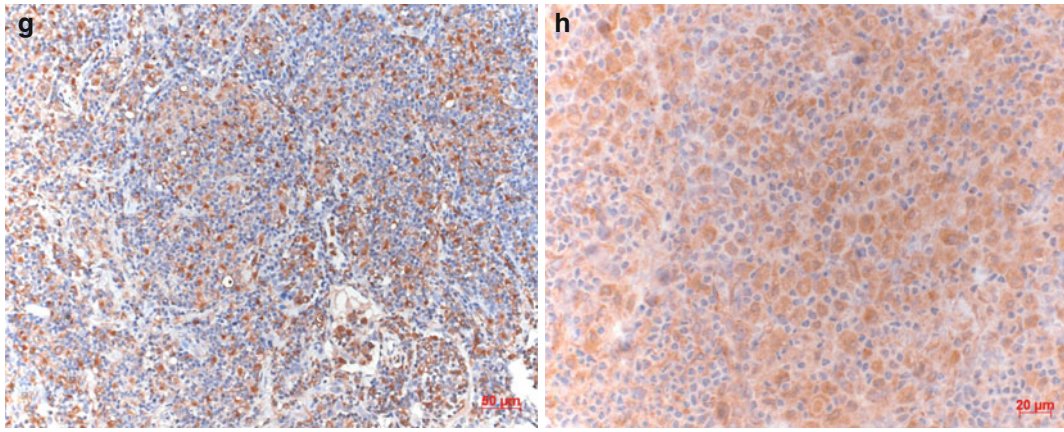

Fig. 17.169 (continued)

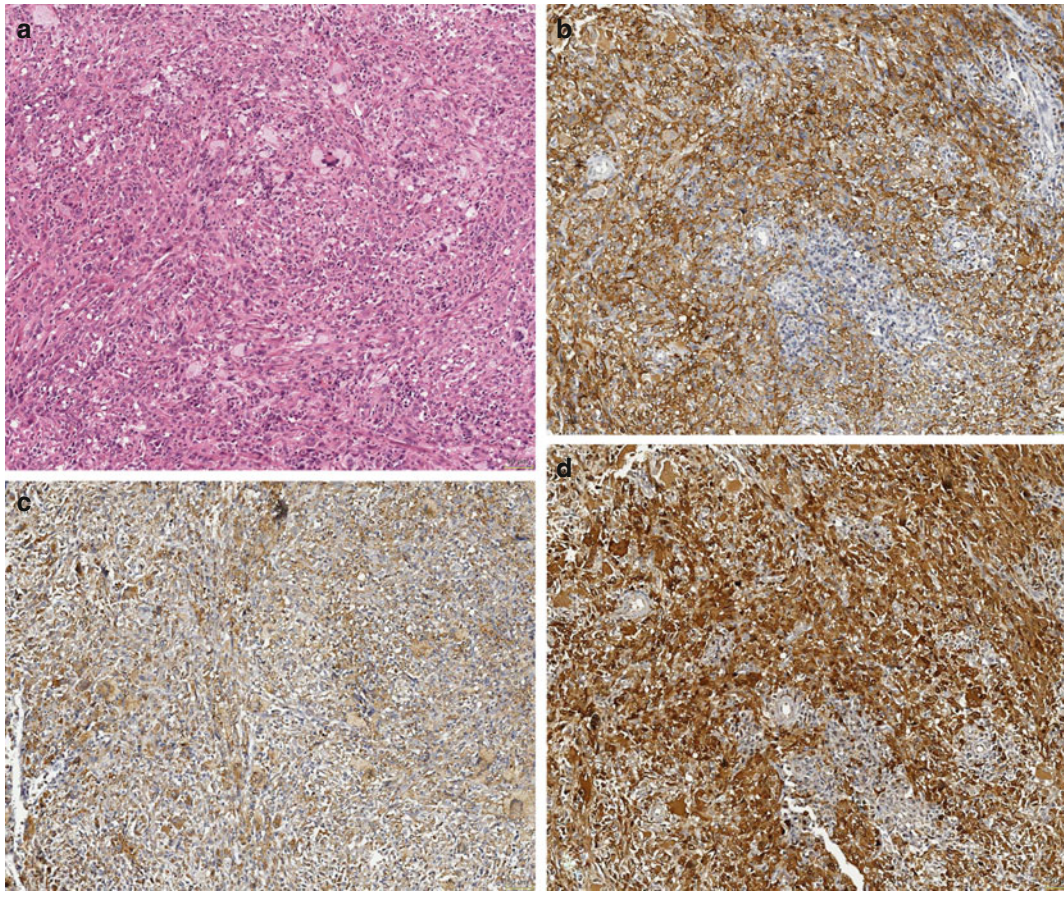

Fig. 17.170 Erdheim-Chester disease, a more typical case is shown here. In (**a**) many large histiocytic cells are seen, all of them with pale pink cytoplasm. Some are multinucleated. By immunohistochemistry these tumor cells stained positively for CD14 (**b**), CD68 (**c**), and S100 protein (**d**). Bars 50 µm

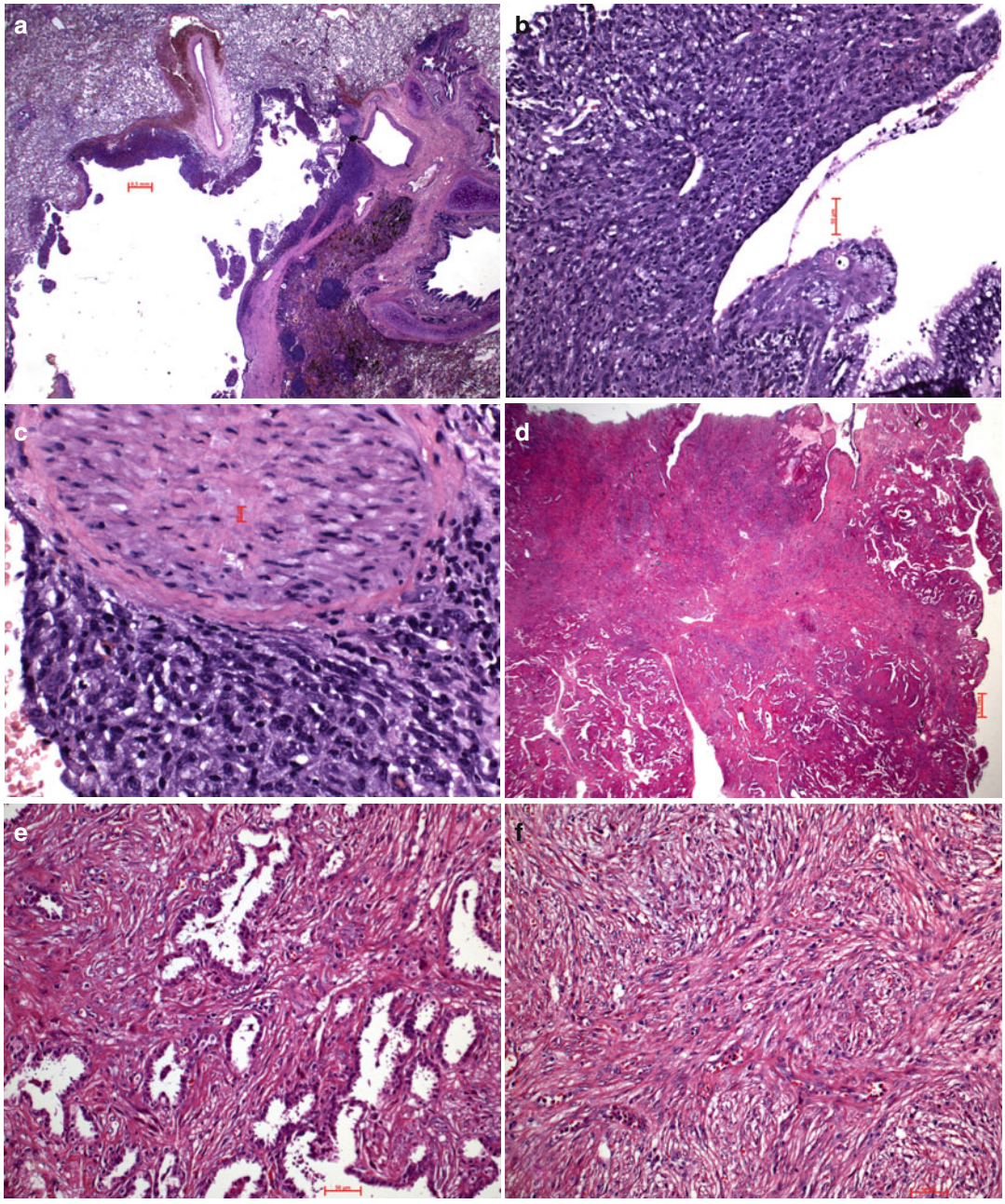

Fig. 17.171 Congenital peribronchial myofibroblastic tumor, two cases are shown: (**a**–**c**) a CPMT is infiltrating the large bronchus and the tumor cells are immature with basophilic cytoplasm and few myofilaments within the cytoplasm. There is not much collagen deposition but an infiltrative destruction of the mucosa and other structures such as a nerve (**c**). The nuclei are plump spindled or ovoid, sometimes epithelioid. Nucleoli are large, chromatin is coarse, and a few mitoses are encountered. The second case (**d**–**f**) shows a CPMT, which is more mature. There is still an infiltrative pattern and destruction of bronchial mucosa leaving only epithelial remnants. This tumor deposited much more collagen. Bars, 500, 50, 10 μm (Case (**a**) courtesy of Bruno Murer)

Differential Diagnosis

Given the age of the patients and the microscopic appearance, there are no differential diagnoses to be considered.

Prognosis and Therapy

Surgical resection is the treatment of choice. If no other complications are present, this should be curative. Most reports regard this tumor as benign.

17.6.2 Fetal Lung Interstitial Tumor (FLIT)

This is a recently described new tumor entity. It occurs in the prenatal period to 3 months of age. The initial description was based on seven male and three female patients [550].

Histopathology

The tumor presents as a solid or mixed solid/cystic lung mass composed of immature interstitial mesenchyme in association with irregular airspace-like structures mimicking abnormal incompletely developed lung at 20–24 weeks gestation [550]. FLIT most often will look like pleuropulmonary blastoma type I; there are also undifferentiated mesenchymal cells, however FLIT lacks rhabdomyoblasts and also primitive cambium-layer cells.

Molecular Biology

In contrast to PPB, FLIT is negative for trisomies 8 and 2 [551]. Onoda and coworkers reported chromosomal rearrangement resulting in alpha-2-macroglobulin (A2M) and anaplastic lymphoma kinase (ALK) gene fusion t(2;12)(p23;p13. Break apart FISH demonstrated chromosomal rearrangement at ALK 2p23. The gene showed exon 22 of A2M to exon 19 of ALK fusion. This provides new insights into the pathogenesis of FLIT and suggests the potential for new therapeutic strategies based on ALK inhibitors [552].

Differential Diagnosis

The only differential diagnosis is type 1 (cystic) pleuropulmonary blastoma; however, cells with rhabdomyoblastic phenotype may help to distinguish PPB from FLIT.

Prognosis and Therapy

Surgical resection is recommended; adjuvant chemotherapy might be added. No recurrences were reported.

17.6.3 Pleuropulmonary Blastoma

Clinical Features

Pleuropulmonary blastoma (PPB) is a malignant primitive mesenchymal childhood tumor, preferentially seen in early childhood, however, sometimes can also affect teens. It can arise in the pleura, the lung, or both. It can present as a predominant cystic, a mixed cystic and solid, or a pure solid lesion. The symptoms are related to compression atelectasis of the lung caused by tumor growth.

Radiologic Features

The cystic variant is well known and can easily be detected by X-ray and CT scan as well. Also ultrasound has been used to detect this tumor, even intrauterine. There are not many other cystic lesions in that age setting; one is congenital emphysema and another bronchogenic cyst.

Gross Findings

A cystic and/or solid tumor not well circumscribed. It can be confined to the pleura or infiltrate the lung too. There are three variants: predominantly cystic, PPB-I; mixed cystic and solid, PPB-II; and predominantly solid, PPB-III. The cystic variant looks like any other cystic lesion and therefore a variety of bronchial and mesothelial cystic lesions enter the differential diagnosis.

Microscopic Findings

The tumor cells form layers of immature small cells with relatively large nuclei with dense, dark-stained, coarse chromatin. These cells form a so-called germinal layer, which is small in PPB-I (Fig. 17.172), even scattered cells can be seen in some cases. Normal stroma sometimes interrupts the tumor, which is confined to the cyst wall.

In addition there are primitive mesenchymal areas quite normal appearing in PPB-I but primitive and atypical in PPB-II (Fig. 17.173). In PPB-III much thicker germinal layers can be seen, and in addition interspersed giant cells, sometimes multinucleated, which show rhabdomyoblastic differentiation. Also areas of chondrosarcoma are usually encountered. Necrosis and bleeding are frequent; however, it depends on the type of PPB, being frequent in type III (Fig. 17.174). PPB-II is in between the two other variants, composed of cysts and solid components. Mitosis is abundant in PPB-III but rare in PPB-I. Type III is mainly composed of solid areas and rapidly progresses [553–555].

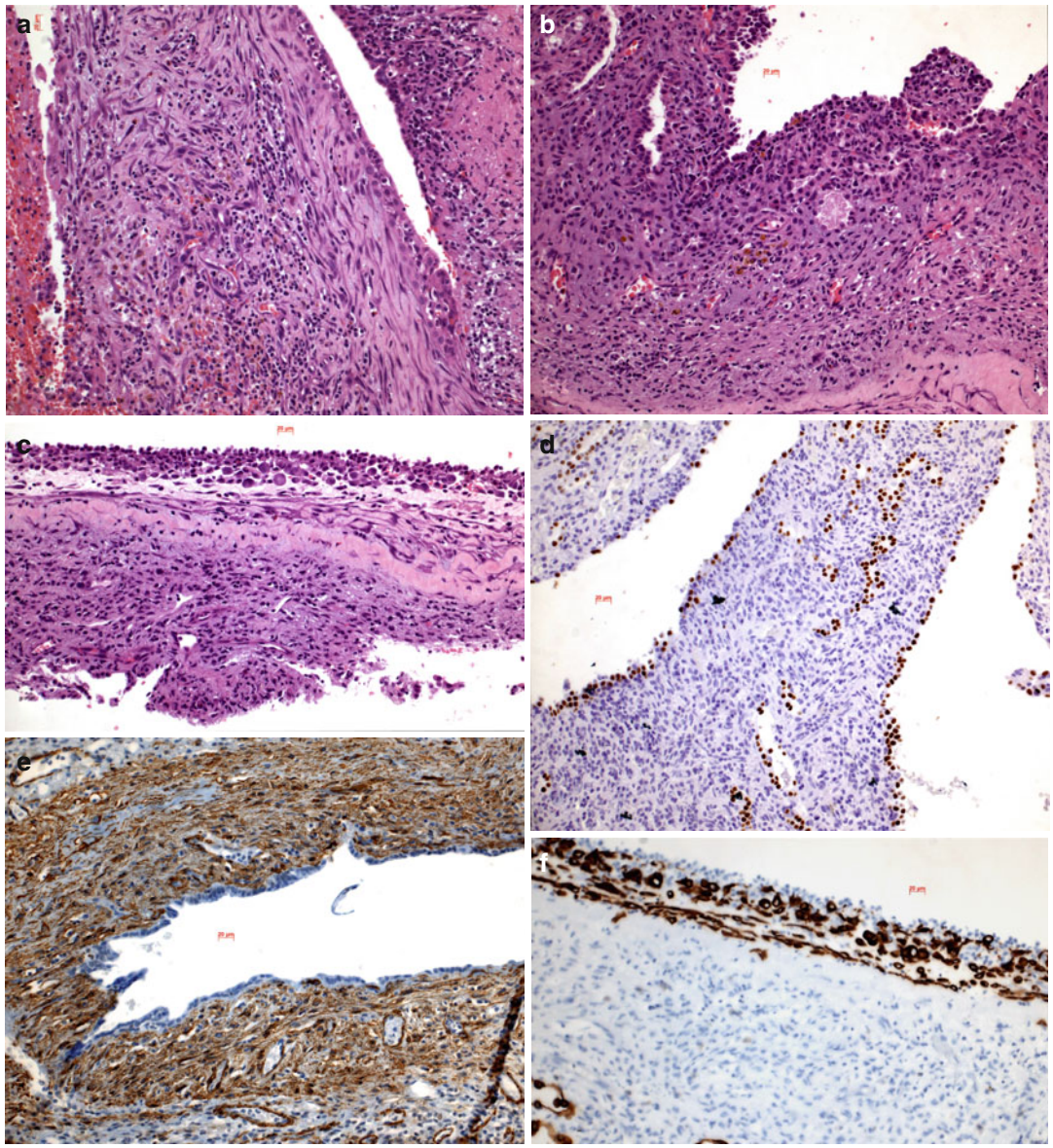

Fig. 17.172 Pleuropulmonary blastoma grade 1, three cases are shown; (**a**–**f**) shows a case where many pitfalls are included. The surface layer in C looked like PPB primarily but by cytokeratin stain turned out to be reactive mesothelium (**f**). Atypical cells in the stroma finally turned out to belong to primitive rhabdomyoblasts (**b**, **c**), negative for TTF1 (**d**), and positive for myogenic markers (SMA in **e**). (**g**, **h**) are classical grade 1 PPBs. Bars, 20, 50, 100 μm

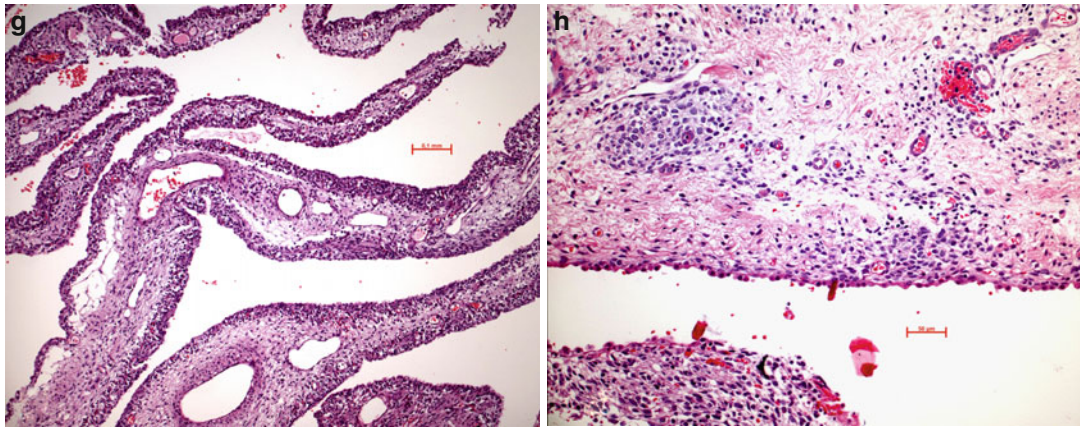

Fig. 17.172 (continued)

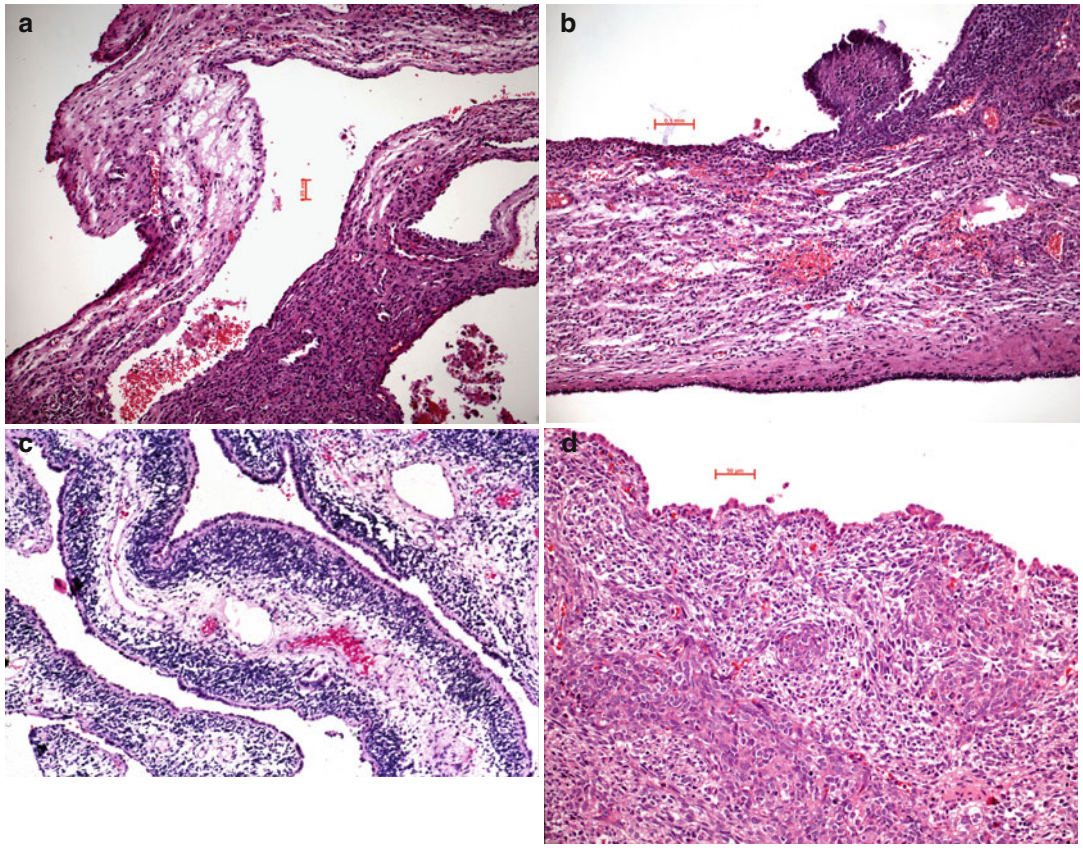

Fig. 17.173 Pleuropulmonary blastoma grade 2, illustrated by four cases. In these the cambium layer is diffusely expanded as in (**b**, **c**), focally with a solid part as in (**a**), or forms solid nodules as in (**d**). Rhabdomyoblasts are still scattered in these cases. Bars, 100, 50 µm

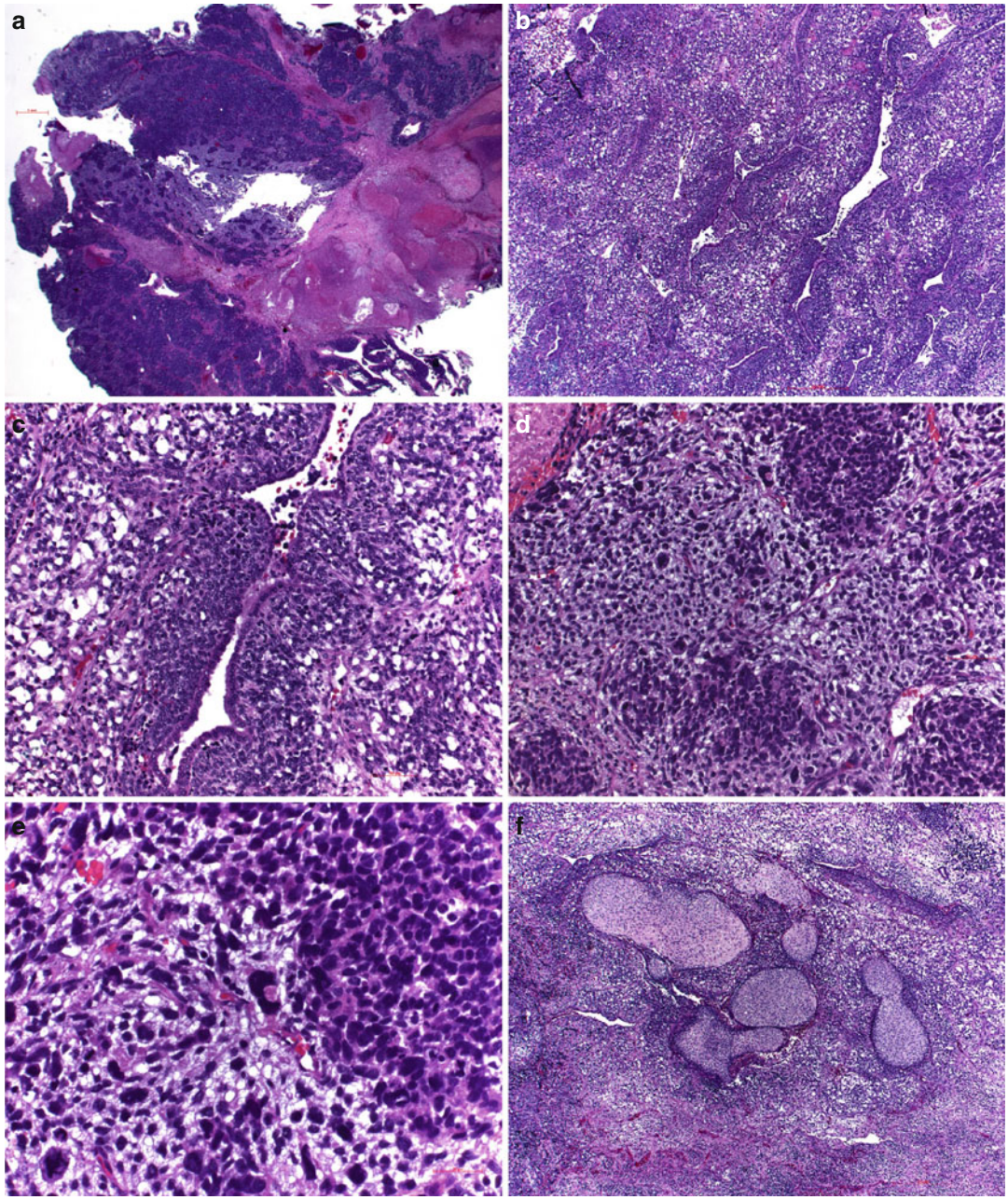

Fig. 17.174 Pleuropulmonary blastoma grade 3, a classical case is shown. In the overview (**a**) the most striking feature are the areas with *dark blue* cells and large areas of *pink* necrosis. On higher power (**b**, **c**) the so-called cambium layer of the cells is seen. These cells represent primitive embryonic mesenchymal cells, which will not stain with any differentiation marker (only vimentin is positive). These cells form a dense band usually underneath regular epithelial or mesothelial remnants of lung and/or pleura. In (**d**, **e**) areas with giant cells are shown, in (**e**) in the center a classical rhabdomyoblast with an inclusion body is illustrated. (**f**, **g**) Are form an area with chondrosarcoma components, also a frequent finding is these tumors. H&E, ×12, 50, 100, 200

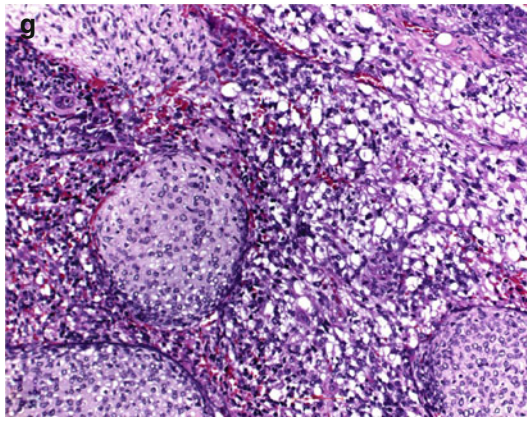

Fig. 17.174 (continued)

Ancillary Studies

By immunohistochemistry the tumor cells are positive for vimentin and negative for cytokeratins. The rhabdomyoblasts stain for desmin. There is no chance for a cytology-based diagnosis.

Molecular Biology

Gain of chromosome 8 is commonly found [556]. Additional abnormalities were loss of 17p; loss of chromosome 10 or 10q; rearrangement of 11p; loss of chromosome X or Xp; gain of chromosomes/arms 1q, 2q, and 7q; and loss of 6q and 18p [557]. In another cytogenetic study, gains were identified at 1q12-q23, 3q23-qter, 8pter-q24.1, 9p13-q21, 17p12-p11, 17q11-q22, 17q23-q25, 19pter-p11, and 19q11-q13.3. Whole chromosome gains were detected at 2 and 7. Loss of genetic material was found at regions 6q13-qter, 10pter-p13, 10q22-qter, and 20p13. The alterations found suggest that a gene or genes of putative relevance in PPB pathogenesis are mapped at 8p11-p12 [558]. This probably resulted in the detection of dicer mutations. Dicer is a protein involved in processing of small inhibitory microRNAs. A mutation has been reported in several families and this was linked to PPB and other childhood tumors [559].

Differential Diagnosis

The major diagnostic problem is with type I: if the cyst walls are not examined carefully, type I is misdiagnosed as simple mesothelial or bronchial cyst. Bronchial cysts are composed of epithelial structures and elements of normal bronchial wall and thus can easily be separated. Mesothelial cysts are much harder to rule out, because the cyst epithelium in PPB-I is also mesothelial derived. The germ cell layer can be inconspicuous, or reduced to small islands, and thus be overlooked. Therefore a careful evaluation of the underlying stroma is relevant. There is not much to differentiate in PPB-II and PB-III. Given the young age of the patients, rhabdomyosarcoma is the only other tumor, which rarely occurs in the lung or metastasizes into it. Especially the germinal layer is quite characteristic for PPB. In PPB-II the combination of cysts and solid areas make the diagnosis easy.

Prognosis and Therapy

PPB is a malignant childhood tumor but with variable degrees of malignancy. Type I is a slow-growing variant, which causes symptoms by enlargement and pulmonary atelectasis, whereas type III is fast growing and infiltrates rapidly adjacent structures. In all types complete resection is essential; in type II and III aggressive chemotherapy might be necessary postoperatively. Type III is the one, which might respond initially to aggressive chemotherapy. Less than half of the patients survive with the diagnosis of PPB-III.

17.6.4 Adenocarcinoma of the Lung Arising in CPAM

Adenocarcinoma of the lung arising in CPAM is extremely rare. A few cases have been identified in a European rare disease study group [12]. These are well-differentiated adenocarcinomas, genotypically different from adenocarcinomas in adults, either smokers or never-smokers. Chromosomal gains on chromosomes 2 and 4 are characteristic major genetic alterations. How these adenocarcinomas are related to CPAM is unclear. The carcinomas arise outside the CPAM lesion (Fig. 17.175). In addition atypical adenomatous hyperplasia has been found too. Within CPAM atypical goblet cell hyperplasia has been identi-

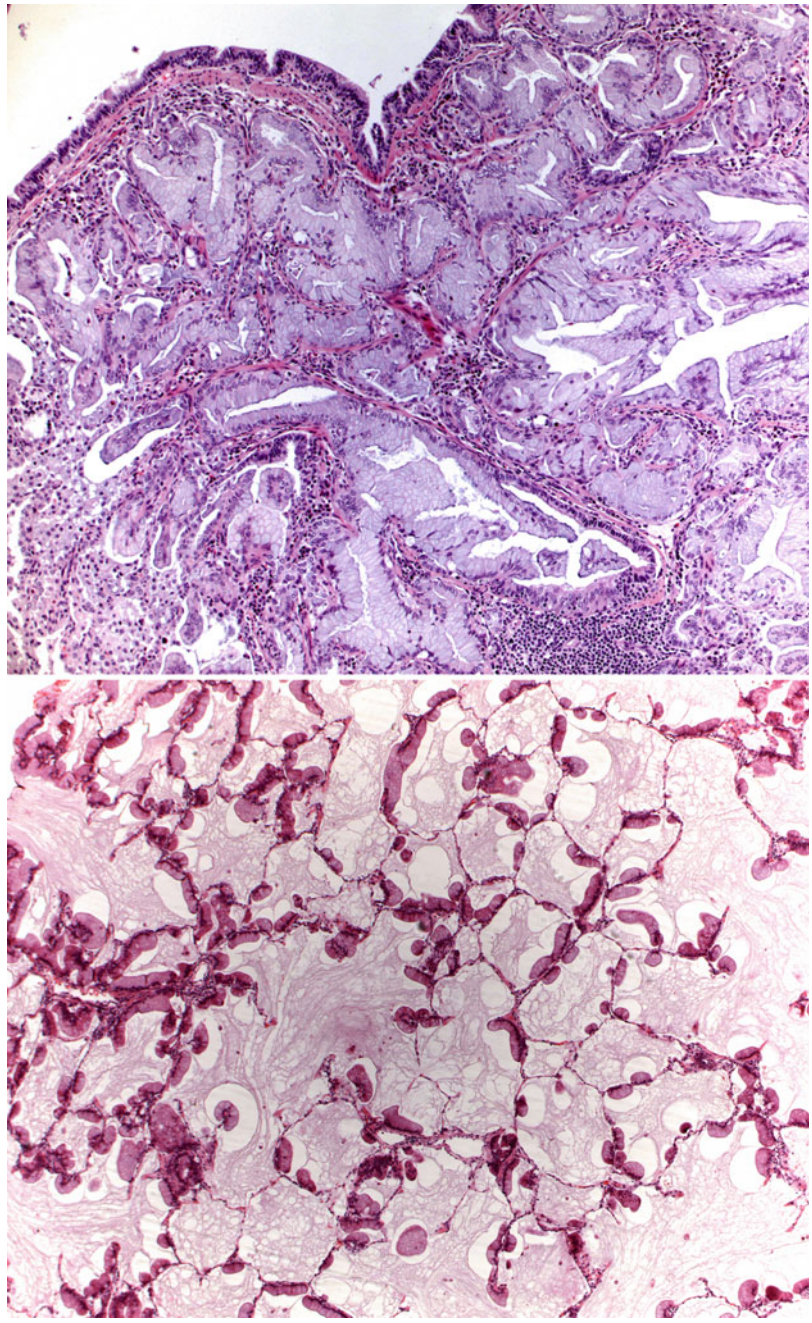

Fig. 17.175
Adenocarcinoma in CPAM, two examples are shown. The *upper* one shows a well-differentiated acinar mucinous adenocarcinoma of goblet cell type, directly underneath the CPAM cyst. The *lower* case is a mucinous lepidic adenocarcinoma again of goblet cell type (Second case courtesy of Mary Sheppard)

fied, which might be the precursor lesion for these adenocarcinomas [12, 560]. In a subsequent report, further molecular abnormalities have been seen: KRAS mutations at codon 12, loss of heterozygosity at p16(INK4) locus, and LOH at FHIT and Rb loci. All three cases expressed MUC5AC [561].

17.6.5 Squamous Cell Papilloma and Papillomatosis

Squamous cell papilloma and papillomatosis in children has been discussed in benign epithelial tumors and therefore does not need to be further discussed.

17.6.6 Capillary Hemangiomatosis

Capillary hemangiomatosis has been already discussed in conjunction with pulmonary arterial hypertension in the chapter on vascular pathology.

References

1. Moran CA, Suster S, Askin FB, Koss MN. Benign and malignant salivary gland-type mixed tumors of the lung. Clinicopathologic and immunohistochemical study of eight cases. Cancer. 1994;73:2481–90.
2. Key BM, Pritchett PS. Mucous gland adenoma of the bronchus. South Med J. 1979;72:83–5.
3. Heard B, Corrin B, Dewar A. Pathology of mucous cell adenomas of the bronchial glands with particular references to ultrastructure. Histopathology. 1985;9:687–701.
4. England D, Hochholzer L. Truly benign "bronchial adenoma". Report of 10 cases of mucous gland adenoma with immunohistochemical and ultrastructural findings. Am J Surg Pathol. 1995;19:887–99.
5. Spencer H. Bronchial mucous gland tumours. Virchows Arch A Pathol Anat Histol. 1979;383:101–15.
6. Tashiro Y, Iwata Y, Nabae T, Manabe H. Pulmonary oncocytoma: report of a case in conjunction with an immunohistochemical and ultrastructural study. Pathol Int. 1995;45:448–51.
7. Ritter JH, Nappi O. Oxyphilic proliferations of the respiratory tract and paranasal sinuses. Semin Diagn Pathol. 1999;16:105–16.
8. de Aquino RT, Magliari ME, Saad Jr R, Neto VD, Filho JE, Neto CD, Capelozzi VL. Bronchial oncocytoma. Sao Paulo Med J. 2000;118:195–7.
9. Mejean-Lebreton F, Barnoud R, de la Roche E, Devouassoux-Shisheboran M. Benign salivary gland-type tumors of the bronchus: expression of high molecular weight cytokeratins. Ann Pathol. 2006;26:30–4.
10. Pfragner R, Ullmann R, Behmel A, Popper HH. Comparative genomic hybridization and cytogenetic analysis in a bronchial adenoma: three clones with different chromosomal aberrations. Int J Oncol. 2001;18:923–8.
11. Kragel PJ, Devaney KO, Meth BM, Linnoila I, Frierson Jr HF, Travis WD. Mucinous cystadenoma of the lung. A report of two cases with immunohistochemical and ultrastructural analysis. Arch Pathol Lab Med. 1990;114:1053–6.
12. Stacher E, Ullmann R, Halbwedl I, Gogg-Kammerer M, Boccon-Gibod L, Nicholson AG, Sheppard MN, Carvalho L, Franca MT, Macsweeney F, Morresi-Hauf A, Popper HH. Atypical goblet cell hyperplasia in congenital cystic adenomatoid malformation as a possible preneoplasia for pulmonary adenocarcinoma in childhood: a genetic analysis. Hum Pathol. 2004;35:565–70.
13. Roux FJ, Lantuejoul S, Brambilla E, Brambilla C. Mucinous cystadenoma of the lung. Cancer. 1995;76:1540–4.
14. Gao ZH, Urbanski SJ. The spectrum of pulmonary mucinous cystic neoplasia: a clinicopathologic and immunohistochemical study of ten cases and review of literature. Am J Clin Pathol. 2005;124:62–70.
15. Monaghan H, Salter DM, Ferguson T. Pulmonary mucinous cystic tumour of borderline malignancy: a rare variant of adenocarcinoma. J Clin Pathol. 2002;55:156.
16. Moran CA. Primary salivary gland-type tumors of the lung. Semin Diagn Pathol. 1995;12:106–22.
17. Sakamoto H, Uda H, Tanaka T, Oda T, Morino H, Kikui M. Pleomorphic adenoma in the periphery of the lung. Report of a case and review of the literature. Arch Pathol Lab Med. 1991;115:393–6.
18. Fitchett J, Luckraz H, Gibbs A, O'Keefe P. A rare case of primary pleomorphic adenoma in main bronchus. Ann Thorac Surg. 2008;86:1025–6.
19. Takeuchi E, Shimizu E, Sano N, Yamaguchi T, Yanagawa H, Sone S. A case of pleomorphic adenoma of the lung with multiple distant metastases – observations on its oncogene and tumor suppressor gene expression. Anticancer Res. 1998;18:2015–20.
20. Carretta A, Libretti L, Taccagni G, Zannini P. Salivary gland-type mixed tumor (pleomorphic adenoma) of the lung. Interact Cardiovasc Thorac Surg. 2004;3:663–5.
21. Pelosi G, Fraggetta F, Maffini F, Solli P, Cavallon A, Viale G. Pulmonary epithelial-myoepithelial tumor of unproven malignant potential: report of a case and review of the literature. Mod Pathol. 2001;14:521–6.
22. Fulford LG, Kamata Y, Okudera K, Dawson A, Corrin B, Sheppard MN, Ibrahim NB, Nicholson AG. Epithelial-myoepithelial carcinomas of the bronchus. Am J Surg Pathol. 2001;25:1508–14.
23. Munoz G, Felipo F, Marquina I, Del Agua C. Epithelial-myoepithelial tumour of the lung: a case report referring to its molecular histogenesis. Diagn Pathol. 2011;6:71.
24. Zawadzka-Glos L, Jakubowska A, Chmielik M, Bielicka A, Brzewski M. Lower airway papillomatosis in children. Int J Pediatr Otorhinolaryngol. 2003;67:1117–21.
25. Soldatski IL, Onufrieva EK, Steklov AM, Schepin NV. Tracheal, bronchial, and pulmonary papillomatosis in children. Laryngoscope. 2005;115:1848–54.
26. Wiatrak BJ, Wiatrak DW, Broker TR, Lewis L. Recurrent respiratory papillomatosis: a longitudinal study comparing severity associated with human papilloma viral types 6 and 11 and other risk factors in a large pediatric population. Laryngoscope. 2004;114:1–23.
27. Popper HH, el-Shabrawi Y, Wockel W, Hofler G, Kenner L, Juttner-Smolle FM, Pongratz MG. Prognostic importance of human papilloma virus

typing in squamous cell papilloma of the bronchus: comparison of in situ hybridization and the polymerase chain reaction. Hum Pathol. 1994;25:1191–7.
28. Syrjanen S, Puranen M. Human papillomavirus infections in children: the potential role of maternal transmission. Crit Rev Oral Biol Med. 2000;11:259–74.
29. Popper HH, Wirnsberger G, Juttner-Smolle FM, Pongratz MG, Sommersgutter M. The predictive value of human papilloma virus (HPV) typing in the prognosis of bronchial squamous cell papillomas. Histopathology. 1992;21:323–30.
30. Abe K, Tanaka Y, Takahashi M, Kosuda S, Hayashi K, Tanabe T, Iwasaki Y, Aida S, Kawauchi T, Yamamoto M, Kita T, Kaji T. Pulmonary spread of laryngeal papillomatosis: radiological findings. Radiat Med. 2006;24:297–301.
31. Assor D. A papillary transitional cell tumor of the bronchus. Am J Clin Pathol. 1971;55:761–4.
32. Smith P, McClure J. A papillary endobronchial tumor with transitional cell pattern. Arch Pathol Lab Med. 1982;106:503–6.
33. Basheda S, Gephardt G, Stoller J. Columnar papilloma of the bronchus. Case report and literature review. Am Rev Respir Dis. 1991;144:1400–2.
34. Popper HHA-SY, Wöckel W, Kenner L, Höfler G. The proof of HPV within bronchial squamous cell papillomas and HPV typing. Comparison of situ hybridization and PCR. Hum Pathol. 1994;11: 1191–7.
35. Lele SM, Pou AM, Ventura K, Gatalica Z, Payne D. Molecular events in the progression of recurrent respiratory papillomatosis to carcinoma. Arch Pathol Lab Med. 2002;126:1184–8.
36. Malanchi I, Accardi R, Diehl F, Smet A, Androphy E, Hoheisel J, Tommasino M. Human papillomavirus type 16 e6 promotes retinoblastoma protein phosphorylation and cell cycle progression. J Virol. 2004;78:13769–78.
37. Tonon SA, Picconi MA, Bos PD, Zinovich JB, Galuppo J, Alonio LV, Teyssie AR. Physical status of the E2 human papilloma virus 16 viral gene in cervical preneoplastic and neoplastic lesions. J Clin Virol. 2001;21:129–34.
38. McGlennen RC, Ghai J, Ostrow RS, LaBresh K, Schneider JF, Faras AJ. Cellular transformation by a unique isolate of human papillomavirus type 11. Cancer Res. 1992;52:5872–8.
39. McBride AA, Schlegel R, Howley PM. The carboxy-terminal domain shared by the bovine papillomavirus E2 transactivator and repressor proteins contains a specific DNA binding activity. Embo J. 1988;7:533–9.
40. Kahn T, Turazza E, Ojeda R, Bercovich A, Stremlau A, Lichter P, Poustka A, Grinstein S, zur Hausen H. Integration of human papillomavirus type 6a DNA in a tonsillar carcinoma: chromosomal localization and nucleotide sequence of the genomic target region. Cancer Res. 1994;54: 1305–12.
41. Coursen JD, Bennett WP, Gollahon L, Shay JW, Harris CC. Genomic instability and telomerase activity in human bronchial epithelial cells during immortalization by human papillomavirus-16 E6 and E7 genes. Exp Cell Res. 1997;235:245–53.
42. DiLorenzo TP, Chen D, Zhang P, Steinberg BM. Evidence for the separate regulation of the human papillomavirus type 11 E7 and E6 promoters by Viral cis sequences near the E6 promoter. Virology. 1998;243:130–9.
43. Cook JR, Hill DA, Humphrey PA, Pfeifer JD, El-Mofty SK. Squamous cell carcinoma arising in recurrent respiratory papillomatosis with pulmonary involvement: emerging common pattern of clinical features and human papillomavirus serotype association. Mod Pathol. 2000;13:914–8.
44. Zobel T, Iftner T, Stubenrauch F. The papillomavirus E8-E2C protein represses DNA replication from extrachromosomal origins. Mol Cell Biol. 2003;23:8352–62.
45. Jiang M, Milner J. Selective silencing of viral gene E6 and E7 expression in HPV-positive human cervical carcinoma cells using small interfering RNAs. Methods Mol Biol. 2004;292:401–20.
46. Li G, He L, Zhang E, Shi J, Zhang Q, Le AD, Zhou K, Tang X. Overexpression of human papillomavirus (HPV) type 16 oncoproteins promotes angiogenesis via enhancing HIF-1alpha and VEGF expression in non-small cell lung cancer cells. Cancer Lett. 2011;311:160–70.
47. Munger K, Baldwin A, Edwards KM, Hayakawa H, Nguyen CL, Owens M, Grace M, Huh K. Mechanisms of human papillomavirus-induced oncogenesis. J Virol. 2004;78:11451–60.
48. Freed GL, Derkay CS. Prevention of recurrent respiratory papillomatosis: role of HPV vaccination. Int J Pediatr Otorhinolaryngol. 2006;70:1799–803.
49. Katz SL, Das P, Ngan BY, Manson D, Pappo AS, Sweezey NB, Solomon MP. Remote intrapulmonary spread of recurrent respiratory papillomatosis with malignant transformation. Pediatr Pulmonol. 2005;39:185–8.
50. Long YT, Sani A. Recurrent respiratory papillomatosis. Asian J Surg. 2003;26:112–6.
51. Hegg CA, Flint A, Singh G. Papillary adenoma of the lung. Am J Clin Pathol. 1992;97:393–7.
52. Yamamoto T, Horiguchi H, Shibagaki T, Kamma H, Ogata T, Mitsui K. Encapsulated type II pneumocyte adenoma: a case report and review of the literature. Respiration. 1993;60:373–7.
53. Dessy E, Braidotti P, Del Curto B, Falleni M, Coggi G, Santa Cruz G, Carai A, Versace R, Pietra GG. Peripheral papillary tumor of type-II pneumocytes: a rare neoplasm of undetermined malignant potential. Virchows Arch. 2000;436:289–95.
54. Baldi A, Santini M, Vicidomini G, Ambrosino F, Vincenzi B, Costanzo R, Di Leo C, Esposito V, Groeger AM, Baldi F. Papillary pneumocytoma of the lung simulating a pleomorphic adenoma. In Vivo. 2002;16:387–90.

55. Mori M, Chiba R, Tezuka F, Kaji M, Kobubo T, Nukiwa T, Takahashi T. Papillary adenoma of type II pneumocytes might have malignant potential. Virchows Arch. 1996;428:195–200.
56. Clark JC, Tichelaar JW, Wert SE, Itoh N, Perl AK, Stahlman MT, Whitsett JA. FGF-10 disrupts lung morphogenesis and causes pulmonary adenomas in vivo. Am J Physiol Lung Cell Mol Physiol. 2001;280:L705–15.
57. Matsumoto M, Sonobe H, Furihata M, Nonami Y, Ohmori Y, Ohtsuki Y. A case of salivary gland-type mixed tumor of the lung differentiating toward type II alveolar epithelial cells in glandular components with a literature review. Virchows Arch. 2002; 441:618–21.
58. Chang T, Husain AN, Colby T, Taxy JB, Welch WR, Cheung OY, Early A, Travis W, Krausz T. Pneumocytic adenomyoepithelioma: a distinctive lung tumor with epithelial, myoepithelial, and pneumocytic differentiation. Am J Surg Pathol. 2007;31: 562–8.
59. Noguchi M, Kodama T, Morinaga S, Shimosato Y, Saito T, Tsuboi E. Multiple sclerosing hemangiomas of the lung. Am J Surg Pathol. 1986;10:429–35.
60. Hanaoka J, Ohuchi M, Inoue S, Sawai S, Tezuka N, Fujino S. Bilateral multiple pulmonary sclerosing hemangioma. Jpn J Thorac Cardiovasc Surg. 2005;53:157–61.
61. Soumil VJ, Navin B, Sangeeta D, Na J, Sharma S, Deshpande R. Multiple sclerosing hemangiomas of the lung. Asian Cardiovasc Thorac Ann. 2004;12: 357–9.
62. Chan NG, Melega DE, Inculet RI, Shepherd JG. Pulmonary sclerosing hemangioma with lymph node metastases. Can Respir J. 2003;10:391–2.
63. Komatsu T, Fukuse T, Wada H, Sakurai T. Pulmonary sclerosing hemangioma with pulmonary metastasis. Thorac Cardiovasc Surg. 2006;54:348–9.
64. Vaideeswar P. Sclerosing hemangioma with lymph nodal metastases. Indian J Pathol Microbiol. 2009;52:392–4.
65. Adachi Y, Tsuta K, Hirano R, Tanaka J, Minamino K, Shimo T, Ikehara S. Pulmonary sclerosing hemangioma with lymph node metastasis: a case report and literature review. Oncol Lett. 2014;7:997–1000.
66. Liebow AA, Hubbell DS. Sclerosing hemangioma (histiocytoma, xanthoma) of the lung. Cancer. 1956;9:53–75.
67. Eggleston JC. The intravascular bronchioloalveolar tumor and the sclerosing hemangioma of the lung: misnomers of pulmonary neoplasia. Semin Diagn Pathol. 1985;2:270–80.
68. Haimoto H, Tsutsumi Y, Nagura H, Nakashima N, Watanabe K. Immunohistochemical study of so-called sclerosing haemangioma of the lung. Virchows Arch A Pathol Anat Histopathol. 1985;407:419–30.
69. Yousem SA, Wick MR, Singh G, Katyal SL, Manivel JC, Mills SE, Legier J. So-called sclerosing hemangiomas of lung. An immunohistochemical study supporting a respiratory epithelial origin. Am J Surg Pathol. 1988;12:582–90.
70. Travis WD, Brambilla E, Burke AP, Marx A, Nicholson AG. WHO classification of tumours of the lung, pleura, thymus and heart. Edited by Bosman FT, E.S. J, S.R. L, H. O. Geneva: IARC, WHO Press; 2015. p. 412.
71. Neuman J, Rosioreanu A, Schuss A, Turi G, Yung E, Trow TK, Williams L, Katz DS. Radiology-pathology conference: sclerosing hemangioma of the lung. Clin Imaging. 2006;30:409–12.
72. Hara M, Iida A, Tohyama J, Miura N, Shiraki N, Itoh M, Ohba S, Tateyama H. FDG-PET findings in sclerosing hemangioma of the lung: a case report. Radiat Med. 2001;19:215–8.
73. Devouassoux-Shisheboran M, de la Fouchardiere A, Thivolet-Bejui F, Sourisseau-Millan ML, Guerin JC, Travis WD. Endobronchial variant of sclerosing hemangioma of the lung: histological and cytological features on endobronchial material. Mod Pathol. 2004;17:252–7.
74. Devouassoux-Shisheboran M, Hayashi T, Linnoila RI, Koss MN, Travis WD. A clinicopathologic study of 100 cases of pulmonary sclerosing hemangioma with immunohistochemical studies: TTF-1 is expressed in both round and surface cells, suggesting an origin from primitive respiratory epithelium. Am J Surg Pathol. 2000;24:906–16.
75. Iyoda A, Hiroshima K, Shiba M, Haga Y, Moriya Y, Sekine Y, Shibuya K, Iizasa T, Fujisawa T. Clinicopathological analysis of pulmonary sclerosing hemangioma. Ann Thorac Surg. 2004; 78:1928–31.
76. Katzenstein AL, Gmelich JT, Carrington CB. Sclerosing hemangioma of the lung: a clinicopathologic study of 51 cases. Am J Surg Pathol. 1980;4:343–56.
77. Niho S, Suzuki K, Yokose T, Kodama T, Nishiwaki Y, Esumi H. Monoclonality of both pale cells and cuboidal cells of sclerosing hemangioma of the lung. Am J Pathol. 1998;152:1065–9.
78. Chan AC, Chan JK. Pulmonary sclerosing hemangioma consistently expresses thyroid transcription factor-1 (TTF-1): a new clue to its histogenesis. Am J Surg Pathol. 2000;24:1531–6.
79. Wang E, Lin D, Wang Y, Wu G, Yuan X. Immunohistochemical and ultrastructural markers suggest different origins for cuboidal and polygonal cells in pulmonary sclerosing hemangioma. Hum Pathol. 2004;35:503–8.
80. Yamazaki K. Type-II pneumocyte differentiation in pulmonary sclerosing hemangioma: ultrastructural differentiation and immunohistochemical distribution of lineage-specific transcription factors (TTF-1, HNF-3 alpha, and HNF-3 beta) and surfactant proteins. Virchows Arch. 2004;445:45–53.
81. Wu CT, Chang YL, Lee YC. Expression of the estrogen receptor beta in 37 surgically treated pulmonary sclerosing hemangiomas in comparison with non-small cell lung carcinomas. Hum Pathol. 2005;36: 1108–12.

82. Dacic S, Sasatomi E, Swalsky PA, Kim DW, Finkelstein SD, Yousem SA. Loss of heterozygosity patterns of sclerosing hemangioma of the lung and bronchioloalveolar carcinoma indicate a similar molecular pathogenesis. Arch Pathol Lab Med. 2004;128:880–4.
83. Yoo SH, Jung KC, Kim JH, Sung SW, Chung JH, Shim YS, Lee SD, Chung DH. Expression patterns of markers for type II pneumocytes in pulmonary sclerosing hemangiomas and fetal lung tissues. Arch Pathol Lab Med. 2005;129:915–9.
84. Sartori G, Bettelli S, Schirosi L, Bigiani N, Maiorana A, Cavazza A, Rossi G. Microsatellite and EGFR, HER2 and K-RAS analyses in sclerosing hemangioma of the lung. Am J Surg Pathol. 2007;31: 1512–20.
85. Lee HJ, Jang SJ, Chun SM, Park SI, Kim DK, Choi J. Comparison of genetic and epigenetic alterations at 11 tumor suppressor loci in pulmonary sclerosing hemangioma and adenocarcinoma. Exp Lung Res. 2011;37:344–53.
86. Amin RM, Hiroshima K, Miyagi Y, Kokubo T, Hoshi K, Fujisawa T, Nakatani Y. Role of the PI3K/Akt, mTOR, and STK11/LKB1 pathways in the tumorigenesis of sclerosing hemangioma of the lung. Pathol Int. 2008;58:38–44.
87. Cho SJ, Jin LJ, Kim BY, Cho SI, Jung WY, Han JH, Ha SY, Kim HK, Kim A. Increased expression of matrix metalloproteinase 9 and tubulin-alpha in pulmonary sclerosing hemangioma. Oncol Rep. 2007; 18:1139–44.
88. Hosaka N, Sasaki T, Adachi K, Sato T, Tanaka T, Miura Y, Sawai T, Toki J, Hisha H, Okamura A, Takasu K, Ikehara S. Pulmonary sclerosing hemangioma associated with familial adenomatous polyposis. Hum Pathol. 2004;35:764–8.
89. Guerra-Gutierrez F, Torres Sanchez I, Gallardo-Madueno G, Marino-Enriquez A, Nistal M. Pulmonary sclerosing hemangioma in a patient with Cowden syndrome. Arch Bronconeumol. 2007;43:418–20.
90. Wei S, Tian J, Song X, Chen Y. Recurrence of pulmonary sclerosing hemangioma. Thorac Cardiovasc Surg. 2008;56:120–2.
91. Yousem SA, Hochholzer L. Alveolar adenoma. Hum Pathol. 1986;17:1066–71.
92. Roque L, Oliveira P, Martins C, Carvalho C, Serpa A, Soares J. A nonbalanced translocation (10;16) demonstrated by FISH analysis in a case of alveolar adenoma of the lung. Cancer Genet Cytogenet. 1996;89:34–7.
93. Popper HH, Juettner-Smolle FM, Pongratz MG. Micronodular hyperplasia of type II pneumocytes – a new lung lesion associated with tuberous sclerosis. Histopathology. 1991;18:347–54.
94. Muir TE, Leslie KO, Popper H, Kitaichi M, Gagne E, Emelin JK, Vinters HV, Colby TV. Micronodular pneumocyte hyperplasia. Am J Surg Pathol. 1998;22:465–72.
95. Maruyama H, Ohbayashi C, Hino O, Tsutsumi M, Konishi Y. Pathogenesis of multifocal micronodular pneumocyte hyperplasia and lymphangioleiomyomatosis in tuberous sclerosis and association with tuberous sclerosis genes TSC1 and TSC2. Pathol Int. 2001;51:585–94.
96. Maruyama H, Seyama K, Sobajima J, Kitamura K, Sobajima T, Fukuda T, Hamada K, Tsutsumi M, Hino O, Konishi Y. Multifocal micronodular pneumocyte hyperplasia and lymphangioleiomyomatosis in tuberous sclerosis with a TSC2 gene. Mod Pathol. 2001;14:609–14.
97. Franz DN, Brody A, Meyer C, Leonard J, Chuck G, Dabora S, Sethuraman G, Colby TV, Kwiatkowski DJ, McCormack FX. Mutational and radiographic analysis of pulmonary disease consistent with lymphangioleiomyomatosis and micronodular pneumocyte hyperplasia in women with tuberous sclerosis. Am J Respir Crit Care Med. 2001;164: 661–8.
98. Popper HH, Gamperl R, Pongratz MG, Kullnig P, Juttner-Smolle FM, Pfragner R. Chromosome typing in lymphangioleiomyomatosis of the lung with and without tuberous sclerosis. Eur Respir J. 1993;6: 753–9.
99. Sampson JR. TSC1 and TSC2: genes that are mutated in the human genetic disorder tuberous sclerosis. Biochem Soc Trans. 2003;31:592–6.
100. Marchevsky AM. Lung tumors derived from ectopic tissues. Semin Diagn Pathol. 1995;12:172–84.
101. Moran CA, Suster S, Fishback NF, Koss MN. Primary intrapulmonary thymoma. A clinicopathologic and immunohistochemical study of eight cases. Am J Surg Pathol. 1995;19:304–12.
102. Myers PO, Kritikos N, Bongiovanni M, Triponez F, Collaud S, Pache JC, Robert JH. Primary intrapulmonary thymoma: a systematic review. Eur J Surg Oncol. 2007;33:1137–41.
103. Srivastava A, Padilla O, Alroy J, Ucci A, Pilichowska M, Daley B, Wolfe HJ. Primary intrapulmonary spindle cell thymoma with marked granulomatous reaction: report of a case with review of literature. Int J Surg Pathol. 2003;11:353–6.
104. Penzel R, Hoegel J, Schmitz W, Blaeker H, Morresi-Hauf A, Aulmann S, Hecker E, Mechtersheimer G, Otto HF, Rieker RJ. Clusters of chromosomal imbalances in thymic epithelial tumours are associated with the WHO classification and the staging system according to Masaoka. Int J Cancer. 2003;105: 494–8.
105. Chang KC, Wu MH, Jones D, Chen FF, Tseng YL. Activation of STAT3 in thymic epithelial tumours correlates with tumour type and clinical behaviour. J Pathol. 2006;210:224–33.
106. Meister M, Schirmacher P, Dienemann H, Mechtersheimer G, Schnabel PA, Kern MA, Herpel E, Xu EC, Muley T, Thomas M, Rieker RJ. Mutational status of the epidermal growth factor receptor (EGFR) gene in thymomas and thymic carcinomas. Cancer Lett. 2007;248:186–91.
107. Tokuoka S. Early cancer and related changes in the bronchial epithelium of former mustard gas workers. Gan To Kagaku Ryoho. 1985;12:708–13.

108. Rock JR, Randell SH, Hogan BL. Airway basal stem cells: a perspective on their roles in epithelial homeostasis and remodeling. Dis Model Mech. 2010;3:545–56.
109. Keith RL, Miller YE, Gemmill RM, Drabkin HA, Dempsey EC, Kennedy TC, Prindiville S, Franklin WA. Angiogenic squamous dysplasia in bronchi of individuals at high risk for lung cancer. Clin Cancer Res. 2000;6:1616–25.
110. Nakayama H, Noguchi M, Tsuchiya R, Kodama T, Shimosato Y. Clonal growth of atypical adenomatous hyperplasia of the lung: cytofluorometric analysis of nuclear DNA content. Mod Pathol. 1990;3:314–20.
111. Weng S, Tsuchiya E, Satoh Y, Kitagawa T, Nakagawa K, Sugano H. Multiple atypical adenomatous hyperplasia of type II pneumonocytes and bronchioloalveolar carcinoma. Histopathology. 1990;16:101–3.
112. Woodruff JM, Chernik NL, Smith MC, Millett WB, Foote Jr FW. Peripheral nerve tumors with rhabdomyosarcomatous differentiation (malignant "Triton" tumors). Cancer. 1973;32:426–39.
113. Mori M, Rao SK, Popper HH, Cagle PT, Fraire AE. Atypical adenomatous hyperplasia of the lung: a probable forerunner in the development of adenocarcinoma of the lung. Mod Pathol. 2001;14:72–84.
114. Ullmann R, Bongiovanni M, Halbwedl I, Petzmann S, Gogg-Kammerer M, Sapino A, Papotti M, Bussolati G, Popper HH. Bronchiolar columnar cell dysplasia – genetic analysis of a novel preneoplastic lesion of peripheral lung. Virchows Arch. 2003;442:429–36.
115. Markel SF, Enzinger FM. Neuromuscular hamartoma – a benign "triton tumor" composed of mature neural and striated muscle elements. Cancer. 1982;49:140–4.
116. Ernst H, Lake SG, Stuart BP, Walter GF, Kamino K, Mohr U. Neuromuscular hamartoma (benign "Triton" tumour) in a mouse. Exp Toxicol Pathol. 1993;45:369–73.
117. Yakulis R, Manack L, Murphy Jr AI. Postradiation malignant triton tumor. A case report and review of the literature. Arch Pathol Lab Med. 1996;120:541–8.
118. Mosca L, Barbareschi M, Mauri MF, Munguia-Barrera J, Frigo B, Muscara M, Valentini L, Mariscotti C. Neuroendocrine lung structures and tumours: immunohistochemical study by specific markers. Histol Histopathol. 1988;3:367–76.
119. Feyrter F. Argyrophilia of bright cell system in bronchial tree in man. Z Mikrosk Anat Forsch. 1954;61:73–81.
120. Feyrter F. A morphologic principle of central and peripheral endocrine regulation. Klin Wochenschr. 1950;28:533–5.
121. Heffner DK, Gnepp DR. Sinonasal fibrosarcomas, malignant schwannomas, and "Triton" tumors. A clinicopathologic study of 67 cases. Cancer. 1992;70:1089–101.
122. De Cauwer H, Bogers JP, Duwel V, den Hauwe V, Croese P, Van Marck E. An intracerebral intraparenchymatous triton tumor in a man with neurofibromatosis. J Neurol. 2007;254:1009–11.
123. Cameron CM, Roberts F, Connell J, Sproule MW. Diffuse idiopathic pulmonary neuroendocrine cell hyperplasia: an unusual cause of cyclical ectopic adrenocorticotrophic syndrome. Br J Radiol. 2011;84:e14–7.
124. Stasik CJ, Tawfik O. Malignant peripheral nerve sheath tumor with rhabdomyosarcomatous differentiation (malignant triton tumor). Arch Pathol Lab Med. 2006;130:1878–81.
125. Wachsmuth W, Viereck HJ. Smoking habits and bronchial cancer. Dtsch Med Wochenschr. 1965;90:708–11.
126. Weston RE, Roberts M. Lung cancer and smoking in Switzerland. Lancet. 1965;1:1057–8.
127. Magnus K, Pedersen E, Mork T, Hougen A, Bjelke E. Lung cancer in Finland and Norway: an epidemiological study. Acta Pathol Microbiol Scand. 1969;Suppl 199:191+.
128. Wynder EL, Muscat JE. The changing epidemiology of smoking and lung cancer histology. Environ Health Perspect. 1995;103 Suppl 8:143–8.
129. Schottenfeld D. In: Pass HI, Minna JB, Johnson DH, Turrisi AT, editors. Epidemiology of lung cancer. Philadelphia: Lippincott-Raven; 1996. p. 307.
130. Boyle P, Ferlay J. Cancer incidence and mortality in Europe, 2004. Ann Oncol. 2005;16:481–8.
131. Thun MJ, Lally CA, Flannery JT, Calle EE, Flanders WD, Heath Jr CW. Cigarette smoking and changes in the histopathology of lung cancer. J Natl Cancer Inst. 1997;89:1580–6.
132. Grimmer G, Naujack KW, Dettbarn G. Gaschromatographic determination of polycyclic aromatic hydrocarbons, aza-arenes, aromatic amines in the particle and vapor phase of mainstream and sidestream smoke of cigarettes. Toxicol Lett. 1987;35:117–24.
133. Zaridze DG, Safaev RD, Belitsky GA, Brunnemann KD, Hoffmann D. Carcinogenic substances in Soviet tobacco products. IARC Sci Publ. 1991;105:485–8.
134. Shields PG. Epidemiology of tobacco carcinogenesis. Curr Oncol Rep. 2000;2:257–62.
135. Smith CJ, Hansch C. The relative toxicity of compounds in mainstream cigarette smoke condensate. Food Chem Toxicol. 2000;38:637–46.
136. Khalili H, Zhang FJ, Harvey RG, Dipple A. Mutagenicity of benzo[a]pyrene-deoxyadenosine adducts in a sequence context derived from the p53 gene. Mutat Res. 2000;465:39–44.
137. White JL, Conner BT, Perfetti TA, Bombick BR, Avalos JT, Fowler KW, Smith CJ, Doolittle DJ. Effect of pyrolysis temperature on the mutagenicity of tobacco smoke condensate. Food Chem Toxicol. 2001;39:499–505.
138. Cloutier JF, Drouin R, Weinfeld M, O'Connor TR, Castonguay A. Characterization and mapping of DNA damage induced by reactive metabolites of 4-(methylnitrosamino)-1-(3-pyridyl)-1-butanone (NNK) at nucleotide resolution in human genomic DNA. J Mol Biol. 2001;313:539–57.

139. Hecht SS. Tobacco carcinogens, their biomarkers and tobacco-induced cancer. Nat Rev Cancer. 2003;3:733–44.
140. Husgafvel-Pursiainen K. Genotoxicity of environmental tobacco smoke: a review. Mutat Res. 2004;567:427–45.
141. Witschi H. Carcinogenic activity of cigarette smoke gas phase and its modulation by beta-carotene and N-acetylcysteine. Toxicol Sci. 2005;84:81–7.
142. Rotunno M, Yu K, Lubin JH, Consonni D, Pesatori AC, Goldstein AM, Goldin LR, Wacholder S, Welch R, Burdette L, Chanock SJ, Bertazzi PA, Tucker MA, Caporaso NE, Chatterjee N, Bergen AW, Landi MT. Phase I metabolic genes and risk of lung cancer: multiple polymorphisms and mRNA expression. PLoS ONE. 2009;4, e5652.
143. Park J, Chen L, Tockman MS, Elahi A, Lazarus P. The human 8-oxoguanine DNA N-glycosylase 1 (hOGG1) DNA repair enzyme and its association with lung cancer risk. Pharmacogenetics. 2004;14:103–9.
144. Xie Y, Yang H, Cunanan C, Okamoto K, Shibata D, Pan J, Barnes DE, Lindahl T, McIlhatton M, Fishel R, Miller JH. Deficiencies in mouse Myh and Ogg1 result in tumor predisposition and G to T mutations in codon 12 of the K-ras oncogene in lung tumors. Cancer Res. 2004;64:3096–102.
145. Olaussen KA, Dunant A, Fouret P, Brambilla E, Andre F, Haddad V, Taranchon E, Filipits M, Pirker R, Popper HH, Stahel R, Sabatier L, Pignon JP, Tursz T, Le Chevalier T, Soria JC. DNA repair by ERCC1 in non-small-cell lung cancer and cisplatin-based adjuvant chemotherapy. N Engl J Med. 2006;355:983–91.
146. Hecht SS, Koh WP, Wang R, Chen M, Carmella SG, Murphy SE, Yuan JM. Elevated levels of mercapturic acids of acrolein and crotonaldehyde in the urine of Chinese women in Singapore who regularly cook at home. PLoS ONE. 2015;10, e0120023.
147. Geles A, Gruber-Moesenbacher U, Quehenberger F, Manzl C, Al Effah M, Grygar E, Juettner-Smolle F, Popper HH. Pulmonary mucinous adenocarcinomas: architectural patterns in correlation with genetic changes, prognosis and survival. Virchows Arch. 2015;467:675–86.
148. Wright DT, Cohn LA, Li H, Fischer B, Li CM, Adler KB. Interactions of oxygen radicals with airway epithelium. Environ Health Perspect. 1994;102 Suppl 10:85–90.
149. Hayes JD, Pulford DJ. The glutathione S-transferase supergene family: regulation of GST and the contribution of the isoenzymes to cancer chemoprotection and drug resistance. Crit Rev Biochem Mol Biol. 1995;30:445–600.
150. Chen G, Gharib TG, Huang CC, Thomas DG, Shedden KA, Taylor JM, Kardia SL, Misek DE, Giordano TJ, Iannettoni MD, Orringer MB, Hanash SM, Beer DG. Proteomic analysis of lung adenocarcinoma: identification of a highly expressed set of proteins in tumors. Clin Cancer Res. 2002;8:2298–305.
151. Christofk HR, Vander Heiden MG, Harris MH, Ramanathan A, Gerszten RE, Wei R, Fleming MD, Schreiber SL, Cantley LC. The M2 splice isoform of pyruvate kinase is important for cancer metabolism and tumour growth. Nature. 2008;452:230–3.
152. Pavanello S, Dioni L, Hoxha M, Fedeli U, Mielzynska-Svach D, Baccarelli AA. Mitochondrial DNA copy number and exposure to polycyclic aromatic hydrocarbons. Cancer Epidemiol Biomarkers Prev. 2013;22:1722–9.
153. Polak JM, Bloom SR. Regulatory peptides and neuron-specific enolase in the respiratory tract of man and other mammals. Exp Lung Res. 1982;3:313–28.
154. Ghatei MA, Sheppard MN, Henzen-Logman S, Blank MA, Polak JM, Bloom SR. Bombesin and vasoactive intestinal polypeptide in the developing lung: marked changes in acute respiratory distress syndrome. J Clin Endocrinol Metab. 1983;57:1226–32.
155. Puzone R, Savarino G, Salvi S, Dal Bello MG, Barletta G, Genova C, Rijavec E, Sini C, Esposito AI, Ratto GB, Truini M, Grossi F, Pfeffer U. Glyceraldehyde-3-phosphate dehydrogenase gene over expression correlates with poor prognosis in non small cell lung cancer patients. Mol Cancer. 2013;12:97.
156. Sasaki H, Shitara M, Yokota K, Hikosaka Y, Moriyama S, Yano M, Fujii Y. Overexpression of GLUT1 correlates with Kras mutations in lung carcinomas. Mol Med Rep. 2012;5:599–602.
157. Takahama M, Tsutsumi M, Tsujiuchi T, Kido A, Sakitani H, Iki K, Taniguchi S, Kitamura S, Konishi Y. Expression of vascular endothelial growth factor and its receptors during lung carcinogenesis by N-nitrosobis(2-hydroxypropyl)amine in rats. Mol Carcinog. 1999;24:287–93.
158. Fontanini G, Calcinai A, Boldrini L, Lucchi M, Mussi A, Angeletti CA, Cagno C, Tognetti MA, Basolo F. Modulation of neoangiogenesis in bronchial preneoplastic lesions. Oncol Rep. 1999;6:813–7.
159. Lee HC, Yin PH, Lin JC, Wu CC, Chen CY, Wu CW, Chi CW, Tam TN, Wei YH. Mitochondrial genome instability and mtDNA depletion in human cancers. Ann N Y Acad Sci. 2005;1042:109–22.
160. Jin X, Zhang J, Gao Y, Ding K, Wang N, Zhou D, Jen J, Cheng S. Relationship between mitochondrial DNA mutations and clinical characteristics in human lung cancer. Mitochondrion. 2007;7:347–53.
161. Matoba S, Kang JG, Patino WD, Wragg A, Boehm M, Gavrilova O, Hurley PJ, Bunz F, Hwang PM. p53 regulates mitochondrial respiration. Science. 2006;312:1650–3.
162. Choi SJ, Kim SH, Kang HY, Lee J, Bhak JH, Sohn I, Jung SH, Choi YS, Kim HK, Han J, Huh N, Lee G, Kim BC, Kim J. Mutational hotspots in the mitochondrial genome of lung cancer. Biochem Biophys Res Commun. 2011;407:23–7.
163. Ocejo-Garcia M, Baokbah TA, Ashurst HL, Cowlishaw D, Soomro I, Coulson JM, Woll PJ. Roles

for USF-2 in lung cancer proliferation and bronchial carcinogenesis. J Pathol. 2005;206:151–9.
164. Shackelford RE, Kaufmann WK, Paules RS. Oxidative stress and cell cycle checkpoint function. Free Radic Biol Med. 2000;28:1387–404.
165. Tang W, Chowdhury AR, Guha M, Huang L, Van Winkle T, Rustgi AK, Avadhani NG. Silencing of IkBbeta mRNA causes disruption of mitochondrial retrograde signaling and suppression of tumor growth in vivo. Carcinogenesis. 2012;33:1762–8.
166. Song MS, Song SJ, Ayad NG, Chang JS, Lee JH, Hong HK, Lee H, Choi N, Kim J, Kim H, Kim JW, Choi EJ, Kirschner MW, Lim DS. The tumour suppressor RASSF1A regulates mitosis by inhibiting the APC-Cdc20 complex. Nat Cell Biol. 2004; 6:129–37.
167. Mascaux C, Laes JF, Anthoine G, Haller A, Ninane V, Burny A, Sculier JP. Evolution of microRNA expression during human bronchial squamous carcinogenesis. Eur Respir J. 2009;33:352–9.
168. Gkirtzimanaki K, Gkouskou KK, Oleksiewicz U, Nikolaidis G, Vyrla D, Liontos M, Pelekanou V, Kanellis DC, Evangelou K, Stathopoulos EN, Field JK, Tsichlis PN, Gorgoulis V, Liloglou T, Eliopoulos AG. TPL2 kinase is a suppressor of lung carcinogenesis. Proc Natl Acad Sci U S A. 2013;110:E1470–9.
169. Robles AI, Linke SP, Harris CC. The p53 network in lung carcinogenesis. Oncogene. 2002;21:6898–907.
170. Mohamed S, Yasufuku K, Hiroshima K, Nakajima T, Yoshida S, Suzuki M, Sekine Y, Shibuya K, Iizasa T, Farouk A, Fujisawa T. Prognostic implications of cell cycle-related proteins in primary resectable pathologic N2 nonsmall cell lung cancer. Cancer. 2007;109:2506–14.
171. Ji H, Ramsey MR, Hayes DN, Fan C, McNamara K, Kozlowski P, Torrice C, Wu MC, Shimamura T, Perera SA, Liang MC, Cai D, Naumov GN, Bao L, Contreras CM, Li D, Chen L, Krishnamurthy J, Koivunen J, Chirieac LR, Padera RF, Bronson RT, Lindeman NI, Christiani DC, Lin X, Shapiro GI, Janne PA, Johnson BE, Meyerson M, Kwiatkowski DJ, Castrillon DH, Bardeesy N, Sharpless NE, Wong KK. LKB1 modulates lung cancer differentiation and metastasis. Nature. 2007;448:807–10.
172. Vasudevan KM, Gurumurthy S, Rangnekar VM. Suppression of PTEN expression by NF-kappa B prevents apoptosis. Mol Cell Biol. 2004;24: 1007–21.
173. Lu Y, Liu Y, Jiang J, Xi Z, Zhong N, Shi S, Wang J, Wei X. Knocking down the expression of Aurora-A gene inhibits cell proliferation and induces G2/M phase arrest in human small cell lung cancer cells. Oncol Rep. 2014;32:243–9.
174. Singh S, Trevino J, Bora-Singhal N, Coppola D, Haura E, Altiok S, Chellappan SP. EGFR/Src/Akt signaling modulates Sox2 expression and self-renewal of stem-like side-population cells in non-small cell lung cancer. Mol Cancer. 2012;11:73.
175. Li L, Yu H, Wang X, Zeng J, Li D, Lu J, Wang C, Wang J, Wei J, Jiang M, Mo B. Expression of seven stem-cell-associated markers in human airway biopsy specimens obtained via fiberoptic bronchoscopy. J Exp Clin Cancer Res. 2013;32:28.
176. Nolte SM, Venugopal C, McFarlane N, Morozova O, Hallett RM, O'Farrell E, Manoranjan B, Murty NK, Klurfan P, Kachur E, Provias JP, Farrokhyar F, Hassell JA, Marra M, Singh SK. A cancer stem cell model for studying brain metastases from primary lung cancer. J Natl Cancer Inst. 2013;105: 551–62.
177. Sarvi S, Mackinnon AC, Avlonitis N, Bradley M, Rintoul RC, Rassl DM, Wang W, Forbes SJ, Gregory CD, Sethi T. CD133+ cancer stem-like cells in small cell lung cancer are highly tumorigenic and chemoresistant but sensitive to a novel neuropeptide antagonist. Cancer Res. 2014;74:1554–65.
178. Gomez-Casal R, Bhattacharya C, Ganesh N, Bailey L, Basse P, Gibson M, Epperly M, Levina V. Non-small cell lung cancer cells survived ionizing radiation treatment display cancer stem cell and epithelial-mesenchymal transition phenotypes. Mol Cancer. 2013;12:94.
179. Ullmann R, Bongiovanni M, Halbwedl I, Fraire AE, Cagle PT, Mori M, Papotti M, Popper HH. Is high-grade adenomatous hyperplasia an early bronchioloalveolar adenocarcinoma? J Pathol. 2003; 201:371–6.
180. Harabayashi T, Kanai Y, Yamada T, Sakamoto M, Ochiai A, Kakizoe T, Koyanagi T, Hirohashi S. Reduction of integrin beta4 and enhanced migration on laminin in association with intraepithelial spreading of urinary bladder carcinomas. J Urol. 1999;161:1364–71.
181. Alt-Holland A, Shamis Y, Riley KN, DesRochers TM, Fusenig NE, Herman IM, Garlick JA. E-cadherin suppression directs cytoskeletal rearrangement and intraepithelial tumor cell migration in 3D human skin equivalents. J Invest Dermatol. 2008;128:2498–507.
182. Inaguma S, Kasai K, Ikeda H. GLI1 facilitates the migration and invasion of pancreatic cancer cells through MUC5AC-mediated attenuation of E-cadherin. Oncogene. 2011;30:714–23.
183. Popper HH. Lung adenocarcinomas: comparison between mice and men. Methods Mol Biol. 2015; 1267:19–43.
184. Chitale D, Gong Y, Taylor BS, Broderick S, Brennan C, Somwar R, Golas B, Wang L, Motoi N, Szoke J, Reinersman JM, Major J, Sander C, Seshan VE, Zakowski MF, Rusch V, Pao W, Gerald W, Ladanyi M. An integrated genomic analysis of lung cancer reveals loss of DUSP4 in EGFR-mutant tumors. Oncogene. 2009;28:2773–83.
185. Pallier K, Cessot A, Cote JF, Just PA, Cazes A, Fabre E, Danel C, Riquet M, Devouassoux-Shisheboran M, Ansieau S, Puisieux A, Laurent-Puig P, Blons H. TWIST1 a new determinant of epithelial to mesenchymal transition in EGFR mutated lung adenocarcinoma. PLoS ONE. 2012;7, e29954.
186. Nakaoku T, Tsuta K, Ichikawa H, Shiraishi K, Sakamoto H, Enari M, Furuta K, Shimada Y,

Ogiwara H, Watanabe S, Nokihara H, Yasuda K, Hiramoto M, Nammo T, Ishigame T, Schetter AJ, Okayama H, Harris CC, Kim YH, Mishima M, Yokota J, Yoshida T, Kohno T. Druggable oncogene fusions in invasive mucinous lung adenocarcinoma. Clin Cancer Res. 2014;20:3087–93.

187. Seo JS, Ju YS, Lee WC, Shin JY, Lee JK, Bleazard T, Lee J, Jung YJ, Kim JO, Yu SB, Kim J, Lee ER, Kang CH, Park IK, Rhee H, Lee SH, Kim JI, Kang JH, Kim YT. The transcriptional landscape and mutational profile of lung adenocarcinoma. Genome Res. 2012;22:2109–19.
188. Araujo LH, Lammers PE, Matthews-Smith V, Eisenberg R, Gonzalez A, Schwartz AG, Timmers C, Shilo K, Zhao W, Natarajan TG, Zhang J, Yilmaz AS, Liu T, Coombes K, Carbone DP. Somatic mutation spectrum of non-small-cell lung cancer in African Americans: a pooled analysis. J Thorac Oncol. 2015;10:1430–6.
189. Li C, Fang R, Sun Y, Han X, Li F, Gao B, Iafrate AJ, Liu XY, Pao W, Chen H, Ji H. Spectrum of oncogenic driver mutations in lung adenocarcinomas from East Asian never smokers. PLoS ONE. 2011;6, e28204.
190. Dorr C, Janik C, Weg M, Been RA, Bader J, Kang R, Ng B, Foran L, Landman SR, O'Sullivan MG, Steinbach M, Sarver AL, Silverstein KA, Largaespada DA, Starr TK. Transposon mutagenesis screen identifies potential lung cancer drivers and CUL3 as a tumor suppressor. Mol Cancer Res. 2015;13:1238–47.
191. An SJ, Chen ZH, Su J, Zhang XC, Zhong WZ, Yang JJ, Zhou Q, Yang XN, Huang L, Guan JL, Nie Q, Yan HH, Mok TS, Wu YL. Identification of enriched driver gene alterations in subgroups of non-small cell lung cancer patients based on histology and smoking status. PLoS ONE. 2012;7, e40109.
192. Kadota K, Nitadori J, Woo KM, Sima CS, Finley DJ, Rusch VW, Adusumilli PS, Travis WD. Comprehensive pathological analyses in lung squamous cell carcinoma: single cell invasion, nuclear diameter, and tumor budding are independent prognostic factors for worse outcomes. J Thorac Oncol. 2014;9:1126–39.
193. Donaldson AW. The epidemiology of lung cancer among uranium miners. Health Phys. 1969;16:563–9.
194. Enderle GJ, Friedrich K. East German uranium miners (Wismut) – exposure conditions and health consequences. Stem Cells. 1995;13 Suppl 1:78–89.
195. Haus BM, Razavi H, Kuschner WG. Occupational and environmental causes of bronchogenic carcinoma. Curr Opin Pulm Med. 2001;7:220–5.
196. Taeger D, Fritsch A, Wiethege T, Johnen G, Eisenmenger A, Wesch H, Ko Y, Stier S, Michael Muller K, Bruning T, Pesch B. Role of exposure to radon and silicosis on the cell type of lung carcinoma in German uranium miners. Cancer. 2006;106:881–9.
197. Taeger D, Johnen G, Wiethege T, Tapio S, Mohner M, Wesch H, Tannapfel A, Muller KM, Bruning T, Pesch B. Major histopathological patterns of lung cancer related to arsenic exposure in German uranium miners. Int Arch Occup Environ Health. 2009;82:867–75.
198. Scarpatetti M, Tsybrovskyy O, Popper HH. Cytokeratin typing as an aid in the differential diagnosis of primary versus metastatic lung carcinomas, and comparison with normal lung. Virchows Arch. 2002;440:70–6.
199. Rossi G, Pelosi G, Graziano P, Barbareschi M, Papotti M. A reevaluation of the clinical significance of histological subtyping of non – small-cell lung carcinoma: diagnostic algorithms in the era of personalized treatments. Int J Surg Pathol. 2009;17:206–18.
200. Tsuta K, Tanabe Y, Yoshida A, Takahashi F, Maeshima AM, Asamura H, Tsuda H. Utility of 10 immunohistochemical markers including novel markers (desmocollin-3, glypican 3, S100A2, S100A7, and Sox-2) for differential diagnosis of squamous cell carcinoma from adenocarcinoma of the Lung. J Thorac Oncol. 2011;6:1190–9.
201. Righi L, Graziano P, Fornari A, Rossi G, Barbareschi M, Cavazza A, Pelosi G, Scagliotti GV, Papotti M. Immunohistochemical subtyping of nonsmall cell lung cancer not otherwise specified in fine-needle aspiration cytology: a retrospective study of 103 cases with surgical correlation. Cancer. 2011;117:3416–23.
202. Popper H, Wirnsberger G, Hoefler H, Denk H. Immunohistochemical and histochemical markers of primary lung cancer, lung metastases, and pleural mesotheliomas. Cancer Detect Prev. 1987;10:167–74.
203. Wistuba II, Behrens C, Virmani AK, Milchgrub S, Syed S, Lam S, Mackay B, Minna JD, Gazdar AF. Allelic losses at chromosome 8p21–23 are early and frequent events in the pathogenesis of lung cancer. Cancer Res. 1999;59:1973–9.
204. Wistuba II, Behrens C, Milchgrub S, Bryant D, Hung J, Minna JD, Gazdar AF. Sequential molecular abnormalities are involved in the multistage development of squamous cell lung carcinoma. Oncogene. 1999;18:643–50.
205. Petersen S, Aninat-Meyer M, Schluns K, Gellert K, Dietel M, Petersen I. Chromosomal alterations in the clonal evolution to the metastatic stage of squamous cell carcinomas of the lung. Br J Cancer. 2000;82:65–73.
206. Luk C, Tsao MS, Bayani J, Shepherd F, Squire JA. Molecular cytogenetic analysis of non-small cell lung carcinoma by spectral karyotyping and comparative genomic hybridization. Cancer Genet Cytogenet. 2001;125:87–99.
207. Weiss J, Sos ML, Seidel D, Peifer M, Zander T, Heuckmann JM, Ullrich RT, Menon R, Maier S, Soltermann A, Moch H, Wagener P, Fischer F, Heynck S, Koker M, Schottle J, Leenders F, Gabler F, Dabow I, Querings S, Heukamp LC, Balke-Want H, Ansen S, Rauh D, Baessmann I, Altmuller J, Wainer Z, Conron M, Wright G, Russell P, Solomon

B, Brambilla E, Brambilla C, Lorimier P, Sollberg S, Brustugun OT, Engel-Riedel W, Ludwig C, Petersen I, Sanger J, Clement J, Groen H, Timens W, Sietsma H, Thunnissen E, Smit E, Heideman D, Cappuzzo F, Ligorio C, Damiani S, Hallek M, Beroukhim R, Pao W, Klebl B, Baumann M, Buettner R, Ernestus K, Stoelben E, Wolf J, Nurnberg P, Perner S, Thomas RK. Frequent and focal FGFR1 amplification associates with therapeutically tractable FGFR1 dependency in squamous cell lung cancer. Sci Transl Med. 2010;2:62ra93.

208. Goncharuk VN, del-Rosario A, Kren L, Anwar S, Sheehan CE, Carlson JA, Ross JS. Co-downregulation of PTEN, KAI-1, and nm23-H1 tumor/metastasis suppressor proteins in non-small cell lung cancer. Ann Diagn Pathol. 2004;8:6–16.
209. Pros E, Lantuejoul S, Sanchez-Verde L, Castillo SD, Bonastre E, Suarez-Gauthier A, Conde E, Cigudosa JC, Lopez-Rios F, Torres-Lanzas J, Castellvi J, Ramon y Cajal S, Brambilla E, Sanchez-Cespedes M. Determining the profiles and parameters for gene amplification testing of growth factor receptors in lung cancer. Int J Cancer. 2013;133:898–907.
210. Bass AJ, Watanabe H, Mermel CH, Yu S, Perner S, Verhaak RG, Kim SY, Wardwell L, Tamayo P, Gat-Viks I, Ramos AH, Woo MS, Weir BA, Getz G, Beroukhim R, O'Kelly M, Dutt A, Rozenblatt-Rosen O, Dziunycz P, Komisarof J, Chirieac LR, Lafargue CJ, Scheble V, Wilbertz T, Ma C, Rao S, Nakagawa H, Stairs DB, Lin L, Giordano TJ, Wagner P, Minna JD, Gazdar AF, Zhu CQ, Brose MS, Cecconello I, Jr UR, Marie SK, Dahl O, Shivdasani RA, Tsao MS, Rubin MA, Wong KK, Regev A, Hahn WC, Beer DG, Rustgi AK, Meyerson M. SOX2 is an amplified lineage-survival oncogene in lung and esophageal squamous cell carcinomas. Nat Genet. 2009;41:1238–42.
211. Skrzypski M, Dziadziuszko R, Jassem E, Szymanowska-Narloch A, Gulida G, Rzepko R, Biernat W, Taron M, Jelitto-Gorska M, Marjanski T, Rzyman W, Rosell R, Jassem J. Main histologic types of non-small-cell lung cancer differ in expression of prognosis-related genes. Clin Lung Cancer. 2013;14:666–73.e662.
212. Ludovini V, Bellezza G, Pistola L, Bianconi F, Di Carlo L, Sidoni A, Semeraro A, Del Sordo R, Tofanetti FR, Mameli MG, Daddi G, Cavaliere A, Tonato M, Crino L. High coexpression of both insulin-like growth factor receptor-1 (IGFR-1) and epidermal growth factor receptor (EGFR) is associated with shorter disease-free survival in resected non-small-cell lung cancer patients. Ann Oncol. 2009;20:842–9.
213. Au NH, Cheang M, Huntsman DG, Yorida E, Coldman A, Elliott WM, Bebb G, Flint J, English J, Gilks CB, Grimes HL. Evaluation of immunohistochemical markers in non-small cell lung cancer by unsupervised hierarchical clustering analysis: a tissue microarray study of 284 cases and 18 markers. J Pathol. 2004;204:101–9.
214. Cooper WA, Lam DC, O'Toole SA, Minna JD. Molecular biology of lung cancer. J Thorac Dis. 2013;5:S479–90.
215. Wang NJ, Sanborn Z, Arnett KL, Bayston LJ, Liao W, Proby CM, Leigh IM, Collisson EA, Gordon PB, Jakkula L, Pennypacker S, Zou Y, Sharma M, North JP, Vemula SS, Mauro TM, Neuhaus IM, Leboit PE, Hur JS, Park K, Huh N, Kwok PY, Arron ST, Massion PP, Bale AE, Haussler D, Cleaver JE, Gray JW, Spellman PT, South AP, Aster JC, Blacklow SC, Cho RJ. Loss-of-function mutations in Notch receptors in cutaneous and lung squamous cell carcinoma. Proc Natl Acad Sci U S A. 2011;108:17761–6.
216. Drilon A, Rekhtman N, Ladanyi M, Paik P. Squamous-cell carcinomas of the lung: emerging biology, controversies, and the promise of targeted therapy. Lancet Oncol. 2012;13:e418–26.
217. Husgafvel-Pursiainen K, Boffetta P, Kannio A, Nyberg F, Pershagen G, Mukeria A, Constantinescu V, Fortes C, Benhamou S. p53 mutations and exposure to environmental tobacco smoke in a multicenter study on lung cancer. Cancer Res. 2000;60:2906–11.
218. Shields PG. Molecular epidemiology of smoking and lung cancer. Oncogene. 2002;21:6870–6.
219. Spoerke JM, O'Brien C, Huw L, Koeppen H, Fridlyand J, Brachmann RK, Haverty PM, Pandita A, Mohan S, Sampath D, Friedman LS, Ross L, Hampton GM, Amler LC, Shames DS, Lackner MR. Phosphoinositide 3-kinase (PI3K) pathway alterations are associated with histologic subtypes and are predictive of sensitivity to PI3K inhibitors in lung cancer preclinical models. Clin Cancer Res. 2012;18:6771–83.
220. Angulo B, Suarez-Gauthier A, Lopez-Rios F, Medina P, Conde E, Tang M, Soler G, Lopez-Encuentra A, Cigudosa J, Sanchez-Cespedes M. Expression signatures in lung cancer reveal a profile for EGFR-mutant tumours and identify selective PIK3CA overexpression by gene amplification. J Pathol. 2008;214:347–56.
221. Malanga D, Scrima M, De Marco C, Fabiani F, De Rosa N, De Gisi S, Malara N, Savino R, Rocco G, Chiappetta G, Franco R, Tirino V, Pirozzi G, Viglietto G. Activating E17K mutation in the gene encoding the protein kinase AKT1 in a subset of squamous cell carcinoma of the lung. Cell Cycle. 2008;7:665–9.
222. Ma Y, Yu WD, Kong RX, Trump DL, Johnson CS. Role of nongenomic activation of phosphatidylinositol 3-kinase/Akt and mitogen-activated protein kinase/extracellular signal-regulated kinase kinase/extracellular signal-regulated kinase 1/2 pathways in 1,25D3-mediated apoptosis in squamous cell carcinoma cells. Cancer Res. 2006;66:8131–8.
223. Travis WD, Brambilla E, Müller-Hermelink HK, Harris CC. Pathology and genetics of tumours of the lung, pleura, thymus and heart. Lyon: IARC WHO Classification of Tumours IARC Press; 2004. p. 10.

224. Rossi G, Mengoli MC, Cavazza A, Nicoli D, Barbareschi M, Cantaloni C, Papotti M, Tironi A, Graziano P, Paci M, Stefani A, Migaldi M, Sartori G, Pelosi G. Large cell carcinoma of the lung: clinically oriented classification integrating immunohistochemistry and molecular biology. Virchows Arch. 2014;464:61–8.
225. Pelosi G, Rossi G, Cavazza A, Righi L, Maisonneuve P, Barbareschi M, Graziano P, Pastorino U, Garassino M, de Braud F, Papotti M. DeltaNp63 (p40) distribution inside lung cancer: a driver biomarker approach to tumor characterization. Int J Surg Pathol. 2013;21:229–39.
226. Brambilla C, Laffaire J, Lantuejoul S, Moro-Sibilot D, Mignotte H, Arbib F, Toffart AC, Petel F, Hainaut P, Rousseaux S, Khochbin S, de Reynies A, Brambilla E. Lung squamous cell carcinomas with basaloid histology represent a specific molecular entity. Clin Cancer Res. 2014;20:5777–86.
227. Schmidt L, Myers J. Bronchioloalveolar carcinoma and the significance of invasion: predicting biologic behavior. Arch Pathol Lab Med. 2010;134: 1450–4.
228. Borczuk AC, Qian F, Kazeros A, Eleazar J, Assaad A, Sonett JR, Ginsburg M, Gorenstein L, Powell CA. Invasive size is an independent predictor of survival in pulmonary adenocarcinoma. Am J Surg Pathol. 2009;33:462–9.
229. Kurokawa T, Matsuno Y, Noguchi M, Mizuno S, Shimosato Y. Surgically curable "early" adenocarcinoma in the periphery of the lung. Am J Surg Pathol. 1994;18:431–8.
230. Noguchi M, Morikawa A, Kawasaki M, Matsuno Y, Yamada T, Hirohashi S, Kondo H, Shimosato Y. Small adenocarcinoma of the lung. Histologic characteristics and prognosis. Cancer. 1995;75:2844–52.
231. Inoue D, Zen Y, Abo H, Gabata T, Demachi H, Kobayashi T, Yoshikawa J, Miyayama S, Yasui M, Nakanuma Y, Matsui O. Immunoglobulin G4-related lung disease: CT findings with pathologic correlations. Radiology. 2009;251:260–70.
232. Zhang Y, Wang R, Li Y, Pan Y, Hu H, Li H, Shen L, Yu Y, Sun Y, Chen H. Negative thyroid transcription factor 1 expression defines an unfavorable subgroup of lung adenocarcinomas. J Thorac Oncol. 2015;10:1444–50.
233. Inamura K, Satoh Y, Okumura S, Nakagawa K, Tsuchiya E, Fukayama M, Ishikawa Y. Pulmonary adenocarcinomas with enteric differentiation: histologic and immunohistochemical characteristics compared with metastatic colorectal cancers and usual pulmonary adenocarcinomas. Am J Surg Pathol. 2005;29:660–5.
234. Yousem SA. Pulmonary intestinal-type adenocarcinoma does not show enteric differentiation by immunohistochemical study. Mod Pathol. 2005;18:816–21.
235. Wang CX, Liu B, Wang YF, Zhang RS, Yu B, Lu ZF, Shi QL, Zhou XJ. Pulmonary enteric adenocarcinoma: a study of the clinicopathologic and molecular status of nine cases. Int J Clin Exp Pathol. 2014;7:1266–74.
236. Gabor S, Renner H, Popper H, Anegg U, Sankin O, Matzi V, Lindenmann J, Smolle Juttner FM. Invasion of blood vessels as significant prognostic factor in radically resected T1-3N0M0 non-small-cell lung cancer. Eur J Cardiothorac Surg. 2004;25:439–42.
237. Yoshida J, Nagai K, Asamura H, Goya T, Koshiishi Y, Sohara Y, Eguchi K, Mori M, Nakanishi Y, Tsuchiya R, Miyaoka E. Visceral pleura invasion impact on non-small cell lung cancer patient survival: its implications for the forthcoming TNM staging based on a large-scale nation-wide database. J Thorac Oncol. 2009;4:959–63.
238. Smolle-Juttner FM, Popper H, Klemen H, Pinter H, Pongratz-Roeger M, Smolle J, Friehs G. Clinical features and therapy of "typical" and "atypical" bronchial carcinoid tumors (grade 1 and grade 2 neuroendocrine carcinoma). Eur J Cardiothorac Surg. 1993;7:121–4; discussion 125.
239. Moran CA, Suster S, Coppola D, Wick MR. Neuroendocrine carcinomas of the lung: a critical analysis. Am J Clin Pathol. 2009;131:206–21.
240. Petzmann S, Ullmann R, Klemen H, Renner H, Popper HH. Loss of heterozygosity on chromosome arm 11q in lung carcinoids. Hum Pathol. 2001; 32:333–8.
241. Ullmann R, Petzmann S, Klemen H, Fraire AE, Hasleton P, Popper HH. The position of pulmonary carcinoids within the spectrum of neuroendocrine tumors of the lung and other tissues. Genes Chromosomes Cancer. 2002;34:78–85.
242. Klemen HS-JF, Popper HH. Morphological and Immunohistochemical study of typical and atypical carcinoids of the lung, on the bases of 55 cases with clinico-pathological correlation and proposal of a new classification. Endocr Relat Cancer. 1994;1: 53–62.
243. Voortman J, Lee JH, Killian JK, Suuriniemi M, Wang Y, Lucchi M, Smith Jr WI, Meltzer P, Giaccone G. Array comparative genomic hybridization-based characterization of genetic alterations in pulmonary neuroendocrine tumors. Proc Natl Acad Sci U S A. 2010;107:13040–5.
244. Ullmann R, Petzmann S, Sharma A, Cagle PT, Popper HH. Chromosomal aberrations in a series of large-cell neuroendocrine carcinomas: unexpected divergence from small-cell carcinoma of the lung. Hum Pathol. 2001;32:1059–63.
245. Travis WD, Linnoila RI, Tsokos MG, Hitchcock CL, Cutler GB, Nieman L, Chrousos G, Pass H, Doppman J. Neuroendocrine tumors of the lung with proposed criteria for large-cell neuroendocrine carcinoma. An ultrastructural, immunohistochemical, and flow cytometric study of 35 cases. Am J Surg Pathol. 1991;15:529–53.
246. Travis WD, Rush W, Flieder DB, Falk R, Fleming MV, Gal AA, Koss MN. Survival analysis of 200

pulmonary neuroendocrine tumors with clarification of criteria for atypical carcinoid and its separation from typical carcinoid. Am J Surg Pathol. 1998;22:934–44.
247. Vollbrecht C, Werner R, Walter RF, Christoph DC, Heukamp LC, Peifer M, Hirsch B, Burbat L, Mairinger T, Kurt Werner S, Wohlschlaeger J, Mairinger FD. Mutational analysis of pulmonary tumours with neuroendocrine features using targeted massive parallel sequencing: a comparison of a neglected tumour group. Br J Cancer. 2015;113: 1704–11.
248. Karlsson A, Brunnstrom H, Lindquist KE, Jirstrom K, Jonsson M, Rosengren F, Reutersward C, Cirenajwis H, Borg A, Jonsson P, Planck M, Jonsson G, Staaf J. Mutational and gene fusion analyses of primary large cell and large cell neuroendocrine lung cancer. Oncotarget. 2015;6: 22028–37.
249. Bari MF, Brown H, Nicholson AG, Kerr KM, Gosney JR, Wallace WA, Soomro I, Muller S, Peat D, Moore JD, Ward LA, Freidin MB, Lim E, Vatish M, Snead DR. BAI3, CDX2 and VIL1: a panel of three antibodies to distinguish small cell from large cell neuroendocrine lung carcinomas. Histopathology. 2014;64:547–56.
250. Petzmann S, Ullmann R, Halbwedl I, Popper HH. Analysis of chromosome-11 aberrations in pulmonary and gastrointestinal carcinoids: an array comparative genomic hybridization-based study. Virchows Arch. 2004;445:151–9.
251. Przygodzki RM, Finkelstein SD, Langer JC, Swalsky PA, Fishback N, Bakker A, Guinee DG, Koss M, Travis WD. Analysis of p53, K-ras-2, and C-raf-1 in pulmonary neuroendocrine tumors. Correlation with histological subtype and clinical outcome. Am J Pathol. 1996;148:1531–41.
252. Sutherland KD, Proost N, Brouns I, Adriaensen D, Song JY, Berns A. Cell of origin of small cell lung cancer: inactivation of Trp53 and Rb1 in distinct cell types of adult mouse lung. Cancer Cell. 2011;19: 754–64.
253. Borges M, Linnoila RI, van de Velde HJ, Chen H, Nelkin BD, Mabry M, Baylin SB, Ball DW. An achaete-scute homologue essential for neuroendocrine differentiation in the lung. Nature. 1997;386:852–5.
254. Chen H, Biel MA, Borges MW, Thiagalingam A, Nelkin BD, Baylin SB, Ball DW. Tissue-specific expression of human achaete-scute homologue-1 in neuroendocrine tumors: transcriptional regulation by dual inhibitory regions. J Clin Invest. 1997;99: 2979–91.
255. Ball DW, Azzoli CG, Baylin SB, Chi D, Dou S, Donis-Keller H, Cumaraswamy A, Borges M, Nelkin BD. Identification of a human achaete-scute homolog highly expressed in neuroendocrine tumors. Int J Cancer. 1993;54:784–92.
256. McFadden DG, Papagiannakopoulos T, Taylor-Weiner A, Stewart C, Carter SL, Cibulskis K, Bhutkar A, McKenna A, Dooley A, Vernon A, Sougnez C, Malstrom S, Heimann M, Park J, Chen F, Farago AF, Dayton T, Shefler E, Gabriel S, Getz G, Jacks T. Genetic and clonal dissection of murine small cell lung carcinoma progression by genome sequencing. Cell. 2014;156:1298–311.
257. Kitamura H, Yazawa T, Sato H, Okudela K, Shimoyamada H. Small cell lung cancer: significance of RB alterations and TTF-1 expression in its carcinogenesis, phenotype, and biology. Endocr Pathol. 2009;20:101–7.
258. Miki M, Ball DW, Linnoila RI. Insights into the achaete-scute homolog-1 gene (hASH1) in normal and neoplastic human lung. Lung Cancer. 2012;75:58–65.
259. Jiang SX, Kameya T, Asamura H, Umezawa A, Sato Y, Shinada J, Kawakubo Y, Igarashi T, Nagai K, Okayasu I. hASH1 expression is closely correlated with endocrine phenotype and differentiation extent in pulmonary neuroendocrine tumors. Mod Pathol. 2004;17:222–9.
260. Westerman BA, Breuer RH, Poutsma A, Chhatta A, Noorduyn LA, Koolen MG, Postmus PE, Blankenstein MA, Oudejans CB. Basic helix-loop-helix transcription factor profiling of lung tumors shows aberrant expression of the proneural gene atonal homolog 1 (ATOH1, HATH1, MATH1) in neuroendocrine tumors. Int J Biol Markers. 2007;22:114–23.
261. Wang XY, Dakir el H, Naizhen X, Jensen-Taubman SM, DeMayo FJ, Linnoila RI. Achaete-scute homolog-1 linked to remodeling and preneoplasia of pulmonary epithelium. Lab Invest. 2007;87:527–39.
262. Kawai T. Histopathological studies on experimentally induced pulmonary, pleural and peritoneal neoplasms in mice by intraperitoneal injection of chrysotile asbestos and N-methyl-N-nitrosourethane. Acta Pathol Jpn. 1979;29:421–33.
263. Xie M, Zhang L, He CS, Xu F, Liu JL, Hu ZH, Zhao LP, Tian Y. Activation of Notch-1 enhances epithelial-mesenchymal transition in gefitinib-acquired resistant lung cancer cells. J Cell Biochem. 2012;113:1501–13.
264. Hamid QA, Addis BJ, Springall DR, Ibrahim NB, Ghatei MA, Bloom SR, Polak JM. Expression of the C-terminal peptide of human pro-bombesin in 361 lung endocrine tumours, a reliable marker and possible prognostic indicator for small cell carcinoma. Virchows Arch A Pathol Anat Histopathol. 1987;411:185–92.
265. Fathi Z, Way JW, Corjay MH, Viallet J, Sausville EA, Battey JF. Bombesin receptor structure and expression in human lung carcinoma cell lines. J Cell Biochem Suppl. 1996;24:237–46.
266. Cook RM, Miller YE, Bunn Jr PA. Small cell lung cancer: etiology, biology, clinical features, staging, and treatment. Proc Natl Acad Sci U S A. 1993;90: 5648–52.
267. Thomas SM, Grandis JR, Wentzel AL, Gooding WE, Lui VW, Siegfried JM. Gastrin-releasing

peptide receptor mediates activation of the epidermal growth factor receptor in lung cancer cells. Neoplasia. 2005;7:426–31.
268. Mooi WJ, Dewar A, Springall D, Polak JM, Addis BJ. Non-small cell lung carcinomas with neuroendocrine features. A light microscopic, immunohistochemical and ultrastructural study of 11 cases. Histopathology. 1988;13:329–37.
269. Kanazawa H, Ebina M, Ino-Oka N, Shimizukawa M, Takahashi T, Fujimura S, Imai T, Nukiwa T. Transition from squamous cell carcinoma to adenocarcinoma in adenosquamous carcinoma of the lung. Am J Pathol. 2000;156:1289–98.
270. Wong DW-S, Leung EL-H, So KK-T, Tam IY-S, Sihoe AD-L, Cheng L-C, Ho K-K, Au JS-K, Chung L-P, Pik Wong M, University of Hong Kong Lung Cancer Study G. The EML4-ALK fusion gene is involved in various histologic types of lung cancers from nonsmokers with wild-type EGFR and KRAS. Cancer. 2009;115:1723–33.
271. Shukuya T, Takahashi T, Kaira R, Ono A, Nakamura Y, Tsuya A, Kenmotsu H, Naito T, Kaira K, Murakami H, Endo M, Takahashi K, Yamamoto N. Efficacy of gefitinib for non-adenocarcinoma non-small-cell lung cancer patients harboring epidermal growth factor receptor mutations: a pooled analysis of published reports. Cancer Sci. 2011;102:1032–7.
272. Yoshida A, Kohno T, Tsuta K, Wakai S, Arai Y, Shimada Y, Asamura H, Furuta K, Shibata T, Tsuda H. ROS1-rearranged lung cancer: a clinicopathologic and molecular study of 15 surgical cases. Am J Surg Pathol. 2013;37:554–62.
273. Yousem SA, Hochholzer L. Mucoepidermoid tumors of the lung. Cancer. 1987;60:1346–52.
274. Fauroux B, Aynie V, Larroquet M, Boccon-Gibod L, Ducou le Pointe H, Tamalet A, Clement A. Carcinoid and mucoepidermoid bronchial tumours in children. Eur J Pediatr. 2005;164:748–52.
275. Molina JR, Aubry MC, Lewis JE, Wampfler JA, Williams BA, Midthun DE, Yang P, Cassivi SD. Primary salivary gland-type lung cancer: spectrum of clinical presentation, histopathologic and prognostic factors. Cancer. 2007;110:2253–9.
276. Macarenco RS, Uphoff TS, Gilmer HF, Jenkins RB, Thibodeau SN, Lewis JE, Molina JR, Yang P, Aubry MC. Salivary gland-type lung carcinomas: an EGFR immunohistochemical, molecular genetic, and mutational analysis study. Mod Pathol. 2008; 21:1168–75.
277. Serra A, Schackert HK, Mohr B, Weise A, Liehr T, Fitze G. t(11;19)(q21;p12~p13.11) and MECT1-MAML2 fusion transcript expression as a prognostic marker in infantile lung mucoepidermoid carcinoma. J Pediatr Surg. 2007;42:E23–9.
278. O'Neill ID. Gefitinib as targeted therapy for mucoepidermoid carcinoma of the lung: possible significance of CRTC1-MAML2 oncogene. Lung Cancer. 2009;64:129–30.
279. Blaukovitsch M, Halbwedl I, Kothmaier H, Gogg-Kammerer M, Popper HH. Sarcomatoid carcinomas of the lung – are these histogenetically heterogeneous tumors? Virchows Arch. 2006;449:455–61.
280. Gu L, Xu Y, Chen Z, Pan Y, Lu S. Clinical analysis of 95 cases of pulmonary sarcomatoid carcinoma. Biomed Pharmacother. 2015;76:134–40.
281. Oyaizu T, Matsumura Y, Kobayashi S, Sado T, Ishihama H, Chida M. Tumor-related gene expression levels in pulmonary pleomorphic carcinoma. J Cardiothorac Surg. 2015;10:79.
282. Tsubata Y, Sutani A, Okimoto T, Murakami I, Usuda R, Okumichi T, Kakegawa S, Togashi K, Kosaka S, Yamashita Y, Kishimoto K, Kuraki T, Isobe T. Comparative analysis of tumor angiogenesis and clinical features of 55 cases of pleomorphic carcinoma and adenocarcinoma of the lung. Anticancer Res. 2015;35:389–94.
283. Velcheti V, Rimm DL, Schalper KA. Sarcomatoid lung carcinomas show high levels of programmed death ligand-1 (PD-L1). J Thorac Oncol. 2013;8:803–5.
284. Kesler KA, Brooks JA, Rieger KM, Fineberg NS, Einhorn LH, Brown JW. Mediastinal metastases from testicular nonseminomatous germ cell tumors: patterns of dissemination and predictors of long-term survival with surgery. J Thorac Cardiovasc Surg. 2003;125:913–23.
285. Policarpio-Nicolas ML, de Leon EM, Jagirdar J. Cytologic findings of NUT midline carcinoma in the hilum of the lung. Diagn Cytopathol. 2015;43:739–42.
286. Sholl LM, Nishino M, Pokharel S, Mino-Kenudson M, French CA, Janne PA, Lathan C. Primary pulmonary NUT midline carcinoma: clinical, radiographic, and pathologic characterizations. J Thorac Oncol. 2015;10:951–9.
287. Wartchow EP, Moore TS, French CA, Mierau GW. Ultrastructural features of NUT midline carcinoma. Ultrastruct Pathol. 2012;36:280–4.
288. Rami-Porta R, Bolejack V, Crowley J, Ball D, Kim J, Lyons G, Rice T, Suzuki K, Thomas Jr CF, Travis WD, Wu YL. The IASLC lung cancer staging project: proposals for the revisions of the T descriptors in the forthcoming eighth edition of the TNM classification for lung cancer. J Thorac Oncol. 2015;10:990–1003.
289. Eberhardt WE, Mitchell A, Crowley J, Kondo H, Kim YT, Turrisi 3rd A, Goldstraw P, Rami-Porta R. The IASLC lung cancer staging project: proposals for the revision of the M descriptors in the forthcoming eighth edition of the TNM classification of lung cancer. J Thorac Oncol. 2015;10:1515–22.
290. Reynolds JV, Kealy WF, O'Sullivan GC. Multiple pulmonary leiomyomatous hamartomas. Ir Med J. 1984;77:106–7.
291. Rossi G, Cavazza A, Valli R, Torricelli P, Richeldi L, Rivasi F, Brambilla E. Atypical lipomatous tumour (lipoma-like well-differentiated liposarcoma) arising in a pulmonary hamartoma and clinically presenting with pneumothorax. Lung Cancer. 2003;39:103–6.
292. Fletcher JA, Pinkus GS, Donovan K, Naeem R, Sugarbaker DJ, Mentzer S, Pinkus JL, Longtine J.

Clonal rearrangement of chromosome band 6p21 in the mesenchymal component of pulmonary chondroid hamartoma. Cancer Res. 1992;52:6224–8.
293. Kazmierczak B, Rosigkeit J, Wanschura S, Meyer-Bolte K, Van de Ven WJ, Kayser K, Krieghoff B, Kastendiek H, Bartnitzke S, Bullerdiek J. HMGI-C rearrangements as the molecular basis for the majority of pulmonary chondroid hamartomas: a survey of 30 tumors. Oncogene. 1996;12:515–21.
294. Rogalla P, Lemke I, Kazmierczak B, Bullerdiek J. An identical HMGIC-LPP fusion transcript is consistently expressed in pulmonary chondroid hamartomas with t(3;12)(q27-28;q14-15). Genes Chromosomes Cancer. 2000;29:363–6.
295. Mak BC, Yeung RS. The tuberous sclerosis complex genes in tumor development. Cancer Invest. 2004;22:588–603.
296. Johansson M, Dietrich C, Mandahl N, Hambraeus G, Johansson L, Clausen PP, Mitelman F, Heim S. Recombinations of chromosomal bands 6p21 and 14q24 characterise pulmonary hamartomas. Br J Cancer. 1993;67:1236–41.
297. Blank C, Schoenmakers EF, Rogalla P, Huys EH, van Rijk AA, Drieschner N, Bullerdiek J. Intragenic breakpoint within RAD51L1 in a t(6;14)(p21.3;q24) of a pulmonary chondroid hamartoma. Cytogenet Cell Genet. 2001;95:17–9.
298. Vera-Roman JM, Sobonya RE, Gomez-Garcia JL, Sanz-Bondia JR, Paris-Romeu F. Leiomyoma of the lung. Literature review and case report. Cancer. 1983;52:936–41.
299. Karnak I, Akcoren Z, Senocak ME. Endobronchial leiomyoma in children. Eur J Pediatr Surg. 2000;10:136–9.
300. Yellin A, Rosenman Y, Lieberman Y. Review of smooth muscle tumours of the lower respiratory tract. Br J Dis Chest. 1984;78:337–51.
301. White SH, Ibrahim NB, Forrester-Wood CP, Jeyasingham K. Leiomyomas of the lower respiratory tract. Thorax. 1985;40:306–11.
302. Gotti G, Haid MM, Paladini P, Di Bisceglie M, Volterrani L, Sforza V. Pedunculated pulmonary leiomyoma with large cyst formation. Ann Thorac Surg. 1993;56:1178–80.
303. Attanoos RL, Appleton MA, Gibbs AR. Primary sarcomas of the lung: a clinicopathological and immunohistochemical study of 14 cases. Histopathology. 1996;29:29–36.
304. Cramer SF. Pulmonary lymphangiomyomatosis and metastasizing leiomyoma. N Engl J Med. 1981;305:587–8.
305. Abramson S, Gilkeson RC, Goldstein JD, Woodard PK, Eisenberg R, Abramson N. Benign metastasizing leiomyoma: clinical, imaging, and pathologic correlation. AJR Am J Roentgenol. 2001;176:1409–13.
306. Gladish GW, Sabloff BM, Munden RF, Truong MT, Erasmus JJ, Chasen MH. Primary thoracic sarcomas. Radiographics. 2002;22:621–37.
307. Gal AA, Brooks JS, Pietra GG. Leiomyomatous neoplasms of the lung: a clinical, histologic, and immunohistochemical study. Mod Pathol. 1989;2:209–16.
308. Moran CA, Suster S, Abbondanzo SL, Koss MN. Primary leiomyosarcomas of the lung: a clinicopathologic and immunohistochemical study of 18 cases. Mod Pathol. 1997;10:121–8.
309. Schneider BF, Lovell MA, Golden WL. Cytogenetic abnormalities in primary bronchopulmonary leiomyosarcoma of childhood. Cancer Genet Cytogenet. 1998;105:145–51.
310. Patton KT, Cheng L, Papavero V, Blum MG, Yeldandi AV, Adley BP, Luan C, Diaz LK, Hui P, Yang XJ. Benign metastasizing leiomyoma: clonality, telomere length and clinicopathologic analysis. Mod Pathol. 2006;19:130–40.
311. Wang R, Lu YJ, Fisher C, Bridge JA, Shipley J. Characterization of chromosome aberrations associated with soft-tissue leiomyosarcomas by twenty-four-color karyotyping and comparative genomic hybridization analysis. Genes Chromosomes Cancer. 2001;31:54–64.
312. Yang J, Du X, Chen K, Ylipaa A, Lazar AJ, Trent J, Lev D, Pollock R, Hao X, Hunt K, Zhang W. Genetic aberrations in soft tissue leiomyosarcoma. Cancer Lett. 2009;275:1–8.
313. Nuovo GJ, Schmittgen TD. Benign metastasizing leiomyoma of the lung: clinicopathologic, immunohistochemical, and micro-RNA analyses. Diagn Mol Pathol. 2008;17:145–50.
314. Canzonieri V, D'Amore ES, Bartoloni G, Piazza M, Blandamura S, Carbone A. Leiomyomatosis with vascular invasion. A unified pathogenesis regarding leiomyoma with vascular microinvasion, benign metastasizing leiomyoma and intravenous leiomyomatosis. Virchows Arch. 1994;425:541–5.
315. Lee HJ, Choi J, Kim KR. Pulmonary benign metastasizing leiomyoma associated with intravenous leiomyomatosis of the uterus: clinical behavior and genomic changes supporting a transportation theory. Int J Gynecol Pathol. 2008;27:340–5.
316. Diao XL, Su Q, Wang SF, Zhang W, Gong L, Liu J, Feng YM. X-chromosome inactivation patterns of different tumor nodules in multiple leiomyomas of uterus. Zhonghua Bing Li Xue Za Zhi. 2003;32:308–13.
317. Capron F, Ameille J, Leclerc P, Mornet P, Barbagellata M, Reynes M, Rochemaure J. Pulmonary lymphangioleiomyomatosis and Bourneville's tuberous sclerosis with pulmonary involvement: the same disease? Cancer. 1983;52:851–5.
318. Sullivan EJ. Lymphangioleiomyomatosis: a review. Chest. 1998;114:1689–703.
319. Chu SC, Horiba K, Usuki J, Avila NA, Chen CC, Travis WD, Ferrans VJ, Moss J. Comprehensive evaluation of 35 patients with lymphangioleiomyomatosis. Chest. 1999;115:1041–52.
320. Abbott GF, Rosado-de-Christenson ML, Frazier AA, Franks TJ, Pugatch RD, Galvin JR. From the archives of the AFIP: lymphangioleiomyomatosis: radiologic-pathologic correlation. Radiographics. 2005;25:803–28.

321. Kitaichi M, Nishimura K, Itoh H, Izumi T. Pulmonary lymphangioleiomyomatosis: a report of 46 patients including a clinicopathologic study of prognostic factors. Am J Respir Crit Care Med. 1995;151:527–33.
322. Matsui K, Beasley MB, Nelson WK, Barnes PM, Bechtle J, Falk R, Ferrans VJ, Moss J, Travis WD. Prognostic significance of pulmonary lymphangioleiomyomatosis histologic score. Am J Surg Pathol. 2001;25:479–84.
323. Kumasaka T, Seyama K, Mitani K, Sato T, Souma S, Kondo T, Hayashi S, Minami M, Uekusa T, Fukuchi Y, Suda K. Lymphangiogenesis in lymphangioleiomyomatosis: its implication in the progression of lymphangioleiomyomatosis. Am J Surg Pathol. 2004;28:1007–16.
324. Martignoni G, Pea M, Reghellin D, Zamboni G, Bonetti F. PEComas: the past, the present and the future. Virchows Arch. 2008;452:119–32.
325. Pan CC, Chung MY, Ng KF, Liu CY, Wang JS, Chai CY, Huang SH, Chen PC, Ho DM. Constant allelic alteration on chromosome 16p (TSC2 gene) in perivascular epithelioid cell tumour (PEComa): genetic evidence for the relationship of PEComa with angiomyolipoma. J Pathol. 2008;214:387–93.
326. Astrinidis A, Khare L, Carsillo T, Smolarek T, Au KS, Northrup H, Henske EP. Mutational analysis of the tuberous sclerosis gene TSC2 in patients with pulmonary lymphangioleiomyomatosis. J Med Genet. 2000;37:55–7.
327. Carsillo T, Astrinidis A, Henske EP. Mutations in the tuberous sclerosis complex gene TSC2 are a cause of sporadic pulmonary lymphangioleiomyomatosis. Proc Natl Acad Sci U S A. 2000;97:6085–90.
328. Goncharova EA, Goncharov DA, Eszterhas A, Hunter DS, Glassberg MK, Yeung RS, Walker CL, Noonan D, Kwiatkowski DJ, Chou MM, Panettieri Jr RA, Krymskaya VP. Tuberin regulates p70 S6 kinase activation and ribosomal protein S6 phosphorylation. A role for the TSC2 tumor suppressor gene in pulmonary lymphangioleiomyomatosis (LAM). J Biol Chem. 2002;277:30958–67.
329. Krymskaya VP. Tumour suppressors hamartin and tuberin: intracellular signalling. Cell Signal. 2003;15:729–39.
330. Krymskaya VP. Smooth muscle like cells in pulmonary lymphangioleiomyomatosis. Proc Am Thorac Soc. 2008;5:119–26.
331. Yu J, Parkhitko A, Henske EP. Autophagy: an 'Achilles' heel of tumorigenesis in TSC and LAM. Autophagy. 2011;7:1400–1.
332. Matsui K, Takeda K, Yu ZX, Valencia J, Travis WD, Moss J, Ferrans VJ. Downregulation of estrogen and progesterone receptors in the abnormal smooth muscle cells in pulmonary lymphangioleiomyomatosis following therapy. An immunohistochemical study. Am J Respir Crit Care Med. 2000;161:1002–9.
333. Banner AS, Carrington CB, Emory WB, Kittle F, Leonard G, Ringus J, Taylor P, Addington WW. Efficacy of oophorectomy in lymphangioleiomyomatosis and benign metastasizing leiomyoma. N Engl J Med. 1981;305:204–9.
334. Schiavina M, Contini P, Fabiani A, Cinelli F, Di Scioscio V, Zompatori M, Campidelli C, Pileri SA. Efficacy of hormonal manipulation in lymphangioleiomyomatosis. A 20-year-experience in 36 patients. Sarcoidosis Vasc Diffuse Lung Dis. 2007;24:39–50.
335. Pechet TT, Meyers BF, Guthrie TJ, Battafarano RJ, Trulock EP, Cooper JD, Patterson GA. Lung transplantation for lymphangioleiomyomatosis. J Heart Lung Transplant. 2004;23:301–8.
336. Bittmann I, Dose TB, Muller C, Dienemann H, Vogelmeier C, Lohrs U. Lymphangioleiomyomatosis: recurrence after single lung transplantation. Hum Pathol. 1997;28:1420–3.
337. O'Brien JD, Lium JH, Parosa JF, Deyoung BR, Wick MR, Trulock EP. Lymphangiomyomatosis recurrence in the allograft after single-lung transplantation. Am J Respir Crit Care Med. 1995;151:2033–6.
338. Nine JS, Yousem SA, Paradis IL, Keenan R, Griffith BP. Lymphangioleiomyomatosis: recurrence after lung transplantation. J Heart Lung Transplant. 1994;13:714–9.
339. Bittmann I, Rolf B, Amann G, Lohrs U. Recurrence of lymphangioleiomyomatosis after single lung transplantation: new insights into pathogenesis. Hum Pathol. 2003;34:95–8.
340. Goncharova EA, Goncharov DA, Lim PN, Noonan D, Krymskaya VP. Modulation of cell migration and invasiveness by tumor suppressor TSC2 in lymphangioleiomyomatosis. Am J Respir Cell Mol Biol. 2006;34:473–80.
341. Bissler JJ, McCormack FX, Young LR, Elwing JM, Chuck G, Leonard JM, Schmithorst VJ, Laor T, Brody AS, Bean J, Salisbury S, Franz DN. Sirolimus for angiomyolipoma in tuberous sclerosis complex or lymphangioleiomyomatosis. N Engl J Med. 2008;358:140–51.
342. Davies DM, de Vries PJ, Johnson SR, McCartney DL, Cox JA, Serra AL, Watson PC, Howe CJ, Doyle T, Pointon K, Cross JJ, Tattersfield AE, Kingswood JC, Sampson JR. Sirolimus therapy for angiomyolipoma in tuberous sclerosis and sporadic lymphangioleiomyomatosis: a phase 2 trial. Clin Cancer Res. 2011;17:4071–81.
343. McCormack FX, Inoue Y, Moss J, Singer LG, Strange C, Nakata K, Barker AF, Chapman JT, Brantly ML, Stocks JM, Brown KK, Lynch 3rd JP, Goldberg HJ, Young LR, Kinder BW, Downey GP, Sullivan EJ, Colby TV, McKay RT, Cohen MM, Korbee L, Taveira-DaSilva AM, Lee HS, Krischer JP, Trapnell BC. Efficacy and safety of sirolimus in lymphangioleiomyomatosis. N Engl J Med. 2011;364:1595–606.
344. Bongiovanni M, Viberti L, Pecchioni C, Papotti M, Thonhofer R, Hans Popper H, Sapino A. Steroid hormone receptor in pleural solitary fibrous tumours

and CD34+ progenitor stromal cells. J Pathol. 2002;198:252–7.
345. Kishi K, Homma S, Tanimura S, Matsushita H, Nakata K. Hypoglycemia induced by secretion of high molecular weight insulin-like growth factor-II from a malignant solitary fibrous tumor of the pleura. Intern Med. 2001;40:341–4.
346. Doyle LA, Fletcher CD. Predicting behavior of solitary fibrous tumor: are we getting closer to more accurate risk assessment? Ann Surg Oncol. 2013;20:4055–6.
347. Morimitsu Y, Nakajima M, Hisaoka M, Hashimoto H. Extrapleural solitary fibrous tumor: clinicopathologic study of 17 cases and molecular analysis of the p53 pathway. APMIS. 2000;108:617–25.
348. Magdeleinat P, Alifano M, Petino A, Le Rochais JP, Dulmet E, Galateau F, Icard P, Regnard JF. Solitary fibrous tumors of the pleura: clinical characteristics, surgical treatment and outcome. Eur J Cardiothorac Surg. 2002;21:1087–93.
349. Schirosi L, Lantuejoul S, Cavazza A, Murer B, Yves Brichon P, Migaldi M, Sartori G, Sgambato A, Rossi G. Pleuro-pulmonary solitary fibrous tumors: a clinicopathologic, immunohistochemical, and molecular study of 88 cases confirming the prognostic value of de Perrot staging system and p53 expression, and evaluating the role of c-kit, BRAF, PDGFRs (alpha/beta), c-met, and EGFR. Am J Surg Pathol. 2008;32:1627–42.
350. Hu Y, Mahar TJ, Hicks DG, Raymond D, Jones C, Wandtke JC, Powers JM, Xu H. Malignant solitary fibrous tumor: report of 3 cases with unusual features. Appl Immunohistochem Mol Morphol. 2009;17:451–7.
351. Rao N, Colby TV, Falconieri G, Cohen H, Moran CA, Suster S. Intrapulmonary solitary fibrous tumors: clinicopathologic and immunohistochemical study of 24 cases. Am J Surg Pathol. 2013;37:155–66.
352. van de Rijn M, Lombard CM, Rouse RV. Expression of CD34 by solitary fibrous tumors of the pleura, mediastinum, and lung. Am J Surg Pathol. 1994;18:814–20.
353. Mohajeri A, Tayebwa J, Collin A, Nilsson J, Magnusson L, von Steyern FV, Brosjo O, Domanski HA, Larsson O, Sciot R, Debiec-Rychter M, Hornick JL, Mandahl N, Nord KH, Mertens F. Comprehensive genetic analysis identifies a pathognomonic NAB2/STAT6 fusion gene, nonrandom secondary genomic imbalances, and a characteristic gene expression profile in solitary fibrous tumor. Genes Chromosomes Cancer. 2013;52:873–86.
354. Schweizer L, Koelsche C, Sahm F, Piro RM, Capper D, Reuss DE, Pusch S, Habel A, Meyer J, Gock T, Jones DT, Mawrin C, Schittenhelm J, Becker A, Heim S, Simon M, Herold-Mende C, Mechtersheimer G, Paulus W, Konig R, Wiestler OD, Pfister SM, von Deimling A. Meningeal hemangiopericytoma and solitary fibrous tumors carry the NAB2-STAT6 fusion and can be diagnosed by nuclear expression of STAT6 protein. Acta Neuropathol. 2013;125:651–8.
355. Robinson DR, Wu YM, Kalyana-Sundaram S, Cao X, Lonigro RJ, Sung YS, Chen CL, Zhang L, Wang R, Su F, Iyer MK, Roychowdhury S, Siddiqui J, Pienta KJ, Kunju LP, Talpaz M, Mosquera JM, Singer S, Schuetze SM, Antonescu CR, Chinnaiyan AM. Identification of recurrent NAB2-STAT6 gene fusions in solitary fibrous tumor by integrative sequencing. Nat Genet. 2013;45:180–5.
356. Rodriguez-Gonzalez M, Novoa NM, Gomez MT, Garcia JL, Ludena D. Factors influencing malignant evolution and long-term survival in solitary fibrous tumours of the pleura. Histol Histopathol. 2014;29:1445–54.
357. Soon L, Flechner L, Gutkind JS, Wang LH, Baserga R, Pierce JH, Li W. Insulin-like growth factor I synergizes with interleukin 4 for hematopoietic cell proliferation independent of insulin receptor substrate expression. Mol Cell Biol. 1999;19:3816–28.
358. Choi Y, Shimogawa H, Murakami K, Ramdas L, Zhang W, Qin J, Uesugi M. Chemical genetic identification of the IGF-linked pathway that is mediated by STAT6 and MFP2. Chem Biol. 2006;13:241–9.
359. Filosso PL, Asioli S, Ruffini E, Rovea P, Macri L, Sapino A, Bretti S, Lyberis P, Oliaro A. Radical resection of a giant, invasive and symptomatic malignant Solitary Fibrous Tumour (SFT) of the pleura. Lung Cancer. 2009;64:117–20.
360. Fiorello A, Vicidomini G, Santini M. Giant solitary fibrous tumors of the pleura: two case reports. Thorac Cardiovasc Surg. 2007;55:458–9.
361. Sakurai H, Hasegawa T, Watanabe S, Suzuki K, Asamura H, Tsuchiya R. Inflammatory myofibroblastic tumor of the lung. Eur J Cardiothorac Surg. 2004;25:155–9.
362. Moran CA, Suster S. Unusual non-neoplastic lesions of the lung. Semin Diagn Pathol. 2007;24:199–208.
363. Farris 3rd AB, Mark EJ, Kradin RL. Pulmonary "inflammatory myofibroblastic" tumors: a critical examination of the diagnostic category based on quantitative immunohistochemical analysis. Virchows Arch. 2007;450:585–90.
364. Kazmierczak B, Dal Cin P, Sciot R, Van den Berghe H, Bullerdiek J. Inflammatory myofibroblastic tumor with HMGIC rearrangement. Cancer Genet Cytogenet. 1999;112:156–60.
365. Coffin CM, Patel A, Perkins S, Elenitoba-Johnson KS, Perlman E, Griffin CA. ALK1 and p80 expression and chromosomal rearrangements involving 2p23 in inflammatory myofibroblastic tumor. Mod Pathol. 2001;14:569–76.
366. Chan JK, Cheuk W, Shimizu M. Anaplastic lymphoma kinase expression in inflammatory pseudotumors. Am J Surg Pathol. 2001;25:761–8.
367. Antonescu CR, Suurmeijer AJ, Zhang L, Sung YS, Jungbluth AA, Travis WD, Al-Ahmadie H, Fletcher CD, Alaggio R. Molecular characterization of inflammatory myofibroblastic tumors with frequent

ALK and ROS1 gene fusions and rare novel RET rearrangement. Am J Surg Pathol. 2015;39:957–67.
368. Zen Y, Kitagawa S, Minato H, Kurumaya H, Katayanagi K, Masuda S, Niwa H, Fujimura M, Nakanuma Y. IgG4-positive plasma cells in inflammatory pseudotumor (plasma cell granuloma) of the lung. Hum Pathol. 2005;36:710–7.
369. Yamamoto H, Yamaguchi H, Aishima S, Oda Y, Kohashi K, Oshiro Y, Tsuneyoshi M. Inflammatory myofibroblastic tumor versus IgG4-related sclerosing disease and inflammatory pseudotumor: a comparative clinicopathologic study. Am J Surg Pathol. 2009;33:1330–40.
370. Cerfolio RJ, Allen MS, Nascimento AG, Deschamps C, Trastek VF, Miller DL, Pairolero PC. Inflammatory pseudotumors of the lung. Ann Thorac Surg. 1999;67:933–6.
371. Shigemitsu H, Koss MN. IgG4-related interstitial lung disease: a new and evolving concept. Curr Opin Pulm Med. 2009;15:513–6.
372. Yi ES, Sekiguchi H, Peikert T, Ryu JH, Colby TV. Pathologic manifestations of Immunoglobulin(Ig) G4-related lung disease. Semin Diagn Pathol. 2012;29:219–25.
373. Campbell SN, Rubio E, Loschner AL. Clinical review of pulmonary manifestations of IgG4-related disease. Ann Am Thorac Soc. 2014;11:1466–75.
374. Cai D, Li H, Wang R, Li Y, Pan Y, Hu H, Zhang Y, Gong R, Pan B, Sun Y, Chen H. Comparison of clinical features, molecular alterations, and prognosis in morphological subgroups of lung invasive mucinous adenocarcinoma. Onco Targets Ther. 2014;7:2127–32.
375. Berntsen NL, Klingenberg O, Juran BD, Benito de Valle M, Lindkvist B, Lazaridis KN, Boberg KM, Karlsen TH, Hov JR. Association between HLA haplotypes and increased serum levels of IgG4 in patients with primary sclerosing cholangitis. Gastroenterology. 2015;148:924–7.e922.
376. Zen Y, Inoue D, Kitao A, Onodera M, Abo H, Miyayama S, Gabata T, Matsui O, Nakanuma Y. IgG4-related lung and pleural disease: a clinicopathologic study of 21 cases. Am J Surg Pathol. 2009;33:1886–93.
377. Takahashi H, Yamamoto M, Tabeya T, Suzuki C, Naishiro Y, Shinomura Y, Imai K. The immunobiology and clinical characteristics of IgG4 related diseases. J Autoimmun. 2012;39:93–6.
378. Kitada M, Matuda Y, Hayashi S, Ishibashi K, Oikawa K, Miyokawa N, Ohsaki Y. IgG4-related lung disease showing high standardized uptake values on FDG-PET: report of two cases. J Cardiothorac Surg. 2013;8:160.
379. Ishimoto H, Yatera K, Shimabukuro I, Matsuki Y, Hanaka T, Oda K, Kawanami T, Mukae H. Case of immunoglobulin G4 (IgG4)-related disease diagnosed by transbronchial lung biopsy and endobronchial ultrasound-guided transbronchial needle aspiration. J UOEH. 2014;36:237–42.
380. Tanaka K, Nagata K, Tomii K, Imai Y. A case of isolated IgG4-related interstitial pneumonia: a new consideration for the cause of idiopathic nonspecific interstitial pneumonia. Chest. 2012;142:228–30.
381. Dhobale S, Bedetti C, Killian P, Ilyas M, Liput J, Jasnosz K, Giclas P. IgG4 related sclerosing disease with multiple organ involvements and response to corticosteroid treatment. J Clin Rheumatol. 2009;15:354–7.
382. Onishi Y, Kawamura T, Kagami R, Nakahara Y, Yoshiro M. IgG4-related lung disease with organizing pneumonia effectively treated with azathioprine. Intern Med. 2014;53:2701–4.
383. Juettner FM, Popper H, Sommersgutter K, Smolle J, Friehs GB. Malignant fibrous histiocytoma of the lung: prognosis and therapy of a rare disease. Report of two cases and review of the literature. Thorac Cardiovasc Surg. 1987;35:226–31.
384. Yousem SA, Hochholzer L. Malignant fibrous histiocytoma of the lung. Cancer. 1987;60:2532–41.
385. Doyle LA, Vivero M, Fletcher CD, Mertens F, Hornick JL. Nuclear expression of STAT6 distinguishes solitary fibrous tumor from histologic mimics. Mod Pathol. 2014;27:390–5.
386. Derre J, Lagace R, Nicolas A, Mairal A, Chibon F, Coindre JM, Terrier P, Sastre X, Aurias A. Leiomyosarcomas and most malignant fibrous histiocytomas share very similar comparative genomic hybridization imbalances: an analysis of a series of 27 leiomyosarcomas. Lab Invest. 2001;81:211–5.
387. Keel SB, Bacha E, Mark EJ, Nielsen GP, Rosenberg AE. Primary pulmonary sarcoma: a clinicopathologic study of 26 cases. Mod Pathol. 1999;12:1124–31.
388. Etienne-Mastroianni B, Falchero L, Chalabreysse L, Loire R, Ranchere D, Souquet PJ, Cordier JF. Primary sarcomas of the lung: a clinicopathologic study of 12 cases. Lung Cancer. 2002;38:283–9.
389. Fletcher CDM, Chibon F, Mertens F. In: Fletcher CD, Bridge JAH, Hogendoorn PCW, Mertens F, editors. Undifferentiated/unclassified sarcomas. Lyon: International Agency for Research on Cancer (IARC); 2013. p. 3, 236–238.
390. Halyard MY, Camoriano JK, Culligan JA, Weiland LH, Allen MS, Pluth JR, Pairolero PC. Malignant fibrous histiocytoma of the lung. Report of four cases and review of the literature. Cancer. 1996;78:2492–7.
391. Herrmann BL, Saller B, Kiess W, Morgenroth K, Drochner K, Schroder T, Mann K. Primary malignant fibrous histiocytoma of the lung: IGF-II producing tumor induces fasting hypoglycemia. Exp Clin Endocrinol Diabetes. 2000;108:515–8.
392. Bonetti F, Pea M, Martignoni G, Doglioni C, Zamboni G, Capelli P, Rimondi P, Andrion A. Clear cell ("sugar") tumor of the lung is a lesion strictly related to angiomyolipoma – the concept of a family of lesions characterized by the presence of the perivascular epithelioid cells (PEC). Pathology. 1994;26:230–6.

393. Panizo-Santos A, Sola I, de Alava E, Lozano MD, Idoate MA, Pardo FJ. Angiomyolipoma and PEComa are immunoreactive for MyoD1 in cell cytoplasmic staining pattern. Appl Immunohistochem Mol Morphol. 2003;11:156–60.
394. Dickson BC, Brooks JS, Pasha TL, Zhang PJ. TFE3 expression in tumors of the microphthalmia-associated transcription factor (MiTF) family. Int J Surg Pathol. 2011;19:26–30.
395. Argani P, Aulmann S, Illei PB, Netto GJ, Ro J, Cho HY, Dogan S, Ladanyi M, Martignoni G, Goldblum JR, Weiss SW. A distinctive subset of PEComas harbors TFE3 gene fusions. Am J Surg Pathol. 2010;34:1395–406.
396. Martignoni G, Bonetti F, Chilosi M, Brunelli M, Segala D, Amin MB, Argani P, Eble JN, Gobbo S, Pea M. Cathepsin K expression in the spectrum of perivascular epithelioid cell (PEC) lesions of the kidney. Mod Pathol. 2012;25:100–11.
397. Ferenczi K, Lastra RR, Farkas T, Elenitsas R, Xu X, Roberts S, Brooks JS, Zhang PJ. MUM-1 expression differentiates tumors in the PEComa family from clear cell sarcoma and melanoma. Int J Surg Pathol. 2012;20:29–36.
398. Sekine I, Kodama T, Yokose T, Nishiwaki Y, Suzuki K, Goto K, Nagai K, Kuriyama T. Rare pulmonary tumors – a review of 32 cases. Oncology. 1998;55:431–4.
399. Allan JS. Rare solitary benign tumors of the lung. Semin Thorac Cardiovasc Surg. 2003;15:315–22.
400. Iwabuchi H, Kamura T, Tanaka M, Kato H. A case of endobronchial lipoma. Diagn Ther Endosc. 1999;5:263–7.
401. Muraoka M, Oka T, Akamine S, Nagayasu T, Iseki M, Suyama N, Ayabe H. Endobronchial lipoma: review of 64 cases reported in Japan. Chest. 2003;123:293–6.
402. Erkilic S, Kocer NE, Tuncozgur B. Peripheral intrapulmonary lipoma: a case report. Acta Chir Belg. 2007;107:700–2.
403. Markert E, Gruber-Moesenbacher U, Porubsky C, Popper HH. Lung osteoma – a new benign lung lesion. Virchows Arch. 2006;449:117–20.
404. Kanu A, Oermann CM, Malicki D, Wagner M, Langston C. Pulmonary lipoblastoma in an 18-month-old child: a unique tumor in children. Pediatr Pulmonol. 2002;34:150–4.
405. Mathew J, Sen S, Chandi SM, Kumar NK, Zachariah N, Chacko J, Thomas G. Pulmonary lipoblastoma: a case report. Pediatr Surg Int. 2001;17:543–4.
406. Gonzalez M, Prior JO, Rotman S, Ris HB, Krueger T. Benign intrapulmonary schwannoma: aspect on F-18 fluorodeoxyglucose PET/CT. Clin Nucl Med. 2011;36:465–7.
407. Chang CY, Fan YM, Bai CY, Cherng SC. Schwannoma mimicking lung cancer metastases demonstrated by PET/CT. Clin Nucl Med. 2006;31:644–5.
408. Jang JY, Kim JS, Choe JW, Kim MK, Jung JW, Choi JC, Shin JW, Park IW, Choi BW, Kim JY. A case of giant, benign schwannoma associated with total lung collapse by bloody effusion. Tuberc Respir Dis (Seoul). 2013;75:71–4.
409. Bosch X, Ramirez J, Font J, Bombi JA, Ferrer J, Vendrell J, Ingelmo M. Primary intrapulmonary benign schwannoma. A case with ultrastructural and immunohistochemical confirmation. Eur Respir J. 1990;3:234–7.
410. Roviaro G, Montorsi M, Varoli F, Binda R, Cecchetto A. Primary pulmonary tumours of neurogenic origin. Thorax. 1983;38:942–5.
411. McCluggage WG, Bharucha H. Primary pulmonary tumours of nerve sheath origin. Histopathology. 1995;26:247–54.
412. Simansky DA, Aviel-Ronen S, Reder I, Paley M, Refaely Y, Yellin A. Psammomatous melanotic schwannoma: presentation of a rare primary lung tumor. Ann Thorac Surg. 2000;70:671–2.
413. Boland JM, Colby TV, Folpe AL. Intrathoracic peripheral nerve sheath tumors-a clinicopathological study of 75 cases. Hum Pathol. 2015;46:419–25.
414. Thomas de Montpreville V, Dulmet EM. Granular cell tumours of the lower respiratory tract. Histopathology. 1995;27:257–62.
415. Deavers M, Guinee D, Koss MN, Travis WD. Granular cell tumors of the lung. Clinicopathologic study of 20 cases. Am J Surg Pathol. 1995;19:627–35.
416. van der Maten J, Blaauwgeers JL, Sutedja TG, Kwa HB, Postmus PE, Wagenaar SS. Granular cell tumors of the tracheobronchial tree. J Thorac Cardiovasc Surg. 2003;126:740–3.
417. Jiang M, Anderson T, Nwogu C, Tan D. Pulmonary malignant granular cell tumor. World J Surg Oncol. 2003;1:22.
418. Petrov DB, Vlassov VI, Kalaydjiev GT, Plochev MA, Obretenov ED, Stanoev VI, Danon SE. Primary pulmonary sarcomas and carcinosarcomas – postoperative results and comparative survival analysis. Eur J Cardiothorac Surg. 2003;23:461–6.
419. Kitamura H. Primary epithelioid malignant schwannoma of the lung. Pathol Int. 1994;44:317–24.
420. Hirose T, Sumitomo M, Kudo E, Hasegawa T, Teramae T, Murase M, Higasa Y, Ikata T, Hizawa K. Malignant peripheral nerve sheath tumor (MPNST) showing perineurial cell differentiation. Am J Surg Pathol. 1989;13:613–20.
421. Stamenkovic I, Yu Q. Merlin, a "magic" linker between extracellular cues and intracellular signaling pathways that regulate cell motility, proliferation, and survival. Curr Protein Pept Sci. 2010;11:471–84.
422. Doddrell RD, Dun XP, Shivane A, Feltri ML, Wrabetz L, Wegner M, Sock E, Hanemann CO, Parkinson DB. Loss of SOX10 function contributes to the phenotype of human Merlin-null schwannoma cells. Brain. 2013;136:549–63.
423. Piotrowski A, Xie J, Liu YF, Poplawski AB, Gomes AR, Madanecki P, Fu C, Crowley MR, Crossman

DK, Armstrong L, Babovic-Vuksanovic D, Bergner A, Blakeley JO, Blumenthal AL, Daniels MS, Feit H, Gardner K, Hurst S, Kobelka C, Lee C, Nagy R, Rauen KA, Slopis JM, Suwannarat P, Westman JA, Zanko A, Korf BR, Messiaen LM. Germline loss-of-function mutations in LZTR1 predispose to an inherited disorder of multiple schwannomas. Nat Genet. 2014;46:182–7.

424. Kim YH, Ohta T, Oh JE, Le Calvez-Kelm F, McKay J, Voegele C, Durand G, Mittelbronn M, Kleihues P, Paulus W, Ohgaki H. TP53, MSH4, and LATS1 germline mutations in a family with clustering of nervous system tumors. Am J Pathol. 2014;184:2374–81.
425. Widemann BC, Acosta MT, Ammoun S, Belzberg AJ, Bernards A, Blakeley J, Bretscher A, Cichowski K, Clapp DW, Dombi E, Evans GD, Ferner R, Fernandez-Valle C, Fisher MJ, Giovannini M, Gutmann DH, Hanemann CO, Hennigan R, Huson S, Ingram D, Kissil J, Korf BR, Legius E, Packer RJ, McClatchey AI, McCormick F, North K, Pehrsson M, Plotkin SR, Ramesh V, Ratner N, Schirmer S, Sherman L, Schorry E, Stevenson D, Stewart DR, Ullrich N, Bakker AC, Morrison H. CTF meeting 2012: translation of the basic understanding of the biology and genetics of NF1, NF2, and schwannomatosis toward the development of effective therapies. Am J Med Genet A. 2014;164A:563–78.
426. Gudena V, Verma N, Post G, Kizziah M, Fenning R, Montero AJ. Metastatic chest wall malignant schwannoma responding to sorafenib: case report and literature review. Cancer Biol Ther. 2008;7:810–3.
427. Suzuki T, Suzuki S, Kamio Y, Hori G, Tomita S, Suzuki H, Mitsuya T, Tate G, Sagawa F. A case of malignant Triton tumor of the lung. Thorac Cardiovasc Surg. 1996;44:319–20.
428. Moran CA, Suster S, Koss MN. Primary malignant 'triton' tumour of the lung. Histopathology. 1997;30:140–4.
429. Niho S, Yokose T, Nishiwaki Y, Mukai K. Immunohistochemical and clonal analysis of minute pulmonary meningothelial-like nodules. Hum Pathol. 1999;30:425–9.
430. Woodruff J. Origin of Triton tumor. Am J Dermatopathol. 1993;15:411–2.
431. Ballas K, Kontoulis TM, Papavasiliou A, Pissas D, Pavlidis T, Katsiki E, Venizelos I, Sakadamis A. A rare case of malignant triton tumor with pluridirectional differentiation. South Med J. 2009;102:435–7.
432. Kamiya K, Yoshizu A, Kashizaki F, Hida N, Hayashi H. Minute pulmonary meningothelial-like nodules coexisting with pulmonary cryptococcosis mimicking lung cancer. Gen Thorac Cardiovasc Surg. 2013;61:659–62.
433. Victoria L, McCulloch TM, Callaghan EJ, Bauman NM. Malignant triton tumor of the head and neck: a case report and review of the literature. Head Neck. 1999;21:663–70.
434. Aubertine CL, Flieder DB. Primary paraganglioma of the lung. Ann Diagn Pathol. 2004;8:237–41.
435. Shibahara J, Goto A, Niki T, Tanaka M, Nakajima J, Fukayama M. Primary pulmonary paraganglioma: report of a functioning case with immunohistochemical and ultrastructural study. Am J Surg Pathol. 2004;28:825–9.
436. Jochmanova I, Zelinka T, Widimsky Jr J, Pacak K. HIF signaling pathway in pheochromocytoma and other neuroendocrine tumors. Physiol Res. 2014;63 Suppl 2:S251–62.
437. Hadoux J, Favier J, Scoazec JY, Leboulleux S, Al Ghuzlan A, Caramella C, Deandreis D, Borget I, Loriot C, Chougnet C, Letouze E, Young J, Amar L, Bertherat J, Libe R, Dumont F, Deschamps F, Schlumberger M, Gimenez-Roqueplo AP, Baudin E. SDHB mutations are associated with response to temozolomide in patients with metastatic pheochromocytoma or paraganglioma. Int J Cancer. 2014;135:2711–20.
438. van Berkel A, Rao JU, Kusters B, Demir T, Visser E, Mensenkamp AR, van der Laak JA, Oosterwijk E, Lenders JW, Sweep FC, Wevers RA, Hermus AR, Langenhuijsen JF, Kunst DP, Pacak K, Gotthardt M, Timmers HJ. Correlation between in vivo 18F-FDG PET and immunohistochemical markers of glucose uptake and metabolism in pheochromocytoma and paraganglioma. J Nucl Med. 2014;55:1253–9.
439. Luchetti A, Walsh D, Rodger F, Clark G, Martin T, Irving R, Sanna M, Yao M, Robledo M, Neumann HP, Woodward ER, Latif F, Abbs S, Martin H, Maher ER. Profiling of somatic mutations in phaeochromocytoma and paraganglioma by targeted next generation sequencing analysis. Int J Endocrinol. 2015;2015:138573.
440. Lee CH, Cheung CY, Chow WS, Woo YC, Yeung CY, Lang BH, Fong CH, Kwok KH, Chen SP, Mak CM, Tan KC, Lam KS. Genetics of apparently sporadic pheochromocytoma and paraganglioma in a Chinese population. Horm Metab Res. 2015;47:833–8.
441. Baysal BE, Maher ER. 15 YEARS OF PARAGANGLIOMA: genetics and mechanism of pheochromocytoma-paraganglioma syndromes characterized by germline SDHB and SDHD mutations. Endocr Relat Cancer. 2015;22:T71–82.
442. Pai U, McMahon J, Tomashefski Jr JF. Mineralizing pulmonary elastosis in chronic cardiac failure. "Endogenous pneumoconiosis" revisited. Am J Clin Pathol. 1994;101:22–8.
443. Favier J, Amar L, Gimenez-Roqueplo AP. Paraganglioma and phaeochromocytoma: from genetics to personalized medicine. Nat Rev Endocrinol. 2015;11:101–11.
444. Nakamura R, Ishikawa S, Sakai M, Goto Y, Minami Y. Increased fluorodeoxyglucose-uptake in positron emission tomography with an endobronchial schwannoma occluding the left main stem bronchus. J Thorac Oncol. 2009;4:1183–4.

445. Rowsell C, Sirbovan J, Rosenblum MK, Perez-Ordonez B. Primary chordoid meningioma of lung. Virchows Arch. 2005;446:333–7.
446. Masago K, Hosada W, Sasaki E, Murakami Y, Sugano M, Nagasaka T, Yamada M, Yatabe Y. Is primary pulmonary meningioma a giant form of a meningothelial-like nodule? A case report and review of the literature. Case Rep Oncol. 2012;5:471–8.
447. Bernabeu Mora R, Sanchez Nieto JM, Hu C, Alcaraz Mateos E, Gimenez Bascunana A, Rodriguez Rodriguez M. Diffuse pulmonary meningotheliomatosis diagnosed by transbronchial lung biopsy. Respiration. 2013;86:145–8.
448. Frydrychowicz C, Holland H, Hantmann H, Gradistanac T, Hoffmann KT, Mueller W, Meixensberger J, Krupp W. Two cases of atypical meningioma with pulmonary metastases: a comparative cytogenetic analysis of chromosomes 1p and 22 and a review of the literature. Neuropathology. 2015;35:175–83.
449. Forest F, Berremila SA, Gyenes C, Ginguene C, Kassir R, Sulaiman A, Pasquier B, Porcheron J, Peoc'h M. Metastatic meningiomas: an unusual clinical and pathological diagnosis with highly variable outcome. J Neurooncol. 2014;120:411–21.
450. Tao CY, Wang JJ, Li H, You C. Malignant intraventricular meningioma with craniospinal dissemination and concurrent pulmonary metastasis. World J Surg Oncol. 2014;12:238.
451. Chiarelli M, De Simone M, Gerosa M, Guttadauro A, Cioffi U. An incidental pulmonary meningioma revealing an intracranial meningioma: primary or secondary lesion? Ann Thorac Surg. 2015;99:e83–4.
452. Kayser K, Zink S, Link B, Herth F, Dienemann H, Schrod L, Gabius HJ. Endobronchial juvenile hemangioma – a case report of a neonate including immunohistochemical monitoring and nuclear, cellular, and vascular morphometry. Virchows Arch. 2001;438:192–7.
453. Weissferdt A, Moran CA. Primary vascular tumors of the lungs: a review. Ann Diagn Pathol. 2010;14:296–308.
454. Iwasaki M, Kobayashi H, Nomoto T, Arai T, Kondoh T. Primary racemose hemangioma of the bronchial artery. Intern Med. 2001;40:650–3.
455. Abrahams NA, Colby TV, Pearl RH, Chipps BE, Juris AL, Leslie KO. Pulmonary hemangiomas of infancy and childhood: report of two cases and review of the literature. Pediatr Dev Pathol. 2002;5:283–92.
456. Sirmali M, Demirag F, Aydin E, Karasu S, Kaya S. A pulmonary cavernous hemangioma causing massive hemoptysis. Ann Thorac Surg. 2003;76:1275–6.
457. Fine SW, Whitney KD. Multiple cavernous hemangiomas of the lung: a case report and review of the literature. Arch Pathol Lab Med. 2004;128:1439–41.
458. Quijano G, Drut R. Multiple congenital infantile hemangiomas of the lung in partial trisomy D. J Clin Pathol. 2007;60:943–5.
459. de Perrot M, Waddell TK, Chamberlain D, Hutcheon M, Keshavjee S. De novo pulmonary capillary hemangiomatosis occurring rapidly after bilateral lung transplantation. J Heart Lung Transplant. 2003;22:698–700.
460. Umezu H, Naito M, Yagisawa K, Hattori A, Aizawa Y. An autopsy case of pulmonary capillary hemangiomatosis without evidence of pulmonary hypertension. Virchows Arch. 2001;439:586–92.
461. Havlik DM, Massie LW, Williams WL, Crooks LA. Pulmonary capillary hemangiomatosis-like foci. An autopsy study of 8 cases. Am J Clin Pathol. 2000;113:655–62.
462. Varnholt H, Kradin R. Pulmonary capillary hemangiomatosis arising in hereditary hemorrhagic telangiectasia. Hum Pathol. 2004;35:266–8.
463. Lippert JL, White CS, Cameron EW, Sun CC, Liang X, Rubin LJ. Pulmonary capillary hemangiomatosis: radiographic appearance. J Thorac Imaging. 1998;13:49–51.
464. Sullivan A, Chmura K, Cool CD, Keith R, Schwartz GG, Chan ED. Pulmonary capillary hemangiomatosis: an immunohistochemical analysis of vascular remodeling. Eur J Med Res. 2006;11:187–93.
465. Assaad AM, Kawut SM, Arcasoy SM, Rosenzweig EB, Wilt JS, Sonett JR, Borczuk AC. Platelet-derived growth factor is increased in pulmonary capillary hemangiomatosis. Chest. 2007;131:850–5.
466. Best DH, Sumner KL, Austin ED, Chung WK, Brown LM, Borczuk AC, Rosenzweig EB, Bayrak-Toydemir P, Mao R, Cahill BC, Tazelaar HD, Leslie KO, Hemnes AR, Robbins IM, Elliott CG. EIF2AK4 mutations in pulmonary capillary hemangiomatosis. Chest. 2014;145:231–6.
467. Tenorio J, Navas P, Barrios E, Fernandez L, Nevado J, Quezada CA, Lopez-Meseguer M, Arias P, Mena R, Lobo JL, Alvarez C, Heath K, Escribano-Subias P, Lapunzina P. A founder EIF2AK4 mutation causes an aggressive form of pulmonary arterial hypertension in Iberian Gypsies. Clin Genet. 2015;88:579–83.
468. Nayyar D, Muthiah K, Kumarasinghe G, Hettiarachchi R, Celermajer D, Kotlyar E, Keogh A. Imatinib for the treatment of pulmonary arterial hypertension and pulmonary capillary hemangiomatosis. Pulm Circ. 2014;4:342–5.
469. Weiss SW, Ishak KG, Dail DH, Sweet DE, Enzinger FM. Epithelioid hemangioendothelioma and related lesions. Semin Diagn Pathol. 1986;3:259–87.
470. Eskenasy A. Primary lung sarcomas. A histopathologic study of 118 cases. Morphol Embryol (Bucur). 1979;25:27–38.
471. Wagoner JK, Infante PF, Apfeldorf RB. Toxicity of vinyl chloride and polyvinyl chloride as seen through epidemiologic observations. J Toxicol Environ Health. 1980;6:1101–7.

472. Landrigan PJ. Occupational and community exposures to toxic metals: lead, cadmium, mercury and arsenic. West J Med. 1982;137:531–9.
473. Doll R. Effects of exposure to vinyl chloride. An assessment of the evidence. Scand J Work Environ Health. 1988;14:61–78.
474. Ishikawa Y, Wada I, Fukumoto M. Alpha-particle carcinogenesis in Thorotrast patients: epidemiology, dosimetry, pathology, and molecular analysis. J Environ Pathol Toxicol Oncol. 2001;20: 311–5.
475. Fagen K, Silverman ED, Cole RL. Detection of a pulmonary epithelioid hemangioendothelioma by FDG PET scan. Clin Nucl Med. 2004;29:758–9.
476. Hristova EN, Krishnamurthy S, Ro JY, Ayala AG. Pulmonary epithelioid hemangioendothelioma with prominent signet ring cell features mimicking metastatic adenocarcinoma. Ann Diagn Pathol. 2003;7:160–4.
477. Anderson T, Zhang L, Hameed M, Rusch V, Travis WD, Antonescu CR. Thoracic epithelioid malignant vascular tumors: a clinicopathologic study of 52 cases with emphasis on pathologic grading and molecular studies of WWTR1-CAMTA1 fusions. Am J Surg Pathol. 2015;39:132–9.
478. Stacher E, Gruber-Mosenbacher U, Halbwedl I, Dei Tos AP, Cavazza A, Papotti M, Carvalho L, Huber M, Ermert L, Popper HH. The VEGF-system in primary pulmonary angiosarcomas and haemangioendotheliomas: new potential therapeutic targets? Lung Cancer. 2009;65:49–55.
479. Sheppard MN, Hansell DM, Du Bois RM, Nicholson AG. Primary epithelioid angiosarcoma of the lung presenting as pulmonary hemorrhage. Hum Pathol. 1997;28:383–5.
480. Cao Y, Zou SM, Zhang KT, Lu N, Liu Y, Feng L, Wen P, Han NJ, Lin DM. Genetic alterations in pulmonary epithelioid hemangioendothelioma and epithelioid angiosarcoma. Histol Histopathol. 2011;26:491–6.
481. Ray-Coquard I, Italiano A, Bompas E, Le Cesne A, Robin YM, Chevreau C, Bay JO, Bousquet G, Piperno-Neumann S, Isambert N, Lemaitre L, Fournier C, Gauthier E, Collard O, Cupissol D, Clisant S, Blay JY, Penel N. Sorafenib for patients with advanced angiosarcoma: a phase II Trial from the French Sarcoma Group (GSF/GETO). Oncologist. 2012;17:260–6.
482. Tamiya H, Kamo R, Kumei A, Yanagihara S, Ishii M, Kobayashi H. Partial response of angiosarcoma of the scalp to sorafenib: association with decreased expression of vascular endothelial growth factors and their receptors. Clin Exp Dermatol. 2012;37:749–52.
483. Eng J, Murday AJ. Leiomyosarcoma of the pulmonary artery. Ann Thorac Surg. 1992;53:905–6.
484. Gurbuz A, Yetkin U, Yilik L, Ozdemir T, Turk F. A case of leiomyosarcoma originating from pulmonary vein, occluding mitral inflow. Heart Lung. 2003; 32:210–4.
485. Bode-Lesniewska B, Zhao J, Speel EJ, Biraima AM, Turina M, Komminoth P, Heitz PU. Gains of 12q13-14 and overexpression of mdm2 are frequent findings in intimal sarcomas of the pulmonary artery. Virchows Arch. 2001;438:57–65.
486. Burke AP, Virmani R. Sarcomas of the great vessels. A clinicopathologic study. Cancer. 1993; 71:1761–73.
487. Tavora F, Miettinen M, Fanburg-Smith J, Franks TJ, Burke A. Pulmonary artery sarcoma: a histologic and follow-up study with emphasis on a subset of low-grade myofibroblastic sarcomas with a good long-term follow-up. Am J Surg Pathol. 2008;32:1751–61.
488. Dewaele B, Floris G, Finalet-Ferreiro J, Fletcher CD, Coindre JM, Guillou L, Hogendoorn PC, Wozniak A, Vanspauwen V, Schoffski P, Marynen P, Vandenberghe P, Sciot R, Debiec-Rychter M. Coactivated platelet-derived growth factor receptor {alpha} and epidermal growth factor receptor are potential therapeutic targets in intimal sarcoma. Cancer Res. 2010;70:7304–14.
489. Hoskote SS, Patel VP. Pulmonary Kaposi sarcoma in AIDS. Mayo Clin Proc. 2012;87, e77.
490. Gasparetto TD, Marchiori E, Lourenco S, Zanetti G, Vianna AD, Santos AA, Nobre LF. Pulmonary involvement in Kaposi sarcoma: correlation between imaging and pathology. Orphanet J Rare Dis. 2009;4:18.
491. Miettinen M, Wang ZF. Prox1 transcription factor as a marker for vascular tumors-evaluation of 314 vascular endothelial and 1086 nonvascular tumors. Am J Surg Pathol. 2012;36:351–9.
492. Catrina SB, Botusan IR, Rantanen A, Catrina AI, Pyakurel P, Savu O, Axelson M, Biberfeld P, Poellinger L, Brismar K. Hypoxia-inducible factor-1alpha and hypoxia-inducible factor-2alpha are expressed in kaposi sarcoma and modulated by insulin-like growth factor-I. Clin Cancer Res. 2006;12:4506–14.
493. Hilliard RI, McKendry JB, Phillips MJ. Congenital abnormalities of the lymphatic system: a new clinical classification. Pediatrics. 1990;86:988–94.
494. Hamada K, Ishii Y, Nakaya M, Sawabata N, Fukuda K, Suzuki H. Solitary lymphangioma of the lung. Histopathology. 1995;27:482–3.
495. Nagayasu T, Hayashi T, Ashizawa K, Muraoka M, Tagawa T, Akamine S, Oka T. A case of solitary pulmonary lymphangioma. J Clin Pathol. 2003;56:396–8.
496. Limmer S, Krokowski M, Kujath P. Pulmonary lymphangioma. Ann Thorac Surg. 2008;85:336–9.
497. Scalzetti EM, Heitzman ER, Groskin SA, Randall PA, Katzenstein AL. Developmental lymphatic disorders of the thorax. Radiographics. 1991;11:1069–85.
498. Bhatti MA, Ferrante JW, Gielchinsky I, Norman JC. Pleuropulmonary and skeletal lymphangiomatosis with chylothorax and chylopericardium. Ann Thorac Surg. 1985;40:398–401.
499. Yekeler E, Dursun M, Yildirim A, Tunaci M. Diffuse pulmonary lymphangiomatosis: imaging findings. Diagn Interv Radiol. 2005;11:31–4.

500. Kruglik GD, Reed JC, Daroca PJ. Radiologic-pathologic correlation from the Armed Forces Institute of Pathology. Lymphangiomyomatosis. Radiology. 1976;120:583–8.
501. Tazelaar HD, Kerr D, Yousem SA, Saldana MJ, Langston C, Colby TV. Diffuse pulmonary lymphangiomatosis. Hum Pathol. 1993;24:1313–22.
502. Ramani P, Shah A. Lymphangiomatosis. Histologic and immunohistochemical analysis of four cases. Am J Surg Pathol. 1993;17:329–35.
503. Brown M, Pysher T, Coffin CM. Lymphangioma and congenital pulmonary lymphangiectasis: a histologic, immunohistochemical, and clinicopathologic comparison. Mod Pathol. 1999;12:569–75.
504. Kandil A, Rostom AY, Mourad WA, Khafaga Y, Gershuny AR, el-Hosseiny G. Successful control of extensive thoracic lymphangiomatosis by irradiation. Clin Oncol (R Coll Radiol). 1997;9:407–11.
505. Kinnier CV, Eu JP, Davis RD, Howell DN, Sheets J, Palmer SM. Successful bilateral lung transplantation for lymphangiomatosis. Am J Transplant. 2008;8:1946–50.
506. Laverdiere C, David M, Dubois J, Russo P, Hershon L, Lapierre JG. Improvement of disseminated lymphangiomatosis with recombinant interferon therapy. Pediatr Pulmonol. 2000;29:321–4.
507. Pfleger A, Schwinger W, Maier A, Tauss J, Popper HH, Zach MS. Gorham-Stout syndrome in a male adolescent-case report and review of the literature. J Pediatr Hematol Oncol. 2006;28:231–3.
508. Aman J, Thunnissen E, Paul MA, van Nieuw Amerongen GP, Vonk-Noordegraaf A. Successful treatment of diffuse pulmonary lymphangiomatosis with bevacizumab. Ann Intern Med. 2012;156:839–40.
509. Sordillo PP, Chapman R, Hajdu SI, Magill GB, Golbey RB. Lymphangiosarcoma. Cancer. 1981;48:1674–9.
510. Heitmann C, Ingianni G. Stewart-Treves syndrome: lymphangiosarcoma following mastectomy. Ann Plast Surg. 2000;44:72–5.
511. Kayser K, Bauer M, Luellig H, Berberich H, Schaaf S. Long-term development of a primary lung sarcoma, probably lymphangiosarcoma – a case report. Thorac Cardiovasc Surg. 1984;32:178–81.
512. Mukhopadhyay S, El-Zammar OA, Katzenstein AL. Pulmonary meningothelial-like nodules: new insights into a common but poorly understood entity. Am J Surg Pathol. 2009;33:487–95.
513. Shotton JC, Stafford ND, Breach NM. Malignant triton tumour of the palate – a case report. Br J Oral Maxillofac Surg. 1988;26:120–3.
514. Shajrawi I, Podoshin L, Fradis M, Boss JH. Malignant triton tumor of the nose and paranasal sinuses: a case study. Hum Pathol. 1989;20:811–4.
515. Ionescu DN, Sasatomi E, Aldeeb D, Omalu BI, Finkelstein SD, Swalsky PA, Yousem SA. Pulmonary meningothelial-like nodules: a genotypic comparison with meningiomas. Am J Surg Pathol. 2004;28:207–14.
516. Pai R, Manipadam MT, Singh P, Ebenazer A, Samuel P, Rajaratnam S. Usefulness of Succinate dehydrogenase B (SDHB) immunohistochemistry in guiding mutational screening among patients with pheochromocytoma-paraganglioma syndromes. APMIS. 2014;122:1130–5.
517. Hansen CP, Francis D, Bertelsen S. Primary hemangiopericytoma of the lung. Case report. Scand J Thorac Cardiovasc Surg. 1990;24:89–92.
518. Rusch VW, Shuman WP, Schmidt R, Laramore GE. Massive pulmonary hemangiopericytoma. An innovative approach to evaluation and treatment. Cancer. 1989;64:1928–36.
519. Yousem SA, Hochholzer L. Primary pulmonary hemangiopericytoma. Cancer. 1987;59:549–55.
520. Gengler C, Guillou L. Solitary fibrous tumour and haemangiopericytoma: evolution of a concept. Histopathology. 2006;48:63–74.
521. Gaertner EM, Steinberg DM, Huber M, Hayashi T, Tsuda N, Askin FB, Bell SW, Nguyen B, Colby TV, Nishimura SL, Miettinen M, Travis WD. Pulmonary and mediastinal glomus tumors – report of five cases including a pulmonary glomangiosarcoma: a clinicopathologic study with literature review. Am J Surg Pathol. 2000;24:1105–14.
522. Katabami M, Okamoto K, Ito K, Kimura K, Kaji H. Bronchogenic glomangiomyoma with local intravenous infiltration. Eur Respir J. 2006;28:1060–4.
523. Lie CH, Chao TY, Chung YH, Lin MC. Primary pulmonary malignant melanoma presenting with haemoptysis. Melanoma Res. 2005;15:219–21.
524. Miller DL, Allen MS. Rare pulmonary neoplasms. Mayo Clin Proc. 1993;68:492–8.
525. Ost D, Joseph C, Sogoloff H, Menezes G. Primary pulmonary melanoma: case report and literature review. Mayo Clin Proc. 1999;74:62–6.
526. Fairweather PM, Williamson R, Tsikleas G. Pulmonary extranodal marginal zone lymphoma with massive crystal storing histiocytosis. Am J Surg Pathol. 2006;30:262–7.
527. Barrie JR, English JC, Muller N. Castleman's disease of the lung: radiographic, high-resolution CT, and pathologic findings. AJR Am J Roentgenol. 1996;166:1055–6.
528. Spedini C, Lombardi C, Lanzani G, Di Fabio D, Chiodera PL. Castleman's disease presenting as an asymptomatic solitary pulmonary nodule. Monaldi Arch Chest Dis. 1995;50:363–5.
529. Tokunaga T, Kadota Y, Utsumi T, Inoue M, Minami M, Okumura M. Castleman's disease arising from an intrapulmonary lymph node. Gen Thorac Cardiovasc Surg. 2009;57:562–5.
530. Okuda M, Okuda Y, Ogura T, Kashio M, Masuno T, Oji Y, Miyazaki M. Primary lung involvement with amyloid deposition in Waldenstom's macroglobulinemia: observations from over 20 years. Respirology. 2004;9:414–8.

531. Girard N, Vasiljevic A, Cottin V, Falchero L, Meyronet D, Thivolet-Bejui F, Cordier JF. Respiratory failure with diffuse bronchiectases and cryoglobulinaemia. Eur Respir J. 2008; 31:1374–8.
532. Consuegra A, Marcos PJ, Vazquez R, Pombo J, Deben G, Verea-Hernando H. Diffuse interstitial lung disease as a first manifestation of Waldenstrom's macroglobulinemia: case report and review of the literature. Arch Bronconeumol. 2014;50:151–3.
533. Mikolaenko I, Listinsky CM. Systemic CD5+ MALT lymphoma: presentation with Waldenstrom syndrome. Ann Diagn Pathol. 2009;13:272–7.
534. Ben-Ezra J, Bailey A, Azumi N, Delsol G, Stroup R, Sheibani K, Rappaport H. Malignant histiocytosis X. A distinct clinicopathologic entity. Cancer. 1991;68:1050–60.
535. Hornick JL, Jaffe ES, Fletcher CD. Extranodal histiocytic sarcoma: clinicopathologic analysis of 14 cases of a rare epithelioid malignancy. Am J Surg Pathol. 2004;28:1133–44.
536. Vos JA, Abbondanzo SL, Barekman CL, Andriko JW, Miettinen M, Aguilera NS. Histiocytic sarcoma: a study of five cases including the histiocyte marker CD163. Mod Pathol. 2005;18:693.
537. Stacher E, Beham-Schmid C, Terpe HJ, Simiantonaki N, Popper HH. Pulmonary histiocytic sarcoma mimicking pulmonary Langerhans cell histiocytosis in a young adult presenting with spontaneous pneumothorax: a potential diagnostic pitfall. Virchows Arch. 2009;455:187–90.
538. Song SY, Lee SW, Ryu KH, Sung SH. Erdheim-Chester disease with multisystem involvement in a 4-year-old. Pediatr Radiol. 2012;42:632–5.
539. Egan AJ, Boardman LA, Tazelaar HD, Swensen SJ, Jett JR, Yousem SA, Myers JL. Erdheim-Chester disease: clinical, radiologic, and histopathologic findings in five patients with interstitial lung disease. Am J Surg Pathol. 1999;23:17–26.
540. Rush WL, Andriko JA, Galateau-Salle F, Brambilla E, Brambilla C, Ziany-bey I, Rosado-de-Christenson ML, Travis WD. Pulmonary pathology of Erdheim-Chester disease. Mod Pathol. 2000;13:747–54.
541. Gatalica Z, Bilalovic N, Palazzo JP, Bender RP, Swensen J, Millis SZ, Vranic S, Von Hoff D, Arceci RJ. Disseminated histiocytoses biomarkers beyond BRAFV600E: frequent expression of PD-L1. Oncotarget. 2015;6:19819–25.
542. Cives M, Simone V, Rizzo FM, Dicuonzo F, Cristallo Lacalamita M, Ingravallo G, Silvestris F, Dammacco F. Erdheim-Chester disease: a systematic review. Crit Rev Oncol Hematol. 2015;95:1–11.
543. Chakraborty R, Hampton OA, Shen X, Simko SJ, Shih A, Abhyankar H, Lim KP, Covington KR, Trevino L, Dewal N, Muzny DM, Doddapaneni H, Hu J, Wang L, Lupo PJ, Hicks MJ, Bonilla DL, Dwyer KC, Berres ML, Poulikakos PI, Merad M, McClain KL, Wheeler DA, Allen CE, Parsons DW. Mutually exclusive recurrent somatic mutations in MAP2K1 and BRAF support a central role for ERK activation in LCH pathogenesis. Blood. 2014;124:3007–15.
544. Emile JF, Diamond EL, Helias-Rodzewicz Z, Cohen-Aubart F, Charlotte F, Hyman DM, Kim E, Rampal R, Patel M, Ganzel C, Aumann S, Faucher G, Le Gall C, Leroy K, Colombat M, Kahn JE, Trad S, Nizard P, Donadieu J, Taly V, Amoura Z, Abdel-Wahab O, Haroche J. Recurrent RAS and PIK3CA mutations in Erdheim-Chester disease. Blood. 2014;124:3016–9.
545. Dishop MK, Kuruvilla S. Primary and metastatic lung tumors in the pediatric population: a review and 25-year experience at a large children's hospital. Arch Pathol Lab Med. 2008;132:1079–103.
546. Hicks J, Mierau G. The spectrum of pediatric fibroblastic and myofibroblastic tumors. Ultrastruct Pathol. 2004;28:265–81.
547. McGinnis M, Jacobs G, el-Naggar A, Redline RW. Congenital peribronchial myofibroblastic tumor (so-called "congenital leiomyosarcoma"). A distinct neonatal lung lesion associated with nonimmune hydrops fetalis. Mod Pathol. 1993;6:487–92.
548. Alobeid B, Beneck D, Sreekantaiah C, Abbi RK, Slim MS. Congenital pulmonary myofibroblastic tumor: a case report with cytogenetic analysis and review of the literature. Am J Surg Pathol. 1997;21:610–4.
549. Sirvent N, Perrin C, Lacour JP, Maire G, Attias R, Pedeutour F. Monosomy 9q and trisomy 16q in a case of congenital solitary infantile myofibromatosis. Virchows Arch. 2004;445:537–40.
550. Dishop MK, McKay EM, Kreiger PA, Priest JR, Williams GM, Langston C, Jarzembowski J, Suchi M, Dehner LP, Hill DA. Fetal lung interstitial tumor (FLIT): a proposed newly recognized lung tumor of infancy to be differentiated from cystic pleuropulmonary blastoma and other developmental pulmonary lesions. Am J Surg Pathol. 2010;34:1762–72.
551. de Chadarevian JP, Liu J, Pezanowski D, Stefanovici C, Guzman M, Katz DA, Pascassio JM. Diagnosis of "Fetal lung interstitial tumor" requires a FISH negative for trisomies 8 and 2. Am J Surg Pathol. 2011;35:1085; author reply 1086–1087.
552. Onoda T, Kanno M, Sato H, Takahashi N, Izumino H, Ohta H, Emura T, Katoh H, Ohizumi H, Ohtake H, Asao H, Dehner LP, Hill AD, Hayasaka K, Mitsui T. Identification of novel ALK rearrangement A2M-ALK in a neonate with fetal lung interstitial tumor. Genes Chromosomes Cancer. 2014;53:865–74.
553. Dehner LP. Pleuropulmonary blastoma is THE pulmonary blastoma of childhood. Semin Diagn Pathol. 1994;11:144–51.
554. Priest JR, McDermott MB, Bhatia S, Watterson J, Manivel JC, Dehner LP. Pleuropulmonary blastoma: a clinicopathologic study of 50 cases. Cancer. 1997;80:147–61.
555. Hachitanda Y, Aoyama C, Sato JK, Shimada H. Pleuropulmonary blastoma in childhood. A tumor

of divergent differentiation. Am J Surg Pathol. 1993;17:382–91.
556. Vargas SO, Nose V, Fletcher JA, Perez-Atayde AR. Gains of chromosome 8 are confined to mesenchymal components in pleuropulmonary blastoma. Pediatr Dev Pathol. 2001;4:434–45.
557. Taube JM, Griffin CA, Yonescu R, Morsberger L, Argani P, Askin FB, Batista DA. Pleuropulmonary blastoma: cytogenetic and spectral karyotype analysis. Pediatr Dev Pathol. 2006;9:453–61.
558. Roque L, Rodrigues R, Martins C, Ribeiro C, Ribeiro MJ, Martins AG, Oliveira P, Fonseca I. Comparative genomic hybridization analysis of a pleuropulmonary blastoma. Cancer Genet Cytogenet. 2004;149:58–62.
559. Slade I, Bacchelli C, Davies H, Murray A, Abbaszadeh F, Hanks S, Barfoot R, Burke A, Chisholm J, Hewitt M, Jenkinson H, King D, Morland B, Pizer B, Prescott K, Saggar A, Side L, Traunecker H, Vaidya S, Ward P, Futreal PA, Vujanic G, Nicholson AG, Sebire N, Turnbull C, Priest JR, Pritchard-Jones K, Houlston R, Stiller C, Stratton MR, Douglas J, Rahman N. DICER1 syndrome: clarifying the diagnosis, clinical features and management implications of a pleiotropic tumour predisposition syndrome. J Med Genet. 2011;48.
560. West D, Nicholson AG, Colquhoun I, Pollock J. Bronchioloalveolar carcinoma in congenital cystic adenomatoid malformation of lung. Ann Thorac Surg. 2007;83:687–9.
561. Lantuejoul S, Nicholson AG, Sartori G, Piolat C, Danel C, Brabencova E, Goldstraw P, Brambilla E, Rossi G. Mucinous cells in type 1 pulmonary congenital cystic adenomatoid malformation as mucinous bronchioloalveolar carcinoma precursors. Am J Surg Pathol. 2007;31:961–9.

Metastasis

18

Lung carcinomas are frequently metastasizing to other organs. Metastasis is the most common cause of death in lung cancer patients. In this chapter, we will focus on two different aspects: mechanisms of metastasis of lung carcinomas and on metastasis to the lung by other malignant tumors.

Lung carcinomas when detected are most often in a metastatic stage IV. Lung carcinomas metastasize by lymphatic as well as blood vessels. When careful evaluation is done in resected lung carcinomas, vascular invasion is often seen in low-stage tumors, which usually results in increased incidence of recurrence as well as shortened survival of the patient [1]. Whereas metastasis via the lymphatic route usually takes longer until distant metastases are set, spreading via blood vessels will set early on distant metastases. Lung carcinomas have some preferential sites for metastasis, such as the brain, bones, and adrenal glands. Other organs are involved usually in late stage of the disease. Within the different types of lung carcinomas, there is also a preferential metastatic site, such as liver metastasis in SCLC and brain metastasis in SCLC and adenocarcinoma [2–4]. In recent years, brain metastasis is increasingly seen in adenocarcinomas with EGFR mutations and EML4-ALK1 rearrangement, whereas squamous cell carcinomas in many cases have a tendency to locally invade the thoracic wall [4, 5]. This opens a variety of questions on metastasis in lung carcinomas, which we aim to address in this review.

When dissecting metastasis into developmental steps, there are several ways to approach this theme, including the first step of invasion into the stroma. As this has been discussed already in the tumor chapter, we will not discuss the process of precursor to in situ carcinoma transition and also will not focus on stroma invasion.

18.1 Tumor Establishment and Cell Migration

After tumor cells have invaded the stroma, several tasks have to be organized. To promote tumor growth, the tumor cells need to organize vascular supply for nutrition and oxygen uptake. For movement within the stroma, this needs to be restructured, the tumor cells have to escape lymphocytic attacks, and finally for migration, the tumor cells have to adapt to a migratory cell structure.

18.1.1 Angiogenesis, Hypoxia, and Stroma (Microenvironment)

When tumor cells start to form nodules within the stroma, they need to communicate with the surrounding microenvironment, which is composed mainly by macrophages, fibroblasts/myofibroblasts,

© Springer-Verlag Berlin Heidelberg 2017
H. Popper, *Pathology of Lung Disease*, DOI 10.1007/978-3-662-50491-8_18

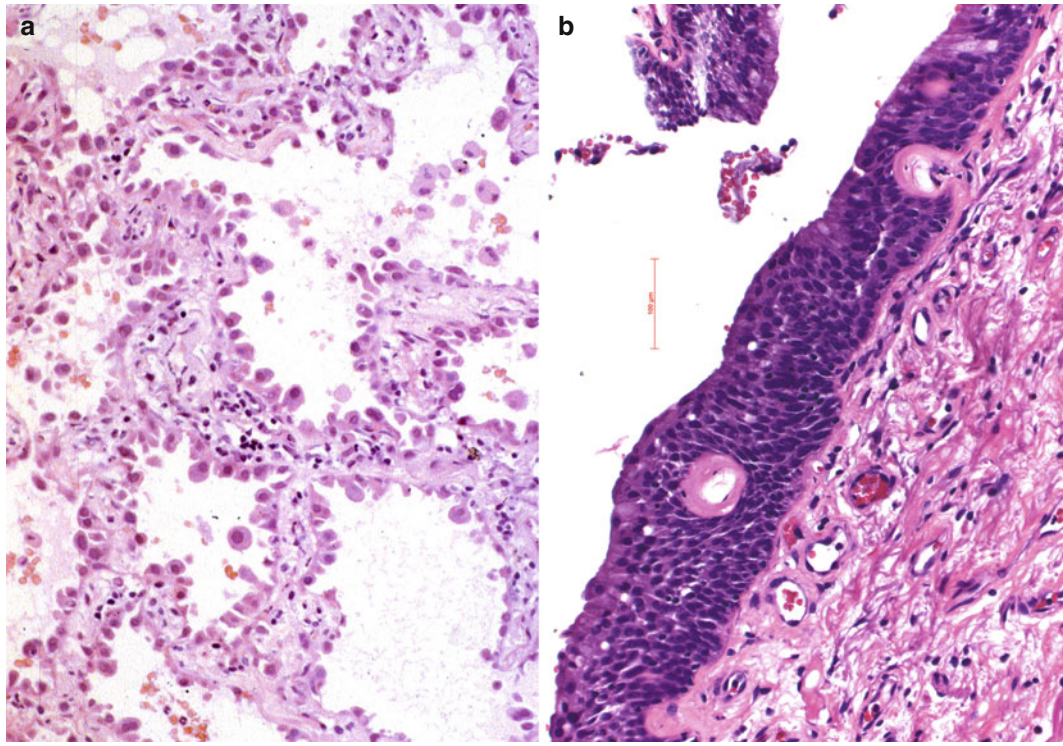

Fig. 18.1 In angiogenesis in preneoplastic lesions, (**a**) atypical adenomatous hyperplasia has no new vessels, but instead relies on the normal vascular architecture of pre-existing alveolar septa; in the vascular variant of squamous cell dysplasia (**b**), the preneoplastic cells induce angiogenesis using vascular growth factors produced by the dysplastic cells

neutrophils, lymphocytes, and dendritic cells. To facilitate angiogenesis tumor cells can either directly release angiogenic factors such as VEGFs to directly stimulate the formation of new blood vessels, or tumor cells cooperate with macrophages, which can release angiogenic growth factors [6–8]. A good example for angiogenesis induced by tumor cells is the vascular variant of squamous cell dysplasia, whereas in atypical adenomatous hyperplasia (AAH) and in well-differentiated adenocarcinomas, angiogenesis seems to relay on cooperating macrophages [9–12] (Figs. 18.1a, b and 18.2a). To understand the function of macrophages, it is necessary to briefly discuss the two different populations of macrophages, the M1 and M2 type. M1 macrophages are acting against tumor cell invasion by secreting interleukin 12 (IL12) which function as tumoricidal by an interaction with cytotoxic lymphocytes and NK cells. M2 macrophages produce IL10, which promote tumor progression. The differentiation of naïve macrophages into either M1 or M2 types is facilitated by Notch, where low Notch via SOCS3 drives macrophages into M2 types [13]. M1 macrophages act pro-inflammatory, inactivate autophagy by production of radical oxygen species, and can also induce apoptosis of tumor cells [14–16]. Notably mutation and inactivation of Notch is found in neuroendocrine carcinomas, whereas activation in other non-small cell carcinomas, which questions the function of this gene as either oncogene or tumor suppressor [17–20]. Most probably different members of the Notch family proteins function differently in squamous cell, small cell, and adenocarcinomas, and in addition act differently during tumor development [21–23].

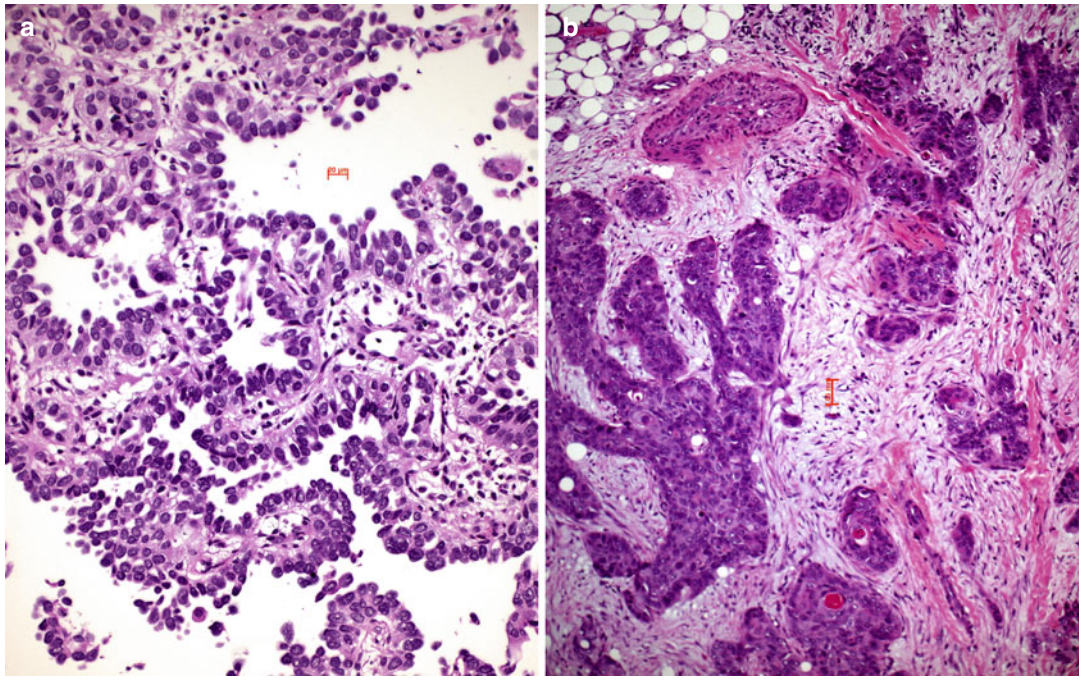

Fig. 18.2 Desmoplastic stroma reaction is almost absent in this well-differentiated lepidic-predominant adenocarcinoma (**a**) whereas prominent in this squamous cell carcinoma (**b**)

18.1.2 The Role of Hypoxia in Tumor Cell Migration and Metastasis

As the primary tumor grows, usually the formation of new blood vessels cannot keep with this resulting in hypoxia. This is the time when tumor cells are faced with this problem and try to escape apoptosis induced by hypoxia. Some of these mechanisms have been elucidated. HIF-1α is upregulated in areas of tumor hypoxia [24–28] and if translocated into the nucleus and bind to HIF-1β can induce transcription of VEGF, thus increasing the formation of more blood vessels. Apoptosis is also inhibited by growth factors such as IGF and EGF, which are also induced by hypoxia [24, 29]. Carcinoma cells also escape apoptosis and cell death in hypoxic areas by reducing their metabolism and cell division [30]. In mouse models of lung adenocarcinomas driven by the mutated RAS oncogene, invasion was exclusively seen starting in areas of necrosis and hypoxia [31] (Fig. 18.3a, b). This fits well with published data from human tumor research, showing that migration and EMT are increased in hypoxic areas by the release of different proteins [32–36]. If each of these enzymes/proteins act in concert together, or if each of these factors can act independently is presently unknown.

Macrophages also act together with fibroblasts and myofibroblasts to form either a stroma suitable for tumor cell invasion and migration (Fig. 18.2b) or might inhibit migration. This can easily be evaluated by morphology: in case the stroma cells form a classical scar, this means inhibition for the tumor cells to migrate, whereas desmoplastic stroma is a form of stroma remodeling done by myofibroblasts, which enable tumor cells to migrate (Fig. 18.4a, b). Usually fibroblasts in scars do not cooperate with tumor cells, myofibroblasts in contrary cooperate [37, 38]. In some cases even tumor cells undergoing epithelial to mesenchymal transition (EMT) directly form part of the desmoplastic stroma as in pleomorphic carcinomas (Fig. 18.5a, b) and occasionally also in SCLC [39]. Several studies have shown that tumor-associated "fibroblasts" (essentially myofibroblasts in the lung) are different from normal fibroblasts in the lung. They

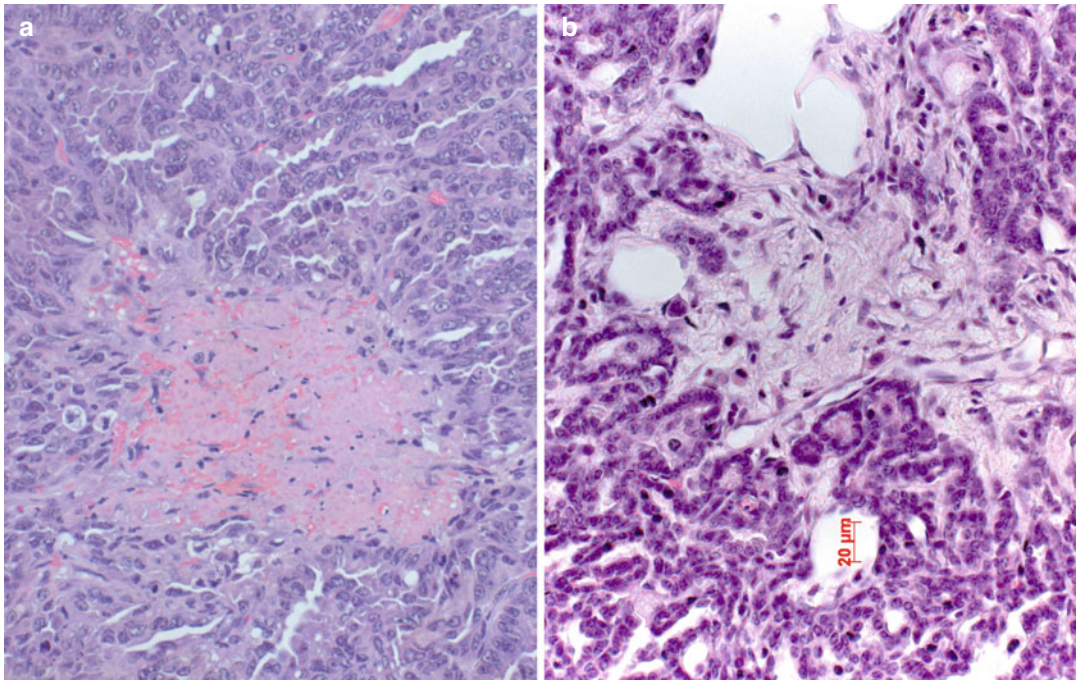

Fig. 18.3 Experimental adenocarcinoma in a mouse. Carcinoma is induced by mutant KRAS. At a certain size of the in situ adenocarcinoma, central hypoxic necrosis develops (**a**), which is the prerequisite for invasion (**b**)

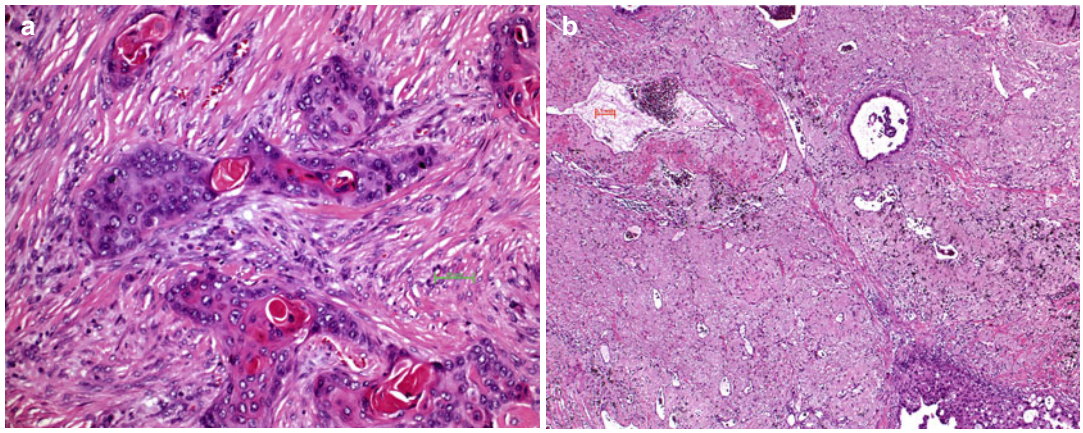

Fig. 18.4 Desmoplastic stroma supports invasion and guides the carcinoma cells in this squamous cell carcinoma (**a**), whereas scar tissue inhibit invasion as in this adenocarcinoma example (**b**). The only way for the carcinoma cells are invasion into lymphatics, which happened in the center

express different genes and proteins related to their function in cancer development. Specifically MLH1 was upregulated, whereas COX1, FGFR4, SMAD3, and p120 were downregulated [40]. Factors have been identified, which drive this differentiation of mesenchymal stem cells into myofibroblasts, namely, TGF-β and IL1β. TGF-β also induces the expression of α–SMA and FAP-α expression [41]. FAP (serine protease fibroblast activation protein) promote tumor growth in an endogenous mouse model of lung cancer driven by the K-rasG12D mutant. On the contrary FAP depletion inhibits tumor cell proliferation indirectly by increasing collagen accumulation,

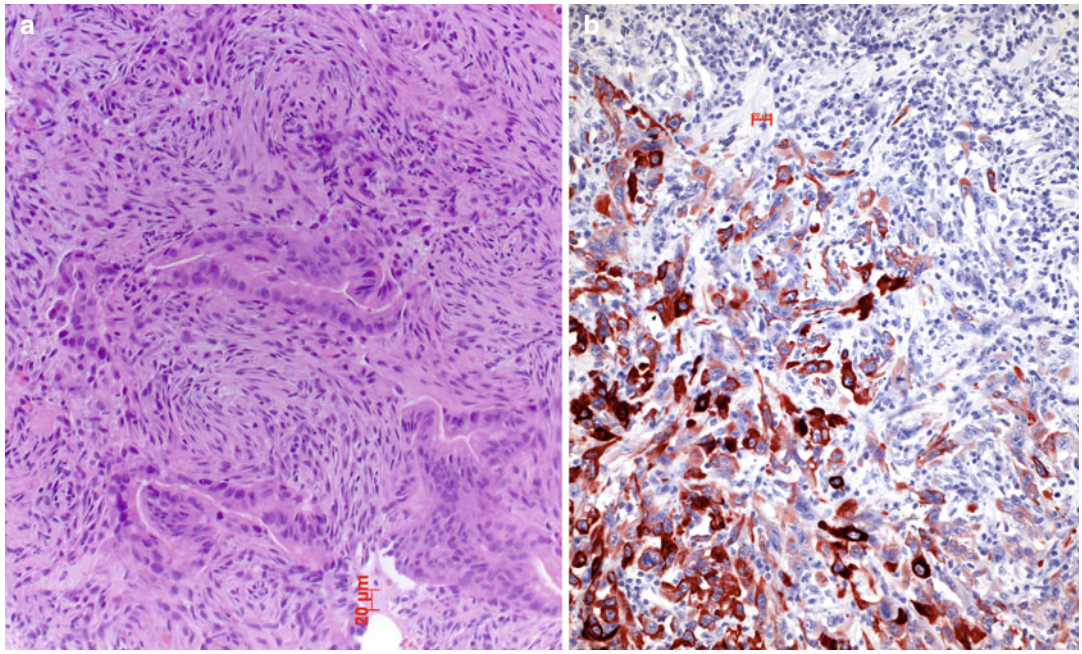

Fig. 18.5 Epithelial to mesenchymal transition (EMT) is common in pleomorphic carcinomas of the lung (**a**); this can also be demonstrated by cytokeratin immunohistochemistry, showing epithelial tumor cells positively stained on the left side, whereas tumor cells at the right side have lost cytokeratin and acquired vimentin (**b**)

decreasing myofibroblasts in number, and decreasing blood vessel density in tumors [42]. Most importantly myofibroblasts also express metalloproteinases (MMP) such as MMP-2, MMP-9, MMP-8, and MMP-7. So these cells actively take part in remodeling of matrix proteins. In addition MMP-8 actively participates in the process of fibrocyte migration [43].

In this context also changes of matrix proteins, their composition, and their orientation are important for tumor cell migration. Usually the matrix is composed of several proteins such as different types of collagen (I, III, IV, V; predominant collagen I), fibronectin, laminin, elastin, and osteonectin. These proteins provide stability to the stroma by their oriented deposition and network formation by cross-linking. They also serve as orientation molecules providing ligands for migrating leukocytes expressing adhesion molecules. Migrating tumor cells also uses this mechanism. As a further benefit, adhesion of SCLC cells to fibronectin, laminin, and collagen IV through β1 integrins confers resistance to apoptosis induced by standard chemotherapeutic agents. Adhesion to ECM proteins stimulated protein tyrosine kinase (PTK) activity in both untreated and etoposide-treated cells [44]. In NSCLC cells of the tumor, stroma selectively synthesize osteonectin (SPARC, normally only in bronchial cartilages) in case of intratumoral hypoxia and acidity. Osteonectin proven by immunohistochemistry favors cancer cell invasion and migration [45].

Another important factor is the orientation and composition of matrix proteins: high amounts of elastin favor resistance for tumor cell migration, whereas high collagen and organized oriented deposition promote tumor cell migration. Conversely direct cell contacts between tumor cells and fibroblasts can also create migratory-inhibitory matrix composed of unorganized collagens (I, III, IV, and V) and proteoglycans (biglycan, fibromodulin, perlecan, and versican). Thick desmoplastic fiber bundles inhibit the migration and invasion of tumor cells [46]. Matrix protein deposition seems to be in addition regulated by a tumor suppressor gene, frequently lost in lung cancer, RBM5 (RNA binding motif protein 5, chromosome 3p21.3). The encoded

protein plays a role in the induction of cell cycle arrest and apoptosis. Loss of RBM5 causes upregulation of Rac1, β-catenin, collagen, and laminin, which in turn increase cell movement. Consequently Rac1 and β-catenin correlate positively with lymph node metastasis in lung cancer patients [47]. Two other matrix proteins are less explored. Expression of periostin is associated with vimentin expression in the stroma or tumor epithelia and correlates with higher stage. The correlation of periostin expression with that of versican and collagen in advanced tumors was less obvious. Opposite to periostin expression of elastin was associated with less advanced disease [39]. However, this observation still needs confirmation as well as more in deep investigation for the function of these proteins.

So invasion, tumor growth, and tumor cell migration of lung cancer cells are regulated by many different factors, as cytokines, adhesion molecules and receptors, and genes acting either directly on tumor cells or cells of the microenvironment.

18.1.3 Escaping Immune Cell Attack

Usually tumor cells produce many modified proteins, which are recognized as foreign by dendritic cells and lymphocytes. Tumor cells are therefore attacked and destroyed by cytotoxic lymphocytes (CD8+). However, pulmonary carcinoma cells have developed different escape mechanisms to prevent this cytotoxic attack. By modulating the innate immune system, macrophages are preferentially forced to differentiate into M2 types as already explained. Another mechanism to protect tumor cell is to modify the pool of antigen-presenting dendritic cells (DC). Within dendritic cells, several functional quite opposite acting cell populations are discerned: conventional DC will present tumor antigens to T lymphocytes and force the production of cytotoxic T cells, whereas plasmacytoid and monocytoid DCs act as tumor protective cells. For example, bombesin derived from SCLC inhibits IL12 production by DC and their ability to activate T cells [48]. Tumor cells by secretion of TGF-β and prostaglandin E2 induce DCs to differentiate into regulatory DCs with a CD11c(low) CD11b(high) phenotype (also named plasmacytoid DC) and high expression of IL10, VEGF, and arginase I. These regulatory plasmacytoid DCs inhibited CD4+ T-cell proliferation [49] and thus act protumorigenic. Another action to prevent cytotoxic lymphocyte attack is to induce an influx of regulatory T cells (Treg). Treg downregulate the production and influx of cytotoxic T cells and NK cells and promote immune tolerance [50–52]. Finally also bone marrow-derived myeloid precursor cells (MDSC) may downregulate a T-cell-based immune reaction toward growing tumor cells by secreting arginase I [53]. Indoleamine 2,3-dioxygenase (IDO) and IL6 seem to play a regulatory role for these MDSC, as downregulation of IDO resulted in reduced lung tumor burden and improved survival in experimental settings. Loss of IDO resulted in an impairment of protumorigenic MDSC, whereas IL6 recovered both MDSC suppressor function and metastasis susceptibility. In addition vascular density was significantly reduced in Ido1-nullizygous mice [54].

In some carcinomas, preferentially in pulmonary squamous cell carcinomas, eosinophils are found in abundance. The role eosinophilic granulocytes play in NSCLC is not fully understood. It may be that variants of IL17 (IL17E) induce a helper two type of immune response, which in turn by the release of IL4 and IL5 causes tissue eosinophilia. In one study it was shown that IL17E has antitumor activity. Injections of recombinant IL17E resulted in significant antitumor activity. Combining IL17E with chemotherapy increased the antitumor efficacy in a xenograft model [55]. Eosinophils are directly acting cytotoxic against the tumor cells, for example, by releasing cytotoxic basic proteins, which was not explored in this study.

18.1.4 Migration

After having established the primary tumor and organized nutrition as well as protection for immune cell attacks, the tumor cells have to acquire changes to migrate to distant sites and

establish metastasis. There are two different forms how tumor cells migrate: single cell or small cell cluster movement as it is seen in small cell carcinoma as well as undifferentiated NSCLC and movement by large clusters of organized cells such as in acinar adenocarcinoma or some cases of squamous cell carcinoma (Figs. 18.6a, b, 18.7a, b, and 18.8a, b). For single cell and small clusters, migration seems to be much easier since single cells can more easily adapt, for example, a spindle cell morphology, which enables better movement. Tumor cells during migration reduce or even abolish cytokeratin filaments and increase or de novo express α-actin and vimentin; this is commonly seen in pleomorphic carcinomas (Fig. 18.5b), carcinosarcomas, high-grade squamous cell and adenocarcinomas, and SCLC. Lung adenocarcinomas with high smooth muscle actin gene ACTA2 expression showed significantly enhanced distant metastasis and unfavorable prognosis. ACTA2 downregulation remarkably impaired in vitro migration, invasion, clonogenicity, and transendothelial penetration of adenocarcinoma cells without affecting proliferation. ACTA2 upregulation in lung adenocarcinoma cells was also connected to expression of c-MET and focal adhesion kinase (FAK), whereas ACTA2 targeting by siRNAs and shRNAs resulted in loss of mesenchymal characteristics [56]. Migration within the stroma requires several changes in tumor cells; one of these is formation of invadopodia. Tyrosine kinase substrate 5 (Tks5) is a scaffolding protein necessary for the formation of invadopodia. There are different isoforms, some of them (short isoforms) associated with reduced others (long isoforms) with increased metastasis [57–59]. Expression of Tks5 together with the expression of α-actin is further regulated by cortactin and neural Wiskott-Aldrich syndrome protein (N-WASP), which also regulate the expression of metalloprotease membrane type 1 matrix metalloprotease (MMP-14) [58]. However, migration of tumor cells seems to be regulated by different genes, so probably there is not a single mechanism for each tumor type, but more likely that tumor cells individually have adapted different mechanisms of migration protocols and used it during carcinogenesis. As an example myosin heavy chain 9 (MYH9) and copine III (CPNE3) positively correlate with the migration and invasion properties of lung cancer cell lines. If CPNE3 was knocked down, the metastatic abilities were inhibited in a mouse model. Also CPNE3 protein expression levels were positively correlated with the clinical stage in NSCLC [60]. In another study, nestin protein expression significantly correlated with tumor size and lymph node metastasis in NSCLC and also poor survival in patients with adenocarcinoma. Nestin inhibition by shRNA decreased proliferation, migration, invasion, and sphere formation in

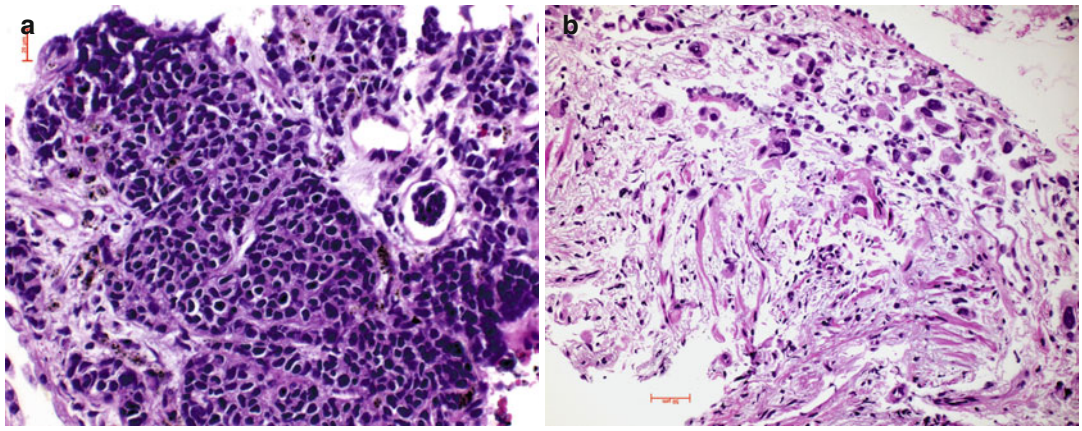

Fig. 18.6 Tumor cell migration: (**a**) The small cells in this neuroendocrine carcinoma move in small cell groups, whereas the adenocarcinoma cells (**b**) move almost as single cells

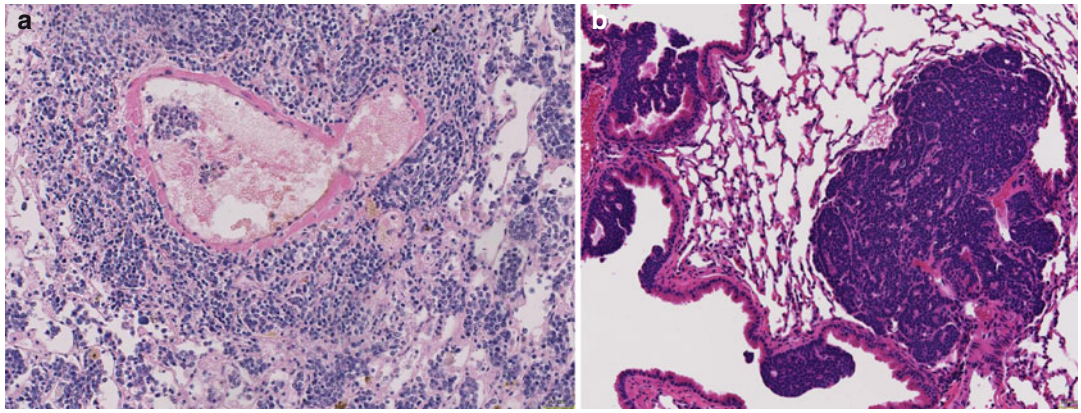

Fig. 18.7 Tumor cell migration: (**a**) This mixed small and large cell neuroendocrine carcinoma migrate as single or small cell clusters, whereas the small cell neuroendocrine carcinoma in (**b**) migrate in small complexes in this very early stage; experimental mouse model (Cases courtesy of Adi Gazdar)

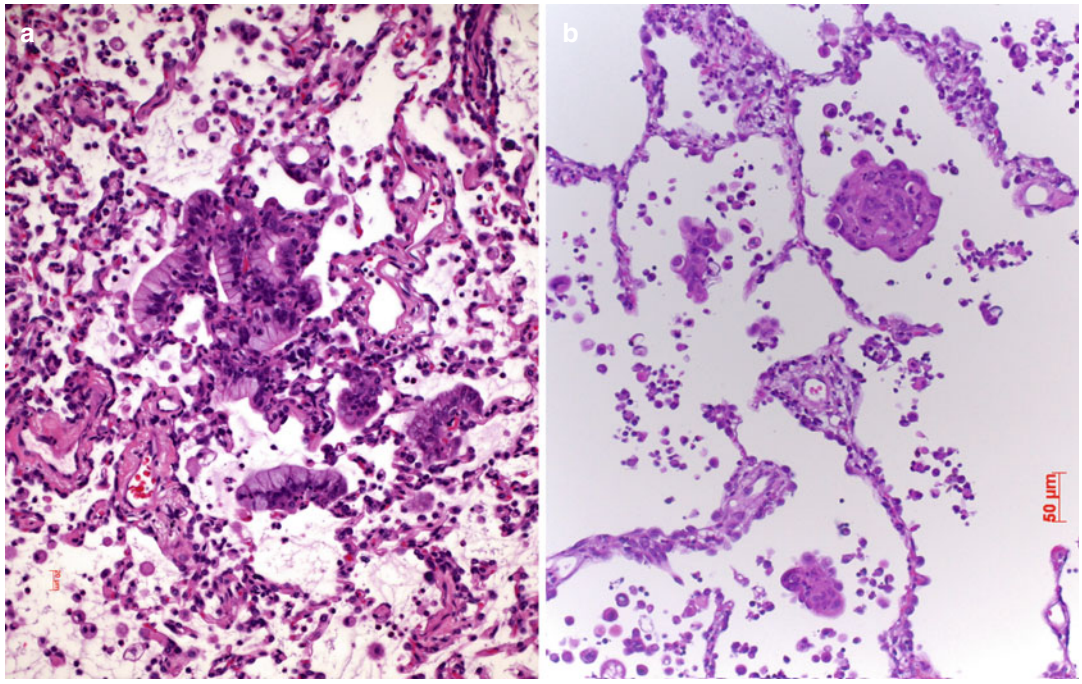

Fig. 18.8 Tumor cell migration: (**a**) A mucinous adenocarcinoma moves in larger cell complexes along the alveolar walls, still using the supply by the alveolar septa; in (**b**) an unusual 3D complex of squamous cells moving as spheroids

adenocarcinoma cells [61]. One of the major studied mechanisms of tumor cell migration is EMT, which again is seen in tumors with single cell or small cluster migration type (Fig. 18.9a–c).

When looking up studies on EMT, a huge amount of published article can be found in databases. The major surprise is that different genes are associated with EMT. And even when focusing on lung cancer studies, there are still different genes found to trigger EMT. One of the most often found EMT-associated genes are Twist, Snail, and TGFβ1.

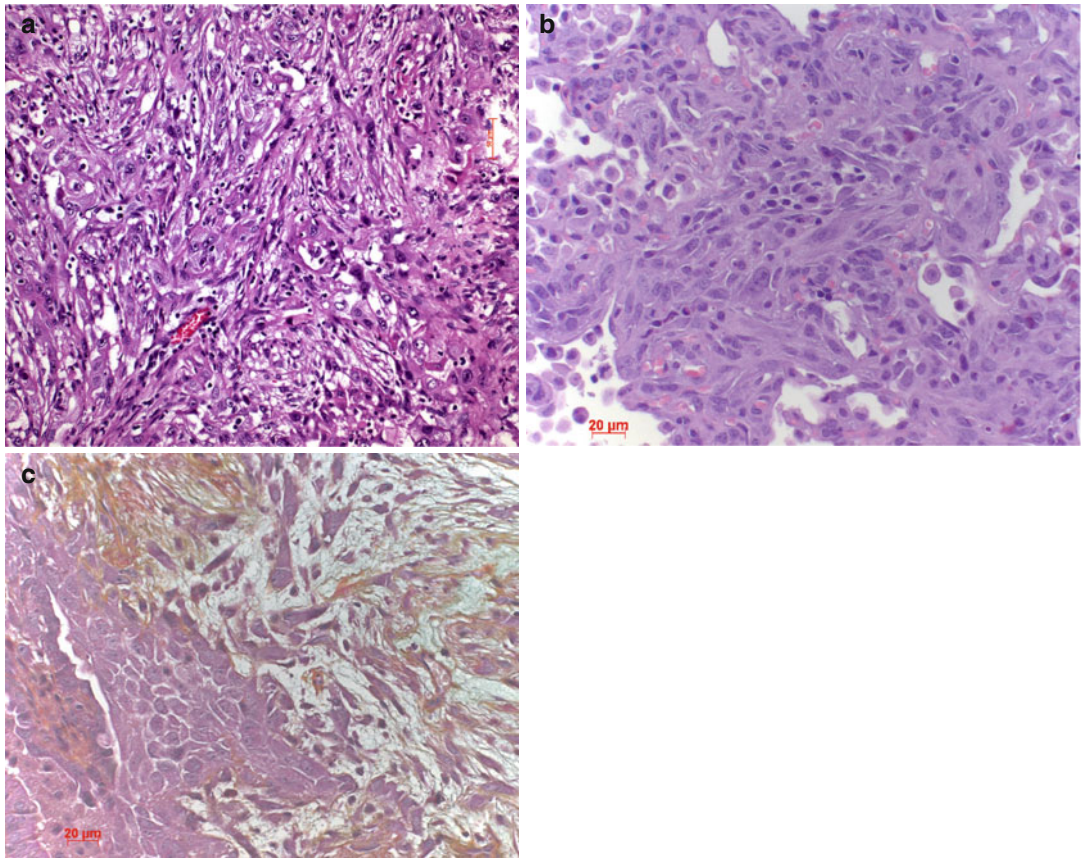

Fig. 18.9 (**a**) EMT in a pleomorphic carcinoma with spindle cells, (**b**, **c**) EMT in mouse model of KRAS-induced adenocarcinomas with additional expression of mutant TP53. In (**c**) the Movat stain better demonstrates the invasion of the spindle tumor cells into the desmoplastic stroma

Suppression of Twist expression in metastatic mammary carcinoma cells inhibits their ability to metastasize from the mammary gland to the lung. Ectopic expression of Twist resulted in loss of E-cadherin-mediated adhesion, activation of mesenchymal markers, and induction of cell motility, suggesting that Twist promotes EMT [62]. In another study, Twist was selectively associated with EGFR-mutated adenocarcinomas. Twist expressed in lung adenocarcinoma cell lines with EGFR mutation showed increased cell mobility. A decrease of EGFR pathway through EGF retrieval or inhibition of Twist expression by small RNA reversed the phenomenon. These findings supported that Twist promotes EMT in EGFR-mutated lung adenocarcinoma [63]. In the study by Pirozzi, the focus was on TGFβ1. They used two epithelial cell lines, which acquired a fibroblast-like appearance when treated by TGFβ1. By inhibiting TGFβ1, vimentin and CD90 were downregulated and cytokeratin, E-cadherin, and CD326 upregulated. TGFβ1 also upregulated Slug, Twist, and β-catenin, thus confirming its EMT property. Interestingly also some stem cell markers as Oct4, Nanog, Sox2, and CD133 were overexpressed too, linking EMT to tumor stem cells [64]. Adhesion plays a major role in EMT, therefore not surprisingly studies have focused on Wnt, Catenin, and GSK3β pathway. Loss of SARI (suppressor of AP-1, also called BATF2) expression initiates EMT, causing repression of E-cadherin and upregulation of vimentin in lung adenocarcinoma cell lines and in human lung adenocarcinomas. By knockdown endogenous SARI in a human lung xenograft mouse model, multiple lymph node metastases

developed. SARI has been shown to regulate EMT by modulating the (GSK)-3β-β-catenin signaling pathway [65]. In the study by Blaukovitsch, another pathway for EMT was shown: Snail and Twist were not involved in pulmonary sarcomatoid carcinomas but instead upregulation of c-Jun and consecutive overexpression of vimentin and fascin was seen [66].

When dissecting sites of metastasis, the way EMT is regulated gets more diverse: PREP1 accumulation was found in a large number of human brain metastases of various solid tumors, including NSCLC. PREP1 induces the expression of multiple activator protein 1 components including Fos-related antigen 1 (FRA-1). FRA-1 and PBX1 are required for EMT triggered by PREP1 in lung tumor cells [67]. The study by Shen showed that increased levels of long noncoding RNA MALAT1 promotes lung cancer brain metastasis by EMT, whereas silencing of MALAT1 inhibits lung cancer cell migration and metastasis in the brain [68]. So far nothing similar was investigated for bone metastasis by pulmonary carcinomas.

We have now focused on single cell and small cluster migration. However, in surgical pathology routine, most well-differentiated carcinomas including lung carcinomas move in large cell clusters, for example, acinar adenocarcinomas will show nicely structured acini deep within the stroma and even within blood vessels (Fig. 18.10a, b). The mechanisms how these tumor cells manage their coordinated movement by retaining their epithelial structure is almost unknown. These carcinomas do not undergo EMT. Recently in an investigation using *Drosophila* border cells as a model, the process of migration of large cell complexes were elucidated. By RNAi silencing 360, conserved signaling transduction genes were knocked down to identify essential pathways for border cell migration. Four genes associated with TGF-β signaling were identified: Rack1 (receptor of activated C kinase), brk (brinker), mad (mother against dpp), and sax (saxophone). Inhibition of Src activity by Rack1 may be important for border cell migration and cluster cohesion maintenance. Although this study focused on signaling pathways involved in collective migration during embryogenesis and organogenesis, these data could be the first step in understanding migration of carcinoma cell complexes in metastasis [69].

18.2 Vascular Invasion: Lymphatic/Hematologic

18.2.1 Blood Vessels

Tumor cells orient themselves along adhesion molecules as expressed by matrix proteins, but in addition they also sense for oxygen and most probably also orient themselves for higher oxygen tension [70]. Invasion into blood vessels is

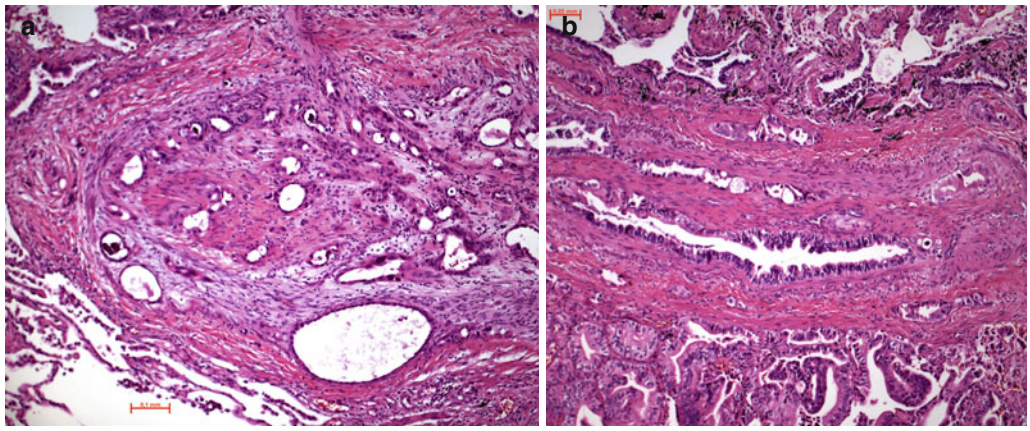

Fig. 18.10 Vascular invasion: In (**a**) tumor cells are scattered in acinar complexes within the intima of this pulmonary artery; in (**b**) large acinar and papillary adenocarcinoma complexes can be seen within this blood vessels, demonstrating the other example of invasion as large tumor cell complexes

very similar to invasion into the stroma: tumor cells have already learned to degrade proteins of the basal lamina at the epithelial border, and similar proteins form the matrix of small blood vessels. Forming holes into the basal lamina of these blood vessels is therefore easily done and tumor cells migrate into the intima. However, a new problem arises for tumor cells within the circulation: shear stress due to tumor cell deformation in small blood vessels and the problem with coagulation.

Shear stress is usually well tolerated by those tumor cells which underwent EMT: tumor cells expressing vimentin and α-actin can adapt to the capillary diameters, but cells still expressing cytokeratins might burst. This is one of the reasons why a majority of tumor cells do not survive within the circulation [71]. With respect to coagulation, tumor cells on one hand have to avoid being trapped within a blood clot, but on the other hand will need a clot to slow down the speed of the bloodstream, attach to the clot, and use it for extravasation [72]. Clot formation might be induced by tissue factors being produced and released by macrophages. Impairment of macrophage function decreased tumor cell survival without altering clot formation, demonstrating that the recruitment of functional macrophages was essential for tumor cell survival [73]. Another way how tumor cells might trigger clot formation has been demonstrated in mucinous adenocarcinomas. Mucins secreted by the tumor cells induced platelet aggregation and furthermore interacted with L-selectin and platelet-derived P-selectin without thrombin generation [74]. This interaction already points to the next step: adherence to vascular walls for extravasation. Coming back to tumor cell trapping by blood clots, it seems that carcinoma cells require the assistance of macrophages and granulocytes for fibrinolysis. In a study of lung carcinomas, fibrinolytic components as tissue plasminogen activators (tPA) and the inhibitors PAI-1 and PAI-2 were all negative in tumor cells, whereas urokinase-specific antibodies stained loosely packed tumor cells and macrophages. Both PAI-1 and PAI-2 were most prominently expressed within interstitial and alveolar macrophages [75]. In another study analyzing pulmonary adenocarcinomas, a positive correlation was found between Ets-1 and urokinase-type plasminogen activator (u-PA) expression [76].

18.2.2 Lymphatic Vessels

Invasion into lymph vessels is easier than into blood vessels due to the tiny wall of the former. In addition carcinoma cells might already enter the lymphatic stream by the interstitial channels of the lymph draining system. On the contrary tumor cells can easily congest lymph vessels. This can reverse the lymph flow, which might explain unusual sites of lymph node metastasis and so-called skip lesions. In contrast to the situation within blood vessels, carcinoma cells in lymphatics have to deal with the immune system. So survival is dependent on induction of immune cell escape mechanisms (see above).

Whereas carcinoma cells entering the bloodstream might cause early-onset distant metastasis and thus shorten overall survival of the patient [1], propagation of carcinoma cells along the lymphatics will set distant metastasis later. These tumor cells will set primarily metastasis within regional lymph nodes.

18.3 Extravasation

Carcinoma cells have to escape the circulation. However, the process how tumor cells select their final destination is still not clear. A lot of information was gained from studies on homing mechanisms of lymphocytes and extravasation of granulocytes. The most important sites are venules with high endothelia. First of all the blood flow is reduced, which enables tumor cells to roll over the endothelia and express adhesion molecules. These adhesion molecules need to find their respective and specific receptors for adhesion. Once adhering to the endothelia, tumor cells have to activate the coagulation system for better and firm adherence, followed by production of holes between endothelia for migration out of the vessel lumen. Several factors have been

identified, such as caveolin, which increases cell permeability. Loss of caveolin results in increased phosphorylation of VEGFR-2 and decreased association with the adherens junction protein, VE-cadherin. Loss of caveolin increases endothelial permeability and tumor growth [77]. Tumor cells might use different selectins such as E- and P-selectin to adhere to specific sites on the endothelia of venules. Also other selectins might be used, as has been shown by knockout of these selectins: PSGL-1, CD44, and CEA could be detected in SCLC cells. By intravital microscopy SCLC cells were shown to roll along vessel walls mimicking leukocyte behavior [78].

18.4 Preparing the Distant Metastatic Focus

It is well known that few tumor cells survive within the circulation. Even more, from those tumor cells, which survive and finally leave the circulation and settle at a distant site, only a small proportion progress and form metastatic nodules [71]. Usually single tumor cells die (probably with the exception of small cell carcinoma cells); small clusters form micronodules but do not grow further. Another enigma is the selection of metastatic sites: in general lung, cancer cells prefer the lung, brain, bones, and adrenal glands, and within lung carcinoma types, small cell neuroendocrine carcinomas as well as adenocarcinomas metastasize into the brain, whereas squamous cell carcinomas prefer bones. What homing mechanisms are in action? And, moreover, how did carcinoma cells communicate with this new stroma? For example, in the brain, carcinoma cells need to organize their new homing by communicating with glia cells and also to manipulate microglia to prevent attacks by immune cells and finally induce angiogenesis for their supply in nutrients and oxygen.

In the following paragraphs, we will focus on different aspects of homing, extravasation, and creation of a metastatic niche in different organs.

To leave the circulation, lung cancer cells need signals, which seem to be specific for each organ. Some of these such as E-selectin are used in several carcinomas including breast and lung. Systemic inflammation may increase the expression of E-selectin, which mediate lung metastasis of an experimental breast cancer model [79]. Hyperpermeability is also a factor important for homing, because this slows down the blood flow and enables rolling of the tumor cells over the endothelia. Hyperpermeability is mediated by endothelial cell-focal adhesion kinase (FAK), which upregulates E-selectin, leading to preferential homing of metastatic cancer cells to these foci [80]. Attachment of tumor cells, however, needs an activation of several other adhesion molecules. Once tumor cell attach on endothelia, they cause the induction of vascular cell adhesion molecule-1 (VCAM-1) and vascular adhesion protein-1 (VAP-1), which is dependent on tumor cell clot formation, induced by tissue coagulation factors [81]. Also changes in the cell-to-cell junctions of endothelia are necessary for the tumor cells, to move through interendothelial gaps. This is facilitated by an overexpression of angiopoietin-2 [82]. In addition also MD-2, a coreceptor for Toll-like receptor 4, triggers the formation of regions of hyperpermeability in mice by upregulating C-C chemokine receptor type 2 (CCR2) expression. The CCR2-CCL2 system induces the abundant secretion of permeability factors such as serum amyloid A3 and S100A8 [83].

Since all these investigations use different models and analyze different tumor tissues or none, it is not surprising that different investigators found different acting molecules. Using cell cultures from an aggressive human squamous cell carcinoma, Chen subcultured different tumor clones and showed a different expression profile for members of the β1 integrin family. By the intravenous inoculation into scid mice, the clonotypes differed in VLA-1 and VLA-2 expression, where high levels of VLA-1 and VLA-2 displays an increase in metastasis [84]. The group by Sadanandam identified 11 unique peptides specific for homing to the lung, liver, bone marrow, or brain. Semaphorin 5A and its receptor plexin B3 were identified as relevant for homing to these organ sites [85]. A major factor for homing of carcinoma cells, including the colon, lung, and breast, is the chemokine receptor CXCR4. The

unique function of CXCR4 is to promote the homing of tumor cells to their microenvironment at the distant organ sites [86]. Acute inflammations seems to promote CXCR4 expression and may alter the lung microenvironment and prepare it for a metastatic "niche" [87]. CXCR4 inhibition reduced the influx of myeloid-derived cells and impaired lung metastases. CXCR4 is specifically expressed in stromal cells that prepare the pro-tumor microenvironment [88].

Several other signaling proteins are also involved in metastatic homing and formation of a metastatic focus; however, how these different molecules interact with each other is not known. In a study looking for the relationship of miRNA and metastasis, Liu et al. found that expression of miR-26a dramatically enhanced lung cancer cell migration and invasion. Matrix metallopeptidase 2 (MMP-2), vascular endothelial growth factor (VEGF), Twist, and β-catenin were upregulated. Phosphatase and tensin homolog (PTEN) was a direct target of miR-26a. They found that miR-26a increased AKT phosphorylation and nuclear factor kappa B (NFκB) activation. So miR-26a enhanced lung cancer metastasis via activation of AKT pathway by PTEN suppression [89]. MALAT1 (metastasis-associated lung adenocarcinoma transcript 1)-deficient cells are impaired in migration and form fewer tumor nodules in a mouse xenograft. Gene expression of MALAT1 is critical for lung cancer metastasis [90]. In addition in another investigation, it was shown that MALAT1 cooperates with eIF4A1 and thymosin-β4 in promoting metastasis in NSCLC [91].

18.4.1 Angiogenesis

Angiogenesis at the metastatic site in one part follows the same principles as in the primary focus; however, there is one major problem: whereas at the primary focus, lung carcinoma cells cross talk with stroma cells by mechanisms and transmitters which have been developed during the process of developing from the precursor lesion to in situ carcinoma to invasive carcinoma, this cross talk is different in the new metastatic site. Brain glia cells or bone marrow stroma cells might respond to other signals than those stroma cells within the lung. So the major developmental step to establish a metastatic focus is communication with the stroma, and further more communication might be different depending on the location. In one investigation a bridge was built between angiogenesis at the primary and metastatic site. CXCL12 was expressed in tumor cells and in tumor vessels; CXCR7 was expressed by tumor and endothelial cells in the primary tumor and in the brain metastasis. CXCR4 showed a nuclear positivity in all samples, but only CXCL12 expression in tumor endothelial cells was significantly correlated with shorter survival [92].

Interaction with stroma: There are no published data, which could highlight general mechanisms by which lung carcinoma cell communicates with their stromal counterparts; however, communication at different organ sites have been studied and therefore will be discussed in this paragraphs.

18.5 Metastasis

When discussing metastasis many questions arise, which are still incompletely answered: when does metastasis occur? Is there a need for a certain size of the primary tumor that cells leave and start migrating? Is hypoxia the clue? Are tumor cells randomly moving out from the tumor or are these selective clones, and are these genetically different from the dominant clone? Do carcinoma cells move collectively or as single cells? These questions have been discussed extensively in the literature, but especially when comparing metastasis in lung cancer, several good examples are there to answer at least some of these questions.

Small cell neuroendocrine carcinoma has some unique features: when looking at the invasion front, it is evident that this carcinoma prefers migration of single cells and small cell clusters composed of three to five cells (Figs. 18.6a and 18.7a). In blood and lymphatic vessels, SCLC usually presents with single cells or small clusters of cells. Quite common is the finding of several large brain metastases and a very small primary tumor, which might even

escape the detection by HRCT. This raises the question of early migration of carcinoma cells from the initial focus and setting metastasis early in the tumor development. In contrast squamous cell carcinoma can form a large primary tumor and when surgically removed has not formed metastasis; even some cases have not set regional lymph node metastasis. Migrating SCC often form large complexes of cells and when seen intravascular again present with large cell complexes. So both extremes do occur in lung carcinomas. In adenocarcinomas both types of migration and metastasis do occur, usually large migrating complexes of well-differentiated acinar or papillary adenocarcinomas (Fig. 18.11a) and small cell clusters of solid or mucinous adenocarcinomas. The aspect of genetic heterogeneity in primary and metastatic tumor clones has been investigated in studies comparing primary and metastatic carcinomas. More important it seems that not only primary carcinomas are different from metastasis, but also metastases differ among each other. To be clear, driver mutations or general genetic aberrations in primary and secondary tumors are still identical, but additional genetic modifications arise within the metastases.

When looking up the frequency of metastasis of lung carcinomas, there are some preferential sites, as the bone 34.3 %, lung 32.1 %, brain 28.4 %, adrenals 16.7 %, and liver 13.4 % [3]. Since specific driver gene mutations have been detected in adenocarcinomas, a lot of speculations about the frequency of brain metastasis in EGFR-mutated and ALK1-rearranged adenocarcinomas were raised. Not many reports have addressed this question. Hendriks et al. reported that in their cohort of 189 patients, there was no difference between EGFR-mutated, KRAS-mutated, or WT adenocarcinomas. There was only a longer post metastatic bone disease survival in EGFR-mutated patients [93]. In another investigation the authors analyzed the frequency of the major types of pulmonary carcinomas. The most frequent metastatic sites were the nervous system, bone, liver, respiratory system, and adrenal gland. Liver (35 %) and nervous system (47 %) metastases were common in small cell lung cancer and bone (39 %) and respiratory system (22 %) metastases in adenocarcinoma. Women and younger patients presented with more metastases to the nervous system. Liver metastases conferred the worst prognosis in large cell carcinomas [94].

This correlates quite well with the study by Shin et al., where the authors analyzed adenocarcinoma metastasis in the brain for EGFR mutations. A strong association between EGFR mutation status and brain metastasis was observed, whereas no association was observed between EGFR mutation status and extracranial metastases. In addition, the number of brain metastases was significantly correlated with the EGFR mutation status [95]. This fits with the study cited above because EGFR mutations are more frequently seen in females as compared to men.

18.5.1 Brain Metastasis

Research coming from brain metastasis of breast and NSCLC has raised several important findings. First metastatic carcinomas can colonize the brain in different ways. Renal cell carcinomas most often form metastases which are well circumscribed and do not grow out of the microglia pseudocapsule, whereas SCLC tend to form small metastatic foci and tumor cells grow into the microglia pseudocapsule and beyond into brain parenchyma. This has nicely been demonstrated by a coculture system consisting of an organotypic mouse brain slice and epithelial cells embedded in matrigel (3D cell sphere) [96]. In addition the same group of researchers has shown that microglia support invasion and colonization of brain tissue by breast and lung cancer cells (Fig. 18.11a, b). This is under the control of the Wnt pathway, as upregulation of Dickkopf-2 an inhibitor of Wnt inactivates the prometastatic function of microglia. Similar to tumor-dendritic cell interaction, bacterial lipopolysaccharide shifts tumor-educated microglia into a classical M1 phenotype, reduces their proinvasive function, and unmasks inflammatory and Wnt signaling as the most strongly regulated pathways [97]. Several factors have been identified as being specifically involved in regulating brain metastasis,

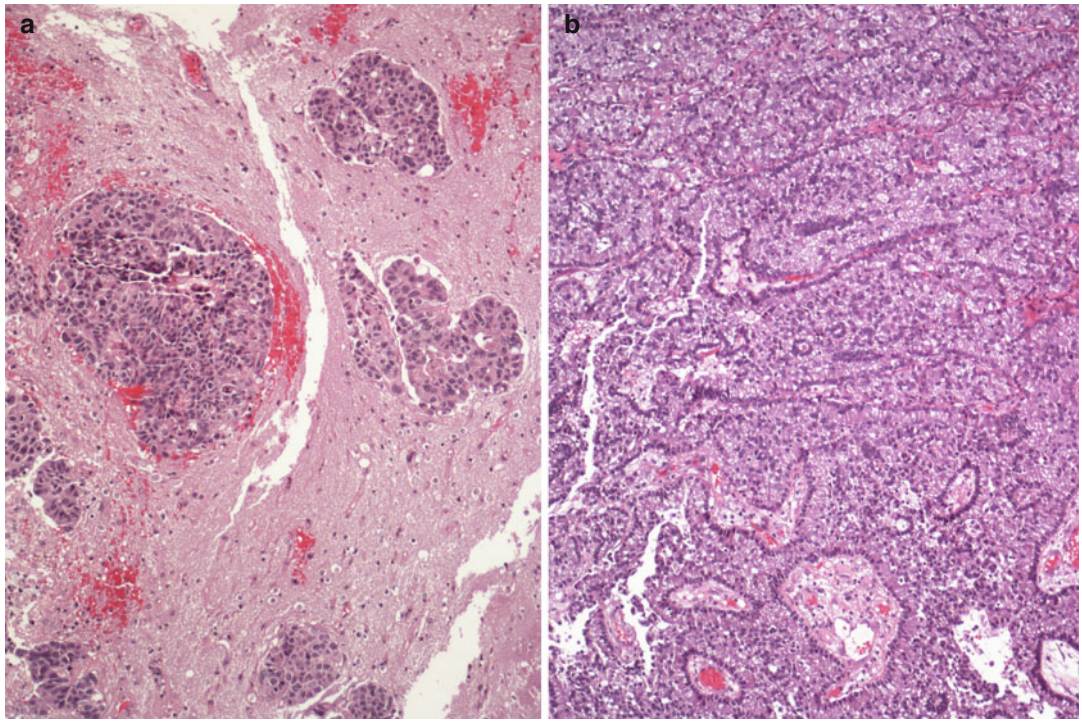

Fig. 18.11 Brain metastasis: (**a**) Cells of an adenocarcinoma interacting with astrocytes and microglia cells; (**b**) large adenocarcinoma complexes have acquired huge areas of the brain, but in addition imitate ependymal structures (Courtesy of Ulrike Gruber-Moesenbacher, Feldkirch)

but so far these are still isolated factors, and the main question, how these different factors interact, remains unanswered.

Among the different cells of the brain, astrocytes seem to serve invading carcinoma cells. Astrocytes secrete matrix metalloprotease-2 (MMP-2) and MMP-9 that proactively induced human lung and breast tumor cell invasion and metastasis formation [98]. In addition factors from the coagulation cascade are important. Plasmin acts as a defense against metastatic invasion by converting membrane-bound astrocyte FasL into a paracrine death signal for cancer cells and by inactivating the axon pathfinding molecule L1CAM, which metastatic cells express for spreading along brain capillaries and for metastatic outgrowth. But metastatic carcinoma cells from lung and breast secrete neuroserpin and serpin B2, to prevent plasmin generation and its metastasis-suppressive effects [99]. Within the Wnt pathway, LEF1/TCF4 acts independently of β-catenin in cerebrally metastasized human lung adenocarcinomas [100]. Downregulation of E-cadherin was also observed in a majority of adenocarcinoma and small cell lung cancer samples. LOH of the CDH1 gene was frequently found in SCLC. Altered expression of Dishevelled-1, Dishevelled-3, E-cadherin, and beta-catenin was present in brain metastases of SCLC and adenocarcinoma, again pointing to the importance of the Wnt signaling [101]. In another study, peritumoral brain edema was shown to be associated with increased β-catenin and E-cadherin and decreased CD44v6 and caspase-9 expression in brain metastatic squamous cell carcinoma [102]. These findings were confirmed in another study showing a significant correlation of increased collagen XVII in adenocarcinoma and increased caspase-9 and CD44v6 and decreased cellular apoptosis susceptibility protein (CAS) and Ki-67 in squamous cell carcinoma in brain metastasis [103].

Interestingly when looking up, adenocarcinomas with ALK1 rearrangement FGFR1 gene

amplification correlated significantly with brain metastases. Although in these cases there were also higher numbers of visceral metastases, FGFR1 amplifications in brain metastases of adenocarcinomas were fivefold more frequent than in the primary tumors [68]. Also a cross talk of EGFR-MET was reported in adenocarcinomas with brain metastasis. This was not a direct interaction, but a signaling via the activation of mitogen-activated protein kinases (MAPK). EGFR-MET cross talk was independent from the mutation status of EGFR. MET signaling promoted migration and invasion. MET inhibition decreased the incidence of brain metastasis [104]. Also CXCR4 seems to play a role in brain metastasis. CXCR4 protein was highly overexpressed in patients with brain-specific metastasis, but significantly less in NSCLC patients with other organ metastases and without metastases [105].

ADAM9 levels were relatively higher in brain metastases than the levels observed in primary lung tumors. ADAM9 regulates lung cancer metastasis to the brain by facilitating the tPA-mediated cleavage of CDCP1 [106]. In a subsequent study, it was shown that ADAM9 regulated miR-218, which targets CDH2 in aggressive lung cancer cells. The downregulation of ADAM9 upregulated SLIT2 and miR-218, which together downregulated CDH2 expression. This study revealed that ADAM9 activates CDH2 through the release of miR-218 inhibition on CDH2 in lung adenocarcinoma [107].

A lot of interesting studies focused on the comparison of genomic alterations between primary lung carcinomas versus brain and bone metastasis. The hypothesis is that there might be a clonal diversity between these two. It is still not clear if genetic differences between the primary tumor and the metastatic site are a primary event, i.e., clones are existing within the primary tumor or, if these are secondary events, reflecting the interaction of the carcinoma cells with the microenvironment and the cells therein. Mock et al. found gene copy number variations between primary and CNS metastasis by array CGH. Genes with amplified copy numbers in primary and metastatic tumors were related to DNA replication and mismatch repair. Genes only amplified in the metastatic tumor were related to leukocyte migration and organ development. Genes with a lower copy number in the metastatic tumor were related to proteolysis, negative regulation of cell proliferation, and cell adhesion [108].

Many more studies focused on specific genes associated with brain metastasis. Lower LKB1 copy number variations and KRAS mutation were significantly associated with more brain metastasis, even predicted brain metastasis [109]. In the study by Gao, miR-95-3p suppressed tumorigenicity and brain metastasis in vivo and increased overall survival and brain metastasis-free survival. Accordingly the levels of miR-95-3p, pri-miR-95, and ABLIM2 mRNA were decreased, and cyclin D1 was increased in brain metastatic tissues [110]. In another study the expression of ACTN4 (actinin α4) was associated with lung cancer metastasis to the brain. The protein essential for cytoskeleton organization and cell motility was significantly elevated in the metastatic brain tumor but not in the primary lung cancer [111].

As with many marker studies focusing on single genes/proteins, a selection bias or just an over interpretation does occur. We already discussed MALAT1 in the setting of invasion and metastasis. Shen and coworkers found higher levels of MALAT1 in brain metastases compared to other extrapulmonary sites. In the in vitro experiments, it turned out that the major function of this lnRNA is EMT [68]. What can be concluded is that EMT seems to be required for tumor cells invading brain tissues, but MALAT1 is not a brain metastasis gene "per se." A similar investigation searched for brain metastasis genes and came up with an EMT regulator: pre-B-cell leukemia homeobox (Pbx)-regulating protein-1 (Prep1) overexpression triggered EMT, whereas PREP1 downregulation inhibits the induction of EMT in response to TGF-β. PREP1 modulates the sensitivity to SMAD3 and induces the expression of Fos-related antigen 1 (FRA-1). Both FRA-1 and PBX1 are required for the mesenchymal changes triggered by PREP1 in lung tumor cells. PREP1-induced mesenchymal transformation correlates with increased lung colonization and PREP1 accumulation was found in human brain metastases [67]. Similarly migration seems to play a role

in brain metastasis, not surprisingly, since migration is often associated with EMT. Han et al. showed that knockdown of KDM5B and SIRT1 genes specifically inhibits lung cancer cell migration in vitro. SIRT1 was highly expressed in brain metastasis. Using other lung cancer cell lines, the authors showed that the function of SIRT1 correlates with cell migration [112]. There are not many studies looking for the influence of molecules of the adhesin family. Nasser and colleagues investigated E-cadherin expression. Low E-cadherin expression was associated with increased risk of developing brain metastasis. By treating tumor in a mouse model with pioglitazone, a peroxisome proliferator-activated receptor γ-activating drug prevented loss of E-cadherin expression and reduced expression of MMP-9 and fibronectin and furthermore the development of brain metastasis [113].

Two studies showed an association of genotypic variants with brain metastasis: in the study by Li et al., genotypes for AKT1 and PI3K were associated with brain metastasis risk (AKT1, rs2498804; AKT1, rs2494732; and PIK3CA, rs2699887) [114]. In the study of Kanteti, genotype variations for SMAD6 (rs12913975) and INHBC (rs4760259) were associated with risk of brain metastasis [115].

Whereas most studies on brain metastasis focused on the most common lung adenocarcinoma, Riihimaki and coworkers studied squamous cell carcinomas, which rarely present with brain metastasis. They found "truncal" PTEN loss and PI3K-aberrant tumors to be associated with brain metastases. There was also a genetic heterogeneity between lung primaries and brain metastases [116].

18.5.2 Lung Metastasis

Although pulmonary metastasis is common in adenocarcinomas as well as SCLC, not much is known about specific molecular mechanisms. In the study by Ruoslahti, connexin-43 was identified as adhesion molecule facilitating "homing" to the lung endothelial cells. Connexin-43 was highly upregulated in tumor cells during endothelial cell contact [117].

18.5.3 Bone Metastasis

In bone metastasis research reports focused on two different aspects of colonization, homing mechanisms and interaction of carcinoma cells with the bone/bone marrow stroma. In the work of Yang, PDGFRβ was found to be the main tyrosine kinase expressed in BM stromal ST-2 and MC3T3-E1 preosteoblastic cells. In incubation of ST-2 and human BM endothelial cells with sunitinib, a PDGFRβ inhibitor led to growth inhibition and induction of apoptosis. Sunitinib produced extensive disruption of tissue architecture and vessel leakage in the BM cavity. Pretreatment of ST-2 cells with sunitinib hindered adhesion to lung cancer cell lines. Pretreatment of mice with sunitinib before intracardiac inoculation of A549M1 or H460M5 cells caused marked inhibition of tumor cells homing to bone, whereas no effect was found when tumor cells were pretreated before inoculation [118]. Several studies focused on the reaction of osteoclasts, which cell type seems to be important for creating a metastatic "niche" for tumor cells in the bone.

Knockdown of DDR1 by siRNA showed reduced invasiveness in collagen matrices and increased apoptosis. Conditioned media of DDR1 knockdown cells decreased osteoclastogenic activity in vitro. In a bone metastasis model lacking DDR1, decreased metastatic activity and reduced tumor burden and osteolytic lesions were achieved. These resulted also in a substantial reduction of tumor cells reaching the bone compartment [119]. Vincent et al. showed induction of TGF-β-dependent osteoclastogenic bone resorption and enhanced stroma-dependent metalloproteolytic activities by TCF4 and PRKD3 and anchorage-related proteins MCAM and SUSD5 resulting in aggressive osseous colonization [120]. In another study stromal cell-derived factor-1 (SDF-1) secreted by osteoblasts and bone marrow stromal cells enhanced the invasiveness of lung cancer cells by increasing MMP-9 expression through the CXCR4/ERK/NFκB signal transduction pathway [121]. In another approach researchers focused on miRNAs associated with bone metastasis of lung cancer. Seven miRNAs

were downregulated and 21 miRNAs were upregulated in lung adenocarcinoma. Functional bioinformatics annotation analysis indicated that the MAPK, Wnt, and NFκB signaling pathways, as well as pathways involving the matrix metalloproteinase, cytoskeletal protein, and angiogenesis factors, are involved in orchestrating bone metastasis [122]. Finally in the study by Luis-Ravelo, the function of RHOB, a small GTPase, was investigated. Gene silencing of RHOB prevented metastatic activity in a systemic murine model of bone metastasis. Consistently, high RHOB levels promote metastasis progression [123]. Interestingly changes in the cellular composition of blood and bone marrow, namely, thrombocytosis but also weight loss and increased AKP and CEA levels, were correlated with bone metastasis in patients with pulmonary adenocarcinoma [124].

A new promising aspect came with the demonstration that the RANK-RANK ligand system regulates the activity of osteoclasts. CCL22 upregulated receptor activator of nuclear factor-κB ligand (RANKL) in osteoclast-like cells which subsequently induced cell migration and also enhanced phosphorylation of protein kinase B/Akt and extracellular signal-regulated kinase (ERK). This suggests that osteoclasts may promote bone metastasis of cancer cells expressing CCR4 in the bone marrow by producing its ligand CCL22 [125]. Lung cancer metastases to bone produce a primarily mixed osteolytic/osteoblastic lesions (Fig. 18.12a, b). Treatment with RANK antibody limited the formation of lytic lesions and inhibited the rate of in vivo tumor growth [126]. The study by Kuo and coworkers studied the regulation and interaction of parathyroid hormone-related protein (PTHrP). The authors showed that miR-33a levels are inversely correlated with PTHrP expression. The reintroduction of miR-33a reduces the production of osteoclastogenesis activator RANKL and macrophage colony-stimulating factor (M-CSF) on osteoblasts, while the expression of PTHrP was decreased. In addition, miR-33a-mediated PTHrP downregulation results in decreased IL8 secretion and contributes to decreased lung cancer-mediated osteoclast differentiation and bone resorption in experimental setting [127]. Peng and colleagues showed upregulated RANKL, RANK, and OPG in NSCLC cell lines and in tumor tissues with bone metastasis. Migration and invasion was significantly enhanced by recombinant human RANKL and transfection of RANKL cDNA and was impaired after OPG was added. Differential expression of RANKL, RANK, and OPG was shown to be associated with the metastatic potential of human NSCLC to skeleton [128]. This was confirmed by the study of Miller. Tumor cell-mediated osteolysis occurs through induction of RANKL. The authors tested this hypothesis in novel NSCLC bone metastasis mouse models. They found that OPG-Fc reduced the development and progression of osteolytic lesions. OPG-Fc plus docetaxel in combination resulted in significantly greater inhibition of skeletal tumor growth compared to either single agent alone. The inhibition of RANKL reduced osteolytic bone destruction and skeletal tumor burden [129].

Dougall and coworkers used denosumab, a fully human monoclonal antibody against RANKL, and demonstrated prevention or delay of skeletal-related events in patients with solid tumors that have metastasized to the bone. Besides the role of RANKL in tumor-induced osteolysis, bone destruction, and skeletal tumor progression, the authors also provided arguments for a direct prometastatic effect of RANKL, as RANKL also stimulates metastasis via activity on RANK-expressing cancer cells, resulting in increased invasion and migration [130].

18.5.4 Pleural Metastasis

Lung carcinomas frequently metastasize to the pleura. Especially adenocarcinomas because of their peripheral location invade early on the pleura. Interestingly when comparing adenocarcinomas with known driver mutation, it is evident that adenocarcinomas with EML4-ALK1 rearrangement have a higher propensity for pleura metastasis and malignant effusion [131]. In one study it was proposed that the 216G/T polymorphism of the EGF receptor may play a role in pleural metastasis by overexpressing the protein [132].

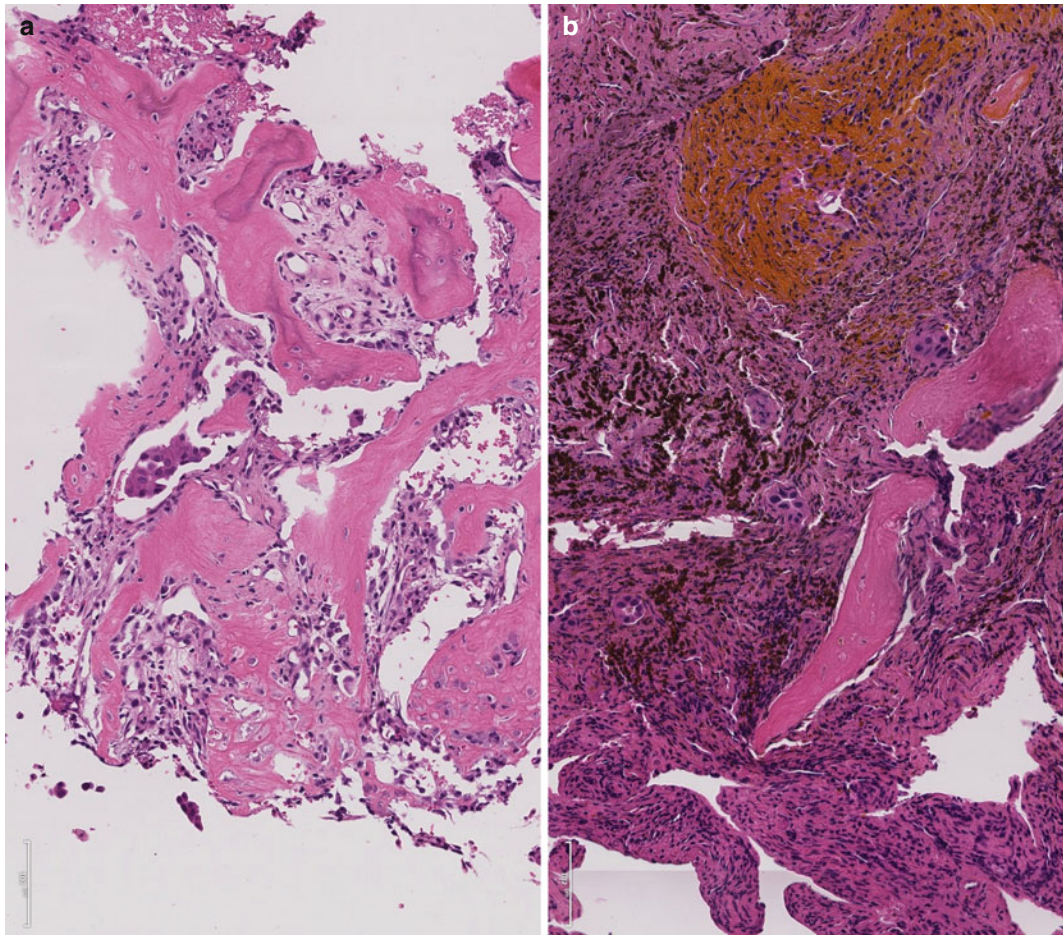

Fig. 18.12 Bone metastasis: (**a**) Adenocarcinoma cell complexes have induced an impressive activity of osteoclasts, resulting in lytic bone lesions; (**b**) adenocarcinoma metastases have induced bleeding and a massive inflammatory reaction, which also results in lytic bone lesions (Courtesy of Ulrike Gruber-Moesenbacher)

18.5.5 Lymph Node Metastasis

Although lymph nodes are among the first metastatic foci of lung carcinomas, much less is known about specific molecular events in facilitating this colonization. Peng et al. studied the effect of hypoxia and chemokines. CCR7 expression correlated positively with HIF-1α and HIF-2α and all together correlated with lymph node metastasis. It was shown that hypoxia induced HIF-1α and HIF-2α expression, which upregulated CCR7; inhibiting HIF-1α or HIF-2α resulted in decreased CCR7 expression and furthermore in inhibition of tumor cell migration and invasion [133]. However, it seems obvious that more than three molecules are involved, which has been shown by a study on genetic aberrations. Gains at 7q36, 8p12, 10q22, and 12p12, loss at 4p14, and the homozygous deletions at 4q occurred significantly more frequent in SCC from patients with lymph node metastases only. Gains at 7q, 8p, and 10q were restricted to SCC with lymph node metastasis and gain at 8q was restricted to patients with distant metastasis [134].

In summarizing our knowledge in the metastatic process in lung carcinomas, it can be stated that many mechanisms and involved genes/proteins have been identified, but the major breakthrough is still not achieved. The major problem is that the process of metastasis has so many steps

that we still do not overlook the interactions of hypoxia, migration, EMT and MET, homing, interaction with stoma cells, and preparation of the metastatic niche, which probably occur not as a time sequence, but more likely in parallel.

18.6 Metastasis to the Lung

The lung is the primary metastatic site of many malignant tumors. Almost all sarcomas primarily metastasize into the lung due to the fact that they prefer hematogenous spreading via veins. Many carcinomas too metastasize primarily into the lung, especially carcinomas from the GI tract. In these cases metastasis can occur either via vascular invasion or via lymphatics. Carcinoma cells travel via ductus thoracicus into left venous confluence further on via vena cava superior into the pulmonary circulation and finally get trapped in pulmonary capillaries.

Morphologically metastasis shows an arrangement around pulmonary arteries (tumor emboli) from where they extravasate. They also can obstruct small blood vessels and again will grow out from the vessels. So a central blood vessel within a malignant tumor focus can be taken as a sign of metastatic growth. Quite common are infarcts due to tumor emboli.

However, also homing mechanisms as described in the previous paragraphs are important. Similar to lung carcinomas, also other malignant tumors use homing mechanisms to attach to pulmonary blood vessels in a specific way. One of these examples is exclusive metastasis of glioblastomas and meningiosarcomas to the lung in the rare instance of metastasis outside the brain.

Most common carcinomas metastasizing to the lung are lung carcinomas itself and colon, kidney, breast, and stomach carcinomas; others are liver, ovary, prostate, endometrium, and germ cell tumors.

Differentiation of Metastasis from Primary Lung Carcinomas

In addition to angiocentricity of metastases, markers can be used to separate carcinomas from primary lung carcinomas. In the table are some useful markers for the differentiation of primary carcinoma versus metastasis to the lung (Table 18.1).

Table 18.1 Expression profiles of different carcinoma types with respect to metastasis versus primary lung carcinoma

Origin	Positive	Negative
Colon	CK20, CDX2*	CK7, TTF1, NapsinA
Breast	MFG1, MFG2, ER**, PR, CK7	NapsinA, SurfApoA/B
Pancreas	Pancreatic stone protein, CK7	SurfApoB, NapsinA±
Prostate	PSA	CK5/CK6
Ovary	CK7	TTF1, SurfApoA/B
Larynx	CK5/CK6	CK7
Esophagus	CK4, CK5/CK6	CK7
Stomach	CK7, ß-catenin, E-cadherin	TTF1, SurfApoA/B, NapsinA

*CDX2 can sometimes be positive in a minority of cells in pulmonary adenocarcinoma
**ER positivity can occur in pulmonary adenocarcinoma

Examples of Common Carcinoma Metastasis to the Lung

Colonic adenocarcinoma: There are some common features which help to separate colonic from primary lung adenocarcinomas: cribriform pattern is common in colonic AC and rare in lung AC, metastasis is usually centered around a pulmonary artery, and often there is extensive necrosis due to infarct induced by the carcinoma embolus (Fig. 18.13). In those cases, which are not primarily easy to diagnose, expression of cytokeratin 20 and CDX2 in colonic AC will establish the correct diagnosis (Fig. 18.14)

Adenocarcinoma of the breast: Breast carcinomas regularly metastasize to the lung and pleura. All types can be seen. Most often ductal and lobular AC will show a diffuse infiltration pattern, which is unusual in primary lung AC. However, in many cases evaluation of expression of markers is required for the diagnosis. Immunohistochemistry for estrogen receptor is not helpful as pulmonary AC can express this receptor too. Progesterone receptor expression is rare in pulmonary AC, but more specific is the expression of both types of milk fat globulins, as coexpression is neither seen in lung AC nor those from the ovary (Fig. 18.15).

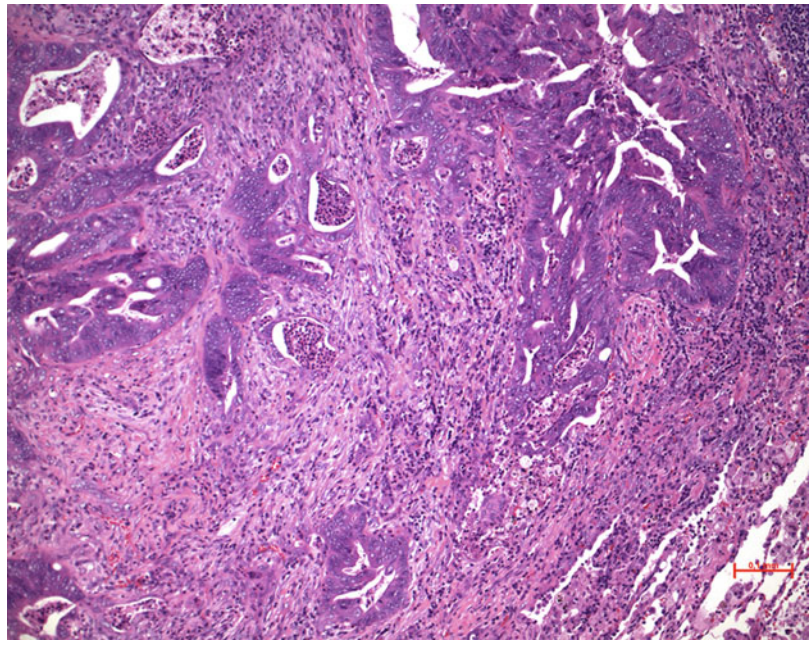

Fig. 18.13 Classic example of colon carcinoma metastasis to the lung. The carcinoma shows the typical pattern of a cribriform adenocarcinoma with secondary and tertiary glands. In such a case, immunohistochemistry is not necessary. H&E, bar 100 µm

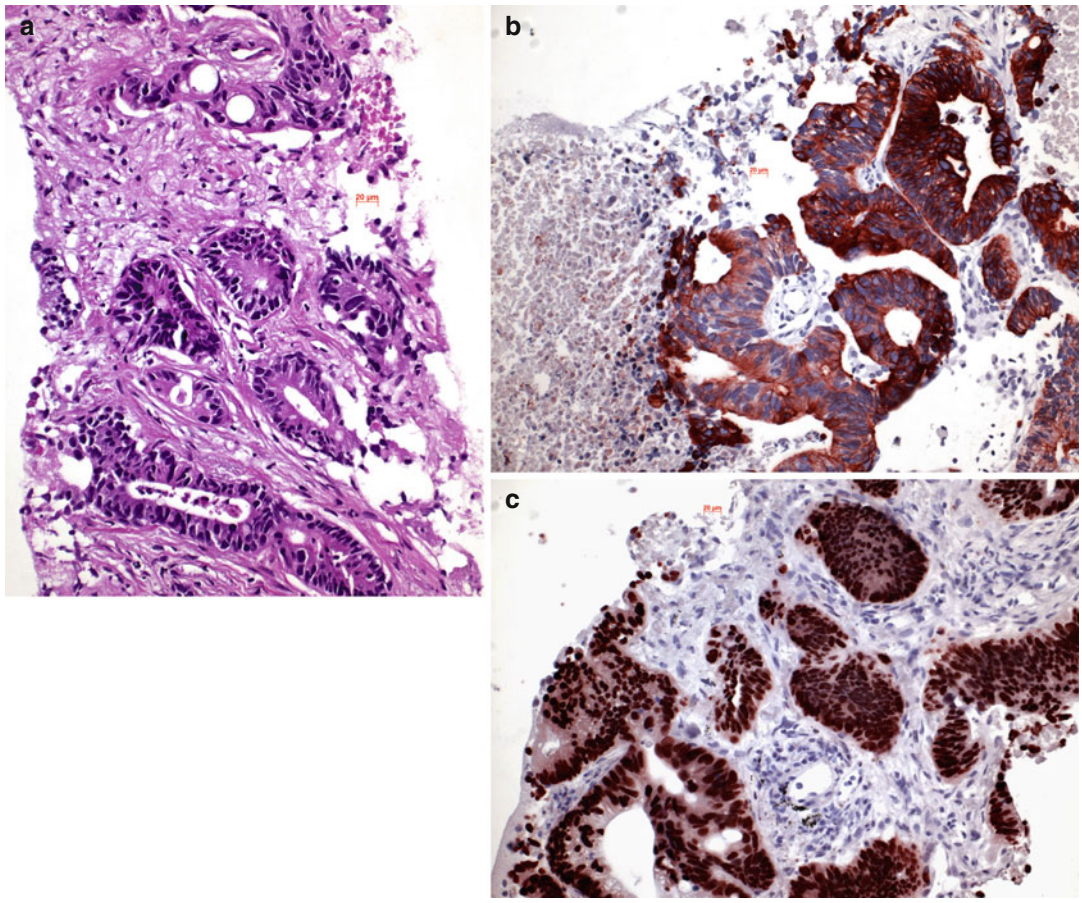

Fig. 18.14 Transthoracic needle biopsy with formations of an acinar adenocarcinoma (**a**). Positive immunohistochemistry for cytokeratin 20 (**b**) and CDX2 (**c**) confirmed a metastasis from the colon. H&E, immunohistochemistry for CK20 and CDX2, bars 20 µm

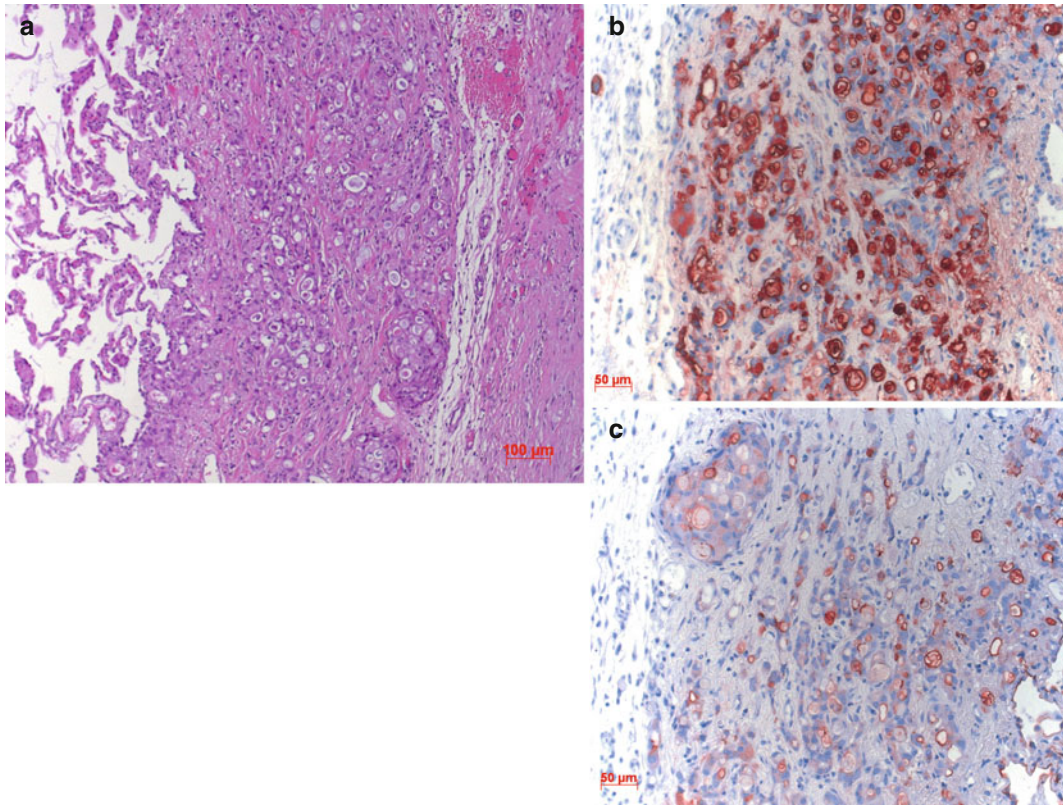

Fig. 18.15 Adenocarcinoma of the breast metastasizing to the lung and pleura (**a**). To confirm the diagnosis, immunohistochemistry for milk fat globulin 1 (**b**) and 2 (**c**) was performed and both antibodies positively stained the carcinoma cells. H&E, immunohistochemistry for milk fat globulin 1 + 2, bars 100 and 50 µm, respectively

Squamous cell carcinoma of the larynx and those from other locations in the upper respiratory and digestive tract are hard to differentiate from primary lung SCC. Esophageal SCC expresses cytokeratin 4, which is not seen in lung SCC, but laryngeal SCC looks similar to lung primary and expresses the same markers. In this instance, only the morphology and CT images will help: more than two nodules and angiocentric growth pattern are in favor of metastasis (Fig. 18.16). In cases where the primary tumor is available, a comparison of the morphology will also assist in making the correct diagnosis.

Renal clear cell carcinoma: Clear cell carcinomas do occur in the lung and many carcinomas show clear cell pattern focally. However, carcinomas entirely composed of clear cells are most likely metastasis from renal cell carcinoma. Localization of the tumor is of no help, as metastasis can occur centrally in bronchi with an endobronchial component. Expression of markers can help: CD10, PAX8, and coexpression of cytokeratin and vimentin are in favor of renal carcinoma metastasis (Fig. 18.17).

Gastric adenocarcinoma: Gastric adenocarcinoma of enteric type rarely metastasizes to the lung. In these rare cases, expression of markers is not very helpful as the same cytokeratin peptides are expressed. TP53 might sometimes assist, as a mutation is most often present, whereas some pulmonary AC can be negative. Expression of villin might be of help. Adenocarcinoma of signet ring cell type more frequently metastasize to the lung. As there is also mucinous AC of signet ring cell type in the lung, the differentiation will need

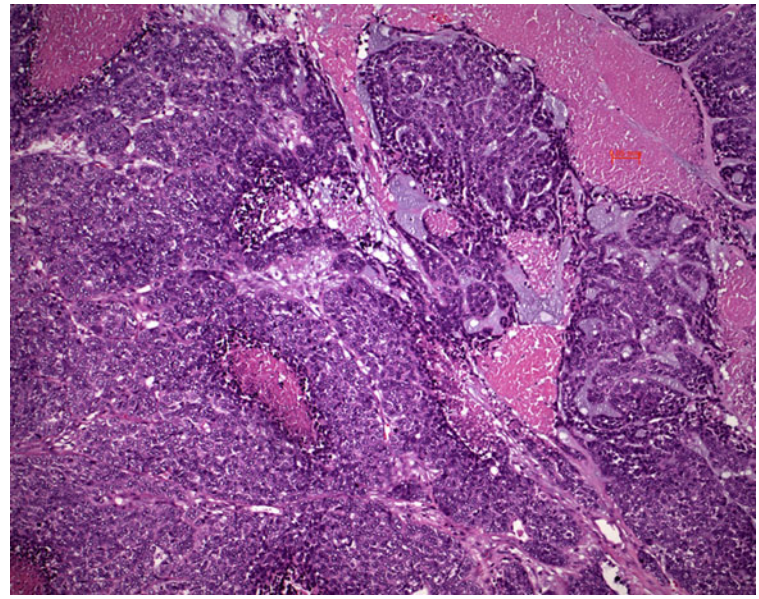

Fig. 18.16 Metastasis of an undifferentiated squamous cell carcinoma in the lung; in this case several nodules were seen on CT scan. Note some unusual features as pseudomucinous stroma depositions and typical large necrosis with apoptotic figures. Comparison of metastasis with the primary tumor also helped in this case. H&E, bar 50 µm

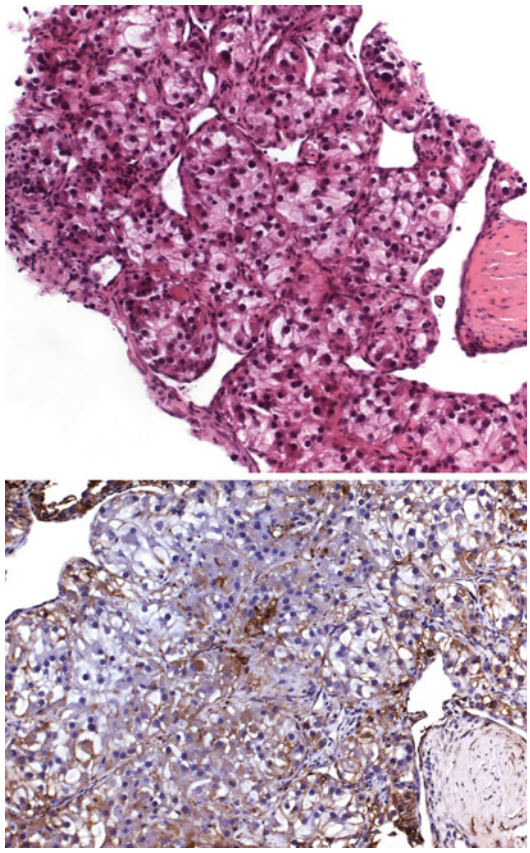

Fig. 18.17 Transthoracic needle biopsy of a large tumor. On histology it was diagnosed as clear cell carcinoma (*upper panel*). To confirm the suspected diagnosis of metastatic renal cell carcinoma immunohistochemistry was performed, CD10 and vimentin were positive in this case. Shown here is the stain for vimentin (*lower panel*). H&E, immunohistochemistry, ×250

immunohistochemistry for the separation. Mutation of E-cadherin results in nuclear expression of β-catenin, which is uncommon in pulmonary AC, and TTF1 is negative.

Adenocarcinoma of the prostate: Usually this AC present with small cribriform glands, uncommon in pulmonary AC. However, sometimes expression of PSA or racemase is necessary to separate metastasis from primary lung AC (Fig. 18.18).

Adenocarcinoma of the ovary: Adenocarcinomas of the ovary, especially cystadenocarcinomas, preferentially metastasize to the pleura, less often to the lung. As these carcinomas are positive for cytokeratin 7 as pulmonary ones, only TTF1 will help to sort the primary location.

Adenocarcinoma of the Endometrium

Among the rare metastasis are those from lacrimal and salivary glands. However, this can occur, and often these carcinomas present with the classical salivary gland-type carcinomas (Fig. 18.19, Table 18.2).

Metastasis of germ cell tumors has been seen frequently in former times, but became rare with the much more efficient chemotherapeutics used today. Most frequently metastasis from embryonic carcinoma and mixed germ cell tumors were seen in former times.

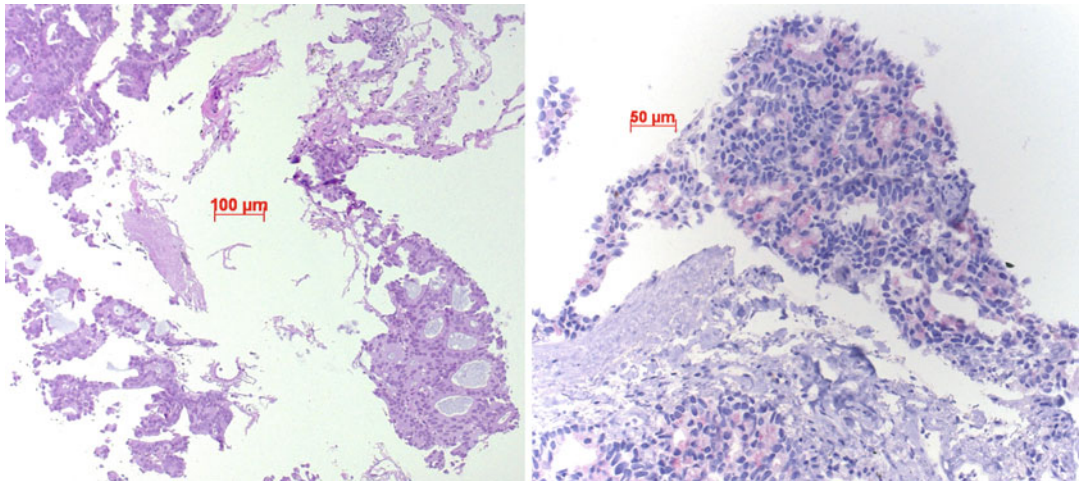

Fig. 18.18 Transthoracic needle biopsy. Adenocarcinoma with small glands and some cribriform pattern was seen (*left*). Immunohistochemistry for racemase (*right*) and PSA confirmed the diagnosis of metastatic adenocarcinoma of the prostate. H&E, immunohistochemistry, bars 100 and 50 µm

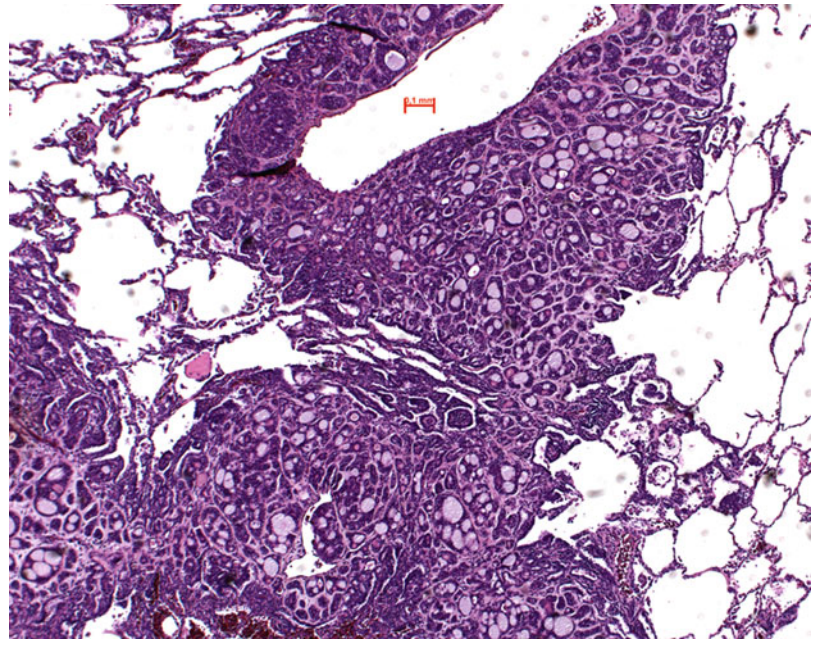

Fig. 18.19 Metastasis from an adenoid-cystic adenocarcinoma of the lacrimal gland. In such a case, the diagnosis of metastasis is easy, as lung primary does not occur in the peripheral lung. However, the primary can only be defined if clinical information or pathological records are available from the primary tumor location. H&E, bar 100 µm

Table 18.2 Overview of the frequency of metastasis from different carcinomas seen in a single institution

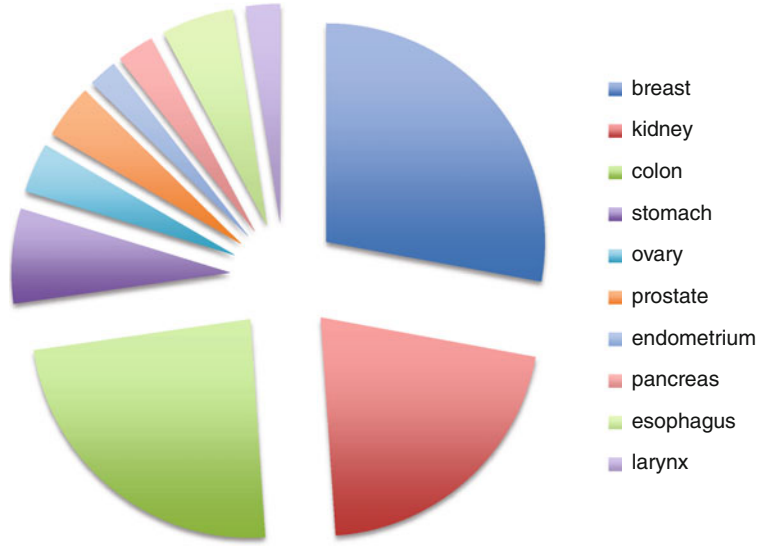

Sarcomas from soft tissue usually metastasize to the lung. Most common are osteosarcomas (Fig. 18.20), but also leiomyosarcoma and liposarcoma. Occasionally some of the rare sarcoma types will be encountered in the lung. Whereas osteosarcoma diagnosis is most often easy, because it affects a young-aged population, and is most often known from the primary surgery, the differential diagnosis of leiomyosarcoma can be difficult (Fig. 18.21). The differential diagnosis in these sarcomas is more difficult as primary leiomyosarcomas arise in the lung, pleomorphic carcinomas can express smooth muscle actin, and metastasizing leiomyoma is another differential diagnosis. Primary leiomyosarcomas of the lung arise in central bronchi, whereas metastasis occurs in the lung periphery. Pleomorphic carcinomas in case of spindle cell carcinoma will focally express also cytokeratin and thus can be separated from leiomyosarcoma. In addition in contrast to the sarcoma, these carcinomas will be negative for desmin. Finally metastasizing leiomyoma will look much more like a benign or low-grade tumor, although like a metastasis it will occur in the periphery. Pleomorphic liposarcoma is another sarcoma, which metastasize to the lung. Other rare examples will be encountered, such as myxofibrosarcoma (Fig. 18.22) and uterine stroma sarcoma (Fig. 18.23, Table 18.3).

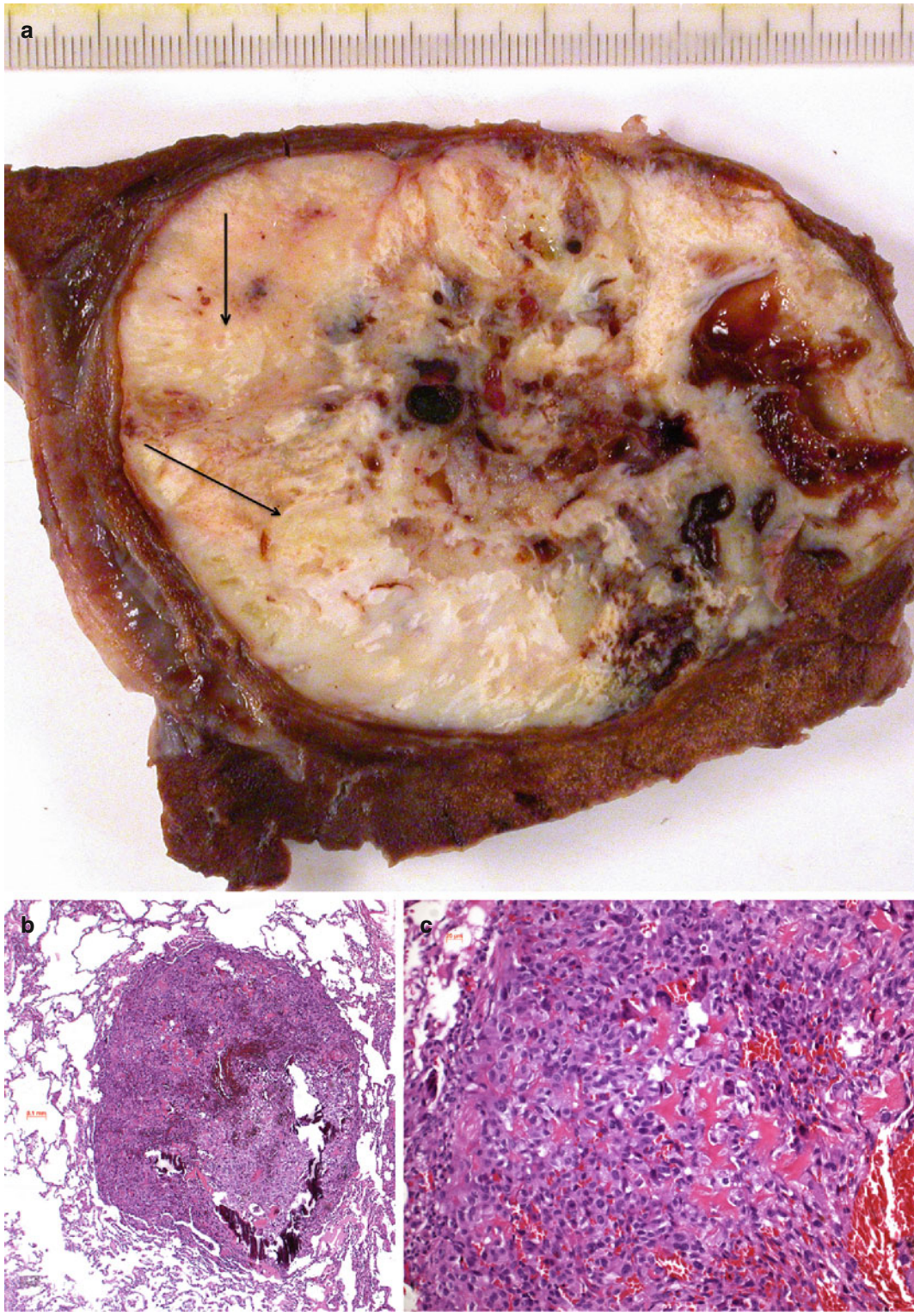

Fig. 18.20 Metastasis of an osteosarcoma. Already at gross morphology, this tumor looks suspicious for a sarcoma, as there are bone-like spicules seen (*arrows*, **a**). In (**b**) a malignant mesenchymal tumor is seen with calcifications but also reddish-stained osteoid. In (**c**) osteoid formation by the tumor cells is seen as well as spindle and epithelioid cells. H&E, bars 100 and 20 μm

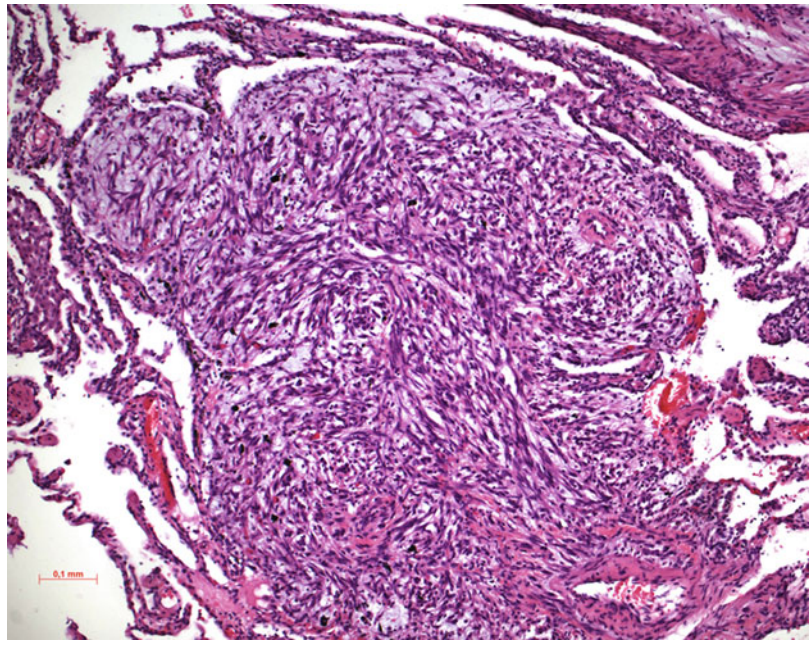

Fig. 18.21 Metastasis from a leiomyosarcoma to the lung. In this case the primary was known and therefore only confirmation of the suspected clinical diagnosis was required. Usually immunohistochemical stains for smooth muscle actin and desmin should be performed. H&E, bar 100 µm

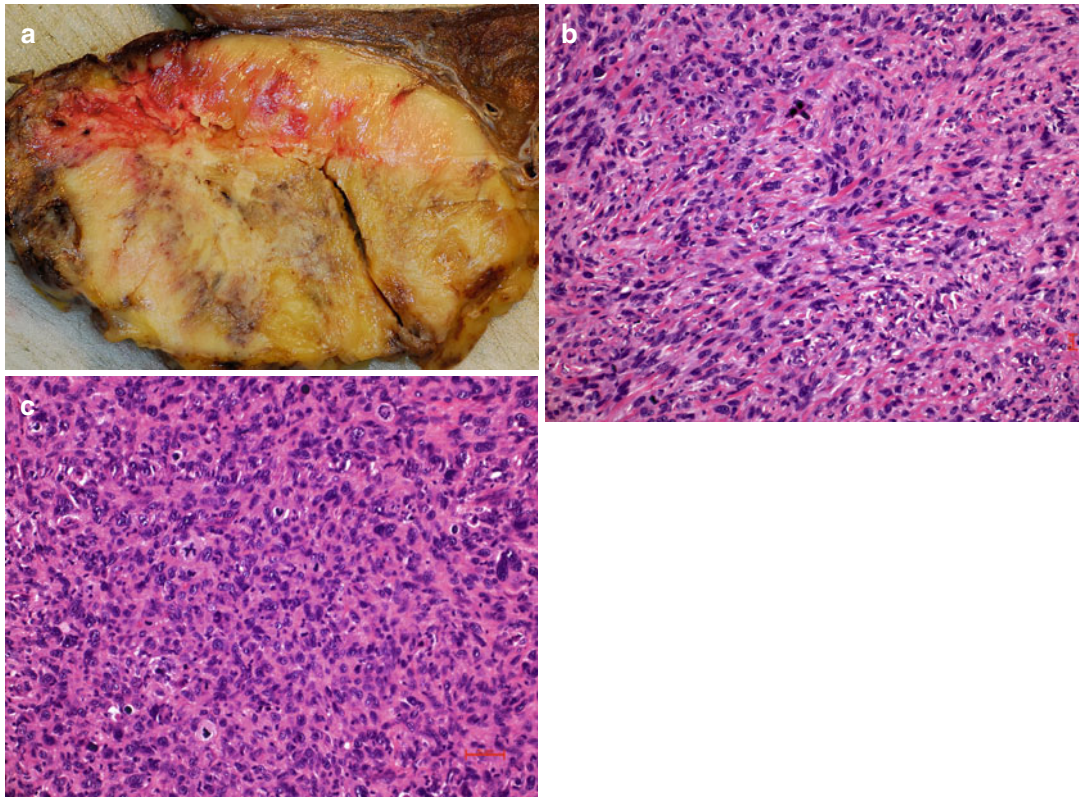

Fig. 18.22 Metastasis from myxofibrosarcoma. (**a**) Gross morphology suggestive of a mesenchymal tumor. (**b**, **c**) Two different areas of the sarcoma showing a more spindle cell pattern and a more round cell pattern. The diagnosis was confirmed by immunohistochemistry in the primary as well as in the metastasis. H&E, ×200

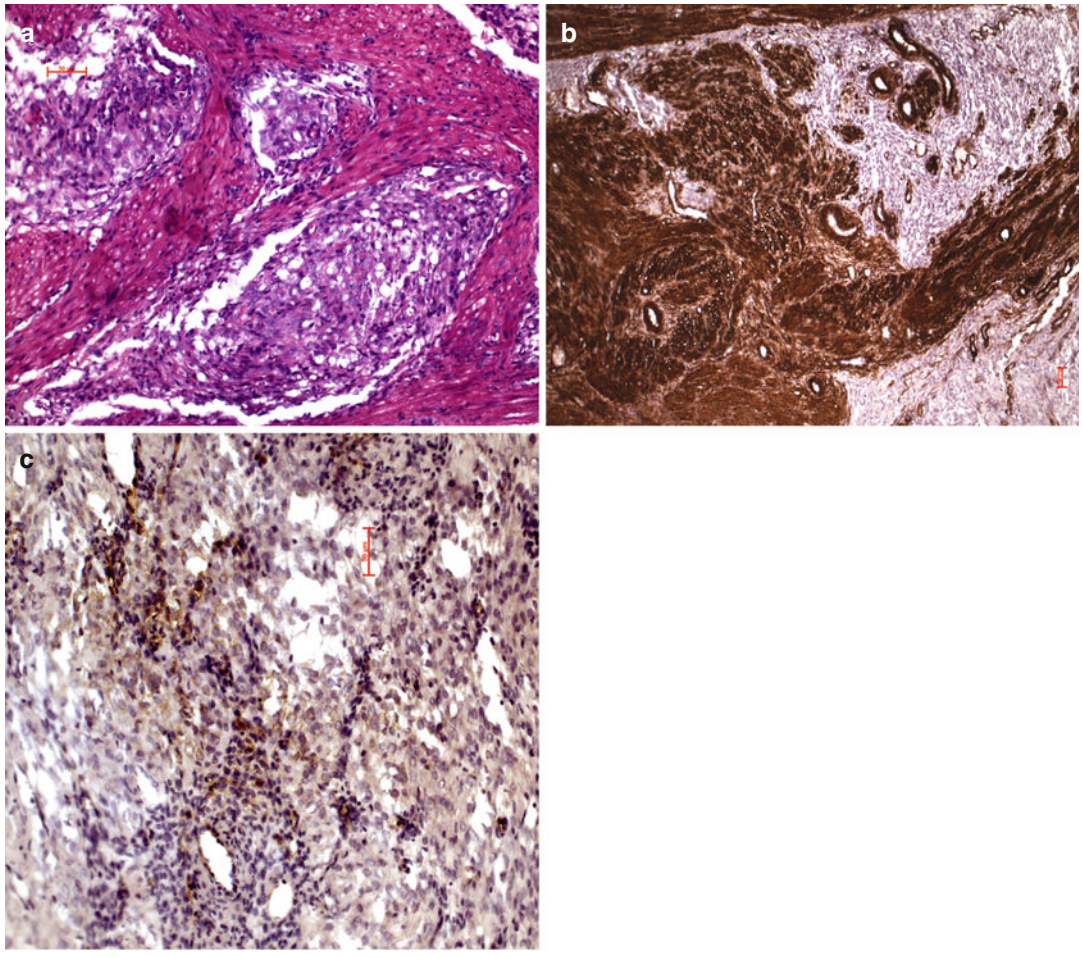

Fig. 18.23 Metastasis of an uterine stroma sarcoma to the lung. (**a**) Shows an in part spindle cell and also epithelioid tumor with lots of stroma between the tumor complexes. Immunohistochemistry for smooth muscle actin (**b**) and CD10 (**c**) among other markers confirmed the diagnosis. H&E, immunohistochemistry, bars 50 μm

Table 18.3 Overview of the frequency of metastasis from different sarcomas seen in a single institution

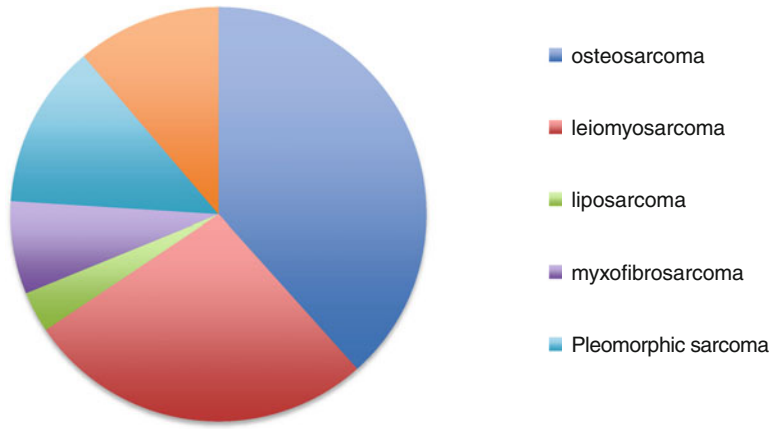

References

1. Gabor S, Renner H, Popper H, Anegg U, Sankin O, Matzi V, Lindenmann J, Smolle Juttner FM. Invasion of blood vessels as significant prognostic factor in radically resected T1-3N0M0 non-small-cell lung cancer. Eur J Cardiothorac Surg. 2004;25:439–42.
2. Tamura T, Kurishima K, Nakazawa K, Kagohashi K, Ishikawa H, Satoh H, Hizawa N. Specific organ metastases and survival in metastatic non-small-cell lung cancer. Mol Clin Oncol. 2015;3:217–21.
3. Faoro L, Hutto JY, Salgia R, El-Zayaty SA, Ferguson MK, Cheney RT, Reid ME, Armato 3rd SG, Krausz T, Husain AN. Lymphatic vessel density is not associated with lymph node metastasis in non-small cell lung carcinoma. Arch Pathol Lab Med. 2008;132:1882–8.
4. Putora PM, Ess S, Panje C, Hundsberger T, van Leyen K, Plasswilm L, Fruh M. Prognostic significance of histology after resection of brain metastases and whole brain radiotherapy in non-small cell lung cancer (NSCLC). Clin Exp Metastasis. 2015;32:143–9.
5. Wilbertz T, Wagner P, Petersen K, Stiedl AC, Scheble VJ, Maier S, Reischl M, Mikut R, Altorki NK, Moch H, Fend F, Staebler A, Bass AJ, Meyerson M, Rubin MA, Soltermann A, Lengerke C, Perner S. SOX2 gene amplification and protein overexpression are associated with better outcome in squamous cell lung cancer. Mod Pathol. 2011;24:944–53.
6. Decaussin M, Sartelet H, Robert C, Moro D, Claraz C, Brambilla C, Brambilla E. Expression of vascular endothelial growth factor (VEGF) and its two receptors (VEGF-R1-Flt1 and VEGF-R2-Flk1/KDR) in non-small cell lung carcinomas (NSCLCs): correlation with angiogenesis and survival. J Pathol. 1999;188:369–77.
7. Yen L, You XL, Al Moustafa AE, Batist G, Hynes NE, Mader S, Meloche S, Alaoui-Jamali MA. Heregulin selectively upregulates vascular endothelial growth factor secretion in cancer cells and stimulates angiogenesis. Oncogene. 2000;19:3460–9.
8. Niethammer AG, Xiang R, Becker JC, Wodrich H, Pertl U, Karsten G, Eliceiri BP, Reisfeld RA. A DNA vaccine against VEGF receptor 2 prevents effective angiogenesis and inhibits tumor growth. Nat Med. 2002;8:1369–75.
9. Guedj N, Couvelard A, Arcangeli G, Dubois S, Thabut G, Leseche G, Fournier M, Degott C, Groussard O. Angiogenesis and extracellular matrix remodelling in bronchioloalveolar carcinomas: distinctive patterns in mucinous and non-mucinous tumours. Histopathology. 2004;44:251–6.
10. Merrick DT, Haney J, Petrunich S, Sugita M, Miller YE, Keith RL, Kennedy TC, Franklin WA. Overexpression of vascular endothelial growth factor and its receptors in bronchial dysplasia demonstrated by quantitative RT-PCR analysis. Lung Cancer. 2005;48:31–45.
11. Ramos AH, Pugh TJ, Stransky N, Helman E, Kim J, Sougnez C, Ambrogio L, Nickerson E, Shefler E, Cortes ML, Auclair D, Saksena G, Voet D, Noble M, DiCara D, Lin P, Lichtenstein L, Heiman DI, Fennell T, Imielinski M, Hernandez B, Hodis E, Baca S, Dulak AM, Lohr J, Landau DA, Wu CJ, Melendez-Zajgla J, Hidalgo-Miranda A, Koren A, McCarroll SA, Mora J, Lee RS, Crompton B, Onofrio R, Parkin M, Winckler W, Ardlie K, Gabriel SB, Roberts CW, Biegel JA, Stegmaier K, Bass AJ, Garraway LA, Meyerson M, Golub TR, Gordenin DA, Sunyaev S, Lander ES, Getz G. Mutational heterogeneity in cancer and the search for new cancer-associated genes. Nature. 2013;499:214–8.
12. Suzuki K, Sun R, Origuchi M, Kanehira M, Takahata T, Itoh J, Umezawa A, Kijima H, Fukuda S, Saijo Y. Mesenchymal stromal cells promote tumor growth through the enhancement of neovascularization. Mol Med. 2011;17:579–87.
13. Wang YC, He F, Feng F, Liu XW, Dong GY, Qin HY, Hu XB, Zheng MH, Liang L, Feng L, Liang YM, Han H. Notch signaling determines the M1 versus M2 polarization of macrophages in antitumor immune responses. Cancer Res. 2010;70:4840–9.
14. Nicholson AG, Detterbeck FC, Marino M, Kim J, Stratton K, Giroux D, Asamura H, Crowley J, Falkson C, Filosso PL, Giaccone G, Huang J, Kondo K, Lucchi M, Marom EM, Okumura M, Ruffini E, Van Schil P. The IASLC/ITMIG thymic epithelial tumors staging project: proposals for the T component for the forthcoming (8th) edition of the TNM classification of malignant tumors. J Thorac Oncol. 2014;9:S73–80.
15. Kaminskyy VO, Piskunova T, Zborovskaya IB, Tchevkina EM, Zhivotovsky B. Suppression of basal autophagy reduces lung cancer cell proliferation and enhances caspase-dependent and -independent apoptosis by stimulating ROS formation. Autophagy. 2012;8:1032–44.
16. Rao S, Tortola L, Perlot T, Wirnsberger G, Novatchkova M, Nitsch R, Sykacek P, Frank L, Schramek D, Komnenovic V, Sigl V, Aumayr K, Schmauss G, Fellner N, Handschuh S, Glosmann M, Pasierbek P, Schlederer M, Resch GP, Ma Y, Yang H, Popper H, Kenner L, Kroemer G, Penninger JM. A dual role for autophagy in a murine model of lung cancer. Nat Commun. 2014;5:3056.
17. Westhoff B, Colaluca IN, D'Ario G, Donzelli M, Tosoni D, Volorio S, Pelosi G, Spaggiari L, Mazzarol G, Viale G, Pece S, Di Fiore PP. Alterations of the Notch pathway in lung cancer. Proc Natl Acad Sci U S A. 2009;106:22293–8.
18. Kunnimalaiyaan M, Chen H. Tumor suppressor role of Notch-1 signaling in neuroendocrine tumors. Oncologist. 2007;12:535–42.
19. Wang NJ, Sanborn Z, Arnett KL, Bayston LJ, Liao W, Proby CM, Leigh IM, Collisson EA, Gordon PB, Jakkula L, Pennypacker S, Zou Y, Sharma M, North JP, Vemula SS, Mauro TM, Neuhaus IM, Leboit PE, Hur JS, Park K, Huh N, Kwok PY, Arron ST, Massion PP, Bale AE, Haussler D, Cleaver JE, Gray JW, Spellman PT, South AP, Aster JC, Blacklow SC, Cho RJ. Loss-of-function mutations in Notch receptors in cutaneous and lung squamous cell carcinoma. Proc Natl Acad Sci U S A. 2011;108:17761–6.

20. Osanyingbemi-Obidi J, Dobromilskaya I, Illei PB, Hann CL, Rudin CM. Notch signaling contributes to lung cancer clonogenic capacity in vitro but may be circumvented in tumorigenesis in vivo. Mol Cancer Res. 2011;9:1746–54.
21. Licciulli S, Avila JL, Hanlon L, Troutman S, Cesaroni M, Kota S, Keith B, Simon MC, Pure E, Radtke F, Capobianco AJ, Kissil JL. Notch1 is required for Kras-induced lung adenocarcinoma and controls tumor cell survival via p53. Cancer Res. 2013;73:5974–84.
22. Xie M, Zhang L, He CS, Xu F, Liu JL, Hu ZH, Zhao LP, Tian Y. Activation of Notch-1 enhances epithelial-mesenchymal transition in gefitinib-acquired resistant lung cancer cells. J Cell Biochem. 2012;113:1501–13.
23. Chen S, Xu Y, Chen Y, Li X, Mou W, Wang L, Liu Y, Reisfeld RA, Xiang R, Lv D, Li N. SOX2 gene regulates the transcriptional network of oncogenes and affects tumorigenesis of human lung cancer cells. PLoS ONE. 2012;7:e36326.
24. Kothari S, Cizeau J, McMillan-Ward E, Israels SJ, Bailes M, Ens K, Kirshenbaum LA, Gibson SB. BNIP3 plays a role in hypoxic cell death in human epithelial cells that is inhibited by growth factors EGF and IGF. Oncogene. 2003;22:4734–44.
25. Chen YQ, Zhao CL, Li W. Effect of hypoxia-inducible factor-1Œ± on transcription of surviving in non-small cell lung cancer. J Exp Clin Cancer Res. 2009;28:29.
26. Wan J, Ma J, Mei J, Shan G. The effects of HIF-1alpha on gene expression profiles of NCI-H446 human small cell lung cancer cells. J Exp Clin Cancer Res. 2009;28:150.
27. Eliasz S, Liang S, Chen Y, De Marco MA, Machek O, Skucha S, Miele L, Bocchetta M. Notch-1 stimulates survival of lung adenocarcinoma cells during hypoxia by activating the IGF-1R pathway. Oncogene. 2010;29:2488–98.
28. Tung KH, Lin CW, Kuo CC, Li LT, Kuo YH, Wu HC. CHC promotes tumor growth and angiogenesis through regulation of HIF-1alpha and VEGF signaling. Cancer Lett. 2013;331:58–67.
29. Gharib TG, Chen G, Huang CC, Misek DE, Iannettoni MD, Hanash SM, Orringer MB, Beer DG. Genomic and proteomic analyses of vascular endothelial growth factor and insulin-like growth factor-binding protein 3 in lung adenocarcinomas. Clin Lung Cancer. 2004;5:307–12.
30. Brader S, Eccles SA. Phosphoinositide 3-kinase signalling pathways in tumor progression, invasion and angiogenesis. Tumori. 2004;90:2–8.
31. Popper HH. Lung adenocarcinomas: comparison between mice and men. Methods Mol Biol. 2015;1267:19–43.
32. Liu YL, Yu JM, Song XR, Wang XW, Xing LG, Gao BB. Regulation of the chemokine receptor CXCR4 and metastasis by hypoxia-inducible factor in non small cell lung cancer cell lines. Cancer Biol Ther. 2006;5:1320–6.
33. Paliwal S, Kovi RC, Nath B, Chen YW, Lewis BC, Grossman SR. The alternative reading frame tumor suppressor antagonizes hypoxia-induced cancer cell migration via interaction with the COOH-terminal binding protein corepressor. Cancer Res. 2007;67:9322–9.
34. Monnier Y, Farmer P, Bieler G, Imaizumi N, Sengstag T, Alghisi GC, Stehle JC, Ciarloni L, Andrejevic-Blant S, Moeckli R, Mirimanoff RO, Goodman SL, Delorenzi M, Ruegg C. CYR61 and alphaVbeta5 integrin cooperate to promote invasion and metastasis of tumors growing in preirradiated stroma. Cancer Res. 2008;68:7323–31.
35. Wei L, Song XR, Sun JJ, Wang XW, Xie L, Lv LY. Lysyl oxidase may play a critical role in hypoxia-induced NSCLC cells invasion and migration. Cancer Biother Radiopharm. 2012;27:672–7.
36. Kim B, Sohn EJ, Jung JH, Shin EA, You OH, Im J, Kim SH. Inhibition of ZNF746 suppresses invasion and epithelial to mesenchymal transition in H460 non-small cell lung cancer cells. Oncol Rep. 2014;31:73–8.
37. Kawashiri S, Tanaka A, Noguchi N, Hase T, Nakaya H, Ohara T, Kato K, Yamamoto E. Significance of stromal desmoplasia and myofibroblast appearance at the invasive front in squamous cell carcinoma of the oral cavity. Head Neck. 2009;31:1346–53.
38. Noguchi M, Shimosato Y. The development and progression of adenocarcinoma of the lung. Cancer Treat Res. 1995;72:131–42.
39. Soltermann A, Tischler V, Arbogast S, Braun J, Probst-Hensch N, Weder W, Moch H, Kristiansen G. Prognostic significance of epithelial-mesenchymal and mesenchymal-epithelial transition protein expression in non-small cell lung cancer. Clin Cancer Res. 2008;14:7430–7.
40. Nakamura N, Iijima T, Mase K, Furuya S, Kano J, Morishita Y, Noguchi M. Phenotypic differences of proliferating fibroblasts in the stroma of lung adenocarcinoma and normal bronchus tissue. Cancer Sci. 2004;95:226–32.
41. Chen H, Yang WW, Wen QT, Xu L, Chen M. TGF-beta induces fibroblast activation protein expression; fibroblast activation protein expression increases the proliferation, adhesion, and migration of HO-8910PM [corrected]. Exp Mol Pathol. 2009;87:189–94.
42. Santos AM, Jung J, Aziz N, Kissil JL, Pure E. Targeting fibroblast activation protein inhibits tumor stromagenesis and growth in mice. J Clin Invest. 2009;119:3613–25.
43. Garcia-de-Alba C, Becerril C, Ruiz V, Gonzalez Y, Reyes S, Garcia-Alvarez J, Selman M, Pardo A. Expression of matrix metalloproteases by fibrocytes: possible role in migration and homing. Am J Respir Crit Care Med. 2010;182:1144–52.
44. Rintoul RC, Sethi T. Extracellular matrix regulation of drug resistance in small-cell lung cancer. Clin Sci (Lond). 2002;102:417–24.
45. Koukourakis MI, Giatromanolaki A, Brekken RA, Sivridis E, Gatter KC, Harris AL, Sage EH. Enhanced expression of SPARC/osteonectin in

the tumor-associated stroma of non-small cell lung cancer is correlated with markers of hypoxia/acidity and with poor prognosis of patients. Cancer Res. 2003;63:5376–80.
46. Coulson-Thomas VJ, Coulson-Thomas YM, Gesteira TF, de Paula CA, Mader AM, Waisberg J, Pinhal MA, Friedl A, Toma L, Nader HB. Colorectal cancer desmoplastic reaction up-regulates collagen synthesis and restricts cancer cell invasion. Cell Tissue Res. 2011;346:223–36.
47. Oh JJ, Taschereau EO, Koegel AK, Ginther CL, Rotow JK, Isfahani KZ, Slamon DJ. RBM5/H37 tumor suppressor, located at the lung cancer hot spot 3p21.3, alters expression of genes involved in metastasis. Lung Cancer. 2010;70:253–62.
48. Makarenkova VP, Shurin GV, Tourkova IL, Balkir L, Pirtskhalaishvili G, Perez L, Gerein V, Siegfried JM, Shurin MR. Lung cancer-derived bombesin-like peptides down-regulate the generation and function of human dendritic cells. J Neuroimmunol. 2003;145:55–67.
49. Liu Q, Zhang C, Sun A, Zheng Y, Wang L, Cao X. Tumor-educated CD11bhighIalow regulatory dendritic cells suppress T cell response through arginase I. J Immunol. 2009;182:6207–16.
50. Xu L, Xu W, Jiang Z, Zhang F, Chu Y, Xiong S. Depletion of CD4(+)CD25(high) regulatory T cells from tumor infiltrating lymphocytes predominantly induces Th1 type immune response in vivo which inhibits tumor growth in adoptive immunotherapy. Cancer Biol Ther. 2009;8:66–72.
51. Li L, Chao QG, Ping LZ, Xue C, Xia ZY, Qian D, Shiang H. The prevalence of FOXP3+ regulatory T-cells in peripheral blood of patients with NSCLC. Cancer Biother Radiopharm. 2009;24:357–67.
52. Bremnes RM, Al-Shibli K, Donnem T, Sirera R, Al-Saad S, Andersen S, Stenvold H, Camps C, Busund LT. The role of tumor-infiltrating immune cells and chronic inflammation at the tumor site on cancer development, progression, and prognosis: emphasis on non-small cell lung cancer. J Thorac Oncol. 2011;6:824–33.
53. Feng PH, Lee KY, Chang YL, Chan YF, Kuo LW, Lin TY, Chung FT, Kuo CS, Yu CT, Lin SM, Wang CH, Chou CL, Huang CD, Kuo HP. CD14(+)S100A9(+) monocytic myeloid-derived suppressor cells and their clinical relevance in non-small cell lung cancer. Am J Respir Crit Care Med. 2012;186:1025–36.
54. Smith C, Chang MY, Parker KH, Beury DW, DuHadaway JB, Flick HE, Boulden J, Sutanto-Ward E, Soler AP, Laury-Kleintop LD, Mandik-Nayak L, Metz R, Ostrand-Rosenberg S, Prendergast GC, Muller AJ. IDO is a nodal pathogenic driver of lung cancer and metastasis development. Cancer Discov. 2012;2:722–35.
55. Benatar T, Cao MY, Lee Y, Lightfoot J, Feng N, Gu X, Lee V, Jin H, Wang M, Wright JA, Young AH. IL-17E, a proinflammatory cytokine, has antitumor efficacy against several tumor types in vivo. Cancer Immunol Immunother. 2010;59:805–17.
56. Lee HW, Park YM, Lee SJ, Cho HJ, Kim DH, Lee JI, Kang MS, Seol HJ, Shim YM, Nam DH, Kim HH, Joo KM. Alpha-smooth muscle actin (ACTA2) is required for metastatic potential of human lung adenocarcinoma. Clin Cancer Res. 2013;19:5879–89.
57. Davidson B. Prognostic factors in malignant pleural mesothelioma. Hum Pathol. 2015;46:789–804.
58. Murphy DA, Courtneidge SA. The 'ins' and 'outs' of podosomes and invadopodia: characteristics, formation and function. Nat Rev Mol Cell Biol. 2011;12:413–26.
59. Li CM, Chen G, Dayton TL, Kim-Kiselak C, Hoersch S, Whittaker CA, Bronson RT, Beer DG, Winslow MM, Jacks T. Differential Tks5 isoform expression contributes to metastatic invasion of lung adenocarcinoma. Genes Dev. 2013;27:1557–67.
60. Lin HC, Zhang FL, Geng Q, Yu T, Cui YQ, Liu XH, Li J, Yan MX, Liu L, He XH, Li JJ, Yao M. Quantitative proteomic analysis identifies CPNE3 as a novel metastasis-promoting gene in NSCLC. J Proteome Res. 2013;12:3423–33.
61. Narita K, Matsuda Y, Seike M, Naito Z, Gemma A, Ishiwata T. Nestin regulates proliferation, migration, invasion and stemness of lung adenocarcinoma. Int J Oncol. 2014;44:1118–30.
62. Yang J, Mani SA, Donaher JL, Ramaswamy S, Itzykson RA, Come C, Savagner P, Gitelman I, Richardson A, Weinberg RA. Twist, a master regulator of morphogenesis, plays an essential role in tumor metastasis. Cell. 2004;117:927–39.
63. Pallier K, Cessot A, Cote JF, Just PA, Cazes A, Fabre E, Danel C, Riquet M, Devouassoux-Shisheboran M, Ansieau S, Puisieux A, Laurent-Puig P, Blons H. TWIST1 a new determinant of epithelial to mesenchymal transition in EGFR mutated lung adenocarcinoma. PLoS ONE. 2012;7:e29954.
64. Pirozzi G, Tirino V, Camerlingo R, Franco R, La Rocca A, Liguori E, Martucci N, Paino F, Normanno N, Rocco G. Epithelial to mesenchymal transition by TGFbeta-1 induction increases stemness characteristics in primary non small cell lung cancer cell line. PLoS ONE. 2011;6:e21548.
65. Wang C, Su Y, Zhang L, Wang M, You J, Zhao X, Zhang Z, Liu J, Hao X. The function of SARI in modulating epithelial-mesenchymal transition and lung adenocarcinoma metastasis. PLoS ONE. 2012;7:e38046.
66. Blaukovitsch M, Halbwedl I, Kothmaier H, Gogg-Kammerer M, Popper HH. Sarcomatoid carcinomas of the lung – are these histogenetically heterogeneous tumors? Virchows Arch. 2006;449:455–61.
67. Risolino M, Mandia N, Iavarone F, Dardaei L, Longobardi E, Fernandez S, Talotta F, Bianchi F, Pisati F, Spaggiari L, Harter PN, Mittelbronn M, Schulte D, Incoronato M, Di Fiore PP, Blasi F, Verde P. Transcription factor PREP1 induces EMT and metastasis by controlling the TGF-beta-SMAD3 pathway in non-small cell lung adenocarcinoma. Proc Natl Acad Sci U S A. 2014;111:E3775–84.

68. Shen L, Chen L, Wang Y, Jiang X, Xia H, Zhuang Z. Long noncoding RNA MALAT1 promotes brain metastasis by inducing epithelial-mesenchymal transition in lung cancer. J Neurooncol. 2015;121:101–8.
69. Marek LA, Hinz TK, von Massenhausen A, Olszewski KA, Kleczko EK, Boehm D, Weiser-Evans MC, Nemenoff RA, Hoffmann H, Warth A, Gozgit JM, Perner S, Heasley LE. Nonamplified FGFR1 is a growth driver in malignant pleural mesothelioma. Mol Cancer Res. 2014;12:1460–9.
70. de Reynies A, Jaurand MC, Renier A, Couchy G, Hysi I, Elarouci N, Galateau-Salle F, Copin MC, Hofman P, Cazes A, Andujar P, Imbeaud S, Petel F, Pairon JC, Le Pimpec-Barthes F, Zucman-Rossi J, Jean D. Molecular classification of malignant pleural mesothelioma: identification of a poor prognosis subgroup linked to the epithelial-to-mesenchymal transition. Clin Cancer Res. 2014;20:1323–34.
71. Luzzi KJ, MacDonald IC, Schmidt EE, Kerkvliet N, Morris VL, Chambers AF, Groom AC. Multistep nature of metastatic inefficiency: dormancy of solitary cells after successful extravasation and limited survival of early micrometastases. Am J Pathol. 1998;153:865–73.
72. Im JH, Fu W, Wang H, Bhatia SK, Hammer DA, Kowalska MA, Muschel RJ. Coagulation facilitates tumor cell spreading in the pulmonary vasculature during early metastatic colony formation. Cancer Res. 2004;64:8613–9.
73. Gil-Bernabe AM, Ferjancic S, Tlalka M, Zhao L, Allen PD, Im JH, Watson K, Hill SA, Amirkhosravi A, Francis JL, Pollard JW, Ruf W, Muschel RJ. Recruitment of monocytes/macrophages by tissue factor-mediated coagulation is essential for metastatic cell survival and premetastatic niche establishment in mice. Blood. 2012;119:3164–75.
74. Wahrenbrock M, Borsig L, Le D, Varki N, Varki A. Selectin-mucin interactions as a probable molecular explanation for the association of Trousseau syndrome with mucinous adenocarcinomas. J Clin Invest. 2003;112:853–62.
75. Mairinger FD, Walter RF, Werner R, Christoph DC, Ting S, Vollbrecht C, Zarogoulidis K, Huang H, Li Q, Schmid KW, Wohlschlaeger J, Zarogoulidis P. Activation of angiogenesis differs strongly between pulmonary carcinoids and neuroendocrine carcinomas and is crucial for carcinoid tumourgenesis. J Cancer. 2014;5:465–71.
76. Takanami I, Takeuchi K, Karuke M. Expression of ETS-1 is correlated with urokinase-type plasminogen activator and poor prognosis in pulmonary adenocarcinoma. Tumour Biol. 2001;22:205–10.
77. Lin MI, Yu J, Murata T, Sessa WC. Caveolin-1-deficient mice have increased tumor microvascular permeability, angiogenesis, and growth. Cancer Res. 2007;67:2849–56.
78. Heidemann F, Schildt A, Schmid K, Bruns OT, Riecken K, Jung C, Ittrich H, Wicklein D, Reimer R, Fehse B, Heeren J, Luers G, Schumacher U, Heine M. Selectins mediate small cell lung cancer systemic metastasis. PLoS ONE. 2014;9:e92327.
79. Tang CH, Tan TW, Fu WM, Yang RS. Involvement of matrix metalloproteinase-9 in stromal cell-derived factor-1/CXCR4 pathway of lung cancer metastasis. Carcinogenesis. 2008;29:35–43.
80. Chen FA, Alosco T, Croy BA, Narumi K, Percy DH, Bankert RB. Clones of tumor cells derived from a single primary human lung tumor reveal different patterns of beta 1 integrin expression. Cell Adhes Commun. 1994;2:345–57.
81. Ruoslahti E. Vascular zip codes in angiogenesis and metastasis. Biochem Soc Trans. 2004;32:397–402.
82. Holopainen T, Saharinen P, D'Amico G, Lampinen A, Eklund L, Sormunen R, Anisimov A, Zarkada G, Lohela M, Helotera H, Tammela T, Benjamin LE, Yla-Herttuala S, Leow CC, Koh GY, Alitalo K. Effects of angiopoietin-2-blocking antibody on endothelial cell-cell junctions and lung metastasis. J Natl Cancer Inst. 2012;104:461–75.
83. Hiratsuka S, Ishibashi S, Tomita T, Watanabe A, Akashi-Takamura S, Murakami M, Kijima H, Miyake K, Aburatani H, Maru Y. Primary tumours modulate innate immune signalling to create pre-metastatic vascular hyperpermeability foci. Nat Commun. 2013;4:1853.
84. Onoda T, Kanno M, Sato H, Takahashi N, Izumino H, Ohta H, Emura T, Katoh H, Ohizumi H, Ohtake H, Asao H, Dehner LP, Hill AD, Hayasaka K, Mitsui T. Identification of novel ALK rearrangement A2M-ALK in a neonate with fetal lung interstitial tumor. Genes Chromosom Cancer. 2014;53:865–74.
85. Tavora F, Miettinen M, Fanburg-Smith J, Franks TJ, Burke A. Pulmonary artery sarcoma: a histologic and follow-up study with emphasis on a subset of low-grade myofibroblastic sarcomas with a good long-term follow-up. Am J Surg Pathol. 2008;32:1751–61.
86. Liang Z, Zhan W, Zhu A, Yoon Y, Lin S, Sasaki M, Klapproth JM, Yang H, Grossniklaus HE, Xu J, Rojas M, Voll RJ, Goodman MM, Arrendale RF, Liu J, Yun CC, Snyder JP, Liotta DC, Shim H. Development of a unique small molecule modulator of CXCR4. PLoS ONE. 2012;7:e34038.
87. Horak CE, Steeg PS. Metastasis gets site specific. Cancer Cell. 2005;8:93–5.
88. Takenaka K, Shibuya M, Takeda Y, Hibino S, Gemma A, Ono Y, Kudoh S. Altered expression and function of beta1 integrins in a highly metastatic human lung adenocarcinoma cell line. Int J Oncol. 2000;17:1187–94.
89. Liu B, Wu X, Wang C, Liu Y, Zhou Q, Xu K. MiR-26a enhances metastasis potential of lung cancer cells via AKT pathway by targeting PTEN. Biochim Biophys Acta. 2012;1822:1692–704.
90. Gutschner T, Hammerle M, Eissmann M, Hsu J, Kim Y, Hung G, Revenko A, Arun G, Stentrup M, Gross M, Zornig M, MacLeod AR, Spector DL, Diederichs S. The noncoding RNA MALAT1 is a critical regulator of the metastasis phenotype of lung cancer cells. Cancer Res. 2013;73:1180–9.

91. Ji P, Diederichs S, Wang W, Boing S, Metzger R, Schneider PM, Tidow N, Brandt B, Buerger H, Bulk E, Thomas M, Berdel WE, Serve H, Muller-Tidow C. MALAT-1, a novel noncoding RNA, and thymosin beta4 predict metastasis and survival in early-stage non-small cell lung cancer. Oncogene. 2003;22:8031–41.
92. Seiter S, Arch R, Reber S, Komitowski D, Hofmann M, Ponta H, Herrlich P, Matzku S, Zoller M. Prevention of tumor metastasis formation by anti-variant CD44. J Exp Med. 1993;177:443–55.
93. Hendriks LE, Smit EF, Vosse BA, Mellema WW, Heideman DA, Bootsma GP, Westenend M, Pitz C, de Vries GJ, Houben R, Grunberg K, Bendek M, Speel EJ, Dingemans AM. EGFR mutated non-small cell lung cancer patients: more prone to development of bone and brain metastases? Lung Cancer. 2014;84:86–91.
94. Riihimaki M, Hemminki A, Fallah M, Thomsen H, Sundquist K, Sundquist J, Hemminki K. Metastatic sites and survival in lung cancer. Lung Cancer. 2014;86:78–84.
95. Shin DY, Na II, Kim CH, Park S, Baek H, Yang SH. EGFR mutation and brain metastasis in pulmonary adenocarcinomas. J Thorac Oncol. 2014;9:195–9.
96. Kafka A, Tomas D, Beros V, Pecina HI, Zeljko M, Pecina-Slaus N. Brain metastases from lung cancer show increased expression of DVL1, DVL3 and beta-catenin and down-regulation of E-cadherin. Int J Mol Sci. 2014;15:10635–51.
97. Sinkevicius KW, Kriegel C, Bellaria KJ, Lee J, Lau AN, Leeman KT, Zhou P, Beede AM, Fillmore CM, Caswell D, Barrios J, Wong KK, Sholl LM, Schlaeger TM, Bronson RT, Chirieac LR, Winslow MM, Haigis MC, Kim CF. Neurotrophin receptor TrkB promotes lung adenocarcinoma metastasis. Proc Natl Acad Sci U S A. 2014;111:10299–304.
98. Fabian K, Nemeth Z, Furak J, Tiszlavicz L, Papay J, Krenacs T, Timar J, Moldvay J. Protein expression differences between lung adenocarcinoma and squamous cell carcinoma with brain metastasis. Anticancer Res. 2014;34:5593–7.
99. Sakamoto S, Inoue H, Ohba S, Kohda Y, Usami I, Masuda T, Kawada M, Nomoto A. New metastatic model of human small-cell lung cancer by orthotopic transplantation in mice. Cancer Sci. 2015;106:367–74.
100. Bleckmann A, Siam L, Klemm F, Rietkotter E, Wegner C, Kramer F, Beissbarth T, Binder C, Stadelmann C, Pukrop T. Nuclear LEF1/TCF4 correlate with poor prognosis but not with nuclear beta-catenin in cerebral metastasis of lung adenocarcinomas. Clin Exp Metastasis. 2013;30:471–82.
101. Fontanini G, Calcinai A, Boldrini L, Lucchi M, Mussi A, Angeletti CA, Cagno C, Tognetti MA, Basolo F. Modulation of neoangiogenesis in bronchial preneoplastic lesions. Oncol Rep. 1999;6:813–7.
102. Lin LC, Hsu SL, Wu CL, Hsueh CM. TGFbeta can stimulate the p(38)/beta-catenin/PPARgamma signaling pathway to promote the EMT, invasion and migration of non-small cell lung cancer (H460 cells). Clin Exp Metastasis. 2014;31:881–95.
103. Pereda J, Sulz L, San Martin S, Godoy-Guzman C. The human lung during the embryonic period: vasculogenesis and primitive erythroblasts circulation. J Anat. 2013;222:487–94.
104. Lin CY, Chen HJ, Huang CC, Lai LC, Lu TP, Tseng GC, Kuo TT, Kuok QY, Hsu JL, Sung SY, Hung MC, Sher YP. ADAM9 promotes lung cancer metastases to brain by a plasminogen activator-based pathway. Cancer Res. 2014;74:5229–43.
105. Sellon RK, Johnson JL, Leathers CW, Sporn T, Beckley JC. Tracheobronchopathia osteochondroplastica in a dog. J Vet Intern Med. 2004;18:359–62.
106. Kranenburg AR, de Boer WI, Alagappan VK, Sterk PJ, Sharma HS. Enhanced bronchial expression of vascular endothelial growth factor and receptors (Flk-1 and Flt-1) in patients with chronic obstructive pulmonary disease. Thorax. 2005;60:106–13.
107. Sher YP, Wang LJ, Chuang LL, Tsai MH, Kuo TT, Huang CC, Chuang EY, Lai LC. ADAM9 upregulates N-cadherin via miR-218 suppression in lung adenocarcinoma cells. PLoS ONE. 2014;9:e94065.
108. Li F, Sun L, Zhang S. Acquirement of DNA copy number variations in nonsmall cell lung cancer metastasis to the brain. Oncol Rep. 2015;34:1701–7.
109. Zhao N, Wilkerson MD, Shah U, Yin X, Wang A, Hayward MC, Roberts P, Lee CB, Parsons AM, Thorne LB, Haithcock BE, Grilley-Olson JE, Stinchcombe TE, Funkhouser WK, Wong KK, Sharpless NE, Hayes DN. Alterations of LKB1 and KRAS and risk of brain metastasis: comprehensive characterization by mutation analysis, copy number, and gene expression in non-small-cell lung carcinoma. Lung Cancer. 2014;86:255–61.
110. Hwang SJ, Lee HW, Kim HR, Song HJ, Lee DH, Lee H, Shin CH, Joung JG, Kim DH, Joo KM, Kim HH. Overexpression of microRNA-95-3p suppresses brain metastasis of lung adenocarcinoma through downregulation of cyclin D1. Oncotarget. 2015;6:20434–48.
111. Gao Y, Li G, Sun L, He Y, Li X, Sun Z, Wang J, Jiang Y, Shi J. ACTN4 and the pathways associated with cell motility and adhesion contribute to the process of lung cancer metastasis to the brain. BMC Cancer. 2015;15:277.
112. Han L, Liang XH, Chen LX, Bao SM, Yan ZQ. SIRT1 is highly expressed in brain metastasis tissues of non-small cell lung cancer (NSCLC) and in positive regulation of NSCLC cell migration. Int J Clin Exp Pathol. 2013;6:2357–65.
113. Yoo JY, Yang SH, Lee JE, Cho DG, Kim HK, Kim SH, Kim IS, Hong JT, Sung JH, Son BC, Lee SW. E-cadherin as a predictive marker of brain metastasis in non-small-cell lung cancer, and its

regulation by pioglitazone in a preclinical model. J Neurooncol. 2012;109:219–27.
114. Li Q, Yang J, Yu Q, Wu H, Liu B, Xiong H, Hu G, Zhao J, Yuan X, Liao Z. Associations between single-nucleotide polymorphisms in the PI3K-PTEN-AKT-mTOR pathway and increased risk of brain metastasis in patients with non-small cell lung cancer. Clin Cancer Res. 2013;19:6252–60.
115. Li Q, Wu H, Chen B, Hu G, Huang L, Qin K, Chen Y, Yuan X, Liao Z. SNPs in the TGF-beta signaling pathway are associated with increased risk of brain metastasis in patients with non-small-cell lung cancer. PLoS ONE. 2012;7:e51713.
116. Paik PK, Shen R, Won H, Rekhtman N, Wang L, Sima CS, Arora A, Seshan V, Ladanyi M, Berger MF, Kris MG. Next-generation sequencing of stage IV squamous cell lung cancers reveals an association of PI3K aberrations and evidence of clonal heterogeneity in patients with brain metastases. Cancer Discov. 2015;5:610–21.
117. Cagle PD. In: Travis WD, Brambilla E, Burke AP, Marx A, Nicholson AG, editors. Epithelioid haemangioendothelioma, vol. 2. Lyon: International Agency for Research on Cancer (IARC); 2015. p. 123–4.
118. Hofmann M, Rudy W, Gunthert U, Zimmer SG, Zawadzki V, Zoller M, Lichtner RB, Herrlich P, Ponta H. A link between ras and metastatic behavior of tumor cells: ras induces CD44 promoter activity and leads to low-level expression of metastasis-specific variants of CD44 in CREF cells. Cancer Res. 1993;53:1516–21.
119. Valencia K, Ormazabal C, Zandueta C, Luis-Ravelo D, Anton I, Pajares MJ, Agorreta J, Montuenga LM, Martinez-Canarias S, Leitinger B, Lecanda F. Inhibition of collagen receptor discoidin domain receptor-1 (DDR1) reduces cell survival, homing, and colonization in lung cancer bone metastasis. Clin Cancer Res. 2012;18:969–80.
120. Vicent S, Luis-Ravelo D, Anton I, Garcia-Tunon I, Borras-Cuesta F, Dotor J, De Las Rivas J, Lecanda F. A novel lung cancer signature mediates metastatic bone colonization by a dual mechanism. Cancer Res. 2008;68:2275–85.
121. Burke AP, Yi ES In: Pulmonary artery intimal sarcoma. In: Travis WD, Brambilla E, Burke AP, Marx A, Nicholson AG, editors. WHO Classification of Tumours of the Lung, Pleura, Thymus and Heart. Lyon: International Agency for Research on Cancer (IARC); 2015.
122. Xie L, Yang Z, Li G, Shen L, Xiang X, Liu X, Xu D, Xu L, Chen Y, Tian Z, Chen X. Genome-wide identification of bone metastasis-related microRNAs in lung adenocarcinoma by high-throughput sequencing. PLoS ONE. 2013;8:e61212.
123. Luis-Ravelo D, Anton I, Zandueta C, Valencia K, Pajares MJ, Agorreta J, Montuenga L, Vicent S, Wistuba, II, De Las Rivas J, Lecanda F. RHOB influences lung adenocarcinoma metastasis and resistance in a host-sensitive manner. Mol Oncol. 2014;8:196–206.
124. Zhang W, Yu C, Huang B, Zhou FL, Huang HD, Li Q. Correlation between bone metastasis and thrombocytosis in pulmonary adenocarcinoma patients. Oncol Lett. 2015;9:762–8.
125. Nakamura ES, Koizumi K, Kobayashi M, Saitoh Y, Arita Y, Nakayama T, Sakurai H, Yoshie O, Saiki I. RANKL-induced CCL22/macrophage-derived chemokine produced from osteoclasts potentially promotes the bone metastasis of lung cancer expressing its receptor CCR4. Clin Exp Metastasis. 2006;23:9–18.
126. Feeley BT, Liu NQ, Conduah AH, Krenek L, Roth K, Dougall WC, Huard J, Dubinett S, Lieberman JR. Mixed metastatic lung cancer lesions in bone are inhibited by noggin overexpression and rank:Fc administration. J Bone Miner Res. 2006;21:1571–80.
127. Kuo PL, Liao SH, Hung JY, Huang MS, Hsu YL. MicroRNA-33a functions as a bone metastasis suppressor in lung cancer by targeting parathyroid hormone related protein. Biochim Biophys Acta. 1830;2013:3756–66.
128. Peng X, Guo W, Ren T, Lou Z, Lu X, Zhang S, Lu Q, Sun Y. Differential expression of the RANKL/RANK/OPG system is associated with bone metastasis in human non-small cell lung cancer. PLoS ONE. 2013;8:e58361.
129. Miller RE, Jones JC, Tometsko M, Blake ML, Dougall WC. RANKL inhibition blocks osteolytic lesions and reduces skeletal tumor burden in models of non-small-cell lung cancer bone metastases. J Thorac Oncol. 2014;9:345–54.
130. Dougall WC, Holen I, Gonzalez Suarez E. Targeting RANKL in metastasis. Bonekey Rep. 2014;3:519.
131. Kim S, Kim TM, Kim DW, Go H, Keam B, Lee SH, Ku JL, Chung DH, Heo DS. Heterogeneity of genetic changes associated with acquired crizotinib resistance in ALK-rearranged lung cancer. J Thorac Oncol. 2013;8:415–22.
132. Guo H, Xing Y, Liu R, Chen S, Bian X, Wang F, Yang C, Wang X. 216G/T (rs712829), a functional variant of the promoter, is associated with the pleural metastasis of lung adenocarcinoma. Oncol Lett. 2013;6:693–8.
133. Hofmann M, Rudy W, Zoller M, Tolg C, Ponta H, Herrlich P, Gunthert U. CD44 splice variants confer metastatic behavior in rats: homologous sequences are expressed in human tumor cell lines. Cancer Res. 1991;51:5292–7.
134. Boelens MC, Kok K, van der Vlies P, van der Vries G, Sietsma H, Timens W, Postma DS, Groen HJ, van den Berg A. Genomic aberrations in squamous cell lung carcinoma related to lymph node or distant metastasis. Lung Cancer. 2009;66:372–8.

Molecular Pathology of Lung Tumors

19

19.1 Introduction

Within the last decade, many important discoveries were made in the regulation of growth, differentiation, apoptosis, and metastasis of lung cancers. These findings have dramatically changed the "ignorance" in the oncology community about the classification of lung carcinomas. A decade ago, oncologists were mainly interested to get the differentiation between small cell (SCLC) and non-small cell carcinomas (NSCLC) of the lung. With the findings of different responses for cisplatin and anti-angiogenic treatment in adenocarcinomas versus squamous cell carcinomas, this simple clinical lung carcinoma classification schema was abolished. Now oncologists want to know the differentiation within NSCLC, and the near future will even increase subtyping of the different NSCLC entities. In this review, we will first focus on general aspects of molecular pathology in lung carcinomas and then discuss different genetic abnormalities within the different entities. These abnormalities will be ordered according to their importance such as targeted therapy and impact on outcome.

19.2 Therapy Relevant Molecular Changes in Pulmonary Carcinomas

19.2.1 NSCLC and Angiogenesis

In the last decade, humanized antibodies have been developed to interfere with the neoangiogenesis in primary as well as metastatic carcinomas [1, 2]. However, anti-angiogenic drugs can cause severe bleeding, especially when administered in patients with centrally located squamous cell carcinomas [3, 4]. However, it is still not clear if the reported bleeding episodes in these patients are due to the squamous histology or more logically to the centrally located tumors, which are usually supported by arteries and veins arising from large branches. In addition it was reported that cavitation within the tumor is prone to hemorrhage, again something more common in central tumors located close to large blood vessels [5].

Angiogenesis, better neoangiogenesis, is a process by which primary tumors get access to nutrients and oxygen. The process of neoangio-

© Springer-Verlag Berlin Heidelberg 2017
H. Popper, *Pathology of Lung Disease*, DOI 10.1007/978-3-662-50491-8_19

genesis is still not fully understood. In some cases, the tumor cells themselves produce angiogenic factors such as vascular endothelial growth factors (VEGFs); in other cases, these growth factors are produced by macrophages present in the tumor microenvironment [6]. However, once new blood vessels (capillaries, small arteries, veins) are formed, this provides advantage for the tumor cells over their normal neighbor cells in getting better oxygen and nutrient supply. Nutrients and oxygen are not the only important factor for better growth; also purine and pyrimidine bases are essential for a dividing tumor cell [7–10]. A good example on how this can influence the progression from preinvasive to invasive lesions is the vascular variant of squamous cell dysplasia. It seems that the early access to blood vessels promotes rapid progression into squamous cell carcinoma [11]. In another preneoplasia, atypical adenomatous hyperplasia (AAH) vascularization is a late event, usually at the transition from in situ to invasive adenocarcinoma [12, 13]. This might explain why AAH can persist for several years without progression [14]. In addition there seems to exist a difference between mucinous and non-mucinous adenocarcinomas with respect to neoangiogenesis [15]. Increased angiogenesis itself in invasive adenocarcinomas has a negative impact on survival and progression of these patients [16].

Angiogenesis is essential for the primary tumor as well as for metastasis. The secretion of VEGFs facilitates most often neoangiogenesis. Tumor blood vessels are fragile and are prone to rupture. Using antibodies against VEGF (bevacizumab), the vascularization can be inhibited, and regression of the tumor is induced. In centrally located tumors, therapy can result in severe hemorrhage. Therefore, the use of bevacizumab is recommended for adenocarcinomas and large cell carcinomas, but squamous cell carcinomas are excluded – SCC is most often a centrally located tumor.

New developments are focusing on the inhibition of the VEGF receptors and also on the role of HIF and hypoxia in tumor development and metastasis. In several studies, the importance of VEGF and VEGFR axis was stated for vascular invasion and metastasis, mainly involving VEGF-C and VEGFR3 [16–19]. Studies aiming to target this axis showed positive results in experimental settings [20–23]. Bringing these targeted therapies into clinical trials is still in its infancy [24, 25]. A major problem in targeting VEGF-VEGFR is the fact that its regulation is under the major influence of the hypoxia pathway. Hypoxia is an important factor in invasion and angioinvasion, and HIF1α signaling will result in the upregulation of VEGF [26, 27]. So the hypoxia pathway might constantly overrule a blockade of VEGF-VEGFR unless also HIF1α production is also inhibited [28].

19.2.2 NSCLC and Cisplatin Drugs: The Effect of Antiapoptotic Signaling

In a large multi-institutional study, the effect of cisplatin chemotherapy was investigated. High expression of DNA repair enzymes, especially nucleotide excision repair enzyme (ERCC1), was found to be responsible for failure of cisplatin chemotherapy, and this expression correlated predominantly with squamous cell histology [29, 30]. ERCC1 is part of the excision repair machinery involved in the repair of damaged DNA. In NSCLC showing a high expression of this enzyme, the action of cisplatin-based chemotherapeutics is inefficient, most probably because DNA damage induced by the drug is immediately repaired. Therefore, ERCC1 should be investigated by immunohistochemistry to predict response to therapy especially in squamous cell carcinomas.

19.2.3 Thymidylate Synthase Blocker

Pemetrexed is an inhibitor of thymidylate synthase (TS) less for the other enzymes in the thymidine cycle. Thymidine uptake is essential for rapidly dividing carcinoma cells. In tumors with low expression of TS, pemetrexed can block the enzyme resulting in growth inhibition. TS expression most often is low in adenocarcinomas, but is

highly expressed in many squamous cell carcinomas. Thus, pemetrexed is efficient in most adenocarcinomas and not in squamous cell carcinomas [31]. However, the action of pemetrexed is still not entirely clear: thymidylate metabolism does not only rely on enzymes of the thymidylate cycle but also needs active and passive uptake mechanisms; and thymidine uptake might also be influenced by pemetrexed [32, 33].

19.2.4 Receptor Tyrosine Kinases in Lung Carcinomas

Receptor tyrosine kinases (RTK) are membrane-bound protein receptor composed of an external receptor domain, a transmembrane spanning portion, and an internal domain, which at its C-terminal end contains the kinase domain. The external receptor domain has a specific configuration for the binding of growth factors, where usually two molecules form homo- or heterodimer with the receptor domain. This specific binding changes the configuration of the whole receptor and leads to the activation of the kinase domain. There are two ways of activation of receptor tyrosine kinases in lung cancer: overproduction of ligands either by the tumor cell or by cells within the microenvironment, such as macrophages, and activation by a mutation of the receptor gene, most often within the kinase domain. The receptor kinase itself can act also in two different ways: one is transfer of phosphorylation to transfer molecules [34–38], like GAB1 or Grb2, and the kinase splits into fragments, where one activated protein fragment translocates into the nucleus and binds to specific DNA elements and induces transcription of proteins [39–41]. In lung cancer, RTKs can be constantly activated by different mechanisms: amplification of the RTK gene, mutations of the RTK gene, and gene rearrangements (translocation/inversion) with constant activation or inactivation of regulatory proteins. Another mechanism is downregulation of regulatory proteins by miRNAs, so a tumor suppressor or a negative feedback protein is not synthesized because of mRNA inactivation by miRNA [42–48].

19.2.5 TP53: The Tumor Suppressor Gene

TP53 was one of the first tumor suppressor genes detected as being mutated in almost every cancer type. TP53 is located on chromosome 17p13-12, contains 11 exons, and has two promoters (one upstream of noncoding first exon and another within first intron) [49]. The protein p53 functions as a cell cycle control, which can send cells with defective DNA directly into apoptosis [50]. TP53 is either mutated or methylated in most lung carcinomas, especially in all tobacco smoke-associated variants. Analysis of these types of mutations highlighted some nonfunctional mutations most probably due to interaction with some tobacco genotoxic compounds [51–56], whereas other mutations resulted in truncation of the protein, defect of protein degradation, and loss of function [57–60]. Mutations and methylation-induced silencing are common in SCLC and squamous cell carcinomas and less frequently in adenocarcinomas [52, 61, 62]. There is still an ongoing debate if p53 inactivation is related to a metastatic phenotype [63–65].

Next we will focus more specifically on tumor entities and what molecular profiles are known in each entity.

19.3 Adenocarcinomas

Adenocarcinomas in highly industrialized countries are the most common lung carcinoma, with a percentage of 40 % of all lung carcinomas. In addition what was previously regarded as a single entity has become a huge diversity of carcinomas. Adenocarcinomas in never-smokers most probably represent a separate entity with different gene signatures and a slower progression rate compared to adenocarcinomas in smokers. Also gene signatures have contributed to a more heterogeneous picture. Morphologically adenocarcinomas can show a variety of patterns, which in part correlate with gene signatures, although our knowledge in this respect is still in its infancy.

Adenocarcinoma is defined by the formation of papillary, micropapillary, cribriform, acinar,

and solid structures, the latter with mucin synthesis – mucin-containing vacuoles in at least 10 % of the tumor cells. Adenocarcinomas can be either mucinous or non-mucinous. Both will show the above mentioned patterns. Some rare variants are fetal, colloid, and enteric adenocarcinomas. Most often a mixed pattern is seen with a predominance of at least one component.

Tumor cells in adenocarcinomas can show differentiations along well-known cell types as Clara cells, pneumocyte type II, columnar cells, and goblet cells. Due to the importance of targeted therapy, the exact classification of adenocarcinomas and their differentiation from other NSCLCs have become a major task in pulmonary pathology. Differentiation factors are used to prove the nature of the carcinoma especially in less well-differentiated examples. A variety of useful markers for have been tested; the most important ones are TTF1 and Napsin A.

19.3.1 EGFR

In 2004 an epidermal growth factor receptor (EGFR) mutation was detected in a patient with lung adenocarcinoma and responded to tyrosine kinase inhibitor treatment – a new era of targeted therapy in NSCLC was invented [66, 67].

Mutation of EGFR has been detected in a small percentage of lung cancer patients in the Caucasian population. In Southeast Asians the percentage can rise to 60 %. These are activating mutations found in exons 18, 19, 20, and 21 of the EGFR gene (kinase domain) [68]. Mutations are most often found in never-smokers, females, and patients with adenocarcinoma histology. Mutations change the configuration of the kinase, which does not need anymore the ligand-based activation from the receptor domain. The receptor stays in an activated stage and constantly signals downstream. Carcinomas with this activating mutation can be growth inhibited by small receptor tyrosine kinase inhibitors (TKI) such as gefitinib, erlotinib, and afatinib. These TKIs bind either reversible or irreversible into the ATP pocket of the mutated EGFR kinase and thus inhibit phosphor-transfer to downstream molecules, thus blocking the signaling cascade [69]. The most common mutations are deletions within exon 19 with a variation of 9–18 nucleotides and a point mutation at exon 21. Other less common mutations are point mutations in exon 18 and insertions in exon 20.

However, mainly within exon 20, there are also resistance mutations; the best known is T790M. This type of mutation inhibits or reverses the binding of the TKIs gefitinib and erlotinib and prevents the receptor blockade. The irreversible TKI afatinib might overrule some of these resistance mutations, but more data are needed to prove this [70, 71].

For targeted therapy with TKIs, tissue samples of NSCLC have to be analyzed for these mutations. Within the different subtypes of adenocarcinomas, some will show a higher percentage of EGFR mutations, whereas others do not. In Caucasian population, adenocarcinomas with acinar or papillary pattern are up to 27 % mutated, whereas mucinous adenocarcinomas are constantly negative for EGFR mutations. Carcinomas with biphasic morphology such as adenosquamous carcinomas and mixed small cell and adenocarcinomas can show mutations but usually in a very small percentage.

Another therapy approach was tested with humanized monoclonal antibodies for EGF. By competitive binding to the receptor, this antibody replaces EGF and thus inhibits transactivation of the kinase. This type of therapy seems to be especially promising in EGFR-naïve (wild-type) adenocarcinomas and in addition also in squamous cell carcinomas [72, 73].

19.3.2 KRAS

KRAS was one of the early detected oncogenes in adenocarcinomas of the lung. KRAS belongs to the family of small GTPases located close to the inner cell membrane. They can be activated by tyrosine receptor kinases either membrane bound as EGFR or also by cytosolic kinases as SRC. Usually phosphorylated transfer molecules activate them as GRB2 [74–76]. Once activated, they can signal downstream into three major cascades: RAL-RAF,

MEK-ERK, and PI3K-AKT. These different activation cascades have different effects on tumor cells; however, the exact interaction and the mechanisms, which select a specific signaling pathway, are not clear [77, 78].

Mutations of KRAS in lung adenocarcinomas are found in the codon 12, 13, and 61. These mutations result in constant activation of KRAS and consecutively activation of the downstream cascades. KRAS in this situation does not need an upstream activation.

KRAS mutations occur at an average of 30 % of all pulmonary adenocarcinomas, but this percentage rises to 50 % in mucinous adenocarcinomas [79]. In one study, KRAS mutations were more frequently seen in solid adenocarcinomas [80]. Whereas KRAS mutations are frequent in Caucasian, these are rare in Southeast Asian population, opposite to the situation of the frequency of EGFR mutations [81–84].

Targeted therapy this moment does not exist for patients with mutated adenocarcinomas, but there are trials going on, which aim to inhibit the downstream signaling pathway with MEK, ERK, and mTOR inhibitors [25].

19.3.3 EML4ALK1 and Additional Fusion Partners

Inversion (erroneously called translocation) of the ALK1 kinase gene and fusion with the EML4 gene have been recently shown in patients with NSCLC, especially in solid adenocarcinomas with focal differentiation into signet ring cells. Subsequently other patterns have been associated with this type of gene rearrangement, such as micropapillary. Both genes are on chromosome 2; the chromosomal break is inversely rearranged whereby the kinase domain of ALK and EML4 is fused together. The ALK kinase thus is under the control of EML4, which results in a constant activation of the kinase. ALK similar to EGFR stimulates proliferation and inhibits apoptosis [85]. Patients with this inversion respond excellently to crizotinib treatment, which is now the second example of targeted therapy in NSCLC [86]. Proof of EML4ALK1 inversion can be done with different methods: the most common is FISH where two probes (3′ and 5′) detecting the ALK gene on both sides of the breakpoint are used. In normal situation, this probes will detect the two portions close together or overlapping within the tumor nucleus. In cases of rearrangement, the probes will highlight each of the splitted portions of the ALK1 gene, so instead of two overlapping signals the signals split apart. In the Caucasian population, EML4ALK1 rearrangement is usually found in 4–6 % of NSCLC; in adenocarcinomas, this might be increased to 8 %.

Other genes joining the ALK1 gene in the same way can replace the EML4 gene. If KIF5B joins to ALK1, the overexpression of KIF5B-ALK [45] in mammalian cells led to the activation of signal transducer and activator of transcription 3 (STAT3) and protein kinase B and enhanced cell proliferation, migration, and invasion [45]. Another fusion partner recently described is ALK-KLC1 [87]. These other ALK1 fusions are rare; the incidence is about 1 %.

Resistance mechanisms in EML4ALK-rearranged lung adenocarcinomas do exist; however, the exact mechanisms are still under investigation [88–91].

19.3.4 ROS1

ROS1 is another kinase involved as a driver gene in adenocarcinomas of the lung [92]. Usually the rearrangement of ROS1 is evaluated by two FISH probes for the 3′- and the 5′ ends. Only few fusion partners have been identified so far, CD74, SLC34A2, EZR, and GOPC/FIG [93–95]. This gene rearrangement has no influence on outcome, but similar to ALK1, this is usually a younger population of cancer patients [96]. The incidence of ROS1 rearrangement is in the range of 1 %. The function of one of the fusion genes EZR-ROS was studied in a mouse model and showed that in this experimental setting the fusion gene acted as an oncogene inducing multiple tumor nodules in mice [95]. Most important patients with this type of gene aberrations responded well to the ALK1 inhibitor crizotinib [97–99].

19.3.5 KIF5B and RET

KIF5B is one of the fusion partners for either ALK1 or RET. The KIF5B-RET fusion gene is caused by a pericentric inversion of 10p11.22-q11.21. This fusion gene overexpresses chimeric RET receptor tyrosine kinase, which can spontaneously induce cellular transformation [100]. Besides KIF5B, CCDC6, and NCOA4 can form fusion genes with RET. Patients with lung adenocarcinomas with RET fusion gene had more poorly differentiated tumors, are younger, and are more often never-smokers. Solid adenocarcinomas predominate, tumors are smaller, but lymph node incidence is higher. The incidence of RET fusion is about in 1% of NSCLCs and almost 2% of adenocarcinomas [100–102].

19.3.6 MET

MET is another receptor tyrosine kinase bound to cell membranes in NSCLC. The ligand for MET is HGF, originally found in hepatic carcinomas. This receptor came into consideration in NSCLC because amplification of MET or alternatively upregulation of HGF was identified as a mechanism of the resistance in EGFR-mutated adenocarcinomas [43, 103]. A search for the role of MET in other NSCLCs excluding EGFR-mutated adenocarcinomas showed that MET amplification was rare, but upregulation of MET is a common event: approximately 20% of NSCLC including adenocarcinomas and squamous cell carcinomas showed high protein expression, but only 2% MET amplification (Popper et al. in preparation). Clinical studies are in progress to evaluate the possibility to interfere with MET signaling using monoclonal antibodies. Other studies use small molecule inhibitors for MET. Since MET expression is common in EGFR-mutated adenocarcinomas, these studies aim to inhibit both EGFR and MET signaling pathways [104–106].

19.3.7 Others Genes

Histone acetylases and deacetylases (HAT, HDAC) regulate the access of the DNA by methylation and demethylation. Thus, these enzymes are important for DNA silencing [107–109]. In addition heavily methylated DNA tends to switch into a supercoiled form, which cannot be read by the transcription machinery. Histones themselves are in addition important for the correct positioning of the DNA, fixing the DNA to specific areas of the nuclear membrane [110–113]. Attempts to interfere with this system have been made quite a while ago, but the results were not convincing, probably because there are several types of HATs and HDACs with different functions. Recently treatment with HDAC inhibitors in combination with other drugs has shown promising results, resulting in apoptosis and tumor cell necrosis [114–116].

In a study focusing on molecular alterations in pulmonary adenocarcinomas, many additional genes were identified: well known are losses of one allele of the tumor suppressor PTEN in 9%, often associated with upregulation of PIK3CA; however, PI3KCA mutations were also detected in 5%. Two other genes mutated in 3% and 2% were identified as STK11 and BRAF, respectively [117]. Interestingly these gene alterations could be sorted by smoking habits to either smokers (STK11) or nonsmokers (PIK3CA). In addition squamous cell carcinoma morphology was associated with PTEN, STK11, and PIK3CA [117].

In a study analyzing Korean lung cancer patients by transcriptome sequencing, the authors identified the well-known candidates, EGFR, KRAS, NRAS, BRAF, PIK3CA, MET, and CTNNB1, but also new driver mutations such as LMTK2, ARID1A, NOTCH2, and SMARCA4 [65]. Besides these mutated genes, also fusion genes were detected as ALK, RET, and ROS1 and new ones as FGFR2, AXL, and PDGFRA. We also found an association between lymph node metastasis and somatic mutations in TP53 (mutations of TP53 will be discussed later on, since this is found in several lung cancer types).

Elevated levels of insulin-like growth factor (IGF)-II are associated with a poor prognosis in human pulmonary adenocarcinoma. Moorehead et al. succeeded to establish pulmonary adenocarcinoma in mice by transgenic overexpression of IGF-II in lung epithelium. These tumors expressed TTF-1, SP-B, and proSP-C. Activation of IGF-IR resulted in the downstream activation of either the Erk1/Erk2 or p38 MAPK pathways [118].

Within this IGF/IGFR system, also binding protein plays a prominent role: IGFBP3 expression resulted in upregulation of VEGF and HIF1, pointing to an important fact of neoangiogenesis, important for accelerated growth and invasion [119]. In contrast IGFBP1 seems to act like a tumor suppressor decreasing colony formation of cell cultures and increasing apoptosis. IGFBP1 has been found methylated in pulmonary adenocarcinomas [120]. The IGFR1 pathway is also involved in resistance mechanisms in EGFR-mutated adenocarcinomas [121]. Treatment with monoclonal antibodies for IGFR1 is also in clinical studies [122–124].

19.4 Squamous Cell Carcinomas

Squamous cell carcinoma (SCC) is defined by a platelike layering of cells, keratinization of at least single cells, intercellular gaps and bridges (represented by desmosomes and hemidesmosomes), and positive staining for high molecular weight cytokeratins (CK 3/5, 13/14). There are some morphologic variants as small cell and basaloid, but these have not been associated with gene signatures and therefore are only important in diagnostics.

The incidence of SCC has dropped in the last three decades from a major entity representing 35 % of lung carcinomas to around 17 %. One of the major reasons is the shift from filter-less to filter cigarettes. This has resulted in the reduction of particle-bound carcinogens and increase of vaporized carcinogens, which more easily reach the bronchioloalveolar terminal unit, inducing mainly adenocarcinomas.

In the past, SCC was mainly a diagnosis required to exclude several therapeutic options in the clinic: no pemetrexed therapy, no anti-angiogenic drugs, and less responsiveness to cisplatin treatment. However, this has changed within the last 3 years.

19.4.1 FGFR1

Fibroblast growth factor receptor 1 was identified being amplified in about 20 % of squamous cell carcinomas [125] (and personal unpublished data). In experimental studies as well as in ongoing clinical trials, it was found that only amplification, proven by in situ hybridization methods, identified patients, which respond to small molecule inhibitor treatment [126, 127] (and unpublished communication from R. Thomas, Cologne, Germany).

19.4.2 DDR2 and FGFR2

DDR2 and FGFR2 mutations are found exclusively in squamous cell carcinomas, however, in a small percentage, 4 % and 2 %, respectively [117]. For FGFR2 multikinase inhibitors might be an option for specific treatment [128–130].

19.4.3 SOX2 Amplification

SOX2 gene located on chromosome 3q26.3 is a factor for the maintenance of stem cell-like properties in lung cancer cells [131]. SOX2 amplification has been reported to be specifically associated with SCC morphology [132–134]. However, other investigations have claimed also an importance for small cell carcinomas and adenocarcinomas [135, 136]. Amplification in SCC was associated with better prognosis [137] whereas with poor prognosis in adenocarcinomas and SCLC [135, 138]. So far no specific therapies do exist for patients with this genetic abnormality.

19.4.4 PTEN Mutation-Deletion

PTEN deletions are quite common in NSCLC, usually associated with the subsequent upregulation of PI3K and downstream activation of the AKT pathway [62, 139]. In the past, therapies were conducted with inhibitors of mTOR, but failed due to the subsequent upregulation of a negative feedback loop of mTOR, which in turn activates AKT and this time results in a circumvention of mTOR via other pathways [140–142]. Recent work, however, has shown a benefit of mTOR inhibition, when applied in the right context [143, 144]. PTEN mutation is more rare, but can be found more often in squamous cell carcinomas [117]. If patients with this genetic abnormality can also be treated by a combined modality is still an unsolved issue.

19.4.5 PDGFRA Amplification

Amplification of the PDGFR alpha was found predominantly in squamous cell carcinomas [145–147]. Although this is not a frequent event in these carcinomas, specific inhibitors have shown a growth-inhibiting effect in cell lines and might be considered in patient treatment.

19.4.6 CDKN2A (p16) Mutation, Deletion, and Methylation

Another uncommon genetic modification is found in the CDKN2A gene coding for the p16 protein. P16 is regarded as a tumor suppressor protein and is involved in cell cycle regulation in many pulmonary carcinomas including SCLC, SCC, and adenocarcinoma [148–150]. It closely interacts with Rb and p53 protein.

19.4.7 Notch1 Mutation

NOTCH-1 regulates cell specification and homeostasis of stem cell compartments, and it is counteracted by the cell fate determinant Numb. Notch signaling is altered in approximately one third of NSCLCs. Loss of Numb expression results in increased Notch activity; in a smaller fraction of cases, gain-of-function mutations of the NOTCH-1 gene are present. Inhibitors of Notch can selectively kill epithelial cell cultures harboring constitutive activation of the Notch pathway [151]. In a subsequent study, NOTCH-1 and NOTCH-2 frame shift and nonsense mutations were identified in pulmonary squamous cell carcinomas [152]. More importantly NOTCH-1 has an important role in carcinogenesis by suppressing p53-mediated apoptosis and regulating the stability of p53 protein. NOTCH-1 also plays an important role in KRAS-induced mouse adenocarcinoma models [153].

19.4.8 REL Amplification

Inducing lung adenocarcinoma in a mouse model, it was shown that different downstream activation of RAS pathways is necessary to induce an invasive and more important angioinvasive phenotype. Only the combined activation of the PI3K, RAS-MAPK-ERK, and the RAL and REL pathway could induce an aggressive phenotype [78]. Whereas REL-A seems to be exclusively expressed in SCLC, REL-B was shown to be processed in NSCLC cell lines. REL-B was shown to suppress the expression of ß1-integrin and thus prevented adherence of the carcinoma cell [154].

19.5 Large Cell Carcinoma

Large cell carcinoma (LC) is defined by large cells (>25 mμ) devoid of any cytoplasmic differentiation and large vesicular nuclei. They have a well-ordered solid structure. By electron microscopy, differentiation structures can be seen such as hemidesmosomes, tight junctions, intracytoplasmic vacuoles with microvilli, and ill-formed cilia. This fits clearly into the concept of a carcinoma, at the doorstep of adenocarcinoma and squamous cell carcinoma differentiation. LC numbers have dramatically decreased due to the use of immunohistochemistry for differentiation. Using TTF1 low molecular cytokeratins as well as

p63 and cytokeratin 5/6, most cases of LC were either shifted into adenocarcinoma or squamous cell carcinoma, respectively [155]. These recent changes make an evaluation of genetic aberrations in LC quite difficult, since genetic studies were based on previous classifications.

Not surprisingly EGFR mutations, MET amplifications, and EML4ALK1 fusions have been reported in LCC [156, 157]. LKB1 a gene mutated in a small percentage of adenocarcinomas was also shown in squamous and large cell carcinomas [158]. LKB1, also known as STK11, is involved in the negative regulation of mTOR and closely cooperates with TSC1 and TSC2 genes [159].

19.6 Other Types of Large Cell Carcinomas

In contrast to LC, which is negatively defined by exclusion criteria, these are positively defined.

LC with rhabdoid phenotype is characterized by a solid growth pattern, often overlaid by a reactive proliferation of pneumocytes, which can give these tumors a pseudoalveolar pattern and a pseudo-composition of two cell populations. Within the cytoplasm of the tumor cells, eosinophilic inclusion bodies can be found, similar to those seen in rhabdomyosarcomas. These inclusion bodies are stained by eosin and are negative for striated muscle markers, but positive for vimentin. The production of vimentin filaments, which seem to have no function because of package into a cytoplasmic vacuole, is the only known abnormality for this tumor type. In a single study, KRAS mutations were found in some cases of this tumor type [155].

Sheets of undifferentiated tumor cells embedded in a lymphocyte-rich stroma characterize *lymphoepithelial-like LC*. The carcinoma cells are positive for cytokeratins 13/14; the lymphocytes in most cases are B cells. In cases from Southeast Asia, most lymphoepithelial-like LCs are positive for EBV, and EBV seems to play a role in carcinogenesis, whereas in Caucasians, these carcinomas are negative for EBV [160, 161]. Only one study looked up genetic changes in this tumor entity: they found unusual mutations in TP53 at exon 8 and EGFR mutations in few patients within their large series. These were exon 21 (not L858R) and exon 18 and 20 mutations [162].

Pulmonary clear cell carcinoma is another rare variant of LCC, defined by abundant glycogen in the cytoplasm of the tumor cells. Tissue processing usually dissolves glycogen, thus leaving the impression of a clear/empty cytoplasm. Only one study examined molecular changes in this tumor type and found predominantly KRAS mutations [155].

19.7 The Neuroendocrine Carcinomas

19.7.1 Small Cell Neuroendocrine Carcinoma

Small cell carcinoma is defined by nuclear size of 16–23 mμ (not so small!), dark stained nuclei (mainly composed of heterochromatin), inconspicuous or lacking nucleoli, small cytoplasmic rim, often invisible in light microscopy, and fragile nuclei.

SCLC is regularly positive for the neuroendocrine markers NCAM and synaptophysin, but most often negative for chromogranin A. The best marker is NCAM with a strong membranous staining. SCLC is positive for low molecular weight cytokeratins. SCLC produces hormones, such as adrenocorticotropin (ACTH), but also substances interfering with the blood coagulation system. In contrast to carcinoids, SCLC more often is positive for heterotopic hormones (i.e., hormones usually not found in adult lung). In our experience, a positive reaction for gastrin-releasing peptide (GRP) and ACTH is most often seen. The secretion of ACTH can cause Cushing syndrome. Some of the hormones especially GRP act as an autocrine loop: the peptide is produced by the cancer cells, is released, and binds back to their respective membrane-bound receptors, which themselves signal back into the nucleus with a growth stimulation [163].

Genetic abnormalities in SCLC are quite common; usually over 50% of the SCLC chromosomes are affected [164–166]. These many

genomic alterations made a search for driver gene mutations/alterations complicated, which consequently resulted that besides classical chemotherapy, no targeted therapy emerged yet.

However, some genetic alterations are known for a long time, not resulting in a therapeutic intervention strategy. Two genetic alterations have been long known, RB loss or mutation and TP53 mutation. Since both genes are involved in cell cycle checkpoint controls, this might explain the high numbers of genetic alterations [167–169]. Other genes involved in SCLC are the tumor suppressor FHIT and RASSF1, both on chromosome 3p, RARbeta, and Myc genes [169]. RASSF1 mRNA expression was lost in all SCLC cell lines tested, whereas its promoter was methylated in some NSCLC cell lines [170]. In SCLC also apoptotic and immunogenic mechanisms seem to be inactivated. In a study by Senderowicz, FasL was overexpressed in almost all SCLC cases examined. The ratio of Fas/FasL was decreased. The authors concluded that FasL overexpression in the context of Fas downregulation might allow tumor cells to induce paracrine killing of cytotoxic T cells [171]. Since the PI3K-Akt signaling pathway is activated in almost all cases of SCLC, this system might also be associated with inhibition of apoptosis via upregulation of TNFRSF4, DAD1, BCL2L1, and BCL2L2 and with chemoresistance [172, 173]. These data demonstrate that several systems are involved in SCLC growth, survival, and resistance to chemotherapy.

ASH1 was identified as the gene responsible for the neuroendocrine phenotype in both high-grade carcinomas [174]. Together with other genes (ATOH1, NEUROD1, and NEUROD4) involved in neurogenic differentiation, they are also expressed in NSCLC with neuroendocrine phenotype. As SCLC, these NSCLC cases expressed mRNA for dopa decarboxylase and stained positively for neuroendocrine markers [175]. ASH1 seems to be an early differentiation gene in the developing lung. In embryonic development, ASH1 was found in neuroepithelial bodies and solitary neuroendocrine cells, but vanishes with maturation of the lung. Therefore, ASH1 might be an early program for neuroendocrine cell differentiation [176]. If there is another function of ASH1 is not entirely clear. ASH1 seems to repress tumor suppressor such as DKK1 and 3, which are regulators of the Wnt-βcatenin pathway. ASH1 also inactivates E-cadherin and integrinß1 by de-acetylation and methylation of the DKK1 and E-cadherin promoters [177]. In an animal lung cancer model, the expression of ASH1 enhances the carcinogenic effect of SV40 large T antigen, suggesting that ASH1 might cooperate with pRB [178].

19.7.2 Large Cell Neuroendocrine Carcinoma

Large cell neuroendocrine carcinoma is defined by a neuroendocrine pattern, i.e., rosettes and trabecules. On low power, they look similar to carcinoids, but on higher magnification, abundant mitoses are obvious. The prognosis of LCNEC is similar to that of SCLC; both are grouped as the high-grade neuroendocrine carcinomas.

Genetic analysis of LCNEC showed similar alterations as found in SCLC. However, allelic losses at 5q and abnormalities in the p16 gene may differentiate LCNEC from SCLC [179]. Another difference between both high-grade neuroendocrine carcinomas is seen at chromosome 3q: gains of 3q are frequently seen in SCLC, whereas gains of 3q were absent in LCNEC. However, gains of 6p were frequent in LCNEC; deletions within 10q, 16q, and 17p were more common in SCLC [180]. ASH1 mRNA is found higher in SCLC, whereas its counteracting gene HES1 was more frequently expressed in LCNEC [181].

19.7.3 Carcinoids

Typical carcinoid is defined by neuroendocrine structures, such as rosettes, trabecules, and solid nests, 0 or 1 mitosis per 2 mm^2, and absence of necrosis. Atypical carcinoid is defined by two to ten mitoses per 2 mm^2 and/or presence of necrosis and again neuroendocrine structures. In both

carcinoids, there is an invasive growth into the lung, and lymphatic and blood vessel invasion can be found in some cases. Some carcinoids can metastasize, but so far there are no predictive markers for the biological behavior.

Those carcinoids, which have more than two losses on distal chromosome 11q, and those with multiple chromosomal losses (<10), also show a worse outcome. Based on genetic studies, it can be speculated that the 140 kDa isoform precursor of NCAM, Zinc-finger protein-like 1, and sorting Nexin 15 might be involved in the genesis of carcinoids [182].

19.8 Salivary Gland Type Carcinomas

Salivary gland tumors can occur in the lung, usually in a central location. Within the spectrum are mucoepidermoid carcinomas, adenoid cystic carcinomas, and epithelial-myoepithelial carcinomas. These are rare carcinomas with a wide range of affected ages, from children as early as 3 years of age, as well as in old patients.

19.8.1 Mucoepidermoid Carcinoma

Due to their central location, they may grow as a polypoid mass occluding large bronchi and thus causing obstruction – this is often the cause for the main clinical symptoms (poststenotic bronchopneumonia).

In low-grade carcinomas, cystic and solid areas are found. In both, mucin-producing columnar cells form glands, tubules, and cysts. Within the glandular areas, squamous epithelium is interspersed; the tumor cells are usually nonkeratinizing. In high-grade carcinomas, the distinction from adenosquamous carcinoma might sometimes be impossible, due to overlapping features. The proof is the mixture of squamous and mucin-producing columnar cells within a gland, endobronchial growth, and absence of keratin pearls and an in situ component. The prognosis of high-grade mucoepidermoid carcinomas is similar to other NSCLCs.

EGFR was studied in mucoepidermoid carcinomas of the lung. Protein expression was frequently found, whereas mutations in exon 18–21 were absent. Polysomy of the EGF receptor was seen in a small percentage of cases [183]. In another study, the authors reported EGFR mutations and also a response to tyrosine kinase inhibitor treatment. One of the patients in this study showed a response to treatment without alterations of the EGFR [184]. A third study probably presents the explanation for this behavior: the authors showed a translocation t(11;19) resulting in a fusion oncogene CRTC1-MAML2. CRTC1-MAML2 was shown to upregulate the EGFR ligand, amphiregulin, and thus activate the receptor [185].

19.8.2 Adenoid Cystic Carcinoma

Similar to the salivary counterpart, adenoid cystic carcinoma of the bronchus is a slowly growing tumor with late lymph node and distant organ involvement. However, recurrence is frequent. They occur in the trachea and the large bronchi as far as normal bronchial glands are found. The tumor forms pseudotubules filled with mucin-like material, which is composed of matrix proteins of the basal lamina as collagen type 4 and fibronectin.

In an experimental model of adenoid cystic carcinoma, it was shown that dual inhibition of EGFR and VEGFR2 resulted in apoptosis, decreased angiogenesis, and metastasis [186]. In an array-CGH study, a gain was found on chromosome 4q12, which contains a cluster of receptor tyrosine kinases such as KIT, PDGFRA [152]; however, in another study looking up this area, KIT mutations or amplifications were not found [187]. Also mutations of EGFR could not be demonstrated in adenoid cystic carcinomas, but upregulation of the protein was a constant feature [183, 188]. In another study, experimental inhibition of phospho-ERK1/2 resulted in inhibition of tumor cell growth and metastasis [189], and in a clinical study, growth of adenoid cystic carcinoma could be inhibited by a multikinase inhibitor [190]; however, in a subsequent clinical trial,

this inhibition could not be confirmed [191]. Recently new investigations came up with genetic aberrations in these carcinomas. The MYB-NFIB fusion resulting in overexpression of MYB was found in the majority of these carcinomas [192, 193]. Copy number alterations including down-regulated suppressor genes were in addition associated with behavior of these carcinomas [192]. Newly identified mutations in adenoid cystic carcinomas, some of which might lead to a targeted therapy, are FGF-IGF-PI3K mutations and mutations in NOTCH-1/NOTCH-2 signaling regulator SPEN, which might be a new cancer gene in this type of tumors, and finally within a subset of these carcinomas also FGFR2 mutations [193, 194].

Another rare salivary gland tumor is acinar cell carcinoma. Uniform tumor cells showing acidophilic/azurophilic granules in their cytoplasm characterize it. So far no specific genetic abnormality has been reported in pulmonary variants.

19.9 Sarcomatoid Carcinomas (SC)

The sarcomatoid carcinomas are a group of carcinomas with sarcomatoid features. This group is composed of pleomorphic carcinoma, spindle and giant cell carcinoma, pulmonary blastoma, and carcinosarcoma.

Pleomorphic carcinoma is defined as a carcinoma with either a spindle or giant cell component and any other NSCLC component. Pulmonary blastoma is composed of a fetal-type adenocarcinoma and an embryonic type of stroma. Most often this stroma component is benign; however, in rare cases, the stroma can exhibit atypia and even malignancy. Finally carcinosarcoma is composed of any type of NSCLC with a sarcoma with osseous, rhabdomyoblastic, or chondroblastic differentiation.

Few studies have focused on this tumor types. In the study by Pelosi, the epithelial components of SC showed expression of epithelial markers and cell cycle inhibitors p21Waf1 and p27Kip1 and the loss of FHIT, whereas the sarcomatoid components expressed mesenchymal markers and differently reacted for molecules involved in cell differentiation, cell cycle control, and tumor cell growth and motility [195]. In another study, the mechanisms of epithelial-mesenchymal transition were explored. The classical pathways NOTCH-1 and Snail and the Wnt pathway could be excluded, but a possible alternative pathway including Jun-Vimentin-Fascin was found [196]. Looking up EGFR and KRAS mutations in SC, no mutations were found for EGFR, but KRAS in almost half of the cases. However, EGFR was constantly overexpressed at the protein level, which might suggest the possibility of an EGF antibody treatment [197].

19.10 Preneoplastic Lesions

Actually our knowledge is very small on preneoplastic lung lesions: for a few carcinomas, the preneoplastic lesion is known; for most carcinomas discussed above, we know nothing. And most important even for those well-known lesions, we cannot predict if these lesions will progress into carcinoma or not. The factors responsible for progression and invasion are unknown. Research on preneoplastic lesions faces two major problems:

When the neoplastic process starts? And what to analyze?

From our current understanding, the neoplastic transformation has some important requirements, which usually precede morphologic changes: nutrition, nucleotides for DNA replication, and oxygen for metabolism. Preneoplastic cells need increased access to nutrients for building up an energy reserve for the increase of cell divisions, they need to get access to higher levels of purine and pyrimidine bases to facilitate their increased DNA replications during mitosis, and for an increased metabolism, also an increase of oxygen might be required [10, 198, 199]. Increased oxygen consumption, however, is controversially discussed: hypoxia seems to be critical for invasion and metastasis, so probably increased oxygen and oxidative metabolism might be required only in the early intraepithelial expansion of the preneoplastic cells, whereas

glycolysis seems more common in invasive carcinomas [198, 200, 201].

19.10.1 Hyperplasia of Goblet Cells and Squamous Metaplasia/Dysplasia

For squamous cell carcinomas, the preneoplastic lesion is known since a while. In the large bronchi, there exists a protection program for toxin/carcinogen exposure, which starts with goblet cell hyperplasia and proceeds to squamous cell metaplasia and further on to squamous cell dysplasia or intraepithelial neoplasia. A vascular variant of dysplasia has been described characterized by an ingrowth of capillaries into the squamous epithelium. Atypia and mitosis might be mild or absent, respectively; however, this represents a rapid progressive lesions [11] most probably due to the expression and release of VEGF (unpublished personal observation).

A few factors influencing this progression have been identified, such as a p63 splice variant; amplification of PI3KCA; increased NFκB p65 nuclear expression; gradual increases of caspase-8, STAT 5, and p70s6K; or decrease of E-cadherin [202–205]. Angiogenic stimuli seem to play a role in progression, since it is upregulated in rapid progressive squamous cell dysplasia with prominent vascular intraepithelial growth pattern [11]. However, the interrelation of genes upregulated and downregulated has not been elucidated, so we are presently limited to single studies looking for different genetic abnormalities.

Atypical adenomatous hyperplasia and *bronchiolar columnar cell dysplasia* are two preneoplastic lesions confined to the alveolar and bronchiolar periphery, respectively. Atypical alveolar hyperplasia is visible already at low power magnification. The normal epithelium is replaced by pneumocyte type II-like atypical cells. Between the cells, lined up as a single row, there are usually gaps left. When these gaps are lost, and cell pile up close to each other, or form cell papillae without stroma, this already fulfills the criteria of adenocarcinoma in situ (AIS). AAH is regarded as the precursor for some non-mucinous adenocarcinomas, especially acinar and papillary types.

19.10.2 Genetic Aberrations in AAH

Genomic aberrations were found to increase from AAH to AIS and invasive adenocarcinoma; the chromosomes involved in the AAH lesions were still present in the high-grade lesions, suggesting an AAH to AIS to invasive adenocarcinoma sequence [206, 207]. KRAS mutations were found in one third of AAHs studied and seem to be an early event in carcinogenesis [208, 209]. A loss of either TSC1 or TSC2 genes was another finding in well-differentiated adenocarcinomas and their associated AAH lesions [210, 211]. EGFR mutations as well as amplifications could not be detected in AAH, but were found in adjacent well-differentiated adenocarcinomas and less frequently in less-differentiated ones [212, 213]. In another study comparing KRAS and EGFR mutations in AAH, AIS, and invasive adenocarcinomas, the percentage of KRAS mutations decreased from AAH to AIS to invasive adenocarcinomas, whereas EGFR mutations increased from AAH to AIS and to invasive adenocarcinomas. This study concluded that two different pathways of AAH exist, one driven by KRAS and the other by EGFR mutations, respectively [214].

In contrast to AAH, bronchiolar columnar cell dysplasia (BCCD) can only be identified at high magnification. In BCCD atypical cells gradually replace normal bronchiolar epithelium. In early stages of BCCD, a monomorphous proliferation of cells replaces these differentiated cells and gradually expands up to the surface. If completely replaced, more atypia is recognized.

In a study of genetic aberrations, Ullmann found an increase of genetic alterations from 2.6 in BCCD to 14.7 in the concomitant adenocarcinoma. Unbalanced numerical aberrations were losses of 3p, 9, 13, and 14 and gains of 1q, 17, 19q, and 20q [215]. Another study demonstrated loss of P16INK4a protein in 70 % of cases. P53 accumulation was found in 26 % of the cases [216].

Atypical goblet cell hyperplasia (AGCH) is much more difficult to recognize: the nuclei are compressed at the cell border, and the chromatin structure is invisible. Atypical, signet ring-like cells are replacing the normal epithelium resulting in a monotonous pattern. Atypical goblet cell hyperplasia might give rise to the different mucinous adenocarcinomas of the lung. AGCH was studied in cystic pulmonary adenomatous malformation (CPAM). In this study, chromosomal gains on chromosomes 2 and 4 were found as the major genetic alteration [217]. The same genetic alterations were demonstrated in three associated adenocarcinomas of children. So most probably oncogenes located on these chromosomes are involved in carcinogenesis.

19.10.3 Neuroendocrine Cell Hyperplasia

Neuroendocrine cell hyperplasia is divided into NE hyperplasia associated with fibrosis and bronchiectasis or in the vicinity of a carcinoid and diffuse NE hyperplasia without known cause; in addition a nodular proliferation is described, and finally there is tumorlet, which is different from carcinoid by size and separation of tumor cell groups by fibrous bands. Tumorlets and diffuse neuroendocrine hyperplasia are often found in the vicinity of carcinoids, and therefore it is speculated that they may represent preneoplastic lesions for carcinoids. A few studies focused on molecular changes in these lesions. Since neuroendocrine lesions and low-grade tumors are usually rich in capillaries, one study focused on angiogenetic factors. VEGF was found highly expressed in diffuse proliferations, but there were no correlations with progression, but rather an association with fibrosis [218]. N-cadherin was found in a high proportion of diffuse hyperplasia and carcinoids, but less in SCLC and LCNEC. In carcinoids N-cadherin expression was associated with negative lymph node status [219].

19.11 Selected Examples of Benign and Mesenchymal Lung Tumors

19.11.1 Benign Epithelial Tumors

Papillomas posses a stroma with thin-walled and fragile capillaries and veins, branching in a tree-like manner, accompanied by few fibrocytes, and covered by metaplastic epithelium. The epithelium is most often composed of squamous cells, sometimes with certain degrees of dysplasia. In rare cases, a transitional and a columnar epithelium or mixtures of all three can occur. In squamous cell papilloma, koilocytes are seen, and by immunohistochemistry, in situ hybridization, or PCR, human papillomavirus can be detected [220, 221]. A bizarre outline of nuclei is usually detected in cases of HPV 16- or 18-positive cases. Many HPV types are known; in general they are divided into oncogenic and non-oncogenic types. They all have in common to promote growth of the epithelial cells when integrated into the cell genome. Also recurrence of papillomas is common. The most important function of HPV genome is its interference with the cell cycle control proteins p53 and RB protein. Specific parts of the HPV genome induce stabilization of the p53 and RB proteins preventing apoptosis induced by genetic aberrations. Therefore, the DNA repair machinery is ineffective, and mitosis progresses despite DNA defects and gene aberrations [222, 223]. Integration of oncogenic HPV types (16, 18) will induce a rapid progression of the papilloma into invasive squamous cell carcinoma [221, 224].

19.11.2 Sclerosing Pneumocytoma

Sclerosing pneumocytoma is a benign epithelial tumor. This is an epithelial neoplasm composed of immature and mature pneumocytes. A few genetic abnormalities have been described in sclerosing pneumocytoma. Aberrant nuclear and cytoplasmic expression of beta-catenin was found in both cellular elements of sclerosing pneumocytoma [225].

Overexpression of estrogen receptor beta was seen in almost 50% of these tumors in another study [226]. One study looking for EGFR, HER2, and KRAS abnormalities did not reveal molecular alterations; however, allelic losses of p16 and Rb were observed [227].

19.12 Tumors Induced by Mutations of the TSC Genes (Related to Tuberous Sclerosis)

TSC genes code for the two proteins hamartin (TSC1) and tuberin (TSC2). Both are embedded into a signaling chain involving LKB1 (STK11), AMPKα, and both upstream of TSC and Rheb and mTOR and downstream of TSC1/TSC2. Normally LKB1 and cyclic AMP stimulate AMPKα, which in turn stimulates TSC1 and TSC2. The translated proteins hamartin and tuberin form a dimer and inhibit Rheb, which stimulates mTOR and mTORC formation. mTOR in sequence can either form the mTORC1 complex (with GβL and raptor) or the mTORC2 complex (with GβL and rictor) [228, 229]. Both TORC complexes signal into different downstream cascades, but altogether induce proliferation and influence cytoskeleton formation in cells and many more functions. In tuberous sclerosis, one of the genes is mutated and no functional protein is translated. This results in uncontrolled mTOR upregulation and tumor formation.

19.12.1 Multifocal Nodular Pneumocyte Hyperplasia (MNPH)

MNPH is characterized by an adenoma-like proliferation of immature and mature pneumocyte type II-like cells without atypia. The cells are positive for surfactant apoprotein A. These lesions form multiple micronodules. There is no progression into malignant tumors known and even no progression of these lesions into larger tumors [230]. Mutation of the TSC1 and TSC2 genes has been proven, so these lesions represent an adenomatous proliferation, induced by genetic instability, caused by mutations of TSC genes [231, 232].

19.12.2 Lymphangioleiomyomatosis (LAM)

LAM is characterized by an uncontrolled proliferation of mature and immature smooth muscle cells. The muscular proliferation is confined to bronchioles and alveoli and also occurs subpleurally and in the vicinity of vascular walls. By compression of lymphatics and airways, cystic spaces are formed, some are dilated lymphatics, and others are dilated bronchioles and alveoli [233]. The disease predominantly affects young woman and often starts after the first delivery. LAM can recur after lung transplantation and therefore present with some features of a systemic malignant disease (repopulation of transplanted lungs from outside) [234–237].

Genetically LAM is related to the tuberous sclerosis complex. Mutations of the TSC1 and TSC2 have been demonstrated in almost all cases evaluated. LAM is one of the many "benign" tumor lesions associated with somatic mutations found in this disease characterized by genetic instability [238–240]. Therapeutic approaches have been invented, first by an antiestrogen therapy including oophorectomy. Despite recurrences reported, lung transplantation has emerged as the best treatment. Recently a treatment with a mTOR inhibitor has shown promising results [241, 242].

19.12.3 Clear Cell Tumor (Sugar Tumor, PEComa = Perivascular Epithelioid Cell Tumor)

PEComa is composed of large polygonal tumor cells with inconspicuous nuclei and usually invisible nucleoli. On formalin-fixed paraffin-

embedded material, the cytoplasm is clear. By PAS stain, abundant glycogen is seen. Another characteristic feature is the prominent vascular network. Most of these tumors will behave benign. However, there is a rare malignant variant with marked nuclear atypia [243, 244]. PEComas are part of the spectrum of the tuberous sclerosis complex. It can be associated with angiomyolipoma of the kidney and LAM and carries a similar spectrum of mutations [245, 246]. Recently another genetic abnormality was demonstrated in a subset of PEComas without tuberous sclerosis association, namely, a TFE gene rearrangement, resulting in an upregulation of the TFE3 protein [247].

19.13 Malignant Tumors of Childhood

19.13.1 Pleuropulmonary Blastoma

Pleuropulmonary blastoma (PPB) is a malignant mesenchymal tumor, which can arise in the pleura, the lung, or both. It can present as a predominant cystic, a mixed cystic and solid, or a pure solid lesion, which is also reflected by an increased aggressive behavior. The tumor cells form layers of immature small cells with relatively large nuclei with dense chromatin. These cells form a so-called germinal layer. In addition interspersed giant cells with rhabdomyoblast differentiation and areas of chondrosarcoma are usually seen [248, 249].

Genetically gains of large parts or whole chromosome 8 are often found in PPB [250–252]. A few other aberrations have been reported: losses on 6q13-qter, 10pter-p13, 10q22-qter, and 20p13 and gains of chromosomes 2 and 8p11-p12 [253]. In some reports, mutations of the TP53 gene were described [254, 255]. Recently DICER 1 syndrome has been linked to PPB: Dicer is a protein involved in processing of small inhibitory microRNAs. A mutation has been reported in several families, and this was linked to the development of PPB and other childhood tumors [256].

19.13.2 Congenital Myofibroblastic Tumor

Congenital myofibroblastic tumor is another rare childhood tumor composed of proliferating myofibroblastic cells, sometimes with marked cellularity and mitotic activity. The tumor cells proliferate within the interstitium and peribronchiolar and thus cause bronchiolar obstruction. They can behave biologically like malignant tumors [257, 258]. A single genetic analysis was reported, under the other name of the tumor, namely, leiomyosarcoma of childhood. The authors reported gains of chromosomes 2 and 11 and losses of chromosomes 9, 19, 20, and 22 [259].

19.14 Final Remarks

Due to the vast amount of knowledge in the epidemiology of lung cancer, we did not include these aspects. Several other topics, which are more general and not organ based in the development of cancer, are not discussed herein, such as the stem cell theory in cancer development and metastasis. Another aspect is invasion and metastasis of lung cancer. This is discussed in Chap. 20 on metastasis.

References

1. Langer CJ, Natale RB. The emerging role of vascular endothelial growth factor receptor tyrosine kinase inhibitors. Semin Oncol. 2005;32:S23–9.
2. Mae M, O'Connor TP, Crystal RG. Gene transfer of the vascular endothelial growth factor receptor flt-1 suppresses pulmonary metastasis associated with lung growth. Am J Respir Cell Mol Biol. 2005;33:629–35.
3. Samadikuchaksaraei A, Cohen S, Isaac K, Rippon HJ, Polak JM, Bielby RC, Bishop AE. Derivation of distal airway epithelium from human embryonic stem cells. Tissue Eng. 2006;12:867–75.
4. Kotton DN, Fabian AJ, Mulligan RC. Failure of bone marrow to reconstitute lung epithelium. Am J Respir Cell Mol Biol. 2005;33:328–34.
5. Kumar RK, Li W, O'Grady R. Maintenance of differentiated phenotype by mouse type 2 pneumocytes in serum-free primary culture. Exp Lung Res. 1995;21:79–94.

6. Decaussin M, Sartelet H, Robert C, Moro D, Claraz C, Brambilla C, Brambilla E. Expression of vascular endothelial growth factor (VEGF) and its two receptors (VEGF-R1-Flt1 and VEGF-R2-Flk1/KDR) in non-small cell lung carcinomas (NSCLCs): correlation with angiogenesis and survival. J Pathol. 1999;188:369–77.
7. Adjei AA. Pharmacology and mechanism of action of pemetrexed. Clin Lung Cancer. 2004;5 Suppl 2:S51–5.
8. Benjamin H, Lebanony D, Rosenwald S, Cohen L, Gibori H, Barabash N, Ashkenazi K, Goren E, Meiri E, Morgenstern S, Perelman M, Barshack I, Goren Y, Edmonston TB, Chajut A, Aharonov R, Bentwich Z, Rosenfeld N, Cohen D. A diagnostic assay based on microRNA expression accurately identifies malignant pleural mesothelioma. J Mol Diagn. 2010; 12:771–9.
9. Ivanov SV, Goparaju CM, Lopez P, Zavadil J, Toren-Haritan G, Rosenwald S, Hoshen M, Chajut A, Cohen D, Pass HI. Pro-tumorigenic effects of miR-31 loss in mesothelioma. J Biol Chem. 2010;285: 22809–17.
10. Koukourakis MI, Giatromanolaki A, Sivridis E, Gatter KC, Harris AL. Pyruvate dehydrogenase and pyruvate dehydrogenase kinase expression in non small cell lung cancer and tumor-associated stroma. Neoplasia. 2005;7:1–6.
11. Keith RL, Miller YE, Gemmill RM, Drabkin HA, Dempsey EC, Kennedy TC, Prindiville S, Franklin WA. Angiogenic squamous dysplasia in bronchi of individuals at high risk for lung cancer. Clin Cancer Res. 2000;6:1616–25.
12. Takahama M, Tsutsumi M, Tsujiuchi T, Nezu K, Kushibe K, Taniguchi S, Kotake Y, Konishi Y. Enhanced expression of Tie2, its ligand angiopoietin-1, vascular endothelial growth factor, and CD31 in human non-small cell lung carcinomas. Clin Cancer Res. 1999;5:2506–10.
13. Chang CC, Lin MT, Lin BR, Jeng YM, Chen ST, Chu CY, Chen RJ, Chang KJ, Yang PC, Kuo ML. Effect of connective tissue growth factor on hypoxia-inducible factor 1alpha degradation and tumor angiogenesis. J Natl Cancer Inst. 2006;98:984–95.
14. Maeshima AM, Tochigi N, Yoshida A, Asamura H, Tsuta K, Tsuda H. Clinicopathologic analysis of multiple (five or more) atypical adenomatous hyperplasias (AAHs) of the lung: evidence for the AAH-adenocarcinoma sequence. J Thorac Oncol. 2010;5: 466–71.
15. Guedj N, Couvelard A, Arcangeli G, Dubois S, Thabut G, Leseche G, Fournier M, Degott C, Groussard O. Angiogenesis and extracellular matrix remodelling in bronchioloalveolar carcinomas: distinctive patterns in mucinous and non-mucinous tumours. Histopathology. 2004;44:251–6.
16. Kojima H, Shijubo N, Yamada G, Ichimiya S, Abe S, Satoh M, Sato N. Clinical significance of vascular endothelial growth factor-C and vascular endothelial growth factor receptor 3 in patients with T1 lung adenocarcinoma. Cancer. 2005;104:1668–77.
17. Kajita T, Ohta Y, Kimura K, Tamura M, Tanaka Y, Tsunezuka Y, Oda M, Sasaki T, Watanabe G. The expression of vascular endothelial growth factor C and its receptors in non-small cell lung cancer. Br J Cancer. 2001;85:255–60.
18. Niki T, Iba S, Yamada T, Matsuno Y, Enholm B, Hirohashi S. Expression of vascular endothelial growth factor receptor 3 in blood and lymphatic vessels of lung adenocarcinoma. J Pathol. 2001;193: 450–7.
19. Arinaga M, Noguchi T, Takeno S, Chujo M, Miura T, Uchida Y. Clinical significance of vascular endothelial growth factor C and vascular endothelial growth factor receptor 3 in patients with nonsmall cell lung carcinoma. Cancer. 2003;97:457–64.
20. Li Y, Wang MN, Li H, King KD, Bassi R, Sun H, Santiago A, Hooper AT, Bohlen P, Hicklin DJ. Active immunization against the vascular endothelial growth factor receptor flk1 inhibits tumor angiogenesis and metastasis. J Exp Med. 2002;195:1575–84.
21. Abdollahi A, Lipson KE, Sckell A, Zieher H, Klenke F, Poerschke D, Roth A, Han X, Krix M, Bischof M, Hahnfeldt P, Grone HJ, Debus J, Hlatky L, Huber PE. Combined therapy with direct and indirect angiogenesis inhibition results in enhanced antiangiogenic and antitumor effects. Cancer Res. 2003; 63:8890–8.
22. Lin J, Lalani AS, Harding TC, Gonzalez M, Wu WW, Luan B, Tu GH, Koprivnikar K, VanRoey MJ, He Y, Alitalo K, Jooss K. Inhibition of lymphogenous metastasis using adeno-associated virus-mediated gene transfer of a soluble VEGFR-3 decoy receptor. Cancer Res. 2005;65:6901–9.
23. Yano S, Muguruma H, Matsumori Y, Goto H, Nakataki E, Edakuni N, Tomimoto H, Kakiuchi S, Yamamoto A, Uehara H, Ryan A, Sone S. Antitumor vascular strategy for controlling experimental metastatic spread of human small-cell lung cancer cells with ZD6474 in natural killer cell-depleted severe combined immunodeficient mice. Clin Cancer Res. 2005;11:8789–98.
24. Cabebe E, Wakelee H. Role of anti-angiogenesis agents in treating NSCLC: focus on bevacizumab and VEGFR tyrosine kinase inhibitors. Curr Treat Options Oncol. 2007;8:15–27.
25. Takahashi O, Komaki R, Smith PD, Jurgensmeier JM, Ryan A, Bekele BN, Wistuba II, Jacoby JJ, Korshunova MV, Biernacka A, Erez B, Hosho K, Herbst RS, O'Reilly MS. Combined MEK and VEGFR inhibition in orthotopic human lung cancer models results in enhanced inhibition of tumor angiogenesis, growth, and metastasis. Clin Cancer Res. 2012;18:1641–54.
26. Das B, Yeger H, Tsuchida R, Torkin R, Gee MF, Thorner PS, Shibuya M, Malkin D, Baruchel S. A hypoxia-driven vascular endothelial growth factor/Flt1 autocrine loop interacts with hypoxia-inducible

factor-1alpha through mitogen-activated protein kinase/extracellular signal-regulated kinase 1/2 pathway in neuroblastoma. Cancer Res. 2005;65: 7267–75.
27. Boreddy SR, Sahu RP, Srivastava SK. Benzyl isothiocyanate suppresses pancreatic tumor angiogenesis and invasion by inhibiting HIF-alpha/VEGF/Rho-GTPases: pivotal role of STAT-3. PLoS ONE. 2011;6:e25799.
28. Goyal A, Poluzzi C, Willis CD, Smythies J, Shellard A, Neill T, Iozzo RV. Endorepellin affects angiogenesis by antagonizing diverse vascular endothelial growth factor receptor 2 (VEGFR2)-evoked signaling pathways: transcriptional repression of hypoxia-inducible factor 1alpha and VEGFA and concurrent inhibition of nuclear factor of activated T cell 1 (NFAT1) activation. J Biol Chem. 2012;287: 43543–56.
29. Olaussen KA, Dunant A, Fouret P, Brambilla E, Andre F, Haddad V, Taranchon E, Filipits M, Pirker R, Popper HH, Stahel R, Sabatier L, Pignon JP, Tursz T, Le Chevalier T, Soria JC. DNA repair by ERCC1 in non-small-cell lung cancer and cisplatin-based adjuvant chemotherapy. N Engl J Med. 2006;355:983–91.
30. Sbarbati A, Osculati F. A new fate for old cells: brush cells and related elements. J Anat. 2005;206: 349–58.
31. Zinner RG, Novello S, Peng G, Herbst R, Obasaju C, Scagliotti G. Comparison of patient outcomes according to histology among pemetrexed-treated patients with stage IIIB/IV non-small-cell lung cancer in two phase II trials. Clin Lung Cancer. 2010;11:126–31.
32. Giovannetti E, Lemos C, Tekle C, Smid K, Nannizzi S, Rodriguez JA, Ricciardi S, Danesi R, Giaccone G, Peters GJ. Molecular mechanisms underlying the synergistic interaction of erlotinib, an epidermal growth factor receptor tyrosine kinase inhibitor, with the multitargeted antifolate pemetrexed in non-small-cell lung cancer cells. Mol Pharmacol. 2008; 73:1290–300.
33. Racanelli AC, Rothbart SB, Heyer CL, Moran RG. Therapeutics by cytotoxic metabolite accumulation: pemetrexed causes ZMP accumulation, AMPK activation, and mammalian target of rapamycin inhibition. Cancer Res. 2009;69:5467–74.
34. Imada K, Leonard WJ. The jak-STAT pathway. Mol Immunol. 2000;37:1–11.
35. Uddin S, Sassano A, Deb DK, Verma A, Majchrzak B, Rahman A, Malik AB, Fish EN, Platanias LC. Protein kinase C-delta (PKC-delta) is activated by type I interferons and mediates phosphorylation of Stat1 on serine 727. J Biol Chem. 2002;277: 14408–16.
36. Grant S, Qiao L, Dent P. Roles of ERBB family receptor tyrosine kinases, and downstream signaling pathways, in the control of cell growth and survival. Front Biosci. 2002;7:d376–89.
37. McBride KM, Reich NC. The ins and outs of STAT1 nuclear transport. Sci STKE. 2003;2003:RE13.
38. Rajadurai CV, Havrylov S, Zaoui K, Vaillancourt R, Stuible M, Naujokas M, Zuo D, Tremblay ML, Park M. Met receptor tyrosine kinase signals through a cortactin-Gab1 scaffold complex, to mediate invadopodia. J Cell Sci. 2012;125:2940–53.
39. Mitola S, Brenchio B, Piccinini M, Tertoolen L, Zammataro L, Breier G, Rinaudo MT, den Hertog J, Arese M, Bussolino F. Type I collagen limits VEGFR-2 signaling by a SHP2 protein-tyrosine phosphatase-dependent mechanism 1. Circ Res. 2006;98:45–54.
40. Heath CM, Stahl PD, Barbieri MA. Lipid kinases play crucial and multiple roles in membrane trafficking and signaling. Histol Histopathol. 2003;18: 989–98.
41. Kim J, Ahn S, Guo R, Daaka Y. Regulation of epidermal growth factor receptor internalization by G protein-coupled receptors. Biochemistry. 2003;42: 2887–94.
42. Nomura M, Shigematsu H, Li L, Suzuki M, Takahashi T, Estess P, Siegelman M, Feng Z, Kato H, Marchetti A, Shay JW, Spitz MR, Wistuba II, Minna JD, Gazdar AF. Polymorphisms, mutations, and amplification of the EGFR gene in non-small cell lung cancers. PLoS Med. 2007;4:e125.
43. Yano S, Wang W, Li Q, Matsumoto K, Sakurama H, Nakamura T, Ogino H, Kakiuchi S, Hanibuchi M, Nishioka Y, Uehara H, Mitsudomi T, Yatabe Y, Sone S. Hepatocyte growth factor induces gefitinib resistance of lung adenocarcinoma with epidermal growth factor receptor-activating mutations. Cancer Res. 2008;68:9479–87.
44. Palmer RH, Vernersson E, Grabbe C, Hallberg B. Anaplastic lymphoma kinase: signalling in development and disease. Biochem J. 2009;420: 345–61.
45. Wong DW, Leung EL, Wong SK, Tin VP, Sihoe AD, Cheng LC, Au JS, Chung LP, Wong MP. A novel KIF5B-ALK variant in nonsmall cell lung cancer. Cancer. 2011;117:2709–18.
46. Zhang B, Pan X, Cobb GP, Anderson TA. microRNAs as oncogenes and tumor suppressors. Dev Biol. 2007;302:1–12.
47. Kumar MS, Lu J, Mercer KL, Golub TR, Jacks T. Impaired microRNA processing enhances cellular transformation and tumorigenesis. Nat Genet. 2007;39:673–7.
48. Raponi M, Dossey L, Jatkoe T, Wu X, Chen G, Fan H, Beer DG. MicroRNA classifiers for predicting prognosis of squamous cell lung cancer. Cancer Res. 2009;69:5776–83.
49. Bourdon J-C, Fernandes K, Murray-Zmijewski F, Liu G, Diot A, Xirodimas DP, Saville MK, Lane DP. p53 isoforms can regulate p53 transcriptional activity. Genes Dev. 2005;19:2122–37.
50. Vogelstein B, Kinzler KW. p53 function and dysfunction. Cell. 1992;70:523–6.

51. Husgafvel-Pursiainen K, Boffetta P, Kannio A, Nyberg F, Pershagen G, Mukeria A, Constantinescu V, Fortes C, Benhamou S. p53 mutations and exposure to environmental tobacco smoke in a multicenter study on lung cancer. Cancer Res. 2000;60:2906–11.
52. Rodin SN, Rodin AS. Human lung cancer and p53: the interplay between mutagenesis and selection. Proc Natl Acad Sci U S A. 2000;97:12244–9.
53. Sanchez-Cespedes M, Ahrendt SA, Piantadosi S, Rosell R, Monzo M, Wu L, Westra WH, Yang SC, Jen J, Sidransky D. Chromosomal alterations in lung adenocarcinoma from smokers and nonsmokers. Cancer Res. 2001;61:1309–13.
54. Zienolddiny S, Ryberg D, Arab MO, Skaug V, Haugen A. Loss of heterozygosity is related to p53 mutations and smoking in lung cancer. Br J Cancer. 2001;84:226–31.
55. Ahrendt SA, Chow JT, Yang SC, Wu L, Zhang MJ, Jen J, Sidransky D. Alcohol consumption and cigarette smoking increase the frequency of p53 mutations in non-small cell lung cancer. Cancer Res. 2000;60:3155–9.
56. Hashimoto T, Tokuchi Y, Hayashi M, Kobayashi Y, Nishida K, Hayashi S, Ishikawa Y, Nakagawa K, Hayashi J, Tsuchiya E. Different subtypes of human lung adenocarcinoma caused by different etiological factors. Evidence from p53 mutational spectra. Am J Pathol. 2000;157:2133–41.
57. Bartkova J, Horejsi Z, Koed K, Kramer A, Tort F, Zieger K, Guldberg P, Sehested M, Nesland JM, Lukas C, Orntoft T, Lukas J, Bartek J. DNA damage response as a candidate anti-cancer barrier in early human tumorigenesis. Nature. 2005;434:864–70.
58. Hollstein M, Sidransky D, Vogelstein B, Harris CC. p53 mutations in human cancers. Science. 1991;253:49–53.
59. Takahashi T, Nau MM, Chiba I, Birrer MJ, Rosenberg RK, Vinocour M, Levitt M, Pass H, Gazdar AF, Minna JD. p53: a frequent target for genetic abnormalities in lung cancer. Science. 1989;246:491–4.
60. Takahashi T, D'Amico D, Chiba I, Buchhagen DL, Minna JD. Identification of intronic point mutations as an alternative mechanism for p53 inactivation in lung cancer. J Clin Invest. 1990;86:363–9.
61. Iggo R, Gatter K, Bartek J, Lane D, Harris AL. Increased expression of mutant forms of p53 oncogene in primary lung cancer. Lancet. 1990;335:675–9.
62. Yokota J, Kohno T. Molecular footprints of human lung cancer progression. Cancer Sci. 2004;95:197–204.
63. Yokota J, Nishioka M, Tani M, Kohno T. Genetic alterations responsible for metastatic phenotypes of lung cancer cells. Clin Exp Metastasis. 2003;20:189–93.
64. Gibbons DL, Lin W, Creighton CJ, Zheng S, Berel D, Yang Y, Raso MG, Liu DD, Wistuba II, Lozano G, Kurie JM. Expression signatures of metastatic capacity in a genetic mouse model of lung adenocarcinoma. PLoS ONE. 2009;4:e5401.
65. Seo JS, Ju YS, Lee WC, Shin JY, Lee JK, Bleazard T, Lee J, Jung YJ, Kim JO, Yu SB, Kim J, Lee ER, Kang CH, Park IK, Rhee H, Lee SH, Kim JI, Kang JH, Kim YT. The transcriptional landscape and mutational profile of lung adenocarcinoma. Genome Res. 2012;22:2109–19.
66. Paez JG, Janne PA, Lee JC, Tracy S, Greulich H, Gabriel S, Herman P, Kaye FJ, Lindeman N, Boggon TJ, Naoki K, Sasaki H, Fujii Y, Eck MJ, Sellers WR, Johnson BE, Meyerson M. EGFR mutations in lung cancer: correlation with clinical response to gefitinib therapy. Science. 2004;304:1497–500.
67. Sordella R, Bell DW, Haber DA, Settleman J. Gefitinib-sensitizing EGFR mutations in lung cancer activate anti-apoptotic pathways. Science. 2004;305:1163–7.
68. Lynch TJ, Bell DW, Sordella R, Gurubhagavatula S, Okimoto RA, Brannigan BW, Harris PL, Haserlat SM, Supko JG, Haluska FG, Louis DN, Christiani DC, Settleman J, Haber DA. Activating mutations in the epidermal growth factor receptor underlying responsiveness of non-small-cell lung cancer to gefitinib. N Engl J Med. 2004;350:2129–39.
69. Isobe T, Herbst RS, Onn A. Current management of advanced non-small cell lung cancer: targeted therapy. Semin Oncol. 2005;32:315–28.
70. Monnier Y, Farmer P, Bieler G, Imaizumi N, Sengstag T, Alghisi GC, Stehle JC, Ciarloni L, Andrejevic-Blant S, Moeckli R, Mirimanoff RO, Goodman SL, Delorenzi M, Ruegg C. CYR61 and alphaVbeta5 integrin cooperate to promote invasion and metastasis of tumors growing in preirradiated stroma. Cancer Res. 2008;68:7323–31.
71. Sun L, Liu Y, Lin S, Shang J, Liu J, Li J, Yuan S, Zhang L. Early growth response gene-1 and hypoxia-inducible factor-1alpha affect tumor metastasis via regulation of tissue factor. Acta Oncol. 2013;52:842–51.
72. Morelli MP, Cascone T, Troiani T, Tuccillo C, Bianco R, Normanno N, Romano M, Veneziani BM, Fontanini G, Eckhardt SG, De Pacido S, Tortora G, Ciardiello F. Anti-tumor activity of the combination of cetuximab, an anti-EGFR blocking monoclonal antibody and ZD6474, an inhibitor of VEGFR and EGFR tyrosine kinases. J Cell Physiol. 2006;208:344–53.
73. Pirker R, Pereira JR, von Pawel J, Krzakowski M, Ramlau R, Park K, de Marinis F, Eberhardt WE, Paz-Ares L, Storkel S, Schumacher KM, von Heydebreck A, Celik I, O'Byrne KJ. EGFR expression as a predictor of survival for first-line chemotherapy plus cetuximab in patients with advanced non-small-cell lung cancer: analysis of data from the phase 3 FLEX study. Lancet Oncol. 2012;13:33–42.
74. Siegfried JM, Gillespie AT, Mera R, Casey TJ, Keohavong P, Testa JR, Hunt JD. Prognostic value of

specific KRAS mutations in lung adenocarcinomas. Cancer Epidemiol Biomarkers Prev. 1997;6:841–7.
75. Wislez M, Fujimoto N, Izzo JG, Hanna AE, Cody DD, Langley RR, Tang H, Burdick MD, Sato M, Minna JD, Mao L, Wistuba I, Strieter RM, Kurie JM. High expression of ligands for chemokine receptor CXCR2 in alveolar epithelial neoplasia induced by oncogenic kras. Cancer Res. 2006;66:4198–207.
76. To MD, Wong CE, Karnezis AN, Del Rosario R, Di Lauro R, Balmain A. Kras regulatory elements and exon 4A determine mutation specificity in lung cancer. Nat Genet. 2008;40:1240–4.
77. Zhou Y, Rideout 3rd WM, Zi T, Bressel A, Reddypalli S, Rancourt R, Woo JK, Horner JW, Chin L, Chiu MI, Bosenberg M, Jacks T, Clark SC, Depinho RA, Robinson MO, Heyer J. Chimeric mouse tumor models reveal differences in pathway activation between ERBB family- and KRAS-dependent lung adenocarcinomas. Nat Biotechnol. 2010;28:71–8.
78. Musteanu M, Blaas L, Zenz R, Svinka J, Hoffmann T, Grabner B, Schramek D, Kantner HP, Muller M, Kolbe T, Rulicke T, Moriggl R, Kenner L, Stoiber D, Penninger JM, Popper H, Casanova E, Eferl R. A mouse model to identify cooperating signaling pathways in cancer. Nat Methods. 2012;9:897–900.
79. Geles A, Gruber-Moesenbacher U, Quehenberger F, Manzl C, Al Effah M, Grygar E, Juettner-Smolle F, Popper HH. Pulmonary mucinous adenocarcinomas: architectural patterns in correlation with genetic changes, prognosis and survival. Virchows Arch. 2015;467:675–86.
80. Rekhtman N, Ang DC, Riely GJ, Ladanyi M, Moreira AL. KRAS mutations are associated with solid growth pattern and tumor-infiltrating leukocytes in lung adenocarcinoma. Mod Pathol. 2013;26:1307–19.
81. Li C, Fang R, Sun Y, Han X, Li F, Gao B, Iafrate AJ, Liu XY, Pao W, Chen H, Ji H. Spectrum of oncogenic driver mutations in lung adenocarcinomas from East Asian never smokers. PLoS ONE. 2011;6:e28204.
82. Gao B, Sun Y, Zhang J, Ren Y, Fang R, Han X, Shen L, Liu XY, Pao W, Chen H, Ji H. Spectrum of LKB1, EGFR, and KRAS mutations in Chinese lung adenocarcinomas. J Thorac Oncol. 2010;5:1130–5.
83. Ren S, Kuang P, Zheng L, Su C, Li J, Li B, Chen X, Wang Y, Kimcurran V, Liu L, Hu Q, Zhang J, Tang L, Zhou C. Analysis of driver mutations in female nonsmoker Asian patients with pulmonary adenocarcinoma. Cell Biochem Biophys. 2012;64:155–60.
84. Koivunen JP, Kim J, Lee J, Rogers AM, Park JO, Zhao X, Naoki K, Okamoto I, Nakagawa K, Yeap BY, Meyerson M, Wong KK, Richards WG, Sugarbaker DJ, Johnson BE, Janne PA. Mutations in the LKB1 tumour suppressor are frequently detected in tumours from Caucasian but not Asian lung cancer patients. Br J Cancer. 2008;99:245–52.
85. Wagner JC, Sleggs CA, Marchand P. Diffuse pleural mesothelioma and asbestos exposure in the North Western Cape Province. Br J Ind Med. 1960;17:260–71.
86. Scagliotti G, Stahel RA, Rosell R, Thatcher N, Soria JC. ALK translocation and crizotinib in non-small cell lung cancer: an evolving paradigm in oncology drug development. Eur J Cancer. 2012;48:961–73.
87. Ikeda K, Nomori H, Mori T, Sasaki J, Kobayashi T. Novel germline mutation: EGFR V843I in patient with multiple lung adenocarcinomas and family members with lung cancer. Ann Thorac Surg. 2008;85:1430–2.
88. Zucali PA, Giaccone G. Biology and management of malignant pleural mesothelioma. Eur J Cancer. 2006;42:2706–14.
89. Nakao M, Yoshida J, Goto K, Ishii G, Kawase A, Aokage K, Hishida T, Nishimura M, Nagai K. Long-term outcomes of 50 cases of limited-resection trial for pulmonary ground-glass opacity nodules. J Thorac Oncol. 2012;7:1563–6.
90. Zhang S, Wang F, Keats J, Zhu X, Ning Y, Wardwell SD, Moran L, Mohemmad QK, Anjum R, Wang Y, Narasimhan NI, Dalgarno D, Shakespeare WC, Miret JJ, Clackson T, Rivera VM. Crizotinib-resistant mutants of EML4-ALK identified through an accelerated mutagenesis screen. Chem Biol Drug Des. 2011;78:999–1005.
91. Yano S, Takeuchi S, Nakagawa T, Yamada T. Ligand-triggered resistance to molecular targeted drugs in lung cancer: roles of hepatocyte growth factor and epidermal growth factor receptor ligands. Cancer Sci. 2012;103:1189–94.
92. Janne PA, Meyerson M. ROS1 rearrangements in lung cancer: a new genomic subset of lung adenocarcinoma. J Clin Oncol. 2012;30:878–9.
93. Suehara Y, Arcila M, Wang L, Hasanovic A, Ang D, Ito T, Kimura Y, Drilon A, Guha U, Rusch V, Kris MG, Zakowski MF, Rizvi N, Khanin R, Ladanyi M. Identification of KIF5B-RET and GOPC-ROS1 fusions in lung adenocarcinomas through a comprehensive mRNA-based screen for tyrosine kinase fusions. Clin Cancer Res. 2012;18:6599–608.
94. Rimkunas VM, Crosby KE, Li D, Hu Y, Kelly ME, Gu TL, Mack JS, Silver MR, Zhou X, Haack H. Analysis of receptor tyrosine kinase ROS1-positive tumors in non-small cell lung cancer: identification of a FIG-ROS1 fusion. Clin Cancer Res. 2012;18:4449–57.
95. Arai Y, Totoki Y, Takahashi H, Nakamura H, Hama N, Kohno T, Tsuta K, Yoshida A, Asamura H, Mutoh M, Hosoda F, Tsuda H, Shibata T. Mouse model for ROS1-rearranged lung cancer. PLoS ONE. 2013;8: e56010.
96. Bergethon K, Shaw AT, Ou SH, Katayama R, Lovly CM, McDonald NT, Massion PP, Siwak-Tapp C, Gonzalez A, Fang R, Mark EJ, Batten JM, Chen H, Wilner KD, Kwak EL, Clark JW, Carbone DP, Ji H, Engelman JA, Mino-Kenudson M, Pao W, Iafrate AJ. ROS1 rearrangements define a unique molecular class of lung cancers. J Clin Oncol. 2012;30: 863–70.

97. Chin LP, Soo RA, Soong R, Ou SH. Targeting ROS1 with anaplastic lymphoma kinase inhibitors: a promising therapeutic strategy for a newly defined molecular subset of non-small-cell lung cancer. J Thorac Oncol. 2012;7:1625–30.
98. Komiya T, Thomas A, Khozin S, Rajan A, Wang Y, Giaccone G. Response to crizotinib in ROS1-rearranged non-small-cell lung cancer. J Clin Oncol. 2012;30:3425–6. author reply 3426.
99. Yasuda H, de Figueiredo-Pontes LL, Kobayashi S, Costa DB. Preclinical rationale for use of the clinically available multitargeted tyrosine kinase inhibitor crizotinib in ROS1-translocated lung cancer. J Thorac Oncol. 2012;7:1086–90.
100. Ju YS, Lee WC, Shin JY, Lee S, Bleazard T, Won JK, Kim YT, Kim JI, Kang JH, Seo JS. A transforming KIF5B and RET gene fusion in lung adenocarcinoma revealed from whole-genome and transcriptome sequencing. Genome Res. 2012;22:436–45.
101. Wang R, Hu H, Pan Y, Li Y, Ye T, Li C, Luo X, Wang L, Li H, Zhang Y, Li F, Lu Y, Lu Q, Xu J, Garfield D, Shen L, Ji H, Pao W, Sun Y, Chen H. RET fusions define a unique molecular and clinicopathologic subtype of non-small-cell lung cancer. J Clin Oncol. 2012;30:4352–9.
102. Takeuchi K, Soda M, Togashi Y, Suzuki R, Sakata S, Hatano S, Asaka R, Hamanaka W, Ninomiya H, Uehara H, Lim Choi Y, Satoh Y, Okumura S, Nakagawa K, Mano H, Ishikawa Y. RET, ROS1 and ALK fusions in lung cancer. Nat Med. 2012;18:378–81.
103. Bean J, Brennan C, Shih JY, Riely G, Viale A, Wang L, Chitale D, Motoi N, Szoke J, Broderick S, Balak M, Chang WC, Yu CJ, Gazdar A, Pass H, Rusch V, Gerald W, Huang SF, Yang PC, Miller V, Ladanyi M, Yang CH, Pao W. MET amplification occurs with or without T790M mutations in EGFR mutant lung tumors with acquired resistance to gefitinib or erlotinib. Proc Natl Acad Sci U S A. 2007;104:20932–7.
104. Janssen HL, Reesink HW, Lawitz EJ, Zeuzem S, Rodriguez-Torres M, Patel K, van der Meer AJ, Patick AK, Chen A, Zhou Y, Persson R, King BD, Kauppinen S, Levin AA, Hodges MR. Treatment of HCV infection by targeting microRNA. N Engl J Med. 2013;368:1685–94.
105. Zhang YW, Staal B, Essenburg C, Lewis S, Kaufman D, Vande Woude GF. Strengthening context-dependent anticancer effects on non-small cell lung carcinoma by inhibition of both MET and EGFR. Mol Cancer Ther. 2013;12:1429–41.
106. Spigel DR, Ervin TJ, Ramlau RA, Daniel DB, Goldschmidt Jr JH, Blumenschein Jr GR, Krzakowski MJ, Robinet G, Godbert B, Barlesi F, Govindan R, Patel T, Orlov SV, Wertheim MS, Yu W, Zha J, Yauch RL, Patel PH, Phan SC, Peterson AC. Randomized phase II trial of onartuzumab in combination with erlotinib in patients with advanced non-small-cell lung cancer. J Clin Oncol. 2013;31:4105–14.
107. Borczuk AC, Gorenstein L, Walter KL, Assaad AA, Wang L, Powell CA. Non-small-cell lung cancer molecular signatures recapitulate lung developmental pathways. Am J Pathol. 2003;163:1949–60.
108. Villar-Garea A, Esteller M. Histone deacetylase inhibitors: understanding a new wave of anticancer agents. Int J Cancer. 2004;112:171–8.
109. Sengupta N, Seto E. Regulation of histone deacetylase activities. J Cell Biochem. 2004;93:57–67.
110. Melhuish TA, Gallo CM, Wotton D. TGIF2 interacts with histone deacetylase 1 and represses transcription. J Biol Chem. 2001;276:32109–14.
111. Beisel C, Imhof A, Greene J, Kremmer E, Sauer F. Histone methylation by the drosophila epigenetic transcriptional regulator Ash1. Nature. 2002;419:857–62.
112. Soejima H, Joh K, Mukai T. Gene silencing in DNA damage repair. Cell Mol Life Sci. 2004;61:2168–72.
113. Dehm SM, Bonham K. SRC gene expression in human cancer: the role of transcriptional activation. Biochem Cell Biol. 2004;82:263–74.
114. Sasaki H, Moriyama S, Nakashima Y, Kobayashi Y, Kiriyama M, Fukai I, Yamakawa Y, Fujii Y. Histone deacetylase 1 mRNA expression in lung cancer. Lung Cancer. 2004;46:171–8.
115. Chen MC, Chen CH, Wang JC, Tsai AC, Liou JP, Pan SL, Teng CM. The HDAC inhibitor, MPT0E028, enhances erlotinib-induced cell death in EGFR-TKI-resistant NSCLC cells. Cell Death Dis. 2013;4:e810.
116. Pal SK, Figlin RA, Reckamp K. Targeted therapies for non-small cell lung cancer: an evolving landscape. Mol Cancer Ther. 2010;9:1931–44.
117. An SJ, Chen ZH, Su J, Zhang XC, Zhong WZ, Yang JJ, Zhou Q, Yang XN, Huang L, Guan JL, Nie Q, Yan HH, Mok TS, Wu YL. Identification of enriched driver gene alterations in subgroups of non-small cell lung cancer patients based on histology and smoking status. PLoS ONE. 2012;7:e40109.
118. Moorehead RA, Sanchez OH, Baldwin RM, Khokha R. Transgenic overexpression of IGF-II induces spontaneous lung tumors: a model for human lung adenocarcinoma. Oncogene. 2003;22:853–7.
119. Gharib TG, Chen G, Huang CC, Misek DE, Iannettoni MD, Hanash SM, Orringer MB, Beer DG. Genomic and proteomic analyses of vascular endothelial growth factor and insulin-like growth factor-binding protein 3 in lung adenocarcinomas. Clin Lung Cancer. 2004;5:307–12.
120. Chen Y, Pacyna-Gengelbach M, Ye F, Knosel T, Lund P, Deutschmann N, Schluns K, Kotb WF, Sers C, Yasumoto H, Usui T, Petersen I. Insulin-like growth factor binding protein-related protein 1 (IGFBP-rP1) has potential tumour-suppressive activity in human lung cancer. J Pathol. 2007;211:431–8.
121. Morgillo F, Kim WY, Kim ES, Ciardiello F, Hong WK, Lee HY. Implication of the insulin-like growth factor-IR pathway in the resistance of non-small cell lung cancer cells to treatment with gefitinib. Clin Cancer Res. 2007;13:2795–803.

122. Gualberto A, Karp DD. Development of the monoclonal antibody figitumumab, targeting the insulin-like growth factor-1 receptor, for the treatment of patients with non-small-cell lung cancer. Clin Lung Cancer. 2009;10:273–80.
123. Gridelli C, Rossi A, Bareschino MA, Schettino C, Sacco PC, Maione P. The potential role of insulin-like growth factor receptor inhibitors in the treatment of advanced non-small cell lung cancer. Expert Opin Investig Drugs. 2010;19:631–9.
124. Hurbin A, Wislez M, Busser B, Antoine M, Tenaud C, Rabbe N, Dufort S, de Fraipont F, Moro-Sibilot D, Cadranel J, Coll JL, Brambilla E. Insulin-like growth factor-1 receptor inhibition overcomes gefitinib resistance in mucinous lung adenocarcinoma. J Pathol. 2011;225:83–95.
125. Weiss J, Sos ML, Seidel D, Peifer M, Zander T, Heuckmann JM, Ullrich RT, Menon R, Maier S, Soltermann A, Moch H, Wagener P, Fischer F, Heynck S, Koker M, Schottle J, Leenders F, Gabler F, Dabow I, Querings S, Heukamp LC, Balke-Want H, Ansen S, Rauh D, Baessmann I, Altmuller J, Wainer Z, Conron M, Wright G, Russell P, Solomon B, Brambilla E, Brambilla C, Lorimier P, Sollberg S, Brustugun OT, Engel-Riedel W, Ludwig C, Petersen I, Sanger J, Clement J, Groen H, Timens W, Sietsma H, Thunnissen E, Smit E, Heideman D, Cappuzzo F, Ligorio C, Damiani S, Hallek M, Beroukhim R, Pao W, Klebl B, Baumann M, Buettner R, Ernestus K, Stoelben E, Wolf J, Nurnberg P, Perner S, Thomas RK. Frequent and focal FGFR1 amplification associates with therapeutically tractable FGFR1 dependency in squamous cell lung cancer. Sci Transl Med. 2010;2:62ra93.
126. Dutt A, Ramos AH, Hammerman PS, Mermel C, Cho J, Sharifnia T, Chande A, Tanaka KE, Stransky N, Greulich H, Gray NS, Meyerson M. Inhibitor-sensitive FGFR1 amplification in human non-small cell lung cancer. PLoS ONE. 2011;6:e20351.
127. Lovly CM, Heuckmann JM, de Stanchina E, Chen H, Thomas RK, Liang C, Pao W. Insights into ALK-driven cancers revealed through development of novel ALK tyrosine kinase inhibitors. Cancer Res. 2011;71:4920–31.
128. Cai ZW, Zhang Y, Borzilleri RM, Qian L, Barbosa S, Wei D, Zheng X, Wu L, Fan J, Shi Z, Wautlet BS, Mortillo S, Jeyaseelan Sr R, Kukral DW, Kamath A, Marathe P, D'Arienzo C, Derbin G, Barrish JC, Robl JA, Hunt JT, Lombardo LJ, Fargnoli J, Bhide RS. Discovery of brivanib alaninate ((S)-((R)-1-(4-(4-fluoro-2-methyl-1H-indol-5-yloxy)-5-methylpyrrolo[2,1-f][1,2,4] triazin-6-yloxy) propan-2-yl)2-aminopropanoate), a novel prodrug of dual vascular endothelial growth factor receptor-2 and fibroblast growth factor receptor-1 kinase inhibitor (BMS-540215). J Med Chem. 2008;51:1976–80.
129. Antoniu SA, Kolb MR. Intedanib, a triple kinase inhibitor of VEGFR, FGFR and PDGFR for the treatment of cancer and idiopathic pulmonary fibrosis. IDrugs. 2010;13:332–45.
130. Sakamoto H, Tsukaguchi T, Hiroshima S, Kodama T, Kobayashi T, Fukami TA, Oikawa N, Tsukuda T, Ishii N, Aoki Y. CH5424802, a selective ALK inhibitor capable of blocking the resistant gatekeeper mutant. Cancer Cell. 2011;19:679–90.
131. Huang MH, Lee JH, Chang YJ, Tsai HH, Lin YL, Lin AM, Yang JC. MEK inhibitors reverse resistance in epidermal growth factor receptor mutation lung cancer cells with acquired resistance to gefitinib. Mol Oncol. 2013;7:112–20.
132. Mantripragada K, Khurshid H. Targeting genomic alterations in squamous cell lung cancer. Front Oncol. 2013;3:195.
133. Li L, Yu H, Wang X, Zeng J, Li D, Lu J, Wang C, Wang J, Wei J, Jiang M, Mo B. Expression of seven stem-cell-associated markers in human airway biopsy specimens obtained via fiberoptic bronchoscopy. J Exp Clin Cancer Res. 2013;32:28.
134. Martinez VD, Thu KL, Vucic EA, Hubaux R, Adonis M, Gil L, MacAulay C, Lam S, Lam WL. Whole-genome sequencing analysis identifies a distinctive mutational spectrum in an arsenic-related lung tumor. J Thorac Oncol. 2013;8:1451–5.
135. Lee YY, Kim HP, Kang MJ, Cho BK, Han SW, Kim TY, Yi EC. Phosphoproteomic analysis identifies activated MET-axis PI3K/AKT and MAPK/ERK in lapatinib-resistant cancer cell line. Exp Mol Med. 2013;45:e64.
136. Politi K, Fan PD, Shen R, Zakowski M, Varmus H. Erlotinib resistance in mouse models of epidermal growth factor receptor-induced lung adenocarcinoma. Dis Model Mech. 2010;3:111–9.
137. Chen Y, Huang Y, Chen J, Wang S, Zhou J. The prognostic value of SOX2 expression in non-small cell lung cancer: a meta-analysis. PLoS ONE. 2013;8:e71140.
138. Yu HA, Arcila ME, Rekhtman N, Sima CS, Zakowski MF, Pao W, Kris MG, Miller VA, Ladanyi M, Riely GJ. Analysis of tumor specimens at the time of acquired resistance to EGFR-TKI therapy in 155 patients with EGFR-mutant lung cancers. Clin Cancer Res. 2013;19:2240–7.
139. Olaussen KA, Soria JC, Morat L, Martin A, Sabatier L, Morere JF, Khayat D, Spano JP. Loss of PTEN expression is not uncommon, but lacks prognostic value in stage I NSCLC. Anticancer Res. 2003;23:4885–90.
140. Sarbassov DD, Guertin DA, Ali SM, Sabatini DM. Phosphorylation and regulation of Akt/PKB by the rictor-mTOR complex. Science. 2005;307:1098–101.
141. Zhang F, Zhang X, Li M, Chen P, Zhang B, Guo H, Cao W, Wei X, Cao X, Hao X, Zhang N. mTOR complex component rictor interacts with PKCzeta and regulates cancer cell metastasis. Cancer Res. 2010;70:9360–70.
142. Sarbassov DD, Ali SM, Sengupta S, Sheen JH, Hsu PP, Bagley AF, Markhard AL, Sabatini DM. Prolonged rapamycin treatment inhibits mTORC2 assembly and Akt/PKB. Mol Cell. 2006;22:159–68.

143. Jia P, Jin H, Meador CB, Xia J, Ohashi K, Liu L, Pirazzoli V, Dahlman KB, Politi K, Michor F, Zhao Z, Pao W. Next-generation sequencing of paired tyrosine kinase inhibitor-sensitive and -resistant EGFR mutant lung cancer cell lines identifies spectrum of DNA changes associated with drug resistance. Genome Res. 2013;23:1434–45.
144. Dearden S, Stevens J, Wu YL, Blowers D. Mutation incidence and coincidence in non small-cell lung cancer: meta-analyses by ethnicity and histology (mutMap). Ann Oncol. 2013;24:2371–6.
145. Han AJ, Xiong M, Zong YS. Association of Epstein-Barr virus with lymphoepithelioma-like carcinoma of the lung in southern China. Am J Clin Pathol. 2000;114:220–6.
146. Pros E, Lantuejoul S, Sanchez-Verde L, Castillo SD, Bonastre E, Suarez-Gauthier A, Conde E, Cigudosa JC, Lopez-Rios F, Torres-Lanzas J, Castellvi J, Ramon y Cajal S, Brambilla E, Sanchez-Cespedes M. Determining the profiles and parameters for gene amplification testing of growth factor receptors in lung cancer. Int J Cancer. 2013; 133:898–907.
147. Han AJ, Xiong M, Gu YY, Lin SX. Lymphoepithelioma-like carcinoma of the lung with a better prognosis. A clinicopathologic study of 32 cases. Am J Clin Pathol. 2001;115:841–50.
148. Hou M, Morishita Y, Iljima T, Inadome Y, Mase K, Dai Y, Noguchi M. DNA methylation and expression of p16(INK4A) gene in pulmonary adenocarcinoma and anthracosis in background lung. Int J Cancer. 1999;84:609–13.
149. Osada H, Takahashi T. Genetic alterations of multiple tumor suppressors and oncogenes in the carcinogenesis and progression of lung cancer. Oncogene. 2002;21:7421–34.
150. Toyooka S, Toyooka KO, Maruyama R, Virmani AK, Girard L, Miyajima K, Harada K, Ariyoshi Y, Takahashi T, Sugio K, Brambilla E, Gilcrease M, Minna JD, Gazdar AF. DNA methylation profiles of lung tumors. Mol Cancer Ther. 2001;1:61–7.
151. Licciulli S, Avila JL, Hanlon L, Troutman S, Cesaroni M, Kota S, Keith B, Simon MC, Pure E, Radtke F, Capobianco AJ, Kissil JL. Notch1 is required for kras-induced lung adenocarcinoma and controls tumor cell survival via p53. Cancer Res. 2013;73:5974–84.
152. Bernheim A, Toujani S, Saulnier P, Robert T, Casiraghi O, Validire P, Temam S, Menard P, Dessen P, Fouret P. High-resolution array comparative genomic hybridization analysis of human bronchial and salivary adenoid cystic carcinoma. Lab Invest. 2008;88:464–73.
153. McDermott U, Ames RY, Iafrate AJ, Maheswaran S, Stubbs H, Greninger P, McCutcheon K, Milano R, Tam A, Lee DY, Lucien L, Brannigan BW, Ulkus LE, Ma XJ, Erlander MG, Haber DA, Sharma SV, Settleman J. Ligand-dependent platelet-derived growth factor receptor (PDGFR)-alpha activation sensitizes rare lung cancer and sarcoma cells to PDGFR kinase inhibitors. Cancer Res. 2009;69: 3937–46.
154. Zhang L, Mitani Y, Caulin C, Rao PH, Kies MS, Saintigny P, Zhang N, Weber RS, Lippman SM, El-Naggar AK. Detailed genome-wide SNP analysis of major salivary carcinomas localizes subtype-specific chromosome sites and oncogenes of potential clinical significance. Am J Pathol. 2013;182: 2048–57.
155. Rossi G, Mengoli MC, Cavazza A, Nicoli D, Barbareschi M, Cantaloni C, Papotti M, Tironi A, Graziano P, Paci M, Stefani A, Migaldi M, Sartori G, Pelosi G. Large cell carcinoma of the lung: clinically oriented classification integrating immunohistochemistry and molecular biology. Virchows Arch. 2014;464:61–8.
156. Tsao MS, Liu N, Chen JR, Pappas J, Ho J, To C, Viallet J, Park M, Zhu H. Differential expression of met/hepatocyte growth factor receptor in subtypes of non-small cell lung cancers. Lung Cancer. 1998; 20:1–16.
157. Kim HR, Shim HS, Chung JH, Lee YJ, Hong YK, Rha SY, Kim SH, Ha SJ, Kim SK, Chung KY, Soo R, Kim JH, Cho BC. Distinct clinical features and outcomes in never-smokers with nonsmall cell lung cancer who harbor EGFR or KRAS mutations or ALK rearrangement. Cancer. 2012;118:729–39.
158. Strazisar M, Mlakar V, Rott T, Glavac D. Somatic alterations of the serine/threonine kinase LKB1 gene in squamous cell (SCC) and large cell (LCC) lung carcinoma. Cancer Invest. 2009;27:407–16.
159. Mak BC, Yeung RS. The tuberous sclerosis complex genes in tumor development. Cancer Invest. 2004; 22:588–603.
160. Wockel W, Hofler G, Popper HH, Morresi A. Lymphoepithelioma-like carcinoma of the lung. Pathol Res Pract. 1995;191:1170–4.
161. Chang YL, Wu CT, Shih JY, Lee YC. New aspects in clinicopathologic and oncogene studies of 23 pulmonary lymphoepithelioma-like carcinomas. Am J Surg Pathol. 2002;26:715–23.
162. Chang YL, Wu CT, Shih JY, Lee YC. Unique p53 and epidermal growth factor receptor gene mutation status in 46 pulmonary lymphoepithelioma-like carcinomas. Cancer Sci. 2011;102:282–7.
163. Uchida K, Kojima A, Morokawa N, Tanabe O, Anzai C, Kawakami M, Eto Y, Yoshimura K. Expression of progastrin-releasing peptide and gastrin-releasing peptide receptor mRNA transcripts in tumor cells of patients with small cell lung cancer. J Cancer Res Clin Oncol. 2002;128:633–40.
164. Levin NA, Brzoska PM, Warnock ML, Gray JW, Christman MF. Identification of novel regions of altered DNA copy number in small cell lung tumors. Genes Chromosom Cancer. 1995;13:175–85.
165. Schwendel A, Langreck H, Reichel M, Schrock E, Ried T, Dietel M, Petersen I. Primary small-cell lung carcinomas and their metastases are characterized by a recurrent pattern of genetic alterations. Int J Cancer. 1997;74:86–93.

166. Ullmann R, Schwendel A, Klemen H, Wolf G, Petersen I, Popper HH. Unbalanced chromosomal aberrations in neuroendocrine lung tumors as detected by comparative genomic hybridization. Hum Pathol. 1998;29:1145–9.
167. Harbour JW, Lai SL, Whang-Peng J, Gazdar AF, Minna JD, Kaye FJ. Abnormalities in structure and expression of the human retinoblastoma gene in SCLC. Science. 1988;241:353–7.
168. Lai SL, Brauch H, Knutsen T, Johnson BE, Nau MM, Mitsudomi T, Tsai CM, Whang-Peng J, Zbar B, Kaye FJ, et al. Molecular genetic characterization of neuroendocrine lung cancer cell lines. Anticancer Res. 1995;15:225–32.
169. Wistuba II, Gazdar AF, Minna JD. Molecular genetics of small cell lung carcinoma. Semin Oncol. 2001;28:3–13.
170. Burbee DG, Forgacs E, Zochbauer-Muller S, Shivakumar L, Fong K, Gao B, Randle D, Kondo M, Virmani A, Bader S, Sekido Y, Latif F, Milchgrub S, Toyooka S, Gazdar AF, Lerman MI, Zabarovsky E, White M, Minna JD. Epigenetic inactivation of RASSF1A in lung and breast cancers and malignant phenotype suppression. J Natl Cancer Inst. 2001; 93:691–9.
171. Senderowicz AM, Viard-Leveugle I, Veyrenc S, French LE, Brambilla C, Brambilla E. Small-molecule cyclin-dependent kinase modulators frequent loss of fas expression and function in human lung tumours with overexpression of FasL in small cell lung carcinoma. Oncogene. 2003;22:6609–20.
172. Kim YH, Girard L, Giacomini CP, Wang P, Hernandez-Boussard T, Tibshirani R, Minna JD, Pollack JR. Combined microarray analysis of small cell lung cancer reveals altered apoptotic balance and distinct expression signatures of MYC family gene amplification. Oncogene. 2006;25:130–8.
173. Krystal GW, Sulanke G, Litz J. Inhibition of phosphatidylinositol 3-kinase-Akt signaling blocks growth, promotes apoptosis, and enhances sensitivity of small cell lung cancer cells to chemotherapy. Mol Cancer Ther. 2002;1:913–22.
174. Ball DW, Azzoli CG, Baylin SB, Chi D, Dou S, Donis-Keller H, Cumaraswamy A, Borges M, Nelkin BD. Identification of a human achaete-scute homolog highly expressed in neuroendocrine tumors. Int J Cancer. 1993;54:784–92.
175. Westerman BA, Breuer RH, Poutsma A, Chhatta A, Noorduyn LA, Koolen MG, Postmus PE, Blankenstein MA, Oudejans CB. Basic helix-loop-helix transcription factor profiling of lung tumors shows aberrant expression of the proneural gene atonal homolog 1 (ATOH1, HATH1, MATH1) in neuroendocrine tumors. Int J Biol Markers. 2007;22: 114–23.
176. Miki M, Ball DW, Linnoila RI. Insights into the achaete-scute homolog-1 gene (hASH1) in normal and neoplastic human lung. Lung Cancer. 2012; 75:58–65.
177. Osada H, Tomida S, Yatabe Y, Tatematsu Y, Takeuchi T, Murakami H, Kondo Y, Sekido Y, Takahashi T. Roles of achaete-scute homologue 1 in DKK1 and E-cadherin repression and neuroendocrine differentiation in lung cancer. Cancer Res. 2008;68: 1647–55.
178. Linnoila RI, Zhao B, DeMayo JL, Nelkin BD, Baylin SB, DeMayo FJ, Ball DW. Constitutive achaete-scute homologue-1 promotes airway dysplasia and lung neuroendocrine tumors in transgenic mice. Cancer Res. 2000;60:4005–9.
179. Hiroshima K, Iyoda A, Shibuya K, Haga Y, Toyozaki T, Iizasa T, Nakayama T, Fujisawa T, Ohwada H. Genetic alterations in early-stage pulmonary large cell neuroendocrine carcinoma. Cancer. 2004; 100:1190–8.
180. Ullmann R, Petzmann S, Sharma A, Cagle PT, Popper HH. Chromosomal aberrations in a series of large-cell neuroendocrine carcinomas: unexpected divergence from small-cell carcinoma of the lung. Hum Pathol. 2001;32:1059–63.
181. Nasgashio R, Sato Y, Matsumoto T, Kageyama T, Hattori M, Iyoda A, Satoh Y, Ryuge S, Masuda N, Jiang SX, Saegusa M. The balance between the expressions of hASH1 and HES1 differs between large cell neuroendocrine carcinoma and small cell carcinoma of the lung. Lung Cancer. 2011;74:405–10.
182. Petzmann S, Ullmann R, Halbwedl I, Popper HH. Analysis of chromosome-11 aberrations in pulmonary and gastrointestinal carcinoids: an array comparative genomic hybridization-based study. Virchows Arch. 2004;445:151–9.
183. Macarenco RS, Uphoff TS, Gilmer HF, Jenkins RB, Thibodeau SN, Lewis JE, Molina JR, Yang P, Aubry MC. Salivary gland-type lung carcinomas: an EGFR immunohistochemical, molecular genetic, and mutational analysis study. Mod Pathol. 2008;21: 1168–75.
184. Han SW, Kim HP, Jeon YK, Oh DY, Lee SH, Kim DW, Im SA, Chung DH, Heo DS, Bang YJ, Kim TY. Mucoepidermoid carcinoma of lung: potential target of EGFR-directed treatment. Lung Cancer. 2008;61:30–4.
185. O'Neill ID. Gefitinib as targeted therapy for mucoepidermoid carcinoma of the lung: possible significance of CRTC1-MAML2 oncogene. Lung Cancer. 2009;64:129–30.
186. Younes MN, Park YW, Yazici YD, Gu M, Santillan AA, Nong X, Kim S, Jasser SA, El-Naggar AK, Myers JN. Concomitant inhibition of epidermal growth factor and vascular endothelial growth factor receptor tyrosine kinases reduces growth and metastasis of human salivary adenoid cystic carcinoma in an orthotopic nude mouse model. Mol Cancer Ther. 2006;5:2696–705.
187. Aubry MC, Heinrich MC, Molina J, Lewis JE, Yang P, Cassivi SD, Corless CL. Primary adenoid cystic carcinoma of the lung: absence of KIT mutations. Cancer. 2007;110:2507–10.

188. Dahse R, Driemel O, Schwarz S, Kromeyer-Hauschild K, Berndt A, Kosmehl H. KRAS status and epidermal growth factor receptor expression as determinants for anti-EGFR therapies in salivary gland carcinomas. Oral Oncol. 2009;45:826–9.
189. Hu JA, Li Y, Fang J. Effect of ERK inhibitor on pulmonary metastasis of inoculated human adenoid cystic carcinoma cells in nude mice. Oral Surg Oral Med Oral Pathol Oral Radiol Endod. 2010;109:117–23.
190. Dammrich DJ, Santos ES, Raez LE. Efficacy of sorafenib, a multi-tyrosine kinase inhibitor, in an adenoid cystic carcinoma metastatic to the lung: case report and review of literature. J Med Case Rep. 2011;5:483.
191. Chau NG, Hotte SJ, Chen EX, Chin SF, Turner S, Wang L, Siu LL. A phase II study of sunitinib in recurrent and/or metastatic adenoid cystic carcinoma (ACC) of the salivary glands: current progress and challenges in evaluating molecularly targeted agents in ACC. Ann Oncol. 2012;23:1562–70.
192. Persson M, Andren Y, Moskaluk CA, Frierson Jr HF, Cooke SL, Futreal PA, Kling T, Nelander S, Nordkvist A, Persson F, Stenman G. Clinically significant copy number alterations and complex rearrangements of MYB and NFIB in head and neck adenoid cystic carcinoma. Genes Chromosom Cancer. 2012;51:805–17.
193. Ho AS, Kannan K, Roy DM, Morris LG, Ganly I, Katabi N, Ramaswami D, Walsh LA, Eng S, Huse JT, Zhang J, Dolgalev I, Huberman K, Heguy A, Viale A, Drobnjak M, Leversha MA, Rice CE, Singh B, Iyer NG, Leemans CR, Bloemena E, Ferris RL, Seethala RR, Gross BE, Liang Y, Sinha R, Peng L, Raphael BJ, Turcan S, Gong Y, Schultz N, Kim S, Chiosea S, Shah JP, Sander C, Lee W, Chan TA. The mutational landscape of adenoid cystic carcinoma. Nat Genet. 2013;45:791–8.
194. Stephens PJ, Davies HR, Mitani Y, Van Loo P, Shlien A, Tarpey PS, Papaemmanuil E, Cheverton A, Bignell GR, Butler AP, Gamble J, Gamble S, Hardy C, Hinton J, Jia M, Jayakumar A, Jones D, Latimer C, McLaren S, McBride DJ, Menzies A, Mudie L, Maddison M, Raine K, Nik-Zainal S, O'Meara S, Teague JW, Varela I, Wedge DC, Whitmore I, Lippman SM, McDermott U, Stratton MR, Campbell PJ, El-Naggar AK, Futreal PA. Whole exome sequencing of adenoid cystic carcinoma. J Clin Invest. 2013;123:2965–8.
195. Pelosi G, Fraggetta F, Nappi O, Pastorino U, Maisonneuve P, Pasini F, Iannucci A, Solli P, Musavinasab HS, De Manzoni G, Terzi A, Viale G. Pleomorphic carcinomas of the lung show a selective distribution of gene products involved in cell differentiation, cell cycle control, tumor growth, and tumor cell motility: a clinicopathologic and immunohistochemical study of 31 cases. Am J Surg Pathol. 2003;27:1203–15.
196. Blaukovitsch M, Halbwedl I, Kothmaier H, Gogg-Kammerer M, Popper HH. Sarcomatoid carcinomas of the lung – are these histogenetically heterogeneous tumors? Virchows Arch. 2006;449:455–61.
197. Italiano A, Cortot AB, Ilie M, Martel-Planche G, Fabas T, Pop D, Mouroux J, Hofman V, Hofman P, Pedeutour F. EGFR and KRAS status of primary sarcomatoid carcinomas of the lung: implications for anti-EGFR treatment of a rare lung malignancy. Int J Cancer. 2009;125:2479–82.
198. Henske EP, McCormack FX. Lymphangioleiomyomatosis – a wolf in sheep's clothing. J Clin Invest. 2012;122:3807–16.
199. Burger JA, Stewart DJ, Wald O, Peled A. Potential of CXCR4 antagonists for the treatment of metastatic lung cancer. Expert Rev Anticancer Ther. 2011; 11:621–30.
200. Fan TW, Lane AN, Higashi RM, Farag MA, Gao H, Bousamra M, Miller DM. Altered regulation of metabolic pathways in human lung cancer discerned by (13)C stable isotope-resolved metabolomics (SIRM). Mol Cancer. 2009;8:41.
201. Malchers F, Dietlein F, Schottle J, Lu X, Nogova L, Albus K, Fernandez-Cuesta L, Heuckmann JM, Gautschi O, Diebold J, Plenker D, Gardizi M, Scheffler M, Bos M, Seidel D, Leenders F, Richters A, Peifer M, Florin A, Mainkar PS, Karre N, Chandrasekhar S, George J, Silling S, Rauh D, Zander T, Ullrich R, Reinhardt HC, Ringeisen F, Buttner R, Heukamp LC, Wolf J, Thomas RK. Cell-autonomous and non-cell-autonomous mechanisms of transformation by amplified FGFR1 in lung cancer. Cancer Discov. 2014;4:246–57.
202. Massion PP, Taflan PM, Jamshedur Rahman SM, Yildiz P, Shyr Y, Edgerton ME, Westfall MD, Roberts JR, Pietenpol JA, Carbone DP, Gonzalez AL. Significance of p63 amplification and overexpression in lung cancer development and prognosis. Cancer Res. 2003;63:7113–21.
203. Massion PP, Taflan PM, Shyr Y, Rahman SM, Yildiz P, Shakthour B, Edgerton ME, Ninan M, Andersen JJ, Gonzalez AL. Early involvement of the phosphatidylinositol 3-kinase/Akt pathway in lung cancer progression. Am J Respir Crit Care Med. 2004; 170:1088–94.
204. Tang X, Liu D, Shishodia S, Ozburn N, Behrens C, Lee JJ, Hong WK, Aggarwal BB, Wistuba II. Nuclear factor-kappaB (NF-kappaB) is frequently expressed in lung cancer and preneoplastic lesions. Cancer. 2006;107:2637–46.
205. Shen J, Behrens C, Wistuba II, Feng L, Lee JJ, Hong WK, Lotan R. Identification and validation of differences in protein levels in normal, premalignant, and malignant lung cells and tissues using high-throughput Western Array and immunohistochemistry. Cancer Res. 2006;66:11194–206.
206. Ullmann R, Bongiovanni M, Halbwedl I, Fraire AE, Cagle PT, Mori M, Papotti M, Popper HH. Is high-grade adenomatous hyperplasia an early bronchioloalveolar adenocarcinoma? J Pathol. 2003;201: 371–6.

207. Mori M, Rao SK, Popper HH, Cagle PT, Fraire AE. Atypical adenomatous hyperplasia of the lung: a probable forerunner in the development of adenocarcinoma of the lung. Mod Pathol. 2001; 14:72–84.
208. Westra WH, Baas IO, Hruban RH, Askin FB, Wilson K, Offerhaus GJ, Slebos RJ. K-ras oncogene activation in atypical alveolar hyperplasias of the human lung. Cancer Res. 1996;56:2224–8.
209. Cooper CA, Carby FA, Bubb VJ, Lamb D, Kerr KM, Wyllie AH. The pattern of K-ras mutation in pulmonary adenocarcinoma defines a new pathway of tumour development in the human lung. J Pathol. 1997;181:401–4.
210. Suzuki K, Ogura T, Yokose T, Nagai K, Mukai K, Kodama T, Nishiwaki Y, Esumi H. Loss of heterozygosity in the tuberous sclerosis gene associated regions in adenocarcinoma of the lung accompanied by multiple atypical adenomatous hyperplasia. Int J Cancer. 1998;79:384–9.
211. Takamochi K, Ogura T, Suzuki K, Kawasaki H, Kurashima Y, Yokose T, Ochiai A, Nagai K, Nishiwaki Y, Esumi H. Loss of heterozygosity on chromosomes 9q and 16p in atypical adenomatous hyperplasia concomitant with adenocarcinoma of the lung. Am J Pathol. 2001;159:1941–8.
212. Haneda H, Sasaki H, Shimizu S, Endo K, Suzuki E, Yukiue H, Kobayashi Y, Yano M, Fujii Y. Epidermal growth factor receptor gene mutation defines distinct subsets among small adenocarcinomas of the lung. Lung Cancer. 2006;52:47–52.
213. Awaya H, Takeshima Y, Furonaka O, Kohno N, Inai K. Gene amplification and protein expression of EGFR and HER2 by chromogenic in situ hybridisation and immunohistochemistry in atypical adenomatous hyperplasia and adenocarcinoma of the lung. J Clin Pathol. 2005;58:1076–80.
214. Sakamoto H, Shimizu J, Horio Y, Ueda R, Takahashi T, Mitsudomi T, Yatabe Y. Disproportionate representation of KRAS gene mutation in atypical adenomatous hyperplasia, but even distribution of EGFR gene mutation from preinvasive to invasive adenocarcinomas. J Pathol. 2007;212:287–94.
215. Ullmann R, Bongiovanni M, Halbwedl I, Petzmann S, Gogg-Kammerer M, Sapino A, Papotti M, Bussolati G, Popper HH. Bronchiolar columnar cell dysplasia – genetic analysis of a novel preneoplastic lesion of peripheral lung. Virchows Arch. 2003;442: 429–36.
216. Casiraghi M, Travaini LL, Maisonneuve P, Tessitore A, Brambilla D, Agoglia BG, Guarize J, Spaggiari L. Lymph node involvement in T1 non-small-cell lung cancer: could glucose uptake and maximal diameter be predictive criteria? Eur J Cardiothorac Surg. 2011;39:e38–43.
217. Stacher E, Ullmann R, Halbwedl I, Gogg-Kammerer M, Boccon-Gibod L, Nicholson AG, Sheppard MN, Carvalho L, Franca MT, Macsweeney F, Morresi-Hauf A, Popper HH. Atypical goblet cell hyperplasia in congenital cystic adenomatoid malformation as a possible preneoplasia for pulmonary adenocarcinoma in childhood: a genetic analysis. Hum Pathol. 2004;35:565–70.
218. Sartelet H, Decaussin M, Devouassoux G, Nawrocki-Raby B, Brichon PY, Brambilla C, Brambilla E. Expression of vascular endothelial growth factor (VEGF) and its receptors (VEGF-R1 [Flt-1] and VEGF-R2 [KDR/Flk-1]) in tumorlets and in neuroendocrine cell hyperplasia of the lung. Hum Pathol. 2004;35:1210–7.
219. Zynger DL, Dimov ND, Ho LC, Laskin WB, Yeldandi AV. Differential expression of neural-cadherin in pulmonary epithelial tumours. Histopathology. 2008;52:348–54.
220. Popper HH, Wirnsberger G, Juttner-Smolle FM, Pongratz MG, Sommersgutter M. The predictive value of human papilloma virus (HPV) typing in the prognosis of bronchial squamous cell papillomas. Histopathology. 1992;21:323–30.
221. Popper HH, El-Shabrawi Y, Wockel W, Hofler G, Kenner L, Juttner-Smolle FM, Pongratz MG. Prognostic importance of human papilloma virus typing in squamous cell papilloma of the bronchus: comparison of in situ hybridization and the polymerase chain reaction. Hum Pathol. 1994;25: 1191–7.
222. Solinas-Toldo S, Durst M, Lichter P. Specific chromosomal imbalances in human papillomavirus-transfected cells during progression toward immortality. Proc Natl Acad Sci U S A. 1997;94: 3854–9.
223. Lele SM, Pou AM, Ventura K, Gatalica Z, Payne D. Molecular events in the progression of recurrent respiratory papillomatosis to carcinoma. Arch Pathol Lab Med. 2002;126:1184–8.
224. Dishop MK, McKay EM, Kreiger PA, Priest JR, Williams GM, Langston C, Jarzembowski J, Suchi M, Dehner LP, Hill DA. Fetal lung interstitial tumor (FLIT): a proposed newly recognized lung tumor of infancy to be differentiated from cystic pleuropulmonary blastoma and other developmental pulmonary lesions. Am J Surg Pathol. 2010;34:1762–72.
225. Hosaka N, Sasaki T, Adachi K, Sato T, Tanaka T, Miura Y, Sawai T, Toki J, Hisha H, Okamura A, Takasu K, Ikehara S. Pulmonary sclerosing hemangioma associated with familial adenomatous polyposis. Hum Pathol. 2004;35:764–8.
226. Wu CT, Chang YL, Lee YC. Expression of the estrogen receptor beta in 37 surgically treated pulmonary sclerosing hemangiomas in comparison with non-small cell lung carcinomas. Hum Pathol. 2005;36: 1108–12.
227. Sartori G, Bettelli S, Schirosi L, Bigiani N, Maiorana A, Cavazza A, Rossi G. Microsatellite and EGFR, HER2 and K-RAS analyses in sclerosing hemangioma of the lung. Am J Surg Pathol. 2007;31: 1512–20.
228. Astrinidis A, Cash TP, Hunter DS, Walker CL, Chernoff J, Henske EP. Tuberin, the tuberous sclerosis complex 2 tumor suppressor gene product, regu-

lates Rho activation, cell adhesion and migration. Oncogene. 2002;21:8470–6.
229. Finlay GA, Malhowski AJ, Liu Y, Fanburg BL, Kwiatkowski DJ, Toksoz D. Selective inhibition of growth of tuberous sclerosis complex 2 null cells by atorvastatin is associated with impaired Rheb and Rho GTPase function and reduced mTOR/S6 kinase activity. Cancer Res. 2007;67:9878–86.
230. Popper HH, Juettner-Smolle FM, Pongratz MG. Micronodular hyperplasia of type II pneumocytes – a new lung lesion associated with tuberous sclerosis. Histopathology. 1991;18:347–54.
231. Muir TE, Leslie KO, Popper H, Kitaichi M, Gagne E, Emelin JK, Vinters HV, Colby TV. Micronodular pneumocyte hyperplasia. Am J Surg Pathol. 1998; 22:465–72.
232. Maruyama H, Ohbayashi C, Hino O, Tsutsumi M, Konishi Y. Pathogenesis of multifocal micronodular pneumocyte hyperplasia and lymphangioleiomyomatosis in tuberous sclerosis and association with tuberous sclerosis genes TSC1 and TSC2. Pathol Int. 2001;51:585–94.
233. Carrington CB, Cugell DW, Gaensler EA, Marks A, Redding RA, Schaaf JT, Tomasian A. Lymphangioleiomyomatosis. Physiologic-pathologic-radiologic correlations. Am Rev Respir Dis. 1977;116:977–95.
234. Nine JS, Yousem SA, Paradis IL, Keenan R, Griffith BP. Lymphangioleiomyomatosis: recurrence after lung transplantation. J Heart Lung Transplant. 1994; 13:714–9.
235. Bittmann I, Dose TB, Muller C, Dienemann H, Vogelmeier C, Lohrs U. Lymphangioleiomyomatosis: recurrence after single lung transplantation. Hum Pathol. 1997;28:1420–3.
236. Bittmann I, Rolf B, Amann G, Lohrs U. Recurrence of lymphangioleiomyomatosis after single lung transplantation: new insights into pathogenesis. Hum Pathol. 2003;34:95–8.
237. Crooks DM, Pacheco-Rodriguez G, DeCastro RM, McCoy Jr JP, Wang JA, Kumaki F, Darling T, Moss J. Molecular and genetic analysis of disseminated neoplastic cells in lymphangioleiomyomatosis. Proc Natl Acad Sci U S A. 2004;101:17462–7.
238. Carsillo T, Astrinidis A, Henske EP. Mutations in the tuberous sclerosis complex gene TSC2 are a cause of sporadic pulmonary lymphangioleiomyomatosis. Proc Natl Acad Sci U S A. 2000;97:6085–90.
239. Sampson JR. TSC1 and TSC2: genes that are mutated in the human genetic disorder tuberous sclerosis. Biochem Soc Trans. 2003;31:592–6.
240. Sietsema KE, McCormack FX. Lymphangioleiomyomatosis: insights about, and from, a rare disease. Am J Respir Crit Care Med. 2003;168:1405–6.
241. Davies DM, de Vries PJ, Johnson SR, McCartney DL, Cox JA, Serra AL, Watson PC, Howe CJ, Doyle T, Pointon K, Cross JJ, Tattersfield AE, Kingswood JC, Sampson JR. Sirolimus therapy for angiomyolipoma in tuberous sclerosis and sporadic lymphangioleiomyomatosis: a phase 2 trial. Clin Cancer Res. 2011;17:4071–81.
242. McCormack FX, Inoue Y, Moss J, Singer LG, Strange C, Nakata K, Barker AF, Chapman JT, Brantly ML, Stocks JM, Brown KK, Lynch 3rd JP, Goldberg HJ, Young LR, Kinder BW, Downey GP, Sullivan EJ, Colby TV, McKay RT, Cohen MM, Korbee L, Taveira-DaSilva AM, Lee HS, Krischer JP, Trapnell BC. Efficacy and safety of sirolimus in lymphangioleiomyomatosis. N Engl J Med. 2011;364:1595–606.
243. Harris GC, McCulloch TA, Perks G, Fisher C. Malignant perivascular epithelioid cell tumour ("PEComa") of soft tissue: a unique case. Am J Surg Pathol. 2004;28:1655–8.
244. Martignoni G, Pea M, Reghellin D, Zamboni G, Bonetti F. PEComas: the past, the present and the future. Virchows Arch. 2008;452:119–32.
245. Astrinidis A, Henske EP. Tuberous sclerosis complex: linking growth and energy signaling pathways with human disease. Oncogene. 2005;24:7475–81.
246. Dabora SL, Franz DN, Ashwal S, Sagalowsky A, DiMario Jr FJ, Miles D, Cutler D, Krueger D, Uppot RN, Rabenou R, Camposano S, Paolini J, Fennessy F, Lee N, Woodrum C, Manola J, Garber J, Thiele EA. Multicenter phase 2 trial of sirolimus for tuberous sclerosis: kidney angiomyolipomas and other tumors regress and VEGF- D levels decrease. PLoS ONE. 2011;6:e23379.
247. Su H, Bodenstein C, Dumont RA, Seimbille Y, Dubinett S, Phelps ME, Herschman H, Czernin J, Weber W. Monitoring tumor glucose utilization by positron emission tomography for the prediction of treatment response to epidermal growth factor receptor kinase inhibitors. Clin Cancer Res. 2006;12: 5659–67.
248. Hachitanda Y, Aoyama C, Sato JK, Shimada H. Pleuropulmonary blastoma in childhood. A tumor of divergent differentiation. Am J Surg Pathol. 1993;17:382–91.
249. Dehner LP. Pleuropulmonary blastoma is THE pulmonary blastoma of childhood. Semin Diagn Pathol. 1994;11:144–51.
250. Novak R, Dasu S, Agamanolis D, Herold W, Malone J, Waterson J. Trisomy 8 is a characteristic finding in pleuropulmonary blastoma. Pediatr Pathol Lab Med. 1997;17:99–103.
251. Barnard M, Bayani J, Grant R, Teshima I, Thorner P, Squire J. Use of multicolor spectral karyotyping in genetic analysis of pleuropulmonary blastoma. Pediatr Dev Pathol. 2000;3:479–86.
252. Vargas SO, Nose V, Fletcher JA, Perez-Atayde AR. Gains of chromosome 8 are confined to mesenchymal components in pleuropulmonary blastoma. Pediatr Dev Pathol. 2001;4:434–45.
253. Roque L, Rodrigues R, Martins C, Ribeiro C, Ribeiro MJ, Martins AG, Oliveira P, Fonseca I. Comparative genomic hybridization analysis of a pleuropulmonary blastoma. Cancer Genet Cytogenet. 2004;149: 58–62.

254. Kusafuka T, Kuroda S, Inoue M, Ara T, Yoneda A, Oue T, Udatsu Y, Osugi Y, Okada A. P53 gene mutations in pleuropulmonary blastomas. Pediatr Hematol Oncol. 2002;19:117–28.
255. Yang P, Hasegawa T, Hirose T, Fukumoto T, Uyama T, Monden Y, Sano T. Pleuropulmonary blastoma: fluorescence in situ hybridization analysis indicating two PPBs were confirmed to harbor p53 mutations. One was a Val to Leu substitution at codon 173, and another was a ArgArg to TrpCys substitution at codons 282 and 283. In each tumor, only the mutated allele was detected, suggesting inactivation of p53. Am J Surg Pathol. 1997;21:854–9.
256. Slade I, Bacchelli C, Davies H, Murray A, Abbaszadeh F, Hanks S, Barfoot R, Burke A, Chisholm J, Hewitt M, Jenkinson H, King D, Morland B, Pizer B, Prescott K, Saggar A, Side L, Traunecker H, Vaidya S, Ward P, Futreal PA, Vujanic G, Nicholson AG, Sebire N, Turnbull C, Priest JR, Pritchard-Jones K, Houlston R, Stiller C, Stratton MR, Douglas J, Rahman N. DICER1 syndrome: clarifying the diagnosis, clinical features and management implications of a pleiotropic tumour predisposition syndrome. J Med Genet. 2011;48:273–8.
257. Alobeid B, Beneck D, Sreekantaiah C, Abbi RK, Slim MS. Congenital pulmonary myofibroblastic tumor: a case report with cytogenetic analysis and review of the literature. Am J Surg Pathol. 1997;21:610–4.
258. McGinnis M, Jacobs G, El-Naggar A, Redline RW. Congenital peribronchial myofibroblastic tumor (so-called “congenital leiomyosarcoma”). A distinct neonatal lung lesion associated with nonimmune hydrops fetalis. Mod Pathol. 1993;6:487–92.
259. Schneider BF, Lovell MA, Golden WL. Cytogenetic abnormalities in primary bronchopulmonary leiomyosarcoma of childhood. Cancer Genet Cytogenet. 1998;105:145–51.

Immunotherapy of Lung Tumors 20

After being used in the therapy of melanomas, immunotherapy is now also used in NSCLC. A major breakthrough in establishing this type of therapy was the finding of immunomodulation of T-cell response through immune checkpoints inducing immune evasion of cancer cells. Cytotoxic T-lymphocyte antigen-4 (CTLA-4) was found in dendritic cells and regulatory T cells (Tregs) in lymph nodes but also circulating in the blood inducing apoptosis and cell death of cytotoxic T lymphocytes [1]. Programmed cell death 1 (PD1) and its ligand PDL1 were found on tumor cells as well as on lymphocytes inducing immune tolerance [2]. Based on these findings, antibodies for PDL1 and PD1 were tested for their ability to interfere with this mechanism of immune tolerance against tumor antigens. Important efforts are under way and have focused on this new treatment modality [2–10]. At present several pharmaceutical companies have developed checkpoint inhibitors (humanized monoclonal antibodies) for treatment of NSCLC patients, and numerous phase II and III studies have been performed. The FDA and EMA have recently approved three of these drugs for treatment of NSCLC. Whereas some drugs are selectively approved for SCC, others may be used in all NSCLC [9, 11–14].

Like other solid tumors, pulmonary carcinomas have developed several mechanisms by which they escape the attack of cytotoxic immune cells. Some of these mechanisms have recently gained special attention, the programmed death 1 – programmed death ligand 1 and 2 (PDL1/2-PD1) – and the CTLA-4 system. Tumor cells as well as lymphocytes can express ligands for PD1 [4]. By this they interact with surface molecules on CD8+ T cells causing apoptosis and further more influence also the microenvironment via orchestration by cytokines, which all together cause immune tolerance. Therapy using antibodies against PDL1 has shown significant improvement experimentally as well as in clinical studies to restore the cytotoxic attack of T lymphocytes toward tumor cells in several solid malignancies [3, 6, 10]. Parallel to targeting PDL1 by anti-PDL1 antibodies, also antibodies against the receptor PD1 have been created and used experimentally and in clinical trials with success [2, 4, 5, 7, 8]. In some clinical trials, specific immunohistochemistry tests for the expression of PD1 and PDL1 were used to select those patients, who might best respond to the antibody-based therapy. A strong staining in at least 5 % of tumor cells and/or lymphocytes – or 50 % in another trial [15] – was regarded as a positive result and predictive for outcome. Looking up clinical data of these trials, it is evident that the majority of patients are detected by this simple stain. However, there exist also a not to be neglected amount of patients, which do not respond to treatment although being positive for PD1/PDL1 as well as patients who do respond despite being negative or low positive for these molecules [16–18].

© Springer-Verlag Berlin Heidelberg 2017
H. Popper, *Pathology of Lung Disease*, DOI 10.1007/978-3-662-50491-8_20

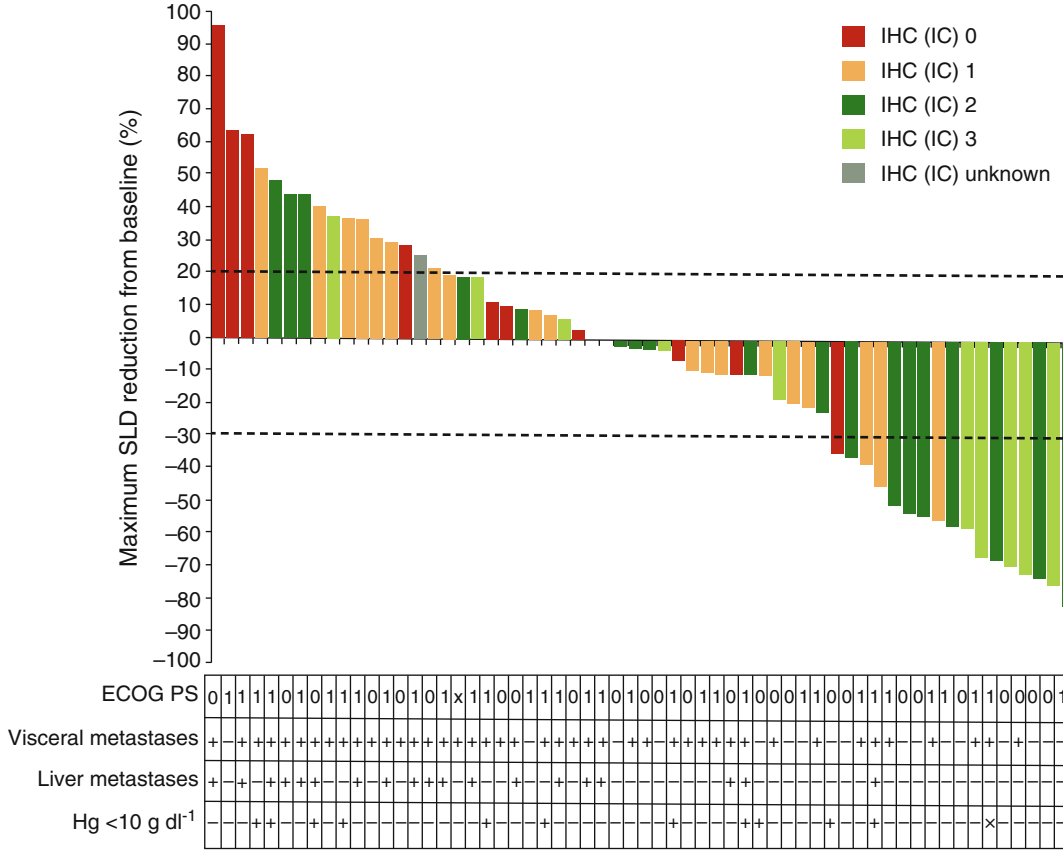

Waterfall plot of patient response and immunohistochemical staining for PDL1 according to J. Brahmer (Presentation AACR 2015, Philadelphia)

Although proving PD1-PDL1 as targetable molecules within the immune regulatory system (Fig. 20.1), it is well known from nonneoplastic diseases that there are many more ways the immune system can be shifted toward antigen tolerance or even lymphocyte exhaustion. Several of these regulatory mechanisms are also targetable. Subsequent development of resistance toward the PD1-PDL1 therapy might be due to one of these immunomodulatory alterations. In addition patients might have developed tolerance against their tumor cells not only by expression of PD1-PDL1 but in addition by other tolerance mechanisms – this could be due in patients, who do not respond to anti-PDL1 therapy despite having PD1-PDL1 upregulated.

20.1 Systems Known to Be Able to Induce Immune Tolerance Toward Foreign Antigens

One of the most important cell types in this regard are antigen-presenting cells from the dendritic cell lineage. There are several populations, such as conventional dendritic cells, which promote immune attack by processing foreign antigens and present them to CD8+ T lymphocytes. Others such as plasmacytoid and granulocytic dendritic cells in contrary cause immune tolerance by cooperating either with regulatory T cells or by inducing an inflammatory environment, which promotes tumor cell invasion, spreading, and finally metastasis [19, 20]. The function of

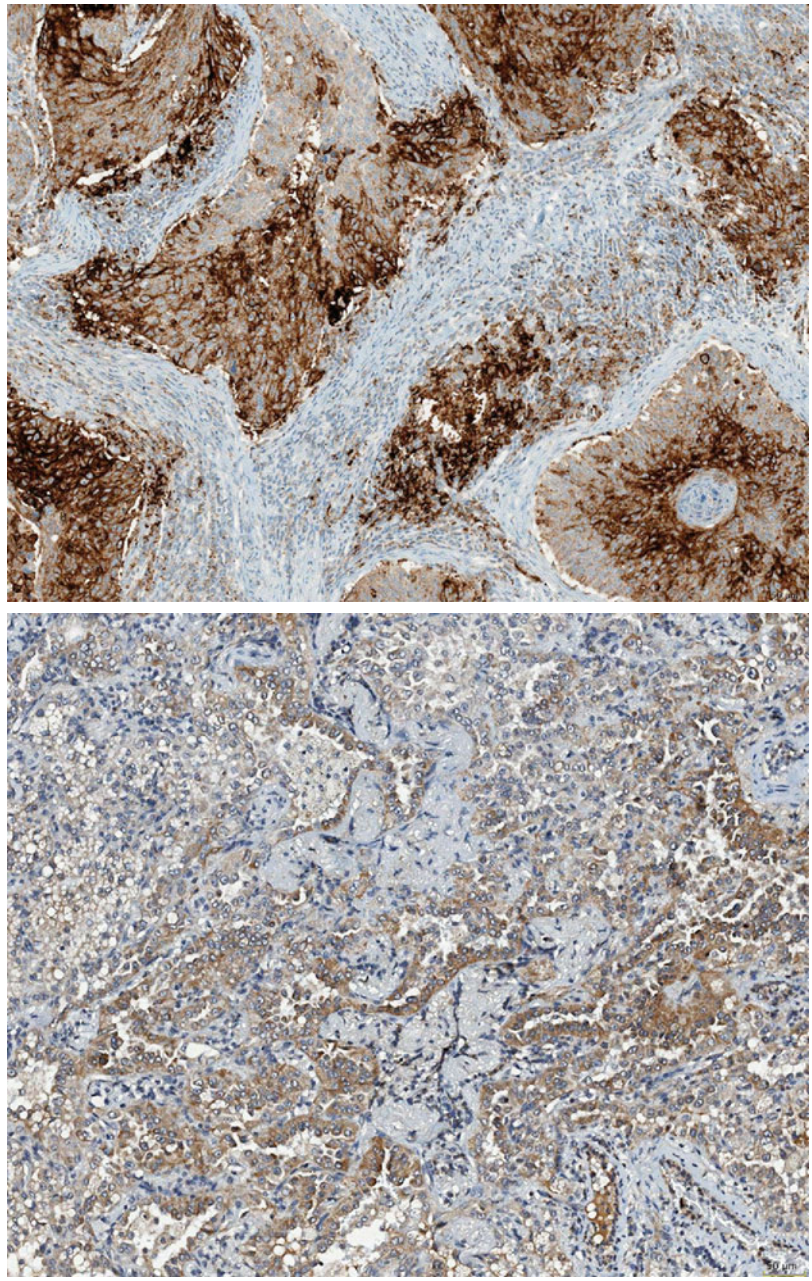

Fig. 20.1 Immunohistochemistry for PDL1 in a squamous cell (*top panel*) and an adenocarcinoma (*bottom panel*). There are differences in the expression of PDL1 between adenocarcinomas and squamous cell carcinomas, but also between the individual tumor cells. Bars 50μm

Langerhans cells, another dendritic cell type, is entirely unknown, but most probably acts against tumor antigens.

Plasmacytoid dendritic cells can also interact with monocytoid cells promoting the differentiation of macrophages into the tumor-promoting M2 lineage. Macrophages play a major role early on in carcinogenesis. Macrophages can induce angiogenesis and prepare and modulate stroma proteins in favor for invading tumor cells, thus promoting tumor growth, invasion, and metastasis [21, 22]. In contrary M1 macrophages might inhibit tumor

progression not only in the early phase but also during metastasis formation [23, 24].

There are additional pathways by which tumor cells can influence the differentiation of M0 macrophages into M2 lineage. Whereas activation of Notch signaling increased M1 macrophages, blocking of Notch induced a M2 response. Wang et al. showed that RBP-J-mediated Notch signaling regulates the M1 versus M2 polarization through SOCS3 [23]. Notch is mutated in several lung carcinomas; however, if this also applies to tumor-associated macrophages has not been studied so far. Tumor cells might use SOCS3 signaling to induce M2 macrophage polarization.

Regulatory T cells (Tregs) can accumulate at the tumor site and block CD8+ T lymphocytes and NK cells in their antitumor action as well as inhibit influx of the cells into the tumor [25, 26].

Autophagy is another mechanism associated with immune cell modulation, although this mechanism is presently not fully understood. Autophagy is seen in many lung cancer types. Increase of autophagy in cancer cells liberates nutrients, decreases the formation of reactive oxygen species, and aids in the clearance of misfolded proteins. This provides a survival advantage for cancer cells in the tumor microenvironment. However, also immune cells infiltrate the tumor environment and encounter hypoxia, resulting in hypoxia-induced autophagy. Due to the fact that autophagy is crucial for immune cell proliferation as well as antigen presentation and T-cell-mediated killing of tumor cells, anticancer treatment strategies based on autophagy modulation will need to consider the impact of autophagy on the immune system [27]. In melanoma it has been shown that hypoxia leads to instability of gap junctional Cx43 and impairs melanoma cell killing by NK cells. Inhibition of autophagy by pharmacological approaches might restore NK-cell-mediated lysis of hypoxic melanoma cells [28].

Since a long time, bronchoalveolar lavage (BAL) is a tool used in the evaluation of inflammatory diseases of the lung. By BAL cells are washed out from lung lobes affected by an inflammatory/immune disease. Typing of lymphocytes allows to evaluate disease activity, impact of therapy, and in few diseases also the diagnosis of the disease [29–33]. In lung tumor BAL is most often used to collect tumor cells from peripheral tumors not otherwise accessible. However, this tool might be used to analyze also the percentages of immune cells in lung lobes bearing lung carcinomas.

References

1. Dall'Era M, Davis J. CTLA4Ig: a novel inhibitor of costimulation. Lupus. 2004;13:372–6.
2. Peggs KS, Quezada SA. PD-1 blockade: promoting endogenous anti-tumor immunity. Expert Rev Anticancer Ther. 2012;12:1279–82.
3. Velcheti V, Rimm DL, Schalper KA. Sarcomatoid lung carcinomas show high levels of programmed death ligand-1 (PD-L1). J Thorac Oncol. 2013;8:803–5.
4. Sznol M, Chen L. Antagonist antibodies to PD-1 and B7-H1 (PD-L1) in the treatment of advanced human cancer. Clin Cancer Res. 2013;19:1021–34.
5. Hamid O, Carvajal RD. Anti-programmed death-1 and anti-programmed death-ligand 1 antibodies in cancer therapy. Expert Opin Biol Ther. 2013;13:847–61.
6. Brahmer JR, Tykodi SS, Chow LQ, Hwu WJ, Topalian SL, Hwu P, Drake CG, Camacho LH, Kauh J, Odunsi K, Pitot HC, Hamid O, Bhatia S, Martins R, Eaton K, Chen S, Salay TM, Alaparthy S, Grosso JF, Korman AJ, Parker SM, Agrawal S, Goldberg SM, Pardoll DM, Gupta A, Wigginton JM. Safety and activity of anti-PD-L1 antibody in patients with advanced cancer. N Engl J Med. 2012;366:2455–65.
7. Topalian SL, Hodi FS, Brahmer JR, Gettinger SN, Smith DC, McDermott DF, Powderly JD, Carvajal RD, Sosman JA, Atkins MB, Leming PD, Spigel DR, Antonia SJ, Horn L, Drake CG, Pardoll DM, Chen L, Sharfman WH, Anders RA, Taube JM, McMiller TL, Xu H, Korman AJ, Jure-Kunkel M, Agrawal S, McDonald D, Kollia GD, Gupta A, Wigginton JM, Sznol M. Safety, activity, and immune correlates of anti-PD-1 antibody in cancer. N Engl J Med. 2012;366:2443–54.
8. Akbay EA, Koyama S, Carretero J, Altabef A, Tchaicha JH, Christensen CL, Mikse OR, Cherniack AD, Beauchamp EM, Pugh TJ, Wilkerson MD, Fecci PE, Butaney M, Reibel JB, Soucheray M, Cohoon TJ, Janne PA, Meyerson M, Hayes DN, Shapiro GI, Shimamura T, Sholl LM, Rodig SJ, Freeman GJ, Hammerman PS, Dranoff G, Wong KK. Activation of the PD-1 pathway contributes to immune escape in EGFR-driven lung tumors. Cancer Discov. 2013;3:1355–63.

9. Davies M. New modalities of cancer treatment for NSCLC: focus on immunotherapy. Cancer Manag Res. 2014;6:63–75.
10. Yang CY, Lin MW, Chang YL, Wu CT, Yang PC. Programmed cell death-ligand 1 expression in surgically resected stage I pulmonary adenocarcinoma and its correlation with driver mutations and clinical outcomes. Eur J Cancer. 2014;50:1361–9.
11. Ohaegbulam KC, Assal A, Lazar-Molnar E, Yao Y, Zang X. Human cancer immunotherapy with antibodies to the PD-1 and PD-L1 pathway. Trends Mol Med. 2015;21:24–33.
12. Pan ZK, Ye F, Wu X, An HX, Wu JX. Clinicopathological and prognostic significance of programmed cell death ligand1 (PD-L1) expression in patients with non-small cell lung cancer: a meta-analysis. J Thorac Dis. 2015;7:462–70.
13. Karachaliou N, Cao MG, Teixido C, Viteri S, Morales-Espinosa D, Santarpia M, Rosell R. Understanding the function and dysfunction of the immune system in lung cancer: the role of immune checkpoints. Cancer Biol Med. 2015;12:79–86.
14. Teixido C, Karachaliou N, Gonzalez-Cao M, Morales-Espinosa D, Rosell R. Assays for predicting and monitoring responses to lung cancer immunotherapy. Cancer Biol Med. 2015;12:87–95.
15. Ochoa CE, Mirabolfathinejad SG, Ruiz VA, Evans SE, Gagea M, Evans CM, Dickey BF, Moghaddam SJ. Interleukin 6, but not T helper 2 cytokines, promotes lung carcinogenesis. Cancer Prev Res (Phila). 2011;4:51–64.
16. Lu J, Lee-Gabel L, Nadeau MC, Ferencz TM, Soefje SA. Clinical evaluation of compounds targeting PD-1/PD-L1 pathway for cancer immunotherapy. J Oncol Pharm Pract. 2014;21:451–67.
17. O'Byrne K. Stimulating immune responses to fight cancer: basic biology and mechanisms. Asia Pac J Clin Oncol. 2015;11 Suppl 1:9–15.
18. Brahmer J, Reckamp KL, Baas P, Crino L, Eberhardt WE, Poddubskaya E, Antonia S, Pluzanski A, Vokes EE, Holgado E, Waterhouse D, Ready N, Gainor J, Aren Frontera O, Havel L, Steins M, Garassino MC, Aerts JG, Domine M, Paz-Ares L, Reck M, Baudelet C, Harbison CT, Lestini B, Spigel DR. Nivolumab versus docetaxel in advanced squamous-cell non-small-cell lung cancer. N Engl J Med. 2015;373:123–35.
19. Enk AH. Dendritic cells in tolerance induction. Immunol Lett. 2005;99:8–11.
20. Liu Q, Zhang C, Sun A, Zheng Y, Wang L, Cao X. Tumor-educated CD11bhighIalow regulatory dendritic cells suppress T cell response through arginase I. J Immunol. 2009;182:6207–16.
21. Suzuki K, Sun R, Origuchi M, Kanehira M, Takahata T, Itoh J, Umezawa A, Kijima H, Fukuda S, Saijo Y. Mesenchymal stromal cells promote tumor growth through the enhancement of neovascularization. Mol Med. 2011;17:579–87.
22. Yoshimura A. Signal transduction of inflammatory cytokines and tumor development. Cancer Sci. 2006;97:439–47.
23. Wang YC, He F, Feng F, Liu XW, Dong GY, Qin HY, Hu XB, Zheng MH, Liang L, Feng L, Liang YM, Han H. Notch signaling determines the M1 versus M2 polarization of macrophages in antitumor immune responses. Cancer Res. 2010;70:4840–9.
24. Wu H, Shang LQ, Chen RL, Yang SM, Wang SL, Wang J, Sun G. Significance of trask protein interactions in brain metastatic cohorts of lung cancers. Tumour Biol. 2015;36:4181–7.
25. Wang Y, Sparwasser T, Figlin R, Kim HL. Foxp3+ T cells inhibit antitumor immune memory modulated by mTOR inhibition. Cancer Res. 2014;74:2217–28.
26. Kim PS, Jochems C, Grenga I, Donahue RN, Tsang KY, Gulley JL, Schlom J, Farsaci B. Pan-Bcl-2 inhibitor, GX15-070 (obatoclax), decreases human T regulatory lymphocytes while preserving effector T lymphocytes: a rationale for its use in combination immunotherapy. J Immunol. 2014;192:2622–33.
27. Schlie K, Spowart JE, Hughson LR, Townsend KN, Lum JJ. When cells suffocate: autophagy in cancer and immune cells under low oxygen. Int J Cell Biol. 2011;2011:470597.
28. Tittarelli A, Janji B, Van Moer K, Noman MZ, Chouaib S. The selective degradation of synaptic connexin 43 protein by hypoxia-induced autophagy impairs natural killer cell-mediated tumor cell killing. J Biol Chem. 2015;290:23670–9.
29. Popper H, Pongratz M. Value and indications for bronchoalveolar lavage combined with transbronchial lung biopsy. Wien Klin Wochenschr. 1987;99:848–55.
30. Robinson PC, Watters LC, King TE, Mason RJ. Idiopathic pulmonary fibrosis. Abnormalities in bronchoalveolar lavage fluid phospholipids. Am Rev Respir Dis. 1988;137:585–91.
31. Oshima M, Maeda A, Ishioka S, Hiyama K, Yamakido M. Expression of C-C chemokines in bronchoalveolar lavage cells from patients with granulomatous lung diseases. Lung. 1999;177:229–40.
32. Magi B, Bini L, Perari MG, Fossi A, Sanchez JC, Hochstrasser D, Paesano S, Raggiaschi R, Santucci A, Pallini V, Rottoli P. Bronchoalveolar lavage fluid protein composition in patients with sarcoidosis and idiopathic pulmonary fibrosis: a two-dimensional electrophoretic study. Electrophoresis. 2002;23:3434–44.
33. Bozinovski S, Jones JE, Vlahos R, Hamilton JA, Anderson GP. Granulocyte/macrophage-colony-stimulating factor (GM-CSF) regulates lung innate immunity to lipopolysaccharide through Akt/Erk activation of NFkappa B and AP-1 in vivo. J Biol Chem. 2002;277:42808–14.

Diseases of the Pleura 21

21.1 Hemorrhage

Hematothorax in most cases is caused by an injury such as street accidents. Either one side or both pleural cavities are filled with blood. The pleura is smooth and shiny.

21.2 Effusion

Pleural effusion is a common event caused by various underlying diseases. In general transudation should be clearly separated from exudation. The first is an equivalent of lung edema, whereas exudation is an inflammation-associated accumulation of fluid in the pleural cavity.

A transudate is a water clear fluid, composed of water, electrolytes, low molecular weight peptides, and proteins, essential in a similar composition as plasma. The underlying causes are heart diseases with low ejection fraction, albuminemia, renal insufficiency, and some rare conditions. A bilateral pleural transudate can cause compression of the lung, resulting in hypoxemia, which can aggravate a heart disease. The main therapy is to treat the underlying disease.

An exudate is caused by any kind of pneumonia with concomitant pleuritis. The exudate can show different colors from yellow in purulent inflammation to red in hemorrhagic pleuritis. Within the exudate, the protein fraction is increased, also higher molecular weight proteins are present, and fibrin clots might be seen.

21.3 Inflammation: Pleuritis

Pleuritis is in almost all cases induced by an underlying pneumonia. Rarely pleuritis is induced by inflammatory processes in the mediastinum of processes within the thoracic wall. In contrast to pneumonia, pleuritis always causes pain when breathing. An exudate is present in most cases.

Fibrinous pleuritis is the most common form of pleuritis. Viral- and bacterial-induced pneumonias will show a fibrinous pleuritis at the beginning and also localized to the areas of the underlying pneumonia. In viral infections, hemorrhage can occur later on, leading to fibrinous-hemorrhagic pleuritis. Fibrin forms fine nets on the surface of the pleura, which is no longer shiny, and caused by respiration, the fibrin is condensed to wavelike structures. Within the pleura and at the surface, there are scattered neutrophilic granulocytes and lymphocytes. The mesothelium is most often denuded. Besides infections, toxins from the circulation cause fibrinous and fibrinous-hemorrhagic pleuritis. An endogenous cause is uremia, where uremic acid and urea are taken up by the mesothelial cells and secreted into the pleural cavity. Exogenous causes are toxins coming from inhaled toxins but also from metabolites from drugs, such as cytotoxic drugs.

21.3.1 Purulent Pleuritis

In purulent pleuritis, neutrophils predominate within the pleura as well as at the surface, and a

© Springer-Verlag Berlin Heidelberg 2017
H. Popper, *Pathology of Lung Disease*, DOI 10.1007/978-3-662-50491-8_21

lot of debris is within the pleural cavity, altogether forming the purulent exudate. Often in bacterial infection, the inflammation is mixed fibrinous-purulent.

21.3.2 Hemorrhagic Pleuritis

Hemorrhagic pleuritis is caused by endogenous toxins such as urea and uremic acid, by metabolites of cytotoxic drugs, as well as by viral infections. A rare cause is autoimmune disease, as systemic lupus erythematosus and autoimmune hemolytic anemia. At the surface as well as within the pleura, bleeding is seen, centered on small blood vessels. In SLE also neutrophils are encountered, and emperipolesis can be seen (lupus phenomenon).

21.3.3 Chronic Pleuritis

In chronic pleuritis, the exudate is organized by a granulation tissue (Fig. 21.1). Newly formed blood vessels are growing perpendicular toward the surface. At the surface, debris is still seen, either fibrinous-purulent or fibrinous-hemorrhagic, mixed with leukocytes. Accompanying the blood vessels, undifferentiated mesenchymal cells and fibroblasts can be seen, which can exhibit marked reactive atypia (Fig. 21.2). From the basal layer of the pleura, fibrosis starts. In this state, the granulation tissue with fibrosis can mimic sarcomatoid mesothelioma, especially the desmoplastic form. In addition the mesenchymal cells can express pan-cytokeratin, which makes this differentiation even more complicated. The major criteria for this reactive proliferation are:

(a) Collagen deposition is ordered in parallel to the surface (Fig. 21.2a, b); this organization starts from the basis and extend toward the surface – in mesothelioma, there is no ordered collagen deposition; the bundles are disoriented.
(b) Atypia of the mesenchymal cells is more pronounced in reactive proliferating pleuritis compared to mesothelioma (Fig. 21.2c, d); in mesothelioma, the cells are more uniform.
(c) Necrosis is uncommon in proliferating pleuritis, but common in mesothelioma.
(d) Mitosis is infrequent in proliferating pleuritis and MIB1-positive cells are scarce, whereas this is higher in mesothelioma; be aware of positivity for MIB1 by the lymphocytes.
(e) In case the underlying fat tissue is present, invasion of mesothelioma cells is the most reliable feature to differentiate it from reactive proliferating pleuritis, which will stop at the pleura-fat interphase.

Granulomatous pleuritis is seen in many infectious epithelioid cell pneumonias, such as tuberculosis, mycobacteriosis, and rare bacterial infections (as discussed in the pneumonia chapter). A common epithelioid cell granulomatous pleuritis is found in sarcoidosis. Within the pleura, confluent epithelioid cell granulomas are encountered. When a necrotic center is present, this is usually caused by an infection. Exudate in granulomatous pleuritis is not always seen.

Hyalinosis or hyaline plaques are frequently seen in the pleura. Hyaline can be focal and even can form bizarre structures (Fig. 21.3) or is found symmetrically on both sides, which should cause a careful investigation for exposure to asbestos fibers (Fig. 21.4).

21.4 Tumors

A few primary benign and malignant tumors do occur in the pleura: malignant mesothelioma, solitary fibrous tumor (fibrohistiocytic tumor of the pleura), calcifying pleuratumor, desmoid tumor, adenomatoid tumor, cystic mesothelioma, and very rarely primary squamous cell carcinoma as well as fibrosarcoma of the pleura. Pleuropulmonary blastoma can occur as a primary tumor of the pleura, but also in the lung, and has been discussed in the lung tumor chapter.

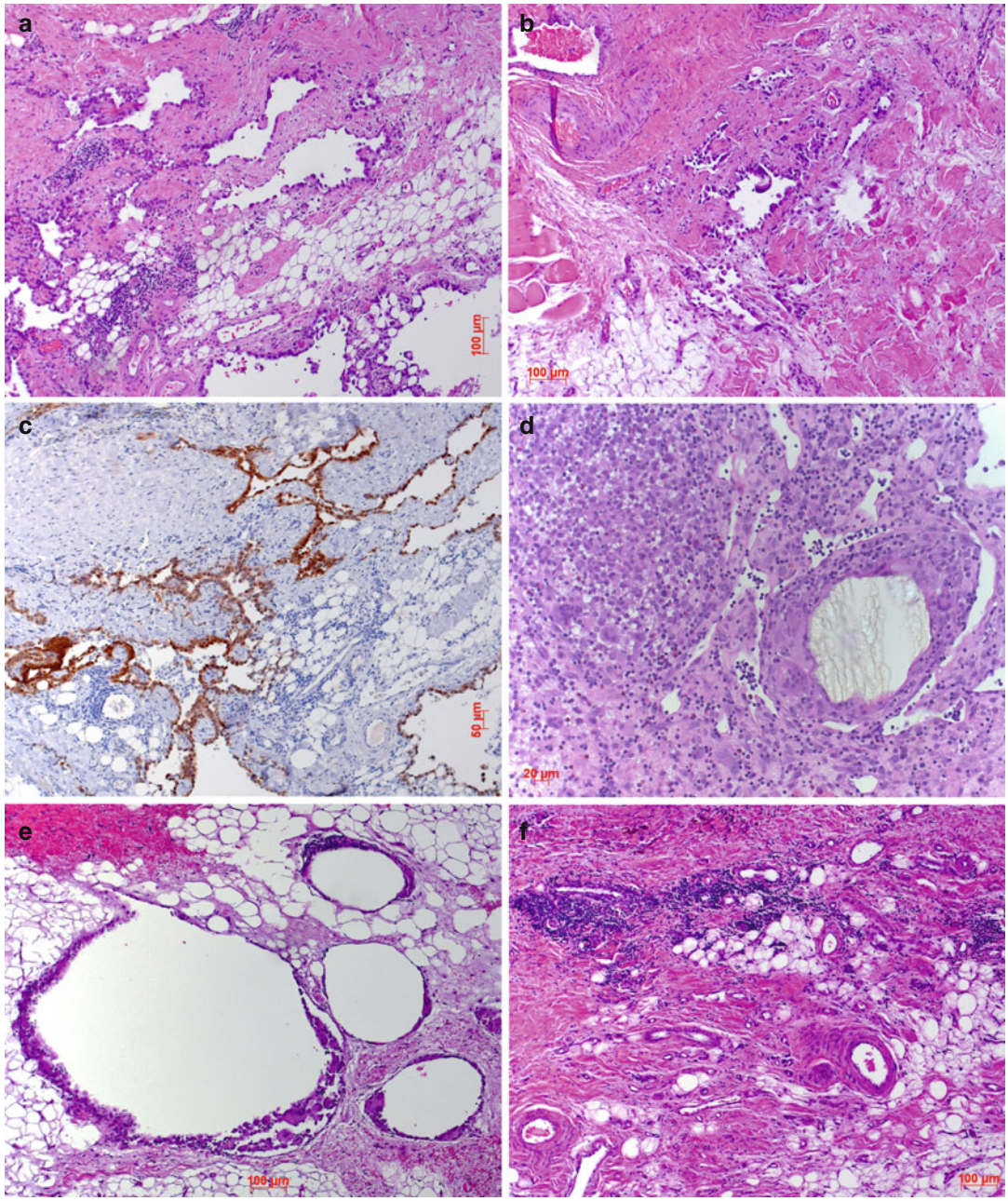

Fig. 21.1 In (**a**, **b**) chronic pleuritis is associated with inclusions of mesothelial cells forming small cystic spaces. This is most often seen after a trauma or recurrent pleuritis. In (**c**) an immunohistochemical stain will not solve the problem, as calretinin will be positive in mesothelial cells. (**d**) Shows a recurrent pleuritis with polarizing material within foreign body giant cells. In (**e**) a foreign body reaction is seen in a cystic structure, a so-called oil cyst after trauma of the fat tissue with necrosis. (**f**) Shows a classical chronic pleuritis. H&E, immunohistochemistry for calretinin, bars 100, 50, 20 µm

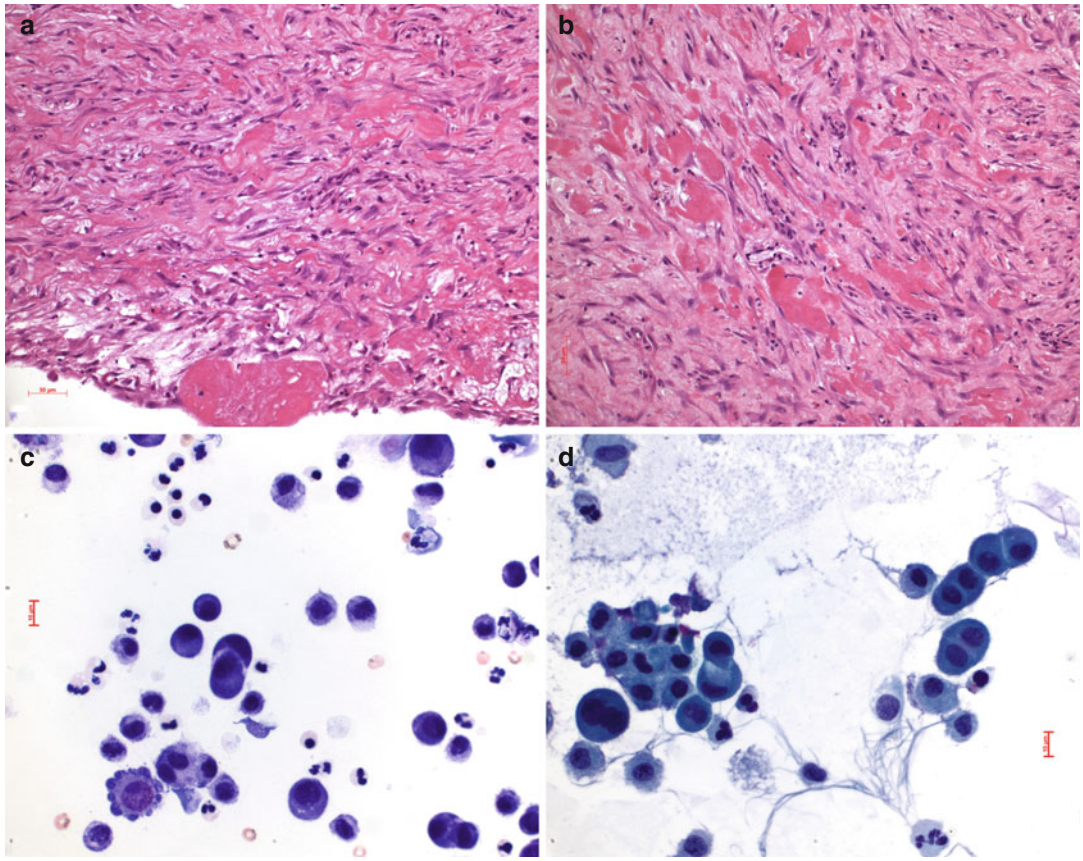

Fig. 21.2 (**a**, **b**) Reactive proliferation of mesenchymal cells in the pleura. Note the parallel orientation of the cells in (**a**) and lots of fibrin between the cells in (**b**). (**c**, **d**) Reactive atypia of mesothelial cells can mimic tumor cells. The nature of mesothelial cells is evident by the long microvilli, which are clearly visible in (**d**), whereas the rosette formed by a mesothelial cell with nuclear debris seen in (**c**) is a sign of a reactive process. H&E, Giemsa, PAP, bars 50 and 10 μm

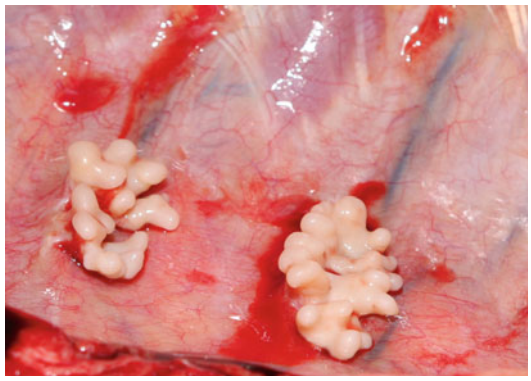

Fig. 21.3 Localized hyaline found at autopsy. Probably a remnant after recurrent exudation

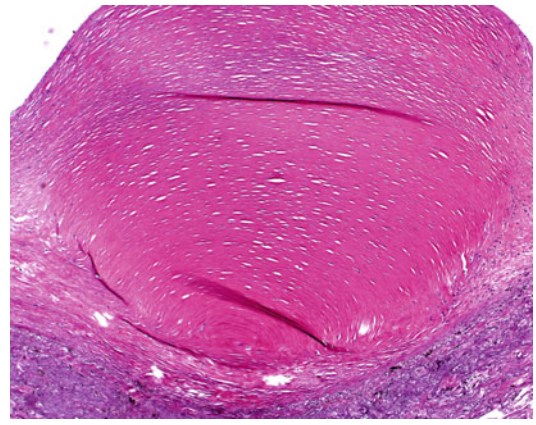

Fig. 21.4 Multiple hyaline nodules and plaques should cause a careful investigation for asbestos exposure. Here collagen bundles form a concentric nodule. A few scattered cells can be found within this nodule. H&E, X25

21.4.1 Mesothelioma

21.4.1.1 Epidemiology

Malignant mesothelioma is caused in more than 80 % by chronic exposure to asbestos fibers. There is a dose-exposure time relationship: a high dose will result in a mesothelioma within 3–5 years, whereas a medium to medium-low dose will cause mesothelioma only if there is a long duration of exposure [1]. The latency period in these cases can be up to 35 years after cessation of exposure. Different types of asbestos fibers also show differences in the required accumulative dose until mesothelioma development starts [2–6].

There are rare familial cases, for which recently BAP1 gene alteration has been found as a possible cause [7, 8].

Other possible causes are radiation and other inhaled carcinogenic fibers including manmade fibers, SV40 viral antigen, and erionite [6, 9–14]. The contribution of SV40 is controversially discussed, as there are arguments for and against its role in inducing mesothelioma [15–21]. From these investigations and discussions, it is likely that SV40 plays a role as a cocarcinogen, enhancing the development of asbestos fiber-induced mesothelioma [10, 11, 22]. For a more detailed discussion, the reader is referred to the article by Roggli et al. summarizing the current understanding on the epidemiology of mesothelioma and asbestosis [23].

Erionite has gained much interest in the past, because in some villages in Anatolia, Turkey, mesothelioma occurred with high frequency. Even immigrants from these villages presented with mesothelioma after exposure cessation. In the meanwhile, it has been shown that erionite can induce mesothelioma with high penetrance; however, also some genetic abnormalities might be involved too [9, 24–31].

21.4.1.2 Clinical and Radiological Findings

Recurrent pleural effusion is the most common clinical sign of mesothelioma. As a rule recurrence of the effusion within 3 months should raise the suspicion of mesothelioma. Resulting from effusion atelectasis of the lung will cause hypoxia. On X-ray and CT scan, effusion and thickening of the pleura or pleural nodules are the prominent findings. On CT invasion of the chest wall can be seen in advanced disease.

21.4.1.3 Gross Morphology

Mesothelioma usually starts from the parietal pleura forming multiple firm white nodules, which later on form white dense plaques. In this stage, mesothelioma might be indistinguishable from pleural metastasis. In late stages, the visceral pleura is involved too and the whole lung can be encased by the tumor (Fig. 21.5). Mesothelioma tends to primarily spread along the lobar fissures and interlobular septa, but invades the lung in late stages. This is usually the gross picture seen at autopsy or sometimes on resection specimen (pleuropneumonectomy). There are few cases of lung carcinomas, which might spread to the pleura in a similar way causing the impression of pseudomesotheliomatous metastasis.

Fig. 21.5 Mesothelioma, the upper example, is from autopsy cases showing almost complete encasement of the lung by the mesothelioma. The lower example is a resection specimen; the tumor involves parietal as well as visceral pleura

21.4.1.4 Histology

Malignant mesothelioma comes in three forms: epithelioid, mixed biphasic, or sarcomatoid mesothelioma. These varieties also carry different prognoses; sarcomatoid variant has the worst prognosis of an average of 6–8 months survival after diagnosis. Epithelioid mesotheliomas can mimic almost every other tumor: most often epithelioid mesotheliomas will present as tubulo-papillary tumors with abundant acid mucopolysaccharides, positively stained by PAS and Alcian blue. They sometimes form slit-like spaces resembling normal mesothelial structures. On the surface, well-differentiated mesothelioma will form papillae, garland-like rows of cells connecting papillae (Fig. 21.6).

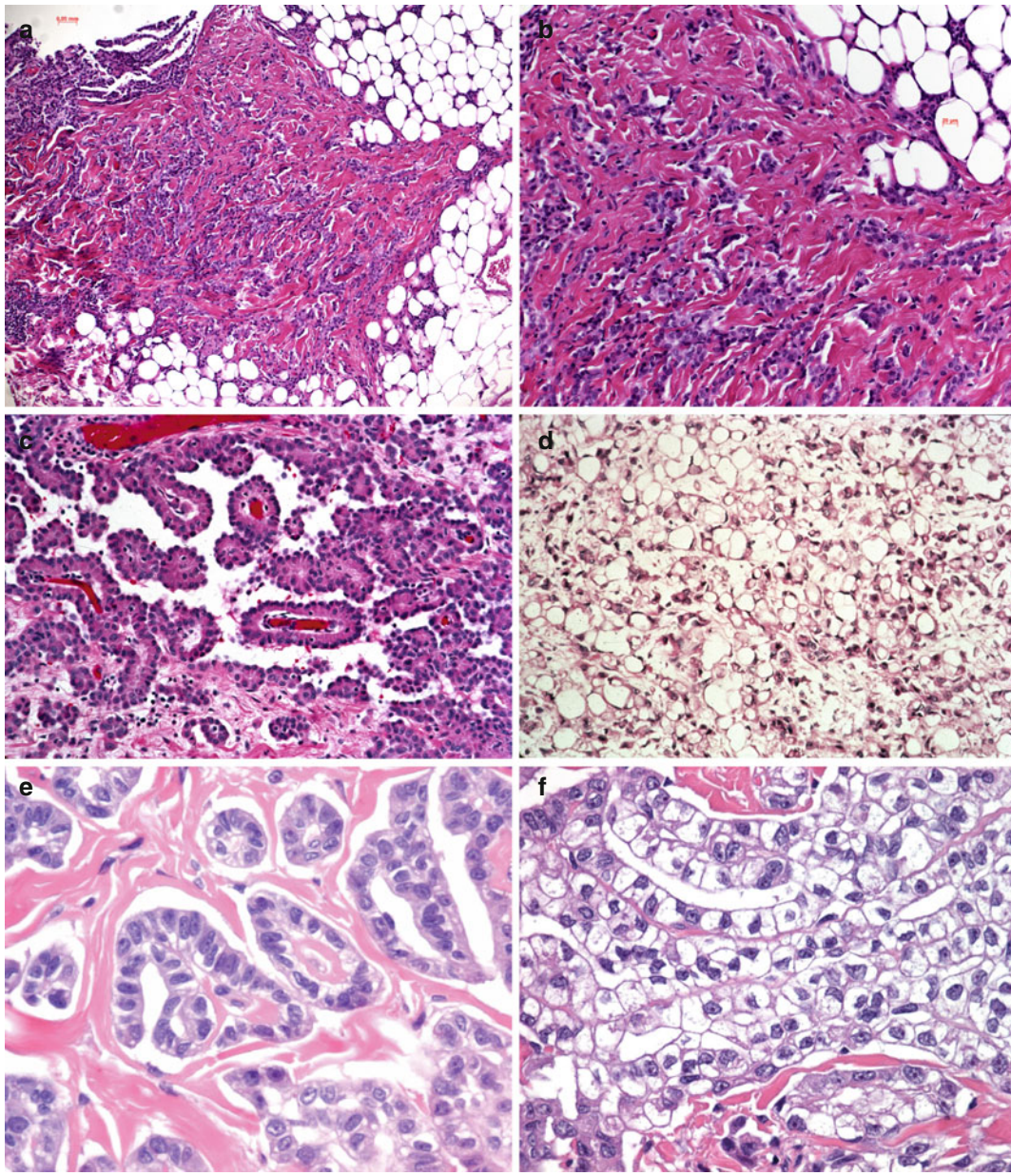

Fig. 21.6 Epithelioid mesothelioma with different patterns: (**a**, **b**) classical pattern with slit-like spaces, (**c**) papillary pattern, (**d**) adenomatoid pattern, (**e**) acinar pattern, (**f**) clear cell pattern, (**g**) deciduoid pattern, (**h**) acinar and solid pattern, (**i**) solid pattern

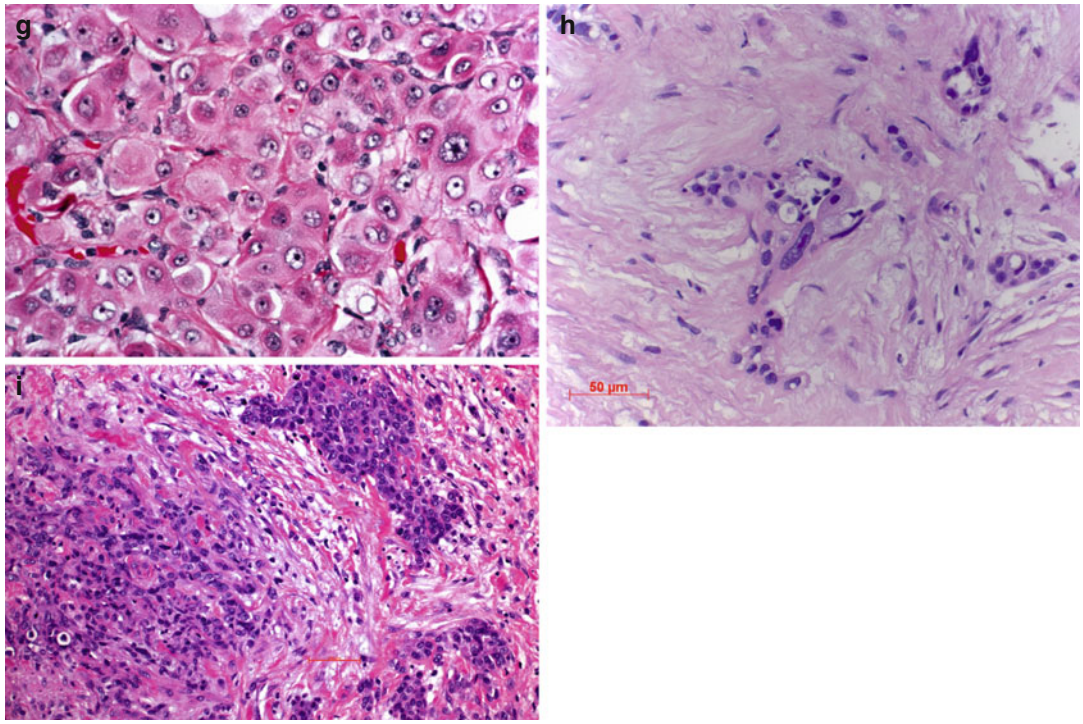

Fig. 21.6 (continued)

By electron microscopy but also in cytological specimen, long microvilli can be seen (Figs. 21.7, 21.8, and 21.9). However, these are not the mesotheliomas, which cause diagnostic problems. It is the variation of structures and patterns, which mesothelioma can form. Epithelioid mesotheliomas can be papillary, acinar, solid, deciduoid, and clear cell. They can mimic pulmonary adenocarcinomas, metastasis from ovarian cystadenocarcinomas, breast carcinomas, and ductal as well as lobular, renal clear cell carcinomas, just to name a few. The sarcomatoid mesotheliomas most often present as a spindle cell proliferation; can be embedded in an inflammatory background (inflammatory sarcomatoid mesothelioma), almost obscuring the tumor cells; and can be pleomorphic like true sarcomas (pleomorphic sarcomatoid mesothelioma). There are even rare forms of mesotheliomas, where the sarcomatoid component simulates an osteosarcoma with osteoid formation. A hard to diagnose sarcomatoid mesothelioma variant is desmoplastic mesothelioma, because tumor cells are scarce and hidden within a fibrous and hyalinized matrix (Fig. 21.10). In mixed mesotheliomas, a combination of epithelioid and sarcomatoid components is present.

21.4.1.5 Variants

Well-Differentiated Papillary Mesothelioma

WDPM is a rare variant, which does have a favorable course, even when it is focally microinvasive. WDPM does occur in the pleura, peritoneum, and serous cavities of the genital tract, the pleura being the most rare location. Most often this tumor is found in young woman in the peritoneal cavity or associated in the serosa of the female

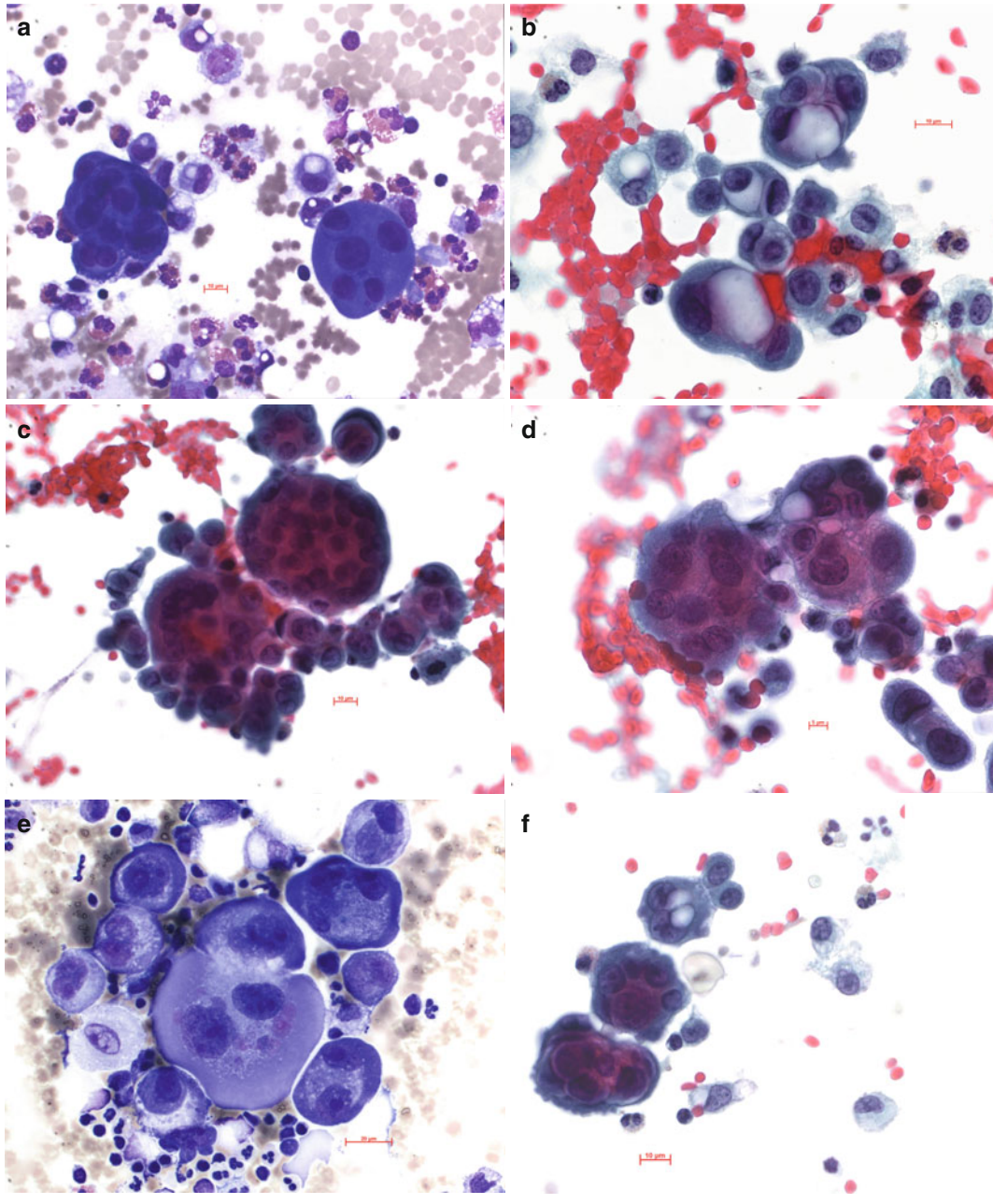

Fig. 21.7 Cytology of epithelioid mesothelioma: the cells form three-dimensional complexes as seen in (**a**, **c**) and can show cytoplasmic vacuoles with mucin as in (**b**, **d**); most important is to look for microvilli, which can be seen in good cytological preparations as (**e**, **f**). Giemsa, PAP, H&E, bars 20, 10, 5 μm

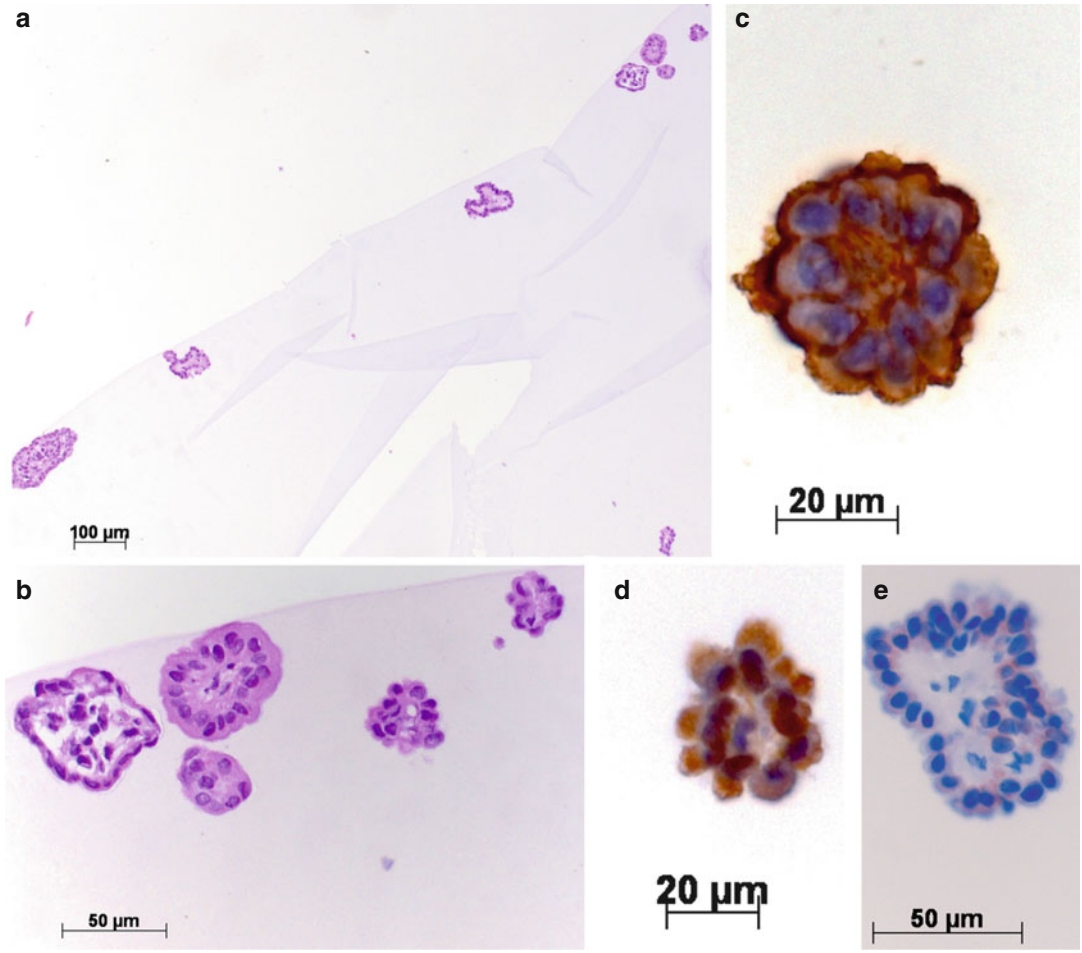

Fig. 21.8 Mesothelioma diagnosis using cytoblock preparations, which allow several immunohistochemical stains to be performed. (**a**, **b**) H&E histology, (**c**) podoplanin, (**d**) WT1, (**e**) cytokeratin 5/6. Bars 100, 50, 20 µm

genital tract (Fig. 21.11). Asbestos exposure is seen in some cases but also patients without asbestos exposure can present with this tumor. In the majority of cases, the outcome is favorable. However, recurrence and in a few cases a fatal outcome can occur [32]. Recurrence and fatal outcome are related to invasive foci and multifocality [33].

WDPM is defined by a single row of mesothelial cells with uniform nuclei, sometimes bland looking, covering stroma papillae. Tumors can show back-to-back papillae, a pattern mimicking invasion but discernible on pan-keratin stain as compressive crowding. True invasive patterns ranged from simple bland-appearing glands invading the stalks of the papillae to solid foci of invasive tumor. These cases usually present with higher cytological grade. The tumor is positive for pan-cytokeratin but negative for p16 deletion.

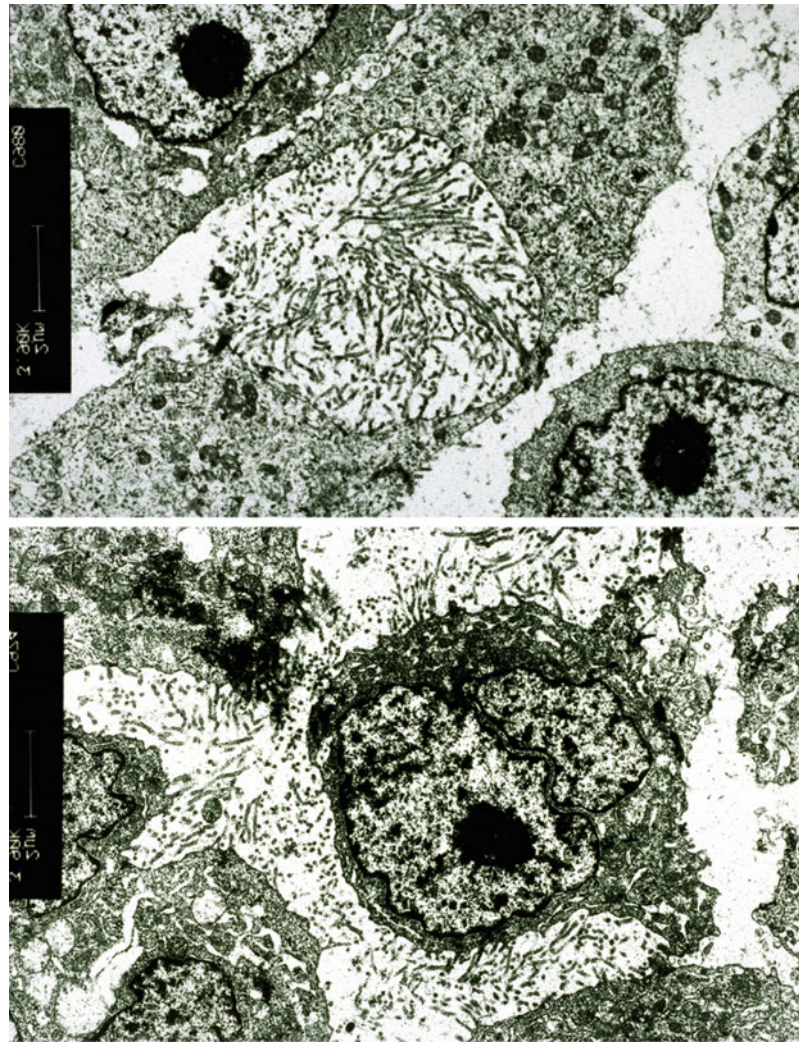

Fig. 21.9 Well-differentiated epithelioid mesothelioma on electron microscopy: note the long slender microvilli, which are not seen in other epithelial malignancies. Bars 5 nm

Localized Mesothelioma

This mesothelioma presents as a solitary mass at the pleura and might be clinically and radiologically misdiagnosed as metastasis (Fig. 21.12).

21.4.1.6 Diagnosis: Differential Diagnosis

Due to the wide variation of patterns, the diagnosis of malignant mesothelioma need to be confirmed by immunohistochemical stains. Many different schemas are currently used; however, a few antibodies have proven to be most reliable: a positive reaction for calretinin, podoplanin, cytokeratin 5/6, vimentin, and thrombomodulin and a negative reaction for monoclonal CEA. Claudin4 and BerEP4 are useful to confirm the diagnosis of malignant epithelioid mesothelioma (Fig. 21.13). As a recommendation, one should use those sets of antibodies, which reliably and reproducibly work in the laboratory. Do not switch to new published antibodies unless these have been validated in several studies against several of the mimickers of mesothelioma.

By cytology the diagnosis is possible, but should not be made straight forward: if there is

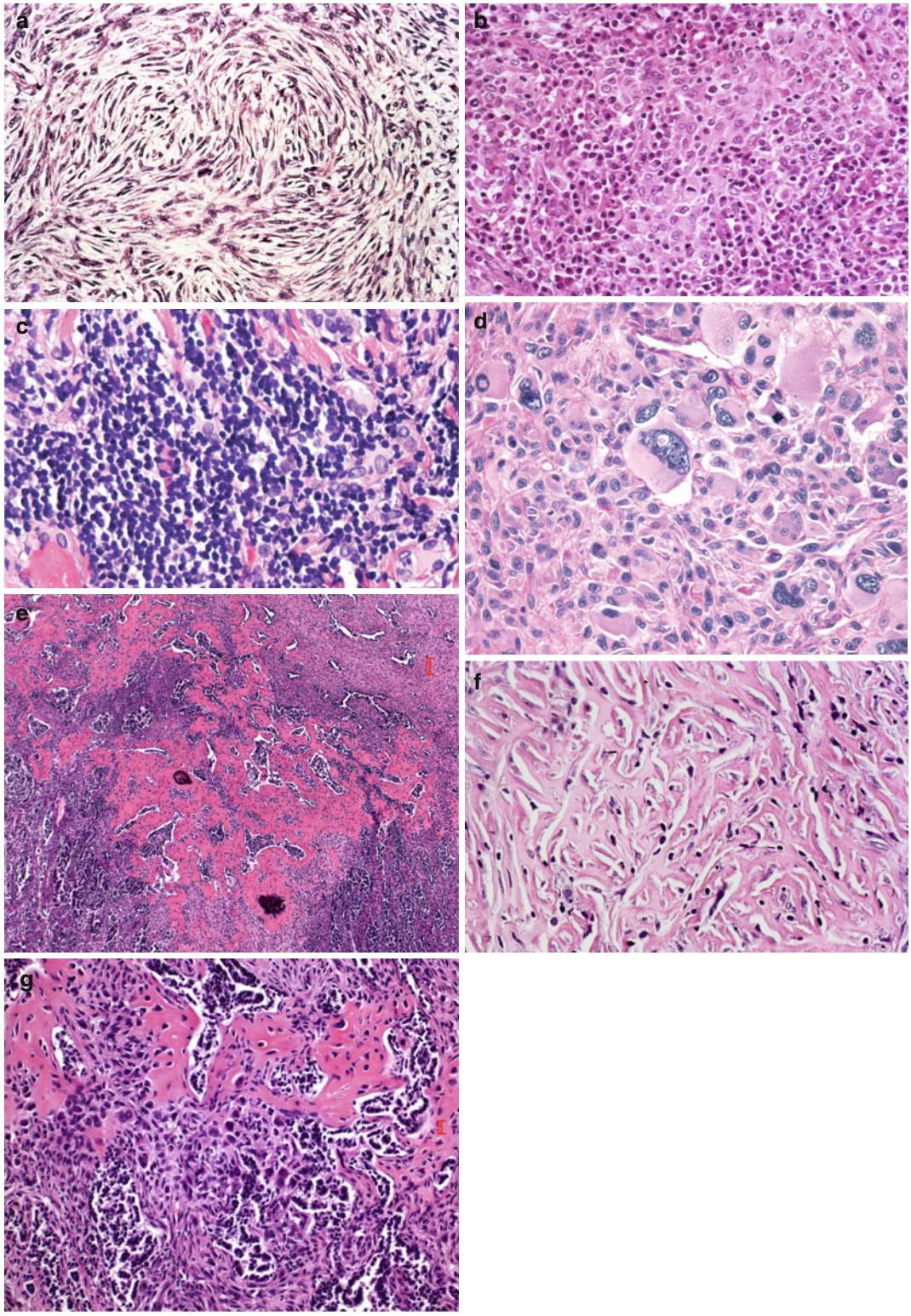

Fig. 21.10 Sarcomatoid mesothelioma variants: (**a**) spindle cell pattern, (**b**) histiocytic pattern, (**c**) inflammatory pattern with scattered histiocyte-like cells, (**d**) pleomorphic pattern, (**e**, **f**) mesothelioma with osteosarcoma component, (**g**) desmoplastic pattern. H&E, ×50, 100, 200, 400

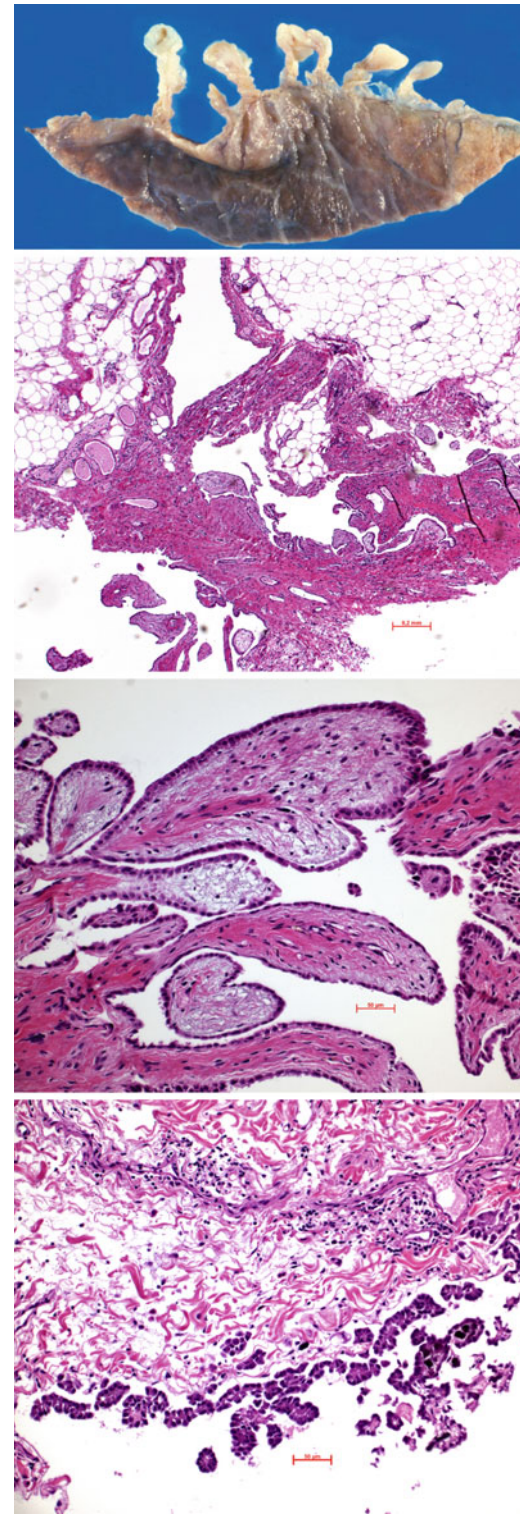

Fig. 21.11 Well-differentiated papillary mesothelioma. From top to bottom: macroscopic appearance of WDPM (Courtesy Philip Cagle) and overview and higher magnification of a case showing a single row of bland-looking mesothelial cells covering a fibrous stroma; second case (*bottom*) with some epithelial papillae in a case with recurrence, but no invasion. H&E, bars 200 and 50 μm (Courtesy Philip Cagle, Houston)

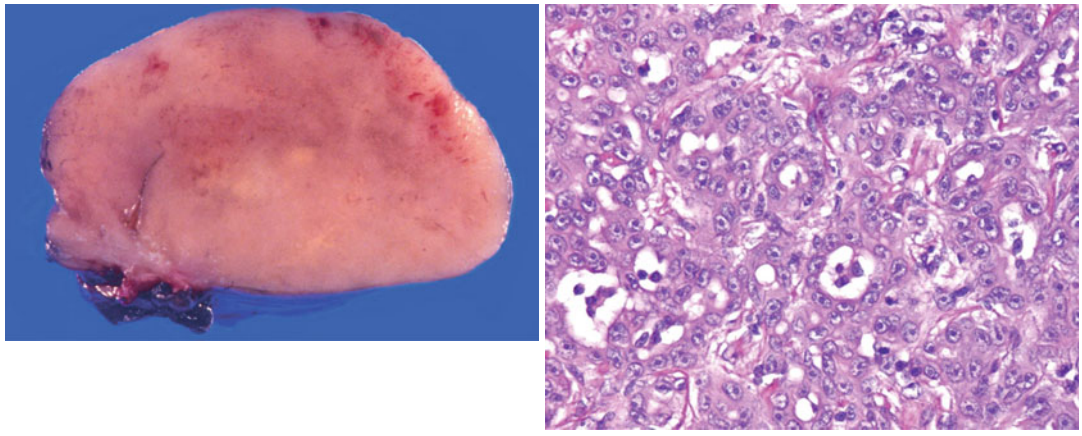

Fig. 21.12 Localized mesothelioma, *left*: macroscopic appearance of such a tumor, which in contrast to solitary fibrous tumor is soft. *Right*: histology shows an acinar and solid mesothelioma with high-grade atypia. H&E, ×400 (Courtesy of Philip Cagle)

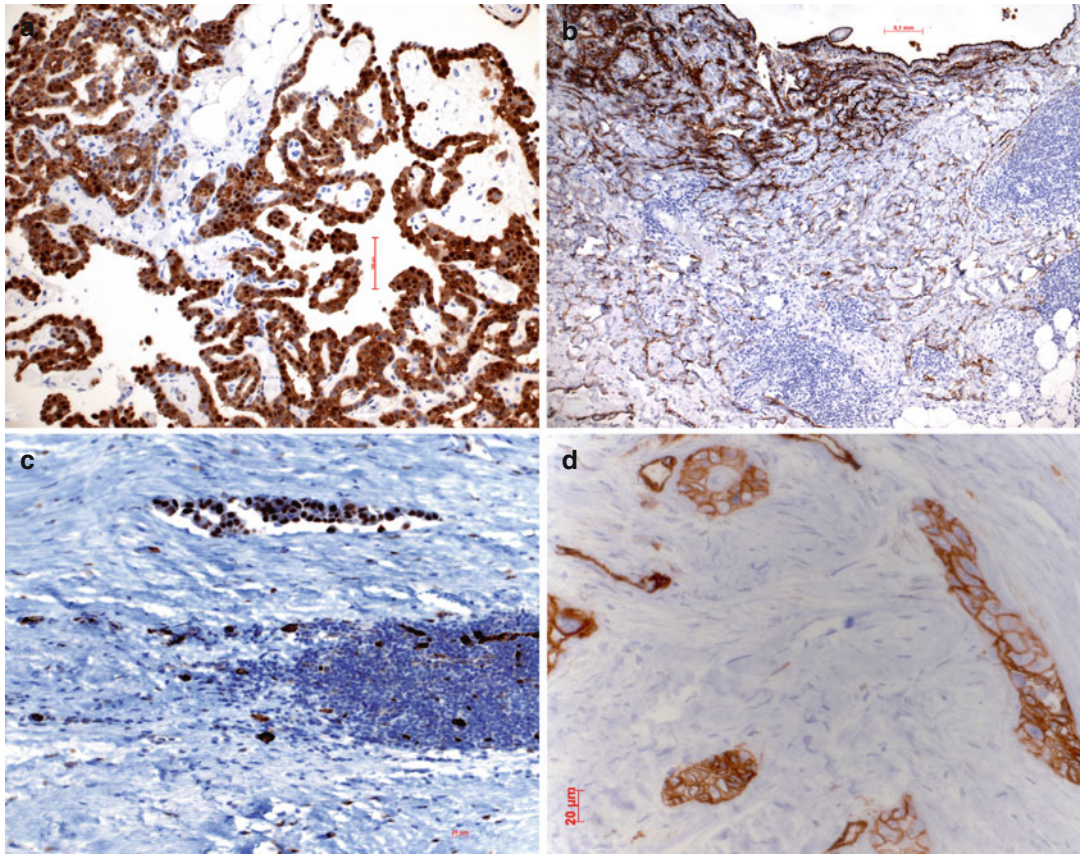

Fig. 21.13 Immunohistochemistry for mesothelioma diagnosis: (**a**) calretinin, (**b**) podoplanin, (**c**) WT1, (**d**) CD146, (**e**) cytokeratin 7, (**f**) thrombomodulin, (**g**) cytokeratin 5/6, bars 200, 100, 50, 20 µm

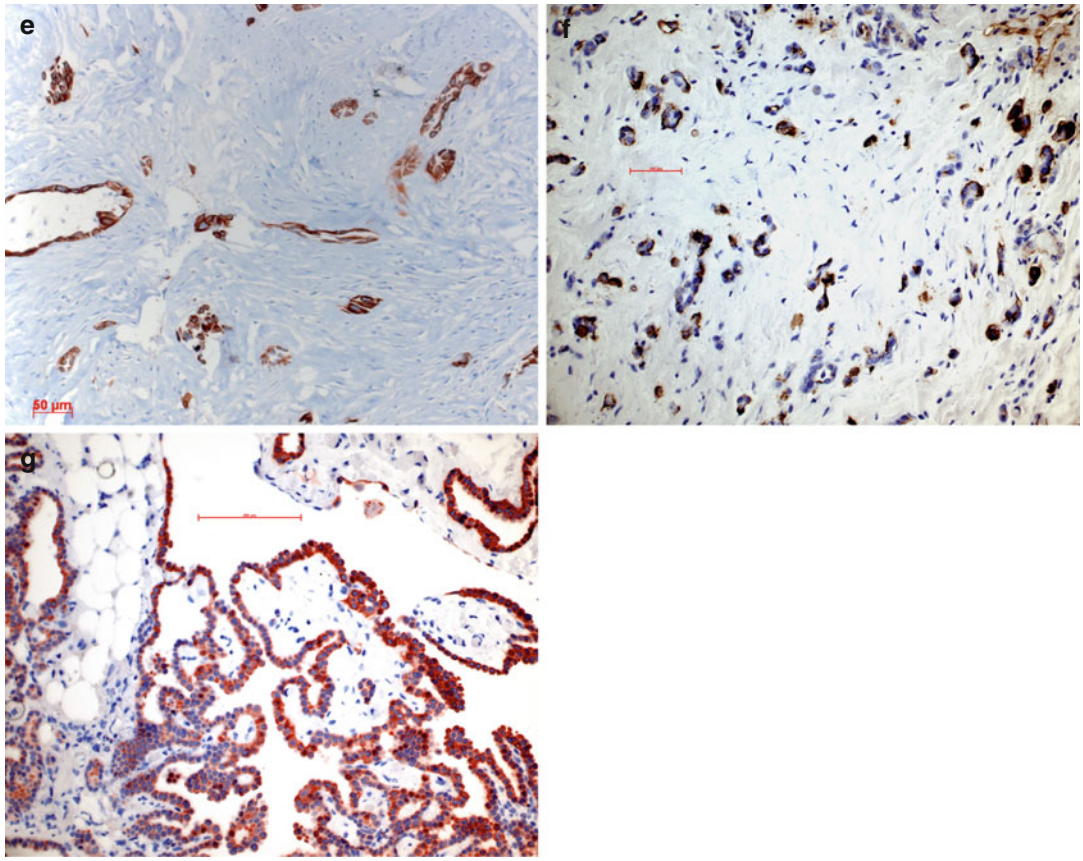

Fig. 21.13 (continued)

Table 21.1 Immunohistochemical markers for the differentiation of mesothelioma versus the most common epithelial metastasis

	CK 5/6	Calretinin	Podoplanin	Thrombomodulin	BerEP4	CEA	MFG1/2	Vim	WT1
Mesothelioma, epithelioid	+	+	+	F+ (spindle cells)	–	–	–	±	+ Nuclear
Adenocarcinoma lung	–	–	–	–	+	±	±	–	–
Breast	–	–	–	–	+	±	+/+	–	–
Ovary	–	± is often pos in cytoplasm	±	–	+	+	–/+	–	±
Kidney	–	–	–	±	+	?	–/–	±	–

recurrent effusion and atypical cells are found, I would make a tentative diagnosis of malignant mesothelioma. Immunocytochemistry can be done, preferentially using cell block techniques (Table 21.1).

Besides the commonly used markers for the differentiation of lung and breast adenocarcinomas versus mesotheliomas, the antibodies' panel might be adapted according to the question addressed. A comprehensive review on marker

expression can be found in the articles by N. Ordonez [34–39].

In sarcomatoid mesothelioma, the use of immunohistochemistry is less helpful, as there are no specific markers for mesothelioma. Most sarcomatoid mesotheliomas will express pan-cytokeratin, which is the most useful marker. In cases of coexpression of pan-cytokeratin and vimentin, this constellation is quite specific for malignant sarcomatoid mesothelioma. Calretinin is often negative, thrombomodulin and WT1 are positive in some sarcomatoid mesotheliomas, whereas podoplanin is most often negative. The negative markers as they are focused on epithelial differentiation are useless.

21.4.1.7 The Hyperplasia-Dysplasia-In Situ Mesothelioma-Mesothelioma Sequence

Due to the long latency period of developing mesotheliomas, there are well-documented precursor lesions. Hyperplasia of the mesothelium is the earliest event to be seen on biopsies; however, this is unspecific. Hyperplasia does occur in regeneration after infectious pleuritis. There have been some attempts to better separate regenerative hyperplasia from hyperplasia in developing mesothelioma: in the study by Attanoos et al., desmin and EMA were reported to be most useful in distinguishing benign from malignant mesothelial proliferations, where desmin was preferentially expressed in reactive mesothelium and EMA in neoplastic mesothelium. Immunohistochemical detection of mutated p53 was less useful, but may be used as a second-line marker of neoplastic mesothelium [40]. In the study by Zimmerman, the use of a chromosome 17α probes turned out as another marker for mesothelioma, showing an average CI of 2.23 with less than 44 % diploid nuclei and 50 % of specimens exhibited bizarre signals [41]. In my own experience as well as in two studies, CD146 turned out to be a reliable marker differentiating reactive from malignant mesothelial proliferations [42, 43]. Mesothelioma in situ was used by David Henderson, but usually in the setting adjacent to an already invasive mesothelioma. In situ mesothelioma is defined as an atypical mesothelial proliferation at the pleural surface without invasion into deeper layers (Fig. 21.14). These mesotheliomas in situ may have abundant myxoid stroma and protrude from the surface as small nodular lesions. It is still debated if one should use this term in cases where invasion is absent. Many pathologists use instead the term atypical mesothelial proliferation and ask for additional biopsies. In any case, either mesothelioma in situ or atypical mesothelial proliferation should not cause surgical intervention.

21.4.1.8 Molecular Biology

From several studies, it is well established that asbestos fibers first stick to the small bronchi and bronchioles causing chronic inflammation. Fibers

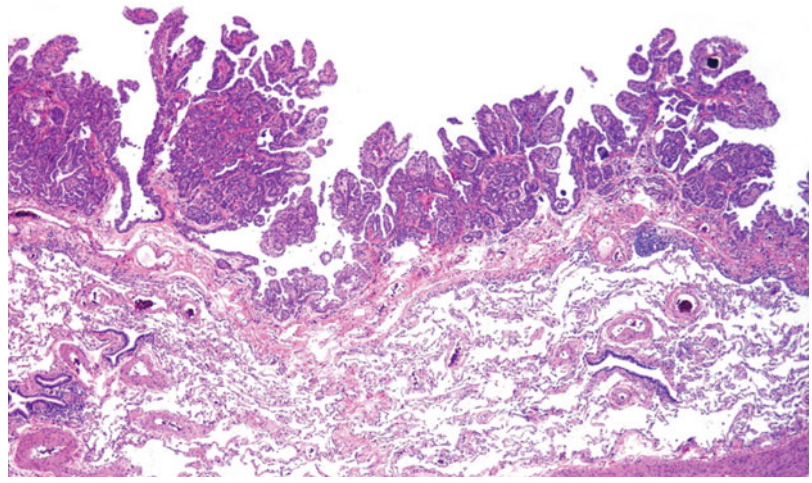

Fig. 21.14 In situ mesothelioma. The proliferation is confined to the surface of the pleura; no invasion is seen. The tumor forms papillary projections into the pleural cavity. In those cases where no invasive mesothelioma is present, one should request rebiopsy or use the term atypical mesothelioma proliferation of uncertain dignity to avoid overtreatment. H&E, X50 (Courtesy Philip Cagle)

transverse the bronchial walls and move through the lung by the respiration movement and finally reach the pleura, where these fibers are deposited, again causing chronic inflammation and damage to the mesothelium but also to the mesenchymal cells of the deeper pleural layer. By recurrent inflammation, aberrations of the DNA occur. Despite this knowledge, the molecular biology of mesothelioma is still not understood. There are many studies focusing on single genes, chromosomal aberrations, mechanisms by miRNA, and also posttranslational protein modifications. Unfortunately none of these studies could be repeated and verified by other studies, leaving many different gene modifications, but no common genetic alterations for a majority of mesothelioma cases.

21.4.1.9 Chromosomal Abnormalities

Several studies have focused on chromosomal abnormalities in mesotheliomas. Loss of copies of chromosomes 8, 16, 20, and 18 were found. Translocations were seen in chromosomes 5, 10, and 13 [44]. In another study, partial or total losses of chromosomes 22, 1, 3, 9, and 14 as well as gains of 7 and 11 were reported. Translocations and deletions involving a breakpoint at 1p11-p22 were most common structural aberrations. Copy numbers of chromosome 7p were inversely correlated with survival [45]. Losses of chromosomal regions in 1p, 8p, 14q, and 22q and gains of 5p, 6p, 8q, 15q, 17q, and 20 were also reported in the study by Kivipensas [46].

Subsequent studies focused on aberrations in losses of the short arm of chromosome 9p21-pter. Other losses were frequently detected in the long arms of chromosomes 4q31.1-qter, 6q22-q24, 13, 14q24-qter, and 22q13. A gain was found in the long arm of chromosome 1cen-qter [47]. In the study by Taguchi, chromosomal losses were found in 1p and 9p. The shortest regions of overlap of these losses were at 1p21-p22 and 9p21-p22, respectively. Other common abnormalities included losses of 3p21 and 6q15-q21 and numerical losses of chromosomes 14, 16, 18, and 22 [48]. Losses in 9p21-p22 were more precisely characterized by the markers D9S171 and IFNA/IFNW [49]. It finally turned out that the most frequent lost region was 9p21.3, the locus of CDKN2A and CDKN2B. Other recurrent minimal regions of losses were 1p31.1-p13.2, 3p22.1-p14.2, 6q22.1, 9p21.3, 13cen-q14.12, 14q22.1-qter, and 22qcen-q12.3. Previously unreported gains included 9p13.3, 7p22.3-p22.2, 12q13.3, and 17q21.32-qter [50]. Losses of the p16 protein are a common occurrence in mesotheliomas (Fig. 21.15). Further deletions of 9p21-p22 outside the p16 locus may reflect the involvement of other putative tumor suppressor genes that could also contribute to the pathogenesis [51, 52]. Codeletion of p15 and p16 was found in many mesotheliomas, including all cases with spindle cell components [53].

Allelic loss of 3p21 is another frequent finding in malignant mesothelioma. And one or more putative tumor suppressor genes might contribute to the pathogenesis [54]. Furthermore three independent regions on 6q14, 6q22, and 6q24 are commonly deleted, most likely containing tumor suppressor genes [55]. Underrepresented segments were seen

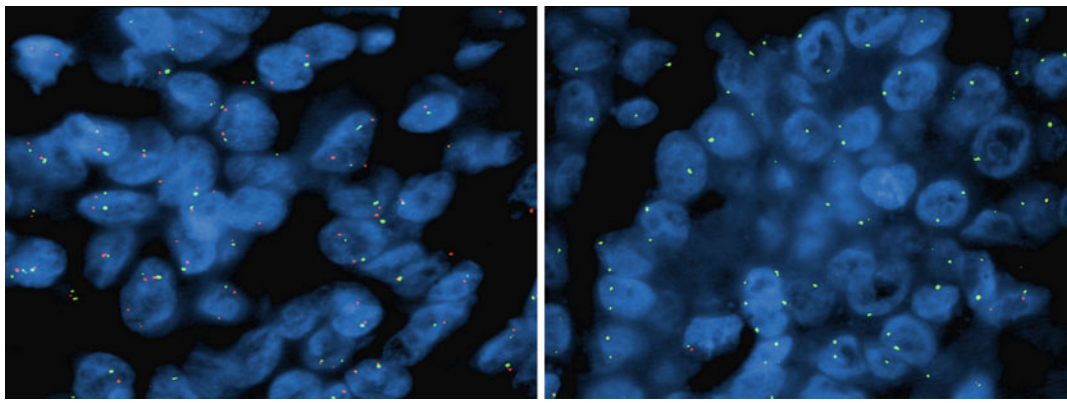

Fig. 21.15 FISH analysis for the loss of chromosome 9p. *Left* a case with retained 9p, *right* a mesothelioma with loss of 9p. ×1,000 (Courtesy of Sanja Dacic, Pittsburgh)

at 22q and 15q1.1-21. The most commonly overrepresented segment was on 5p. A new recurrent site of chromosomal loss within 15q was reported by Balsara et al. The minimal region of chromosomal loss was identified at 15q11.1-15 [56].

21.4.1.10 Pathway Analysis in Mesothelioma

In this context of these differences in the reported genetic abnormalities, it does not make sense to focus on single markers but instead focus on pathways activated in mesotheliomas. One of the most common activated pathways is Wnt signaling through Dvl overexpression and downstream signaling through β-catenin [57].

Through the mechanism by asbestos fibers, inflammation plays a major role in the pathogenesis. Yang et al. presented important data that TNFα signaling through NFkB increases the percent of mesothelial cells that survive asbestos fiber exposure, thus increasing the pool of mesothelial cells susceptible to malignant transformation [58]. Moreover, loss of Faf1 and downregulation of Faf1 protein showed that Faf1 regulates TNFα-mediated NFkB signaling in mesothelioma [59]. The importance of asbestos-induced inflammation in the initiation and growth of mesothelioma has been highlighted by the identification of HMGB1 and Nalp3 inflammasomes as key initiators. Asbestos fibers induce necrosis and cause release of HMGB1, which in turn activate Nalp3 inflammasome – a process that is enhanced by asbestos-induced production of reactive oxygen species. HMGB1 and Nalp3 lead to interleukin 1β and TNFα secretion and NFkB activity, thereby promoting cell survival and tumor growth [31].

Within this scenario, STAT1 is highly expressed in mesothelioma. STAT1 seems to function like an oncogene, and its action may be prolonged by a loss of its negative regulator SOCS1. The main function might be antiapoptosis by signaling into survivin [60, 61]. Another important function for mesothelioma cells is adhesion to stroma proteins. Inactivation of merlin is common in mesotheliomas by inactivating mutation of NF2, the gene coding for merlin. Inactivation of merlin promotes mTORC1 signaling resulting in integrin-mediated adhesion [62].

Other signaling pathways in mesotheliomas are associated with angiogenesis, like IGF stimulatory pathways and VEGF and COX overexpression [63]. Another mechanism by which angiogenesis might be achieved is PDGFR signaling. Expression of TIE2/Tek, a tyrosine kinase receptor for angiogenesis, was differentially regulated via PDGFR [61]. Besides genetic inactivation of p16(INK4a)/p14(ARF) and neurofibromatosis type 2 (NF2), also epigenetic inactivation of RASSF1A does occur. Activation of multiple receptor tyrosine kinases including EGFR family and MET and subsequent deregulations of mitogen-activated protein kinase (MAPK) and PI3K-AKT signaling cascades are frequently observed in mesothelioma cells [64]. Mesothelioma cells are also dependent on NOTCH-1 signaling, resulting in negative regulation of PTEN, which in turn leads to activation of PI3K/Akt/mTOR signaling pathway [65].

21.4.1.11 Familial Cases and Long Survivor Cases

Although in most mesotheliomas an exposure anamnesis for asbestos fibers can be established, in some mesotheliomas, no asbestos exposure is found. In some cases, exposure to other environmental or manmade fibers is seen. In a few cases, mesothelioma occurs as a familial disease. Usually mesotheliomas are found over two to three generations within a family [7, 8, 66, 67]. It seems that loss of function of BAP1 might be the main genetic factor contributing to the development of malignant mesothelioma in this setting (Fig. 21.16).

Within mesothelioma patients a small cohort of long survivors exists. These patients are characterized by prolonged survival beyond 3 years after diagnosis [61, 68]. There are some molecular features, which characterize these mesotheliomas: EGFR was expressed stronger; antiapoptosis was not upregulated by STAT1-survivin. Proliferative activity was significantly lower, and expression for p27(kip1) was high.

21.4.1.12 Treatment

There are different treatment options in malignant mesothelioma: combined chemotherapy and radiotherapy, pleurectomy in early stages, pleuropneumonectomy, and sometimes combinations of three of these. In general the outcome in mesothelioma is poor. Most patients will not survive more than 2 years after diagnosis. There

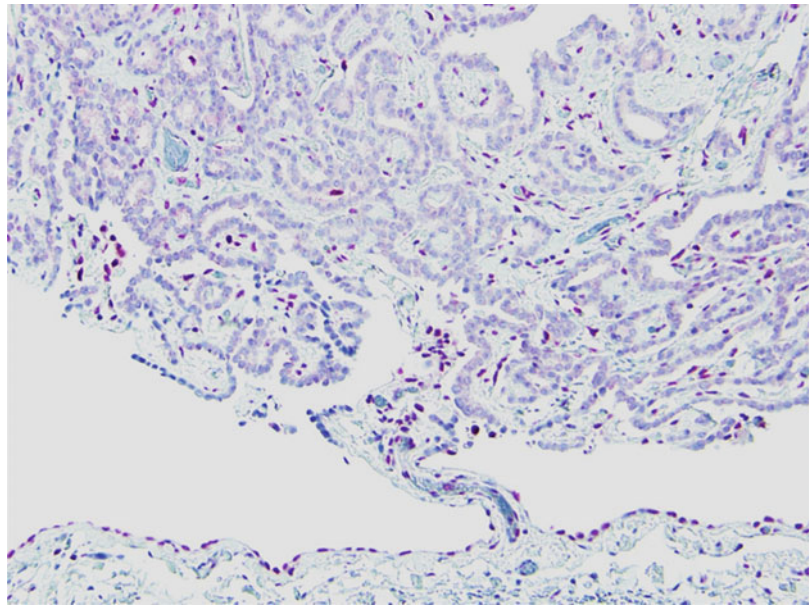

Fig. 21.16 Loss of BAP1 expression in a case of familial mesothelioma. The tumor cells are negative, whereas mesothelial cells and lymphocytes show nuclear positivity. Immunohistochemistry for BAP1, ×200

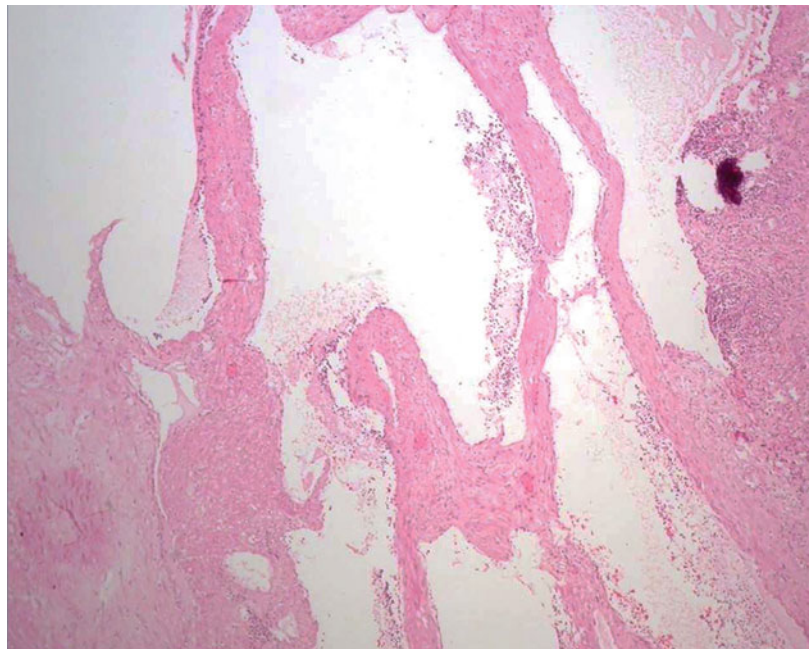

Fig. 21.17 Multicystic mesothelioma is characterized by cysts lined by a single layer of flat mesothelial cells. A translucent fluid usually fills the lumen. H&E, ×50

are few patients who survive longer (>3 years), which are so-called long survivors. In these patients, there are few molecular changes, which separate them from classical cases [60, 61]. In addition there are also familial cases of mesothelioma in which BAP1 suppressor gene deletion seems to play a major role; however, this same gene seems to act differently in non-familial cases of mesothelioma [7, 8, 69, 70].

21.4.2 Multicystic Mesothelioma

MM is found most frequently in young to middle-aged women and affects predominantly the pelvic peritoneum but rarely the pleura. In these cases, it can cause pneumothoraces [71]. It grows along the serosa as multiple, translucent, fluid-filled cysts (Fig. 21.17). Occasionally, it manifests as a solitary or free-floating mass.

The tumor is made up of clusters of mesothelial-lined cysts embedded in a delicate fibrovascular stroma. The mesothelial cells may be flattened or cuboidal. Adenomatoid features or squamous metaplasia of the mesothelium occurs in one third of cases. In a significant number of cases, the stroma shows marked inflammatory changes that make it difficult to recognize the underlying neoplastic proliferation. In most patients, the tumor behaves benign; only few patients died of tumor [72]. Mucin stains, immunohistochemistry, and electron microscopy are consistent with a mesothelial origin. Usually there is absence of stromal invasion and lack of mitotic activity [73].

21.4.3 Adenomatoid Tumor

Adenomatoid tumor is a mesothelial tumor usually found in the serosa of the spermatic cord and also arising from the serosa at the ovary and tube. Peritoneal adenomatoid tumor is also seen; however, in the pleura, this is rare. Adenomatoid tumor presents as small nodule(s) arising from the pleura. Histologically there is a focal proliferation of epithelioid cells forming vacuoles and tubular spaces in a fibrous stroma (Fig. 21.18). The differential diagnosis includes metastatic signet ring cell carcinoma. The cells react with mesothelial markers such as cytokeratin 5/6, calretinin, and vimentin, but are negative for carcinoembryonic antigen and BER-EP4. In the report by Kaplan et al., electron microscopy showed well-developed basal lamina, desmosomes, and numerous slender microvilli along the luminal surfaces of the tumor cells [74].

Adenomatoid tumors are benign mesothelial tumors; resection is the appropriate treatment.

21.4.4 Solitary Fibrous Tumor of the Pleura (Fibroma, SFT)

21.4.4.1 Clinical and Radiological Findings

SFT of the pleura is most often found in the costodiaphragmatic angle, but also in other locations. SFT can grow quite large, up to more than 10 cm, sometimes called giant fibroma. In large tumors, hypoglycemia might be seen, even hypoglycemic coma. Otherwise the symptoms are related to compression of the lung and mediastinal shift. On X-ray and CT scan, a tumor is seen, and due to its characteristic location in most cases, the radiologist makes a correct diagnosis. However, there are cases of SFT that arise within the lung from lobar and interlobar fissures, and thus these tumors are interpreted as malignant mesenchymal tumors or metastasis.

21.4.4.2 Gross Morphology

The tumor is firm, the cut surface is whitish gray, and fascicular structures can be discerned (Fig. 21.18).

21.4.4.3 Histology

SFT is composed of areas rich in collagen bundles, often hyalinized, forming short crossed

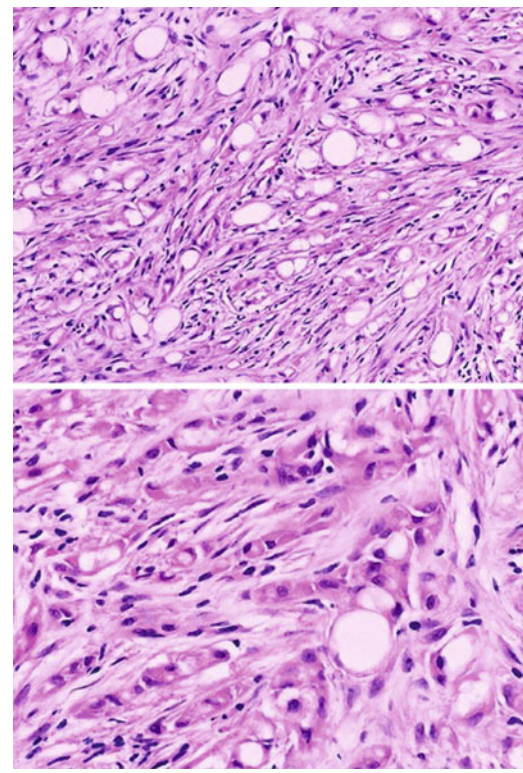

Fig. 21.18 Adenomatoid tumor of the pleura. The tumor is characterized by short cords of cells infiltrating a fibrous stroma and in addition forms small cystic structures, filled with fluid. H&E, ×100 and 200

structures, in some tumors almost acellular. The cellular areas are composed of spindle cells (fibroblasts and fibrocytes). The most common pattern has been called "pattern less pattern." There are recognized variants, such as hemangiopericytic, neurofibromatous, and phyllodes variant (Fig. 21.19a–d). Focal degeneration of collagen simulating tumor necrosis can be seen. Other less frequently observed features are the formation of "amianthoid" fibers, multinucleated giant cells, and foci of metaplastic ossification. In case more than five mitoses are found in 2 mm^2, a malignant SFT should be diagnosed (Fig. 21.19e, f). So far the outcome in these malignant variants is neither clear nor predictable [75–77]. In some cases metastasis has been found, in others a higher incidence of recurrence [78–80].

21.4.4.4 Immunohistochemistry

Insulin-like growth factors and their receptors play an important role in these tumors, as they act as autocrine growth factors [81]. As a side effect, they also induce hyperinsulinemia, which sometimes is the leading and only symptom in these patients (hypoglycemia). Some markers do exist for SFT: they are positive for CD34 (Fig. 21.19g), vimentin, ILG1+2, and ILGRα+β, but are negative for most other markers. A new specific marker is STAT6 [82–86] based on the fusion of STAT6 and NAB2 genes. This results in high expression of STAT6 protein in these tumors.

21.4.4.5 Differential Diagnosis

Given the characteristic pattern in most cases and the bland cytomorphology, most cases of SFT can be diagnosed without any additional immunohistochemical stains. Only those variants mentioned above will require additional investigations. Sarcomas can be sorted out due to their nuclear atypia and frequent mitosis, neurogenic tumors show different morphology of the nuclei, but here STAT6 stain will help. Desmoid tumor usually will show more cellular polymorphism compared to the monomorphic appearance of SFT. Malignant SFT can be difficult to diagnose, as the characteristic collage pattern might be absent. Helpful are the comma-shaped nuclei and the immunohistochemical profile with CD31 and STAT6.

Fig. 21.19 Solitary fibrous tumor of the pleura: *top panel* shows a small tumor with a peduncle of lung tissue; at the *bottom* a large SFT arising from an interlobar septum is shown

21.4.5 Desmoid Tumor

A repair tissue, sometimes granulation tissue, characterizes desmoid tumor of the pleura. This is most probably a reactive or reparative growth following a trauma [87] (and B. Murer, personal communication). Intrathoracic desmoid tumors often exhibit clinical and radiographic features similar to localized fibrous tumor of the pleura. This tumor infiltrates adjacent structures. In contrast to SFT, there are different cells involved, such as histiocytes, fibroblasts, fibrocytes, and a variable amount of inflammatory cells (Fig. 21.20). There are no mitoses. There is abundant repair tissue leading to the appearance of a tumor. The tumor cells are immunoreactive for vimentin, desmin, smooth muscle actin, and muscle-specific actin and β-catenin and are negative for S-100 protein. Local excision will result in complete recovery.

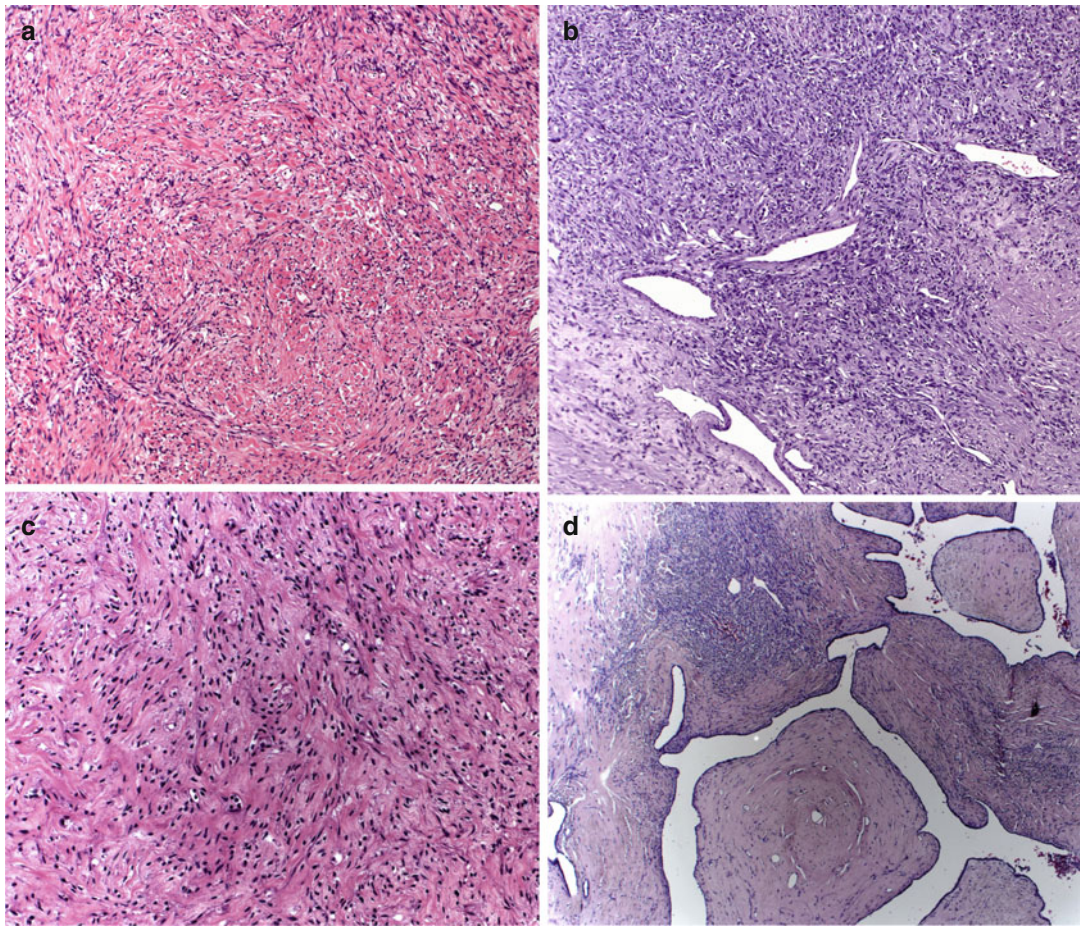

Fig. 21.20 Solitary fibrous tumor (SFT) with different patterns, (**a**) classical patternless pattern with irregular deposited collagen fiber bundles, (**b**) hemangioma-like pattern, (**c**) neurofibroma-like pattern, (**d**) lobular pattern similar to phyllodes tumor of the breast, (**e**, **f**) malignant SFT with high cellularity and increased mitosis, (**g**) immunohistochemistry for CD34. H&E, IHC, ×50, 100, 200

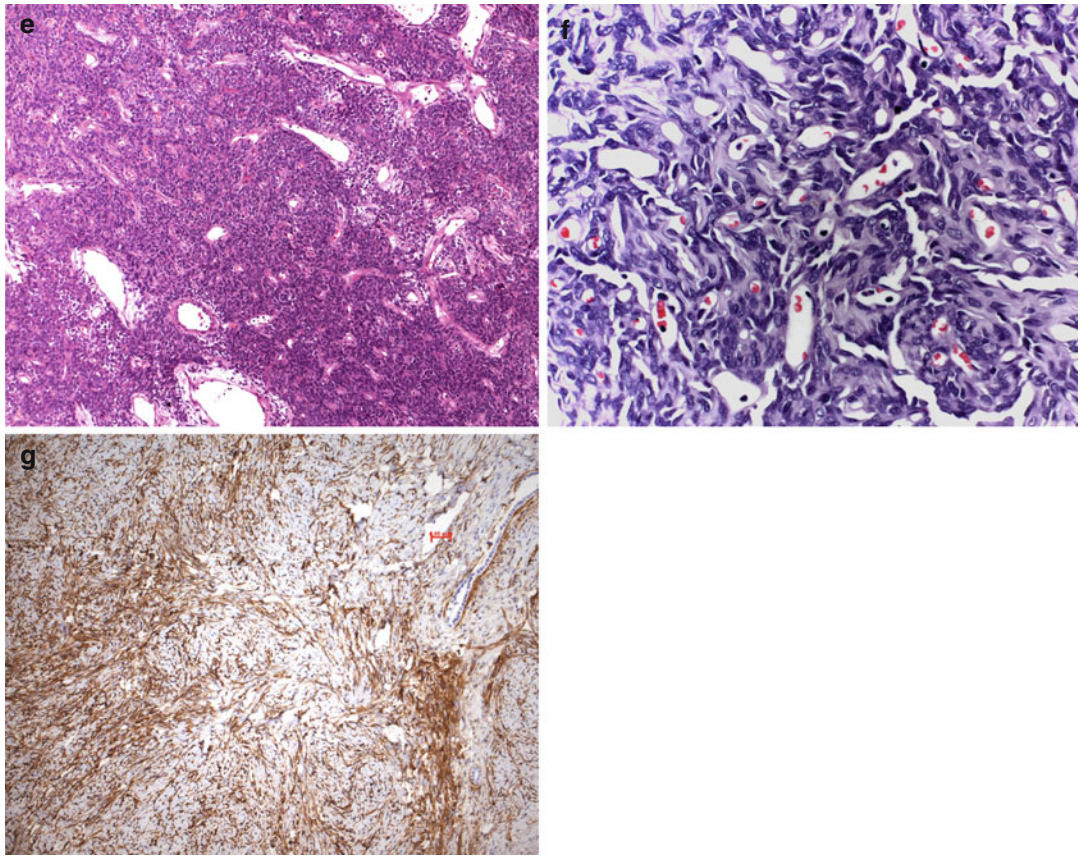

Fig. 21.20 (continued)

21.4.6 Calcifying (Fibrous) Pleura Tumor (CPT)

Calcifying tumor of the pleura is a rare fibrous tumor, most probably arising from deeper layers of the pleura. It is characterized by a plaque-like macroscopic appearance. Histologically there are fibrocytes and fibroblasts with numerous calcified bodies. The tumor is benign and very slow growing. Tumor size can be from 0.6 to 25 cm. Lesions are well-circumscribed hypocellular spindle cell proliferations with dense stromal collagen. A lymphoplasmacytic infiltrate and stromal calcifications are diagnostic features (Fig. 21.21). The tumor cells are positive for CD34; rare cells are positive for smooth muscle actin and desmin and consistently negative for ALK-1 and S-100 protein [88].

21.4.7 Primary Squamous Cell Carcinoma of the Pleura

Primary squamous cell carcinoma of the pleura is a rare tumor. It has features as any other squamous cell carcinoma. Therefore the diagnosis can only be made, when every other primary location is excluded (Fig. 21.22).

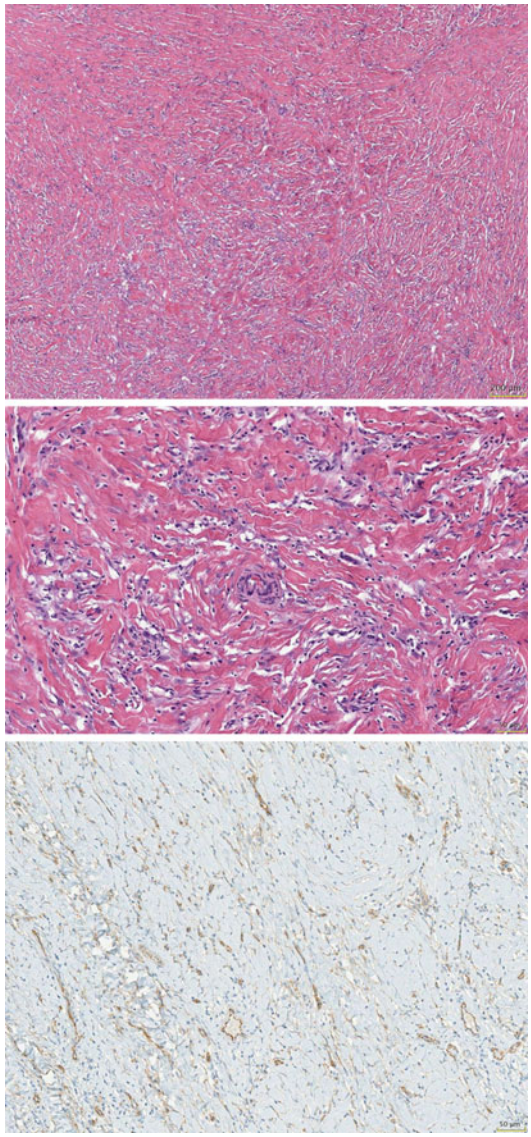

Fig. 21.21 Desmoid tumor of the pleura, *top panel* shows an overview; at this magnification, the tumor resembles granulation tissue or SFT. *Middle panel* shows a higher magnification, where the impression of granulation tissue is clearer with capillaries, primitive mesenchymal cells, and scattered inflammatory cells, predominantly lymphocytes. In the *bottom panel*, immunohistochemistry for β-catenin is shown, which shows nuclear expression. H&E, IHC, bars 200 and 50 μm

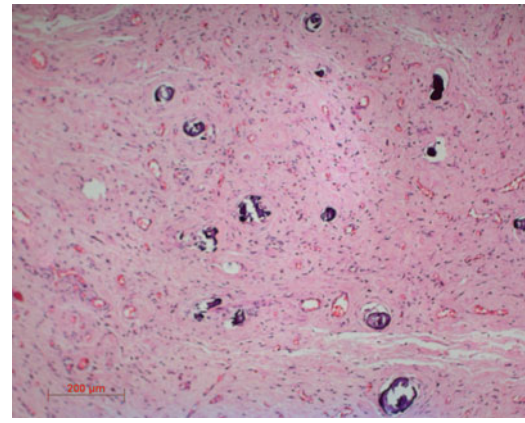

Fig. 21.22 Calcifying tumor of the pleura with numerous calciferous embedded in a fibrous stroma. H&E, bar 200 μm

21.4.8 Primary Fibrosarcoma

Primary fibrosarcoma is another rare tumor of the pleura. It has to be separated from malignant SFT by its more uniform appearance. Fibrosarcoma forms long small bundles of streaming cells, arranged like swimming schools of young fish. There are usually long bundles of collagen between the tumor cell groups. The collagen deposition is unlike that seen in SFT. Mitoses are scarce, the cells are uniform fibroblast-like, chromatin is irregularly distributed within the nucleus, and nucleoli are small or invisible.

21.4.9 Undifferentiated Sarcoma Arising in the Lung and/or Pleura (Formerly Malignant Fibrous Histiocytoma, MFH)

This entity has been already shortly discussed in the tumor chapter. We will add some interesting aspects here. I had the opportunity to review a consultation case, which has three different patterns in one tumor: classical SFT, malignant SFT, and finally a pleomorphic sarcoma (Fig. 21.23). The

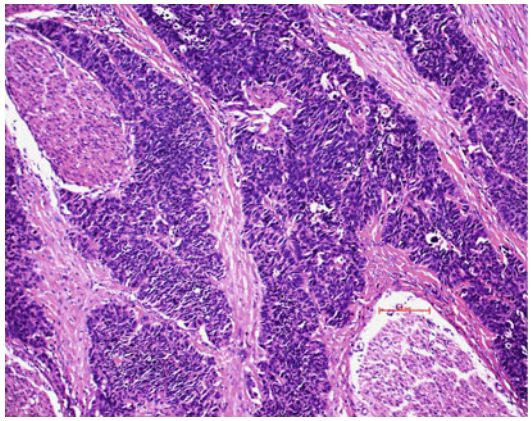

Fig. 21.23 Primary squamous cell carcinoma of the pleura. The major problem in this diagnosis is that metastasis has to be excluded before the diagnosis can be made. Otherwise this looks like any other squamous cell carcinoma. H&E, bar 200 µm

tumor was localized to the pleura and did not invade the lung. As discussed in the tumor chapter, undifferentiated pleomorphic sarcomas do exist in the lung too; however, to my knowledge, they do not metastasize. This case illustrated here raises the possibility that this entity is the highly malignant variant of SFT, pleomorphic SFT, and has nothing to do with soft tissue pleomorphic sarcomas.

21.4.10 Desmoplastic Round Cell Tumor

This is a malignant mesenchymal tumor characterized by small round cells. This tumor preferentially occurs in children and young adults and presents with chest pain and pleural effusion. On gross morphology, the tumor looks like any mesenchymal tumor; there are no specific features.

On histology the tumor is composed of small round cells forming strands and sometimes pseudoacini with mesenchymal matrix protein in the center. The nuclei are round, chromatin is irregularly dispersed, nuclear inclusions are seen, and nucleoli are slightly enlarged. The cytoplasm is basophilic (Fig. 21.24). Mitosis is common.

The tumor is characterized by a translocation of EWSR1-WT1, which should be demonstrated by PCR for the fusion gene or by FISH.

Therapy with cytostatics should be initiated; however, many of these tumors get resistant and will recur.

21.5 Metastasis to the Pleura

The pleura is a common location for metastasis, most often from lung carcinomas (Figs. 21.25 and 21.26). However, many other carcinomas such as ovarian cystadenocarcinomas, ductal and lobular breast carcinomas, and adenocarcinomas of the prostate, stomach, and pancreas are also seen. The main differential diagnosis for carcinoma metastases is mesothelioma as discussed above.

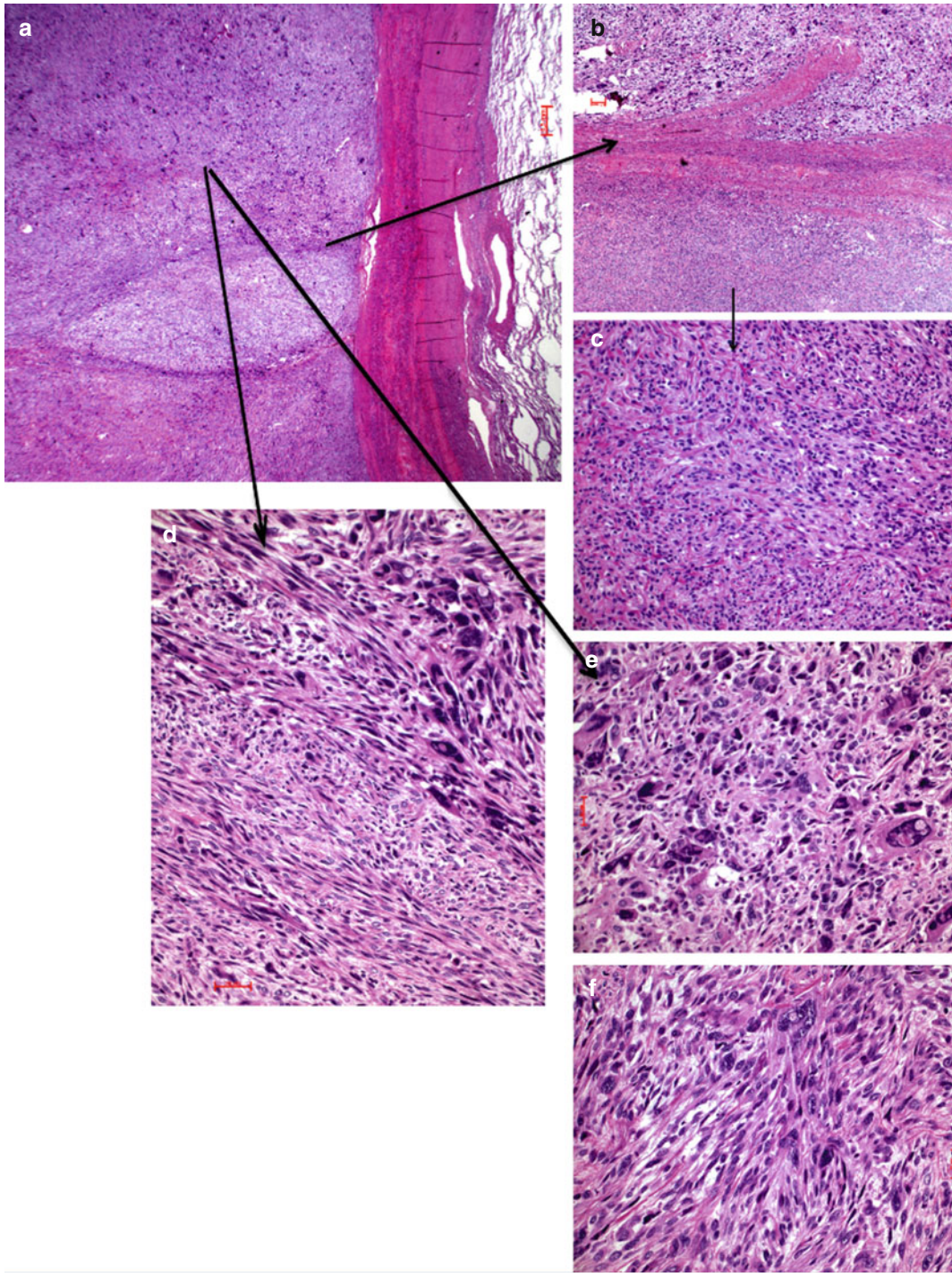

Fig. 21.24 Pleomorphic SFT, this case shows several features of an SFT but also features, which are more common in pleomorphic sarcomas. (**a**) Overview, at the *bottom* a classical SFT, in the *middle* malignant cell rich SFT, and at the *top* the area with pleomorphic features. (**b** and **d**) shows the transition zone between malignant SFT and pleomorphic SFT, in (**c**) the malignant SFT is shown, (**e**) shows the pleomorphic component, and in (**f**) a mixture of spindle cell and pleomorphic cell pattern is visible. *Arrows* from the overview point to the magnified illustration. H&E, 500, 100, 50, 20 µm

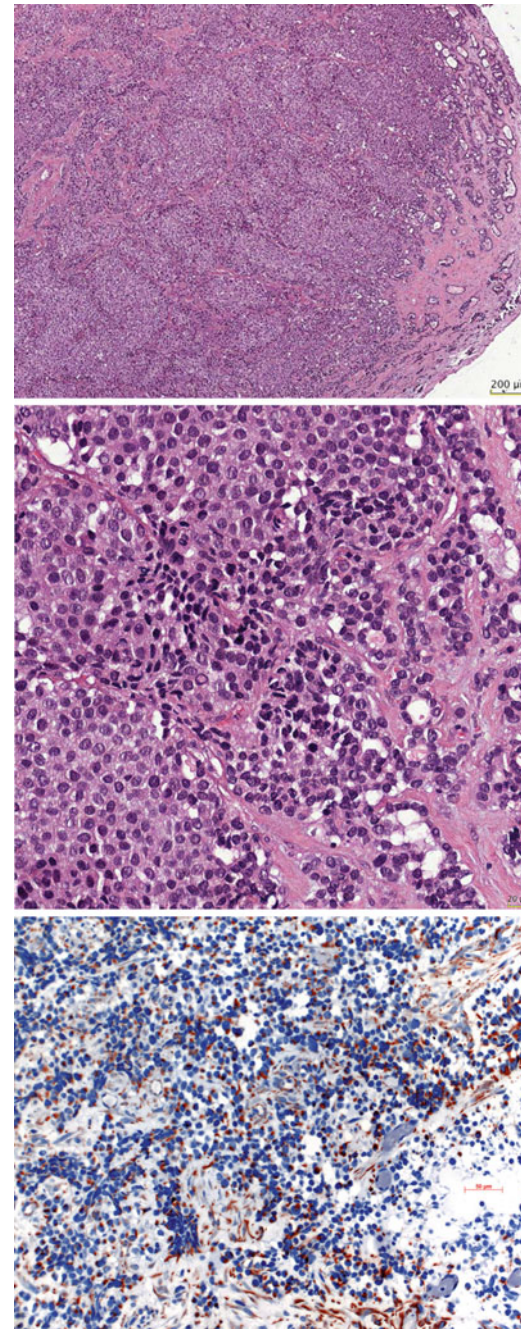

Fig. 21.25 Desmoplastic round cell tumor. On low power a very cellular solid tumor is seen; focally there is dense fibrous stroma (*upper panel*). On higher magnification, the small round cells with round nuclei are seen forming single strands; clusters and pseudoacinar structures can be appreciated. There is also a dense desmoplastic stroma (*middle panels*). These tumors are usually positive for β-catenin (*lower panel*), which however is not associated with E-cadherin. Bars 200, 50, 20 µm

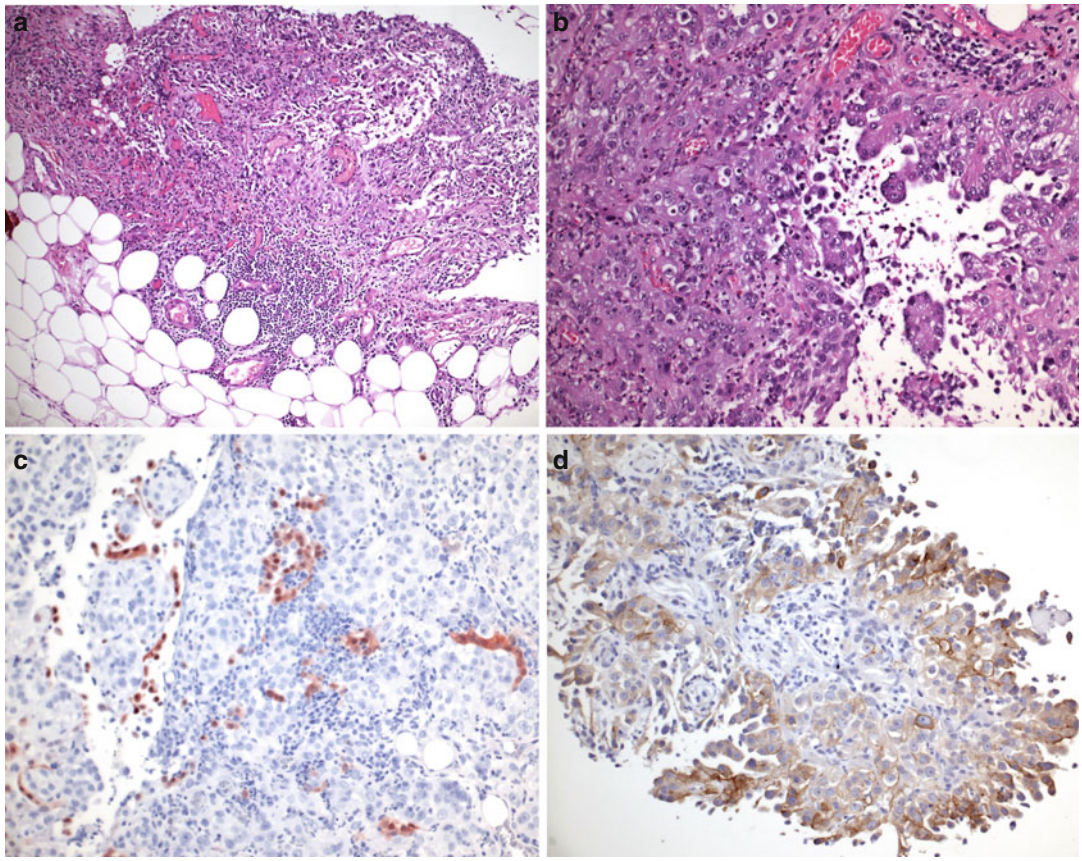

Fig. 21.26 Metastasis of pulmonary adenocarcinoma to the lung (**a**, **b**, two different cases). By immunohistochemistry, the tumor is negative for calretinin, but entrapped mesothelial cells are positive (**c**). The tumor cells reacted positively for claudin 4 (**d**). ×100, 200, 400

References

1. Roggli VL. Malignant mesothelioma and duration of asbestos exposure: correlation with tissue mineral fibre content. Ann Occup Hyg. 1995;39:363–74.
2. Wheeler CS. Exposure to man-made mineral fibers: a summary of current animal data. Toxicol Ind Health. 1990;6:293–307.
3. Churg A, Vedal S. Fiber burden and patterns of asbestos-related disease in workers with heavy mixed amosite and chrysotile exposure. Am J Respir Crit Care Med. 1994;150:663–9.
4. Proietti L, Spicuzza L, Di Maria A, Polosa R, Sebastian Torres E, Asero V, Di Maria GU. Non-occupational malignant pleural mesothelioma due to asbestos and non-asbestos fibres. Monaldi Arch Chest Dis. 2006;65:210–6.
5. Gibbs GW, Berry G. Mesothelioma and asbestos. Regul Toxicol Pharmacol. 2008;52:S223–31.
6. Yang H, Testa JR, Carbone M. Mesothelioma epidemiology, carcinogenesis, and pathogenesis. Curr Treat Options Oncol. 2008;9:147–5.
7. Testa JR, Cheung M, Pei J, Below JE, Tan Y, Sementino E, Cox NJ, Dogan AU, Pass HI, Trusa S, Hesdorffer M, Nasu M, Powers A, Rivera Z, Comertpay S, Tanji M, Gaudino G, Yang H, Carbone M. Germline BAP1 mutations predispose to malignant mesothelioma. Nat Genet. 2011;43:1022–5.
8. Wiesner T, Fried I, Ulz P, Stacher E, Popper H, Murali R, Kutzner H, Lax S, Smolle-Juttner F, Geigl JB, Speicher MR. Toward an improved definition of the tumor spectrum associated with BAP1 germline mutations. J Clin Oncol. 2012;30:e337–40.
9. Metintas M, Hillerdal G, Metintas S, Dumortier P. Endemic malignant mesothelioma: exposure to erionite is more important than genetic factors. Arch Environ Occup Health. 2010;65:86–93.
10. Henzi T, Blum WV, Pfefferli M, Kawecki TJ, Salicio V, Schwaller B. SV40-induced expression of calretinin protects mesothelial cells from asbestos cytotoxicity and may be a key factor contributing to mesothelioma pathogenesis. Am J Pathol. 2009;174:2324–36.
11. Carbone M, Bedrossian CW. The pathogenesis of mesothelioma. Semin Diagn Pathol. 2006;23:56–60.

12. Baris YI, Grandjean P. Prospective study of mesothelioma mortality in Turkish villages with exposure to fibrous zeolite. J Natl Cancer Inst. 2006;98:414–7.
13. Churg A. Deposition and clearance of chrysotile asbestos. Ann Occup Hyg. 1994;38:625–33, 424–625.
14. De Vuyst P, Dumortier P, Swaen GM, Pairon JC, Brochard P. Respiratory health effects of man-made vitreous (mineral) fibres. Eur Respir J. 1995;8:2149–73.
15. Leithner A, Weinhaeusel A, Windhager R, Schlegl R, Waldner P, Lang S, Dominkus M, Zoubek A, Popper HH, Haas OA. Absence of SV40 in Austrian tumors correlates with low incidence of mesotheliomas. Cancer Biol Ther. 2002;1:375–9.
16. Manfredi JJ, Dong J, Liu WJ, Resnick-Silverman L, Qiao R, Chahinian P, Saric M, Gibbs AR, Phillips JI, Murray J, Axten CW, Nolan RP, Aaronson SA. Evidence against a role for SV40 in human mesothelioma. Cancer Res. 2005;65:2602–9.
17. Lopez-Rios F, Illei PB, Rusch V, Ladanyi M. Evidence against a role for SV40 infection in human mesotheliomas and high risk of false-positive PCR results owing to presence of SV40 sequences in common laboratory plasmids. Lancet. 2004;364:1157–66.
18. Jaurand MC, Fleury-Feith J. Pathogenesis of malignant pleural mesothelioma. Respirology. 2005;10:2–8.
19. Cacciotti P, Barbone D, Porta C, Altomare DA, Testa JR, Mutti L, Gaudino G. SV40-dependent AKT activity drives mesothelial cell transformation after asbestos exposure. Cancer Res. 2005;65:5256–62.
20. Cristaudo A, Foddis R, Vivaldi A, Buselli R, Gattini V, Guglielmi G, Cosentino F, Ottenga F, Ciancia E, Libener R, Filiberti R, Neri M, Betta P, Tognon M, Mutti L, Puntoni R. SV40 enhances the risk of malignant mesothelioma among people exposed to asbestos: a molecular epidemiologic case-control study. Cancer Res. 2005;65:3049–52.
21. Gordon GJ, Rockwell GN, Jensen RV, Rheinwald JG, Glickman JN, Aronson JP, Pottorf BJ, Nitz MD, Richards WG, Sugarbaker DJ, Bueno R. Identification of novel candidate oncogenes and tumor suppressors in malignant pleural mesothelioma using large-scale transcriptional profiling. Am J Pathol. 2005;166:1827–40.
22. Kroczynska B, Cutrone R, Bocchetta M, Yang H, Elmishad AG, Vacek P, Ramos-Nino M, Mossman BT, Pass HI, Carbone M. Crocidolite asbestos and SV40 are cocarcinogens in human mesothelial cells and in causing mesothelioma in hamsters. Proc Natl Acad Sci U S A. 2006;103:14128–33.
23. Roggli VL, Sharma A, Butnor KJ, Sporn T, Vollmer RT. Malignant mesothelioma and occupational exposure to asbestos: a clinicopathological correlation of 1445 cases. Ultrastruct Pathol. 2002;26:55–65.
24. Selcuk ZT, Coplu L, Emri S, Kalyoncu AF, Sahin AA, Baris YI. Malignant pleural mesothelioma due to environmental mineral fiber exposure in Turkey. Analysis of 135 cases. Chest. 1992;102:790–6.
25. Simonato L, Baris R, Saracci R, Skidmore J, Winkelmann R. Relation of environmental exposure to erionite fibres to risk of respiratory cancer. IARC Sci Publ. 1989;90:398–405.
26. Baris I, Simonato L, Artvinli M, Pooley F, Saracci R, Skidmore J, Wagner C. Epidemiological and environmental evidence of the health effects of exposure to erionite fibres: a four-year study in the Cappadocian region of Turkey. Int J Cancer. 1987;39:10–7.
27. Roushdy-Hammady I, Siegel J, Emri S, Testa JR, Carbone M. Genetic-susceptibility factor and malignant mesothelioma in the Cappadocian region of Turkey. Lancet. 2001;357:444–5.
28. Dumortier P, Gocmen A, Laurent K, Manco A, De Vuyst P. The role of environmental and occupational exposures in Turkish immigrants with fibre-related disease. Eur Respir J. 2001;17:922–7.
29. Fraire AE, Greenberg SD, Spjut HJ, Dodson RF, Williams G, Lach-Pasko E, Roggli VL. Effect of erionite on the pleural mesothelium of the Fischer 344 rat. Chest. 1997;111:1375–80.
30. Bertino P, Marconi A, Palumbo L, Bruni BM, Barbone D, Germano S, Dogan AU, Tassi GF, Porta C, Mutti L, Gaudino G. Erionite and asbestos differently cause transformation of human mesothelial cells. Int J Cancer. 2007;121:12–20.
31. Carbone M, Yang H. Molecular pathways: targeting mechanisms of asbestos and erionite carcinogenesis in mesothelioma. Clin Cancer Res. 2012;18:598–604.
32. Butnor KJ, Sporn TA, Hammar SP, Roggli VL. Well-differentiated papillary mesothelioma. Am J Surg Pathol. 2001;25:1304–9.
33. Churg A, Allen T, Borczuk AC, Cagle PT, Galateau-Salle F, Hwang H, Murer B, Murty VV, Ordonez N, Tazelaar HD, Wick M. Well-differentiated papillary mesothelioma with invasive foci. Am J Surg Pathol. 2014;38:990–8.
34. Ordonez NG. Podoplanin: a novel diagnostic immunohistochemical marker. Adv Anat Pathol. 2006;13:83–8.
35. Ordonez NG. Value of immunohistochemistry in distinguishing peritoneal mesothelioma from serous carcinoma of the ovary and peritoneum: a review and update. Adv Anat Pathol. 2006;13:16–25.
36. Ordonez NG. The diagnostic utility of immunohistochemistry in distinguishing between epithelioid mesotheliomas and squamous carcinomas of the lung: a comparative study. Mod Pathol. 2006;19:417–28.
37. Ordonez NG. Mesothelioma with rhabdoid features: an ultrastructural and immunohistochemical study of 10 cases. Mod Pathol. 2006;19:373–83.
38. Ordonez NG. Immunohistochemical diagnosis of epithelioid mesothelioma: an update. Arch Pathol Lab Med. 2005;129:1407–14.
39. Ordonez NG. What are the current best immunohistochemical markers for the diagnosis of epithelioid mesothelioma? A review and update. Hum Pathol. 2007;38:1–16.
40. Attanoos RL, Griffin A, Gibbs AR. The use of immunohistochemistry in distinguishing reactive from neoplastic mesothelium. A novel use for desmin and comparative evaluation with epithelial membrane antigen, p53, platelet-derived growth factor-receptor, P-glycoprotein and Bcl-2. Histopathology. 2003;43:231–8.
41. Zimmerman RL, Bibbo M. Clinical utility of chromosome 17 alpha satellite probe in distinguishing

benign mesothelium from malignant cells: a pilot study using routinely fixed specimens. Oncol Rep. 1999;6:695–8.
42. Bidlingmaier S, He J, Wang Y, An F, Feng J, Barbone D, Gao D, Franc B, Broaddus VC, Liu B. Identification of MCAM/CD146 as the target antigen of a human monoclonal antibody that recognizes both epithelioid and sarcomatoid types of mesothelioma. Cancer Res. 2009;69:1570–7.
43. Sato A, Torii I, Okamura Y, Yamamoto T, Nishigami T, Kataoka TR, Song M, Hasegawa S, Nakano T, Kamei T, Tsujimura T. Immunocytochemistry of CD146 is useful to discriminate between malignant pleural mesothelioma and reactive mesothelium. Mod Pathol. 2010;23:1458–66.
44. Libbus BL, Craighead JE. Chromosomal translocations with specific breakpoints in asbestos-induced rat mesotheliomas. Cancer Res. 1988;48:6455–61.
45. Tiainen M, Tammilehto L, Rautonen J, Tuomi T, Mattson K, Knuutila S. Chromosomal abnormalities and their correlations with asbestos exposure and survival in patients with mesothelioma. Br J Cancer. 1989;60:618–26.
46. Kivipensas P, Bjorkqvist AM, Karhu R, Pelin K, Linnainmaa K, Tammilehto L, Mattson K, Kallioniemi QP, Knuutila S. Gains and losses of DNA sequences in malignant mesothelioma by comparative genomic hybridization. Cancer Genet Cytogenet. 1996;89: 7–13.
47. Bjorkqvist AM, Tammilehto L, Anttila S, Mattson K, Knuutila S. Recurrent DNA copy number changes in 1q, 4q, 6q, 9p, 13q, 14q and 22q detected by comparative genomic hybridization in malignant mesothelioma. Br J Cancer. 1997;75:523–7.
48. Taguchi T, Jhanwar SC, Siegfried JM, Keller SM, Testa JR. Recurrent deletions of specific chromosomal sites in 1p, 3p, 6q, and 9p in human malignant mesothelioma. Cancer Res. 1993;53:4349–55.
49. Cheng JQ, Jhanwar SC, Lu YY, Testa JR. Homozygous deletions within 9p21–p22 identify a small critical region of chromosomal loss in human malignant mesotheliomas. Cancer Res. 1993;53:4761–3.
50. Lindholm PM, Salmenkivi K, Vauhkonen H, Nicholson AG, Anttila S, Kinnula VL, Knuutila S. Gene copy number analysis in malignant pleural mesothelioma using oligonucleotide array CGH. Cytogenet Genome Res. 2007;119:46–52.
51. Cheng JQ, Jhanwar SC, Klein WM, Bell DW, Lee WC, Altomare DA, Nobori T, Olopade OI, Buckler AJ, Testa JR. p16 alterations and deletion mapping of 9p21-p22 in malignant mesothelioma. Cancer Res. 1994;54:5547–51.
52. Dacic S, Kothmaier H, Land S, Shuai Y, Halbwedl I, Morbini P, Murer B, Comin C, Galateau-Salle F, Demirag F, Zeren H, Attanoos R, Gibbs A, Cagle P, Popper H. Prognostic significance of p16/cdkn2a loss in pleural malignant mesotheliomas. Virchows Arch. 2008;453:627–35.
53. Xio S, Li D, Vijg J, Sugarbaker DJ, Corson JM, Fletcher JA. Codeletion of p15 and p16 in primary malignant mesothelioma. Oncogene. 1995;11:511–5.
54. Lu YY, Jhanwar SC, Cheng JQ, Testa JR. Deletion mapping of the short arm of chromosome 3 in human malignant mesothelioma. Genes Chromosom Cancer. 1994;9:76–80.
55. Jensen RH, Tiirikainen M, You L, Ginzinger D, He B, Uematsu K, Xu Z, Treseler P, McCormick F, Jablons DM. Genomic alterations in human mesothelioma including high resolution mapping of common regions of DNA loss in chromosome arm 6q. Anticancer Res. 2003;23:2281–9.
56. Balsara BR, Bell DW, Sonoda G, De Rienzo A, du Manoir S, Jhanwar SC, Testa JR. Comparative genomic hybridization and loss of heterozygosity analyses identify a common region of deletion at 15q11.1–15 in human malignant mesothelioma. Cancer Res. 1999;59:450–4.
57. Uematsu K, Kanazawa S, You L, He B, Xu Z, Li K, Peterlin BM, McCormick F, Jablons DM. Wnt pathway activation in mesothelioma: evidence of Dishevelled overexpression and transcriptional activity of beta-catenin. Cancer Res. 2003;63:4547–51.
58. Yang H, Bocchetta M, Kroczynska B, Elmishad AG, Chen Y, Liu Z, Bubici C, Mossman BT, Pass HI, Testa JR, Franzoso G, Carbone M. TNF-alpha inhibits asbestos-induced cytotoxicity via a NF-kappaB-dependent pathway, a possible mechanism for asbestos-induced oncogenesis. Proc Natl Acad Sci U S A. 2006;103:10397–402.
59. Altomare DA, Menges CW, Pei J, Zhang L, Skele-Stump KL, Carbone M, Kane AB, Testa JR. Activated TNF-alpha/NF-kappaB signaling via down-regulation of Fas-associated factor 1 in asbestos-induced mesotheliomas from Arf knockout mice. Proc Natl Acad Sci U S A. 2009;106:3420–5.
60. Arzt L, Kothmaier H, Halbwedl I, Quehenberger F, Popper HH. Signal transducer and activator of transcription 1 (STAT1) acts like an oncogene in malignant pleural mesothelioma. Virchows Arch. 2014;465: 79–88.
61. Kothmaier H, Quehenberger F, Halbwedl I, Morbini P, Demirag F, Zeren H, Comin CE, Murer B, Cagle PT, Attanoos R, Gibbs AR, Galateau-Salle F, Popper HH. EGFR and PDGFR differentially promote growth in malignant epithelioid mesothelioma of short and long term survivors. Thorax. 2008;63: 345–51.
62. Lopez-Lago MA, Okada T, Murillo MM, Socci N, Giancotti FG. Loss of the tumor suppressor gene NF2, encoding merlin, constitutively activates integrin-dependent mTORC1 signaling. Mol Cell Biol. 2009;29:4235–49.
63. Whitson BA, Kratzke RA. Molecular pathways in malignant pleural mesothelioma. Cancer Lett. 2006; 239:183–9.
64. Sekido Y. Genomic abnormalities and signal transduction dysregulation in malignant mesothelioma cells. Cancer Sci. 2010;101:1–6.
65. Graziani I, Eliasz S, De Marco MA, Chen Y, Pass HI, De May RM, Strack PR, Miele L, Bocchetta M. Opposite effects of Notch-1 and Notch-2 on mesothelioma cell survival under hypoxia are exerted

through the Akt pathway. Cancer Res. 2008;68: 9678–85.
66. Musti M, Cavone D, Aalto Y, Scattone A, Serio G, Knuutila S. A cluster of familial malignant mesothelioma with del(9p) as the sole chromosomal anomaly. Cancer Genet Cytogenet. 2002;138:73–6.
67. Betti M, Casalone E, Ferrante D, Romanelli A, Grosso F, Guarrera S, Righi L, Vatrano S, Pelosi G, Libener R, Mirabelli D, Boldorini R, Casadio C, Papotti M, Matullo G, Magnani C, Dianzani I. Inference on germline BAP1 mutations and asbestos exposure from the analysis of familial and sporadic mesothelioma in a high-risk area. Genes Chromosom Cancer. 2015;54:51–62.
68. Bongiovanni M, Cassoni P, De Giuli P, Viberti L, Cappia S, Ivaldi C, Chiusa L, Bussolati G. p27(kip1) immunoreactivity correlates with long-term survival in pleural malignant mesothelioma. Cancer. 2001;92: 1245–50.
69. Arzt L, Quehenberger F, Halbwedl I, Mairinger T, Popper HH. BAP1 protein is a progression factor in malignant pleural mesothelioma. Pathol Oncol Res. 2014;20:145–51.
70. Alakus H, Yost SE, Woo B, French R, Lin GY, Jepsen K, Frazer KA, Lowy AM, Harismendy O. BAP1 mutation is a frequent somatic event in peritoneal malignant mesothelioma. J Transl Med. 2015;13:122.
71. Oks M, He T, Palkar A, Esposito MJ, Koenig SJ. Benign multicystic mesothelioma causing bilateral pneumothoraces. Ann Am Thorac Soc. 2015;12: 1106–9.
72. Weiss SW, Tavassoli FA. Multicystic mesothelioma. An analysis of pathologic findings and biologic behavior in 37 cases. Am J Surg Pathol. 1988;12: 737–46.
73. Ball NJ, Urbanski SJ, Green FH, Kieser T. Pleural multicystic mesothelial proliferation. The so-called multicystic mesothelioma. Am J Surg Pathol. 1990; 14:375–8.
74. Kaplan MA, Tazelaar HD, Hayashi T, Schroer KR, Travis WD. Adenomatoid tumors of the pleura. Am J Surg Pathol. 1996;20:1219–23.
75. Magdeleinat P, Alifano M, Petino A, Le Rochais JP, Dulmet E, Galateau F, Icard P, Regnard JF. Solitary fibrous tumors of the pleura: clinical characteristics, surgical treatment and outcome. Eur J Cardiothorac Surg. 2002;21:1087–93.
76. Fiorello A, Vicidomini G, Santini M. Giant solitary fibrous tumors of the pleura: two case reports. Thorac Cardiovasc Surg. 2007;55:458–9.
77. Harrison-Phipps KM, Nichols FC, Schleck CD, Deschamps C, Cassivi SD, Schipper PH, Allen MS, Wigle DA, Pairolero PC. Solitary fibrous tumors of the pleura: results of surgical treatment and long-term prognosis. J Thorac Cardiovasc Surg. 2009;138:19–25.
78. Hu Y, Mahar TJ, Hicks DG, Raymond D, Jones C, Wandtke JC, Powers JM, Xu H. Malignant solitary fibrous tumor: report of 3 cases with unusual features. Appl Immunohistochem Mol Morphol. 2009;17:451–7.
79. Imai K, Hirayama K, Matsuzaki I, Minamiya Y, Saito H, Mitsui M, Hosono Y, Ogawa J. Resection of a giant, invasive malignant solitary fibrous tumor of pleura. Gen Thorac Cardiovasc Surg. 2012;60:859–62.
80. Bongiovanni M, Viberti L, Pecchioni C, Papotti M, Thonhofer R, Hans Popper H, Sapino A. Steroid hormone receptor in pleural solitary fibrous tumours and CD34+ progenitor stromal cells. J Pathol. 2002;198: 252–7.
81. Kishi K, Homma S, Tanimura S, Matsushita H, Nakata K. Hypoglycemia induced by secretion of high molecular weight insulin-like growth factor-II from a malignant solitary fibrous tumor of the pleura. Intern Med. 2001;40:341–4.
82. Doyle LA, Vivero M, Fletcher CD, Mertens F, Hornick JL. Nuclear expression of STAT6 distinguishes solitary fibrous tumor from histologic mimics. Mod Pathol. 2014;27:390–5.
83. Vogels RJ, Vlenterie M, Versleijen-Jonkers YM, Ruijter E, Bekers EM, Verdijk MA, Link MM, Bonenkamp JJ, van der Graaf WT, Slootweg PJ, Suurmeijer AJ, Groenen PJ, Flucke U. Solitary fibrous tumor – clinicopathologic, immunohistochemical and molecular analysis of 28 cases. Diagn Pathol. 2014;9:224.
84. Mohajeri A, Tayebwa J, Collin A, Nilsson J, Magnusson L, von Steyern FV, Brosjo O, Domanski HA, Larsson O, Sciot R, Debiec-Rychter M, Hornick JL, Mandahl N, Nord KH, Mertens F. Comprehensive genetic analysis identifies a pathognomonic NAB2/STAT6 fusion gene, nonrandom secondary genomic imbalances, and a characteristic gene expression profile in solitary fibrous tumor. Genes Chromosom Cancer. 2013;52: 873–86.
85. Schweizer L, Koelsche C, Sahm F, Piro RM, Capper D, Reuss DE, Pusch S, Habel A, Meyer J, Gock T, Jones DT, Mawrin C, Schittenhelm J, Becker A, Heim S, Simon M, Herold-Mende C, Mechtersheimer G, Paulus W, Konig R, Wiestler OD, Pfister SM, von Deimling A. Meningeal hemangiopericytoma and solitary fibrous tumors carry the NAB2-STAT6 fusion and can be diagnosed by nuclear expression of STAT6 protein. Acta Neuropathol. 2013;125:651–8.
86. Robinson DR, Wu YM, Kalyana-Sundaram S, Cao X, Lonigro RJ, Sung YS, Chen CL, Zhang L, Wang R, Su F, Iyer MK, Roychowdhury S, Siddiqui J, Pienta KJ, Kunju LP, Talpaz M, Mosquera JM, Singer S, Schuetze SM, Antonescu CR, Chinnaiyan AM. Identification of recurrent NAB2-STAT6 gene fusions in solitary fibrous tumor by integrative sequencing. Nat Genet. 2013;45:180–5.
87. Wilson RW, Gallateau-Salle F, Moran CA. Desmoid tumors of the pleura: a clinicopathologic mimic of localized fibrous tumor. Mod Pathol. 1999;12:9–14.
88. Nascimento AF, Ruiz R, Hornick JL, Fletcher CD. Calcifying fibrous 'pseudotumor': clinicopathologic study of 15 cases and analysis of its relationship to inflammatory myofibroblastic tumor. Int J Surg Pathol. 2002;10:189–96.

Experimental Lung Tumors

22

22.1 History

Mice, rats, and hamsters have been used as models for human lung cancer since several decades [1, 2]. In the past, mainly inhalation of tobacco smoke and other carcinogenic substances has been applied to these rodent species [3–6]. In most instances, lung carcinomas resembling the human counterpart could not be simulated with the exception of urethane-induced murine models. Moreover, rodents easily and spontaneously develop adenomas but not invasive carcinomas [7]. A cystic squamous lesion was induced in some experiments, which has been labeled as squamous cell carcinoma; however, this represents in essence bronchiectasis with squamous metaplasia and dysplasia, but never progressed into invasive squamous cell carcinoma [8, 9]. In recent time, genetically engineered lung carcinomas in mice became a tool to study carcinogenesis in adenocarcinomas and small-cell carcinomas. In this chapter, we will discuss progress as well as drawback by these different approaches in understanding human pulmonary carcinogenesis.

22.2 Tobacco Inhalation Experiments

In the 1950s and 1960s, many experimental tobacco inhalation studies were performed, some of them funded by the tobacco industry. In these experiments, mice and rats were exposed to tobacco smoke using standardized cigarettes. Inhalation was most often done by nose-only exposure: mice or rats were kept in an inhalation device with their head fixed and had to breathe through their nose tobacco smoke-enriched air for several hours. In other experiments, rats and mice were exposed to tobacco smoke through a tracheal tube inserted surgically into their trachea, thus circumventing breathing through their nose. In these experiments, pulmonary adenomas and adenocarcinomas developed, in rare instances also cystic bronchiectasis with squamous metaplasia and focal dysplasia. The results of these experiments were taken as a proof that tobacco smoking does not cause squamous cell carcinomas nor small-cell carcinomas – at that time regarded as the smoking-induced carcinomas.

22.3 Why Adenocarcinomas in Mice and Rats?

Rodents when exposed to noxious substances in the air will recirculate the air within their large upper respiratory tract especially their large sinuses and clean the air before inhaling it into their lower respiratory tract. When exposed to tobacco smoke via the trachea, the content, including particulates, will be inhaled into the lung periphery, acting on Clara cells and peripheral precursor/stem cells. The airway branching

© Springer-Verlag Berlin Heidelberg 2017
H. Popper, *Pathology of Lung Disease*, DOI 10.1007/978-3-662-50491-8_22

in rodents is dichotomous, which results in an almost ideal laminar flow of the air with tobacco smoke content, in contrast to the asymmetric branching of primate and human airways, where particulates will be trapped at bifurcations by turbulences. Therefore if humans inhale tobacco smoke with particulates (filterless cigarette), these substances will primarily act on the epithelium of large airways, where a program exists for squamous metaplasia and where also precursor cells for SCLC are located – one of the reasons for the occurrence of SCC and SCLC in patients smoking filterless cigarettes. So these inhalation experiments preceded the occurrence of adenocarcinomas in human in the era of the filter cigarette.

22.4 Xenograft Transplantation of Human Carcinomas/Cell Cultures into Nude Mice

New experimental strategies are focusing on xenograft transplantation [10–13]. Human pulmonary carcinomas are transplanted into nude mice, and their behavior and biology are studied. In addition also genetically modified cell lines are also used in xenograft experiments [14–17]. This experimental design has advantages as well as disadvantages: Advantages are the tumors studied are real human tumors, which are biologically identical to the tumor in patients. Their genetic makeup is identical. The disadvantage is that there is no tumor-stroma interaction. So the mouse stroma cells do not recognize the tumor cells, neither cooperate nor act against the tumor. The same is true for the mouse immune system. Therefore the modification of the tumor induced by the stroma and immune system is missing, which makes prediction of behavior impossible.

However, the real advantage of genetically modified cell lines is in the ability to test new drugs. For example, EGFR-mutated adenocarcinoma cell lines can be tested in vitro and in addition also by using xenograft transplantation [16, 18–21].

22.5 Differences in Chemically Induced Lung Tumors Compared to Humans

The use of different carcinogenic substances to induce lung carcinomas goes back to the early 1960s [22, 23]. By using chemical carcinogens, carcinomas could be induced in laboratory animals, especially mice [22, 24]; benzo-a-pyrene was one of the early substances by which pulmonary carcinomas could be induced in different animal models [25–29]. These chemically induced lung carcinomas have regained interest in recent years [30–33]. Some of these models when an intratracheal instillation technology was used developed squamous cell and undifferentiated pulmonary carcinomas. Other substances such as urethane when injected induce adenocarcinomas. The advantage of chemically induced carcinogenesis in laboratory animals is that the chemicals induce a similar spectrum of genetic aberrations as tobacco smoking-induced carcinomas in humans. However, the genetic spectrum of aberrations is not constant.

Another problem of inducing lung tumors by chemical substances is the formation of spontaneous adenomas in mice.

22.6 The Urethane Model

In the 1980s and 1990s, lung carcinomas were induced by injections of different chemicals such as urethane. It took some time until it was discovered that the selection of the mouse strain also is important, as in some strains this did not work. In A/J strain of mice, urethane (ethyl carbamate) induced lung hyperplasia, adenoma, and adenocarcinoma. These morphologic stages correlated with sequential molecular genetic changes where KRAS mutations arose early and p53 mutations late in tumorigenesis. KRAS mutations were predominantly seen at codon 61 and p53 mutations in exons 5–8 [34]. A comparison of genetic changes between the mouse model and human tumor samples showed 409 genes common in the mouse model and in human tissues. A number of

changes were recapitulated such as changes in glycolytic enzymes and cell cycle proteins. However, genes coding for angiogenesis were differently expressed. Therefore the A/J mouse-urethane model reflects several but not all molecular details of human lung AC [6]. A further study using this model in combination with tobacco smoke exposure failed. The results of this study showed no significant difference in the number of nodules and hyperplasia between a urethane-only and three urethane and cigarette smoke-exposed groups of Balb/c mice in the lung [35]. Another study compared exposure of methyl-nitrosourea (MNU) or urethane with mutated KRAS-induced lung carcinomas. Although the MNU-induced tumors carried exactly the same initiating mutation in KRAS as seen in the KRAS model (G12D), MNU tumors had 192 somatic single-nucleotide variants, compared to six in tumors from the KRAS model. But the KRAS tumors exhibited a significantly higher level of aneuploidy and copy number alterations compared with the carcinogen-induced tumors, suggesting that carcinogen-induced and genetically engineered models lead to tumor development through different routes. In addition the urethane-induced tumors carry predominantly KRAS Q61R mutations, whereas those from KRAS animals carry predominantly KRAS Q61L mutations [36]. Another aspect of urethane-induced carcinomas is the fact that besides lung carcinomas also tumors in other organs are induced.

22.7 Genetically Engineered Mouse Models of Lung Cancer

In recent times, genetically engineered mouse models, which express oncogenes or have lost tumor suppressor genes for lung cancer formation, have been developed. The genetically induced lung tumors in these models closely resemble human tumors [37–41].

Descriptions of these types of tumors have been published by experimental and veterinary pathologists, which, however, are not experienced in human pathology. On the other hand, most pulmonary pathologists have no experience with these experimental models or with differences of the architecture of the rodent compared to human lung. One of the aims therefore is to answer the question to which extent human lung cancer can be histopathologically modeled in mice.

We have already discussed the spectrum of human pulmonary carcinomas. So here we have to discuss comparative morphology in diseased and healthy lungs from mammalians, but also across the animal kingdom. To evaluate genetically engineered lung tumors in laboratory animals and to interpret them require the understanding of normal lung anatomy and histology with respect to differences and similarities in the architecture as well as the distribution of epithelial and mesenchymal cells in the human lung. For example, the delivery of carcinogens by inhalation will result in a high concentration at the bronchioloalveolar junction and in alveoli due to the dichotomous branching of the rodent lung and the almost laminar airstream.

Lung tumors in mice can be genetically induced by expression of oncogenes in pulmonary cells. A popular model is LSL-KRAS^{G12D} mice that express the KRAS^{G12D} oncogene in pulmonary cells after Adeno-Cre or Lenti-Cre inhalation [37–39, 42–45]. Oncogenes can also be stochastically expressed after Cre-mediated activation, which allows investigation of gene cooperation [46]. These efforts have resulted in the generation of adenocarcinomas, but not squamous cell carcinomas. Moreover, five laboratories have described mouse models for small-cell lung cancer that are based on double deletion of TP53/RB [43] or triple deletion of TP53/RB/PTEN tumor suppressors [47].

22.7.1 The Pulmonary Adenocarcinoma Models

Lung tumors were induced in HRAS-driven Multi-Hit mice, which allow stochastic activation of MAPK, RAL, and PI3K effector pathways

[46] and LSL-KRAS^{G12D} mice harboring additional genetic modifications (knockout of RANK, apelin, or ATG5) using inhalation of Cre-expressing viruses. In a subset of HRAS-driven Multi-Hit mice, TP53 or PTEN genes were deleted. In each of the above experiments between 7 and 70 lungs, tumors developed in mouse lungs. A morphologic sequence from hyperplasia to atypical proliferation to adenoma to adenocarcinoma in situ and invasive adenocarcinoma was found.

22.7.2 Histopathology of Adenocarcinomas

In all KRAS oncogene activated mice – regardless of additional genetic alterations – hyperplasia of type II pneumocytes could be found (Fig. 22.1), in several experiments also nodular aggregates of pneumocytes (nodular hyperplasia; Fig. 22.2). These proliferations, however, never progressed into high-grade malignancies. In these proliferations, the morphologic differentiation of type II pneumocytes could be seen, sometimes also a cuboidal transformation of pneumocytes, which is well known in human lung pathology as reactive, reparative, or preneoplastic. Nuclear to cytoplasmic ratio was only slightly increased, but not that amount one will see in neoplasia.

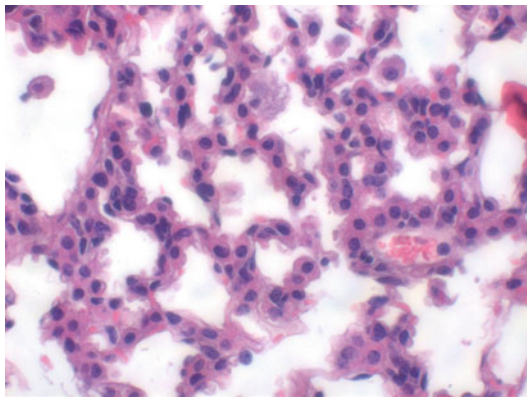

Fig. 22.1 Diffuse hyperplasia of pneumocytes type II in the mouse, induced by expressing mutant KRAS or HRAS. H&E, ×400

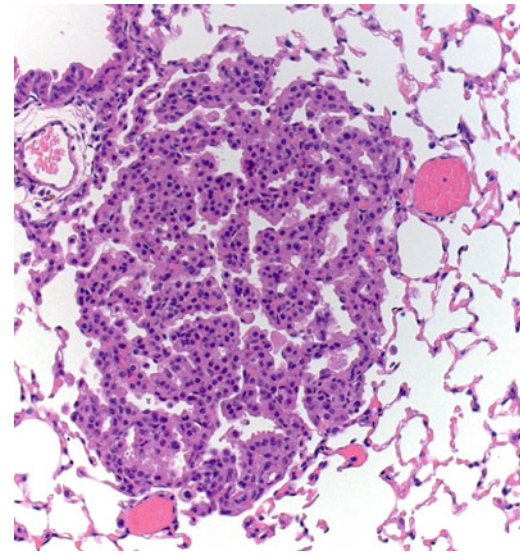

Fig. 22.2 Nodular hyperplasia of pneumocytes and slit-like spaces of alveoli in some areas. H&E, ×200

KRAS as well as HRAS oncogenes induced another type of proliferation at the bronchioloalveolar junction. This type of proliferation started as an expansion of epithelial cells at the basal layer of the terminal bronchiolar epithelium (basal or reserve/stem cells). The cells were polygonal or cuboidal and had larger than normal nuclei with still regularly distributed chromatin. Nucleoli were inconspicuous; the cells looked similar to regenerating epithelia (Figs. 22.3, 22.4, and, 22.5). In some cases, atypia was seen early on, the polymorphous nuclei were enlarged, the chromatin was coarse, and nucleoli were enlarged (Fig. 22.6). This proliferation later on developed into a micropapillary epithelial proliferation and further on acquired a mesenchymal stalk with newly formed capillary loops and primitive mesenchymal stroma cells, thus presenting as a papillary preneoplasia. This proliferation extended into the peripheral alveoli, completely filling the air spaces (Fig. 22.7). Since the alveoli in mice are smaller compared to human lung, but the mouse transformed epithelial cells are not as small, these lesions often appeared solid (the ratio of cell diameter of pneumocytes II and alveolar diameter is different across the different mammalian species). Only at high magnification, a slit-like alveolar lumen could be seen. Nodules

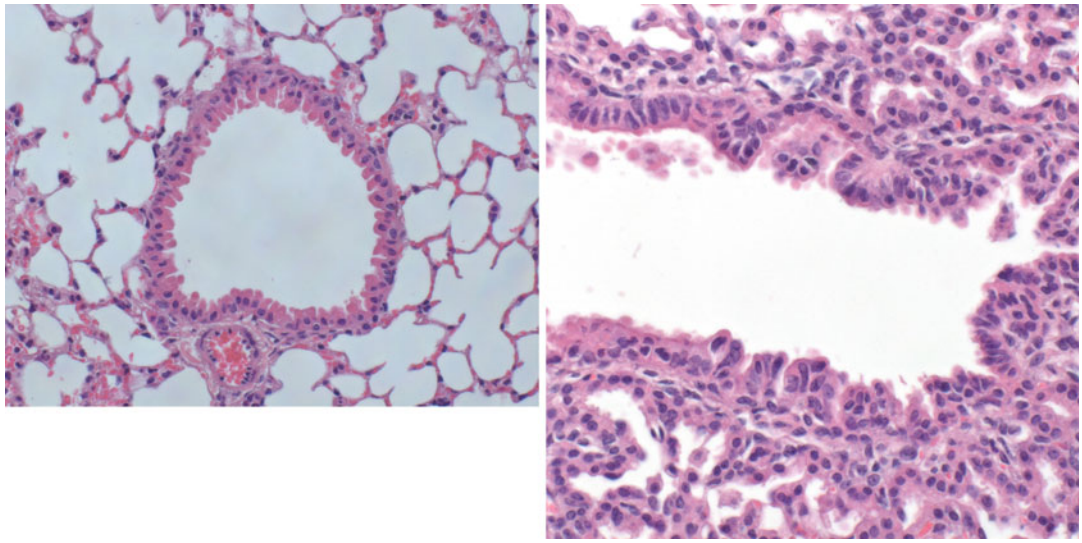

Fig. 22.3 Preneoplastic proliferation of cells at the bronchioloalveolar junction. *Left* normal bronchiolar epithelium (single cell row, few reserve cells). *Right* expansion of preneoplastic cells at the basis of a bronchioles (at least double layers of cells). H&E, ×200

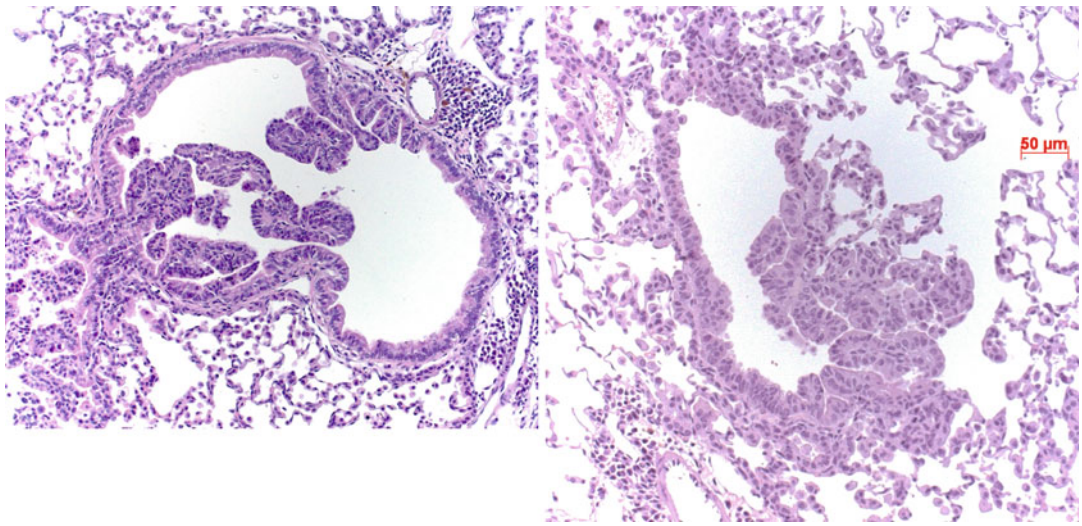

Fig. 22.4 Later stage with papillary proliferations into the bronchiolar lumen (*left*) and expansion into the adjacent alveoli (*right*). Note stroma formation and newly formed capillaries. H&E, bar 50 µm

grew larger (up to 1 cm) and developed central necrosis, most probably due to hypoxia (Fig. 22.8). However, no invasion occurred at this time, but the cytological atypia qualified these lesions as an in situ adenocarcinoma: nuclear to cytoplasmic ratio was >50 %, nuclear chromatin was irregular distributed, nucleoli were increased in size, and few mitotic figures were found.

Within these larger nodules of in situ adenocarcinomas, necrosis did occur. Almost concomitant with necrosis, neoangiogenesis started (Fig. 22.9). Primitive stroma cells were seen expressing CD31 and CD34, deposition of newly synthesized matrix proteins occurred, primitive capillaries were formed, and the stroma developed features of a desmoplastic stroma reaction comparable to

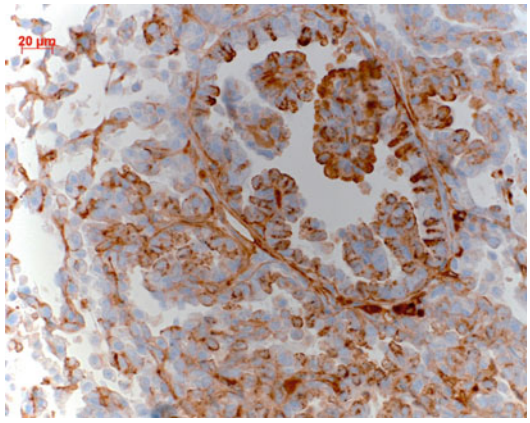

Fig. 22.5 Preneoplastic papillary proliferation at the bronchioloalveolar junction zone (BAJ) shows still a differentiation toward bronchiolar epithelium demonstrated by positivity for Clara cell protein 10. Bar 20 µm

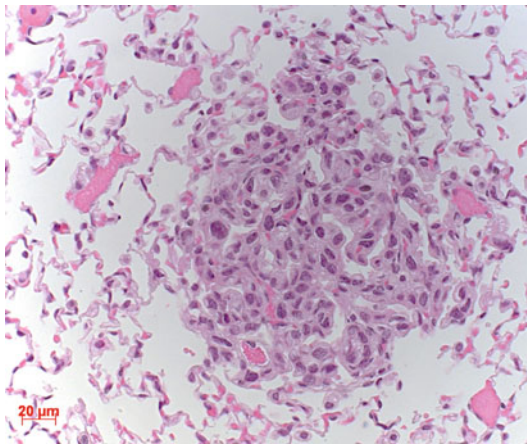

Fig. 22.6 Atypia early on in this preneoplastic proliferation at the bronchioloalveolar junction. H&E, bar 20 µm

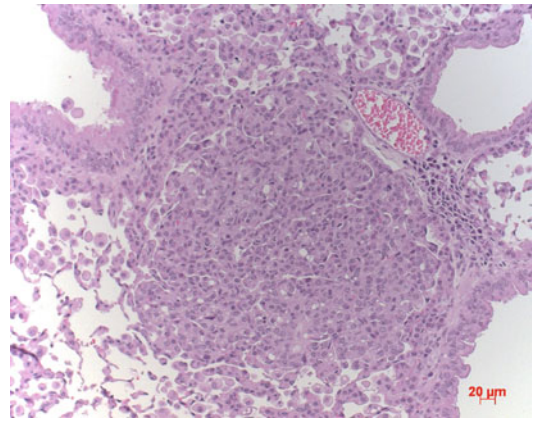

Fig. 22.7 Extension of the papillary proliferation into the alveolar tissue, completely filling the lumina. H&E, bar 20 µm

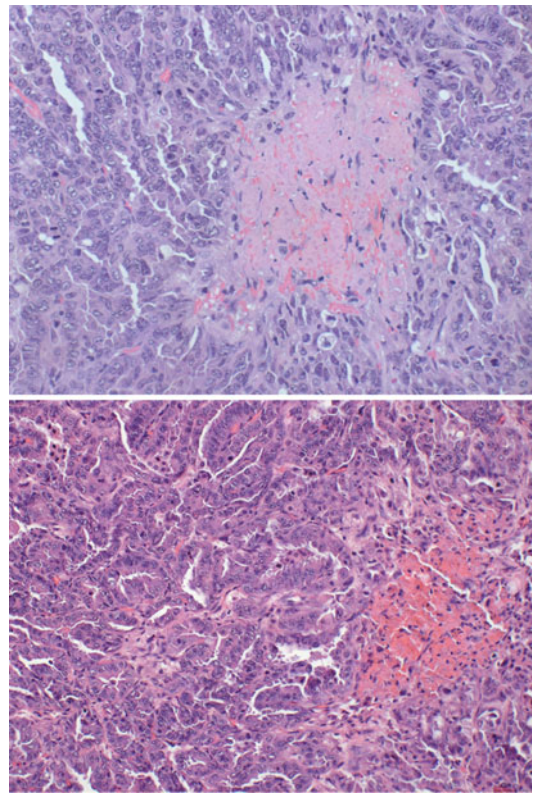

Fig. 22.8 Adenocarcinoma in situ with central necrosis, in the case to the right additionally bleeding into the necrosis. H&E, ×200

that seen in human carcinomas (Fig. 22.9). Once desmoplastic stroma has developed, the tumor cells started to invade this stroma, developing into invasive adenocarcinomas (Fig. 22.9). Angioinvasion was found in some cases (Fig. 22.10), but it seems that an interaction of different genes is necessary: in the HRAS Multi-Hit model, angioinvasion was only seen in those adenocarcinomas, which harbored activation of all three RAS effectors (MAPK, RAL, and PI3K) or additional TP53 or PTEN inactivation [48].

In some models, peripheral adenomas developed in addition to nodular hyperplasia. The difference between nodular hyperplasia and adenoma is preservation of the alveolar structure in nodular

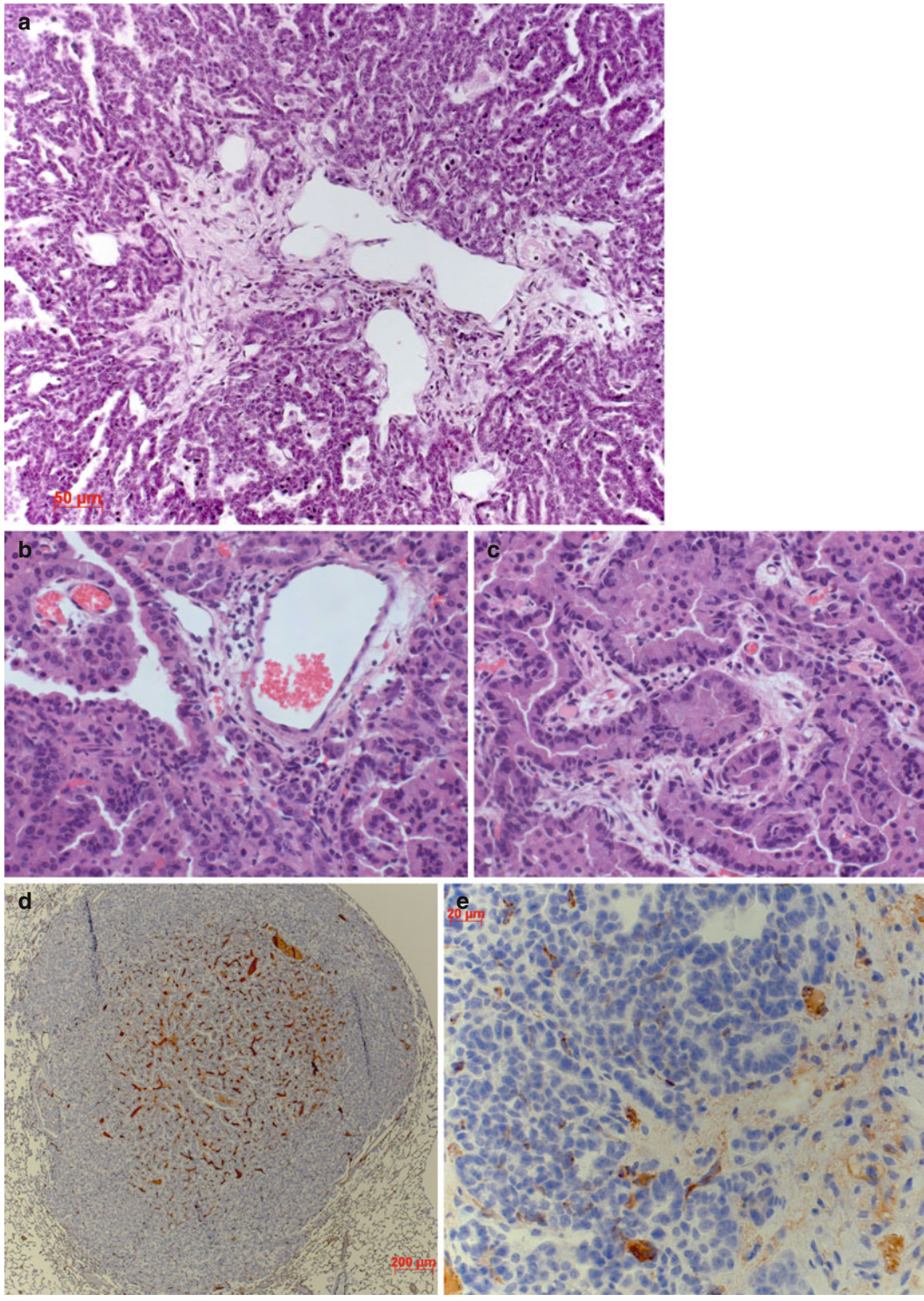

Fig. 22.9 (**a**) Invasive adenocarcinoma, note the desmoplastic stroma in the center, which had replaced the necrosis. (**b**, **c**) Details of areas of invasion. There are single cells (**b**) as well as small complexes of adenocarcinoma invading the stroma. (**d**) Neoangiogenesis is seen in the necrotic center of an adenocarcinoma and specifically at the border of invasion (**e**). H&E, immunohistochemistry with CD31 antibodies, bars 200, 50, and 20 µm

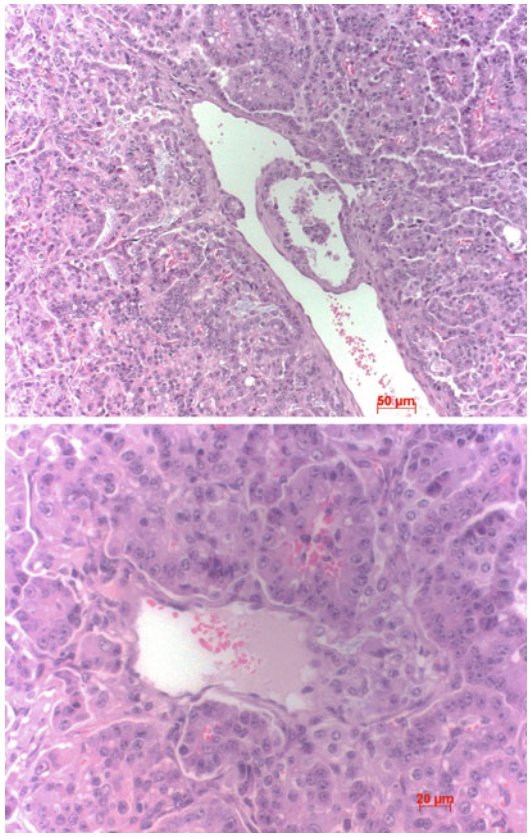

Fig. 22.10 Invasive adenocarcinoma with angioinvasion, two different examples are shown. H&E, bars 50 and 20 µm

hyperplasia and the original capillary network confined to the alveolar septa, whereas in adenomas the alveolar architecture is lost, and new capillaries are formed. In all models studied, these adenomas never progressed into a malignant lesion.

22.7.3 Immunohistochemistry as an Aid to Identify the Precursor Cell Population

Clara cells expressed Clara cell protein 10 (CC10) in normal bronchi and bronchioles. During the papillary proliferations starting from the bronchioloalveolar junction, the expression of CC10 was still retained within the cuboidal cells but, however, was lost in most cells, when adenocarcinomas in situ were formed (Fig. 22.11). Only single cells still expressed this protein. A similar reaction was

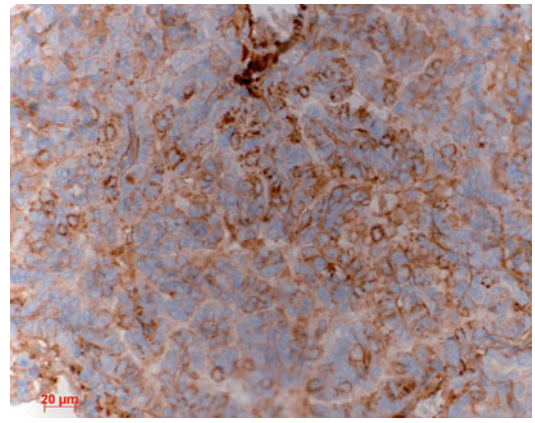

Fig. 22.11 Loss of Clara cell protein 10 expression during the development of an in situ adenocarcinoma. Some cells still express CC10; others are negative. Immunohistochemistry for CC10 protein

seen for surfactant apoproteins (SApo): type II pneumocytes expressed SApoA and SApoB, and this expression was retained in pneumocyte hyperplasia, diffuse as well as nodular. In peripheral adenomas, this expression was lost in almost all cells. Few proliferating cells in the papillary bronchioloalveolar junction expressed SApoB. In adenocarcinomas in situ, this expression was lost; however, in invasive adenocarcinomas, SApoB could be demonstrated in the more differentiated cells in the center of the adenocarcinoma, especially in the papillary component. SApoC was expressed in pneumocytes type II in hyperplasia, but single cells also expressed SApoC in the bronchioloalveolar junction papillary proliferations. Also in adenocarcinomas in situ and in invasive adenocarcinomas, single cells and small-cell clusters expressed SApoC.

Using double staining for CC10 and SApoC in selected cases, double staining for these markers occurred in very few or only single cells (Fig. 22.12). Cells coexpressing CC10 and SApoC are regarded as peripheral stem cells residing in the niches of bronchioloalveolar junctions [49]. There was no expansion of these cells indicating that the tumor proliferation most probably started from more differentiated cells and not peripheral stem cells. The proliferation starting from the bronchioloalveolar junction was constantly positive for pan-cytokeratin, ruling

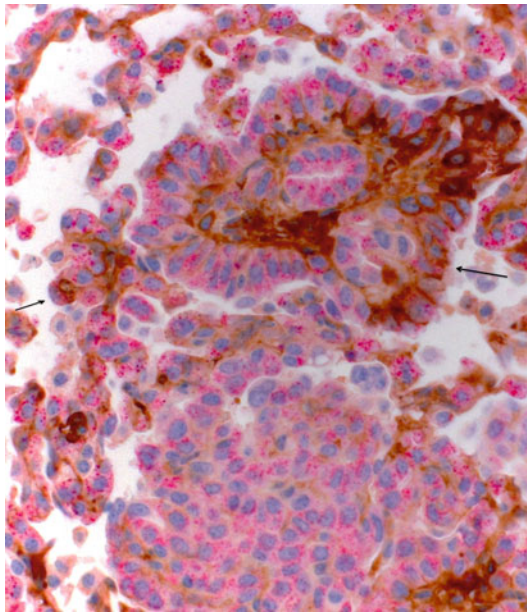

Fig. 22.12 Coexpression of CC10 and SApoC in cells of an in situ adenocarcinoma. Only a few cells coexpressed both markers (*arrows*), which characterize them as peripheral lung stem cells. Immunohistochemistry with antibodies for CC10 (*brown*) and SApoC (*red*), ×400

out the presence of newly invading hematopoietic stem cells as the source of tumor cells [48].

Within the necrotic centers, newly formed blood vessels could be seen using immunohistochemistry for CD31 and CD 34. When immunohistochemistry was applied for podoplanin, which is a marker of endothelia of small blood vessels and lymphatics, dilated lymphatics were seen at the periphery of the in situ adenocarcinomas, but not in the necrotic centers (Fig. 22.9d, e). Neoangiogenesis of lymphatics was only seen after new blood vessels already appeared in the hemorrhagic or necrotic centers of the carcinomas. Lymphangiogenesis accompanied the invasion of the carcinomas, but did not precede it.

22.7.4 Progression of Adenocarcinomas

Stromal invasion in all mouse models depended on tumor size, the occurrence of hypoxia in the center, necrosis, desmoplastic stroma reaction, and angiogenesis. Invasion occurred only in large nodules within their center. The morphologic changes preceding invasion were hemorrhage and infarct-like necrosis suggesting a prominent role of hypoxia. Necrosis and hemorrhage were followed by formation of desmoplastic stroma and primitive blood vessels. Carcinoma cells invaded predominantly into the newly formed modified stroma. Importantly, hypoxia seems to promote invasiveness of human carcinomas [50–53] as well indicating that the mouse models could be an ideal tool to study the association of hypoxia, invasion, and metastasis.

Epithelial to mesenchymal transition (EMT) is a mechanism, which facilitates invasion and oriented tumor cell movement within the stroma. It can be easily diagnosed by the spindle cell morphology of the tumor cells, which express cytokeratin, vimentin, and smooth muscle actin (cytokeratin expression can even be lost). In humans, the most instructive lung cancer type displaying features for EMT is sarcomatoid carcinoma (spindle cell and pleomorphic carcinoma). The molecular basis for EMT in lung carcinomas might be pleiotropic and cannot be attributed to single genes [20, 54–66]. In the investigated mouse models, EMT seemed to play a minor role and was only represented in a single tumor by a small focus of cells with less than 1 mm in diameter. Here tumor cells acquired typical spindle cell morphology, but still retained expression of cytokeratin (Fig. 22.13) [48].

Invasion into blood vessel required additional genetic aberrations such as TP53 or PTEN deletion in HRAS Multi-Hit mice. Interestingly none of the adenocarcinomas in various mice displayed metastasis, which might be due to tumor overload. Up to 70 foci in lungs and additional pneumocyte hyperplasia might have reduced the ability of oxygenation, because type II pneumocytes are large and increased the distance between alveolar and capillary lumina. Therefore, even in cases with angioinvasion, the animals might have died due to respiratory insufficiency before metastasis could occur. Moreover, as pointed out above, induction of metastasis might require additional genetic modifications [67, 68].

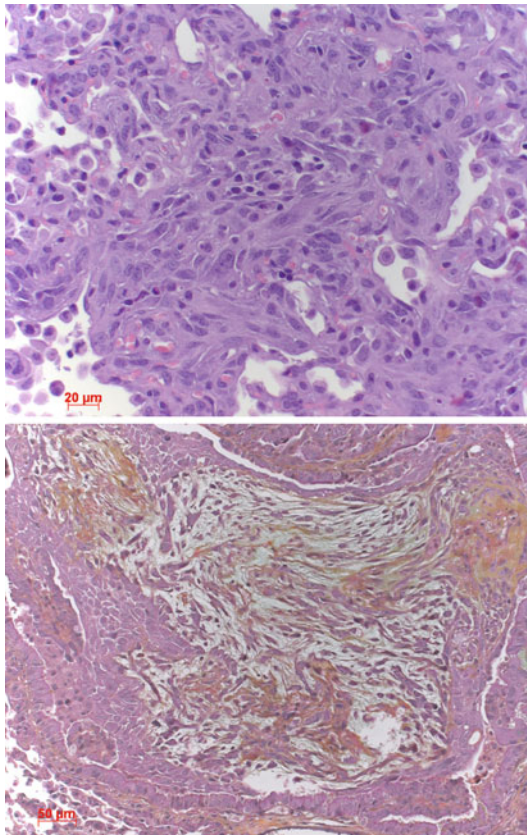

Fig. 22.13 Epithelial to mesenchymal transition (EMT) in a small invasive adenocarcinoma. The spindle cells in the center showed longitudinal microfilaments illustrated by immunohistochemistry for vimentin (not shown). There are a few lymphocytes within the central stroma where tumor cells already have invaded (*upper panel*). In the *lower* panel, EMT is associated with invasion in this adenocarcinoma. It is difficult to sort desmoplastic stroma cells versus adenocarcinoma cells with spindle cell morphology. However, the large atypical nuclei in the latter help for the separation. H&E, Movat, bars 50 and 20 µm

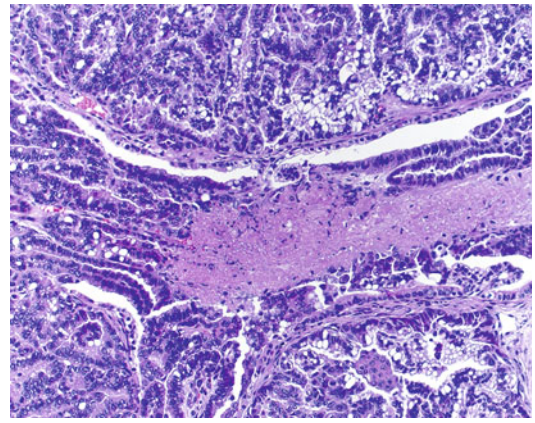

Fig. 22.14 Pseudo-signet ring cell formation in the KRAS-induced mouse model with knockout of apelin. H&E, ×200

22.7.5 Specific Changes Induced by Genetic Modifications

22.7.5.1 Signet Ring Cell Formation

Signet ring cell formation was not observed in the bronchioloalveolar junction papillary hyperplasia. It should be noted that signet ring cell morphology in the mouse models did not exactly reflect signet ring cell carcinomas in humans: most human signet ring cell carcinomas show accumulation of mucins within vacuoles formed within the cell cytoplasm. In the mouse models, no mucinous material is present, although the morphologic features are almost identical to human tumors. In mice the content in the cytoplasmic vacuole is more likely composed of lipids, which are usually dissolved during tissue processing. However, there was a wide variation in numbers of signet ring cells in mouse models, which correlated with genetic manipulations. Only a few signet ring cells could be encountered in HRAS Multi-Hit mice and in KRAS models with deletion of RANK or ATG5, whereas substantial and sometimes even dominant signet ring cell differentiation was found in KRAS-induced adenocarcinomas with deletion of apelin (Fig. 22.14).

22.7.5.2 Oxyphilic/Oncocytic Changes

In the KRAS model with deletion of ATG5, an oncocytic transformation was seen across the whole sequence of tumor progression, starting with pneumocyte hyperplasia, peripheral adenomas, in situ adenocarcinomas, and invasive adenocarcinomas. Oxyphilic/oncocytic transformation was absent in all other mouse models.

22.7.6 Do Mouse Adenocarcinomas Resemble Human Adenocarcinomas?

The morphology of mouse lung carcinomas, induced by exposure to carcinogens, has been described in previous reports [8, 69, 70]. These chemical models never simulated adenocarcinomas of humans although rare cases of mucinous tumors were reported. Even squamous cell carcinomas were predominantly characterized as cystic tumors surrounded by an atypical squamous epithelium without signs of invasiveness. Genetically induced mouse lung tumors [5, 71] resembled human adenocarcinomas more precisely, but the sequence of events in mouse models was most often described by basic researchers not familiar with human lung carcinoma morphology. Recently, a consensus conference established a nomenclature for proliferative lesions evolving in mouse models [72]. This classification is a first step to precisely define the different sequences of proliferation in mouse models, but some aspects are still missing:

1. Human lung adenocarcinomas arise after decades of carcinogen exposure, whereas tumors in mouse models develop within weeks.
2. Only a few genetic changes give rise to mouse adenocarcinomas, which is in contrast to human tumors.
3. Differences in the anatomy and histology of mouse and human lungs have not been taken into account.

Human adenocarcinomas can be separated into the common peripheral types, presenting with a lepidic, acinar, micropapillary, cribriform, and/or solid pattern. Usually one pattern is predominant but rarely only one pattern is present. In addition, peripheral adenocarcinomas can be further separated into mucinous and non-mucinous types. Rarely, a mixed mucinous and non-mucinous morphology can be observed. In addition, some rare variants exist such as fetal-, intestinal-, or colloid-type adenocarcinomas [73, 74]. Moreover, rare central adenocarcinomas with a morphologic pattern resembling bronchial glands but also solid and acinar adenocarcinomas can occur.

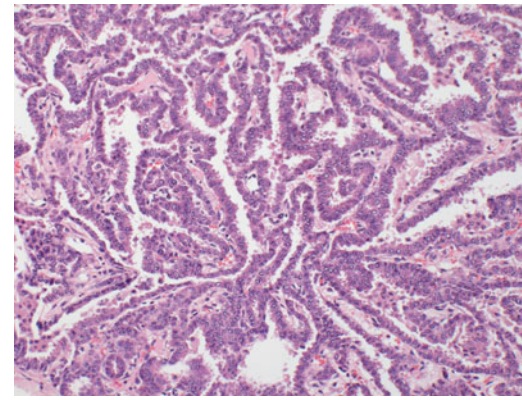

Fig. 22.15 Invasive adenocarcinoma with differentiation into papillary subtype. H&E, ×200

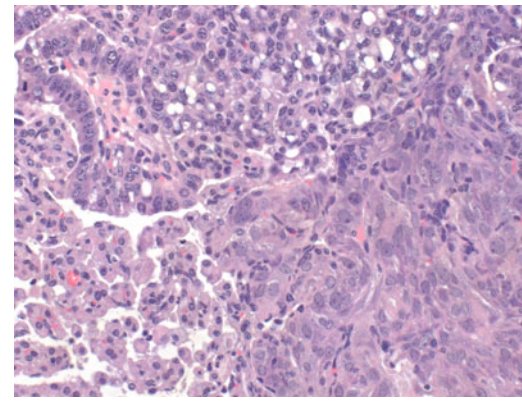

Fig. 22.16 Invasive adenocarcinoma with a solid highly atypical component in the right lower area and a better differentiated one on *top*. H&E, ×200

Adenocarcinomas in different mouse models morphologically present as papillary (Fig. 22.15) and solid types, where solid forms (Fig. 22.16) have to be carefully evaluated, because they are often pseudo-solid due to the filling of the alveoli with tumor cells. This is a common morphology of in situ adenocarcinomas. Lepidic, micropapillary, cribriform non-mucinous, and various forms of mucinous adenocarcinomas are never observed.

Lepidic adenocarcinomas probably could not develop in a mouse lung because of the small diameter of alveoli and the relatively large size of the tumor cells. Therefore, in situ adenocarcinomas often showed a pseudo-solid morphology, but slit-like spaces of alveolar remnants are identified on higher magnification. Other types of adenocarcinomas are not formed because additional stimuli (e.g., for goblet cell formation) are missing during early steps of carcinogenesis [75–79]. Thus, only a small percentage of human pulmonary adenocarcinomas are morphologically represented in the mouse models, and for the vast majority, no suitable model exists.

The histopathology of HRAS- and KRAS-induced tumors suggests that these mice represent a model for non-mucinous peripheral thyroid transcription factor-1 (TTF1)-positive human adenocarcinomas. Papillary and solid differentiation was most commonly found in KRAS models, whereas solid and acinar adenocarcinomas were predominantly seen in HRAS models. Additional genetic modifications might be needed for development of micropapillary or cribriform non-mucinous adenocarcinomas as observed in human patients.

22.7.7 Differences in Mouse and Human Lung Morphology as Explanation for Different Adenocarcinoma Appearance

The fate of inhaled material is quite different in humans and mice: particulate materials are predominantly cleared in the upper respiratory tract of mice. The inhaled air circulates within the large sinusoidal areas where particulates are deposited. Therefore, inhaled particulates being either toxic and/or carcinogenic will act primarily in the upper respiratory tract [80, 81]. In addition, the airways of the mouse lung branch in a dichotomous manner, i.e., each bronchus divides into two equally sized bronchial branches. This results in an almost laminar airflow, and particles with an aerodynamic diameter of <2 μm will be deposited in the peripheral lung. In contrast, there is not much clearance of particulates in the nose and nasal sinuses of humans, but due to an asymmetric bronchial branching (a bronchus divides into a main branch with two thirds of the diameter and a minor bronchus with one-third diameter), particulates are deposited in the larger bronchi due to turbulences at the bifurcations. Therefore, even particulates with a small aerodynamic diameter might already be filtered out at central bronchial bifurcations. In human bronchi, the number of branches outnumbers those of mice more than three times, and the cell composition and distribution are different: in human bronchi, the ratio of ciliated to goblet cells is 6–8:1, whereas the number of goblet cells in the mouse is significantly lower. Ciliated cells occur in human lungs down to the larger bronchioles, whereas in mouse lungs, bronchioles are almost devoid of ciliated cells. In contrast, Clara cells in mouse lungs do not only occur in a substantial number in bronchioles, but also larger bronchi, whereas in human lungs, these cells are mainly confined to the terminal bronchioles and alveolar ducts. Secretory cells are forming one compartment in human and mouse bronchioles, but have been renamed as tuft cells or pneumocytes type III in mice. Short microvilli and secretory granules in the cytoplasm characterize these cells [82, 83]. Their function is unknown, but they can be found in well-differentiated peripheral human lung adenocarcinomas. These morphologic differences might partially explain some of the differences between human and mouse adenocarcinomas.

22.7.8 Genetic Differences Between Mouse and Human Adenocarcinomas

Most genetic lung cancer mouse models are based on mutations of RAS genes, in particular KRAS. In humans, KRAS mutations are found

in ~50 % of mucinous [84] and less frequently in non-mucinous adenocarcinomas (<25 %), whereas adenocarcinomas in KRAS mouse models are all non-mucinous. As stated above, KRAS-induced mouse adenocarcinomas show papillary and pseudo-solid morphologic differentiation. In contrast, human non-mucinous adenocarcinomas of papillary or acinar morphology display mutations of EGFR in >25 % of cases.

Mucinous differentiation in carcinogenesis starts early on as goblet cell metaplasia and dysplasia. The genetic basis of this kind of differentiation is only marginally understood. Takeyama showed that MUC5AC production and goblet cell proliferation are regulated by EGFR ligands EGF and TGFα [85]. However, if EGFR activation results in goblet cell proliferation, why do mucinous adenocarcinomas not harbor EGFR mutations? In an animal model of asthma, IL13 and IL4 stimulated MUC5AC mRNA expression and induced goblet cell proliferation. Similarly, airway inflammation had a similar effect via stimulation of IL4 and IL13 release [86–88]. Related to carcinogenesis, expression of IL4, IL4R, and MUC2 proteins was demonstrated in proliferating goblet cells of pulmonary cystic adenomatoid malformations [78]. Inflammatory changes preceding carcinoma formation are commonly observed in human patients indicating that different interleukins may be involved [79, 85, 89–91]. RAS mutations could act synergistically with tumor-promoting effects of inflammation. Human mucinous adenocarcinomas harboring KRAS mutations usually arise in cigarette smokers. Airway inflammation is a common phenomenon in these patients. Many of them develop lung cancer but also chronic obstructive lung disease (COPD). One of the clinical characteristics of COPD is mucus expectoration long before lung carcinomas arise. This indicates that mucinous differentiation manifests early in precursor lesions and is retained in developing adenocarcinomas. KRAS mutation might be a later event, after goblet cell hyperplasia has occurred.

22.7.9 Cellular Origin of Adenocarcinomas

In human lungs and in other mammalian species, peripheral stem cells are found within the bronchioloalveolar junction. These cells have been characterized by concomitant expression of CC10, surfactant apoprotein B/C, and stem cell markers CD34 and CD133 [92–95]. In contrast, pneumocytes type II have regenerative capacity (cell division, differentiation into Clara cells and type I pneumocytes) but are not stem cells. The same is true for Clara cells within the bronchiolar epithelium, which has been demonstrated by ablation of these cells with specific toxic compounds [96]. Clara cells in mice and other mammalians (but not humans) can also be found in larger bronchi and even the trachea.

Although the bronchioloalveolar junction was the location where papillary bronchiolar hyperplasia started in genetic mouse models, more differentiated cells with Clara and basal cell morphology, but not peripheral stem cells, gave rise to in situ adenocarcinomas and invasive adenocarcinomas. This is evident by the scarce presence of tumor cells stained by CC10 and SurfApoC. This might reflect the mode of induction of these tumors, which is based on oncogene activation but not intoxication. Activation of an oncogene might result in expansion of more differentiated cells that accumulate additional mutations. In contrast, a stem cell proliferation within the peripheral lung needs a regenerative stimulus such as eradication of large amounts of alveolar and bronchiolar cells by toxins [97–100].

22.7.10 The Small-Cell Carcinoma Models

Several attempts were made to create a small-cell carcinoma model [47, 101–104]. A few of them succeeded in this attempt and created a centrally located small-cell carcinoma in

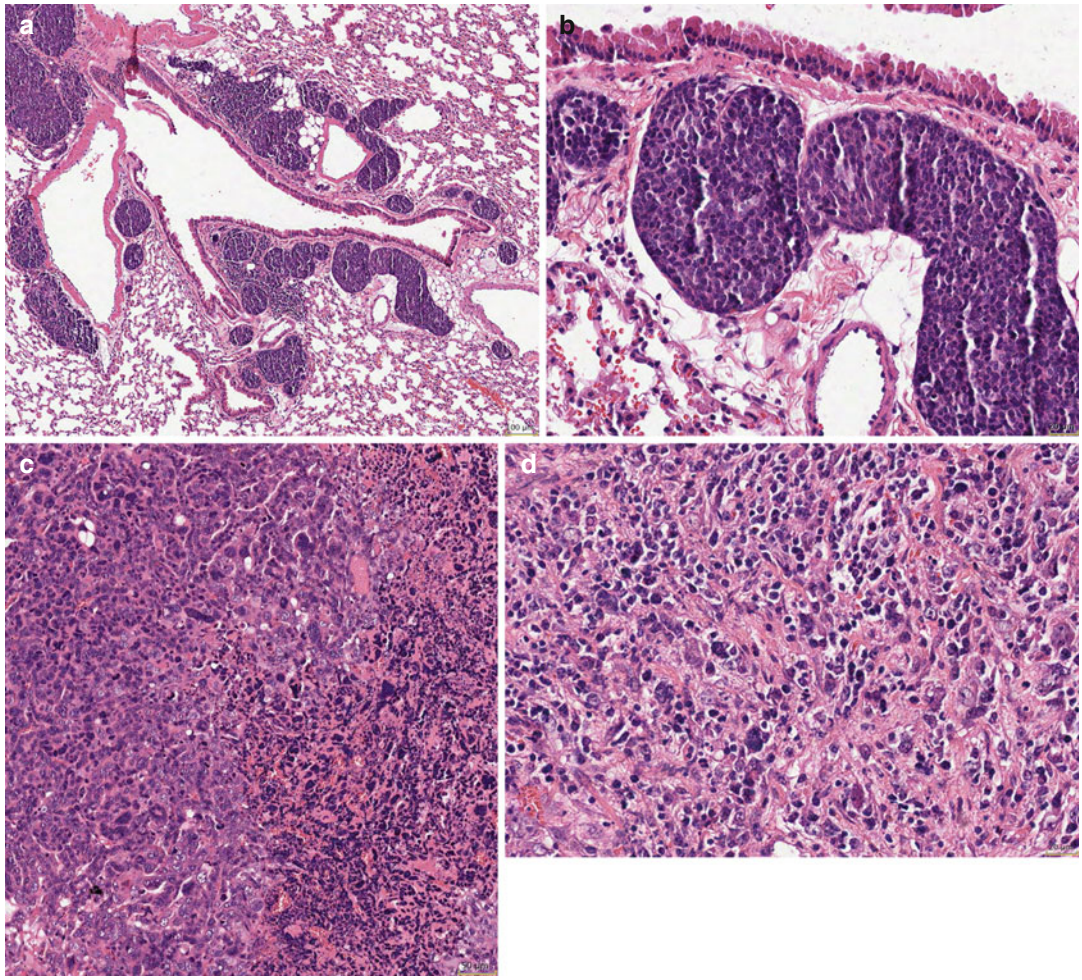

Fig. 22.17 Undifferentiated and high-grade solid adenocarcinoma created in an attempt for SCLC. In (**a**) it is evident that the tumor developed not out of the bronchial mucosa but underneath – this is shown in higher magnification in (**b**). The tumor cells have large nuclei and enlarged nucleoli; the chromatin pattern is coarse granular and not dense as in SCLC. In (**c**) there are formations of an adenocarcinoma, whereas what looks like SCLC is apoptosis. In (**b**–**d**) the nuclear features are seen, which do not fit with those of a SCLC. Due to the expression of ASH1, several of these carcinomas express neuroendocrine markers, but this would only shift them into NSCLC with neuroendocrine features. H&E, bars 100, 50, and 20 μm

mice. When looking up these models, three of them created small-cell carcinoma analogs based on conditional deletion of RB and TP53, however, in peripheral stem cells or Clara cells. Not surprisingly these carcinomas looked like undifferentiated solid adenocarcinomas, presenting with large visible nucleoli and a coarse chromatin pattern (Fig. 22.17). Some expressed neuroendocrine markers, especially if there was also an expression for ASH1 [47]. In one of those cases, the tumor resembled morphologically a SCLC, but lacked the expression of neuroendocrine markers. In a few of these cases not unexpectedly, also adenocarcinomas were induced. A few of these experiments succeeded in the induction of a centrally located SCLC [103, 105]. These carcinomas showed early foci of carcinomas with small round and spindle cell nuclei, dense chromatin pattern, and almost invisible nucleoli (Fig. 22.18). Other carcinomas were more comparable to large-cell

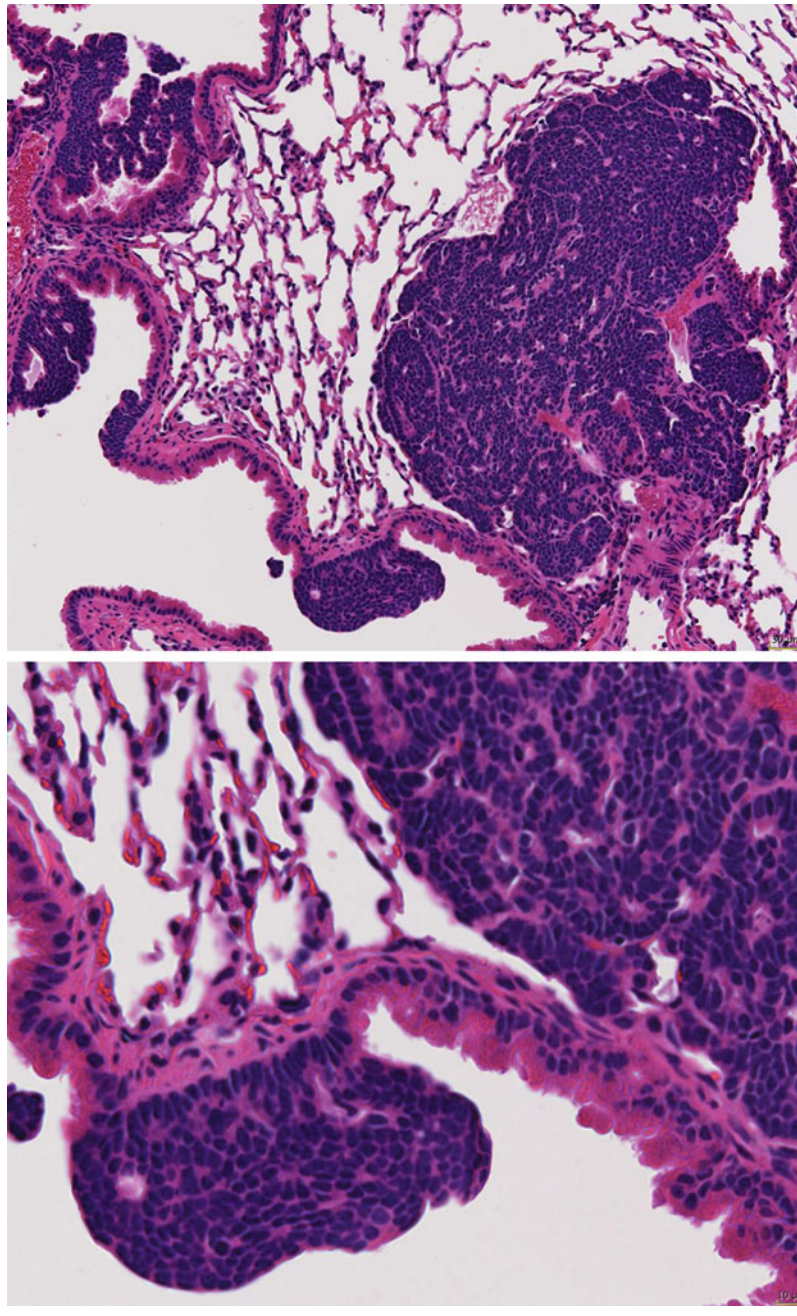

Fig. 22.18 Small-cell neuroendocrine carcinoma in a mouse induced by RB loss and TP53 mutation. In some also PTEN loss was induced. The nuclei show dense dark chromatin, nucleoli are invisible, and cytoplasm is small. The carcinoma foci start within central airways, similar to what is seen in human SCLC. Interestingly in the mouse tumors, the neuroendocrine structures, especially rosettes, are nicely formed. *Upper* panel shows an overview and *lower* panel a higher magnification of two foci. H&E, bars 30 and 10 μm (Courtesy of Adi Gazdar, Dallas)

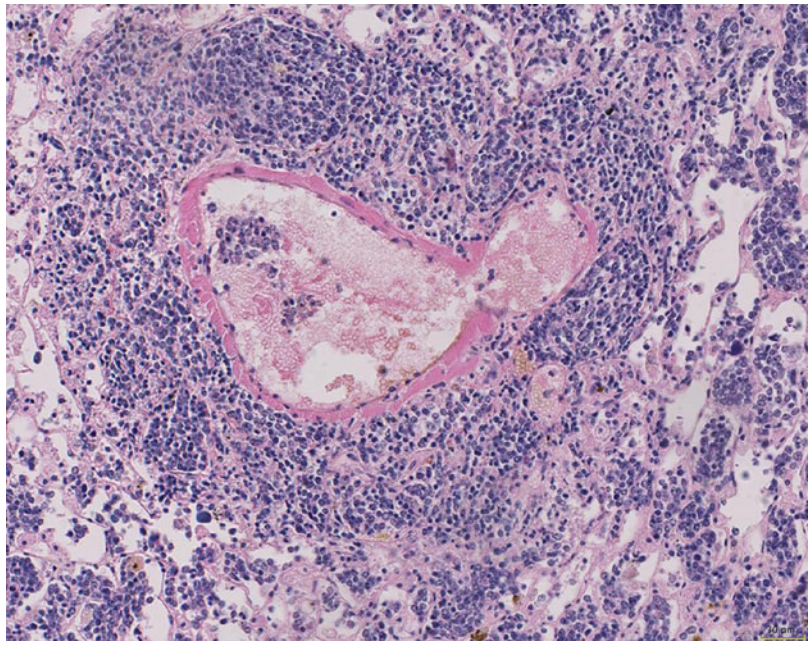

Fig. 22.19 Other examples of a neuroendocrine carcinoma, here differentiated into a large-cell neuroendocrine carcinoma with large nuclei and enlarged nucleoli. Also chromatin pattern is vesicular and not dense. H&E, bar 30 μm

neuroendocrine carcinomas with larger nuclei, more cytoplasm, and enlarged nucleoli (Fig. 22.19). The tumors expressed neuroendocrine markers. In subsequent studies, several important findings were reported such as paracrine signaling between SCLC subclones as critical for metastasis, local invasion, and intravasation. The most important genes were fibroblast growth factor 2 (FGF2) and MAPK, causing enhanced expression of the Pea3 (polyomavirus enhancer activator 3) transcription factor [105].

Another finding is that besides RB and p53 deletions also p130 is an important tumor suppressor and is usually deleted in SCLC. A conditional mutant mice with p130, Rb, and TP53 deletion resulted in increased proliferation and significant acceleration of SCLC development in this mouse model. Genome-wide expression profiling experiments further showed that Rb/p53/p130-mutant mouse tumors were similar to human SCLC [106].

22.8 Models of Metastasis

There are several attempts to create models of lung carcinomas, which regularly metastasize [107–110]. The neuroendocrine carcinomas discussed above usually metastasize, and also those undifferentiated carcinomas in an attempt to create SCLC did metastasize (Fig. 22.20). Meaningful models should identify genes that are important for invasion and metastasis of human carcinomas. These genes should be evaluated in paired samples of human primary carcinomas and metastases and also by comparison of tumors with different metastatic capacities.

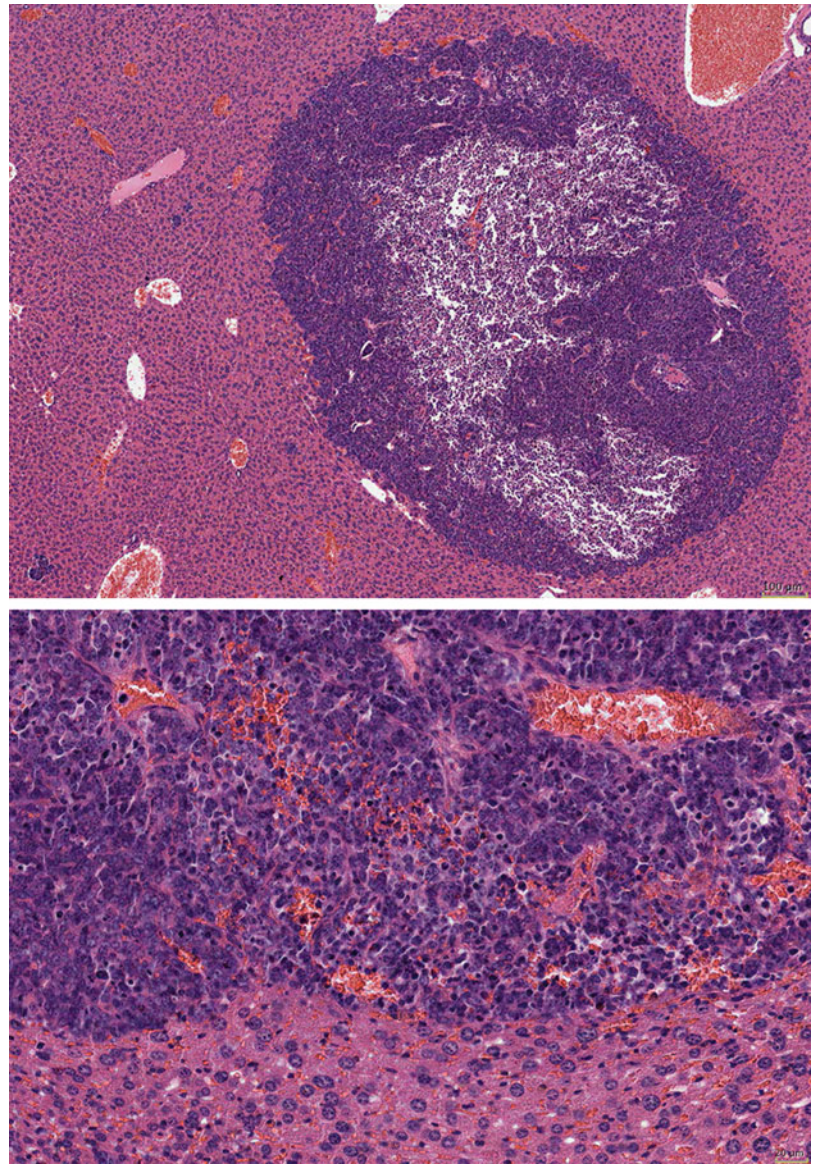

Fig. 22.20 Liver metastasis of an undifferentiated carcinoma with neuroendocrine features. H&E, bars 100 and 20 μm

References

1. Oomen LC, Van der Valk MA, Den Engelse L. Tumour susceptibility in mice in relation to H-2 haplotype. IARC Sci Publ. 1983;51:205–21.
2. Schepers GW. Lung tumors of primates and rodents. II. IMS Ind Med Surg. 1971;40:23–31.
3. Miller MS, Gressani KM, Leone-Kabler S, Townsend AJ, Malkinson AM, O'Sullivan MG. Differential sensitivity to lung tumorigenesis following transplacental exposure of mice to polycyclic hydrocarbons, heterocyclic amines, and lung tumor promoters. Exp Lung Res. 2000;26:709–30.
4. Yang G, Wang ZY, Kim S, Liao J, Seril DN, Chen X, Smith TJ, Yang CS. Characterization of early pulmonary hyperproliferation and tumor progression and their inhibition by black tea in a 4-(methylnitrosamino)-1-(3-pyridyl)-1-butanone-induced lung tumorigenesis model with A/J mice. Cancer Res. 1997;57:1889–94.

5. Malkinson AM. Primary lung tumors in mice: an experimentally manipulable model of human adenocarcinoma. Cancer Res. 1992;52:2670s–6.
6. Stearman RS, Dwyer-Nield L, Zerbe L, Blaine SA, Chan Z, Bunn Jr PA, Johnson GL, Hirsch FR, Merrick DT, Franklin WA, Baron AE, Keith RL, Nemenoff RA, Malkinson AM, Geraci MW. Analysis of orthologous gene expression between human pulmonary adenocarcinoma and a carcinogen-induced murine model. Am J Pathol. 2005;167:1763–75.
7. Chen Y, Thai P, Zhao YH, Ho YS, DeSouza MM, Wu R. Stimulation of airway mucin gene expression by interleukin (IL)-17 through IL-6 paracrine/autocrine loop. J Biol Chem. 2003;278:17036–43.
8. Heinrich U, Pott F, Mohr U, Fuhst R, Konig J. Lung tumours in rats and mice after inhalation of PAH-rich emissions. Exp Pathol. 1986;29:29–34.
9. Grimmer G, Abel U, Brune H, Deutsch-Wenzel R, Emura M, Heinrich U, Jacob J, Kemena A, Misfeld J, Mohr U, et al. Evaluation of environmental carcinogens by carcinogen-specific test systems. Exp Pathol. 1986;29:65–76.
10. Kitamura H, Tsubakihara M, Inayama Y, Ito T, Kanisawa M. Long-term maintenance of human distal airway epithelial cells in nude mice: a potentially useful model for the study of pulmonary carcinogenesis and lung cell biology. Lab Invest. 1990;62:383–9.
11. Kool H, Mous D, Tibboel D, de Klein A, Rottier RJ. Pulmonary vascular development goes awry in congenital lung abnormalities. Birth Defects Res C Embryol Today. 2014;102:343–58.
12. Erlandsson A, Forssell-Aronsson E, Seidal T, Bernhardt P. Binding of TS1, an anti-keratin 8 antibody, in small-cell lung cancer after 177Lu-DOTA-Tyr3-octreotate treatment: a histological study in xenografted mice. EJNMMI Res. 2011;1:19.
13. Weiss ID, Ella E, Dominsky O, Smith Y, Abraham M, Wald H, Shlomai Z, Zamir G, Feigelson SW, Shezen E, Bar-Shai A, Alon R, Izhar U, Peled A, Shapira OM, Wald O. In the hunt for therapeutic targets: mimicking the growth, metastasis, and stromal associations of early-stage lung cancer using a novel orthotopic animal model. J Thorac Oncol. 2015;10:46–58.
14. Gao Y, Li G, Sun L, He Y, Li X, Sun Z, Wang J, Jiang Y, Shi J. ACTN4 and the pathways associated with cell motility and adhesion contribute to the process of lung cancer metastasis to the brain. BMC Cancer. 2015;15:277.
15. Truesdell P, Ahn J, Chander H, Meens J, Watt K, Yang X, Craig AW. CIP4 promotes lung adenocarcinoma metastasis and is associated with poor prognosis. Oncogene. 2015;34:3527–35.
16. Stewart EL, Mascaux C, Pham NA, Sakashita S, Sykes J, Kim L, Yanagawa N, Allo G, Ishizawa K, Wang D, Zhu CQ, Li M, Ng C, Liu N, Pintilie M, Martin P, John T, Jurisica I, Leighl NB, Neel BG, Waddell TK, Shepherd FA, Liu G, Tsao MS. Clinical utility of patient-derived xenografts to determine biomarkers of prognosis and map resistance pathways in EGFR-mutant lung adenocarcinoma. J Clin Oncol. 2015;33:2472–80.
17. Gallagher-Colombo SM, Miller J, Cengel KA, Putt ME, Vinogradov SA, Busch TM. Erlotinib pretreatment improves photodynamic therapy of non-small cell lung carcinoma xenografts via multiple mechanisms. Cancer Res. 2015;75:3118–26.
18. Gotz R, Sendtner M. Cooperation of tyrosine kinase receptor TrkB and epidermal growth factor receptor signaling enhances migration and dispersal of lung tumor cells. PLoS ONE. 2014;9:e100944.
19. Huang MH, Lee JH, Chang YJ, Tsai HH, Lin YL, Lin AM, Yang JC. MEK inhibitors reverse resistance in epidermal growth factor receptor mutation lung cancer cells with acquired resistance to gefitinib. Mol Oncol. 2013;7:112–20.
20. Pallier K, Cessot A, Cote JF, Just PA, Cazes A, Fabre E, Danel C, Riquet M, Devouassoux-Shisheboran M, Ansieau S, Puisieux A, Laurent-Puig P, Blons H. TWIST1 a new determinant of epithelial to mesenchymal transition in EGFR mutated lung adenocarcinoma. PLoS ONE. 2012;7:e29954.
21. Bryant JL, Britson J, Balko JM, Willian M, Timmons R, Frolov A, Black EP. A microRNA gene expression signature predicts response to erlotinib in epithelial cancer cell lines and targets EMT. Br J Cancer. 2012;106:148–56.
22. Slaga TJ. Overview of tumor promotion in animals. Environ Health Perspect. 1983;50:3–14.
23. Sunderman Jr FW. Nickel carcinogenesis. Dis Chest. 1968;54:527–34.
24. Nuzum EO, Malkinson AM, Beer DG. Specific Ki-ras codon 61 mutations may determine the development of urethan-induced mouse lung adenomas or adenocarcinomas. Mol Carcinog. 1990;3:287–95.
25. Watanabe M, Watanabe K, Konno K, Sato H. Genetic differences in the induction of aryl hydrocarbon hydroxylase and benzo(a)pyrene carcinogenesis in C3H/He and DBA/2 strains of mice. Gan. 1975;66:217–26.
26. Henry MC, Port CD, Kaufman DG. Importance of physical properties of benzo(a)pyrene-ferric oxide mixtures in lung tumor induction. Cancer Res. 1975;35:207–17.
27. Saffiotti U, Montesano R, Sellakumar AR, Cefis F, Kaufman DG. Respiratory tract carcinogenesis in hamsters induced by different numbers of administrations of benzo(a)pyrene and ferric oxide. Cancer Res. 1972;32:1073–81.
28. Toth B, Shubik P. Carcinogenesis in AKR mice injected at birth with benzo(a)pyrene and dimethylnitrosamine. Cancer Res. 1967;27:43–51.
29. Miller L, Smith WE, Berliner SW. Tests for effect of asbestos on benzo[a]pyrene carcinogenesis in the respiratory tract. Ann N Y Acad Sci. 1965;132:489–500.
30. Bodduluru LN, Kasala ER, Barua CC, Karnam KC, Dahiya V, Ellutla M. Antiproliferative and antioxidant potential of hesperetin against benzo(a)pyrene-

induced lung carcinogenesis in Swiss albino mice. Chem Biol Interact. 2015;242:345–52.
31. Ravichandran N, Suresh G, Ramesh B, Manikandan R, Choi YW, Vijaiyan Siva G. Fisetin modulates mitochondrial enzymes and apoptotic signals in benzo(a)pyrene-induced lung cancer. Mol Cell Biochem. 2014;390:225–34.
32. Zuo J, Brewer DS, Arlt VM, Cooper CS, Phillips DH. Benzo pyrene-induced DNA adducts and gene expression profiles in target and non-target organs for carcinogenesis in mice. BMC Genomics. 2014;15:880.
33. Yeo CD, Kim JW, Ha JH, Kim SJ, Lee SH, Kim IK, Kim YK. Chemopreventive effect of phosphodiesterase-4 inhibition in benzo(a)pyrene-induced murine lung cancer model. Exp Lung Res. 2014; 40:500–6.
34. Horio Y, Chen A, Rice P, Roth JA, Malkinson AM, Schrump DS. Ki-ras and p53 mutations are early and late events, respectively, in urethane-induced pulmonary carcinogenesis in A/J mice. Mol Carcinog. 1996;17:217–23.
35. Santiago LN, de Camargo FJ, Braga LC, Cordeiro JA, Cury PM. The effect of different doses of cigarette smoke in a mouse lung tumor model. Int J Clin Exp Pathol. 2009;2:176–81.
36. Westcott PM, Halliwill KD, To MD, Rashid M, Rust AG, Keane TM, Delrosario R, Jen KY, Gurley KE, Kemp CJ, Fredlund E, Quigley DA, Adams DJ, Balmain A. The mutational landscapes of genetic and chemical models of Kras-driven lung cancer. Nature. 2015;517:489–92.
37. Lee HY, Suh YA, Lee JI, Hassan KA, Mao L, Force T, Gilbert BE, Jacks T, Kurie JM. Inhibition of oncogenic K-ras signaling by aerosolized gene delivery in a mouse model of human lung cancer. Clin Cancer Res. 2002;8:2970–5.
38. Jackson EL, Olive KP, Tuveson DA, Bronson R, Crowley D, Brown M, Jacks T. The differential effects of mutant p53 alleles on advanced murine lung cancer. Cancer Res. 2005;65:10280–8.
39. Sweet-Cordero A, Mukherjee S, Subramanian A, You H, Roix JJ, Ladd-Acosta C, Mesirov J, Golub TR, Jacks T. An oncogenic KRAS2 expression signature identified by cross-species gene-expression analysis. Nat Genet. 2005;37:48–55.
40. Wootton SK, Metzger MJ, Hudkins KL, Alpers CE, York D, DeMartini JC, Miller AD. Lung cancer induced in mice by the envelope protein of jaagsiekte sheep retrovirus (JSRV) closely resembles lung cancer in sheep infected with JSRV. Retrovirology. 2006;3:94.
41. Lee GH. The Kras2 oncogene and mouse lung carcinogenesis. Med Mol Morphol. 2008;41:199–203.
42. Kim CF, Jackson EL, Kirsch DG, Grimm J, Shaw AT, Lane K, Kissil J, Olive KP, Sweet-Cordero A, Weissleder R, Jacks T. Mouse models of human non-small-cell lung cancer: raising the bar. Cold Spring Harb Symp Quant Biol. 2005;70:241–50.
43. Minna JD, Kurie JM, Jacks T. A big step in the study of small cell lung cancer. Cancer Cell. 2003;4:163–6.
44. DuPage M, Dooley AL, Jacks T. Conditional mouse lung cancer models using adenoviral or lentiviral delivery of Cre recombinase. Nat Protoc. 2009;4:1064–72.
45. Zhou Y, Rideout 3rd WM, Zi T, Bressel A, Reddypalli S, Rancourt R, Woo JK, Horner JW, Chin L, Chiu MI, Bosenberg M, Jacks T, Clark SC, Depinho RA, Robinson MO, Heyer J. Chimeric mouse tumor models reveal differences in pathway activation between ERBB family- and KRAS-dependent lung adenocarcinomas. Nat Biotechnol. 2010;28:71–8.
46. Musteanu M, Blaas L, Zenz R, Svinka J, Hoffmann T, Grabner B, Schramek D, Kantner HP, Muller M, Kolbe T, Rulicke T, Moriggl R, Kenner L, Stoiber D, Penninger JM, Popper H, Casanova E, Eferl R. A mouse model to identify cooperating signaling pathways in cancer. Nat Methods. 2012;9:897–900.
47. McFadden DG, Papagiannakopoulos T, Taylor-Weiner A, Stewart C, Carter SL, Cibulskis K, Bhutkar A, McKenna A, Dooley A, Vernon A, Sougnez C, Malstrom S, Heimann M, Park J, Chen F, Farago AF, Dayton T, Shefler E, Gabriel S, Getz G, Jacks T. Genetic and clonal dissection of murine small cell lung carcinoma progression by genome sequencing. Cell. 2014;156:1298–311.
48. Popper HH. Lung adenocarcinomas: comparison between mice and men. Methods Mol Biol. 2015;1267:19–43.
49. Banerjee ER, Henderson Jr WR. Characterization of lung stem cell niches in a mouse model of bleomycin-induced fibrosis. Stem Cell Res Ther. 2012;3:21.
50. Koukourakis MI, Giatromanolaki A, Brekken RA, Sivridis E, Gatter KC, Harris AL, Sage EH. Enhanced expression of SPARC/osteonectin in the tumor-associated stroma of non-small cell lung cancer is correlated with markers of hypoxia/acidity and with poor prognosis of patients. Cancer Res. 2003;63:5376–80.
51. O'Byrne KJ, Dalgleish AG, Browning MJ, Steward WP, Harris AL. The relationship between angiogenesis and the immune response in carcinogenesis and the progression of malignant disease. Eur J Cancer. 2000;36:151–69.
52. Galaup A, Cazes A, Le Jan S, Philippe J, Connault E, Le Coz E, Mekid H, Mir LM, Opolon P, Corvol P, Monnot C, Germain S. Angiopoietin-like 4 prevents metastasis through inhibition of vascular permeability and tumor cell motility and invasiveness. Proc Natl Acad Sci U S A. 2006;103:18721–6.
53. Liu YL, Yu JM, Song XR, Wang XW, Xing LG, Gao BB. Regulation of the chemokine receptor CXCR4 and metastasis by hypoxia-inducible factor in non small cell lung cancer cell lines. Cancer Biol Ther. 2006;5:1320–6.
54. Taki M, Kamata N, Yokoyama K, Fujimoto R, Tsutsumi S, Nagayama M. Down-regulation of Wnt-4 and up-regulation of Wnt-5a expression by

epithelial-mesenchymal transition in human squamous carcinoma cells. Cancer Sci. 2003;94:593–7.
55. Eger A, Stockinger A, Park J, Langkopf E, Mikula M, Gotzmann J, Mikulits W, Beug H, Foisner R. beta-Catenin and TGFbeta signalling cooperate to maintain a mesenchymal phenotype after FosER-induced epithelial to mesenchymal transition. Oncogene. 2004;23:2672–80.
56. Gotzmann J, Mikula M, Eger A, Schulte-Hermann R, Foisner R, Beug H, Mikulits W. Molecular aspects of epithelial cell plasticity: implications for local tumor invasion and metastasis. Mutat Res. 2004;566:9–20.
57. Timmerman LA, Grego-Bessa J, Raya A, Bertran E, Perez-Pomares JM, Diez J, Aranda S, Palomo S, McCormick F, Izpisua-Belmonte JC, de la Pompa JL. Notch promotes epithelial-mesenchymal transition during cardiac development and oncogenic transformation. Genes Dev. 2004;18:99–115.
58. Lan M, Kojima T, Osanai M, Chiba H, Sawada N. Oncogenic Raf-1 regulates epithelial to mesenchymal transition via distinct signal transduction pathways in an immortalized mouse hepatic cell line. Carcinogenesis. 2004;25:2385–95.
59. Grego-Bessa J, Diez J, Timmerman L, de la Pompa JL. Notch and epithelial-mesenchyme transition in development and tumor progression: another turn of the screw. Cell Cycle. 2004;3:718–21.
60. Zavadil J, Cermak L, Soto-Nieves N, Bottinger EP. Integration of TGF-beta/Smad and Jagged1/Notch signalling in epithelial-to-mesenchymal transition. Embo J. 2004;23:1155–65.
61. Yao HW, Xie QM, Chen JQ, Deng YM, Tang HF. TGF-beta1 induces alveolar epithelial to mesenchymal transition in vitro. Life Sci. 2004;76:29–37.
62. Zhou BP, Deng J, Xia W, Xu J, Li YM, Gunduz M, Hung MC. Dual regulation of Snail by GSK-3beta-mediated phosphorylation in control of epithelial-mesenchymal transition. Nat Cell Biol. 2004;6:931–40.
63. Blaukovitsch M, Halbwedl I, Kothmaier H, Gogg-Kammerer M, Popper HH. Sarcomatoid carcinomas of the lung – are these histogenetically heterogeneous tumors? Virchows Arch. 2006;449:455–61.
64. Gibbons DL, Lin W, Creighton CJ, Rizvi ZH, Gregory PA, Goodall GJ, Thilaganathan N, Du L, Zhang Y, Pertsemlidis A, Kurie JM. Contextual extracellular cues promote tumor cell EMT and metastasis by regulating miR-200 family expression. Genes Dev. 2009;23:2140–51.
65. Ramos C, Becerril C, Montano M, Garcia-De-Alba C, Ramirez R, Checa M, Pardo A, Selman M. FGF-1 reverts epithelial-mesenchymal transition induced by TGF-{beta}1 through MAPK/ERK kinase pathway. Am J Physiol Lung Cell Mol Physiol. 2010;299:L222–31.
66. Masszi A, Kapus A. Smaddening complexity: the role of Smad3 in epithelial-myofibroblast transition. Cells Tissues Organs. 2011;193:41–52.
67. Borczuk AC, Kim HK, Yegen HA, Friedman RA, Powell CA. Lung adenocarcinoma global profiling identifies type II transforming growth factor-beta receptor as a repressor of invasiveness. Am J Respir Crit Care Med. 2005;172:729–37.
68. Gibbons DL, Lin W, Creighton CJ, Zheng S, Berel D, Yang Y, Raso MG, Liu DD, Wistuba II, Lozano G, Kurie JM. Expression signatures of metastatic capacity in a genetic mouse model of lung adenocarcinoma. PLoS ONE. 2009;4:e5401.
69. Matsuzaki O. Histogenesis and growing patterns of lung tumors induced by potassium 1-methyl-1,4-dihydro-7-(2-(5-nitrofuryl)vinyl)-4-oxo-1,8-naphthyridine-3-carboxylate in ICR mice. Gann. 1975;66:259–67.
70. Rehm S, Kelloff GJ. Histologic characterization of mouse bronchiolar cell hyperplasia, metaplasia, and neoplasia induced intratracheally by 3-methylcholanthrene. Exp Lung Res. 1991;17:229–44.
71. Malkinson AM. Molecular comparison of human and mouse pulmonary adenocarcinomas. Exp Lung Res. 1998;24:541–55.
72. Nikitin AY, Alcaraz A, Anver MR, Bronson RT, Cardiff RD, Dixon D, Fraire AE, Gabrielson EW, Gunning WT, Haines DC, Kaufman MH, Linnoila RI, Maronpot RR, Rabson AS, Reddick RL, Rehm S, Rozengurt N, Schuller HM, Shmidt EN, Travis WD, Ward JM, Jacks T. Classification of proliferative pulmonary lesions of the mouse: recommendations of the mouse models of human cancers consortium. Cancer Res. 2004;64:2307–16.
73. Travis WD, Brambilla E, Noguchi M, Nicholson AG, Geisinger KR, Yatabe Y, Beer DG, Powell CA, Riely GJ, Van Schil PE, Garg K, Austin JH, Asamura H, Rusch VW, Hirsch FR, Scagliotti G, Mitsudomi T, Huber RM, Ishikawa Y, Jett J, Sanchez-Cespedes M, Sculier JP, Takahashi T, Tsuboi M, Vansteenkiste J, Wistuba I, Yang PC, Aberle D, Brambilla C, Flieder D, Franklin W, Gazdar A, Gould M, Hasleton P, Henderson D, Johnson B, Johnson D, Kerr K, Kuriyama K, Lee JS, Miller VA, Petersen I, Roggli V, Rosell R, Saijo N, Thunnissen E, Tsao M, Yankelewitz D. International association for the study of lung cancer/american thoracic society/european respiratory society international multidisciplinary classification of lung adenocarcinoma. J Thorac Oncol. 2011;6:244–85.
74. Travis WD. Update on small cell carcinoma and its differentiation from squamous cell carcinoma and other non-small cell carcinomas. Mod Pathol. 2012;25 Suppl 1:S18–30.
75. Maeshima A, Miyagi A, Hirai T, Nakajima T. Mucin-producing adenocarcinoma of the lung, with special reference to goblet cell type adenocarcinoma: immunohistochemical observation and Ki-ras gene mutation. Pathol Int. 1997;47:454–60.
76. Dabbagh K, Takeyama K, Lee HM, Ueki IF, Lausier JA, Nadel JA. IL-4 induces mucin gene expres-

sion and goblet cell metaplasia in vitro and in vivo. J Immunol. 1999;162:6233–7.
77. Yamamoto H, Bai YQ, Yuasa Y. Homeodomain protein CDX2 regulates goblet-specific MUC2 gene expression. Biochem Biophys Res Commun. 2003;300:813–8.
78. Stacher E, Ullmann R, Halbwedl I, Gogg-Kammerer M, Boccon-Gibod L, Nicholson AG, Sheppard MN, Carvalho L, Franca MT, Macsweeney F, Morresi-Hauf A, Popper HH. Atypical goblet cell hyperplasia in congenital cystic adenomatoid malformation as a possible preneoplasia for pulmonary adenocarcinoma in childhood: a genetic analysis. Hum Pathol. 2004;35:565–70.
79. Maeda Y, Tsuchiya T, Hao H, Tompkins DH, Xu Y, Mucenski ML, Du L, Keiser AR, Fukazawa T, Naomoto Y, Nagayasu T, Whitsett JA. Kras(G12D) and Nkx2-1 haploinsufficiency induce mucinous adenocarcinoma of the lung. J Clin Invest. 2012;122:4388–400.
80. Popper HH, Woldrich A. Oxygen radical formation a probable mechanism for chromate toxicity. Prog Histochem Cytochem. 1991;23:220–6.
81. Popper HH, Wiespainer G, Leingartner E, Weybora W, Ratschek M. Short term chromate inhalation in a computer-assisted inhalation chamber: immediate toxicity and late cancer development. Environ Hyg. 1992;3:127–31.
82. Reid L, Meyrick B, Antony VB, Chang LY, Crapo JD, Reynolds HY. The mysterious pulmonary brush cell: a cell in search of a function. Am J Respir Crit Care Med. 2005;172:136–9.
83. Sbarbati A, Osculati F. A new fate for old cells: brush cells and related elements. J Anat. 2005;206:349–58.
84. Geles A, Gruber-Moesenbacher U, Quehenberger F, Manzl C, Al Effah M, Grygar E, Juettner-Smolle F, Popper HH. Pulmonary mucinous adenocarcinomas: architectural patterns in correlation with genetic changes, prognosis and survival. Virchows Arch. 2015;467:675–86.
85. Takeyama K, Dabbagh K, Lee HM, Agusti C, Lausier JA, Ueki IF, Grattan KM, Nadel JA. Epidermal growth factor system regulates mucin production in airways. Proc Natl Acad Sci U S A. 1999;96:3081–6.
86. Rose MC, Piazza FM, Chen YA, Alimam MZ, Bautista MV, Letwin N, Rajput B. Model systems for investigating mucin gene expression in airway diseases. J Aerosol Med. 2000;13:245–61.
87. Johnson DH, Fehrenbacher L, Novotny WF, Herbst RS, Nemunaitis JJ, Jablons DM, Langer CJ, DeVore 3rd RF, Gaudreault J, Damico LA, Holmgren E, Kabbinavar F. Randomized phase II trial comparing bevacizumab plus carboplatin and paclitaxel with carboplatin and paclitaxel alone in previously untreated locally advanced or metastatic non-small-cell lung cancer. J Clin Oncol. 2004;22:2184–91.
88. Zuhdi Alimam M, Piazza FM, Selby DM, Letwin N, Huang L, Rose MC. Muc-5/5ac mucin messenger RNA and protein expression is a marker of goblet cell metaplasia in murine airways. Am J Respir Cell Mol Biol. 2000;22:253–60.
89. Yamauchi K, Piao HM, Nakadate T, Shikanai T, Nakamura Y, Ito H, Mouri T, Kobayashi H, Maesawa C, Sawai T, Ohtsu H, Inoue H. Enhanced goblet cell hyperplasia in HDC knockout mice with allergic airway inflammation. Allergol Int. 2009;58:125–34.
90. Zhang X, Zhang Y, Tao B, Wang D, Cheng H, Wang K, Zhou R, Xie Q, Ke Y. Docking protein Gab2 regulates mucin expression and goblet cell hyperplasia through TYK2/STAT6 pathway. FASEB J. 2012;26:4603–13.
91. Abdullah LH, Wolber C, Kesimer M, Sheehan JK, Davis CW. Studying mucin secretion from human bronchial epithelial cell primary cultures. Methods Mol Biol. 2012;842:259–77.
92. Linnoila RI, Sahu A, Miki M, Ball DW, DeMayo FJ. Morphometric analysis of CC10-hASH1 transgenic mouse lung: a model for bronchiolization of alveoli and neuroendocrine carcinoma. Exp Lung Res. 2000;26:595–615.
93. Giangreco A, Reynolds SD, Stripp BR. Terminal bronchioles harbor a unique airway stem cell population that localizes to the bronchoalveolar duct junction. Am J Pathol. 2002;161:173–82.
94. Berns A. Stem cells for lung cancer? Cell. 2005;121:811–3.
95. Kim CF, Jackson EL, Woolfenden AE, Lawrence S, Babar I, Vogel S, Crowley D, Bronson RT, Jacks T. Identification of bronchioalveolar stem cells in normal lung and lung cancer. Cell. 2005;121:823–35.
96. Volckaert T, Dill E, Campbell A, Tiozzo C, Majka S, Bellusci S, De Langhe SP. Parabronchial smooth muscle constitutes an airway epithelial stem cell niche in the mouse lung after injury. J Clin Invest. 2011;121:4409–19.
97. Van Winkle LS, Buckpitt AR, Nishio SJ, Isaac JM, Plopper CG. Cellular response in naphthalene-induced Clara cell injury and bronchiolar epithelial repair in mice. Am J Physiol. 1995;269:L800–18.
98. Buckpitt A, Boland B, Isbell M, Morin D, Shultz M, Baldwin R, Chan K, Karlsson A, Lin C, Taff A, West J, Fanucchi M, Van Winkle L, Plopper C. Naphthalene-induced respiratory tract toxicity: metabolic mechanisms of toxicity. Drug Metab Rev. 2002;34:791–820.
99. Abdo KM, Grumbein S, Chou BJ, Herbert R. Toxicity and carcinogenicity study in F344 rats following 2 years of whole-body exposure to naphthalene vapors. Inhal Toxicol. 2001;13:931–50.
100. Park KS, Wells JM, Zorn AM, Wert SE, Laubach VE, Fernandez LG, Whitsett JA. Transdifferentiation of ciliated cells during repair of the respiratory epithelium. Am J Respir Cell Mol Biol. 2006;34:151–7.
101. Meuwissen R, Linn SC, Linnoila RI, Zevenhoven J, Mooi WJ, Berns A. Induction of small cell lung cancer by somatic inactivation of both Trp53 and Rb1 in a conditional mouse model. Cancer Cell. 2003;4:181–9.

102. Calbo J, Meuwissen R, van Montfort E, van Tellingen O, Berns A. Genotype-phenotype relationships in a mouse model for human small-cell lung cancer. Cold Spring Harb Symp Quant Biol. 2005;70:225–32.
103. Gazdar AF, Savage TK, Johnson JE, Berns A, Sage J, Linnoila RI, MacPherson D, McFadden DG, Farago A, Jacks T, Travis WD, Brambilla E. The comparative pathology of genetically engineered mouse models for neuroendocrine carcinomas of the lung. J Thorac Oncol. 2015;10:553–64.
104. Linnoila RI, Naizhen X, Meuwissen R, Berns A, DeMayo FJ. Mouse lung neuroendocrine carcinomas: distinct morphologies, same transcription factors. Exp Lung Res. 2005;31:37–55.
105. Kwon MC, Proost N, Song JY, Sutherland KD, Zevenhoven J, Berns A. Paracrine signaling between tumor subclones of mouse SCLC: a critical role of ETS transcription factor Pea3 in facilitating metastasis. Genes Dev. 2015;29:1587–92.
106. Schaffer BE, Park KS, Yiu G, Conklin JF, Lin C, Burkhart DL, Karnezis AN, Sweet-Cordero EA, Sage J. Loss of p130 accelerates tumor development in a mouse model for human small-cell lung carcinoma. Cancer Res. 2010;70:3877–83.
107. Kitamura T, Qian BZ, Pollard JW. Immune cell promotion of metastasis. Nat Rev Immunol. 2015;15:73–86.
108. Chen S, Sanjana NE, Zheng K, Shalem O, Lee K, Shi X, Scott DA, Song J, Pan JQ, Weissleder R, Lee H, Zhang F, Sharp PA. Genome-wide CRISPR screen in a mouse model of tumor growth and metastasis. Cell. 2015;160:1246–60.
109. Li CM, Chen G, Dayton TL, Kim-Kiselak C, Hoersch S, Whittaker CA, Bronson RT, Beer DG, Winslow MM, Jacks T. Differential Tks5 isoform expression contributes to metastatic invasion of lung adenocarcinoma. Genes Dev. 2013;27:1557–67.
110. Calbo J, van Montfort E, Proost N, van Drunen E, Beverloo HB, Meuwissen R, Berns A. A functional role for tumor cell heterogeneity in a mouse model of small cell lung cancer. Cancer Cell. 2011;19:244–56.

Handling of Tissues and Cells 23

23.1 Biopsies

There are different types of biopsies one can receive: bronchial biopsies, transbronchial biopsies, ultrasound-guided needle biopsies, and transthoracic needle biopsies. Bronchial biopsies, ultrasound-guided needle biopsies, and transthoracic needle biopsies are usually taken because of clinically suspected tumor. Three cylinders are recommended for transthoracic needle biopsy, four to eight pieces are recommended for bronchial biopsies, and three to five punches should be done in ultrasound-guided needle biopsy. Rapid on-site evaluation (ROSE) is recommended if logistically possible. This will enable to control the quality of the FNA-derived material, and in case of insufficient tissues, the procedure can be repeated. Transbronchial biopsies are most often taken for the diagnosis of nontumor diseases. At least four to six pieces are recommended. Ideally these are taken under radiological control. Video-guided or ultrasound-guided systems are available, which increase the sensitivity of this method. However, if the transbronchial biopsy is not representative or nondiagnostic, we recommend to proceed to videothoracic surgery.

The biopsies should be fixed in 4 % neutral buffered formalin for at least 8 h. After that, they should be processed using automated systems. In case of transthoracic needle biopsies, the cylinders should be placed each in separate cassettes. This will enable to select the most appropriate cylinder for molecular analysis and save additional tissue for further analysis.

23.2 Videothoracic Lung Biopsy (VATS) and Open Lung Biopsy (OLB)

The thoracic surgeon, the radiologist, and the pathologist should discuss the selection of the biopsy site. It is important to take the biopsy at a site, where the most important radiologic changes are seen. In interstitial pneumonias, these are nodular densities, granulomas, ground-glass opacities, cystic spaces, etc. The tissue should measure at least 3×5×3 cm. Biopsies from children including newborn can be smaller. The tissue should be fixed by formalin instillation. Take a small syringe and fill it with formalin. Insert the needle into the lung biopsy and gently inflate it by floating the lung with formalin. The tissue should look like lung tissue in full inspiration. Place the tissue into a container with ample formalin and let it fix for at least 8 h before sectioning it.

After fixation, remove the clamps and section the tissue into 6–8 mm thick slices and describe macroscopically whatever morphologic abnormalities are present. Slicing the tissue may be dictated by the probable diagnoses suspected: slicing in a 90° angle against the pleura surface is most often appropriate; however, in cases of suspected vascular diseases, it is recommended to

© Springer-Verlag Berlin Heidelberg 2017
H. Popper, *Pathology of Lung Disease*, DOI 10.1007/978-3-662-50491-8_23

section the tissue parallel to the pleura surface, to get cross sections of the vessels (see schematic drawing below). After macroscopic inspection, process the slices each in a separate cassette and number them consecutively.

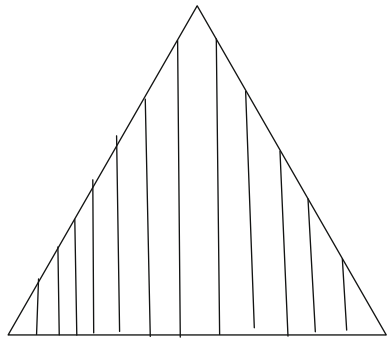

Pleura surface

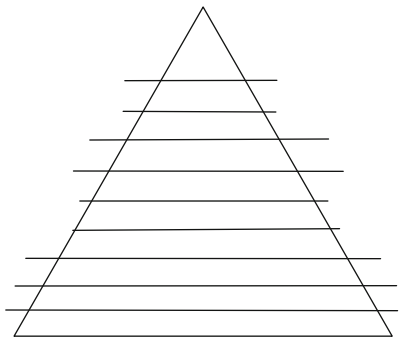

Pleura surface

23.3 Resection Specimen

Lobectomy and pneumonectomy specimen are filled with formalin from the airways. This can be done by a pressure pump from a formalin container or simply by a glass reservoir above the specimen (at least 25 cm above). Insert a tip of a pipette into the respective bronchus, and fill the lobes one by one until the whole lung looks like in maximal inspiration. Place this resection specimen into a large container filled with formalin, and cover the lung by paper towels soaked in formalin to avoid drying of the surface. Let the tissue fix overnight (at least 10 h).

After fixation, section the lung either horizontally or vertically depending on the needs. Resection margins (bronchial, vascular, mediastinal) should be painted with colors. In case you need a correlation with a CT, it is recommended to section the tissue horizontally in slices corresponding to the CT slices. Section the lung into 6–8 mm thick slices and place them one after another on your table for detailed inspection. Describe whatever macroscopic abnormalities are present. Then start to cut out lymph nodes and place them accordingly to their stage into separate cassettes. If the nodes are resected separately, section and count them individually and place them into separate cassettes. Take sections from the tumor, at least one section from each slice of lung tissue; in large tumors, take two instead of one from each slice. Give measurements on all abnormalities in cm or mm. Include at least three to four pieces of lung tissue from areas outside the tumor for controls or for evaluation of concomitant lung diseases, such as emphysema, COPD, etc.

23.4 Frozen Section Handling and Evaluation

Frozen section analysis of lung diseases is a preferred way to preselect tissue, to plan ancillary investigations, and to plan for storage in biobanks. This can be done in resection specimen as well as VATS. In resection specimen, this is useful for the evaluation of resection margins. From the fresh tissue, bronchial and vascular margins are sectioned and covered by the freezing medium, frozen, and sectioned. The rest can be fixed and processed for paraffin histology.

In VATS the process is different: mix the freezing medium with phosphate-buffered saline solution 1:1. Aspirate this mixture into a syringe. Insert the needle into the fresh VATS specimen, and gently instill the mixture into the lung until it appears as in full inspiration. Cut the suture and cut the tissue into 6 mm thick slices. Inspect the slices for morphologic abnormalities and select one to two slices for frozen section evaluation. These sections can be stained by H&E and Giemsa; both stains together will provide a maximum of information to reach a diagnosis. At least

the information about a sufficient amount of tissue and tissue, which contains the looked after pathology, can be submitted to the clinician.

In these cases, appropriate tissue can be separated and stored in a tissue bank. We had good experiences with three types of preparations:

1. Small cubes of tissue are immersed into deep frozen isobutene and stored in liquid nitrogen. Isobutene is primarily frozen in liquid nitrogen; after the alcohol is white and frozen, let it thaw shortly; this lowers the temperature into −196 °C. Immerse the tissue into this melting alcohol. Under this temperature, water freezes amorphous; therefore, no ice crystals will appear when the tissue is thawed.
2. Another batch of tissue cubes are placed into RNAlater® and stored in a refrigerator until next morning. After that, the vial with the tissue cubes is stored in a refrigerator at −70 °C.
3. A third batch of tissue cubes is immersed into the freezing medium and after that immediately snap frozen and stored in liquid nitrogen.

Samples under 1 are optimal for genetic analysis but also for FISH. Samples under 2 are optimal for RNA analysis providing even full-length mRNA. Samples under 3 are optimal for protein analysis and can also be used for immunohistochemistry and for preparing a frozen tissue microarray block.

23.5 Handling of Cells

Different types of cytological material are submitted to pathology: smears on glass slides, brush cytology, fine needle aspirates, bronchoalveolar lavage, and pleural fluid. Smears are usually stained by Giemsa (including different modifications), H&E, and Papanicolaou. Even stained slides can sometimes be successfully used for molecular analysis in case no other tumor material is available. Brush cytology often also comes already smeared on glass slides and therefore can only be processed by staining. Aspirates from different sites including EBUS- and EUS-derived cells should be processed into cell blocks if possible. It is recommended that all aspiration material should be submitted unfixed. The material is centrifuged. The cell pellet is immersed into dissolved 7 % agarose in PBS. After cooling, the whitish cell-containing part is dissected, fixed in formalin for 10 min, and embedded in paraffin. Sections can be made as in tissues.

Pleural fluid should be processed similarly into cell blocks in case of suspected tumor/metastasis.

The preparation of bronchoalveolar lavage has already been explained in Chap. 15.

23.6 Microbiology

For microbiological analysis, take swaps from tissue sections and process it for microbiological analysis as usual. Use a new knife for sectioning to avoid contamination. For immediate analysis, a smear can be produced in addition and stained by Gram or acid-fast stains.